EAWAG
Swiss Federal Institute for Environmental Science and Technology

SWAT Team
USDA-ARS Research Lab, Temple, Texas
TAES, Temple, Texas
SSL, Texas A&M University, College Station

3rd International SWAT Conference July 11-15, Zürich

Held at EAWAG, ETH, Switzerland

ISBN: 1-933570-43-1

2005 3rd International SWAT Conference Proceedings

Edited by

Raghavan Srinivasan
Jennifer Jacobs
Danya Day
Karim Abbaspour

Sponsored by the

EAWAG, Swiss Federal Institute for Environmental Science and Technology
www.eawag.ch/

DEZA, Swiss Agency for Development and Cooperation
www.deza.ch/

Swiss National Science Foundation, Switzerland
www.snf.ch/

ESRI++, Switzerland

Co-sponsored by the

USDA-ARS Grassland, Soil & Water Research Laboratory
Temple, Texas, USA

Blackland Research and Extension Center
Texas Agricultural Experiment Station
Temple, Texas, USA

Spatial Sciences Laboratory, Texas A&M University
College Station, Texas, USA

July 13-15, 2005 • Zurich, Switzerland

ISBN: 1-933570-43-1

Foreword

This proceeding presents papers that were given at the 3rd International SWAT Conference, SWAT 2005, which convened at Eawag in Duebendorf, Switzerland.

The focus of this conference was to allow an international community of researchers and scholars to discuss the latest advances in the use of the SWAT (Soil Water Assessment Tool) model to assess water quality trends.

The SWAT model was developed by researchers Jeff Arnold of the United States Department of Agriculture Research Service (USDA-ARS) in Temple, Texas and Raghavan Srinivasan at the Texas Agricultural Experiment Station (TAES), who is the Director of the Texas A&M University Spatial Sciences Laboratory.

SWAT is a comprehensive computer simulation tool that can be used to simulate the effects of point and nonpoint source pollution from watersheds, in the streams, and rivers. SWAT is integrated with several readily available databases and Geographic Information Systems (GIS).

Because of the versatility of SWAT, the model has been utilized to study a wide range of phenomena throughout the world. At the same time, the research community is actively engaged in developing new improvement to SWAT for site-specific needs and linking SWAT results to other simulation models.

This conference provided an opportunity for the international research community to gather and share information about the latest innovations developed for SWAT and to discuss challenges that still need to be resolved.

This proceedings includes papers covering a variety of themes, including new developments associated with SWAT, applications of the SWAT model, the use of related modeling tools, how SWAT can be calibrated or compared to other models, the use of other simulation models and tools, and integrating SWAT with other models. In addition to papers presented at SWAT 2005, posters shown at the conference are also included in this proceeding.

The organizers of the conference—Karim Abbaspour and Raghavan Srinivasan — want to express thanks to organizations and individuals who made this conference successful. Organizations that played a key role in this conference include USDA-ARS, TAES, Texas A&M University, Swiss Federal Institute for Aquatic Sciences and Technology (Eawag), Swiss Agency for Development and Cooperation (SDC), and Swiss National Science Foundation (SNF). We also thank ESRI++ for their involvement and cooperation with the conference

Individuals that should be acknowledged in the proceedings include Iswarya Srinivasan.

To learn more about SWAT, go to http://www.brc.tamus.edu/swat/ or contact Raghavan Srinivasan at r-srinivasan@tamu.edu.

Conference Objective

Soil and Water Assessment

Natural watershed systems maintain a balance between precipitation, runoff, infiltration, and water which either evaporates from bare soil and open water surfaces or evapotranspires from vegetated surfaces, completing the natural cycle. The understanding of this hydrologic cycle at a watershed scale, and the fate and transport of nutrients, pesticides and other chemicals affecting water quality is essential for development and implementation of appropriate watershed management policies and procedures.

In recent years, application of models has become an indispensable tool for the understanding of the natural processes occurring at the watershed scale. As the natural processes are more and more modified by human activities, application of integrated modelling to account for the interaction of practices such as agricultural management, water removals from surface bodies and groundwater, release of swage into surface and sub-surface, urbanization, etc., has becomes more and more essential.

The program SWAT (Soil and Water Assessment Tool) due to its continuous time scale, distributed spatial handling of parameters and integration of multiple processes such as climate, hydrology, nutrient and pesticide, erosion, land cover, management practices, channel processes, and processes in water bodies has become an important tool for watershed-scale studies.

The third international SWAT conference to be held at EAWAG in Zurich, Switzerland will devote itself to discussions around the application of SWAT to watershed problems world wide. The 5-day program will include 2 days of hands on learning of the SWAT program at the introductory and advanced levels, followed by three days of conference covering a variety of topics related to watershed modelling such as hydrology, water quality, landuse management, erosion, and system analytic topics in calibration, optimization, and uncertainty analysis techniques.

Scientists associated with research institutes and those associated with government agencies and centers for policy making are encouraged to take part in this international conference in order to become familiar with the latest advances and developments in the area of watershed-scale modelling and applications.

Conference Organizing Committee

Karim Abbaspour
abbaspour@eawag.ch
EAWAG, Dübendorf, Switzerland

Rosi Siber
rosi.siber@eawag.ch
EAWAG, Dübendorf, Switzerland

Jürgen Schuol
juergen.Schuol@eawag.ch
EAWAG, Dübendorf, Switzerland

Karin Ghilardi
karin.ghilardi@eawag.ch
EAWAG, Dübendorf, Switzerland

Peter Reichert
reichert@eawag.ch
EAWAG, Dübendorf, Switzerland

Jing Yang
jing.yang@eawag.ch
EAWAG, Dübendorf, Switzerland

Raghavan Srinivasan
r-srinivasan@tamu.edu
Texas A&M University, Texas, USA

Jeff Arnold
jgarnold@spa.ars.usda.gov
USDA ARS, Texas, USA

Scientific Panel Members

Karim Abbaspour
abbaspour@eawag.ch
(EAWAG, Switzerland)

Majid Afyuni
afyuni@cc.iut.ac.ir
(Isfahan University of Technology, Iran)

Jeff Arnold
jgarnold@spa.ars.usda.gov
(USDA ARS, Texas, USA)

Lutz Breuer
Lutz.Breuer@agrar.uni-giessen.de
(Giessen University, Germany)

Mauro DiLuzio
diluzio@brc.tamus.edu
(Texas A&M University, USA)

Nicola Fohrer
nfohrer@hydrology.uni.kiel.de
(Kiel University, Germany)

Jochen Froebrich
jofr@fggm.uni-hannover.de
(Hannover University, Germany)

Ann van Griensven
avgriens@vub.ac.be
(University of Ghent, Belgium)

Valentina Krysanova
krysanova@pik-potsdam.de
(Potsdam Institute for Climate Impact Research, Germany)

Antonio Lo Porto
loporto@area.ba.cnr.it
(IRSA-CNR, Italy)

Farhad Mousavi
mousavi@cc.iut.ac.ir
(Isfahan University of Technology, Iran)

Peter Reichert
reichert@eawag.ch
(EAWAG, Switzerland)

Raghavan Srinivasan
r-srinivasan@tamu.edu
(Texas A&M University, USA)

Martin Volk
martin.volk@ufz.de
(UFZ-Centre for Environmental Research, Germany)

CONTENTS

Foreword i
Conference Organizing Committee iii
Scientific Panel Members iv

Invited Paper

Conservation Effects Assessment Project-ARS Watershed Assessment Study xiii
Clarence Richardson

Session I

1. **SWAT peer-reviewed literature: A review** 1
Philip Gassman, Manuel R. Reyes, Colleen H. Green and Jeffrey G. Arnold

2. **Application of SWIM model in the Elbe Basin: Experience and new developments** 19
Valentina Krysanova, Fred Hattermann, Joachim Post, Anja Habeck and Frank Wechsung

3. **Catchment scale modelling of pesticide losses with imperfect data: A case study from the UK** 30
S.M. White, N. Kannan, B. Grizzetti and J. Hollis

4. **Limitations, problems and solutions in the setup of SWAT for a large-scale hydrological application** 40
Jürgen Schuol and Karim Abbaspour

5. **Assessment of water use in a small watershed in northern Syria, using SWAT** 50
Adriana Bruggeman and Geerte van der Meijden

Session II

6. **The suitability of SWAT model in sediment yield modeling for ungauged catchments: A case of Simiyu River Subcatchment, Tanzania** 61
P.M. Ndomba, F.W. Mtalo and A. Killingtveit

7. **Predicting diffuse-source transfers of sewage sludge-associated chemicals to surface waters using SWAT** 70
N. Kannan, S.M. White and M.J. Whelan

8. **SDA SWAT edition: Efficient spatial data analysis & visualization for SWAT results** **80**
Theresa Possley and Qimiao Lu

Session III

9. **Optimal experimental design in river water quality modelling** **88**
Veronique Vandenberghe, Ann van Griensven, Willy Bauwens and Peter A. Vanrolleghem

10. **Application of SWAT in developing countries using readily available data** **98**
J.H. Jacobs and R. Srinivasan

11. **SWAT-DEG and channel restoration of urban streams** **107**
P.M. Allen and J.G. Arnold

Session IV

12. **Integrated river basin modeling including wetlands and riparian zones in the German Elbe River Basin** **114**
Fred F. Hatterman, Valentina Krysanova, Anja Habeck and Joachim Post

13. **Adapting SWAT for riparian wetlands in an Ontario watershed** **123**
Amanjot Singh, Ramesh Rudra and Wanhong Yang

14. **Developing parameters to simulate trees with SWAT** **132**
Doug MacDonald, Jim Kiniry, Jeff Arnold, Ruth McKeown, Ivan Whitson, Gordan Putz and Ellie Prepas

15. **Integration of 3-PG into SWAT to simulate the growth of evergreen forests** **142**
B.M. Watson, N. Coops, S. Selvalingam and M. Ghafouri

16. **A user friendly multi-catchments tool for the SWAT model** **153**
E. Lorrai and P. Cau

Session V

17. **Towards a process-oriented HRU concept in SWAT: Catchment-related control on baseflow and storage of landscape units in medium to large river basins** **159**
Martin Volk, Peter M. Allen, Jeffrey G. Arnold, Pei-Yu Chen

18. **Interfacing SWAT with systems analysis tools: A generic platform** **169**
Jing Yang, Karim C. Abbaspour and Peter Reichert

19. **Evaluation Methods for SWAT Models** **179**
A. van Griensven, T. Meixner, S. Grunwald and R. Srinivasan

20. **Modifications of the Soil Water and Assessment Tool (SWAT-C) for streamflow modeling in a small, forested watershed on the Canadian Boreal Plain** **189**
Ruth A. McKeown, Gordon Putz, Jeff Arnold and Mauro Di'Luzio

Session VI

21. **The power of multi-objective calibration: Two case studies with SWAT** **200**
Johan A. Huisman, Thorsten Pohlert, Lutz Breuer and Hans-Georg Frede

22. **Comparison of optimization algorithms for the automatic calibration of SWAT2000** **210**
Bryan A. Tolson and Christine A. Shoemaker

23. **A comparison of parameter regionalisation strategies for the water quantity module of the SWAT with application to the Scheldt River Basin** **221**
Griet Heuvelmans, Bart Muys and Jan Feyen

24. **Vulnerability assessment of climate change impact on Indian water resources using the SWAT model** **231**
A.K. Gosain, Sandhya Rao and Debajit Basu Ray

Session VII

25. **Effects of input data resolution on SWAT simulations – A case study at the Ems River Basin (Northwestern Germany)** **241**
Gerd Schmidt and Martin Volk

26. Application of water management models to Mediterranean temporary rivers **251**
Antonio Lo Porto, Anna Maria Girolamo, Filomena De Luca and Giuseppe Pappagallo

27. Evaluation of the SWAT model in a small experimental Mediterranean basin **261**
Feliciana Licciardello, Raghavan Srinivasan and Santo Marcello Zimbone

28. Comparison of runoff responses between SWAT and sequentially coupled SWAT-MODFLOW model **271**
Do Hun Lee, Nam Won Kim and IL Moon Chung

29. Hydrological modelling using SWAT for effective management of a small agricultural watershed **279**
M.P. Tripathi

Session VIII

30. An analysis of the 2004 Iowa diffuse pollution needs assessment using SWAT **291**
Philip W. Gassman, Silvia Secchi, Cathy L. Kling, Manoj Jha, Lyubov A. Kurkalova and Hong-Li Feng

31. Potential accuracy of water quality estimates based on non-calibrated SWAT simulations **301**
Claire Baffaut, Todd D. Farrand and Verel W. Benson

32. An approach to assess SWAT model performance in evaluating management actions in a Finnish catchment **310**
Ilona Bärlund and Teija Kirkkala

33. Application of SWAT model to the decision support framework of the Mekong River Commission **320**
Kittipong Jirayoot and Le Duc Trung

34. The European Common Agriculture Policy and feasible hydrological impacts for the Dill Catchment, Germany **330**
L. Breuer, J.A. Huisman and H.-G. Frede

Session IX

35. On the use of SWAT for the identification of the most cost-effective nitrogen abatement measures for river basins 339
Jan Cools and Willy Bauwens

36. Downstream sediment response to conservation practice implementation 349
Michael W. Van Liew and Jeffrey G. Arnold

37. Development of complex hydrologic response unit (HRU) schemes and management scenarios to assess environmental concentrations of agricultural pesticides using SWAT 359
Michael F. Winchell, Raghavan Srinivasan, Tammara L. Estes and Susan S. Alexander

Posters

38. A decision support system based on the SWAT model for the Sardinian Water Authorities 369
P. Cau and E. Lorrai

39. Use of hydrological models at the catchment scale to predict the effect of different land management practices and point source pollution 379
I. Contu, A. Carucci and P. Cau

40. Scale issues, hydrological pathways, and nitrogen runoff from Agriculture-Results from the Mellupite Catchment, Latvia 390
Johannes Deelstra, Kaspars Abramenko, Nils Vagstad and Viesturs Jansons

41. Evaluation of SWAT for use in development of a river basin management plan for the Ythan Catchment, UK 398
Caroline F. Dilks, Sarah M. Dunn and Robert C. Ferrier

42. Distributed watershed modeling of a mountainous catchment-A case study in the Amameh Catchment in Iran 408
Shaaban-Ali Gholami

43. SWAT model development for a large agricultural watershed in Iowa 414
C.H. Green, M. Di Luzio, J.G. Arnold and M.D. Tomer

44. An analysis of non-point source pollution in a stock breeding area of the Heihe River Basin 423
Fanghua Hao, Hongguang Cheng, Shengtian Yang, Ye Qi and Xiyan Ren

45. **Modeling the effects of land use and climate change on hydrology and soil erosion in a sub-humid African catchment** 434
H. Busche, Claudia Hiepe and B. Diekkrüger

46. **An assessment of alternative conservation practice and land use strategies on the hydrology and water quality of the Upper Mississippi River Basin** 444
Manoj Jha, Philip W. Gassman, Silvia Secchi, Jeff G. Arnold, Lyubov A. Kurkalova, Hong-Li Feng and Cathy L. Kling

47. **Macro-scale catchment modeling in Northwest Russia** 454
S.A. Kondratyev

48. **Sensitivity of the SWAT model to spatial variability of land use and soil data: A Lake Balaton Catchment case study** 464
Peter Laszlo, Laszlo Pasztor and Jozsef Szabo

49. **Impact of precipitation data interpolation on the quality of SWAT simulations** 472
Roberta Maletta, Johan A. Huisman, Lutz Breuer, Hans-Georg Frede and Giuseppe Mendicino

50. **SWAT modeling response of soil erosion and runoff to changes in precipitation and cover** 482
Claire Baffaut, M.A. Nearing, V. Jetten, O. Cerdan, A. Couturier, M. Hernandez, Y. Le Bissonnais, M.H. Nichols, J.P. Nunes, C.S. Renschler, V. Souchère and K. van Oost

51. **Hydrologic modeling of a semi-arid region in Brazil** 491
Maria Quiteria C. de Oliveira, Ramon C. de Oliveira and Yvonilde D P Medeiros

52. **Evaluation of the soil nitrogen balance model in SWAT with lysimeter data** 498
Thorsten Pohlert, Johan A. Huisman, Lutz Breuer and Hans-Georg Frede

53. **Modeling soil carbon cycle for the assessment of carbon sequestration potentials at the river basin scale** 509
Joachim Post, Felicitas Suckow, Valentina Krysanova and Fred F. Hattermann

54. **Evaluation of soil infiltration in furrow irrigation and determination of Kostiakov and Kostiakov-Lewis equations coefficients** 518
A.Rahimi, H.A. Kashkuli and S. Boroomand

55. **Assessment of agricultural management practices in the Upper Maquoketa River Watershed using SWAT** 522
Pipat Reungsang, R.S. Kanwar, M. Jha, P.W. Gassman, K. Ahmad and A. Saleh

56. Evaluation of SWAT streamflow components for the Grote Nete River Basin (Flanders, Belgium) **532**
Hamed Rouhani, Patrick Willems and Jan Feyen

57. Impact of land use changes on stream flows using the SWAT model; Case study: Kasilian Catchment **542**
Hossein Saadati, S.H. Gholami and S.A. Ayyoubzadeh

58. Imitating model water-salt balance (IWSBM) in large watershed basins **549**
Javad Sadatinejad and A. Ranjbarfordoi

59. Application of SWAT and APEX models using SWAPP (SWAT/APEX program) for Upper North Bosque River Watershed in Texas **559**
Ali Saleh

60. A modeling approach for evaluating the water quality benefits of conservation practices at the national level **568**
C. Santhi, N. Kannan, M. Di Luzio, S.R. Potter, J.G. Arnold, J.D. Atwood and R.L. Kellogg

61. Transport and uptake of Cd, Cu, Pb and Zn in calcareous soil of Central Iran under wheat and safflower cultivation: A column study **577**
Gholamabbas Sayyad, Majid Afyuni, Sayed-Farhad Mousavi, Karim C. Abbaspour Rainer Schulin

62. Prioritizing watershed development programmes in developing countries **588**
Sucharita Sen and Ms. Poulomi Banerjee

63. Climate change impacts on the hydrology and water quality of the Upper Mississippi River Basin **599**
Eugene S. Takle, Manoj Jha, Philip W. Gassman, Christopher J. Anderson and Silvia Secchi

64. Model for nitrogen leaching from a watershed using field scale models **609**
Anatoli Vassiljev

65. Calibration and validation of the SWAT model to predict atrazine in streams in Northeast Indiana **616**
Gabriel G. Vazquez–Amábile and Bernard A. Engel

66. A procedure to compute groundwater table depth using SWAT **627**
Gabriel G. Vazquez–Amabile, Bernard A. Engel and Dennis C. Flanagan

67. Methods for analyzing calibration parameter uncertainty **637**
T.L. Veith, L. T. Ghebremichael, M. W. Van Liew and J. G. Arnold

68. The TERRACE Project: SWAT application for diffuse chemical pollution modeling **657**
S.M. White, N. Kannan, I. Beaudin, J. Hollis, A.R. Young, V. Keller and M. Whelan

69. Ensuring appropriate hydrological response for past and future nutrient load modeling in the Norfolk Broads **666**
J. Whitehead, S.M. White and I. Holman

70. Groundwater resource management on the urban environment **674**
Eyilachew Yitayew

Non-SWAT Related Papers

71. Sugarcane crop coefficient (Ratoon) in Haft tappeh of Iran **684**
Saeed Boroomand Nasab, Heidarali Kashkuli and Mohamad Reza

72. Floodwater effect on infiltration rate of a floodwater spreading system in Moosian gravelly piedmont plain in Dehloran, West Central Iran **691**
Saeed Boroomand Nasab, Hossain Charkhabi and Ayoub Pirani

73. Soil physical and chemical properties as indicators of land degradation in the Kouhrang (Chelgerd) Region, Chahar-Mahal & Bakhtiary Province, Iran **697**
A. Jalalian, M. Azarbin, M.K. Eghbal and S.F. Mousavi

74. Depasturation effects on soil physical and chemical properties is Isfahan and CharMahal Bakhtiari Region
Mohammad Hajabbasi

APPENDIX

Author Index **708**

2005 SWAT Conference Agenda **710**

Conference Group Picture **717**

Conservation Effects Assessment Project-ARS Watershed Assessment Study

C. W. Richardson[1]
[1]USDA Agricultural Research Service, Temple, TX

The United States Department of Agriculture (USDA) has provided financial and technical assistance to farmers to implement soil and water conservation practices during the last 60 years. These USDA conservation initiatives are currently conducted through several programs. The Farm Security and Rural Investment Act of 2002 (the 2002 Farm Bill) authorized an increase in funding for the Environmental Quality Incentives Program (EQIP). The Conservation Reserve Program (CRP) authorized continued funding for other conservation programs, and established new conservation programs. Overall, the 2002 Farm Bill authorized federal expenditures for conservation practices on farms and ranches in the U.S. at a level about 80 percent greater than levels set by the 1996 Farm Bill. It is widely recognized that these conservation programs will protect millions of acres of agricultural land from degradation and will enhance environmental quality. The environmental benefits of the programs, however, have not been quantified. Tracking the environmental benefits of the programs will allow policymakers and program managers to implement and modify existing programs and design new programs to more effectively and efficiently meet Congressional goals.

The Natural Resources Conservation Service (NRCS) and the Agricultural Research Service (ARS) are leading a project to quantify the effects of the USDA conservation programs. The project, known as the Conservation Effects Assessment Project (CEAP), has two major components: 1) a National Assessment and 2) a Watershed Assessment Study. The National Assessment will be conducted using NRCS data and watershed-scale models, such as the Soil Water Assessment Tool (SWAT) and will provide estimates of conservation benefits at the national scale. The ARS Watershed Assessment Study (WAS) is designed to provide a detailed assessment of conservation programs on selected watersheds.

Objectives of the Watershed Assessment Study

Previous research has established effects of conservation practices at the plot or field-scale. The results are limited in that they have not captured the complexities and interactions of conservation practices, landscape characteristics, and other land uses at watershed and landscape scales. The WAS was designed to assess the effects and benefits of conservation practices at the watershed scale. The results will advance our knowledge of watershed-scale assessment methodology to capture impacts at multiple scales. These studies will also improve our understanding of the effects of conservation practices beyond the edge of the farm field. The primary objectives are to support the National Assessment by providing detailed research findings for a few intensively studied watersheds and to provide a framework for improving the performance of the models that will be used in the National Assessment. Within these primary objectives the specific objectives are:

1. Develop and implement a data system to organize, document, manipulate and compile water, soil, management, and socio-economic data for assessment of conservation practices.

2. Measure and quantify water quality, water quantity, soil quality, and ecosystem effects of conservation practices at the watershed scale in a variety of hydrologic and agronomic settings.

3. Validate models and quantify uncertainties of model predictions at multiple scales by comparing predictions of water quality to measured water, soil, and land management effects of conservation practices.

4. Develop and apply policy-planning tools to aid selection and placement of conservation practices to optimize profits, environmental quality, and conservation practice efficiency.

5. Develop and verify regional watershed models that quantify environmental outcomes of conservation practices in major agricultural regions.

Research Approach

Twelve ARS Benchmark Watersheds are being used to support watershed-scale assessment of the environmental effects of USDA conservation program implementation. The underlying approach to the research is the acquisition, analysis, and interpretation of data from 12 benchmark watersheds (Figure 1) and the testing and evaluation of models that will be used in the National Assessment. Conservation practices have been, or will be, applied on the 12 watersheds. The Benchmark Watersheds are at different stages of research implementation, ranging from little or no existing data on a few watersheds to fully implemented experiments in place and water quality and discharge monitoring ongoing on several watersheds. Development and testing of regional watershed models will be associated primarily with the 12 benchmark watersheds. The 12 watersheds provide a cross-section of climate, soils, land use, topography, and crops across major rainfed production regions of the U.S. The watersheds represent primarily rainfed cropland, although some of the watersheds also contain irrigated cropland, grazingland, wetlands, and confined animal feeding operations. Conservation practices (or best management practices, BMPs) to be emphasized will include NRCS CORE 4 practices for croplands (conservation buffers, nutrient management, pest management, and tillage management), drainage management systems, and manure management practices. Environmental effects and benefits will be estimated primarily for water and soil resources, with some assessment of wildlife habitat and air quality benefits on selected watersheds. The measurements to be made and the conservation practices to be evaluated for each watershed are summarized in Table 1.

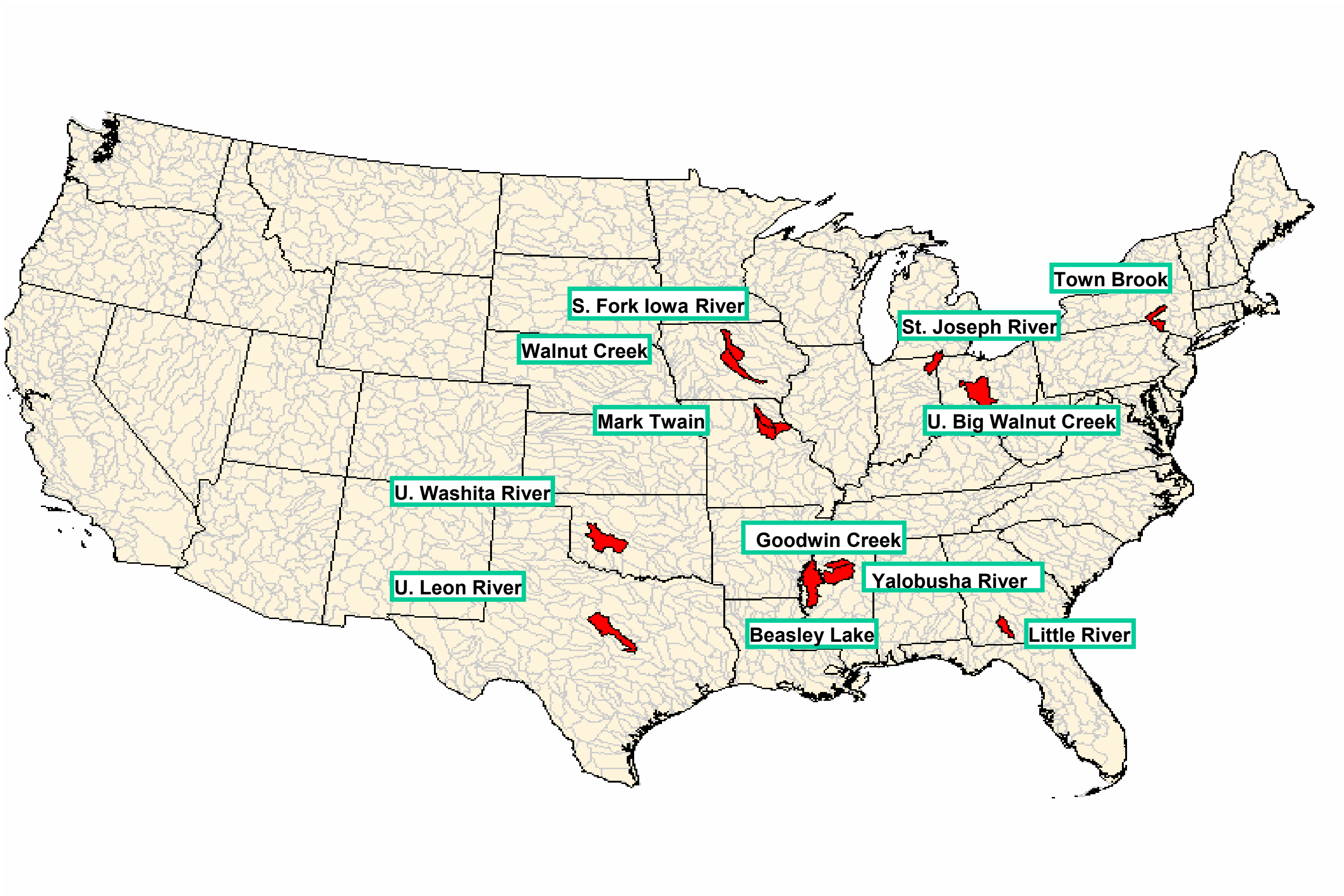

Figure 1. Location of ARS Benchmark Watersheds.

Table 1. Resource Measurements and Conservation Practices Underway or Planned for ARS Benchmark Watersheds for CEAP Watershed Assessment Study.

Watershed	Resource Measurements					Conservation Practices
	Water Quality[1]	Water Quantity[2]	Soil [3]	Ecosystem [4]	Economics [5]	
S. Fork, Iowa River, IA	N, P, S, Pa, T, DO	D, A, P, G,	AS, B, O, E, total N, P		E, O, P	M, N, T
Walnut Creek, IA	N, P, Pe, S	D, A, P			E	N, D
Salt River, Mark Twain Lake, MO	N, P, Pa, Pe, S	D, G, P	AS, E, O, P, AM, D		O, P	B, N, P, T
Upper Washita River, OK	N, P, S	D, G, P, I, S, C	AS, AW, B, O, N, P	H		C, L
Goodwin Creek, MS	N*, P*, Pa*, S*	C, D, P, S	AS, E, O, P	C*, D*, H*, R*		B, C, N, T, L
Yalobusha, MS	N, P, S,	D, C, P, S, G	AW, B			B, C, T
Beasley Lake, MS	N, P, S, DO, Pa, Pe, T	D, P	O	C, D, R		B, D, N, T, L
Upper Leon River, TX	N, P, S, Pa	D, P	AS, B, E, O, P			B, N, M, R, T
Little River, GA	N, P, Pe, DO, S, T	D, G, P, S	AW, B, M, O			B, C, M, N, P, R, T
Town Brook, NY	P, S	D, G, P	AW, B, P		E, O, P	B, C, M, N, T
St. Joseph River, IN	N, P, S, Pe		AS, AW, B, C, E, M, N, O, P		E, P	B, D, M, N, P, T
Upper Big Walnut Creek, OH	N, P, S, Pe	A, D, P	AW, B, E, O, P	H, D, C	E	B, D, L, N, P, T

[1] **Water Quality Measurements:**
DO - dissolved oxygen
N - nitrate-nitrogen
P – phosphorus
Pa – pathogens

[2] **Water Quantity Measurements:**
A – Artificial drainage
C – Channel geomorphology
D – Discharge
I – Irrigation

[3] **Soil Measurements:**
AS – Aggregate Stability
AW – Available Water Holding Capacity
B – Bulk Density
C – C mineralization potential
E – Electrical Conductivity

Pe – pesticides
S – sediments
T – temperature

[4] Ecosystem Measurements:
C – Community Structure
D – Species Diversity
H – Habitat Quality
N – Native vegetation Cover
P – Patchiness Index
R – Species Richness
S – Soil flora and fauna

G – Groundwater
P – Precipitation
S – Soil Water

[6] Conservation Practice Categories:
B – Buffers
C – Channel Management
D – Drainage Management
M – Manure Management
N – Nutrient Management
P – Pest
R – Range
T – Tillage
L – Land conversion

M – microbial biomass Carbon
N – N species and min. potential
O – Organic Carbon
P – Soil-test Phosphorus
AM – Microbial Activity
D – Microbial Diversity

[5] Economic Measurements:
E – Program Efficiency
O – Optimal Placement
P – Profit

* From previously collected data.

The goal for the WAS is to provide detailed assessments of conservation programs in a few selected watersheds, provide a framework for improving the performance of the national assessment models, and support coordinated research on the effects of conservation practices across a range of resource characteristics (such as climate, terrain, land use, and soils).

The research is being conducted by more than 60 scientists from 11 ARS research locations. The scientists are organized into six teams with specific responsibilities for collecting, analyzing, and interpreting the data as well as developing, validating, and applying models. The teams are: 1) Data Management, 2) Watershed Design for Determining Environmental Effects, 3) Model Validation, Evaluation and Uncertainty Analysis, 4) Economic Analysis, 5) Model Development and Regionalization, and 6) Data Quality and Assurance. Teams 1 through 5 are primarily responsible for leading research conducted under objectives 1 through 5, respectively. It is essential that compatible data be obtained across all field sites and laboratories in order to make valid comparisons of the effects of conservation practices across regions. Team 6 is providing support to the other five teams by providing data quality guidelines for methods and procedures to be used for data collection and analysis.

The objectives and team activities are tightly linked. Figure 2 is a graphical description of the relationship among the five teams that are charged with achieving their respective objectives and delivering the products to NRCS for use in the National Assessment. Team 1 is charged with developing a data system for storing and managing the basic data and delivering the data system to NRCS. The data system will be populated with data collected by Team 2 on the 12 watersheds. Team 6 will provide guidelines for methods and procedures to be used for data collection and analysis. Close coordination among Teams 1, 2, and 6 is required to ensure that meaningful data are obtained from the watersheds and entered into the data system. Team 2 is also responsible for delivering a quantification of the effects of various conservation practices as determined on the watersheds to the National Assessment team.

Team 3 is responsible for evaluating the performance of the models that will be used in the National Assessment and delivering estimates of uncertainty in model outputs. The model evaluations will be performed using data collected on the watersheds. To accomplish this objective, scientists in Team 3 will work closely with field researchers in Team 2 to evaluate the models on specific watersheds and with Team 1 to access data in the data system for model evaluation.

Team 4 will be involved with developing economic planning tools for delivery to the National Assessment team. The work involves coupling physical models from Team 3 with economic models to form a tool for determining optimal multi-objective decisions regarding selection and placement of conservation practices; therefore, coordination between Team 3 and Team 4 is required. Economic data will be collected jointly by Teams 2 and 4 on selected watersheds that will become part of the data system, thus requiring cooperation among Teams 1, 2, and 4. The economic planning tools developed by Team 4 will be provided to the National Assessment team.

Team 5's primary responsibility is the development of region-specific models in modular form. The team will use models developed by Team 3 as legacy models for development of regional modular models. Coordination with Team 3 will be required to determine which features are needed for specific regions and to ensure that modular versions of models produce appropriate results. Teams 3 and 5 will work together to test the new models. Team 5 will also work closely with Team 1 to obtain data for testing the new regional modular models. The regional modular models developed by Team 5 are expected to be available at the end of this project. The new modular models will be provided to the National Assessment team for future assessments.

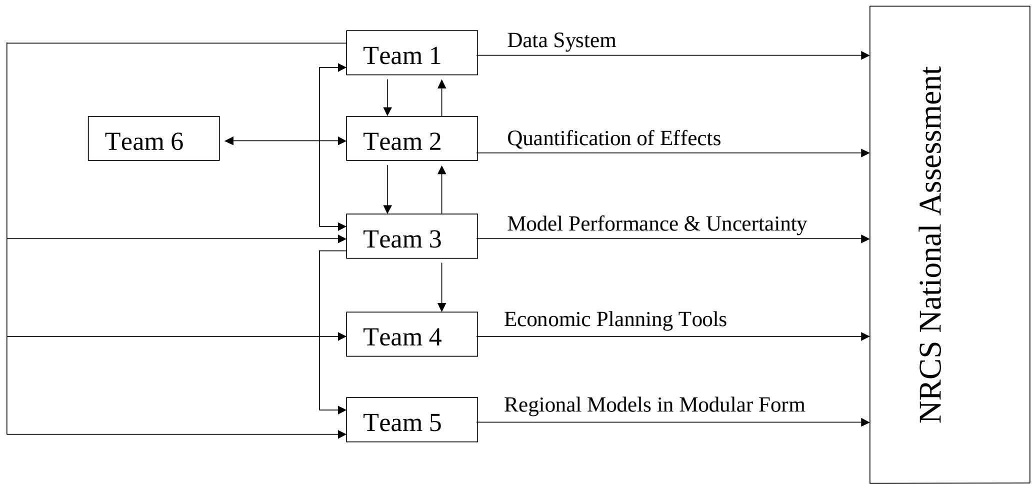

Figure 2. Relationship among six CEAP research teams.

Anticipated Products

The purpose of the WAS is to provide a scientific basis and validation for the National Assessment. Five specific products, or deliverables, are to be provided to NRCS and other stakeholders to meet the demands of the National Assessment and other similar activities designed to quantify the effects of USDA conservation programs. The five products are:

1. Water, soil, management, and socio-economic data system to document the effects of conservation practices.
2. Quantification, at multiple scales, of the effects of conservation practices on water quality, water quantity, soil quality, and ecosystems.
3. Validation of model performance through quantifying uncertainties of model predictions at multiple scales.
4. Planning tools to evaluate the environmental and cost effectiveness of selection and placement of conservation practices at multiple scales.
5. New regional software tools (Object Modeling Systems) that can be used to quantify environmental outcomes of conservation practices in major agricultural regions.

Progress

A detailed project plan for the Watershed Assessment Study was developed in 2004. The project plan contains specific tasks that are necessary to accomplish the objectives and deliver the products. Each task has been assigned to a specific scientist and has an identified completion date. The structured organization is designed to ensure that the products are delivered in time for the National Assessment schedule. The six teams are actively pursuing their respective objectives. The data system has been designed and implementation of the system is underway. Data collection is underway on all 12 watersheds. The models to be used by the National Assessment are being validated on several watersheds and model improvements are being implemented as needed. Economic data are being collected on selected watersheds, and the policy-planning economic tools are being developed and tested. Regions have been identified that need specific modeling capabilities.

Additional Information

The comprehensive analysis of resources, the quality of the environment, and social and economic benefits that accrue to rural communities and the nation from implementing conservation programs will assist those responsible for developing conservation policy and managing the USDA Farm Bill conservation programs. Additional details about both the CEAP National Assessment and Watershed Assessment can be found at the following web site:

http://www.nrcs.gov/technical/nri/ceap/

Session I

1. **SWAT peer-reviewed literature: A review** **1**
   Philip Gassman, Manuel R. Reyes, Colleen H. Green and Jeffrey G. Arnold

2. **Application of SWIM model in the Elbe Basin: Experience and new developments** **19**
   Valentina Krysanova, Fred Hattermann, Joachim Post, Anja Habeck and Frank Wechsung

3. **Catchment scale modelling of pesticide losses with imperfect data: A case study from the UK** **30**
   S.M. White, N. Kannan, B. Grizzetti and J. Hollis

4. **Limitations, problems and solutions in the setup of SWAT for a large-scale hydrological application** **40**
   Jürgen Schuol and Karim Abbaspour

5. **Assessment of water use in a small watershed in northern Syria, using SWAT** **50**
   Adriana Bruggeman and Geerte van der Meijden

SWAT Peer-Reviewed Literature: A Review

Philip W. Gassman[1], Manuel R. Reyes[2], Colleen H. Green[3], & Jeffrey G. Arnold[3]
[1]Center for Agricultural and Rural Development (CARD), Dept. of Economics, 578 Heady Hall, Iowa State Univ., Ames, Iowa, 10011-1070, USA. Email: pwgassma@iastate.edu
[2]Bioenvironmental Engineering, Dept. of Natural Resources and Environmental Design, North Carolina A&T State University, Greensboro, North Carolina, USA
[3]Grassland, Soil and Water Research Laboratory, USDA-ARS, Temple, Texas, USA

Abstract

The Soil and Water Assessment Tool (SWAT) model is a continuation of nearly 30 years of modeling efforts conducted by the United States Department of Agriculture (USDA) Agricultural Research Service (ARS). SWAT has gained international acceptance as a robust interdisciplinary watershed modeling tool as evidenced by international SWAT conferences, SWAT-related papers presented at numerous other scientific meetings, and dozens of articles published in peer-reviewed journals. The model has also been adopted as part of the U.S. Environmental Protection Agency (USEPA) Better Assessment Science Integrating Point & Nonpoint Sources (BASINS) software package and is being used by many U.S. federal and state agencies, including the USDA within the Conservation Effects Assessment Project (CEAP). At present, over 160 peer-reviewed published articles have been identified that report SWAT applications, reviews of SWAT components, or other research that includes SWAT. Many of these peer-reviewed articles are summarized here according to relevant application categories such as streamflow calibration and related hydrologic analyses, climate change impacts on hydrology, pollutant load assessments, comparisons with other models, and sensitivity analyses and calibration techniques. Recommended research needs for SWAT are also presented.

Introduction

The SWAT model (Arnold et al., 1998; Arnold and Fohrer, 2005) has proven to be an effective tool for assessing water resource and diffuse pollution problems for a wide range of scales and environmental conditions across the globe. In the U.S., SWAT is increasingly being used to support Total Maximum Daily Load (TMDL) analyses (Di Luzio et al., 2002; http://www.epa.gov/ owow/tmdl/), research the effectiveness of conservation practices in CEAP (http://www.nrcs.usda.gov/technical/NRI/ceap/; Mausbach and Dedrick, 2004), perform "macro-scale studies" such as Upper Mississippi River Basin (e.g., Arnold et al., 2000; Jha et al., 2004b) and entire U.S. (e.g., Arnold et al., 1999a; Rosenberg et al., 2003) assessments, and a wide variety of other water use and water quality applications. Similar SWAT application trends have also emerged in Europe as indicated by the variety of studies presented in two previous European international SWAT conferences; these are reported in part for the first conference in a special issue of *Hydrological Processes* (vol. 19, issue 3) and in the SWAT2003 2nd International Conference Proceedings (http://www.brc.tamus.edu/swat/ /2ndswatconf/2ndswatconfproceeding.pdf).

Reviews of SWAT applications and/or components have been previously reported, sometimes in conjunction with comparisons with other models (e.g., Borah and Bera, 2003; Borah and Bera, 2004; Steinhardt and Volk, 2003; Arnold and Fohrer, 2005; Jayakrishnan et al., 2005). However, these previous reviews do not provide a comprehensive overview of the complete body of SWAT applications that have been reported in the peer-reviewed literature. Thus the primary objective of this research is to fill the gap by providing a review of the full range of studies that have been conducted with SWAT. Research findings or methods are summarized here for most of the 160-plus peer-reviewed articles that have been identified in the literature, based on relevant application categories. Brief overviews of SWAT development history and current research needs are also provided.

SWAT Development History

The development of SWAT is a continuation of USDA-ARS modeling experience that spans a period of roughly 30 years. Early origins of SWAT can be traced to previously developed USDA-ARS models as described by Arnold and Fohrer (2005) and Krysanova et al. (2005). The current SWAT model is a direct descendant of the SWRRB model (Williams et al., 1985), which was designed to simulate management impacts on water and sediment movement for ungaged rural basins across the U.S. The historical development of SWAT by specific model version up to SWAT2000 is chronicled by Arnold and Fohrer (2005). SWAT2000's capabilities include: bacteria routines, urban routines, the Green and Ampt infiltration equation, an improved weather generator, the ability to read in daily solar radiation, relative humidity, wind speed and potential ET, Muskingum channel routing, and modified dormancy calculations for tropical areas. Snow fall and melt equations were also refined and improved. Other recent enhancements that have been incorporated in SWAT2003 include: bacteria (E. coli and fecal coliform), tile flow, potholes, CN option based on antecedent weather, automated sensitivity and calibration, a sub-hourly time step, adjustment of phosphorus availability timing, and the provision for stream channels to down cut and widen as the channel is eroded following the approach described by Allen et al. (1999; 2002).

Two other notable trends that are interwoven with the ongoing development of SWAT are the emergence of "spin-off SWAT models" and Geographic Information System (GIS) interface tools. Several adaptations of SWAT have been created to provide improved simulation of specific processes, which in some cases have been focused on specific regions. Examples of spin-off models include: (1) Extended SWAT (ESWAT), which features enhanced in-stream kinetics and other modifications (van Griensven and Bauwens, 2001; 2005), (2) the Soil and Water Integrated Model (SWIM) which is partially based on SWAT (Krysanova et al., 1998; 2005), (3) SWAT-G, a modified version of SWAT99.2 (Eckhardt et al., 2002; Lenhart et al., 2003; 2005), and (4) SWATMOD, a version of SWAT that has been linked to MODFLOW to simulate detailed surface/groundwater interaction (Sophocleus et al., 2000). The first GIS interface program developed for SWAT was SWAT/GRASS, which was built within the GRASS raster-based GIS (Srinivasan and Arnold, 1994). The ArcView-SWAT (AVSWAT) interface tool (Di Luzio et al., 2004a; 2004b) was constructed later, which supports data inputs from ArcView and model execution within the same framework. SWAT2000 has also been incorporated within the USEPA BASINS 3.0 package, which provides GIS utilities that support automatic data input using ArcView (Di Luzio et al., 2002). Other interface tools have been developed to support specific applications including the Automated Geospatial Watershed Assessment (AGWA) software package (Miller et al., 2002) and InputOutputSWAT (IOSWAT), which incorporates SWAT/GRASS and several other tools into a single framework (Haverkamp et al., 2005).

SWAT Applications

Hydrologic Studies

Several hydrologic components (surface runoff, ET, recharge, and streamflow) that are currently in SWAT have been developed and validated at smaller scales within the EPIC, GLEAMS and SWRRB models. Interactions between surface flow and subsurface flow in SWAT are based on a linked surface-subsurface flow model developed by Arnold et al. (1993). Characteristics of this flow model include non-empirical recharge estimates, accounting of percolation, and applicability to basin-wide management assessments with a multi-component basin water budget. The flow model was validated in a 471 km^2 watershed in the Grand Prairie region near Waco, Texas. Current SWAT reach and reservoir routing routines are based on the ROTO approach (Arnold et al., 1995b), which was developed to estimate flow and sediment yields in large basins using sub-area inputs from SWRRB. Configuration of routing schemes in SWAT is based on the approach given by Arnold et al. (1994).

The surface runoff, ET, and streamflow components have been refined and validated at larger scales within SWAT including a U.S. national assessment of streamflow and ET (Arnold et al., 1999a). Arnold and Allen (1996) used measured data from three Illinois watersheds to successfully validate surface runoff, groundwater flow, groundwater ET, ET in the soil profile, groundwater recharge, and groundwater height parameters. Groundwater recharge and discharge (baseflow) results from SWAT were compared to filtered estimates for the 491,700 km^2 Upper Mississippi River Basin (Arnold et al., 2000). Chu and Shirmohammadi (2004) evaluated SWAT's capability to predict surface and subsurface flow for a 33.4 km^2 watershed in Maryland. They found that SWAT was unable to simulate an extremely wet year; with the wet year removed, the surface runoff, baseflow and streamflow results were within acceptable accuracy on a monthly basis. Subsurface flow results improved with the baseflow corrected. Spruill et al. (2000) calibrated and validated SWAT with one year of data each. Nash-Sutcliffe Efficiency (NSE) values reflected poor peak flow values and recession rates. The NSE values for monthly total flows were 0.58 and 0.89 for 1995 and 1996, respectively. Their analysis confirmed the results of a dye trace study in a central Kentucky karst watershed, indicating that a much larger area contributed to streamflow than was described by topographic boundaries.

Rosenthal et al. (1995) linked GIS to SWAT and with no calibration simulated 10 years of monthly streamflow. SWAT underestimated the extreme events but had a significant relationship (R^2=0.75). Rosenthal and Hoffman (1999) successfully used SWAT and a spatial database to simulate flows, sediment, and nutrient loadings on a 9,000 km^2 watershed in central Texas to locate potential water quality monitoring sites. SWAT was successfully validated for streamflow and sediment loads for the Mill Creek watershed in Texas for 1965-68 and 1968-75 (Srinivasan et al., 1998a). Monthly streamflow rates were well predicted but the model overestimated streamflows in a few years during the spring/summer months (Srinivasan et al., 1998b). The overestimation may be accounted for by variable rainfall during those months. SWAT also predicted soil erosion and sediment transport satisfactorily considering the model's limitations.

As part of the HUMUS (Hydrologic Unit Model for the United States) project, annual runoff and ET were validated across the entire continental U.S. (Arnold et al., 1999a). Monthly streamflow was also validated against measured USGS flow at several gaging stations across the U.S. (Arnold et al., 2000; Arnold et al., 1999). Bingner (1996) simulated runoff for 10 years for a watershed in northern Mississippi. The SWAT model produced reasonable results in the simulation of runoff on a daily and annual basis from multiple subbasins, with the exception of a wooded subbasin.

Arnold et al. (1999) integrated GIS with SWAT to evaluate streamflow and sediment yield data in the Texas Gulf Basin with drainage areas ranging from 10,000 to 110,000 km^2. Streamflow data from approximately 1,000 stream monitoring gages from 1960 to 1989 were used to calibrate and validate the model. Predicted average monthly streamflow data from three six-digit HUA were 5% higher than measured flows with standard deviations between measured and predicted within 2%. SWAT simulated sediment yields compared reasonably well to estimated yields (from the rating curve) considering input uncertainties, sampling errors, and model assumptions. Benaman and Shoemaker (2004) found that significant uncertainty remained with the SWAT sediment routine.

Arnold et al. (2001) found that a simulated wetland near Dallas, Texas needed to be at or above 85% capacity for 60% of a 14-year simulation period. Conan et al. (2003b) found that SWAT adequately simulated the changing from wetlands to dry land for the Upper Guadiana river basin in Spain. SWAT, however, was unable to represent all of the discharge details impacted by land use alterations. Hernandez et al (2000) utilized existing data sets (i.e. STATSGO soil database and NALC land cover classification) for parameterizing SWAT to simulate hydrologic response to land cover change for a small semi-arid watershed (150 km^2) in southeastern Arizona. These authors found that calibration was required to improve model efficiency for simulation of runoff depth. Mapfumo et al. (2004) tested the model's ability to simulate soil-water patterns in small watersheds under three grazing intensities in Alberta, Canada. They observed that SWAT had a tendency to over-predict soil-water in dry soil conditions and to under-predict in wet soil conditions. Overall, the model was adequate in simulating soil-water patterns for all three watersheds with a daily time-step. Van Liew and Garbrecht (2003) evaluated SWAT's ability to predict streamflow under varying climatic conditions for three nested subwatersheds in the Little Washita River Experimental Watershed in southwestern Oklahoma. They found that SWAT could adequately simulate runoff for dry, average, and wet climatic conditions in one subwatershed, following calibration for relatively wet years in two of the subwatersheds. Govender and Everson (2005) also found that the model performed better in drier years than in a wet year.

Deliberty and Legates (2003) used SWAT to simulate soil moisture conditions in Oklahoma. Arnold et al. (2005) validated a crack flow model for SWAT, which simulates soil moisture conditions with depth to account for flow conditions in dry weather. The crack flow model is impacted by crack potential, soil depth, and soil moisture. Seasonal trends were in agreement with simulated crack volume (R^2=0.84). Measured daily surface runoff was regressed with simulated data resulting in an R^2=0.87.

Chanasyk et al. (2002) simulated the impacts of grazing on hydrology and soil moisture, respectively, using small grassland watersheds under three grazing intensities in Alberta, Canada. They evaluated SWAT's ability to simulate low flow conditions that included snowmelt events. Chanasyk et al. and Peterson and Hamlet (1998) found that SWAT was better suited for long simulation periods and suggested that the snowmelt routine be improved. The modifications performed by Fontaine et al. (2002) have clearly improved the snowmelt routine, as evidenced by an NSE increase from -0.70 to 0.86 for a six-year SWAT simulation of the Upper Wind River Basin in Wyoming.

Sun and Cornish (2005) simulated 30 years of bore data from a 437 km^2 catchment. They used SWAT to estimate recharge in the headwaters of the Liverpool Plains in NSW, Australia. These authors determined that SWAT could estimate recharge and incorporate land use and land management at the catchment scale as compared to using the point source modeling approach. Gosain et al. (2005) assessed SWAT's ability to simulate return flow after the introduction of canal irrigation in a basin in Andra Pradesh, India. SWAT provided the assistance water managers needed in planning and managing their water resources under various scenarios.

The impact of flood-retarding structures on streamflow with varying climatic conditions in Oklahoma was investigated with SWAT by Van Liew et al. (2003b). It was found that flood-retarding structures are effective at reducing annual peak runoff events. Low streamflow was also impacted, showing that maintenance of a minimum baseflow is vital for stream habitat preservation.

Climate Change Impact Studies

Climate change impacts can be simulated directly in the standard SWAT model by accounting for: (1) the effects of increased atmospheric CO_2 concentrations, in the range of 330-660 ppmv, on plant development and transpiration, and (2) changes in climatic inputs that are usually determined by downscaling climate change projections generated by general circulation models (GCMs) or GCMS coupled with regional climate models (RCMs). Eckhardt and Ulbrich (2003) have directly addressed variable stomatal conductance and leaf area responses by incorporating different stomatal conductance decline factors and leaf area index (LAI) values in SWAT-G, as a function of five main vegetation types; a similar approach could be a useful enhancement for the standard SWAT model.

Stonefelt et al. (2000) and Fontaine et al. (2001) assessed climate change impacts with SWAT for the 5,000 km^2 Upper Wind River Watershed in northwest Wyoming and the 427 km^2 Spring Creek Watershed in the Black Hills of South Dakota, respectively, using arbitrary changes in climatic inputs that were based, in part, on previous GCM/RCM projections. Eheart and Tornil (1999) also report arbitrary climatic change impacts on Illinois water resources.

Cruise et al. (1999), Ritschard et al. (1999), and Limaye et al. (2001) describe climate change impacts on the hydrology of selected watersheds in the U.S. southeast region, using SWAT and downscaled climate projections from the HadCM2 GCM. Ritschard et al. found that future water availability could decline up to 10% within 20-40 years during critical agricultural growing season periods in the Gulf Coast. A second key finding (Limaye et al.) was that GCM interfaces with hydrologic models may only work for regional assessments of seasonal and annual climate change rather than for short-term watershed-level analyses. Rosenberg et al. (2003) simulated the effect of downscaled HadCM2 climate projections (CO_2 = 560 ppmv) on the hydrology of the 18 major U.S. water resource regions (MWRRs) with SWAT within the HUMUS framework; predicted water yields changed from -11 to 153% and 28 to 342% across the MWRRs in 2030 and 2095, respectively, relative to the baseline. Thomson et al. (2003) used a similar approach to evaluate El Niño/Southern Oscillation (ENSO) scenario effects on the 18 MWRRs while Rosenberg et al. (1999) evaluated GCM projection impacts on the Ogallala Aquifer within two MWRRs. Other studies that used downscaled GCM projections include Muttiah and Wurbs (2002), Eckhardt and Ulbrich (2003), and Krysanova et al. (2005).

Stone et al. (2001) predicted the impact of climate change on Missouri River Basin water yields by inputting downscaled climate projections, estimated by nesting the RegCM RCM within the CISRO GCM, into a modified SWAT model (Hotchkiss et al., 2000) that more accurately simulated major Missouri River reservoirs. Water yields declined at the basin outlet by 10 to 20% during the spring and summer months, but increased during the rest of the year. Significant shifts in Missouri River Basin water yield impacts were found when SWAT was driven by downscaled CISRO GCM projections only versus the nested RegCM-CISRO GCM approach (Stone et al., 2003). Jha et al. (2004b) found that Upper Mississippi River Basin streamflows increased by 50% for the period of 2040-49, when climate projections generated by a nested RegCM2-HadCM2 approach were used to drive SWAT.

Hanratty and Stefan (1998), Varanou et al. (2002), and Boorman (2003) report climate change impacts on both hydrology and pollutant losses. Hanratty and Stefan found that streamflows, and P, organic N, nitrate, and sediment yields, generally decreased for a 3,400 km^2 watershed in southwest Minnesota in response to a downscaled $2xCO_2$ GCM climate change scenario. Varanou et al. also found that average streamflows, sediment yields, organic N losses, and nitrate losses decreased during most months in response to nine different climate change scenarios downscaled from three GCMs for a 2,796 km^2 watershed in Greece. Boorman evaluated climate change impacts on flow and nutrient loses with SWAT for four different watersheds located in Italy, France, Finland, and the UK.

Pollutant Loss Studies

Pollutant loss estimations are described in roughly 50 of the peer-reviewed papers, many of which are discussed in other sections. Papers focused on validation efforts of SWAT pollutant loss routines and/or evaluation of best management practices (BMP) are discussed in this section.

Initial comparisons of SWRRB-ROTO sediment output compared favorably with measured data for three watersheds in Texas (Arnold et al., 1995a). SWAT predictions of sediment loss were further tested in nine watersheds in Texas (Srinivasan et al., 1998b; Arnold et al., 1999; Santhi et al., 2001a; Saleh et al., 2000) and single watersheds in Indiana (Arnold and Srinivasan, 1998; Engel et. al., 1993), New York (Benaman and Shoemaker, 2005), Maryland (Chu et al., 2004), and India (Tripathi et al., 2004). These studies varied in watershed sizes, interval and duration of measured sediment loss, validation criteria, and other factors. All of the studies concluded that the SWAT sediment predictions showed general agreement with measured values, except for the New York and Maryland experiments. The analysis in the New York watershed concentrated on high-flow sediment event data, and SWAT underestimated 34 of the 35 observed sediment loads and underestimated erosion caused by snowmelt. In Maryland, monthly sediment predictions were poor but annual sediment predictions strongly agreed with annual observed sediment loss. SWAT nitrogen and phosphorous predictions were evaluated in two watersheds in Texas (Santhi et al., 2001a; Saleh et al., 2000), two watersheds in Finland (Frances et al., 2001; Grizzetti et al., 2003), a watershed in Indiana (Arnold and Srinivasan, 1998; Engel et al. 1993) and a watershed in Maryland (Chu et al., 2004). These studies all concluded that SWAT reasonably predicted measured nitrogen and phosphorus losses, except for poor monthly predictions for the study in Maryland. In addition, Veith et al. (2005) found that measured watershed exports of dissolved P and total P during a 7 month sampling period from a Pennsylvania watershed were similar in magnitude to SWAT predicted losses.

SWAT has been used to evaluate the environmental or economic impacts of BMPs or land use changes at a variety of scales. SWAT was used within HUMUS to conduct a national-scale analysis of the effect of management scenarios on water quantity and quality (Jayakrishnan et al., 2005). Atwood et al. (1999) used SWAT to determine the effects of reducing nitrogen fertilizer on corn and sorghum in the Upper Mississippi River valley, as a function of crop nitrogen stress over 5 or 10% of the growing season. The 10% stress level resulted in reducing fertilizer needs by 30% and N transport in the Upper Mississippi and Ohio rivers by 3%, while having only a modest impact on agricultural prices and income. SWAT results indicated that implementation of improved tillage practices can reduce sediment yields by almost 20% in the Rock River in Wisconsin (Kirsch et al., 2002). Chaplot et. al. (2004) found that adoption of no tillage, changes in nitrogen application rates, and land use changes could greatly impact nitrogen losses in the Walnut Creek Watershed in central Iowa. Further analysis of BMPs by Vache et al. (2002) for Walnut Creek and a second Iowa watershed indicated that large sediment reductions could be obtained, depending on BMP choice. Gitau et. al (2004) determined cost-effective pollution reduction through farm level optimization of BMP placement using SWAT. The effects of BMPs related to dairy manure management and municipal wastewater treatment plant effluent were evaluated by Santhi et al. (2001b) with SWAT for the Bosque River Watershed in Texas. Water quality impacts associated with converting farmland and forests to turfgrass were assessed by King and Balogh (2001) using SWAT. SWAT studies in India include identification of critical or priority areas for soil and water management in a watershed (Kaur et al., 2004 and Tripathi et al., 2003), the impact of different tillage systems on nitrogen and sediment losses, and the effects of replacing rice with peanut and soybean on soil loss (Tripathi et al., 2005).

Calibration Technique Studies

SWAT input parameters are physically based and are allowed to vary within a realistic uncertainty range for calibration. Calibration techniques are generally referred to as either manual or automated. With manual calibration, the user compares measured and simulated values and better judgment is used to determine which variables to adjust, how much to adjust them, and when the results are reasonable. Santhi et al. (2001a) calibrated and validated SWAT for streamflow, sediment, nitrogen and phosphorus loss simulations for the Bosque River in Texas. They present a general procedure for manual calibration suggesting sensitive input parameters, realistic uncertainty ranges and reasonable regression results (i.e., satisfactory R^2 and NSE values). Lenhart et al. (2002) report on the effects of two different sensitivity analysis schemes using SWAT-G, in which an alternative approach of varying parameter values within a fixed percentage of the valid parameter range was compared with the more usual method of varying each initial parameter by the same fixed percentage. Spruill et al. (2000) performed a sensitivity analysis which showed that saturated hydraulic conductivity, alpha baseflow factor, drainage area, channel length, and channel width were the most sensitive parameters. Coffey et al. (2004) recommended using the R^2 and modeling efficiency objective functions for daily streamflow data. NSE and R^2 coefficients are their suggested methods for analyzing monthly data.

Automated methods link SWAT with an optimization scheme to automate the calibration procedure. Applications of a shuffled complex evolution optimization scheme are described by van Griensven and Bauwens (2001; 2003; 2005) and van Griensven et al. (2002) for ESWAT simulations, primarily for the Dender River in Belgium. The user inputs calibration parameters and ranges along with measured daily flow and pollutant data. The automated calibration scheme controls up to several thousand model runs to find the optimum input data set. Vandenberghe et al. (2002) describe further ESWAT autocalibrations for the Dender River basin. A similar automatic calibration was performed with the SCE genetic algorithm by Eckhardt and Arnold (2001) for an 81 km^2 watershed in Germany; Eckhardt et al. (2005) identify this approach as a shuffled complex evolution algorithm in a second analysis.

In addition to total streamflow, it is important to calibrate individual hydrologic processes. Because of pollutant transport processes, it is particularly important to simulate proper surface and groundwater flow ratios. To aid in estimating surface and ground water flows, automated baseflow separation techniques were compared with manual techniques (Arnold et al., 1995a). Arnold and Allen (1999) successfully utilized an automated digital filter technique for estimating baseflow and annual groundwater recharge from streamflow hydrographs. The automated technique is used as a check on mass balance methods for shallow water table aquifers. The automated filter was validated with data from six watersheds in the Midwest and eastern U.S.

Benaman and Shoemaker (2004) developed a method that applies Monte Carlo runs to reduce uncertain parameter ranges. After parameter range reduction, their method reduced the model output range by an order of magnitude, resulting in reduced uncertainty and the amount of calibration required for SWAT. However, significant uncertainty remained with the SWAT sediment routine. As an alternative to using the Monte Carlo method, Whittaker

(2004) used a Beowulf cluster parallel computer with specialized application information for simulations with SWAT. Twelve hundred annual simulations including 102 years of sediment load and flow out of each basin outlet were run with varying computational nodes, which nearly reached the theoretical speed increase. Govender and Everson (2005) evaluated SWAT to assess if it could reasonably simulate hydrologic processes in daily time steps from two small South African catchments. SWAT's inability to grow Mexican Weeping Pine (*Pinus patula*) was reflected in the lack of simulating increased ET rates in mature plantations. They used the PEST parameter estimation program and identified soil moisture variables, initial groundwater variables, and runoff curve numbers to be some of the sensitive parameters in SWAT. Di Luzio and Arnold (2004) described the background, formulation, and results of an hourly input-output calibration approach to potentially be used by SWAT. This approach was tested on 24 representative storm events between 1994 and 2000 in a 1,233 km^2 watershed in Oklahoma.

Effects of Subwatershed Delineation and Other Inputs on SWAT Predictions

Binger et al. (1997), Manguerra and Engel (1998), FitzHugh and Mackay (2000), Jha et al. (2004), and Chen and Mackay (2004) found that SWAT flow predictions were generally insensitive to HRU and/or subwatershed delineations, with no changes in input data. However, Binger et al. found that the number of subwatersheds affected predicted sediment yields; FitzHugh and Mackay, Jha et al., and Chen and Mackay found similar results when varying both HRUs and subwatersheds. Jha et al. also found that SWAT nitrate predictions were sensitive to HRU and subwatershed configurations but mineral P estimates were not. Binger et al. suggested that sensitivity analyses should be performed to determine the appropriate level of subwatersheds. Suggestions on selecting appropriate numbers of subwatersheds are given by Jha et al. Chen and Mackay suggest that errors in MUSLE sediment estimates can be avoided by using only subwatersheds, instead of using HRUs within subwatersheds.

Bosch et al. (2004) found that SWAT streamflow estimates for a 22.1 km^2 subwatershed of the Little River Watershed in Georgia were more accurate using high-resolution topographic, land use, and soil data versus low-resolution data obtained from BASINS. Cotter et al. (2004) report that DEM resolution was the most critical input for a SWAT simulation of the 1,890 ha Moores Creek Watershed in Arkansas, and that minimum DEM resolution should be between 30 and 300 m and minimum land use and soil resolutions should be between 300 and 500 m to obtain accurate flow, sediment, NO_3-N, and TP estimates. Di Luzio et al. (2005) also found that DEM resolution was the most critical for SWAT simulations of the 21.3 km^2 Goodwin Creek Watershed in Mississippi; land use resolution effects were also significant but the resolution of soil inputs was not.

Simulated hydrologic responses in SWAT or SWAT-G have also been shown to be sensitive to historical land use changes (Miller et al., 2002), hypothetical land use changes (Fohrer et al., 2001; Eckhardt et al., 2003; Heuvelmans et al., 2004; Huisman et al., 2004; Heuvelmans et al., 2005), and similar results have been found with the SWIM model (Krysanova et al., 2005). Other studies have shown that SWAT hydrologic responses are sensitive to choice of climatic inputs (Harmel et al., 2000; Moon et al., 2004) or choice of surface runoff estimation technique (King et al., 1999).

Haverkamp et al. (2002) established a relationship between SWAT's efficiency and the number of subwatersheds modeled. A statistically based approach/tool called the SUbwatershed Spatial Analysis Tool (SUSAT) was used to find an appropriate level of discretization to be applied to the three watersheds before running SWAT. Further application of SUSAT in combination with SWAT-G, IOSWAT, and other software tools are described by Fohrer et al. (2005) and Haverkamp et al. (2005).

Comparisons of SWAT with Other Models

Borah and Bera (2003; 2004) compared SWAT with several other watershed-scale models. In their 2003 paper, they report that DWSM, HSPF, SWAT, and other models have hydrology, sediment, and chemical routines applicable to watershed scale catchments, and concluded that SWAT is a promising model for continuous simulations in predominantly agricultural watersheds. In their 2004 paper, they compiled 17 SWAT, 12 HSPF, and 18 DWSM applications and concluded that SWAT and HSPF were suitable for predicting yearly flow volumes, sediment loads, and nutrient losses, were adequate for monthly predictions except for months having extreme storm events and hydrologic conditions, and poor in simulating daily extreme flow events. In contrast, DWSM reasonably predicted distributed flow hydrographs and concentration or discharge graphs of sediment, nutrient, and pesticides at small time intervals. Shepherd et al. (1999) evaluated 14 models and found SWAT to be the most suitable for estimating phosphorus loss from a lowland English catchment.

Van Liew et al. (2003a) compared the streamflow predictions of SWAT and HSPF on eight nested agricultural watershed within the Washita River Basin in southwestern Oklahoma. They found that differences in model performance were mainly attributed to the runoff production mechanisms of the two models. Furthermore, they concluded that SWAT gave more consistent results than HSPF in estimating streamflow for agricultural watersheds under various climatic conditions and may thus be better suited for investigating the long term impacts of climate variability on surface water resources. Saleh and Du (2004) calibrated SWAT and HSPF with daily flow, sediment, and nutrients measured at five stream sites of the Upper North Bosque River Watershed located in Central Texas. They concluded that the average daily flow, sediment, and nutrient loading simulated by SWAT were closer to measured values than HSPF during both the calibration and verification periods. El-Nasr et al. (2005) found that both SWAT and MIKE-SHE simulated the hydrology of Belgium's Jeker River Basin in an acceptable way. However, MIKE SHE predicted the overall variation of river flow slightly better.

Interfaces of SWAT with Other Models

Innovative applications have been performed by interfacing SWAT with other environmental and/or economic models. Evaluation of irrigation management strategies for three watersheds in Kansas have been performed with SWATMOD (Sophocleus et al., 2000) and two similar SWAT-MODFLOW interface applications (Sophocleus et al., 1999; Perkins and Sophocleus, 1999). A combined SWAT-MODFLOW approach was also used to study runoff and water balance for a 5,000 km^2 basin in central New Mexico (Menking et al., 2003) and flow and nitrate movement for a 12 km^2 watershed in Brittany, France (Conan et al., 2003). Osei et al. (2003a; 2003b) simulated the impacts of nutrient losses from dairy manure applications for the Lake Fork Reservoir Watershed (LFRW) in northeast Texas and the Upper North Bosque River Watershed (UNBRW) in north central Texas, respectively, by interfacing a Farm Economic Model (FEM) with the APEX model and SWAT. It was concluded that appropriate pasture nutrient management including stocking density adjustments and more efficient application of commercial fertilizer could lead to significant reductions in nutrient losses in the LFRW, and that manure incorporation reduced phosphorus losses at a relatively small to moderate cost to producers in the UNBRW. Lemberg et al. (2002) evaluated the economic impacts of brush control in the Frio River Basin in Texas by linking the PHYGROW model with SWAT and using two economic models. Economic evaluations of riparian buffer benefits in regards to reducing atrazine concentration and other factors were performed by Qiu and Prato (1998; 2001). The performance of a salmon habitat remediation policy was evaluated by Whittaker (2005) by linking SWAT to a farm operator model. Whittaker et al. (2003) determined whether or not a nutrient input tax is better in reducing agricultural fertilizer application than a command and control policy by interfacing SWAT with an economic policy model. Evaluation of different policies were demonstrated by Attwood et al. (2000) by showing economic and environmental impacts at the U.S. national scale and for Texas by linking SWAT with an agricultural sector model. Weber et al. (2001) studied the effects of land use changes on landscape structures and functions using SWAT and the ecological model ELLA. Fohrer et al. (2002) used SWAT-G, the YELL ecological model, and the Proland Agricultural Economic model to assess the effects of land use changes and associated hydrologic impacts on habitat suitability for the Yellowhammer bird species. Frede et al. (2002) describe the importance of soil relationships for studies that interface SWAT with the ELLA, YELL, Proland, and related models.

Research Needs

The worldwide application of SWAT reveals that it is a versatile model that can be used to integrate multiple environmental processes, which support more effective watershed management and the development of better-informed policy decisions. The SWAT model will continue to evolve as users determine needed improvements that will enable more accurate simulation of currently supported processes or provide new functionality that will expand the SWAT simulation domain. Key SWAT research needs and emerging model developments include:

1. Development of concentrated animal feeding operations and related manure application routines that support simulation of surface and integrated manure application techniques and their influence on nutrient fractionation, distribution in runoff and soil, and sediment loads.
2. Water flow between hydrologic response units has been initiated so that landscape position between HRUs will influence the water balance as well as nutrient and sediment loads.
3. Stream channel degradation and sediment deposition need improvement to better describe sediment transport and demonstrate nutrient loads associated with sediment movement.
4. Autocalibration and uncertainty analysis tools are currently being improved in SWAT; however, refinements are needed to lessen user calibration time.
5. Development of a GIS interface using ArcGIS has been initiated, which will have the same functionality as AVSWAT (Di Luzio et al., 2002).
6. Improved simulation of riparian zones and other conservation practices is needed in SWAT, to better support watershed-based BMP evaluations.

Conclusions

The wide range of SWAT applications that have been described here underscores that the model is a very flexible and robust tool that can be used to simulate a variety of watershed problems. The ability of SWAT to replicate hydrologic and/or pollutant loads at a variety of spatial scales on an annual or monthly basis has been confirmed in numerous studies. However, the model performance has been inadequate in some studies, especially when comparisons of predicted output were made with a time series of measured daily flow and/or pollutant loss data. Some users have addressed weaknesses in SWAT by component modifications, which support more accurate simulation of specific processes or regions. This is a trend that will likely continue. Creation of additional support tools to facilitate various applications of SWAT can also be expected. The SWAT model will continue to evolve in response to the needs of the ever-increasing worldwide user community and to provide improved simulation accuracy of key processes.

References

Allen, P.M., J.G. Arnold, and E. Jakubowski. 1999. Prediction of stream channel erosion potential. *Environ. Engr. Geosci.* 5(3):339-351.

Allen, P.M., J.G. Arnold, and W. Skipworth. 2002. Assessment of bedrock channel erosion in urban watersheds. *J. of Amer. Water Res. Assoc*. 38(5):1477-1492.

Arnold, J.G., and P.M. Allen. 1999. Automated methods for estimating baseflow and groundwater recharge from streamflow records. *J. of Amer. Water Res. Assoc*. 35(2):411-424.

Arnold, J.G., and P.M. Allen. 1996. Estimating hydrologic budgets for three Illinois watersheds. *J. Hydrol.* 176:57-77.

Arnold, J.G., and Allen, P.M. 1993. A comprehensive surface-ground water flow model. *J. Hydrol.* 142:47-69.

Arnold, J.G., P.M. Allen, and D. Morgan. 2001. Hydrologic model for design of constructed wetlands. *Wetlands* 21(2):167-178.

Arnold, J.G., P.M. Allen, R.S. Muttiah, and G. Bernhardt. 1995a. Automated baseflow separation and recession analysis techniques. *Groundwater* 33(6):1010-1018.

Arnold, J.G. and N. Fohrer. 2005. SWAT2000: current capabilities and research opportunities in applied watershed modeling. *Hydrol. Process.* 19(3):563-572.

Arnold, J.G., R.S. Muttiah, R. Srinivasan, and P.M. Allen. 2000. Regional estimation of baseflow and groundwater recharge in the upper Mississippi basin. *J. Hydrol.* 227:21-40.

Arnold, J.G., K.N. Potter, K.W. King, and P.M. Allen. 2005. Estimation of soil cracking and the effect on surface runoff in a Texas Blackland Prairie Watershed. *Hydrol. Process.* 19(3):589-603.

Arnold, J.G. and R. Srinivasan. 1998. A continuous catchment-scale erosion model. In *Modelling Soil Erosion by Water*, NATO ASI Series, Vol. I 55:413-427. J. Boardman and D. Favis-Mortlock, eds. Springer-Verlag Berlin Heidelberg.

Arnold, J. G., R. Srinivasan, and B.A. Engel. 1994. Flexible watershed configurations for simulation models. American Institute of Hydrology. *Hydrol. Sci.Technol.* 30(1-4):5-14.

Arnold, J.G., R. Srinivasan, R.S. Muttiah, P.M. Allen and C. Walker. 1999a. Continental scale simulation of the hydrologic balance. *J. of Amer. Water Res. Assoc*. 35(5):1037-1052.

Arnold, J.G., R. Srinivasan, R.S. Muttiah, and J.R. Williams. 1998. Large area hydrologic modeling and assessment part I: model development. *J. of Amer. Water Res. Assoc*. 34(1):73-89.

Arnold, J.G., R. Srinivasan, T.S. Ramanarayanan, and M. Di Luzio. 1999b. Water resources of the Texas gulf basin. *Water Sci. Technol.* (39)3:121-133.

Arnold, J.G., J.R. Williams, and D.A. Maidment. 1995b. A continuous time water and sediment routing model for large basins. *J. Hydraulics Div., ASCE* 121(2): 171--183.

Atwood, J.D., V.W. Benson, R. Srinivasan, C. Walker, and E. Schmid. 1999. Simulated nitrogen loading from corn, sorghum, and soybean production in the Upper Mississippi Valley. In *Sustaining the Global Farm: Selected Papers from the 10th International Soil Conservation Organization Meeting*, 344-348 (Eds.: D.E. Stott, R.H. Mohtar, and G.C. Steinhardt). West Lafayette, IN: USDA-ARS, National Soil Erosion Lab., Purdue Univ.

Available at: http://topsoil.nserl.purdue.edu/nserlweb /isco99/pdf/ISCOdisc/tableofcontents.htm.

Attwood, J.D., B. McCarl, C.C. Chen, B.R. Eddleman, B. Nayda, and R. Srinivasan. 2000. Assessing regional impacts of change: linking economic and environmental models. *Agric. Syst.* 63:147-159.

Benaman, J. and C. A. Shoemaker. 2004. Methodology for analyzing ranges of uncertain model parameters and their impact on total maximum daily load processes. *J. Environ. Engr.* 130(6):648-656.

Benaman, J. and C.A. Shoemaker. 2005. An analysis of high-flow sediment event data for evaluating model performance. *Hydrol. Process.* 19(3):605-620.

Bingner, R. L. 1996. Runoff Simulated from Goodwin Creek Watershed Using SWAT. *Trans. ASAE* 39(1):85-90.

Bingner, R.L., J. Garbrecht, J.G. Arnold, and R. Srinivasan. 1997. Effect of watershed subdivision on simulated runoff and fine sediment yield. *Trans. ASAE* 40(5):1329-1335.

Boorman, D.B. 2003. Climate, Hydrochemistry and Economics of Surface-water Systems (CHESS): adding a European dimension to the catchment modelling experience developed under LOIS. *Sci. Total Environ.* 314-316:411-437.

Borah, D.K. and M. Bera. 2004. Watershed-scale hydrologic and nonpoint-source pollution models: review of applications. *Trans. ASAE* 47(3):789-803.

Borah, D.K. and M. Bera. 2003. Watershed-scale hydrologic and nonpoint-source pollution models: review of mathematical bases. *Trans. ASAE* 46(6):1553-1566.

Bosch, D.D., J.M. Sheridan, H. L. Batten, J. G. Arnold. 2004. Evaluation of the SWAT Model on a Coastal Plain Agricultural Watershed. *Trans. ASAE* 47(5):1493-1506.

Chanasyk, D.S., E. Mapfumo, and W. Willms. 2003. Quantification and simulation of surface runoff from fescue grassland watersheds. *Agric. Water Manage.*59:137-153.

Chaplot, V., A. Saleh, D.B. Jaynes, and J. Arnold. 2004. Predicting water, sediment and NO_3-N loads under scenarios of land-use and management practices in a flat watershed *Water Air Soil Pollut.* 154(1-4):271-293.

Chen, E. and D.S. Mackay. 2004. Effects of distribution-based parameter aggregation on a spatially distributed agricultural nonpoint source pollution model. *J. Hydrol.* 295:211-224.

Chu, T.W. and A. Shirmohammadi. 2004. Evaluation of the SWAT model's hyrodology component in the piedmont physiographic region of Maryland. *Trans. ASAE* 47(4):1057-1073.

Chu, T.W., A. Shirmohammadi, H. Montas, and A. Sadeghi. 2004. Evaluation of the SWAT model's sediment and nutrient components in the Piedmont Physiographic Region of Maryland. *Trans. ASAE* 47(5):1523-1538.

Coffey, M.E., S.R. Workman, J.L. Taraba, and A.W. Fogle. 2004. Statistical procedures for evaluating daily and monthly hydrologic model predictions. *Trans. ASAE* 47(1):59-68.

Conan, C., F. Bouraoui, N. Turpin, G. de Marsily, and G. Bidoglio. 2003a. Modeling flow and nitrate fate at catchment scale in Brittany (France). *J. Environ. Qual.* 32:2026-2032.

Conan, C., G. de Marsily, F. Bouraoui, and G. Bidoglio. 2003b. A long-term hydrological modelling of the Upper Guadiana river basin (Spain). *Phys. Chem. Earth* 28:193-200.

Cotter, A.S., I. Chaubey, T.A. Costello, T.S. Soerens, and M.A. Nelson. 2003. Water quality model output uncertainty as affected by spatial resolution of input data. *J. of Amer. Water Res. Assoc.* 39(4): 977-986.

Cruise, J.F., A.S. Limaye, and N. Al-Abed. 1999. Assessment of impacts of climate change on water quality in the Southeastern United States. *J. of Amer. Water Res. Assoc.* 35(6): 1539-1550.

Deliberty, T.L. and D.R. Legates. 2003. Interannual and seasonal variability of modelled soil moisture in Oklahoma. *Int. J. Climatol.* 23:1057-1086.

Di Luzio, M. and J.G. Arnold. 2004. Formulation of a hybrid calibration approach for a physically based distributed model with NEXRAD data input. *J. Hydrol.* 298(1-4):136-154.

Di Luzio, M., R. Srinivasan, and J.G. Arnold. 2002. Integration of watershed tools and SWAT model into BASINS. *J. of Amer. Water Res. Assoc*. 38(4): 1127-1141.

Di Luzio, M., R. Srinivasan, and J.G. Arnold. 2004a. A GIS-coupled hydrological model system for the watershed assessment of agricultural nonpoint and point sources of pollution. *Trans.GIS* 8(1):113-136.

Di Luzio, M., J.G. Arnold, and R. Srinivasan 2004b. Integration of SSURGO maps and soil parameters within a geographic information system and nonpoint source pollution model system. *J. Soil Water Conser.* 59(4):123-133.

Di Luzio, M., J.G. Arnold and R. Srinivasan. 2005. Effect of GIS data quality on small watershed streamflow and sediment simulations. *Hydrol. Process.* 19(3): 629-650.

Eckhardt, K. and J.G. Arnold. 2001. Automatic calibration of a distributed catchment model. *J. Hydrol.* 251(1-2):103-109.

Eckhardt, K., L. Breuer, and H.-G. Frede. 2003. Parameter uncertainty and the significance of simulated land use change effects. *J. Hydrol.* 273:164-176.

Eckhardt, K., N. Fohrer, and H.-G. Frede. 2005. Automatic model calibration. *Hydrol. Process.* 19(3): 651-658.

Eckhardt, K., S. Haverkamp, N. Fohrer, and H.-G. Frede. 2002. SWAT-G, a version of SWAT99.2 modified for application to low mountain range catchments. *Phys. Chem. Earth* 27(9-10):641-644.

Eckhardt, K. and U. Ulbrich. 2003. Potential impacts of climate change on groundwater recharge and streamflow in a central European low mountain range. *J. Hydrol.* 284(1-4):244-252.

Eheart, J.W. and D.W. Tornil. 1999. Low-flow frequency exacerbation by irrigation withdrawals in the agricultural midwest under various climate change scenarios. *Water Resour. Res.* 35(7):2237-224.

El-Nasr, A. J.G. Arnold, J. Feyen, and J. Berlamont. 2005. Modelling the hydrology of a catchment using a distributed and a semi-distributed model. *Hydrol. Process.* 19(3):573-587.

Engel, B.A., R. Srinivasan, J.G. Arnold, C. Rewerts, and S.J. Brown. 1993. Nonpoint Source (NPS) Pollution Modeling Using Models Integrated with Geographic Information Systems (GIS). *Water Sci. Tech.* 28(3-5):685-690.

FitzHugh, T. W., and D.S. Mackay. 2000. Impacts of input parameter spatial aggregation on an agricultural nonpoint source pollution model. *J. Hydrol.* 236:35-53.

Fohrer, N., S. Haverkamp, K. Eckhardt, and H.-G. Frede. 2001. Hydrologic response to land use changes on the catchment scale. *Phys. Chem. Earth* (*B*), 26(7-8): 577-582.

Fohrer, N., S. Haverkamp, and H.-G. Frede. 2005. Assessment of the effects of land use patterns on hydrologic landscape functions: development of sustainable land use concepts for low mountain range areas. *Hydrol. Process.* 19(3): 659-672.

Fohrer, N., D. Möller, and N. Steiner. 2002. An interdisciplinary modelling approach to evaluate the effects of land use change. *Phys. Chem. Earth* 27(9-10): 655-662.

Fontaine, T.A., T.S. Cruickshank, J.G. Arnold and R.H. Hotchkiss. 2002. Development of a snowfall-snowmelt routine for mountainous terrain for the soil water assessment tool (SWAT). *J. Hydrol.* 262(1-4):209-223.

Fontaine, T.A., J.F. Klassen, T.S. Cruickshank, and R.H. Hotchkiss. 2001. Hydrological response to climate change in the Black Hills of South Dakota, USA. *Hydrological Sci. J.* 46(1):27-40.

Francos, A., G. Bidoglio, L. Galbiati, F. Bouraoui, F.J. Elorza, S. Rekolainen, K. Manni, and K. Granlund. 2001. Hydrological and water quality modelling in a medium-sized coastal basin. *Phys. Chem. Earth (B)* 26(1):47-52.

Frede, H.-G., M. Bach, N. Fohrer, and L. Breuer. 2002. Interdisciplinary modeling and the significance of soil functions. *J. Plant Nutrition Soil Sci. (Zeitschrift fur Pflanzenernahrung und Bodenkunde*) 165(4):460-467.

Gitau, M.W., T.L. Veith, and W.J. Gburek. 2004. Farm-level optimization of BMP placement for cost-effective pollution reduction. *Trans. ASAE* 47(6):1923-1931.

Gosain, A.K., S. Rao, R. Srinivasan, and N. Gopal Reddy. 2005. Return-flow assessment for irrigation command in the Palleru river basin using SWAT model. *Hydrol. Process.* 19(3): 673-682.

Govender, M. and C.S. Everson. 2005. Modelling streamflow from two small South African experimental catchments using the SWAT model. *Hydrol. Process.* 19(3): 683-692.

Grizzetti, B., F. Bouraoui, K. Granlund, S. Rekolainen, and G. Bidoglio. 2003. Modelling diffuse emission and retention of nutrients in the Vantaanjoki watershed (Finland) using the SWAT model. *Ecol. Modell.*169:25-38.

Hanratty, M.P. and H.G. Stefan. 1998. Simulating climate change effects in a Minnesota agricultural watershed. *J. Environ. Qual.* 27:1524-1532.

Harmel, R. D., C.W. Richardson, and K.W. King. 2000. Hydrologic response of a small watershed model to generated precipitation. *Trans. ASAE* 43(6):1483-1488.

Haverkamp, S., R. Srinivasan, H.-G. Frede and C. Santhi. 2002. Subwatershed spatial analysis tool: discretization of a distributed hydrologic model by statistical criteria. *Journal of the American Water Resour. Assoc.* 38 (6):1723-1733.

Haverkamp, S., N. Fohrer, and H.-G. Frede. 2005. Assessment of the effect of land use patterns on hydrologic landscape functions: a comprehensive GIS-based tool to minimize model uncertainty resulting from spatial aggregation. *Hydrol. Process.* 19(3):715-727.

Hernandez, M., S.C. Miller, D.C. Goodrich, B.F. Goff, W.G. Kepner, C.M. Edmonds, and K.B. Jones. 2000. Modeling runoff response to land cover and rainfall spatial variability in semi-arid watersheds. *Environ. Monitoring Assess.* 64:285-298.

Heulvelmans, G., J. F. Garcio-Qujano, B. Muys, J. Feyen, and P. Coppin. 2005. Modelling the water balance with SWAT as part of the land use impact evaluation in a life cycle study of CO_2 emission reduction scenarios. *Hydrol. Process.* 19(3):729-748.

Heuvelmans, G., B. Muys, and J. Feyen. 2004. Evaluation of hydrological model parameter transferability for simulating the impact of land use on catchment hydrology. *Phys. Chem. Earth, Parts A/B/C* 29(11-12):739-747.

Hotchkiss, R.H., S.F. Jorgensen, M.C. Stone, and T.A. Fontaine. 2000. Regulated river modeling for climate change impact assessment: The Missouri River. *J. of Amer. Water Res. Assoc*. 36(2): 375-386.

Huisman, J.A., L. Breuer, and H.G. Frede. 2004. Sensitivity of simulated hydrological fluxes towards changes in soil properties in response to land use change. *Phys. Chem. Earth, Parts A/B/C* 29(11-12): 749-758.

Jayakrishnan, R., R. Srinivasan, C. Santhi, and J.G. Arnold. 2005. Advances in the application of the SWAT model for water resources management. *Hydrol. Process.* 19(3): 749-762.

Jha, M., P.W. Gassman, S. Secchi, R. Gu, and J. Arnold. 2004a. Effect of watershed subdivision on SWAT flow, sediment, and nutrient predictions. *J. of Amer. Water Res. Assoc.* 40(3):811-825.

Jha, M., Z. Pan, E.S. Takle, and R. Gu. 2004b. Impacts of climate change on streamflow in the Upper Mississippi River Basin: a regional climate model perspective. *J. Geophys. Res.* 109:D09105.

Kaur, R., O. Singh, R. Srinivasan, S.N. Das, and K. Mishra. 2004. Comparison of a subjective and a physical approach for identification of priority areas for soil and water management in a watershed – a case study of Nagwan watershed in Hazaribagh District of Jharkhand, India. *Environ. Model. Assess.* 9(2):115-127.

King, K.W., J.G. Arnold, and R.L. Bingner. 1999. Comparison of Green-Ampt and curve number methods on Goodwin creek watershed using SWAT. *Trans. ASAE* 42(4):919-925.

King, K.W. and J.C. Balogh. 2001. Water quality impacts associated with converting farmland and forests to turfgrass. *Trans. ASAE* 44(93):569-576.

Kirsch, K., A. Kirsch, and J.G. Arnold. 2002. Predicting sediment and phosphorus loads in the Rock River Basin using SWAT. *Trans. ASAE* 45(6):1757-1769.

Krysanova, V., D.-I.Müller-Wohlfeil, and A. Becker. 1998. Development and test of a spatially distributed hydrological/water quality model for mesoscale watersheds. *Ecol. Modell.* 106:261-289.

Krysanova, V., F. Hatterman, and F. Wechsung. 2005. Development of the ecohydrological model SWIM for regional impact studies and vulnerability assessment. *Hydrol. Process.* 19(3):763-783.

Lemberg, B., J.W. Mjelde, J.R. Conner, R.C. Griffin, W.D. Rosenthal, and J.W. Stuth. 2002. An interdisciplinary approach to valuing water from brush control. *J. of Amer. Water Res. Assoc*. 38(2):409-422.

Lenhart, T., K. Eckhardt, N. Fohrer and H.-G. Frede. 2002. Comparison of two different approaches of sensitivity analysis. *Phys. Chem. Earth* 27:645-654.

Lenhart, T., N. Fohrer, and H.-G. Frede. 2003. Effects of land use changes on the nutrient balance in mesoscale catchments. *Phys. Chem. Earth, Parts A/B/C* 28(33-36):1301-1309.

Lenhart, T., A. Van Rompaey, A. Steegen, N. Fohrer, H.-G. Frede, and G. Govers. 2005. Considering spatial distribution and deposition of sediment in lumped and semi-distributed models. *Hydrol. Process.* 19(3): 785-794.

Limaye, A.S., T.M. Boyington, J.F. Cruise, A. Bulus, and E. Brown. 2001 Macroscale hydrologic modeling for regional climate assessment studies in the southeastern United States. *J. of Amer. Water Res. Assoc.* 37(3):709-722.

Manguerra, H.B., and B.A. Engel. 1998. Hydrologic parameterization of watersheds for runoff prediction using SWAT. *J. of Amer. Water Res. Assoc*. 34(5):1149-1162.

Mapfumo, E., D.S. Chanasyk, and W.D. Willms. 2004. Simulating daily soil water under foothills fescue grazing with the soil and water assessment tool model (Alberta, Canada). *Hydrol. Process.* 18:2787-2800.

Mausbach, M.J. and A.R. Dedrick. 2004. The length we go: measuring environmental benefits of conservation practices. *J. Soil Water Cons.* 59(5): 96A-103A.

Menking, K.M., K.H. Syed, R.Y. Anderson, N.G. Shafike, and J.G. Arnold. 2003. Model estimates of runoff in the closed, semiarid Estancia basin, central New Mexico, USA. *Hydrological Sci. J.*, 48(6): 953-970.

Miller, S. N., W.G. Kepner, M.H. Mehaffey, M. Hernandez, R.C. Miller, D.C. Goodrich, K.K Devonald, D.T. Heggem, and W.P. Miller . 2002. Integrating landscape assessment and hydrologic modeling for land cover change analysis. *J. of Amer. Water Res. Assoc.* 38(4):915-929.

Moon, J., R. Srinivasan, and J.H. Jacobs. 2004. Streamflow estimation using spatially distributed rainfall in the Trinity River Basin, Texas. *Trans. ASAE* 47(5):1445-1451.

Muttiah, R. S. and R. A. Wurbs. 2002. Modeling the impacts of climate change on water supply reliabilities. International Water Resources Association, *Water International* 27(3):407-419.

Osei, E., P.W. Gassman, L.M. Hauck, R. Jones, L. Beran, P.T. Dyke, D.W. Goss, J.D. Flowers, and A.M.S. McFarland. 2003a. Environmental benefits and economic costs of manure incorporation on dairy waste application fields. *J. Envr. Manage.* 68(1):1-11.

Osei, E., P.W. Gassman, L.M. Hauck, S. Neitsch, R.D. Jones, J. Mcnitt, and H. Jones. 2003b. Using nutrient management to control nutrient losses from dairy pastures. *J. of Range Manage.* 56:218-226.

Perkins, S.P. and M. Sophocleous. 1999. Development of a comprehensive watershed model applied to study stream yield under drought conditions. *Groundwater* 37(3):418-426.

Peterson, J.R. and J.M. Hamlet. 1998. Hydrologic calibration of the SWAT model in a watershed containing fragipan soils. *J. of Amer. Water Res. Assoc*. 34(3):531-544.

Qiu, Z., and T. Prato. 1998. Economic evaluation of riparian buffers in an agricultural watershed. *J. of Amer. Water Res. Assoc*. 34(4):877-890.

Qiu, Z., and T. Prato. 2001. Physical determinants of economic value of riparian buffers in an agricultural watershed. *J. of Amer. Water Res. Assoc.* 37(2):295-303.

Ritschard, R. L., J.F. Cruise, and L.U. Hatch. 1999. Spatial and temporal analysis of agricultural water requirements in the Gulf Coast of the United States. *J. of American Water Resources Assoc.* 35(6):1585-1596.

Rosenberg, N.J., R.A. Brown, R.C. Izaurralde, and A.M. Thomson. 2003. Integrated assessment of Hadley Centre (HadCM2) climate change projections in agricultural productivity and irrigation water supply in the conterminous United States: I. climate change scenarios and impacts on irrigation water supply simulated with the HUMUS model. *Agricultural and Forest Meteorology* 117(1-2):73-96.

Rosenberg, N.J., D.L. Epstein, D. Wang, L. Vail, R. Srinivasan, and J.G. Arnold. 1999. Possible impacts of global warming on the hydrology of the Ogallala aquifer region. *Climatic Change* 42(4):677-692.

Rosenthal, W.D., and D.W. Hoffman. 1999. Hydrologic modeling/GIS as an aid in locating monitoring sites. *Trans. ASAE* 42(6):1591-1598.

Rosenthal, W.D., R. Srinivasan, and J.G. Arnold. 1995. Alternative river management using a linked GIS-hydrology model. *Trans. ASAE* 38(3):783-790.

Saleh, A., J.G. Arnold, P.W. Gassman, L.W. Hauck, W.D. Rosenthal, J.R. Williams, and A.M.S. McFarland. 2000. Application of SWAT for the upper north Bosque watershed. *Trans. ASAE* 43(5):1077-1087.

Saleh, A. and B. Du. 2004. Evaluation of SWAT and HSPF within BASINS program for the Upper North Bosque River watershed in central Texas. *Trans. ASAE* 47(4):1039-1049.

Santhi, C., J.G. Arnold, J.R. Williams, W.A. Dugas, R. Srinivasan, and L.M. Hauck. 2001a. Validation of the SWAT model on a large river basin with point and nonpoint sources. *J. of Amer. Water Res. Assoc*. 37(5):1169-1188.

Santhi, C., J.G. Arnold, J.R. Williams, L.M. Hauck, and W.A. Dugas. 2001b. Application of a watershed model to evaluate management effects on point and nonpoint source pollution. *Trans. ASAE* 44(6):1559-1570.

Shepherd, B., D. Harper, and A. Millington. 1999. Modelling catchment-scale nutrient transport to watercourses in the U.K. *Hydrobiologia* 395-396:227-237.

Sophocleous, M.A., J.K. Koelliker, R.S. Govindaraju, T. Birdie, S.R. Ramireddygari, and S.P. Perkins. 1999. Integrated numerical modeling for basin-wide water management: The case of the Rattlesnake Creek basin in south-central Kansas. *J. Hydrol.* 214:179-196.

Sophocleous, M. and S. P. Perkins 2000. Methodology and Application of Combined Watershed and Ground-water Models in Kansas. *J. Hydrol.* 236 (3-4):185-201.

Spruill, C.A., S.R. Workman, and J.L. Taraba. 2000. Simulation of daily and monthly stream discharge from small watersheds using the SWAT model. *Trans. ASAE* 43(6):1431-1439.

Srinivasan, R. and J.G. Arnold. 1994. Integration of a basin-scale water quality model with GIS. *Water Resour. Bull.* (30)3:453-462.

Srinivasan, R.S., J.G. Arnold, and C.A. Jones. 1998a. Hydrologic modeling of the United States with the soil and water assessment tool. *Water Resour. Develop.* 14(3):315-325.

Srinivasan, R., T.S. Ramanarayanan, J.G. Arnold, and S.T, Bednarz. 1998b. Large area hydrologic modeling and assessment part II: model application. *J. of Amer. Water Res. Assoc*. 34(1):91-101.

Steinhardt, U. and M. Volk. 2003. Meso-scale landscape analysis based on landscape balance investigations: problems and hierarchical approaches for their resolution. *Ecol. Modell.* 168(3):251-265.

Stone, M.C., R.C. Hotchkiss, and L.O. Mearnes. 2003. Water yield responses to high and low spatial resolution climate change scenarios in the Missouri River Basin. Geophys. Res. Lett., 30(4):1186,doi:10.1029/2220GLO16122.

Stone, M.C., R.H. Hotchkiss, C.M. Hubbard, T.A. Fontaine, L.O. Mearns, and J.G. Arnold. 2001. Impacts of climate change on Missouri river basin water yield. *J. of Amer. Water Res. Assoc*. 37(5):1119-1130.

Stonefelt, M. D., T.A. Fontaine, and R.H. Hotchkiss. 2000. Impacts of climate change on water yield in the upper wind river basin. *J. of Amer. Water Res. Assoc*. 36(2):321-336.

Sun, H. and P.S. Cornish. 2005. Estimating shallow groundwater recharge in the headwaters of the Liverpool Plains using SWAT. *Hydrol. Process.* 19(3): 795-807.

Thomson, A.M., R.A. Brown, N.J. Rosenberg, R.C. Izaurralde, D.M. Legler, and R. Srinivasan. 2003. Simulated impacts of El Nino/southern oscillation on United States water resources. *J. of Amer. Water Res. Assoc*. 39(1):137-148.

Tripathi, M.P., R.K. Panda, and N.S. Raghuwanshi. 2005. Development of effective management plan for critical watersheds using SWAT model. *Hydrol. Process.* 19(3): 809-826.

Tripathi, M.P., R.K. Panda, N.S. Raghuwanshi, and R. Singh. 2004. Hydrological modelling of a small watershed using generated rainfall in the soil and water assessment tool model. *Hydrol. Process.* 18:1811-1821.

Tripathi, M.P., R.K. Panda, and N.S. Raghuwanshi. 2003. Identification and Prioritisation of Critical Sub-watersheds for Soil Conservation Management using the SWAT Model. *Biosystems Engineering* (2003) 85(3):365-379, doi:10.1016/S1537-5110(03)00066-7.

Vaché, K.B., J.M. Eilers, and M.V. Santelman. 2002. Water quality modeling of alternative agricultural scenarios in the U.S. Corn Belt. *J. of Amer. Water Res. Assoc*. 38(2):773-787.

Vandenberghe V., A. van Griensven and W. Bauwens. 2001. Sensitivity analysis and calibration of the parameters of ESWAT: Application to the river Dender. *Water Sci. Technol.* 43(7):295-301.

van Griensven, A., and W. Brauwens. 2001. Integral water quality modeling of catchments. *Water Sci. Technol.* 43(7):321-328.

van Griensven, A., and W. Bauwens. 2003. Multiobjective autocalibration for semidistributed water quality models. *Water Resour. Res. 39*(12):1348, doi:10.1029/2003WR002284.

Van Griensven, A. and W. Buawens. 2005. Application and evaluation of ESWAT on the Dender basin and Wister Lake basin. *Hydrol. Process.* 19(3):827-838.

van Griensven A., A. Francos and W. Bauwens. 2002. Sensitivity analysis and auto-calibration of an integral dynamic model for river water quality. *Water Sci. Technol.* 45(9):325-332.

Van Liew, M.W., J.G. Arnold, and J.D. Garbrecht. 2003a. Hydrologic simulation on agricultural watersheds: choosing between two models. *Trans. ASAE* 46(6):1539-1551.

Van Liew, M.W. and J. Garbrecht. 2003. Hydrologic simulation of the Little Washita River experimental watershed using SWAT. *J. of Amer. Water Res. Assoc*. 39(2):413-426.

Van Liew, M.W., J.D. Garbrecht, and J.G. Arnold. 2003c. Simulation of the impacts of flood retarding structures on streamflow for a watershed in southwestern Oklahoma under dry, average, and wet climatic conditions. *J. Soil Water Conser.* 58(6):340-348.

Varanou, E, E. Gkouvatsou, E. Baltas, and M. Mimikou. 2002. Quantity and quality integrated catchment modelling under climatic change with use of Soil and Water Assessment Tool model. J. Hydrologic Engr. 7(3):228-244.

Veith, T. L., A. N. Sharpley, J. L. Weld, W.J. Gburek. 2005. Comparison of measured and simulated phosphorus losses with indexed site vulnerability. *Trans. ASAE* 48(2):557-565.

Weber, A., N. Fohrer and D. Moller. 2001. Long-term land use changes in a mesocale watershed due to socio-economic factors – effects on landscape structures and functions. *Ecol. Model.* 140:125-140.

Whittaker, G.R. 2004. Use of a Beowulf cluster for estimation of risk using SWAT. *Agron. J.* 96:1495-1497.

Whittaker, G. 2005. Application of SWAT in the evaluation of salmon habitat remediation policy. *Hydrol. Process.* 19(3): 839-848.

Whittaker, G., R. Fare, R. Srinivasan, and D.W. Scott. 2003. Spatial evaluation of alternative nonpoint nutrient regulatory instruments. *Water Resour. Res.* 39(4): 1079, doi:10.1029/2001 WR001119.

Williams, J.R., A.D. Nicks, and J.G. Arnold. 1985. Simulator for water resources in rural basins. *J. Hydr. Engr.* 111(6): 970-986.

Application of SWIM Model in the Elbe Basin: Experience and New Developments

Valentina Krysanova*, Fred Hattermann, Joachim Post, Anja Habeck, and Frank Wechsung
Potsdam Institute for Climate Impact Research, P.O. Box 601203, Telegrafenberg, 14412 Potsdam, Germany. E-mail: krysanova@pik-potsdam.de

Abstract

The need for assessment of water resources availability and quality in large, ungauged river basins and large regions is a frequent topic of discussion. It is becoming increasingly important for water resources evaluation in countries with poor data availability, and for climate and land use change impact assessment at the regional scale. The main objective of this study is to discuss prerequisites and conditions for such applications using ecohydrological river basin models like SWIM (**S**oil and **W**ater **I**ntegrated **M**odel) and SWAT (Soil and Water Assessment Tool). SWIM was developed based on SWAT-1993 for climate and land use change impact studies. SWIM has several improved/modified subroutines and several new modules in comparison with SWAT-2000, e.g. the crop generator to distribute crop rotations; the riparian zone module as an interface between upland areas, groundwater, and river networks; the forest growth module; the module for CO_2 adjustment of plant growth; and the carbon cycle module.

The choice of strategy for model validation and analysis of uncertainty related to model parameterization and input data are discussed in this paper. The purpose is to discuss the multi-site, multi-scale, and multi-criteria validation method of a regional-scale ecohydrological model based on uncertainty analysis performed in advance. This method was successfully applied for modelling with SWIM in the Elbe River Basin in Germany (drainage area of about 100,000 km^2) and its subbasins. The basin is representative of semi-humid landscapes in Europe, where water availability during the summer season is the limiting factor for plant growth and crop yield. Analysis of parameter sensitivity and analysis of uncertainty related to model parameterization and input data should be performed before the validation in order to optimize the validation strategy. The prerequisites of the model application in ungauged basins are discussed.

Introduction

Ecohydrology combines the studies of hydrological, biogeochemical, and ecological processes and their interrelations in soil and water bodies. It aims at a better understanding of hydrological factors determining the development of natural and human-driven terrestrial ecosystems, and of ecological factors controlling water fluxes. River catchments can be considered as integrators of the effects of many climatic and terrestrial forces, as they have hierarchical structure and natural boundaries, and therefore represent an appropriate scale for ecohydrological modelling.

A physically based hydrological/ecohydrological model describes the natural system using mainly basic mathematical representations of the flow of mass, momentum, and energy. At the catchment scale, a physically-based model has to be fully distributed by accounting for spatial variations in all variables and parameters. However, the fact that a model is physically based does not necessarily mean that it is based only on fundamental physical laws. Conceptual approaches that mathematically describe the general process behavior may also be included.

It has been shown that the inclusion of physical laws in a model does not, by itself, guarantee its quality. Even if physical laws included in the model are proven to represent a good mathematical description for a soil column under laboratory conditions where soil has been well mixed, this may not automatically be the case at the scale of grid elements used in distributed hydrological models (Beven, 1996). These equations usually require application with parameters and variables assumed to be uniform over a spatial scale of hundreds of meters or even kilometers. On the other hand, description of physical processes is lacking in conceptual hydrological models (e.g. water movement through soil layers), and therefore it is difficult to integrate biogeochemical processes in them.

The continuous dynamic models that include mathematical descriptions of physical, biogeochemical, and hydrochemical processes, and combine significant elements of both physical and conceptual semi-empirical nature can be called *process-based ecohydrological models*. Numerous studies have demonstrated that such models are able to adequately represent natural processes at the catchment scale.

An ecohydrological model for a river catchment inevitably contains a hydrological module as a basic element. Another necessary part is a vegetation submodel. Also, such a model usually includes submodels for biogeochemical cycles (carbon, nitrogen, phosphorus) with a certain level of complexity. The hydrological, vegetation, and biogeochemical submodels are usually coupled in order to include important interactions and feedbacks between the processes, like water and nutrient drivers for plant growth, water transpiration by plants, nutrient transport with water, etc. Usually, vertical and lateral fluxes of water and nutrients in catchments are modelled separately, whereas climate parameters are not modelled but used as external drivers. The models SWAT (Arnold *et al*., 1993) and SWIM (Krysanova *et al*., 1998a) can be classified as the process-based modelling tools.

In this paper, the following problems related to regional applications of ecohydrological models SWIM and SWAT are discussed: choice of strategy for model validation, and analysis of uncertainty related to model parameterization and input data.

Short Description of SWIM

The modelling system SWIM is a continuous-time spatially semi-distributed model, integrating hydrological processes, vegetation growth (agricultural crops and natural vegetation), nutrient cycling (carbon, C, nitrogen, N, and phosphorus, P), and sediment transport at the river basin scale. In addition, the system includes the interface to the Geographic Information System GRASS (Geographic Resources Analysis Support System, GRASS 4.1, 1993), which allows the extraction of spatially distributed parameters for elevation, land use, soil, and vegetation, and creation of the hydrotope structure and the routing structure for the basin under study.

SWIM is based on two previously developed tools – SWAT (Arnold *et al.*, 1993), and MATSALU (Krysanova *et al.*, 1989). The model MATSALU was developed in Estonia for the agricultural basin of the Matsalu Bay, with an area of about 3,500 km^2, and the Matsalu Bay ecosystem in order to evaluate different management scenarios for the eutrophication control of the bay. The MATSALU model has a three-level spatial disaggregation and consists of four externally coupled submodels for the basin hydrology, the basin geochemistry, the river transport of water and nutrients, and the nutrient dynamics in the bay ecosystem. Both SWAT and the catchment submodel MATSALU were based on the CREAMS model (Knisel, 1980), like many other hydrological/water quality models.

A three-level scheme of spatial disaggregation (basin – subbasins – hydrotopes or region – climate zones – hydrotopes) plus vertical subdivision of the root zone into a maximum of 10 soil layers are used in SWIM. A hydrotope is a set of elementary units in a subbasin or climate zone, which have the same land use and soil. During the simulation,

(1) water, nutrients, and plant biomass were initially calculated for every hydrotope/soil layer in a hydrotope,
(2) the outputs from hydrotopes were then integrated to estimate the subbasin outputs, and
(3) the routing procedure was applied to the subbasin lateral flows for water, nutrients, and sediments, taking into account transmission losses.

The latest developments in SWIM include:

(1) additional functions describing dependence of photosynthesis and transpiration on atmospheric CO_2 for climate change impact assessment;
(2) implementation of the method of sensitivity and uncertainty analysis in SWIM;
(3) implementation of a multi-criteria, multi-site, and multi-scale validation method of SWIM;
(4) thorough validation of SWIM in a lowland catchment for water quality;
(5) improved forest ecosystem module and crop generator;
(6) implementation of riparian zone module in SWIM to improve water quality modelling;
(7) direct inclusion of a carbon cycle module in SWIM.

This paper describes the methods of sensitivity, uncertainty, and validation (for details see Hattermann et al., 2005a). The equations for climate change impact assessment are presented in Krysanova and Wechsung, 2002a. The implementation of the riparian zone module and application of SWIM for water quality modelling is described in Hattermann et al., 2005b and Habeck et al., 2004. The carbon cycle module in SWIM and its verification are described in Post et al., 2004.

The Basin under Study

The Elbe River Basin covers large parts of the Czech Republic and Eastern Germany. The total length of the Elbe River is 1,092 km, the drainage area is approximately 148,268 km² (approximately 2/3 belongs to Germany and 1/3 to the Czech Republic). About 25 million inhabitants live in the basin, which includes the cities of Prague, Berlin, Hamburg, Dresden, and Leipzig. Many tributaries of the Elbe are controlled with dams and weirs, whereas the main channel of the Elbe in Germany is in a semi-natural status.

The river discharge is characterized by winter and spring high water periods. Buffer storages of glacial snow to mitigate against both flood discharge and low flow are missing in the upstream reaches of the Elbe due to the lack of high mountain regions. Therefore, the span between monthly low flow and high flow in the Elbe is 1:21. The long-term mean annual precipitation in the basin is 659 mm. The long-term mean annual discharge of the Elbe River is 716 $m^3\ s^{-1}$ at the gauge Neu Darchau, the specific discharge is 6.2 $l\ s^{-1}\ km^{-2}$, which corresponds 29.7% of the annual precipitation.

The German part of the Elbe drainage area is subdivided into three typical subregions based on relief and soils, namely, (1) the Pleistocene lowland, covering the Havel basin and the area to the west and northwest of it; (2) the loess subregion in the lower parts of the Saale and the Mulde basins; and (3) the mountainous subregion in the upper parts of the Saale and the Mulde basins. Agricultural areas that occupy about 56% of the total area of the German part of the drainage basin represent one of the most important sources of diffuse nutrient pollution. The Elbe and its tributaries are intensively used for fresh water supply for domestic, industrial, and agricultural purposes.

A primary reason for selecting the Elbe Basin as a case study is its vulnerability to water stress during dry periods. Due to the position of the basin between the relatively “wet” maritime climate in Western Europe and the more continental climate in Eastern Europe with longer dry periods, the annual long-term average precipitation is relatively small. In the lowland of the German part of the basin it is less than 600 mm yr^{-1}. The Elbe River Basin is therefore classified as the driest among the five largest river basins in Germany (Rhine, Danube, Elbe, Weser, and Ems). Taking into account the existing centers of urbanization in the basin (Berlin, Hamburg, etc.), and a possibility of decreasing precipitation in the future due to climate change (Werner & Gerstengarbe, 1997), the resulting potential problems and conflicts are escalating, and a comprehensive climate impact study is becoming increasingly important. In the Global Change impact studies, particular interest is placed in valuating the effects of expected changes in climate and land use on hydrological processes, water quality, and crop yield.

Pollution of surface and groundwater in the basin caused by the high intensity of water use, excessive application of fertilizers and pesticides in agriculture, and discharge of domestic and industrial wastes are yet other reasons for implementing an impact study for the Elbe Basin. Nutrient pollution (nitrogen and phosphorus) is one of the most widespread forms of water pollution in the region. Even though emissions from point sources were notably decreased in the basin since the 1990’s due to reduction of industrial sources and introduction of new and better sewage treatment facilities, the diffuse sources of pollution represented mainly by agriculture are still not sufficiently controlled. The simulation experiments provide a valuable tool to analyse how different factors and management options influence nutrient fluxes from upland areas to the basin outlet.

Four Steps of Model Verification for a Basin

The model validation includes four major steps:

(1) *Sensitivity analysis* to define a set of most important parameters.

(2) *Uncertainty analysis* to evaluate the model uncertainty related to input data and model parameters defined in Step 1.

(3) *Multi-scale and multi-site hydrological validation*: simulated and measured water discharges are compared in the outlet and intermediate gauges in representative subregions and at different scales.

(4) *Multi-criteria model validation*, including other model outputs, like groundwater table, evapotranspiration, crop yield, nutrient concentration and load, and erosion.

Sensitivity Analysis Method

Three subbasins of the Elbe: the upper Saale (1,013 km^2 located in the mountainous subregion), the Mulde (2,091 km^2 located in the mountainous and loess subregions), the Löcknitz (447 km^2 located in lowland), and the entire Elbe Basin were selected to investigate the model sensitivity and uncertainty related to parameters and input data.

The sensitivity analysis included different global parameters responsible for the model behavior, which were chosen after the preliminary test on sensitivity. They are:

- soil-related parameters: correction factors for saturated soil conductivity, for soil depth, and curve number coefficient;
- vegetation-related parameters: correction factors for LAI, for biomass-energy ratio, for albedo coefficient, for base temperature of plant growth, and for root depth;
- hydrology-related parameters: correction factors for river routing coefficients, for groundwater return flow, for groundwater delay, for channel slope and for channel Manning coefficient.

In addition, climate correction factors for temperature, radiation, and precipitation were considered in order to investigate the model sensitivity to climate input.

The calibration parameters were sampled randomly within their physically meaningful limits. Most of the parameters were sampled from the normal distribution with a mean of one, and then multiplied with their initial values in order to assess the sensitivity of the model to higher or lower values of parameters. The routing correction parameter was sampled from the triangular distribution.

300 parameter sets were generated for each of the four basins using the Latin Hypercupe method (Richter *et al*., 1996). Each parameter set was the input for a four-year simulation run. Two major model outputs were taken into consideration: the deviation in water balance and the Nash & Sutcliffe efficiency (1970) for the daily simulated against daily observed water discharge. The sensitivity of model results to the parameters was estimated using the Partial Correlation Coefficients of the rank transformed data (the simulation results, Tarantola 2001), and a set of most important parameters was chosen.

Method of Model Validation

First, the model was applied separately to 12 subbasins of the Elbe located in different subregions with drainage areas varying from 280 to 23,690 km^2. The hydrological processes were calibrated with a daily time-step using the observed river discharge for comparison. A rough non-generic automatic calibration was performed using a Monte Carlo method combined with the Latin Hypercupe method (Tarantola 2000) in order to assure that all physically meaningful parameter combinations are considered in the modelling procedure. Afterwards, fine-tuning of the model was done.

Then the best 20 results of the automatic calibration for each subregion of the Elbe were statistically evaluated applying cluster analysis, where the parameter sets of the simulation results were used as independent values to classify them. This allowed for an investigation of typical parameter sets for the subregions of the Elbe Basin. Besides the initial storage values and the radiation correction factor, the following three parameters were used to calibrate the hydrological processes in the model: the parameter *rcor* to tune river flow routing, the parameter *sccor* to calibrate the saturated soil conductivity, and the groundwater reaction factor *alph* to adjust the baseflow.

The simulated river discharge was compared with the measured discharge for an eight year period. Statistical evaluation of the results was done by analysing the long-term deviation in water balance and the efficiency criteria after Nash & Sutcliffe (1970). Based on the calibration results, the hydrology of the selected subbasins and the entire Elbe Basin was validated. Based on the information gained from the mesoscale catchments, the parameter sets were taken and used to validate the hydrological processes over the entire basin.

The validation in the Elbe and its subbasins resulted in the Nash & Sutcliffe efficiency varying between 0.72 and 0.92 with the daily time-step, and between 0.81 and 0.94 with the monthly time-step. The deviation of runoff volume was usually lower than ±3%, with a single maximum value of 9.7% for a dry period. The stable results in all three subregions and at different scales assure that multi-scale and multi-site validation of SWIM in the Elbe Basin was successful.

The multicriterial validation included other hydrological variables, like groundwater table and evapotranspitration, and other variables related to water quality, erosion, and crops. For example, the spatial behaviour of hydrological processes inside the basins was analysed using contour maps of the water table and observed time series of groundwater levels. The long-term mean water table dynamics in three lowland basins: the Stepenitz basin with an area of 574 km^2, the Löcknitz basin with an area of 447 km^2, and the Nuthe basin with an area of 1,993 km^2, were simulated and compared with the measured ones.

The sequential model validation continued by including vegetation, erosion, and nitrogen dynamics. Nitrogen dynamics was examined using data from two basins and two lysimeters, erosion was validated using data from two basins, and crop growth using data from the state of Brandenburg and the total German part of the Elbe (Krysanova *et al*., 1999a, 1999b, 2002b, Krysanova & Becker, 1999, Dreyhaupt, 2001).

Uncertainty Analysis and Robustness

Based on the calibration results, the hydrology of three selected subbasins: one subbasin in the lowlands (the Löcknitz basin, gauge station Gadow), one in the loess area (the Mulde basin, gauge station Wechselburg), and one from the mountains (the Upper Saale basin, gauge station Blankenstein), and the entire Elbe Basin were further analysed. The uncertainty was investigated using histograms of the two criteria: the model efficiency and the deviation in water balance, based on the 300 simulations for every basin. Figure 1 shows eight histograms demonstrating the results of the uncertainty analysis. Each graph has four histograms, three for the subbasins from the mountains, the loess area and the lowlands, and one for the entire Elbe Basin.

As one can see, the model provides a good reproduction of water balance. The mean value of 300 simulations was around zero for all catchments except those in the loess area, where the model tends to slightly overestimate water discharge (and hence, underestimates evapotranspiration). In our view, the hydraulic parameterization of loess soils involves a lot of uncertainties when the parameters are transferred from the lab measurements to the basin scale, so that the inherent heterogeneity of the soils (cracks, macropores, textural characters) cannot be represented in macroscale polygon covers.

The model efficiency was always above 0.3, the mean values were above 0.6. The conclusion is that the model was able to reproduce satisfactory dynamic flow patterns of river discharge in different basins even if sensitive parameters were sampled stochastically and not calibrated. The best performance with the highest efficiencies was in the mountainous catchment, which was quite natural. The lowest efficiencies, with higher standard deviation, were obtained for the loess and lowland catchments. This result agrees with the outcome of the model validation, where the nested lowland catchments produced the poorer results.

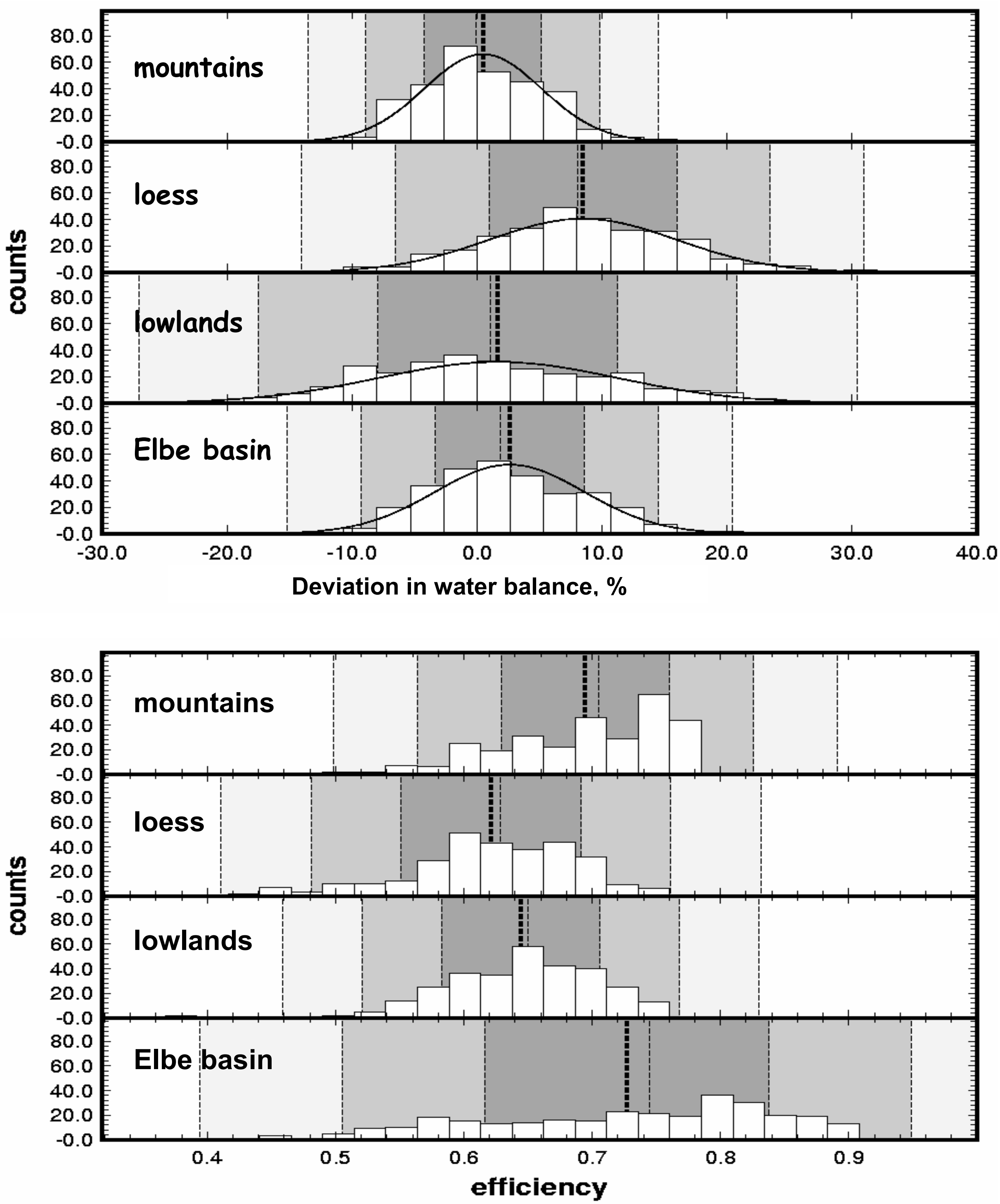

Figure 1. Histograms demonstrating the results of the uncertainty analysis for three subbasins and the total Elbe Basin.

The distributions for the Elbe Basin represent a composite of the results of the nested subbasins. The simulated discharge was slightly overestimated. The average of the efficiency distribution was better than the ones in the smaller subbasins, but had higher variation.

The overall result of the uncertainty analysis in macroscale applications of SWIM is the following: 90% of the simulations have an efficiency above 0.53 and an absolute deviation of water balance lower than 9.9%. The uncertainty in simulating the hydrological processes in lowland and loess subareas was higher, whereas the results in mountainous parts of the basin show a robust and stable performance.

Conclusions and Outlook

The model validation described in the paper has shown that SWIM is able to illustrate with a reasonable accuracy the basic hydrologic processes (including the spatial and temporal variability of the main water balance components), the cycling of nutrients in the soil and their transport with water, the growth and yield of major crops, and the dynamic features of soil erosion and sediment transport under different environmental conditions in catchments of temperate climate zones.

This provides a justification and a sound base for studying the effects of changes in climate and land use on all these interrelated processes and characteristics, and for the model transfer to ungauged basins, assuming that climatic, topographical, land use, and soil conditions are similar (for example, in the temperate zone). For application in other conditions and climatic zones, a preliminary test and validation in representative subbasins could be recommended.

The prerequisites of the model application in ungauged basins are:

- analysis of the model sensitivity to input data and model parameters, outlining the most critical input data and parameters;
- analysis of uncertainty related to input data and model parameters;
- thorough validation of the model based on the sensitivity analysis performed in advance, whereas the method of validation should be multi-scale, multi-site, and multi-criteria.

After such a procedure, if the model validation was successful and uncertainty is not high, the model can be applied in ungauged basins belonging to the same climate zone, or in a larger river basin or region. If a new region has essentially different geomorphological or climate characteristics, the model application is possible only after its preliminary validation in a representative catchment.

References

Arnold J.G., Allen P.M., Bernhardt G., 1993. A comprehensive surface-groundwater flow model, *Journal of Hydrology* 142: 47-69.

Beven K.J., 1996. A discussion of distributed hydrological modelling. In: M.B.Abbott, J. CH. Refsgaard (eds.) *Distributed hydrological Modelling*, Kluwer Acad. Publ.: Dordrech, Boston, London.

Dreyhaupt J. (ed.), 2001. Stickstoffmodellierung für Lysimeter des Parthegebietes. Ergebnisse des Workshops vom 8 bis 10 Juni 1999, *UFZ-Bericht* 17, Umweltforschungszentrum Leipzig-Halle GmbH, Leipzig.

GRASS4.1. Reference Manual, 1993. US Army Corps of Engineers. Construction Engineering Research Laboatories, Champaign, Illinois.

Habeck Habeck, A., Krysanova, V., Hattermann, F., 2004. - Integrierte Analysen zur Wasserqualita"t in mesoskaligen Einzugsgebieten des Tieflandes. - In: Wasser- und Stofftransport in heterogenen Einzugsgebieten. - Beitra"ge zum Tag der Hydrologie 2004. - Hydrologische Wissenschaften. -H. 5/2004.

Hattermann, F.F., Krysanova, V, Wechsung, F, Wattenbach, M., 2004. Integrating groundwater dynamics in regional hydrological modelling. Environmental Modelling and Software 19(11): 1039-1051.

Hattermann F, Krysanova V., Wechsung F., Wattenbach, M. 2005a. Macroscale validation of the ecohydrological model SWIM for hydrological processes in the Elbe basin with uncertainty analysis. . In: Fohrer, N. and Arnold, J. (Editors), 2005. Regional Assessment of Climate and Management Impacts Using the SWAT Hydrological Model. Hydrological Processes (in print).

Hattermann, F.F., Krysanova, V., Habeck, A., Bronstert, A., 2005b. Integrating wetlands and riparian zones in river basin modelling. Ecological Modelling (submitted).

Knisel W.G. (ed.), 1980. CREAMS: A field scale model for chemicals, runoff, and erosion from agricultural management systems. *USDA Conservation Research Report* 26: 643.

Krysanova V., Meiner A., Roosaare J., Vasilyev A., 1989. Simulation modelling of the coastal waters pollution from agricultural watershed, *Ecological Modelling* 49: 7-29.

Krysanova V., Müller-Wohlfeil D.I., Becker A., 1998. Development and test of a spatially distributed hydrological / water quality model for mesoscale watersheds. *Ecological Modelling* 106: 261-289.

Krysanova V., Becker A. 1999. Integrated Modelling of Hydrological Processes and Nutrient Dynamics at the River Basins Scale, *Hydrobiologia* 410: 131-138.

Krysanova V., Wechsung F., Becker A., Poschenrieder W., Gräfe, J., 1999a. Mesoscale ecohydrological modelling to analyse regional effects of climate change. *Environmental Modelling and Assessment,* 4, (4): 259-271.

Krysanova V., Gerten D., Klöcking B., Becker A., 1999b. Factors affecting nitrogen export from diffuse sources: A modelling study in the Elbe basin. In: L. Heathwaite (ed.) Impact of Land-Use Change on Nutrient Loads from Diffuse Sources, *IAHS Publ*. 257: 201-212.

Krysanova V., Wechsung F., Arnold J., Srinivasan R., Williams J., 2000. SWIM (Soil and Water Integrated Model). User Manual, PIK Report 69. Potsdam Institute for Climate Impact Research: Potsdam.

Krysanova, V. and F. Wechsung, 2002a. Impact of Climate Change and higher CO_2 on hydrological processes and crop productivity in the state of Brandenburg, Germany. In: M. Beniston (ed.) Advances in Global Change Research,, v. 10, 271-300

Krysanova V., Williams J., Bürger G., Österle H., 2002b. Linkage *between hydrological processes and sediment transport at the river basin scale - a modelling study.* UNESCO Technical Report on Hydrological Processes and Soil Erosion *(in print).*

Nash, J.E. and J.V. Sutcliffe, 1970. River flow forecasting through conceptional models, 1. A discussion of principles. *J. Hydrol*., 10: 282-290.

Post, J., V. Krysanova & F. Suckow, 2004. Simulation of water and carbon fluxes in agro- and forest ecosystems at the regional scale. In: C. Pahl-Wostl, S. Schmidt, A. E. Rizzoli & T. Jakeman (Eds.) Complexity and Integrated Resources Management. Transactions of the 2nd Biennial Meeting of the International Environmental Modelling and Software Society (iEMSs), Manno, Switzerland, pp. 730-736.

Richter, O, Diekkrüger, B, Nörtersheuser, P., 1996. Environmental Fate Modeling of Pesticides. From the Laboratory to the Field Scale. Weinheim, New York, Basel, Cambridge, Tokyo.

Tarantola, S. 2000. SimLab 1.1, Reference Manual. USDA: United States Department of Agriculture, 2001. AGNPS 2001 Output Processor Model (version 1.0). National Sedimentation Laboratory. USA.

Werner P.C., Gerstengarbe F.-W. 1997., A proposal for the development of climate scenarios. *Climate Research* 8, (3): 171-182.

Catchment Scale Modelling of Pesticide Losses with Imperfect Data – A Case Study from the UK

S.M. White[1*], N. Kannan[2], B. Grizzetti[3] and J. Hollis[4]
[1]Institute of Water and Environment, Cranfield University, Silsoe, Bedfordshire, MK45 4DT, U.K. E-mail: Sue.White@cranfield.ac.uk
[2]Blackland Research and Extension Centre, 720, East Blackland Road, Temple, TX, 76502, U.S.A.
[3]JRC-Ispra, Via E. Fermi 1, I-21020 Ispra (VA), Italy
[4]National Soil Resources Institute, Cranfield University, Silsoe, Bedfordshire, MK45 4DT, U.K.

Abstract

Data on pesticide application rates and locations in the UK are sparse. The most precise data are available at high costs. However, regional estimates of average monthly inputs for each crop type and pesticide are available for England and Wales from the national Department of Environment Food and Rural Affairs (Defra). The main shortcomings of this data source are that precise locations of application are not available and average application rates are calculated as the total pesticide usage in the region divided by the total area of a particular crop type. Typically, these average application rates will be at levels considerably lower than 0.1 kg ha^{-1}, which is clearly not a reflection of the way that pesticides are applied in the real world. Using a hydrologically calibrated and validated SWAT model for the Exe River Basin in southwest England, a range of methods for estimation of pesticide application rates and locations were tested. Some calibration data were available from a water treatment plant at the basin outlet.

The study has shown that SWAT can be successfully applied using the regional Defra data, although calibration of the *percop* parameter in SWAT is required. The values of *percop* changes are substantially dependent on the method used to locate pesticide applications in time and space.

Introduction

The modelling of pesticide losses from land to water bodies has traditionally required detailed knowledge about land cover, land management, and pesticide applications (e.g. Jarvis et al, 1991). When modelling at the river basin scale, such data are difficult if not impossible to find. As part of the TERRACE study (White *et al*, 2005a) there was a requirement to demonstrate the capability of the Soil and Water Assessment Tool (SWAT) (Arnold *et al*, 1998a; Arnold *et al*, 1998b; Neitsch *et al*, 2001) in modelling chemical transfers from land to water. Although data on pesticides are sparse, there is more information available than for other diffuse source chemicals. Thus, given some data and previous work, pesticides were chosen as the trial vehicle to demonstrate SWAT's capabilities in chemical modelling.

The pesticide modelling was carried out for a previously calibrated and validated set-up of the USDA Soil and Water Assessment Tool (SWAT) for the Exe Catchment in southwest England (White *et al*, 2003; White *et al*, 2005a).

Study Area

The Exe Catchment has a total area of 1,530 km^2 and is located in southwest England (White *et al*, 2005a). It extends from nearly the north Devon coast to the south coast, reaching its tidal limit (the downstream end of hydrological catchment models) at Trews Weir in Exeter, the county town. It is a largely rural, agricultural catchment, dominated by intensive livestock grazing over most of the area, with a small region of rough moorland grazing in the north, and an area of arable agriculture in the south and west (Figure 1). Soils vary from peat in the north to a mixture of poorly to well drained soils in the south. Many of the soils have a high surface stone content. The climate of the area is best described as warm and wet. Annual rainfall for the catchment as a whole is 1,097mm. There are few frost days during the year, but agricultural activity is constrained by the wetness of soils which can remain at field capacity well into the spring. There are minor aquifers in the centre of the basin.

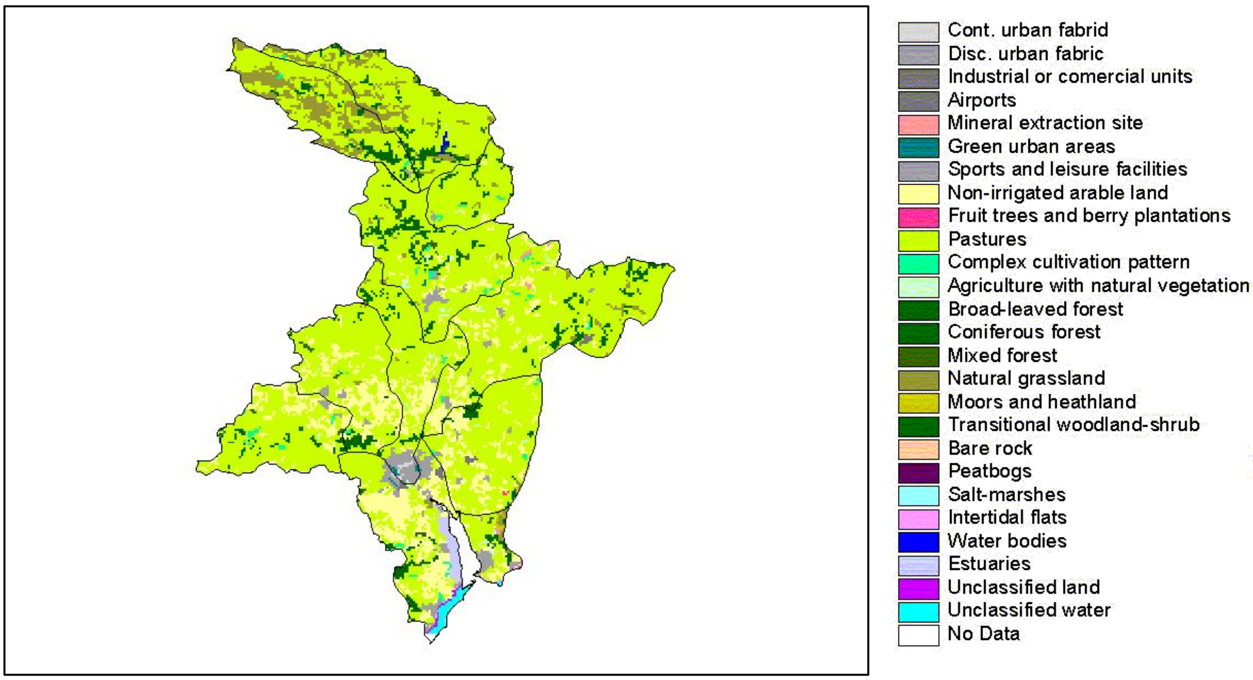

Figure 1. Land use in the Exe Catchment (1990).

Methodology

The Exe Catchment model was set up, calibrated, verified, and validated as part of a contract for the European Chemicals Industries Council (CEFIC). SWAT was used as the basis for the diffuse pollution modelling of catchments in Europe in the TERRACE study (White *et al*, 2005a). Hydrology was calibrated, verified, and validated at the HRU, sub-catchment, and catchment scale (White *et al*, 2005-UK) using data for river flow separated into baseflow and rapid response, soil moisture variation, and crop growth and yield. Once the hydrology was performing well, contaminants could be added to the system.

The distributed modelling of pesticide losses from fields to rivers and water bodies requires information on pesticide input rates and dates. However, in the UK (and much of Europe) data are only routinely available at a regional level. This provides the modeller with a dilemma. The data that are routinely available are expressed as total usage of a pesticide per month in a region, divided by the total hectares of the crop of interest in that region. This means that the data values in kg ha^{-1} terms are very low, and do not represent what any farmer would do in reality. Example data for permanent pasture for two years are shown in Table 1.

This study investigated methods of using such regional data in diffuse pollution modelling. The data, supplied by the Department of Environment, Food and Rural Affairs (Defra), in the UK, are given as average monthly application rates for a specific crop, pesticide, and region (see Table 1 for example data). In contrast, the manufacturer's recommendations supplied information about the required application rate for effective control of pests or weeds, and more closely reflect what farmers will do in practice. Two methods were therefore devised to use these two sets of information in modelling pesticide loss in the Exe Catchment. The pesticide chosen was Mecoprop, as it is used on both improved grassland and cereal fields, which are the dominant land cover and arable crop type, respectively, in the catchment. This meant that expected losses of Mecoprop were likely to be higher than for other pesticides, an expectation which was confirmed on inspection of the limited water quality data for model validation. The use of Mecoprop added a further complication in that some farmers were switching from Mecoprop to Mecoprop-P during the period for which the model was being applied. However, recommended application rates of Mecoprop-P are half of those for Mecoprop and thus where Mecoprop-P usage was suggested this was converted to a Mecoprop application at twice the Mecoprop-P rate.

Table 1. Defra pesticide application statistics for spring barley in the southwestern region.

1994 data			1996 data		
Pesticide	Month of application	Average application rate (kgha^{-1})	Pesticide	Month of application	Average application rate (kgha^{-1})
Mecoprop	4	0.0336384	Mecoprop	4	0.023194
Mecoprop	5	0.1728617	Mecoprop	5	0.1411155
Mecoprop	6	0.0283121	Mecoprop-P	4	0.0194712
Mecoprop	8	0.004478	Mecoprop-P	5	0.125503
Mecoprop-P	3	0.0393891	Mecoprop-P	6	0.0339376
Mecoprop-P	4	0.0205927			
Mecoprop-P	5	0.113266			

Two methods were developed which use the available data in different ways.

Method 1

Regional data from Defra were used to calculate the cumulative monthly application rates of Mecoprop. Within SWAT the catchment was divided into sub-catchments and then into hydrological response units (HRUs). Management actions, such as pesticide application are carried out at the HRU level. Therefore, HRUs were randomly selected for pesticide application from the pasture and cereal HRUs in order to match both the cumulative monthly pattern and the monthly regional usage rates for these land uses based on the Defra statistics (Figure 2). Those HRUs selected for pesticide application received a realistic dosage (according to manufacturer's instructions: 1-2.4 kg active substance ha^{-1} for pasture, 1.4-2.4 kg active substance ha^{-1} for cereals) selected randomly from the range of recommended dosage rates on a randomly selected date in the appropriate month. In practice this meant that HRUs were selected and their areas summed until the percentage of the area receiving Mecoprop gave an average application rate equivalent to the Defra statistics. Ten different random selections were made, meaning that pesticides were applied at realistic rates but at different times and locations for each of the ten scenarios. The random selection was thus threefold – HRU, date within the month, and dosage rate. In addition, one run was made with the same random selection process but with a much more complex pattern of HRUs. This was achieved by defining many more sub-catchments in the original SWAT model, to investigate whether more complexity in the model resulted in better predictive capability.

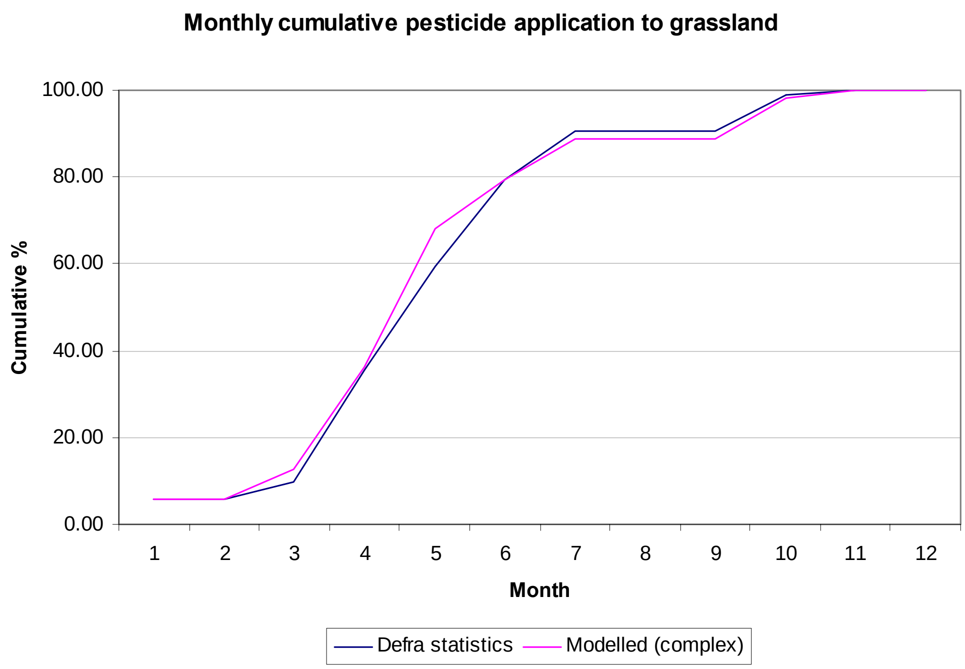

Figure 2. Monthly cumulative pesticide application to grassland in the southwest region showing Defra statistics (average for 1994 and 1996) and modelled inputs using the complex model set-up.

Method 2

Method 1 involved considerable pre-processing of data outside of the SWAT run and only gave scenarios of possible pesticide application rates rather than a true pattern of application (i.e. it was a representation of a possible reality but it was not what really happened). This caused a high overhead in computing and staff requirements for possibly little benefit. It was therefore decided to investigate application of pesticide to ALL potential fields where Mecoprop may be used at the regional rate given in the Defra statistics. While being a completely unrealistic representation of actual farm practice, this is a much simpler modelling procedure. In this case a random element was also introduced by selecting dates for pesticide application within a given month. Thus, pesticides were applied at the monthly regional rate for each land use concerned. Again, ten random selections of date within the month were made.

Results

Very few measurements of Mecoprop concentration are available for all catchments across the UK. The Environment Agency, which has responsibility for routine water quality monitoring, takes samples from some 8,000 water bodies across the UK at four weekly intervals. These samples are analysed for a range of contaminants, including several pesticides. However, because pesticide concentrations in rivers tend to peak at times of maximum application and high surface or drain flow, such a sampling procedure often misses peaks in such event base contaminant concentrations. The same is true for sediment and phosphate. For pesticides the consequence is that they are only present in samples at concentrations lower than the detection limit. In the Exe Catchment there were some data available from the Water Treatment Works (WTW) at the outlet of the catchment. Here the local water company, South-West Water, monitors pesticides at times when high concentrations are expected, according to detailed farm statistics. Thus, their data reflect a much higher range of concentrations than those seen in the EA data. These WTW data have been used to verify model results.

No calibration of the pesticide component of SWAT has been carried out. Once the model was calibrated, verified, and validated for hydrology this was taken as a sufficient basis for contaminant modelling. This will reflect the situation in most catchments where more information is available for hydrological verification than for contaminants. The logic is that if water is moving realistically, both in amount and path, then providing contaminants that are well parameterised in terms of their physical characteristics should provide reasonable concentrations of the pesticide as it is transported with the relevant flow. Pesticide characteristic data were taken from the Institut National de Recherche Agronomique (NRA) – “Agritox” website (http://www.inra.fr/agritox/).

Given the methods used to determine pesticide application date and rate, it is not reasonable to expect good time series predictions of pesticide concentrations in rivers. More important, from a management point of view, is to be able to predict the frequency at which various concentrations may occur. Results are thus presented as both time series and exceedance curves.

Method 1 gives a very poor representation of time series (Figure 3), but a much better representation of the frequency curve (Figure 4). Some improvement in predictive ability is achieved as the catchment representation is made more complex, but at the cost of greater time inputs for model set-up and runs.

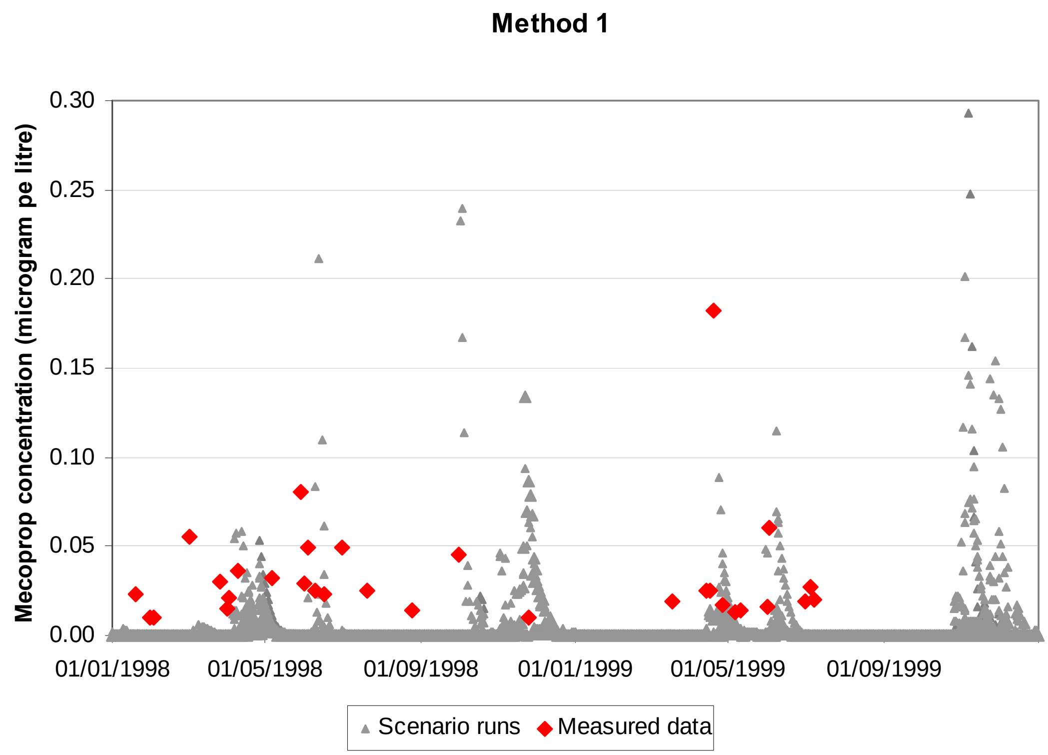

Figure 3. Time series of pesticide predictions – method 1.

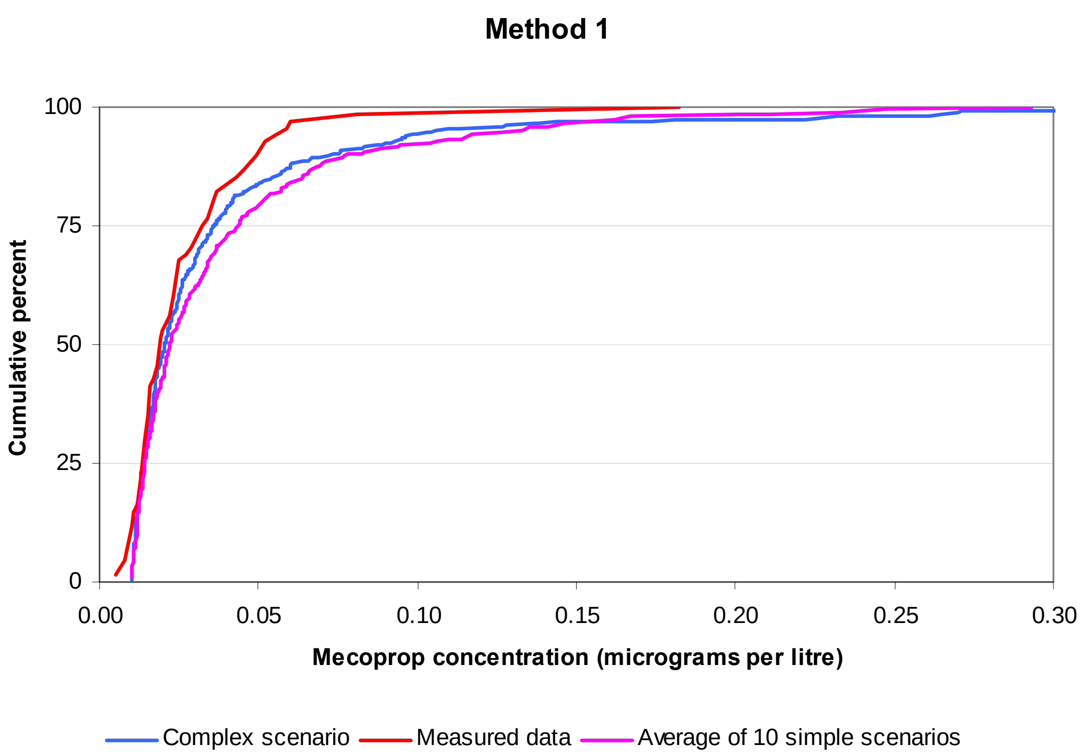

Figure 4. Pesticide exceedance curves – method 1.

Method 2 gives a much better representation of the time series (Figure 5), although it provides a slightly poorer representation of the pesticide frequency curve (Figure 6). However, higher concentrations, which it can be argued are the most important to model correctly, are better represented with this method.

In order to achieve these results in SWAT it was necessary to change one of the model parameters, PERCOP. This controls the percentage of pesticide reaching the soil which is available for transport in surface flow. For Method 1 PERCOP was set at 0.0001 and for Method 2 PERCOP was set at 0.2. This represents a reduction in pesticide availability for Method 1. All other model parameters were left the same for both sets of model runs.

Discussion and Conclusions

These results are important in terms of the feasibility of pesticide modelling over large scales and for multiple catchments in Europe. While research studies for small areas may have data on pesticide usage, this will not be the case for larger areas. Data on pesticides, such as those provided by Defra, are available at the European level and the ability to use this information within a modelling framework, such as SWAT, represents a step change in contaminant modelling. It may also open the possibility of modelling other contaminants for which only regional data are available.

Clearly, the results obtained have been verified using only a limited set of monitored pesticide concentrations. Lack of data for model validation continues to be the biggest hindrance to catchment level contaminant modelling in Europe. Only through improved data can the effectiveness of existing models be judged. Politicians require models to provide information about the impacts of different land management strategies or policies. It must be made clear to them that models can only be as good as the data available to set them up and validate results.

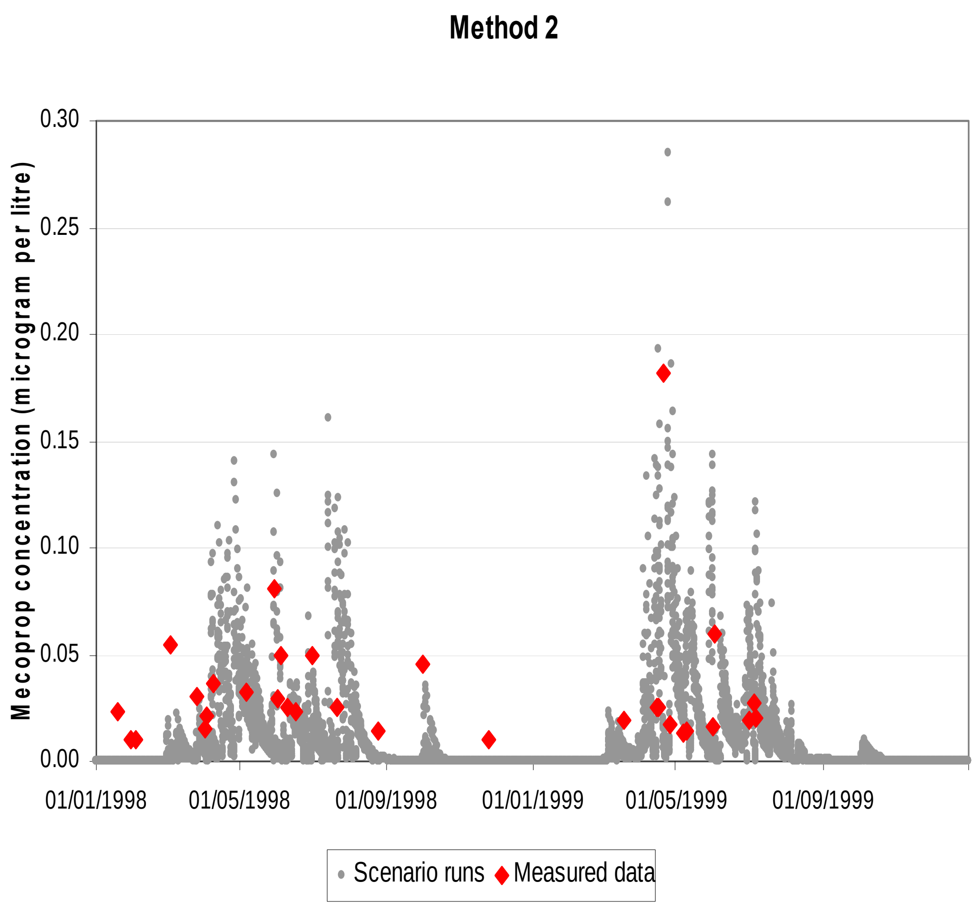

Figure 5. Time series of pesticide predictions – method 2.

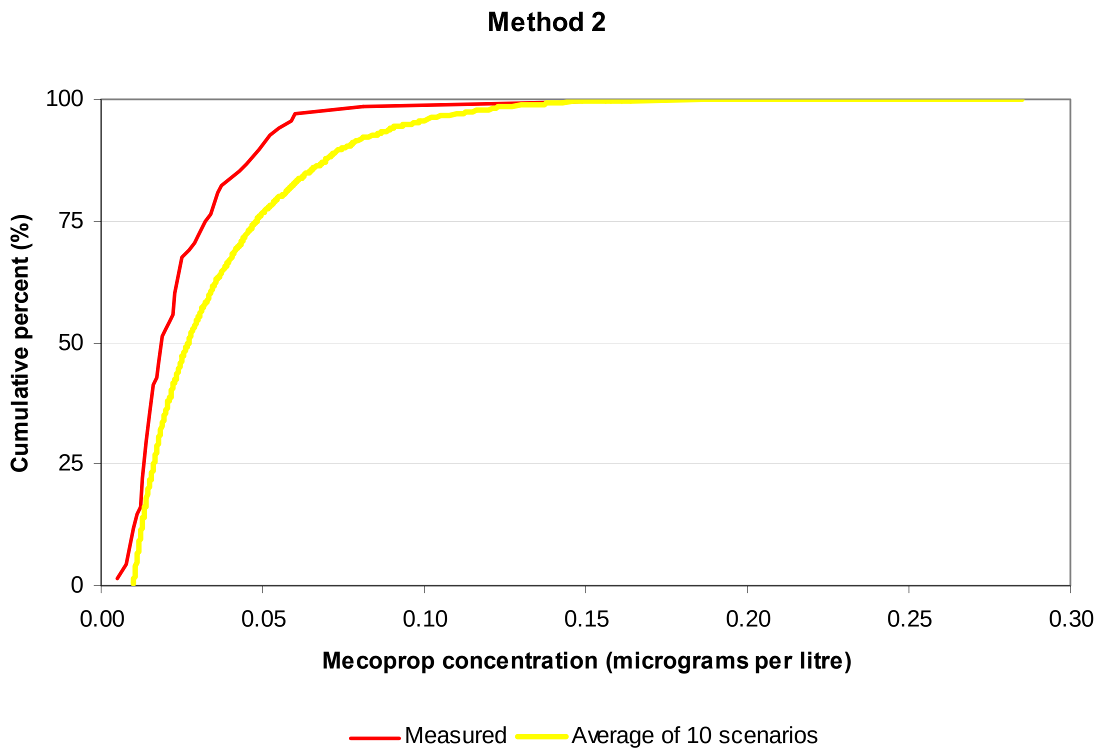

Figure 6. Pesticide exceedance curves – method 2.

References

Arnold, J.G., Srinivasan, R., Muttiah, R.S., & Williams, J.R., 1998a Large area hydrologic modelling and assessment Part I: Model development. *Journal of the American Water Resources Association*, 34(1), 73-89.

Arnold, J.G., Srinivasan, R., Muttiah, R.S., & Williams, J.R., 1998b Large area hydrologic modelling and assessment Part Ii: Model application. *Journal of the American Water Resources Association*, 34(1), 91-101.

Jarvis, N.J., Bergström, L. & Stenström, J., 1991 A model to predict pesticide transport in macroporous field soils. In: *Proceedings of the National Symposium on Preferential Flow*, (eds. T.J. Gish and A. Shirmohammadi), December, Chicago, IL, American Society of Agricultural Engineers, St. Joseph, MI, 308-317.

Neitsch, S.L., Arnold, J.G., Kiniry, J.R., Williams, J.R. 2001. *Soil and Water Assessment Tool - Theoretical Documentation. Version 2000.*

White, S.M., Beaudin, I., Kannan, N., Hollis, J.M., Worrall, F. & Hallet, S. TERRACE: Terrestrial Runoff modelling for Risk Assessment of Chemical Exposure. Year three report, Version 1.0. Final report on the TERRACE project. Unpublished report, Cranfield University.

White, S.M., Kannan, N., Beaudin, I., Hollis, J., Young, A.K., Keller, V. & Whelan, M., 2005a. The TERRACE project: SWAT application for diffuse chemical pollution modelling. *Proceedings SWAT 2005, 3rd International Conference*, Zurich, Switzerland, July 11th – 15th 2005.

White, S.M., Kannan, N., Holman, I., Whitehead, J., Beaudin, I., Carter, J. & Hollis, J.M., 2005b. Using SWAT in English catchments: experience and lessons. *Proceedings SWAT 2005, 3rd International Conference*, Zurich, Switzerland, July 11th – 15th 2005.

Limitations, Problems and Solutions in the Setup of SWAT for a Large-Scale Hydrological Application

Jürgen Schuol and Karim Abbaspour
Swiss Federal Institute of Aquatic Science and Technology, Department of Systems Analysis, Integrated Assessment and Modelling, Überlandstrasse 133, 8600 Dübendorf, Switzerland.
E-Mail: juergen.schuol@eawag.ch

Abstract

Although the SWAT model has been applied to many basins around the world, little research has been undertaken on the model's applicability in very large-scale (millions of sqkm) watersheds. The goal of this study was to quantify the amount of the global country-based available freshwater starting with a sub-continental appraisal. Special emphasis was given to the quantification of the spatial and temporal distribution of the total available water as well as the soil water, considering its importance for rain-fed agriculture.

Setting up the SWAT model for an entire continent using the ArcView interface was not possible, as the interface is not able to calculate the geomorphic subbasin parameters for such a large area with more than 1,500 subbasins. Therefore, a four million km^2 area in West Africa, including the Niger, Volta, and Senegal River Basins was first modeled. During this setup additional AVSWAT-specific problems were encountered, mainly due to the limited ability to manually process stream definitions and subbasin delineations. The DEM had to be manipulated in order to avoid a misrouting of the streams. Furthermore, many of the necessary SWAT soil and land use parameters do not exist on a global/continental scale, making it necessary to use pedotransfer functions and assumptions based on similar classes in order to assign reasonable parameter values. Weather station density, and thus climatic data availability, is often not sufficient in many parts of the world. In addition, this data are often of meagre quality, making the use of a weather generator inevitable. While WXGEN (the weather generator model included in SWAT) needs daily measured values as input, an automated procedure was developed in this study for which gridded monthly climate data is sufficient. Using a daily weather generator algorithm (DWGA), the annual and monthly model output was clearly improved.

Once the initial SWAT and data shortcomings for the West Africa case study had been overcome, model calibration was completed using SUFI-2, a multi-site automated calibration procedure. Preliminary annual and monthly simulations showed promising results with respect to the freshwater quantification goal of this study; however, these results also pointed out the uncertainty of the conceptual model. Reservoirs and wetlands, amongst others, are important processes not included in the model up to now, due to limited information on a global scale. Further model improvements, challenging calibration efforts, and a proper uncertainty analysis are still necessary.

Introduction

Two years ago "GIS-based hydrological modelling of global freshwater availability" project was started. The objective of this project was to quantify the country-based freshwater availability at a sub-continent scale. To better manage the limited water resources, it is imperative to have a good estimate of the availability of freshwater at a national scale. This figure is widely sought after in many global studies, ranging from studies of food and water security, sectoral water planning, national economic and social policies, to desertification, forced migration, and the effects of climate change and population growth. The available estimates of freshwater are imprecise and do not quantify the temporal and spatial distributions of available water, which in some cases are more important than the available water figure itself. Therefore, the goal of this study was to provide monthly figures, not only for the river discharges (blue water), but also for the soil water (green water), which is the main source of water for rain-fed agriculture. Furthermore, there are no reliable measures of uncertainty associated with the available figures, which makes uncertainty and risk analysis extremely difficult.

To accomplish the objectives, the integrated, continuous, large-scale daily water balance model SWAT (Soil and Water Assessment Tool – Arnold et al., 1998, Arnold et al., 1999) was used. SWAT was selected because of its capability to simulate the hydrologic balance as simply and yet as realistically as possible. The model accounts for differences in soils, land use, crops, topography, and climate. Furthermore, SWAT provides the possibility to extend the hydrological model with sediment and nutrient sub-models, an issue that could be of interest in a follow-up project.

The first step in this project was to collect, compile, and examine globally, digitally available data sets, which are necessary in order to run a hydrological model. Initially, the intent was to model freshwater availability continent by continent, starting with Africa. Due to severe problems within the setup of the continental model using the ArcView–SWAT interface, it was decided to first apply SWAT to a four million km^2 area in West Africa in order to gain experience in large-scale modelling. One major challenge was the insufficient daily climate data. Therefore, a daily weather generator algorithm (DWGA) that uses the currently available 0.5° monthly weather statistics was developed and successfully tested. The calibration of the model is an ongoing process using a multi-site automated global search procedure. Preliminary results will be shown and discussed.

Input Data for Global SWAT Simulations

The basic data sets required to develop the SWAT model input are: topography, soil, land use, and climatic data. The following GIS maps and databases were collected mainly from freely available sites on the Internet, followed by an accurate compilation and analysis of quality and integrity:

(i) A *Digital global elevation model (DEM) and stream network*, produced by the U.S. Geological Survey's (USGS) public domain geographic database HYDRO1k. This data provides consistent global coverage of topography and streams at a resolution of 1 km.

(ii) A *Soil map*, produced by the Food and Agriculture Organization of the United Nations (FAO), which differentiates almost 5,000 soil types at a spatial resolution of 10 km and provides some soil properties. Further soil properties for two layers of depth (e.g. particle-size distribution, bulk density, organic carbon content, available water capacity, and saturated hydraulic conductivity) were obtained from Reynolds et al. (1999) and through the use of pedotransfer functions implemented in the program Rosetta (Schaap, 1999).

(iii) A *Land use map* produced by the U.S. Geological Survey (USGS). This 1 km spatial resolution Global Land Cover Characterization (GLCC) map represents 24 classes. Plant parameters (e.g. leaf area index (LAI), maximum stomatal conductance, maximum root depth, and optimal and minimum temperature for plant growth) were determined for the 24 classes based on available SWAT land use classes.

(iv) *Climate data* published daily by the National Climatic Data Center (NCDC, 1994) for approximately 10,000 worldwide stations for the period of 1977 to 1991. The Global Daily Climatology Network (NCDC, 2002) collected climate data at over 30,000 stations for different time periods. However, it should be noted that the global distribution of the climate stations is fairly uneven, and both quantity and quality of the data vary noticeable. The Climatic Research Unit (CRU) provides complete global 0.5° climate grids for the time period 1901 to 1995 with, among other parameters, monthly values of precipitation, minimum and maximum temperature, and number of wet days per month (New et al., 2000, Mitchell et al. 2003).

Daily and monthly time series for river discharge were obtained for calibration purposes from the Global Runoff Data Center (GRDC, 2004) which provides data for approximately 6,500 gauging stations around the world. Furthermore, a global database of lakes, reservoirs, and wetlands (Lehner and Döll, 2004), and a global map of irrigated areas (Siebert et al., 2005) are useful sources of additional information.

Basic Setup of the West Africa Model

The idea for this modelling exercise was to approach the global goal continent by continent and start with Africa because the water problem here is among the most severe in the world. It is also one of the most challenging regions in the world because of the comparably small amounts of available data for this continent. Using the ArcView interface, Africa was delineated into about 1,500 subbasins with a threshold drainage area of 10,000 km^2. The following step, the automatic calculation of the geomorphic subbasin parameters (e.g. elevation distribution, area, slope, and stream length) failed within the interface, possibly due to some internal ESRI ArcView memory problem. As the ArcView source code is not freely available, this problem could not be solved. A preliminary version of the newly developed ArcGIS-SWAT interface was also tested, and this version can handle a great number of subbasins. Unfortunately, there are still other limitations to using this new interface, but according to the developers these will be resolved in the near future.

In order to gain experience in large-scale hydrological SWAT modeling, a four million km^2 area in West Africa (approx. one-seventh of Africa) was chosen as the study area for this project. This area included the Niger, Volta, and Senegal River Basins (Figure 1). Portions of 18 countries are included in the modeled basin.

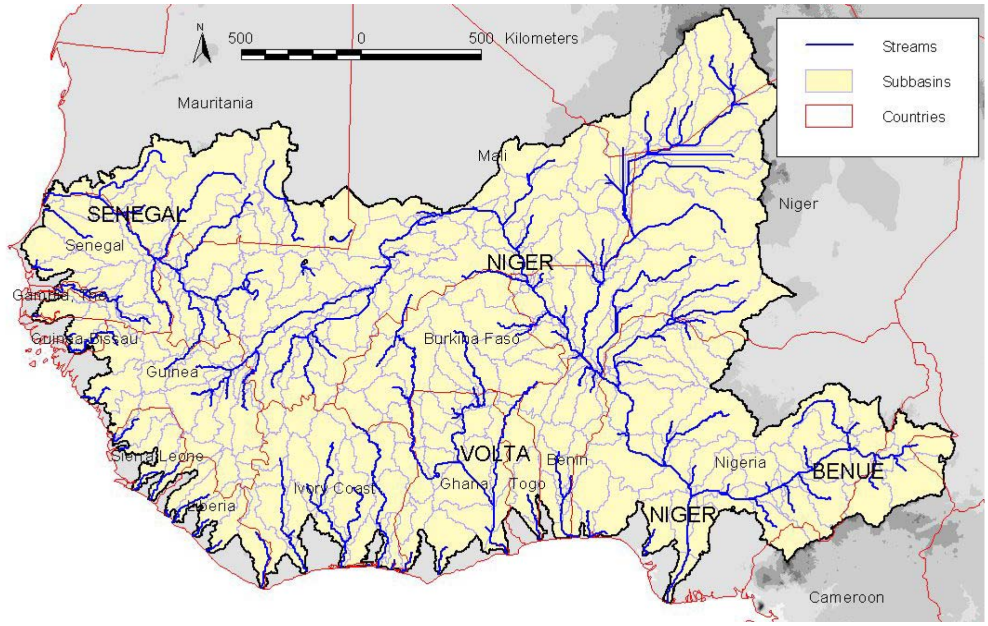

Figure 1: West Africa SWAT model study area.

This area is also of great interest from a technical modelling point of view, as it covers climatic zones from hyper-arid to humid. While the greatest part of the area is characterized by savannah, the land use varies from barren/sparsely vegetated deserts to evergreen rainforests. Ultimately, the subbasins within the political boundaries of each country will be integrated to allow a country-based assessment of freshwater availability.

The watershed was subdivided into 292 subbasins (Figure 1), again with a minimum threshold drainage area of 10,000 km^2. The fact that the ArcView-SWAT interface does not allow for inland sinks/deltas is problematic. The entire basin was routed to outlets flowing to the sea; however, this deficiency was overcome by manipulating the DEM. Artificial holes were cut in the DEM, imitating the border of the DEM. In order to find inland sinks it was essential to have a digitized stream network.

The global land use and soil maps that used were provided in a gridded form. Loading and overlaying them within the ArcView-SWAT interface did not work properly for such a large watershed. For instance, at least one triangular area within the basin was never covered. This problem could be solved by converting the gridded soil and land use layer into shapefiles and then loading them again.

Due to the large scale and the resulting long computation time, it was decided to use only the dominant land use and soil type for the HRU (Hydrological Response Unit) generation. At this point, the basic model setup was finished.

Climate Input and the Daily Climate Generator Algorithm

The climate data is one of the most fundamental inputs to SWAT but in many areas of the world, such as West Africa, the gauging station network is not dense and the time periods with measured data are short and/or have many missing and sometimes even erroneous data (Figure 2).

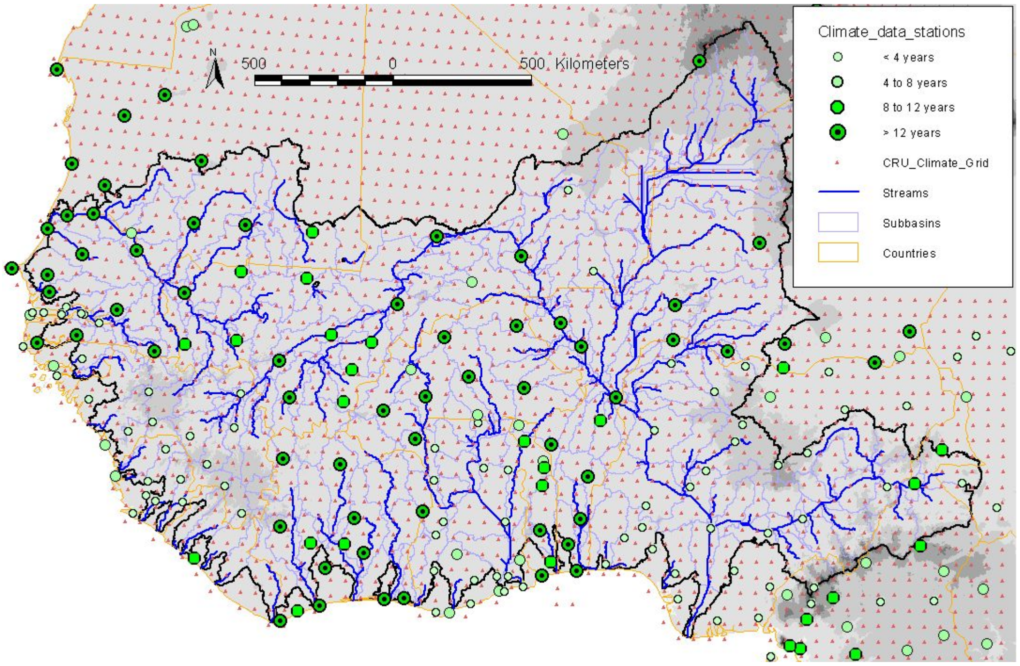

Figure 2: Climate stations and the associated number of years of data as well as the centres of the gridded monthly climate data.

Missing daily climate values at the existing stations were filled within the SWAT program using the included weather generator model, WXGEN (Sharpley and Williams, 1990). It was developed for the contiguous U.S. and needs daily measured values in order to determine monthly statistical values based on which new values are generated. Unrealistic weather data can be generated if a weather station has only a few measured or many erroneous values, as was the case in this study, and missing values can be generated from untrustworthy statistics. A careful manual analysis of the measured values at all stations would be necessary, but was not practical in this study with continental models and many hundred of stations.

In SWAT, the climate data for each subbasin is obtained from the nearest climate station. If the nearest station is far away, the SWAT simulation quality is adversely affected. Due to the clustering of suitable stations and the selection of the closest station as the representative for every subbasin, only 104 stations were included as weather input for the 292 subbasins. Furthermore, it should be noted that for the rest of Africa, with the exception of South Africa, the database is even worse, making a reasonable continental hydrological model based only on globally available weather station data almost impossible.

The CRU developed a complete, global 0.5° monthly climate grid (Figure 2) based on measured values using an anomalies interpolation technique. Fekete et al. (2004) compared the CRU precipitation dataset with five other datasets and showed that it performed quite well in a water balance model and had the longest temporal coverage and best spatial resolution. In looking for a daily weather generator that could sufficiently provide monthly summaries, we found SIMMETEO (Geng et al., 1986). Hartkamp et al. (2003) and Soltani and Hoogenboom (2003) compared SIMMETEO with other stochastic weather generators that need a higher temporal resolution input (daily measured values) and found a similar performance.

As existing daily weather generators were not directly applicable to the data in this study and could not be automated in order to generate values for many stations at once, a new daily climate generation algorithm (DWGA, see *Schuol and Abbaspour, 2005 for details*) for rainfall as well as maximum and minimum temperature (Fig. 3) was developed based on

SIMMETEO. First, it was necessary to overlay the climate grids with the subbasins and aggregate the values in order to obtain one value per month for each subbasin. This step was performed using *ArcGIS*. After DWGA is used to simulate daily values, they are scaled with respect to the total monthly CRU averages, as these values are assumed to be the best available data.

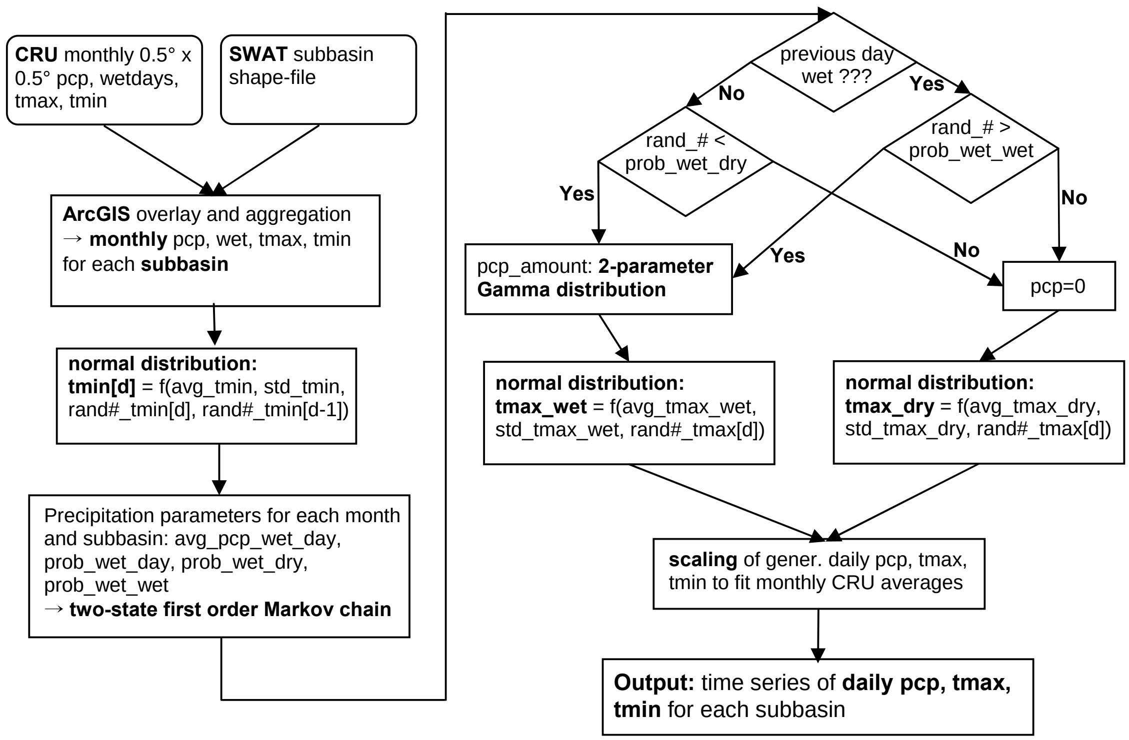

Figure 3: Flowchart of the Daily Climate Generation Algorithm.

Using this procedure a time series of daily precipitation and minimum and maximum temperature for each subbasin was obtained and assigned to the subbasin centeroid. After this step, model setup was finished and an initial simulation for a 25-year period from 1971 to 1995 was completed. In addition, a 25-year simulation using the climate station data was completed and the runoff results from the two uncalibrated models was compared at 12 generally evenly distributed discharge stations, each of which had a database for a comparatively long time period. While both uncalibrated models clearly overestimated the measured runoff, the R-squared value between measured and simulated runoff improved significantly using the new generated weather data as opposed to the SWAT generated weather (Figure 4).

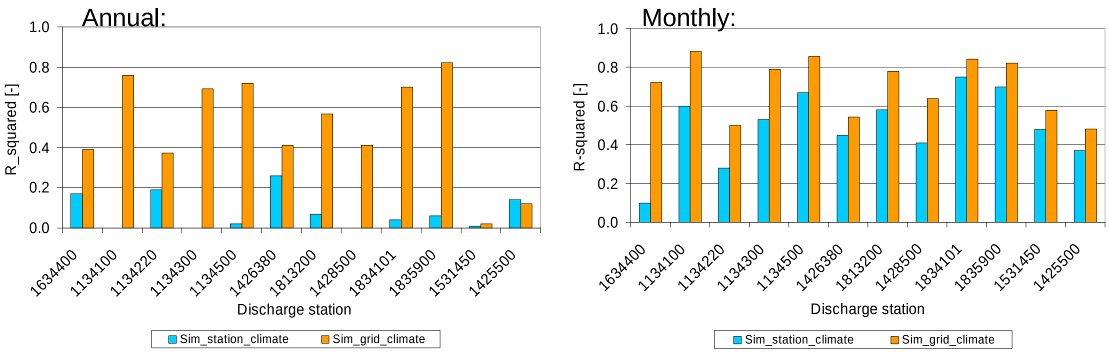

Figure 4: Annual and monthly R-squared values between measured and simulated discharge using both climate input from weather stations and grid data.

Calibration Procedure

The initial simulations have shown that using our generated daily weather, the annual and monthly runoff is not well represented, making calibration inevitable. Measured river discharge at 68 stations in West Africa was used for calibration purposes. At many stations the available data does not cover the entire simulation period, but the available years/months were always split into equal time periods for calibration and validation. An initial annual calibration was followed by a monthly calibration.

The calibration procedure that was used for parameter estimation was the inverse modelling routine SUFI-2 (Abbaspour et al., 2004). It is a multi-site, automated global search procedure and the RMSE was selected as an objective function. Initial uncertainty ranges, equal to the physical parameter bounds, were assigned to each parameter included in the calibration procedure and within these ranges Latin hypercube sampling was used for the selection of *n* parameter combinations. The SWAT-SUFI-Interface developed by Yang et al. (2005) helped to assign and update the parameters, and thus the model could be run and results could be analyzed automatically for all *n* combinations. Based on the parameter combination(s) that resulted in the best representation of measured runoff, new, narrower parameter ranges were determined and the procedure was rerun. This step could be repeated several times, thus the initial uncertainties in the model parameters are progressively reduced.

The goal of this parameter fitting procedure was to bracket most of the measured data within the 95% prediction uncertainty (95PPU). If upon reaching this goal a significant $R2$ and coefficient of efficiency (Nash-Sutcliff) exits between the observed and measured runoff data then the model can be referred to as calibrated. Nevertheless, the question of when the model is calibrated remains, it is apparent that the words “most” and “significant” in the goal definition are indeterminate. This definition is project dependent and there is not one definition that can be applied to all kinds of models/projects. For this large-scale project, given the imprecise quality of the measured data, it was sufficient to bracket (account for) 80 percent of the measured data within the 95PPU, and obtain a Nash-Sutcliff coefficient (NS) of larger than 0.5. The 95PPU represents also the parameter uncertainty resulting from the non-uniqueness of effective model parameters.

Sensitive parameters, to be included in the fitting procedure, were determined by looking at the absolute sensitivities (one-at-a-time sensitivity analysis) and the relative sensitivities (Jacobian/sensitivity matrix) determined within SUFI-2.

Results and Discussion

The results presented are preliminary and rather a basis for discussion of further improvements. Ten parameters were included in the calibration procedure: the CN value of grassland and savannah, the available water capacity of the dominant soil type sandy-clay-loam, some groundwater parameters (GWQMN, REVAPMN, RCHRG_DP), the soil evaporation compensation factor ESCO, the surface runoff lag coefficient SURLAG, and the two Muskingum routing calibration coefficients MSK_CO1 and MSK_CO2. Figure 5 shows the NS coefficient of the monthly runoff calibration at the included 68 stations.

At first glance, the results are quite diverse, but a closer look reveals the emergence of some clear patterns. While most of the stations in the west have a positive NS and many of them also posses a significant NS higher than 0.7, stations further downstream the River Niger are not well represented. The stations with a positive NS in the east are all at tributaries of the River Niger that have a comparatively small watershed. Figure 6 illustrates the wide range of quality in the model fit, taking two stations as an example. It also emphasizes that the parameter uncertainty is not the sole source of uncertainty; the model structure uncertainty is also important. It seems that not all processes were included in the model, especially some that are important further downstream on the River Niger. These processes are mainly associated with the existing large reservoirs regulating the runoff of the River Niger and also the large Niger Inland Delta delaying the runoff and significantly contributing to higher evaporation losses. Furthermore, all types of water use, especially irrigation, have local importance. It would be ideal to include reservoirs, wetland, and water use in the model, but readily available, detailed information on the management of the reservoirs and on stored water in the wetlands are almost nonexistent.

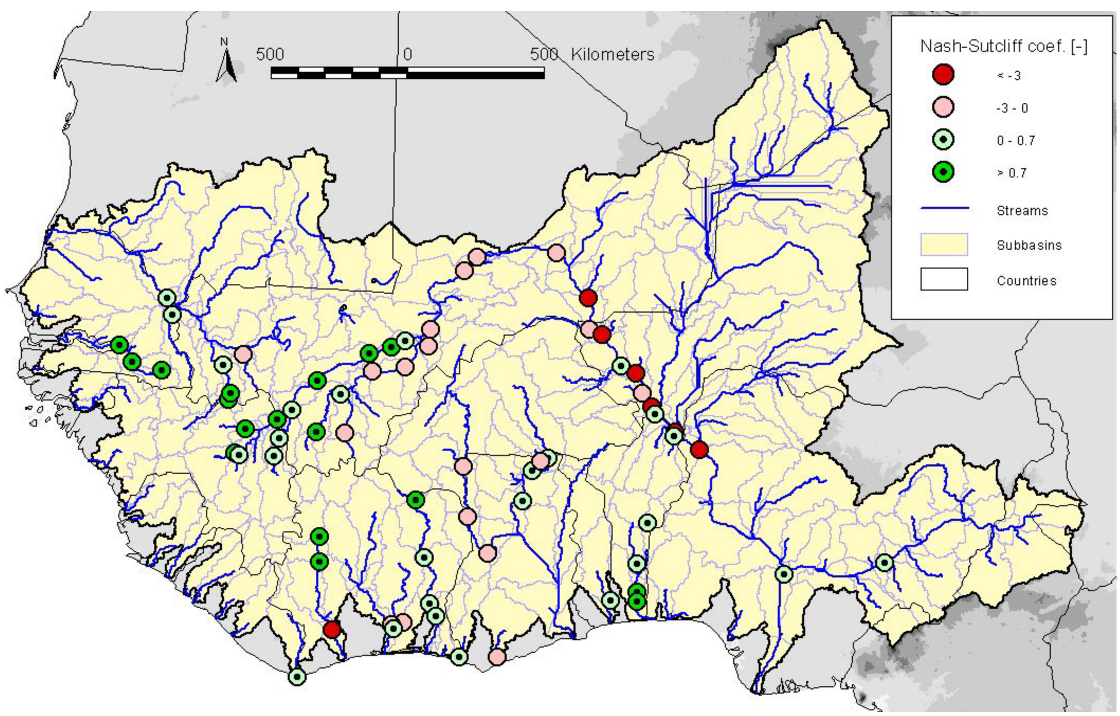

Figure 5: Coefficient of efficiency (NS) between the monthly measured and simulated runoff at the 68 calibration stations.

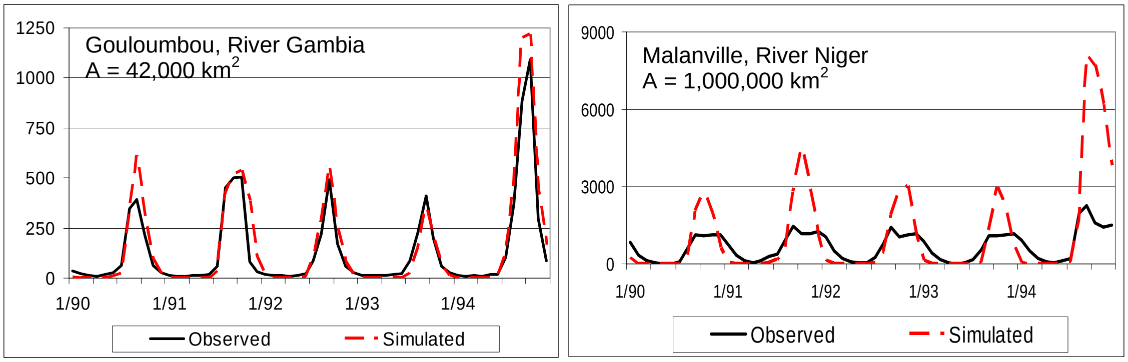

Figure 6: Exemplary calibration results for runoff at two of the 68 stations: Gouloumbou at the River Gambia and Malanville at the River Niger.

Conclusions

This study showed that the SWAT model can be used for extremely large-scale water quantity investigations, but there are quite a few stumbling blocks in the model setup. The minor problems, such as misrouting of streams, can be resolved, as for the major problem, the inability of the existing AVSWAT interface to calculate the geomorphic subbasin parameters for very large areas, the new ArcGIS interface will be a solution. The dilemma between the need for daily weather station data in the SWAT model and the relative non-existence of sufficient high-quality station data could be overcome by using monthly climate data and the Daily Climate Generator Algorithm developed in this study.

The modelled annual and monthly runoff is quite promising in some areas, but in others further model improvements are inevitable. An improved calibration is realistic but due to the non-uniqueness of effective parameters there will never be one best fit. Further research on the characterization and inclusion of typical reservoir management patterns as well as the inclusion of wetlands is necessary.

In the near future we will create a model for the entire continent of Africa, making use of the experience gained in West Africa, and further approach our global freshwater quantification goal. We will also emphasize proper quantification of the uncertainty in the freshwater availability estimates.

References

Abbaspour, K.C., Johnson, C.A. and van Genuchten, M.T., 2004. Estimating uncertain flow and transport parameters using a sequential uncertainty fitting procedure. Vadose Zone Journal 3, 1340-1352.

Arnold, J.G., Srinivasan, R., Muttiah, R.S. and Allen, P.M. (1999). Continental scale simulation of the hydrologic balance. In: Journal of the American Water Resources Association 35 (5): 1037-1051.

Arnold, J.G., Srinisvan, R., Muttiah, R.S., Williams, J.R., 1998. Large area hydrologic modeling and assessment part I: model development. Journal of American Water Resources Association, 34 (1), 73-89.

DiLuzio, M., Srinisvasan, R., Arnold, J.G., Neitsch, S.L., 2002. ArcView Interface for SWAT2000, Blackland Research&Extension Center, Texas Agricultural Experiment Station and Grassland, Soil and Water Research Laboratory, USDA Agricultural Research Service.

Fekete, B.M., Vörösmarty, C.J., Roads, J.O. and Willmott, C.J., 2004. Uncertainties in precipitation and their impacts on runoff estimates. Journal of Climate 17 (2), 294-304.
Geng, S., Penning de Vries, F.W.T., Supit, I., 1986. A simple method for generating daily rainfall data. Agricultural and Forest Meteorology 36, 363-376.
Global Runoff Data Centre (GRDC), 2004. GRDC station catalogue. Online: http://grdc.bafg.de/servlet/is/Entry.987.Display/.
Hartkamp, A.D., White, J.W., Hoogenboom, G., 2003. Comparison of three weather generators for crop modeling: a case study for subtropical environments. Agricultural Systems 76, 539-560.
Lehner, B. and Döll, P. 2004. Development and validation of a global database of lakes, reservoirs and wetlands. Journal of Hydrology 296 (1-4), 1-22.
Mitchell, T.D., Carter, T.R., Jones, P.D., Hulme M., New, M., 2003. A comprehensive set of high-resolution grids of monthly climate for Europe and the globe: the observed record (1901-2000) and 16 scenarios (2001-2100). Journal of Climate: submitted.
National Climatic Data Centre (NCDC), 1994. Global daily summary: Temperature and precipitation 1977-1991, CD-ROM, Version 1.0.
National Climatic Data Centre (NCDC), 2002. Global daily climatology network (GDCN), CD-ROM, Version 1.0.
New, M., Hulme, M., Jones, P.D., 2000. Representing twentieth century space-time climate variability. Part 2: development of 1901-96 monthly grids of terrestrial surface climate. Journal of Climate 13, 2217-2238.
Reynolds, C.A., Jackson, T.J., Rawls, W.J., 1999. Estimating available water content by linking the FAO soil map of the world with global soil profile database and pedo-transfer functions. Proceedings of the AGU 1999 spring conference, Boston, MA.
Schaap, M., 1999. Rosetta Version 1.0. Online: http://www.ussl.ars.usda.gov/models/rosetta/rosetta. HTM
Schuol, J., and K.C. Abbaspour, 2005. A Daily Weather Generator for Predicting Rainfall and Maximum-Minimum Temperature using Monthly Statistics Based on a Half-Degree Climate Grid. Being prepared for Ecological Modelling
Sharpley, A.N., Williams J.R., eds., 1990. EPIC-Erosion Productivity Impact Calculator, 1. model documentation. U.S. Department of Agriculture, Agricultural Research Service, Tech. bull. 1768.
Stefan Siebert, Petra Döll, Sebastian Feick and Jippe Hoogeveen (2005), Global map of irrigated areas version 3.0 Johann Wolfgang Goethe University, Frankfurt am Main, Germany / Food and Agriculture Organization of the United Nations, Rome, Italy
Soltani, A., Hoogenboom, G., 2003. A statistical comparison of the stochastic weather generators WGEN and SIMMETEO. Climate research 24, 215-230.
Yang, J, Abbaspour, K.C., and Reichert, P. 2005. Interfacing Watershed Models with Systems Analysis Tools: Implementation for SWAT. Submitted to Water Science and Technology

Assessment of Water Use in a Small Watershed in Northern Syria, Using SWAT

Adriana Bruggeman[1] and Geerte van der Meijden[2]
[1]International Center for Agricultural Research in the Dry Areas (ICARDA), P.O. Box 5466, Aleppo, Syria. E-mail: a.bruggeman@cgiar.org
[2]ARCADIS Euroconsult, Arnhem, The Netherlands; formerly: Erosion and Soil & Water Conservation Group, Wageningen University, The Netherlands.

Abstract

In large parts of West Asia and North Africa, rainfall is not sufficient for crop production. Water harvesting, the collection and storage of surface runoff, provides critical water supplements for crops in these areas. However, the collection of water in the upstream areas affects the downstream users of the resource. The objective of this paper was to evaluate the use of SWAT for simulating water flows and productivity of different land uses in arid watersheds. The model was applied to a small arid watershed (28 km2) in northern Syria. The area has a Mediterranean climate, with a long-term average annual rainfall of 222 mm. This paper presents some model modifications and suggestions for using SWAT to model resource management processes in dry Mediterranean watersheds, including grazing of crop residues, olive orchard management, water harvesting, and degradation of rangelands. With these modifications SWAT was found to be a useful tool for evaluating land and water management options in arid environments.

Introduction

Water is a continuous concern of the communities in the dry, rain-fed areas of the Mediterranean region. When rainfall is barely sufficient to support crops, the natural variability of the climate has especially critical effects. The International Center for Agricultural Research in the Dry Areas (ICARDA) has adopted the Khanasser Valley in northern Syria as an integrated research site for testing sustainable agricultural production and resource management options with farming communities in marginal dry environments (ICARDA, 2005). Although the farmers in these environments are not averse to trying out new land use and resource management options, they are constrained by a system that has traditionally very low input in terms of natural, financial, and human resources. Changes witnessed during the last decade in Khanasser Valley are an exponential growth in the number of olive trees (Tubeileh et al, 2004), a significant increase in lamb fattening units, and a continuous construction of new family homes. These developments are associated with various resource management issues, such as changes in surface runoff flows, nutrient pollution due to inadequate storage and use of manure, and increased competition for the limited groundwater resources. Simulation models can help to understand the long-term effects of land use changes, which are critical in helping to provide better advice on agricultural development in these marginal environments.

Many mathematical models that simulate watershed processes exist (Singh, 1995; Singh and Woolhiser, 2002), but a relatively small number are in general use. The Soil and Water Assessment Tool (SWAT) (Neitsch et al, 2002b) was selected for this case study, because (i) it has many useful features that accommodate the simulation of hydrologic processes in arid environments; (ii) it includes a full water balance processes, such as crop growth, which allows the assessment of water productivity; (iii) it has a GIS interface that facilitates the preparation of the large amount of highly variable spatial data required for watershed simulations; (iv) it is freely available, including documentation and source code; and (v) last but not least, it has an active development and user community.

The functioning of watershed models and parameters is usually evaluated using surface runoff records. However, there are very few watersheds in the dry marginal areas of West Asia and North Africa where surface runoff is measured. The rarity and immensity of wadi floods in these environments makes runoff monitoring a difficult and costly venture. Because of the scarcity of monitoring records, the demand for tools that predict water flows in ungauged watersheds is high, but the judicious application of these tools is critical.

In dry areas, evapotranspiration is the most significant use of precipitation and drives the water balance. However, almost all published SWAT applications focus on surface runoff and water quality, whereas very few studies evaluate or report simulated evapotranspiration and crop production results. Notable exceptions are Kannan et al. (2003), Watson et al. (2003), and Baffault et al. (2003), but these papers provide few specifics. Evaluating actual evapotranspiration and crop production in watersheds is, of course, more involved than comparing simulated runoff with the automatically monitored runoff at the watershed outlet. In this regard, an interesting study was presented by Narasimham et al. (2005). These authors evaluated soil moisture contents simulated with SWAT for six watersheds in Texas with normalized difference vegetation index (NDVI) data from the NOAA-AVHRR satellite. Although they obtained good correlations between simulated soil moisture and NDVI values for agricultural land and pasture, no clear relations could be found between the simulated soil moisture contents and NDVI values for brushy rangelands and forests.

Van der Meijden (2004) used SWAT to assess the prospects and effects for water harvesting practices in the Habs-Harbakiyah watershed, a small side valley of the Khanasser Valley. During this work, the need to modify SWAT to better simulate the processes in this typical arid Mediterranean environment became clear. The objective of the study presented here was to review, test, and modify the SWAT processes related to water flow and productivity in arid Mediterranean environments, using the Habs-Harbakiyah watershed in northern Syria as an application case. This study focuses on water; nitrogen and phosphorus processes are not evaluated.

Methodology

Model Description

The model version used in this study was SWAT2000. The input data were prepared with the help of the SWAT ArcView interface (Di Luzio at al., 2002). To understand the model modifications and parameter values presented in the next sections, the main crop growth equations and processes are summarized here. This information was taken from Neitsch et al. (2002a; 2002b); some additional information, which was gleaned from the SWAT2000 source code, was added. The term crop is used here to refer to all agricultural and natural plants, including trees and rangeland species.

Actual evapotranspiration is modeled as a function of the potential evapotranspiration and the amount of water available in the soil. SWAT offers different methods for estimating potential evapotranspiration. For the Penman-Monteith method, the daily-computed LAI and crop height are included in the canopy resistance term of the equation to directly compute potential crop transpiration. For the Hargreaves and Priestley Taylor equations, the potential plant transpiration is assumed to be equal to the potential evapotranspiration. But when the LAI is less than 3, it is computed as follows:

$$= \frac{\quad}{\quad}$$

where ET_c is the potential transpiration; LAI is the leave area index; and ET is the potential evapotranspiration. Potential soil evaporation is computed as a function of the ET and the surface cover, and adjusted when evapotranspiration is high.

Although the Penman-Monteith equation has been generally recommended for the computation of crop evapotranspiration (Allen et al, 1998), the Hargreaves equation was selected for this application, because it provides a clear relation of the effect of crop characteristics on evapotranspiration. The Hargreaves equation has been found to give similar ET values as the Penman-Monteith equation in Khanasser Valley, except that Hargreaves ET is lower than Penman-Monteith ET during the dry summer months. In summer, the valley (including the climate station) is not under the fully-watered reference conditions required for these equations. However, during these months soil moisture, not evaporative demand, is the limiting factor. Although an under-estimation of the potential evapotranspiration affects the simulated crop water stress, the drought tolerant species that are growing in these environments during summer, such as olives, may actually experience less stress than computed on the base of the Penman-Monteith equation.

Daily increase in leaf area index is computed as a function of the fraction of the potential heat units of the crop. The fraction of the potential heat units are the ratio of the heat units (HU) accumulated by the crop to the total heat units required to bring the crop to maturity, or potential heat units (PHU). The accumulation of heat units starts at planting. The accumulated heat units are set back to zero at the end of the year for all crops in the northern hemisphere, and for annuals and trees also at dormancy.

Total biomass production (including roots) is computed from the crop's radiation use efficiency (RUE) and the intercepted photosynthetically active radiation (PAR). The intercepted PAR is computed from the incident photosynthetically active radiation (assumed to be 50% of the incoming solar radiation), a light extinction coefficient, and the LAI, following Beer's law:

$$\Delta \quad = \qquad - \quad - \quad +$$

where Δbio is the increase in total plant biomass on a given day (kg/ha); RUE is the radiation-use efficiency of the plant expressed in kg ha^{-1} MJ^{-1} m^2 (equal to 10^{-1} g MJ^{-1}); $0.5*H_{day}$ is the incident photosynthetically active radiation (MJ m^{-2}); and k is the light extinction coefficient. SWAT uses a light extinction coefficient of 0.65 for all plants. The fraction of the total biomass in the roots is computed as a function of the accumulated heat units, varying linearly from 0.4 at the start of growth to 0.2 at maturity.

Each day water, temperature, and nutrient stress factors are computed, varying between zero for no stress and one for maximum stress. To adjust the daily biomass production for stress, it is multiplied with a plant growth factor. The plant growth factor is computed as one minus the maximum of the three stress factors (water, temperature and nutrient stress). Similarly, the LAI growth is adjusted for stress by multiplying it with the root of the plant growth factor.

To calculate the grain, or so-called economic yield, the above ground biomass is multiplied with the harvest index (HI). The user-specified harvest index is adjusted daily, as a function of the potential heat units accumulated. The HI is also adjusted for the evapotranspiration deficit during the second part of the growing season and before the start of leave senescence (DLAI).

The above equations provide a robust and flexible system for the simulation of crop production. However, the processes are more geared towards the growth of annual crops than to trees. In addition, a concern for the application of the model to the dry areas is that the performance of these equations under severely water limited conditions has not been well studied.

Study Area

The main agricultural activities in the Habs-Harbakiyah watershed are rain-fed barley and small ruminant production. In spring, the sheep graze the stony limestone hill-slopes that border the watershed. The hill-slopes are dissected by gullies, which carry runoff water down the steep, stony slopes. The runoff often disperses on the flat, deep soils of the crop land before it reaches the main wadi system. Farmers plough over these gullies, but they have not built diversions for spreading the runoff water on their land. A number of olive orchards have been established during the last six years. The trees are planted both on the stony slopes and on the flatter valley soils. Some farmers prepare v-shaped or semi-circular earth bunds in their orchards to harvest runoff water for the trees. The government has recently constructed a small reservoir, just south of Harbakiyah village, which diverts the flow from the main wadi. We consider this the outlet of the watershed. Long-term annual precipitation, occurring mainly during the October-May cropping season, is 222 mm.

The weather generator in the SWAT model was used to allow the simulation of long-term effects. Data from stations in Khanasser Valley were used for the weather generator (Van der Meijden et al., 2004). For the rainfall distribution parameters, we used a 7-year record from a tipping bucket rain gauge in the nearby Qurbatiyah station (1998-2005). The monthly data of this station were similar to the long-term monthly data from the manual rain gauge in Khanasser town (1929-2001), but the daily data were considered much more reliable.

A Digital Elevation Model (DEM) of the watershed was made using data from the Shuttle Radar Topography Mission (USGS, 2005) an ortho-rectified landsat 7 ETM+ image covering the whole area, an ikonos image of part of the watershed, and field data of the gullies and wadis, collected with a handheld GPS (Constantinos, 2003; Van der Meijden, 2004).

A soil map (scale 1:50,000) of the Khanasser Valley was made by Ruysschaert (2001). The main soils in the Habs-Harbakiyah watershed are Calcisols in the valley floor, Calcaric Leptosols on the slopes, and Cambisols on the plateau. Soil textures are mainly clay loam and loam, and infiltration rates are high. The main differences in the physical characteristics of the different soil units are due to the soil depth and stoniness, which are related to the land slope. Therefore, the soil map was adjusted with the help of the DEM, as described by Van der Meijden (2004). The soil physical characteristics were taken from soil samples collected by various ICARDA studies, complemented with properties computed by the soil water characteristics calculator from texture data (Saxton et al., 1986). The available water capacity and bulk density were adjusted for the stone content of the soil, with consideration of the retention properties of the calcareous stones (Cousin et al., 2003).

A land-use map of the Khanasser Valley was made by d'Altan (2003), based on a visual interpretation of an Aster image (August 28, 2001), the DEM, and a survey of the olive fields in 2003 (Tubeileh et al., 2004). The main crop in the Habs-Harbakiyah watershed is rain-fed barley, while natural rangelands are covering the stony slopes. Olive orchards occupied almost 4% of the cultivated land in the watershed in 2003. A few fields of wheat (both rain-fed and under supplemental irrigation), legumes, and cumin can also be found in the watershed. Some farmers irrigate small plots of vegetables in summer. The water for irrigation and domestic use is pumped from a rather low-yielding limestone aquifer, with a water level of at least 18 m below the surface. For this study only the main land uses, barley, olives, and rangeland, were considered.

The runoff curve number (CN) values (Table 1) were taken from tables provided by USDA-NRCS (1986). For the footslopes and the edges the CN was adjusted for slope, using the equation from Williams (1995), as provided by Neitsch et al. (2002b). To represent the almost bare condition of the land during the dry summer and before the establishment of a vegetative cover during the winter growing season (January), two curve numbers were used for each land use. The CN values for barley are changed after harvest and grazing in May, for rangeland and orchards values are changed in April as a result of heavy grazing and tillage, respectively.

Table 1. Main soil and land use characteristics in the Habs-Harbakiyah Watershed.

Land use	Soil unit	Slope %	Soil depth m	Rock content %	Available water %	Soil group	Curve Number Jan-April	Curve Number May-Dec
Barley	plateau	< 2	0.6	50	0.10	B	81	86
Barley	valley floor	< 2	1.5	10	0.15	A	72	77
Olive	footslopes	2-10	1.0	40	0.10	C	83	92
Rangeland	edges	10-25	0.4	60	0.07	D	90	95

Crop and Management Parameters

In northern Syria, barley is generally planted in November, although farmers delay planting until the first good rains have been received. After harvesting in May, the stubble is grazed by sheep. To prevent re-growth of the crop, we specified all residue to be grazed in one day with a kill operation set on the next day. Most farmers do not apply fertilizer to their rain-fed fields, except during wet years. To reduce the effect of nutrient stress we applied 50 kg ha^{-1} yr^{-1} both N and P. To allow the simulation of the run-on of surface water from the adjacent slopes, we used the option irrigation from reach.

The SWAT crop database (Neitsch et al., 2002) does not provide data for winter barley. To evaluate crop parameters and production values for barley, we reviewed the work of Goyne et al. (1993) and Kiniry et al. (1995), and studies conducted by ICARDA scientists in Khanasser Valley and nearby locations in northern Syria (e.g., Keatinge and Chapanian, 1991; Jones and Singh, 1995; Pala et al., 1996; Schweers et al., 2004). Values for the maximum potential leaf area index (BLAI) leaf area development (FRGRW1, LAIMX1, FRGRW2, LAIMX2, DLAI), radiation use efficiency (BIO_E), crop height (CHTMX), root depth (RDMX), optimal temperature for leaf development (T_OPT), and the harvest index under optimum (HVSTI) and stressed conditions (WSYF), presented in Table 2, were selected based on local observations, expert knowledge, and information from the cited studies. The other parameter values were taken from spring barley in the SWAT crop database.

Table 2. Crop parameter values used for the Habs-Harbakiyah watershed, see text for abbreviations.

	BLAI	FRGRW1	LAIMX1	FRGRW2	LAIMX2	DLAI
Barley	4	0.42	0.20	0.75	0.95	0.91
Olives	1	0.45	0.75	0.87	0.98	1.00
Rangeland	2	0.47	0.20	0.77	0.95	1.00
	BIO_E	CHTMAX	RDMAX	T_OPT	HVSTI	WSYF
Barley	30	0.70	1.00	25	0.46	0.10
Olives	15	3.00	2.00	35	0.60	0.15
Rangeland	10	0.50	1.00	30	na [a]	na [a]

[a] not applicable.

The olive is an evergreen plant with a biennial growing cycle. The alternate bearing results in low yields during off years, which can not easily be represented by SWAT. To derive crop parameter values for olive, we reviewed the work of various authors (e.g., Villalobos et al., 1995; Pastor et al., 1998; Kiniry, 1998; Fernandez and Moreno, 1999; Tous et al., 1999; Dichio et al. 2000; Mariscal et al. 2000a, 2000b; Gomez et al., 2001; Morales, 2002; Tubeileh et al, 2004).

Olive growing practices in the Khanasser Valley have been described by Tubeileh et al. (2004). Trees are typically planted at spacings of seven by seven or eight by eight m. Farmers commonly prune their trees every other year, although once every three or four years would be sufficient (Tubeileh et al., 2004). Trees are sometimes pruned during harvest in November or December, but mid or late February would be preferred to limit the chance of frost damage. Most farmers provide supplemental irrigation to their trees in summer, applying three to 12 irrigations for a total of 500 to 1,000 L per tree. Some farmers apply sheep manure to their trees in winter. Under good management and summer irrigation, yields of 30 kg/tree were obtained in the Khanasser Valley area (Tubeileh et al., 2004).

For this SWAT application it was assumed that the trees have matured, but are kept small by pruning. Spacing was approximately eight by eight m (150 trees ha^{-1}). Manure was applied in January at a recommended rate of 25 kg per tree (Tubeileh et al., 2004). An irrigation of 1,000 L per tree, equal to a 15 mm application, was given in July. It was assumed that the olives were harvested in December, with half the yield representing pruned branches and leaves. This assumption was based on the average yearly values computed from the pruning and yield data provided by Morales (2002). The initial total (above and below-ground) biomass was set to 30 ton ha^{-1}. The values of the radiation use efficiency (BIO_E) and the harvest indices (HVSTI, WSYF) were adjusted (calibrated) by trial and error to match biomass production data from local studies and the cited papers.

For micro-catchment water harvesting systems, almost all precipitation will remain on the field, but the field does not generally receive water from upstream land units. Micro-catchment harvesting is somewhat difficult to represent in SWAT because evapotranspiration and soil water use are modeled as one-dimensional processes. However, in micro-catchment systems trees are normally planted at wider spacing, resulting in a low LAI. In SWAT a low LAI would result in low potential plant transpiration, less water stress, and less reduction of biomass production. Micro-catchment water harvesting was simulated by reducing the curve number to 70. Because the trees had matured and were planted at similar spacing, we assumed the same LAI for olive trees with and without water harvesting practices.

The natural vegetation of the Khanasser Valley belongs to the Mediterranean Irano-Turanian botanical region (Al-Oudat et al, 2005). The rangelands include annuals, biennials, perennials, and semi-shrubs. Due to heavy grazing, cutting, and plowing many valuable fodder shrubs have been replaced by spiny species. On the stony slopes, grasses are dominant. The development of the rangeland vegetative cover is similar to that of the barley. The rangelands are generally grazed during the period of February to April. Typical above-ground biomass production values for the degraded slopes of the Khanasser Valley are 900, 500, and 300 kg ha^{-1} for wet, average and dry years, respectively (J.A. Tiedeman, personal.communication, 2004). Because the grazing in the watershed is a rather destructive practice, a minimum biomass for grazing was set equal to the assumed biomass of the roots (500 kg ha^{-1}).

Growth and production parameters of rangeland species in Texas have been measured and analyzed by Kiniry et al (1999; 2002). This information was also used for the SWAT crop database (Neitsch et al., 2002a). Values from the database were used for range (grasses), unless specified otherwise (Table 2). The radiation use efficiency and the potential heat units (PHU) were adjusted (calibrated) by trial and error. The PHU was adjusted because the accumulated heat units are affected by grazing. The potential heat units for all crops were computed using 100 years of daily temperature data generated by SWAT. The base temperature of all crops was zero.

Results and Discussion

SWAT Modifications

To facilitate the growth and management of winter crops, including subsequent harvest, graze, and kill operations for barley, and the change of the runoff curve number during the growing season simulated as a tillage operation with zero mixing; the indices of the management operations were adjusted. The call to subroutine dormant was removed because although the crops in this watershed are affected by cold, they do not become dormant during the winter season. Accumulated heat units for trees and perennials were set to zero in the grow subroutine on February 1 and on November 1, respectively. The accumulated heat units of the crops were no longer set to zero at the end of the year.

For harvest and grazing operations, the leaf area index was adjusted with the ratio of the removed versus the above-ground biomass. For trees the root fraction was considered to be equal to half of the biomass, whereas for rather degraded rangelands (perennials), the biomass of the roots was considered to be equal to the minimum biomass required for grazing. Adjustments were made to summarize the grazed biomass of perennials as annual yield. The annual biomass and yield of barley should not be summarized during the grazing operation, because these were already summarized during the harvest operation.

The irrigation-from-reach option was used to model the natural or man-made diversion of surface runoff water in an HRU, with the runoff generated by upstream HRUs within the same sub-watershed. Modifications for taking the surface runoff water were made in the virtual subroutine, and in the irr_rch subroutine for application to the identified downstream HRU.

Case Study Results

The average annual precipitation for the 100-year simulation was 225 mm. The crop production and water balance components for the main HRUs in the watershed are summarized in Table 3.

Table 3. Average annual crop production and water balance components, expressed as a percentage of the precipitation, for the main HRUs in the Habs-Harbakiyah Watershed.

Land use	Soil unit	Total biomass[a] ton ha^{-1}	Grain yield ton ha^{-1}	Crop transpiration %	Soil evaporation %	Runoff %	Percolation %
Barley	plateau	2.8	0.9	34	49	6	11
Barley	valley floor	3.1	1.0	43	57	0	0
Olive	footslopes	48.9	3.0	70	19	7	4
Olive WH[b]	footslopes	50.1	3.1	72	18	1	9
Rangeland	edges	0.5[c]	na	9	58	24	9

[a] Total above and below ground biomass before harvest.
[b] Orchards with micro-catchment water harvesting.
[c] Total above ground biomass grazed by the sheep.

Simulated biomass production and yields confirmed the data from local studies. The simulated water productivity of the barley grain in the valley was high, 1.0 kg m^{-3}. Due to its low cover and continuous grazing, the water productivity of the rangeland was very low. The precipitation was mainly lost to soil evaporation and runoff. Due to their year-round cover, the water productivity of the olives was high. An average yield of 20 kg per tree was harvested. The differences in yield for the olives with and without micro-catchment systems were small. Because water harvesting occurs under wet conditions, the percolation to the groundwater from the soils on the foot slopes was high. This confirms the importance of deep soils for water harvesting systems for crop production (Oweis et al., 2001). The olive orchards with water harvesting practices on the footslopes reduced the runoff to the barley fields. The effect of the reduced runoff on the barley yields still needs to be analyzed. The runoff from the barley fields in the valley was very low (0.3%).

Groundwater was an important resource in the dry areas. The groundwater recharge that takes place by percolation from the barley fields on the plateau was 11% of the average annual rainfall. These relatively high recharge rates are caused by the shallow depth and the low water holding capacity of the soils, which have high stone contents. Additional field data collection and model simulations with the upper and lower boundary values for these parameters should be conducted.

Conclusions

We can conclude from this study that SWAT is a powerful tool for evaluating water flows and productivity of different land uses in arid and semi-arid watersheds. In these environments, where the majority of the precipitation is being used for evapotranspiration, accurate modeling of the crop growth processes is critical. There is an obvious need to test the performance of crop models under severely water-stressed conditions. The work presented here was only a humble first step; further review of studies, analysis of data, mining of expert knowledge, and experimental work is needed.

Modifications and additions to the code included an option for simulating water harvesting practices and improved simulation of winter crop management and production. Some of the implemented modifications of the code were specific to this application. Attempts to make these modifications generic, without any changes in the current input file structure of SWAT are a somewhat insurmountable task. The widespread user community of SWAT would certainly benefit from an adjustment of the crop growth and management processes to facilitate the seamless production of winter crops. However, this requires a thorough understanding of the diverse needs of the users. Furthermore, an option for routing surface runoff between hydrologic response units within the same sub-watershed could also be a useful enhancement for the application of the model in arid environments, but this seems to go against the nature of SWAT somewhat.

Model developers often struggle to find a balance between offering the user too many options and not enough. SWAT has found a reasonable middle ground, and the GIS-interface and the included databases and default value options greatly assist the input preparation process. This, in turn, also reduces the need for the user to try to understand the actual functioning of the model. Obviously, the general increased interest in models and expert systems has not come with an increased interest in the reading of model documentation and experimental data collection. This may at times lead to dubious efforts and results.

Acknowledgements

We would like to express our sincere appreciation to the SWAT development team not only for providing a very comprehensive watershed model, but even more so for making the source code accessible for use. Special thanks are due to Jim Kiniry for providing additional information on crop growth models and parameter values. We are also very grateful to the editors of the proceedings for their support. We would like to acknowledge current and past colleagues at ICARDA, who shared data and expert knowledge used in this study. We are grateful to Piero d'Altan for his preparation and assistance with the GIS data layers. Operational funds for data collection related to this study were provided by the German Ministry of Development Cooperation (BMZ).

References

Allen, R., L. Pereira, D. Raes, and M. Smith 1998. Crop evapotranspiration. Guidelines for computing crop water requirements. FAO Irrigation and Drainage Paper 56. FAO, Rome.

Al-Oudat, M., A. Khatib Salkini, J. Tiedeman. 2005. Major native plant species in Khanasser area, Syria (Al-Hass and Shbeith mountains). ICARDA, Aleppo, Syria.

Baffault, C., J.R. Arnold, and J.S. Schumacher. 2003. Fecal coliform fate and transport simulation with SWAT. p. 4-9. *In* R. Srinivas et al. (ed.) Second International SWAT Conference Proceedings. Texas Water Resources Institute. TWRI Technical Report 266. Texas Water Resources Institute, College Station, TX.

Cousin, C., B. Nicoullaud, and C. Coutadeur. 2003. Influence of rock fragments on the water retention and water percolation in a calcareous soil. Catena, 53:97-114.

Constantinos, B. 2003. Developing methodology to assess gully processes using AV GIS in dryland Khanasser Valley, Syria. Thesis report. Agricultural University of Norway, Centre for International Environment and Development Studies, Oss, Norway.

D'Altan, P. 2003. Land use map of Khanasir Valley. ICARDA, Aleppo, Syria.

Dichio, B. M. Roman, V. Nuzzo, and C. Xiloyannis. 2000. Soil water availability and relationship between canopy and roots in young olive trees (cv Coratina). Acta Hortic., 586:225-258.

Di Luzio, M., R. Srinivasan, J.G. Arnold, S.L. Neitsch. 2002. Arcview interface for SWAT 2000: User's guide. Texas Water Resources Institute, College Station, TX.

Fernandez, J.E., and F. Moreno. 1999. Water use by the olive tree. Journal of crop production, 2(2):101-162.

Gomez, J.A., J.V. Giráldez, and E. Fereres. 2001. Rainfall interception in olive trees in relation to leaf area. Agricultural Water Management, 49:65-76.

Goyne, P.J., S.P. Milroy, J.M. Lilley, and J.M. Hare. 1993. Radiation interception, radiation use efficiency and growth of barley cultivars. Aust. J. Agric. Res., 44:1351-1366.
ICARDA. 2005. Sustainable agricultural development for marginal dry areas. Khanasser Valley Integrated Research Site. ICARDA, Aleppo, Syria.
Jones, M.J. and M. Singh. 1995. Yields of crop dry matter and nitrogen in long-term barley rotation trials at two sites in northern Syria. J. Agric. Sci., 124:389-402.
Kannan, N, S. White, F. Whorral, and M. Whellan. 2003. Modeling pollutants in runoff from the Colworth experimental catchment. p. 149-154. *In* R. Srinivas et al. (ed.) Second International SWAT Conference Proceedings. Texas Water Resources Institute. TWRI Technical Report 266. Texas Water Resources Institute. College Station, TX.
Keatinge, J.D.H., and N. Chapanian. 1991. The effect of improved management on the yield and nitrogen content of legume hay/barley crop rotations in West Asia. J. Agron. Crop Sci., 167:61-69.
Kiniry, J.R. 1998. Biomass accumulation and radiation use efficiency of honey mesquite and eastern red cedar. Biomass Bioenergy, 15(6):467-473.
Kiniry, J.R., D.J. Major, R.C. Izaurralde, J.R. Williams, P.W. Gassman, M. Morrison, R. Bergentine, and R.P. Zentner. 1995. EPIC model parameters for cereal, oilseed, and forage crops in the northern Great Plains region. Can. J. Plant Sci., 75:679-688.
Kiniry, J.R., H. Sanchez, J. Greenwade, E. Seidensticker, J.R. Bell, F. Pringle, G. Peacock, Jr., and J. Rives. 2002. Simulating grass productivity on diverse range sites in Texas. Journal Soil Water Conserv., 57:144-150.
Kiniry, J.R., C.R. Tischler, G.A. van Esbroeck. 1999. Radiation use efficiency and leaf CO_2 exchange for diverse C_4 grasses. Biomass Bioenergy, 17:95-112.
Narasimham, B., R. Srinivasan, J.G. Arnold, and M. DiLuzio. 2005. Estimation of long-term soil moisture using a distributed parameter hydrologic model and verification using remotely sensed data. Trans. Am. Soc. Agric. Eng, 48(3):1101-1113.
Neitsch, S.L., J.G. Arnold, J.R. Kiniry, R. Srinivasan, J.R. Williams. 2002a. Soil and Water Assessment Tool user's manual: version 2000. TWRI Report TR-192. Texas Water Resources Institute, College Station, Texas, USA.
Neitsch, S.L., J.G. Arnold, J.R. Kiniry, J.R. Williams, and K.W. King. 2002b. Soil and Water Assessment Tool theoretical documentation: version 2000. Texas Water Resources Institute, College Station, TX.
Mariscal, M.J., F. Orgaz, F.J. Villalobos. 2000a. Radiation-use efficiency and dry matter partitioning of a young olive (Olea europaea) orchard. Tree Physiology, Vol 20, 65-72.
Mariscal, M.J., F. Orgaz, F.J. Villalobos. 2000b. Modelling and measurement of radiation interception by olive canopies. Ag. Forest Meteo 100: 183-197.
Morales Bernardino, J. 2002. Pruning management in traditional olive orchards. Olivae, 92:38-43.
Oweis, T., D. Prinz, and A. Hachum. 2001. Water harvesting: Indigenous knowledge for the future of the drier environments. ICARDA, Aleppo, Syria.
Pala, M., C.O. Stockle, and H.C. Harris. 1996. Simulation of durum wheat (Triticum turgidum ssp. Durum) growth under different water and nitrogen regimes in a Mediterranean environment using CropSyst. Agric. Systems, 51:147-163.
Pastor, M, J. Hidalgo, V. Vega, and J. Castro. 1998. Olive irrigation in the district of La Loma in the province of Spain. Olivae, 71:39-49.
Ruysschaert, G. 2001. Bodemkartering en fysische landevaluatie van het Khanassergebied, Syrie. Eindwerk voor de graad van bio-ingenieur, Katholieke Universiteit Leuven, Belgium.
Saxton, K. E., W.J. Rawls, J.S. Romberger, and R.I. Papendick. 1986. Estimating generalized soil-water characteristics from texture. Soil Sci. Soc. Amer. J., 50(4),1031-1036.

Singh, V. P. (ed.). 1995. Computer models of watershed hydrology. Water Resources Publications, Highlands Ranch, CO.

Singh, V.P. and D.A. Woolhiser. 2002. Mathematical modeling of watershed hydrology. J. Hydrol. Eng., 7(4):270-292.

Schweers, W., A. Bruggeman, A. Rieser, T. Oweis. 2004. Irrigation practice and water-use efficiency in Khanasser valley, northwest Syria. J. Applied Irrig. Sci., 39(2):241-252.

Tubeileh, A, A.Bruggeman, and F.Turkelboom. 2004. Growing olives and other tree species in marginal dry areas. ICARDA, Aleppo, Syria.

Tous, J., A. Romero, J. Plana, and F. Baiges. 1999. Planting density trial with Arbequina olive cultivar in Catalonia, Spain. Act Hort. 474:177-108.

U.S. Geological Survey. 2005. Shuttle radar topography mission [Online]. Available at http://srtm.usgs.gov/ (accessed 5 May 2005), USGS, Washington, DC.

USDA-NRCS. 1986. Urban Hydrology for Small Watersheds, TR55 [Online]. Available at http://ftp.wcc.nrcs.usda.gov/hydro/hydro-tools-models-wintr55.html (accessed 4 Oct, 2005). USDA, Washington, DC.

Watson, B.M., M. Ghafouri, and S. Selvalingam. 2003. Application of SWAT to model the water balance of the Woady Yaloak River catchment, Australia. p. 94-110. *In* R. Srinivas et al. (ed.) Second International SWAT Conference Proceedings. TWRI Technical Report 266. Texas Water Resources Institute. College Station, TX.

Williams, J.R. 1995. The EPIC model. p. 909-1000. *In* V.P. Singh (ed.) Computer models of watershed hydrology. Water Resources Publications, Highlands Ranch, CO.

Session II

6. **The suitability of SWAT model in sediment yield modeling for ungauged catchments: A case of Simiyu River Subcatchment, Tanzania** **61**
P.M. Ndomba, F.W. Mtalo and A. Killingtveit

7. **Predicting diffuse-source transfers of sewage sludge-associated chemicals to surface waters using SWAT** **70**
N. Kannan, S.M. White and M.J. Whelan

8. **SDA SWAT edition: Efficient spatial data analysis & visualization for SWAT results** **80**
Theresa Possley and Qimiao Lu

The Suitability of SWAT Model in Sediment Yield Modeling for Ungauged Catchments: A Case of Simiyu River Subcatchment, Tanzania

P.M. Ndomba[1*], F.W. Mtalo[2], and A. Killingtveit[3]
[1]Doctoral student, University of Dar es Salaam (UDSM), P.O. BOX 35131 Dar es Salaam, Tanzania. E-mail: pmndomba@ucc.ac.tz
[2]Associate Professor, University of Dar es Salaam (UDSM), Tanzania
[3]Professor, Norges teknisk-naturvitenskapelige universitet (NTNU), Norway

Abstract

Different approaches to erosion control measures and modeling techniques have been applied in Tanzania. They included government campaigns or enforcement, experimentation (runoff plots), and mathematical modeling. In order to cope with soil erosion problems in the Uluguru Mountains, Morogoro region, the former government of Tanganyika Territory introduced a series of conservation measures. These involved compulsory bench terracing on all fields of medium slopes, with re-forestation in steeper slopes, grass barriers, and firebreaks around all fields. The assumption behind the measures was that sheet wash and flush runoff were major problems and that large terraces were the most effective structures for controlling soil erosion. New techniques imposed on indigenous farmers did not succeed. It is no doubt the methods that require experimentation are demanding in terms of resources and transferability.

Models that require large calibration data from runoff plots have not been found to be a reliable tool in the region. Nevertheless, some researchers tried to use renowned empirical models such as USLE, to estimate sediment yield and the results of the model were validated with reservoir sedimentation surveys. However, in some studies it was difficult to model inter-annual erosion rates, sediment deposition, gully and riverbank erosion, and to simulate individual erosion processes in the catchment. Lack of calibration data prohibited the ascertaining of findings. As a result, researchers in Tanzania and elsewhere in the tropics could not have a common tool for assessing the erosion rates in catchments.

The results of sediment yield modeling using the SWAT model in the Simiyu River Basin suggests that the model can be applied in ungauged catchments (i.e. poor data regions). For instance, daily flow data, which was used to calibrate the water balance equation in the model, was found to be adequate to reduce the error between simulated and scanty observed sediment loads. The long-time annual flows between observed and simulated were comparable with means of 12.93m^3/s and 12.67m^3/s respectively. Simulation of inter-annual flows, between 1970 and 1971, gave a Nash and Suttcliffe efficiency of 58%. The long-term specific yield of 0.523t/ha/year was simulated. It was also found that the use of free available Internet geo-spatial data for the SWAT model development highlighted an opportunity for the applicability of complex models such as SWAT in the ungauged catchment. A set of factors that cause erosion in the catchment could be determined. This paper recommends that sediment yield modeling researchers from the tropical regions to customize the SWAT model in their local area for improved watershed management. It proposes an improved SWAT model structure by coupling the model with hydraulic channel network models such that flood routing could be handled and thus sediment loads be routed.

Introduction

Soil erosion is a worldwide environmental problem that degrades soil productivity and water quality, causes sedimentation in reservoirs, and increases the probability of floods (Ouyung, 2001). Most of the countries in the tropics have no appropriate and accurate soil erosion prediction models, although the Soil Loss Estimation Model for Southern Africa (SLEMSA) and the Universal Soil Loss Equation (USLE) are used in different tropical countries (Mulengera, 1999). The SLEMSA, which was developed initially for Zimbabwe, still needs some modifications. It has not yet been widely used or tested outside Zimbabwe and in some instances has given unrealistic soil loss values (Mulengera, 1999).

Sediment transport rate is affected by hydrological as well as hydraulic characteristics. Since the former cannot be adequately taken into account quantitatively, a high degree of accuracy in sediment load computations cannot be expected (Garde and Rangaraju, 2000). Watershed management programs frequently fail to reduce sediment yield because either the physical nature of the problem is not properly diagnosed or the economic and cultural conditions leading to accelerated erosion are not addressed and erosion control practices are abandoned as soon as government subsidies are removed (Gregory and Fan, 1998). Besides, the development of a comprehensive sediment yield model requires substantial funding, extensive time and expertise, which are often unavailable in developing countries (Mulengera, 1999).

Studies on erosion problems in Tanzania date back as early as in the 19th century in the era of East African caravan trade (Christianson, 1981). For instance, the growing gullies in the foot slopes of Mount Meru in the Arusha region are typical evidence of the existing high levels of erosion rates (Semu *et al.*, 1992). Evidence of high erosion rates in Tanzania have been reported in other past studies (Young and Forsbrooke, 1960; Little, 1963; Rapp *et al.*, 1973; Mtalo and Ndomba, 2001)

Different approaches to erosion control and modeling techniques have been applied. They include government campaigns or enforcement, physical, geographical, experimentation (runoff plots), and mathematical model applications. The methods that require experimentation are demanding, in terms of resources and transferability (i.e. scale) (Yanda, 1995). During the colonial rule, the indigenous inhabitants of Uluguru Mountains, in Morogoro region, by the former Tanganyika Territory were forced to adopt erosion prevention solutions such as terracing without their consent, and hence the exercise failed. Models that require large calibration data from runoff plots were not reliable in the region (Yanda, 1995). Other researchers have used empirical models such as USLE to estimate sediment yield, whereas the results of the model were validated with reservoir trapping and sedimentation surveys. In the Pangani River Basin for instance, only half of the estimated upland erosion is found to reach catchment outlet (Mtalo and Ndomba, 2001).

In these previous studies, however, it was difficult to account for sediment deposition within the catchment and to model the individual erosion processes. Therefore, this study aimed at assessing the suitability of SWAT2000 model (Neitsch, 2002) as one of the watershed erosion models in modeling sediment yield in an ungauged catchment called Simiyu. The model was used to assess its suitability in modeling sediment yield in the data scarce catchments, located in this northern part of Tanzania.

Description of the Study Area

The Simiyu Catchment covers an area of 10,659 km^2. It is located between 33.46^oE – 34.84^oE and 2.36^oS – 3.27^oS (Figure 1). The Simiyu River discharges its waters into Lake Victoria. Before it enters the lake, its main tributary, the Duma River, joins the main Simiyu River. This is a result of the confluence of Ngasamo and Bariadi Rivers. The road-bridge gauging station located at the confluence of the two rivers, Simiyu and Duma, forms the lowest point of the study area (Figure 1).

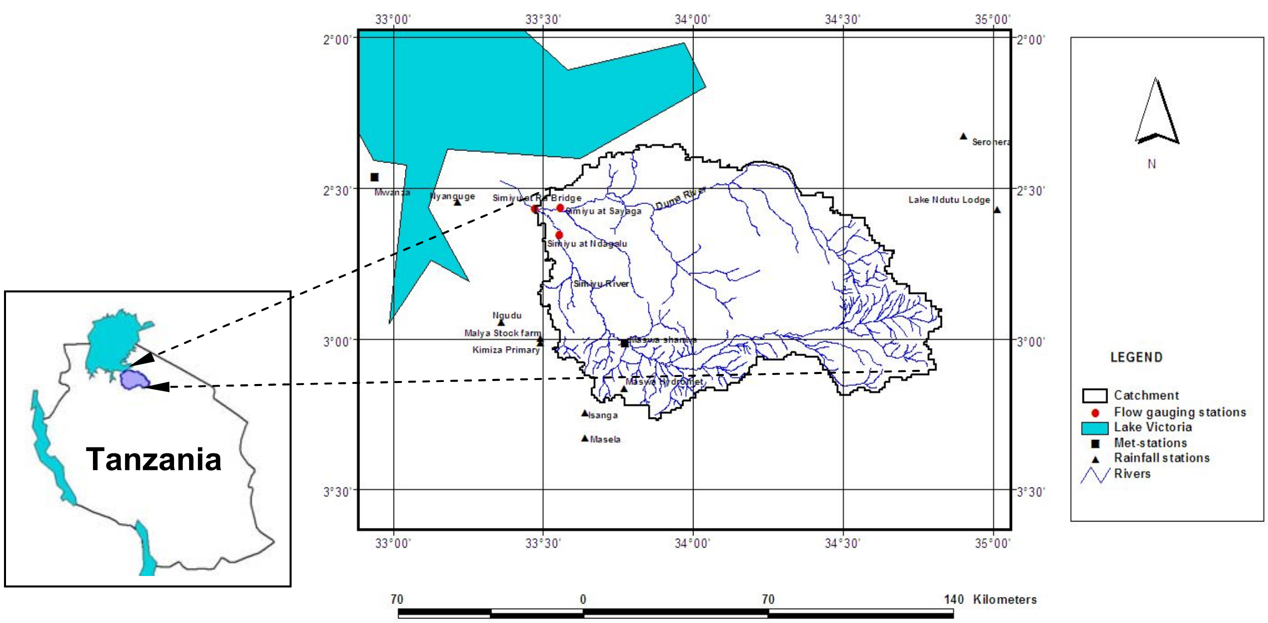

Figure 1. **A location map of the Simiyu River basin.**

Data and Data Analysis

Land cover data was acquired from Lake Victoria Environmental Management Project (LVEMP) database, whereas Digital Elevation Models (DEM) and soil texture coverage were obtained online from the United States Geological Survey (USGS) website with a resolution of 30 arc second (approx. 1 km). The maximum and minimum elevations are 2021m.a.s.l and 1135m.a.s.l respectively. The longest flow path is 222km while the average slope is 0.4 percent. Deep sandy soils dominate the study area with coverage of about 86 percent. The main land use categories are pastureland, cultivation, and rangeland, with coverage of 52, 25, and 20 percent respectively. Other land use classes such as forest, urban, and water covers the remaining 3 percent.

Concurrent data sets of river flows between 1970 and 1978 are available at three gauging stations (i.e. 112012 - Ndagalu gauging station, 112022 - Simiyu near the road-bridge, and 112032 - Sayaga gauging station) (Figure 1). Ndagalu and Simiyu main outlet stations flow data series have missing values of 47 and 22 percent respectively. The data at 112012 was used for model calibration while that at 112022 for model validation. The long-term average annual flow at the Simiyu sub-catchment main outlet is 12.93 m3/s. Data analysis indicate that Simiyu River can be categorized as ephemeral, as it dries up completely between July and October.

Meteorological data sets from two stations (i.e. Mwanza and Maswa-Shanwa) include daily temperatures, humidity, radiation, wind, and pan evaporation, which span the period 1970-1974. Daily rainfall data was also acquired. The missing data in rainfall records reach up to 32% while records of other climatic variables were relatively continuous with less than 1% missing. The mean annual rainfall is 1,000 mm.

A short record of daily sediment data was available at station 112022 as Total Suspended Solids (TSS) for seven days spanning the period between December 7, 2000 and December 13, 2000. The data was obtained from the database at the Water Resources Engineering Department of the University of Dar es Salaam. However, the quality of this record is doubtful since neither the method of sediment sampling nor quality report was available. The data was considered vital for this study because in ungauged catchments, lack of data description, scarcity, and unreliability are common features.

Methodology

The SWAT model under GIS environment, (i.e. AVSWAT2000), was used for watershed modeling. The calibration procedure incorporated in the model was used in this study for the selection of a few relevant parameters. They included the Curve number (CN2), Channel transmission losses (CH_K2), Threshold depth of water (REVAPMN) in shallow aquifer for controlling the movement of water into the soil zone in response to water deficiencies within a day (i.e. revap) to occur, Groundwater “revap” coefficient (GW_REVAP), Baseflow Alpha factor (ALPHA_BF), and Soil Available Water Capacity (SOL_AWC). The model was calibrated using data in the catchment of Simiyu-Ndagalu. Only the flow component of SWAT was calibrated. Sediment loads were not calibrated due to a lack of measured sediment loads in the catchment. The calibration was done based on long time averages of annual runoff, surface runoff, and baseflow. Also, a temporal calibration was carried out in order to simulate the seasonal variability of fluxes.

A lack of continuous sediment flow data indicated the need for validating the available scanty data so as to give an insight into the performance of the developed model. The calibrated model was applied to the entire catchment, using optimum parameter values, as determined during the model training. Scanty sediment loads measured at the station 112022 validated the performance of the developed model. Therefore, a relative comparison between observed sediments loads, as sampled during the start of rains season between December 7 and 13, 2000, and simulated fluxes in the similar seasons was adopted. In the latter, a match of flow discharge and season of the year was used to select comparable records from observed and simulated data sets. Therefore, in this study the assessment of the model suitability is based on its ability to simulate long-term hydrological fluxes and their seasonal variability.

Results and Discussion

Results of model calibration for the Simiyu-Ndagalu Catchment are presented in Table 1, and Figures 2 and 3. Generally, the results indicate that simulated and observed annual volumes are comparable (Table 1). However groundwater or baseflow (GWQ) component is better simulated than the surface runoff (SURF). The model was capable of capturing about 58% of the variance in observed records (Figure 2). The model inefficiencies were due to its failure to capture some runoff peaks such as those on January 22, 1971 and February 9, 1971. Besides, low flows are well estimated. A general observation of Figure 3 suggests a well-simulated annual flow with a mean of 12.67 m^3/s, which differs slightly from that of observed annual flows (12.93 m^3/s). A long-term simulation of the sediment model in the Simiyu-Ndagalu Catchment gave an average specific sediment yield of 0.523 t/ha/year. Using the derived specific yield for the entire catchment, the average daily sediment yield at the station 112022 outlet was 1439 ton/day.

Table 1. Long-term average annual volumes calibration results.

	Total Water Yield WYD (mm)	Surface Flow SURF (mm)	Baseflow GWQ (mm)
Observed	84.30	58.40	25.90
Simulated	77.64	52.41	25.15

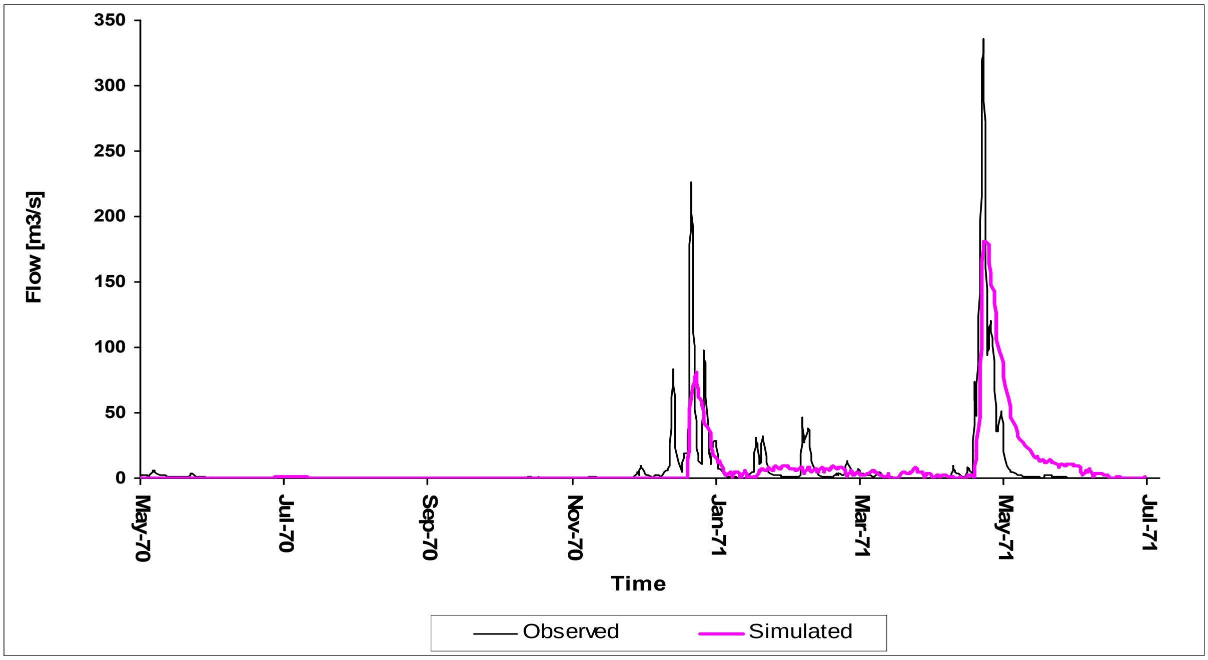

Figure 2: Temporal calibration results (seasonal variability of flow) between May 1, 1970 and April 30, 1971 (Nash, R^2=58%).

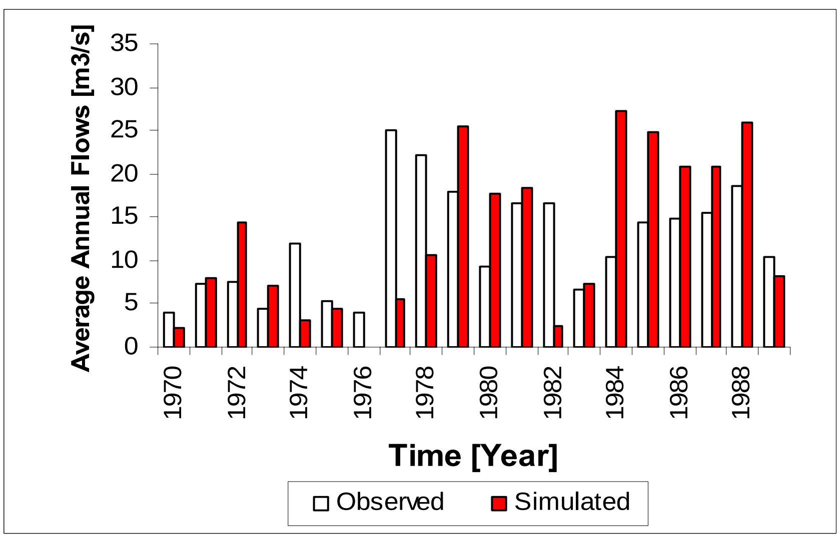

Figure 3: Long-term simulation results for Simiyu-Ndagalu Sub-catchment.

The underestimation of the runoff peaks (Figure 2) was attributed to assumption of uniform deep sandy soils in the entire basin. In reality, the basin consists of a variety of soil units which are not mapped. Figure 3 indicates that simulation results compares well with observed flow between 1970 and 1974. The reason is the use of observed data in this period during model calibration. However, between 1975 and 1988, the model uses only simulated weather data sets to simulate runoff.

The results (Table 2) are reasonable although no concurrent data sets were used. For instance, sediment yields in the catchment during the 1970s were expected to differ from those in 2000 due to significant changes in the land use and land cover hydrological patterns in the catchment. As a result, a comparison of seasons of the year was considered appropriate. Moreover, it should be noted that the results presented in this study assume a number of factors: 1) The predictions by SWAT so far can be viewed as “natural” flow without the influence of human factor (e.g. irrigation). 2) The model assumed that land use does not change and only static land use coverage of 1990s was used to develop the computation units (HRU). 3) The dominant source of sediment is from rill and inter-rill (sheet erosion) while other forms of erosion such as gullying have not been considered. Based on the hypothesis that the sediment yield is mainly influenced by surface runoff, accurate calibration of the water balance equation gives comparable estimates of the sediment loads in the catchment.

Table 2. Model validation results at Simiyu Catchment main bridge outlet.

Observed			Simulated			Remarks
Date (d/m/y)	Flow (m^3/s)	Sediment loads (ton/day)	Date (d/m/y)	Flow (m^3/s)	Sediment loads (ton/day)	
7/12/2000	152.7	5673.5	2/4/1975	151.2	4444.3	Rainy season
8/12/2000	122.8	3871.8	3/4/1975 22/2/1989	122.9 121.9	2924.8 3350.0	Rainy season
9/12/2000	71.2	1323.2	15/4/1974 26/4/1977	71.6 70.8	1853.2 1856.5	Rainy season
10/12/2000	97.0	3605.2	26/12/1982 29/1/1985 24/1/1987 26/12/1989	99.8 97.1 98.4 94.6	3658.2 3762.8 3084.6 2528.0	Rainy season
11/12/2000	134.5	10750.8	20/1/1987 16/3/1978	132.2 131.7	7117.0 6114.3	Rainy season
12/12/2000	139.1	11020.4	7/4/1978 30/12/1979	133.6 135.8	11815.0 9844.4	Rainy season
13/12/2000	91.0	1966.0	15/4/1978 30/12/1982 31/12/1988	91.4 90.0 89.5	1953.9 1401.2 1595.1	Rainy season

Conclusions

Despite the course resolution of spatial data such as soil data, the hydrological model developed gave reasonable estimates for ungauged catchments. An Index of Volmetric Fit (IVF) of 98% was obtained for long-term simulation of runoff while the Nash and Suttcliffe Model efficiency was 58% during the simulation of seasonal flow variability. This model and the spatial inputs could reasonably simulate temporal variability of hydrological fluxes in ungauged catchments. Parameters of this water balance model estimated at one sub-catchment with good data were used in developing a sediment yield model for the entire basin. The sediment yield model gave a long-term specific sediment yield of 0.523t/ha/year, which gave reasonable results despite sediment data problems.

The results indicate the suitability of the freely available geo-spatial data for the development of complex models like the SWAT model for use in the estimation of hydrological variables in the ungauged catchments. The approach presented in this paper is comparatively cheaper to other methods of sediment yield modeling applied elsewhere in Tanzania and therefore, this paper calls for sediment yield modeling researchers from the tropical regions to customize the SWAT model in their local area for improved watershed management. However, since sediment data used were of low quality, it is strongly recommended to install sediment samplers in various parts along the rivers in the basin to regularly sample the sediment rates.

References

Christianson C., (1981). “Soil Erosion and sedimentation in semi-arid Tanzania”. Ph.D Thesis. Scandinavian Institute of African Studies, Uppsala and Department of Physical Geography, University of Stockholm.Garde, R.J., and Rangaraju, K.G., (2000).
“Mechanics of Sediment Transportation and Alluvial Stream Problems.” Third Edition, 5p. New Age International (P) Limited, Publishers. New Delhi, India.

Gregory, L. M. and Jiahua Fan, (1998). “Design and Management of Dams, Reservoirs, and Watersheds for Sustainable Use”. Reservoir Sedimentation Handbook. McGraw-Hill companies, Inc.

Little, B. G. (1963). “Report on the condition of rivers rising in the Uluguru Mountains and their catchments”. Unpubl. report, W.D.&I.D. Tanzania.

Mtalo, F.W., and Ndomba, P.M., (2001). “Estimation of Soil erosion in the Pangani basin upstream of Nyumba ya Mungu reservoir.” Water Resources Management: The case of Pangani Basin. Issues and Approaches; Workshop Proceedings Edited by J. O. Ngana. pp196-210. Dar es Salaam University Press.

Mulengera, M.K., (1999). “Estimating the USLE-Soil Erodibility factor in developing tropical countries”. *Trop. Agric. (Trinidad)*, 76 (1), 17 - 22

Neitsch S.L., J.G. Arnold, J.R. Kiniry, J.R. Williams, (2002). “Soil and Water Assessment Tool Theoretical Documentation”, Version 2003, Grassland, Soil and Water Research Laboratory Agricultural Research Service 808 East Blackland Road, Temple, Texas 76502

Ouyung, D. and Bartholic, J. (2001). “Web-based GIS Application for Soil Erosion Prediction.” Proceedings of An International Symposium. Soil Erosion Research for the 21st Century Honolulu, HI. Jan. 3-5, 2001. Institute of Water Research, Michigan State University.

Rapp, A., Axelsson, V., Berry, L. and Murray-Rust, D. H. (1973). “Soil erosion and sediment transport in the Morogoro river catchment, Tanzania”. In: Rapp, A., Berry, L. and Temple, P. 1973. Studies of soil erosion and sedimentation in Tanzania. Bureau of Resource Assessment and Land use Planning, University of Dar es Salaam. Research Monograph no. 1. 125-156.

Semu, E., Göran Bergman, and Erik Skoglund, (1992). “Evaluation of Soil Conservation and Agroforestry Programme - Arusha (SCAPA) in Tanzania.”

Yanda, P.Z, (1995). “Temporal and Spatial Variations of Soil Degradation in Mwisanga Catchment, Kondoa, Tanzania”. Doctoral Dissertation 1995. Department of Physical Geography. Stockholm University.

Young, R. and Forsbrooke, H., (1960). “Land and politics among the Luguru of Tanganyika”. Routledge & kegan Paul, London. 196pp.

Predicting Diffuse-Source Transfers of Sewage Sludge-Associated Chemicals to Surface Waters Using SWAT

N. Kannan*, S.M. White and M.J. Whelan
*Blackland Research and Extension Centre, 720, East Blackland Road, Temple, TX, 76502. U.S.A. kannan@brc.tamus.edu Fax: 254-774-6001.

Abstract

Chemicals present in domestic wastewater can adsorb to solid phase materials during sewage treatment. If sewage sludge (or biosolids) is applied to land, these chemicals can be transferred to the soil. Under some circumstances they can also be transferred to surface waters during storm events, either in solution or attached to sediments. In this paper we describe the utility of the SWAT 2000 model to estimate diffuse-source surface water exposure to "down-the-drain" chemicals. The model was applied hypothetically to predict the behavior of linear alkylbenzene sulphonate (LAS), an anionic surfactant commonly used in household detergents, in a small catchment in Bedfordshire, UK, where it has previously been validated successfully for streamflow, sediments and pesticides. LAS transfers were estimated for two scenarios: (1) realistic and (2) worst case, based on assumptions about sludge application rates and the concentration of LAS in sludge. In addition, the sensitivity of the model output to the proportion of the catchment to which sludge is applied was established. Soil wetness and the total quantity of biosolids applied were the biggest determinants of chemical transport from the catchment. The potential for SWAT to serve as a higher-tier tool in environmental risk assessments is also discussed.

Key words: Sewage sludge, LAS, SWAT, diffuse source, modelling, biosolids

Introduction

The main route of environmental exposure for the ingredients of personal and household care products is via the wastewater stream after use by the consumer, principally to surface waters receiving treated and untreated effluents. However, some chemicals present in domestic wastewater can adsorb to solid phase materials during sewage treatment and if sewage sludge (or biosolids) is applied to land, these chemicals can be transferred to soil. As a consequence, the resulting concentrations and potential effects of sludge-associated chemicals in soil are considered in the generic methodology described in the Technical Guidance Document (TGD) on Risk Assessment (2003). However, very little attention has been given to the potential transfer of sludge-applied chemicals from land to surface waters. To some extent this is due to the difficulties in representing this route of exposure in simple generic models, since the transport processes are uncertain and highly variable – both spatially and temporally. Significant transfers (in solution or attached to sediment) are likely to occur only when high magnitude storm events coincide with high chemical availability (e.g. soon after application). Nevertheless, such site-management and weather-specific processes can be modelled in higher-tier exposure assessments. Such assessments are routinely performed for pesticides as part of the registration procedure in Europe, using detailed process-based models developed under FOCUS (http://viso.ei.jrc.it/focus/index.html). As part of its Long Range Research Initiative (LRI) the European chemical industry (CEFIC) has been sponsoring a number of projects to enhance higher-tier exposure assessment in different environmental compartments. One of these projects (TERRACE) has developed a methodology for predicting the diffuse-source transfer of chemicals from land to surface waters (White et al., 2001). The TERRACE methodology is based on SWAT 2000 (Soil and Water Assessment Tool) (Arnold et al., 1993, Neitsch et al., 2001a), a conceptual model developed to quantify the impact of land management practices on water quality in large, complex catchments. It has been shown to provide reasonable predictions for the fate of pesticides and nutrients (e.g. Kirsh and Kirsh, 2002, Santhi et al., 2002, Kannan, 2003) but has never been used to explore the potential for surface water exposure to sludge-associated chemicals. In this paper we describe an application of SWAT 2000 to predict the transfer of a well-studied sludge-applied chemical (linear alkylbenzene sulphonate: LAS) to surface waters in a number of hypothetical scenarios in a small catchment for which the model has been shown to predict streamflow, sediment and pesticide transfers satisfactorily (Kannan, 2003). To our knowledge this is the first attempt to estimate the transfer of sludge-applied LAS to surface waters using a semi-distributed hydrological model. It should be stressed at this stage that sewage sludge has never actually been applied to the study catchment described in this paper and, therefore, from the point of view of surfactant transfers the results are purely theoretical.

Study Area

SWAT was applied to the 141.5 ha Colworth Catchment in Bedfordshire, U.K. (in an area bounded by National Grid References SP 495000, SP 263000 and SP 499000, SP 263000). The catchment is predominantly underlain by the Hanslope soil series, consisting of a clay loam soil over stony, calcareous clay (NSRI/DEFRA/LANDIS)**.** Generic soils data including horizon depths, texture, organic carbon content, bulk density, saturated hydraulic conductivity, and water retention curves were obtained from the National Soil Resources Institute (http://www.silsoe.cranfield.ac.uk/nsri/services/cf/gateway/pdf/bibliography.pdf). With the exception of a small area of unused land and a very small area of deciduous woodland on the northern edge of the catchment (Figure 1), the land use is entirely arable with a rotation of wheat, oilseed rape, grass, beans, and peas. Data for all management operations (dates and rates of fertilizer application, tillage, pesticide application, planting, and harvest) conducted on the arable land in the catchment has been recorded. Tile drains (approximately every 40 m with gravel backfill) have been installed in all but one of the arable fields in the catchment. Secondary drainage treatments (mole drainage and sub-soiling) are applied where needed. All field drains eventually discharge into a main stream running through the centre of the catchment.

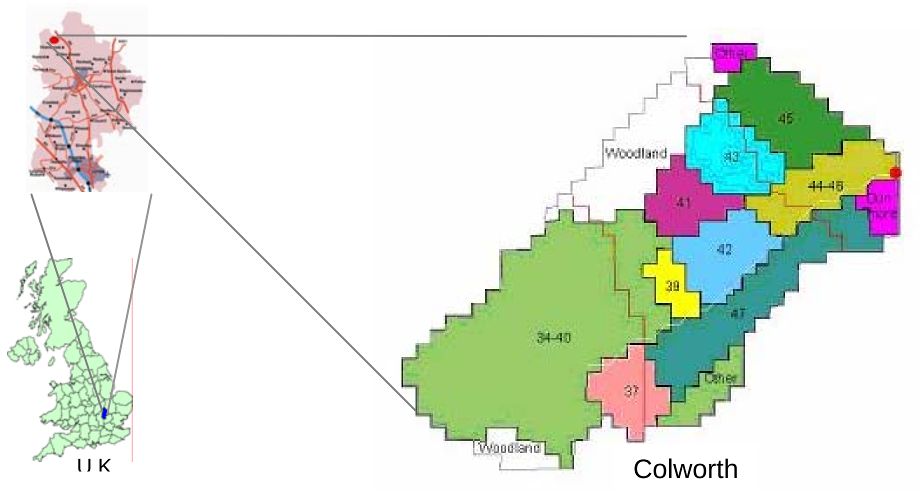

Figure 1. Location of study area.

Sub-daily (30 minute) rainfall data and daily maximum and minimum temperature values were available for the catchment over the monitoring period. Solar radiation, wind speed, and dew point temperature (used to calculate relative humidity) were obtained from the British Atmospheric Data Centre (BADC) (http://badc.nerc.ac.uk/home/) for the nearest station (Bedford – about 10 km away). An automatic flow recording system was installed at the catchment outlet in 1999 by the Agriculture Development and Advisory Service (ADAS). The system continuously recorded discharge using a Wessex flume equipped with an ultrasonic level sensor linked to a Campbell Scientific CR10 data logger, which could be downloaded remotely by ADAS.

Substance Information

Linear alkylbenzene sulphonate (LAS) is a major anionic surfactant used in household detergent products such as laundry powders, liquids, dishwashing detergents, and all-purpose cleaners. Its widespread use has prompted the collection of a range of data on its fate and effects in different environmental compartments. Its selection as a hypothetical test compound in this study is based largely on the good availability of suitable input data for the model. The physical-chemical properties of LAS are available (TGD, 2003; HERA 2002). In raw sewage, the LAS concentration can be in the range of 1-15 mg/L and treatment of sewage in activated sludge treatment plants can decrease the concentration to 0.009-0.14 mg/L (HERA, 2002). Removal in sewage treatment is predominantly due to biodegradation, although there is also some adsorption to solids. As a consequence, there is often some LAS associated with sewage sludge (hereafter biosolids). Since biosolids are often applied to farmland as an alternative to commercial fertilisers or manures, there is a need to assess the risk of deleterious impacts of LAS in soil and of the transfer of LAS to surface waters in solution or via soil erosion.

Normally LAS degrades rapidly under aerobic conditions. Typical degradation half-life of LAS in amended soils ranges from 3-35 days depending on soil type and season (Ward and Larson, 1989, Waters et al., 1989, Berna et al., 1989). For the UK, Holt et al., (1991) observed half lives of 7-22 days in soil. The default soil half-life for LAS recommended by the TGD (2003) is 30 days, based on performance in standard ready biodegradation tests.

The sludge partition coefficient (log K_p) ranges from 3 to 3.5 and the soil-water absorption coefficient (K_d) takes a value between 2 and 300 L/kg. Freundlich isotherms have been reported to represent sorption data reasonably well. LAS mobility in soils is generally low due to its fairly high sorptive capacity but may leach to lower soil depths in sandy soils with low organic matter contents. Kuchler and Schneek (1997) detected LAS down to 35 cm in column experiments, although they did not observe accumulation and also found that LAS was readily degraded ($t_{½}$ 3-7 days).

Hydrological Modelling

Hydrological modelling was carried out for the catchment from October 1999 to December 2002. Model performance was evaluated by comparing predicted and gauged discharge using Percent BIAS (PBIAS), Persistence Model Efficiency (PME), Nash and Sutcliffe Efficiency (NSE), and Daily Root Mean Square estimation criterion (DRMS) (Gupta et al., 1999). On the basis of these measures of fit, the best model performance for the Colworth Catchment was obtained using SCS CN combined with the Hargreaves evapotranspiration equation (Table 1; Kannan, 2003). Note that care was taken to ensure that crop growth, evapotranspiration, surface runoff, tile drainage, and baseflow predictions were sensible (Kannan, 2003), in addition to obtaining a reasonable match between predicted and observed streamflow values.

Table 1. Performance of hydrological modelling.

Period	**Method**	**PBIAS**	**PME**	**NSE**	**DRMS**
Oct. 1999 to Dec. 2000	Calibration	16.85	56.17	60.12	0.81
Jan. 2001 to May 2002	Validation	3.17	51.15	59.32	0.74

Since LAS has a fairly high soil adsorption coefficient, soil erosion is likely to be an important transport mechanism for diffuse-source transfers to surface waters. It is, therefore, necessary to model both the dissolved and adsorbed phase transport of LAS and a necessary first step is to correctly represent the loss of soil from fields and through the river system.

Figure 2 shows the predicted (uncalibrated) and observed daily suspended sediment (SS) concentrations in the Colworth stream for a few runoff events in which SS was measured. With the exception of two events (in February and March 2002) the predicted concentrations matched the observations reasonably well and suggested that the model was predicting SS fluxes satisfactorily. In addition, the sediment yield values predicted by SWAT appeared to be reasonable for the rainfall and cropping pattern seen at Colworth (e.g. Walling et. al., 2002) although there is no similar observed time series for a comparison.

Definition of Biosolids and LAS Application in SWAT

Since SWAT does not allow for the simulation of sludge-associated chemicals directly, application of biosolids to agricultural fields was represented as separate manure and chemical applications. The nutritional content of biosolids was represented in the SWAT-fertiliser database as manure, with a nitrogen (N) content of 3.91% and a phosphorus (P) content of 4.82%. These values are representative of nutritional content of biosolids in this region (Anglian Water, Pers comm.).

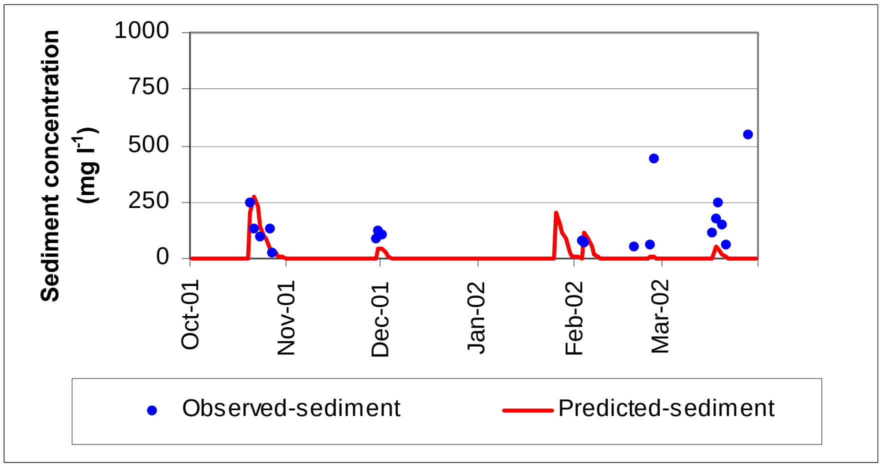

Figure 2. Comparison of sediment concentration.

The rate of application of biosolids needed to replace commercial fertiliser applications was calculated as the annual nutrient application rate in fertiliser divided by the nutrient content of biosolids. Since the phosphorus content of biosolids in the Anglian region is high, crop demand is based solely on N. For a crop receiving a total fertiliser input of 100 kg N ha^{-1} yr^{-1}, biosolids with a nitrogen content of 3.91% N would need to be applied at 2558 kg ha^{-1}yr^{-1} (2500 kg ha^{-1}yr^{-1} approximately). This calculation assumes that the nutrients in biosolids and fertiliser would be equally available, which will not actually be the case, but was simple and convenient. The normal rate of application of biosolids ranges from 5,000 to 5,800 kg/ha (Anglian Water, Pers comm.), which will take care of the nutritional demand of crops for two agricultural seasons.

Two scenarios were evaluated: realistic and worst-case were conducted to model biosolid application for different fields (individual fields and all the possible fields together). For both scenarios the physical-chemical properties of the chemical were kept constant. However, the soil half-life of LAS, the content of LAS in biosolids, and rate of biosolids application were varied. For two fields in the catchment, biosolid application was not modeled because of the type of land use (woodland). All scenarios were evaluated for three hydrologically different cropping seasons (average, wet, and dry) with varying rainfall amounts (663.8, 755.4 and 527.2 mm, respectively). There is only one soil type in the catchment; however, the cropping pattern varies widely for the arable fields. To conduct scenario trials easily and to reach important conclusions, the crop grown was kept the same (winter wheat) for all the fields in all three cropping seasons considered for LAS modelling. Also the dates for tillage, planting, fertiliser, manure, pesticide applications, and harvest were kept the same for all the winter wheat cropping seasons. In connection with another study, the crop growth of winter wheat was modelled more realistically than other crops grown in the catchment (Kannan, 2003).

The following properties of LAS were assumed in all scenarios: K_{OC} = 615.98 L/kg (from K_{OW} using the TGD method for K_{OC}); water solubility = 250 mg/L (HERA, 2002).

Table 2. Properties of LAS and application details for different scenarios.

Scenario	Half life (days)	LAS in bio-solids (g/kg)	Application rate (kg/ha)	% of nutrient demand met	Apply to
Realistic case	7	5	2500	100	All fields together and each field individually
Worst case	30	10	5000	TGD	All fields together and each field individually

Results

Model predictions are expressed as loads of LAS leaving the catchment for each scenario, i.e. (a) three hydrologically different seasons (b) different rates of biosolids application (realistic/worst case) and (c) proportion of catchment area vs. load. The realistic scenario with average rainfall conditions was considered the benchmark, unless otherwise stated. The results under the categories (a) and (b) are applicable for biosolid application for all the possible fields (Figure 1).

Predictions of LAS load leaving the catchment are presented in Table 3 and Figure 3. The lowest LAS flux was predicted for the water year 2001-2002 which was also the year with the lowest annual rainfall. The LAS flux from the year 1999-2000 was the highest of the three years considered, due to a high predicted soil water content and rainfall soon after biosolid application (Figure 4) which favored LAS transport. In the 2000-2001 cropping season, soil water content at the time of biosolids application was much lower, resulting in a lower propensity for drainage, runoff, and associated contaminant transport. A similar pattern was observed for the worst-case scenario. In all cases LAS transport was less than 1% of LAS applied (Table 3).

Table 3. Predicted total load of LAS leaving the catchment for three hydrologically different cropping seasons (total load for 100 days from the date of application).

Season	Realistic case			Worst case		
	Applied (kg)	Load (kg)	% applied	Applied (kg)	Load (kg)	% applied
1999 Winter	1556.25	8.993	0.58	6225	55.908	0.900
2000 Winter	1556.25	3.376	0.22	6225	26.113	0.420
2001 Winter	1556.25	0.085	0.01	6225	3.032	0.050

The predicted flux of LAS from the catchment in the worst-case scenario was always much greater than for the realistic scenario (Table 3). The difference was not proportional to the amount of LAS applied, which suggests a non-linear relationship between application rate and flux.

As expected, an increase in the area of biosolid application resulted in an increase in total LAS load (Figure 5). For both the realistic and worst-case scenarios, the increase in LAS load per unit increase in application area was highest for the year 1999-2000 (average annual rainfall) due to the specific hydrological conditions predicted for this year (wet soil at the time of application followed by rainfall).

The predicted total LAS load for different application areas is shown in Figure 5. A similar pattern was also predicted for the worst-case assumptions. Although there was a general increase in LAS flux with increase in the area of biosolid application, there was no consistent difference in the predicted flux as a percentage of LAS applied. Higher fluxes were always predicted for the year 1999-2000 compared to the other two years.

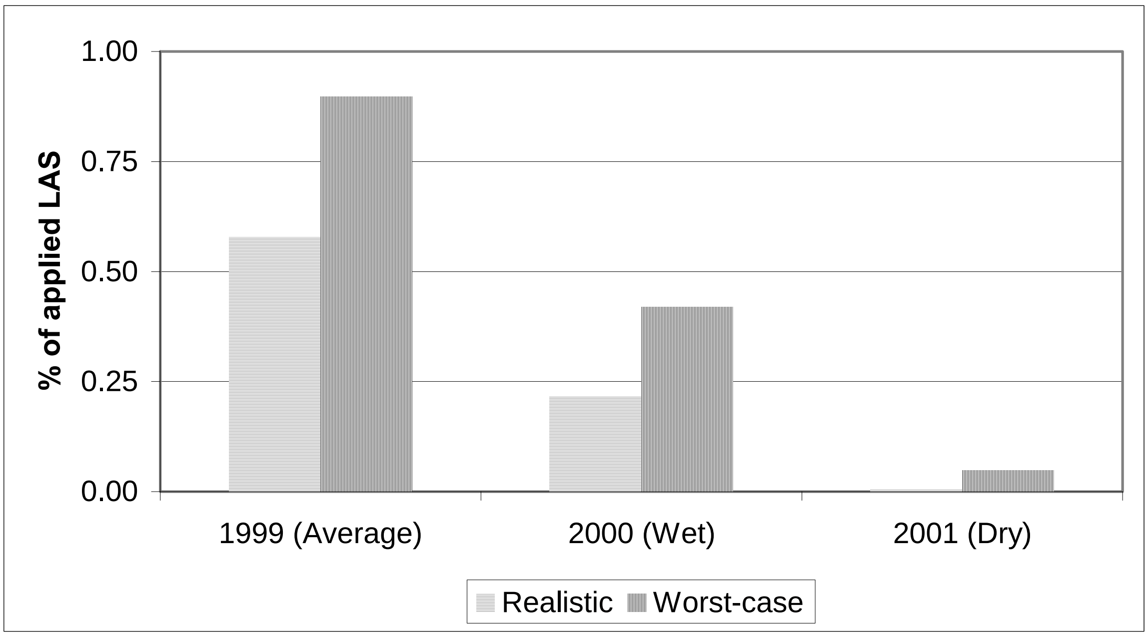

Figure 3. Predicted total loads of LAS for three hydrologically different cropping seasons.

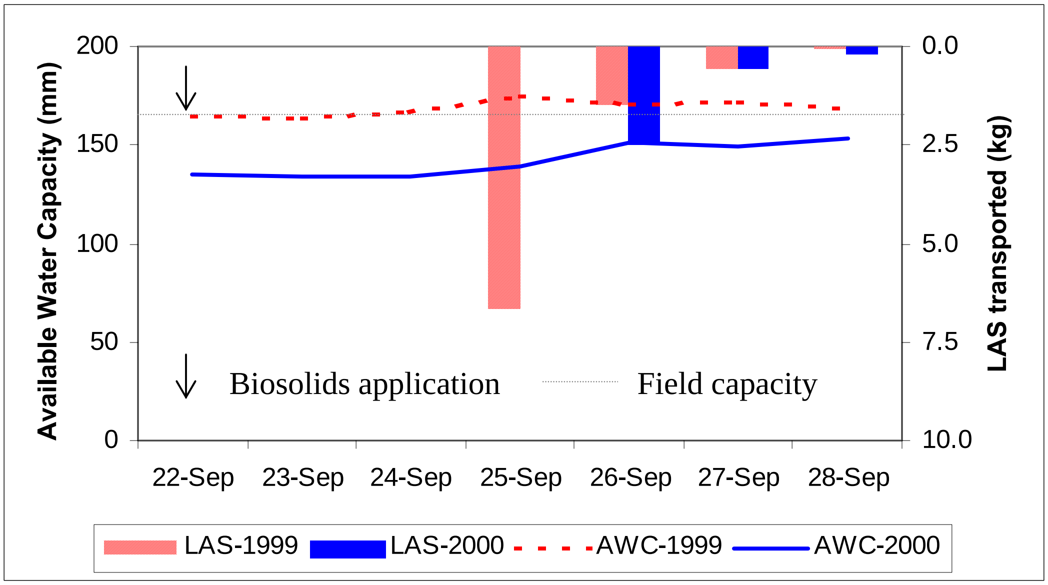

Figure 4. Relationship between predicted available soil water and predicted transport of LAS in realistic case scenario.

Conclusions

The SWAT 2000 model was used to predict the diffuse-source transfer of linear alkylbenzene sulphonate (LAS) to surface waters resulting from the application of biosolids (sewage sludge) to land. The model was applied hypothetically to the Colworth Catchment in a number of scenarios to different fields. Biosolids are represented in SWAT as two components: one with nutritional value and the other representing sludge-associated chemicals. The flexibility offered by SWAT to analyse the consequences of changing management operations was fully utilised.

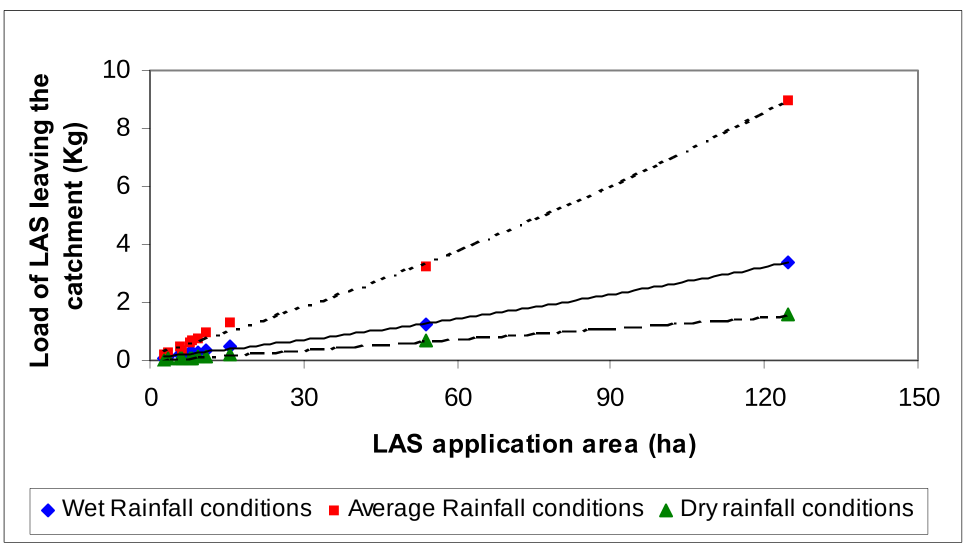

Figure 5. Relationship between area of application and predicted load of LAS leaving the catchment for various rainfall conditions-realistic case.

Based on the results obtained from this study the following conclusions can be drawn:

1. SWAT 2000 can, in principle, be used to model the transport of LAS to rivers, although its transport via tile drains and groundwater are not fully functional.
2. Although all the scenarios examined were hypothetical (and thus the accuracy of the predictions could not be checked) the model has been successfully applied to predict measured flows and pesticide concentrations in the Colworth Catchment. This lends credibility to the predictions for LAS.
3. The model predicted that soil water content at the time of biosolid application and the total quantity of biosolids applied had the greatest control over LAS transfer to the catchment outlet.
4. The model results suggest that loss of surfactants from the application of biosolids to land will probably not result in a deleterious impact on water quality even for extreme worst-case scenarios.

Acknowledgements

We are very grateful to ADAS and, in particular, to Simon Groves for the supply of hydrological, meteorological and water quality data and to the Unilever Sustainable Agriculture team, particularly Jos van Oostrum and Innes McEwan, for providing land use and other essential information. The work was conducted with the help of financial support from the CEFIC LRI and Unilever.

References

Arnold, J.G., Allen, P.M., and Bernhardt, G. (1993) A comprehensive surface-groundwater flow model. Journal of Hydrology, 142, 47-69.

Berna L., Ferrer A., Moreno A., Prats D., and Ruiz Bevia F. (1989) The fate of LAS in the environment. Tenside Surfactants Detergents, 26, 101-107.

FOCUS (2001) "FOCUS Surface Water Scenarios in the European Union Evaluation Process under 91/414/EEC". Report of the FOCUS Working Group on Surface Water Scenarios, EC Document Reference SANCO/4802/2001-rev.1. 221.

Gupta, H.V., Sorooshian, S., and Yapo, P.O. (1999). Status of automatic calibration for hydrologic models: Comparison with multilevel expert calibration, Journal of Hydrologic Engineering, 4(2), 135-143.

http://www.silsoe.cranfield.ac.uk/nsri/services/cf/gateway/pdf/bibliography.pdf (Last accessed: Oct. 21, 2005)

British Atmospheric Data Centre - http://badc.nerc.ac.uk/home/ (Last accessed: Oct. 21, 2005)

HERA methodology document (2002), Human and Environmental Risk Assessment on ingredients of European household cleaning products-Linear Alkylbenzene Sulphonate, LAS, CAS No. 68411-30-3 http://www.heraproject.com/RiskAssessment.cfm?SUBID=4 (Last accessed on 21-01-2005).

Holt M.S. and Bernstein S.L. (1991) Linear Alkylbenzenes in sewage sludges and sludge amended soils. Water Research, 26(5) 613-624.
http://www.usatoday.com/weather/whumcalc.htm (Last accessed : Oct. 21, 2005)

Kannan, N. (2003). A robust methodology to predict diffuse source pollution in the aquatic environment: A case study for the Colworth catchment, Bedfordshire. Ph.D. thesis, Cranfield University, Silsoe, MK45 4DT, Bedfordshire, U.K.

Kirsh, K., Kirsh, A., and Arnold, J.G. (2002). Predicting sediment and phosphorus loads in the Rock River Basin using SWAT. Trans ASAE, 45(6), 1757-1769.

Kuchler T. and Schneek W. (1997) Behaviour of LAS in sandy soils with low amounts of organic matter. Chemosphere 35(12), 153-167.

LandIS-National soil database of England and Wales (NSRI/DEFRA/LANDIS). National Soil Resources Institute, Silsoe, Bedfordshire, U.K.

Neitsch, S.L., Arnold, J.G., Kiniry, J.R. and Williams, J.R. (2001a) Soil and Water Assessment Tool-Version2000-User's manual, Temple, Texas, U.S.A.

Neitsch, S.L., Arnold, J.G., Kiniry, J.R. and Williams, J.R. (2001b). Soil and Water Assessment Tool-Version 2000-Theoretical Documentation, Temple, Texas, U.S.A.

Roberts D.W. (1991). QSAR issues in aquatic toxicity of surfactants. Science of Total Environment, 109-110 557-568

Santhi, C., Arnold, J.G., Williams, J.R., Hauck, L.M. and Dugas, W.A. and (2001). Application of a watershed model to evaluate management effects on point and non-point source pollution. Trans ASAE, 44(6), 1559-1570.

Soil Conservation Service. (1972). Section 4: Hydrology In National Engineering Handbook. SCS.

TGD (2003) Technical Guidance Document on Risk Assessment in support of Directive-93/67/EEC, European Commission, JRC, Italy

Walling, D.E., Russell, M.A., Hodgkinson, R.A., and Zhang, Y. (2002). Establishing sediment budgets for two small lowland agricultural catchments in the UK. Catena, 47(4), 323-353.

Ward, T.E. and Larson R.J. (1989) Biodegradation Kinetics of Linear Alkylbenzene Sulfonate in Sludge-Amended Agricultural Soils Ecotoxicology and Environmental Safety 17 (1), 119-130

Waters J., Holt M.S. and Matthijs E. (1989) fate of LAS in sludge-amended soils. Tenside Surfactants Detergents, 26, 129-135.

White, S.M., Anderton, S.P., Ishemo, C., Worrall, F., Hollis, J., and Hallet, S. (2001) TERRACE: TErrestrial Runoff modelling for Risk Assessment of Chemical Exposure. Review of State of the Art: Assessment of modelling software and available geodata. University of Durham, Unpublished report.

SDA *SWAT Edition*: Efficient Spatial Data Analysis & Visualization for SWAT Results

Theresa Possley[1] and Qimiao Lu[2]
[1]W.F. Baird & Associates, Madison, WI, USA, Email: tpossley@baird.com
[2]W.F. Baird & Associates, Oakville, ON, Canada, Email: qlu@baird.com

Abstract

SDA *SWAT Edition* is a customized version of Spatial Data Analyzer (SDA), a GIS-based data visualization and analysis tool, developed specifically for the SWAT model output. SDA animates time series and spatial data over GIS maps with rapid display speed, even for very large model output file sizes. It can manipulate commonly used GIS data layers, most SWAT model results and any additional data (such as input and observed datasets) in ASCII format. All spatial and temporal data can be interpreted graphically as vectors, contours, color-mappings or hill-shadings. SDA generates sub-maps, which can be used for multi-angle map views, profile plots, and time series plots, that can be animated simultaneously. This includes the capability to view model results from more than one model run simultaneously, enabling quick comparison of different model scenarios. The data can be explored and edited in four-dimensional space (three dimensions in space plus time) with fully-functioning GIS navigation tools. Movies may be recorded in various formats, and high-resolution maps of model results can be generated for use in reports or public presentations. SDA has been applied for modeling and other studies in the fields of hydrology, hydraulics, hydrodynamics, sediment transport, water quality, oceanography, meteorology, biology, and others. It has been used to animate 1D/2D/3D hydrodynamic models, hydrologic models, wave models, sediment transport models, meteorological models, particle tracking models, and animal and fish tracking models. SDA is an efficient tool for SWAT model development, calibration, verification, and results analysis.

SDA Background

Spatial Data Analyzer (SDA) is a GIS-based data visualization and analysis tool developed by Dr. Qimiao Lu. It animates time series and spatial data over GIS data layers with impressive display speed and can load the most commonly used GIS databases, any numerical model results based on commonly used grids, and any time series data in ASCII format. All loaded spatial and temporal data can be graphically and dynamically visualized as vectors, barbs, contours, color-mappings or hill-shadings over a GIS map (Figure 1). The data can be graphically explored and edited in four-dimensional space (three dimensions in space plus time) with fully functional GIS navigation tools. Models currently supported in SDA include: STWAVE, MIKE21, MIKE3, ADCIRC, RMA2/SED2D, ECOM-SED, MISED, HEC6, GSSHA, and SWAT.

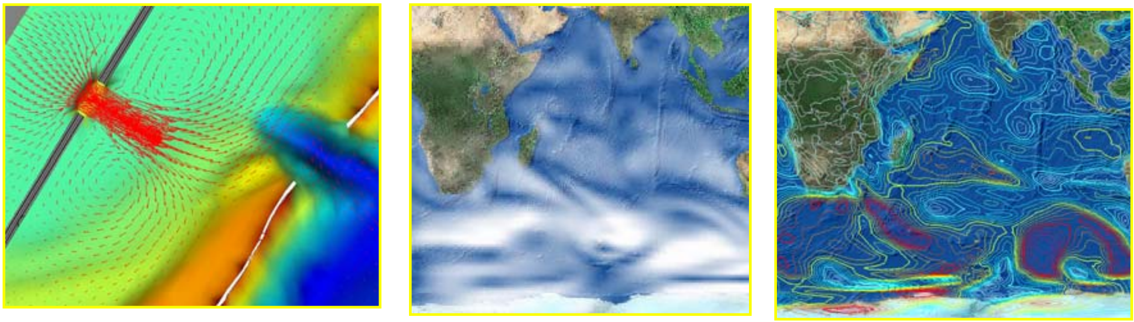

Hill-shading layer and vector layer *Color mapping layer using partial transparency* *Contour layer*

Figure 1: SDA visualization options.

SDA has been widely applied for modeling and other studies in the fields of hydrology, hydraulics, hydrodynamics, sediment transport, water quality, oceanography, meteorology, biology, and others. It is designed for visually pre- and post-processing numerical modeling data, as well as any kind of spatially or temporally relevant data analysis. It has been used to animate 1D/2D/3D hydrodynamic models, hydrologic models, wave models, sediment transport models, meteorological models, particle tracking models and fish tracking models.

SDA *SWAT Edition*

Purpose

SDA *SWAT Edition* was developed to fill a need for more powerful and efficient model output analysis and visualization for SWAT model results, specifically addressing the needs for handling of large file sizes and mapping and sharing of model results with those outside the SWAT modeling community.

Efficient handling of large datasets is essential to the SWAT modeling community, as file sizes for SWAT model runs with daily output can quickly approach several hundred megabytes and even several gigabytes. Manipulation of these large datasets is required in order to plot and further analyze the SWAT results of interest. Using the AVSWAT interface (Di Luzio et. al., 2002) the user is able to read SWAT model results to a .dbf file, though this is not recommended for long simulations with daily results (R. Srinivasan, personal communication, SWAT Beginner Workshop, May 17-19, 2005) as it can corrupt the project (.apr) file. Also, if using Microsoft Excel's text import wizard for viewing output results, the user is limited to 65,536 rows of data, which is easily exceeded. Beyond writing one's own code to view and reformat large SWAT output datasets, the SWAT user community has few options for large dataset manipulation.

Mapping of model results is also an important part of SWAT model output analysis. The SWAT model results can be mapped within the AVSWAT interface, provided the user selects to read the results to a .dbf file; though, there are some limitations to this option. First, only subbasin results can be mapped; results for reaches, reservoirs, and other model output and input cannot be mapped automatically within the AVSWAT interface. Also, only one time-step can be mapped at a time. If the user is interested in viewing the results spatially over numerous time-steps, there is no efficient way to do this within the AVSWAT interface. These limitations put constraints on how the model results can be shared and communicated with those outside the SWAT modeling community.

SDA *SWAT Edition* was developed with features designed to address these limitations, as well as to provide a more complete tool for SWAT output analysis and visualization.

Features

A custom conversion tool was developed specifically for SWAT model results, allowing the user to read in subbasin, reach, and reservoir output files, as well as precipitation inputs. Additionally, the user can specify which output variables to read in; thus reducing the amount of data to only that of interest to the user (Figure 2). SDA *SWAT Edition* can handle SWAT output file sizes of 10 GB or greater; the user is limited only by their computer hardware. Therefore, daily results for several years on large watersheds can be imported with no trouble. In addition to SWAT model results, the user has the ability to import any time series data (such as observed records) into SDA *SWAT Edition* and view those values along with SWAT results. Once the data is converted and imported into SDA *SWAT Edition*, all data can be quickly and easily viewed and edited within the Data Editor window.

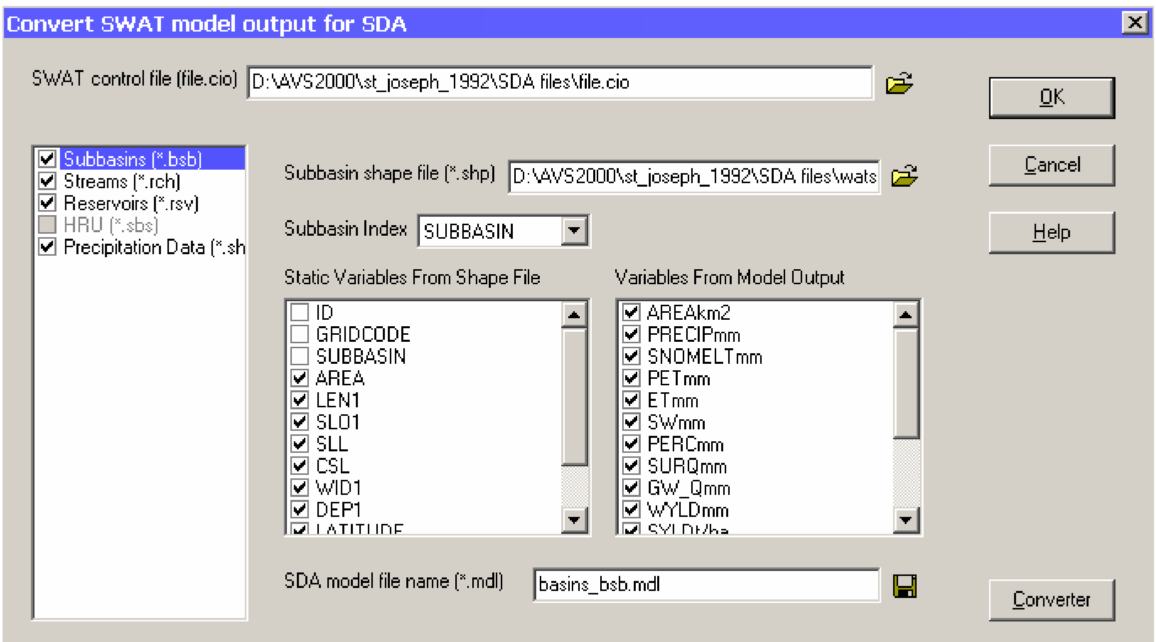

Figure 2: SDA SWAT model conversion program dialog box.

With SDA *SWAT Edition* any SWAT variable can quickly be viewed on a map by simply dragging and dropping. Results can be overlaid on GIS map layers to better visualize the results spatially. The maps can then be animated to quickly view the entire time series of results.

Another feature of SDA *SWAT Edition* is the ability to display submaps in a main map, or child windows in a main window. A submap is totally independent of the main map and has its own graphic content or viewing parameters (view center and scale) that may be different from the main map. Submaps are animated simultaneously with the main map. There are three kinds of submaps: index map, subviewer, and time series plotter.

The index map shows the entire map and the current viewing area of the main map. It is generally used to quickly pan the main map. The subviewer is similar to the main map, but its graphic content or viewing extent may be completely different from the main map. For instance, datasets shown in a subviewer may be different from that shown in the main map or other subviewers. It is useful when comparing two sets of model results that may have been calculated in two different scenarios. Viewing parameters such as scale factor and viewing center in a subviewer may be different from the main map or other subviewers. It is useful to look closely at the area of interest without missing the overview. The time series plotter is used to plot time series data. This data is generally extracted from model results at specific points or from any ASCII file (e.g., observed data). The time series plotter illustrates the temporal variation associated with the animation and is useful for model calibration when model results are compared against observed values. The time series plotter supports several different styles: lines, points, bars, areas, combinations of the former and plots with numerous Y-axes.

Other SDA *SWAT Edition* features include a math parser, results export, and movie and image creation. The built-in math parser, which compiles and evaluates user-specified mathematical equations, allows users to dynamically create a new variable from their SWAT time series results. For example, area loadings can quickly be calculated from the unit area loads by multiplying by the area and a unit conversion factor, if necessary. This powerful tool allows any variable to be dynamically created and visualized without any additional programming or change to model output.

All results can be exported to an ASCII file by simply choosing the location of interest (such as a river mouth) and selecting the Export option from the File menu. This allows the user to export data of particular interest to be viewed/analyzed using other software. SDA *SWAT Edition* provides a variety of media outputs for animation such as on-screen animation, off-screen movie recording, high-resolution static image export, and high quality print. Users can choose between AVI and MPEG movie format and can set the movie length, playback speed, and movie quality. The map can be captured as an image using the copy/paste operation through the clipboard, exported with high resolution or sent to printers directly for high quality output. This provides several options for sharing model results with those outside the SWAT modeling community.

Example Results

Figures 3-7 demonstrate some of the visualization capabilities of the SDA *SWAT Edition* software.

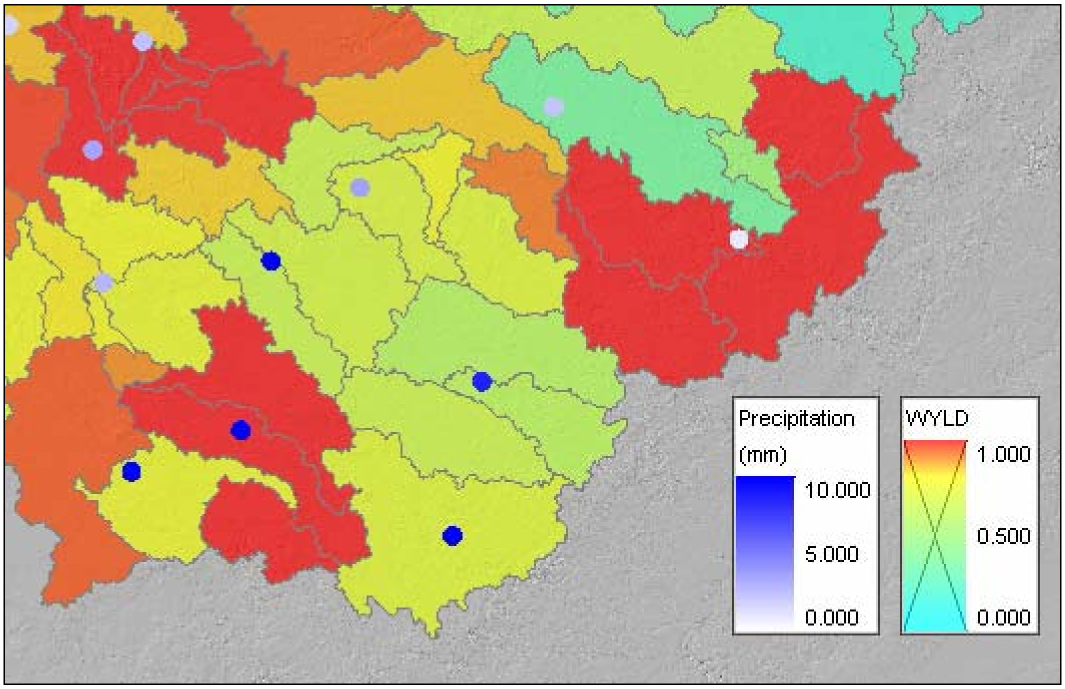

Figure 3: SWAT subbasin results and precipitation station input.

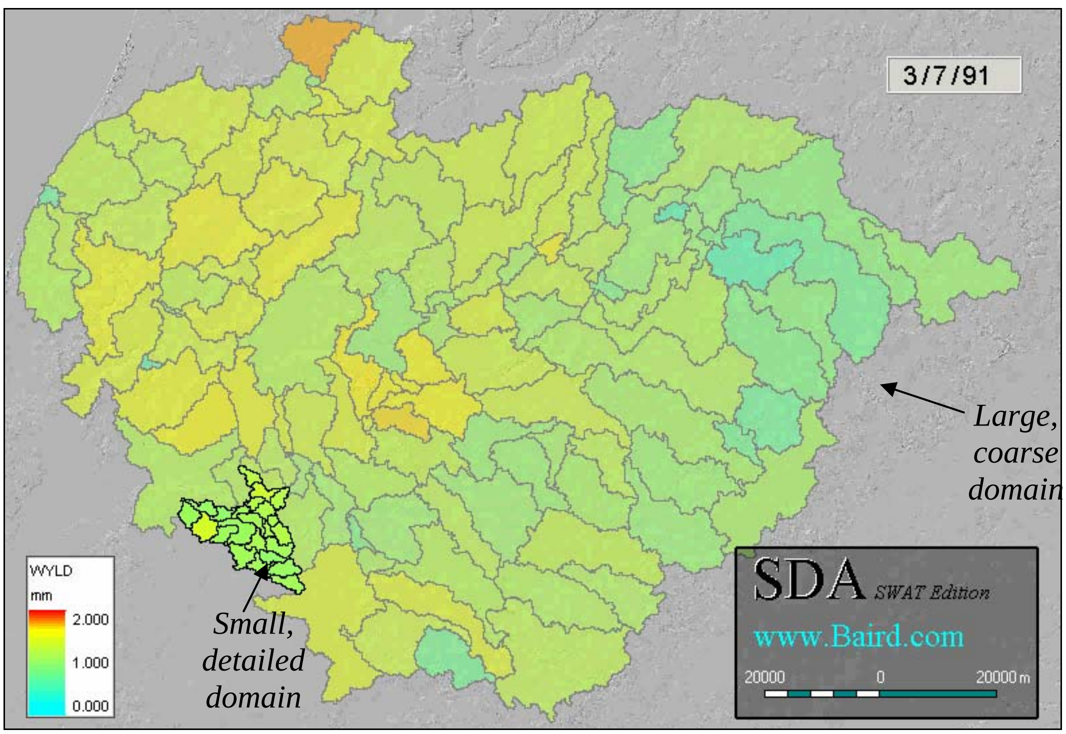

Figure 4: SWAT subbasin results for two different model domains.

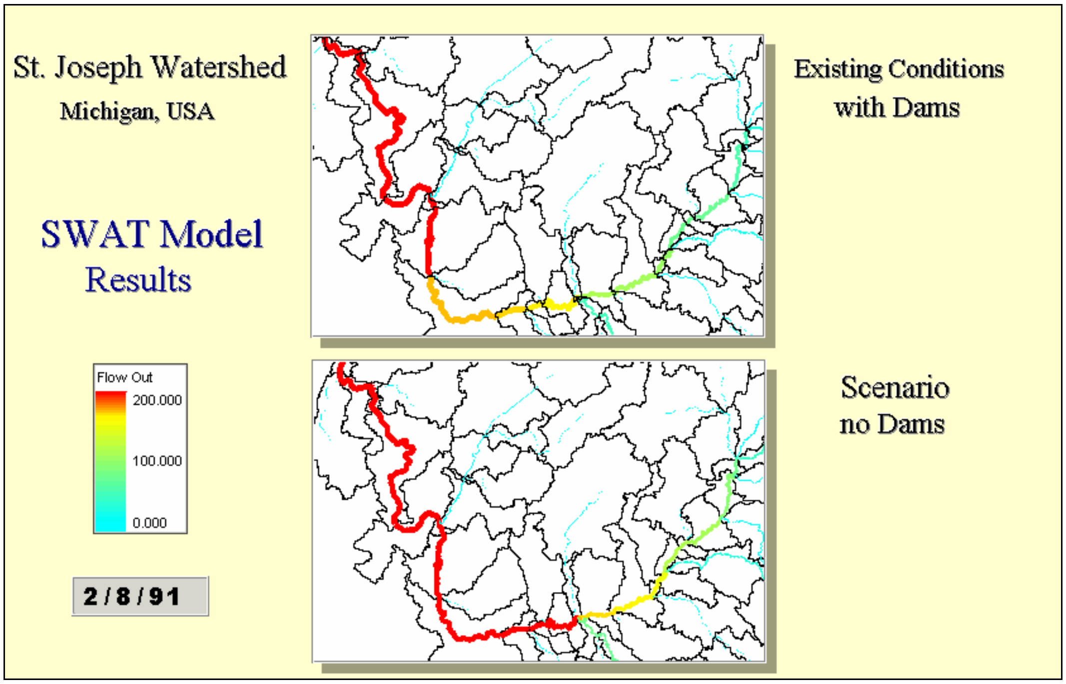

Figure 5: SWAT reach results for two different scenarios.

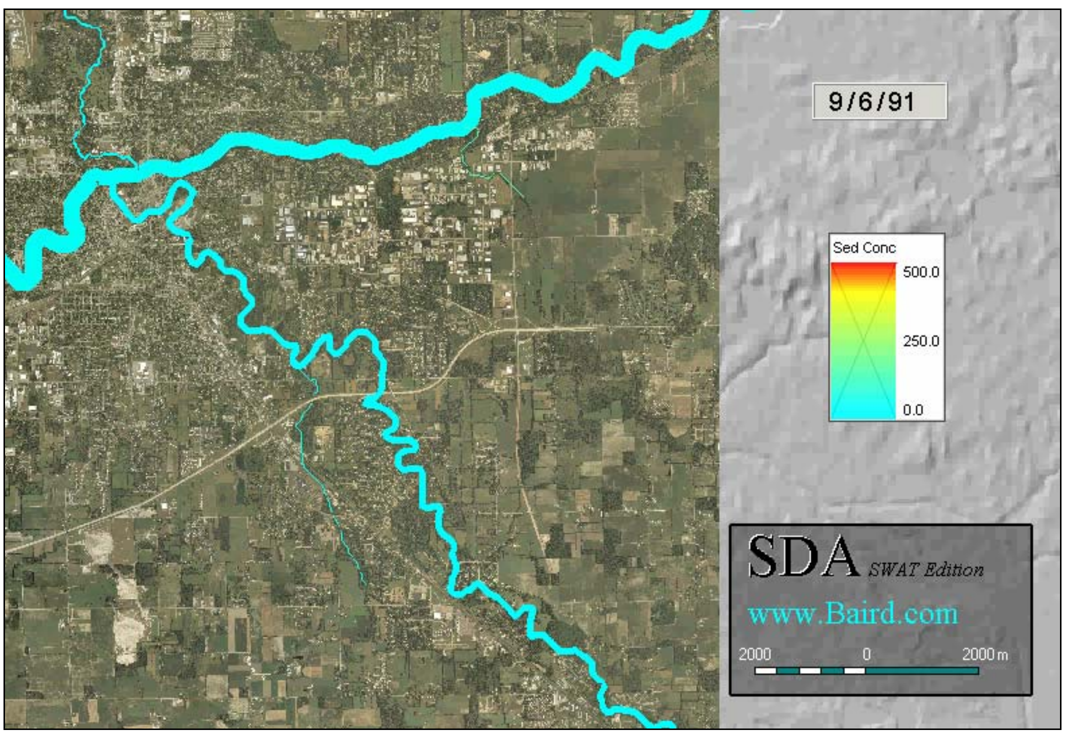

Figure 6: SWAT reach results overlaid on an aerial photo.

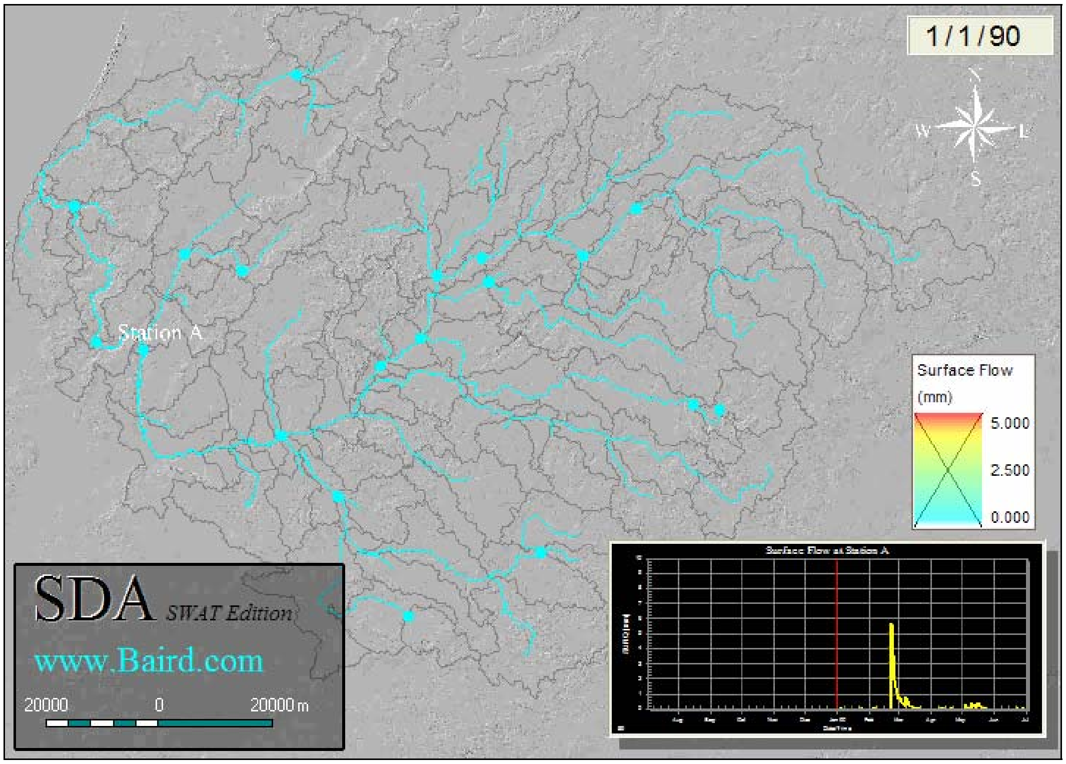

Figure 7: SWAT reach results with time series plot viewer of results at Station A.

Conclusions

SDA *SWAT Edition* is a GIS-based visualization and analysis tool customized specifically for SWAT model results. It has the ability to quickly and efficiently import large SWAT datasets and map and animate that data in a GIS environment. In addition to various analysis tools, the software enables SWAT modelers to easily share and convey their model results with those outside the SWAT user community. SDA *SWAT Edition* is an incredibly valuable tool for viewing and analyzing complex dynamic data sets in a flexible, efficient, and robust environment.

Future Development

Future development of SDA *SWAT Edition* may incorporate several new features including calculation of dataset and calibration statistics, such as average over a specified time period, Nash-Sutcliffe efficiency and r-squared; import and visualization of results by HRU; custom line plots, such as cumulative values and exceedence probability; and visualization of NEXRAD rainfall data grids. Depending on funding sources, these and other potential features may be incorporated into SDA *SWAT Edition* to make it a complete tool for SWAT model results analysis and visualization.

References

Di Luzio, M., R. Srinivasan, J.G. Arnold, and S.L. Neitsch. 2002. Soil and Water Assessment Tool. ArcView GIS Interface Manual: Version 2000. GSWRL Report 02-03, BRC Report 02-07, Published by Texas Water Resources Institute TR-193, College Station, TX. 346p.

Session III

9. **Optimal experimental design in river water quality modelling** **88**
   Veronique Vandenberghe, Ann van Griensven, Willy Bauwens and Peter A. Vanrolleghem

10. **Application of SWAT in developing countries using readily available data** **98**
    J.H. Jacobs and R. Srinivasan

11. **SWAT-DEG and channel restoration of urban streams** **107**
    P.M. Allen and J.G. Arnold

Optimal Experimental Design in River Water Quality Modelling

Vandenberghe Veronique[1], Ann van Griensven[1], Willy Bauwens[2] and Peter A. Vanrolleghem[1]
[1]Ghent University, Department of Applied Mathematics, Biometrics and Process Control (BIOMATH) Coupure Links 653, B-9000 Ghent, Belgium. E-mail: vero@biomath.Ugent.be
[2]Free University of Brussels, Laboratory of Hydrology and Hydraulic Engineering, Pleinlaan 2, B-1050 Brussels, Belgium

Abstract

This paper presents a methodology for the definition of an optimal set of sampling data for the calibration of a river water quality model. Starting with an extensive set of measurements, it is the aim of this study to reduce those data to obtain minimum data necessary for a calibration with acceptable uncertainty in the parameters. This method requires a model for the river under examination and availability of samples for a first calibration of the model. Synthetic time series data are generated using the model, which can be used as virtual observations. Then, the method of D-optimal design is applied. The amount, frequency, period, place, and type of variables measured for the water samples with the most reliable parameter estimates are considered to be the best observations for the river. Also, the percentage of improvement in reliability can be defined as a function of the observations taken. This method is applied to the River Dender, Belgium.

Introduction

Parameters for a river water quality model are not always practically identifiable due to a lack of data or the fact that data are taken during periods or in places that are not suitable for calibration of the model. Optimal experimental design (OED) techniques are a useful tool to construct experiments that contain information necessary for model calibration of the system under consideration. OED applications exist in many disciplines such as modelling of waste water treatment plants (Vanrolleghem et al., 1995), modelling of pyruvate production (Zelic et al., 2004), groundwater modelling experiments (Catania et al., 2004), systems biology (Faller et al. 2003), food technology (Nahor et al., 2001), pharmacology (Fedorov and Leonov, 2001) and electrical engineering (Ko et al., 2004). A common element in all of these applications is that the experimental conditions such as temperature, time, pH, measurement frequency, initial concentration, etc., are controllable. For a natural river system, things become more complicated as a combination of different factors like temperature, flow, and concentration do not occur at the desired time and as such, a method must be found which maximises the content of information of experiments, without knowing the exact situations under which those measurements will occur. Further, external conditions such as weather, river discharges, or diffuse pollution into the river can change year after year, so measurements that are likely to be optimal for a particular year can appear to be sub-optimal the next year. All of these reasons mean that a straightforward, optimal experimental design cannot be used for river water quality modelling, and extensions of those designs are needed to find a good measurement set-up.

It is the aim of this study to find a good set-up for measurements for the calibration of a river water quality model, based on a set of previous measurements and a model calibrated with those measurements. It is assumed that the calibrated model gives good results but that the uncertainty bounds are too wide to draw reliable conclusions for management decisions. Another goal is to find a cost-effective solution, so the obtained amelioration with more or better measurements will be linked and compared to costs and practical considerations. The methods are applied in a practical case study on the River Dender in Flanders, Belgium.

The River Dender

The River Dender, a tributary of the River Scheldt, drains an area of 1,384 km^2. The flow of the river is very irregular with high peak discharges (100 m^3/s) during intense rainfall and very low discharges (1 m^3/s) during dry periods. To suit navigation and to temper the high flows, the Dender is canalized and regulated by 14 sluices. Due to this, during dry periods the river reacts as a succession of reservoirs with a typical depth of 3 to 5 m, a width of 12 to 50 m and lengths of 2 to 8 km. In periods of high flow, all sluices are opened and the river regains its natural stream profile (Bervoets et al., 1989). The river is heavily polluted by domestic, industrial, and agricultural pollution (Demuynck et al., 1997).

ESWAT

An extended version of the Soil Water and Assessment Tool (SWAT) (Arnold et al., 1996), ESWAT, was applied to the River Dender. In ESWAT (van Griensven and Bauwens, 2001), an in-stream water quality model based on QUAL2E (Brown and Barnwell, 1987) has been implemented. Moreover, the processes were represented on a sub-daily time basis to allow for applications to smaller river basins and for the simulation of the impacts of eutrophication (e.g. diurnal dissolved oxygen dynamics due to algal growth). The model was calibrated, using a multi-objective calibration technique, based on high frequency water quality observations during the last four months of 1994 (van Griensven et al., 2002). The water quality calibration parameters included oxygen, BOD, ammonia, nitrate, and phosphate at a downstream location (Denderbelle). A sensitivity analysis showed that the water quality module implemented in ESWAT for the Dender requires the calibration of eight parameters (Vandenberghe et al., 2002)

Methodology

The purpose of this study is to maximize the practical identification of critical datat sets by defining an optimal experiment that increases the information content of the data. Different experiments (sampling schemes) will reveal more or less information and more or less parameter reliability, e.g. schemes that lack dynamics will provide less information than schemes with more. Optimal sampling design techniques aim at the identification of sampling schemes to improve different aspects of the mathematical modeling process, according to explicitly stated objectives (Dochain and Vanrolleghem, 2001; De Pauw and Vanrolleghem, 2004). The objective considered here is to increase the precision of the parameters for the water quality module ESWAT. The method used here is the D-optimal experimental design (Goodwin and Payne, 1977; Walter and Pronzato, 1999), because this method is the most general method for minimising the error on all estimated parameters. In a D-optimal experimental design, the precision of the parameters is assessed by considering the determinant of the inverse of the covariance matrix of the parameter estimates (*C*) or Fisher Information Matrix (FIM) (Godfrey and Distefano, 1985) (Equation 1).

$$C(b) = \sigma^2 \left(S^T Q S\right)^{-1} \qquad FIM(b) = C^{-1}(b) \tag{1}$$

where *b* represents the model parameter vector, *Q* a diagonal matrix, with the elements being the squares of the observation weights and *S* is the sensitivity matrix of outputs to parameters. Calculation of the covariance matrix based on the Jacobian matrix, instead of the Hessian, is acceptable when assuming linearity and observations with constant standard deviations (Bard 1974). The determinant of the FIM, Det(FIM) is proportional to the volume of the confidence region. Thus, by maximizing Det(FIM), the volume of the confidence ellipsoids, and, correspondingly, the geometric average of the parameter errors is minimized. D-optimal experiments also have the advantage of being invariant with respect to any scaling of the parameters (Petersen 2000). For non-linear models the FIM is parameter dependent. The OED technique thus requires an initial data set to calibrate the model. Non-accurate parameter estimates may therefore lead to an inefficient experimental layout. This means that for the processes related to the non-accurate parameters better measurements could be identified. The design can only be approached by an iterative process of data collection and design refinement, known as a “sequential design” (Casman et al., 1988). Parameter values are adapted after every measuring campaign and thus, the parameter values converge at the end to the best estimates. Figure 1 shows the iterative scheme that is used to find the optimal measurements starting with a model that is calibrated with the currently available data. Next, each step is explained in more detail.

Generating Synthetic Data Series

The evaluation of different sampling schemes requires the availability of a long time series of high frequency water quality data at different locations along the river. Because such historical series were not available, synthetic observation data were generated by simulations with the ESWAT model. For realism, these were subsequently altered by the addition of pseudo-random noise. Noise was generated from a normal distribution with variations that are consistent with the accuracy of the measuring devices used to measure the variables (Vandenberghe *et al.* 2005). These variations include 3% for Dissolved Oxygen (DO); 10% for Biological Oxygen Demand (BOD) and 5% for NO_3 and NH_4. Then the parameters for the sampling layout were defined. Examples of such parameters are the sampling frequency, e.g. every two hours, location of the measurements, e.g. downstream and 6 km more upstream, and the kind of measured variables, e.g. DO + NH_3.

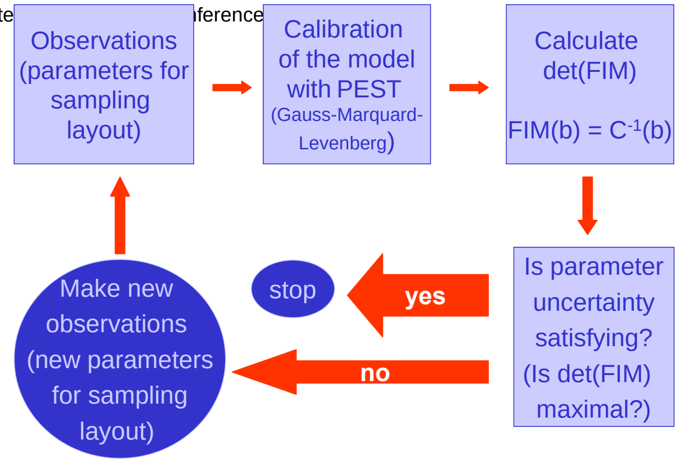

Figure 1. Optimal experimental design for river water quality modelling (PEST = Parameter ESTimation model (Pest Manual, 1994)).

Calibration of the Model

With the data selected from the synthetic time series on the basis of a certain sample layout, the model can be calibrated again. To be sure that the calibration process does not end in a local optimum, the initial parameter values are taken in the neighbourhood of the final parameter values obtained during the calibration with the available data. The purpose of this step is not to find the parameter values (as they are already known) but rather to obtain the Jacobian matrix during the calibration with a derivative-based method. Here the PEST (Parameter ESTimation) program (Pest Manual, 1994) is used. The PEST program calculates the covariance matrix of the parameters at the best estimate. This is the same as the inverse of the FIM, so the optimisation program in fact calculates the FIM.

Calculate the Determinant of the FIM

In this stage, one obtains the parameter uncertainty and the FIM from the calibration process. The parameter uncertainty can be propagated through the model to see the influence on the model results. In this step the determinant of the FIM, which is proportional to the volume of the confidence region around the parameters, is calculated.

Evaluation of the Det(FIM) and the Parameter Uncertainty

The loop can be continued by selecting different observations characterized by a different sampling layout or the program can stop when it is decided that the Det(FIM) is maximal or that the parameter uncertainty is satisfying. In this study, the loop will end once the observation set that maximizes the Det(FIM) is found.

Maximization of the Det(FIM) by Changing the Sampling Layout

The Shuffled Complex Method (SCE-UA) (Duan et al., 1992) is used here to optimize the parameters of the sample layout until a maximum of the Det(FIM) is found. The parameters of the sample layout are the parameters that are changed to obtain a maximisation of the objective function, the Det (FIM). After several evaluations of the Det(FIM), the shuffled complex method finds the optimum quite fast because the method searches the whole parameter space in an efficient and effective manner.

Results

As an illustration of the applicability of the method, a simple case, whereby only DO is considered at one specific location is presented first. The synthetic observation series consists of one year of hourly data. The optimization is limited to the measuring frequency, the number of samples, and the period of the year for sampling. The sampling time-step was allowed to vary between one hour and two days; the minimum number of samples was one and the maximum number was 365*24. Samples could be taken during winter, summer or a mixed summer-winter period, depending on the start of the period and the total number of samples that are taken. In Figure 2, the optimization process is shown. SCE-UA used 136 runs to find the optimum for which the Det(FIM) is largest. As was expected, the results show that the uncertainty in the parameters became minimal for the smallest sampling interval (Figure 3 left), a large number of samples (Figure 3 right) and a longer period, mainly spring and summer months (data not shown). A sample every hour, starting in February and ending on August 30th, representing a total of 5,804 samples appears to provide the best results.

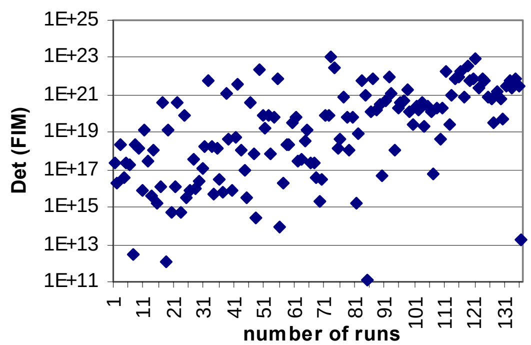

Figure 2. Optimization of the Det (FIM) (3 parameters of sampling layout).

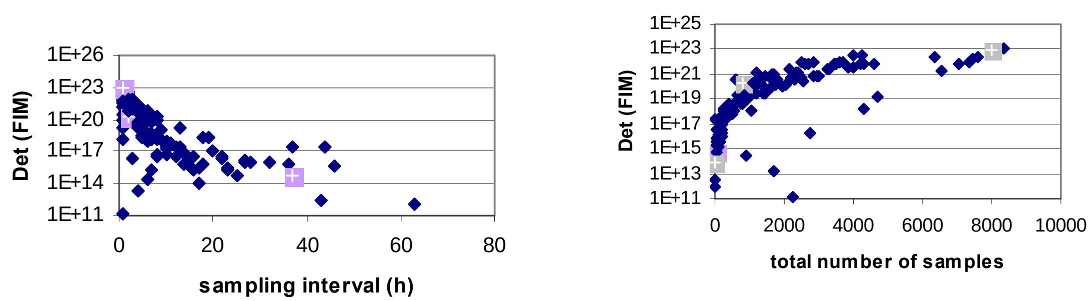

Figure 3. The Det(FIM) as a function of the total number of samples (left) and sampling interval (right) (points marked with an ⊞ are investigated further).

A second example shows a more complex case, whereby the data type (only DO or combined DO-NO_3, DO-NO_3-BOD, or DO-NO_3-BOD-NH_4) and sample locations (four possible combinations of three possible locations: upstream, halfway, downstream) are considered as parameters for the sampling layout. A substantial increase in the number of iterations for the optimization was observed (Figure 4). The best way to take samples is on an hourly time basis (Figure 5 left), over nearly the entire year (8,730 samples) (Figure 5 right), on two locations (data not shown) and with measurements of the four variables (data not shown). This is again a very logical result. However, Figure 5 depicts other possible sampling schemes that provide a quasi-similar accuracy, with fewer samples or a lower frequency. As can be seen in Figure 5, e.g. the confidence regions around the parameters do not differ much in the range of 5,000 to 8,000 samples. This is explained by other factors that influence the accuracy, such as the period of the year during which the samples were taken.

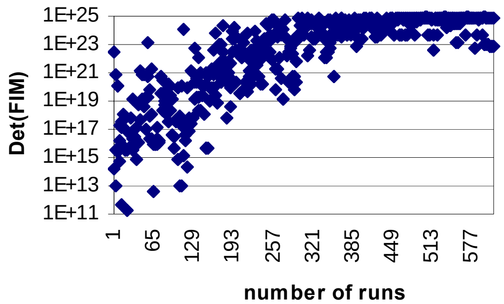

Figure 4. The optimization of the Det(FIM) with variation of five parameters.

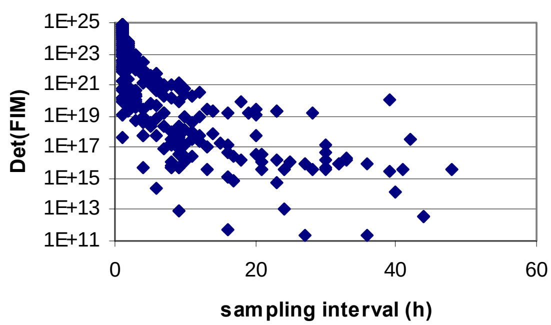

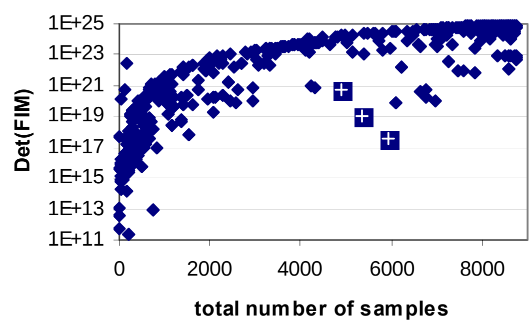

Figure 5. The inverse of the Det(FIM) as a function of the sampling interval (left) and the total number of samples (right).

Alternatively, some sampling schemes clearly appear as non-optimal (such schemes are indicated by squares in Figure 5). These schemes require large numbers of samples, but due to the wrong choice of other factors, the information content of these schemes is poor. More details on these schemes are given in Table 1. The reason for the poor performance of these schemes is related to the sampling location (upstream) and to the fact that the sampling period does not include the spring, which seems here to be important for the calibration process.

Table 1. Non-optimal sampling designs.

Sampling interval (h)	Number of samples	Period	Location	Observed variables	Det(FIM)
1	5972	16 Apr.-31 Dec.	Geraardsbergen	DO-NO_3	4,08E+17
1	5340	22 May-15 Nov.	Geraardsbergen	DO-NO_3-BOD	1,19E+19
1	4902	11 May-31 Dec.	Geraardsbergen	DO-NO_3-BOD	5,92E+20

The Search for the Optimal Experimental Design Including Practical Considerations

The value of the Det(FIM) has no physical meaning. A further analysis is needed to check the improvement of the calibration with the optimal set of measurements in contrast with (for calibration purposes) a weaker measurement set, which is characterized by lower costs and efforts to improve feasibility. The performance of the calibration is evaluated by looking at the final uncertainty of the model results, taking into account the variances and correlation between the parameters after calibration. This is because, in practice, one may only be interested in the model results and not in the parameters themselves. The uncertainty of the results is then evaluated in view of acceptability towards the purpose of the model.

To illustrate the procedure, three sampling schemes from the first test case are considered (indicated by squares in Figure 3). More details about the schemes are given in Table 2. The model outputs and the 95% confidence intervals for the considered schemes for one day (February 22), chosen because of the low oxygen content that increases during the day, are given in Figures 6 and 7. The results of the uncertainty analysis show that the average width of the confidence interval in the model output is reduced by 45% for scheme 2 when compared to scheme 1 and by 60% if scheme 3 is compared to scheme 1. The results illustrate the possibilities of the method to define a dedicated sampling strategy, in view of a given modelling accuracy.

Table 2: Selected sampling schemes for evaluation of resulting uncertainty in model output.

Sampling interval (h)	Number of samples	Period	Det(FIM)
37	42	26 Oct.-31 Dec.	4,93E+14
2	818	23 Oct.-31 Dec.	1,69E+20
1	8008	2 Feb.-30 Aug.	9,62E+22

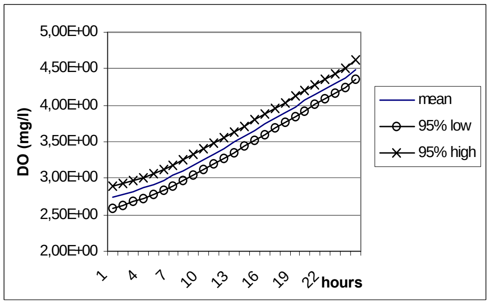

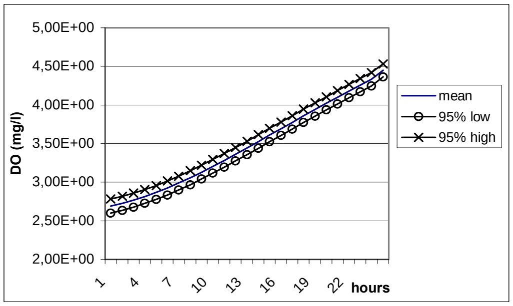

Figure 6. DO with confidence bounds for February 22, sampling scheme 1 (l) and 2 (rt).

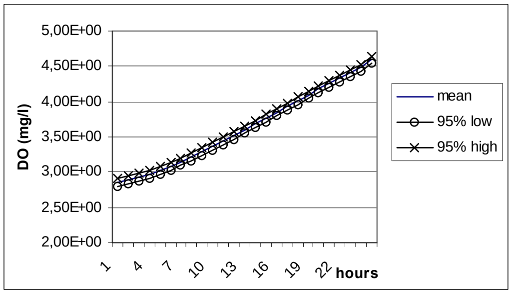

Figure 7. DO with confidence bounds on February 22, sampling scheme 3.

Based on the results of OED it is possible to determine to what extent more expensive measurements can be substituted with less expensive ones. Therefore, a comparison is of the Det(FIM) based on the number of measured water quality variables can be made (Figure 8).

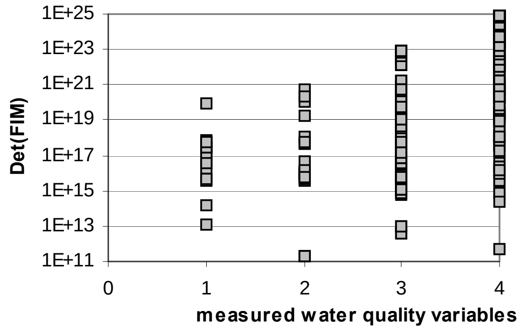

Figure 8. Det(FIM) as a function of the measured water quality variables. (1= DO; 2 = DO + NO_3; 3 = DO + NO_3 + BOD; 4 = DO+NO_3 +BOD + NH_4)

As shown in Figure 8, the highest Det(FIM) that can be obtained without measuring BOD is 1E+21, or 1E+25 including the BOD measurement . Again, the uncertainty on the simulated DO concentrations must be checked. In addition, a cost analysis is needed, as it is possible that measuring DO at high frequency during the entire year is more expensive than measuring BOD during three months at a low frequency.

Conclusions and Recommendations

It has been shown that OED methods can be used for an iterative, sequential design of a strategy for measuring water quality variables in a river, in view of the calibration of water quality models. First, a relatively extensive set of measurements is needed to set up a model for the river. Using this model, the OED method enables the definition of efficient measurement strategies to find better model parameter estimates and reduce the uncertainty in those estimates. In subsequent stages, the measurement strategy can be updated in an iterative way.

This method has been successfully applied to the River Dender. If the goal is maximal accuracy, the optimal sampling strategy has the highest number of samples and the highest sampling frequency, at the maximal number of locations, and whereby a maximal number of variables are measured. The usefulness of the method, however, resides in its ability to evaluate sub-optimal sampling strategies, whereby strategies are evaluated in view of the limitations of costs and other practical considerations. This can be of great importance for some costly and time-consuming analysis of samples, e.g. for pesticide modeling and monitoring. By extending the OED method with a procedure for the definition of the modeling uncertainty, it becomes possible to define the optimal sampling strategy to obtain a given modeling accuracy.

Further extensions of the OED can be considered according to the objectives or possibilities of the experimental design. A first extension can be the addition of more or additional parameters for the sampling layout. Those can be other measurable variables such as suspended solids and water temperature or additional sampling locations. One may also try to determine whether or not a distinction must be made between the different variables in relation to their sampling frequency and period. As such, sampling schemes can become extremely efficient. Another extension may be the use of different evaluation criteria for the OED because criteria other than the maximization of the Det(FIM) could be more suitable for other studies. For example, the reliability of the parameter estimates can be less important than the final uncertainty on critical values of certain parameters. Therefore, it is evident that in such cases other schemes for the OED can be applied (or a combination of different criteria).

Acknowledgements

The authors would like to give special thanks to the financial support of the EU Harmoni-CA project (EVKI-CT-2002-20003) and the EU CD4WC project (EVK1-CT-2002-00118).

References

Arnold, J.G., Williams, J.R., Srinivasan, R. and King, K.W. (1996). *SWAT manual*. USDA, Agricultural Research Service and Blackland Research Center.

Bard, Y. (1974). *Nonlinear parameter estimation*, Academic Press, New York and London.

Bervoets, L., Schneiders, A. and Verheyen, R.F. (1989). *Onderzoek naar de verspreiding en de typologie van ecologisch waardevolle waterlopen in het Vlaams gewest. Deel 1 - Het Denderbekken*. Universitaire Instelling Antwerpen. (in dutch)

Brown, L.C. and Barnwell, T.O. (1987). *The enhanced stream water quality models, QUAL2E and QUAL2E-UNCAS: Documentation and User Manual.* U.S. EPA.

Casman, E.A., Naiman, D.Q. and Chamberlain, C.E. (1988). Confronting the ironies of optimal design: nonoptimal sampling designs with desirable properties. *Water. Resour. Res.* **24** (3), 409-415.

Catania, F., Massabò, M., Minciardi, R., Paladino, O. and Robba, M. (2004). Optimal sampling for parameters estimation. In: *Proceedings of iEMSs 2004 International Congress: Complexity and Integrated Resources Management*, Osnabrueck, Germany, June 2004.

De Pauw, D. and Vanrolleghem, P.A. (2004). Optimal experimental design for model calibration: general procedure. In: *Proceedings of PhD symposium*, Ghent, Belgium.

Demuynck, C., Bauwens, W., De Pauw, N., Dobbelaere, I. and Poelman, E. (1997). Evaluation of pollution reduction scenarios in a river basin: application of long term water quality simulations. *Water Sci. Tech.* **35** (9), 65-75.

Dochain, D. and Vanrolleghem, P.A. (2001). *Modelling and estimation in wastewater treatment processes*, London, UK.

Duan, Q., Gupta, V.K. and Sorooshian, S. (1992). Effective and efficient global minimalization for conceptual rainfall-runoff models. *Water Resour. Res.* **28**, 1015-1031.

Faller, D., Klingmüller, U. and Timmer, J. (2003). Simulation methods for optimal experimental design in systems biology. *Simulation* **79** (12), 717-725.

Fedorov, V.V. and Leonov, S.L. (2001). Optimal design of dose response experiments: A model-oriented approach. *Drug Information J.* **35** (4), 1373-1383.

Godfrey, K.R. and Distefano, J.J. (1985). Identifiability of model parameters. In: *Identification and System Parameter Estimation*(ed.), Pergamon Press, Oxford, pp. 89-144.

Goodwin, G.C. and Payne, R.L. (1977). *Dynamic system identification. Experiment design and data analysis*, Academic Press, New York.

Ko, Y., Kim, Y., Park, D. and Yun, I. (2004). Nonlinear diffusion process modeling using response surface methodology and variable transformation. *Robotics and computer-integrated manufacturing* **20** (2), 121-125.

Nahor, H.B., Scheerlinck, N., Verniest, R., De Baerdemaeker, J. and Nicolai, B.M. (2001). Optimal experimental design for the parameter estimation of conduction heated foods. *J. Food Eng.* **48** (2), 109-119.

Pest Manual (1994). Model independent parameter estimation. Watermark computing.

Petersen, B. (2000). Calibration, identifiability and optimal experimental design of activated sludge models. PhD-thesis, Ghent University.

van Griensven, A. and Bauwens, W. (2001). Integral water quality modelling of catchments. *Water Sci. Tech.* **43** (7), 321-328.

van Griensven, A., Francos, A. and Bauwens, W. (2002). Sensitivity analysis and auto-calibration of an integral dynamic model for river water quality. *Water Sci. Tech.* **45** (9), 325-332.

Vandenberghe, V., Goethals, P., van Griensven, A., Meirlaen, J., De Pauw, N., Vanrolleghem, P.A. and Bauwens, W. (2005). Application of automated measurement stations for continuous water quality monitoring of the Dender river in Flanders, Belgium. *Env. Monit. Assess.* (in press).

Vandenberghe, V., Van Griensven, A. and Bauwens, W. (2002). Detection of the most optimal measuring points for water quality variables: Application to the river water quality model of the river Dender in ESWAT. *Water Sci. Tech.* **46** (3), 1-7.

Vanrolleghem, P.A., Van Daele, M. and Dochain, D. (1995). Practical identifiability of a biokinetic model of activated sludge respiration. *Water Res.* **29**, 2561-2570.

Walter, E. and Pronzato, L. (1999). *Identification of parametric models from experimental data*, Springer Verlag, Heidelberg.

Zelic, B., Vasic-Racki, D., Wandrey, C. and Takors, R. (2004). Modeling of the pyruvate production with Escherichia coli in a fed-batch bioreactor. *Bioproc. Biosys. Eng.* **26** (4), 249-258.

Application of SWAT in Developing Countries using Readily Available Data

J.H. Jacobs* and R. Srinivasan
Spatial Sciences Laboratory, Texas A&M University, 1500 Research Parkway, Suite B223, College Station, TX 77845

*Corresponding author: phone: 979-458-8051; fax: 979-862-2607; e-mail: jhjacobs@tamu.edu

Abstract

The Upper Tana River Basin is strategically one of the most critical resource areas of Kenya. The Masinga Reservoir, at the outlet of the basin, provides water and hydroelectric power for 65% of the nation. Unregulated deforestation and expansion of cultivation practices onto marginal soils in this critical river basin has resulted in significant reservoir siltation and reduced water quality. Reforestation of zones moving down slope from 2,000 m, to 1,950 m, 1,900 m and 1,850 m elevation would represent a 30 to 55% increase in reforested area in the Upper Tana River Catchments. The Soil and Water Assessment Tool (SWAT) model was used to evaluate these various reforestation scenarios. The results of this analysis show that full implementation of reforestation down to 1,850 m would result in a 7% decrease in sediment loading in the Masinga Reservoir. These results were obtained through the modification and merging of datasets from a wide variety of existing sources to create complete model inputs. In addition, these scenario models were run in a "relative" comparison mode due to the lack of high quality observed sediment data. However, the model was rudimentarily calibrated for flow on a monthly basis. This study demonstrates a successful application of SWAT with limited readily available data, such as in developing countries.

Key Words: hydrology, reforestation, Kenya, Tana River, SWAT, erosion, runoff, impact assessment

Introduction

During the last 100 years, the amount of forested area in Kenya has dwindled, with approximately 1.7% of forest land area remaining (UNEP, 2001). Causes of the deforestation are related to land tenure policies, logging of indigenous species, charcoal production, cultivation, and land settlement (Lambrechts et al. 2003). From a hydrological standpoint, these forests are located in the upper catchments of the major watersheds that provide water for hydroelectric power generation, agriculture, and industrial and household use.

The Tana River and its tributaries form the major water flow outlet from Mount Kenya and the Aberdares. This river system is the largest river in Kenya and its catchment area occupies approximately 17% of the country. The Masinga Dam is by far the greatest regulator of the Tana River system, given its size and strategic location in the upper reaches of the system (Pacini et al. 1998). In addition, most of the highland forests of the Tana system occur in the Upper Tana Catchment above the Masinga Dam (Schneider and Brown, 1998). The dam serves as a storage reservoir which helps control the flow of water through a series of downstream hydro-electric reservoirs. The Masinga Dam does generate electricity, however, at lower capacity than those downstream.

Study Area

Model simulations for this study were conducted in the Upper Tana River Basin in Kenya. The study area catchment is northeast of Nairobi and comprises approximately 10,000 km^2 of the total 100,000 km^2 area of the entire basin. This is the headwaters of the Tana River, an important source of water and hydroelectric power in the area. The major tributaries arise on the slopes of Mt. Kenya and the Aberdare Range, and the river then travels approximately 1,000 km to the eastern coast of Kenya and empties into the Indian Ocean.

The elevation of the study area ranges from 4,700 m on Mt. Kenya to a low of 730 m near the Masinga Dam. Soils, rainfall, and therefore land use generally follow this elevation gradient. The soils in the area consist of Andosols (M2) in the upper elevations, Nitosols (R1, R2, and R3) in the mid-elevations, and Ferallsols (Um19) and Vertisols (L11, Up4) in the lower elevations of the catchment. Mt. Kenya and the Aberdare Ranges receive greater than 1,800 mm/yr rainfall. Forests and tea crops are predominately found in this area. The mid-elevations, between 1,200 and 1,800 m, receive between 1,000 and 1,800 mm/yr rainfall. This area supports most of the intensive agriculture. Crops include coffee, maize, bananas, napier grass, and beans. The lower elevations, below 1,000 m, receive less than 700 mm/yr rainfall. This area consists mainly of rangelands which are used for livestock grazing (Otieno and Maingi, 2000). At all elevations, however, there is a distinct seasonal variation in river flow. There are two wet periods of three months separated by dry periods, with most of the rain falling from March through May and slightly less in the period from September through November. During the dry periods, there is a high demand on water for irrigation, urban consumption, and hydroelectric power. The Masinga Dam was constructed to address this need for a consistent water supply to the area. This dam is situated at the outlet of the study area catchment. It regulates the flow of water to a chain of downstream reservoirs (Kamburu, Gitaru, Kindaruma and Kiambere) and serves as a water supply to the surrounding area (Watermeyer et al., 1976).

Materials and Methods

Obtaining physically-based data for hydrologic modeling is often difficult, even in developed countries, where data of high quality are generally collected and analyzed. However, in developing countries it is always a challenge to assemble the data needed to complete a rigorous watershed assessment. In many cases, the data that are available were collected for different purposes and may have been manipulated before publication based on the original project needs. The result, therefore, is often low spatial and temporal resolution of the natural resource information needed for hydrologic modeling. For example, available data may have been aggregated to a large scale that is difficult to disaggregate to a more local scale without making assumptions. Furthermore, compiling complete datasets for meaningful analysis of an entire study area can be even more challenging. For this study data was obtained from a wide variety of sources, including government agencies, NGOs, and other world organizations, and it was not well organized.

Data and Processing

The main datasets used in hydrologic analysis include elevation, climate, land use, and soils. Modification and pre-processing of these datasets for use in model applications was the most challenging part of this analysis. Elevation data was obtained from the Blackland Research and Extension Center in Temple, Texas. A USGS 1 km DEM which was refined by the Shuttle Radar Topography Mission (SRTM) DEM data, was resampled to a 100 m resolution using an ArcView spline routine (Paul Dyke, personal communication). All other datasets required more extensive manipulation for use in the model.

Climate data is one of the most critical datasets for watershed analysis. In this case, developing an adequate spatial and temporal coverage for the study area was a challenge, considering the vast differences in elevation from mountain tops to lowland areas. In addition, most of the actual observed data were available only at the highest elevations. Therefore, this data was obtained from several sources, each of which only covered portions of the watershed study area. These data were individually processed and then merged to create a complete weather data input for the model. First, historical precipitation and air temperature data were collected from the two World Meteorological Organization (WMO) stations located in the study area. These were the Nyeri and Embu stations, and data was only available for the period from 1978-1997. Additional rainfall data was obtained for the northern portions of the watershed from the Natural Resources Management Trust, Nanyuki, Kenya. This historical data was collected from towns, farms, and plantations in the Laikipia region of Kenya. Finally, rainfall data for the southern portions of the watershed were obtained from the Collaborative Historical African Rainfall Model (CHARM) dataset. The CHARM data was derived from combined daily rainfall reanalysis fields, monthly interpolated rainfall, and an orographic precipitation model to allow for spatial and temporal representation of daily rainfall on an 11 x 11 km grid for the entire African continent for the period from 1961-1996 (Funk et al., 2003). The CHARM rainfall data represent a smoothed daily rainfall since it is derived from 10-day accumulated historical data. Because the smoothed data had a tendency to over or underestimate daily events, the data were “event corrected” using event statistics from the WMO stations, thus allowing the CHARM data to behave in a more hydrologically correct manner.

Raingauge stations for this analysis were identified by location and in order of importance (WMO, Laikipia and CHARM) based on the accuracy of the dataset. In all, 20 stations were used in this analysis (Figure 1).

Land use classifications and the management thereof are key factors in simulating runoff and sediment loss, and it can again be difficult to produce meaningful model results without accurate spatial and temporal information. Land use for this analysis was derived from a combination of Kenya Department of Resource and Survey and Remote Sensing (DRSRS) and the Japan International Co-operation Agency (JICA, 1987) data. DRSRS surveys were conducted in medium and high potential agricultural areas (Njuguna, 2001). These surveys resulted in the identification of point locations for a 2,400 x 4,800m irregular grid of percent land use classifications. These points were converted to ESRI grid format, and only land use types that comprised greater than 90% for a given point were used for further analysis. At most, four land uses were defined for each grid cell and then weighted based on percent contribution. Data obtained from JICA was used in low agricultural potential areas, i.e. forested areas in the north western and rangelands in the southeastern portions of the watershed. These data were merged

with processed DRSRS survey data to create a continuous land use layer for model application. A total of 1,100 unique land use combinations were used in this analysis (Figure 2).
The Kenya 1:1 million scale Soil and Terrain (KENSOTER) database developed by the Kenya Soil Survey (KSS) and the International Soils Reference and Information Centre (ISRIC) was used to define soil units for the study area. In the KENSOTER spatial database, soil map units represent a soil series or association of several soils. For this study, the dominant soil type within each map unit was extracted, along with the associated attribute data, for use in the model. The soil parameter estimator from the EPIC crop model and the Soil Water Characteristics calculator (http://www.bsyse.wsu.edu/saxton/soilwater/) were used to fill in gaps for soils with missing or no attribute data.

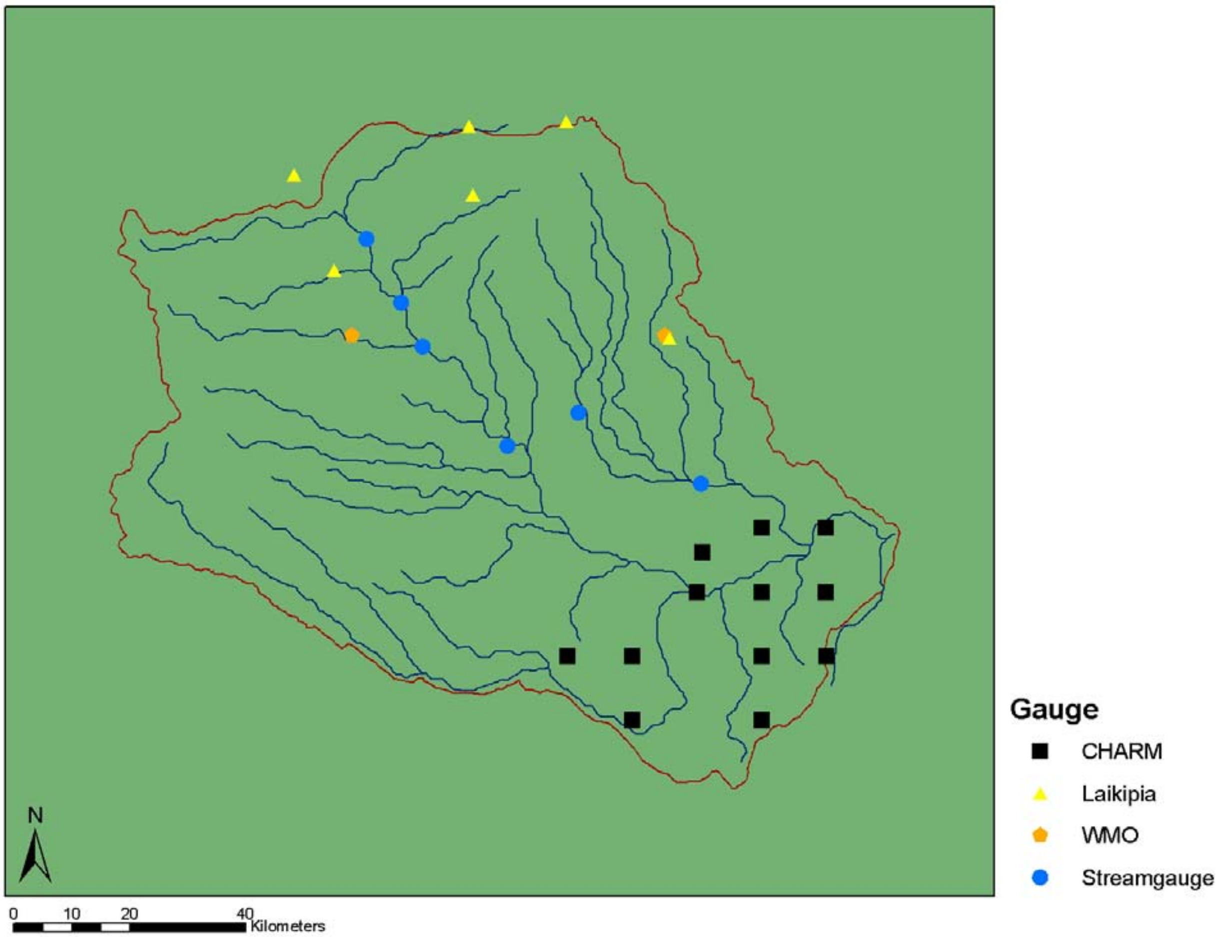

Figure 1. Rain and streamgauge locations for the study area simulations.

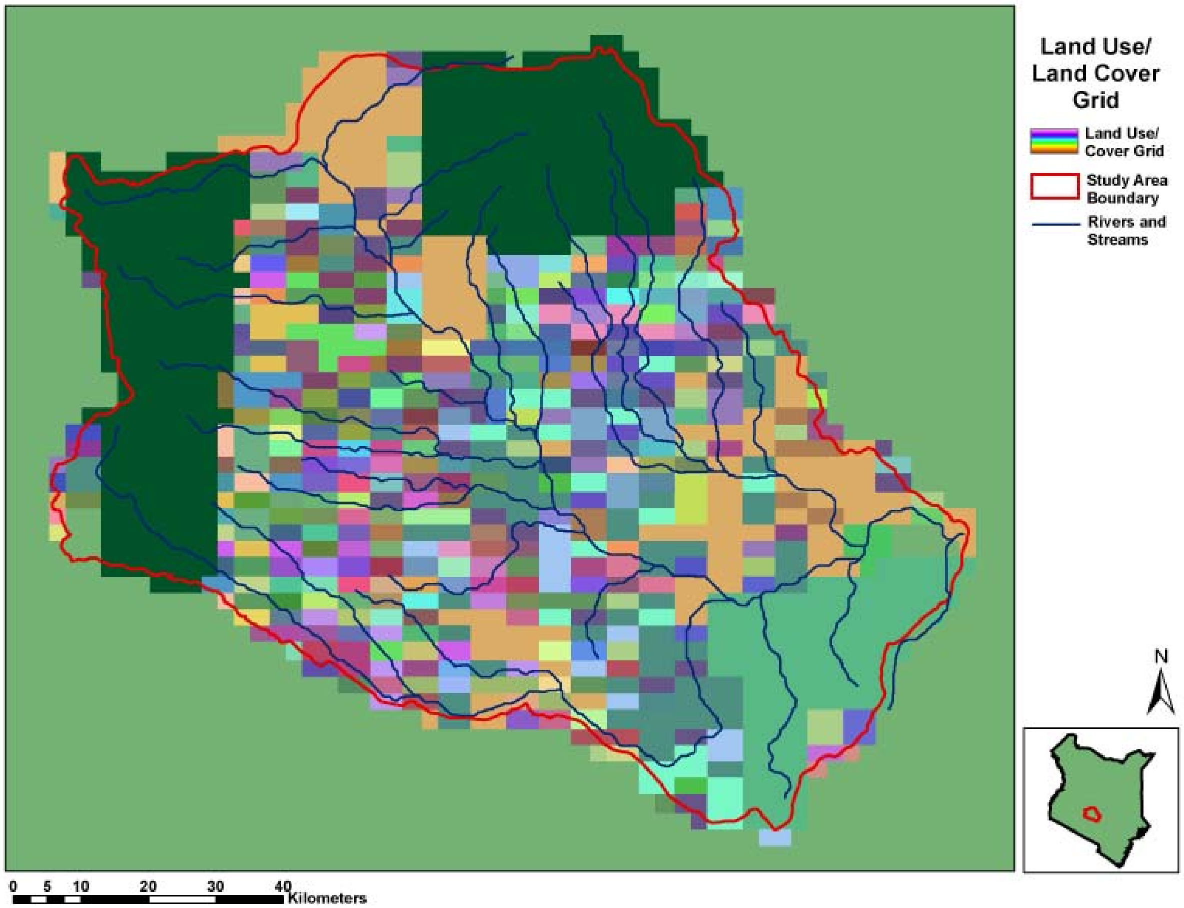

Figure 2. Land use grid used for the base hydrology analysis. Each grid cell (2400 x 4800 meters) represents a combination of up to 4 dominant land uses. Colors represent unique combinations of land uses.

Model and Setup

In this study, the Soil and Water Assessment Tool (SWAT) model was used to simulate the environmental implications of reforestation in the higher elevations of the Upper Tana River Basin. The basin was represented by 60 subbasins with a 9,752.82 km^2 area for the model simulations. The time period for analysis was from 1978-1995; however, the first three years of the simulation were used as a "warm-up" period in which the model's initial conditions were established. These years were therefore not included in the final result comparisons. The results reported in this study for various simulations consist of data for the time period from 1981 to 1995. In addition, no model calibration was attempted except for adjustments in the baseflow recession constant.

This study consisted of a two phased approach. In phase I, the model was developed to represent existing conditions. Detailed information concerning runoff and sedimentation were collected during this run. In phase II, the model was configured to reflect various management scenarios, namely zonal reforestation in the upper reaches of the catchment. Graded reforestation scenarios were implemented at the 2,000, 1,950, 1,900, and 1,850 m intervals in which the entire area above a given elevation contour was filled with forest land cover.

Results

Due to the lack of reliable observed streamflow data, it was difficult to calibrate and validate the initial model run before scenario implementation. In this case the model was run in a "relative" mode, i.e. the initial model results were used as a baseline comparison for each of the scenario runs. These results were then reported in terms of percent change rather than actual values.

Baseline Results

For the purposes of this study the catchment was divided into three main branches that combine to create the Masinga Dam inflow. These include the main branch, or Tana River, in the central reaches, the Thiba River in the northeastern reaches, and the Thika River in the southwestern reaches of the watershed. Simulated percent rainfall, runoff, and sediment contributions to the reservoir were calculated for these three branches. These contributions were greatest from the Tana subbasins, followed by the Thiba, then Thika subbasins.

It should be noted that due to the uncertainty in the sources of rainfall inputs and the lack of spatial correlation between these rainfall inputs, comparisons were made with the middle 95% of the data. The observed and predicted streamflow was sorted and the top and bottom 2.5% of the data were removed. This process removed both predicted and observed outliers from statistical analysis. In some cases additional data points were removed based on missing or incomplete observed flow data.

The Tana River subbasins account for 92.91% of the rainfall in the catchment, with 51.66% of the runoff, and 50.36% of the sediment load to the reservoir. This subwatershed comprises 57% of the study area; therefore, these results were expected. The Thiba subbasins account for only 4.25% of the catchment rainfall, but contribute 40% of the catchment runoff, and 43.81% of the sediment load to the reservoir. In addition, this subwatershed accounts for only 22% of the study area. Thika subbasins, on the other hand, play a minor role in the catchment with 2.84% of the rainfall, 8.34% of the catchment runoff, and only 5.83% of the sediment load (Figure 3). Furthermore, this subwatershed makes up the smallest portion of the study area at only 20%. Lastly, the total cumulative reservoir inflow and sediment load was calculated to be 70.94 million m^3 and 46.39 million tons, respectively, for the 14-year study period (1981-1995).

Scenario Results

For the 2,000 m interval simulation, forest cover was 2,932.76 km^2. Forest cover increased over each successive simulation of 1,950m, 1,900m, and 1,850m to include 3,077.22 km^2, 3,253.48 km^2 and 3,453.24 km^2 of forest area, respectively.

In general, grazing lands and tea were the main land use types to be displaced by forest restoration activities at all contour intervals. In addition, areas of displaced maize and coffee increased with each successive scenario.

Based on an examination of simulation results, change in total flow and the variance of flow was relatively insignificant and was therefore omitted from further evaluation. However, the change in sediment load was noticeable over the scenario simulations.

In general, sediment yield decreases with each successive scenario simulation (moving down slope from 2,000 m) or increase in forest cover. Values range from an annual average of 3.43 to 3.18 million tons of sediment to the reservoir (Figure 4). There is, however, a 0.6% increase from the 2,000 to 1,950 m scenario.

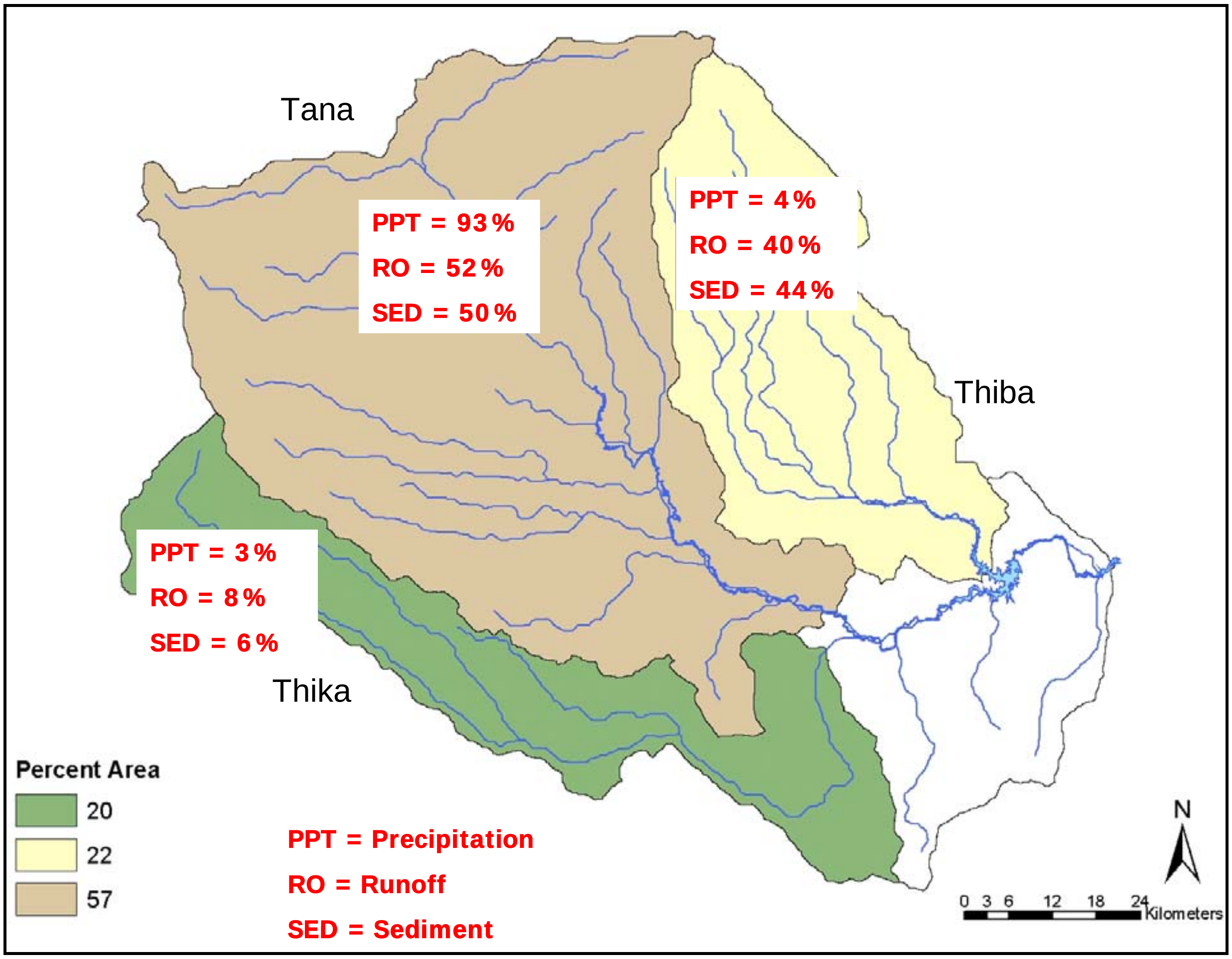

Figure 3. Percent rainfall, runoff, and sediment contributions to the Masinga Reservoir.

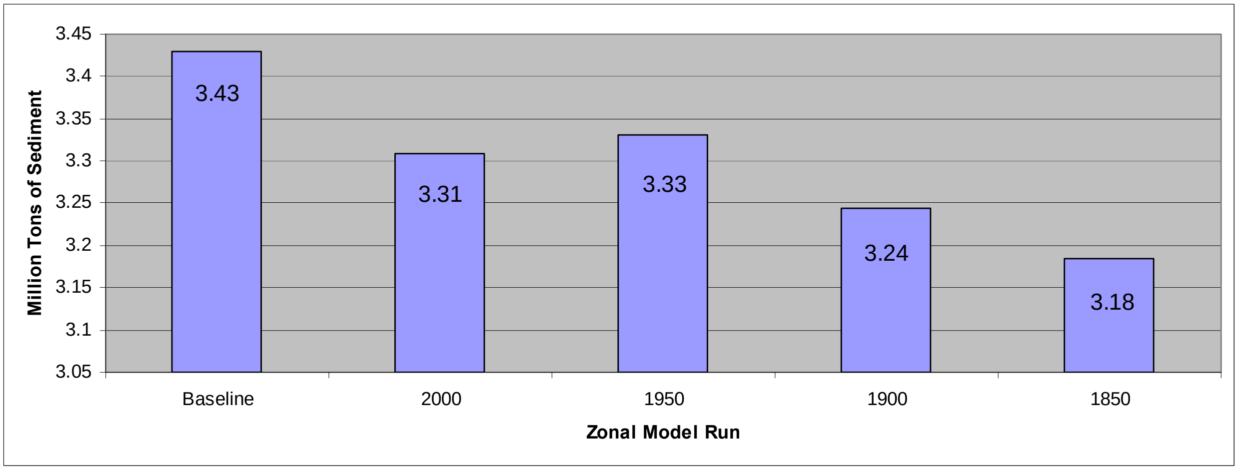

Figure 4. Average annual sediment yield for the catchment for current conditions (Baseline) and subsequent reforestation for the elevational zones going down slope from 2,000 m to 1,850 m.

Summary and Conclusions

Climate and land use data are arguably the two most important or driving factors in any hydrologic analysis. In this study however, these datasets were not readily available in a spatially and temporally explicit framework needed for further analysis. Instead, data was collected from various groups and merged to create complete study area coverage. As these data were merged, the most positive aspects of each were preserved and emphasized over others to produce the most spatially and temporally complete datasets possible. This lack of representative, high quality input data for the study area also prevented rigorous calibration and validation; therefore, the model was run on a relative basis. Despite some inconsistencies between model predictions and observed data (it should be noted that the predicted flow generally tracked the observed flow patterns throughout the study period), the initial results were used as a baseline for the relative comparison between stream flow and sediment transport under current conditions and various forest restoration scenarios.

Based on the relative comparison to baseline conditions, sediment load to the reservoir generally decreased with each successive simulation moving down slope. The only exception to this is in the 1,950 m scenario. The slight increase in sediment load from the 2,000 m to 1,950 m scenario could be attributed to the displacement of tea plantations that are prevalent in this elevation band. Established tea plantations would provide more canopy cover than young forests, and thereby reduce the total amount of sediment loss.

The results of this research suggest that implementation of full forest restoration up to the 1,850 m contour interval, with the exception of tea plantations, would reduce the amount of sediment reaching the reservoir by upwards of 7% per year. This would extend the life of the dam and improve water quality in the catchment as well.

These results were delivered to Kenyan Government Officials for use in policy planning. This would not have been possible except for the combination of data from various sources and modifications to best represent spatial and temporal variability and the use of relative model comparisons.

References

Funk, C., Michaelsen, J., Verdin, J., Artan, G., Husak, G., Senay, G., Gadain, H., Magadazire, T., 2003. The Collaborative Historical African Rainfall Model: Description and Evaluation. International Journal of Climatology 23:47-66.

JICA, 1987. Japan International Co-operation Agency, National Water Master Plan, Kenya.

Lambrechts, C., Woodley, B., Church, C., Gachanja, M., 2003. Aerial survey of the destruction of the Aberdare range forests. Division of Early Warning and Assessment, UNEP.

Njuguna, E.C., 2001. Aerial Survey Sample Photo Interpretation Report on Land Use Land Cover for Medium to High Potential Districts of Kenya. Kenya Department of Resource Surveys and Remote Sensing. Nairobi, Kenya. 8 pgs.

Otieno, F.A.O., Maingi, S.M., 2000. Sedimentation problems of Masinga Reservoir. In: Land and Water Management in Kenya. Eds. Gichuki, F.N., Mungai, D.N., Gachene C.K. and Thomas D.B. Published by Soil and Water Conservation Branch, Ministry of Agriculture and Rural development, Nairobi, Kenya.

Pacini, N., Harper, D., Mavuti, K., 1998. Hydrological and ecological considerations in the management of a catchment controlled by a reservoir cascade: The Tana River, Kenya. pp. 239-258. In: D. Harper and T. Brown (eds). The sustainable management of tropical catchments. John Wiley & Sons. Indianapolis, IN.

Schneider, H., Brown, T., 1998. Remote sensing and GIS studies of erosion potential for catchment management: A densely populated agricultural catchment in Kenya. pp. 31-47. In: D. Harper and T. Brown (eds). The sustainable management of tropical catchments. John Wiley & Sons. Indianapolis, IN

UNEP, 2001. Closed canopy forest cover: An Assessment of the Status of the World's Remaining Closed Forest. UNEP, Nairobi.

Watermeyer, Legge, Piesold and Uhlman, 1976. Upper reservoir scheme: Appraisal engineering report, vol. 2. Tana and Athi River Development Authority, Nairobi.

SWAT-DEG and Channel Restoration of Urban Streams

P.M. Allen[1], J.G. Arnold[2]
[1]Dept. Of Geology, Baylor University, Waco, Tx, Peter_Allen@baylor.edu ,(254)710-2189
[2]USDA-ARS/SPA, W. Skipwith, Halff Associates, Inc., Dallas, TX, and S. Berman, Halff Associates, Inc., Dallas, TX.

Introduction

Channel equilibrium occurs when all four variables, sediment discharge, sediment particle size, streamflow, and stream slope, are in balance. Changes in streamflow and sediment variables may occur due to changes in land use. Streams that are free to adjust will generally do so and reestablish new equilibrium conditions over a period ranging from decades to centuries. River and stream restoration seeks to quantify this relationship so that river adjustments, which can cause significant damage to existing urban infrastructure, can be avoided or at least reduced in scope and severity. In this paper, the methodology used to aid in design of urban streams is given to illustrate how the SWAT-DEG (Soil Water Assessment Tool-Degradation) model can be used in design of stable urban channels. Then, several other example applications of using the SWAT-DEG model of channel erosion are discussed.

Methodology

Channel Stability Assessment

a. Design Discharge

The procedure used in the channel stability assessment is illustrated in Figure 1. The soils, land use, channel and landscape slope, and geology of the basin are evaluated from field and mapped data. From this information, the channel forming discharge is calculated using regression equations and routed flood flow obtained from the unit hydrograph models for the watershed. Prior research has shown the active channel discharge is equivalent to approximately the 1.25-year Return Interval (R.I.) flood computed from Dempster's (1974) regression equations or the 0.5-year R.I computed by the unit hydrograph methods (HEC-1). The difference in the above-cited return periods is due to the treatment of antecedent moisture conditions in the model and possibly inferred loss rates for urban storms. Previous studies by the U.S. Geological Survey have shown similar problems of over prediction for high frequency storms using the unit hydrograph models calibrated for large floods. The SWAT-DEG model was also run from this preliminary watershed data.

b. Field Assessment

The field survey includes a visual summary of channel conditions by river reach (photographs of the left and right bed and bank). The length interval chosen for data assimilation for urban channels is 200 feet. Four major areas of information are derived from the channel survey. The bed material is documented and selected samples are taken for sieve analysis or a Wolman's pebble count is performed in the field. Sieve analysis and Wolman's pebble count are conducted to determine the gradation and size of bed material contained in the channel streambed. The geology (stratigraphy) of the reach is noted considering rock type, bedding, degree of weathering, and thickness of alluvial soils. Bank stability (slumps, flows, toppling failures) and degree of erosion is noted, as well as distance to and type of structure that may be impacted by future erosion. Finally, the meander geometry is measured and radius of curvature (Rc) and Rc/(bottom width) is obtained. This information is useful in assessing bend scour and meander migration rates.

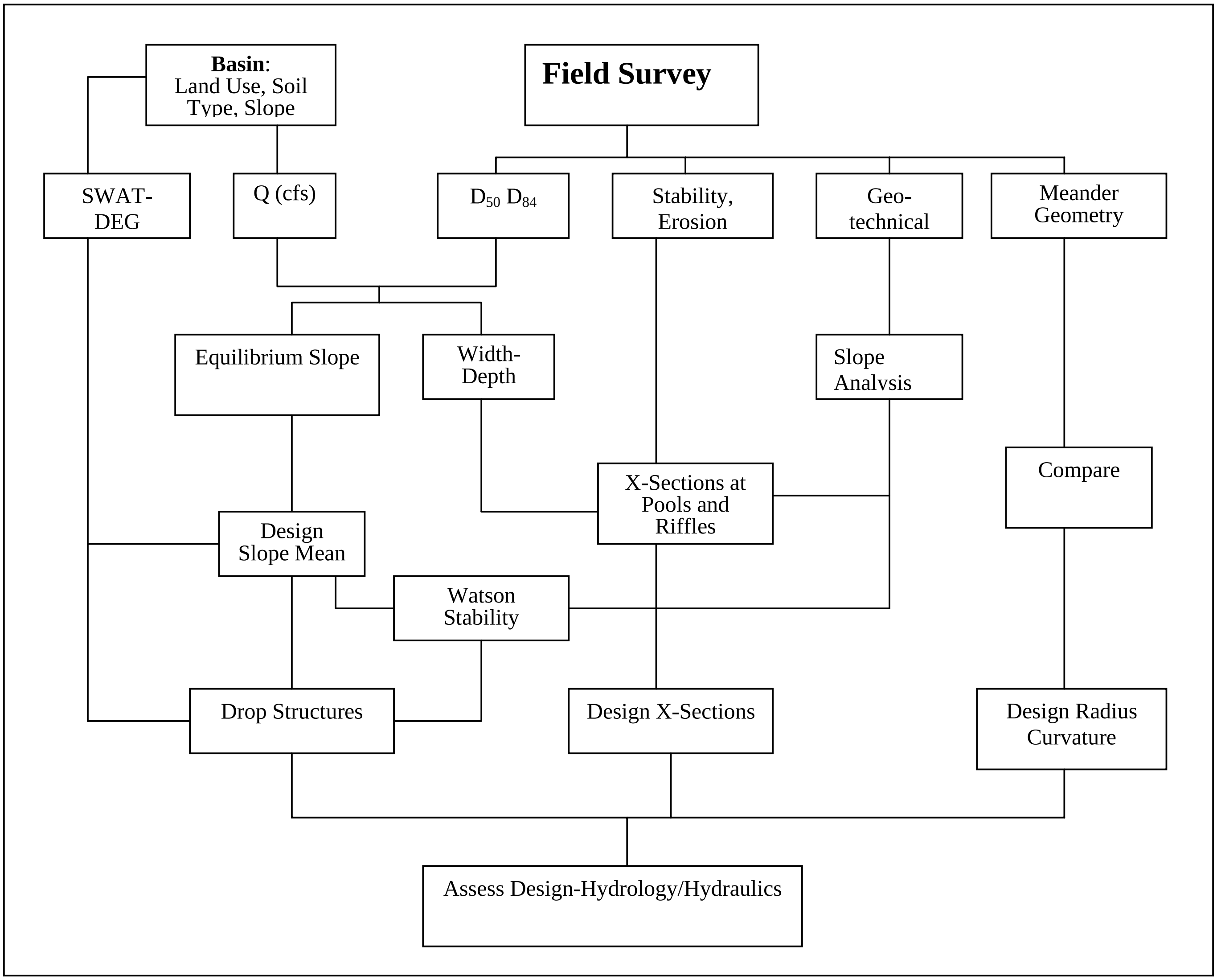

Figure 1. Quantifying river behavior flow chart.

c. SWAT-DEG

The Soil Water Assessment Tool (SWAT) is designed to simulate watershed processes and the impact of land and water management on water quality. Recently, the channel sediment routing model (DEG) has been modified to simulate downcutting and widening (Allen et al, 1999). An erodibility coefficient derived from submerged jet testing (Hanson, et. al., 1990) is multiplied by tractive force to compute downcutting and the channel slope is adjusted accordingly. Widening of the channel is accomplished through local width-depth ratios derived from measurements of streams in the Texas Blackland Prairie.

Three channel dimensions are allowed to vary in the channel downcutting and widening simulations: bankfull depth, width, and slope. The amount of downcutting in each event is:

$$D_{erosion} = 358(D_{water})(K_{ch}) \quad (1)$$

Where $D_{erosion}$ is the depth of downcutting in m, D_{water} is the water depth in m, and K_{ch} is the erodiblity coefficient (cm/hour/Pa). The new bankfull depth is computed with:

$$Depth_{new} = Depth_{bankfull} + Depth_{erosion} \quad (2)$$

The new bank width is computed with:

$$Wbankfull = Width\ /Depth\ Ratio\ (Depth_{new}) \quad (3)$$

The new channel slope is calculated as:

$$Slope_{new} = Slope - (Depth_{erosion})/(1000*Length) \quad (4)$$

Where Length is the channel length in km.

The model makes the basic assumption that over long periods of time, given the constraints of simple channel dimensions and 1D flow, limiting side slope equilibrium is equal to the materials internal angle of friction and the degree of downcutting. Local assessments of over 300,000 feet of channel in the metroplex confirm such assumptions. If more detail is needed within the local reach, the ARS Bank Stability model or the continuous simulation model CONCEPTS is also available.

The model was run on the study watershed using future land use and the local climate station as input. The equilibrium slope was input as the lower boundary condition for downcutting, Figure 2. For example, the time for the stream (15 sq. km) to reach equilibrium under urban conditions is on the order of 40 years. Of note are the periods of static conditions as in the 30-40 year time span. This is due to climatic factors, which is consistent with measured rates in other urban watersheds.

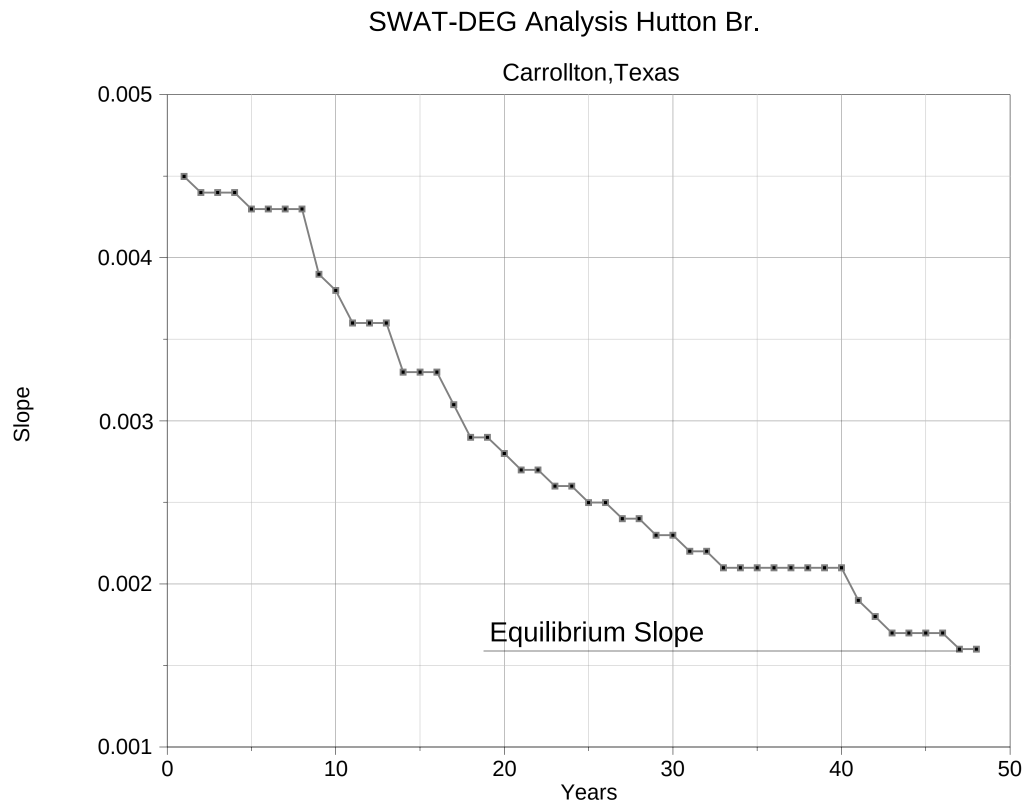

Figure 2. SWAT-DEG results of the modeled watershed.

Channel Design Parameters

The main stem of the creek can be subdivided into two basic geomorphic sections based on field surveys, the results of the SWAT-DEG model, and the Harvey Watson channel evolution assessment of the stream.

From station 4400 upstream (stations 0-6000), the channel is actively downcutting and should be considered in a degrading state. From station 4400 downstream, the channel is aggrading. Evidence for the upstream degradation (downcutting), are oversteepened banks, knickpoints, side channel gullies, and exposed sewer lines. Evidence of downstream aggradation is deposition and formation of large gravel bars and channel widening.

A channel design discharge is determined for the main stem of the stream based on three assumptions: (1) This was the calculated discharge for the fully developed basin derived from Dempster's (1974) regression equations, (2) these equations have been shown to define the active channel dimensions in the Dallas and North Texas area (Allen, Arnold, and Skipwith, 2002), and (3) consistency with HEC model results for the study area. Consistency with the HEC-RAS model results is checked and the proposed channel design parameters altered to produce the desired channel velocities in the range of 4 to 5 ft/s.

Based on this channel discharge and results of the Wolman's pebble count for the reach, stable slope equations were used to calculate the design channel slope. The pebble count indicated a D_{50} of 19.5 mm. The equilibrium channel slope is calculated from six methods.

The average of all the methods indicates a design (equilibrium) slope of 0.0016 for the study area.

The meander geometry is analyzed for the study reach. Stable meander geometry was analyzed using Shields Curve for shear stress and Leopold's sine generated curve function that resulted in a radius of curvature of 114 feet. Williams' empirical equations for river meanders and channel size using active channel width are used to estimate meander dimensions.

The active channel dimensions were based on four criteria: (1) design discharge, (2) stable bank slopes, (3) bankfull velocities, and (4) pool riffle geometry. Based on the routed flood flows and active channel discharge, the channel was modified to account for the remaining criteria. Cross sections were input into the HEC-RAS model for Hutton Branch, and channel velocities were checked against acceptable erosion thresholds (less than 6 feet per second).

To sustain the design equilibrium slope of 0.0016 within the project limits, grade control structures had to be added. These structures allow the new channel design to maintain the desired slope without further downcutting. In addition, bank armor (toe protection) was added along the outside slopes of meander bends. This was done to prevent lateral migration of the channel due to scour during the larger floods.

The resulting plan for Hutton Branch between the two streams is to restore the channel to a natural section and alignment. Stable channel design velocities will be maintained while floodwater surface elevations are kept at or below existing levels. In addition, a more stable, composite channel shape is proposed that will more efficiently pass the lower flood events and minimize channel instability.

In order to achieve a more stable, yet natural channel alignment, meanders will be introduced. The side slope of the inside bank of the channel is flattened to 5:1 to simulate a natural meandering channel section. On the outside bank, loose stone riprap will be placed to protect the slopes. At utility crossings or where right-of-way is being restricted, a gabion wall will be used.

The design slope of 0.0016 is used throughout the reach. To achieve this equilibrium slope, six drop structures will be needed. The drop structures also protect utility crossings

The recommended plan can be implemented without any increase in water surface elevation for the 100-year flood on Hutton Branch. The change in water surface elevation for the 100-year flood ranges from a decrease of 0.02 feet to 1.95 feet.

Proposed work includes 107,000 cubic yards of channel excavation and the placing of 29,000 cubic yards of fill. The total estimated cost for the recommended plan, including clearing, filling, re-grading, and re-vegetating areas along the banks of Hutton Branch, is $2,863,000.

Discussion and Conclusions

A channel restoration design was developed for Hutton Branch that follows the stable channel design process described in this section of the report. Planform geometry was developed and as a result a more natural meandering channel alignment was developed. The proposed stabilized channel satisfied the required velocity limits based upon the Manning's analysis. Verification of the velocities and channel carrying capacity was fulfilled by detailed hydraulic modeling process. The SWAT-DEG model is shown to be an integral part of the channel design and has been used on over five major studies to date in the Dallas-Fort Worth area. The channel restoration plan cost compared favorably with the cost of other, more structural channel stabilization techniques such as channel armoring.

Other applications of the SWAT-DEG model fall into three categories: (1) modeling degradation under various climate conditions, (2) analyzing the effects of erosion coefficients on downcutting, and (3) assessing time to equilibrium conditions. A lawsuit was brought against a suburb of Dallas asserting that the erosion in the channel was caused by the City permitting too much impervious surfaces to be built in the watershed, thus causing increased flooding and channel erosion in the last decade. SWAT was set up under the current land use and the climate was allowed to vary. It was shown that climatic conditions had a far more profound influence on channel erosion than did the recent increase in basin imperviousness as shown in the remarkable difference between the two rates of downcutting. A second example assesses the amount of downcutting which could occur under wet and dry soil conditions. The potential downcutting under dry clay channel conditions and under saturated soil conditions is demonstrated indicating up to a six fold change. The erodibility coefficients were determined from jet index tests on the soil samples derived from the bottom of the stream. The tests were run on soil material starting out at the plastic limit and then at field capacity. The two degradation curves were estimated using an incremental weighted average technique using modeled flood conditions. It was shown that the erodibility coefficient has a profound effect on downcutting rates. The SWAT model was then run for the same stream to compare the continuous simulation to a weighted average. The incremental weighted average technique was useful but fails to show potentially large annual increases in downcutting (up to a meter). Such storm induced downcutting can be important in critical channel areas near large structures. This testing was done to assess the potential for using the simpler incremental technique for a proposed channel setback ordinance in Austin, Texas. The final example illustrates how SWAT-DEG can be a useful tool to determine the projected time to equilibrium in the basin. This of course is simplified but can give engineers a means of prioritizing costly channel stabilization techniques throughout the watershed. Since the average cost of restoration can range up to 50 dollars per square foot of channel, prioritizing the expenditure of funds over multiple bond programs and thus years are essential for urban drainage repair and stream restoration. Future work on the SWAT-DEG model will involve modifications of erodibility coefficients to varying soil moisture regimes in the channel. Multiple runs for varying urban conditions are also planned within the metroplex to allow preliminary assessment of channel downcutting in urban streams with varying slopes, erodibility, land use and drainage basin size.

References

Arnold, J.G., Allen, P.M., and Bernhardt, G., 1993. A Comprehensive Surface/Groundwater Flow Model. Journal of Hydrology, 142, p. 47-69.

Allen, P.M., Arnold, J.G., and Jakabowski, E., 1997. Design and Testing of a Simple Submerged Jet Device for Field Determination of Soil Erodibility. Journal of Environmental and Engineering Gesosciences, 3, pp. 579-584.

Allen, P.M., Arnold, J.G., and Jakabowski, 1999. Prediction of Stream Channel Erosion Potential. Journal of Environmental and Engineering Geoscience, 5, pp. 339-351.

Allen, P.M., and Flannigan, B., 1985. Geology of Dallas, Texas. In: Cities of the World, Eds. Hathaway, A.: Bulletin of the Association of Engineering Geologists, 23, pp. 363-416.

Dempster, G.R., 1974. Effects of Urbanization on Floods in the Dallas,Texas Metropolitan Area. U.S. Geological Survey, Water Resources Inveistgation, 60-73, 51p.

Lane, E.W., 1955. Design of Stable Channels. Trans. Amer. Soc. Civil Engineers, Vol. 120, pp. 12234-1279.

Tinkler, K.J., and Parish, J., 1998. Recent Adjustments to the Long Profile of Cooksville Creek, an Urbanized Bedrock Channel in Mississauga, Ontario. In: Rivers Over Rock:Fluvial Processes in Bedrock Channels. AGU Monograph 107, pp. 167-187.

Neitsch, S.L., Arnold, J.G., Kiniry, J.R., Srinivasan, R., J.R. Williams, 2002. Soil and water assessment Tool User's Manual Version 2000. Blackland Res. Center, TAES, 720 Blackland Road, Temple, Texas 76502.

Leopold , L.B., and Wolman, M.G., 1960. River Meanders. Geol. Soc. Amer. Bull. 71, vol 5, pp. 769-784.

Watson, C.C., Peterson, M.R., Harvey, M.D. Biedenhorn, D.S., and Combs, P. 1988. Geotechnical and Hydraulic Stability Numbers for Channel Rehabilitation; Part II. Hydraulic Engineering. Proceedings of 1988 National Conference. Hy. Div. ASCE, Colorado Springs, Aug. 8-12, 1988.

Session IV

12. **Integrated river basin modeling including wetlands and riparian zones in the German Elbe River Basin** **114**
Fred F. Hatterman, Valentina Krysanova, Anja Habeck and Joachim Post

13. **Adapting SWAT for riparian wetlands in an Ontario watershed** **123**
Amanjot Singh, Ramesh Rudra and Wanhong Yang

14. **Developing parameters to simulate trees with SWAT** **132**
Doug MacDonald, Jim Kiniry, Jeff Arnold, Ruth McKeown, Ivan Whitson, Gordan Putz and Ellie Prepas

15. **Integration of 3-PG into SWAT to simulate the growth of evergreen forests** **142**
B.M. Watson, N. Coops, S. Selvalingam and M. Ghafouri

16. **A user friendly multi-catchments tool for the SWAT model** **153**
E. Lorrai and P. Cau

Integrated River Basin Modeling Including Wetlands and Riparian Zones in the German Elbe River Basin

Fred F. Hatterman[1], Valentina Krysanova[1], Anja Habeck[1], Joachim Post[1]
[1]Potsdam Institute for Climate Impact Research (PIK), Telegrafenberg A51, 14473 Potsdam, Germany. E-mail: hattermann@pik-potsdam.de

Abstract

Riparian wetlands are hydrologically connected to both the surrounding upstream catchment area and river, and represent an interface between them. They intercept surface and subsurface runoff with soluble nutrients and sediments from the upland areas, and therefore function as buffers for the river network. Due to their connection to groundwater and supply of nutrients from upland areas, riparian wetlands have excellent conditions for vegetation development during the whole growth season. As a result, riparian wetlands are highly effective in the reduction of diffuse source pollution and sediment loads to rivers and streams.

Integrating wetlands and riparian zones in eco-hydrological river basin modelling is very challenging. The correct representation of all these processes in the modelling framework with their different characteristic spatial and temporal scales is not a trivial task and includes much inherent uncertainty. Additional problems include the identification of riparian zones based on regionally available data and verification of the results.

Keywords: Riparian zones; wetlands; water quality; groundwater dynamics; nutrient retention

Introduction

The water framework directive of the European Commission demands that water bodies in Europe be brought into “a good ecological status” (EC 2000). Many efforts and improvements have been made, mainly in the implementation of waste water treatment plants. But these measures only help to improve the water quality of point sources, whereas the main origin of some important contaminants are diffuse sources like atmospheric deposition and fertilisation of crop land. Here, riparian zones and wetlands play an important role in the control of the water quality of surface water systems (Dall’O’ et al., 2001).

The paper presents an integrated catchment model with which it is possible to analyse the processes in wetlands and riparian zones in meso- to macroscale river basins, the scale relevant for water management planning and for the implementation of the water framework directive. A simple but comprehensive mechanistic wetland module was developed and coupled with the eco-hydrological model SWIM (**S**oil and **W**ater **I**ntegrated **M**odel, Krysanova et al., 1998), which integrates hydrological processes, vegetation, erosion and nutrient dynamics at the watershed scale. The reliability of the model results was tested under well-defined boundary conditions by comparing the results with those from a two dimensional numeric groundwater model under steady-state and transient conditions (Hattermann et al., 2004b). In addition, results were compared with observed data from a meso-scale basin, using contour maps of the long-term mean water table, observed groundwater level data, and observed river discharge and nutrient concentrations.

The results of the study show that riparian zones and wetlands have a high potential to reduce the nutrient transport into surface water systems, although the uncertainty of the modelling results is very high. Their impact is so large because they are at the interface between catchment and river systems, where the greater part of the nutrients in the catchment originally applied as fertilizers or mineralized from plant residues are already degraded. Restoration and management of wetlands is therefore a high priority for the control of non-point source contamination of surface waters.

Material and Methods

The Model

SWIM A three-level scheme of spatial disaggregation from basin to subbasins and to hydrotopes is used in the model. A hydrotope is a set of elementary units in the subbasin, which have the same geographical features, such as land use, soil type, and average water table depth. Therefore it can be assumed that they behave in a hydrologically uniform way (Krysanova et al., 2000). Water fluxes, plant growth, and nitrogen dynamics are calculated for every hydrotope, where up to 60 vertical soil layers can be considered. The outputs from the hydrotopes are aggregated at the subbasin scale. Mean resistance time and potential retention of water and nutrient fluxes are calculated using spatial features of the hydrotopes, such as distance to the next river, gradient of the groundwater table, and permeability of the aquifer. The approach allows us to consider and investigate the spatial pattern of land use and land use changes. The lateral fluxes are routed over the river network, taking transmission losses into account. Plant dynamics are simulated using a simplified EPIC approach (Williams et al., 1984). A full description of the model can be found in Krysanova et al. (1998, 2000). An extensive hydrological validation of the model in the Elbe Basin including sensitivity and uncertainty analyses is described in Hattermann et al. (2004a).

The Wetland Module

Important for the investigation of meso- to macroscale river basins is to apply methods which are physically sound but simple enough to save computation time and data demand (Arnold et al., 1993). The wetland module described here consists of two parts: one part describes the groundwater fluxes and water table dynamics, where the time scale is in days or weeks. The second part describes the nutrient fluxes and degradation, where the time scale is much larger (years and decades, sometimes centuries, because of the mean residence time of the groundwater).

Important for the hydrological processes and nutrient fluxes in wetlands is a good reproduction of the groundwater dynamics. Smedema & Rycroft (1983) derived a linear storage equation following the Dupuit-Forchheimer assumptions to predict the non-steady-state response of groundwater flow to periodic recharge from Hooghoudt's steady-state formula. It was assumed that the time-derivative of return flow q in mm d^{-1} (the groundwater discharge) at time step t is linearly related to the rate of change in water table height h in m (water table above drainage base). Only headlosses in a horizontal direction are considered:

$$\frac{dq}{dt} = \frac{8*T}{L^2} * \frac{dh}{dt} \quad (1),$$

where T is the transmissivity in $m^2\ d^{-1}$ and L the slope length in m. If the groundwater body is recharged by deep soil percolation or another source (Rc in mm d^{-1}), and is depleted by drain discharge (q), it follows that the water table will rise when $Rc\text{-}q > 0$ and fall when $Rc\text{-}q < 0$. The water table fluctuations can be described as:

$$\frac{dh}{dt} = \frac{(Rc - q)}{C*S} \quad (2).$$

S is again the specific yield. It follows that by assuming that the retention constant $C = 0.8$ (Smedema & Rycroft 1983):

$$\frac{dq}{dt} = \frac{10*T}{S*L^2} * (Rc - q) = \alpha * (Rc - q) \quad (3),$$

The change in drain discharge *dq/dt* is proportional to the excess recharge *Rc-q*, with α being the proportionality factor (reaction factor, see Equation 6). Equation 2 can be transformed to obtain the equation for return flow:

$$q_t = q_{t-1} * \exp(-\alpha * \Delta t) + Rc_{\Delta t} * (1 - \exp(-\alpha * \Delta t) \qquad (4).$$

Using the linear relationship between q and h (Equation 1), we get:

$$h_t = h_{t-1} * \exp(-\alpha * \Delta t)) + \frac{Rc_{\Delta t}}{0.8 * S * \alpha} * (1 - \exp(-\alpha * \Delta t) \qquad (5).$$

The equations are scale independent and the spatial unit for which h and q are calculated can be either the hydrotope or the subbasin. The factor α is a function of the transmissivity T and the slope length L:

$$\alpha = \frac{10 * T}{S * L^2} \qquad (6).$$

Therefore, the reaction factor has a physical meaning and can be estimated directly by using observations of the groundwater head h. This was done using an automatic calibration algorithm by adjusting T and S in physically sound limits.

While it is possible to describe water table dynamics using the mean reaction time, the time scales which have to be considered for the simulation of nutrient retention are much larger (years and decades), because the actual residence time is the crucial value which determines the intensity of degradation. According to Wendland et al. (1993), the degradation of nitrate N (kg ha^{-1}) can be approximated by a linear decay equation, where λ is a function of temperature and available oxygen. The full retention of a landscape is then a function of mean residence time and degradation:

$$\frac{dN_{t,out}}{dt} = N_{t,in} \frac{1}{1 + K\lambda}(1 - e^{-(\frac{1}{K}+\lambda)t}) + N_{t-1,out} e^{-(\frac{1}{K}+\lambda)t} \qquad (7)$$

where K, in days, is the mean residence time. The mean residence time of water in the subbasin to flow from a specific hydrotope to the next river is calculated for each hydrotope using a GIS and digital maps of the groundwater table and geo-hydrology. Since SWIM distinguishes between surface flow, interflow and baseflow, each having different retention characteristics (residence time and oxygen content), there has to be one equation for each of the fluxes.

Plant uptake of water and nutrients from groundwater is only possible in times when the plant roots have access to it and if the plant demand cannot be satisfied by soil water and nutrient recourses. A resistance function controls the ability of plant roots for water and nutrient uptake from groundwater.

The Basin

The northern lowland part of the German Elbe Basin, where the model was tested in the Nuthe Catchment (1,938.0 km^2, see Figure 1), is climatically one of the driest regions in Germany, with a mean annual precipitation of about 600 mm per year. Hence, water availability during the summer season is the limiting factor for plant growth. The lowland is formed by mostly sandy glacial sediments and drained by slowly flowing streams with broad river valleys. The upper sites with deep water tables are covered by sandy, highly permeable soils, and mostly pine forests or arable land on ground moraine with till soils that tend to have layers with lower water permeability.

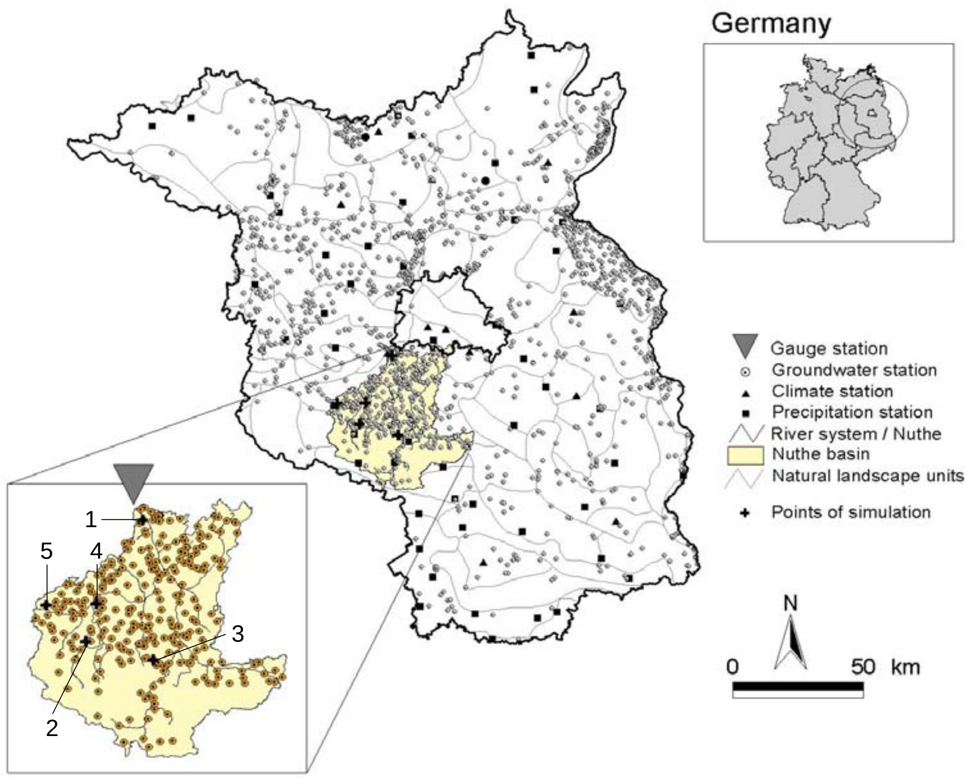

Figure 1. The location of the Nuthe Basin (1938.0 km^2) and the observation points. Valleys are covered by loamy alluvial soils with grassland and riparian forests, where the groundwater is very shallow, and arable land elsewhere.

Results and Discussion

Groundwater and River Flow Dynamics

First, the simulated mean annual water table depth of all subbasins in the Nuthe Basins were calibrated automatically using the permeability in a physically sound range (8 m d^{-1} – 60 m d^{-1}). The mean simulated amplitude was too high and had to be smoothed by a moderate increase in the value of specific yield (2.5% - 30%, as taken from the geo-hydrological map). The Mean Absolute Error of the long term observed data as compared to the simulated water table in all subbasins was 0.026 m.

The observation wells were selected in order to represent a cross-section through the basin from the lowlands in the north to the hilly area in the south-west. Well 1 is located next to the outlet of the Nuthe River Catchment. The curves show a good fit, especially for the early 1980s. The rise of the groundwater level in 1987 and 1988 is slightly overestimated by the model in subbasins 2, 4, and 5. As explained in section 1, the natural flow regime in the Nuthe Basin is influenced by streamflow control (weir and reservoir management), and especially in the lowland areas the water level is controlled by land drainage.

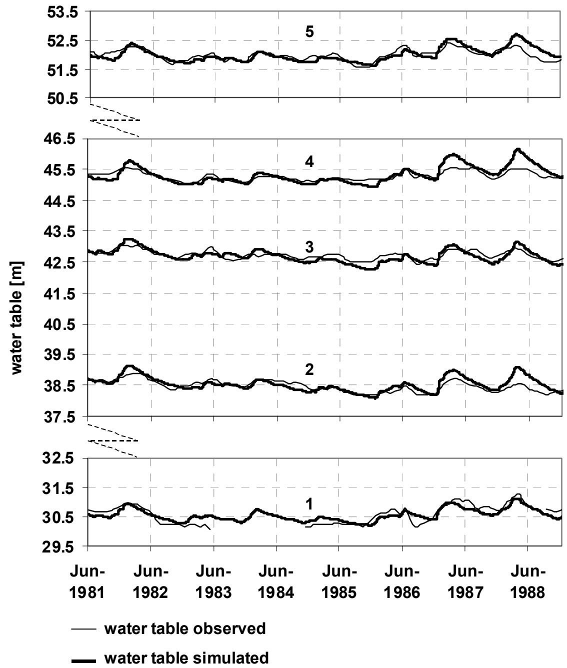

Figure 2. Comparison of observed and simulated groundwater table for five locations in the Nuthe Basin (Hattermann et al., 2004b).

Figure 3 illustrates the impact of plant water uptake on the simulated water table. While the groundwater tables simulated with and without plant water uptake converge during the winter, they separate during the vegetation period, where the plant uptake leads to a decline of the groundwater table. Evapotranspiration and recharge in Figure 3 are calculated with plant water uptake from groundwater.

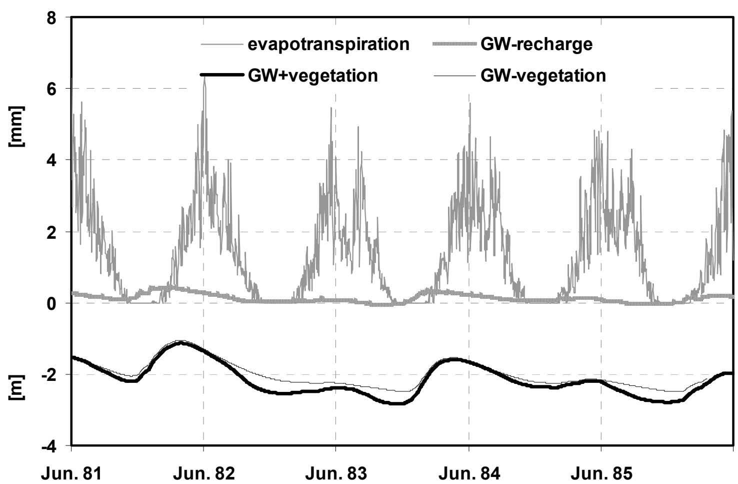

Figure 3. Comparison of simulated and observed groundwater table with (GW+vegetation) and without (GW-vegetation) plant water uptake from groundwater.

The mean long term difference between the observed and simulated river discharge at the basin outlet is 3.0% for the calibration period 1981 - 1988, indicating that the water balance is correctly calculated by SWIM. The daily Nash & Sutcliffe efficiency is 0.7 (only 0.54 for the validation period 1989-2000). The hydraulic regime of the Nuthe Basin is strongly influenced by water management regulations like drainage systems and weir plants, so that it is difficult to reproduce the hydrograph with higher accuracy. The summer discharge is in some years overestimated by the model (see Figure 4).

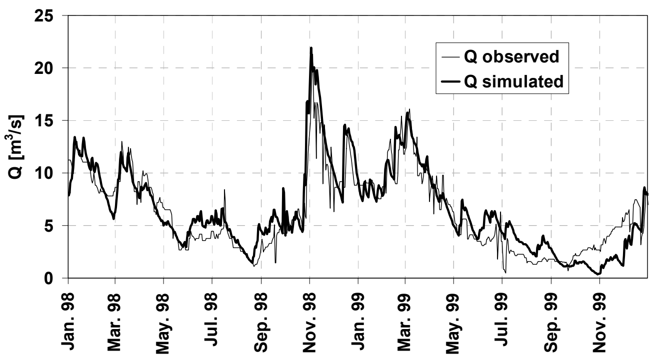

Figure 4. Comparison of daily river flow observed and simulated (gauge Babelsberg).

This can be explained by water abstraction and regulation measures, when a minimum river flow is provided by reservoir management in dry summer periods. It is worth mentioning that the efficiency was notably higher for other meso- and macro-scale subbasins of the Elbe located in hilly and mountainous areas (Hattermann et al., 2004a). Without additional plant water uptake from groundwater, the total evapotranspiration would be 25% lower, leading to an increase in river discharge of about 50%.

Nitrate Concentrations

The nitrate concentration in the Nuthe River during the Eighties was strongly influenced by point sources (irrigation of waste waters in very small areas, municipal waste waters, even direct discharge of liquid manure into surface waters), where the records are vague and incomplete, so that the comparison in Figure 5 is done for a time period in the Nineties, where the impact of point sources is very limited because of the implementation of waste water treatment plants in the basin.

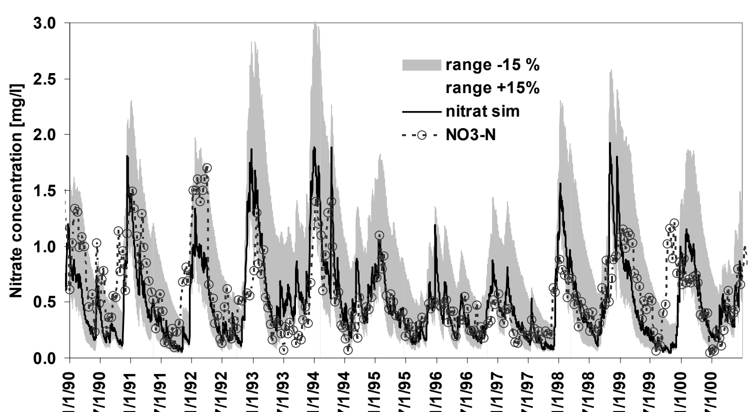

Figure 5. Simulated and observed nitrate concentrations in the Nuthe River with the range of uncertainty because of uncertain geo-hydrological information.

Diffuse sources in this study are fertilizer applications (about 135 kg/ha for winter wheat, a smaller application in late fall, larger in spring), atmospheric depositions (about 25 kg/ha), and plant depositions after harvest and fall.

The comparison shows that the periodicity and amplitude of the observed values is generally reproduced well by SWIM, although the difference between observed and simulated values is large, especially at the end of the year. The reason is that the diffuse sources for nitrate contamination (in particular fertilization) are not very well known, because information about crop rotation schemes and fertilization regimes are not available at the regional scale.

The mean residence time of groundwater is 41 years, with a maximum of approximately 400 years. The values are in positive agreement with Landesumwelamt (2002), who estimated the nutrient loads and retention in the lowland catchments of the Elbe Basin. The range of uncertainty produced by the uncertain geo-hydrological information is also included in Figure 5 by assuming a 15% longer or shorter mean residence time and half life time.

Figure 6 illustrates the impact of plant uptake of nitrate in riparian zones and wetlands. As shown also for the impacts of plants on the water level in Figure 3, the differences are the highest during the summer season when plant demand is high and therefore cannot be satisfied by the soil water concentrations. The difference becomes smaller during the late summer, because the total amount of available nutrients in soils and hence the leaching of nutrients is at a minimum. Figure 7 shows a map of the additional plant nitrate uptake from groundwater in kg ha^{-1}. The values are not large in comparison with the total plant uptake (up to 150 kg ha^{-1}). The additional uptake is only about 1% of the total uptake, but this leads to retention of about 24% of the total river load. The reason is that the additional uptake happens in an area next to the surface water bodies where the largest part of the nitrate which was originally applied by fertilizers, mineralised from plant residues, and decomposed from the atmosphere, is already degraded.

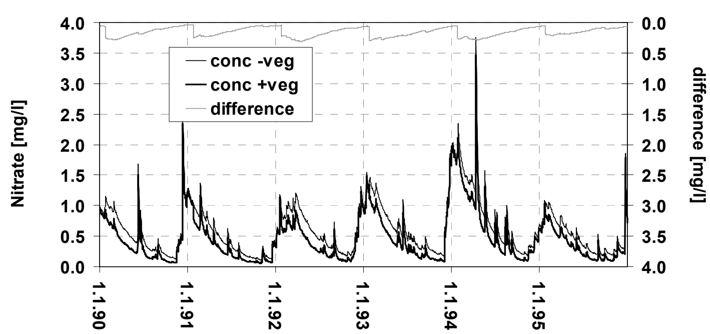

Figure 6. Comparison of simulated and observed nitrate concentration with and without plant water uptake from groundwater.

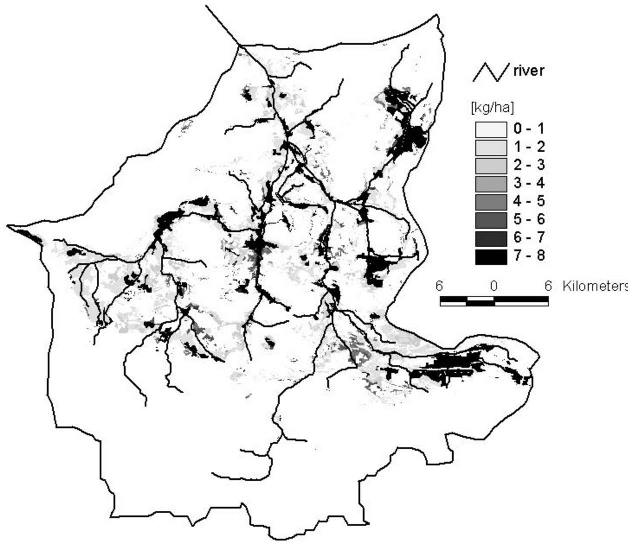

Figure 7. Additional nitrate uptake by plants in riparian zones and wetlands.

Conclusions

The simulation results indicate that relatively small parts of the total catchment area have a high impact on the water and nutrient balance in the catchment (additional evapotranspiration of about 25% and additional nitrate uptake of about 1% leading to a decrease in river discharge of about 50% and a decrease in annual river nitrate load of about 24%), although the uncertainty of the results is high. Riparian zones and wetlands are buffer systems which are able to reduce contamination of surface waters, as long as the vegetation has access to groundwater. On the other hand, restoration of wetlands will lead to increased water losses by evapotranspiration, crucial in a region where river discharge during the summer season is only possible by water regulation through dams and weirs, and where a trend to lower annual precipitation has been observed during the last decades. It follows that water managers have to find a sensitive balance between water quality and water quantity aspects in the planning process.

References

Arnold, J.G., Allen, P.M., Bernhardt, A. (1993) A comprehensive surface-groundwater flow model. *Journal of Hydrology* 142, 47-69.

Dall'O', M., Kluge, W., Bartels, F. (2001) FEUWAnet: a multi-box water level and lateral exchange model for riparian wetlands. *Journal of Hydrology* 250, 40-62.

EC (2000) Establishing a framework for community action in the field of water policy. Directive 2000/60/EC of the European Parliament and of the Council of 23 October 2000, *Official Journal of the European Communities*, Brussels.

Hattermann, F.F., Wattenbach, M., Krysanova, V., Wechsung, F. (2004a) Macroscale validation of the eco-hydrological model SWIM for hydrological processes in the Elbe basin with uncertainty analysis. In: Regional Assessment of Climate and Management Impacts Using the SWAT Hydrological Model (ed. by N. Fohrer and J. Arnold). *Hydrological Processes* (in press).

Hattermann, F.F., Krysanova, V, Wechsung, F, Wattenbach, M. (2004b) Integrating groundwater dynamics in regional hydrological modelling. *Environmental Modelling and Software* 19(11), 1039-1051.

Krysanova, V., Becker, A., Müller-Wohlfeil, D.-I. (1998) Development and test of a spatially distributed hydrological / water quality model for mesoscale watersheds. *Ecological Modelling* 106, 261-289.

Krysanova, V., Wechsung, F., Arnold, J., Srinivasan, R., Williams, J. (2000) *PIK Report Nr. 69* "SWIM (Soil and Water Integrated Model), User Manual".

Landesumweltamt Brandenburg (2002). Stoffeinträge in die Gewässer des Landes Brandenburg. Band 68. Potsdam.

Smedema, L.K., Rycroft, D.W. (1983) *Land Drainage – Planning and Design of Agricultural Drainage Systems*. Cornell University Press, Ithaca, NY.

Wendtland, F., Albert, H., Bach, M., Schmidt, R. (1993) *Atlas zum Nitratstrom in der Bundesrepublik Deutschland*. Springer Verlag, Berlin.

Williams, J.R., Renard, K.G., Dyke, P.T. (1984) EPIC – a new model for assessing erosion's effect on soil productivity. *Journal of Soil and Water Conservation* 38, 381-383.

Adapting SWAT for Riparian Wetlands in an Ontario Watershed

Amanjot Singh, Ramesh Rudra and Wanhong Yang.
School of Engineering, University of Guelph, Guelph, Ontario, Canada N1G 2W1. E-mail: asingh@uoguelph.ca

Abstract

Watershed models like the Soil and Water Assessment Tool (SWAT) are fairly comprehensive in simulating different hydrological processes by dividing subbasins into hydrologic response units (HRU) comprising unique soil and land use combinations. However, the HRUs are not hydraulically interconnected and are lumped at the subbasin level to estimate runoff and pollutants delivered to the reach. This lumping aggregates modeling outputs for various land features, thus making it difficult to examine the effect of some significant components, such as riparian wetlands, which may not be dominant when seen at the subbasin scale. This study adapts SWAT for simulating riparian wetlands by coupling it with the Riparian Ecological Management Model (REMM). This approach is applied to Canagagigue Creek Watershed of the Grand River Basin in Southern Ontario, Canada. The results indicate considerable reduction in surface runoff (33% - 43%) and sediment yield (61% - 90%) when the riparian system is introduced to the subbasin. The coupled system can be used to evaluate the effect of riparian wetlands on stream water quality or as a design tool for restoration or construction of riparian wetlands.

Introduction

Wetlands were spatially widespread in southern Ontario before extensive agriculture began. Over 65% of the wetlands in southern Ontario have been lost through conversion to other land uses within the last 200 years (GRCA 2003). In the past, efficacy of these natural filtering systems was, perhaps, not well perceived. Further, intensive agricultural activities, including application of liquid manure and chemical fertilizers to supplement crop nutrients, is resulting in movement of sediments, nutrients, and pathogens to the streams, ultimately ending up in the Great Lakes.

Wetlands filter sediments and nutrients, improve water quality, attenuate flood control, and provide significant wildlife habitat (Warner, 2002). Ecological benefits include nutrient storage, biological diversity, and critical habitat for fish and wildlife. Carbon, a primary component of the most significant greenhouse gases that contribute to climate change, is sequestered in wetland soils and vegetation (GRCA 2003). Several studies have verified that stream side and flood plain zone vegetation (riparian buffers) is active in reducing nutrient and sediment concentrations in overland and subsurface flows moving to low order streams (Cooper et al., 1987; Lowrance et al., 1997; Vellidis et al., 2002).

Since the 1980s wetland policy in Ontario has evolved in response to the growing concerns about the negative environmental effects in agricultural watersheds. In 1996, the Province issued a Policy statement to deal with wetlands as Natural Heritage (GRCA 2003). This policy was established to ensure that the public planning agencies would have regard for the value of wetlands. Wetland policy is intended to protect Provincially Significant Wetlands (Classes 1 to 3) and encourages the protection of all other wetlands. Because the efforts for preserving wetlands are prioritized, it is important to understand the hydrology and hydraulics of the wetland in watersheds through different modeling approaches.

Numbers of modeling approaches have been developed to understand and simulate wetland hydrology in the context of watersheds. Arnold et al. (2001) modified SWAT to allow ponded water within the prescribed wetland to interact with the soil profile and the shallow aquifer for constructed wetlands. In the study, a wetland was described as a hydrologic response unit and a water balance approach was used to simulate wetland hydrology for non-ponded and ponded conditions. Restrepo et al. (1998) modified the groundwater model MODFLOW (McDonald and Harbough, 1988) to address wetland-groundwater interactions. They considered flow as a combination of sheet flow through dense wetland vegetation and slough flow through a channel. The other models that have been used to simulate some aspects of wetland hydrology include DRAINMOD (Skaggs, 1994), Flatwoods (Sun et al., 1998), a Wetland Dynamic Water Budget Model (Walton et al. 1996), WETMOD (Cetin et al., 2001), WETLAND (Lee et al. 2002), and Soil Water Balance Model (Bidlake and Boetcher, 1996). However, there is a need to explicitly link wetland functions with watershed processes to examine the spatial variations of wetland benefits in agricultural watersheds.

In this paper, the Soil and Water Assessment Tool (SWAT) is adapted for simulating riparian wetlands by coupling it with the Riparian Ecological Management Model (REMM). The model coupling is applied to the upper Canagagigue Creek Watershed of the Grand River Basin in southern Ontario, Canada to estimate the wetland benefits in subbasins in terms of attenuating surface runoff and filtering of sediments. The modeling results will have important policy implications for designing effective wetland policy in agricultural watersheds.

Methodology

For simulating riparian wetland hydrology in watersheds, a number of modeling approaches were reviewed. The SWAT model was selected for simulating watershed hydrology for its wide acceptability for modeling agricultural watersheds. The REMM model was selected for simulating riparian wetlands because of its comprehensive approach in handling riparian processes. The basic modeling approach used in SWAT and REMM is described below:

SWAT Model Description

SWAT is a comprehensive continuous-time watershed model that operates on a daily time-step. The model was developed by the Blackland Research and Extension Center and the USDA-ARS (Arnold et al., 1998). It predicts the impact of land management on water, sediment, and nutrient outflow from an agricultural watershed. Major model components include weather, hydrology, soil temperature, plant growth, nutrients, pesticides, and land management.

SWAT delineates watersheds into subbasins and subbasins are divided further into hydrologic response units (HRU) based upon unique soil/land-use characteristics. Flow, sediment, and nutrient loading from each HRU in a subbasin are summed and the resulting loads are then routed through channels, ponds, and reservoirs to the watershed outlet (Arnold et al., 2001).

SWAT has been widely applied for modeling watershed hydrology and simulating the movement of non-point source pollution. However, the model structure prevents it from explicitly simulating the hydrology of some land components such as riparian wetlands. The HRUs are not hydraulically interconnected and, therefore, marking how much runoff will be received by the riparian buffer system (RBS) is not feasible. Further, SWAT lumps outputs of runoff and pollutants coming from HRUs within one subbasin and delivers it to the reach.

The lumping nullifies the affect of non-dominant land management practices, which may have larger contributions in controlling the outflow of pollutants. Therefore, in the absence of the procedures for these processes, which may be actually controlling hydrology, it may be misleading to force the model to converge to the observed values by calibrating the model parameters.

REMM Description

The Riparian Ecosystem Management Model (REMM) was developed at the USDA-ARS Southeastern Watershed Research Laboratory (Altier et al., 2002; Lowrance et al., 2000). REMM is a comprehensive model that divides riparian buffer zones spatially into three zones. Zone 1 (normally undisturbed native forest area) is a narrow strip adjacent to the stream for stream bank protection and aquatic environment. Zone 2 (normally matured coniferous trees) is managed woody vegetation for sequestering sediment and nutrients from upland runoff. Zone 3 (normally herbaceous strip) receives runoff, sediments, and nutrients from the watershed upland of the riparian system. Although the modeling approach depicts a typical riparian buffer system, it can handle various combinations of vegetation and merging of zones.

Vertically REMM divides soil profiles into three layers and considers a litter layer at the surface of the ground. Water moves both vertically and laterally through these layers. The litter layer acts as a mixing layer and interacts with surface runoff. The mass balance and rate-controlled approaches are used for storage of water in all the three zones and for movement of water between these zones (Altier et al., 2002).

REMM is a continuous-time model operating on a daily time-step. The input files are well structured and parameters are stored in climate, field input, vegetation, buffer, and rate files. The model output provides runoff, sediment, and nutrient loads coming from all the three zones on daily basis.

REMM needs inputs from the upland watershed through measurement of runoff, sediments, and nutrients or simulating those values using some other watershed model and then manually preparing field input files.

Study Site Description

Canagagigue Creek Watershed is a sub-watershed of Grand River Basin, a major river basin that drains into Lake Erie in southern Ontario, Canada. Canagagigue Creek Watershed is under intensive agriculture, which covers 80% - 90% of the watershed (Carey et al., 1983). The creek has a catchment area of about 150 km^2 and is located between $43^0$36’ N – $43^0$42’ N latitude and $80^0$33’ W – $80^0$38’ W longitude. There is a reservoir (Floradale Reservoir) located in the middle of the watershed, which is equipped with a gauging station. The watershed upstream of the reservoir is considered in this study (Figure 1).

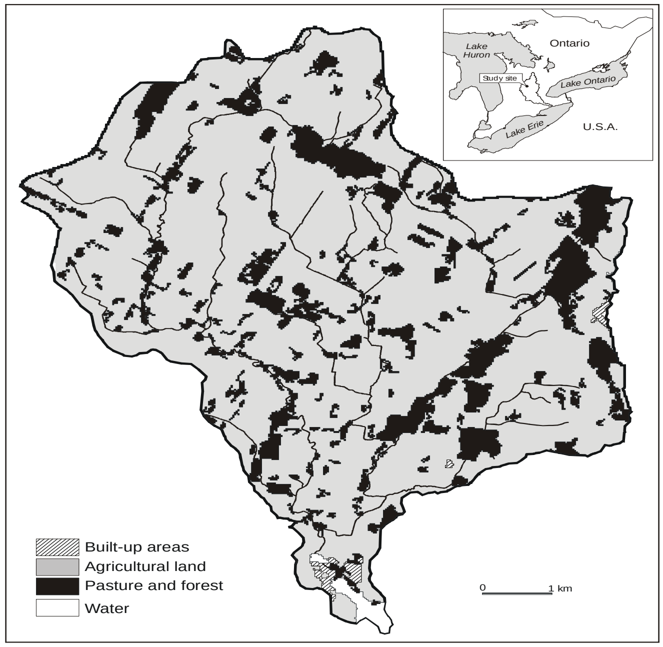

Figure 1. Location of Canagagigue Creek watershed in Grand River basin.

Reports by the Grand River Conservation Authority indicate that some sites in the downstream portions of the Canagagigue Creek Watershed are hyper-eutrophic and rated poor in terms of water quality (GRCA, 2004). This watershed lost more than 70% of its wetlands when the growing population in this region demanded more land for agriculture. Still the eastern tributary of Canagagigue Creek has some riparian wetlands, and in some subbasins, wetlands contribute up to 20% of the area.

SWAT-REMM Coupling Hypothesis

The main requirement for simulation of riparian wetland hydrologic processes is coupling the watershed scale model SWAT and the riparian ecology model REMM. The SWAT structure (Arnold et al. 2001) does not have hydraulically interconnected HRUs within a subbasin. The runoff, sediment, and nutrient output at the outlet of the subbasin is a lumped output of all the HRUs in that subbasin. Since the riparian zones are spatially located along the stream, and the runoff coming from the catchment passes through these buffers before entering the stream, output from a subbasin passed to REMM as an input should reflect the effect of riparian buffers on sequestering runoff, sediments, and nutrients.

The subbasin output file for SWAT gives daily runoff, sediment, and nutrient data for all the subbasins for the entire simulation period. The SWAT subbasin output file was compared with the field input file for REMM (Table 1). Although the SWAT output does not generate the extensive output parameters required by REMM, the major parameters are available and rest may be substituted from other resources.

Table 1. Comparison of parameters required by field data file of REMM and simulated by SWAT.

Parameters required by the REMM Field Data File	Parameters simulated in the SWAT subbasin file
Surface Runoff (mm)	Yes
Subsurface Runoff (mm)	Yes
Sediment loading (kg/ha)	Yes
Sediment-clay fraction	No
Sediment-silt fraction	No
Sediment-sand fraction	No
Sediment-small aggregate fraction	No
Sediment-large aggregate fraction	No
C-humus-active-surface runoff (kg/ha)	No
C:N ratio surface runoff	No
C:P ratio surface runoff	No
C-humus-active-subsurface flow (kg/ha)	No
C:N ratio subsurface flow	No
C:P ratio subsurface flow	No
C-humus-active-sediment (kg/ha)	No
C:N ratio sediment	No
C:P ratio sediment	No
Ammonia-surface runoff (kg/ha)	No
Ammonia-subsurface flow (kg/ha)	No
Ammonia-sediment (kg/ha)	No
Nitrate-surface runoff (kg/ha)	Yes
Nitrate-subsurface flow (kg/ha)	No
Phosphorus-surface runoff (kg/ha)	Yes
Phosphorus -subsurface flow (kg/ha)	No
Phosphorus –sediment (kg/ha)	Yes

Results and Discussion

The SWAT and REMM coupled model was run for a period of seven months, from April 1, 1998 to October 31, 1998, on a portion of the Canagagigue Creek Watershed upstream of the Floradale Reservoir. The results presented in this paper are simulated results. These results could not be validated due to the unavailability of observed data at the subbasin level; however, trends in the results were analyzed to investigate the change of magnitude in runoff and sediment entering the stream in the presence of riparian wetlands.

SWAT Simulation

For the application of SWAT, the Canagagigue Creek Watershed upstream of the Floradale Reservoir was delineated into 27 subbasins using a 10 m DEM. A 100 ha threshold area was used for stream definition. One subbasin (20) was selected for the application of SWAT-REMM coupling (Figure 2). Subbasin 20 has a total area of 445 ha and a 4,800 m stream length, with a 200 m riparian zone passing through it. The riparian buffer zone contributes about 20% of the total subbasin area.

Figure 3 shows the hydrograph and sediment graph of runoff and sediments flowing out of subbasin 20 and entering the stream during the simulation period. The monthly averaged daily runoff rate ranged from 0.00 to 1.68 cm H_2O/ha, and sediment yield ranged from 0.00 to 420 kg/ha. The hydrologic output data was passed on to the REMM model for input as upland data entering the riparian buffer.

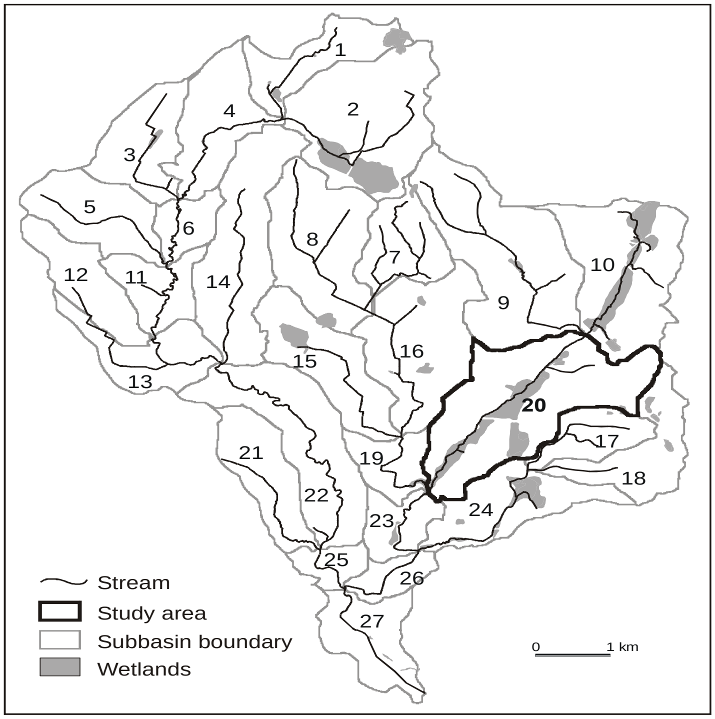

Figure 2. Delineated Canagagigue Creek Watersheds with riparian wetlands.

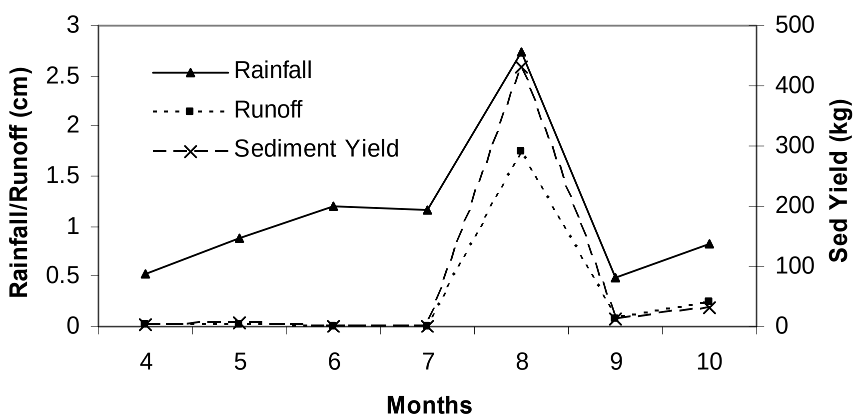

Figure 3. Monthly daily average output of runoff and sediment from SWAT simulations.

REMM Simulation

The REMM model needs input for the upland field data, buffer data, and type of vegetation in the three zones. The upland field input information was extracted for subbasin 20 from the SWAT subbasin output file and formatted for the REMM field input data. The buffer input file requires an area of upland field contributing surface and subsurface runoff and sediments to the riparian buffer, stream depth, and latitude. All the information was extracted from the SWAT output file and fed into the buffer file.

The riparian buffer was divided into three zones. Zone 1 was 30 m all along the stream with deciduous tree type vegetation. Zone 2 was composed of coniferous trees and ran 150 m along the main slope of the watershed. Zone 3 was 20 m long and was composed of herbaceous grass plantation. The subbasin slope was 2.66%.

The output of the REMM model for runoff and sediment yield is presented in Figures 4 and 5, respectively. Tables 2 and 3 present the role of the three zones in reducing the amount of runoff and sediment entering the stream. The results reveal that riparian wetlands significantly decrease runoff and sediment loads entering the stream. Zone 3 was most effective in reducing the entry of sediment to the stream and Zone 2 was most effective in sequestering runoff. The runoff was reduced from 4% to 9% through Zone3, 17% to 38% in Zone 2, 10% to 18% in Zone 1, and 28% to 50% in total before reaching the stream (Table 2). Similarly, sediments were filtered from 41% to 82% in Zone3, 28% to 66% in Zone 2, 7% to 12% in Zone 1, and 61% to 90% in total (Table 3). This shows that the presence of riparian wetlands helped in sequestering up to 50% of runoff and 90% of sediments. The results are supported by a study done by Sheridan et al. (1999).

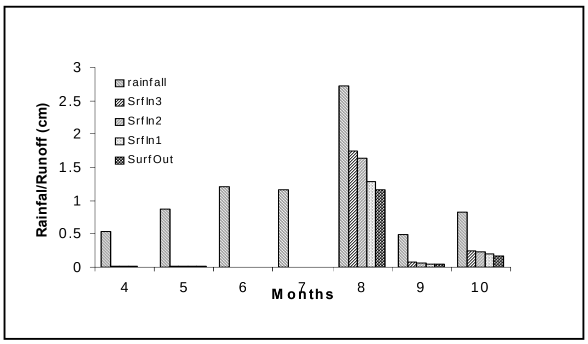

Figure 4. Bar graph showing sequestration of runoff in the three riparian zones.

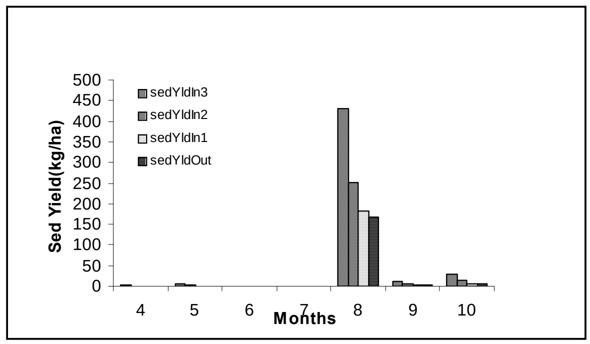

Figure 5. Bar graph showing sediment filtration through the three riparian zones.

Table 2. Variation in surface runoff as it passes through the three riparian zones.

1	2	3	4	5	6	7	8	9	10
4	15.86	0.01	0.01	7.48	0.01	33.54	0.01	14.66	43.28
5	27.20	0.02	0.02	7.15	0.01	32.15	0.01	13.69	41.44
6	36.20	0.00	0.00	8.63	0.00	38.31	0.00	18.34	49.63
7	36.00	0.00	0.00	0.00	0.00	0.00	0.00	0.00	0.00
8	84.60	1.68	1.59	5.62	1.25	25.68	1.12	10.15	33.22
9	14.60	0.07	0.07	6.72	0.05	30.37	0.04	12.50	39.07
10	25.60	0.23	0.22	4.11	0.19	17.29	0.16	13.34	28.33

1. Month; 2. Rainfall (cm); 3. Surface Runoff Entering Zone 3 (cm); 4. Surface Runoff Entering Zone 2 (cm); 5. Pecent Reduction through Zone 3; 6. Surface Runoff Entering Zone 1 (cm); 7. Percent Reduction through Zone 2; 8. Surface Runoff Leaving Zone 1 (cm); 9. Percent Reduction through Zone 1; 10. Percent Total Reduction.

Table 3. Variation in sediment yield through three riparian zones.

1	2	3	4	5	6	7	8	9
4	2.63	0.98	62.92	0.44	55.05	0.39	11.93	85.32
5	5.10	2.21	56.65	0.75	65.95	0.70	7.59	86.36
6	0.07	0.01	82.43	0.01	41.81	0.01	0.00	90.5
7	0.00	0.00	0.00	0.00	0.00	0.00	0.00	0.00
8	417.29	244.12	41.50	175.56	28.09	163.01	7.15	60.94
9	12.17	6.15	49.44	2.47	59.89	2.28	7.52	81.24
10	29.03	15.04	48.21	6.88	54.25	6.24	9.29	78.51

1. Month; 2. Sediment Yield Entering Zone 3 (kg); 3. Sediment Yield Entering Zone 2 (kg); 4. Percent Reduction through Zone 3; 5. Sediment Yield Entering Zone 1 (kg); 6. Percent Reduction through Zone 2; 7. Sediment Yield Leaving Zone 1 (kg); 8. Percent Reduction through Zone 1; Percent Total Reduction.

Conclusions

Contamination of the Great Lakes with the pollutants coming from the agricultural watersheds draining into the lakes leads to growing concerns in protecting the source water. Wetland conservation has become an important effort in addressing these concerns. The province of Ontario has made it a policy to prioritize and protect existing wetlands and has proposed the option of constructing more wetlands. For constructing and protecting wetlands, it is essential to understand the effects of wetlands in the context of hydrology and hydraulics of the watershed through different modeling procedures. Most of the existing models work either for watersheds or for wetlands and lack interaction. This study presents an effort to couple a watershed scale model with a wetland model and understand the role of wetlands on watershed hydrology and hydraulics.

A subbasin of Canagagigue Creek Watershed with 20% riparian wetland area was selected for modeling. The watershed scale model SWAT and the riparian wetland model REMM were coupled for simulation. The SWAT model was used to generate upland information for REMM, which was used for the riparian system simulation.

The results indicated considerable reduction in surface runoff (28% - 50%) and sediment yield (60% - 90%) when the riparian system was introduced to the subbasin. Zone 3, with herbaceous grass strips, filters most of the sediments, and Zone 2, the managed forest, sequesters runoff. This coupling procedure could be used to assess the efficiency of existing riparian wetlands or to design riparian zone dimensions for constructed wetlands.

References

Altier L S, Lowrance R, Williams R G, Inamder, J M Bosch D D, S P Sheridan, Hubbard R K and Thomas D L 2002. The Riparian Ecosystem Management Model, Simulator for Ecological Processes in Riparian Zones. USDA-ARS Conservation Report 46. Washington D.C.

Arnold J G, Allen P M and Morgan D S 2001. Hydrologic model for design and constructed wetlands. Wetlands. 21(2): 167 – 178.

Arnold J G, Srinivassan R, Muttiah R S and Williams J R 1998. Large area hydrologic modeling and assessment part I: model development. J American Water resources Association 34: 73 – 89.

Bidlake W R, and Boetcher P F. 1996, Simulation of the soil water balance of an undeveloped prairie in West Central Florida: U.S. Geological Survey Water Supply Paper 2472.

Brinson, M M. 1988. Strategies for assessing the cumulative effects of wetland alteration on water quality. Environmental Management 12:655–662.

Carey J H, Fox M E, Brownlee B G, Metcalfe J L, Mason P D and Yerex W H 1983. The fate and effects of contaminants in Canagagigue Creek-1. Stream ecology and identification of major contaminants. Environment Canada. Scientific series No. 135. 37p.

Cetin L, Recknagel F and Boumans R. 2001. Validation of the Model WETMOD for Lower Murray Wetlands: Core for Restoration Scenarios at Landscape Scale. Fenner. Conference on the Environment 2001 on Biodiversity Conservatiuon in Freshwaters. Canberra, Australia.

Cooper J R, Gilliam J W, Daniels R B and Robarge W P. 1987. Riparian areas as filters for agricultural sediment. Soil Science Society of America Journal 51: 416–420.

GRCA 2003. GRCA Wetlands Policy. Grand River Conservation Authority. Online: http://www.grandriver.ca/WetlandsPolicy/pdf/Wetlands_%20Policy_2003.pdf.

GRCA 2004. Water quality in the Grand River: Current Conditions and Historic Trends. Grand River Conservation Authority Report No. P-08-04-65, Ontario, Canada.

Lee E R, Mostaghimi S and Wynn T M 2002. A model to enhance weland design and optimize nonpoint source pollution control. J of The American Water Resources Association, 38(1): 17-32.

Lowrance R, Altier L S, Williams R G Inamder S P Sheridan J M Bosch D D, Hubbard R K and Thomas D L 2000. REMM: The Riparian Ecosystem Management Model. J of Soil and Water Conservation: First Quarter; 55(1): 27 – 34.

Lowrance R, Vellidis G, Wauchope R D, Gay P, and Bosch D D. 1997. Herbicide transport in a riparian forest buffer system in the coastal plain of Georgia. Transactions of the ASAE 40:1047–1057.

McDonald M G A and Harbraug A W 1988. A Modular, Three Dimensional Finite-Difference Ground Water Flow Model. Techniques of Water Resources Investigations of U.S. Geological Survey, Book 6, U.S. Government Printing Office, Washington D.C.

Restrepo J I, Montoya A N and Obeysekera J 1998. A wetland simulation module for the MODFLOW ground water model. Groundwater, 36(5): 764-770.

Sheridan, J. M., R. R. Lowrance, and D. D. Bosch., 1999. Management Effects on Runoff and Sediment Transport in Riparian Forest Buffers. Transactions of the ASAE 42(1): 55-64.

Skaggs, R W 1984, DRAINMOD—A water management model for shallow water table soils-user's guide: North Carolina State University, Raliegh, NC, USA.

Sun, G., Riekerk H, and Comerford N B. 1998, Modeling the forest hydrology of wetland-upland ecosystems in Florida: Journal of the American Water Resources Association. 34, 827–841.

Vellidis G, Lowrance R, Gay P and Wauchope R D. 2002. Herbicide transport in a restored riparian forest buffer system. Transactions of the ASAE 45:89–97.

Walton, R., Chapman R S, and Lewis J E. 1996, Development and application of the wetlands dynamic water budget model: Wetlands. 16, 347–357.

Warner B G 2002. Canada’s Wetland Industry. Wetlands Research Centre, University of Waterloo, Ontario, Canada.

Developing Parameters to Simulate Trees with SWAT

Doug MacDonald[1*], Jim Kiniry[3], Jeff Arnold[3], Ruth Mckeown[2], Ivan Whitson[4] Gordan Putz[2], Ellie Prepas.[1]
[1]Department of the Forest Environment, Lakehead University, Thunder Bay, ON, P7B 5E1. *(jmacdon6@lakeheadu.ca, (418)-840-2902).
[2]Department of Civil and Geological Engineering, University of Saskatchewan, Saskatoon, SK.
[3]Grassland, Soil, and Water Research. Laboratory, USDA, Temple TX.
[4]Millar Western Forest Products Ltd., Edmonton, AB.

Abstract

Deterministic watershed scale models such as SWAT can be adapted for forest management. As a part of the **For**est **W**atershed **a**nd **R**iparian **D**isturbance (FORWARD) study, SWAT is being used to estimate the impacts of different harvest patterns on streamflow and water quality in the Forest Management Area of Millar Western Forest Products Ltd. on the Boreal Plain of North America. Application of SWAT in a forested environment requires a detailed description of forest growth dynamics. We have modified SWAT to bypass its crop model and use data simulated by a more complete growth model, ALMANAC. In this paper we discuss the modifications that were made to ALMANAC to simulate forest growth on the Boreal Plain. We built on published work using the plant growth model ALMANAC to simulate tree growth. Our efforts were aimed at developing parameters for white spruce, black spruce, lodgepole pine, and trembling aspen and their competition with shrubs, grasses, and herbaceous vegetation in young stands after forest disturbance, such as harvests and fires. The modified version of ALMANAC simulated light competition, and variations in forest stand structure (tree density), and produced reasonable estimates of variations in tree height and biomass in 55 permanent sample plots maintained by Millar Western. Initial SWAT simulations of a forested watershed suggest that forest disturbance and regrowth may be simulated by passing data between the two models. FORWARD will evaluate the potential for SWAT to estimate the impact of forestry practices on watershed hydrology and water quality.

Introduction

Watershed scale models, such as SWAT, have the potential to predict the changes to streamflow caused by forest harvest. SWAT has simulated catchment discharge and water quality in large catchments that include forest over short time periods assuming static forest conditions (Santhi et al., 2001). McKeown et al., (2004) modified the SWAT model for the Boreal Plain and simulated discharge in a watershed with greater than 90% forest. Their results were promising and suggest that SWAT is capturing the dominant hydrological processes in these watersheds. However, to provide predictions for the impacts of forest harvest on watershed hydrology, the static forest growth model in SWAT is inadequate (Watson et al., 2005). Due to the complexity and dynamic nature of forest growth over time and in particular over the first 20 years after stand establishment, a more dynamic forest growth model is required for SWAT.

SWAT incorporates equations to simulate plant growth from the crop growth model EPIC (Williams et al., 1983). ALMANAC is also a modified version of the EPIC model with equations that account for the competition for light, water, and nutrients between multiple species growing simultaneously (Kiniry et al., 1992). The ALMANAC model has reproduced low perennial/tree competition for light, water and nutrients (Kiniry, 1998) to estimate losses in grazing capacity due to shading. We feel that ALMANAC has the potential to simulate the dynamics of early forest stand growth where competition is occurring between perennial grasses, woody shrubs, and crop trees. Like SWAT, ALMANAC functions on a daily time-step and uses the same water balance equations, the same nutrient release equations and the same weather generator as the SWAT crop model, making the two models compatible.

Forests of the western Boreal Plain of North America contain any variety of pure or mixed stands of lodgepole pine (*pinus contorta*) white and black spruce (*picea glauca and mariana*), balsam fir (*Abies balsamea*), and rapid growing deciduous forests dominated by *Populus* species. Forest productivity ranges from productive stands with mean annual increments of wood production from 4.5 $m^3 ha^{-1} yr^{-1}$ to unproductive sites of less than 1 $m^3 ha^{-1} yr^{-1}$. After harvest, invading grasses and woody shrubs compete strongly with crop trees. The climate rests on the borderline of being able to sustain forests in terms of yearly moisture, with annual precipitation ranging from 300 mm in the north western extreme of the Plains to 625 mm per year in the eastern extreme. Forest stands occur on dry uplands where forest growth is limited largely by available soil water. Other forests stands are in fens, bogs, and seepage zones, where water tables are perched and adequate soil water is available. The relief is flat to gently sloping and catchment areas are large with first-order watersheds occupying 5 km^2. Water flow is dominated by rainfall and occasionally spring run-off, and rainfall occurs largely in June and early July (Smith et al., 2001).

We have modified ALMANAC and estimated growth parameters that provide simulations of the variation in forest growth over the life of a stand in dry, moist, productive and unproductive sites. One of the preferred methods to calculate evapotranspiration in forested environments is the Penmen-Monteith equation (Amthor et al., 2001), which requires good estimates of plant leaf area index (LAI), and canopy height. We bypassed the SWAT crop growth model and used the ALMANAC model predictions of canopy height and leaf area transferred to SWAT to simulate evapotranspiration using the Penmen-Monteith equation. The FORWARD study consists of 12 forested watersheds that have been gaged at least since 2001, five of which have been more than 50% harvested during the winter of 2003-2004. The objective of this work will be to use SWAT with ALMANAC as the crop growth model to simulate the impacts of forest harvest on the hydrology in these watersheds.

Initial attempts to use ALMANAC to simulate forest growth suggested that modifications were required to certain aspects of the model's equations to reproduce the variability of forest growth on the Boreal Plain. In this paper we describe equations integrated into the boreal forest version of the ALMANAC model ($ALMANAC_{BF}$) and demonstrate our initial results simulating the height and biomass of forested sites on the Boreal Plain as observed in data from Millar Western Forest Product's permanent sample plot program.

Material and Methods

Calibration Data

A subset of data from Millar Western Forest Products permanent sample plots were used to refine the growth parameters for boreal forest trees in $ALMANAC_{BF}$. Permanent sample plots are forest inventory plots in which the number, height, and diameter at breast height (DBH) of all trees in a 400 m^2 area are monitored. From these data sets, overstorey tree biomass was calculated with the use of allometric equations (Ter-Mikaelian et al., 1992) that relate the DBH of a tree to the total and foliar biomass. The subset of PSP data consisted of pure stands and mixtures of deciduous trees (aspen, birch and balsam poplar), lodgepole pine, and black and white spruce. A summary of the basic characteristics of the 55 sites is presented in Table 1. In addition to tree data, PSP data includes soil texture and drainage. The Alberta vegetation index (AVI) and ecosite maps of the areas were used to define the site index of the forest stand in which the PSP was established, and the ecosite phase of the site.

Table 1. General characteristics of calibration data set broken down by age classes and site indices.

Site Index	Age Class	Biomass ($Mg\ ha^{-1}$) Ave.	(Range)	Height (m) Ave.	(Range)	n
Good	<40	-	-	-	-	-
	40-50	100	(40-120)	14.8	(7.5-19)	8
	50-70	80	(20-140)	16.0	(7.5-15)	4
	70-100	181	(150-210)	19.6	(8.5-24)	5
	>100	155	(75-240)	19.6	(13-27)	6
Medium	<40	-	-	-	-	-
	40-50	125	(120-130)	9.1	(8.5-9.5)	2
	50-70	108	(90-130)	11.4	(9.0-14)	2
	70-100	172	-	23.1	-	1
	>100	126	(100-175)	18.1	(12-25)	6
Fair	<40	4	-	4.3	-	1
	40-50	87	(80-130)	7.9	(5.0-10)	8
	50-70	78	(20-160)	10.8	(7.5-15)	7
	70-100					0
	>100	96	(50-130)	17.0	(8.5-28)	5

Model Input

ALMANAC$_{BF}$ simulates forest growth from the first year after forest disturbance. Each of the 55 PSP sites were treated as individual input files. Vegetation input for ALMANAC simulations consisted of the current percent cover of tree species identified in the PSP data, and estimates of the maximum percent covers of shrub, forb and grass species in the first 20 years after stand initiation. The percent cover of these competing species present at stand initiation were estimated based on statistical relationships between ecosite and vegetation cover developed specifically for the Millar Western FMA (Doyon and MacLeod, 2000). Soil input data consisted of the physical and chemical characteristics for the four dominant soil series from this region of Alberta, taken from the Alberta Soils Database (Knapik, 1983). These were representative of the range of texture observed in the PSP data sets. Average monthly weather data were taken from a nearby Environment Canada weather station and were used to simulate a 180 year daily weather file.

Simulation of the Calibration Data Set

A batch processing script was written that ran ALMANAC for each of the 55 input files representing the individual PSP sites. The radiation use efficiency (RUE), maximum leaf area index (LAI) and empirical parameters used in the equations that describe the relationships between growth and heat unit accumulation (see Kiniry et al., 1992) for trees were modified to create the best fit relationship to the calibration data set.

ALMANAC, Model Functions

The ALMANAC model is a modification of the EPIC model (Williams et al., 1983) and the crop growth equations are very similar to those in the current SWAT crop model.

ALMANAC was initially developed to simulate competition of weeds on crop yield and includes a simple light competition model to simulate reductions in biomass due to shading (Kiniry et al., 1992). ALMANAC uses Beer's law (Monsi and Saeki, 1953) to simulate the photosynthetically active radiation (PAR) intercepted by the entire canopy,

$$FRACTION(PAR) = 1 - \exp\left(\sum_{\text{A to n}} k_n * LAI_n\right)$$

where FRACTION (PAR) refers to the fraction of PAR intercepted by the complete canopy, LAI_n is the LAI of n species making up the canopy and k_n is their light extinction coefficients as defined by Beer's Law.

ALMANAC simulates light competition by calculating the RATIO of the total FRACTION of PAR that each species intercepts based on their height relative to the height of the entire plant canopy. For example, for species "A" of the canopy the RATIO of the total FRACTION of PAR is calculated as:

$$RATIO_A = \frac{LAI_A * k_A * \exp\left(-\kappa_A * LAIHF_A\right)}{\sum_{\text{A to n}} LAI_n * k_n * \exp\left(-\kappa_n * LAIHF_n\right)}$$

where RATIO refers to the relative proportion of PAR that species A intercepts, LAI_n and k_n are the same as above, $LAIHF_n$ is the value of the combined LAI above half the height of the species and κ_n is the extinction coefficient of the combined canopy above half the height of the species. The conceptual development of this equation is based on the work of Spitters and Aerts (1983).

These equations allow ALMANAC to distribute PAR among the different species of the canopy based on their relative height with the assumption that shorter species will be shaded by the taller species in the canopy. The LAI and k values of each species are also accounted for in the partitioning of intercepted PAR among competing species.

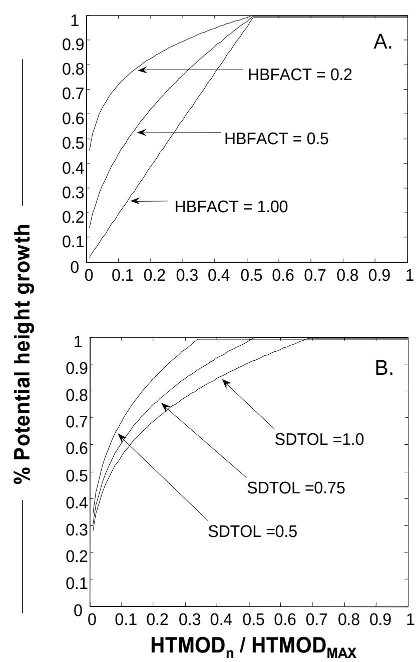

Figure 1A and 1B. The effect of factors (HBFACT and SDTOL) used in height reduction equations on potential height growth.

Modifications to ALMANAC for Boreal Forest Trees: Development of ALMANAC$_{BF}$

To simulate the development of mixed tree canopies of forest stands on the Boreal Plain, no changes were made to the fundamental model equations. However, it was necessary to make three changes to the model code to describe the variability in growth patterns observed across the Millar Western landbase on the Boreal Plain.

Height Growth Reductions with Light Competition

ALMANAC was initially developed to simulate the competition between annual or perennial weeds and crops in homogenous fields. While, competition effects on height growth of weeds and crops is not an issue, in forest stands, accurate simulation of height growth and the reduction of height growth associated with shading by other species is important. The tree height growth equations follow a sigmoid curve. We have incorporated a simple equation into ALMANAC that relates reductions in the RATIO of intercepted PAR to reductions in height growth. The equation is normalized for the percent occupancy of the canopy of a species to ensure that height reductions are only associated with differences in height between species. The calculation begins with a selection of the dominant shading species, i.e. that species that receives the greatest amount of PAR and whose height growth is not limited by other species occupying the canopy ($HTMOD_{MAX}$)

$$HTMOD_{MAX} = MAX\left(HTMOD_{1 \text{ to } n} = RATIO_{1 \text{ to } n} * \frac{LAI_{PC100_{1 \text{ to } n}}}{LAI_{PC_{1 \text{ to } n}}} \right)$$

where $HTMOD_{1 \text{ to } n}$ is the RATIO of PAR intercepted by species 1 to n and normalized by the ratio of the maximum potential LAI of the species (LAI_{MAX}) at 100% cover to the LAI at the percent cover defined by the user in the input file (LAI_{PC}).

Height growth of other species is reduced relative to the species that dominates the canopy identified as $HTMOD_{MAX}$

$$HTINCR_{A(n)} = HTINCR_{P(n)} * \left(\frac{HTMOD_{(n)}}{HTMOD_{MAX} * SDTOL_{(n)}} \right)^{HBFACT_{(n)}}$$

where $HTINCR_{A(n)}$ is the actual daily height increment corrected for the effect of shading, $HTINCR_{P(n)}$ is the potential height increment calculated as a function of the ideal sigmoid height growth curve, $HTMOD_{(n)}$ and $HTMOD_{MAX}$ are defined as above and $SDTOL_{(n)}$ and $HBFACT_{(n)}$ are species specific plant parameters that define how individual species react to shading. The factor $HBFACT_{(n)}$ accounts for the observation that reduced biomass associated with reduced PAR interception is not directly proportional to height growth to account for higher allocations of biomass to diameter growth (King, 2005). As $HBFACT_{(n)}$ increases species "*n*" will invest less biomass in height growth and more in diameter growth (Figure 1A). The factor $SDTOL_{(n)}$ allows species "*n*" to tolerate a certain amount of shading without reducing height growth to account for species that maintain investment in height growth (Perry, 1994) when shaded, to the detriment of diameter growth (Figure 1B). As $SDTOL_{(n)}$ decreases species "*n*" will tolerate a certain amount of shading without reducing height growth (Figure 1B).

Stem Number and Tree Allometrics

Tree growth in the original ALMANAC was focussed on light competition impacts on understorey perennials and annuals. Consequently, the differences between net primary production and gross primary production for trees were largely ignored, with the exception of estimates of annual leaf fall. We have incorporated a function into $ALMANAC_{BF}$ that calculates annual foliar return (leaf fall) based on species allometry, and stem exclusion (stemfall) in the early stages of stand development. The function also accounts for variations in stem density with site indices[1] that are based on local forest inventory yield tables.

---

[1] Site index is a commonly used classification system that separates stands based on productivity. Vegetation indices for forest areas classify stands according to site index as good, medium, fair and poor. Site indices are calculated for each forest stand in as forest management area from aerial photos and are a part of vegetation indices that Foresters use to evaluate the productivity of their landbase.

Changes in stem number with stand maturity were incorporated into the model by fitting an exponential decay curve with a single species specific crop parameter to the Alberta Phase 3 Forest Inventory.

$$STMX_{(n)} = \left(YTS_{MAX(n)} - YTS_{MIN(n)}\right) * \left(f(Y) * \exp\left(\frac{Y - YYTD_{(n)}}{SCM_{(n)}} \right)\right) + YTS_{MIN_{(n)}}$$

where $STMX_{(n)}$ is the maximum number of stems per hectare for species *"n"*, $YTS_{MAX(n)}$ is the maximum number of stems reported in yield tables, $YTS_{MIN(n)}$ is the minimum number of trees reported in yield tables, Y is the year after stand establishment, $YYTD_{(n)}$ is the first year that data is available in yield tables, and $SCM_{(n)}$ is a species specific crop parameter that defines the steepness of the exponential decrease in stem number after stand establishment. The $ALMANAC_{BF}$ user enters the values for $YTS_{MAX(n)}$, $YTS_{MIN(n)}$, and $YYTD_{(n)}$ as input taken directly from common forester's yield tables that provide stem numbers for different site indices at different stand ages. The model will then calculate decreases in stem number with stand maturity that vary with changes in site index based on these inputs. For example, with pure aspen stands, a good site will be reduced from 10,000 stems per hectare at year 10 after stand initiation to 400 stems at 180 years, whereas a fair site will decrease from 40,000 stems to 900 stems, respectively (Figure 2).

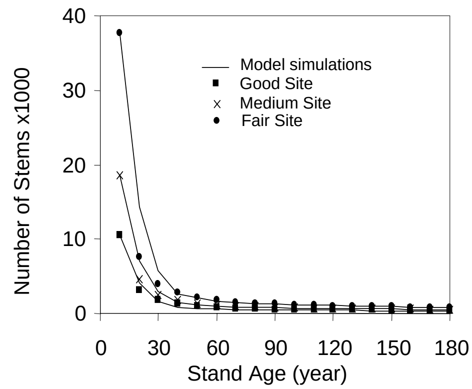

Figure 2. Model simulations of reductions in aspen stem number with increasing stand age at different site indices.

In mixed stands the actual stem numbers ($STM_{A(n)}$) for species *"n"* at any period during the development of the forest stand are modified based on the ratio of the actual calculated LAI and the maximum LAI at 100 percent cover (LAI_{PC100}).

$$STM_{A_{(n)}} = STM_{MAX} * \frac{LAI_{PC_{(n)}}}{LAI_{PC100_{(n)}}}$$

Once we have calculated number of stems in a given stand we can calculate tree mortality and loss of woody biomass due to tree mortality. First, we back-calculate an average DBH for the forest stand, using species specific allometric equations (Ter-Mikaelian 1993),

$$DBH_{(n)} = \left(\frac{AVB_{T_{(n)}}}{ABC1_{(n)}} \right)^{\frac{1}{ABC2_{(n)}}}$$

where $AVB_{T(n)}$ is the average biomass per tree calculated as biomass per hectare and $STM_{A(n)}$ and ABC1 and ABC2 are coefficients used in allometric equations relating biomass to DBH. Foliar biomass can then be calculated using allometric equations from the calculated DBH. Net annual aboveground biomass (NPP) production can then be calculated by subtracting losses of annual foliar biomass (100% for deciduous plants, 30% for coniferous species) and annual stem loss from gross annual production (GPP).

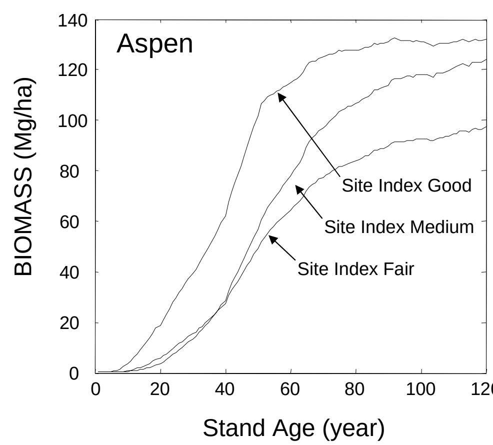

Figure 3. Average changes in biomass production associated with changes in site index in simulated pure Aspen stands.

$$NPP = GPP - FOL_n - \left((STMLY_{A(n)} - STM_{A(n)}) * AVB_{T(n)}\right)$$

where $STMLY_{A(n)}$ is stem number from the previous year and $STM_{A(n)}$ and $AVB_{T(n)}$ are as defined above.

Leaf Area Index, Relationships with Stem Density

A final modification to the ALMANAC code was required to account for differences in NPP that were observed on the landscape of the Boreal Plain. Some reductions in productivity may simply be related to stand structure. Other physiological models have accounted for decreases in NPP due to the increase in stem density (Landsberg and Waring, 1997; Zhou et al., 2004). As stem density increased, the DBH and foliar biomass of individual trees decreased. Consequently, as investment in foliar biomass decreased, LAI, total light interception, and biomass production was reduced. We incorporated these stand dynamics in a simplistic manner based on relative differences between stem density in good sites, versus medium and fair sites. The model calculates stem density, DBH and foliar biomass for the defined site index as above and then in parallel calculates an optimum foliar biomass based on the *"ideal"* stem density (i.e. as if the site was classified as a good site).

$$LAI_{PCA(n)} = LAI_{PC(n)} * \frac{BFOL_{SI(n)}}{BFOL_{SIO(n)}}$$

The actual leaf area index (LAI_{PCA}) for species *"n"* used to calculate species growth is a function of the maximum potential LAI_{PC} at a given percent cover, reduced by the fraction of foliar biomass at the user defined site index ($BFOL_{SI}$) over the optimum foliar biomass ($BFOL_{SIO}$) in a good site at lower stem density and with higher DBH trees. Biomass in fair sites can be reduced by up to 30% compared to good sites, due to the simulated differences in investment of biomass between foliage and stems captured in this relationship (Figure 3).

Results

Biomass and Height in Permanent Sample Plot Data

Without the changes incorporated into $ALMANAC_{BF}$ the model overestimated tree biomass at combinations of RUE and LAI that would be considered reasonable for boreal forest conditions (between 1 and 2 g MJ^{-1} and 2 to 5 m^2 m^{-2}, respectively) due to underestimates of annual stem and leaf fall. Furthermore, height growth did not vary from site to site. With the basic changes we incorporated into the model code, the model simulations of PSP data reproduced the difference in average biomass for different age classes and site indices reported in Table 1 with an r^2 of 0.73 (Figure 4A) and the average heights with an r^2 of 0.83 (Figure 4B). When the observed and simulated biomass and height of all individual PSPs are compared the r^2s are only 0.49 and 0.55, respectively (data not shown). The model does not

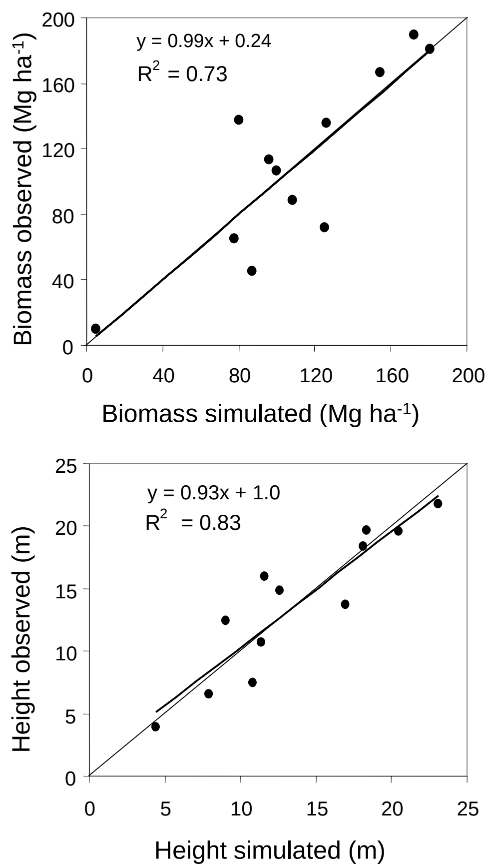

Figure 4A and 4B. Simulated average biomass (A) and height for different age classes in the calilbration data set

reproduce all the variability observed in the PSP data. However, it produced a reasonable reproduction of the average trends observed on the landscape at different stand ages and in different productivity classes (site indices).

There are many sources of error in such a simulation. A portion of the error is associated with input error. The competition that is occurring after stand initiation from grasses/forbs and shrubs is, at best, an estimate since we have no real data on the initial conditions of the stand. Also, the use of site indices that are estimated from aerial photos can lead to misinterpretations about the productivity of a site. Furthermore, we have not yet attempted to simulate the limitations on growth associated with nutrient limitations. Nonetheless, the fact that we were able to reproduce the general trends in biomass and height growth with limited input data is promising and the model is a measurable improvement over the current crop model in SWAT for simulating forest growth dynamics.

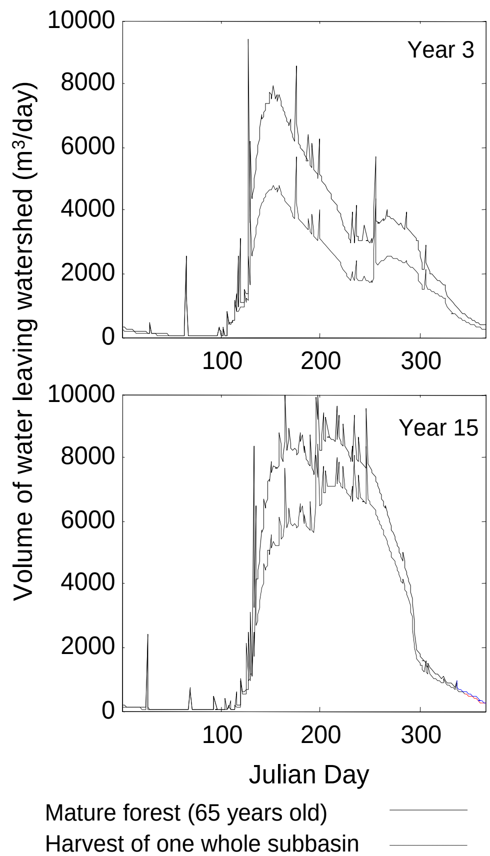

Figure 5. The outflow of a generic watershed simulated by SWAT in year 3 and year 15 of a 15 year simulation using ALMANAC as the growth model with the entire watershed modeled as a mature forest and with one subbasin harvested and regrowing after harvest.

SWAT-ALMANAC Interface

The objective of bypassing the SWAT crop growth model and using ALMANAC input data was to be able to reproduce changes in evapotranspiration when forests are disturbed. We have set up a 200 ha Boreal Plain watershed with three subbasins and simulated outflow for 15 years with SWAT using ALMANAC as the crop growth model. In one case, we simulated the watershed entirely covered with mature (65 year old) forest and in the second case with a complete harvest of one of the watershed's subbasins using identical weather input. In this example, we observed a decrease in peak outflow with the forest harvest of nearly 100% in year three after harvest increasing to about 25% of the original harvest in year 15 (Figure 5). It is evident from this result that we are able to use ALMANAC as the SWAT crop growth model to create modifications in forest growth that can have measurable impacts on evapotranspiration.

Conclusions and Continued Work

ALMANAC$_{BF}$ has been modified to provide reasonable simulations of the variability in biomass and height of forest stands ranging from the age of 28 to greater than 100 years of age on the Boreal Plain. The model shows promise for simulating forest growth on the Boreal Plain. The parameters developed in the calibration routine will be verified against an independent data set from Millar Western's PSP data. However, we have only begun to work with simulations of forest growth in the first 20 years. Other data sets will allow us to validate plant parameters for forbs, grasses and woody shrubs. Thus we will be able to reproduce the relationships between the leaf area index, biomass, and evapotranspiration on sites immediately after forest harvest (the first 20 years) to provide estimates of the impacts of forest harvest on evapotranspiration. Furthermore, subroutines that are associated specifically with forest practices, such as herbicide application and thinning operations, must be incorporated into the model.

Modifications in evapotranspiration due to forest harvest can be simulated by transferring plant growth data from ALMANAC to SWAT. The interface between the two models must be further refined. In addition, there is a need to verify whether or not the soil water balance equations are providing similar estimates of soil water content and water stress on plants on a daily basis. Work will begin soon on simulation of the impacts of forest harvest on watershed hydrology in the FORWARD gaged watersheds.

References

Amthor, J.S., J.M. Chen, J.S. Clein, S.E. Frolking, M.L. Goulden, R.F. Grant, J.S. Kimball, A.W. King, A.D. McGuire, N.T. NIkolov, C.S. Potter, S. Wang and S.C. Wofsy. 2001. Boreal forest CO_2 exchange and evapotranspiration predicted by nine ecosystem process models: Intermodal comparisons and relationships to field measurements. J. Geophys. Res. 106: 33623-33648.

Doyon, F. and H.L. MacLeod. 2000. BAP Report #5 Special habitat element model development. Insitut Quebecois d'Amenagement de la Foret Feuillue St Andre, QC and KBM consultants, ThunderBay, ON, Canada.

King, D. 2005. Linking tree form allocation and growth with an allometrically explicit model. Ecol. Model. 185: 77-91.

Kiniry J.R., J.R. Williams, P.W. Gassman and P. Debaeke. 1992. A general process-oriented model for two competing plant species. Trans. ASAE 35: 801-810.

Kiniry, J.R. 1998. Biomass accumulation and radiation use efficiency of honey mesquite and eastern red cedar. Biomass Bioenergy, 15: 467-473.

Knapik, L.J. and J.D. Lindsay. 1983. Reconnaissance soil survey of the Iosequn Lake Area, Alberta. Report Umber 43, Alberta Research Council, Edmonton, AB. Canada.

Landsberg, J.J. and R.H. Waring. 1997. A generalised model of forest productivity using simplified concepts of radiation use efficiency, carbon balance and partitioning. For. Ecol. Management. 95: 209-228.

McKeown, R., Putz, G., Arnold, J. and Whitson, I. 2004. Streamflow modelling in a small forested watershed on the Canadian Boreal Plain using a modified version of the soil and water assessment tool (SWAT). 1st Water and Environment Specialty conference of the Canadian Society for Civil Engineering. Saskatoon, Canada, June 2-5 2004.

Monsi, M. and T. Saeki. 1953. Uber den Lictfaktor in den Pflanzengesellschaften und sein Bedeutung fur die Stoffproduktion. Japan J. Bot. 14:22-52.

Perry, D. 1994. Forest Ecosystems. The Johns Hopkins University Press, Baltimore. 649 pp.

Santhi, C., J.G. Arnold, J.R. Williams, W.A. Dugas and L. Hauck. 2001. Validation of the SWAT model on a large river basin with point and nonpoint sources. J. Amer. Water Resourc. Assoc. 37: 1169-1188.

Spitters, C.J.T. and R. Aerts. 1983. Simulation of competition for light and water in crop-weed associations. Aspects of Appl. Biol. 4: 467-483.

Smith, D.W., E.E. Prepas, G. Putz, J.M. Burke, W.L. Meyer and I. Whitson. 2003. The forest watershed and riparian disturbance study: a multi-disciplinary initiative to evaluate and manage watershed disturbance on the Boreal Plain of Canada. J. Environ. Eng. Sci. 2: S1-S13.

Ter-Mikaelian, M.T. and M.D. Korzukhin. 1997. Biomass equations for sixty-five North American tree species. For. Ecol. Man. 97: 1-24.

Watson, B.M. N. Coops, M. Ghafouri and S. Selvalingam. 2005. Simulating leaf area index of eucalyptus forest and pine plantations for a catchment-scale water balance model. 29th Hydrology and Water Resources Symposium. Feb 21-23, Canberra, Australia.

Williams, J.R., Renard, K.G., and Dyke, P.T. 1983. A new method for assessing the effect of erosion on productivity—The EPIC model.

Zhou, X., Peng, C and Dang, Q. 2004. Assessing the generality and accuracy of the TRIPLEX model using in situ data of boreal forests in central Canada. Environ. Model Software 19: 35–46

Integration of 3-PG into SWAT to Simulate the Growth of Evergreen Forests

B.M. Watson[1*], N. Coops[2], S. Selvalingam[1] and M. Ghafouri[1]
[1]School of Engineering and Technology, Deakin University, Geelong, Victoria, Australia, 3217. E-mail: bmwatson@deakin.edu.au
[2]Department of Forest Resource Management, University of British Columbia, Vancouver, Canada.

Abstract

SWAT cannot accurately simulate the seasonal fluctuations or the long-term trend of the Leaf Area Index (LAI) of evergreen forests. This deficiency has detrimental impacts for the prediction of interception and transpiration, two processes that have a significant influence on catchment water yield. This paper details the integration of the forest growth model 3-PG with SWAT to improve the simulation of LAI for evergreen forests. The integrated model, called SWAT/3-PG, was applied to the Woady Yaloak River Catchment in southern Australia where eucalyptus forests and pine plantations account for 30% of the total land use. SWAT/3-PG simulated the LAI of eucalypts and pines more accurately and realistically than the original version of SWAT. Forest LAI simulated by SWAT/3-PG agreed reasonably well with estimates of forest LAI derived independently from a Landsat satellite image. SWAT/3-PG has considerable value as a tool that managers can utilise to predict the impacts of land use change in catchments where evergreen forests are prevalent.

Introduction

SWAT is a hydrologic model than can be used to predict the long-term impacts of land use change on the water balance and water quality of large scale catchments. It is a powerful tool that is utilised by numerous catchment management authorities around the world to manage land and water resources at a regional scale. SWAT is becoming increasingly popular in Australia with numerous applications of the model reported recently. One of the main reasons for the growing popularity of SWAT is that very few large scale catchment models have been developed in Australia for predictive purposes. There is an urgent need for catchment management authorities to have access to tools that will enable them to predict the impacts of impending land use changes. SWAT is regarded by many to be a suitable model that can fill the void.

Watson et al. (2003) identified a deficiency with the vegetation growth component of SWAT from an application of the model to the Woady Yaloak River Catchment in southern Australia. They found that the leaf area index (LAI) and biomass of mature eucalyptus and pine trees was not simulated accurately. Figure 1 shows the LAI and biomass of the eucalyptus trees growing in subcatchment 1 of the Woady Yaloak River Catchment as simulated by SWAT. It can be observed that the LAI and biomass of the eucalyptus trees fluctuates significantly on an annual basis. These patterns in LAI and biomass are totally unrealistic and do not accurately represent the long-term trends normally associated with these types of trees. Several SWAT users in Australia and overseas have reported to the first author through personal communications that they have encountered the same problem.

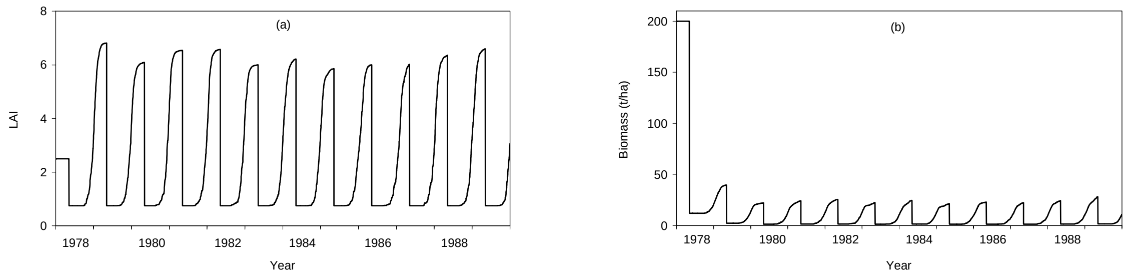

Figure 1(a)-(b). LAI and biomass of eucalyptus trees as simulated by SWAT.

The cause of these fluctuations is attributed to the model forcing all trees, regardless of the species, to go dormant for several months of the year in response to shortened day length. Dormancy is a mechanism that definitely needs to be accounted for in explaining the growth of deciduous trees. However, this is not the case for evergreen trees because they do not lose all their leaves every autumn and they do not enter a prolonged dormant period in winter. When the dormancy mechanism in the model was deactivated for the trees, it was found that the large fluctuations were no longer a problem. However the long-term trend in LAI normally associated with eucalypts and pines was still not reproduced adequately.

SWAT utilises a single plant growth model to simulate a variety of vegetation types including pasture, crops, and trees. The plant growth model used in SWAT is a simplified version of the EPIC (Williams, 1995) plant growth model, which was originally developed to simulate the growth of annual and perennial crops. The model was later used to predict the growth of pine trees (Williams, 1995) but it would appear that no significant modifications were made to the model to accommodate its extension from crops to trees. Therefore, tree growth is seemingly differentiated from crop growth simply by the utilisation of a different set of parameters. In SWAT, phenological plant development is based on daily accumulated heat units. This theory postulates that plants have heat requirements that can be quantified and linked to the time it takes to reach maturity. The heat unit approach has been in use for over two centuries and has been applied by researchers to a wide variety of plants (Wang, 1960). There are also a number of tree growth models that involve some use of the heat unit theory (Schenk, 1996). It should be noted that there are significant differences between these tree growth models and the plant growth module of SWAT. Wang (1960) remarked that "the heat unit system has been widely adopted because of its value in satisfying practical needs, rather than for its accuracy or its theoretical soundness." In fact, utilisation of the heat unit theory in plant growth models has been severely criticised for a variety of reasons (see Schenk, 1996). It is unlikely that the current plant growth module of SWAT could be used to accurately predict the growth of evergreen forests. It is undoubtedly a complex issue which needs to be reviewed in the near future.

The realistic long-term, large scale spatio-temporal characterisation of LAI is of great importance in studies concerning land use change and its effect on hydrology (Watson, 1999). The processes of interception and transpiration, both of which play a key role in catchment hydrology, are highly dependant on LAI (Vertessy, 2001). Therefore, the inability of SWAT to correctly simulate the LAI of evergreen forests has serious implications for its application to Australian catchments. Large eucalypt and pine plantations are expected to be established across Australia in the coming decades to prevent further degradation of land and water resources. The results from an application of SWAT to predict the impacts arising from these changed conditions would have to be reviewed with extreme caution, otherwise erroneous conclusions may be reached and as a consequence the management strategies to be implemented could be seriously flawed. Given that catchment managers in Australia are expected to rely heavily on SWAT for routine planning and decision making in the future, it is vital that LAI be predicted with sufficient accuracy. Harris (2003) stated "in an environment of massive degradation it is very important that we get our basic assumptions and tools correct." After careful consideration, it was concluded that it would be more practical to integrate a soundly based, well-established and technically supported forest growth model into SWAT instead of modifying the existing plant growth module to simulate the growth of evergreen forests more accurately. The latter option would have been a very difficult, expensive, and time consuming task. This paper describes the integration of the forest growth model 3-PG (Physiological Principles in Predicting Growth) (Landsberg & Warring, 1997) with SWAT.

Description of 3-PG

3-PG is a dynamic, process-based model of forest growth that predicts the net photosynthesis by forest stands on a monthly basis using climate, soil, and management factors. The model utilises a number of simple relationships derived from earlier research that allows process-based calculations to estimate forest growth in terms of a few variables (Coops and Waring, 2001). 3-PG is a generalized stand model which means applications of the model are not restricted to a particular site or a single species. It can be applied to plantations and even-aged, relatively homogenous forests. The parameters required by the model are related to tree physiology and can be derived from field measurements or the literature. The input data required are mean monthly values of maximum and minimum temperature, rainfall, solar radiation, and vapour pressure deficit as well as estimates of the soil storage capacity and soil fertility. 3-PG can be run for a nominated period of years using long-term monthly averages or monthly data for each year. Figure 2 shows the LAI and biomass of the eucalyptus forest in subcatchment 1 of the Woady Yaloak River Catchment as simulated by 3-PG using long-term average climate data. The seasonal fluctuations in LAI can be clearly observed, as can the long-term trend. It should be noted that these patterns in LAI are also observed for pine trees.

The model is essentially comprised of a set of calculations that lead to biomass values and another set that then distribute the biomass to the leaves, roots, and stems (Kirschbaum et al., 2001). Gross primary production in 3-PG is the product of the canopy quantum efficiency coefficient and the utilisable absorbed photosynthetically active radiation, which is obtained through the reduction of the absorbed photosynthetically active radiation by an amount determined by a series of modifiers. The modifiers reflect the constraints imposed on the utilisation of absorbed radiation by leaves of the canopy due to stomatal closure caused by high atmospheric pressure deficits, changes in soil water content, the effects of sub-freezing temperature, and stand age (Landsberg & Waring, 1997).

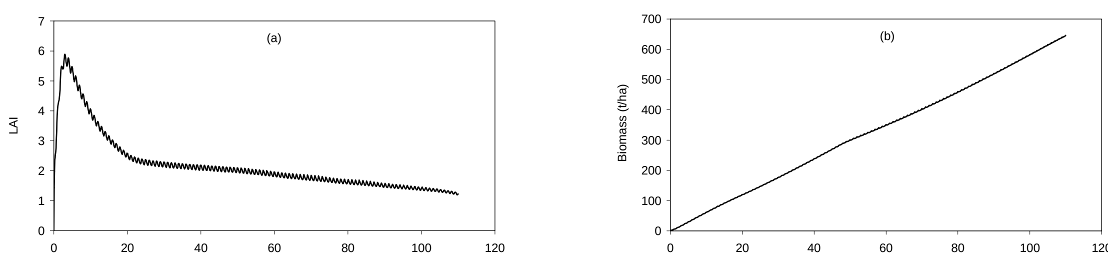

Figure 2(a)-(b). Long-term LAI and biomass of eucalypts simulated by 3-PG.

Research has shown that the ratio of net to gross primary production is relatively constant (0.45 ± 0.05) for a wide variety of forests, including deciduous hardwoods and evergreen conifers (Landsberg & Waring, 1997). This simplifying assumption eliminates the need to calculate respiration. Net primary production, which is the net amount of carbon converted to biomass, is then partitioned into root and above ground biomass. The amount of carbon allocated to the roots below ground is estimated using a simple relationship derived from information in the literature on root growth and turnover while the amount of carbon allocated between the foliage and stems is determined using a procedure based on allometric ratios (Landsberg & Waring, 1997). The model accounts for the effects of nutrition on the amount of carbon allocated to the roots, with less carbon being allocated to the roots of trees on fertile sites. 3-PG uses a procedure based on the -3/2 power law and stem growth rates to compute changes in stem populations (self-thinning) (Landsberg & Waring, 1997). Litterfall and the decline in forest growth rates due to age have also been incorporated into the model.

Although there are numerous process-based models available, most have limited practical value to forest managers and can only be used for research purposes. According to Landsberg & Waring (1997), the reason for this is "the calculation of forest growth from physiological processes is complicated and has necessarily involved the use of detailed, multi-variable models that generally require a great deal of information and careful parameterisation before they can be run." In contrast, 3-PG is considerably less complex than most other process-based models, yet it is soundly based on a number of well-established physiological principles and biophysical processes. Therefore, the model is of considerable value to practitioners involved in the management of forests and plantations as well as to scientists who can use it as a research tool. 3-PG has been widely evaluated in Australia as well as in other countries such as the USA, Canada, China, Brazil, South Africa, and the U.K.

Incorporation of 3-PG into SWAT

3-PG is a public domain model so the source code, which is written in Visual Basic, is freely available. The source code was converted from Visual Basic into Fortran90 and incorporated into SWAT as a separate subroutine. It is important to note that SWAT was operated on a daily time-step whereas a monthly time-step was utilised for 3-PG. Although versions of 3-PG that operate on a daily time-step have been developed (M. Battaglia, CSIRO FFP, personal communication, 2004), extreme caution needs to be exercised with their use because the assumptions and coefficients pertaining to 3-PG are relevant at a monthly time scale. Therefore, retaining the monthly time-step for 3-PG in SWAT was regarded to be a compulsory measure. Although there may be scaling issues associated with this arrangement, it was not considered critical because the LAI and biomass of evergreen forests can be predicted more accurately by the integration of 3-PG into SWAT than by using the original plant growth module in SWAT. Sophocleous & Perkins (2000) were confronted with the same issue when they integrated the groundwater model MODFLOW into SWAT. SWAT was operated on a daily time-step, whereas MODFLOW was utilised on a monthly time-step. They reported that "ideally, streamflow and ground-water movement should be calculated with the same time-step because of their interactions." However, due to computational constraints, a monthly time-step was utilised for MODFLOW simulations. Although they acknowledged that using a monthly time-step to represent groundwater processes was a limitation, they did not consider it critical because the integrated model allowed the seasonal variation of watertable levels and recharge to be predicted over a period of several years with sufficiently greater accuracy than what could be achieved with the original version of SWAT. In light of this, it was deemed adequate to use a monthly time-step for 3-PG in SWAT.

On the first day of every month, the 3-PG subroutine was called to compute the LAI and biomass for the HRUs comprised of eucalypts and pines. The value of the LAI and biomass calculated on the first day of the month was assumed to be constant for the rest of the month. This assumption is quite reasonable given that fluctuations in LAI and biomass of eucalyptus and pine trees are minimal from one month to the next (see Figure 2). For the first month of the simulation period, initial values had to be assigned for several site factors including the initial number of stems, stand age, and the biomass of the foliage, stems, and roots.

One of the modifiers utilised by 3-PG to reduce the absorbed photosynthetically active radiation is the soil water modifier. The equation used to calculate this variable requires the ratio between the soil water content and the storage capacity of the soil to be known (referred to here as the moisture ratio). The original 3-PG model employs a simple monthly water balance model to compute the soil water content. It does not explicitly account for the soil water content of the individual horizons in the soil profile. Instead the soil profile is simply treated as a single layer. In contrast, SWAT computes the soil water content for the individual horizons in the profile. In the integrated model, the soil water content calculated for each horizon by SWAT was summed to give the total soil water content of the profile, which was then used to compute the soil water modifier for the 3-PG component. The average soil water content of the previous month was used to calculate the soil water modifier. It is possible to utilise the value of the soil water content on the same day that the 3-PG subroutine is activated. However, it was found that when this approach was implemented, the occurrence of large rainfall events towards the end of the month could raise the soil water content substantially, which would cause larger than expected LAI and biomass values to be computed in the following month. Apart from the fact that using the average soil water content of the previous month returned better results, this approach is also more consistent with the original 3-PG model because the modifiers used to calculate the utilisable radiation are applied to monthly averages (Landsberg & Waring, 1997).

Study Area

The Woady Yaloak River Catchment is located in southwest Victoria, Australia. Human activities such as gold mining and agriculture are largely responsible for the massive environmental degradation observed today. A remedial measure that has been proposed to prevent further degradation is the widespread planting of trees in the worse affected areas of the catchment. The consequences of this could be devastating because the Woady Yaloak River Catchment is home to more than 200 farmers and is a significant contributor to Australia's agricultural output. Native eucalyptus forests and commercial pine plantations account for more than 30% of the total land use at the present time. Given that they cover almost one-third of the catchment, the forests and plantations undoubtedly play an important role in the overall water balance of the study area.

Numerous eucalyptus species are found in the native forests of the Woady Yaloak River Catchment. Basic information on the distribution of species within the forests is given in DSE (2004a), with nearly all forests being comprised of more than one species. 3-PG does not permit the growth of multiple species to be modelled within the same plot, nor does SWAT allow HRUs to be comprised of more than one species. In most of the native forests across the study area, *Eucalyptus obliqua* is the dominant species. For simplicity it was assumed all native forests were comprised of *E. obliqua*. The exact age of the eucalyptus forests in the study area is largely unknown, although DSE (2004b) have classified most as mature (DSE, 2004b). The eucalyptus trees were estimated to be approximately 70 years old from field observations. The pine plantations, comprised mainly of *Pinus radiata*, were established in the mid 1960s (LCC, 1980). It was assumed they were all established in 1965.

Setup and Calibration of SWAT/3-PG

The Woady Yaloak River Catchment was discretised into 29 subcatchments and 92 HRUs. The number of HRUs identified as eucalyptus and pine were 10 and two, respectively. A threshold level of 10% was used to define the land use and soils of the HRUs. SWAT/3-PG was calibrated and validated for the periods 1978-1989 and 1990-2001, respectively. The model was calibrated against streamflow recorded at the two gauging stations located along the river: Pitfield (306 km^2) and Cressy (1157 km^2). The 3-PG component was parameterised for *E. obliqua* and *P. radiata* by using parameter values supplied by the CSIRO.

Remote Sensing Data

In recent years, the use of remote sensing to estimate the LAI of forests has become widespread because it is a relatively simple and cost-effective method. A number of studies have reported good correlations between ground-based measurements of LAI and estimates of LAI derived from satellite images (for example Coops et al., 1997). Estimates of LAI for the study area were derived from a Landsat 7 ETM Path Image taken in January 2001. Using bands 4 and 5, which are the near infrared (NIR) and red (R) wavelengths of the electromagnetic spectrum, an image of Normalised Difference Vegetation Index (NDVI) was calculated. LAI was estimated directly from NDVI using a predictive regression relationship (Coops et al., 1997). The LAI derived from the resultant image at several sites across the catchment were compared to the LAI predicted by SWAT/3-PG in January 2001.

Results and Discussion

Figure 3 shows the LAI and biomass of the eucalypts and pines growing in subcatchment 1 simulated by SWAT-3PG and the original 3-PG model for the calibration period. The LAI and biomass simulated by SWAT/3-PG was in good agreement with the LAI and biomass simulated by 3-PG. Due to the integration of 3-PG into SWAT, the predicted LAI and biomass of the forests is clearly more realistic than the LAI and biomass produced by the original SWAT plant growth module (see Figure 1). The large disparity between the LAI and biomass of the eucalypts and pines is attributed to the significant age difference (approximately 35 years) between the two tree types.

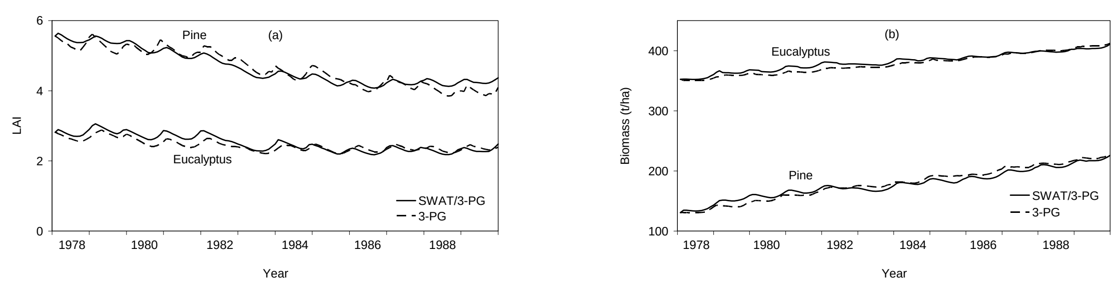

Figure 3(a)-(b). Simulated LAI and biomass of eucalypts and pines in subcatchment 1.

The slight differences between the LAI and biomass simulated by SWAT/3-PG and 3-PG are attributed to the different soil water balance components of the two models. The utilisation of different soil water balance components leads to variations in the soil water content simulated by the models over time. Any variations in the soil water content will result in different values for the soil water modifier being computed. Therefore, the absorbed photosynthetically active radiation will not be reduced by the same quantity in the case of each model. As discussed earlier, the moisture ratio is determined from the soil water content. The discrepancy between the moisture ratios simulated by the two models over time is shown in Figure 4. It is evident that the moisture ratio simulated by SWAT/3-PG varies considerably from that simulated by 3-PG. The long-term trend indicates that the moisture ratio is highest in winter and lowest in summer. This is not surprising because prolonged rainfall over the winter months replenishes the soil water which is then depleted over the hot, dry summer months. 3-PG has a tendency to produce higher values for the moisture ratio in winter. However, it is in summer that the greatest discrepancies exist. Values for the moisture ratio predicted by SWAT/3-PG in summer are considerably lower than those predicted by 3-PG.

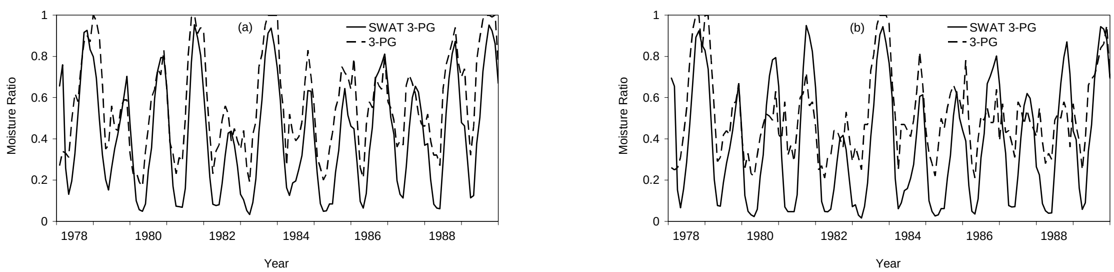

Figure 4(a)-(b). Simulated moisture ratio for eucalypts and pines growing in subcatchment 1.

For six sites across the study area, an average value of LAI was determined from the image of computed LAI. The six sites, which were several square kilometres in area, were selected from subcatchments that had large tracts of native forests or plantations growing in them. In each of those subcatchments, HRUs had been created with either eucalypts or pines as the land use. One hundred values of LAI were obtained from the image at each of the six sites, with each value of LAI corresponding to the value of one pixel (100 m x 100 m). Selection of the values was a random procedure and therefore somewhat subjective. Care was taken to ensure low LAI readings, which in all likelihood corresponded to cleared areas or thin stands which are not representative of the surrounding forest, were not selected and included in the analysis. Inclusion of these low readings would result in the LAI of a site being underestimated. Presented in Figure 5 are 'box and whisker' plots of the statistics for the LAI derived from the Landsat satellite image. The plots present the mean, 25 and 75 percentiles, and the range (maximum and minimum) of the 100 values of LAI selected at each site. Also presented in Figure 5 are the values of LAI predicted by SWAT/3-PG in January 2001 from the subcatchments in which the six sites were selected.

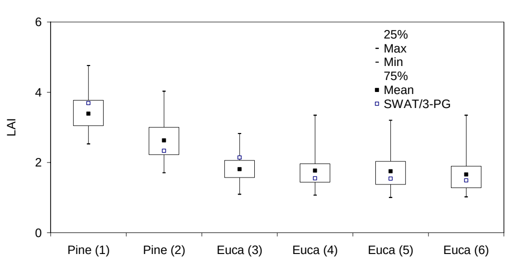

Figure 5. 'Box and whisker' plots of statistics for LAI derived from Landsat satellite image and LAI predicted by SWAT/3-PG.

Figure 5 reveals that there is considerable spread in LAI at each of the six sites analysed. However, the LAI predicted by SWAT/3-PG fell within the 25 and 75 percentiles of the LAI derived from the Landsat image at five out of the six sites. The LAI predicted by SWAT/3-PG was just above the 75 percentile at site 3. Differences between the simulated LAI and the mean LAI estimated from the satellite image ranged from 6% to 19% across the six sites. It is acknowledged that this analysis involving the LAI derived from the remote sensing image is somewhat crude compared to other analyses reported in the literature (e.g. Coops et al., 1997), but given the financial and time constraints imposed on this project little else could be done. It is highly recommended that a more detailed study of this nature be conducted in the future for the study area.

Soil evaporation, transpiration, and canopy evaporation are the three main components of evapotranspiration (Vertessy, 2001). The annual values for each component as predicted by SWAT/3-PG are shown in Figure 6 for the eucalypts in subcatchment 1 over the calibration period. Transpiration is the largest component accounting for 71.2% of the total amount of evapotranspiration over the calibration period. For the same period, soil evaporation and canopy evaporation comprised 13.5 and 15.3%, respectively, of the total amount of evapotranspiration. White et al. (2002) have shown that more water is lost through transpiration from eucalyptus stands than through soil evaporation and canopy interception. They measured the canopy evaporation, transpiration, and soil evaporation from a tree belt in Western Australia, which contained five different species of eucalypts, for one year. It was found that transpiration accounted for 73.9% of the total amount of evapotranspiration over this period, whereas canopy evaporation and soil evaporation accounted for 17.0 and 9.1%, respectively.

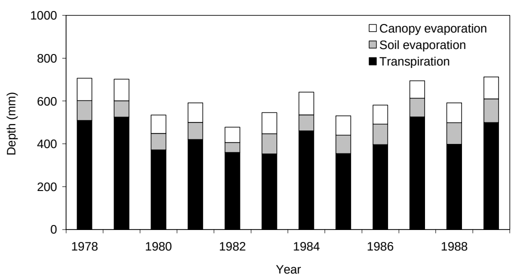

Figure 6. Annual soil evaporation, canopy evaporation, and transpiration from eucalypts in subcatchment 1.

The observed and predicted hydrographs for the annual and monthly runoff at Cressy are shown in Figure 7 for the calibration period. The performance of SWAT/3-PG for predicting annual runoff was exceptionally good. It is important to note that the model has accounted for the considerable variability in runoff on an annual time scale. Very good results were also achieved for monthly predictions, with the model capturing the seasonal trends extremely well.

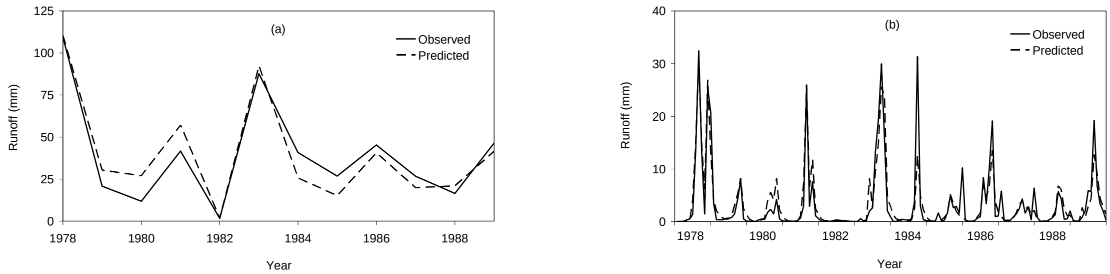

Figure 7(a)-(b). Observed and predicted hydrographs for annual and monthly runoff at Cressy.

This study has shown that the integration of 3-PG into SWAT has lead to considerable improvements in the simulation of LAI and biomass for the native eucalyptus forests and commercial pine plantations in the Woady Yaloak River Catchment. Given the demonstrated suitability of 3-PG for simulating the growth of forests in Australia, the integrated model described in this paper, SWAT/3-PG, has the potential to be applied to other catchments in Australia where eucalypts and pines comprise a significant proportion of the total land use. SWAT/3-PG also has value as a practical tool for forest managers who may need to consider the impacts of forestry activities on runoff, groundwater recharge, and evapotranspiration. This cannot be achieved by the stand-alone version of 3-PG at the current time due to the very simple water balance component embedded in its formulation. SWAT/3-PG is not limited to applications in Australia, but can be applied to catchments around the world where evergreen forests are found. It is important to remember that SWAT/3-PG is not a universally applicable model because 3-PG cannot be used to simulate the growth of deciduous forests. Although 3-PG has been applied to diverse forest types (see Coops and Waring, 2001), there are still many species that have yet to be assigned parameter values. However, in these circumstances it would be sufficient to adopt values from a similar species, particularly since improved estimates of LAI can be achieved from using SWAT/3-PG over SWAT. The fact that 3-PG cannot handle mixed-species forest stands is not considered to be a limitation at the present time because almost every forest growth model currently available cannot simulate the growth of plots containing more than one species (Schenk, 1996). It is also important to point out that there are several disadvantages associated with the integration of 3-PG with SWAT. These include an increase in model complexity, greater data requirements, and the need for a more experienced user. However, it is felt that these disadvantages are outweighed by the main advantage of the integrated model, which is the ability to provide accurate and reliable predictions of LAI and biomass for evergreen forests.

Conclusions

The original version of SWAT is not able to simulate the long-term trend of LAI and biomass for eucalyptus and pine trees adequately. 3-PG, which is a process-based, forest growth model, was integrated with SWAT to overcome this deficiency. SWAT/3-PG was shown to predict the LAI and biomass of the evergreen forests in the Woady Yaloak River Catchment more accurately than the original version of SWAT. The LAI and biomass predicted by SWAT/3-PG compared well with the LAI and biomass simulated by the original 3-PG model. It was also shown that forest LAI modelled by SWAT/3-PG compared well to forest LAI derived from a Landsat satellite image. LAI needs to be predicted with sufficient accuracy because transpiration and interception, two processes that have a significant influence on catchment water yield, are highly dependent on LAI. SWAT/3-PG is able to provide reliable estimates of LAI for long periods of time, which means it can be used with greater confidence than SWAT as a tool for making management decisions in catchments where evergreen forests occupy large areas of land. The results from this preliminary application of SWAT/3-PG are very promising and warrant further research be carried out to further evaluate and test the model. In general, it is strongly recommended that extensive research be conducted in the near future on forest growth in SWAT, given the widespread occurrence of evergreen forests in many regions of the world. However, this does not imply that the integrated model described in this paper, SWAT/3-PG, should be the sole focus of any future research efforts.

References

Coops, N., Delahaye, A., & Pook, E. (1997). Estimation of eucalyptus forest leaf area index on the south coast of New South Wales using Landsat MSS data. *Australian Journal of Botany*, *45*, 757–769.

Coops, N.C., & Waring, R. (2001). The use of multiscale remote sensing imagery to derive regional estimates of forest growth capacity using 3-PGS. *Remote Sensing of Environment*, *75*, 324-334.

DSE. (2004a). Forest Maps & Facts, Department of Sustainability and Environment, Midlands FMA, www.dse.vic.gov.au, Accessed 5 April 2004.

DSE. (2004b). Victorian Forest Resources – Interactive Maps, Department of Sustainability and Environment, Relative Age Layer, www.dse.vic.gov.au, Accessed 5 April 2004.

Harris, G. (2003). Ecological paradigms, change detection and prediction. In: D. Post (Ed.), *Proceedings of MODSIM 2003*, MSSANZ, 1-10.

Kirschbaum, M.U.F., Carter, J.O., Grace, P.R., Keating, B.A., Keenan, R.J., Landsberg, J.J., McKeon, G.M., Moore, A.D., Paul, K.I., Pepper, D..A, Probert, M.E., Richards, G.P., Sands P.J. & Skjemstad, J.O. (2001). Brief description of several models for simulating net ecosystem exchange in Australia. In: M.U.F. Kirschbaum & R. Mueller (Eds.), *Net Ecosystem Exchange*, CRC for Greenhouse Accounting, Canberra, 8–29.

Landsberg, J.J. & Waring, R.H. (1997). A generalised model of forest productivity using simplified concepts of radiation-use efficiency, carbon balance and partitioning. *Forest Ecology and Management*, *95*, 209–228.

LCC. (1980). *Report on the Ballarat Area*, Land Conservation Council, Melbourne.

Schenk, H.J. (1996). Modeling the effects of temperature on growth and persistence of tree species: A critical review of tree population models. *Ecological Modelling*, *92*, 1–32.

Sophocleous, M., & Perkins, SP. (2000). Methodology and application of combined watershed and ground-water models in Kansas. Journal of Hydrology, 236, 185-201.

Vertessy, R.A. (2001). Impacts of plantation forestry on catchment runoff. In: E.K.S. Nambiar, & A.G. Brown (Eds.), *Plantations, Farm Forestry and Water*, RIRDC Publication No. 01/20, 7–19.

Wang, J. (1960). A critique of the heat unit approach to plant response studies. *Ecology*, *41*, 785–790.

Watson, B.M., Ghafouri, M., & Selvalingam, S. (2003). Application of SWAT to model the water balance of the Woady Yaloak River catchment, Australia. In: R. Srinivasan, J.H. Jacobs & R. Jensen (Eds.), *2nd International SWAT Conference Proceedings*, 94–110.

Watson, F.G.R. (1999). *Large scale, long term, physically based modelling of the effects of land cover change on forest water yield*. PhD Thesis, The University of Melbourne, Australia.

White, D.A., Dunin, F.X., Turner, N.C., Ward, B.H., & Galbraith, J.H. (2002). Water use by contour-planted belts of trees comprised of four eucalyptus species. *Agricultural Water Management*, *53*, 133-152.

Williams, J.R. (1995). The EPIC Model. In: V.P. Singh (Ed.), *Computer Models of Watershed Hydrology*, Water Resources Publications, Colorado, 909–1000.

A User Friendly Multi-catchments Tool for the SWAT Model

E. Lorrai & P. Cau
CRS4, Center for advanced studies in Sardinia, Parco Scientifico e Tecnologico, POLARIS, Edificio1, 09010 Pula (CA – Italy). E-mail: eva@crs4.it

Abstract

A software system to manage SWAT results (*bsb.dbf* and *rch.dbf*) has been developed on a multi-catchment scale. Regions such as Sardinia, Sicily, Portugal, etc. are, in fact, characterized by a large variety of ecosystems within complex catchments. The AVS2000 interface deals with one watershed at a time, but the aggregation of SWAT results for adjacent basins may be necessary for an integrated water resources management. To achieve this goal, an ArcView extension, called *multi-catch.avx*, has been developed.

The extension allows the user to select the subbasins within the basins under investigation and obtain statistical reports of the model output, from the rch and bsb tables, in the form of charts, statistics, and maps. The tool helps water managers in the demanding problem of water management by automating the post-processing operation when dealing with many catchments within a region. *Multi-catch.avx* uses the bsb and rch files of all the projects and dynamically permits temporal and spatial analysis at the widest scale and helps to create maps in the ArcView environment. A project view is created where all the watersheds under study are displayed along with their subbasins. The user can dynamically visualize and analyze the spatial distribution of a chosen model output for all the active subbasins within the given basin, at a monthly or yearly time-step. Moreover, the bsb file of each project is aggregated to represent the whole basin under study and statistical indicators such as mean, standard deviation, etc. are calculated. The newly developed ArcView extension has been utilized to map and analyze 15 Swat projects within the Sardinian Region.

Introduction

Water resources management is a complex task in regions where no natural hydraulic connection between streams exists. Each watershed in such a region must be analyzed separately. Still, water resources management must deal with the hydrological systems as a whole. SWAT has demonstrated its potential in analyzing the water cycle and the related hydrologic fluxes at the catchment scale, but only one watershed at a time can be simulated. The result of each simulation is printed in a general form (at a daily, monthly or yearly time-step), letting the user decide how to treat the results, which statistics to generate, etc. To get a global view of the entire system and the results obtained for various catchments would require the user to post-process the results from the individual SWAT projects. We therefore developed a new ArcView extension called *multi-catch.avx* to enable SWAT users to make concurrent comparisons of different hydrological fluxes of the water budget for multiple SWAT projects. This will be extremely important when, within a region, a large number of watersheds are modeled and all watersheds must be analyzed together in order to identify critical situations within the entire system.

ArcView Extension Description

The development of the *multi-catch.avx* extension addresses two issues: 1) how to deal with situations when multiple catchments are present and need to be analyzed, and 2) how to organize the SWAT results for optimum use by water managers.

The *multi-catch.avx* (version 1) has been developed in the Avenue programming language, and incorporates an external program, called *Extract_results.pl*, written in Perl (www.perl.org). The Perl script, dedicated to the treatment of the bsb SWAT output, uses the following algorithms:

$$X_{basin} = \sum_{s=1}^{N} \left(\frac{X_s \cdot A_s}{A_{tot}} \right)$$

where X_{basin} is the value of the specific parameter (precipitation, evapotranspiration, etc.) aggregated at the basin scale, X_s is the value of the corresponding parameter for the active subbasin *s*, A_s is the area of the subbasin, A_{tot} is the total area of investigation, and N is the total number of active subbasins.

Extract_results.pl enables the user to merge the monthly results on a yearly basis. The program needs the Perl environment to be installed (ActivePerl, with XBase and DBD-XBase modules). The ArcView extension can be loaded directly in ArcView 3.1 or later versions. After the file *multi-catch.avx* is copied in the ARCVIEW EXT32 directory, it can be loaded in an ArcView project from the File drop down menu, selecting Extensions and Multi-catchments Swat Extension. The multi-catchment tool is visible within the Project, View, and Table sessions. The *multi-catch.avx* works with the bsb files contained in the directory *\scenarios\default\tablesout* and the shapefiles contained in *\watershed\shapes* of each SWAT project (Figure 1). To make the extension work, it is necessary for the user to set an environment variable having the value of the directory where all the SWAT projects are located. The results created by the *multi-catch.avx* extension are automatically placed in the same directory.

The tool works in 4 phases:

1) The user chooses the SWAT projects to be analyzed via the command Load basin (Figure 2). Once the projects are chosen, the waters and watersub shapefiles are loaded from the projects directory (*\watershed\shapes*) in a View, along with the associated bsb and rch tables.
2) The user can choose which subbasins of each basin should be considered active, so that all the statistics will refer only to these subbasins. This is achieved by creating two tables (*define_bsb.dbf* and *bsb.refer.dbf*) that the user can modify in order to:
    a) Select which subbasins must be considered active in terms of contribution to the water balance by clicking the extension command and then Modify active subbasins. If the user skips this command, all the subbasins are considered active.
    b) Choose or later modify which parameters are significant for the statistics by clicking the extension command and then Modify active parameters. By default, the active parameters are PreCiPitation, Snowmelt, Potential EvapoTranpiration, EvapoTranspiration, Water YieLD, Sediment YieLD, ORGanic Nitrogen, ORGanic Phosphorous, and NO3 in SURface runoff.
3) The user can now run the Perl program and load the results into the project. In this phase the following operations are performed:
    a) For each project two files are created (*Project_name_monthly* and *Project_name_yearly*). They have the same format as the bsb table.

b) The monthly table is then reorganized and saved in a new table, where the years are in rows and the monthly values are in columns. This is important to show the hydrological regime and to design water management plans. This phase is quite time consuming because of the computational time needed to transpose tables.
c) The active subbasins are merged and one polygon is created. A new shapefile is then created where each feature (one polygon) represents a basin.

4) The user is asked to choose which statistics should be calculated. The results are displayed in the active View as a new theme, and a graduated legend is created.

The user can select the time period for statistical evaluation and the required statistical measures such as mean, standard deviation, 25th percentile, or 75th percentile (Figure 3).

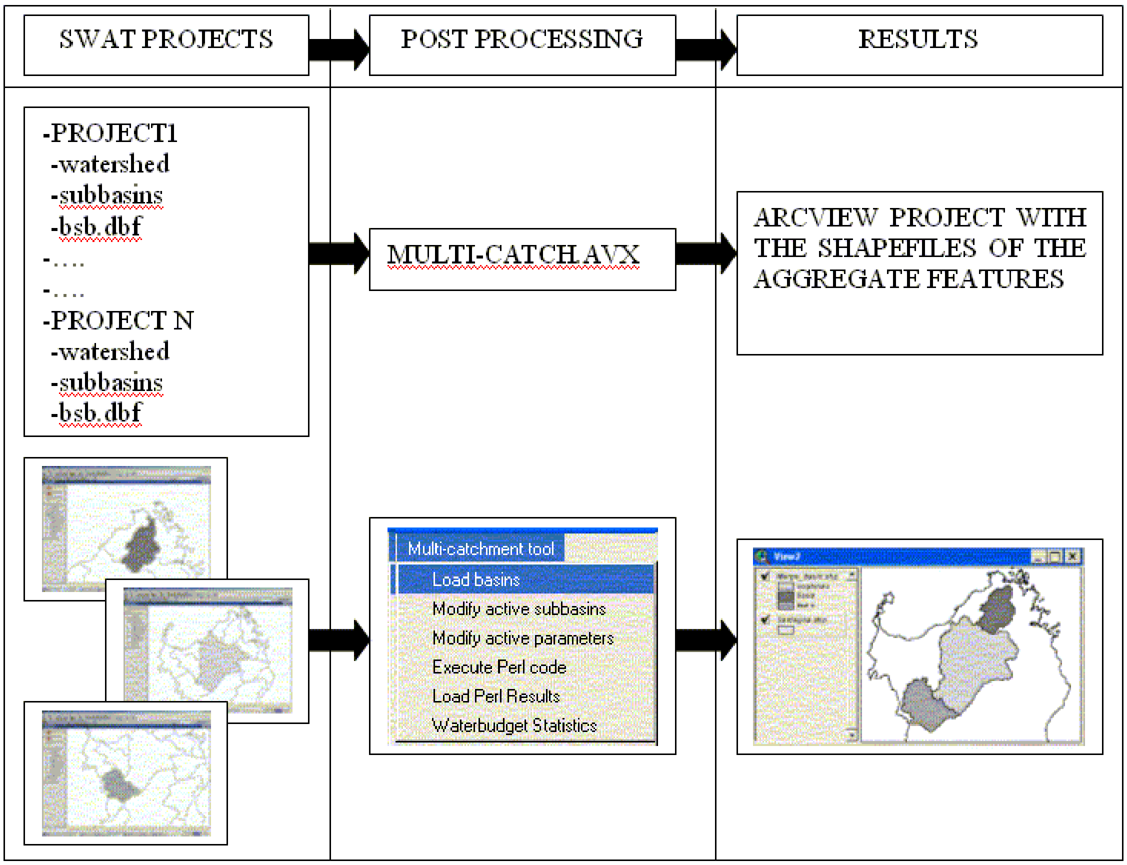

Figure 1. The ArcView *multi-catch.avx* uses the geographical information (watershed and subbasin) and the bsb tables to calculate statistics and create maps.

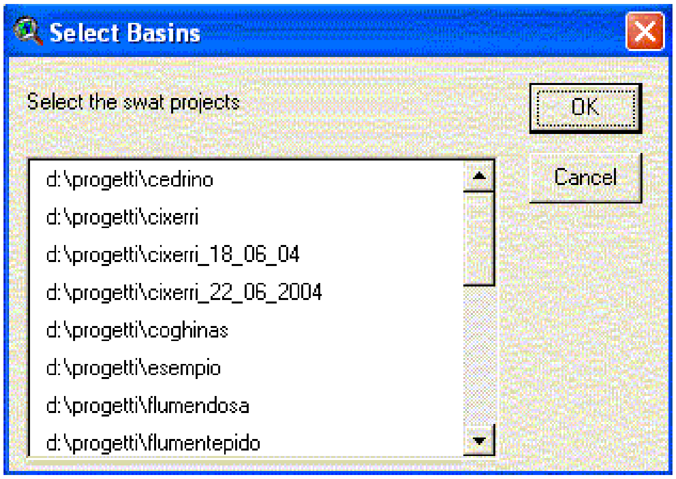

Figure 2. Through simple interfaces the user can choose the basins and the subbasins to be analyzed.

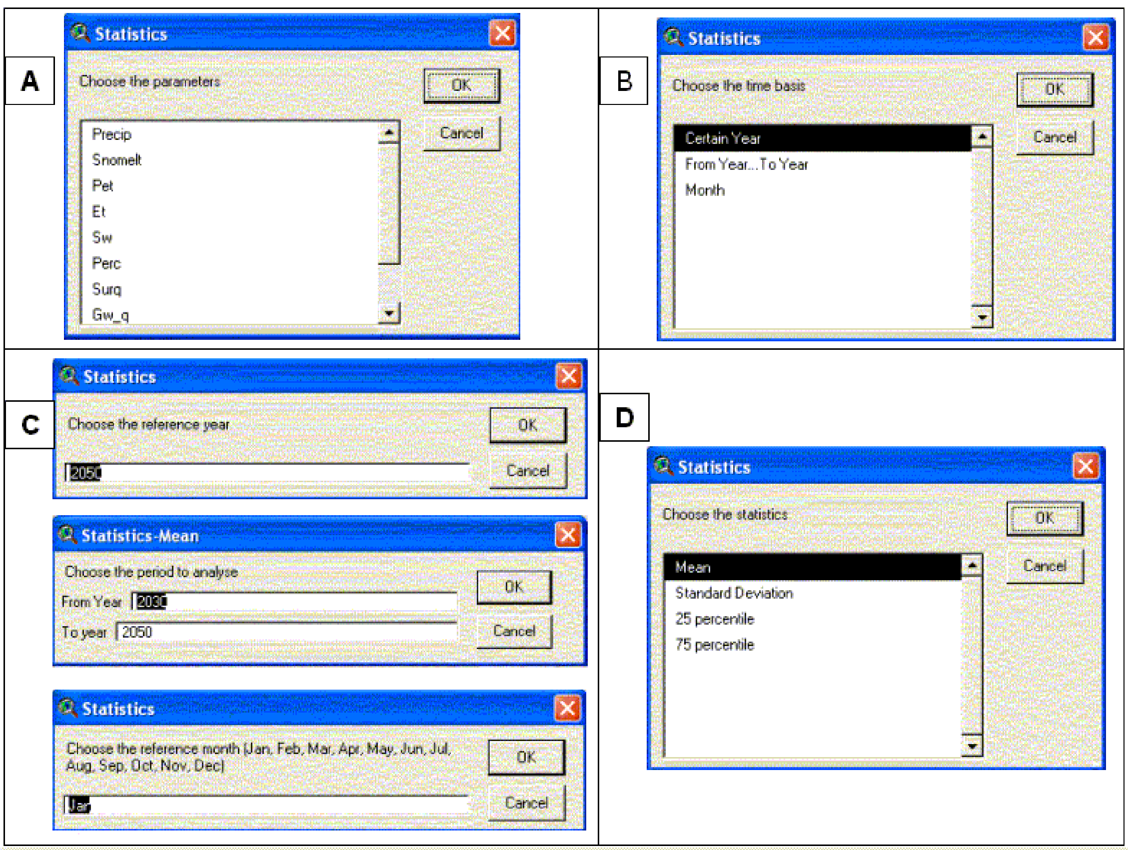

Figure 3. (A) The user can choose the parameters to be evaluated and (B) the time period to be analyzed. Note: For the yearly time resolution the user can choose one year (e.g. 2050) or a range of years (e.g. from 2030 to 2050). (C) For the monthly time resolution the user can choose which months to analyze. (D) Finally, the user can choose the statistical measures of interest.

Application of the Extension

In 2002, a consortium made up of CRS4, TEI, PROGEMISA, and NAUTILUS was created for a three-year project called "Piano di Tutela delle Acque" (PTA). One of the main focuses of the project was the development of a multisectorial, integrated, and operational Decision Support System (DSS) for the sustainable use of water resources at the catchment scale. A more detailed description of the PTA can be found in the article "A Decision Support System based on the SWAT model for the Sardinian Water Authorities" (P. Cau and E. Lorrai). The *multi-catch.avx* program has been used in the PTA to analyze and map the SWAT results. The main catchments of the island (15 basins) have been analyzed to gain an overview of the spatial distribution of the water cycle components of the whole system (Figure 4). In the following example, all of the subbasins were considered active. The parameters under investigation are precipitation, potential evapotranspiration, and water yield.

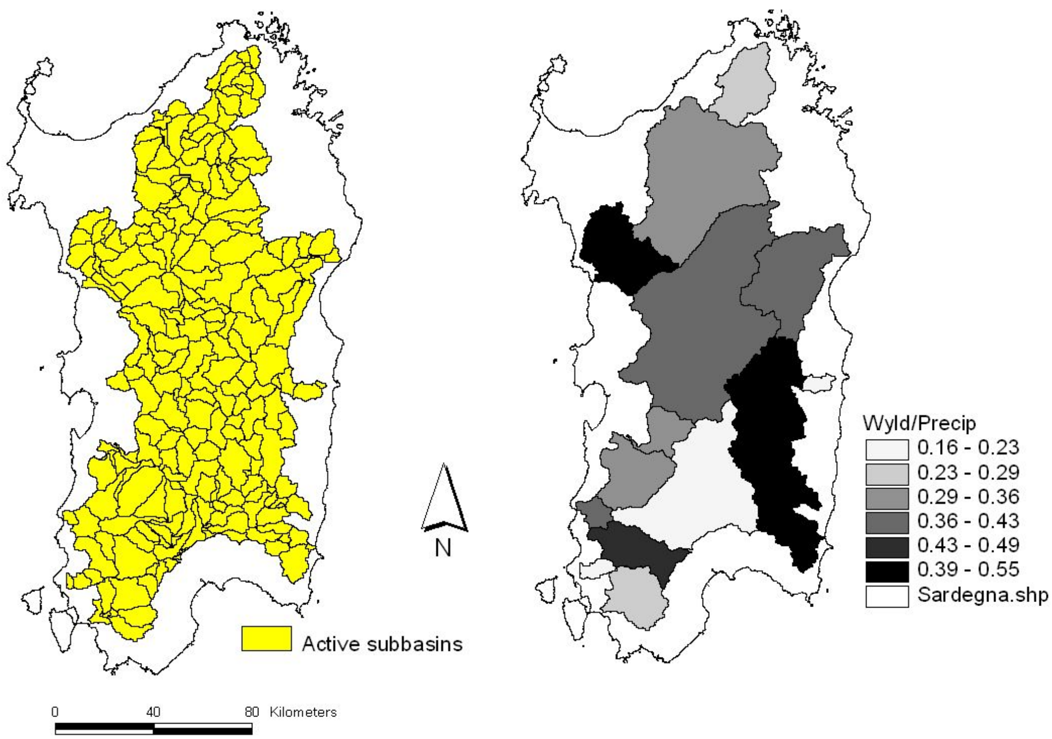

Figure 4. Application of the *multi-catch.avx* to a real case. The active subbasins (left) and the spatial distribution of the average water yield normalized by rainfall (right) for the time period from 1922-1992 are shown.

Conclusions

The ArcView extension *multi-catch.avx* has been developed to facilitate water resources management in complex regions where a wide variety of watersheds are investigated. Currently, SWAT only allows users to analyze independent watersheds separately. Still, water resources management should treat the hydrological systems as a whole. The procedures implemented in *multi-catch.avx* make use of the bsb, rch tables, and watershed and subbasin shapefiles to allow for a more dynamic spatial analysis at the regional scale. In addition, maps can be visualized in the ArcView environment. Future versions will enforce spatial analysis at the subbasin scale.

Acknowledgments
The Perl script *Extract_results.pl* has been written by Claudio Gallo, CRS4.

References

Neitsch, S.l., Arnold, J.G., Kiniry, J.R, Williams, J.R. *Soil and Water Assessment Tool. Theoretical documentation. Version 2000.* Blackland research center - Texas agricultural experiment station. Grassland, soil and water research laboratory - USDA agricultural research service (2001).

Neitsch, S.l., Arnold, J.G., Kiniry, J.R, Williams, J.R. *Soil and Water Assessment Tool. User's manual. Version 2000.* Blackland research center - Texas agricultural experiment station. Grassland, soil and water research laboratory - USDA agricultural research service (2001).

Cau P., Cadeddu A., Gallo C., Lecca G. & M. Marrocu. *Estimating available water resources of the Sardinian island using the SWAT model.* Atti della conferenza Second International SWAT conference, Bari, Italy, pag. 64 - 70, Luglio 2003.

Cau P., E. Lorrai . *A Decision Support System based on the SWAT model for the Sardinian Water Authorities.* Third International SWAT conference, Zurich, Switzerland, July 2005.

Session V

17. **Towards a process-oriented HRU concept in SWAT: Catchment-related control on baseflow and storage of landscape units in medium to large river basins** **159**
Martin Volk, Peter M. Allen, Jeffrey G. Arnold, Pei-Yu Chen

18. **Interfacing SWAT with systems analysis tools: A generic platform** **169**
Jing Yang, Karim C. Abbaspour and Peter Reichert

19. **Evaluation Methods for SWAT Models** **179**
A. van Griensven, T. Meixner, S. Grunwald and R. Srinivasan

20. **Modifications of the Soil Water and Assessment Tool (SWAT-C) for streamflow modeling in a small, forested watershed on the Canadian Boreal Plain** **189**
Ruth A. McKeown, Gordon Putz, Jeff Arnold and Mauro Di'Luzio

Towards a Process-Oriented HRU-Concept in SWAT: Catchment-Related Control on Baseflow and Storage of Landscape Units in Medium to Large River Basins

Martin Volk, Peter M. Allen, Jeffrey G. Arnold, Pei-Yu Chen
UFZ-Centre for Environmental Research, Department of Applied Landscape Ecology, Permoserstr. 15, D-4318 Leipzig, Germany. E-mail: martin.volk@ufz.de

Abstract

A principle of a new HRU concept for SWAT is based on the integration of basic and most significant spatial landscape units characterized by different hydrological properties and functions. Delineation of these units requires their reproducible description by easily obtained physical parameters and indicators. The authors suggest a method based on (i) the delineation of the basic units valley floors, hill slopes, and ridge top areas from a DEM, (ii) the calculation of terrain-based parameters in the basin area, total channel length, drainage density, slope angle, hypsometric integral and climate index, and (iii) verification of the hydrological significance of the spatial response units by comparing observations of their hydrological characteristics by automated baseflow separation and recession analysis of streamflow data. These data have been compiled in 49 gauge-related subbasins of different sizes (< 50 to 23,000 km²) in relation to landscape units, geology, basin relief, land use, and soil conditions. A macro model was developed on the basis of the strongest correlated parameters (basin area, channel length, climate index, baseflow index, drainage density, and percent proportion of valley floors) to predict storage by using these six variables. The test of the model showed the best suitability for subbasins >300 km^2 in size and indicated scale-specific significance and change of the controlling factors for storage. Next, different methods are used to quantify the storage volume of the landscape units, especially for valley floors, which is important for an accurate description in the model. The studies are essential for characterizing response units on larger scales, and represent the basis for an improved spatial description of hydrology and transport processes for river basin management by modifying the HRU concept in SWAT.

Introduction

The spatial description of basin hydrology and nutrient transport processes in SWAT (Arnold et al., 1998) is presently realized by summarizing the flows from overlaid soil and land use patches in subbasins with averaged slope angles. Current and future river basin management requires a more spatially distributed description of these processes to enable land use management as a process-controlling factor to realize a sound river basin management (Volk and Steinhardt, 2001). Many concepts, with different degrees of complexity, have been developed in river basin modelling to aggregate units with similar hydrologic behaviour (Hydrological Response Units, Flügel and Staudenrausch, 1999). Knowledge about the significant controlling factors for hydrological processes and functions is needed on different spatio-temporal scales to delineate such response units (Lacey and Grayson, 1998). This requires a sound description of the characteristics by using physically-based parameters and indicators, but also more simplified solutions even on larger scales. Beside the use of indices, this study also includes a method to

delineate three basic landscape units, valley floors, hill slopes, and ridge top areas, in order to investigate their importance on the hydrological processes at the concerned scale-levels.
Our hypothesis is that storage is both a product of the basin morphology as well as basin geology. In addition, the control exerted by the landscape on the baseflow system varies with watershed size and potential moisture availability. Large basins show linear behaviour, integrating many storage factors, while smaller basins tend to behave in a non-linear fashion, with increasing significance of single hydrologic controls.

The watershed morphology in this study is analyzed in the following way; (i) terrain-based parameters such as basin area, slope angle, total channel length, drainage density, and hypsometric integral as well as the climate index, are analyzed for the entire watershed, and (ii) the watershed landscape is then delineated into three basic units, valley floors, hill slopes and ridge top areas, from a DEM for a more detailed delineation of watershed function. These watershed descriptors are then compared with observations of the hydrological characteristics of baseflow as derived from automated recession analysis of streamflow data and subsurface storage calculation in the different river basins. Next, a correlation analysis shows the main relations between storage and the proportion of the landscape units of the basin and the morphometric parameters. As a result, the authors develop a model based on a regression analysis that allows the calculation of the storage under different landscape conditions. Finally, different methods are used to quantify the storage volume of the landscape units especially for valley floors, which is important for an accurate description in the model. The studies are essential for investigating the significance of storage and other hydrological functions of landscape units on larger scales and represent the base for improved river basin management by modifying the HRU concept in SWAT.

Controlling Factors of Baseflow and Storage on Different Scales

Following the theory that different physical processes may dominate at different scales (Dooge, 1989; Lacey and Grayson, 1998), work has to be done to define the dominating factors on the different scale levels, which also may differ in various climate and topographic zones (Wooldridge and Kalma 2001). This is also needed in order to find linkages between process descriptions at the hill slope and watershed scales (Sivapalan, 2003). By knowing the relevant process-influencing factors on each spatio-temporal level, measures to prevent environmental impairments by land use or use of the natural filter and storage capabilities of the landscape (especially floodplains) could be planned and implemented more effectively. This study tries to find the impact of catchment-related terrain and climate metrics and indices as well as geology-land use distributions on baseflow and storage in a large river basin and its subbasins. The study also includes a new approach to relating delineated landscape units to the hydrological characteristics to prove the idea of a process-based HRU concept.

Study Area

The Saale River Basin (Central Germany) is located in Central Germany. The basin can be subdivided in three sub-regions, the Pleistocene lowlands, the loess sub-region, and the mountainous sub-region. The length of the river is about 320 km. Precipitation varies from 500 mm in the dry loess areas to 1,200 mm in the forested mountain regions. Figure 1 shows the location of the river basin in Germany, including the gauges used and the main geological units.

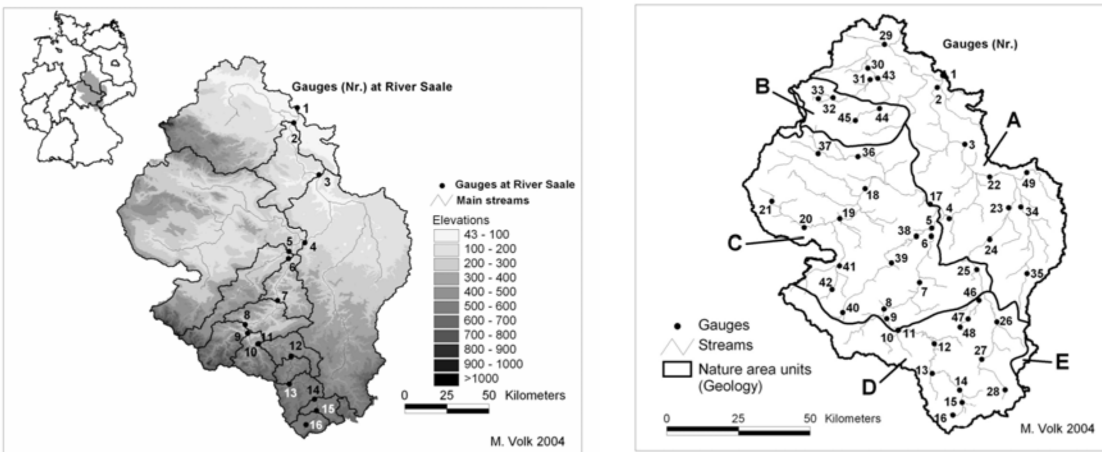

Figure 1. Location of the Saale River Basin in Germany and its 16 gauge-related subbasins (left). The map on the right shows the location of 49 gauges of the main tributaries with the main geological units: A = northwestern and southeastern loess region, B = Harz mountains, C = Thuringian Basin and uplands, D = Thuringian Mountains, Fichtelgebirge and Vogtland Mountains, E = Erzgebirge Mountains.

Methods

Delineation of the Landscape Units and Validation

Landscape units or landscape positions are important hydrologic, geomorphic, and environmental features. Distinguishing between hill slopes and valley bottoms, for instance, is necessary because of the substantial differences in hydrological processes (surface and sub-surface flow and storage) and related transport mechanisms for sediments and nutrients between the two landforms (Gallant and Dowling, 2003). The *slope position method* (USDA Forest Service, 1999) has been selected as a useful method to delineate the landscape units, where the slope position of a cell is its relative position between the valley floor and the ridge top. Downhill and uphill flow accumulation values greater than user specified limits are used to identify valleys and ridges, respectively. A detailed description of the method is given in Volk et al. (2005). Slope position is calculated for the cells in the output grid as the elevation of each cell relative to the elevation of the valley that the cell flows down to and the ridge it flows up to (vertical distance z). This is presented as a ratio, ranging from 0 (valley floor) to 100 (ridge top). However, the selection of the threshold values and the validation of the delineated landscape units represent a general problem (Gallant and Dowling, 2003). Thus, several calculations for the study area with different sizes have been carried out to find the threshold values and optimal value range for valley floors, hill slope areas, and ridge tops that represent the data resolution and the terrain conditions of the study area (Volk et al., 2005). The results have been compared and proved by calculated topographic factors, relief amplitude, and soil maps. The delineated valley floors are shown in Figure 2.

Calculation of Terrain Based Metrics and Dimensionless Indices

Terrain-based metrics and dimensionless indices are used to describe physical characteristics and process-controlling factors of river basins (Dowling et al., 1998; Hurtrez et al., 1999; Layson and Grayson, 1998). For this study, we have calculated the metrics and indices listed in Table 1.

Table 1. Calculated terrain based metrics and dimensionless indices.

Basin area	
Slope angle	
Drainage density	*(Dd = total channel length / basin area)*
Hypsometric Integral	$(Int = (Elev_{mean} - Elev_{min}) / (Elev_{max} - Elev_{min}))$
Climate Index	*(CI = rainfall / PET)*
Mean Soil Available Water Capacity (AWC)	
Baseflow Index	*(BI = baseflow / streamflow)*

Baseflow Separation and Recession Analysis

Automated baseflow separation and recession analysis techniques have been applied to the streamflow data to derive information about the baseflow contribution and the recession constant (α) and thus the storage of the basins (Arnold and Allen, 1999). The recession constant α is calculated as an indicator for transmissivity and storage of the aquifer. The alpha factor is a direct index of the intensity with which the baseflow drainage rate responds to changes in the recharge. It is directly related to the permeability and thickness of the aquifer and inversely related to aquifer storage and length of the flow path to the stream. While "alpha" shows the slope of the recession curve, baseflow days describe the time it takes for the baseflow recession to pass through one log cycle. Thus, a low number of baseflow days indicate a rapid drainage and/or little storage, whereas a high number of baseflow days indicate slow drainage and/or high storage. Though "alpha" and baseflow days indicate the same item (alpha = 2.3*(1/BFD), baseflow days have been chosen for the further analysis for a clearer presentation.

Correlation Analysis

Linear regression analysis has been carried out to investigate the relationships between baseflow and storage to the proportion of the landscape units and the used metrics and indices statistically. A clear trend of an increasing storage capability (increasing number of baseflow days and percentage of baseflow contribution, expressed with the baseflow index) with increasing basin size can be observed. Drainage density, average slope angle, and hypsometric integral are similarly shown to decrease downstream. The relative increase in proportion of valleys and decreasing proportion of hill slopes fits in well with this result. Decreasing slope angles, drainage densities, and hypsometric integrals of the following upstream basins indicate plateau-like terrain conditions in the southern portions of the river basin. The southern mountainous parts of the basin show partly-permeable weathering gravel, locally supporting high baseflow contribution to the streamflow.

Multiple correlation analysis showed a ranking of the relationships between baseflow days and a combination, and strongly correlated variables. As a result of the multiple regression analysis, the following macro model is developed that describes storage of the basin by using the most significant parameters (Equation 1):

$$BFD = 32.36 + 0.011 * A + (-0.020) * L + (-39.40) * CI + 71.15 * BI + 21.41 * Dd + 0.56 * VF \quad (1)$$

where A is the area of the basin, L is the total channel length, CI is the climate index, BI is the baseflow index, Dd is the drainage density and VF is the area of the valley floor.

The comparison of predicted and calculated baseflow days using the 16 gauges of the River Saale showed a very high correlation ($r^2 = 0.93$) and thus confirms the significance of the selected variables. High deviations are observed with the subbasins in the uplands with low storage capability. The regression indicates that the continuity of groundwater flow in the basin is a function of basin area, length, overland flow distance, and valley width, or more simply, a function of hill slope length and valley width integrated over the basin. The model has been successfully applied with 49 other gauges in different geological units of the basin (Figure 1, and Volk et al., 2005). In our recent studies we have worked on the use of maximum baseflow (Q_{max}) and the recession constant “alpha” to quantify landscape storage.

Quantification of Landscape-Specific Water Storage on Different Scale Levels

The relevance of the delineated landscape units for the process behavior of watersheds and subbasins can be shown by demonstrating the relationship between water storage and delineated landscape units. One should assume that hill slopes are areas of recharge and valleys are areas of discharge to the stream. Since the regression equations indicate that baseflow is related to valley storage, then one must establish a relationship between floodplain and valley dimensions and baseflow storage. Here, water storage is calculated for the valley landscape unit using two different methods.

The Valley Cross Profile Level: A Numerical Approach to Calculating Bank Storage

Large scale calculations have to be proved on a smaller scale. Thus, we used a numerical approach (Whiting & Pomeranets, 1997) to calculate bank storage at three valley cross profiles of the Saale River (Figure 2).

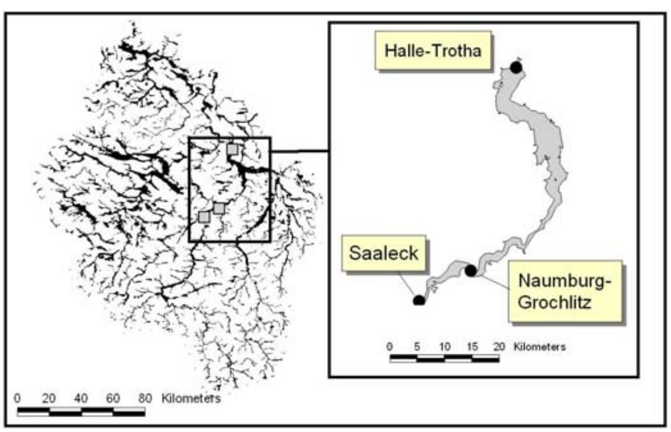

Figure 2. Delineated valley floors and location of the considered cross profiles in the Saale River Basin.

The valley cross profiles are located at the gauges Naumburg-Grochlitz and 15.3 km south of it, at the gauge Saaleck (Saale River). The third profile lies at the gauge Halle-Trotha (70 river-km North of Naumburg –Grochlitz). The floodplain width has been estimated from the results of the delineation of the landscape units using the slope position method. The recession parameter (*B*) below is a floodplain width – channel width ratio. It is expressed as (Equation 2):

$$B = 2L/W \qquad (2)$$

where 2L is the distance between valley sides at the level of the floodplain and W is the channel width (Whiting & Pomeranets, 1997). Thus, the large values below for α are the result of the wide, flat floodplains at the sites of the profiles in comparison to the relatively narrow channels (Table 2).

Table 2. River channel and valley geometries of the selected sections.

Profile	River-km	Max. channel depth [m]	Average channel depth [m]	Channel width [m]	Valley width (delineated) [m]	Recession parameter (*B*)
Halle-Trotha	88.5	3.36	1.95	54.26	1,520	28
Naumburg-Gr.	158.5	4.23	3.55	43.49	1,005	23
Saaleck	173.	3.00	2.26	42.66	740	17

Maximum bank storage has been calculated by using the equation provided by Whiting & Pomeranets (1997) (Equation 3):

$$V_s = Sy\ YW\ (B - 1 + (Y / w \tan\beta) \qquad (3)$$

where *Sy* is the Specific Yield, *Y* is the difference in elevation streambottom and banktop, *β* is the bank angle, and *W* is the bankfull channel width. Bank angle is assumed to be 2.

Specific Yield is estimated by using a regression equation provided by the U.S. Department of the Interior (1978). The equation uses saturated hydraulic conductivity of the soil (K) as an input variable. The results of calculations of the Specific Yield (Sy) for the floodplain soils of the gauge related subbasins of Halle-Trotha (Sy = 6.5% (fraction 0.065)), Naumburg-Grochlitz (Sy = 5.7% (fraction 0.057)) and Saaleck (Sy = 7.1% (fraction 0.071) are in the range of sandy clays to silt (Johnson, 1967), and thus represent the conditions of the area quite well.

The following results (Table 3) were obtained from the calculations of the maximum storage (V_s) by using Equation 3 (Whiting & Pomeranets, 1997).

Table 3. Bank storage of the selected valley sections.

Profile	Equation	V_s (m³/m channel)
Halle-Trotha	0.0654 * 3.36 * 54.26 * (28 – 1 + (3.36 / 54.26 * 2))	323.4
Naumburg-Grochlitz	0.057 * 4.23 * 43.49 * (23 – 1 + (4.23 / 43.49 * 2)	232.7
Saaleck	0.071 * 3.00 * 42.66 * (17 – 1 + (3.00 / 42.66*2))	146.7

The high bank storage values are a result of the wide valleys, relatively small channels, and mostly silty-clay soils. The calculated maximum storage volumes of Halle-Trotha and Naumburg-Grochlitz have been multiplied by the distance to the next upstream gauge in order to estimate the floodplain storage of both valley sections (distance Naumburg-Grochlitz: 70 km, distance Naumburg-Grochlitz and Saaleck: 15.3 km). By assuming the same valley width from the profiles for the entire valley section (multiplying distance in m by floodplain width), results in a floodplain area of 106.4 km^2 for the section between Halle and Naumburg and 15.7 km^2 for the area of the floodplain between Naumburg and Saaleck. The results of the described storage calculation are shown in Table 4.

Table 4. Water storage of the valley sections, derived by multiplying the results of the bank storage calculation [m^3/m channel] with the distance between the gauges.

Valley section	Area [km^2]	Storage volume [m^3]
Halle - Naumburg	106.4	22,638,000
Naumburg – Saaleck	15.7	3,560,310

The Floodplain Storage Level

This method simply assumes that the storage volume can be described by floodplain area, soil depth, and specific yield. In order to compare the water storage, resulting from the multiplied river cross profiles, with our large-scale floodplain storage estimations, the valley sections of interest need to been selected from our delineated valley floors by using GIS operations. The comparison between the area sizes of the valley sections derived from the multiplied river cross profiles, and the sections that have been delineated by GIS, showed 3.9% for the Halle-Naumburg section, and only 1.9% for the Naumburg section, and thus verified the results of the delineation. The selected valley areas have been intersected with the soil map of Germany (scale 1:1,000,000, BGR, 1995). Saturated hydrologic conductivity (K) was extracted from the map and related to the area. Specific Yield was then calculated by again using the above mentioned regression equation: Halle-Trotha, Sy = 6.5% (fraction 0.065) and Naumburg-Grochlitz, Sy = 5.7% (fraction 0.057). The estimation of the required floodplain depths or hydrological effective soil depth is a problem and becomes even more critical on large scales due to the lack of sufficient soil information. Thus, an empirical approach has been applied by using the following Equation (4) to estimate floodplain depth (Allen and Arnold, 1994):

$$\textit{Floodplain depth (ft.)} = 0.3287 * Q^{0.34} * (RI^{0.142}) \tag{4}$$

where Q is the streamflow at bankfull depth in cubic feet per second (cfs) and RI is the recurrence interval in years. One ft. corresponds to 0.3048 m and 35.31467 cfs corresponds to 1 m^3/s.

The estimation of the floodplain depth has been carried out on the example of the three selected river cross profiles. Streamflow (Q) at bankfull depth is derived from official hydrological records (STAU 1994). Floodplain depth is assumed here to be the hydrological effective soil depth. After investigating the streamflow records in detail, and according to Haase et al. (2000) and Jordan & Weder (1995), the resulting floodplain depths using a recurrence interval of 25 years have been assumed to be most realistic for the region (Table 5).

Table 5. Estimated floodplain depths using a recurrence interval of 25 years.

Gauge	Bankfull river stage [cm]	Bankfull Streamflow [m³/s]	Estimated floodplain depth [m] (Recurrence Interval: 25 years)
Halle-Trotha	336	200	3.22
Naumburg-Grochlitz	423	215	3.30
Saaleck	300	166	3.02

Floodplain storage volume (V_{FP}) was also calculated by using the following simple Equation (5):

$$V_{FP} = \textit{Floodplain area} * \textit{floodplain depth} * \textit{Specific Yield} \quad (5)$$

The results of the calculation are presented in Table 6.

Table 6. Estimated floodplain storage using a simple approach based on floodplain area, soil depth, and specific yield.

Valley section	Area [km²]	Storage volume [m³]
Halle - Naumburg	110.5	23,483,460
Naumburg – Saaleck	15.4	2,953,170

Comparison of the Results

The comparison of the results (converted in mm) for both methods (Table 7) shows that for the larger valley section, Halle to Naumburg, values are similar, with a very slight deviation of 0.1%. The higher deviations at the Naumburg – Saaleck section might be caused by the much smaller area, where single and local special factors and conditions have much more impact on the storage behaviour. The used relative coarse soil data and the derived soil depth might not be fully representative of these special conditions. In consideration of the coarse and simple approach that we used for the large-scale estimation, the results are satisfactory.

Table 7. Comparison of the storage volume calculation using a numerical method and a simple approach on the basis of area, soil depth, and specific yield.

Valley section	Storage “Profile” [mm]	Storage “Floodplain Area” [mm]	Deviation [%]
Halle - Naumburg	212.8	212.5	0.1
Naumburg – Saaleck	231.2	188.1	18.6

Conclusions

This study illustrates the interrelationships of baseflow response with basin size, total channel length, climate index, baseflow index, drainage density, and valley floor for a large-scale river basin and its gauge-related subbasins. The relationship between floodplain (valley floor unit) and valley dimensions and baseflow storage has been established by water storage calculations using two different methods.

The results confirm, in general, the statements of Marani et al. (2001) and Zecharias and Brutsaert (1988) concerning the significance of valleys and drainage density for controlling baseflow and storage. However, in contrast to Marani et al. (2001), this study shows drainage density to have a significant correlation to the baseflow days. The calculated morphometric and hydrologic parameters and the predicted baseflow days for the gauge-related subbasins showed the best results for the larger basins, and thus showed a quasi-linear behavior (see also Sjodin et al., 2001). The integrating functions controlling baseflow response or storage is, in this case, best represented and averaged by basin size, drainage density, and proportion of the basin occupied by valley floors for basins over 300 km^2.

Lacey and Grayson (1998) found no correlation between baseflow and basin size for watersheds up to 100 km^2. This leads us to the assumption that, with decreasing basin size, the significance of individual subbasin-specific factors becomes more important. These factors were not represented by our combination of six variables. This study used a baseflow separation and recession analysis technique that assumes a priori, a linear baseflow recession. In this regard, the best results were achieved with this method within the larger basins. Thus, we are planning comparative studies in basins of different size and characteristics with our method and non-linear methods such as BNL (Wittenberg, 1999) in order to optimize the application of such methods. Additionally, future work will include the development of methods for a ruled-based delineation of the landscape units. Also, comparative analyses using the automated “multiresolution index of valley bottom flatness” (MRVBF) by Gallant and Dowling (2003) and other methods, in addition to the applied “Slope position” method are planned. The presented method will be applied to study areas of different sizes with hydrologic instrumentation in order to (i) find the transitions between linearity and non-linearity, (ii) specify the storage behavior, and (iii) to better quantify the landscape-specific storage. The results will be used for the new, more catchment-related, HRU concept of SWAT. Current plans for the routing of water from one landscape unit to another include streamorder-based cascading systems, among others.

References

Allen, P.M., J.G. Arnold and B. Byars (1994): Downstream channel geometry for use in planning-level models. – Water Resources Bulletin 30, 3: 663-671.

Arnold, J.G. and P.M. Allen (1999): Automated methods for estimating base flow and ground water recharge from streamflow records. J. American Water Resources Association 35(2):411-424.

Arnold, J. G., R. Srinivasan, R. S. Muttiah and J.R. Williams (1998): Large area hydrologic modeling and assessment, Part I: Model development. J. American Water Resources Association 34(1):73-89.

Bundesanstalt für Geowissenschaften und Rohstoffe (BGR), (Ed., 1995): Bodenübersichtskarte der Bundesrepublik Deutschland 1:1,000,000. Hannover.

Dooge, J.C.I. (1989): Scale problems in hydrology. Chester C. Kisiel Fifth Memorial Lecture, 1986, Department of Hydrology and Water Resources, University of Arizona.

Dowling, T.I., D.P. Richardson, A. O’Sullivan, G.K. Summerwell and J. Walker (1998): Application of the hypsometric integral and other terrain based metrics as indicators of catchment health. A preliminary analysis. CSIRO Land and Water, Canberra. Technical Report 20/98: 49 pp.

Flügel, W.-A. and H. Staudenrausch (1999): Hydrological networkin modelling using GIS for supporting integrated water resources management. - Proc. of the International Congress on Modelling and Simulation, Vol. 4, pp. 1087-1092, University of Waikato, Hamilton, New Zealand.

Gallant, J.C. and T.I. Dowling (2003): A multiresolution index of valley bottom flatness for mapping depositional areas. – Water Resources Res. 39, 12, 1347, doi:10.1029/2002WR001426, 2003.

Haase, D., B. Schneider & H. Neumeister (2000): Processes in Fluvisoils caused by artificial floodings in floodplain forest ecosystems. – Geoökodynamik 21: 185-198.

Hurtrez, J.-E., C. Sol and F. Lucazeau (1999): Effect of drainage area on hypsometry from an analysis of small-scale drainage basins in the Siwalik Hills (Central Nepal). Earth Surface Processes and Landforms 24:799-808.

Institute of Hydrology (1980): Low flow studies. Wallingford, UK.

Jordan, H. and H.-J. Weder (Eds., 1995): Hydrogeologie. Grundlagen und Methoden. Regionale Hydrogeologie : Mecklenburg-Vorpommern, Brandenburg und Berlin, Sachsen-Anhalt, Sachsen, Thüringen. – 2. Ed., Enke, 603 pp.

Lacey, G.C. and R.B. Grayson (1998): Relating base flow to catchment properties in south-eastern Australia. J. Hydrology 204:231-250.

Marani, M., E. Eltahir and A. Rinaldo (2001): Geomorphic Controls on regional Base flow. Water Resouces Res. 37(10):2619-2630.

Sivapalan, M. (2003): Process complexity at hillslope scale, process simplicity at the watershed scale: is there a connection. Hydrological Processes 17: 1037-1041.

Sjodin, A., W.M. Lewis Jr. and J.F. Saunders (2001): Analysis of groundwater exchange for a large plains river in Colorado (USA). Hydrological Processes 15: 609-620.

USDA Forest Service (1999): Digital Visions Enterprise Unit. Tools. AML scripts. http://www.fs.fed.us/digitalvisions/tools/index.php?shortcat=GridTools

Volk, M. and U. Steinhardt (2001): Landscape balance. In: Kroenert, R., U. Steinhardt and M. Volk, (Eds., 2001): Landscape balance and landscape assessment, Springer-Verlag: 163-202.

Volk, M., P.M. Allen and J.G. Arnold (2005): Analysis of catchment-related control on baseflow and storage of landscape units in medium to large river basins. – J. Hydrology (submitted).

Whiting, P. and M. Pomeranets (1997): A numerical study of bank storage and its contribution to streamflow. J. Hydrology 202: 121-136.

Wittenberg, H. (1999): Base flow recession and recharge as nonlinear storage processes. – Hydrological Processes 13: 715-726.

Wooldridge, S.A., and J.D. Kalma (2001): Regional-scale hydrological modelling using multiple-parameter landscape zones and a quasi-distributed water balance model. Hydrology and Earth System Sciences 5(1): 59-74.

Zecharias, Y.B. and W. Brutsaert (1988): Recession characteristics of groundwater outflow and base flow from mountainous watersheds. Water Resources Res. 24(10):1651–1658.

Interfacing SWAT with Systems Analysis Tools: A Generic Platform

Jing Yang, Karim C. Abbaspour, and Peter Reichert
Swiss Federal Institute for Aquatic Science and Technology (eawag), 8600 Dübendorf, Switzerland. E-mail: jing.yang@eawag.ch

Abstract

Due to the complex structure of model input and output files, watershed models are in need of a flexible interface for model calibration, sensitivity analysis, and uncertainty analysis. As there are many systems analysis programs (SAP) in use, an interface based on a generic platform enabling easy coupling of a watershed model to any SAP is highly desirable. The suggested interface for the hydrologic model, Soil and Water Assessment Tool (SWAT), uses the concept of "parameter identifiers" where the initial parameter values are spatially scaled either locally within each subbasin, or regionally according to soil hydrological group, soil texture, or land use category. This interface opens the opportunity for the application of a large class of model investigation techniques. In this paper, the concepts underlying this interface are discussed and a simple application demonstrates its use in the Chaohe Basin in northern China. The freely available interface should be useful for all SWAT users, and the description of the underlying concepts could stimulate similar developments for other watershed simulation programs.

Introduction

Mechanistic watershed models (such as SWAT) that account for hydrologic processes such as rainfall, runoff, evaporation, infiltration, redistribution, and aquifer and river flows need a large amount of input data. The main data needs consist of information about climate, topography, surface structure, soil, aquifer, landuse, and land management. Most of these input data are available only at certain points in the catchment and have to be extrapolated to larger land units or subbasins. This requires extrapolating the point measurements to spatially averaged precipitation intensities, surface roughness factors and soil properties, and extrapolating sample information about land management to the whole catchment. This cannot be done without a calibration procedure that takes into account the point measurements, but fine tunes the parameters to obtain a good model fit. Measurements often used for model calibration include discharge at basin outlets, water levels in aquifers, lakes and reservoirs, sediment loads, and water quality indicators such as nitrate or phosphate concentrations. Using various measurements to calibrate a model would generally lead to a model with larger applicability.

There are significant methodological problems associated with such a calibration procedure (Duan *et al.*, 2002). A major problem is that a large number of parameters need to be estimated with data from a relatively small number of gauging stations. This leads to the non-uniqueness of effective model parameters which can be associated with a flat objective function in a certain direction in parameter space or with the existence of multiple local minima with similarly good values of the objective function. These problems have been addressed on the one hand by global optimization algorithms (Duan et al., 1992) and multiple criteria optimization strategies (Gupta *et al.*, 2002) and, on the other hand, by procedures that search for adequate parameter sets or parameter regions instead of a single optimum value (Beven and Binley, 1992; Vrugt *et al.*, 2002, Abbaspour et al., 2004).

As a consequence of these methodological problems, there is not a single, best procedure that could apply to all watershed model calibrations. This makes the availability of different calibration procedures for the same model and data set beneficial. As uncertainty in the conceptual model is always a serious concern, application of different calibration procedures to different watershed models or different aggregation levels of a model could help to identify the adequate level of aggregation for a certain problem. Such a multi-calibration study would, therefore, profit significantly from a standard interface between simulation programs and systems analysis programs (SAP). Such an interface was recently proposed (Reichert, 2005a) and implemented in the systems analysis program UNCSIM (Reichert, 2005b; http://www.uncsim.eawag.ch) and the inverse modelling routine SUFI-2 (Abbaspsour *et al.*, 2004). This collection of systems analysis techniques is very useful, but it would be beneficial if more algorithms would become available in an implementation that supports this interface.

It is the goal of this paper to discuss the specific requirements of an interface between watershed models and systems analysis tools and to describe the concepts underlying an implementation of such an interface (SWAT_SA_Interface) for the Soil and Water Assessment Tool (SWAT) model (Arnold *et al.*, 1998; http://www.brc.tamus.edu/swat). This is a widely used simulation program for hydrological and water quality modelling at the catchment scale.

SWAT_SA_Interface

1. Requirements of a system analysis interface for watershed models

Automated model calibration requires that the uncertain model parameters are systematically changed, the model is run, and the required outputs (corresponding to measured data) are extracted from the model output files. The main function of a system analysis interface is to provide a link between the input/output of a SAP and a model. The simplest way of handling the file exchange is through text file formats. A schematic of the SWAT_SA_Interface is illustrated in Figure 1. The SWAT_SA_Interface consists of two executable programs “sw_edit” and “sw_extract” (Figure 1). The SAP generates values for the uncertain model parameters (or parameter identifiers as explained later) and writes them to the file “model.in”. The “sw_edit” program places these values (according to the specification of the identifiers) in the model’s input files, and after running the SWAT model, “sw_extract” extracts the required simulation results from the SWAT output files and writes them to the file “model.out”. This file is subsequently read by the SAP, new parameters are generated, and the procedure continues until a satisfactory model simulation is reached.

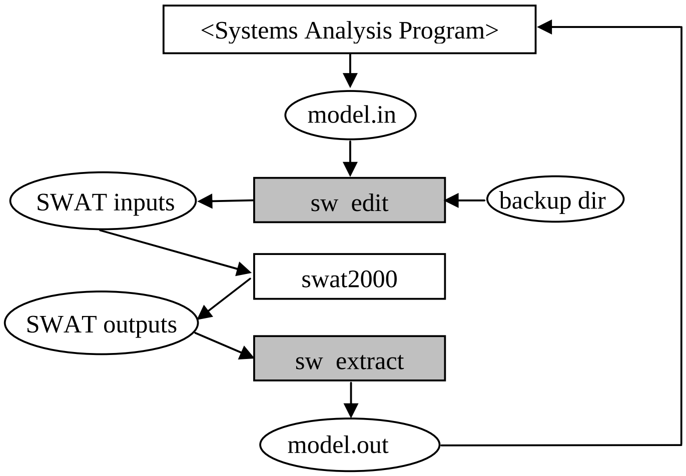

Figure 1. Schematic of information and procedures in the SWAT_SA_Interface program.

2. Overview of the SWAT simulation program

SWAT (Arnold et al., 1998) is a watershed simulation model that was originally developed by the US Department of Agriculture. SWAT solves water balances in hydrologic response units (HRUs) which are defined by unique landuse – soil type combinations within subbasins of the watershed. For each HRU the water balance is calculated considering precipitation, evapotranspiration, runoff, infiltration, interflow, and percolation into a shallow aquifer. River flow is routed downstream to the outlet of the watershed. The current version of SWAT (SWAT 2000) is linked to ArcView GIS (ESRI, http://www.esri.com) in order to facilitate handling of input and output. SWAT also has a water quality component describing transport of sediment, and transport and transformation of nutrients and pesticides. Running SWAT is based on a three-step procedure:

1. In the first step, an ArcView GIS interface of SWAT (AVSWAT) is used to delineate subbasins from digital elevation data, and then generate HRUs within each subbasin by overlaying the soil and land use maps. As a final step, AVSWAT produces a large number of input text files. The content of these input text files and their correspondence with spatial levels are summarized in Table 1.
2. In the second step, the FORTRAN program "swat2000" reads these text input files, performs the simulation, and writes text output files.
3. ArcView-SWAT (AVSWAT) provides limited post processing capabilities and other programs must be used for output manipulation and display.

After the initial setup of a SWAT project, the text file-based project can be run and analyzed independent of the AVSWAT interface. This text file-based project provides the easiest access for the implementation of an interface with systems analysis programs.

3. Text input and output files

There are three levels of SWAT input files: basin, subbasin, and HRU level input files. Basin level input files are used to specify model definitions and parameters valid for the whole watershed. Subbasin level inputs are used to specify values at the subbasin levels. The parameters in the HRU level apply to all HRUs in different subbasins. Table 1 also lists the type, name, and level of each file. There are additional input files, not relevant to calibration, which are not mentioned here.

There are several types of output data. These include output data at the outlets of subbasins (such as discharge time series), output data from within the subbasins (such as ground water level), output data from HRUs (such as precipitation), and summaries of the input and output data (such as precipitation and sediment loads).

Table 1. Example of the file types, file levels and corresponding parameter information.

File type	Level	Description
.bsn	Basin level	Basin input file, with parameters used for the whole basin, such as snowmelt factor.
.wwq	Basin level	Watershed water quality input file with parameters used by the QUAL2E model applied in the main channels.
.crp	Basin level	Land cover / plant growth database file with plant growth parameters for all land covers simulated in the watershed.
.rte	Subbasin level	Main channel routing input file with parameters governing water and sediment movement in the main channel of the sub-basin.
.sub	Subbasin level	Subbasin input file with information related to features within the subbasin, such as properties of tributary channels.
.swq	Subbasin level	Stream water quality input file with parameters used to model pesticide and nutrient transformations in the main channel
.wgn	Subbasin level	Weather generator input file with the statistical data needed to generate representative daily climate data for the subbasin.
.wus	Subbasin level	Water use input file with information for consumptive water use in the subbasin.
.chm	HRU level	Soil chemical input file with information about initial nutrient and pesticide levels of the soil in the HRU.
.hru	HRU level	HRU input file with information related to a diversity of features within the HRU, such as parameters affecting surface water flow.
.mgt	HRU level	Management input file with management scenarios simulated.
.sol	HRU level	Soil input file with parameters about the physical characteristics

4. Specification of uncertain parameters using parameter identifiers

In SWAT, the HRU is the smallest unit of spatial disaggregation. As a watershed is divided into HRUs based on elevation, soil, and land use, a distributed parameter such as hydraulic conductivity can potentially be defined for each HRU. An analyst is, hence, confronted with the difficult task of collecting or estimating a large number of input parameters, which are usually not available. An alternative approach for the estimation of distributed parameters is calibrating a single global modification term that can scale the initial estimates by a multiplicative, or an additive term. This leads to the proposed parameter identifiers.

An important consideration for applying parameter identifiers is that the changes made to the parameters should have physical meanings and should reflect physical factors such as soil, landuse, elevation, etc. Therefore, the following scheme is suggested for the parameter identifiers:

x__<parname>.<ext>__<hydrogrp>__<soltext>__<landuse>__<subbsn>

where x = Code to indicate the type of change to be applied to the parameter:
v – means the existing parameter value is be replaced by the given value,
a – means the given value is added to the existing parameter value, and
r– means the existing parameter value is multiplied by (1 + the given value);
<parname> = SWAT parameter name;
<ext> = SWAT file extension code for the file containing the parameter;
<hydrogrp> = soil hydrological group (‘A’, ‘B’, ‘C’ or ‘D’);
<soltext> = soil texture;
<landuse> = name of the landuse category;
<subbsn> = subbasin number or crop index. When <parname> describes a parameter that is applied at the subbasin or HRU level, this code represents the number or combination of numbers of subbasins; when <ext> is “crp”, it represents a crop index or combination of crop indices.

Any combination of the above factors can be used to describe a parameter identifier. If the parameters are used globally, the identifiers <hydrogrp>, <soltext>, <landuse>, and <subbsn> can be omitted. The presented encoding scheme allows the user to make distributed parameters dependent on important influential factors such as: hydrological group, soil texture, and landuse. The parameters can be kept regionally constant to modify a prior spatial pattern, or be changed globally. This gives the analyst more freedom in selecting the complexity of a distributed parameter. By using this flexibility, a calibration process can be started with a small number of parameters that only modify a given spatial pattern with more complexity and regional resolution added in a stepwise learning process.

The program “sw_edit” in the SWAT_SA_Interface implements the above scheme. The program can easily be linked to any calibration program with components shown in Figure 1. The file “model.in” contains a list of parameter identifiers to be estimated, “backup dir” is a directory containing SWAT input files with the prior model parameters, “SWAT inputs” are the modified SWAT input files, “SWAT2000” is the SWAT execution program, “SWAT outputs” are the SWAT output files, “sw_extract” extracts the required (compatible with measurements) data from the SWAT output files, and finally, “model.out” is the output file of the “sw_extract” program containing a set of data that can be compared with the measurements.

5. SWAT_SA_Interface implementation

There are a large number of SWAT model parameters distributed over a large number of input files. The number of files increases as the watershed disaggregation into subbasin, and consequently the number of HRUs increases. To make the process of modifying input files efficient, this interface was implemented in C++. In a first step, a library of classes corresponding to the input files listed in Table 1 was built. The common functions for reading and writing parameter values from and to the text files are declared in a base class (CBaseParaFile) and implemented in the file-type specific classes. The functions for reading the output files are implemented in a separate class (CMethodSet). This leads to the class hierarchy described in Table 2 and shown in Figure 2.

Table 2. Declared and implemented methods of the classes for modifying/extracting the SWAT input/output files.

Class	Description	Declared methods not yet realized	Realized methods
CMethodSet	common functions and, extracting SWAT information outputs		- Procedure for common functions - Procedure for collecting general SWAT project information - Procedures for extracting SWAT outputs
CBaseParaFile	Base class for swat input files	- Procedure for reading a parameter - Procedure for changing a parameter	- Procedure for retrieving file name, getting or checking the range of a given parameter
CBasinBSNFile CCropFile CHruHRUFile … CSubSUBFile	- Related to .bsn - Related to crop.dat - Related to .hru … - Related to .sub		- Procedure for reading a parameter value - Procedure for changing a parameter value

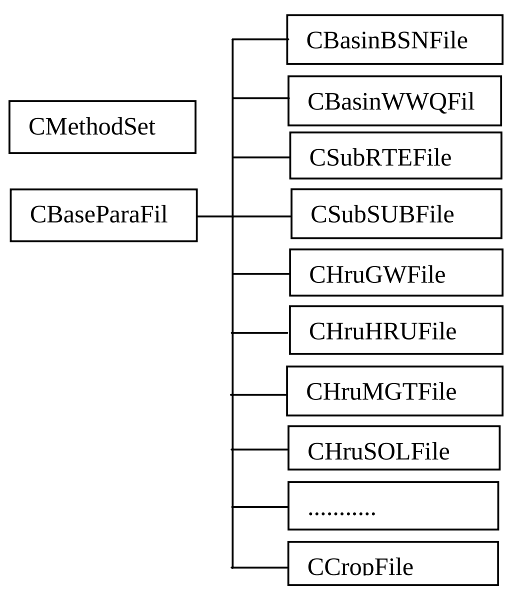

Figure 2. Class hierarchy for modifying or extracting the SWAT.

Figure 3. The locations of the Chaohe Basin and the Xiahui station.

Application to the Chaohe Basin

The Chaohe Basin is part of the catchment of the Miyun Reservoir (Figure 3), which is an important drinking water reservoir for the city of Beijing. With an average yearly precipitation of 530 mm from 1973-1990, this basin is part of the arid region of North China.

Average yearly runoff per surface area is about 60 mm; this is only about 12% of the precipitation. The ratio of surface runoff to precipitation deceased from 24% in 1973 to 9% in 1990 because of its use for drinking water. Water quality is also an important concern in this river basin; hence, a hydrologic and water quality model for this basin can provide useful information for water management.

Daily discharge data and daily sediment load data are available for the watershed outlet, i.e., Xiahui station with a drainage area of 5,340 km^2. A simulation with initial estimates of the parameters led to over-estimation of discharge peaks and sediment loads, emphasizing the need for model calibration.

The SWAT model for the Chaohe Basin was calibrated and tested based on the discharge and sediment data at the basin outlet (Xiahui station) using a typical split sample procedure. The data from the period of 1980-1986 was used for calibration, and data from 1987-1990 was used for model validation. The R^2 and the Nash-Sutcliffe coefficient, NS, (Nash and Sutcliffe, 1970) were used to assess the goodness of fit. The Shuffled Complex Evolution (SCE-UA) algorithm (Duan et al., 1992) as implemented in UNCSIM was used to perform the calibration. In this application, 14 parameter identifiers were selected based on a preliminary sensitivity analysis. The parameter identifiers and their calibrated values are listed in Table 3.

Table 3. Calibrated parameter identifiers used for calibration.

parameter identifier	calibrated value	parameter identifier	calibrated value
a__CN2.mgt	-14.88	v__GW_DELAY.gw	182.667
v__ESCO.hru	0.502	r__SLSUBBSN.hru	-0.027
r__SOL_K.sol	0.281	a__CH_K2.rte	33.644
a__SOL_AWC.sol	0.044	a__OV_N.hru	0.06
v__ALPHA_BF.gw	0.293	a__USLE_K.sol	0.086
v__USLE_C.crp________19	0.315	v__SPCON.bsn	0.00128
r__USLE_C.crp________103,105,106,108,109	14.258	a__SPEXP.bsn	-0.4764

The calibrated parameter identifiers mean that, for example, all curve numbers (CN2) had to be decreased by 14.88, the soil evaporation compensation factors (ESCO) had to be set to a global value of 0.502, all prior soil hydraulic conductivity values (SOL_K) had to be multiplied by (1 + 0.281), and USLE_C factors had to be multiplied by (1 + 14.258) for crop indices 103,105,106,108, and 109.

The calibration and validation statistics are reported in Table 4. In general, the statistics are quite significant. In Figures 4 and 5 measurement and model simulation results are illustrated. The simulation of sediment load is not as good as that for flow. One reason is that the universal soil loss equation (USLE) implemented in SWAT does not account for all the complex activities, such as construction, crop growing, and soil dumping, taking place in the flood plains in the Chaohe region. The decrease in the CN2 parameter (Table 4) from the initial estimates and the increase in SOL_AWC reflect the decreasing percentage of runoff. The increase in USLE_C and USLE_K parameters, however, reflects the high sediment erosion in the region. A more detailed discussion of the calibration procedure and parameter uncertainties is reported in Yang et al. (2005).

Table 4. Statistics of calibration and verification results for flow and sediment load.

	R^2	NS coefficient
Flow Calibration (1980-1986)	0.75	0.75
Validation (1987-1990)	0.80	0.77
Sediment Calibration (1980-1986)	0.53	0.53
Validation (1987-1990)	0.40	0.37

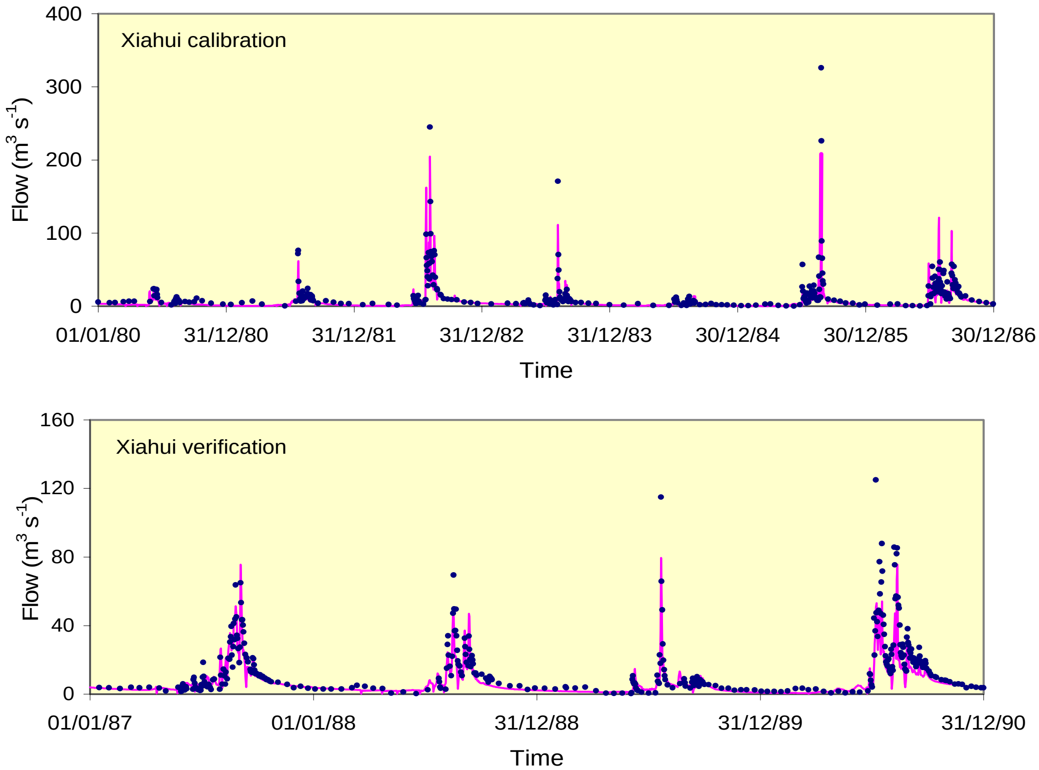

Figure 4. Comparison of the simulated (lines) and observed (points) at the Xiahui station for calibration and validation periods.

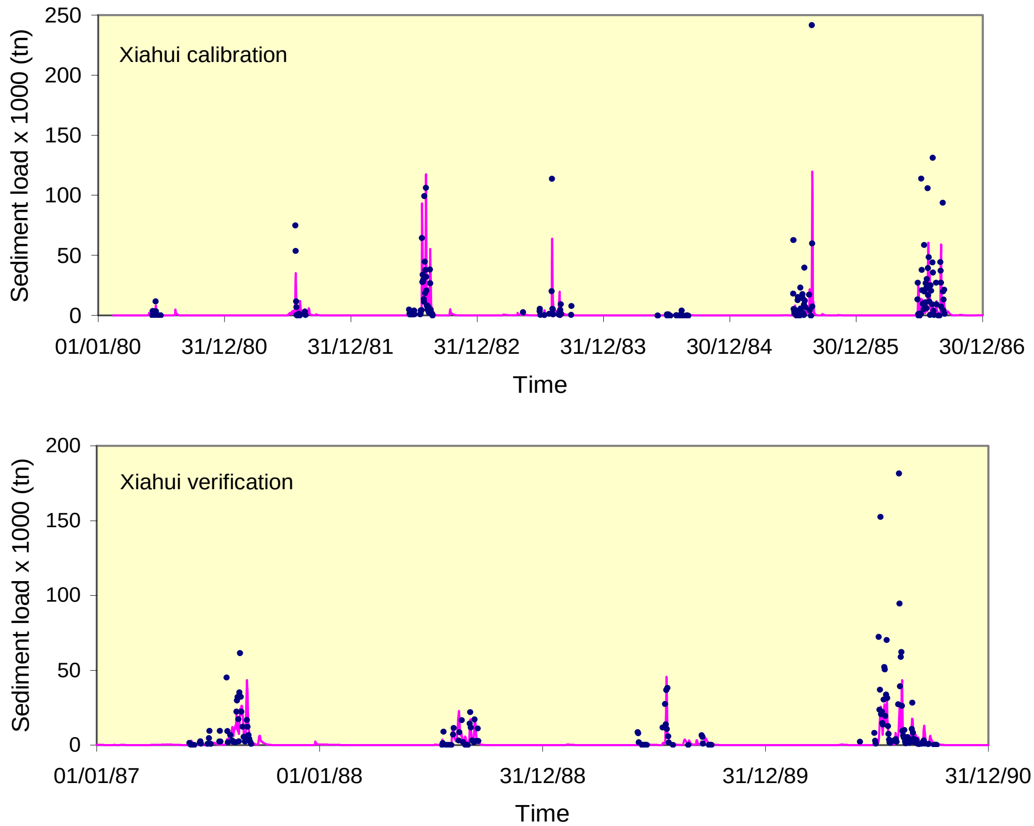

Figure 5. Comparison of the simulated (lines) and observed (points) daily sediment load at the Xiahui station for calibration and validation periods.

Conclusions

The SWAT_SA_Interface greatly facilitates the process of calibration. Introduction of the parameter identifiers is essential for dealing with the large number of parameters and the assignment of meaningful spatial distributions to them. If more systems analysis programs adhere to the suggested standard interface, then more analysis techniques can be brought to bear on the calibration of watershed models.

References

Abbaspour, K.C., Johnson, A., van Genuchten, M.Th, 2004. Estimating uncertain flow and transport parameters using a sequential uncertainty fitting procedure. Vadose Zone Journal 3(4), 1340-1352

Arnold, J.G., Srinivasan R., Muttiah R.S., Williams J.R., 1998. Large area hydrologic modeling and assessment - Part 1: Model development. Journal of the American Water Resources Association 34(1), 73-89.

Beven, K.J. and Binley, A.M., 1992. The future of distributed models: model calibration and uncertainty prediction. Hydrological Processes 6(3), 279-298.

Duan, Q., Gupta, H.V., Sorooshian, S., 1992. Effective and efficient global optimization for conceptual rainfall-runoff models. Water Resources Research 28(4), 1015-1031.

Duan, Q., Gupta, H.V., Sorooshian, S., Rousseau, A.N. and Turcotte, R., eds., 2002. Calibration of Watershed Models. American Geophysical Union, Washington, DC, USA.

Gupta, H.V., Bastidas, L.A., Vrugt, J.A., Sorooshian, S., 2002. Multiple criteria global optimization for watershed model calibration. In: Duan, Q., Gupta, H.V., Sorooshian, S., Rousseau, A.N. and Turcotte, R., (eds.), Calibration of Watershed Models. American Geophysical Union, Washington, DC, USA, pp. 125-132.

Nash, J. E., J. V. Sutcliffe, 1970. River Flow Forecasting through Conceptual Models 1. A Discussion of Principles. Journal of Hydrology 10(3), 282-290.

Reichert, P., 2005a. A standard interface between simulation programs and systems analysis software. Water Science and Technology, in print.

Reichert, P., 2005b. UNCSIM – A program for statistical inference and sensitivity, identifiability and uncertainty analysis, in preparation.

Vrugt, J. A., H. V. Gupta, et al., 2003. A Shuffled Complex Evolution Metropolis algorithm for optimization and uncertainty assessment of hydrologic model parameters. Water Resources Research 39(8), art.no.-1021

Yang, J., Reichert, P., Abbaspour, K.C., Yang, H., 2005. Calibration and uncertainty analysis of a hydrological model for the Chaohe Basin in China, in preparation.

Evaluation Methods for SWAT Models

A. van Griensven[1] , T. Meixner[2], S. Grunwald[3], R. Srinivasan[4]
[1]Biomath, Ghent University, Coupure links 653, 9000 Gent, Belgium. E-mail: ann.vangriensven@Ugent.be
[2]Environmental Sciences, University of California, Riverside
[3]Soil and Water Science Department, University of Florida
[4]Spatial Sciences Laboratory, Texas A&M University

Abstract

Worldwide, water quality regulators increasingly rely on water quality models at the catchment scale, such as the SWAT model, to aid in decision making. These models are able to integrate several sources of pollution at large scales and conduct long-term predictions for pollution abatement scenarios. However, for the practical use of these models, it is important to know the reliability of model results. Traditionally, reliability is quantified by uncertainty analysis methods within a statistical framework. Whereas a wide range of statistical theories exist, it has not yet been possible to conduct a complete and robust uncertainty analysis for these complex models, as there are too many unknowns associated with the modelling problem. For this reason, we propose evaluation methods that are not based on statistics but instead evaluate models on a fit-to-purpose basis.

Within SWAT2005, both a statistical method for uncertainty analysis, ParaSol, and an evaluation method, SUNGLASSES, are incorporated. ParaSol estimates the uncertainty originating from parameter uncertainty that is associated with the calibration procedure. Poor identification of the parameters is propagated to uncertainty bounds on the model results. SUNGLASSES evaluates the correctness of the model predictions to be used for decision making. Failure to make accurate predictions results in wider uncertainty bounds on the model outputs. The application of these methods is illustrated with SWAT2005 simulations for flow and sediment loads in Honey Creek, a tributary of the Sandusky River Basin (Ohio).

Introduction

Model uncertainty analysis aims to quantitatively assess the reliability of model outputs. Many of the water quality modelling applications used to support policy and land management decision making lack this information, and thereby lose credibility (Beck, 1987). Several sources of modelling unknowns and uncertainties result in the fact that model predictions are not a certain value, but should be represented with a confidence range of values (Gupta et al., 1998; Vrugt et al. 2003; Kuczera, 1983a; Kuczera 1983b; Beven, 1993). These sources of uncertainty are often categorized as input uncertainties (such as errors in rainfall or pollutant source inputs), model structure/model hypothesis uncertainties (uncertainties caused by inappropriateness of the model to reflect reality or the inability to identify the model parameters), and uncertainties in the observations used to calibrate/validate the model outputs.

Over the last decade, model uncertainty analysis has been investigated by several research groups from a variety of perspectives. These methods have typically focused on methodologies that look at model parametric uncertainty, but investigators have had a more difficult time assessing model structural and data errors, and properly accounting for these sources of model prediction error (e.g. see commentaries (Beven and Young, 2003; Gupta et al., 2003)). Many researchers have shown that parameter uncertainty was much smaller than expected for the level of trust in the model (Thiemann et al., 2001; Beven and Freer, 2001;

Freer et al., 2003). The focus on parametric uncertainty in model calibration and uncertainty methodologies does not address overall model predictive uncertainty, which encompasses uncertainty introduced by data errors (in input and output observations), model structural errors, and uncertainties introduced by the likelihood measure or objective function used to develop a model and its particular application to a single location (Gupta et al., 2003; Thiemann et al., 2001). It is well known that hydrologic models, particularly those of the rainfall-runoff process and even more so for models of water quality, are not perfect and thus the assumption that the model being used in the calibration process is correct does not hold for the application of hydrologic models (for examples compare Mroczkowski et al., 1997; Boyle et al., 2001; Meixner et al., 2002; Beven, 1993).

The traditional way in which hydrologists assess models, and whether or not the calibration process was valuable and meaningful, includes conducting an evaluation of the model via some methodology. A fundamental necessity noted by many is that the model must be evaluated using data not used for model calibration (Klemes, 1986). This concept typically goes under the name split sample methodology. Typically, this split sample approach is conducted using one half of the time series to calibrate the model and the second half of the time series to evaluate the calibration results. This approach represents the minimum bar over which a model must pass to be considered suitable for further application (Mroczkowski et al., 1997). Here we present a methodology that utilizes a split sample approach to estimate overall model predictive uncertainty with regard to the output variables to be used in the decision making process. We compare these results to those garnered using a parametric uncertainty method based on the statistical approaches ParaSol (Parameter Solutions) using the Soil and Water Assessment Tool (SWAT).

Methods

ParaSol is an optimization and statistical uncertainty method that assesses model parameter uncertainty. On top of ParaSol, SUNGLASSES uses all parameter sets and simulations. Additional sources of uncertainty are detected using an evaluation period, in addition to the calibration period.

Description of ParaSol

The ParaSol (Parameter Solutions) method was developed to perform optimization and model parameter uncertainty analysis for complex models such as distributed (water quality) models, typically having a high number of parameters, high parameter correlations, several output variables, and a complex structure leading to multiple minima in the objective function response surface. The ParaSol method calculates objective functions (OFs) based on model outputs and observation time series, it aggregates these objective functions to a global optimization criterion (GOC), minimizes the OF or a GOC using the Shuffled Complex Evolution (SCE-UA) algorithm, and performs uncertainty analysis with a choice between two statistical concepts.

The Shuffled Complex Evolution (SCE-UA) Algorithm

The SCE-UA algorithm is a global search algorithm for the minimization of a single function with up to 16 parameters (Duan et al., 1992). It combines the direct search method of the simplex procedure with the concept of a controlled random search of Nelder and Mead (1965), a systematic evolution of points in the direction of global improvement, competitive evolution (Holland, 1975), and the concept of complex shuffling. In a first step (zero-loop), SCE-UA selects an initial ‘population’ by random sampling throughout the feasible parameter space for p parameters to be optimized (delineated by given parameter ranges). The population is portioned into several "complexes" that consist of 2p+1 points. Each complex evolves independently using the simplex algorithm. The complexes are periodically shuffled to form new complexes in order to share information between the complexes. SCE-UA has been widely used in watershed model calibration and other areas of hydrology, such as soil erosion, subsurface hydrology, remote sensing, and land surface modelling (Duan, 2003). It was generally found to be robust, effective, and efficient (Duan, 2003). The SCE-UA has also been applied with success to SWAT for the hydrologic parameters (Eckardt and Arnold, 2001) and hydrologic and water quality parameters (van Griensven and Bauwens, 2003).

Objective Functions

Within an optimization algorithm it is necessary to select a function that must be minimized or optimized that replaces the expert perception of curve-fitting during the manual calibration. There are a wide array of possible error functions to choose from, and many reasons to pick one versus another (for further discussion on this topic see (Legates and McCabe, 1999; Gupta et al., 1998)). The types of objective functions selected for ParaSol are limited to the following, due to the statistical assumptions made in determining the error bounds in ParaSol.

Sum of the squares of the residuals (SSQ): similar to the Mean Square Error method (MSE), it aims at matching a simulated series to a measured time series (Equation 1).

$$SSQ = \sum_{n=1,N} \left[x_{n,sim} - x_{n,obs} \right]^2 \qquad (1)$$

with N the number of pairs consisting of the simulation $x_{n,sim}$ and the corresponding observation $x_{n,obs}$.

The sum of the squares of the difference of the measured and simulated values after ranking (SSQR): The SSQR method aims at the fitting of the frequency distributions of the observed and the simulated series. After independent ranking of the measured and the simulated values, new pairs are formed and the SSQR is calculated as (Equation 2):

$$SSQR = \sum_{j=1,N} \left[x_{j,sim} - x_{j,obs} \right]^2 \qquad (2)$$

where j represents the rank. As opposed to the SSQ method, the time of occurrence of a given value of the variable is not accounted for in the SSQR method (van Griensven and Bauwens, 2003).

Multi-objective Optimization

Since the SCE-UA minimizes a single function, it cannot be applied directly for multi-objective optimization. There are several methods available in the literature to aggregate objective functions to a global optimization criterion (Madsen, 2003; van Griensven and Bauwens, 2003) for multi-objective calibration, but they do not provide uncertainty analysis. By using the Bayesian theory (Box and Tiao, 1973) under the assumption that the objective functions are independent of each other, it is possible to define a Global Optimization Criterion (GOC) (Equation 3):

$$GOC = \sum_{m=1}^{M} \frac{SSQ_m * N_m}{SSQ_{m,\min}} \qquad (3)$$

Thus, the sum of the squares of the residuals gets weights that are equal to the number of observations divided by the minimum. The minima of the individual objective functions (SSQ

or SSQR) are, however, initially not known. After each loop in the SCE-UA optimization, an update is performed for the minima of the objective functions using the newly gathered information within the loop and consequently, the GOC values are recalculated.
The main advantage of using Equation 3 to calculate the GOC is that it allows for a global uncertainty analysis considering all objective functions as described below.

Uncertainty Analysis Method

The uncertainty analysis divides the simulations that have been performed by the SCE-UA optimization into 'good' simulations and 'not good' simulations, and in this way is similar to the GLUE methodology (Beven and Binley, 1992). The simulations gathered by SCE-UA are very valuable as the algorithm samples over the entire parameter space with a focus of solutions near the optimum/optima. To increase the usefulness of the SCE-UA samples for uncertainty analysis, some adaptations were made to the original SCE-UA algorithm, to allow for a better exploration of the full parameter range and to prevent the algorithm from focusing on a very narrow set of solutions. The worst results are replaced by random sampling (where k is equal to the number of complexes).

The ParaSol Algorithm uses a threshold value for the objective function (or Global Optimization Criterion) to select the 'good' simulations by considering all of the simulations that give an objective function below this threshold. The threshold value can be defined by χ^2-statistics, where the selected simulations correspond to the confidence region (CR). For a single objective calibration for the SSQ, the SCE-UA will find a parameter set Θ^*, consisting of the p free parameters (θ^*_1, θ^*_2,… θ^*_P), which corresponds to the minimum of the sum the squares (SSQ). According to χ^2-statistics (Bard, 1974), we can define a threshold "c" for a 'good' parameter set using the Equation (4):

$$c = OF(\theta^*) * (1 + \frac{\chi^2_{P,0.95}}{N - P}) \quad (4)$$

where the $\chi^2_{P,0.95}$ gets a higher value for more free parameters P.

For multi-objective calibration, the selections are made using the GOC of Equation 3 that normalizes the sum of the squares for the total of observations, N_T, equal to the sum of $N_{1,\ldots}$,N_m,…N_M observation. A threshold for the GOC is calculated by (Equation 5):

$$c = GOC(\theta^*) * (1 + \frac{\chi^2_{P,0.95}}{\sum_{m=1}^{M} N_m - P}) \quad (5)$$

thus all simulations with GOC < c are deemed acceptable.

Description of SUNGLASSES

The Sources of Uncertainty Global Assessment using Split SamplES (SUNGLASSES) was designed to assess predictive uncertainty that is not captured by parameter uncertainty, in order to get a stronger evaluation of model prediction power,. The method accounts for strong increases in model prediction errors when simulations are done outside the calibration period by using a split sample strategy whereby the evaluation period is used to define the model output uncertainties. The assessment on the evaluation period should depend on a criterion related to the sort of decision the model is being used for.

These uncertainty ranges depend on the GOC, representing the objective functions, on one side, to calibrate the model and develop an initial estimate of model parameter sets, and an evaluation criterion (to be used in decision making) on the other, that is used to estimate uncertainty bounds. The GOC is used to assess the degree of error on the process dynamics, while the evaluation criteria define a threshold on the GOC. This threshold should be as small as possible, but the uncertainty ranges on the criterion should include the "true" value for both the calibration and the validation period. For example, when model bias is used as the criterion, these "true" values are then a model bias equal to zero. Thus, the threshold for the GOC would be increased until the uncertainty ranges on the total mass flux include zero bias. SUNGLASSES operates by ranking the GOCs (Figure 1). Statistical methods can be used to define a threshold considering parameter uncertainty. In this case, ParaSol was used to define such a threshold. However, when we look at the predictions, it is possible that unbiased simulations are not within the ParaSol uncertainty range, other than parameter uncertainty. This result means that there are additional uncertainties acting on the model outputs (Figure 2). Thus, a new, higher threshold is needed in order to have unbiased simulations included within the uncertainty bounds (Figures 1 and 2). This methodology is flexible in the sense that different combinations of objective functions can be used within the GOC. Also, alternatives for the bias as the criterion for the model evaluation period are possible, depending on the model outputs to be used for decision making. Examples of alternative criteria are the percentage of time a certain output variable is higher or lower than a certain threshold (being common for water quality policy) or the maximum value of a certain model prediction percentile (often important for flood control).

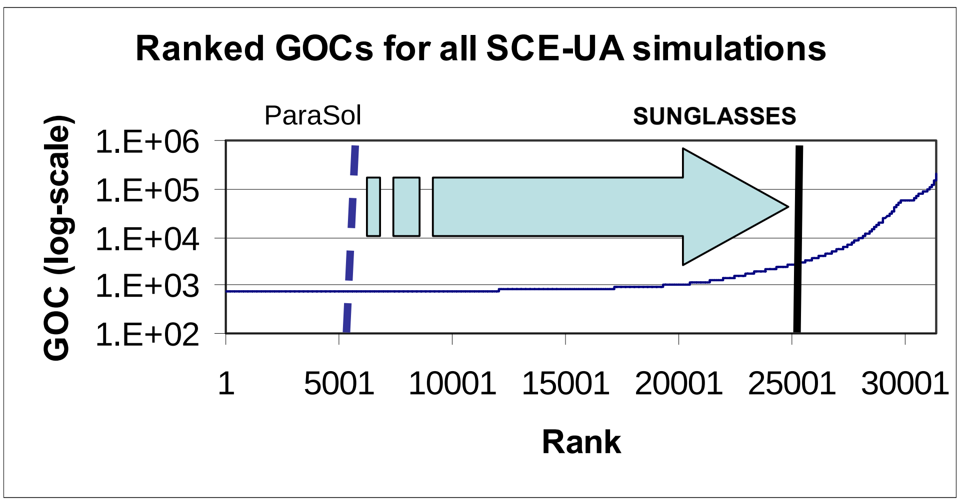

Figure 1. Selection of good parameter sets using a threshold imposed by ParaSol or by SUNGLASSES.

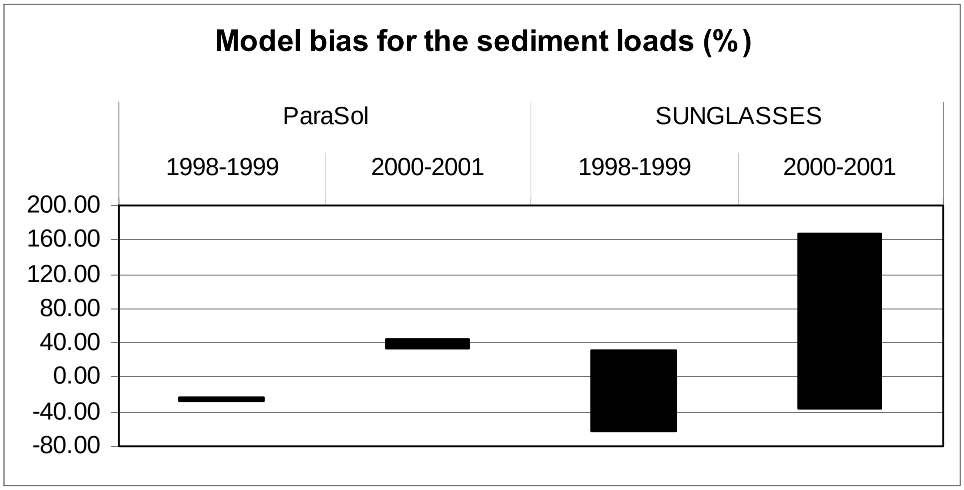

Figure 2. Confidence regions for the sediment loads calculations according to ParaSol and SUNGLASSES.

Application on a SWAT Model

SUNGLASSES was programmed within SWAT (to be part of SWAT2005) and was applied on a small model for evaluation purposes of the methodology and for comparison purposes to the ParaSol method.

SWAT

The Soil and Water Assessment Tool (SWAT) (Arnold et al., 1998) is a semi-distributed and semi-conceptual program that calculates water, nutrient, and pesticide transport at the catchment scale on a daily time-step. It represents hydrology and soil processes by interception, evapotranspiration, surface runoff (SCS curve number method (USDA Soil conservation Service, 1972)), soil percolation, lateral and groundwater flow, and river routing, as well as erosion, crop, and pesticide processes. The catchment is divided into subbasins, river reaches, and Hydrological Response Units (HRUs). While the subbasins can be delineated and located spatially, the further sub-division into HRUs is performed in a stochastic way by considering a certain percentage of subbasin area for each combination of soil and land use classes, without any specified location in the subbasin.

Parameter Change Options for SWAT

In the ParaSol algorithm, as implemented with SWAT2005, parameters affecting hydrology or pollution can be changed either in a lumped way (over the entire catchment), or in a distributed way (for selected subbasins or HRUs). They can be modified by replacement, by addition of an absolute change, or by a multiplication of a relative change. A relative change means that the parameters, or several distributed parameters simultaneously, are changed by a certain percentage. However, a parameter is never allowed to go beyond the predefined parameter ranges. For instance, all soil conductivities for all HRUs can be changed simultaneously over a range of -50 to +50% of their initial values which are different for the HRUs according to their soil type. This mechanism allows for a lumped calibration of distributed parameters while these parameters keep their relative physical meaning (soil conductivity of sand will be higher than soil conductivity of clay).

Honey Creek Model Description

Honey Creek is a subbasin within the Sandusky River Watershed (Ohio) within the Erie Watershed and Great Lakes Basin. The SWAT model for Honey Creek has been abstracted from the SWAT model of the Sandusky that was provided by the University of Florida to the research group at the University of California, Riverside. It covers an area of 338 km^2 and consists of one subbasin, represented by five HRUs, a river reach, and a single point source. Daily observations for the period 1998-1999 were used to calibrate the model. These consisted of 661 flow observations and 518 sediment concentration estimates. The model was developed for use in managing sediment transport. Therefore, calibrations and uncertainty analysis were applied on daily series of flow and sediment loads. Sensitivity results were used to select the ten most important parameters for flow and sediments (van Griensven et al., 2005). These parameters are listed in Table 1. The distributed parameters are changed in a lumped way by considering a single relative change that is applied to all parameters.

Table 1. Parameters used in calibration with sensitivity rank, according to SSQ, the daily flows, and the sediment concentrations.

Parameter	Description		Q	SS (conc)
SMFMX	Maximum melt rate for snow during (mm/°C/day)	Lumped	2	17
ALPHA_BF	Baseflow alpha factor (days).	Lumped	8	1
ch_k2	Channel conductivity (mm/hr)	Distributed	5	14
USLE-P	USLE equation support practice (P) factor.	Distributed	No effect	4
CN2	SCS runoff curve number for moisture condition II.	Distributed	3	2
sol_awc	Available water capacity of the soil layer (mm/mm soil).	Distributed	10	3
surlag	Surface runoff lag coefficient	Lumped	1	7
SFTMP	Snowfall temperature (°C)	Lumped	15	6
SMTMP	Snow melt base temperature (°C)	Lumped	7	5
Sol_z	Soil depth	Lumped	9	10

Objective functions

SWAT was applied to the Honey Creek Catchment in order to estimate sediment export from the catchment. Therefore, the joint calibration included the SSQ for the streamflow and sediment concentrations with a Box-Cox transformation to reduce the heteroscedastic nature of the residuals. Therefore, the Global Optimization Criterion represents the errors associated with both flow and water quality variables.

Evaluation criterion

Based on the assumption that the purpose of the model was to assess global fluxes in sediments loads at the outlet of the creek, the evaluation criteria was described by the model biases on the mass flux that were calculated as (Equation 6):

$$BIAS = \left[\frac{\sum_{n=1}^{N} SIM_n - \sum_{n=1}^{N} OBS_n}{\sum_{n=1}^{N} OBS_n} \right] * 100. \qquad (6)$$

where N is the number of pairs (simulation, observation), SIM_n is the simulation at day n and OBS_n is the observation of day n. The bias was calculated for the water flow and the sediment loads in the calibration and validation period.

Results

ParaSol and SUNGLASSES Confidence Space

A total of 34,669 simulations were performed to minimize the GOC. The ParaSol results, using χ^2-statistics for 97.5% confidence probability, show a clear bias to the sediment load during the calibration period, between -23% and -27%, and an opposite bias for the validation period, 34 to 43% (Figure 2). This suggests that the bias depends on the period of observations. It is also clear that the uncertainty method within ParaSol does not foresee this strong bias and that the zero-bias is not captured. This result is probably due to the compromises that must be made between the different objective functions. An application of SUNGLASSES shows that the sediment load calculations can have an overestimation of up to 167%. This means that the model, when calibrated on a period of two years, is not performing well, and is thus highly uncertain in assessing total mass fluxes. The confidence ranges for the time series give much wider bounds for SUNGLASSES and they capture more of the observations as well (Figure 3). For instance, the missed observations in early 1999 are not captured in ParaSol while they are with SUNGLASSES (Figure 3). We therefore conclude that SUNGLASSES gives an overall more liberal estimation of the confidence regions.

Conclusions

It can be stated that the uncertainty due to poor identification of parameters is rather low according to χ^2-statistics, and that the length of the data is not a problem in this regard. Other sources of uncertainty however cause a bias in the model outputs when run in a predictive mode. Such bias is explained by errors in the model structure or the inability of the data to represent important variabilities that are inherent to environmental systems.

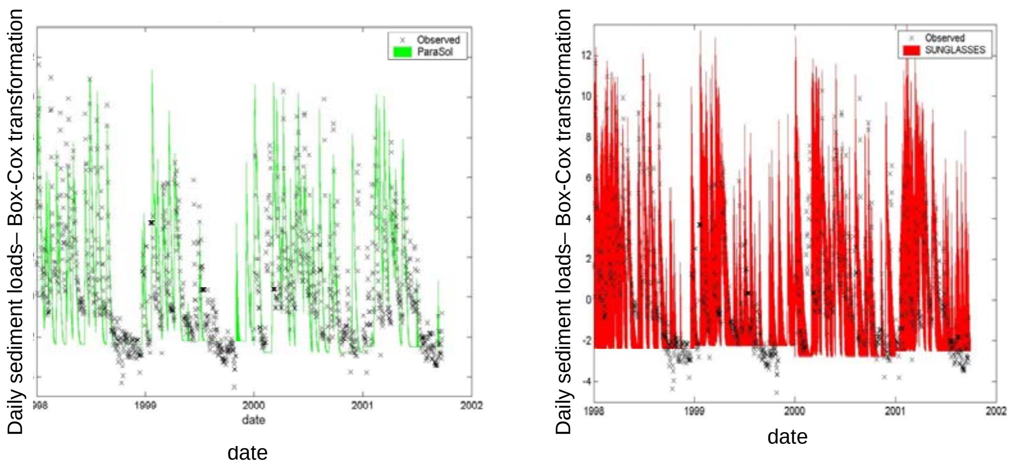

Figure 3. Confidence regions for the time series of the daily sediment loads according to ParaSol and SUNGLASSES.

Acknowledgements

The results presented in this publication have been supported by the US National Science Foundation (EAR-0094312) and the EU project Harmoni-CA (EVK1-CT-2002-20003).

References

Arnold J. G., R. Srinivasan, R. S. Muttiah, and J. R. Williams. Large area hydrologic modelling and assessment part I: model development. Journal of the American Water Resources Association, 34(1), 73-89, 1998.

Beck, M.B. Water quality modelling: a review of the analysis of uncertainty. Water Res. Research, 23(6), 1393-1441, 1987.

Beven, K., Prophecy, reality and uncertainty in distributed hydrological modelling, Advances in Water Resources, 16:41-51, 1993.

Beven, K. and P. Young, Comment on "Bayesian recursive parameter estimation for hydrologic models" by M. Thiemann, M. Torsset, H. Gupta, and S. Sorroshian, Water. Resourc. Res., 39(5):COM 1-1-COM 1-4, 2003.

Beven, K. and A. Binley, The Future of Distributed Models: Model Calibration and Uncertainty Prediction, Hydrol. Processes, 6:279-298, 1992.

Beven, K. and J. Freer, Equifinality, data assimilation, and uncertainty estimation in mechanistic modelling of complex environmental systems using the GLUE methodology, J. Hydrol., 249:11-29, 2001.

Boyle, D. P., H. V. Gupta, S. Sorooshian, V. Koren, Z. Zhang, and M. Smith, Toward improved streamflow forecasts: Value of semidistributed modelling, Water. Resourc. Res., 37:2749-2759, 2001.

Duan, Q., Gupta, V. K. and Sorooshian, S. (1992) Effective and efficient global optimisation for conceptual rainfall-runoff models, Water. Resourc. Res., 28:1015-1031.Eckhardt K and Arnold, J.G. (2001) Automatic calibration of a distributed catchment model, J. Hydrol., 251: 103-109.

Duan, Q., Sorooshian, S. Gupta, H. V., Rousseau, A. N. and Turcotte, R. (2003) Advances in Calibration of Watershed Models, AGU, Washington, DC.Grayson, R. B. and G. Bloschl, Spatial Modelling of Catchment Dynamics, in Spatial Patterns in Catchment Hydrology:

Observations and Modelling, edited by R. B. Grayson and G. Bloschl, pp. 51-81, Cambridge University Press, Cambridge, 2001.

Gupta, H., M. Thiemann, M. Trosset, and S. Sorooshian, Reply to comment by K. Beven and P. Young on "Bayesian recursive parameter estimation for hydrologic models, Water. Resourc. Res., 39(5):COM 2-1-COM 2-5, 2003.

Gupta, H. V., S. Sorooshian, and P. O. Yapo, Toward improved calibration of hydrologic models: multiple and noncommensurable measures of information, Water. Resourc. Res., 34:751-763, 1998.

Holland, J.H. (1995) Adaptation in Natural and Artificial Systems. The University of Michigan Press, Ann Arbor, MI, 183 p, 975.Klemes, V., Dilettantism in Hydrology: Transition or Destiny?, Water. Resourc. Res., 22:177S-188S, 1986.

Kuczera, G., Improved Parameter Inference in Catchment Models: 1. Evaluating Parameter Uncertainty, Water. Resourc. Res., 19:1151-1162, 1983a.

Kuczera, G., Improved Parameter Inference in Catchment Models: 2. Combining Different Kinds of Hydrologic Data and Testing Their Compatibility, Water. Resourc. Res., 19:1163-1172, 1983b.

Kuczera, G. and M. Mroczkowski, Assessment of hydrologic parameter uncertainty and the worth of multiresponse data, Water. Resourc. Res., 34:1481-1489, 1998.

Legates, D. R. and McCabe, G. J. (1999) Evaluating the use of "goodness-of-fit" measures in hydrologic and hydroclimatic model validation, Water. Resourc. Res., 35:233-241.

Meixner, T., H. V. Gupta, L. A. Bastidas, and R. C. Bales, Estimating Parameters and Structure of a Hydrochemical Model Using Multiple Criteria, in Calibration of Watershed Models, edited by Q. Duan, S. Sorooshian, H. V. Gupta, A. N. Rousseau, and R. Turcotte, pp. 255-295, AGU, Washington, DC, 2003.

Mroczkowski, M., G. P. Raper, and G. Kuczera, The quest for more powerful validation of conceptual catchment models, Water. Resourc. Res., 33:2325-2335, 1997.

Nelder, J.A. and Mead R. A. (1965) Simplex method for function minimisation, Computer Journal, 7, 308-313.

Thiemann, M., M. Trosset, H. V. Gupta, and S. Sorooshian, Bayesian recursive parameter estimation for hydrological models, Water. Resourc. Res., 37:2521-2535, 2001.

USDA Soil Conservation Service. National Engineering Handbook Section 4 Hydrology, Chapter 19, 1983.

van Griensven A. and Bauwens W. Integral modelling of catchments. Water Science and Technol., 43(7), 321-328, 2001.

van Griensven A., T. Meixner, S. Grunwald, T. Bishop and R. Srinivasan. A global sensitivity analysis method for the parameters of multi-variable watershed models, submitted to J. Hydrol., 2005.

Vrugt, J. A., H. V. Gupta, W. Bouten, and S. Sorooshian. A shuffled Complex Evolution Metropolis Algorithm for Estimating Posterior Distribution of Watershed Model Parameters, in Calibration of Watershed Models , ed. Q. Duan, S. Sorooshian, H. V. Gupta, A. N. Rousseau, and R. Turcotte, AGU Washington DC, DOI: 10.1029/006WS07, 2003.

Modifications of the Soil Water and Assessment Tool (SWAT-C) for Streamflow Modeling in a Small, Forested Watershed on the Canadian Boreal Plain

Ruth A. McKeown[1], Gordon Putz[1], Jeff Arnold[2], Mauro Di'Luzio[2]
[1]Civil and Geological Engineering, University of Saskatchewan, 57 Campus Drive, Saskatoon, SK, S7N 5A9, Canada. E-mail: rum196@engr.usask.ca
[2]United States Department of Agriculture, Blackland Research Center, Temple, Texas, USA

Abstract

The SWAT model was developed to simulate streamflow and water quality for watersheds composed of agricultural cropland and rangeland. More recently, efforts have been made to utilize SWAT2000 for hydrologic simulations in forested watersheds. The Forest Watershed and Riparian Disturbance (FORWARD) project is studying the impact of fire and harvesting disturbances on streamflow in several small (6 – 16 km^2) forested watersheds located on the Boreal Plain in central Alberta, Canada. Streamflow simulations using the existing representation of hydrologic processes within SWAT2000 were not completely satisfactory for forested conditions. In order to improve the streamflow simulations in a forested environment, the SWAT2000 model code was modified. A surface litter layer under the forest canopy was incorporated into the soil layer representation and a modified version of the SWAT "potholes" facility was used to simulate the effect of water storage and release by Boreal Forest wetlands. The solar radiation input code was modified to account for watershed aspect and slope in the calculation of the Penman-Monteith potential evapotranspiration. The prediction of soil temperature based upon solar radiation input was modified to account for watershed aspect, slope, and canopy cover because a better representation of soil temperature is particularly important for simulation of streamflow associated with the spring thaw. The damping effect of the surface litter layer on soil temperatures was also incorporated. Model results using SWAT2000-C (the modified version of SWAT) and SWAT2000 are presented and discussed in comparison to measured streamflow.

Introduction

The Forest Watershed and Riparian Disturbance (FORWARD) project is investigating and modeling the impact of fire and harvesting disturbances on streamflow in several small (6 - 16 km^2) and large (150 – 250 km^2) forested watersheds located on the Boreal Plain in central Alberta, Canada. The four objectives of the FORWARD project include: 1) assessing the impact of harvesting with and without riparian zone buffers on the streamflow and water quality downstream of the disturbance; 2) determining the impact of fire on streamflow and water quality of flow downstream of the disturbance; 3) assessing the difference in watershed response to harvesting and fire; and 4) providing a modeling tool for industry to manage the impact of harvesting.

Harvesting and fire disturbances can potentially result in significant impacts on downstream water quantity and quality. Numerous studies have reviewed the impact of harvesting (Bowling et al. 2000; Buttle and Metcalfe 2000; Jones and Grant 2001; Nichols and Verry 2001; Prepas et al. 2001; Thomas 2001) and fire (Bayley et al. 1992; McEachern et al. 2000) and have compared the two disturbance types (Lamontagne et al. 2000) and their relative impact on streamflow and water quality. However, few studies have been conducted in the Boreal Plains forest. Projects conducted in the Boreal Plains forest have focused on the impact of these disturbances on the water quality in lakes (McEachern et al. 2000; Prepas et al. 2001).

Figure 1 shows the location of the FORWARD project in Canada, and the watershed discussed in this paper. In total there are 16 watersheds in the FORWARD project that will be modeled using SWAT2000-C, five harvested, four burned in a wildfire, and seven remaining as reference streams.

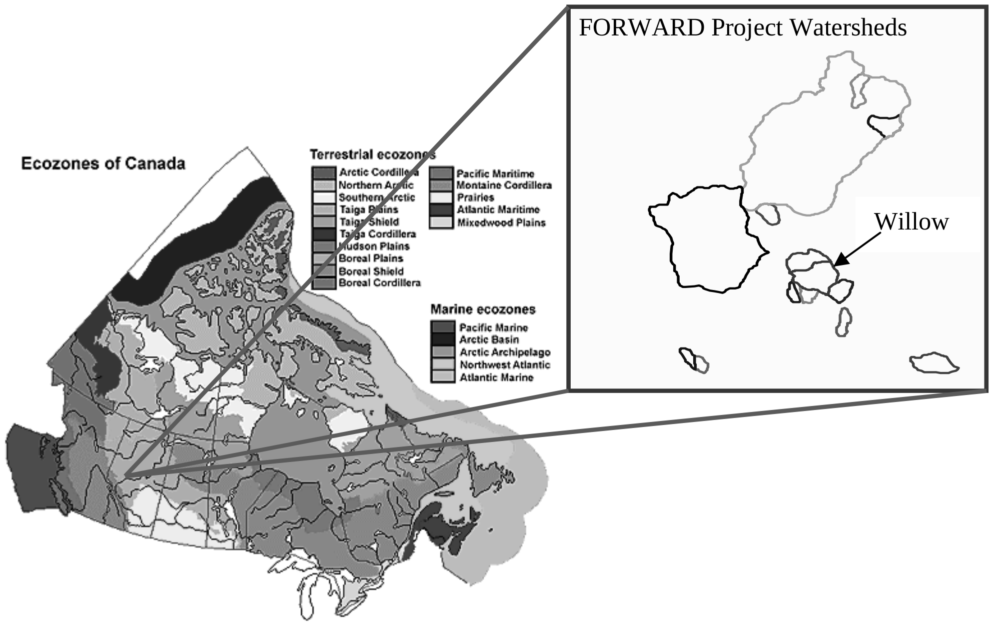

Figure 1. Project location.

Cold winters and cool summers, typical of the Boreal Forest, influence hydrological conditions in ways that are less well-understood than the hydrology of more temperate locations (Buttle et al. 2000). Typically, the total precipitation is less than in more temperate regions. Most of the Boreal Forest receives on the order of 300 to 625 mm of precipitation on an annual basis, with the distribution between rainfall and snowfall being approximately 3 to 1. Snow is typically present in the Boreal Forest from six to eight months of the year (Dingman, 2002). The Boreal Forest experiences a wide range in temperatures, with short summers (Woodwar, 1996), and is classified as sub-arctic and cold continental (GeoGratis, 2003). The average yearly temperature is near $0^{o}C$, with temperatures in the North American Boreal Forest varying from a mean daily average of $15.7^{o}C$ in July to $–19.1^{o}C$ in January (Canada 2002)**.**

The Boreal Forest is composed of deciduous and coniferous species, the composition of which changes over time. In the early successional stages of growth, broadleaf deciduous trees and shrubs are dominant. The most common of the early successional species are alder, birch, and aspen (Woodwar, 1996). As the stand matures, coniferous species are more dominant and include spruce, fir, pine, and deciduous larch or tamarack. Black spruce and larch ring the edge of boggy areas (Woodwar, 1996). Pine forests flourish on sandy outwash plains and areas that used to be dunes. Larch forests are found in areas where the substrate is thin and waterlogged and are underlain by permafrost. The Boreal Forests have open canopies, which are conducive to an understory of shrubs, mosses, and lichens (Woodwar, 1996).

Soil orders found in the Boreal Forest include histosols, spodosols, alfisols, and inceptisols. Spodsols (luvisols) are found primarily in cool, wet climates under deciduous and coniferous forests and are dominant in the study area. These soils have well-developed organic, leached, and accumulation horizons.

The purpose of this paper is to present modifications to SWAT2000, called SWAT2000-C, that have improved the simulation of water movement in forested watersheds. Model output from SWAT2000-C and SWAT2000 is compared to daily streamflow for the Willow Creek Watershed within the FORWARD study area. This watershed has been designated a reference watershed, and will be used to assess the relative impact of disturbance (fire and harvesting) in other watersheds.

Methodology

Study Site

To date, the FORWARD modeling effort has focused on one small watershed, Willow Creek. The watershed is 16 km^2 in size. The elevation ranges from 870 m at the mouth of the watershed to a maximum elevation of approximately 1,061 m. The watershed is primarily covered by forest and has been partitioned using the United States Geological Survey (USGS) classification system. Deciduous forest covers 42% of the total area, while coniferous forest covers 28%. An additional 23% of the land is covered with a mix of deciduous and coniferous trees. The remainder is composed of rangeland and transportation right of ways, forested wetlands, and non-forested wetlands. The soil data for the watershed indicates that approximately 91% is composed of the Soil Conservation Service (SCS) hydrologic soil group C, and the remainder of the watershed is composed of soils group D. These fine to very fine textured soils have a low to very low rate of water infiltration when wet, which results in high runoff potential. Shallow wetlands (<0.5 m) in the watershed cover approximately 10.9% of the land base, with deep wetlands (>6 m) covering an additional 1.2% of the land base.

Source Data

Data used in the modeling was obtained from existing geographical information system (GIS) coverages and meteorological stations, as well as from field data. The existing GIS coverages included land cover, a digital elevation model (DEM), and stream coverages. Field data collected includes soils and streamflow data at the outlet of the watershed. Meteorological data was available from surrounding fire tower installations, an Environment Canada weather station, and in the latter half of 2002, a FORWARD meteorological station was established in the Willow Creek Watershed. Figure 2 shows the location of the meteorological stations in the vicinity of the project as well as the watershed of interest.

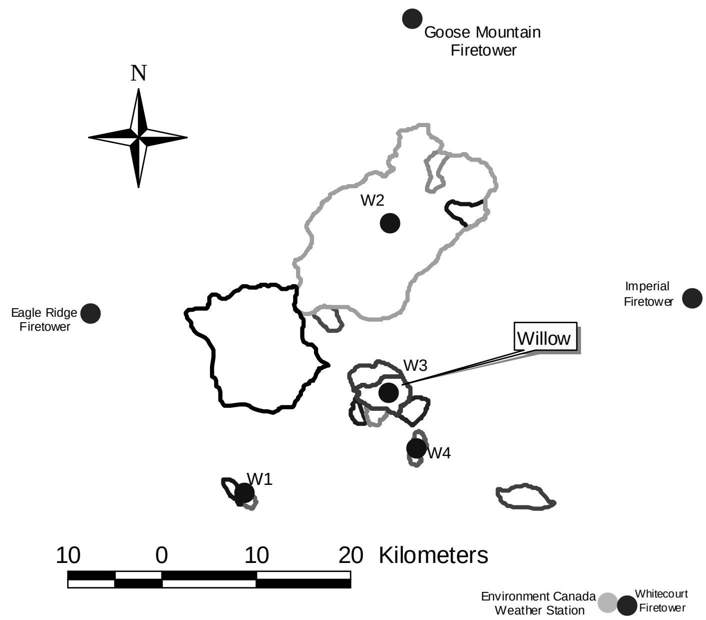

Figure 2: Meteorological stations.

Model Setup

The SWAT2000 model was run in the Better Assessment Science Integrating point and Nonpoint Sources (BASINS) environment. Initial conditions for the model were based upon both SWAT2000 default data and site-specific information. The land use/land cover, reach, and soils coverages were configured to mimic the standard USA classification systems for input into BASINS. The land coverage was determined to be primarily deciduous coniferous and mixed tree species with a minimal content of rangeland bush, forested and non-forested wetlands, and transportation as determined from the USGS classification system. Figure 3a shows the distribution of the forest cover over the basin. Soils information was constructed from available provincial government database information and field reconnaissance. These deep clay-till soils were classified as either SCS soil type “C” or “D”. The number of soil horizons ranged from five to six with one of the layers representing the highly permeable forest litter layer. Lower layers have high clay content and slow the downward movement of moisture. Figure 3b shows the soils distribution over the watershed. The reach data was reviewed and formatted to match the data input requirements for BASINS.

Deep wetlands are located in the uplands of the watershed. Shallow wetlands are under review for potential re-definition and were not incorporated as wetlands into the modeling results presented. Shallow wetland areas were characterized as a forest stand with a thick litter layer.

Data from three different meteorological stations was used in the modeling. For the first 18 months of modeling, the meteorological data was taken from stations approximately 45 km away from the watershed. Data for the summer months was obtained from Eagle Ridge fire tower, with data from the winter months used from the closest Environment Canada Station. In the summer of 2002, the meteorological station W3 was installed in the Willow Creek Watershed and used for the remainder of the modeling period.

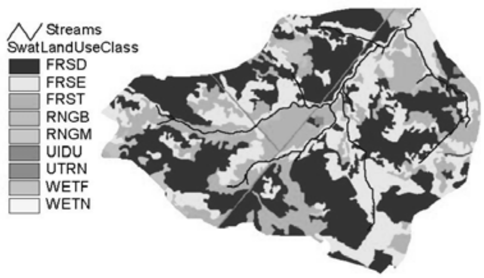

(a)

Figure 3: Willow Creek Watershed (a) land cover distribution; (b) Soils distribution.

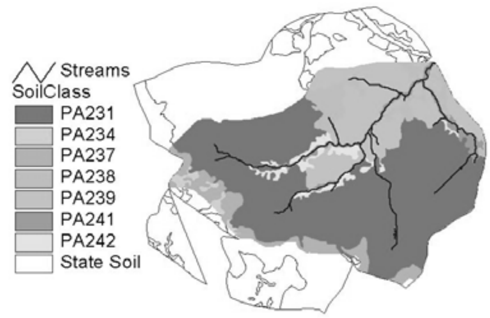

(t

The model was run for 4 years prior to the calibration period in order to remove any potential bias in initial site parameter estimates. The variable storage routing method and the Penman-Monteith evapotranspiration method were used during the modeling.

Model Code Expansion – SWAT2000-C

The SWAT2000 model was originally developed for an agricultural setting. In order to improve the hydrologic simulation for forested conditions, the SWAT2000 model code was modified in three areas, and renamed SWAT2000-C. These areas consist of the inclusion of a litter layer over the soil profile, the improvement of soil temperature modeling, and an enhanced representation of boreal wetlands.

The litter layer under the vegetative canopy better represents the hydrologic processes in a forested environment. The litter layer provides additional storage for water during higher intensity rainstorms thus attenuating peak flows realized at the stream. The parameters used in the development of the litter layer subroutine are shown in Figure 4.

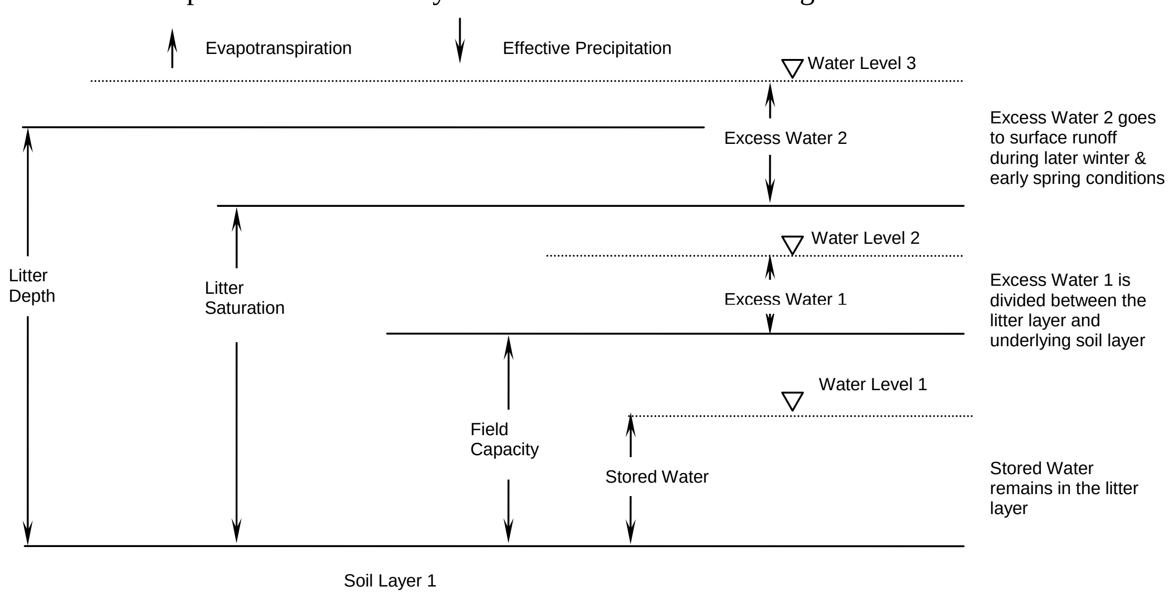

Figure 4: Litter layer description.

The precipitation that reaches the litter layer is reduced by the canopy storage, thus reducing the effective precipitation. The effective precipitation for the day enters the litter layer. If the effective precipitation is less than the field capacity of the litter layer (Water Level 1), the water is stored in the litter layer. If the effective precipitation is greater than the field capacity of the litter layer (Water Level 2), the water in excess of the field capacity, and equal to or less than the saturation level of the litter layer is proportioned between the lateral flow in the litter layer and the percolation into the underlying soil layers. The equation used to proportion the excess water is given in [1].

[1] $$ratio = \frac{k_{sat-soil}}{k_{sat-soil} + k_{sat-litter} * slope}$$

where:

$k_{sat-soil}$ = saturated hydraulic conductivity of the underlying soil layer (mm/hr)
$k_{sat-litter}$ = saturated hydraulic conductivity of the litter layer (mm/hr)
slope = slope of the litter/soil interface (percent)

Surface runoff in a forested environment is assumed to occur only when the underlying soils are frozen, and the litter layer is saturated. The justification for allowing surface runoff only during the conditions described stems from a review of the ability of the underlying soil to transmit water. The saturated hydraulic conductivity has been estimated to range from 100 to 600 mm/hr for the litter layer and from 1 to 100 mm/hr for the underlying mineral soil. This relates to the ability of the litter layer to transmit 2,400 to 14,400 mm during the day, and 24 to 2,400 mm for the first soil layer. It would be unlikely that a rainstorm would occur that would fill the litter layer storage and have a high enough intensity that the soils could not transmit all of the precipitation to lower soil layers during summer conditions. However, when the litter layer is saturated and frozen, the ability to transmit snowmelt through the litter layer is limited. Consequently, surface runoff is allowed in this specific scenario.

The wetland code was added to better represent wetlands within the Boreal Forest. Wetlands are believed to influence water movement by providing baseflow during dry periods, and reducing peak flows in the stream by acting as a buffer during wet periods. Water inflows and outflows incorporated into the model are shown in Figure 5.

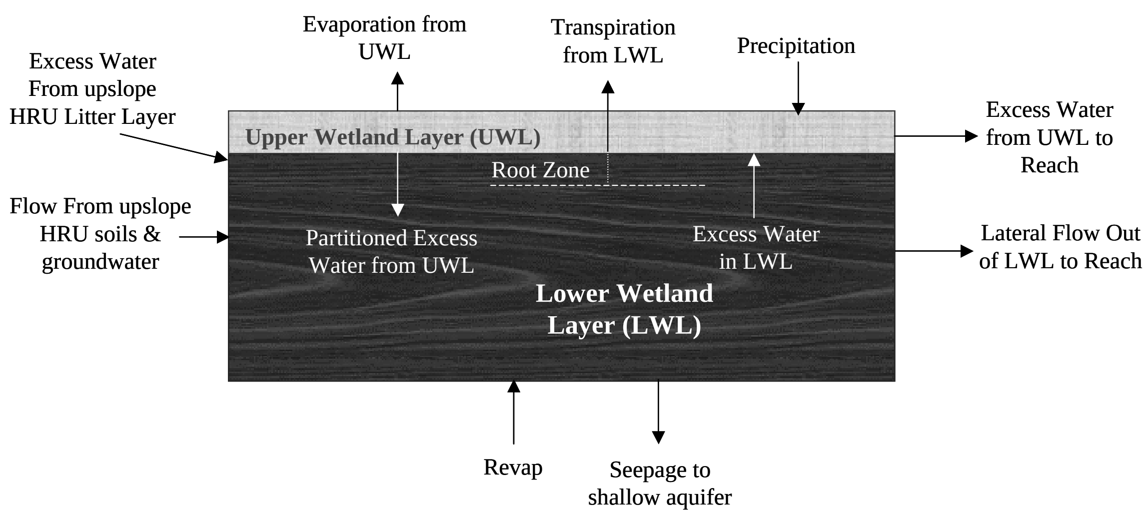

Figure 5: Wetlands code water balance.

The equation for inflow into the lower wetland layer includes the volume of water from contributing hydrologic response units and the precipitation that infiltrates through the upper wetland layer into the lower wetland layer and is shown in [2].

[2] $$V_{end} = V_{stored} + V_{flowin} - V_{flowout}$$

$$V_{end} = V_{stored} + V_{hru\_gw} + V_{hru\_surf} + V_{hru\_lat} + V_{hru\_lit} + V_{pot\_lit} + V_{pot\_revap} - V_{pot\_trans} - V_{pot\_xs} - V_{pot\_seep} - V_{pot\_lat}$$

Where:
V_{end} = depth of water in the lower wetland layer (LWL) at the end of the day (mm H_2O)
V_{stored} = depth of water in the LWL at the start of the day (mm H_2O)
V_{flowin} = depth of water that enters the LWL during the day (mm H_2O)
$V_{flowout}$ = depth of water that exits the LWL during the day (mm H_2O)
V_{hru_gw} = proportional depth of water from the upslope HRU's groundwater flow feeding the LWL (mm H_2O)
V_{hru_surf} = proportional depth of water from the upslope HRU's surface flow feeding the LWL (mm H_2O)
V_{hru_lat} = proportional depth of water from the upslope HRU's lateral flow feeding the LWL (mm H_2O)
V_{hru_lit} = proportional depth of water from the upslope HRU's litter flow feeding the LWL (mm H_2O)
V_{pot_lit} = depth of water from the wetland upper wetland layer (UWL) feeding the LWL (mm H_2O)
V_{pot_revap} = depth of water from the shallow aquifer feeding the LWL (mm H_2O)
V_{pot_trans} = depth of water transpired from the LWL (mm H_2O)
V_{pot_xs} = depth of water in excess of the maximum volume that can be stored in the LWL that is directed back to the UWL (mm H_2O)
V_{pot_seep} = depth of water that seeps from the LWL to the shallow aquifer (mm H_2O)
V_{pot_lat} = depth of water that flows laterally from the LWL (mm H_2O)

The solar radiation incident on the canopy was adjusted to account for aspect and slope. This affects the streamflow reaching the channel during warmer months when using the Penman-Monteith method for evapotranspiration calculation. The aspect and slope of the subbasins was incorporated into the model. South facing slopes in the northern hemisphere thaw earlier than north facing slopes (Murray and Buttle 2002). The radiation reaching the ground varies depending upon the slope orientation (Oke 2000). The equation incorporated into the model (Revfeim 1978; Tian et al. 2001) is shown in [3].

[3] $$G_a = G_m\left[R_d(1-K_r) + f_\beta K_r + 0.2(1-f_\beta)\right]$$

where:
G_a = radiation reaching the sloped ground surface (MJ/m^2)
G_m = radiation measured on a flat surface (MJ/m^2)
R_d = ratio of direct radiation on the slope to direct radiation on a horizontal surface
K_r = ratio of diffuse radiation to global radiation for a horizontal surface
F_β = proportion of the hemisphere above the slope surface that is blocked by the horizontal plane

The ratio of direct radiation on the slope to direct radiation on a horizontal surface is a function of the latitude, aspect, slope, and the declination (the angular position of the sun at solar noon with respect to the plane of the equator)(Tian et al. 2001). The aspect of the subbasins is determined outside of the SWAT2000-C model interface. The results are compiled in an ascii file and read into the model for use.

Soil temperature calculations were adapted to incorporate the aspect and slope using [3], as well as the influence of vegetation and the damping effect of the litter layer. The soil was found to thaw consistently earlier than values measured in the field. This was believed to influence spring flows, where infiltration was excessive with little runoff. Modeled results did not correlate very well with recorded values. Vegetation growing on the landscape intercepts solar radiation reducing the amount reaching the ground surface (Eagleson 1970; Ohta et al. 2001). This in turn impacts the rate at which the soil thaws (Oke 2000). Beer's Law of light extinction was used to attenuate the radiation reaching the ground surface. The equation is shown in [4].

[4] $$G_f = G_a e^{(-K \bullet LAI)}$$

where:

- G_a = actual radiation reaching the sloped ground surface (MJ/m^2)
- G_f = radiation measured on a sloped surface under vegetation (MJ/m^2)
- K = extinction coefficient representing the radiation loss through the vegetation canopy
- LAI = leaf area index of the vegetation canopy

This equation allows for the variation of the extinction coefficient as deemed appropriate while the LAI is calculated on a daily basis by the model.

The damping effect of the litter layer also delays the soil freeze and thaw. An equation was developed using litter and soil temperature data gathered over a short period from the project area. The equation, assumed to generally follow an S-shape, shown in [5], could be further refined with additional site data.

[5] $$bcv_{forest} = \frac{D_{LL}}{D_{LL} + Exp(-2.598 + 0.845 \bullet D_{LL})}$$

where:

- bcv_{forest} = weighing factor for soil cover impacts
- D_{LL} = normalized litter layer depth

Results

Daily stream flows were modeled for the Willow Watershed for 2001 through 2004. A comparison of measured and modeled results for 2001-2004 is shown in Figures 6a through 6d respectively. The modeled results generally follow the measured values for all years of modeling.

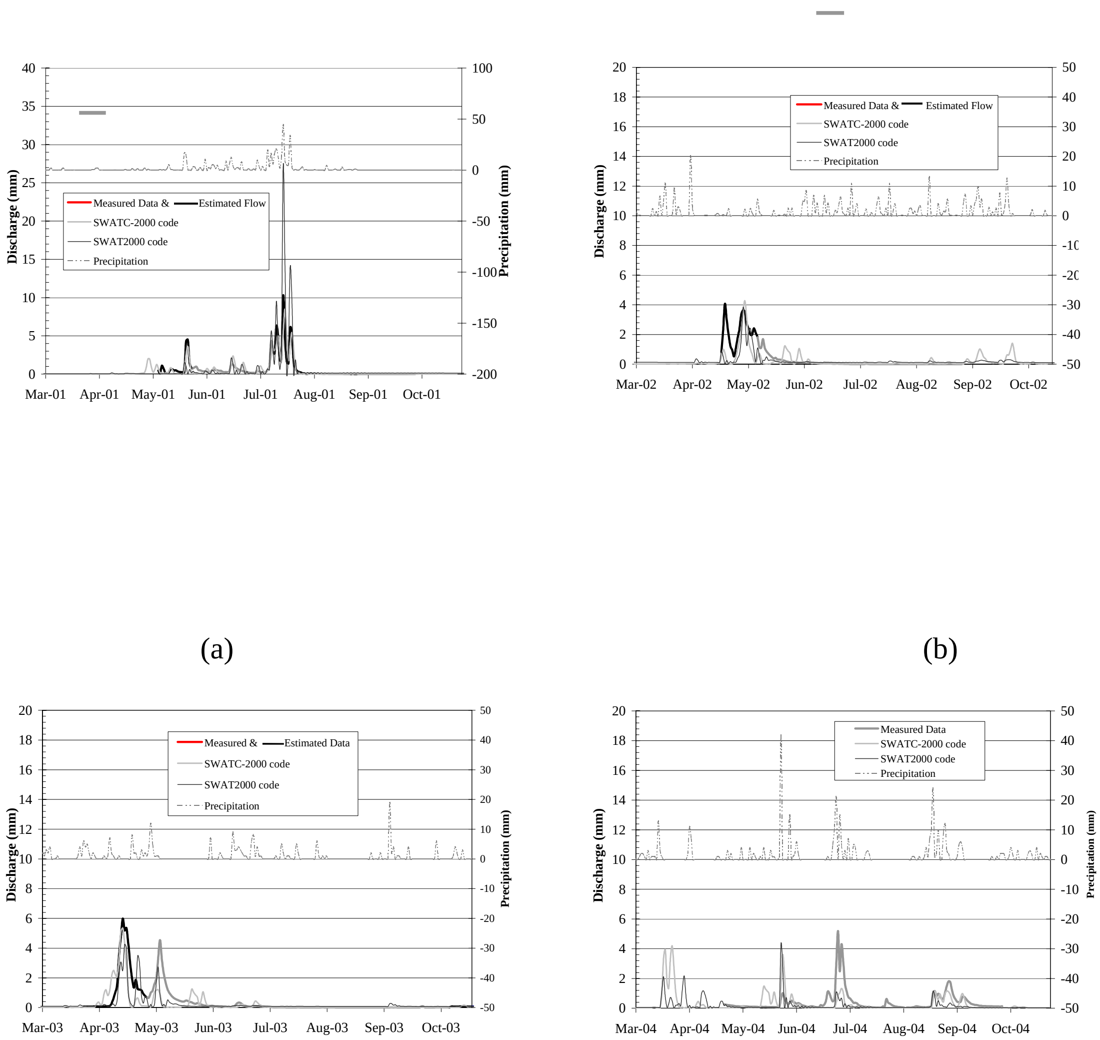

(a) (b)

(c) (d)

Figure 5: Willow Creek Watershed modeled and measured daily discharge for (a) 2001 (b) 2002, (c) 2003, and (d) 2004.

Discussion

The modeled results using SWAT2000-C better match the measured flows compared to SWAT2000 results. The daily and monthly Nash-Sutcliff R^2 values using SWAT2000 were –0.10 and 0.42, respectively. SWAT2000-C daily and monthly Nash-Sutcliff R^2 for the period of modeling was 0.56 and 0.72, respectively.

A significant amount of uncertainty exists in the input precipitation data. Storm precipitation in the project area is often the result of thunder cells, although frontal storms also occur. Consequently, rainfall magnitudes can vary significantly over relatively short distances. The precipitation at meteorological station W3 may not be representative of the precipitation over the entire watershed. An example of this occurs in early August 2004, where runoff was measured with no corresponding precipitation event. Given the uncertainty and variability in the input rainfall data, the results obtained using the SWAT2000-C model are considered reasonable.

Conclusions

SWAT2000-C provides improved simulation results for streamflow from the Willow Creek forested watershed in the Canadian Boreal Plain as compared to SWAT2000. The effort to improve and expand the model to better represent forested watersheds, with particular emphasis on characteristics of the Boreal Forest has been successful in the Willow Watershed. Further modifications of the model could still be implemented to better represent the conditions in the Boreal Forest. These improvements include litter layer growth, more detailed equations for wetlands freeze and thaw, a further refined damping effect equation, and the development of an improved radiation reduction equation specific to the area. A number of the proposed improvements can only be implemented by gathering additional data from the project site.

References

Bayley, S. E., Schindler, D. W., Beaty, K. G., Parker, B. R., and Stainton, M. P., . 1992. Effects of multiple fires on nutrient yields from streams draining boreal forest and fen watersheds: Nitrogen and phosphorus. Canadian Journal of Fisheries and Aquatic Science, 49, 584-596.

Bowling, L. C., Storck, P., and Lettenmaier, D. P. 2000. Hydrologic effects of logging in western washington, united states. Water Resources Research, 36:11, 3223-3240.

Buttle, J. M., Creed, I. F., and Pomeroy, J. W. 2000. Advances in canadian forest hydrology, 1995-1998. Hydrological Processes, 14:9, 1551-1578.

Buttle, J. M., and Metcalfe, R. A. 2000. Boreal forest disturbance and streamflow response, northeastern ontario. Canadian Journal of Aquatic Science, 57 (Suppl. 2), 5-18.

Environment Canada. 2002. Citing online sources: Climate normals 1971 - 2000. Available from http://www.msc.ec.gc.ca/climate/climate_normals/stnselect_e.cfm [cited February 14 2003].

Dingman, S. L. 2002. Physical hydrology, Prentice-Hall Inc., Upper Saddle River, NJ.

Eagleson, P. S. 1970. Dynamic hydrology, McGraw-Hill Book Company.

Natural Resources Canada, Government of Canada. 2003. Citing online sources: Ecozones of canada. Available from http://geogratis.cgdi.gc.ca/Ecosystem/1_ecosys/ecoreg.htm [cited April 23, 2003 1999].

Jones, J. A., and Grant, G. E. 2001. Comment on "peak flow responses to clear-ciutting and roads in small and large basins, western cascades, oregon: A second opinion". Water Resources Research, 37:1, 175-178.

Lamontagne, S., Carignan, R., D'Arcy, P., Prairie, Y. T., and Pare, D. 2000. Element export in runoff from eastern canadian boreal shield drainage basins following forest harvesting and wildfires. Canadian Journal of Aquatic Science, 57 (supp 2.), 118-128.

McEachern, P., Prepas, E. E., Gibson, J. J., and Dinsmore, W. P. 2000. Forest fire induced impacts on phosphorus, nitrogen, and chlorophyll a concentrations in boreal subarctic lakes of northern alberta. Canadian Journal of Fisheries and Aquatic Science, 57 (Suppl. 2), 73-81.

Murray, C. D., and Buttle, J. M. 2002. Impacts of clearcut harvesting on snow accumulation and melt in a northern forest. Journal of Hydrology, 271, 197-212.

Nichols, D. S., and Verry, E. S. 2001. Stream flow and groundwater recharge from small forested watersheds in north central minnesota. Journal of Hydrology, 245, 89-103.

Ohta, T., Hiyama, T., Tanaka, H., Kuwada, T., Maximov, T. C., Ohata, T., and Fukushima, Y. 2001. Seasonal variation in the energy and water exchanges above and below a larch forest in eastern siberia. Hydrological Processes, 15, 1459 - 1476.

Oke. 2000. Boundary layer climates: Second edition, Rutledge.

Prepas, E. E., Pinel-Alloul B., Planas, D., Mthot, G., Paquet, S., and Reedyk, S. 2001. Forest harvest impacts on water quality and aquatic biota on the boreal plain: Introduction to the trols lake program. Canadian Journal of Fisheries and Aquatic Sciences, 58**:**2, 421-436.

Revfeim, K. J. A. 1978. A simple procedure for estimating global daily radiation on any surface. Journal of Applied Meteorology, 17, 1126 - 1131.

Thomas, R. B., Megahan, W.F. 2001. Comment on "peak flow responses to clear-cutting and roads in small and large basins, western cascades, oregon" by j.A. Jones and g.E. Grant - reply. Water Resources Research, 37**:**1, 181-183.

Tian, Y. Q., Davies-Colley, R. J., Gong, P., and Thorrold, B. W. 2001. Estimating solar radiation on slopes of arbitrary aspect. Agricultural and Forest Meteorology, 109, 67-74.

SLW. 1996. Citing online sources: Taiga or boreal forest. Available from [cited October 1996].

Session VI

21. **The power of multi-objective calibration: Two case studies with SWAT** **200**
Johan A. Huisman, Thorsten Pohlert, Lutz Breuer and Hans-Georg Frede

22. **Comparison of optimization algorithms for the automatic calibration of SWAT2000** **210**
Bryan A. Tolson and Christine A. Shoemaker

23. **A comparison of parameter regionalisation strategies for the water quantity module of the SWAT with application to the Scheldt River Basin** **221**
Griet Heuvelmans, Bart Muys and Jan Feyen

24. **Vulnerability assessment of climate change impact on Indian water resources using the SWAT model** **231**
A.K. Gosain, Sandhya Rao and Debajit Basu Ray

The Power of Multi-Objective Calibration: Two Case Studies with SWAT

Johan A. Huisman[1*], Thorsten Pohlert[1], Lutz Breuer[1] and Hans-Georg Frede[1]
Institute of Landscape Ecology and Resources Management, University of Giessen, Heinrich-Buff-Ring 26, D-35392 Giessen, Germany. Email: sander.huisman@agrar.uni-giessen.de

Abstract

Proper calibration procedures for complex eco-hydrological models should use all available measurement time series that provide useful information about the physical system. This is especially true for distributed models that simulate a variety of hydrological and matter fluxes, such as SWAT. There are three well-accepted methods for multi-objective calibration within hydrology. In this contribution, we present two case studies where SWAT is calibrated with these different multi-objective calibration approaches. In the first case study, SWAT is calibrated to percolation, actual evapotranspiration, and nitrate leaching fluxes measured within a lysimeter. With this example, we illustrate several important aspects of multi-objective calibration, such as noncommensurability of different error measures. In the second case study, SWAT is calibrated to measured discharge from three subbasins of the Dill Catchment (Germany). This example shows how multi-objective calibration is used to determine if one set of parameters can provide adequate simulations for all three subbasins. We hope that these case studies illustrate the power of multi-objective calibration.

Introduction

To calibrate a hydrologic model, one must specify values for its parameters in such a way that the behavior of the model closely matches that of the real system. Because of the time-consuming nature of manual trial-and-error calibration, a lot of effort has been dedicated to developing automated calibration methods that can effectively and efficiently find a set of optimal parameters given a single objective function (e.g. Duan et al. 1993; Kuzcera and Parent, 1998; Vrugt et al., 2003). Practical experience with model calibration suggests that there is no single-objective function that adequately measures all aspects deemed important in a manual calibration (Gupta et al., 1998). Furthermore, with the increase in computer power, the number of eco-hydrological models that can simulate several watershed output fluxes at different locations within the catchment has steadily increased. If measurements of other water output fluxes besides discharge are available (e.g. chemical constituents), these should be used in the automated calibration of complex eco-hydrological models, such as SWAT.

In this paper, we present two case studies where SWAT was calibrated with three different multi-objective calibration approaches. In the first case study, SWAT was applied to lysimeter data. With this computationally inexpensive example, we illustrated several important aspects of multi-objective calibration, such as noncommensurability of different error measures and the relevance of new types of data in constraining the model predictions. In the second case study, SWAT was calibrated to measured discharge from three subbasins of the Dill Catchment (Germany). This example shows how multi-objective calibration is used to determine whether or not one set of parameters can provide adequate simulations for all three subbasins. The overall aim of this study was to illustrate that multi-objective calibration is a powerful tool to provide insight in the results of automated model calibration, the complex interactions within a hydrological model, and the system under study.

The Multi-Objective Calibration Problem

There are three accepted methods to perform a multi-objective calibration in eco-hydrology. The most general method is based on Pareto optimality. Pareto optimality recognizes that, in general, the solution of a multi-objective problem will not be unique. Typically, the multi-objective problem will lead to different solutions that are all optimal for one objective function only. Moving from one solution to another will lead to an improvement of one objective function while causing deterioration in the value of at least one other objective function. This is graphically illustrated in Figure 1, where point A indicates the parameters that minimize objective function 2 and point B indicates the parameters that minimize objective function 1. The solution to the multi-objective problem consists of all points that fall on the line connecting A and B. Moving along this line from A to B results in smaller values of objective function 1 and larger values for objective function 2. It is not possible to decide objectively which of these solutions are the best, and such solutions are called non-dominated or Pareto solutions. For more information on Pareto optimality, the reader should refer to Gupta et al. (1998). Recently, Vrugt et al. (2003) have presented an effective and efficient algorithm (MOSCEM-UA) to find the Pareto solutions within a range defined by upper and lower values for each calibrated model parameter, the so-called parameter space.

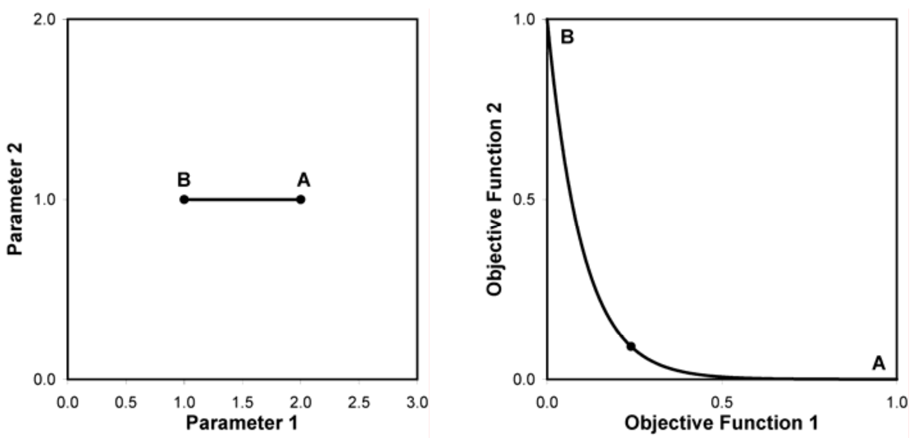

Figure 1. (after Yapo et al., 1998). Illustration of Pareto optimality.

The second method for multi-objective calibration is to aggregate the multiple objectives to a single objective and to optimize this aggregated objective function with a traditional optimization algorithm. The aggregation of the multiple objective functions requires the subjective choice of weighting factors for each objective functions. For example, the point in Figure 1 (right) shows the minimum value of an aggregated objective function where both objective functions are equally weighted. The new SWAT release allows multi-objective calibration based on one aggregated objective function according to the methods proposed by van Griensven and Bauwens (2003). They proposed a weighting scheme called the Global Optimization Criterion (GOC) that sums the position of each objective function in the respective cumulative probability density (Equation 1):

$$GOC_j = \sum_{i=1,m} f_i(OF_{i,j}) \qquad (1)$$

where f_i is a normalization function based on the normal or the lognormal distribution, j is the parameter set under consideration and m is the number of objective functions (OF). The mean and standard deviation of the objective functions required for the normalization function have to be obtained from a set of random draws from the user-defined parameter space.

The third method for multi-objective calibration is based on the philosophy that there are many model structures and many different parameters sets within a chosen model structure that provide an acceptable reproduction of the observed system behavior. This has been called the equifinality concept and the Generalized Likelihood Uncertainty Estimation (GLUE) methodology has been developed to deal with this phenomenon (Beven and Freer, 2001). In the GLUE methodology, random samples are drawn uniformly from a user-defined parameter space. A quantitative measure of performance is used to separate behavioral and non-behavioral parameters sets based on a subjective (but explicit) threshold. In the multi-objective version of the GLUE methodology, behavioral parameter sets have to pass a set of multiple thresholds.

Case Studies

Lysimeter Data

The lysimeter data are from the lysimeterstation Brandis, which is located approximately 15 km southeast from Leipzig, Germany at a altitude of 136 m a.s.l. We used the data from lysimeter group five, which consist of three undisturbed soil monoliths with an area of 1 m^2 and a depth of three m. The soil was classified as an eroded cambisol with a relatively high loam content of 30% in the upper soil layer and a high sand content (>90%) in the parent material below 0.35 cm. Monthly data for percolation, actual evapotranspiration (ET), and nitrate leaching were provided for the hydrological years 1981-1992. Information on daily precipitation, soil properties, and soil management (crop rotation, planting and harvest dates and fertilizer application amounts and timing) was also available.

Table 1. Prior parameter ranges used in the multi-objective calibration for the lysimeter data.

Model Parameter	Lower Limit	Upper Limit
*Bulk density (BD, g cm^{-3})	1.45	1.55
*Available water content (AWC, -)	0.16	0.19
*Saturated hydraulic conductivity (K_{sat}, mm hr^{-1})	0	750
*Moist soil albedo (ALB, -)	0.20	0.30
Maximum rooting depth (RD_{max}, mm)	500	2000
Soil evaporation compensation factor (ESCO, -)	0.1	1.0
Plant uptake compensation factor (EPCO, -)	0.0	1.0
Rate factor for humus mineralization (CMN, -)	0.00	0.01
Residue decomposition factor (RSDCO, -)	0.00	0.10
Maximum daily denitrification rate (MAX_WDN, kg ha^{-1} d^{-1})	0.0	0.3
Maximum daily nitrate uptake (MAX_NUP, kg ha^{-1} d^{-1})	0.0	10.0

For the multi-objective calibration with the lysimeter data, we used a slightly modified version of SWAT2000 with a single hydrological response unit. In the original SWAT2000 model, all excess water above field capacity drains with the velocity of the K_{sat}. The percolation measurements from the lysimeter (described later) showed that this concept overestimates the drainage velocity. Therefore, we introduced an exponential reduction of the K_{sat} as a function of the amount of water above field capacity to calculate the unsaturated hydraulic conductivity. Excess water above field capacity then drained with a velocity dependent on the amount of excess water present. This concept was also used in the SWAT99.2 version, but was removed in the SWAT2000 release. The second modification involved the introduction of two new model parameters limiting the maximum daily denitrification rate (MAX_WDN) and the maximum amount of daily plant nitrate uptake (MAX_NUP). The maximum rates for denitrification and plant uptake were introduced to provide a realistic upper limit on these fluxes. In the original SWAT2000 most of the nitrogen disappeared through denitrification, which caused high nitrogen stress for the plants and unrealistically high plant uptake immediately after fertilizer application. For more details on problems with the N cycling, refer to Pohlert et al. (2005).

The model parameters and the upper and lower boundaries used in the multi-objective calibration are provided in Table 1. The model parameters marked with an * in the table are parameters where the value of the upper soil layer were calibrated and the values for the other layers were adjusted in ratio with the upper soil layer (Eckhardt and Arnold, 2001). The calibration period was from 1981 to 1986 and the validation period was from 1987 to 1992.

We applied both the MOSCEM-UA and the GLUE methodology to the lysimeter data within a MATLAB environment. For the MOSCEM-UA algorithm we defined six objective functions: Nash-Sutcliffe (NS) index and bias for percolation, actual ET and nitrate leaching. In total, we performed 182,000 model runs with MOSCEM-UA. A multi-objective calibration based on an aggregated objective function was emulated with the results of the MOSCEM-UA algorithm. For the GLUE algorithm, we used the same six objective functions with the following thresholds: NS index for percolation and actual ET > 0.7, NS index for nitrate leaching > 0.6, bias lower than 50 mm in six years for percolation and actual ET, and a bias lower than 50 kg/ha in six years for nitrate leaching. The GLUE analysis was terminated when 97 behavioral model runs were found.

Dill Catchment

The Dill Catchment is a low mountainous catchment in Germany (Figure 2) with an area of 693 km^2. The catchment is covered by 30% deciduous forest, 25% coniferous forest, 30% pasture, 6% crop land and 9% urban area, as was determined from a composite of Landsat TM5-scenes from 1994 and 1995 (Nöhles, 2000). Soil data are available in a 1:50000 soil map (HLUG, 1998). For the SWAT simulations, the catchment was divided into 48 subbasins and 765 hydrological response units.

For the multi-objective calibration of the Dill Catchment, we used MOSCEM-UA coupled with a version of SWAT adapted to low mountainous regions in Germany (SWAT-G, Eckhardt et al., 2002). One of the main differences between SWAT-G and other versions of SWAT is that SWAT-G includes an anisotropy factor between vertical and horizontal saturated hydraulic conductivity to account for the strong tendency for lateral flow in this type of catchment. SWAT-G was calibrated to three hydrological years of daily discharge measurements (1983-1985) available for the gauging station at the catchment outlet and to three other stations draining subcatchments of the Dill: Aar (134 km^2), Dietzhölze (81 km^2) and Obere Dill (63 km^2). In the multi-objective calibration, we searched for the Pareto solutions for the sum of squared residuals (SSR) between measured and modeled discharge for the Dill Catchment and the three subcatchments.

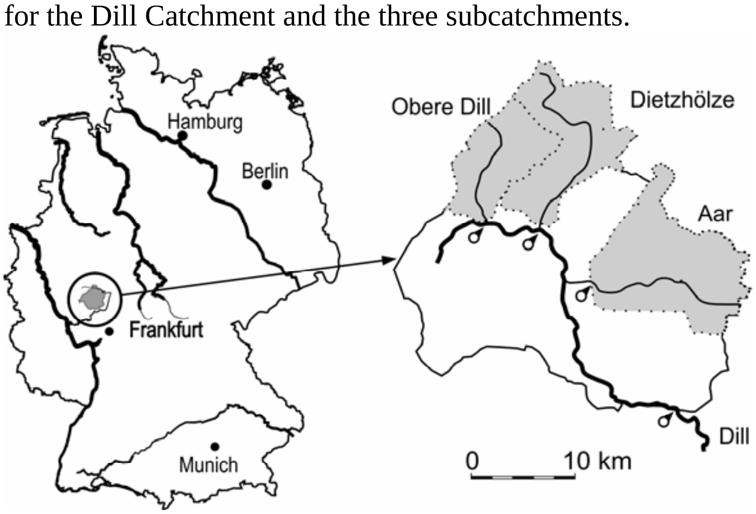

Figure 2. The Dill Catchment and the three subcatchments.

We included 11 model parameters in the multi-objective calibration of the Dill Catchment. The prior parameter ranges for the automatic calibration are given in Table 2 for each of the optimized parameters. The model parameters marked with an * in the table are parameters where the value of the upper soil layer of one particular soil were calibrated and the values for the other layers and other soils were adjusted according to the change ratio of the upper soil layer according to Eckhardt and Arnold (2001).

Table 2. Prior parameter ranges used in the multi-objective calibration of the Dill Catchment.

Model parameter	Lower Bound	Upper Bound
Surface runoff lag time (SURLAG, d)	1.000	5.000
Manning N surface runoff (OV_N, $m^{-1/3}s$)	0.200	0.500
Groundwater recession coefficient (ALPHA_BF, d^{-1})	0.030	0.060
Delay of groundwater recharge (GW_DELAY, d)	1.000	20.000
Deep aquifer percolation factor (RCHRG_DP, -)	0.000	0.800
*Bulk density soil (BD, gcm^{-3})	1.500	1.600
Bulk density bedrock (BD, gcm^{-3})	2.510	2.640
*Available water content (AWC, -)	0.160	0.200
*Saturated hydraulic conductivity Soil I (K_{sat}, mm h^{-1})	1.000	45.000
*Saturated hydraulic conductivity Soil II (K_{sat}, mm h^{-1})	45.000	85.000
*Anisotropy factor (ANISO, -)	2.000	8.000

Results and Discussion

Lysimeter Data

Figure 3 shows the Pareto front between the NS index and the model bias for both the percolation and the nitrate leaching at the bottom of the lysimeter. The figure clearly illustrates the trade-off between these two performance measures. Parameter sets with the highest NS index have a large bias. For both percolation and nitrate leaching, a small decrease in the NS index (~0.05 units) resulted in an enormous improvement in the model bias. This is due to the well-known fact that the NS index is most sensitive to peaks in the observations. Often, attempts to maximize the NS index (or to minimize a sum of squared residuals) overemphasize a correct simulation of the peaks at the cost of the model bias. Obviously, these results already make a good case for multi-objective calibration and provide a good argument against overambitious optimization of a single objective function without consideration of other performance measures.

Figure 4 shows Pareto fronts between NS indices for different combinations of percolation, actual ET and nitrate leaching. This figure shows that there are also strong trade-offs between the correct simulation of single output fluxes, similar to what was shown in Figure 3 for different performance measures and a single output flux. Again, a small decrease in the objective function of one output flux can lead to a strong improvement in another objective function. This is especially true for the Pareto fronts between the NS index of percolation and ET. The other Pareto fronts shown in Figure 4 seem to indicate a more gradual trade-off.

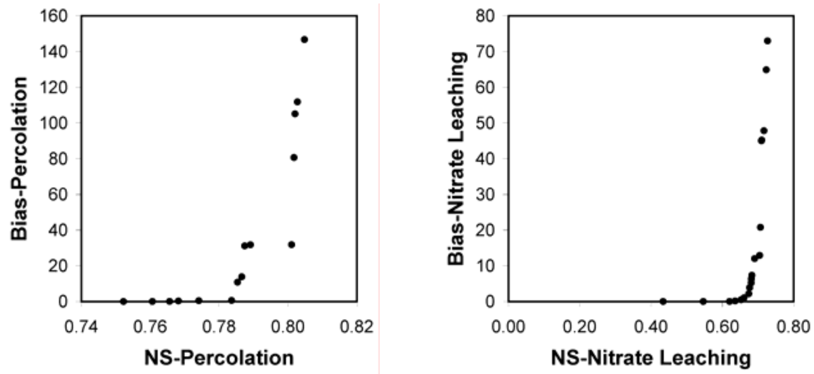

Figure 3. Pareto front of the NS index against bias for percolation (left) and nitrate leaching (right).

The Pareto fronts shown in Figure 4 can be further examined by taking a closer look at the parameters associated with the fronts. For example, in the case of the Pareto front between actual ET and N leaching, the simulations with the highest NS index for actual ET are associated with very low values of MAX_NUP. A strong limitation of the maximum nitrogen uptake will clearly lead to a low NS index for nitrate leaching because too much nitrate will be leached from the soil. The highest NS index for N leaching was achieved with a value of 0.27 kg N/ha for the maximum daily nitrate uptake. The gradual change in the Pareto front of ET against N leaching can, amongst other reasons, be explained by the compromise for the model parameter MAX_NUP. The low value of MAX_NUP for the highest NS index for ET indicates a problem with the evapotranspiration calculations. The model is trying to compensate for an overestimation of actual ET by reducing plant growth. This can be due to a problem with the input data or the inappropriateness of the Penman-Monteith model for this particular locality.

Figure 4 also shows the objective function values that would have been obtained with a multi-objective calibration based on a single aggregated objective function as defined in Equation 1. It should be noted that this is the approach that will be available in the new SWAT release. In two out of three cases, the aggregated objective function has resulted in a reasonable compromise between the two objective functions. Only in the case of percolation and ET does the aggregated objective function seem to result in an awkward compromise. This can be explained by the mean and standard deviations of the random model runs that define the cumulative probability density function required for normalization in Equation 1. Since ET is much more driven by the boundary conditions than the percolation, the initial standard deviation of the NS index is much smaller for ET than for percolation. This results in a high weight for percolation in the aggregated objective function. Nevertheless, aggregation of multiple objectives seems to be a simple method to avoid over-conditioning of the calibration on a single objective function. A further advantage of an aggregated objective function is that algorithms for global optimization of a single objective function are widely available and are usually more efficient than algorithms for multi-objective calibration.

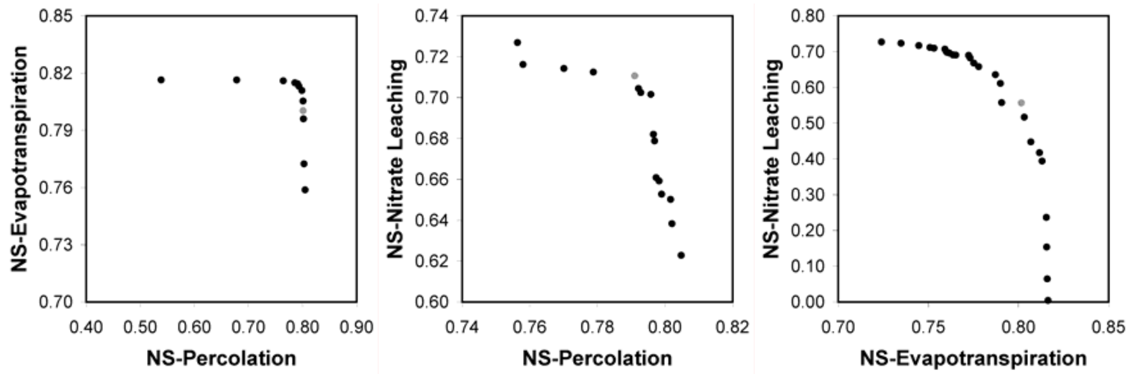

Figure 4. Pareto fronts of the NS index between different combinations of percolation, actual ET and nitrate leaching. Gray dots indicate optimal model runs for multi-objective calibration with an aggregated objective function according to equation 1.

Table 3 shows the number of behavioral model runs in the GLUE analysis after successively considering six objective functions. In total, 157,502 model runs were performed that resulted in 97 model runs that satisfied all six performance criteria. The percentages indicate that two performance criteria were particularly selective. First, Table 3 shows that only a small fraction of the model runs that have a NS index higher than 0.7 have a model bias lower than 50 mm over the entire calibration period. This corresponds well with the results of the analysis which also indicated a strong trade-off between a high NS index and a low model bias for percolation. Second, Table 3 shows that runs that provide behavioral model runs for percolation and actual ET do not necessarily provide behavioral model runs for nitrate leaching.

Table 3. Number of behavioral model runs in the GLUE analysis and the percentage of model runs retained after considering six successive performance criteria.

Total	Percolation (NS > 0.7)	Percolation (Bias < 50)	Actual ET (NS > 0.7)	Actual ET (Bias < 50)	N-leaching (NS > 0.7)	N-leaching (Bias < 50)
157502	78568	3145	2545	2048	157	97
	49.9%	4.0%	80.9%	80.5%	7.7%	61.8%

Figure 5 shows the uncertainty bounds derived with the GLUE methodology after calibration with six objective functions. Although the dynamics of all three variables are adequately modeled with SWAT, there are still a considerable number of measurements that fall outside of the uncertainty bounds, especially for the actual ET. This must be attributed to either model structural uncertainty (error) or input data uncertainty. One might also argue that the thresholds that separate the behavioral from the non-behavioral model runs were set too ambitiously. Assuming a lower threshold will result in wider uncertainty bounds; however, in this case that will not cause the bounds to bracket the measurements, since it was mostly the peaks that were not adequately modeled.

Figure 6 shows the effect of including extra information in the calibration on the uncertainty bounds. In the left panel, the uncertainty bounds after calibration on percolation data and the uncertainty bounds after considering all three output fluxes are compared. Clearly, the uncertainty bounds for percolation are not strongly influenced by the addition of extra information in the calibration. This indicates that SWAT does not have a strong feedback between the N cycling and the water cycling. Apparently, it is possible to accurately simulate water flow without a correct representation of the nitrogen cycle. This is also apparent from the right panel, which shows that there was a wide range of simulated values before calibration to the nitrate leaching data (gray area). Only after consideration of the nitrate leaching data were the parameters related to nitrogen fluxes somewhat constrained (especially the maximum daily rate of denitrification). The middle panel of Figure 6 shows the uncertainty bounds before and after calibration on actual ET data. It can be seen that the uncertainty was not strongly reduced after including actual ET data. Apparently, the model predictions were already strongly constrained after calibration to the percolation, although the dominance of the boundary conditions compared to the influence of the model parameters will certainly be important as well.

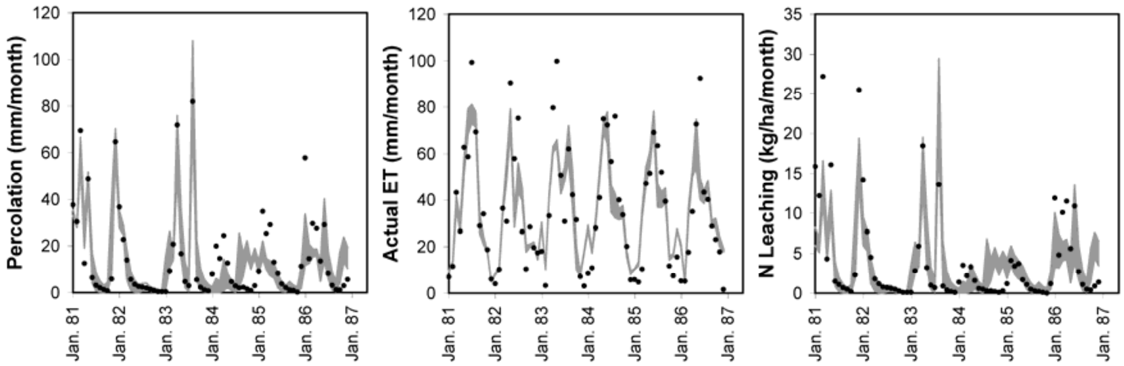

Figure 5. Uncertainty bounds derived with the GLUE methodology after considering six objective functions.

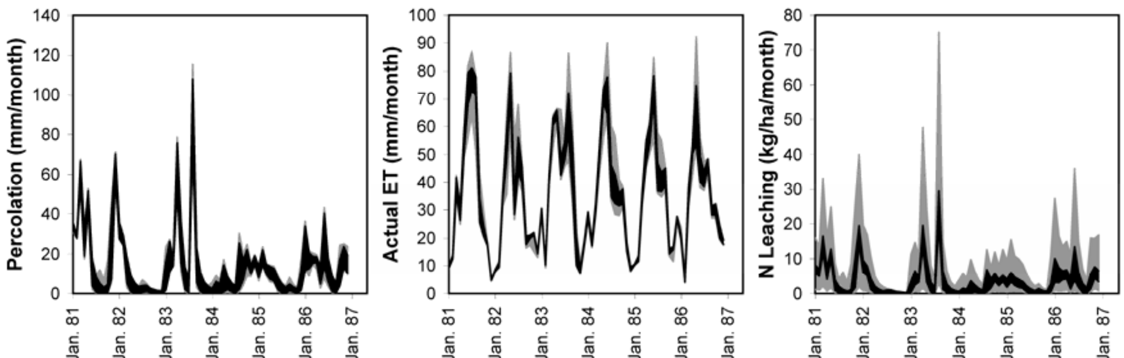

Figure 6. Uncertainty bounds derived with the GLUE methodology. (left) uncertainty bounds after calibration on percolation (gray) and all three fluxes (black). (middle) uncertainty bounds after calibration on percolation (gray) and percolation and actual ET (black). (right) uncertainty bounds after calibration on percolation and actual ET (gray) and all three fluxes (black).

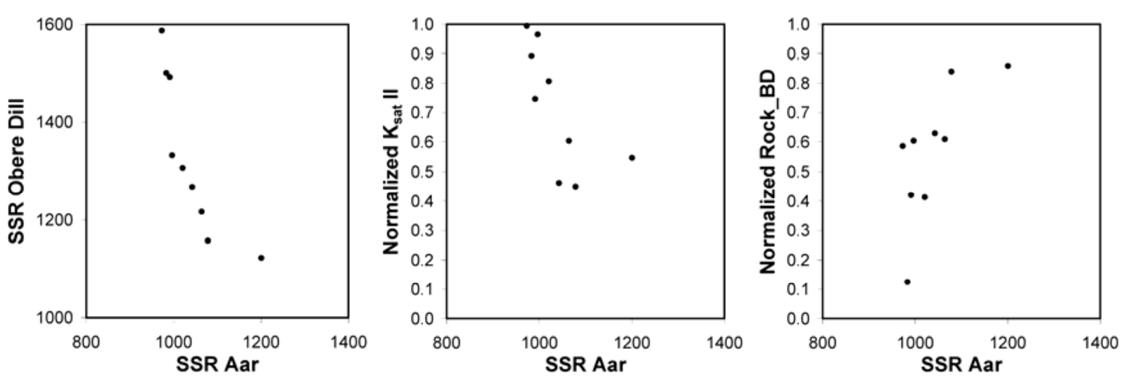

Figure 7. (left) Pareto front between sum of squared residuals of the Aar catchment and the Obere Dill catchment. (middle and right) Scatter plots of sum of squared residuals and model parameters that seem to be different for the two subcatchments.

Dill Catchment

Figure 7 shows the results of the multi-objective calibration on the Dill Catchment. This preliminary analysis was based on only 3,000 model simulations, which means that some of the Pareto fronts have not yet been sampled adequately by the MOSCEM-UA algorithm. However, for some objective functions, relationships were already obvious. The left panel of Figure 7 shows the trade-off between the sum of squared residuals of the Aar Catchment and the Obere Dill Catchment. Clearly, a minimization of the objective function for the Aar Catchment will lead to a strong reduction in the quality of the simulations for the Obere Dill. The scatter plots in the middle and right panel of Figure 7 point at the reasons for the strong trade-off. The parameter sets from the Pareto front with a high normalized saturated hydraulic conductivity (K_{sat}) for soil type II tend to perform well in the Aar Catchment, whereas the simulations seem to be better for the Obere Dill when the normalized K_{sat} for soil type II was lower. The reverse seems to be true for the normalized bulk density of the bedrock layer, where low values provide better simulations in the Aar Catchment and high values provide better simulations in the Obere Dill. This analysis will be extended once more model runs have been completed. The results will be compared to the results of the proxy-catchment test, and the multi-objective calibration based on an aggregated objective function that was presented by Huisman et al. (2003).

Conclusions

We have presented two case studies where we applied three different methods for multi-objective calibration. We hope that the examples convinced the reader that multi-objective calibration is a necessity for good automated model calibration. The multi-objective calibration method based on the aggregation of multiple objectives in a single value, which is implemented in the next release of SWAT, provided a good, but subjective, compromise between the different objective functions.

Acknowledgements

This study has been supported by the Deutsche Forschungsgemeinschaft within the scope of the Collaborative Research Center (SFB) 299.

References

Beven, K. and J. Freer. 2001. Equifinality, data assimilation, and uncertainty estimation in mechanistic modeling of complex environmental systems using the GLUE methodology. Journal of Hydrology, 249, 11-29.

Duan, Q., V.K. Gupta and S. Sorooshian. 1993. A shuffled complex evolution approach for effective and efficient global optimization for conceptual rainfall-runoff models. Water Resources Research, 28(4), 1015-1031.

Eckhardt, K., J.G. Arnold. 2001. Automatic calibration of a distributed catchment model. Journal of Hydrology, 251, 103-109.

Eckhardt, K., S. Haverkamp, N. Fohrer, and H.-G. Frede. 2002. SWAT-G, a version of SWAT 99.2 modified for application to low mountain range catchments. *Physics and Chemistry of the Earth* 27, 641-644.

Gupta, H.V, S. Sorooshian and P.O. Yapo. 1998. Toward improved calibration of hydrologic models: multiple and noncommensurable measures of information. Water Resources Research 35(4), 751-763.

HLUG (Hessisches Landesamt für Umwelt und Geologie). 2002. Digital soil map 1:50000.

Huisman, J.A., L. Breuer, K. Eckhardt and H.G. Frede. 2003. Spatial consistency of automatically calibrated SWAT simulations in the Dill catchment and three of its sub-catchments. Proceedings of the second international SWAT conference, Bari, Italy, 78-81.

Kuzcera, G. and E. Parent. 1998. Monte Carlo assessment of parameter uncertainty in conceptual catchment models: the Metropolis algorithm. Journal of Hydrology, 211, 69-85.

Nöhles, I. 2000. Landnutzungsklassifikation mit multitemporalen Landsat TM-Szenen in einer kleinstrukturierten Agrarregion. PhD-thesis Justus-Liebig Universität Giessen, Germany (in German).

Pohlert, T., J.A. Huisman, L. Breuer and H.-G. Frede. 2005. Evaluation of the soil nitrogen balance model in SWAT with lysimeter data. This conference.

Van Griensven, A., and W. Bauwens. 2003. Multiobjective autocalibration for semidistributed water quality models. Water Resources Research, 39(12), 1348.

Vrugt, J.A., H.V. Gupta, W. Bouten and S. Sorooshian. 2003. A shuffled complex evolution Metropolis algorithm for optimization and uncertainty assessment of hydrologic model parameters. Water Resources Research, 39, 1201.

Vrugt, J.A., H.V. Gupta, L.A. Bastidas, W. Bouten and S. Sorooshian. 2003. Effective and efficient algorithm for multi-objective optimization of hydrologic models. Water Resources Research, 39(8), 1214.

Yapo, P.O., H.V. Gupta and S. Sorooshian. 1998. Multi-objective global optimization for hydrologic models. Journal of Hydrology 204, 83-97.

Comparison of Optimization Algorithms for the Automatic Calibration of SWAT2000

Bryan A. Tolson[1] and Christine A. Shoemaker[2]
[1]Assistant Professor, Department of Civil Engineering, University of Waterloo, 200 University Ave. West, Waterloo, Ontario, Canada, N2L 3G1. Email: btolson@uwaterloo.ca.
[2]Professor, School of Civil and Environmental Engineering, Cornell University.

Abstract

This study compares multiple optimization algorithms for the automatic calibration of the SWAT2000 model. The optimization algorithms considered were the Shuffled Complex Evolution (SCE), real-valued simple Genetic Algorithm (GA), multi-start Simplex algorithm, and Monte Carlo Sampling (MCS) algorithms. In addition, a new algorithm, developed by the authors, called the Global Greedy Search (GGS) algorithm was compared to the popular SCE algorithm. Algorithms were compared for a six and 14 dimensional calibration problem of a simple synthetic SWAT2000 model. Since any modeller that downloads SWAT2000 can easily replicate these two calibration problems, they form two benchmark calibration test problems for consistent testing of calibration algorithms applied to SWAT2000. Unlike most previous studies, all algorithms here were compared so that speed of convergence to their final best solutions was clearly presented. This comparison methodology generalizes performance comparison results so that modellers across a wide range of case studies (i.e. varying model sizes and computational constraints) can interpret the results that are most relevant to their case study. As shown in the majority of previous studies, the SCE algorithm outperforms the Simplex, GA, and MCS algorithms. However, the new GGS algorithm was demonstrated to find comparable or better final solutions than SCE, and GGS found good calibration solutions substantially faster than SCE.

Introduction

Automatic calibration is defined here as an optimization algorithm-based search for a set of environmental simulation model parameter values that result in model predictions which best match the available measured data for the system being modelled. The development of automatic calibration methods for watershed models like SWAT has been an important advancement in environmental simulation modelling and studies have shown the benefits of automatic calibration in terms of saving human time (Ajami et al., 2004). Relatively fewer studies, however, demonstrate that superior modeling results (i.e. predictive accuracy) are achieved through automatic calibration in comparison to the more traditional watershed model calibration approach of manual trial-and-error calibration. Perhaps for this reason, manual calibration remains an acceptable method for model calibration and is often combined with automatic calibration optimization algorithms (Hogue et al., 2000). More importantly, the continued persistence of manual calibration is an implicit reminder that model calibration is mainly about finding good solutions (parameter sets) rather than the absolute best mathematical fit to the measured data (i.e. the optimal solution).

Previous automatic calibration studies do not commonly assess how quickly, in terms of the number of function or model evaluations, the optimization algorithms approach their final best solution. For example, in the seminal papers for the SCE algorithm (Duan et al., 1993; Duan et al., 1992), only the final algorithm solutions after convergence were assessed as to whether they had identified the known globally optimal solutions. Other automatic calibration comparison studies show a similar focus on final algorithm solutions and do not report results before the final best solutions are identified (Franchini et al., 1998; Gan and Biftu, 1996). There are two major problems with such an approach. First, other modellers subject to more restrictive case study specific computational constraints (i.e. fewer available model evaluations) are not presented with comparisons relevant to their case study. Secondly, the ability of algorithms to find good calibration solutions quickly is not assessed. Admittedly, the description 'good solutions' is rather vague but is roughly defined here to be the level of model performance that a typical modeller performing a manual calibration would deem acceptable and thus cease the manual calibration efforts. We believe that human and/or computer-modelling time is better directed to additional analyses (i.e. uncertainty analysis) after finding good calibration solutions, rather than searching for that final improvement in the third decimal place of the coefficient of determination. In this study, we present algorithm performance results in ways that provide more complete information to modellers selecting an optimization algorithm for their case study.

Many benchmark test functions are easily programmed and widely used in the literature to compare optimization algorithm performance (e.g. the Griewank, Hartman, and Rosenbrock functions, etc.). Although there are abundant studies comparing optimization algorithms for automatic calibration of watershed models, replicating these case studies (i.e. the model and specific case study inputs) so that new optimization algorithms can be compared to old results can be time consuming and often impossible without the assistance of the original researchers who defined the case study. Therefore, another purpose of this study is to introduce two SWAT2000 model calibration case studies that are easily replicated so that optimization algorithm results can be compared between independently conducted studies with confidence.

The next section of this paper describes benchmark optimization problems. Additional details for problem replication are in the Appendix. In the Results and Discussion section, we demonstrate simple methods for presenting automatic calibration algorithm comparison results that thoroughly summarize multiple aspects of algorithm performance. Results show that although the SCE algorithm is better than most other algorithms, a newer algorithm developed by the authors, called the Global Greedy Search (GGS) algorithm, performs nearly as well or better than SCE.

Methodology

Case Study

This case study uses the readily available Lakefork SWAT2000 example model that is available in the AVSWAT2000 GIS Interface download (DiLuzio et al., 2001). The Lakefork model case study can be recreated by following the explicit steps in the Appendix that refers to Chapter 15 of DiLuzio et al. (2001). This benchmark case study was defined so that SWAT2000 executed quickly and minimal deviations from the AVSWAT2000 example model data set were necessary. As a result, the two synthetic test problems defined for this case study are more of a curve-fitting exercise and do not represent all aspects or considerations in a real calibration problem. Nonetheless, the test problems are relevant insofar as a good automatic calibration approach requires an effective curve-fitting optimization algorithm. Future work is needed to produce a real calibration case benchmark study.

Two calibration test problems were defined and both calibrate to two years of synthetically generated monthly outputs at the watershed outlet. The default values of the parameters assigned by AVSWAT2000 (except for the change to PHU inputs listed in the Appendix) were the optimal solution for both test problems and the synthetic 'measured' data was created by simulating the model once under these default inputs. The synthetic measured data time series were recorded with four significant figures, which is how outputs are printed in SWAT2000. The upper and lower bounds of the parameter values were assigned based on the SWAT2000 user manual (Neitsch et al., 2001), the UTIL program, or the ranges of inputs listed in the crop database. In addition, lower bounds were never allowed to be zero since for some parameters, zero causes the default value for some parameters to be used. The original SWAT2000.exe file was used to run the model and all parameter modifications and model output synthesis were coded in Matlab© to operate on the SWAT input and output files.

Problem 1. This is a six-dimensional flow calibration problem where the calibration parameters for this problem (see Table 1) were selected so that minimal coding was required to modify the SWAT model parameters (i.e. free format input and/or one file location of parameter input). This problem is not necessarily a reflection of the six most important parameters in SWAT. The objective for this problem was to minimize the sum of squared errors (SSE) for the monthly outlet flows (a global minimum of 0.000).

Problem 2. This is a 14-dimensional simultaneous flow and sediment calibration problem. Calibration parameter ranges and optimal values for this problem are given in Table 2. Although more typical calibration parameters were considered in this problem, modifying some of these 14 parameters in the input files was not as straightforward as in Problem 1. Therefore, when replicating this study, the coding to change some of the parameters should be tested to ensure that after multiple parameter modifications, the model predictions at the optimal solution always result in the output values listed in the Appendix. In order to weight the flow and sediment calibration equally, the objective for this problem was to maximize the sum of the Nash-Suttcliffe coefficients (Nash and Suttcliffe, 1970) for monthly flow and sediment at the watershed outlet (a global maximum of 2.000).

Table 1. Ranges and optimal values of SWAT2000 calibration parameters in test Problem 1.

Short Parameter Name (input file), Long Parameter Name	Lower Bound	Upper Bound	Value at Optimal Solution
SMTMP (.bsn), Snow melt base temperature (ºC)	-5.0	5.0	1.0
SURLAG (.bsn), Surface runoff lag coefficient	1.0	24.0	4.0
GW_DELAY (.gw), Groundwater delay time (days)	0.001	500.0	31.0
ALPHA_BF (.gw), Baseflow alpha factor (days)	0.001	1.0	0.0048
BIO_E (crop.dat), Radiation-use efficiency ((kg/ha)/(MJ/m2))	25.0	40.0	35.0
BLAI (crop.dat), Maximum potential leaf area index	3.0	6.0	4.0

Table 2. Ranges and optimal values of SWAT2000 calibration parameters in test Problem 2.

Short Parameter Name (input file), Long Parameter Name	Lower Bound	Upper Bound	Value at Optimal Solution
TIMP (.bsn), Snow pack temperature lag factor	0.01	1.0	1.0
SURLAG (.bsn), Surface runoff lag coefficient	1.0	24.0	4.0
APM (.bsn), Peak rate factor for subbasin sediment routing	0.5	1.5	1.0
PRF (.bsn), Peak rate factor for main channel sediment routing	0.5	1.5	1.0

SPCON (.bsn), Linear channel sediment reentrainment factor	0.0001	0.01	0.001
SPEXP (.bsn), Exponent channel sediment reentrainment factor	1.0	2.0	1.5
GW_DELAY (.gw), Groundwater delay time (days)	0.001	500.0	31.0
ALPHA_BF (.gw), Baseflow alpha factor (days)	0.001	1.0	0.048
BIOMIX (.mgt) ^{A}, Biological mixing efficiency	0.1	0.4	0.2
CN2 (.mgt) ^{A}, SCS runoff curve number for moisture condition II	79.0	90.0	84.0
AWC_f (.sol) $^{A \& B}$, Available water capacity *factor*	0.5	1.5	1.0
SOL_K_f (.sol) $^{A \& C}$, Saturated hydraulic conductivity	0.5	1.5	1.0
T_OPT (crop.dat), Optimal temperature for plant growth (ºC)	20.0	30.0	25.0
T_BASE (crop.dat), Minimum temperature for plant growth (ºC)	8.0	13.0	12.0

A) Only values in subbasins (or HRUs) 1-13 were calibrated.
B) The base or default values for AWC were multiplied by the calibration factors (AWC_f) to arrive at the .sol input file values. Base AWC values as fractions for HRUs 1-5, 7, 9 and 10 by soil layers (1-5) were [0.12 0.10 0.09 0.16 0.11] and base AWC values for HRUs 6, 8, and 11-13 by soil layers (1-4) were [0.12 0.12 0.14 0.11].
C) The base or default values for SOL_K were multiplied by the calibration factors (SOL_K_f) to arrive at the .sol input file values. Base SOL_K values in mm/hr for HRUs 1-5, 7, 9 and 10 by soil layers (1-5) were [91.00 0.89 0.91 1.70 0.50] and base SOL_K values for HRUs 6, 8, and 11-13 by soil layers (1-4) were [91.00 0.13 1.00 12.00].

Optimization Algorithms

All algorithms used in this study were coded in Matlab and compared to default or recommended algorithm parameter settings. For fair and consistent algorithm comparisons, no attempts were made to optimize algorithm parameters for application to this case study. A maximum of 2,500 SWAT model evaluations were used to solve Formulation 1 while a maximum of 6,000 were used for Formulation 2.

The Monte Carlo Sampling (MCS) algorithm is a uniform random sampling algorithm and was applied to help assess the difficulty of the test problems. MCS was only stopped when the maximum iteration (model evaluation) limit was reached. The multi-start Simplex algorithm was based on restarting the Simplex algorithm available in the Matlab (R13) optimization toolbox (*fminsearch* function). In each optimization trial with multiple restarts, once a Simplex algorithm run stopped after converging, another Simplex run was started at a randomly selected initial solution. This was repeated until it was clear that restarting the Simplex would not improve the current best solutions. A penalty function approach was used to incorporate the SWAT parameter bound constraints. The multi-start Simplex was applied to determine if the test problems were highly non-convex with many local optimums.

A simple real-valued Genetic Algorithm (GA) was also tested in this study. The GA used binary tournament selection, single point crossover with two children produced per pair of parents, a simple normal random variable mutation operator and elitism. Based on previous experience with this GA, the probability of crossover was set at 1.0, the probability of mutation for each decision variable value was 0.04 and the normal random variable for mutation added to the current decision variable value had a standard deviation equal to 20% of the decision variable range. The population size and maximum generation limit were set to 26 and 96, respectively, for Problem 1 and 50 and 200, respectively, for Problem 2. A population of 26 was selected for Problem 1 simply to match the population size used by the SCE algorithm in Problem 1.

The Shuffled Complex Evolution (SCE-UA) algorithm by Duan et al. (1992) was recoded in Matlab and used in this study because it has been demonstrated to be effective relative to many other optimization algorithms. The Matlab SCE algorithm was tested against the Fortran version of SCE (version 2.2) for consistency on multiple test functions, and was found to produce average results that were extremely similar. The only difference between the Matlab and Fortran SCE versions was that the Matlab SCE implementation only stops the SCE algorithm when the maximum iteration limit is reached. SCE default algorithm inputs were used here. Based on recommendations in Duan et al. (1994), the default number of SCE complexes was determined to be two for Problem 1 (6 dimensions) and four for Problem 2 (14 dimensions).

The Global Greedy Search (GGS) algorithm is a single parameter optimization algorithm developed by Tolson (2005). GGS is a greedy search algorithm and is not population based. Neighbouring solutions are sampled at random and the size of the neighbourhood varies dynamically with the number of objective function evaluations. The GGS neighbourhood size parameter was set to the default value of 0.2 for all optimization trials. Full algorithm details were presented at the conference presentation and will be available in a pending journal paper.

Results and Discussion

Algorithm performance results for each problem were compared with two types of plots. The first type shows algorithm convergence behaviour and plots the average best solution found versus the number of model evaluations. The average was measured across the optimization trials (30) and computed at all numbers of model evaluations (e.g. 2,500 times for Problem 1 and 6,000 for Problem 2) for all algorithms except the Simplex. Simplex results by model evaluation were not available and therefore could only be presented at the end of each restart (i.e. the average objective function value versus the average number of model evaluations). The second type of plot summarizes the set of best final solutions found by each algorithm using an empirical cumulative distribution function (CDF) with a plotting position of i/(n+1) where i is the rank and n is the number of optimization trials. Each empirical CDF curve shows the probability that the algorithm will find an equal or better objective function value.

Problem 1

For Problem 1, 30 optimization trials were performed, each trial consisting of a maximum of 2,500 SWAT model evaluations. The Simplex and GGS algorithms were initialized to the same set of 30 uniform random initial solutions. The GA and SCE were initialized to the same 30 initial uniform random population sets.

Figure 1 shows the average convergence behaviour of each algorithm. As expected, MCS performed the worst of all five algorithms. The Simplex algorithm was restarted five times and repeatedly converged to non-optimal solutions. Restarting the Simplex until the maximum of 2,500 model evaluations would not have significantly improved Simplex results. The dashed lines between the six points on the Simplex curve are linear interpolations. Clearly, this problem is not convex and has many local minima and therefore should be solved with more effective global optimization algorithms. SCE and GA results in Figure 1 are only shown after 26 model evaluations (initial populations evaluated). SCE clearly outperforms the GA and the Simplex for any number of model evaluations. However, the new GGS algorithm clearly outperforms the SCE algorithm for any number of model evaluations. An SSE of 1.0 in Problem 1 corresponds to a Nash-Suttcliffe coefficient (E_{NS}) of 0.999. Therefore, the term ‘outperforms’ refers to the mathematical rather than practical calibration result.

The empirical CDFs for the five algorithms are given in Figure 2. The CDF for each algorithm demonstrates the range of objective function values (SSE) found (i.e. clearly shows the maximum and minimum SSE values). For a given SSE value, the algorithm with the highest CDF value performs best. The MCS algorithm is stochastically dominated by the Simplex algorithm (as well as the other three algorithms) because for any SSE value, say SSE*, the Simplex algorithm has a higher probability of finding an SSE that is equal to or better (lower in this case) than SSE*. The GA, SCE and GGS algorithms stochastically dominate the Simplex algorithm. The SCE and GGS algorithms stochastically dominate the GA. Since the GGS and SCE CDFs intersect in Figure 2, neither algorithm dominates the other. The near vertical line between SSE values of 1.E-02 and 1.E-01 for SCE shows that SCE converges early to similar objective function values. In comparison, GGS does not have trouble surpassing this SCE objective function threshold value. Only the SCE algorithm found solutions with SSE less than 1.E-04 (five solutions).

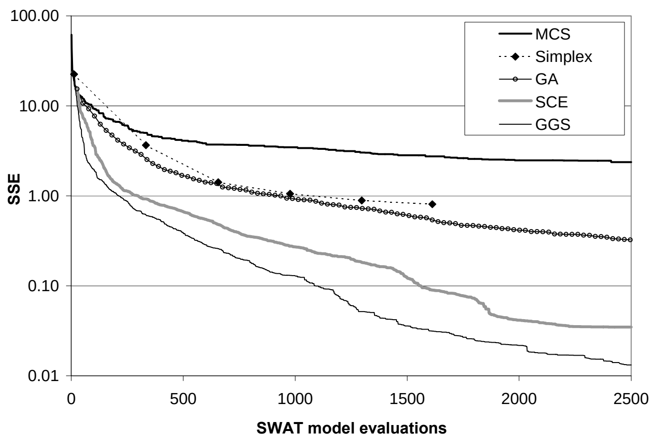

Figure 1. Comparison of algorithm performance for Problem 1. Average Sums of Squared Errors (SSE) over all optimization trials as a function of model evaluations.

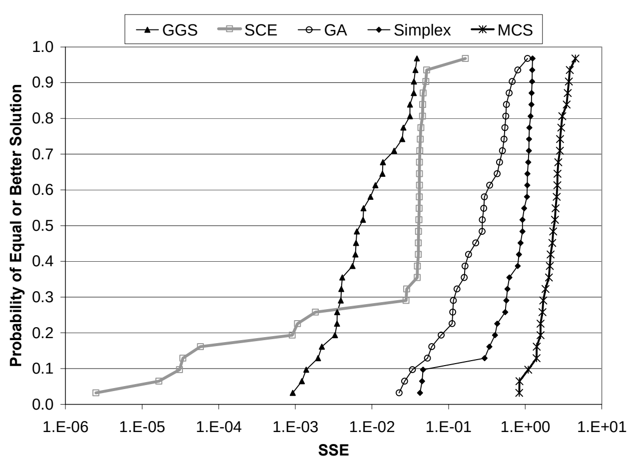

Figure 2. Empirical cumulative distribution function (CDF) for best solutions to Problem 1 (at the maximum number of model evaluations).

Problem 2

For Problem 2, 30 optimization trials were performed with each consisting of a maximum of 6,000 SWAT model evaluations. The Simplex and GGS algorithms were initialized to the same set of 30 uniform random initial solutions. The GA and SCE had different population sizes and were therefore initialized to different uniform random population sets.

Figure 3 compares the average convergence behaviour of all five algorithms. Results are very similar to Problem 1 in terms of algorithm ranking. MCS is the worst algorithm, followed by the Simplex and the GA. As in Problem 1, the Simplex in Problem 2 was only restarted five times since it was apparent that further improvements in the objective function were not likely. After 6,000 model evaluations, SCE produced the highest average objective function value (1.998) while GGS was very close behind with an average of 1.997. However, for any fewer than 2,500 model evaluations, GGS performed substantially better than SCE (i.e. by up to 0.03 or 0.04 objective function units).

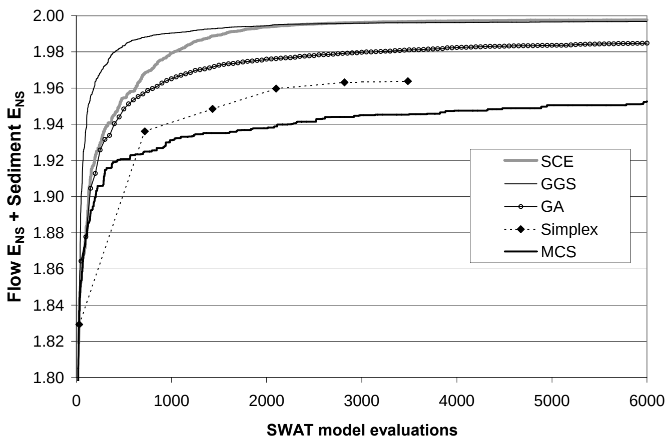

Figure 3. Comparison of algorithm performance for Problem 2. Average objective function value (Flow E_{NS} + Sediment E_{NS}) over all optimization trials as a function of model evaluations.

The empirical CDFs for the five algorithms are given in Figure 4. Figure 4A shows only the MCS, Simplex, GA and SCE algorithm CDFs while Figure 4B shows the GGS and SCE CDFs. As in Problem 1, SCE stochastically dominates the GA, Simplex and MCS algorithms. Figure 4B shows that SCE more reliably finds objective function values greater than 1.996 in comparison to GGS. However, only the GGS algorithm found solutions better than 1.999.

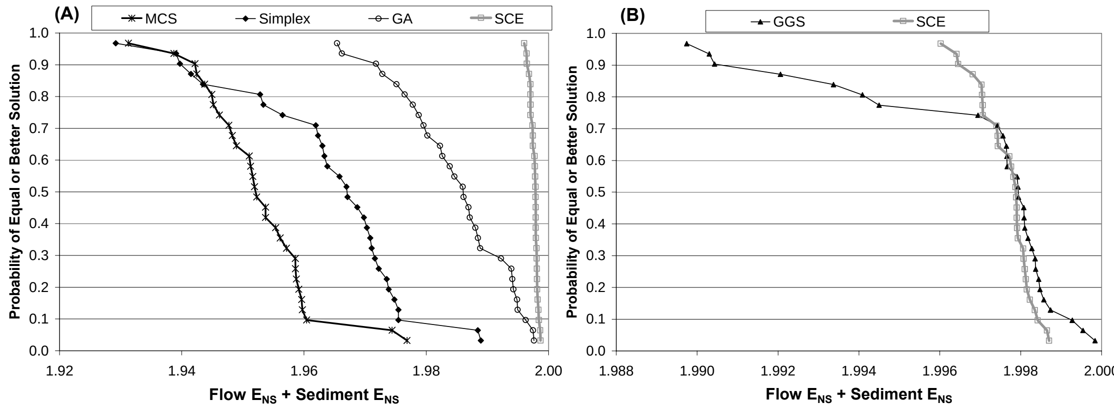

Figure 4. Empirical cumulative distribution function (CDF) for best solutions to Problem 2 (at maximum number of model evaluations).

Discussion

Presenting automatic calibration algorithm performance comparisons using the convergence and CDF plots demonstrated in Figures 1 through 4 provides general information that can be interpreted by future modellers to determine the algorithm that appears best suited to their case study. Convergence plots like Figures 1 and 3 allow modellers to interpret results at the computational scale that is feasible for their case study. CDF plots like Figures 2 and 4 allow modellers to make even more informed decisions based on their specific objective function value targets.

For example, if a SWAT modeller was constrained to less than 2,500 model evaluations for a calibration problem with about 14 parameters, based on Figure 3, they would select the GGS algorithm for their automatic calibration. However, if the same modeller was not constrained by time and wanted to find the best possible solution (i.e. the 0.001 difference in average GGS and SCE objective function values at 6,000 function evaluations in Figure 3 was judged to be practically significant), then based only on Figure 3, the modeller would select the SCE algorithm for automatic calibration. Figure 4B presents results in a way that enables more informed decision-making for this same modeller. For example, if the modeller considered that any calibration yielding an objective function > 1.996 was calibrated adequately for all practical purposes, then that modeller would definitely want to use SCE because only SCE always achieved solutions > 1.996.

We believe the GGS algorithm is a promising alternative to SCE for automatic calibration. When GGS is observed to be better than SCE, the difference in performance is quite significant (See Figures 1 and 3), however, when SCE is better than GGS (as after 6,000 model evaluations in Figure 3), the difference is not significant from a more practical calibration perspective. We have observed extremely similar results for multiple real calibration case studies and multiple optimization test functions of various dimensions. Additional results presented at the conference show that for the Cannonsville Watershed SWAT2000 case study (Tolson and Shoemaker, 2004), which is a real calibration study; the GGS algorithm performs significantly better than the SCE algorithm.

Conclusions

This paper demonstrates two simple ways of graphically comparing algorithm performance. These comparisons generalize results so that modellers across a wide range of case studies (i.e. varying model sizes and computational constraints) can interpret the results that are most relevant to their case study and their calibration goals. In comparison to the popular SCE algorithm, the GGS algorithm was demonstrated to be an attractive alternative optimization algorithm for automatic calibration. In addition to the comparable or better algorithm performance results, GGS is much simpler and thus easier to code than SCE. Furthermore, unlike SCE, the only GGS algorithm parameter does not have to be modified as the dimension of the problem changes. Overall, the much quicker convergence of GGS to good calibration solutions in comparison to SCE demonstrates that GGS will be more effective than SCE for case studies where time and/or computational resources are limited and the SCE algorithm is not allowed to run to convergence.

We hope that in the future, additional real SWAT calibration studies (i.e. with actual measured calibration data) will be available as automatic calibration benchmarks. Synthetic test calibration problems do not, by themselves, form an adequate test problem suite in which to compare various optimization algorithms for automatic calibration. We believe it is important that this model benchmarking is extended to SWAT sensitivity and uncertainty studies. Although the results and methodology in this study are particularly relevant to the SWAT model, they are also just as relevant to the calibration of any mathematical simulation model.

References

Ajami, N.K., Gupta, H., Wagener, T. and Sorooshian, S., 2004. Calibration of a semi-distributed hydrologic model for streamflow estimation along a river system. Journal of Hydrology, 298: 112-135.

DiLuzio, M., Srinivasan, R. and Arnold, J.G., 2001. Arcview Interface for SWAT2000 User's Guide, US Department of Agriculture - Agricultural Research Service, Temple, Texas.

Duan, Q.Y., Gupta, V.K. and Sorooshian, S., 1993. Shuffled Complex Evolution Approach For Effective And Efficient Global Minimization. Journal Of Optimization Theory And Applications, 76(3): 501-521.

Duan, Q.Y., Sorooshian, S. and Gupta, V., 1992. Effective And Efficient Global Optimization For Conceptual Rainfall-Runoff Models. Water Resources Research, 28(4): 1015-1031.

Duan, Q.Y., Sorooshian, S. and Gupta, V.K., 1994. Optimal Use Of The SCE-UA Global Optimization Method For Calibrating Watershed Models. Journal Of Hydrology, 158(3-4): 265-284.

Franchini, M., Galeati, G. and Berra, S., 1998. Global optimization techniques for the calibration of conceptual rainfall-runoff models. Hydrological Sciences Journal-Journal Des Sciences Hydrologiques, 43(3): 443-458.

Gan, T.Y. and Biftu, G.F., 1996. Automatic calibration of conceptual rainfall-runoff models: Optimization algorithms, catchment conditions, and model structure. Water Resources Research, 32(12): 3513-3524.

Hogue, T.S., Sorooshian, S., Gupta, H., Holz, A. and Braatz, D., 2000. A multistep automatic calibration scheme for river forecasting models. Journal Of Hydrometeorology, 1(6): 524-542.

Nash, J.E. and Suttcliffe, J.V., 1970. River flow forecasting through conceptual models, Part I. A discussion of principles. Journal of Hydrology, 10(3): 282-290.

Neitsch, S.L., Arnold, J.G., Kiniry, J.R. and Williams, J.R., 2001. Soil and Water Assessment Tool User's Manual Version 2000: Draft-April 2001, US Department of Agriculture - Agricultural Research Service, Temple, Texas.

Tolson, B. A. (2005). "Automatic calibration, management and uncertainty analysis: phosphorus transport in the Cannonsville Watershed." PhD Dissertation, School of Civil

and Environmental Engineering, Cornell University, Ithaca, NY. 227 pp.
Tolson, B. A. and Shoemaker, C. A. (2004). Watershed modeling of the Cannonsville Basin using SWAT2000: Model development, calibration and validation for the prediction of flow, sediment and phosphorus transport to the Cannonsville Reservoir. Version 1.0. Technical Report, School of Civil and Environmental Engineering, Cornell University. 159 pp. http://techreports.library.cornell.edu:8081/Dienst/UI/1.0/Display/cul.wat/2004-2.

Appendix

The following steps detail how to recreate the base SWAT2000 input files so that the exact calibration case studies can be replicated in order to reliably compare additional algorithm performance.

1. Download the 3/11/2002 version of the AVSWAT2000 interface from the SWAT website. Note that the previous version will not produce the exact same case study input files.
2. Install the AVSWAT2000 interface.
3. Go to chapter 15 in the interface manual and create the example Lakefork model (based on instructions in Section 15.1.1 through 15.1.6). In addition, do the following:
    a) Skip steps 18 and 19 in Section 15.1.1 (do not add manual subbasin outlets).
    b) After running SWAT (section 15.1.6), modify the PHU inputs as follows:
        - Edit Input / Subbasins data / Select Subbasin 1 / Select .Mgt Input file
            - Edit the 'Plant/begin growing season' Operation
            - Change HEATUNITS input to 2039.000; click Save; click OK; Extend the same data set to: select Subbasins 1, 2, 6, 8, 11, 12, 13; select Soils TX633, TX620; click OK;
        - Continue to edit subbasin data: Select Subbasin 3 / Select .Mgt Input file
            - Edit the 'Plant/begin growing season' Operation
            - Change HEATUNITS input to 2060.950; click Save; click OK; Extend the same data set to: select Subbasins 3, 4, 5, 7, 9, 10; click OK;
        - Continue to edit subbasin data: Select Subbasin 15 / Select .Mgt Input file
            - Edit the 'Plant/begin growing season' Operation
            - Change HEATUNITS input to 2039.000; click Save; click OK; Extend the same data set to: select Subbasins 15, 16; click OK; click Exit
    c) Simulation / Run SWAT / click Run SWAT / click NO to read results
4. Now look for the folder containing ASCII text I/O files (something like C:\AVS2000\lakefork\scenarios\default\txtinout)
5. Copy the txtinout folder to a new location called 'basemodel' (or any other name).
6. Locate the SWAT2000.exe file (version with timestamp of 8/31/2001) from the 'AvSwatPr' folder. Copy and paste SWAT2000.exe in your 'basemodel' folder.
7. Now the 'basemodel' folder contains all the necessary case study model input files. Run the model from the 'basemodel' folder by double-clicking on the exe file.
8. Open the output.std file and locate the 'AVE ANNUAL BASIN VALUES' section and check that your outputs are precisely the following:
    - PRECIP=1256.8 MM, SURFACE RUNOFF Q=374.10 MM, TOTAL WATER YLD=455.97 MM, ET=735.7 MM, TOTAL SEDIMENT LOADING=2.504 T/HA
    - ORGANIC N=3.989 KG/HA, ORGANIC P=0.488 KG/HA, NO3 YIELD (SQ)=0.957 T/HA, SOL P YIELD=0.021 KG/HA
9. If your outputs are the same, then you have successfully recreated the benchmark case study model files. If not, see the discussion below.

The base model used in this work was recreated on computers with multiple processors and multiple Windows operating systems, each of which had Arcview© 3.2 and Spatial Analyst 2 software installed. Should the case study creation steps above fail to produce the output in Step 8 above, consider the following actions in order:

- First, check if the SWAT website has the benchmark Lakefork model input files and 8/31/2001 SWAT2000.exe available to download.
- If that fails, contact the first author directly to get a copy of the benchmark model input files.

A Comparison of Parameter Regionalisation Strategies for the Water Quantity Module of the SWAT with Application to the Scheldt River Basin

Griet Heuvelmans[1]*, Bart Muys[1] and Jan Feyen[1]
[1]Department of Land Management, Katholieke Universiteit Leuven, Vital Decosterstraat 102, B-3000 Leuven, Belgium. E-mail: griet.heuvelmans@agr.kuleuven.ac.be

Abstract

Due to uncertainty in model inputs, accurate and realistic rainfall-runoff simulations require structure and observations calibration of the model parameters. A goal of any operational model, like SWAT, is to make extrapolations to ungauged sites and/or to alternative scenarios of land use and climate change. For such applications, a case-specific parameter optimisation is not always possible and a regionalisation strategy is needed. In this research, six regionalisation strategies for the water quantity module of SWAT are compared with application to 25 subcatchments of the Scheldt River Basin. The strategies under consideration are: (1) use of SWAT defaults, (2) use of average parameter optima for the entire study region, (3) linking parameters to physical catchment descriptors by linear regression, (4) linking parameters to physical catchment descriptors with artificial neural nets, (5) delineating zones with a uniform parameterisation following a parameter-per-parameter analysis, and (6) delineating zones based on the parameter set as a whole. The analysis is limited to the seven most sensitive parameters. The linking of parameters to physical catchment descriptors by linear or non-linear models results in the highest model efficiency for daily streamflow simulations, which was completed for more than 60% of the examined catchments. The delineation of zones based on the parameter set as a whole is the preferred regionalisation strategy for almost 25% of the analyzed catchments. The use of SWAT defaults or region-wide average parameter values considerably lowers the model performance, in particular for the simulation of baseflow. In general, long-term average flows are better reproduced than daily streamflow. This trend is more pronounced for the poorest performing strategies, so that the difference in performance of the parameter regionalisation strategies is small for the simulation of 10-year average flows.

Introduction

According to Klemes (1986) model results can be used either as research tools to increase our knowledge about hydrological processes or to support the formulation of policies and regulations. In the first case, study areas are selected as a function of data availability. For practical model applications, study areas are generally predefined and often data for a site-specific optimisation of model parameters are not available. When modelling the impact of hypothetical scenarios of land use or climate change, parameters for post-change conditions are never available. Since SWAT is designed for applied modelling, particularly for the simulation of land use impacts, the question of how the parameters of the SWAT can be quantified in ungauged catchments or under an altered environmental setting arises. Do default parameter values deliver a reliable model output in this case; or does one need a more advanced parameter regionalisation strategy?

Parameter regionalisation is a procedure for deriving parameter estimates from previous model applications to gauged catchments. Despite this fact, this technique was applied a few decades ago (e.g., Magette et al., 1976, James, 1972), and is still an actual topic in applied hydrological modelling (e.g., Croke et al., 2004; Hundecha and Bárdossy, 2004; Kokkonen et al., 2003, Mwakalila, 2003). There exists a wide variety of regionalisation techniques. Some techniques predict parameter values based on the location of a catchment; others link model parameters to catchment attributes like average slope, area, and shape of the catchment. For each of these two categories, the regionalisation scheme can either be continuous or discontinuous. Continuous schemes can be obtained by kriging or by regression analysis using catchment attributes as inputs. Discontinuous schemes can be constructed by delineating spatial zones or intervals of certain catchment attributes wherein a given parameter value or parameter set is valid.

The aim of this paper is to compare the performance of different parameter regionalisation strategies for the water quantity module of the SWAT model with application to 25 subbasins in the Flemish part of the Scheldt River Basin. Specific objectives are (I) to assess whether SWAT defaults fit Flemish conditions, and (II) to quantify the impact of different parameter regionalisation strategies on the accuracy of the model output at different temporal scales (daily, monthly, and yearly streamflow).

Methodology

Study Area

The Flemish part of the Scheldt River Basin has a temperate climate with an average yearly rainfall of 813 mm, an average July temperature of 16°C and an average January temperature of 2°C. Precipitation is evenly distributed over the year. Regionalisation schemes were constructed based on SWAT simulations of 25 catchments, varying in size between two and 210 km². Catchments in the northern part of the study area are flat and mostly covered by sandy soils. The groundwater table occurs at relatively shallow depth. The most common land use types are pasture and forest. The topography of the southern part of the study area is rolling hills covered by fine-textured soils. The groundwater table is situated at greater depths as compared to the northern subbasins. Most of the area is used as cropland (mainly winter wheat and maize). Despite the occurrence of a few larger urban centres, the catchments used for the construction and evaluation of the regionalisation schemes did not contain large cities. In other words, the resulting schemes are only applicable to rural catchments with limited built-up areas.

Model Set-up

Model inputs were gathered from existing databases: climatic data were obtained from the RMI (Royal Meteorological Institute of Belgium), daily streamflow measurements for the period 1990-2001 from the Flemish Environmental Administration (AMINAL), and digital elevation data from the National Geographical Institute (NGI). Digital land use and soil maps are distributed by the Flemish Land Agency (VLM). Basic soil attributes were derived from the AARDEWERK database (Van Orshoven et al., 1993). Soil hydraulic parameters were calculated from these basic attributes using the pedo-transferfunctions of Vereecken et al. (1990).

A sensitivity analysis and preliminary model run identified seven model parameters that need to be adjusted to reach acceptable model behaviour: GW_REVAP, REVAPMN, ALFA_BF, GW_DELAY, SOL_AWC, SOL_K and CN2. GW_REVAP, REVAPMN, ALFA_BF and GW_DELAY mainly influence base flow simulation, whereas CN2 , SOL_K and SOL_AWC primarily affect surface runoff formation. Table 1 summarises the minimum, maximum, and average value of the seven most sensitive parameters as used for the regionalisation of the 25 catchments. CN2 and the soil hydraulic properties were estimated with the curve number table (USDA SCS, 1972) and with pedo-transfer functions (Vereecken et al., 1990), respectively. Because these parameter estimates are known to be error-prone, the estimates were optimised in the calibration. The correction factors were assumed constant for all soil types and soil horizons to facilitate the parameter optimisation process. For the same reason, GW_REVAP, REVAPMN, GW_DELAY and ALFA_BF were considered as constants within every catchment.

Table 1. SWAT parameters adjusted in the model calibration, including the minimal, maximal and average parameter optima for the 25 catchments under study and the name of the input file where these parameters are specified. For SOL_AWC, SOL_K and CN2, 'optimal values' are expressed as correction factors.

Parameter	Input file	Minimum	Maximum	Average
ALPHA_BF	.gw	0.15	0.46	0.28
GW_REVAP	.gw	0.1	0.18	0.14
REVAPMN	.gw	0	45	12
GW_DELAY	.gw	10	31	18
SOL_AWC	.sol	-2	21	8
SOL_K	.sol	-5	25	8
CN2	.mgt	-16	24	4

The seven selected parameters were calibrated manually for all catchments using daily discharge data for the period 1990-1995. Daily streamflow data for the period 1996-2001 were used for model validation. The following objective functions were used: (1) maximisation of the Nash and Suttcliff (1970) model efficiency for daily streamflow simulation, and (2) minimisation of the deviation of simulated yearly flow components with the components obtained from measured streamflow records with the filter developed by Arnold et al. (1995).

Regionalisation of Model Parameters

Six different parameter regionalisation strategies were considered:

(1) use of the default values provided by SWAT: this can be considered as the baseline scenario;
(2) use of average parameter optima for the entire study region (last column of Table 1);
(3) linking parameters to catchment attributes with multiple linear regression;
(4) linking parameters to catchment attributes following a non-linear scheme (implemented with artificial neural networks);
(5) delineating zones with a uniform parameterisation following a parameter-per-parameter analysis; and
(6) delineating zones based on the parameter set as a whole.

Details about the construction of the attribute-based regionalisation schemes (3) and (4) can be found in Heuvelmans et al. (2005). A preliminary list of physical catchment descriptors that could be used as inputs for the regionalisation schemes was composed based on the available data and the physical meaning of the model parameters. The following factors were considered: catchment morphology and physiography, land use, including the spatial distribution of land use within a sub-catchment, texture of the soil profile and substrate, and the depth at which the shallow aquifer occurs. A correlation analysis was carried out to assist the selection of input variables for the regionalisation. The regionalisation schemes based on ANNs and regression equations were then constructed stepwise to find the optimal amount and combination of input variables. The final form of these schemes were as follows:

- GWREVAP and REVAPMN = f(slope, shallow aquifer, %forest, %sand)
- GW_DELAY = f(slope, clay subsoil, shallow aquifer)
- ALFA_BF = f(elongation, shallow aquifer, slope)
- SOL_K and SOL_AWC = f(slope, %forest)
- CN2 = f(drainage density, %forest in buffer area)

Table 2 explains the meaning of the input variables of the attribute-based regionalisation schemes.

Details about the construction of the location-based regionalisation schemes (5) and (6) can be found in Heuvelmans et al. (2004). Spatial zones with a uniform parameterisation were delineated with a hierarchical clustering algorithm. In the single parameter approach, two to four zones were delineated for every parameter. In the parameter set approach, the study area was subdivided into three zones wherein a certain parameter set was valid.

Table 2. Definition and magnitude of the physical catchment descriptors used for calculating the SWAT model parameters.

Physical catchment descriptor	Definition	Min	Max
Slope	Average slope of the catchment (%)	0.18	2.81
Drainage density	Length of rivers and drainage channels per unit area (km/km²)	0.57	1.75
Elongation	The ratio of the diameter of a circle having the same area as the catchment, to the catchment length	0.52	1.02
Forest	% of the area covered with forests	0.36	43.05
Forest buffer	% of the area in a 100 m buffer surrounding the stream network, covered with forests	0.6	53.17
Shallow aquifer	% of the area with a permanent aquifer at <2m depth	0	33.15
Clay subsoil	% of the area with a clay substrate at <2m depth	0	29.9
Sand	% of the area with sand as topsoil texture	0	80.38

Results

Suitability of Default Parameter Values for Flemish Conditions

The upper part of Figure 1 shows the model efficiency obtained with default SWAT parameters for Flemish catchments. The resulting model efficiencies varied significantly throughout the region. In the central part of Belgium, characterised by a rolling relief and fine-textured soils, SWAT defaults gave an acceptable model behaviour for some of the simulated catchments, with model efficiencies for daily and monthly streamflow simulation slightly higher than 0.6. In the north, west, and east, the model performance was unacceptable for all catchments (lower than 0.4). The simulation for baseflow was more problematic than the simulation for peaks; baseflow volumes were generally overestimated.

The spatial pattern of model efficiencies obtained with site-specific parameter optima, depicted in the lower part of Figure 1, resembles the pattern obtained with the default parameters: catchments in the central part generally had higher model efficiencies. However, after calibration, an acceptable model fit was attained for all catchments. The increase in model efficiency due to the use of local parameter optima amounts were on average around 0.3 for monthly flows and 0.4 for daily flows. For the catchments in central Belgium, the increase in model performance after calibration was larger for daily than for monthly flows.

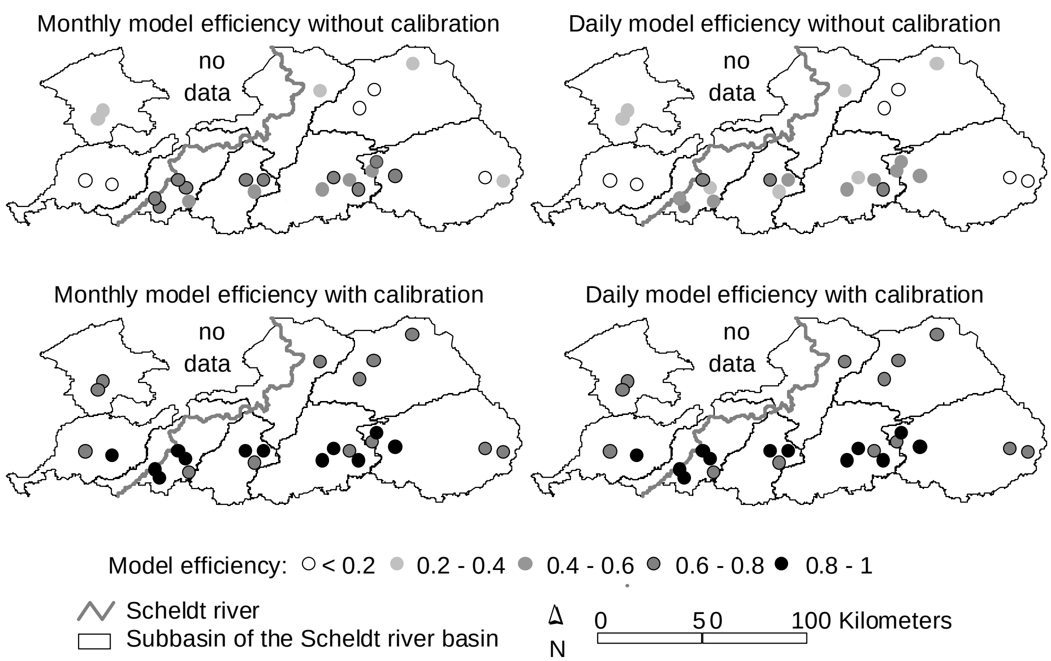

Figure 1. Model efficiency for daily and monthly stream flow simulation using default parameter values and site-specific parameter optima.

Using Parameter Regionalisation Schemes to Predict the Streamflow Regime

Figure 2 indicates the average model efficiency for the 25 studied areas for daily, monthly, and yearly streamflow simulation using the six considered parameter regionalisation strategies for the validation period 1996-2001. Figure 3 presents the relative deviation of the simulated flow components from the ones derived with the filter. Because the filter parameters could not be optimised with respect to locally observed data, the filter results should be treated as ‘orders of magnitude’ instead of exact values. Therefore, only the relative error of yearly and 10-year average flows was considered in this study.

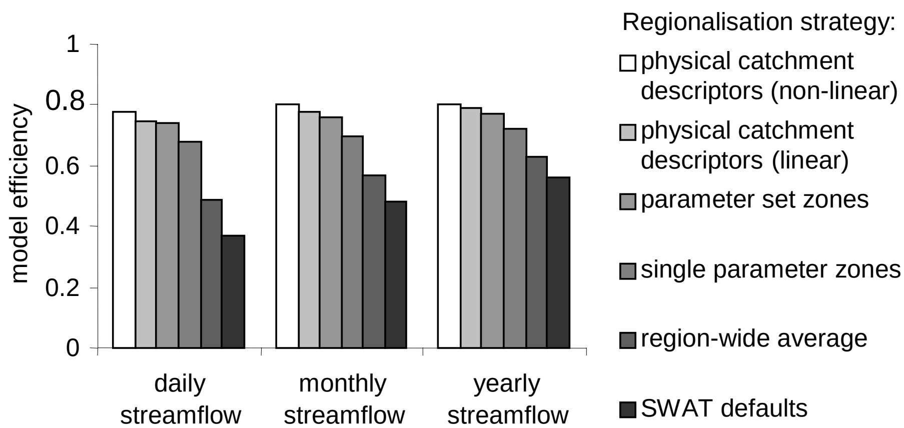

Figure 2. Average model efficiency for the 25 study catchments using six different parameter regionalisation strategies.

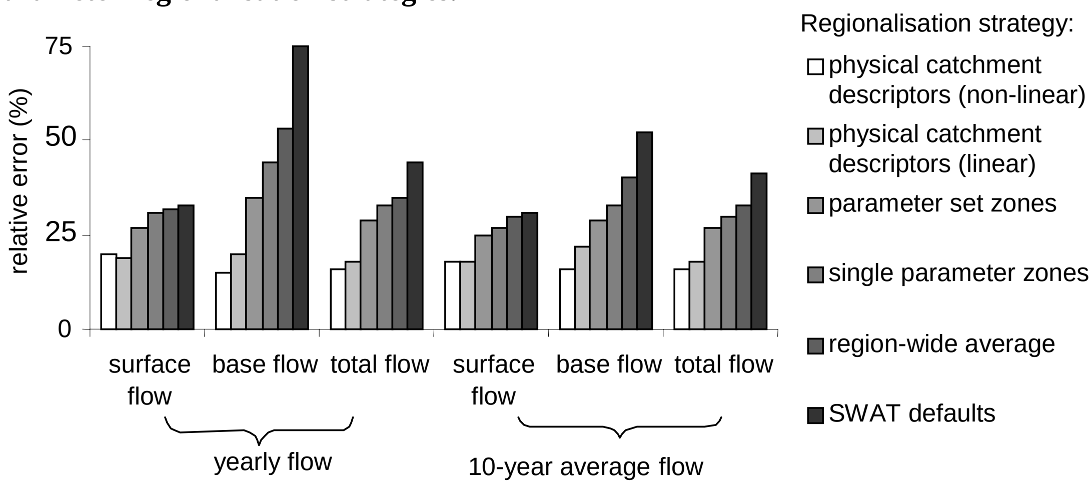

Figure 3. Average deviation of simulated flow components from filtered components for the 25 studied areas using six different parameter regionalisation strategies.

The linking of parameters to physical catchment descriptors by non-linear models resulted in the highest average model efficiency for daily, monthly, and yearly streamflow simulation. For more than 60% of the catchments, these attribute-based regionalisation schemes outperformed all other strategies for most objective functions. The delineation of zones based on the parameter set as a whole was the preferred regionalisation strategy for almost 25% of the studied catchments (Figure 4). The term 'preferred' means in this context that the average performance of the different objective functions (model efficiency for daily and monthly streamflow observations and relative error of yearly and 10-yearly flow components) was the highest for these strategies. The use of default parameter values led to inaccurate predictions, as demonstrated previously. Region-wide average parameter values delivered better results than the defaults, but baseflow simulations remained problematic. Long-term average flows were generally better reproduced than daily flows, especially for the poorest performing regionalisation strategies. Hence, at first sight the errors due to the simple parameter estimation strategies do not accumulate over time.

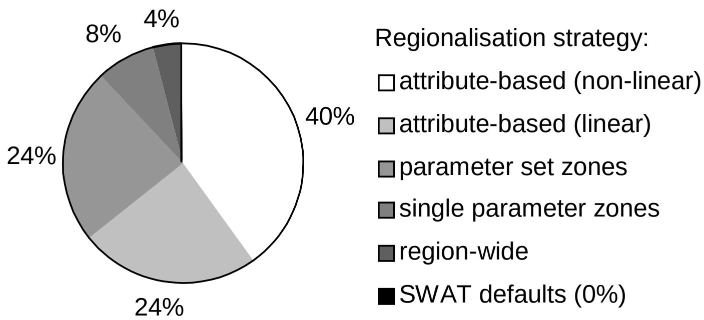

Figure 4. Preferred parameter regionalisation strategy for the 25 studied catchments (in % of the catchments). A regionalisation strategy is preferred for a certain catchment if it results in the highest average score for four criteria: model efficiency for daily and monthly stream flow simulations, and reltive error of yearly and 10-yearly flow components.

Discussion

Default Settings versus Advanced Parameter Regionalisation Strategies

Despite the fact that acceptable model efficiencies were attained for some catchment areas, the default parameter values provided by the SWAT do not particularly suit Flemish conditions. A site-specific model calibration or a regionalisation of parameter estimates is therefore desired. For the northern part of the study area, the overestimation of baseflow with default settings (left part of Figure 5) was mainly due to an inadequate parameterisation of the REVAP process, i.e. the transfer of water between the shallow aquifer and root zone. The amount of REVAP was underestimated with default parameter values, hence evapotranspiration volumes were underestimated and too much water was diverted to the river network as baseflow. Because the attribute-based regionalisation models expressed the REVAP parameters as a function of the presence of a water table at shallow depth, baseflow simulation was considerably enhanced. The zones delineated in the single parameter and the parameter set approach more or less coincided with this catchment attribute, explaining why these strategies also led to accurate baseflow predictions.

Using the default settings, the total flow volumes were well-predicted for catchments in central Belgium, but the timing and the steepness of baseflow recessions were less correct (right part of Figure 5). As a consequence, the efficiency for model streamflow prediction was acceptable but the efficiency for daily stream flow prediction proved doubtful. The attribute-based regionalisation models took the shape of the catchment and subsoil properties into account for the estimation of GW_DELAY and ALPHA_BF, two parameters that influence baseflow recession. This considerably improved the accuracy of daily streamflow simulation.

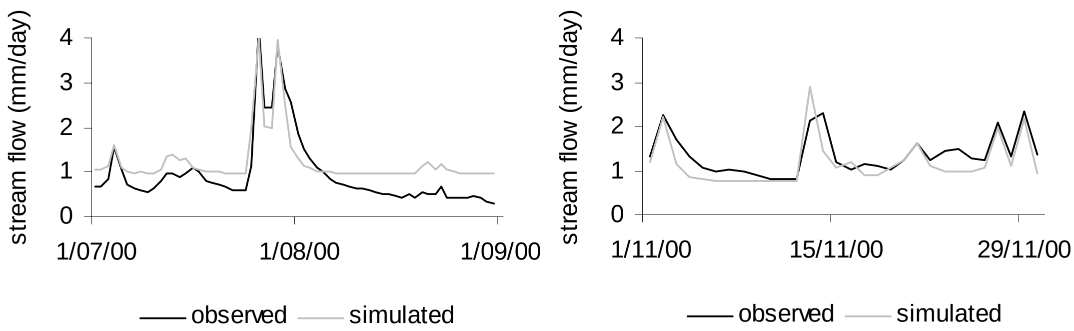

Figure 5. Typical simulation results when using default model settings in the northern part of the study region (left figure) and in central Belgium (right figure).

Attribute-based versus Location-based Parameter Regionalisation

The difference in model performance between attribute-based and location-based regionalisation strategies was small, with a slightly better performance for the attribute-based regionalisation schemes. This conclusion was opposite to the findings of Merz and Blöschl (2004). According to that study, a location-based regionalisation scheme delivered more accurate predictions than an attribute-based model. Previous studies tend to indicate that the relative performance of parameter regionalisation methods is application-specific. The model structure, the objective of the study, and the characteristics of the study area can affect the outcome.

Model Structure

The SWAT model has a clear physical basis and most model parameters relate to one distinguishable hydrological process. Contrary to the SWAT parameters, parameters of conceptual models are often lumped representations of the real-world processes. It is likely that lumped parameters are more difficult to relate to catchment attributes because they may depend on many catchment attributes. Moreover, the effect of one catchment attribute may depend on the value of the other attributes. This problem also arises for the parameters of SWAT, but to a lesser degree. In the case of SWAT, an attribute-based regionalisation can be regarded as a one-to-many projection, with one process linked to many attributes. Similarly, an attribute-based regionalisation of conceptual model parameters can be presented as a many-to-many projection, with many processes (jointly represented by one parameter) linked to many attributes. The latter is far more complex than the one-to-many projection, and consequently, less likely to yield a useful parameter regionalisation model.

Objectives of the Model Application

Attribute-based and location-based regionalisation models differ with respect to their potential fields of application. Both techniques can be used in the study area for estimating model parameters of ungauged catchments. However, the location-based model is easier to use because it does not require any additional inputs, whereas for the attribute-based scheme the inputs need to be derived from (generally available) spatial data. In addition to the parameterisation of ungauged basins, parameter regionalisation schemes can be used to represent the spatial variability in parameter optima in a semi-distributed model application. When a model is applied in semi-distributed mode, non-measurable parameters are often assumed spatially invariant for the sake of simplicity and because data for a semi-distributed parameter specification are lacking. Regionalisation models can be used to derive parameter estimates for ungauged subbasins in this case, leading to a better implementation of the semi-distributed modelling concept. As previously stated, the location-based regionalisation is better suited for this field of application than the attribute-based approach. It not only provides parameter estimates for a given catchment discretisation, but it also indicates which zones have significantly different parameter optima. In other words, it can serve as a guideline for determining an appropriate level of catchment discretisation. The major advantage of the attribute-based regionalisation is that it can also be used outside the conditions for which it was constructed. For example, it can be used to estimate model parameters for alternative land use scenarios or for the modelling of ungauged basins outside the studied area. Of course, the reliability of the regionalisation schemes is questionable for conditions that lie outside the range of the conditions of the catchments used for the construction of the schemes. For modelling the impact of climate change, attribute-based schemes must be derived for a larger area, covering the future climate that one would like to model. Parameter regionalisation schemes are known to perform rather poorly if applied in catchments with climatic conditions that are under-represented in the dataset used for the construction of the regionalisation model (e.g., Abdulla and Lettenmaier, 1997).

Characteristics of the Study Area

The northern part of Belgium is a very heterogeneous region in many respects. There are a wide variety of soil types, not only between the catchments but also within a catchment. Almost all land use types occur in every part of the studied region, albeit in different proportions. Consequently, it is hard to divide the region into sub-regions with unique (hydrological) features. Parameter optima vary significantly over short distances while at the same time one parameter set may suit several distinct locations within the region. This might explain why in this study, a location-based regionalisation model was less successful than the attribute-based model.

Conclusions

Based on a data set of 25 small catchments in the Scheldt River Basin, attribute-based (linear and non-linear) and location-based (single parameter zones or parameter set zones) regionalisation strategies were derived. Comparison of the model efficiencies for these different parameter regionalisation strategies indicated that attribute-based regionalisation was the preferred regionalisation strategy for most catchments. However, the difference in model performance between attribute-based and location-based schemes was small. Both strategies performed considerably better than the use of region-wide average values or the use of SWAT defaults. The latter technique still delivered acceptable model behaviour in the central part of Belgium, but tended to overestimate baseflow volumes for catchments located in the north, east, and west portions of the study area. Therefore, it can be concluded that default parameters do not fit Flemish conditions. The use of a more advanced parameter regionalisation strategy, either based on location or on physical catchment descriptors, is recommended. The exact nature of the best performing parameter regionalisation strategy (linear attribute-based, non-linear attribute-based, single parameter zones and parameter set zones) depends on the objective of the study, the characteristics of the study area and the model structure. In this study, the non-linear attribute-based regionalisation was preferred.

References

Abdulla, F.A., Lettenmaier, D.P. 1997. Development of regional parameter estimation equations for a macroscale hydrologic model. Journal of Hydrology 197, 230-257.

Arnold, J.G., Allen, P.M., Muttiah, R., Bernhardt, G. 1995. Automated base flow separation and recession analysis. Ground Water 33 (6), 1010-1018.
Croke, B.F.W., Merritt, W.S., Jakeman, A.J. 2004. A dynamic model for predicting hydrological response to land cover changes in gauged and ungauged catchments. Journal of Hydrology 291, 115-131.
Heuvelmans, G., Muys, B., Feyen, J. 2004. Analysis of the spatial variation in the parameters of the SWAT with application in Northern Belgium. Hydrology and Earth System Sciences 8(5), 931-939.
Heuvelmans, G., Muys, B., Feyen, J. 2005. Regionalisation of the parameters of a hydrological model: comparison of linear regression models with artificial neural nets. Submitted.
Hundecha, Y., Bárdossy, A. 2004. Modeling the effect of land use changes on the runoff generation of a river basin through parameter regionalization of a watershed model. Journal of Hydrology 292, 291-295.
James, L.D. 1972. Hydrologic modeling, parameter estimation and watershed characteristics. Journal of Hydrology17, 283-307.
Klemes, V. 1986. Operational testing of hydrological simulation models. Hydrological Sciences Journal – Journal des Sciences Hydrologiques 31, 13-24.
Kokkonen, T.S., Jakeman, A.J., Young, P.C., Koivusalo, H.J. 2003. Predicting daily flows in ungauged catchments: model regionalisation from catchment descriptors at the Coweeta Hydrologic Laboratory, North Carolina. Hydrological Processes 17(11), 2219-2238.
Magette, W.L., Shanholtz, V.O., Carr, J.C. 1976. Estimating selected parameters for the Kentucky watershed model from watershed characteristics. Water Resources Research 12(3), 472-476.
Merz, R.& Blöschl, G. 2004. Regionalisation of catchment model parameters. Journal of Hydrology 287, 95-123.
Mwakalila, S. 2003. Estimation of stream flows of ungauged catchments for river basin management. Physics and Chemistry of the Earth 28, 935–942.
Nash, J.E., Sutcliffe, J.V. 1970. River flow forecasting through conceptual models, I, A discussion of principles. Journal of Hydrology 10, 282-290.
USDA SCS, 1972. National engineering handbook. Section 4 Hydrology.
Van Orshoven, J., Deckers, J.A., Vandenbroucke, D., Feyen, J. 1993. The completed database of Belgian soil profile data and its applicability in planning and management of rural land. Bulletin Recherche Agronomie Gembloux 28(2-3), 197-222.
Vereecken, H., Feyen, J., Maes, J. 1990. Estimating the hydraulic conductivity soil water content relationship from easy to measure soil properties. Soil Science 149(1), 1-12.

Vulnerability Assessment of Climate Change Impact on Indian Water Resources Using the SWAT Model

A. K. Gosain[1], Sandhya Rao[2], Debajit Basu Ray[3]
[1] Professor of Civil Engineering, Indian Institute of Technology, Delhi 110 016, India. E-mail: gosain@civil.iitd.ernet.in, (91) (011) 2659 1186, Fax: (91) (011) 2658 1117
[2] Ex. Director, INRM Consultants Pvt Ltd.
[3] Sr. Executive (Technical) INRM Consultants Pvt Ltd

Abstract

A very exhaustive study was conducted as part of the National Communication (NATCOM) project undertaken by the Ministry of Environment and Forests, of the Government of India to quantify the impact of climate change on the water resources of India using a hydrological model. The study uses the HadRM2 daily weather data to determine the control (present) and GHG (future) water availability in space and time. A distributed hydrological model, namely the Soil and Water Assessment Tool (SWAT) has been used on major river basins of the country. The framework predicts the impact of climate change on the water resources with the assumption that the land use shall not change over time and any manmade changes like dams, diversions, etc. have not been incorporated. A total of 40 years of simulation over 12 river basins of the country (leaving out only two major river systems, the Brahmputra and Indus) have been conducted, 20 years were devoted to control (present) and the remaining 20 years devoted to the GHG (future) climate scenario. Each river basin has also been further subdivided into reasonable sized sub-basins so as to account for spatial variability. It has been observed that the impacts of climate change are not uniform over the country and are varying across the river basins as well as across sub-basins. The initial analysis revealed that the GHG scenario may deteriorate the conditions in terms of severity of droughts and intensity of floods in various parts of the country and that there is a general reduction in the quantity of the available runoff under the GHG scenario. This paper presents the detailed analyses of two river basins with maximum effect with respect to drought and floods.

Introduction

Water is a very precious natural resource and very complex to manage. The complexity has further increased due to the possible impacts of global climate change being predicted. The general impacts of climate change on water resources have been identified by the Third Assessment report of the Intergovernmental Panel on Climate Change, (IPCC, 2001). It indicates an intensification of the global hydrological cycle, affecting both ground and surface water supply for domestic and industrial uses, irrigation, hydropower generation, navigation, in-stream ecosystems and water-based recreation. Changes in the total amount of precipitation as well as in its frequency and intensity have also been predicted, which shall in turn affect the magnitude and timing of runoff and soil moisture status. The coping capacity of the societies shall vary with respect to their preparedness. The countries with integrated water-management systems may protect water users from climate change at minimal cost, whereas others may have to bear substantial economic, social, and environmental costs to do the same.

Thus, the climate change impacts are going to be most severe in the developing world, because of their poor capacity to cope with and adapt to climate variability. India falls into this category. At the national level there has not been any significant work on the climatic change impact assessment on water resources. The general philosophy of the implications of climatic change on the water resources of India has been discussed by Lal (2001). A general projection of the water resource demand for 2050 has been worked out by the Central Water Commission, without consideration for the possible impact of climate change (Thatte, 2000). Therefore, in a real sense the NATCOM study (Gosain et. al., 2003) was the first attempt to quantify the impact of the climate change on the water resources of the country. This paper presents detailed results of the study on two extreme river basins affected with respect to the drought and flood severities due to climate change.

Methodology

The SWAT water balance model has been used to carry out the hydrologic modeling of the river basins of the country. The SWAT model (Arnold et al., 1998), developed by the Agricultural Research Service, Blackland, Texas, USA, simulates the hydrologic cycle in daily time steps. The SWAT model has the capability to route water from individual watersheds, through the major river basin systems. SWAT is a semi-distributed, continuous, daily time step hydrological model with an ArcView GIS interface (AVSWAT) for pre- and post-processing of the data and outputs.

This study determines the present water availability in space and time without incorporating any manmade changes like dams, diversions, etc. The same framework is then used to predict the impact of climate change on the availability of water resources (future) with the assumption that the land use shall not change over time.

Data Used for Study

The SWAT model requires the data on terrain, land use, soil, and weather for assessment of water resources availability at desired locations of the drainage basin. These data (1:250,000 scale) for all river basins barring Brahmaputra and Indus have been used. The data used for the modeling includes a Digital Elevation Model (DEM) generated using contours taken from 1:250,000 scale, Classified land cover data of 1 km grid cell size produced using remote sensing by the University of Maryland Global Landcover Facility (Hansen et al., 1999), FAO Digital Soil Map of the World and Derived Soil Properties (ver. 3.5, November 1995) with a resolution of 1:5,000,000 (FAO, 1995). The data generated in transient experiments by the Hadley Centre for Climate Prediction, U.K., at a resolution of 0.44° latitude X 0.44° longitude grid points (depicted in Figure 1) has been obtained from IITM (Indian Institute of Tropical Meteorology), Pune, India. The daily weather data on temperature (maximum and minimum), rainfall, solar radiation, wind speed, and relative humidity at all the grid locations were processed.

Delineation of the River Basins

Automatic delineation of each of the river basins was accomplished by using the DEM as input and the final outflow point on the river basin as the final pour/drainage point. Figure 1 depicts the modeled river basins (automatically delineated using GIS).

The river basins have been divided into sub-basins depending on the selection of the threshold value. Table 1 presents the threshold values used in the process of automatic delineation. It also provides the number of sub-basins the river basin was divided into as a result of this threshold. The total area of the river basin, as obtained from the automatic delineation, has also been provided. The threshold is subjective and is selected iteratively to divide the basin into number of sub-basins. The idea was to account for the spatial variability. But there has to be some tradeoff between the sub-division and the data on other elements that dictate the hydrology such as land use and soil information.

Table 1. Some of the basic details of the basins analyzed in the study.

S. No.	Basin	Threshold Value Used (ha)	Number of Sub-basins	Total Area (ha)
1.	Brahmani	99,700	19	4,999,399
2.	Cauvery	350,000	11	6,467,199
3.	Ganga	2,000,000	29	87,180,000
4.	Godavari	600,000	27	30,003,299
5.	Krishna	600,000	21	24,647,200
6.	Luni	750,000	9	12,793,400
7.	Mahanadi	400,000	21	14,027,300
8.	Mahi	100,000	13	3,579,000
9.	Narmada	350,000	15	9,765,000
10.	Pennar	200,000	11	5,524,600
11.	Sabarmati	48,900	8	1,668,026
12.	Tapi	200,000	13	6,853,799

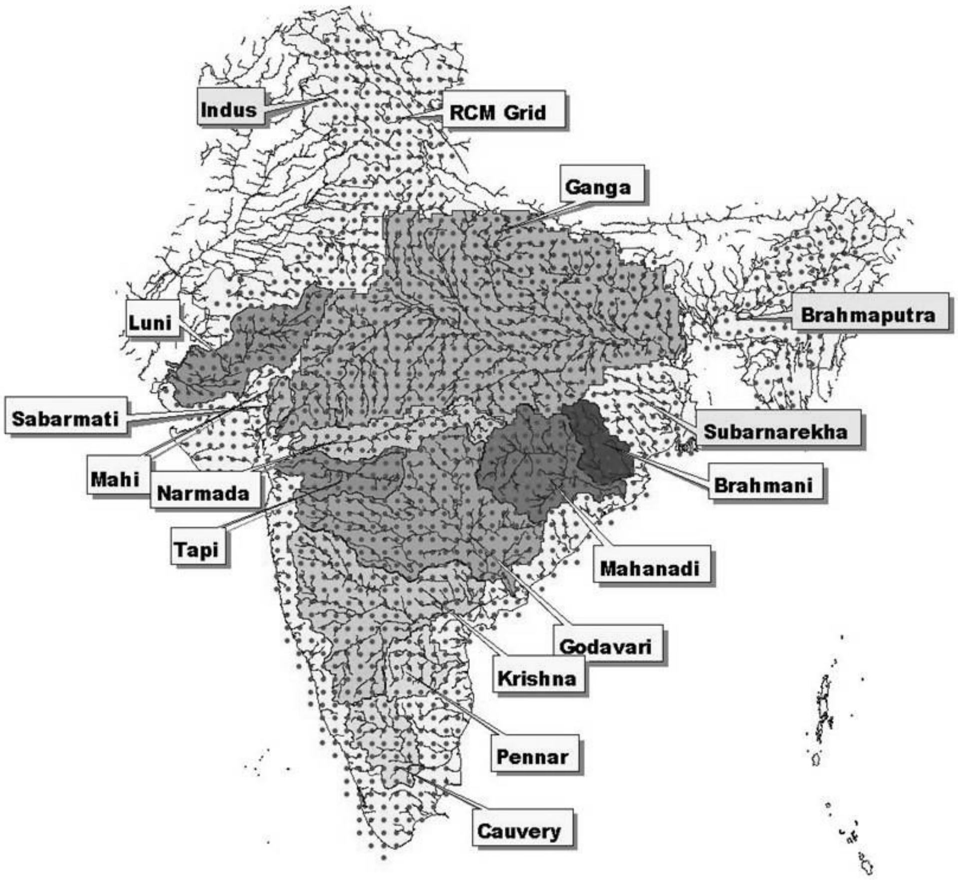

Figure 1. The modeled river basins of the Indian Sub-continent.

Hydrologic Modeling of the River Basins

The SWAT distributed hydrologic model has been used on each of the river basins given in Table 1. The basins have been sub-divided using the threshold values given in Table 1. These values were adapted to divide the basin into a reasonable number of sub-basins so as to account for the spatial variability. After mapping the basins for terrain, land use, and soil, each of the basins has been simulated imposing the weather conditions predicted for control and GHG climate.

Control Climate Scenario

Each of the river basins has been simulated using the SWAT model to generate daily weather by the HadRM2 control climate scenario (1981-2000). Although the SWAT model does not require elaborate calibration, in the present case, any calibration was not meaningful since the simulated weather data was used for the control period which is not the historical data corresponding to the recorded runoff (Gosain et al., 2003). The observed meteorological data at the national scale was unavailable for use. Presently, the model has been used with the assumption that every river basin is a virgin area without any manmade change incorporated, which was reasonable for making the initial national communication to the UNFCCC (the basic objective of this study). The model generates detailed outputs on flow at sub-basin outflow points, actual evapotranspiration, and soil moisture status at daily intervals. Further sub-divisions of the total flow into components such as surface and subsurface runoff are also available. It also provides the recharge to the ground water on a daily basis.

GHG Climate Scenario

The model was again run on each of the basins using GHG climate scenarios (2041-2060) data, without changing the land use. The outputs of these two scenarios have been analyzed first at the basin level with respect to the possible impacts on the precipitation, runoff, soil moisture, and actual evapotranspiration. Subsequently, detailed analyses were performed on two of the river systems, namely Krishna and Mahanadi, to demonstrate the impacts at the sub-basin level. Incidentally, these are the river basins which have been identified to have maximum effect with regard to droughts and floods, respectively.

Summary Results of River Basins Modeled

The percent change in water balance components of rainfall, runoff, and actual evapotranspiration from the control to GHG climate scenarios for the 12 river basins was computed. Table 2 depicts comparison of change in water balance components of rainfall, runoff, and actual evapotranspiration for GHG scenarios. It was observed that the impacts are different in different catchments. A close examination of the table also reveals that the increase in rainfall due to climate change does not always result in an increase in the surface runoff, as may be generally predicted. For example, in the case of the Cauvery River basin an increase of 2.7% of rainfall was predicted, but the runoff in fact decreased by about 2% and the actual evapotranspiration increased by about 7.5%. On the contrary, a predicted reduction in rainfall in Narmada resulted in an increase in runoff, which is again contrary to the usual expectation. Results at the sub-basin level are presented for two sample basins in Table 2.

Table 2. Change in Water Balance Components as % of Control.

Basins	Scenario	Rainfall mm	Change over Control %	Runoff mm	Change over Control %	Actual ET mm	Change over Control%
Cauvery	Control	1309		661		601	
	GHG	1344.0	2.7	650.4	-1.6	646.8	7.5
Brahmani	Control	1384.8		711.5		628.8	
	GHG	1633.7	18.0	886.1	24.5	698.8	11.13
Godavari	Control	1292.8		622.8		624.1	
	GHG	1368.6	5.9	691.5	11.03	628.3	0.67
Krishna	Control	1013.0		393.6		585.0	
	GHG	954.4	-5.8	346.9	-11.86	575.6	-1.61
Luni	Control	317.3		15.5		316.5	
	GHG	195.3	-38.4	6.6	-57.40	207.3	-34.50
Mahanadi	Control	1269.5		612.3		613.5	
	GHG	1505.3	18.6	784.0	28.04	674.1	9.88
Mahi	Control	655.1		133.9		501.0	
	GHG	539.3	-17.7	100.0	-25.31	422.7	-15.63

Basins	Scenario	Rainfall mm	Change over Control %	Runoff mm	Change over Control %	Actual ET mm	Change over Control%
Narmada	Control	973.5		353.4		586.8	
	GHG	949.8	-2.4	359.4	1.69	556.6	-5.15
Pennar	Control	723.2		148.6		556.7	
	GHG	676.2	-6.5	110.2	-28.84	551.7	-0.89
Tapi	Control	928.6		311.2		587.9	
	GHG	884.2	-4.8	324.9	4.40	529.3	-9.97
Ganga	Control	1126.9		495.4		535.0	
	GHG	1249.6	10.9	554.6	11.95	587.2	9.76
Sabarmati	Control	499.4		57.0		433.1	
	GHG	303.0	-39.3	16.6	-70.88	286.0	-33.96

Detailed Results of Two River Basins

Detailed results for two river basins, one with resulting drought conditions and the other with pronounced flood conditions have been selected. These are the Krishna and Mahanadi river basins, respectively.

Krishna River Basin

The Krishna River Basin has been divided into 21 sub-basins as depicted in Figure 1. The annual average precipitation, actual evapotranspiration, and water yield as simulated by the SWAT model over the entire Krishna basin for control and GHG scenarios has been depicted in Figure 2. A close examination reveals that this river basin is expected to receive reduced levels of precipitation, actual evapotranspiration, and water yield.

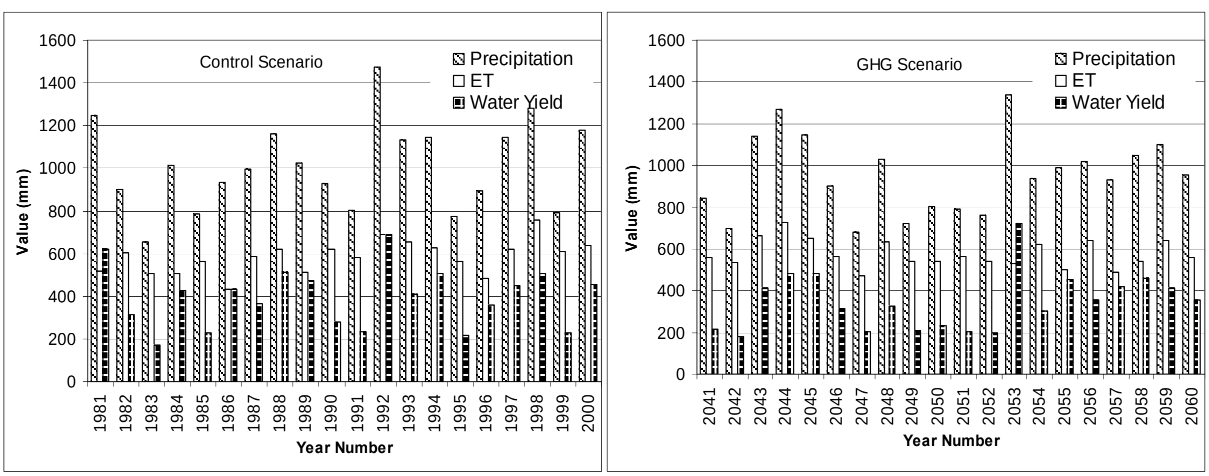

Figure 2. Mean annual water balance components for Krishna under Control and GHG scenarios.

Drought Analysis

Drought indices are widely used for the assessment of drought severity by indicating relative dryness or wetness affecting water-sensitive economies. The Palmer Drought Severity Index (PDSI) is one such widely used index that incorporates information on rainfall, land use, and soil properties in a lumped manner (Palmer 1965). The Palmer index categorizes drought into different classes. A PDSI value below 0.0 indicates the beginning of a drought situation and a value below -3.0 is categorized as severe drought conditions.

Recently, a soil moisture index has been developed (Narasimhan and Srinivasan, 2002) to monitor drought severity using SWAT outputs. This formulation has been employed in the present study to focus on the agricultural drought where severity implies cumulative water deficiency. With this in mind, weekly information has been derived using daily SWAT outputs, which in turn have been used for subsequent analysis of drought severity. The soil moisture index has been computed for all the sub-basins of the River Krishna.

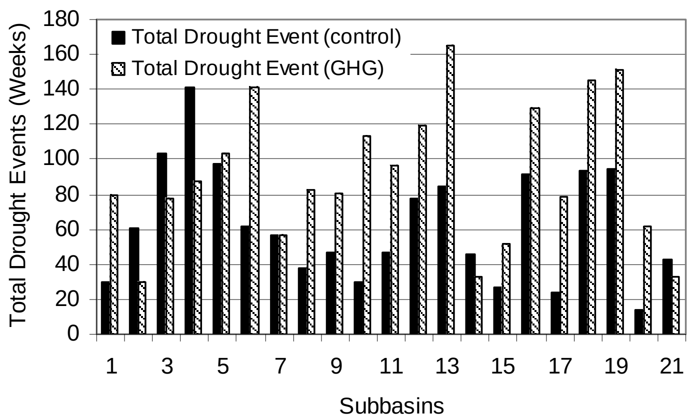

Figure 3. Number of drought weeks in Sub-basins of Krishna for Control to GHG scenarios.

Figure 3 depicts the number of drought weeks in the sub-basins of Krishna consisting of the weeks with SMI of less than or equal to -3.0, for both control and GHG scenarios. The SMI for GHG scenario has been computed using the soil moisture deficit ratio parameters of the control scenario. Figure 3 shows that the number of drought weeks has increased considerably during the GHG scenario, with the exception of approximately five sub-basins.

Mahanadi River Basin

The Mahanadi River Basin has been divided into 21 sub-basins as depicted in Figure 1. The annual average precipitation, actual evapotranspiration, and water yield as simulated by the model over the total Mahanadi basin for control and GHG scenarios has been depicted in Figure 4. A close examination reveals that this river basin is expected to receive comparatively higher levels of precipitation in the future and a corresponding increase in evapotranspiration and water yield.

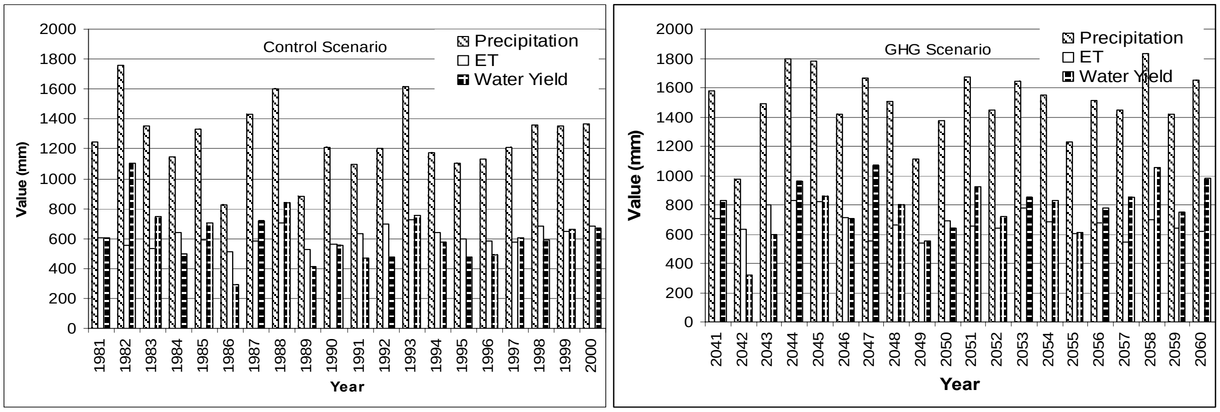

Figure 4. Annual Water Balance components for Control and GHG scenarios.

The impact of climate change on the water yield converted into runoff in cubic meters per second (cumecs) at the outlet of the river system has been analyzed with respect to four arbitrarily selected runoff percentiles (25, 50, 75, and 90%). Table 3 shows the values corresponding to 25, 50, 75, and 90% dependability levels.

Table 3. Runoff percentiles (25, 50, 75, 90 %) for the Control and GHG scenarios.

Dependable Flow (m^3/sec)	25%	50%	75%	90%
Control	4716	1206	15.9	1.5
GHG	6103	1168	43.4	3.2

It may be noticed that the flow for all levels has increased for the GHG scenario over the corresponding control flow magnitude, except for the 50% level of dependability, at which the flow was marginally reduced.

Flood Analysis for Mahanadi Basin

Although the flow duration curve is indicative of severe flood conditions, detailed analysis for one of the sub-basins experiencing the most severe flooding under the GHG scenario have been analyzed and presented in Figure 5.

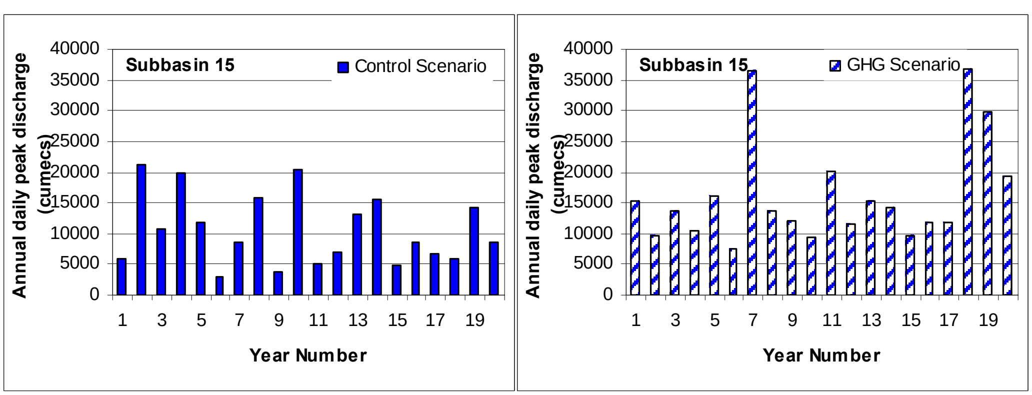

Figure 5. Annual maximum daily peak discharges for Mahanadi sub-basin number 15 for Control and GHG scenarios.

The most affected sub-basins in Mahanadi (Sub-basins 15) have been analyzed for flood severity (Figure 5). In this sub-basin, the annual maximum peak has increased from the present level of about 20,000 cumecs under control scenario to a maximum level of about 37,000 cumecs under the GHG scenario. In the GHG scenario, there have been three years when the peak level of 30,000 cumecs was surpassed. Such an increase in flood peak may be detrimental to structures such as dams and bridges on the drainage systems in the region.

Conclusions

It is a challenge to quantify the impact of climate change. In this case, the water balance simulation modeling approach was used to maintain the dynamics of hydrology and thereby make assessments of vulnerability which are more authentic and reliable than in previous studies. The usefulness of such an approach has been proven by the fact that the results of the GHG scenarios have been dictated by temporal variability at daily levels as well as the spatial state of the land mass in terms of its moisture conditions and land use.

Because the present study was part of the initial communication of the country to UNFCCC, many assumptions were made due to lack of appropriate data, including manmade interventions, detailed land use, and soil. Even the model validation could not be undertaken due to this lack of detailed data. However, the second phase of the study is being initiated soon wherein all of these discrepancies shall be addressed. As a first attempt this study provides a great deal of information that can be utilized to formulate the first adaptation strategies to combat the climate change impacts on water resources.

The initial analysis has revealed that the GHG scenario may deteriorate the conditions in terms of the severity of droughts and intensity of floods in various parts of the country. However, there is a general reduction in the quantity of the available runoff in the GHG scenario. There are definite impacts that may induce additional stresses that will require various additional adaptation strategies. The strategies may include a change in land use, cropping patterns, water conservation, flood warning systems, etc.

Acknowledgements

The authors are grateful to the Ministry of Environment and Forests for supporting this study. Thanks are due to Dr. Subodh Sharma, Dr. Sumana Bhattacharya, and Dr. Amit Garg for their constant help and constructive suggestions.

References

Arnold, J.G., R Srinivasan, R.S. Muttiah, and J.R. Williams. 1998. Large area hydrologic modeling and assessment: Part I. Model development. Journal of the American Water Resources Association, 34(1): 73-89.

Food and Agriculture Organization of the United Nations (FAO). 1995. Digital soil map of the world and derived soil properties (Version 3.5). FAO, Rome, Italy.

Gosain, A.K., Sandhya R., and Basuray D., 2003. Assessment of vulnerability and adaptation for water sector. Proceedings of the Workshop on Vulnerability Assessment and Adaptation Due to Climate Change on Indian Water Resources, Coastal Zones and Human Health, Ministry of Environment and Forests, New Delhi, pp 17-24.

Gosain, A.K., Sandhya R., Srinivasan, R., and Reddy N.G., 2005. "Return-Flow Assessment for Irrigation Command in the Palleru River Basin Using SWAT Model", Hydrological Processes, 19, 673-682.

Hansen, M. C., DeFries, R. S., Townshend, J. R. G., and Sohlberg, R., 1999. 1 km Global Land Cover Data Set Derived from AVHRR. Global Land Cover Facility, University of Maryland Institute for Advanced Computer Studies, College Park, Maryland, U.S.A.).

IPCC (Intergovernmental Panel for Climate Change), 2001. Climate Change 2000, The science of climate change, Assessment report of the IPCC Working Group I, Cambridge University Press, Cambridge.

Lal, M., 2001. Climate Change – Implications for India's Water Resources, J. Indian Water Resources Society, 21(3); 101-119.

Narasiman, B., and Srinivasan, R., 2002.Development of a soil moisture index for agricultural drought monitoring using hydrologic model (SWAT),GIS and Remote Sensing. The 2002 Texas Water Monitoring Congress Proceedings. The University of Texas at Austin, September 9-11, 2002.

Palmer, W.C., 1965. Meteorological drought. Research Paper 45. U.S. Department of Commerce, Weather Bureau, Washington, D.C. 58pp.

Thatte C.D., 2000. Green to Evergreen Revolution through a Blue Revolution, J. Indian Water Resources Society, 20(2); 63-75.

Session VII

25. **Effects of input data resolution on SWAT simulations – A case study at the Ems River Basin (Northwestern Germany)** **241**
Gerd Schmidt and Martin Volk

26. **Application of water management models to Mediterranean temporary rivers** **251**
Antonio Lo Porto, Anna Maria Girolamo, Filomena De Luca and Giuseppe Pappagallo

27. **Evaluation of the SWAT model in a small experimental Mediterranean basin** **261**
Feliciana Licciardello, Raghavan Srinivasan and Santo Marcello Zimbone

28. **Comparison of runoff responses between SWAT and sequentially coupled SWAT-MODFLOW model** **271**
Do Hun Lee, Nam Won Kim and IL Moon Chung

29. **Hydrological modelling using SWAT for effective management of a small agricultural watershed** **279**
M.P. Tripathi

Effects of Input Data Resolution on SWAT Simulations – A Case Study at the Ems River Basin (Northwestern Germany)

Gerd Schmidt and Martin Volk
UFZ-Center of Environmental Research, Department Applied Landscape Ecology, Permoserstraße 15, D-04318 Leipzig, Germany. Email: gerd.schmidt@ufz.de

Abstract

The development and implementation of management plans for river basins requires the analysis of ecological causes/consequences/relationships. An appropriate method for such analyses is the application of simulation models. However, accurate simulations of hydrology, nutrient balance, and matter fluxes require knowledge of the effect of input data resolution on the simulation results. This is essential in order to receive information both about the range of variation and the scale-specific suitability of the simulation results. Thus, this study shows the impact of input data of different spatial resolution on model simulations. The simulations were carried out on the Upper Ems River Basin in Northwestern Germany using AVSWAT2000. The comparative use of input data sets with different spatial resolutions shows that the model starts each simulation with spatially different distributed parameter sets for the same basin. This leads to results with different efficiencies (qualities) – depending on the temporal data resolution in each case. Model applications related to river basin management need appropriate input data sets that are suitable to the spatial and temporal planning and information level in question to allow accurate predictions of land use impacts on water and nutrient fluxes. The simulations using input data with different resolutions show that the suitability of SWAT is problematic in basins with sizes of under 300 to 500 km². In addition, model efficiencies of monthly simulations are in the same range with both the high and low resolution input data and indicate that the use of high resolution data is not in any case necessary. Thus, we recommend intense preliminary considerations about the goal of model application and the necessary quality or information level of the simulation results. Decision support needs tools and predictions that are capable of solving real problems. Thus, especially for meso- to macro-scale applications, simulations using appropriate input data with a defined variation extent of spatio-temporal resolution are generally more effective than the attempted use of the highest resolutions of input data to seemingly eliminate all uncertainties.

Introduction

With the implementation of the European Water Framework Directive (WFD) in the year 2000, the German Ministry of Education and Science started a research program called "River Basin Management". This was done in order to contribute to the solution of problems related to the implementation of this directive. FLUMAGIS (www.flumagis.de) is one of approximately ten integrated research projects in that program. The project aims to an improved participation of stakeholders in the process of river basin management. Its main target is the development of an assessment and visualisation tool to simulate human impacts on the hydrological and ecological conditions in river basins. The WFD requires the development of management strategies to achieve a sound ecological quality of aquatic systems in Europe. The needed management measures, efficiency controls, and reports should therefore be produced at different scales. Thus, it is also essential to analyse the causes/consequences/relationships between land use and ecological conditions and the situation of aquatic systems at relevant scales. One outcome of our work with the FLUMAGIS project is the development of a scale-specific model concept to meet these requirements (Volk & Schmidt, 2004, Gretzschel et. al, 2004). The development of assessment strategies with scale equivalent indicators and the use of different hydrological simulation model systems are closely connected with the realization of that concept. As a consequence, we had to determine on which scales we could usefully apply the SWAT model for our land use scenarios, on the basis of the available governmental data sets. A scale-appropriate use of SWAT in this project depended especially on the spatial resolution and quality of these available input data.

Scale-specific simulation of land use effects on water balance and runoff dynamics requires appropriate data sets for each scale level. Questions of scale-appropriate modelling and effects of data resolution on simulation results have been intensely discussed in recent years (Liang et al, 2004, Muttiah and Wurbs, 2002, Quinn, 2004). However, the integration of homogeneous and scale-equivalent input data sets for hydrological simulation, especially on the meso- to maco-scale, is still a challenge (Quinn, 2004, Liang et al., 2004, Volk and Schmidt, 2004, Muttiah et. al, 2002). Besides the lack of suitable data, one of the most important problems to consider is the compilation of parameter sets for model calibration. Moreover, the problem of estimating the influence of the input data resolution on the quality of simulations is of great importance with regard to the modelling of hydrological processes in ungauged catchments.

Thus, this study shows how the input data resolution influences the simulation results of the SWAT model (Arnold et al., 1993, Neitsch et al., 2002). The AVSWAT2000 (DiLuzio et al., 2001) interface was used in this study and simulations were carried out at different time-steps (annual, monthly, daily) in catchments of varying size. An important goal of the investigation was to find the best data and model combinations to contribute to scale-specific decision support in river basin management. Another problem addressed in this study was determining which spatial and temporal resolution was needed to answer certain questions. Finally, consideration of time exposure for data compilation and management as well as model setup and simulation was necessary. Environmental planners and authorities responsible for river basin management need pragmatic management advice and information concerning causes/consequences and cost-benefit effects of any problem or management decision.

Study Area

The Upper Ems River Basin is a part of the North-German Lowlands and covers an area of approximately 3,800 km² in northwestern Germany (Figure 1). The mostly flat Ems River Basin has been formed mainly by glacial and periglacial processes. The elevation of the catchment ranges from 27 m to 350 m above sea level. Thick layers of sandy sediments are another result of the periglacial processes. These sediments are the base material of the soil development in the region. The soils and sediments have mostly high infiltration capacities with a resulting strong influence on the runoff dynamics in the basin. Table 1 shows the gauges and hydrological characteristics of the Upper Ems River Basin.

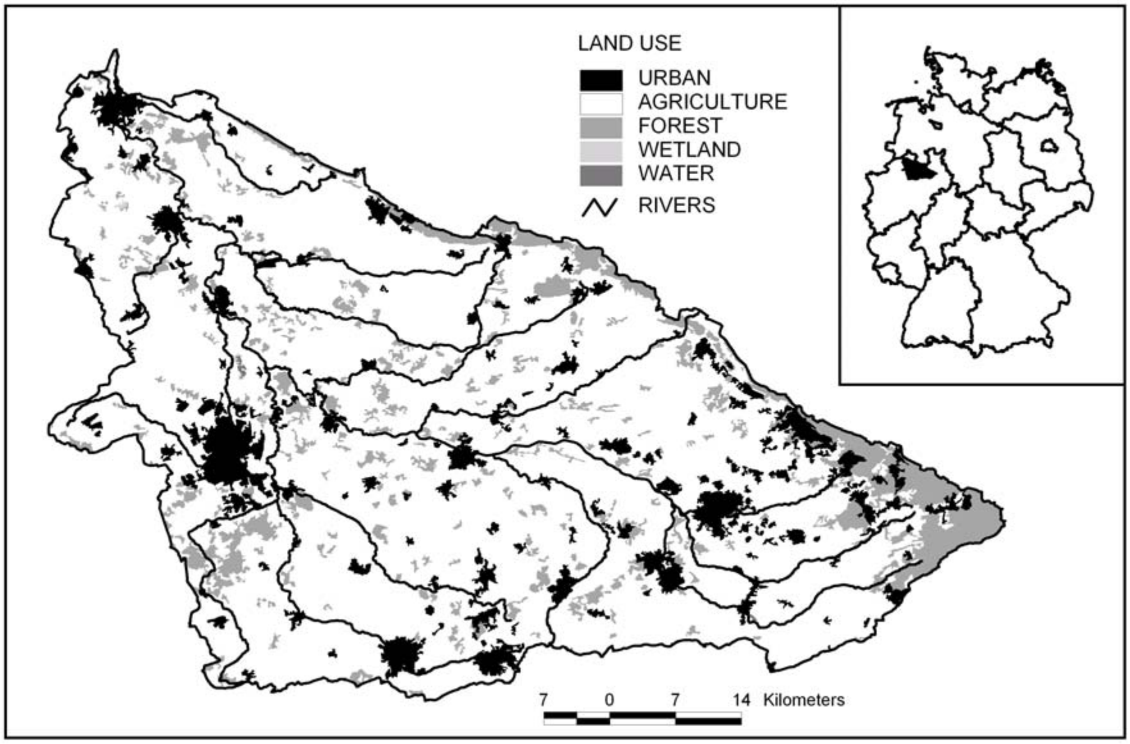

Figure 1. Location of the study area in Germany and overview over the land use situation.

The Ems River Basin is characterized by a mean annual average precipitation of 600 mm in the southwest to 1,200 mm in the mountainous eastern part. The basin is intensively used by agriculture (75% arable land) with livestock numbers of up to 3.8 animal units per ha (SO-NRW 2004). This land use causes high nutrient inputs into the Ems River system. Concentrations of up to 14 mg/l of total nitrogen (measured at the outlet gauge of the Upper Ems Basin Rheine) substantially impair the water quality of the River Ems.

Table 1. Gauges and hydrological characteristics of Ems River Basin.

Gauge	**River**	**Subbasin**	**Mean Streamflow [m³/s]**	**Mean total runoff [l/s/km²]**	**BFI**	**α BF**
Rheine	Ems	3740.0	37.012	9.9	0.59	0.0209
Haskenau	Ems	1845.0	19.011	10.3	0.62	0.0198
Haus Langen	Ems	1616.0	17.355	10.7	0.64	0.0162
Einen	Ems	1485.8	15.987	10.8	0.62	0.0235
Rheda	Ems	342.6	3.221	9.4	0.57	0,0237
Ahlen	Werse	46.6	0.608	13.1	0.48	0.0633
Albersloh	Werse	321.6	3.112	9.7	0.17	0.0410
Roxel	Muenst. Aa	88.2	0.866	9.8	0.42	0.0599
Coermühle	Muenst. Aa	152.3	1.417	9.3	0.36	0.0367
Ladbergen	Glane	350.0	2.125	6.1	0.59	0.0211

Database, Pre-Processing, and Simulation

Database

The comparative analysis is based on two data sets with different spatial resolutions (Table 2). The DEMs used in this analysis are publicly available government data, produced by the Survey of the State of North-Rhine Westfalia. The soil information used is from two different sources. The soil map of Germany (1:1,000,000 scale) BÜK1000 is a product of the German Geological Survey (BGR), whereas the 1:50,000 (BK50) soil map was produced by the State Department of Geology of North-Rhine Westfalia. Both data sets have the same structure and the soils are described by the same classification system. Each soil unit is described by one data set with up to eight layers. The soil hydraulic parameters were calculated using equations provided by the German Soil mapping instructions (BGR – German Geological Survey 1996). The relevant parameter sets had to be transformed from the German classification system into SWAT compatible units. Land use information was based on CORINE Land Cover 1994 (Corine – Co-ordination of Information on the Environment, Statistisches Bundesamt, 1994). The data set is available in three aggregation levels. Both the level I data with five land use types and level II data with 24 land use types were used in the investigation area. The climatic data were obtained from the German Weather Survey (DWD). The Regional Department of the Environment in Muenster and Bielefeld provided streamflow data for ten gauges.

Table 2. Different input data sets.

Data set	Low resolution	High resolution
DEM	200m grid	50m grid
Soil	BÜK1000 – 1:1,000,000 21 soil types	BK50 1:50,000 854 soil types
Land use	Corine Land Cover – aggregated 5 land use types	Corine Land Cover – disaggregated 24 land use types
Climate	All regional stations of the German weather survey 5 full equipped 21 precipitation stations	All regional station of the German weather survey 5 full equipped 21 precipitation stations
Streams	Aggregated river system	Complete river system up to 10 stream orders

Pre-Processing and Simulation

At first, the same parameter adjustments were used for both watershed delineations by using the AVSWAT2000 pre-processing tool. Both delineations were made with the “Burn in” option. The digital stream networks used for this option were obtained from one source, the State Department of the Environment of North-Rhine Wesfalia. For consistency, the stream network in two aggregation levels was used. For simulations with the high resolution input data, the full network with up to ten stream orders was used. To simulate the hydrological conditions based on data with a low resolution, a network that included only the main tributaries was used. The definition of the subbasins was completed by choosing a value of 4,000 ha as the threshold area. The same gauges, used as subbasin outlets (Table 1), and the available sewage plants, identified as inlets into the subbasins in the simulation, were included in both simulations in order to achieve comparability. The use of different data sets resulted in some differences in the catchment characteristics for the simulation (Table 3). This could be one reason for simulation uncertainties based on the input data resolution or quality. The sizes of the delineated catchments differed only slightly. However, the differences in the number of subbasins, and thus the internal differentiation, was a consequence of different subbasin sizes. This is important for the estimation of hydrological characteristics such as specific runoff. The wide difference in numbers of Hydrological Response Units (HRU) in the two simulations gives an idea of the effect of input data resolution on the effort of calibration work (Table 3).

Table 3. Delineated characteristics of the river basin.

	Low resolution	High Resolution	Difference
Catchment area in km²	3708	3785	77
Number of sub-basins	62	76	10
Number of HRUs	387	1950	1563

The results of the automatic watershed delineation with both DEMs come close to the catchment size stated by the water management authorities. In contrast, the gauge-related subbasins inside the catchment were delineated much better using the DEM with a higher spatial resolution (Table 4).

Table 4. Comparison of delineated gauge-related sub-basins of the Ems River Basin based on different resolution input data.

			Low resolution input data		High resolution input data	
Gauge	**River**	**Area km²**	**Area in km²**	**Diff in %**	**Area in km²**	**Diff in %**
Ahlen	Werse	46.6	46.4	-0.43	47.2	1.29
Albersloh	Werse	321.6	298.8	-7.09	360.0	11.94
Rheda	Ems	342.6	278.4	-18.74	340.7	-0.56
Ladbergen	Glane	350.0	132.6	-62.11	173.0	-50.57
Roxel	Münst. Aa	88.2	81.6	-7.48	87.6	-0.68
Coermühle	Münst. Aa	152.3	139.4	-8.47	147.7	-3.02
Einen	Ems	1,485.8	1,502.3	1.11	1,582.6	6.52
Haus Langen	Ems	1,616.0	2,148.3	32.94	1,630.2	0.89
Haskenau	Ems	1,845.0	2,750.9	49.10	1,816.7	-1.53
Rheine	Ems	3,740.0	3,695.3	-1.20	3,784.8	1.20

The existing SWAT parameter database (default) of land use types was adapted to the European conditions using the plant parameter database of Breuer et al (2003). On the basis of a sensitivity analysis using an artificial catchment (Liersch, 2005, Volk & Schmidt, 2004), model calibrations were made manually for the period of 1992 and 1993. The validation period ranged between the years 1994 and 2000. Parameter settings for the swat.gw, swat.sub, and swat.bsn were made with the same values for both simulation types.

Results

This study focused on the comparison of simulation results using two input data sets with different spatial resolutions. The simulation results were compared to streamflow data of ten gauges in the catchment. Moreover, the potential effect of catchment size on the simulation efficiency was investigated. By using the input data with the low resolution, sound simulation results were obtained for mean monthly runoff at the ten gauges of the Upper Ems Basin. The results are presented in Figure 2, which shows the observed and simulated runoff values at the Rheda (342.6 km²) and Rheine (3,740 km²) gauges. A problem arose with the description of the total runoff values where the full equivalency could not be reached.

a) 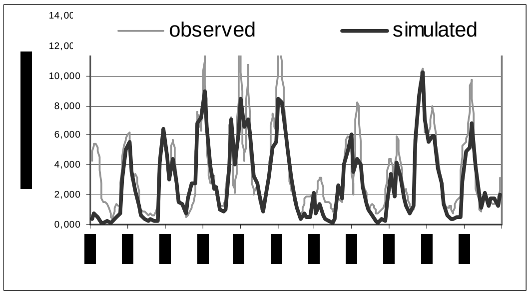

b) 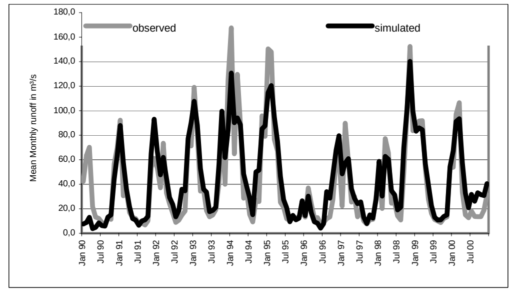

Figure 2. Observed and simulated mean monthly runoff at the Rheda (a) and Rheine (b) gauges (1990 – 2000).

Correlation analysis and coefficient of efficiency (Nash & Sutcliff, 1970) have been used to evaluate the simulation. Results are considered to be good for values $E > 0.75$, while for values of E between *0.75* and *0.36*, the simulation results are considered to be satisfactory (Motovilov et al., 1999). These quality measures have also been used for the analysis of potential effects of catchment size on the simulation results. The goal of the latter issue was to find out applicability limitations of SWAT with respect to the (small) size of catchments.

The efficiencies of the monthly simulations using the input data with low resolutions indicate a good correspondence between simulated and measured data (Table 5). This observation serves as an example for simulations with different input data at different time-steps. A comparison of the efficiencies with the basin sizes shows an interesting relationship. In the large catchments, the model efficiency is higher than in the small ones. This could be caused by: 1) The fact that in large catchments the runoff dynamics or process response is less intensive than in small catchments. 2) SWAT was developed for predictions in meso-scale to macro-scale river basins and might not optimally represent the dynamics of the small basins. The interesting point here was finding a corresponding threshold value of basin size under which SWAT was no longer suitable.

Table 5. Mean runoff and model efficiency of monthly simulations with low input data resolution.

Gauge	Area km²		Mean runoff obs.	Mean runoff calc.	Diff rel in %	Nash-Suttcliff efficiency	r	r²	Relative volume error
Einen	1502,3	cal	15,881	17,635	11	0,922	0,970	0,940	104,280
		val				0,801	0,908	0,824	106,257
Rheda	278,4	cal	3,511	3,019	14	0,836	0,943	0,890	84,951
		val				0,746	0,892	0,796	82,096
Haus Langen	2148,3	cal	17,086	18,477	8,1	0,892	0,949	0,900	102,020
		val				0,775	0,933	0,870	114,023
Haskenau	2750,9	cal	18,869	19,588	3,8	0,939	0,970	0,940	100,217
		val				0,826	0,910	0,827	99,701
Rheine	3695,3	cal	41,062	46,185	12,5	0,945	0,978	0,957	106,672
		val				0,816	0,907	0,823	107,100
Ahlen	46,4	cal	0,600	0,494	17,7	0,792	0,939	0,882	80,681
		val				0,730	0,900	0,809	78,054
Albersloh	298,8	cal	3,021	3,230	6,9	0,861	0,934	0,872	99,081
		val				0,715	0,848	0,720	100,480

Roxel	81,6	cal	0,874	1,150	31,5	0,807	0,940	0,883	123,959
		val				0,652	0,834	0,696	124,003
Coermühle	139,4	cal	1,382	1,867	35,1	0,828	0,966	0,934	128,587
		val				0,703	0,878	0,771	128,763
Ladbergen	132,6	cal	2,162	1,856	14,2	0,876	0,965	0,930	87,822
		val				0,737	0,902	0,813	81,141

As a consequence, a critical basin size for an adequate simulation with SWAT was identified. Figure 3 shows the relationship between the basin size and the Nash-Sutcliff-efficiencies for the monthly simulations. On the basis of only a few numbers of basins one can observe a break in the curve at an area of approximately 300 to 500 km². This is caused by the combination of the low resolution input data used and the insufficient capability of SWAT to simulate the process dynamics in small catchments.

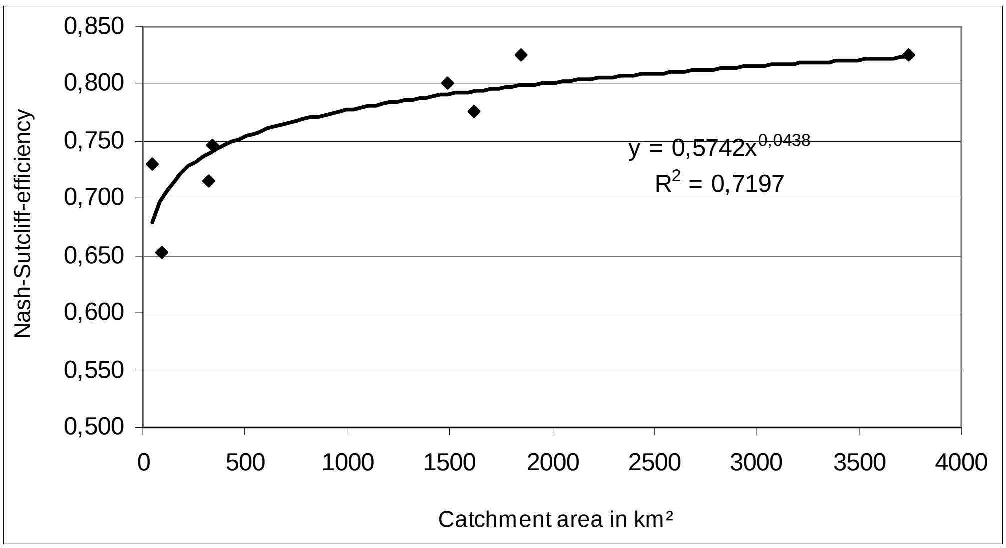

Figure 3. Relationship between basin size and model efficiency (monthly simulations) using input data with a low resolution.

The simulations using the high resolution input data involved much more work and time. This was caused by the higher number of process units (subbasins, HRUs) compared to the low resolution input data (Table 3). Again the relationship between catchment size and Nash-Sutcliff-Efficiency was investigated. Figure 4 shows the same behaviour as observed with the lower resolution input data. The model efficiency increases with the size of the catchments.

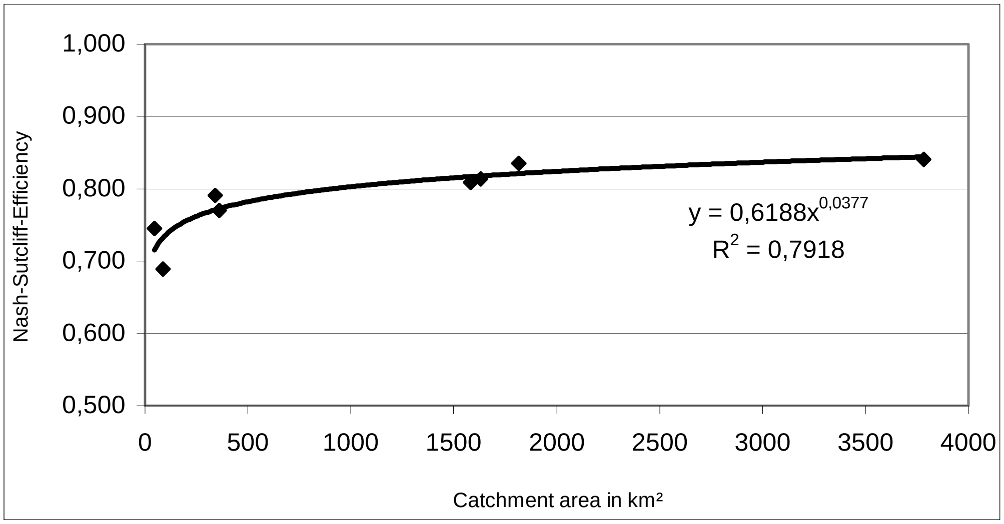

Figure 4. Relation between catchment size and model efficiency for monthly simulations based on high resolution input data.

It can be shown again that the curve has a break with a basin area size of approximately 300 to 500 km². The result provides additional support for the suitability of SWAT for a certain basin size. Even with the use of input data with higher resolutions (mostly of a scale of 1:50,000), efficient simulations could not be achieved with basins smaller than 300 to 500 km².

In addition, the effect of input data resolution on the efficiency of simulation at different time-steps should be addressed. The following figures (Figure 5 and Figure 6) show the model efficiencies, as well as r and r² at a monthly time-step (m) with low (lr) and high (hr) resolution input data.

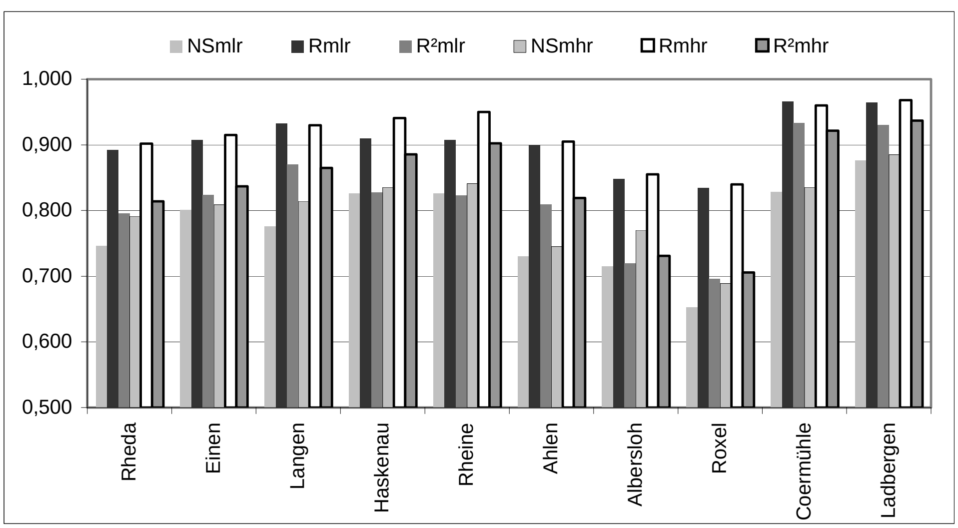

Figure 5. Comparison of the efficiencies of simulations at a monthly time-step with different resolutions of input data.

Based on the monthly time-step, only slightly higher efficiencies were achieved using the high resolution input data. Keeping in mind the increased time and work associated with model parameterization and calibration efforts with many more process units, the results fall short of our expectations. Considering the model efficiencies with the daily simulations (Figure 6), the situation is different. With the higher resolution input data, much better results are achieved as indicated by higher model efficiencies.

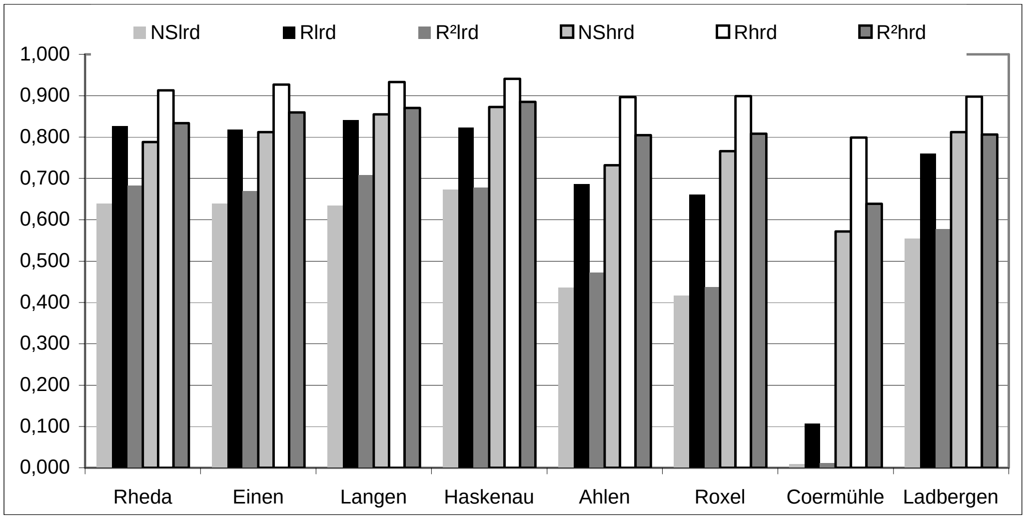

Figure 6, Comparison of efficiency values of simulations at a monthly time-step with different resolution input data.

Conclusions

The results of this study have shown that the input data resolution and the basin size have considerable influences on the model efficiencies, and thus the quality of the SWAT simulations. Simulations using input data with different resolutions have shown that the suitability of SWAT is problematic in basins with sizes less than 300 to 500 km². In addition, model efficiencies for monthly simulations are in the same range with the input data of both high and low resolutions and indicate that the use of high resolution data is not necessary in all cases.

As a consequence, intense data analysis and a target/goal oriented simulation procedure is recommended before using SWAT for the prediction of rainfall-runoff dynamics and land use scenarios. The needed resolution depends on the required information of a certain spatial planning or river basin management level. For instance, aggregated time-steps in large river basins produced good simulation quality using low resolution input data. Such results are sufficient to indicate areas with environmental risks, or hot spots. To predict high resolution dynamics and process quantification, the use of the highest scale-adequate input data resolution available is recommended.

Acknowledgements

The FLUMAGIS research project is funded by the Ministry of Education and Science (BMBF) in Germany.

References

Arnold, J.G., P.M. Allen and G. Bernhardt (1993): A comprehensive surface-groundwater flow model. J. Hydrology 142: 47-69.

BGR – Bundesanstalt für Geowissenschaften und Rohstoffe & GLA – Geologische Landesämter (Eds., 1996): Bodenkundliche Kartieranleitung, 4. Ed., Hannover, 392 pp.

Breuer, L., K. Eckhardt and H.-G. Frede (2003): Plant parameter values formodels in temperate climates. - Ecological modelling 169: 237–293.

Di Luzio, M., R. Srinivasan, J.G. Arnold and S.L. Neitsch (2002): ArcView Interface for SWAT2000. User´s Guide. GSWRL Report 02-03, BRC Report 2-07. Temple, Texas, USA.

Gretzschel, O., G. Schmidt, M. Uhl and M. Volk (2004): Der Umgang mit der Skalenproblematik bei der Modellierung des Wasserhaushaltes im Projekt FLUMAGIS. – In: Bronstert, A., A. Thieken, B. Merz, M. Rode and L. Menzel (Hrsg., 2004): Wasser- und Stofftransport in heterogenen Einzugsgebieten. - Forum für Hydrologie und Wasserwirtschaft 5, 04: 105-108.

Liang, X., J. Guo and L.R. Leung (2004): Assessment of the effects of spatial resolutions on daily water flux simulation. – J. Hydrology 298: 287–310.

Liersch, S. (2005): Auswirkungen von Landnutzungsänderungen und umweltgerechten Bewirtschaftungsmethoden auf den Wasser- und Stoffhaushalt des Einzugsgebietes der Ems in Nordrhein-Westfalen. – Diploma thesis (unpublished), University of Potsdam.

Motovilov, Y.G., L. Gottschalk, K. Engeland and A. Rohde (1999): Validation of a distributed hydrological model against spatial observations. Agricultural and Forest Meteorology 98: 257-277.

Muttiah, R. S. and R.A. Wurbs (2002): Scale dependent soil and climate variability effects on watershed water balance of the SWAT model. – J. Hydrology 256: 264-285

Nash, J.E. and J.V. Sutcliff (1970): River flow forecasting through conceptual models, Part I – A discussion of principles. - J. Hydrology 10: 228-250.

Neitsch, S.L., J.G. Arnold, J.R. Kiniry, R. Srinivasan and J.R. Williams (2002): Soil and Water Assessment Tool. User´s Manual. Version 2000. GSWRL Report 02-02, BRC Report 2-06. Temple, Texas, USA.

Quinn, P. (2004): Scale appropriate modelling: representing sause-and-effect relationships in nitrate pollution at the catchment scale for the purpose of catchment scale planning. – J. Hydrology 291: 197–217.

SO – NRW Statistics Office of Nordrhine Westfalia (2004): Lifestock numbers in nordrhine Westfalia from 1990 to 2001, database published in the internet.

Volk, M. and G. Schmidt (2004): The model concept in the project FLUMAGIS: scales, simulation and integration. - Texas Water Resources Institute Technical Report 266: 236–248.

Application of Water Management Models to Mediterranean Temporary Rivers

Antonio Lo Porto[1*], Anna Maria De Girolamo[1], Filomena De Luca[1], Giuseppe Pappagallo[1]
[1]National Research Council, Water Research Institute (CNR-IRSA), Via F. De Blasio n.5, 70123 Bari, Italy. Email: loporto@area.ba.cnr.it

Abstract

The application of water quality models to areas characterized by periods without runoff and extreme first flush effects with the beginning of the rain period is the aim of the EU project TempQsim (EVK1-CT2002-00112). More specifically, it deals with the evaluation and the improvement of water quality models for temporary streams in Southern European catchments. To this aim, existing water quality models have been tested to evaluate their suitability to describe the dynamics of temporary streams. Within this research area, our work deals with the application of the Soil and Water Assessment Tool (SWAT-2000) model to a Sardinian catchment, Rio Mulargia. The main objective is to observe and accurately predict movements of sediments and nutrients during water routing. We focus particularly on the first flush events in order to highlight the specific features that must be added to the model to make the results more reliable in these situations. The SWAT model has been applied to the Mulargia Catchment where available rain gauge data were not representative of the watershed, and the simulation gave results that matched measured data satisfactorily.

In summary, the SWAT model, applied to a truly intermittent river, such as Mulargia, proved capable of simulating the behaviour of the catchment and of most of the processes therein. Nevertheless, in this paper some limitations of the model have been highlighted and discussed in detail.

Introduction

The Mediterranean region is a bioclimatic, morphogenetic, and hydrologic transition between the temperate, humid northern latitudes and the dry latitudes to the south. Despite the diversity of environments included in the term "Mediterranean" (Mateu, 1988), it still denotes a particular combination of complex climatic, structural, and geomorphological factors.

In this context, intermittent and ephemeral streams are common fluvial systems. Rainfall and runoff processes in such streams have been studied in arid, semiarid, and Mediterranean zones (Osborn and Lane, 1969; Karst, 1960; Rodier, 1981; De Vera, 1984; Schick, 1988; Sorriso-Valvo et al., 1995; Reid and Frostick, 1997; Martýnez-Mena et al. 1998; Meirovich et al., 1998; Shentsis et al., 1999; Lange et al., 1999; etc.).

The importance of the effect of spatial and temporal variability of rainfall on runoff has been described by many authors at many scales (Osborn and Lane, 1969; Woolhiser and Goodrich, 1988; Nouh, 1990; Faures et al., 1995; Goodrich et al., 1995). For small basins, it has a significant influence over peak discharge and total runoff (Osborn, 1984), which explains the difficulties experienced in trying to design models that accurately simulate the peak flows (Nouh, 1990).

To this end, the goal of the TempQsim project is to test existing water quality models to evaluate their suitability to describe the dynamics of temporary streams and to improve the efficiency of tools for integrated water management in the semiarid Mediterranean river catchments.

This paper describes the application of the Soil and Water Assessment Tool (SWAT-2000) model to the Rio Mulargia Catchment. SWAT, after calibration and validation, was used to estimate hydrological balance, quantify the different components, and evaluate the loads of sediments and nutrients that reach the outlet of the watershed. This study focused particularly on the first flush events in order to highlight the specific features that must be added to the model to make the results more reliable..

Watershed Description

Rio Mulargia is an important tributary of the Flumendosa River. Together with the reservoirs built in the catchment, this constitutes a fundamental water resource for urban, industrial, and agricultural uses in the southeastern Sardinian Region. The morphology of the catchment reflects the very complex geology of the area and most of the rocky formations share remote origins. The actions of climatic agents and erosion have been bevelling the roughness to reach the actual softened shapes of the formations. Quite commonly carbonaceous layers come to the light intercalated with volcanic matter of various petrographies that give origin to the lavic-tufaceus formations (Commissione delle Comunità Europee et al., 1993). Surface cover is constituted mostly of sandy-loam and clay soils whose thickness is variable and sometimes reaches or exceeds a meter in depth.

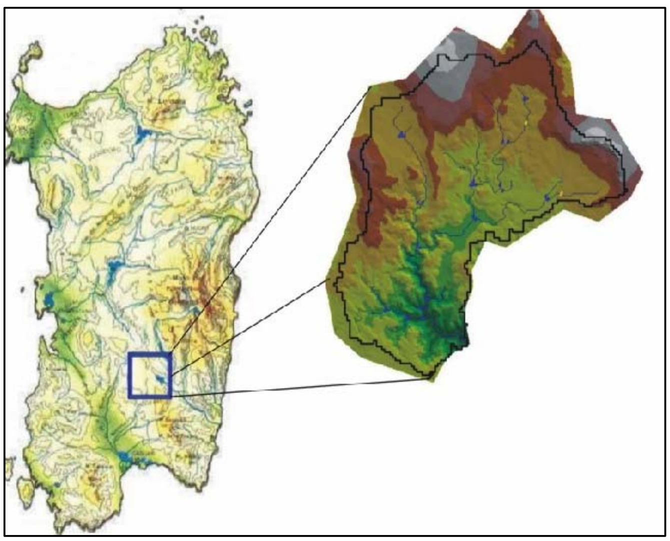

Figure 1: Mulargia Catchment (Sardinia)

The landscape in the Mulargia Catchment constitutes a moderately anthropized part of the Flumendosa Catchment. Most of the surface is used for pasture with some negligible arable land (mostly vineyard); also important is the presence of cattle and ovine breeding that is still managed in a traditional way (animals are allowed to freely move in open pastures) on both natural prairies and cultivated pastures.

In the catchment, industrial settlements are negligible except for one cheese factory and one slaughter-house. Human settlements are restricted to three small villages whose overall population reaches a maximum of 4,500. Wastewater is treated in two treatment plants (all up to a secondary stage) that discharge into the river network. The catchment covers an area of 6,476 ha and spans an elevation range from 250 to 750 m (Figure 1). The river network has an overall length of around 44 km, while the distance from the origin of the stream to the outlet in the reservoir is around 15 km. The climate in the area is characterized by an average annual rainfall of around 530 mm, mostly concentrated in autumn and winter with usually very dry summers. It must be noted, however, that there is great variability in space and time. In fact, the region receives a good deal of storms that account for the concentration of rain amount in few events and, consequently, for the rather pulse flow in the stream. Spatial variability is responsible for the occurrence of localized rain events that are not traced by most of the rain gauges in the area. This also accounts for the relatively low representation of each rain gauge. Several rain stations spread across the landscape are needed to get a meaningful picture of the rainfall in the catchment.

Temperature behaviour is typically Mediterranean, with the maximum reaching 40°C and the minimum rarely below 0°C. The average daily temperature drift is around 10°C and it is usually higher in summer.

Data Availability

Most of the data have been obtained through a close cooperation with the local end user "Ente Autonomo Flumendosa" (EAF, a public administration for the management of water resources in the Flumendosa Watershed), as well as with the other Italian partner, Research and Training Centre "Hydrocontrol" that took part either in the data gathering or in the model database set-up.

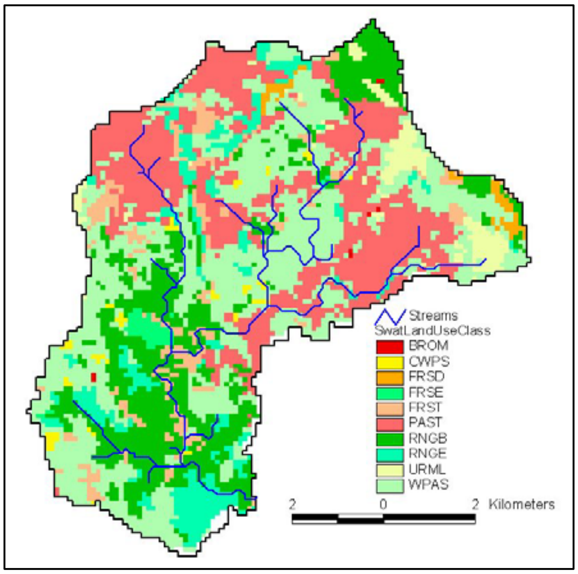

Figure 2: Land use map.

The DEM is in a raster format with a grid resolution of 100 m, which has been clipped from a regional coverage. Originally, the elevation data were available as a point vector file where z-values were present every 80 m along both latitude and longitude. These values were used to obtain a TIN that was eventually converted to a raster format and resampled to a 100 m cell size.

The land use map (Figure 2) has also been clipped from a regional vector coverage (released in 2003) whose legend is based on the CORINE level 4 legend. The original legend entries were reclassified and, in some cases, aggregated to conform to the land use database present in the SWAT model (the watershed results included 10 land use classes.)

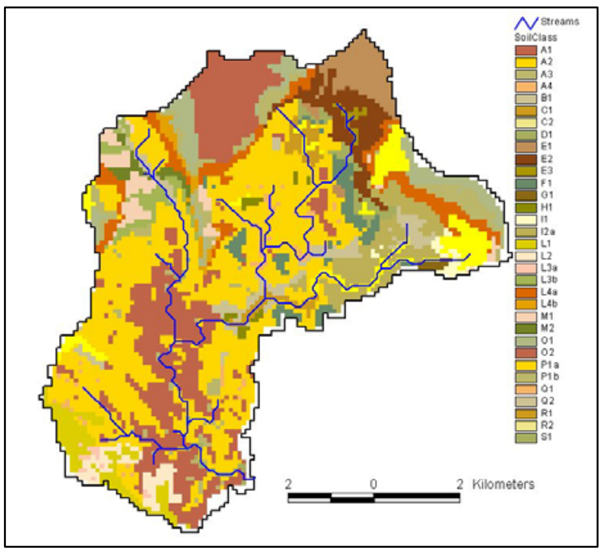

Figure 3: Soil classes.

The soil map (Figure 3) was gathered from EAF in vector form covering the entire Flumendosa Watershed. The results showed that a total of 32 soil classes were present in the Mulargia Catchment. Together with the map, a georeferenced database was made available containing data for several soil samples taken in the field. All soil sample data sets relative to the Mulargia Watershed were sorted and used to derive the values for the physical-chemical parameters needed to fill the SWAT soil database. In the case of some parameters (bulk density and K sat.), transfer functions were used, adopting the specific software "Soil Water Characteristics" developed by the USDA-ARS and the Washington State University (Saxton, version 6.1.51) for texture, organic matter, skeleton, and salinity. Daily climatic data were obtained for several stations in the area; only those having a near-complete time series of at least 10 years were retained. After comparison of rain records against measured flow, the selection was restricted to only three stations located along the watershed border. Daily precipitation values from 1989 to 2004 were obtained for those stations, whereas daily maximum and minimum temperature, solar radiation, wind speed, and relative humidity were available for only one station. Flow and pollutant load from the wastewater treatment plants of Nurri and Orroli were available only as average daily values and were considered constant in the absence of additional data.

Information on agricultural management practices, obtained by local farmers through the colleagues of Hydrocontrol, was included in the environmental database regarding fertilization (date, type, and amount) tillage, and cropping.

Methodology

The SWAT-2000 model with an ArcView interface was used in this study. The model was run on a daily time-step from January 1992 to April 2004. Since it is convenient to allow the model to “warm up” to reach acceptable and stable estimations for some parameters when initial values are not available or filled as first guesses, climate data for the first five years were used to represent data for the time period from 1987-1991. However, results were reported only for the 1992-2004 time period.

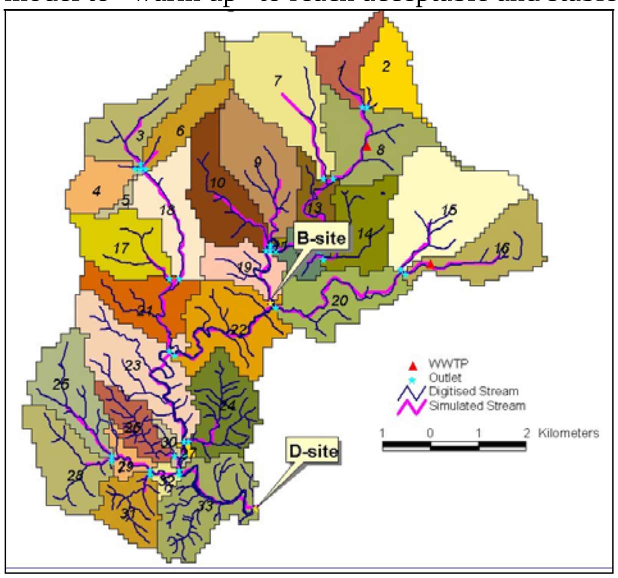

Figure 4: Subcatchments.

Since some holes were present in the climate data, the weather generator included in SWAT was used, based on statistical values (average monthly values for rain, maximum and minimum temperature, standard deviation, skew coefficient, probability of wet day following a dry day in the month, probability of wet day following a wet day, average number of rainy days in the month), and computed on the basis of available daily values.

The modelled catchment was delineated allowing the GIS interface to compute the river network and the catchment boundaries on the basis of the DEM. To achieve better results, the “burn in” option (available in the interface) for digitised river networks was used to “force” the GIS to trace a computed network on the catchment. The model was allowed to trace subbasin boundaries and to locate subcatchment outlets on the basis of geomorphology. However, to force the model to also compute outputs for the sites where Hydrocontrol takes water quality and flow measures, two outlets were added by hand: one (B-site) in the northern part of the river network after the WWTPs discharge, the second (D-site), set as the final outlet of the catchment, corresponding at the inlet of the Mulargia River into the reservoir.

The interface located a total of 33 subcatchments (Figure 4). The land area in each subbasin was divided into hydrologic response units (HRUs) which are portions of subbasins with unique land use/management/soil attributes. Next, for the delineation of these HRUs, the interface was instructed to retain only land uses and soil classes that accounted for a minimum of 35 and 10 percent of each subbasin’s surface, respectively. A total of 92 HRUs were obtained.

Measured water quality and flow were available for the D-site (1992-2004) as daily values for flow and longer time steps for water quality. Due to the varied lengths of the time series and the lack of flow and water quality data for the B-site, the idea of adopting a “split in space” approach for calibration-validation was discarded. A “split in time” approach was preferred, in which measured values for the D-site were used and the model was calibrated for the period 1992-1997 and validated for the period 2003-2004. Hydrological calibration was attempted, operating on the following parameters: curve number (CN2), soil available water capacity (SOL_AWC), soil evaporation compensation factor (ESCO), groundwater “revap” coefficient (GW_REVAP), the threshold depth of water in the shallow aquifer for “revap” to occur (REVAPMN), threshold depth of water in the shallow aquifer required for baseflow to occur (GWQMN), transmission losses/values for channel hydraulic conductivity (CH_K), and the baseflow alpha factor (ALPHA_BF).

Since water quality data were available only for the validation period, a rough water quality calibration was done referring to data of some peaks in that period. Calibration was based on several parameters such as the initial concentration of nutrients in the soil (SOL_NO3, SOL_ORG, SOL_MIN), the percolation coefficients (NPERCO, PPERCO), the fraction of fertilizer applied to the top 10 mm of soil (FERT_LY1), and the biological mixing efficiency (BIOMIX). Regarding sediment, the calibration was based on parameters such as loads from each subbasin (USLE_P and BIOMIX) and the channel erodibility factor (CH_EROD).

Results and Discussion

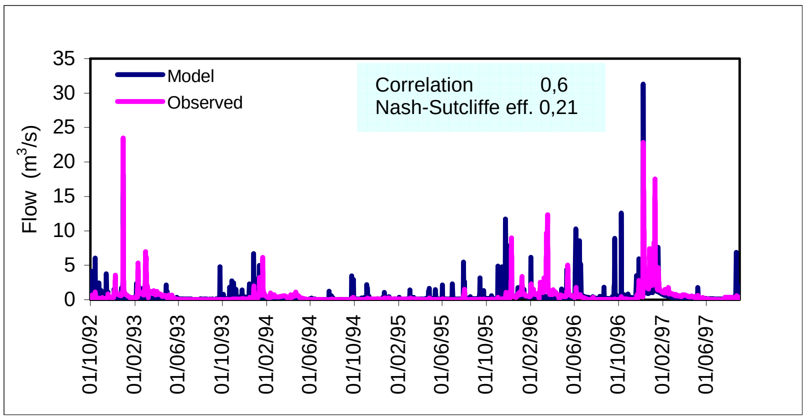

Figure 5: Measured vs. simulated flow for the calibration period.

Simulated flow for the calibration period is reported in Figure 5. It can be noted that during that period the simulated flow, while roughly matching the shape of the measured flow, shows many more peaks than those existing in the recorded data. This is due to the low representation of the available rainfall recording stations because of high spatial variability of the precipitation. This situation notwithstanding, the overall average flow is approached and the order difference of 20% is well below the error threshold in measurements with such a low flow. The correlation is acceptable and the Nash Sutcliffe efficiency coefficient (Nash and Sutcliffe, 1970) is rather low, however it is positive and in line with other values obtained in previous experiences in semi-arid catchments.

After calibration, the model was run for the period September 2003 – April 2004 for validation. Simulated flow is reported in Figure 6 against the measured one. The plot shows that modelled flow greatly overlays the measured line, few peaks are overestimated, and none are missed. The simulation results are quite satisfactory. The correlation is higher and the

Nash Sutcliffe coefficient is more than doubled. Simulated average flow exactly matched the measured flow, while looking at seasonal values, the model slightly overestimates flow in summer and autumn, and underestimates it in winter and spring. This is consistent with what occurred during the calibration period. In Table 1, yearly averages for the water balance components are reported together with an overall average for the simulation period, while Figure 7 shows the monthly averages. It must be stated that the term "baseflow" also includes the contribution of the WWTPs that accounts for around 5% of the water budget. It can be concluded that the water cycle is dominated by evapotranspiration while water yield only accounts for 1/4 of the available budget and percolation for less than 1/5. More than half of the water budget is lost through evapotranspiration. Considering water quality, the average monthly loads for the relevant parameters are reported in Figure 8. Sediment and particle-bound nutrients show maximum values in January and September, while soluble nutrients (NO3 and soluble P) reach their maximum load in November and December. This behaviour is linked with that of precipitation. In fact, in November and December when rainfall reaches its maximum, soluble nutrients are washed from soils, while sediment bound nutrients show maximum load in September probably because of the erosive impact of the first flush events. The average concentrations of nutrients are in accord with values of literature (Commissione delle Comunità Europee et al., 1993).

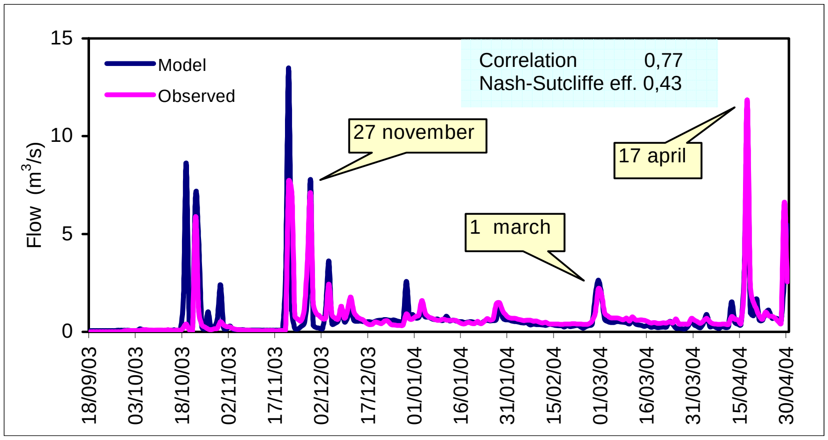

Figure 6: Measured vs. simulated flow for the validation period.

Table 1: Yearly averages of simulated water balance.

Year	Prec	Surface flow	Lateral flow	Baseflow	Percolation	Soil water	Actual ET	Potential ET	Water yield
	mm	mm	mm	mm	mm	mm	mm	mm	mm
1992	575	122	10	12	219	51	214	793	144
1993	512	68	11	39	215	49	220	635	118
1994	358	40	6	14	101	41	219	889	60
1995	510	93	9	35	203	50	196	539	136
1996	838	204	17	138	382	51	235	569	358
1997	568	106	12	138	259	49	194	573	256
1998	421	32	8	51	132	46	252	1231	91
1999	592	95	11	63	241	48	242	582	169
2000	528	94	9	42	218	52	202	859	145
2001	379	30	9	94	137	49	207	928	133
2002	628	100	11	53	236	49	280	869	164
2003	725	166	14	121	326	51	216	1123	301
2004*	305	45	7	75	143	29	133	381	127
*Jan-May									
Average	**553**	**96**	**11**	**67**	**222**	**49**	**223**	**799**	**173**

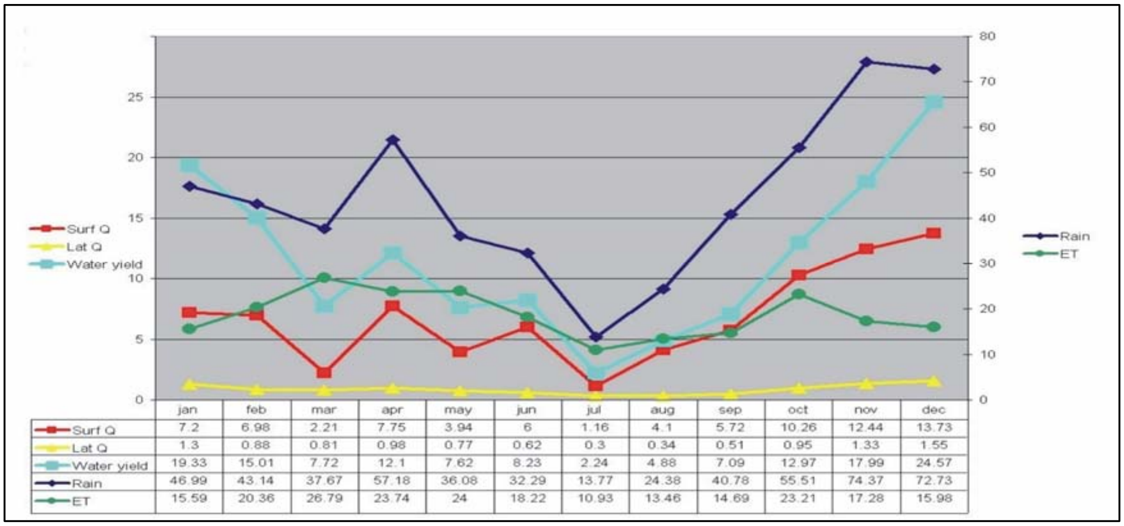

Figure 7: Average monthly water balance.

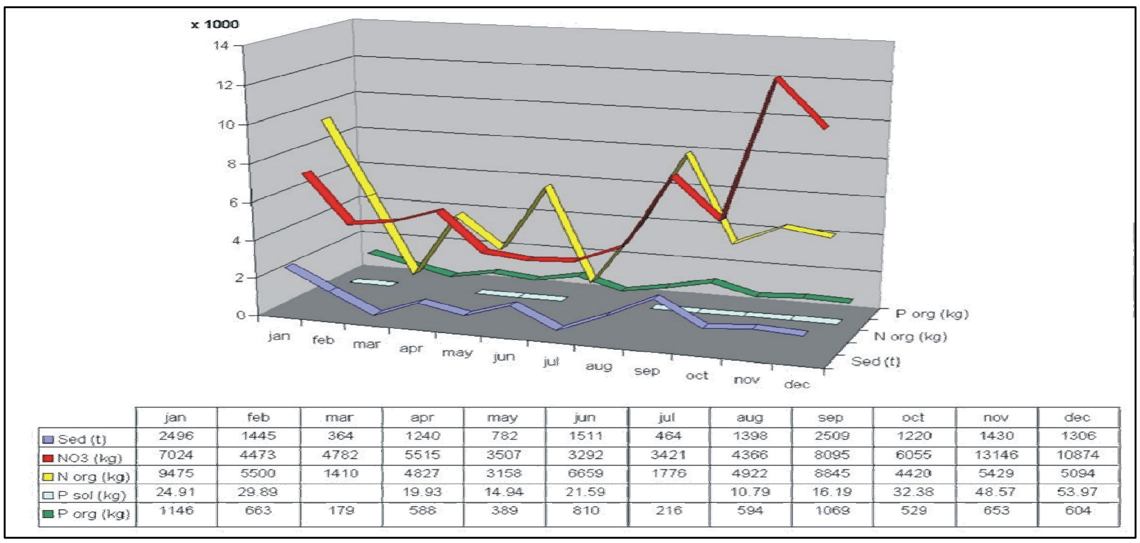

Figure 8: Average monthly load.

To describe the catchment behaviour in correspondence with different flow regimes, flow and pollutant transfer in the period September 2003- May 2004 have been separated into low-flow and high-flow periods. Table 2 shows that the flood events are responsible for half of the flow in all the period while covering only 1/5 of the days. Load generated by floods in sediment, total N and total P is little more that 50% of the load generated for the entire period. It can be concluded that floods are about four times more productive in water and sediment yield, five times in total P load, and six times in total N load with respect to low-flow periods. The model estimation agrees with the measurements conducted by the Research and Training Centre “Hydrocontrol” at the outlet D.

Table 2: Load from high-flow and low-flow in 2003-2004.

	Water Yield Mmc	%	days	%	SED ton	%	N TOT ton	%	P TOT ton	%
Low flow	8	50.0	207	80.5	15,945.5	48.6	84.5	38.7	6.8	45.7
High flow	8	50.0	50	19.5	16,887.8	51.4	134.0	61.3	8.1	54.3
Total	16		257		32,833.3		218.5		14.9	

SWAT gives nutrient and sediment loads produced for each subbasin and allows the creation of relative thematic maps. These are very useful to highlight areas that are determined to be polluted and to establish the associated soil/land use that produces the problem. In our case, the results demonstrate that the west side of the catchment contributes more to the pollutant load, while the upper north-east part is much more clean, despite the steeper slope and the presence in that area of two WWTPs.

An in depth look at three flood events recorded in the D-site and properly selected in the validation period provides further insight. The flood of November 27, 2003 came after another big storm, and was selected as a peak event in a wet period, while the peaks of March 1, 2003 and April 17, 2004 were selected to represent floods of different weight in rather dry periods. For each flood a comparison has been made between measurements and model outputs for water flow and for pollutants, both in terms of concentration and load. One of these comparisons is reported in Figure 9.

Figure 9: Flood events of 11/27/03, 03/01/03 and 4/17/04 (flow and loads).

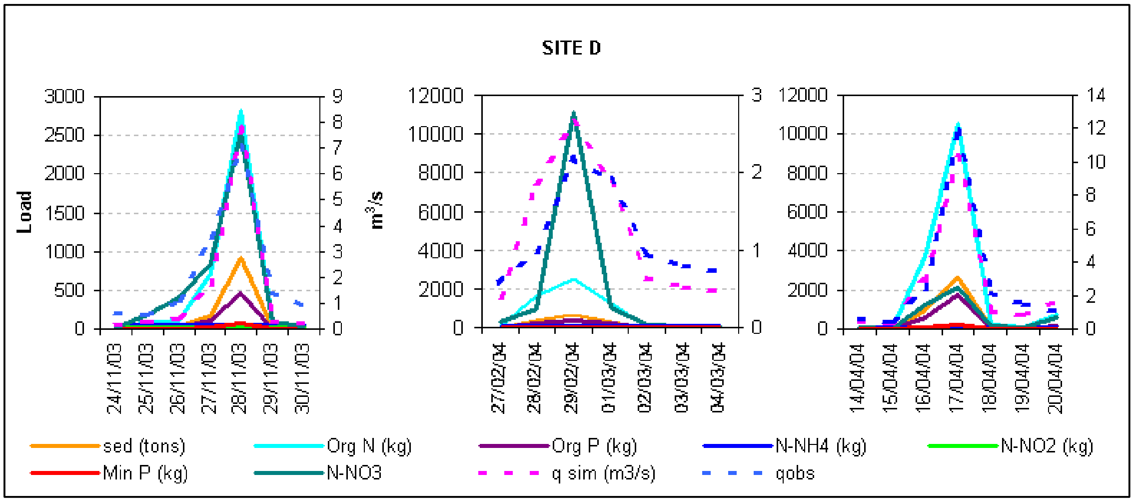

Table 3. Simulated and measured loads.

	27 november 2003		1 march 2003		17 april 2004	
	simulated	*observed*	*simulated*	*observed*	*simulated*	*observed*
Sed (tons)	170	240	320	165	2631	1400
Org P (kg)	112	270			1738	205
Org N (kg)	723	1350			10530	20000
N-NH4 (kg)	54	27	54	41	54	120
N-NO3 (kg)	845	2000	1063	500	2104	1600
Min P (kg)	19.5	90			227	184

Table 3 shows that there is a generally good agreement between the measured and simulated flow in all three flood events. Simulated concentrations and load are of the same magnitude order for all the parameters, and in most cases the values are very close. Sediment concentration was always overestimated, while nutrients concentration showed rather good agreement. Load agreement was somehow lower but in this case it must be considered that some measured values were missing, which can lead to incorrect load calculations in a river, like the one in this study, where flow and concentration (especially for sediment and particle bound nutrients) can vary by a factor of 100 in half an hour. In general, pollutants show concentration peaks that tend to precede flow peaks while load peaks closely follow floods. N-NH4 and N-NO2 show a different behaviour with respect to other nutrients, in that they show a concentrated decrease in correspondence to the flow peaks. This is very likely due to the fact that these compounds are not produced by a diffuse source but are present in WWTP effluent; hence they are diluted during flood events.

A difference can be noticed looking at the shape of the hydrogram of the event of November 27th compared to the others. The first one shows a less steep shape in the growing phase while the other two show a shape that can be defined symmetric to the first one: the steeper side is on the right side, during the decreasing phase. This could be explained on the basis of the different baseline conditions. In fact, the flood event of November happened in a wet period. The soil was probably not dry and with no crust, and the first rain water was allowed to infiltrate in the soil up to saturation, which differs from the floods events of March and April that took place after a period with no precipitation.

Conclusions

The SWAT model has been applied to the Mulargia Catchment, where available rain gauge data were not representative of the catchment. Notwithstanding this, the simulation gave results that satisfactorily matched measured data. Simulated nutrient concentrations and loads were also in agreement with measured values, even though the model had only been calibrated for hydrology. The model proved to be a very useful tool in assessing environmental pressure from human activities (mostly agriculture), and has huge potential from a management point of view, in that it allows the construction and evaluation of different land use scenarios or management strategies in soil and/or water resource uses. Including the crop growth module with an extensive crop parameter database into the model gives it the ability to simulate the water and nutrient cycle with precision. Nevertheless, the model, as applied to a truly intermittent river such as the Mulargia, was able to capture the behaviour of the catchment and of most of the processes therein. A better sediment simulation module could be useful since the current one is based on the Modified USLE that operates on daily rainfall. In semiarid regions, with sparse soil cover, rainfall, often concentrated in a few storms, can feature an intense erosion generating ability. A model that considers the same amount of rainfall diluted in 24 hours can consistently underestimate erosion and, consequently, sediment-bound nutrient movements. We believe that the model would benefit from additional features: 1) tools to generate geographically interpolated rainfall values that also consider differences in statistical distributions of rainfall in the different source measured stations and 2) tools for sub-daily steps in runoff, erosion, and routing calculation.

Acknowledgement

Model application was made possible by Hydrocontrol and EAF collaboration. Particularly we would like to thank Ludovica Diliberto and Giuseppe Canè (Hydrocontrol) for their help in catchment investigation and data availability, and Maria Antonietta Dessena and Paolo Botti (EAF) for their help in land knowledge.

References

A. M. Camarasa Belmonte, F. Segura Beltran, “Flood events in Mediterranean ephemeral streams (ramblas) in Valencia region, Spain”, Catena 45 (2001), pagg. 229–249

C. Santhi, J.G. Arnold, J.R. Williams, W.A. Dugas, R. Srinivasan, L.M. Hauck, “Validation of the SWAT model on large river basin with point and nonpoint sources”; Journal of the american water resources association (JAWRA); vol. 37 no. 5, october 2001 pagg. 1168-1188

William F. Hansen, "Identifying stream types and management implications", Forest Ecology and Management, 143 (2001) 39-46

Shadrack Mwakalila, "Estimation of stream flows of ungauged catchments for river basin management", Physics and Chemistry of the Earth, 28 (2003) 935–942

S. Jubb, P. Hulme, I. Guymer, J. Martin; "Considering the impact of intermittent discharges when modelling overflows", Wat. Sci. Tech. Vol. 38, No. 10, pp. 23-30, 1998 (IAWQ)

Commissione delle Comunità Europee, Regione Autonoma della Sardegna, Ente Autonomo Flumendosa, "Analisi sulle cause dell'eutrofizzazione delle acque del sistema idraulico Flumendosa – Campidano in relazione all'applicabilità della direttiva CEE sulle acque potabili", in Volume A Relazione generale, Cagliari, 1993, 307.

Donigian A. S., Huber W. C., Modeling Nonpoint Source Water Quality in Urban and Non-urban areas, EPA 68-03-3513, U. S. EPA, Athens, GA, 1990.

EAF, Studio dell'Idrologia Superficiale della Sardegna, 1996.

EAF, Carta dei suoli e Carta dell'uso del Suolo del sistema idrogeologico Flumendosa – Flumineddu – Mulargia, 2001.

EAF, TempQsim Project – Principal outlines of Flumendosa catchment, marzo 2004.

Hydrocontrol, Comunicazione personale dott.sa Diliberto L., Ing. Canè G., 2004.

Nash J. E., Sutcliffe J. V., "River flow forecasting through conceptual models", Journal of Hydrology, 10, 1970, 282-290.

Santhi C., Arnold J. G., Williams J. R., Dugas W. A., Srinivasan R., Hauck L. M., "Validation of the SWAT Model on a large river basin with point and nonpoint sources", Jounal of the American Water Resources Association, 37 (5) 2001.

Saxton K. E., "Soil Water Characteristics - Hydraulic Properties Calculator", version 6.1.51, USDA – Agricultural Research Service & Department of Biological System Engineering Washington State University.

Evaluation of the SWAT Model in a Small Experimental Mediterranean Basin

Feliciana Licciardello[1*], Raghavan Srinivasan[2] and Santo Marcello Zimbone[3]
[1*]Dipartimento di Ingegneria Agraria, Università degli Studi di Catania, Italy
[2] Spatial Science Laboratory, Texas A&M University, College Station, Texas, USA
[3] Dipartimento di Scienze e Tecnologie Agro-forestali e Ambientali, Università degli Studi Mediterranea di Reggio Calabria, Italy.

Abstract

This paper reports the results of an evaluation of SWAT (Soil and Water Assessment Tool) based on the recorded data at a small Sicilian mountainous basin, consisting of mainly pasture, which was equipped with monitoring systems ten years ago to further extend model testing to semi-arid Mediterranean conditions. The model showed a good capability in simulating surface runoff when the FAO Penman-Monteith equation was used to calculate the potential evapotranspiration. A reasonable simulation of 25 event suspended sediment yields was found after a calibration/validation process carried out by modifying the USLE-C factor.

Introduction

Water availability, quality, and sediment delivery have become challenging issues threatening food supply, security, human health, and natural ecosystems, especially in light of recent concerns over climate and/or land use changes (Nearing et al., 2004). In order to set-up decision support systems, many attempts have been made to develop predictive erosion models (Renard et al., 1982; Singh, 1995; Morgan et al., 2000). Despite the efforts, more work is needed to assess and improve model reliability in the different environmental contexts, and particularly in the semi-arid Mediterranean environment. The physically-based Soil and Water Assessment Tool (SWAT, Arnold et al., 1998) is a newly developed model that can be applied to large complex basins with varying soils, land use, and management conditions over long periods of time. Applications of SWAT in several countries have shown promising results in the assessment of runoff and sediment yield, mainly at annual and monthly scales (Tripathi et al., 2004), under a wide range of soil types, land uses, and climate conditions (Arnold and Fohrer, 2005). Some applications have been carried out in Mediterranean areas to predict transport of sediments and nutrients during water routing (Lo Porto et al., 2005), analyse forestry and agricultural impacts on water resources quality and quantity (Pappagallo et al., 2003), evaluate water budgets at the regional scale (Lorrai and Cau, 2005), and gain insight into the relative importance of the different flow components (Sulis et al., 2004). Only a few tests of SWAT have been performed in small basins. Model calibration at the daily scale in South Africa provided reasonable predictions of streamflow in a small natural grassland basin (0.68 km^2); the application of the calibrated model to a small afforested basin (1.95 km^2) highlighted an overestimation of streamflow due to the model not accounting for the increased evapotranspiration of maturing pine plantations (Govender and Everson, 2005). Regression analysis provided good results when observed and simulated

---

* ***Correspondence to:*** Feliciana Licciardello, Dipartimento di Ingegneria Agraria, Università degli Studi di Catania, Via Santa Sofia 100, 95123 Catania, Italy. Email: flicciar@unict.it

The contributions of the authors to this work can be considered equivalent.

daily surface runoff was compared for a small basin (0.53 km^2) in Texas after SWAT integration with a soil-cracking subroutine (Arnold et al., 2005). The effects of distributed input data resolution on the uncalibrated runoff and sediment yield were assessed in a small basin (21.3 km^2) in Mississippi (Di Luzio et al., 2005).

A monitoring campaign of a small Sicilian basin started in 1995 in order to contribute to the study of hydrological processes and the evaluation of event and continuous prediction of runoff and sediment yield models in a Mediterranean environment. This work aims to evaluate the SWAT model performance under investigated conditions based on the recorded data.

Materials and Methods

Main Characteristics of the Experimental Basin and 9-year Hydrological Response

The monitored basin, called Cannata, is an ephemeral mountainous tributary of the Flascio River in Eastern Sicily (37°53' N, 14°46' E). The basin covers about 1.3 km^2 between 903 m and 1,270 m a.s.l. with an average slope of 21%; the longest pathway is about 2.4 km, with an average slope of approximately 12%. The Kirpich concentration time (Chow et al., 1988) is 0.29 h. The equipment in the basin (Figure 1) includes a meteorological station (A), recording rainfall, air temperature, wind, solar radiation, and pan evaporation, two pluviometric stations (identified as B and C), as well as a hydrometrograph (D) connected to a runoff water automatic sampler (E) for the control of sediment concentration in the flow.

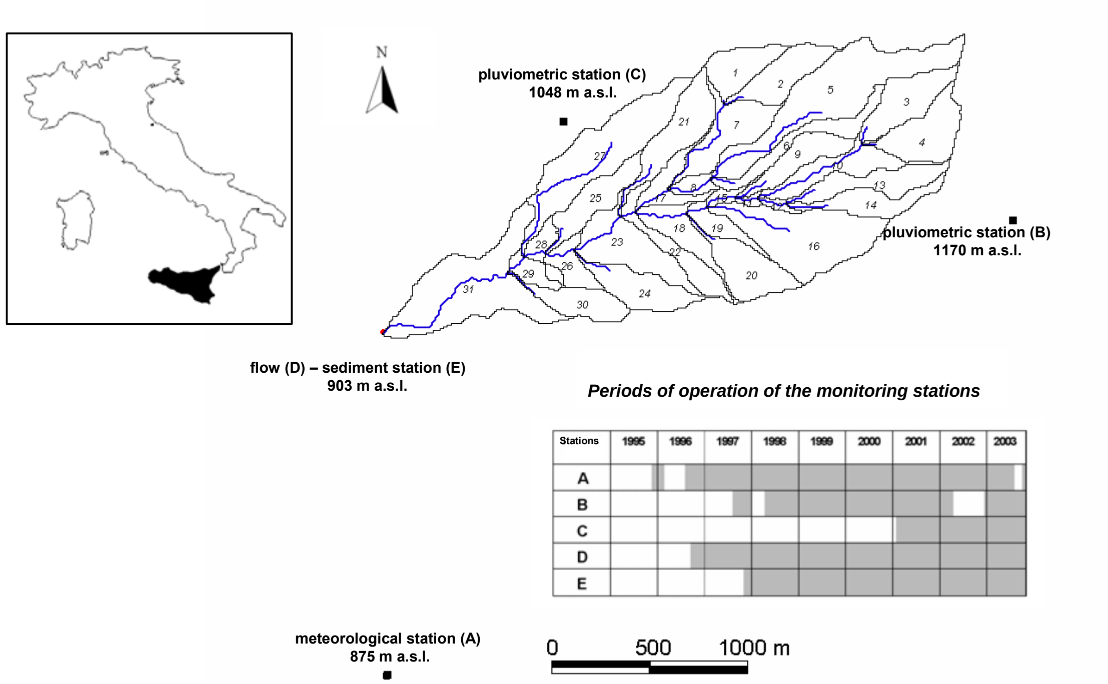

Figure 1. Layout of subdivision and hydrological network of the equipped basin in Sicily.

In a survey conducted in 1996, clay-loam (USDA classification) was identified as the dominant soil texture within the basin (63% of the 57 top-soil samples). The soil saturated hydraulic conductivity, measured by a Guelph permeameter (Eijkelkamp model 2800), is in the range 0.2 to 17.6 mm/h (n = 57; CV = 103%). Land use monitoring has highlighted the prevalence of pasture areas (ranging between 87% and 92% of the basin area) with different vegetation complexes (up to 15 species) and ground covers. In particular, four soil cover situations can be distinguished: a high-density herbaceous vegetation (eventually subjected to tillage operations); a medium density herbaceous vegetation; sparse shrubs; and cultivated winter wheat with a wheat-fallow rotation. More detailed information about basin characteristics and monitoring equipment are reported in a previous paper (Licciardello et al., 2001). The main results of the observations in the period 1996 – 2003 are the following:

- yearly rainfall (station A) between 574 and 895 mm mainly (80 - 90%) falling from September to March;
- yearly runoff between 30.7 mm (1998) and 365.8 mm (2003);
- yearly runoff coefficient (calculated as the ratio between total runoff and total rainfall as recorded by the station A) between 5% and 41%, with an average of 15%;
- occasional high differences in recorded rainfall events between the three gauges; as expected rainfall spatial variability lowers working on a monthly and yearly basis;
- event runoff volume ≥ 1mm with rainfall depths over 6.8 mm;
- maximum event runoff volume of 153 mm;
- generally flash response with a time lag in the range of 41.0 - 84.2 min, as resulting from the analysis of 4-event sample;
- event runoff coefficient characterized by a broad range of variation (up to 84%);
- a maximum recorded discharge of 3.4 m^3/s (2.6 $l/s/km^2$) (a higher uncontrolled discharge occurred in 1996 causing damages to the measuring equipment);
- 25 events with suspended sediment concentrations between 0.1 and 9.2 g/l;
- event sediment yield (estimated on the basis of runoff volume and suspended sediment concentration in the flow) up to $282 \cdot 10^3$ kg (2,168.4 kg/ha).

The results of surface runoff separation from baseflow, as performed by the traditional manual linear method, which was applied to annual observed streamflow data, are summarized in Table 1. These results match reasonably well with those obtained through an automated digital filter (Arnold et al., 1995; Arnold and Allen, 1999); the differences in the surface runoff component extracted by the two methods are up to 16.7% (Table 1).

Table 1. Yearly values of surface runoff and baseflow components at the Cannata Basin, Sicily.

Runoff component	Hydrograph separation method	Yearly volumes (mm)						
		1997	1998	1999	2000	2001	2002	2003
Surface runoff	Manual	60.9	30.8	65.0	52.3	45.8	99.0	278.2
	Automated	67.4	32.6	75.8	54.4	42.5	102.8	283.0
Base flow	Manual	5.6	4.0	26.9	7.0	3.4	11.5	112.9
	Automated	12.3	5.6	37.8	9.0	0.0	15.5	117.6

Brief Description of the SWAT Model

SWAT is a physically-based continuous time hydrologic model developed by the USDA-ARS to predict the impact of land management practices on water, sediment, and agricultural chemical yields in large complex basins with varying soil type, land use, and management conditions over long periods of time. The model has been developed in an ArcView GIS environment. Required spatial data sets include a DEM, land cover and soil maps. In SWAT, a basin is partitioned into a number of subbasins interconnected by a stream network. Each subbasin can be divided into a number of spatially unidentified Hydrologic Response Units (HRUs) having unique land use and soil combinations. SWAT requires daily precipitation and maximum and minimum air temperature data that can be recorded at different sites. The

SWAT2000 version (Neitsch et al., 2002) has options to use observed solar radiation, wind speed, relative humidity, and evaporation data. The model includes a number of storage databases (i.e. soils, land cover/plant growth, tillage, and fertilizer) which can be customized for an individual basin. A single growth model in SWAT is used for simulating all crops based on the simplification of the EPIC crop model (Williams et al., 1984). Phenological development of the crop is based on daily heat unit accumulation. The model can simulate up to 10 soil layers if sufficiently detailed information is available. SWAT2000 is expected to provide useful information across a range of timescales, i.e. hourly, daily, monthly, and yearly time-steps (Neitsch et al., 2002). Full details of the model are given in Neitsch et al. (2002).

SWAT Model Implementation to the Experimental Basin

Elevation, land use, and soil characteristic input data sets for the Cannata Basin were obtained from GIS data layers at different resolutions. The elevation layer was extracted from a 5 m resolution DEM purposely arranged by digitizing 2 m elevation contour lines. The soils and land use layers were obtained from maps at a 25 m resolution of the five soil textures (clay, loam, loam-clay, loam-sand, loam-sand-clay) and two soil managements (pasture and winter wheat cultivation with rotation) in the basin. The basin was divided into 31 subbasins, ranging in size from 0.28 to 11.12 ha (Figure 1). The multiple HRUs option was used to enable the creation of multiple HRUs for each subbasin (thresholds of 5% over the subbasin area for land use and of 10% for soils were used); in total, 63 HRUs were delineated with sizes varying between 0.28 and 8.79 ha. For each texture, a uniform soil profile was modelled with the maximum depth allowed by averaging the required physical characteristics from the 57 field samples (up to 36 samples for each type of soil). For each land use, information about the specific plants and the management practices were set in the management files. The planting, harvest, and tillage operations and irrigation, nutrient, and pesticide applications were scheduled by date. The potential heat unit program provided 2,800 °C as the number of heat units required to bring a plant to maturity for both pasture and winter wheat. A pasture was planted between two winter wheat cultivations to simulate the crop rotation. The Curve Number values were derived by the standard procedure set by the Soil Conservation Service (USDA, 1972). Based on the available distributed samples of soil texture, structure, and field saturated conductivity, the basin was entirely represented by the soil hydrologic groups C and D, characterized by the highest surface runoff yield potential. The CN for the initial condition (AMC-II) for both pasture and winter wheat, taken from the SWAT database tables (USDA, 1986) for arid and semi-arid rangelands and cultivated agricultural lands, were 81 and 89 for pasture and 81 and 84 for winter wheat for hydrologic groups C and D, respectively. A single CN was used throughout the year for both land uses. The three precipitation recording gauges and meteorological station A were used for daily precipitation and climate input data (Figure 1).

Model Simulations

The performance of the hydrological component of the SWAT model was first analysed at a yearly time-step. Four simulations were run, alternately selecting the three optional evapotranspiration (PET) equations in SWAT, Penman-Monteith (Allen et al., 1989; simulation series I), Priestley-Taylor (Priestley and Taylor, 1972; series II) and Hargreaves (Hargreaves et al., 1985; series III), and the FAO Penman-Monteith equation (Allen et al., 1998; series IV) which is not integrated in the SWAT model. The latter equation, recommended as the standard method for the definition and computation of the reference evapotranspiration (Allen et al., 1998), is based on a reference crop with a height of 0.12 m, a fixed surface resistance of 70 s/m, and an albedo of 0.23. The daily FAO Penman-Monteith PET was calculated externally by the validated program PMday.xls (Snyder, 2002).

Following the approach suggested in the SWAT user manual (Neitsch et al., 2002), the best simulation results obtained at the yearly time-step were processed at monthly and daily time-steps.

A calibration was attempted to improve the simulation at a daily time-step by modifying the SCS Curve Number, which is expected to influence most output variables (Lenhart et al., 2002).

An analysis of the performance of the SWAT erosion component was conducted at the event scale. An evaluation process was carried out by modifying the C factor in the Universal Soil Loss Equation using the events during the period 1997-2000 and 2001-2003 for calibration and validation, respectively.

The coefficient of determination (R^2) and the Nash and Sutcliffe (1970) model efficiency (E) were the statistical parameters used to evaluate the performance of the model at the different time-steps.

To allow the model to adjust the initial soil water storage terms, it was necessary to append two years of dummy data to the beginning of the precipitation data set used for the Cannata Basin simulation. A modification of the SLSUBBSN parameter (indicating the distance from the sub-basin divide at which sheet flow is the dominant process) was necessary to obtain reasonable lateral flow values, due to the fact that the values had been assigned by the GIS interface out of the lower limit of the accepted range (10-150 m) for five of the 31 subbasins with the highest slopes (between 25.2 and 34.2%).

Results and Discussion

The best results, in terms of cumulated surface runoff for the period 1997-2003, were obtained when the FAO Penman-Monteith option was selected to calculate the PET (simulation series IV, Table 2). The same behaviour was observed at the yearly time-step. While the simulated streamflows were underestimated for four out of eight years when the FAO Penman-Monteith equation was used, they were overestimated when using the Penman-Monteith equation, and underestimated for six out of eight years when using the Hargreaves and the Priestley-Taylor equations (Table 2). An underestimation for wet years was also observed in a small natural grassland watershed in South Africa (Govender and Everson, 2005).

Table 2. Yearly observed and simulated surface runoff and baseflow at the Cannata Basin, Sicily.

Year	Surface runoff (mm)					Baseflow (mm)				
	Obs	Simulated				Obs	Simulated			
		series I	II	III	IV		series I	II	III	IV
1997	60.9	160.8	72.3	72.3	91.3	12.3	107.0	13.4	13.4	21.5
1998	30.8	103.1	38.8	38.8	53.0	5.6	71.8	9.6	9.6	12.1
1999	65.0	94.7	32.8	32.8	40.5	37.8	13.8	9.1	9.1	9.2
2000	52.3	125.9	51.6	51.6	58.5	9.0	16.6	9.3	9.3	9.5
2001	45.8	64.5	34.2	34.2	39.4	0.0	10.8	10.7	10.7	10.9
2002	99.0	131.6	81.2	81.2	89.7	15.5	12.3	12.4	12.4	12.5
2003	278.2	294.2	200.1	200.1	223.3	117.6	40.2	14.3	14.3	14.8
All years	631.9	974.8	510.9	510.9	595.7	197.7	272.5	78.8	78.8	90.4

The performance in the runoff simulation depended on the actual evapotranspiration (ET) simulated by SWAT based on the PET equation used. The average PET (excluding the year 1996) simulated by the FAO Penman-Monteith equation was 28% larger and 20% smaller than the values calculated using the Penman-Monteith and Hargreaves equations, respectively (Table 3). A similar behaviour was observed at the yearly time-step. The PET values obtained using the Priesty-Taylor equation were the same as those obtained when the Hargreaves equation was used. The long-term average actual evapotranspiration (ET) was less influenced by the choice of PET equation; however, significant differences remain at the yearly time-step (Table 3), especially due to the simulated values during the summer season. Differences of the same order of magnitude between annual ET values calculated by evapotranspiration equations incorporated in SWAT were found by Heuvelmans et al. (2005).

Table 3. Yearly potential and actual evapotranspiration simulated by the SWAT model at the Cannata Basin, Sicily.

Year	Potential evapotranspiration PET (mm)				Actual evapotranspiration ET (mm)			
	series I	II	III	IV	series I	II	III	IV
1997	663.0	1154.7	1154.7	927.5	482.6	686.0	686.0	642.0
1998	633.1	1110.0	1110.0	916.9	459.5	641.5	641.5	620.0
1999	617.4	1196.6	1196.6	936.5	438.0	529.3	529.3	543.3
2000	599.1	1169.5	1169.5	967.8	430.9	519.9	519.9	526.8
2001	793.5	1206.0	1206.0	1053.7	516.9	563.4	563.4	558.9
2002	792.6	1202.2	1202.2	1024.4	520.6	557.7	557.7	547.6
2003	774.6	1171.2	1171.2	984.2	557.7	722.2	722.2	670.3
Average year	696.2	1172.9	1172.9	973.0	486.6	602.8	602.8	587.0

Good results in terms of coefficient of determination (R^2=0.91) and model efficiency (E=0.99) were found for surface runoff at the monthly time-step (Figure 2). The simulation was unsatisfactory for the monthly baseflow volumes with an R^2= 0.07 and E= 0.13.

A calibration of the CN number was attempted in order to reduce the underestimation of surface flow for the seven events having a runoff depth higher than 20 mm. Increasing the default values of the CN parameter up to 3.9%, on the basis of the average slope of the subbasins, did not improve the coefficient of determination and model efficiency (Table 4). Similar underestimation of the highest observed daily runoff depths during the simulation were observed by Govender and Everson (2005), with a model efficiency of 0.68. The coefficient of determination found for the baseflow regression analysis and the model efficiency did non improve by modifying the GW_REWAP, REVAPMN, and GWQMN parameters, as suggested in the SWAT user's manual (Neitsch et al., 2002).

The regression analysis applied to event-scale suspended sediment yields sampled in the period 1997-2003 gave an R^2=0.76 with a low model efficiency; 24 out of 25 cases were underestimated (Table 5). The USLE-C factors for pasture and winter wheat were adjusted to approximate observed and simulated sediment loads, as suggested by Neitsch et al. (2001) and Santhi et al. (2001). The eight events observed during the period 1997-2000 were chosen for model calibration. The best coefficient of determination (R^2=0.96) and model efficiency (E=0.94) (Table 6) were reached by increasing the minimum default USLE-C factors (0.003 for pasture and 0.03 for winter wheat) up to 0.04 and 0.4 for pasture and winter wheat, respectively. The increased USLE-C factor values were used to simulate the 17 events sampled in the period chosen for validation (2001-2003). A coefficient of determination of 0.80 and a model efficiency of 0.41 were obtained (Table 6); a major overestimation of sediment yield was found for three events due to an overestimation of the suspended sediment concentration. High model-data differences in sediment loads (up to 700%) were found by Benaman and Shoemaker (2005) for short events (3 - 5 days) simulated by the SWAT model after a long term calibration/validation.

Three major factors can explain the differences between the observed and simulated sediment yields. First, as the model is run on a daily time-step, it is possible that a small time shift for sediment loading in the model would cause a great error in the comparison to observed loads. The second factor is related to the sensitivity of the model to small sediment loads. Finally, the developers of SWAT did not intend for the model to be used at event scale, but over long time periods.

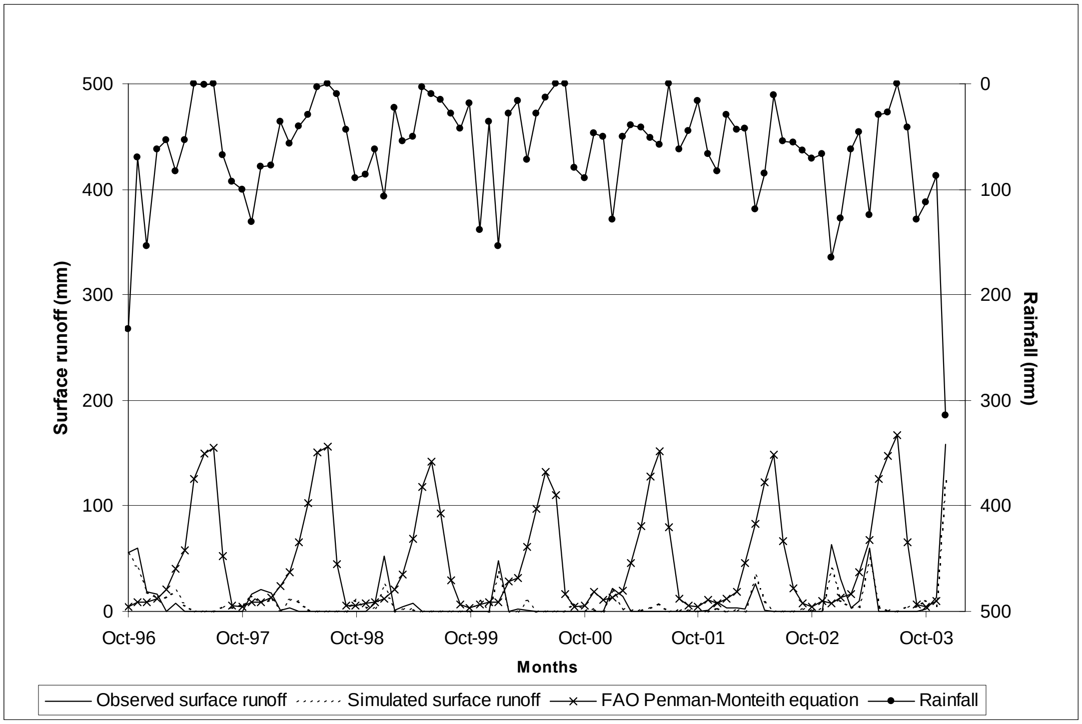

Figure 2. Monthly values of rainfall, surface runoff, and evapotranspiration in the period 1996-2003 at Cannata Basin, Sicily.

Table 4. Statistics of daily surface runoff and baseflow for the simulation series IV performed by SWAT.

	Daily surface runoff						Daily base flow					
	Mean	Median	Max	SD	R^2	E	Mean	Median	Max	SD	R^2	E
	[mm]				-	-	[mm]				-	-
Obs	0.3	0.0	145.3	3.6	-	-	0.1	0.0	7.3	0.4	-	-
Sim	0.3	0.0	113.5	2.8	0.88	0.86	0.0	0.0	0.1	0.0	0.05	0.01

Table 5. Summary of observed and simulated event-scale suspended sediment yields at the Cannata Basin, Sicily.

Event		Rainfall (mm)	Runoff (base+surface) (mm)		Suspended sediment yield (10^3 kg)		Average suspended sediment concentration (g/l)	
n.	date		Obs	Sim	Obs	Sim	Obs	Sim
1	23-24/11/1997	28.2	8.8	10.6	25.7	29.6	2.2	2.5
2	25-26/01/1998	23.0	12.1	0.7	3.2	0.4	0.2	0.4
3	31/01-1/2	19.0	4.3	1.4	7.5	1.3	1.3	0.8
4	12/12	12.4	2.8	0.1	4.8	0.3	1.3	0.7
5	22/12	18.8	4.2	2.6	2.0	5.3	0.4	1.7
6	03-04/01/1999	62.0	43.4	22.9	50.5	36.7	0.9	1.2
7	13-15/01/2000	93.8	45.7	35.7	72.5	69.5	1.2	1.2
8	19/1	9.6	2.8	0.4	0.7	0.3	0.2	0.6
9	28-30/01/2001	21.4	14.6	1.9	18.7	1.9	1.0	0.6
10	17-19/01/2002	11.2	2.4	0.0	0.6	0.0	0.2	0.1
11	03-04/04	23.0	3.0	0.7	5.1	0.7	1.3	0.6
12	4/5	12.8	7.1	0.2	8.8	0.2	1.0	0.5
13	4/6	7.8	6.0	0.0	4.1	0.0	0.5	0.1
14	4/22	66.2	17.8	129.9	25.4	129.9	1.1	3.6
15	25-26/12	37.6	16.1	41.4	43.5	41.4	2.1	1.5
16	18-19/01/2003	20.2	12.9	3.0	4.3	3.0	0.3	0.5
17	25-26/01	25.6	13.2	6.1	11.5	6.1	0.7	0.8
18	03-04/03	20.8	11.9	4.3	1.8	4.3	0.1	1.3
19	04-05/04	67.6	53.4	154.1	8.4	154.1	0.1	3.2
20	09/04	11.0	12.0	4.8	0.7	4.8	0.0	1.5
21	19/10	13.0	1.7	0.3	0.1	0.3	0.0	0.7
22	25-26/11	27.6	13.1	13.0	17.5	13.0	1.0	1.3
23	11-12/12	135.6	159.5	379.8	283.8	379.8	1.4	2.6
24	13/12	5.2	6.1	0.6	7.8	0.6	1.0	0.5
25	29-30/12	11.4	7.9	1.4	20.1	1.4	2.0	1.0

Table 6. Statistics of event sediment yield for the calibration/validation tests of SWAT at the Cannata Basin, Sicily.

	Statistics of event-scale sediment yield after model calibration						Statistics of event-scale sediment yield after model validation					
	Mean	Median	Max	SD	R^2	E	Mean	Median	Max	SD	R^2	E
	[10^3kg]				-	-	[10^3kg]				-	-
Obs	23.3	6.2	72.5	28.3	-	-	27.2	8.4	283.8	67.1	-	-
Sim	17.9	3.3	69.5	25.4	0.95	0.91	43.6	3.0	379.8	98.3	0.80	0.41

Conclusions

The overall results of this SWAT performance evaluation carried out for the Cannata Basin are promising. The model showed a good capability in simulating surface runoff when the FAO Penman-Monteith equation was used to calculate the potential evapotranspiration.

Increasing the default Curve Number values, on the basis of the average slope of the subbasins, did not improve model performance. Further investigations are needed to improve the estimation of baseflow, which is, however, not of particular relevance in the examined conditions. A good simulation of 25 event suspended sediment yields was found after a calibration/validation process was conducted by increasing the default values of the USLE-C factor for both pasture and winter wheat. A major overestimation of sediment yield was found for three events due to an overestimation of the suspended sediment concentration. The differences between the observed and simulated sediment yields could be due to small entities of the sediment loads and the fact that the model was run on a daily time-step to simulate events.

References

Allen, R.G., Jensen, M.E., Wright, J.L., Barman, R.D., 1989. Operational estimates of evapotranspiration. Agronomy Journal, 81:650-662.

Allen, R.G., Pereira, L.S., Raes, D., Smith, M., 1998. Crop evapotranspiration - Guidelines for computing crop water requirements. FAO Irrigation and drainage paper 56, United Nation Food and Agriculture Organization, Rome, Italy.

Arnold, J.G., Allen, P.M., Muttiah, R., Bernhardt, G., 1995. Automated base flow separation and recession analysis techniques, Ground Water, 33(6): 1010-1018.

Arnold, J.G., Srinivasan, R., Muttiah, R., Williams, Jr. 1998. Large area hydrologic modelling and assessment part I: model development. Journal of the American Water resources association 34(1): 73-89.

Arnold, J.G., Allen, P.M, 1999. Automated methods for estimating baseflow and groundwater recharge from streamflow records, Journal of the American Water Resources Association, 35(2): 411-424.

Arnold, J.G., Fohrer, N., 2005. SWAT2000: current capabilities and research opportunities in applied watershed modelling. Hydrological Processes, 19, 563-572.

Arnold, J.G., Potter, K.N., King, K.W., Allen, P.M., 2005. Estimation of soil cracking and the effect on surface runoff in a Texas Blackland Prairie watershed. Hydrological Processes, 19, 589-603.

Benaman, J., Shoemaker, C.A., 2005. An analysis of high-flow sediment event data for evaluating model performance. Hydrological Processes, 19, 605-620.

Di Luzio, M., Arnold, J.G., Srinivasan, R., 2005. Effect of GIS data quality on small watershed stream flow and sediment simulations. Hydrological Processes, 19, 629-650.

Govender, M., Everson, C.S., 2005. Modelling stream flow from two small South African experimental catchments using the SWAT model. Hydrological Processes, 19, 683-692.

Hargreaves, G.L., Hargreaves, G.H., Riley, J.P., 1985. Agricultural benefits for Senegal River Basin. Journal of Irrigation and Drainage Engineering, 111(2):113-124.

Heuvelmans, G., Garcia-Qujano, J.F., Muys, B., Feyen, J., Coppin, P., 2005. Modelling the water balance with SWAT as part of the land use impact evaluation in a life cycle study of CO2 emission reduction scenarios. Hydrological Processes, 19, 729-748.

Lenhart, T., Eckhardt, K., Fohrer, N., Frede, H.G., 2002. Comparison of two different approaches of sensitivity analysis. Physics and Chemistry of the Earth, 27, 645-654.

Licciardello, F., Rizzo, N., Somma, F., Zimbone, S.M., 2001. Runoff and soil erosion in a small Sicilian watershed. Proceedings of International Symposium: Erosion Research for the 21st Century. Honolulu, Hawaii, 363-366.

Lo Porto, A., De Girolamo, A.M., De Luca, F., Pappagallo, G., 2005. Application of water management models to Mediterranean temporary rivers. These proceedings.

Lorrai, E., Cau, P., 2005. A user friendly multi-catchments tool for the SWAT model. These proceedings.
Morgan, R.C.P., Nearing, M.A., 2000. Soil erosion models: present and future. Proceedings of the 3rd International Congress of the European Society for Soil Conservation. 275. Valencia, Spain.
Nash, J.E., Sutcliffe, J.V., 1970. River flow forecasting through conceptual models 1. A discussion of principles. Journal of Hydrology, 10, 282:290.
Nearing, M.A., Pruski, F.F., O'Neal, M.R., 2004. Expected climate change impacts on soil erosion rates: A review. Journal of Soil and Water Conservation. 59 (1): 43-50.
Neitsch, J.G., Arnold, J.G., Kiniry, J.R., Williams, J.R., King, K.W., 2002. SWAT: Soil and Water Assessment tool, Theoretical documentation, version 2000. USDA: Texas.
Neitsch, J.G., Arnold, J.G., Kiniry, J.R., Srinivasan, R., Williams, K.W., 2002. SWAT: Soil and Water Assessment tool, User's manual, version 2000. USDA: Texas.
Pappagallo, G. Leone, A., Lo Porto, A., 2003. Use of management models to study human impact on quality and quantity of water resources in the basin of Celone River (Apulia, Italy). Proceedings of the 3rd International SWAT Conference, July, 1-4, Bari, Italy.
Priestley, C.H.B., Taylor, R.J., 1972. On the assessment of surface heat flux and evaporation using large-scale parameters. Monthly Weather Review, 100:81-92.
Renard, K.G., Rawls, W.J., Fogel, M.M., 1982. Currently available models. In: Haan, C.T., Johnson, H.P. and Brakensiek, D.L. (eds) Hydrologic Modelling of Small Watersheds. ASAE, St. Joseph, Michigan, 507-522.
Santhi, C., Arnold, J.G., Williams, J.R., Dugas, W.A., Srninivasan, R., Hauck, L.M., 2001. Validation of the SWAT model on a large river basin with point and nonpoint sources. Journal of the American Water Resources association, 37 (5), 1169-1188.
Singh, V.P., 1995. Computer models of watershed hydrology. Water Resources Publications LLC, CO, USA.
Snyder, R.L., Eching, S., 2002. Penman-Monteith daily (24-hour) Reference Evapotranspiration Equations for Estimating ETo, ETr and HS ETo with Daily Data. http://biomet.ucdavis.edu/
Sulis, M., Badas, M.G., Deidda, R., Piga, Marrocu, M. Paniconi, C., 2004. Applicazione del modello SWAT al bacino dell'Araxisi. XXIX Convegno Nazionale di Idraulica e Costruzioni Idrauliche. 7-10 settembre, Trento, Italy.
Tripathi, M.P., Panda, R.K., Raghuwanshi, N.S., Singh, R., 2004. Hydrological modelling of a small watershed using generated rainfall in the soil and water assessment tool model. Hydrological Processes, 18, 1811-1821.
USDA, Soil Conservation Service, 1972. National Engineering Handbook, Hydrology, Section 4. Washington D.C., 548.
USDA, Soil Conservation, 1986. Urban Hydrology for Small Watersheds, Service Engineering Division. Technical Release 55.
Williams J.R., Jones, C.A., Dyke, P.T., 1984. A modelling approach to determining the relationship between erosion and soil productivity. Transaction of the ASAE, 21: 129-144.

Comparison of Runoff Responses between SWAT and Sequentially Coupled SWAT-MODFLOW Model

Do Hun Lee[1], Nam Won Kim[2], and IL Moon Chung[2]
[1]Department of Civil Engineering, Kyung Hee University, Seocheon-Ri, Kihung-Eup, Yongin-Si, Gyeonggi-Do, 449-701, Korea. Email: dohlee@khu.ac.kr
[2]Water Resources Department., Korea Institute of Construction Technology, Goyang-Si, Korea

Abstract

The sequentially coupled SWAT-MODFLOW model was developed and applied to Bocheong-cheon IHP experimental watershed in Korea. The performance of the SWAT-MODFLOW coupled model was tested against the measured runoff data and simulation results of the SWAT model for five years between 1992 and 1996. The simulation results of SWAT-MODFLOW indicate that its overall performance in estimating runoff responses is slightly worse than that of the SWAT model. However, the application of SWAT-MODFLOW allows us to identify the spatial distribution of the groundwater table and to estimate the interaction flux between streamflow and groundwater flow. This study suggests that there is a need to reduce the uncertainty associated with identifying MODFLOW model parameters and boundary conditions and characterizing aquifer structure in order to improve its applicability to the medium to large watershed scale.

Keywords: SWAT, MODFLOW, Runoff Response, Bocheong-cheon Watershed

Introduction

This study is concerned with comparing the SWAT model (Neitsch et al., 2001) with the sequentially coupled SWAT-MODFLOW model for simulating the runoff response at the medium to large watershed scale. The sequentially coupled SWAT-MODFLOW model can be formulated by superimposing surface runoff and lateral flow calculated from SWAT on baseflow calculated from MODFLOW (McDonald and Harbaugh, 1988). In the past, a number of studies have been conducted by coupling a semi-distributed watershed model with the MODFLOW groundwater model. Perkins and Sophocleous (1999) developed SWATMOD which dynamically couples SWAT with the MODFLOW model. Davis (2001) also developed ISGW model which integrates HSPF (Bicknell et al. 1997) with the MODFLOW model.

Since the baseflow component of the SWAT model is based on the lumped model structure and the application of the integrated SWAT-MODFLOW model to Korea's watershed has been very limited, there is a need to understand the applicability of the sequentially coupled SWAT-MODFLOW model to simulating runoff responses in Korea's watersheds. The specific objective of this paper is to compare the sequentially coupled SWAT-MODFLOW model with SWAT and to understand the performance of both models for reproducing runoff responses.

Methods and Materials

SWAT Model

The Soil and Water Assessment Tool (SWAT) was used to investigate the runoff response in the Bocheong-cheon watershed in Korea. The Bocheong-cheon watershed is one of the IHP research basins in Korea and the hydrologic data have been collected since 1984. The watershed area being studied is about 350 km^2 and the average elevation of the watershed is about 283 m. The main land use types in the watershed are mixed forest, occupying 63%, and agricultural land, occupying 26%, of the watershed.

Figure 1 shows the raingage and water level stations in the Bocheong-cheon watershed. The daily rainfall data measured at 11 raingage stations, shown in Table 1, were used as input to the SWAT model. The climatic input data at six stations, shown in Table 2, were used to define wind speed, relative humidity, daily maximum and minimum temperature, and solar radiation.

Since the topography, soil, and land use maps are required to prepare the input data of the SWAT model, digital maps of 1:25,000 scale were applied in this study. For the estimation of major flow processes, the SCS curve number equation was used to calculate surface runoff, the Penman-Monteith equation was used for potential evapotranspiration, and the Muskingum-routing method was used to model channel flow for the SWAT model simulations. The soil physical parameters such as bulk density, available water capacity, and saturated hydraulic conductivity of each soil layer were estimated by using a pedo transfer function developed by Saxton et al. (1986).

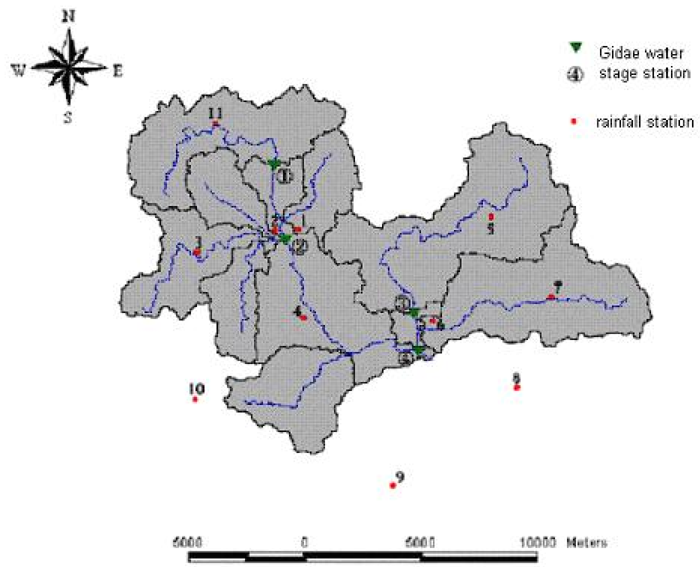

Figure 1. Bocheong-cheon Watershed.

Table 1. Annual average rainfall from 1992 to 1996.

Station	Elevation (m)	Annual precipitation (mm)
An Nae	80	1350.5
Myo Geum	140	1004.5
Cheong San	120	1050.7
Jung Nyul	180	1103.0
Kwan Gi	160	998.1
Pyeong On	200	1102.8
Sam Ga	380	818.7
Song Jug	130	1087.9
Sam San	150	1066.2
Dong Jeong	210	1163.8
Yi Weon	220	1000.5

Table 2. Average and standard deviation of climatic variables in Bocheong-cheon Watershed.

Station	Elevation (m)	Wind speed (m/s)	Relative humidity	Daily maximum temperature (℃)	Daily minimum temperature (℃)	Daily solar radiation (MJ/㎡)
Cheongju	59	1.9(0.87)	0.67(0.11)	18.35(10.25)	7.28(10.49)	12.54(6.24)
Geumsan	67.1	1.15(0.61)	0.7(0.1)	18.48(9.91)	5.26(10.65)	No record
Daejeon	170.7	1.68(0.87)	0.69(0.12)	18.51(9.9)	7.73(10.25)	13.43(6.8)
Chupungryong	245.9	2.59(1.78)	0.67(0.14)	17.58(9.96)	6.61(9.63)	11.82(6.11)
Munkyung	172.1	1.78(0.95)	0.65(0.15)	17.52(10.01)	5.97(9.9)	No record
Boeun	170	1.65(1.14)	0.72(0.1)	17.25(9.98)	4.36(10.7)	No record

Note: The values in the parenthesis indicate a standard deviation.

Sequentially Coupled SWAT-MODFLOW Model

The surface runoff and baseflow responses were examined by sequential coupling of the SWAT and MODFLOW models. Figure 2 shows the conceptualization of the sequential coupling between SWAT and MODFLOW. In the sequential approach, SWAT was simulated before MODFLOW, then the recharge flux calculated from SWAT was used as the recharge input to the MODFLOW model. After MODFLOW was simulated, total runoff was estimated by summing up baseflow calculated from MODFLOW, and surface runoff and lateral flow was estimated from the SWAT model.

For the simulation of the MODFLOW model, the Bocheong-cheon watershed was divided into 10,000 cells and no flow boundary condition was applied to the watershed boundary by assuming that the surface and groundwater divide coincided. The stream boundary condition was treated using the river package of the MODFLOW model.

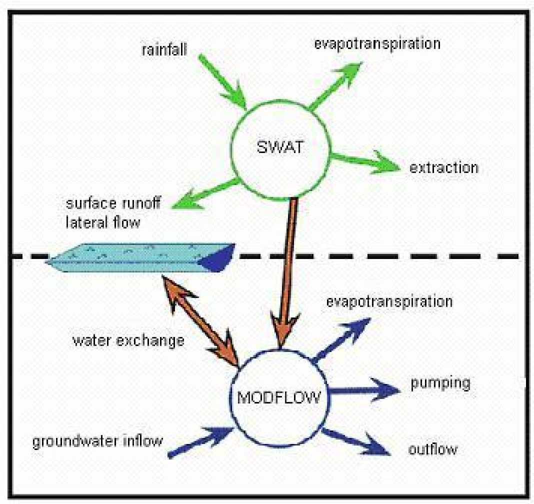

Figure 2. Conceptualization for coupling SWAT and MODFLOW.

Results

The performance of the SWAT model and sequentially coupled SWAT-MODFLOW model was evaluated against the daily streamflow measured at the Gidai station of the Bocheong-cheon watershed. At this phase, the calibrated SWAT model parameters were minimized such that groundwater related parameters (GW_DELAY, ALPHA_BF, and REVAPMN) and the Manning roughness coefficient for main and tributary channels (CH_N2 and CH_N1) were identified by a manual calibration method, and other parameters were specified as default parameters determined by the SWAT GIS interface. The MODFLOW parameters, such as hydraulic conductivity, specific storage, and specific yield, were specified based on the available pumping test results and range of parameters for various porous materials given in Batu (1998).

Table 3 shows the simulated results for the SWAT and SWAT-MODFLOW models against measured runoff. For a comparison measure, Nash-Sutcliffe efficiency index (E.I.) defined by Nash and Sutcliffe (1970) was used along with average and standard deviation of runoff time series. In addition to daily runoff response, three different averaged daily runoff time series were constructed. The SWAT model performed better than the SWAT-MODFLOW model in terms of Nash-Sutcliffe efficiency index and the coefficient of determination, as shown in Table 3 and Figure 3. The Nash-Sutcliffe efficiency index increased from 0.62 to 0.83 as the averaging period for runoff time series increased. However, the average values of runoff time series calculated from both SWAT and SWAT-MODFLOW slightly overestimated the measured average value. The average values of runoff time series estimated from SWAT-MODFLOW exhibited smaller error compared to the average values calculated from the SWAT model. Both the SWAT and SWAT-MODFLOW models underestimated the standard deviation of measured runoff time series. And the SWAT model performed better than SWAT-MODFLOW in reproducing the standard deviation of runoff. Figure 4 shows a comparison of daily runoff between SWAT and SWAT-MODFLOW, in which both models show good agreement with the determination coefficient of 0.88.

Table 3. Performance of SWAT and SWAT-MODFLOW model.

Runoff type	Measure type	SWAT	SWAT-MODFLOW	Measurement
Daily runoff	Average	6.3	6.1	5.5
	Standard deviation	13.0	9.7	19.1
	E.I.	0.62	0.52	-
10 day averaged runoff	Average	6.3	6.1	5.5
	Standard deviation	10.1	6.4	11.8
	E.I.	0.8	0.68	-
20 day averaged runoff	Average	6.4	6.2	5.5
	Standard deviation	9.0	5.4	9.8
	E.I.	0.83	0.7	-
30 day averaged runoff	Average	6.4	6.2	5.5
	Standard deviation	8.2	4.7	8.6
	E.I.	0.83	0.71	-

Note: The units of average and standard deviation are in m^3/s.

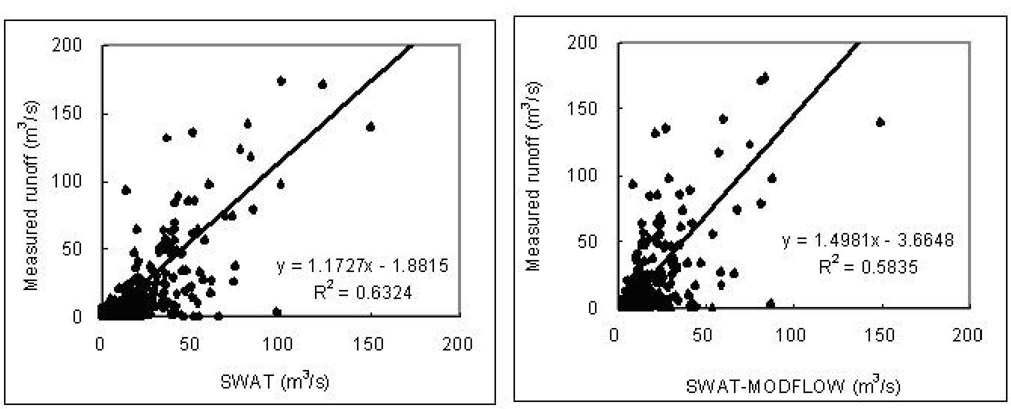

Figure 3. Comparison between measured and simulated daily runoff responses.

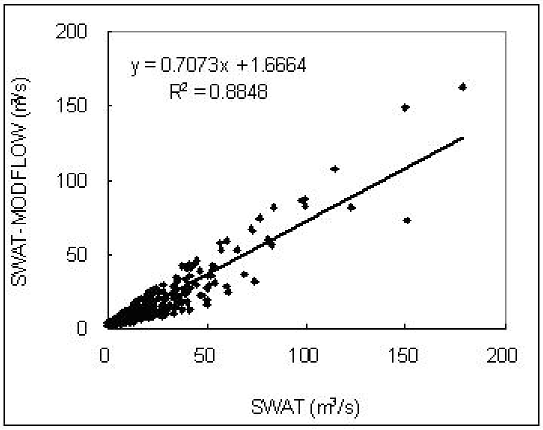

Figure 4. Comparison of daily runoff between SWAT and SWAT-MODFLOW model.

Conclusions

The spatially distributed groundwater flow model, MODFLOW was sequentially coupled with the SWAT model based on the principle of superimposition and tested against the measured runoff time series. The simulation of the SWAT and SWAT-MODFLOW models using five years of daily runoff data from 1992 to 1996 reveals that the SWAT model performs better than the coupled SWAT-MODFLOW model in reproducing runoff responses at the Gidae water stage station within the Bocheong-cheon experimental watershed in Korea. The poorer performance of the coupled SWAT-MODFLOW model is mainly due to uncertainty in conceptualizing aquifer structure and identifying MODFLOW model parameters and boundary conditions. Based on the findings of this study, it would be difficult to apply the coupled SWAT-MODFLOW model at a large watershed scale unless sufficient data for characterizing the groundwater system is available. However, the main advantages in applying the coupled SWAT-MODFLOW model are to predict the spatial distribution of the groundwater table and to better estimate the water flux exchange between stream and groundwater. The simulation of the coupled SWAT-MODFLOW model indicates that the baseflow component of SWAT needs to be further tested since the SWAT model lacks aquifer storage effect in generating baseflow.

Acknowledgements

This research was supported by a grant (2-2-2) from the Sustainable Water Resources Research Center of 21st Century Frontier Research Program.

References

Batu, V., 1998, Aquifer hydraulics, John Wiley & Sons, Inc.

Bicknell, B.R., J.C. Imhoff, J.L. Kittle, A.S. Jr. Donigian, R.C. Johanson, 1997, Hydrological Simulation Program-Fortran, U.S. Environmental Protection Agency, National Exposure Research Laboratory, Athens, GA, EPA/600/R-97/080, 755 p.

Davis, P.R., 2001, Integrated surface and ground water management, Proceedings of the specialty symposium held in conjunction with the world water and environmental resources congress, ASCE, pp. 100-109.

McDonald, M.G. and A.W. Harbaugh, 1988, A modular three-dimensional finite-difference ground-water model, U.S. Geological Survey Open-File Report 83-875.

Nash, J.E. and J.E. Sutcliffe, 1970, River flow forecasting through conceptual models, Part 1- A discussion of principles, Journal of Hydrology, 10, pp. 282-290.

Neitsch, S.L., J.G. Arnold, J.R. Kiniry, J.R. Williams, 2001, Soil and Water Assessment Tool Theoretical Documentation Version 2000. Agricultural Research Service. Texas Agricultural Experiment Station. Temple, Texas.

Perkins, S. and M. Sophocleous, 1999, Development of a comprehensive watershed model applied to study stream yield under drought conditions, Ground Water, 37(3), pp. 418-426,

Saxton, K.E., W.J. Rawls, J.S. Romberger, and R.I. Papendick, 1986. Estimating generalized soil-water characteristics from texture. SOIL Sci. Soc. Am. J., 50, pp. 1031-1036.

Hydrological Modelling using SWAT for Effective Management of a Small Agricultural Watershed

M. P. Tripathi
Associate Professor, Department of Soil and Water Engineering, Faculty of Agricultural Engineering, Indira Gandhi Agricultural University, Raipur- 06 (CG) India. E-mail: drmpt64@hotmail.com

Abstract

The Soil and Water Assessment Tool (SWAT) was tested on a daily and monthly basis and applied for developing the management scenarios for the critical subwatersheds of a small agricultural watershed (Nagwan) in eastern India. Watershed and subwatershed boundaries, drainage networks, slope, and soil texture maps were generated using GIS. Supervised classification methods were used for land use/cover classification from satellite imagery. Manning's n for overland and channel flows were calibrated for the monsoon season of 1996. The model was validated for the year 1997. The model accurately simulated daily and monthly values for runoff and sediment yield from the studied watershed. Simulated values for organic N, P, NO_3-N, and soluble P agreed well with observed values. The model was found to be satisfactory in generating daily and monthly rainfall during the period from 1996 to1998. The predicted values for daily runoff and sediment yield using generated rainfall compared well with observed runoff and sediment yield during those years. An adequately tested model was used for developing the management plan for the critical subwatersheds, which were identified on the basis of average annual sediment yield and nutrient losses. The subwatersheds WS12, WS9, WS7, WS10, and WS6 were found to be critical. Several combinations of treatments including crops, tillage, and levels of fertilizer were considered. The existing practice was considered as the base for evaluating other management practices for rice. It was found that other crops could not replace rice since these crops resulted in higher sediment yield as compared to rice. An MB plough increased sediment yield by about 39 percent and decreased nutrient losses by about 22, 50, 3, and 37 percent N, P, NO_3-N, and soluble P, respectively as compared to the conventional tillage for the existing level of fertilizer. A decrease in sediment yield as compared to conventional tillage was found to be about 19, 11, and 10 percent for zero tillage, conservation tillage, and field cultivator, respectively. The impact of zero and conservation tillage on nutrient losses for all levels of fertilizer doses was found to be more than that of the other tillage practices. It can be concluded that field cultivator followed by conventional tillage is a better option than the other tillage practices. Also, a dose of 40:30 kg/ha of N:P fertilizer proved to be appropriate for rice with either conventional tillage or field cultivator, and therefore is recommended for adoption in the critical subwatersheds of the Nagwan Watershed.

Introduction

Estimation of runoff and sediment yield is necessary for the design of conservation structures to reduce the ill effects of sedimentation and to select the priority watersheds for implementing and evaluating the watershed management programmes with limited resources. Effective control of soil erosion requires implementation of best management practices in critical erosion prone areas. This effort can be enhanced by the use of physically-based computer simulation models, remote sensing data, and a GIS techniques, which can assist management agencies in both identifying the most vulnerable erosion prone areas and selecting appropriate management practices.

Many hydrologic and water quality models like ANSWERS, AGNPS, HSPF, MIKE SHE, SWRRB, SWAT, and WEPP are presently in use to evaluate the parameters involved in hydrological and environmental processes. Among these models, SWAT is a newly developed model, which can be applied to a large ungauged rural watershed with hundreds of small subwatersheds (Arnold et al., 1996). SWAT is a process-based hydrological model; its major components include surface hydrology, weather, sedimentation, soil temperature, crop growth, nutrients, pesticides, ground water, and lateral flow. The compilation and input of hydrologic data that are required by the SWAT model can be extracted with the use of GIS mainly from map layers including land use/cover, DEM, soil, slope, drainage, and watershed/subwatershed boundaries.

Previous applications of SWAT have shown promising results (Srinivasan et al., 1993; Rosenthal et al., 1995; Bingner et al., 1997; Srinivasan et al., 1998; Arnold et al., 1999; Santhi et al., 2001). In these studies, the model was tested mainly on a monthly and annual basis for predicting runoff and sediment yield. A few studies on the application of the SWAT model for developing best management scenarios for critical erosion prone areas of a watershed have been reported. However, no study is available in the literature under Indian conditions for the prediction of surface runoff and sediment yield. In India, very little efforts have been made on the use of hydrologic and water quality models to develop an effective management plan for small agricultural watersheds using a systematic modelling approach.

It is obvious that rainfall data for several years are required for developing the long-term management plan of a watershed. Many process-based hydrological models, including SWAT, have the capability to generate rainfall and thereafter, runoff, sediment yield, and nutrient losses. Adequate procedures to calibrate and validate the SWAT model are an important research issue. A model should be adequately tested before using it in developing effective management plans, specifically when generated rainfall is the basic input. The basic requirement for any watershed hydrology model is an adequate capability to estimate surface runoff because it influences the transport of sediments and agro-chemicals.

Numerous studies have indicated that, for many watersheds, a few critical areas are responsible for a disproportionate amount of the pollution (Maas et al., 1985; Storm et al., 1988; Dickinson et al., 1990). Critical areas of a watershed can be defined both from the land resource and water quality perspectives (Maas et al., 1985). From the land resource perspective, critical areas are those land areas where the soil erosion rate exceeds the soil loss tolerance value. Critical areas from the water quality perspectives are areas where the greatest improvement can be achieved with the least capital investment in best management practices.

The average soil loss value of 16.4 t/ha/yr (Dhruva Narayana, 1993) and permissible soil loss value of 11.2 t/ha/yr (Mannering, 1981) can be taken into consideration for identifying critical subwatersheds. Priorities can be fixed on the basis of ranks assigned to each critical subwatershed according to ranges of soil erosion classes described by Singh et al. (1992) for Indian watersheds. Tim et al. (1992) used an average soil loss tolerance value of 9.0 t/ha/yr in a study to identify critical areas. They also considered a threshold value of 1.12 kg/ha/yr for the loading rate of P. A threshold value of 10 mg/l for nitrate nitrogen and 0.5 mg/l for dissolve phosphorous, as described by EPA (1976), can be considered as a criterion for identifying critical subwatersheds.

This study was undertaken with the major objectives of calibrating and validating the SWAT model for the Nagwan Watershed in eastern India using satellite data and GIS to identify critical subwatersheds and evaluating best management practices.

Materials and Methods

The Nagwan watershed (92.46 km^2) is located in the Upper Damoder Valley Corporation (DVC) in the Hazaribagh district of Jharkhand, India (Figure 1). The watershed lies between 85.25^o to 85.43^o E longitudes and 23.99^o to 24.12^o N latitudes with an elevation ranging from 550 to 640 m above MSL. Rainfall, runoff, and sediment yield data for 12 years (1991 to 2002) were collected from DVC, Hazaribagh. IRS-1B (LISS II) satellite data from October 19, 1996 were collected and used for land use/cover classification. Topographic maps (1:50,000) were collected from Survey of India, Calcutta. Soil resources data were collected from DVC, Hazaribagh for use in the study.

The package EASI-PACE was used for terrain analysis and image processing. The DEM, watershed boundary, drainage networks, and slope map were generated using the procedure described by Jenson & Domingue (1988). The delineated watershed was subdivided into 12 subwatersheds on the basis of topography. A supervised land use classification method was used for land use/cover classification. The land use classes were identified as upland and low land rice (32.95 km^2), orchards (2.94 km^2), deep and shallow water (1.71 km^2), closed and open forest (4.05 km^2), fallow land (8.26 km^2), grasses/shrubs (16.21 km^2), upland crops (7.85 km2), and settlements (13.40 km^2). A soil texture map was generated using soil resource data. Areas with different soil textures were found to be 11.0, 14.6, 12.1, 8.3, 39.0, and 5.2 km^2 for silty clay loam, loam, sandy loam, loamy sand, silt loam, and clay loam, respectively.

The weighted average curve number (CN) for each subwatershed was calculated using the land use/cover map, soil texture map, and standard curve numbers for India. Other input parameters for the delineated subwatersheds were extracted using the various maps. The observed surface runoff and sediment yield for the monsoon season (June to October) in 1996 were used for evaluation of model calibration performance. The input parameters that showed negligible variation in monthly surface runoff and sediment yield were not calibrated and taken as suggested by Arnold et al. (1996). The weighted average values for the parameters such as runoff curve number, surface slope, channel length, average slope length, channel width, channel depth, soil erodibility factor, and other soil layer data were taken for each subwatershed (Table 1). Manning's n values for overland channel flows were calibrated.

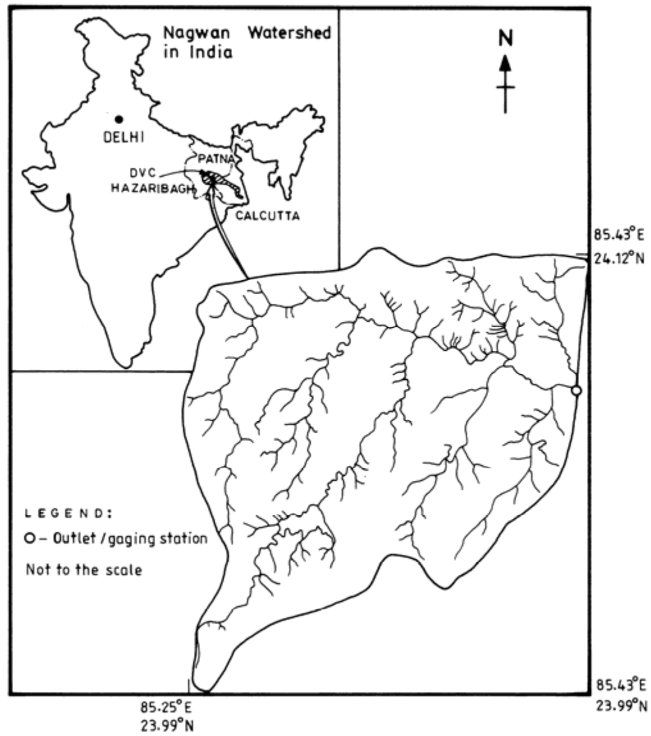

Figure 1. Location of the Nagwan Watershed in India.

Table 1. Subwatershed input data for the SWAT model.

Sub-watershed	Area (km^2)	Slope (%)	Curve Number	Ave. slope length (m)	Channel length (m)	Channel slope (%)	K value	P value
WS1	17.19	2.2	83.6	464.3	9.60	.005	0.28	0.60
WS2	9.33	3.0	71.0	493.8	5.28	.008	0.19	0.50
WS3	6.27	2.1	79.7	481.6	1.80	.001	0.22	0.60
WS4	9.89	2.2	55.0	456.4	5.40	.004	0.26	0.60
WS5	14.67	2.1	68.9	395.8	6.00	.005	0.21	0.60
WS6	3.54	2.8	80.1	492.3	2.25	.001	0.19	0.50
WS7	9.46	3.1	69.0	517.0	5.76	.005	0.24	0.50
WS8	4.24	2.3	68.9	574.3	2.94	.006	0.19	0.60
WS9	3.10	2.9	74.7	437.8	2.25	.008	0.23	0.50
WS10	7.23	3.3	66.5	454.7	5.40	.009	0.23	0.50
WS11	4.80	2.9	79.2	479.4	3.36	.009	0.17	0.50
WS12	0.51	9.1	66.8	290.8	0.90	.006	0.25	0.60
WS	90.23	2.3	72.0	461.7	13.86	.005	0.21	0.60

The model was validated for the year 1997 using rainfall, temperature, and curve numbers for 1996. Frequency distributions for simulated monthly runoff and sediment yield were compared with distributions of their observed counterparts for the years 1998 to 2002. The model's ability to generate rainfall was also evaluated for a three-year period (1996 to 1998). The model performance was evaluated on the basis of test criterion recommended by the ASCE Task Committee (1993). Graphical and statistical methods were also used for evaluating the model performance. The critical subwatersheds were identified on the basis of average annual sediment yield and nutrient losses during the period from 1996 to 1998. The ranges of erosion rates and their classes suggested by Singh et al. (1992) were inferred. The critical subwatersheds were then considered in evaluating the management scenarios to reduce the runoff rate, sediment yield, and nutrient losses from the Nagwan Watershed. A total of 60 combinations of treatment options, which included crops (rice, maize, groundnut, and soybean), tillage (T_1-zero, T_2-conservation, T_3-field cultivator, T_4-MB plough and T_5-conventional), and levels of fertilizer (F_1-existing, F_2-half of the recommended and F_3-recommended) were considered in this study. The values of mixing efficiency 0.05, 0.25, 0.30, 0.90, and 0.50 were considered, for zero, conservation, field cultivator, MB plough, and conventional tillage, respectively.

Results and Discussion

Model Calibration

Manning's n values for overland flow (0.065) and channel flow (0.040) were considered for the Nagwan Watershed during calibration. Results showed that the observed and simulated daily runoff and sediment yield for the calibration period (June to October 1996) matched quite well. A coefficient of determination (r^2) of 0.94 and 0.98 for runoff and sediment yield, respectively, indicated a close relationship between measured and predicted runoff and sediment yield. A Nash-Sutcliffe simulation efficiency (COE) of 0.90 and 0.91 for runoff and sediment yield, respectively, also supported this finding. Comparison of means using the Students t-test also revealed that the means of observed and predicted runoff and sediment yield were not significantly different at a 95% confidence level. The overall percent deviation (Dv) of 5.0 and 14.9% for runoff and sediment yield, respectively, indicated that the model was predicting satisfactorily (Table 2).

Model Validation

Results showed that the magnitude and temporal variation of simulated runoff and sediment yield matched closely with the observed runoff values for the entire monsoon season in 1997. High r^2 values of 0.91 and 0.89 for runoff and sediment yield, respectively, indicated a close match between measured and predicted values. A close agreement between the means and standard deviations of the measured and predicted runoff and sediment yield indicated that the frequency distributions were similar. High COE values of 0.87 and 0.89 and Dv values of 4.6 and 13.3%, indicated that the model was accurately validated for predicting runoff and sediment yield from the Nagwan Watershed (Table 2).

Table 2. Statistical results for daily observed and simulated runoff and sediment yield.

Statistical Parameters	Runoff (mm)				Sediment (t/ha)			
	1996		1997		1996		1997	
	Obs.	Sim.	Obs.	Sim.	Obs.	Sim.	Obs.	Sim.
Mean	1.89	1.79	2.80	2.68	0.028	0.032	0.026	0.022
Std. deviation	6.36	7.51	7.06	8.16	0.170	0.213	0.072	0.067
Max. Peak	50.26	64.29	50.33	57.00	1.960	2.500	0.538	0.460
Total	288.91	274.39	429.07	409.40	4.318	4.960	3.885	3.330
Count	153	153	153	153	153	153	153	153
t-cal	0.556		0.531		0.311		0.063	
t-critical	1.976		1.976		1.976		1.976	
r^2	0.946		0.912		0.980		0.891	
% Deviation	5.0		4.6		-14.9		14.3	
COE	0.90		0.87		0.91		0.89	

Distribution of Monthly Runoff and Sediment Yield

The validation results for measured and simulated monthly surface runoff and sediment yields for the monsoon months during a five-year period were quite good (Figures 2 and 3). A high value of coefficient of determination of 0.84 indicated a good agreement between distributions of monthly runoff values. The means of observed (42.4 mm) and simulated (45.9 mm) monthly runoff were found to be similar at a 95% confidence level. A value of coefficient of simulation efficiency (0.83) also indicated a good agreement between the monthly frequency distributions. An overall deviation of 8.4% indicated that, in general, the simulated monthly surface runoff compared well with measured monthly values. The mean of the observed (1.58 t/ha) and simulated (1.47 t/ha) monthly sediment yield was statistically similar at the 95% confidence level, and high values for the coefficient of determination (0.92) and coefficient of simulation efficiency (0.91) indicated a good agreement between the observed and simulated monthly sediment yield. Overall percent deviation indicated that the model was under-predicting monthly sediment yield values by 7.1%.

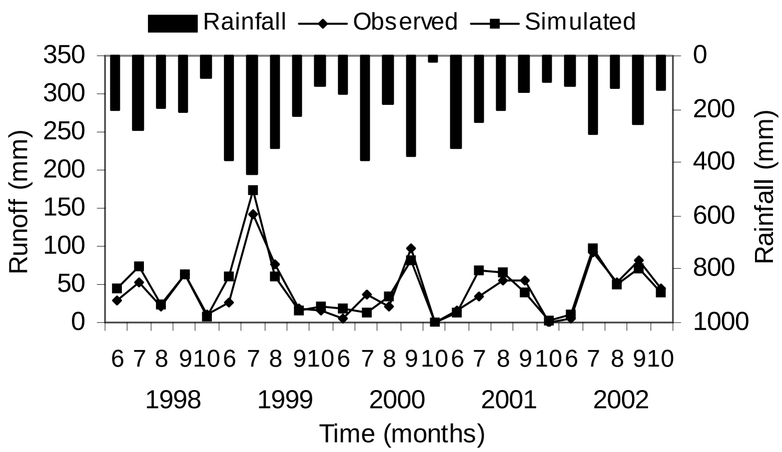

Figure 2. Graphical comparison of observed and simulated monthly runoff.

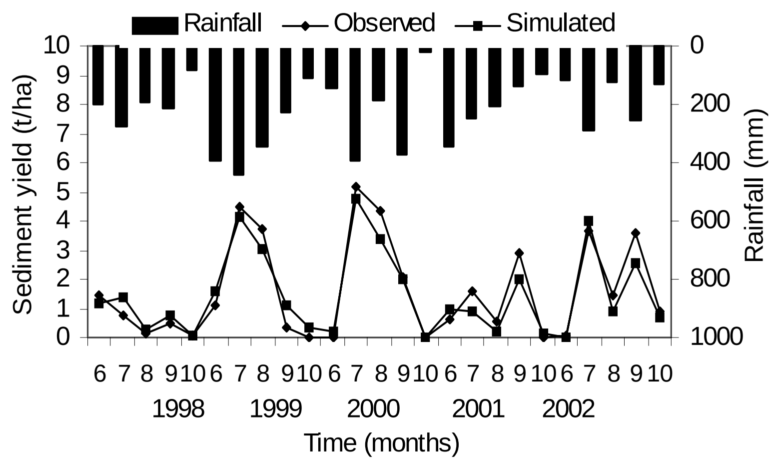

Figure 3. Graphical comparison of observed and simulated monthly sediment yield.

Nutrients

The observed and simulated nutrient losses were tested for the 12 events in the monsoon season during 1997. Observed and simulated mean organic nitrogen, phosphorous, NO_3-N, and soluble P were not significantly different at the 95% level of confidence. The Dv value was found to be 15.8, 11.7, 3.7, and 12.5 percent for organic N, P, NO_3-N, and soluble P, respectively, indicating that the model was predicting nutrient losses satisfactorily. An r^2 value of 0.82, 0.89, 0.86, and 0.82 for organic N, P, NO_3-N, and soluble P, respectively, indicated good agreement between observed and simulated values for nutrient losses for the 12 rainfall events during 1997.

Rainfall Generation

The SWAT model generates rainfall using the first order Markov chain model. Results showed that the predicted daily rainfall values were quite close to the observed rainfall for the monsoon season for the years 1996 to 1998. The scattergram of observed and simulated monthly rainfall indicated that the observed and simulated rainfall values were uniformly distributed along a 1:1 line (Figure 4). A high value for r^2 (0.91) indicated that model was able to generate monthly rainfall close to the observed rainfall. The Student's t-test indicated that the means for monthly observed (101.2 mm) and simulated (109.8 mm) rainfall were similar at the 95% level of confidence. The lower value of deviation (8.5%) indicated that the model predicted monthly rainfall values that were close to the observed values. Further, the model predicted daily runoff and sediment yield for the monsoon seasons for the years 1991 to 1998 using generated rainfall were also in close agreement with the observed runoff and sediment yield (Table 3).

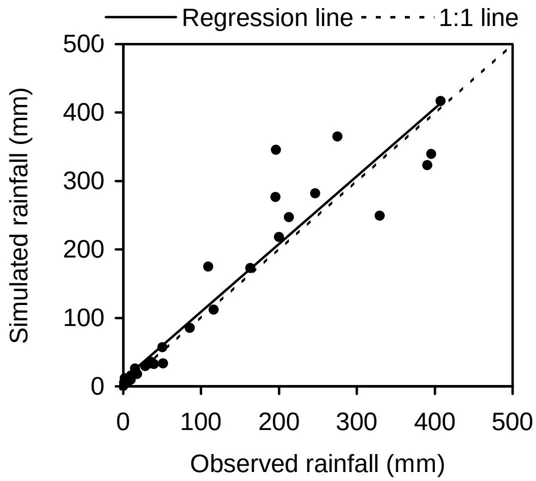

Figure 4. Comparison between observed and simulated monthly rainfall (1996-1998).

Table 3. Statistical results for monthly observed and simulated rainfall, runoff, and sediment yield during monsoon seasons (1991-1998).

Statistical parameters	Rainfall (mm)		Runoff (mm)		Sediment (t/ha)	
	Obs.	Sim.	Obs.	Sim.	Obs.	Sim.
Mean	203.33	226.80	63.68	70.60	0.78	0.82
Standard error	40.83	54.29	16.71	16.74	0.18	0.29
Standard deviation	91.30	121.41	37.36	37.42	0.41	0.64
Maximum	274.64	340.00	107.22	105.50	1.23	1.59
Minimum	51.23	36.00	13.91	22.70	0.13	0.03
Total	1016.65	1134.00	318.40	352.99	3.90	4.09
Count	40	40	40	40	40	40
t-cal		-1.314		-0.893		-0.267
t-critical (two-tail)		2.776		2.776		2.776
r^2		0.938		0.797		0.807
% Deviation		-11.5		-10.9		-5.0

Identification of Critical Subwatersheds

On the basis of soil erosion rates (Singh et al., 1992), the erosion classes were assigned to each subwatershed. The WS5 fell under the moderate (5 to 10 t/ha/yr) soil loss group of soil erosion classes. The WS12, WS9, WS7, WS6, and WS10 fell under the high (10 to 20 t/ha/yr) soil loss group of soil erosion classes, whereas other subwatersheds fell under the slight erosion classes. The nutrient losses obtained from these subwatersheds were also slightly higher in comparison to that of the other subwatersheds (Table 4).

Table 4. Model output for identification of critical subwatersheds (1996-1998).

Sub-Watershed	Area (km^2)	Runoff (mm)	Sediment (t/ha)	Organic N (kg/ha)	Organic P (kg/ha)	NO_3-N (kg/ha)	Soluble P (kg/ha)	Erosion class	Priority
WS1	17.23	467.68	4.41	5.00	2.38	2.71	0.27	Slight	-
WS2	9.29	274.78	3.66	4.15	1.99	1.42	0.17	Slight	-
WS3	6.32	422.14	4.39	5.03	2.39	2.29	0.25	Slight	-
WS4	9.93	143.59	1.68	1.96	0.94	0.75	0.09	Slight	-
WS5	14.71	284.49	7.00	7.50	3.58	1.15	0.18	Moderate	-
WS6	3.52	456.13	12.87	13.26	6.24	2.04	0.28	High	V
WS7	9.47	292.96	13.47	13.85	6.56	1.19	0.18	High	III
WS8	4.24	331.56	3.33	3.84	1.84	1.74	0.20	Slight	-
WS9	2.98	373.98	14.63	14.86	6.99	1.59	0.23	High	II
WS10	7.22	262.27	12.80	13.23	6.27	1.05	0.17	High	IV
WS11	4.78	416.65	4.67	5.30	2.53	2.25	0.25	Slight	-
WS12	0.54	256.34	18.82	18.40	8.79	1.26	0.16	High	I

Effective Management

In order to create an appropriate management strategy suited to the farmers of the watershed, a set of 60 combinations of various treatments were studied for each critical subwatershed and the best management plan was developed. For all critical subwatersheds, runoff, sediment yields, and nutrient losses showed similar trends and thus the results related to one sample subwatershed (WS7) are presented. Results showed that the rice could not be replaced by maize, groundnut, and soybean since these crops resulted in higher sediment yield as compared to rice. The farmers of the watershed generally grow rice using conventional tillage with a 25:15 kg/ha level of N:P fertilizer during the monsoon season. Therefore, the existing management practice was considered as a base for evaluating other management practices for rice.

Average annual runoff increased slightly for all the fertilizer and tillage treatments except for the MB plough, where it decreased as compared to existing tillage. On average, the maximum increase in runoff was identified for zero tillage, followed by conservation tillage, and field cultivator. There was no effect of tillage on rice yield with the recommended fertilizer dose (80:60 kg/ha of N:P). Use of an MB plough increased sediment yield by about 30% as compared to conventional tillage. This high sediment yield was due to the higher mixing efficiency of the MB plough. The lowest sediment yield (about 11 t/ha) was found for zero tillage at all fertilizer levels. The decrease in sediment yield as compared to conventional tillage was found to be about 19, 11, and 10 percent for zero tillage, conservation tillage, and field cultivator, respectively (Table 5).

Considering the existing fertilizer dose, the losses of NO_3-N increased by about 3, 2, and 1%, and decreased by 3% for conservation tillage, zero tillage, field cultivator, and MB plough, respectively. A similar trend was observed with half and full recommended doses of fertilizer for the NO_3-N losses. For the 80:60 kg/ha dose of fertilizer, the soluble P losses were found to be slightly lower than other doses. However, the losses were the same for both zero tillage and conservation tillage. For all doses of fertilizer, soluble P losses were increased by about 30% for the field cultivator and decreased by about by 37% with the MB plough (Table 5). This means that the MB plough inverses and pulverizes the soil and mixes-up the P thoroughly, and thereby it is not available at the surface to dissolve in runoff.

Table 5. Effect of various tillage practices and fertilizer levels on subwatershed (WS7) yield as simulated by SWAT for the monsoon seasons of 1996-1998.

Treatments	Runoff (mm)	Sediment (t/ha)	Rice yield (t/ha)	NO_3-N (kg/ha)	Soluble P (kg/ha)	Organic N (kg/ha)	Organic P (kg/ha)
T_1+F_1	293.18	10.96	1.55	1.21	0.30	26.25	15.67
T_2+F_1	293.02	11.94	1.55	1.22	0.30	28.20	16.84
T_3+F_1	293.04	12.12	1.58	1.20	0.24	18.95	10.39
T_4+F_1	292.82	18.73	1.64	1.15	0.12	10.87	3.26
T_5+F_1	292.96	13.47	1.62	1.19	0.18	13.85	6.56
T_1+F_2	293.28	10.83	1.63	1.26	0.30	27.02	16.55
T_2+F_2	293.13	11.76	1.63	1.27	0.30	28.97	17.74
T_3+F_2	293.13	12.03	1.66	1.24	0.24	19.59	11.08
T_4+F_2	292.93	18.68	1.73	1.16	0.12	11.03	3.43
T_5+F_2	293.04	13.44	1.68	1.21	0.18	14.33	7.05
T_1+F_3	293.41	10.84	1.76	1.40	0.30	29.11	18.63
T_2+F_3	293.27	11.77	1.76	1.41	0.30	31.20	19.97
T_3+F_3	293.24	12.04	1.76	1.35	0.24	21.11	12.59
T_4+F_3	292.96	18.67	1.76	1.19	0.12	11.38	3.79
T_5+F_3	293.12	13.44	1.76	1.29	0.18	15.33	8.04

The losses of N and P in the sediment were found to be 22 and 50% less, respectively, for the MB plough with existing fertilizer doses as compared to conventional tillage. At all fertilizer levels, organic N and P losses were lowest with the use of the MB plough (Table 5). As far as sediment loss was concerned, the zero tillage, followed by conservation tillage, and field cultivator was more suitable than the MB plough and conventional tillage. On the other hand, when nutrient losses were taken into consideration, the MB plough and conventional tillage were found to be suitable for the WS7. Considering both sediment and nutrient losses collectively, the conventional tillage was found to be better than the other tillage practices.

The field cultivator was found to be beneficial, as it was able to reduce the sediment yield by about 10%, as compared to conventional tillage, in each fertilizer application treatment (Table 5). Conversely, use of field cultivator increased nutrient losses. However, the field cultivator could be used since sediment losses were less than the conventional tillage and nutrient losses were within the permissible limit. The results also revealed that the 40:30 kg/ha of N:P level of fertilizer proved to be better for rice with either conventional tillage or the field cultivator.

Conclusions

The SWAT model accurately simulates runoff, sediment yield, and nutrient losses from the Nagwan Watershed on a daily and monthly basis. The SWAT model can successfully be used for identifying critical subwatersheds for management purposes. The model can be used for planning and management of the Nagwan Watershed on a long-term basis using generated daily rainfall. For the existing rice crop, zero and conservation tillage practices along with 40:30 kg/ha of N:P fertilizer can be recommended because the tillage reduces sediment yield by about 12 and 19%, respectively, as compared to existing tillage. The field cultivator is recommended to replace the conventional tillage because it reduces the sediment yield by 10% as compared to conventional tillage.

References

Arnold J G; Williams J R; Srinivasan R; King K W. 1996. Soil and Water Assessment Tool, User's Manual, USDA, Agriculture Research Service, Grassland, Soil and Water Research Laboratory, 808 East Blackland Road Temple, TX 76502.

Arnold J G; Srinivasan R; Muttiah R S; Williams J R. 1998. Large area hydrologic modeling and assessment part I: model development, *J. of Am. Water Resou. Asso., AWRA*, 34(1): 73-89.

Arnold J G; Srinivasan R; Muttiah R S; Allen P M. 1999. Continental scale simulation of the hydrologic balance. *J. of Am. Water Resou. Asso., AWRA*, 35(5):1037-1051.

ASCE Task Committee (1993). Criteria for Evaluation of Watershed Models. *J. of Irrig. and Drain. Engg.*, 119(3): 429-442.

Bingner R L; Garbrecht J; Arnold J G; Srinivasan R. 1997. Effect of watershed division on simulation of runoff and fine sediment yield. *Trans. of ASAE*, 40(5): 1329-1335.

Dhruva Narayana V V. 1993. In Soil and Water Conservation Research in India. Indian Council of Agricultural Research, Krishi Anusandhan Bhavan, Pusa, New Delhi; 146-51.

Dickinson W T; Rudra R P; Wall G J. 1990. Targeting remedial measures to control nonpoint source pollution. *Water Resources Bulletin, AWRA*, 26(3): 499-507.

EPA (1976). Quality Criteria for Water. Environmental Protection Agency, Washington, DC.

Jenson S K; Domingue J O. 1988. Extracting topographic structure from digital elevation data for geographic information system analysis. *Photogram. Engg. and Remote Sen.*, 54(11): 1593-1600.

Maas R P; Smolen M D; Dressing S A. 1985. Selecting critical areas for nonpoint source pollution control. *J. of Soil and Water Cons.*, 40(1): 68-71.

Mannering J V. 1981. The Use of Soil Tolerances as Strategy for Soil Conservation. In Soil Conservation Problem and Prospect. R. P. C. Morgan John Wiley & Sons, Chichester England; 337-349.

Rosenthal W D; Srinivasan R; Arnold J G. 1995. Alternative river management using a linked GIS-hydrology model. *Trans. of ASAE*, 38(3): 783-790.

Santhi C; Arnold J G; Wliiiams J R; Dugas W A; Srinivasan R; Hauck L M. 2001. Validation of the SWAT model on a large river basin with point and nonpoint sources. *J. of Am. Water Resou. Asso., AWRA*, 37(5): 1169-1188.

Singh G; Ram Babu; Pratap Narain; Bhushan L S; Abrol I P. 1992. Soil erosion rate in India. *J. of Soil and Water Cons.*, 47(1): 97-99.

Srinivasan R; Arnold J G; Rosenthal W; Muttiah R S. 1993. Hyrologic modeling of Texas Gulf basin using GIS. In Proc. of 2nd Intl. GIS and Environ. Modeling, Breckinridge, Colorado; 213-217.

Srinivasan R; Ramanarayanan T S; Arnold J G; Bednarz S T. 1998. Large area hydrologic modeling and assessment part II: Model application. *J. of Am. Water Resou. Asso., AWRA*, 34(1): 91-101.

Storm D E; Dillaha T A; Mostaghimi S; Shanholtz V O. 1988. Modeling phosphorous transport in surface runoff. *Trans. of the ASAE*, 31: 117-127

Tim U S; Moostaghimi S; Shanholtz V O. 1992. Identification of critical nonpoint pollution source areas using geographic information systems and water quality modeling. *Water Resources Bulletin, AWRA*, 28(5): 877-887.

Session VIII

30. **An analysis of the 2004 Iowa diffuse pollution needs assessment using SWAT** **291**
Philip W. Gassman, Silvia Secchi, Cathy L. Kling, Manoj Jha, Lyubov A. Kurkalova and Hong-Li Feng

31. **Potential accuracy of water quality estimates based on non-calibrated SWAT simulations** **301**
Claire Baffaut, Todd D. Farrand and Verel W. Benson

32. **An approach to assess SWAT model performance in evaluating management actions in a Finnish catchment** **310**
Ilona Bärlund and Teija Kirkkala

33. **Application of SWAT model to the decision support framework of the Mekong River Commission** **320**
Kittipong Jirayoot and Le Duc Trung

34. **The European Common Agriculture Policy and feasible hydrological impacts for the Dill Catchment, Germany** **330**
L. Breuer, J.A. Huisman and H.-G. Frede

An Analysis of the 2004 Iowa Diffuse Pollution Needs Assessment Using SWAT

Philip W. Gassman, Silvia Secchi, Cathy L. Kling, Manoj Jha, Lyubov A. Kurkalova, and Hong-Li Feng
Center for Agricultural and Rural Development (CARD), Dept. of Economics, 578 Heady Hall, Iowa State Univ., Ames, Iowa, 10011-1070, USA. Email:pwgassma@iastate.edu

Abstract

An economic and environmental analysis for mitigating cropland diffuse pollution was performed for the Iowa Department of Natural Resources (IDNR) to support cost information to be supplied to the U.S. Environmental Protection Agency (USEPA) for the 2004 Clean Watersheds Needs Survey (CWNS). The assessment was performed for 13 major watersheds in Iowa by interfacing economic models with the Soil and Water Assessment Tool (SWAT) model, and utilizing available conservation practice costs and other relevant data. Calibration and validation of SWAT was initially performed for the Raccoon River Watershed; r^2 and model efficiency (E) statistics were greater than 0.7 for most of the comparisons between simulated and measured annual and monthly stream flows, sediment loads, and nitrate losses. The majority of r^2 and E values computed for annual comparisons between simulated and measured stream flows for the 13 study watersheds exceeded 0.85; the corresponding monthly statistics were generally greater than 0.75. The conservation practices that were analyzed included land set aside, terraces, grassed waterways, contouring, conservation tillage, and a simple nutrient reduction strategy. The program costs (net present value) of implementing the set of identified conservation practices over a 10-year phase-in period were estimated to range from \$2.414 to \$4.269 billion, depending on whether new and/or existing adopters are accounted for and if high or low cost estimates are used. The associated SWAT-predicted reductions in sediment, nitrates, total N, and total P for the 13 watersheds ranged from 6 to 65%, 6 to 20%, 14 to 30%, and 28 to 59%, respectively.

Introduction

The U.S. Environmental Protection Agency (USEPA) is required to perform a periodic national Clean Watersheds Needs Survey (CWNS) in response to directives that were established by the 1972 U.S. Clean Water Act. The purpose of the survey is to identify all existing water quality or public health problems, and the corresponding mitigation costs that would quailfy for funding from the Clean Water State Revolving Fund (CWSRF). Categories eligible for CWSRF funding include wastewater treatment systems, sewer and conveyance systems, storm water management programs, and diffuse pollution sources. Cost estimates of mitigating Iowa cropland diffuse pollution were not submitted for the 2000 CWNS (USEPA, 2000) by the the Iowa Department of Natural Resources (IDNR). However, the IDNR wished to submit such cost estimates to the USEPA for the 2004 version of the CNWS, to provide a more accurate accounting of cropland diffuse pollution cost abatement in Iowa. In response, an assessment was performed for 13 major watersheds that cover 87% of Iowa (Figure 1) by interfacing economic models developed in-house at the Center for Agricultural and Rural Development (CARD) with the Soil and Water Assessment Tool (SWAT) model (Arnold et al., 1998), and utilizing available conservation practice cost and other relevant data. The study required: (1) calibration and validation of SWAT, (2) selection of the conservation practices to include in the study and associated program costs, and (3) estimation of the total costs and and environmental impacts of implementing the conservation practices. The objective here is to breifly describe all three key phases of the study and to further discuss the implications of the results found for two different scenarios.

Watershed Descriptions

The SWAT simulations were configured for 13 major watersheds in Iowa that range in size from 2,051 km^2 to 37,496 km^2 and together cover 87% of the state (Figure 1). These watersheds were selected because they were completely or mostly located in Iowa, and they represented the majority of Iowa land area for the SWAT scenarios. The key characteristics of each watershed are given in Table 1. The watersheds consist of one to nine U.S. Geological Survey (USGS) 8-digit Hydrologic Unit Code (HUC), or Cataloging Unit watersheds (Seaber et al., 1987). The 8-digit watersheds were used to define the Des Moines and Iowa River subwatersheds; smaller 10-digit watersheds (IDNR-IGS, 2004) were used to define the subwatersheds for the other 11 watersheds as discussed in the next section.

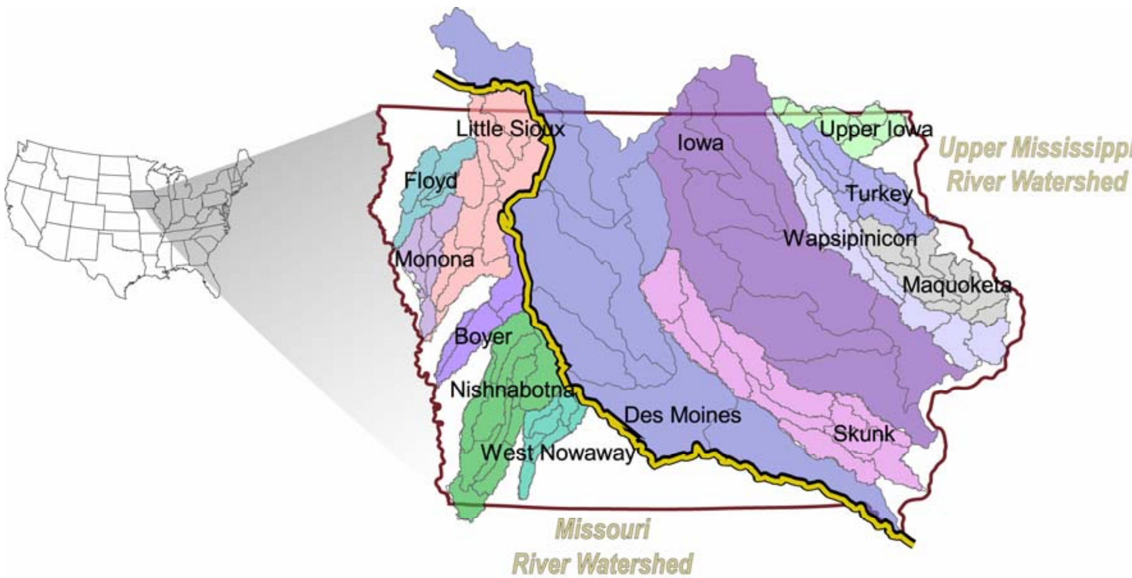

Figure 1. The 13 watersheds (and subwatersheds) included in the study, and the location of each watershed within the Missouri River or Upper Mississippi River Watersheds.

Table 1. Characteristics of the 13 study watersheds.

ID	Watershed	# of 8-digit watersheds	# of sub-watersheds	Drainage area (km^2)	Major land use (%)			
					Cropland	Grassland[b]	Forest	Urban
1	Floyd	1	5	2,376	84	13	0	3
2	Monona	1	5	2,452	78	19	2	1
3	Little Sioux	2	10	9,203	86	13	1	0
4	Boyer	1	5	2,820	68	26	4	2
5	Nishnabotna	3	11	7,718	84	15	1	0
6	Nodaway	1	7	2,051	52	41	5	3
7	Des Moines	9	9	37,496	71	16	6	7

8	Skunk	3	12	11,246	69	25	5	1
9	Iowa	9	9	32,796	77	12	4	8
10	Wapsipinicon	2	11	6,582	77	19	3	1
11	Maquoketa	1	10	4,827	56	32	10	3
12	Turkey	1	9	4,400	56	25	16	3
13	Upper Iowa	1	7	2,569	51	26	19	3

SWAT Baseline Simulation Methodology

The U.S. Department of Agriculture (USDA) 1997 National Resources Inventory (NRI) database (Nusser and Goebel, 1997; http://www.nrcs.usda.gov/technical/NRI/) is a key data source that was used to perform the SWAT simulations for the 13 watersheds. The NRI contains soil type, landscape features, cropping histories, conservation practices, and other data for roughly 800,000 U.S. nonfederal land "points" including 34,120 in Iowa (14,472 of which are cropland points). Each point is assumed to represent a homogeneous area of land use, soil, and other characteristics (averaging about 430 ha in size) and is spatially referenced at the county, 8-digit watershed, Major Land Resource Area (MLRA), and state levels. Crop rotations incorporated in the SWAT simulations are derived from cropping histories reported in the NRI. Other land use data required for the baseline simulation were also obtained from the NRI. The tillage implements simulated for the different levels of tillage (conventional, reduced, mulch, and no-till) incorporated in the analysis were obtained from the USDA 1990-95 Cropping Practices Survey (CPS), which is accessible at http://usda.mannlib.cornell.edu/usda/ess_entry.html. The distribution of tillage practices were based on data obtained from the Conservation Tillage Information Center (CTIC; http://www.ctic.purdue.edu/CTIC/CTIC.html) and were imputed to the NRI points as described by Feng et al. (2004). Historical precipitation, maximum temperature, and minimum temperature data obtained from the Iowa Environmental Mesonet (http://mesonet.agron.iastate.edu/request/coop/fe.phtml) for the 20-year period (1980-2000) were used for the SWAT simulations. The soil layer data required for the SWAT simulations was input from a soil database that contains soil properties consistent with those described by Baumer et al. (1994), with the additional enhancement of ID codes that allowed direct linkage to NRI points.

Delineation of each watershed into smaller spatial units required for the SWAT simulations consists of two steps: (1) subdividing each watershed (Figure 1) into either 8- or 10-digit watersheds, and (2) creating Hydrologic Response Units (HRUs) within each of the subwatersheds. The smaller 10-digit subwatersheds were used for those watersheds that consist of 1 to 3 8-digit watersheds (Figure 1), to avoid potential distortions in predicted pollutant indicators when only a small number of subwatersheds are used in a SWAT application as found by Jha et al. (2004). The HRUs required for the SWAT baseline simulations were created by aggregating NRI points together that possess common land use, soil, and management characteristics; these HRUs represented "lumped" areas of common land use rather than explicit spatial locations, which is the standard approach with SWAT (e.g., Arnold et al., 2000). Further details of the subwatershed and HRU delineation methods used for this study are given in Jha et al. (2005) and Kling et al. (2005).

SWAT Calibration and Validation

A SWAT calibration and validation exercise (Jha et al., 2005) was performed for the Raccoon River Watershed, which is a subwatershed of the Des Moines River Watershed (Figure 2). The Raccoon River Watershed was chosen for the calibration and validation phase because reliable stream flow, sediment, and nitrate data was available (Lutz, 2004). A total of 26 10-digit subwatersheds were delineated for the Raccoon River simulations (Figure 2); each subwatershed was further subdivided into appropriate HRUs. An automated digital filter technique (Arnold and Allen, 1999) was used to estimate baseflow versus surface runoff contributions to stream flow measured near Van Meter, Iowa (Figure 2). This step indicated that the total flow consisted of about 65% baseflow. Calibration of SWAT was first performed for the full 18-year period which resulted in a split of about 60% baseflow and 40% surface runoff, which was similar to the digital filter results. These results were achieved by reducing the curve numbers (CNs) by 8% and the available soil water capacity (SOL_AWC) values by 0.04 mm. Further calibration and validation was then performed for 1981-89 and 1990-99, respectively, by comparing simulated annual and monthly stream flows, sediment yields, and nitrate loads with corresponding measured values collected at Van Meter (the monthly measured sediment and nitrate loads were estimated from single monthly measurements). The 1981-89 stream flow calibration was performed first, by adjusting additional parameters such as the soil evaporation compensation factor (ESCO). Model calibration of sediment yield was then performed by adjusting selected parameters, including the linear (SPCON) and exponent (SPEXP) components of the sediment equation and the channel cover factor, to match measured sediment yield. Calibration of the nitrate predictions primarily involved adjusting the nitrogen percolation coefficient (NPERCO) within an acceptable range. The model was not found to be very sensitive to the NPERCO adjustments. The resulting r^2 and Nash-Sutcliffe modeling efficiency (E) statistics (Table 2) indicated that the model accurately reflected the measured annual and monthly flows, sediment yields, and nitrate loads in both periods, except for the predicted monthly sediment losses in 1981-89. Graphical comparisons shown in Figure 3 underscore that the model realistically tracked the Raccoon River stream flows; similar comparisons are shown for sediment and nitrate in Jha et al. (2005). The calibrated parameters were then used for the 13 watersheds included in the assessment. Further comparisons (Figure 4) show that SWAT predicted the measured stream flows well across all 13 watersheds.

Table 2. Predicted versus measured statistics for the Raccoon River calibration and validation.

Indicator	Calibration Period (1981-89)				Valibration Period (1990-99)			
	Annual		Monthly		Annual		Monthly	
	R^2	E	r^2	E	r^2	E	r^2	E
Stream flow	0.96	0.95	0.78	0.77	0.93	0.87	0.86	0.82
Sediment	0.90	0.88	0.46	0.44	0.96	0.83	0.91	0.90
Nitrate	0.92	0.82	0.78	0.75	0.77	0.70	0.79	0.75

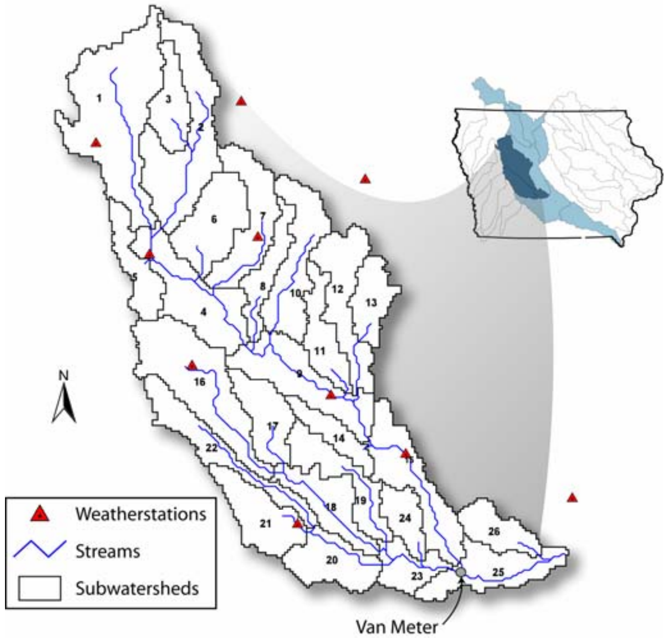

Figure 2. Raccoon River Watershed location, subwatersheds used for the SWAT simulations, and location of the weather stations and town of Van Meter (measured data collection site).

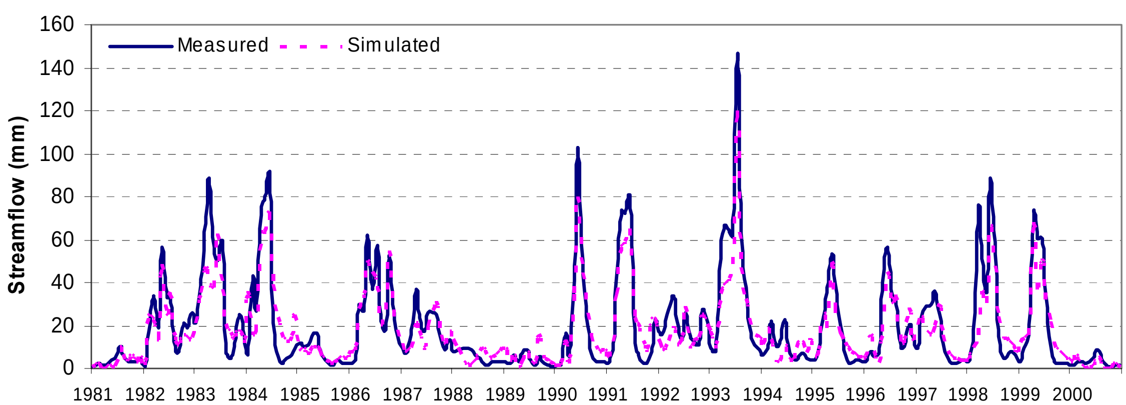

Figure 3. Simulated versus measured monthly flows at Van Meter, IA for the Raccoon River.

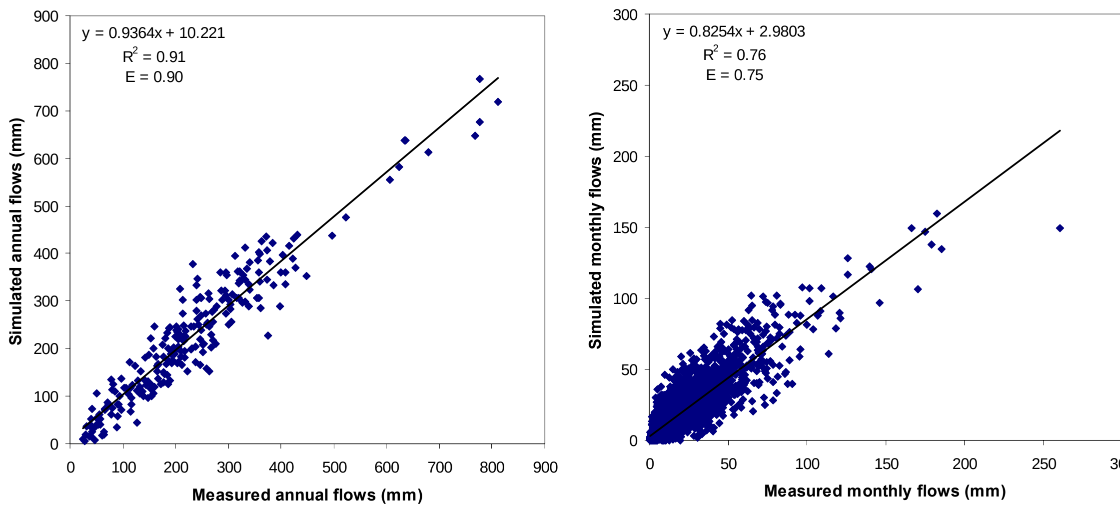

Figure 4. Simulated versus measured annual and monthly stream flows for all 13 watersheds.

Selection and Simulation of Conservation Practices

The choice and extent of conservation practices to include in the analysis was determined in collaboration with the IDNR. The practices selected were Conservation Reserve Program (CRP) land (land set aside), terraces, grassed waterways, contouring, and conservation tillage. The latter four are all established best management practices (BMPs); CRP land also essentially functions as a BMP when applied to highly erodible land, riparian areas or other vulnerable landscapes. Existing cropland managed with these BMPs was identified using NRI or CTIC data, and was accounted for in both the baseline and scenario simulations. The "new BMPs" adopted for the conservation practice scenarios were assumed to be applied primarily to cropland that did not have a prior history of conservation practices, except for some cases in which new BMPs could override existing practices following the criteria given in Kling et al. (2005). The BMPs adopted in the scenarios were simulated simultaneously based on the following algorithm: (1) conversion of all cropland to CRP, that was identified in the NRI to be within 30 m of a waterway, (2) conversion of additional cropland to CRP based on the highest erosion index values given in the NRI, until 10% of the statewide cropland was converted (including step 1), (3) installation of terraces on all remaining cropland with slopes greater than 7% in western Iowa (within the Missouri River Watershed—see Figure 1) and slopes exceeding 5% on all other cropland, (4) implementation of contouring on all cropland with slopes higher than 4%, that were not affected by steps 1-3, (5) installation of grassed waterways on all crop fields that have slopes of at least 2% that were not included in steps 1-4, and (6) adoption of conservation tillage on all cropland with slopes greater than 2% that were not converted to CRP; the conservation tillage mix consisted of 80% mulch tillage (>30% residue coverage) and 20% no-till (>60% residue coverage). The application of the algorithm resulted in a significant increase in the statewide area that would be treated with the five conservation practices as shown in Table 3. The largest increases occurred for conservation tillage, grassed waterways, and terraces. The distribution of the increased area managed with these conservation practices varied greatly between the 13 watersheds as described by Kling et al. (2005).

Table 3. Effect of scenario on statewide areal distributions (ha) of the conservation practices.

Statewide Status	CRP	Conservation Tllage	Contouring	Grassed Waterways	Terraces
Existing	704,211	5,666,518	2,083,765	862,996	782,227
New	346,518	2,929,352	493,117	2,857,126	1,316,356

A second scenario was performed that incorporated the previously described algorithm along with a simple 10% reduction in nitrogen (N) and phoshorus (P) fertilizer application rates, which were assumed to be applied only to corn. The N and P fertilizer application rates were calculated at the 8-digit watershed level, based on total N and P fertilizer loads that were determined for those regions in a nutrient balance study conducted by the Iowa Geological Survey division of the IDNR (C. Wolter. 2004. Personnel communication. IDNR-IGS, Iowa City, IA). The average 8-digit watershed N application rates varied between 94 and 206 kg/ha; the P application rates were considerably lower.

The terrace, contouring, and grassed waterway costs were determined based on available data obtained from USDA and Iowa state agency sources. A range of cost estimates were found for some of the practices, especially for terraces. Computing a cost impact of reducing fertilizer use proved extremely difficult; the prevailing view based on expert opinion was that the crop yield economic impact of the fertilizer reduction would be insignificant. However, a one-time nutrient management cost of about $37/ha was assumed to be incurred by the producers in response to the simulated 10% decrease in fertilizer application rates. Discrete choice tillage and land retirement economic models were used to estimate tillage and CRP costs, as a function of NRI and CPS data, and production costs estimated using methods developed by the AAEA (2000). The selection of which NRI points that CRP, terraces, contouring, grassed waterways, and conservation tillage should be assigned to was based on the conservation practices algorithm. New land use distributions determined with the algorithm were then input to SWAT by aggregating NRI points together that possess common land use, soil, and management characteristics. These NRI clusters served as the HRUs for the two scenarios. Further details on the cost estimation process and modeling framework are given in Kling et al. (2005).

The effect of contouring, terraces, and grassed waterways in SWAT was primarily accounted for by adjusting the support practice (P) factor, which is one of the factors in the Modified Universal Soil Loss Equation (MUSLE) that is used in SWAT. The contouring and terrace P factors are based on values reported by Wischmeier and Smith (1978) as a function of slope range, and ranged between 0.5 to 0.9 for contouring and 0.1 to 0.18 for terraces. A P factor value of 0.4 for grassed waterways was assumed based on the methodology used by Gassman et al. (2003) for simulating the impact of grassed waterways in the Mineral Creek Watershed in eastern Iowa. The impact of grassed waterways was further accounted for by adjusting the Manning's N values for the affected HRUs, to reflect improved vegetation cover in the field channels. Conservation tillage, CRP, and fertilizer reduction effects were simulated directly based on management or land use changes.

Results and Discussion

Both annualized social costs and program costs phased in over a 10-year period were estimated for this study (Kling et al., 2005); the 10-year phase-in period was considered by

IDNR to be a reasonable timeframe to inplement the additional BMPs. The social and program costs were determined for both the existing and new practices, with the recognition that funding most existing practices is probably unlikely. The projected upper and lower bound estimates (where applicable) of the program costs for both the existing and new practices are listed in Table 4. The large increase in terraces was by far the most expensive new practice, followed by the additional land converted to CRP. The high terrace costs reflect the fact that installation of terraces is quite expensive relative to most other BMP options. However, the total CRP and terrace costs were much closer for existing landscapes that were managed with these two practices. The total overall costs are projected to range between \$2.414 and \$4.269 billion, depending on whether the costs for existing practices are included and whether low or high cost estimates are used. It is notable that the Iowa cost estimates in Table 4 are much greater than the 2000 USEPA CNWS "documented national estimate of \$500 million", indicating that a more complete national cost analysis of mitigating diffuse pollution is needed. Distributions of the total CRP, conservation tillage, terrace, and overall total costs are shown by watershed in Figure 4 (high estimates that include both existing and new practice costs). These distributions clearly show that the effects of the scenario algorithm varied greatly across the state.

Table 4. Total projected program costs of existing and new conservation practices for Iowa.

Cost category	Total program costs ($ millions)			
	Existing		New	
	Low	High	Low	High
CRP (land retirement)	640	640	315	315
Conservation tillage	324	324	150	150
Contouring	36	73	21	42
Grassed waterways	27	40	95	142
Terraces (annualized cost at 5%)	709	709	1,712	1,712
Nutrient management	0	0	121	121
Total	1,736	1,786	2,414	2,482

Baseline loadings predicted for each watershed outlet are reported in Kling et al. (2005). The impacts of the scenarios relative to the baseline are shown in Table 6. The predicted sediment and total P relative changes were virtually identical across the 13 watersheds between the two scenarios and thus are shown only for scenario 2. The predicted nitrate and total N losses are shown for both scenarios, due to the increased reductions that occurred in response to the 10% fertilizer reduction that was simulated for scenario 2. Predicted sediment decreases ranged from 6% for the Little Sioux River Watershed to 65% for the Turkey River Watershed. Sediment reductions were estimated to be greater than 30 and 40% for nine and seven of the watersheds, respectively. The predicted decreases in total P losses ranged from 28% for the Upper Iowa Watershed to 59% for the Turkey River Watershed, with the majority of the decreases exceeding 40% relative to the baseline. Relatively small nitrate reduction impacts were predicted for the initial scenario run of -6 to 13% across the 13 watersheds. The negative numbers likely reflects the fact that increased nitrate leaching, followed by subsequent increases in nitrate losses via tile drains, can occur with increased levels of conservation tillage and terraces. Nitrate reductions of 6% for the Des Moines River Watershed to 20% for the Nishnabotna River Watershed were predicted for the second scenario, reflecting the impact of the reduced nitrogen fertilizer applications. The same effect can be seen for the predicted reductions in total N losses between the two scenarios, which were generally much higher for the second scenario.

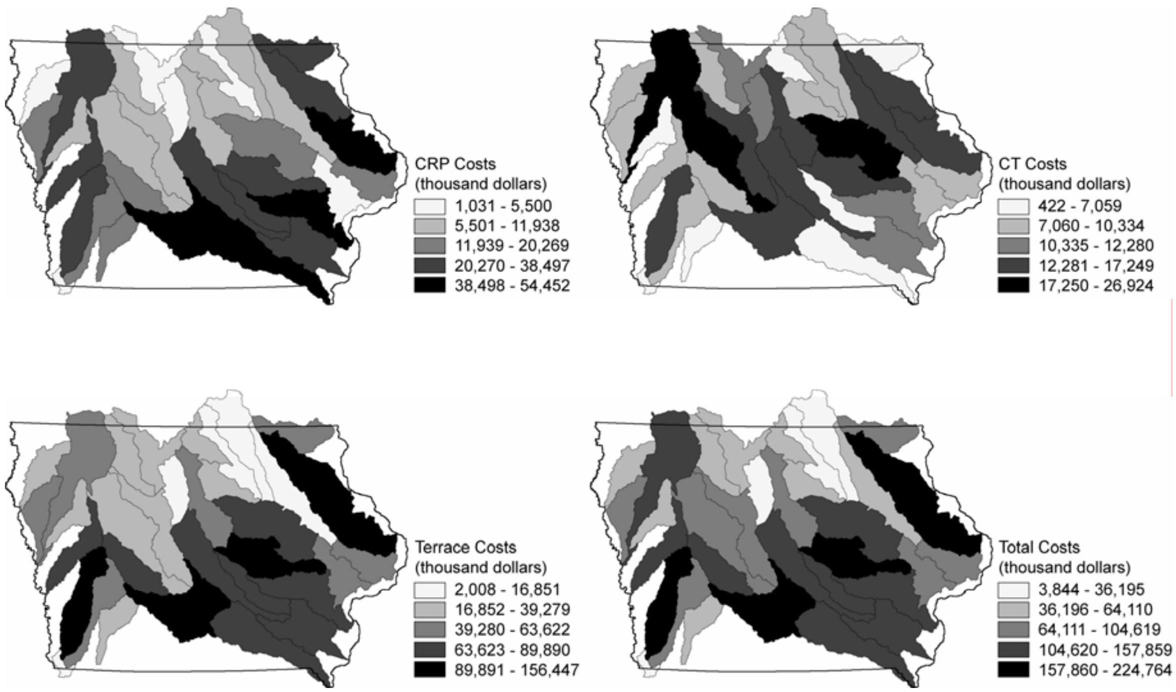

Figure 5. Distribution of selected conservation practice costs and total costs by watershed.

Table 5. Reductions (%) for selected indicators relative to the baseline simulations[a]

Watershed	Sediment	Total P	Total N (scenario 1)	Total N (scenario 2)	Nitrate (scenario 1)	Nitrate (scenario 2)
Floyd	30	52	9	20	-1	13
Monona	10	42	8	20	2	17
Little Sioux	6	49	7	15	2	11
Boyer	35	53	19	27	4	16
Nishnabotna	43	52	25	30	13	20
Nodaway	45	45	17	22	6	11
Des Moines	10	37	14	20	-5	6
Skunk	63	51	12	19	5	13
Iowa	13	48	23	29	-5	6
Wapsipinicon	64	50	6	14	1	9
Maquoketa	46	56	6	19	-6	9
Turkey	65	59	8	19	-3	10
Upper Iowa	50	28	10	17	1	10

[a]Sediment and total P results are from scenario 2, which were virtually identical to scenario 1.

Conclusions

The results of this study suggest that the costs of reducing diffuse pollution to acceptable levels in Iowa could be quite high, and that additional research is needed to accurately estimate such costs at both state and national levels in the U.S. This initial analysis does not begin to address all the potential practices that could be used to improve water quality, such as wetlands and riparian buffers. Thus it is probable that the algorithm used does not result in the most cost-efficient set of conservation practices or the most effective approach for reducing polluntant loads. At present, there is a lack of clarity regarding what target pollutant levels should be in streams, which needs to be addressed for future studies. The modeling system used for this analysis proved to be a generally robust tool for obtaining an initial assessment of the costs and environmental impacts of mitigating cropland nonpoint source pollution in Iowa. The same approach could be adopted in other regions of the country to provide a more accurate accounting of possible costs to reduce cropland nonpoint source pollution. The modeling approach could be improved by incorporating more spatial detail into SWAT, which would allow simulation of conservation practices at explicit locations within different landscapes. Better cost estimates would also strengthen the cost assessment process.

References

AAEA. 2000. Commodity costs and return estimation handbook. Task Force, American Agricultural Economics Association. Ames, Iowa. Available at: http://waterhome.brc.tamus. edu/care/Aaea/.

Arnold, J.G., and P.M. Allen. 1999. Automated methods for estimating baseflow and groundwater recharge from stream flow records. *J. Amer. Water Resour. Assoc.* 35(2):411-424.

Arnold, J.G., R.S. Muttiah, R. Srinivasan, and P.M. Allen. 2000. Regional estimation of base flow and groundwater recharge in the upper Mississippi basin. *J. Hydrol.* 227(2000):21-40.

Arnold, J.G., R. Srinivasan, R.S. Muttiah, and J.R. Williams. 1998. Large area hydrologic modeling and assessment part I: model development. *J. Amer. Water Resour. Assoc.* 34(1):73-89.

Baumer, O., P. Kenyon, and J. Bettis. 1994. MUUF v2.14 User's Manual. U.S. Department of Agriculture, Natural Resources Conservation Service, National Soil Survey Center, Lincoln, Nebraska.

Feng, H., L.A. Kurkalova, C.L. Kling, and P.W. Gassman. 2004. Environmental conservation in agriculture: land retirement versus changing practices on working land. Working paper 04-WP 365. Center for Agricultural and Rural Development, Iowa State Univ., Ames, Iowa. Available at: http://www.card.iastate.edu/facstaff/profile.aspx?id=5&show=pubs

Gassman, P.W., A. Saleh, E. Osei, J. Abraham, and J. Rodecap. 2003. Environmental and economic impacts of alternative management scenarios for the Mineral Creek Watershed. Proceedings of the Total maximum Daily Load (TMDL) Environmental Regulations II, 8-12 November, Albuquerque, New Mexico. ASAE, St. Joseph, Michigan. pp. 323-331.

IDNR-IGS. 2004. Drainage basin data. What's Happenin', The Iowa Geological Survey's Geographic Information Systems Bi-Monthly Section Newsletter. Available at:

http://www.igsb.uiowa.edu/nrgislibx/ newsletters/200408%20GIS%20Newsletter%20 Vol%20III.pdf.

Jha, M., P.W. Gassman, S. Secchi, R. Gu, and J. Arnold. 2004. Effect of watershed subdivision on SWAT flow, sediment, and nutrient predictions. *J. of Amer. Water Res. Assoc*. 40(3):811-825.

Jha, M., P.W. Gassman, S. Secchi, and J.G. Arnold. 2005. Nonpoint source needs assessment for Iowa part I: configuration, calibration and validation of SWAT. Watershed Management to Meet Water Quality Standards and Emerging TMDL (Total Maximum Daily Load), Proceedings of the Third Conference 5-9 March 2005 Atlanta, Georgia. ASAE, St. Joseph, Michigan. pp. 511-521.

Kling, C., S. Secchi, M. Jha, L. Kurkalova, H.F. Hennessy, and P. Gassman. 2005. Report to the Iowa Department of Natural Resources: Nonpoint source needs assessment for Iowa: The cost of improving Iowa's water quality. Center for Agricultural and Rural Development, Dept. of Economics, Iowa State Univ., Ames, Iowa.

Lutz, 2004. Annual Report: Water Quality Studies—Red Rock and Saylorville Reservoirs, Des Moines River, Iowa. Environmental Engineering Section, Dept. of Civil Engineering, Engineering Research Institute, Iowa State Univ., Ames, Iowa. Available at: http://www.ccee.iastate.edu/research/ lutz/homepage.html.

Nusser, S. M., and J.J. Goebel. 1997. The national resources inventory: a long-term multi-resource monitoring programme. *Environ. Ecol. Stat.*. 4:181-204.

Seaber, P.R., F.P. Kapinos, and G.L. Knapp. 1987. Hydrologic Units Maps. U.S. Geological Survey, Water-Supply Paper 2294.

USEPA. 2000. Clean Watersheds Needs Survey. U.S. Environmental Protection Agency, Office of Wasterwater Management, Municipal Support Division, Municipal Policy Branch Washington, D.C. 20460. Available at: http://www.epa.gov/owm/mtb/cwns/2000rtc/toc.htm.

Wischmeier, W. H. and D. D. Smith. 1978. Predicting rainfall erosion losses - A guide to conservation planning. USDA Handbook No. 537. Washington, D. C.

Potential Accuracy of Water Quality Estimates Based on Non-calibrated SWAT Simulations

Claire Baffaut*[1], Todd D. Farrand[1], and Verel W. Benson[1]
[1]Food and Agricultural Policy Research Institute, University of Missouri – Columbia, 101 Park DeVille Drive, Columbia, MO 65203, USA. Email: baffautc@missouri.edu

Abstract

The SWAT model can be used to analyze the impact of alternative management practices on streamflow and water quality indicators; it has been shown to be a good predictor of these indicators when it is calibrated with local flow and water quality data. One draw-back is the need for flow and water quality data that is not always available. The intent of this study is to investigate the possibility of using SWAT for assessing the effectiveness of the environmental and conservation programs when no calibration data is available. The Miami Creek and the Long Branch watersheds in western and northern Missouri, respectively, were modeled with SWAT when no flow data was available. The models were developed in close cooperation with local stakeholders and validated using regional flow data, correlations based on drainage areas, county crop yields, and the results of pesticide analyses in nearby watersheds. Since then flow data was collected in both watersheds and the models were calibrated using this data. The analysis compares the goodness of fit of the model results with the measured flow and the corresponding sediment, nutrient, and chemical loadings when the models are calibrated and when they are not. It also examines whether the calibration of the models leads to different answers in terms of the effectiveness of alternative management practices. Results indicate that average annual flow values predicted by the non-calibrated models were within 15% of the values predicted by the calibrated model; sediment loadings were within 20 to 30% of those predicted by the non-calibrated models, and pollutant loading differences varied from 15% to 50%. In spite of the large differences of results from the calibrated and non-calibrated models, the predicted efficiencies of no-till practices and reduced applications of atrazine are similar with both models. Additional conservation practices such as nutrient management, pasture and grazing management systems, filter strips, and conservation crop rotations will be investigated.

Introduction

The SWAT model can be used to analyze the impact of alternative management practices on streamflow and water quality indicators; in the U.S. it is proposed as a tool to evaluate the impacts of many state and federal conservation programs at the watershed level. SWAT has been shown to be a good predictor of flow, nutrient concentrations, and pesticide concentrations when it is calibrated with local flow and water quality data (Arnold et al. 2000; Peterson and Hamlett, 1998; Baffaut, 2003). During calibration the values of the input parameters are adjusted by comparison of the model results with the measured variables (flow values and pollutant concentrations). One draw-back is the need for flow and water quality data that are not always available.

In the Unites States, water resource managers, planners, and regulators are in need of a tool to evaluate and quantify the environmental benefits of federal and state conservation programs. These programs consist of voluntary measures subsidized by a governmental agency with cost-share or technical assistance. While the practices have often been tested at the field level, it is difficult to estimate the benefits at the watershed level of a range of known practices. Planners need to determine the level of investment needed in a watershed to obtain water quality improvement, the number of hectares to be treated, and where the efforts should be focused. In the absence of flow and water quality data prior to and after the implementation of these measures, water managers only resource is to develop and use a watershed model. Yet, the lack of flow and water quality data also makes model calibration approximate. Practitioners have gone around this problem by asserting that the goal is not to have absolute values of the different pollutant loadings but to estimate the changes that could be achieved by implementing alternative management practices. Thus it is often assumed that the change predicted by a non-calibrated model is a good approximation of what can be expected. To our knowledge, this hypothesis has not been verified.

The intent of this study is to investigate the possibility of using SWAT to assess the effectiveness of the environmental and conservation programs when good physical data (soil, land use, and land management) but no flow or water quality calibration data are available. Two mid-sized agricultural watersheds of Missouri are considered to estimate and analyze the differences in results obtained when proper flow calibration is conducted and when it is not. The analysis utilizes these two watersheds to:

- quantify the differences in water, nutrient, and pesticide loadings, and
- quantify the differences in loading reduction estimated by the models.

Methodology

The two watersheds are the Miami Creek (Figure 1) and the Long Branch (Figure 2) watersheds in western and northern Missouri, respectively. The main characteristics and land use information are summarized in Table 1.

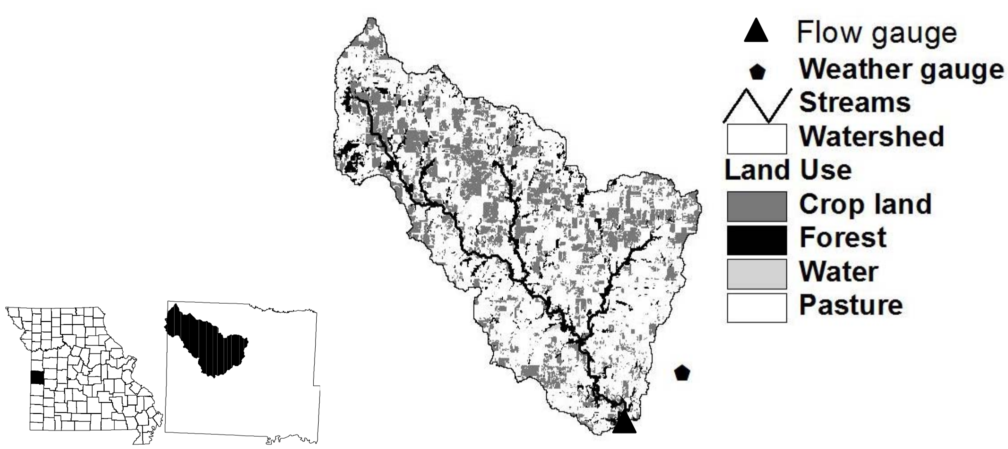

Figure 1. Location and land use distribution of the Miami Creek Watershed.

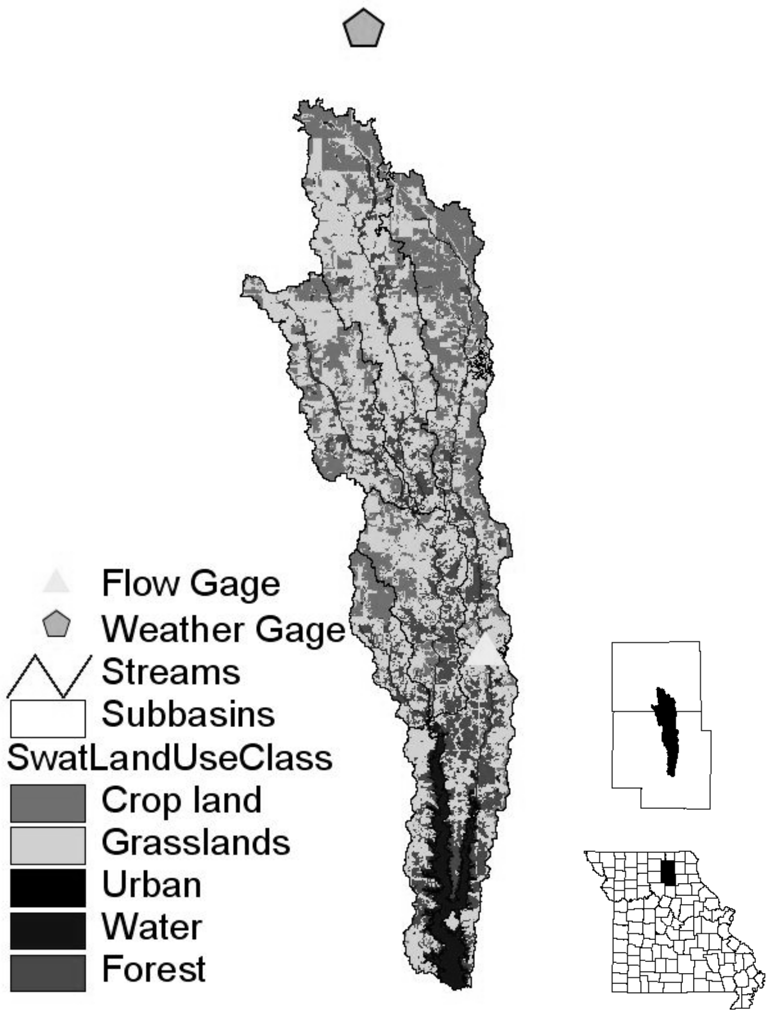

Figure 2. Location and land use distribution of the Long Branch Watershed.

Table 1. Land use distribution in the Long Branch and Miami Creek Watersheds.

	Long Branch	Miami Creek
Watershed area (km^2)	271.0	350.0
Average annual Precipitation (mm)	911	1100
Average annual flow (cms)	0.56	0.90
Crop land	29 %	26 %
Grassland	39 %	66%
Forest	27 %	8%
Water	5%	0%
Soil hydrological group	C and D	D
Ratio of groundwater contribution to total flow	0.17	0.13

Both watersheds were modeled with SWAT when no flow or water quality data were available. The models were developed with the following information:

- Topography: a 30-meter grid with elevation in meters.
- Weather: 30 years or more of measured daily precipitation and temperature.

- Land use: a 30-meter grid land use map developed from a 1992 satellite image and ground proofed by the Missouri Resource Assessment Program.
- Soils: a SSURGO soil map was utilized to determine the dominant soils in each subbasin. Soil characteristics for these soils were established by soil scientists at the Natural Resource Conservation Service.
- Management: a panel of producers, conservationists, and custom applicators was established in each watershed to develop a consensus of the management practices. Input parameters such as operation dates, application rates, and rotations were determined in cooperation with the farm panel. The crop rotations and management operations are described in previously published reports (Heidenreich and Farrand, 2000; Baffaut et al., 2001)
- County crop yields were obtained from the Missouri Agricultural Statistic Service. Yields obtained in the watershed are assumed to be the same as in the county. If the watershed crosses county lines, a weighed average of the county crop yields was calculated that is proportional to the fraction of the watershed that lies in each county. The average annual crop yields for the last eight years were compared to those simulated by the model. The eight year limitation insures that the comparison is only made for those years where the management practices are unlikely to be different from those established by the farm panel.
- Regional flow data and correlations based on drainage areas were utilized to establish an average annual total water yield.

The models were first developed with SWAT 98.1 and transferred to SWAT 2000. Input parameters were adjusted to obtain average annual crop yields over the last eight years and average water yields over the last 30 years that match the measured (for yields) or estimated (for flows) values. The parameters that were adjusted were: curve numbers, evaporation compensation factor, soil bulk density, soil available water capacity, soil hydraulic conductivity, and groundwater threshold parameters (return flow and re-evaporation).

The models used a skewed precipitation distribution. The Penman-Monteith evapo-transpiration estimation method was selected because it proved to give good results in Missouri. In the absence of flow data to estimate the Muskingum routing coefficients, the variable storage routing method was selected. In the rest of this paper, we will characterize these first models as yield-calibrated.

Flow gauges have been installed in the Long Branch and Miami Creek watersheds by the US Geological Survey and daily flow data was collected beginning in 1995 and 2001, respectively. The SWAT2000 models were calibrated using this data. For each watershed, two thirds of the data were used for calibration and one third for validation. In addition to the previously listed input parameters, the following ones were adjusted: groundwater delay and recession constant, snow melt parameters, and soil crack potential. Muskingum routing was used in the Miami Creek Watershed instead of variable storage routing and the coefficients were adjusted. In the rest of this paper, we will characterize these first models as flow-calibrated.

The analysis compares the goodness of fit of the model results with the measured flow and the corresponding sediment, nutrient, and chemical loadings when the models are calibrated and when they are not. The goodness of fit is estimated by two indicators: the relative error in average annual surface runoff, groundwater, and total flow; and the Nash-Sutcliffe coefficient calculated with monthly total flow values. They are given by the following equations:

$$\text{Relative error} = (Q_{simulated} - Q_{measured})/Q_{measured}*100$$

$$\text{Nash-Sutcliffe} = 1 - \Sigma(Q_{simulated} - Q_{measured})^2/\Sigma(Q_{average} - Q_{measured})^2$$

The models are then utilized to simulate 32 years of monthly and annual sediment, nutrient, and pesticide loadings using generated weather. The initial two years of results were ignored and the average annual loadings were calculated.

The models were then altered to represent different crop land management practices proposed to reduce sediment and nutrients in the Miami Creek watershed and to reduce atrazine loadings (an herbicide widely used in the United States for corn production) in the Long Branch watershed. In the Miami Creek watershed, all tillage and cultivation operations before and during the soybean and wheat years of the corn-soybean-wheat rotation were removed. The corn years were left as is because, on clay pans, no-till corn is not thought to be as successful. The initial residue cover is increased from 300 kg/ha to 500 kg/ha on these hydrologic response units (HRU), the biological mixing coefficient in increased to reflect a higher density of soil biological activity, and the minimum value of the C factor for wheat is reduced. In the Long Branch watershed, the 2.2 kg/ha atrazine application on May 8th is replaced by a combination of different pesticides. A later atrazine application is included on June 10th at half the rate, 1.1 kg/ha.

The analysis examines whether the calibration of the models leads to different answers in terms of the effectiveness of alternative management practices. The changes in sediment, nutrient, and pesticide loadings obtained when management practices are implemented are compared between each model.

Results

The calibration of the Miami creek model was performed using flow data from October 2001 to September 2003. The calibration for the Long Branch watershed was performed with data from July 1995 to December 2000, slightly more than 5 years of data. Table 2 shows the calibration indicators for both watersheds before and after flow calibration.

In the Long Branch watershed, the apparent good fit between the measured flow values and the flows predicted by the yield-calibrated model hid larger errors in the prediction of surface runoff and groundwater flow. In spite of a satisfactory percent error in total flow and a Nash-Sutcliffe coefficient greater than 0.7, the percent errors in surface runoff and groundwater flow are very large. Given the small contribution of groundwater flow in this area due to clay pan soil, a large error does not significantly change the pollutant loadings and stream concentrations. However, a 25% error in surface runoff is expected to have large impacts in estimated pollutant loadings.

In the Miami Creek watershed, the use of flow data to calibrate the model did not significantly modify the values of the goodness of fit indicators. The main difference is with the groundwater that was under-estimated in the yield-calibrated model. The groundwater represents a small fraction of the flow, 13%, and is not expected to have a large impact on the results. Flow calibration also resulted in a decrease in estimated surface runoff. The Nash-Sutcliffe coefficient value around 0.6 indicates a satisfactory, although not very good, fit of monthly flow values. This corresponds to an under- and over- prediction of flows during the spring 2002 and 2003, respectively.

Table 2. Goodness of fit obtained with two types of calibration data.

	% error in surface runoff	% error in groundwater	% error in total flow	Nash-Sutcliffe
Long Branch yield-calibrated	-26%	65%	-7%	0.78
Long Branch flow-calibrated	-8%	45%	6%	0.93

Miami Creek yield-calibrated	9%	-24%	6%	0.56
Miami Creek flow-calibrated	-4%	7 %	1%	0.62

The results presented in Table 3 indicate that the average annual flow values predicted by the yield-calibrated and flow-calibrated models were within 15% and 25% of each other; sediment loadings were within 42% to 53%, for the Long Branch and Miami Creek watersheds, respectively. Pollutant loading relative differences varied from 23% to 98%, depending of the pollutant and the watershed. Atrazine was the pollutant for which the difference was the largest, 98% for the Long Branch and 50% for the Miami creek models. A possible explanation for this is that lower predicted surface runoff values transport lower amounts of atrazine, which then remains on the soil and is subject to decay. Indeed, in both cases, the difference in atrazine that is dissolved and transported with surface runoff is counter-balanced by an opposite change in the decayed amount.

Table 3. Differences in sediment, nutrient, and pesticide stream loadings with two types of calibration data.

	Water yield (mm)	Sediment loading (kg/ha)	Nitrogen loading (kg/ha)	Phosphorus loading (kg/ha)	Atrazine loading (kg)
Long Branch yield-calibrated	206	3.2	9.1	3.2	267
Long Branch flow-calibrated	211	4.5	11.3	3.8	529
Ratio to the yield-calibrated result in Long Branch	1.03	1.42	1.23	1.24	1.98
Miami Creek yield-calibrated	275	2.6	9.9	5.3	262
Miami Creek flow-calibrated	204	1.4	6.6	3.3	130
Ratio to the yield-calibrated result in Miami Creek	0.74	0.53	0.67	0.65	0.50

After modifications of the crop land management, the models were run again for 30 years using simulated weather. The predicted efficiencies of reduced tillage and reduced applications of atrazine are presented in Table 4.

Table 4. Changes in pollutant loadings predicted by each model.

	Sediment loading	Total nitrogen loading	Total phosphorus loading	Atrazine loading
Long Branch yield-calibrated	NA	NA	NA	-27%
Long Branch flow-calibrated	NA	NA	NA	-45%
Miami Creek	-16%	-7%	8%	NA

yield-calibrated Miami Creek flow-calibrated	-14%	-6%	11%	NA

Discussion

In the Long Branch watershed, the reduction in atrazine loading due to a later and reduced application is more pronounced with the flow-calibrated model than with the yield-calibrated model. The calibration of the Long Branch model resulted in a 22% increase in surface runoff. These higher surface runoff values result in a 98% increase of the atrazine loading. When the May atrazine application rate of 2.2 kg/ha is replaced by a June application of 1.1 kg/ha, the yield- and flow-calibrated models result in different estimations of the benefits of this practice. The yield- and flow-calibrated models predict a 27% and 45% reduction of the atrazine loading, respectively. Table 5 shows the average annual May and June surface runoff values predicted with both models, indicators that are better correlated with atrazine loading than average annual values. The May surface runoff ratio of the flow-calibrated model to the yield-calibrated model is higher (1.33) than the June ratio (1.2). It is, therefore, expected to see more difference between both models when the herbicide is applied in May than when it is applied in June, and a corresponding higher efficiency of the alternative with the flow-calibrated model.

Table 5. Average annual monthly values in the Long Branch Watershed.

	May	June
Yield-calibrated model	Precipitation: 107 mm Surface runoff: 12 mm	Precipitation: 135 mm Surface runoff: 24 mm
Flow-calibrated model	Precipitation: 107 mm Surface runoff: 16 mm	Precipitation: 135 mm Surface runoff: 29 mm

This finding would emphasize the need to use a well calibrated model to estimate the impacts of management practices that involve a variation of the timing of the management operations. A close observation of the results, however, shows that even though the reduction in loadings predicted by both models is significantly different, the reduction in stream concentrations is not. Figures 3 and 4 show the atrazine concentration-duration curves in May and June with each model and for each management practice. In spite of atrazine loadings predicted with each model being different, the curves predicted with the yield- and flow-calibrated models can be considered identical. If the intent of the practice implementation is to reduce stream concentration, either model could be used. If the intent is to reduce the loading to a threshold value or by a given amount, the models would produce different answers.

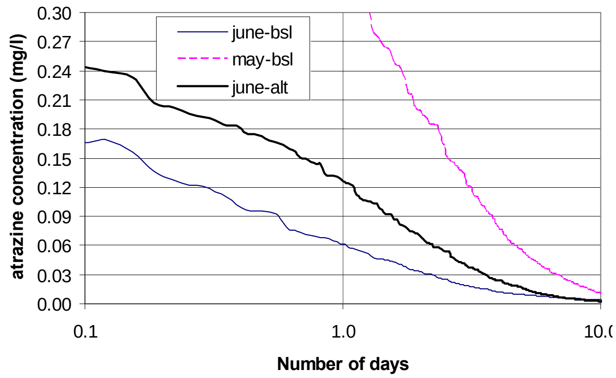

Figure 3. Atrazine concentration-duration curves predicted by the flow-calibrated (a) and the yield-calibrated (b) models for the baseline (bsl) and the alternative (alt) managements.

(a)

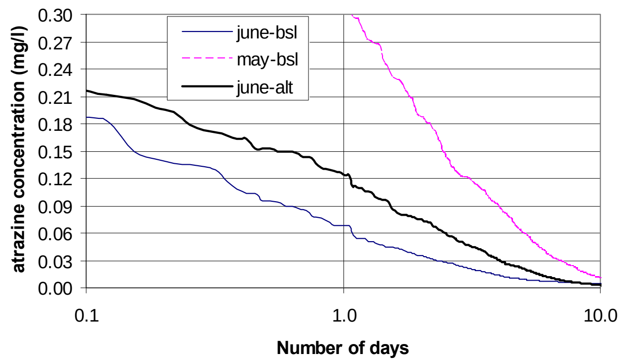

(b)

In the Miami Creek watershed, the 15% reduction of the sediment loadings is similar with each model. The alternatives considered here consisted of removing all tillage and cultivation operations before wheat and soybean planting. The difference between a 16% and 14% reduction with the yield- or flow- calibrated model is small enough that the response of both models can be considered identical. Total nitrogen decreases by 6% and total phosphorus increases by 8% or 11% with the yield- or flow-calibrated models. The total nitrogen decrease is actually the result of a 12% decrease of organic nitrogen that is similar to the decrease of sediment and an increase of nitrates. The prediction of the nitrate increase varies from 4% with the flow-calibrated model to 8% with the yield-calibrated model. Similarly, the total phosphorus increase is the result of changes in organic phosphorus, soluble phosphorus, and mineral phosphorus adsorbed to sediment. The predicted 13% increase in soluble and sediment phosphorus is similar for both models. However, the response of the models for organic phosphorus is different, with the yield-calibrated model predicting a small 3% decrease and the flow-calibrated model predicting a 7% increase.

It is surprising to see how both models respond differently to alternative management practices for nitrates and organic phosphorus and similarly for other forms of nutrients. However, it is conceivable since nitrogen and phosphorus fertilizers are not applied at the same time of the year and the calibration of the model involved the resetting of curve number values at planting and tillage time. A final note, changes are small and additional investigations should be performed when practices that have larger impact are evaluated.

Conclusions

The calibration of the Miami Creek and Long Branch models based on average annual county crop yields and regional flow values resulted in models that simulated monthly total flows for which the percent error and the Nash-Sutcliffe coefficients were within acceptable values. However, the use of flow data to calibrate these models resulted in significant improvements of the respective contributions of surface runoff and groundwater flow. The differences in predicted surface runoff resulted in large differences in the prediction of pollutants.

The calibration of the Miami Creek model did have an impact on the predicted reductions (percent change) due to reduced tillage for some forms of the nutrients. The prediction of the sediment loadings reduction was similar.

In the Long Branch watershed, the predicted percent change in atrazine loading was very different depending on the model used. However, the prediction of stream concentrations was similar with either model.

Given the results of this analysis, we would expect to see larger differences of percent change of pollutant loadings relative to a baseline between a yield- and flow-calibrated model when the calibration involves the adjustment of monthly or seasonal parameter values. Examples would be the adjustment of the curve number after a planting or tillage operation, or snow-melt parameters. Similarly, the predictions of the impact are likely to be different when the alternative management involves a change in the timing of certain operations. An example would be applying herbicides in June rather than in May.

Overall, the assumption that a roughly calibrated model is all that is needed to estimate the relative impact of a change in management practices is not always verified and should be taken lightly. We reiterate the importance of respecting the contribution of surface runoff and groundwater flows to have correct estimations of the pollutant loadings. We also recognize that in the absence of calibration data, a yield-calibrated process-based model may be the best available tool when decisions have to be made.

References

Arnold, J.G., R.S. Muttiah, R. Srinivasan, and P.M. Allen. 2000. Regional estimation of base flow and groundwater recharge in the upper Mississippi basin. J. of Hydrology 227(2000):21-40.

Baffaut C. 2004. Shoal Creek watershed water quality analysis, FAPRI-UMC Report 01-04, Food and Agricultural Policy Research Institute, Columbia, MO.

Baffaut C., D. Schuster, L.K. Heidenreich, D.T. Farrand, A. Bross, V.W. Benson 2001. Miami creek watershed water quality Analysis, FAPRI-UMC Report 01-01, Food and Agricultural Policy Research Institute, Columbia, MO.

Heidenreich L.K. and T.D. Farrand, 2000. Long Branch Lake Environmental Analysis, FAPRI-UMC Report 05-00, Food and Agricultural Policy Research Institute, Columbia, MO.

Peterson, J.R. and J.M. Hamlet. 1998. Hydrologic calibration of the SWAT model in a watershed containing fragipan soils. J. of American Water Resources Association 34(3): 531-544.

An Approach to Assess SWAT Model Performance in Evaluating Management Actions in a Finnish Catchment

Ilona Bärlund[1] and Teija Kirkkala[2]
[1] Finnish Environment Institute (SYKE), P.O. Box 140, FI-00251 Helsinki, email: ilona.barlund@ymparisto.fi
[2] Southwest Finland Regional Environment Centre, Pori

Abstract

The ecological status of Lake Pyhäjärvi may be classified as moderate due to its elevated nutrient concentrations and algal biomass production. Therefore, the Eurajoki River Basin, including Lake Pyhäjärvi, was chosen as the Finnish test catchment in an EU project on benchmarking models for the Water Framework Directive. One aim of the project was to test the suitability of models for the assessment of management options proposed to meet the surface water quality targets. The catchment model SWAT is currently being tested for its capability to analyse the effectiveness of proposed measures to reduce agricultural and sparse settlement nutrient loading. The results indicate that SWAT can be calibrated against measured data, especially for discharge and total nutrient loading. The validations using other monitoring points within the catchment reveal, however, a lack in the model's ability, in the present set-up, to reproduce observed catchment dynamics.

Introduction

The EU Water Framework Directive (WFD) mandates Member States to develop river basin management plans for each river basin district. To achieve this, the responsible authorities must have tools to assess alternative management options. Effects of environmental conditions and agricultural practices on nutrient leaching have been studied in several field trials in Finland (e.g. Puustinen 1999; Turtola and Kemppainen 1998). Due to complexity of the soil-water-plant interactions, the direct up-scaling of results from these singular field scale experiments to regional assessments of losses can be misleading. Therefore, mathematical modelling tools have been developed and modelling strategies set up to generalise the effect of environmental conditions and agricultural practices on nutrient losses at the field and catchment scale. Models like SOIL/SOILN (Johnsson *et al.* 1987), GLEAMS (Knisel 1993) and ICECREAM (Tattari *et al.* 2001) have been used to assess phosphorus (P) and nitrogen (N) losses from agricultural land in Finland (Granlund *et al.* 2000; Knisel and Turtola 2000; Tattari *et al.* 2001). The SWAT model has been applied to the Vantaanjoki Basin to estimate retention of total N and P in this Finnish river basin. The model performance was found to be satisfactory, the Nash-Sutcliffe index for the simulation of discharge and total N and total P loads ranged for validation from 0.43 to 0.57 (Grizzetti *et al.* 2003).

One aim of the EU-funded project 'Benchmark models for the Water Framework Directive' (BMW) was to establish a set of criteria to assess the appropriateness of models for use in the implementation of WFD. This concept progressed from being a set of generic questions (Saloranta *et al.* 2003) to a document that can be used as a basis for the dialogue between a modeller and a water manager (Hutchins *et al.* submitted; Kämäri *et al.* submitted). The dialogue process was supported by modelling case studies in selected catchments. The Finnish test case in the BMW project was the catchment of Lake Pyhäjärvi and it was based on linking models. First, the lake model LakeState was used for setting the targets for the loading reduction for Lake Pyhäjärvi. Based on these results, the catchment model SWAT has been set up to assess the effectiveness of proposed measures to reduce agricultural and sparse settlement nutrient loading (Bärlund *et al.* 2004). In order to test the applicability of SWAT for this purpose, the model was applied to the River Yläneenjoki Catchment draining directly to Lake Pyhäjärvi and contributing over 50% of the P load reaching the lake. The modelling approach comprising calibration and validation is described in this study.

Methodology

Lake Pyhäjärvi, situated in the municipalities of Säkylä, Eura and Yläne in south-western Finland, is one of the most widely studied lakes in Finland. In the 1970s, the water quality of Lake Pyhäjärvi was classified as excellent, but in the classification carried out in the 1990s, the water quality was only estimated as good. The eutrophication of the lake has progressed at a rapid pace over the last few years. Lake Pyhäjärvi is currently mesotrophic. The greatest threat to the lake is the nutrient load which exceeds the tolerance limit of the lake. According to studies and mathematical models, the P load to Lake Pyhäjärvi should be reduced to almost half of the present amount in order to stop the eutrophication process and to gradually improve water quality. The major inflows to Lake Pyhäjärvi are the Rivers Yläneenjoki and Pyhäjoki, which cover 68% of the drainage basin. Of the total area, 22% is cultivated; the remainder comprises forest, peatland and housing areas. Field cultivation and animal husbandry comprise 55% and 39% of the external P and N load to Lake Pyhäjärvi, respectively. Since the drainage basin of the lake is relatively small, atmospheric deposition to the lake is also an important component of the external load: it makes up approximately 20% of the total P load and 30% of the total N load when estimated from the bulk deposition measurements made at three stations adjacent to the lake (Ekholm *et al.* 1997).

The SWAT model (Soil and Water Assessment Tool) is a continuous time model that operates on a daily time step at the catchment scale (Arnold *et al.* 1998; Neitsch *et al.* 2001). It can be used to simulate water and nutrient cycles in agriculturally dominated landscapes. The catchment is generally partitioned into a number of subbasins where the smallest unit of discretisation is a unique combination of soil and land use overlay referred to as a hydrologic response unit (HRU). SWAT is a process based model, also including empirical relationships. One objective of such a model is to assess long-term impacts of management practices. The model has been widely used but also further developed in Europe (e.g. Krysanova *et al.* 1998; Eckhardt *et al.* 2002; van Griensven *et al.* 2002). SWAT was chosen for this case study for three main reasons: its ability to simulate both P and N on catchment scale, its European wide use and its potential to include agricultural management actions. Also, SWAT was evaluated against the diffuse pollution benchmark criteria developed by the BMW project and it was found to have potential with respect to the Water Framework Directive requirements (Dilks *et al.* 2003; Perrin *et al.* submitted).

The Yläneenjoki Catchment, 234 km^2 in area, is located on the coastal plains of south-western Finland, thus the landscape ranges in altitude from 50 to 100 m a.s.l. The soils in the river valley are mainly clay and silt, whereas tills and organic soils dominate elsewhere in the catchment. Long-term (1961-1990) average annual precipitation is 630 mm of which approximately 11% falls as snow (given as the maximum water equivalent of the snow cover, assuming no sublimation) (Hyvärinen *et al.* 1995). The average monthly temperature for the period November to March ranges from –0.5 and –6.5 ^{o}C. The warmest month is generally July when the average temperature is 16.2 ^{o}C (1980-2000). Average discharge in the Yläneenjoki main channel is 2.1 m^{3}s^{-1} (Mattila *et al.* 2001), which equates to an annual water yield of 242 mm (1980-1990). The highest discharges occur in the spring and late autumn months. Groundwater contributions to streamflow are small. Agriculture in the Yläneenjoki Catchment consists of mainly cereal production and poultry husbandry. According to surveys performed from 2000-2002, 75% of the agricultural area is planted for spring cereals and 5-10% for winter cereals (Pyykkönen *et al.* 2004). Agriculture in the Yläneenjoki Catchment is intensive for Finland.

Data for only one precipitation and temperature gauge were available for the Yläneenjoki Catchment (MSt, Figure 1). The station for global radiation was located approximately 60 km outside the catchment. The regular monitoring of water quality of river loads was started as early as the 1970s in the Yläneenjoki Catchment. Monitoring of ditches and brooks entering the river or lake started at the beginning of the 1990s. The nutrient load has been monitored in the Yläneenjoki River by taking and analysing, in general bi-weekly, water samples and measuring the daily water flow at one point (Vanhakartano: outlet of subbasin 39, P2 in Figure 1). Furthermore, water quality was monitored on a monthly basis at three additional points in the main channel and in 13 open ditches running into the River Yläneenjoki in the 1990s.

For the SWAT simulations the available data on land use and soil types had to be aggregated. The SWAT parameterisation was performed for seven land use types: water, field, forest cuts and recently planted forest, active forest, old forest, peat bog and sealed areas. The soil was divided into six general types: clay (44%), till and other coarse soils (23%), open bedrock (21%), turf (13%) and silt (0.6%), using the 25m raster database for Finnish subsoils (depth >25cm) provided by the Geological Survey of Finland. Coarse soils (tills, till ridges, eskers, gravel and coarse sand) that showed a great variety but only patchwork locations within the catchment were grouped and parameterised according to the dominant type, till. The fields were parameterised to be spring barley since spring cereals are the most common crop type in the catchment. The classification of the Yläneenjoki Catchment resulted in 43 subbasins. A threshold value of 10% for land use and soil types resulted in 267 HRUs. The parameterisation of soils and vegetation was based on measurements, expert judgement and previous field scale modelling work (i.e. using the ICECREAM model, e.g. Tattari et al., 2001; Rankinen et al., 2001). Clear information gaps were identified for a wide range of parameters in the Yläneenjoki data set (Bärlund et al., 2004) where model default values are now used. Calibration took place against discharge and sediment and nutrient concentration measurements as well as calculated daily loads at Vanhakartano (P2, Figure 1), which is situated approximately 4 km from the river mouth. This was performed for the years 1990-1994.

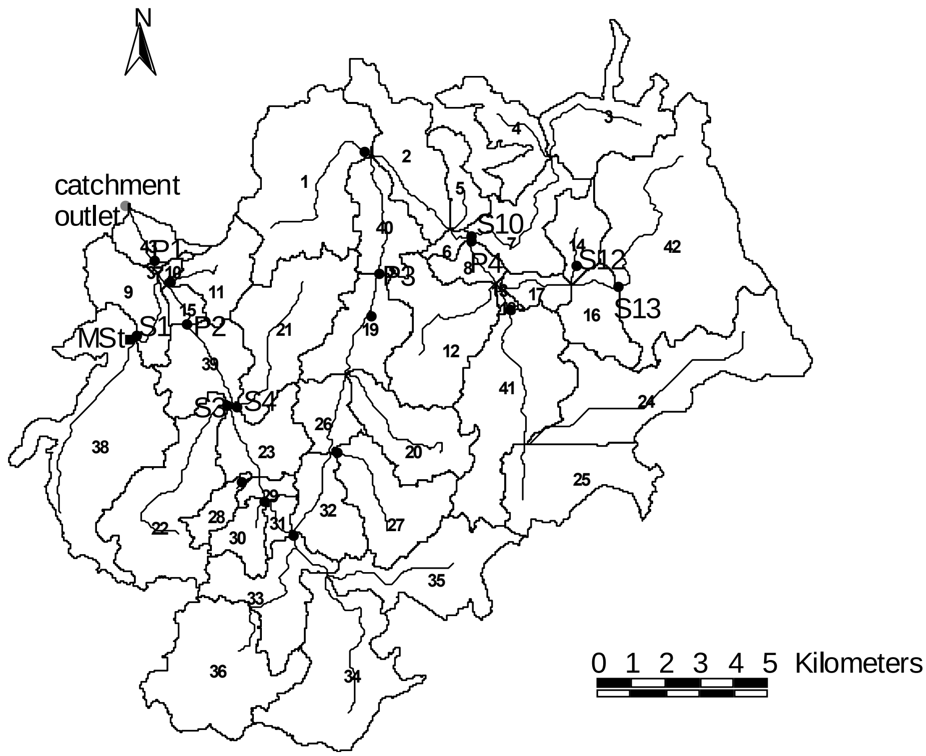

Figure 1. SWAT set-up, location of the meteorological station (MSt) and the utilised monitoring points in the mainstream (P1-P4) and in selected subbasins (S1, S3, S4, S10, S12 and S13) in the Yläneenjoki Catchment.

Results and Discussion

The uncalibrated SWAT run showed clear faults in the ability to describe observed discharge behaviour. This concerned mainly three phenomenon: too much snow melt during winter months, timing and amount of snow melt in spring, and too many and partially over-predicted peaks during summer (Bärlund et al., 2004). These were addressed in the calibration procedure, where in the first phase only basin-wide parameters were changed. The basin scale water balance components (average for 1990-1994) were roughly inline with expert judgement. The actual evapotranspiration was assessed to be too low, whereas surface runoff was perceived as being too high. This meant that parameters governing surface runoff, such as the SCS runoff curve number, and parameters governing the interaction between surface water and groundwater needed to be calibrated in the second step. A reasonable fit was acquired using 13 parameters (Table 1).

The simulations were conducted without the in-stream processes option. It was discovered that the annual denitrification amounts were unreasonably high. In the model code the denitrification limit is set at 0.99 × FC (field capacity). For the clay soil that dominates for agricultural land in Yläneenjoki, this limit is clearly too low. The annual denitrification values appeared reasonable with a new limit of 1.1 × FC. After an initial assumption, it was later decided that crop residue removal is closer to actual conditions and the parameter HVSTI (crop residues removed) was changed from 0.5 to 0.9. Except for the sum of nitrite and nitrate nitrogen (NO_{23}-N), the calibration of the nutrients was mainly concentrated on point sources and initial values of the P pools in soil.

Table 1. SWAT parameters used to calibrate discharge and nutrients at Vanhakartano.

No.	Parameter	Starting value	End value	Calibrated against
1	SFTMP	-3.2	-0.2	discharge
2	SMTMP	-0.3	-0.1	discharge
3	SNOCOVMX	1	10	discharge
4	SURLAG	4	1	discharge
5	GW_DELAY	31	25	discharge
6	RECHRG_DP	0	0.1	discharge
7	CANMX (forest)	5 & 10	50 & 70	discharge
8	T_BASE (forest)	2, 5	0	discharge
9	BLAI (forest)	5	9	discharge
10	PHU (forest)	2000, 2500	3500	discharge
11	OV_N (agricultural land)	0.04	0.19	discharge
12	CH_N (tributaries)	0.05	0.08	discharge
13	GDRAIN	12	48	discharge
14	PRF	0.8	1	sediment conc.
15	CN2 (forest on clay, silt and turf)	78, 77, 70	55	discharge, NO_{23}-N
16	CN2 (forest on moraine, open rock)	25	34	discharge, NO_{23}-N
17	CN2 (agricultural land on clay)	83	70	discharge, NO_{23}-N
18	CN2 (agricultural land on clay, tillage)	83, 89	75	discharge, NO_{23}-N
19	CLAY (agric. subsoil, clay)	74	55	discharge, NO_{23}-N
20	BD (agric. subsoil, clay)	1.1	1.3	discharge, NO_{23}-N
21	AWC (agric. subsoil, clay)	0.25	0.17	discharge, NO_{23}-N
22	CLAY (agric. subsoil & forest topsoil, turf)	33	3	discharge, NO_{23}-N
23	AWC (agric. subsoil & forest topsoil, turf)	0.60	0.50	discharge, NO_{23}-N
24	NPERCO	0.2	0.9	NO_{23}-N
25	MINPCNST (point sources)	*1	*0.25	PO_4-P
26	SOL_LABP1 (moraine, clay)	30, 40	20, 30	PO_4-P
27	ORGPCNST (point sources)	*1	*0.25	total P
28	SOL_ORGP1 (all soils)	465	207 (calc. intern.)	total P

The calibration result was evaluated using the Nash-Sutcliffe index (NSI) and the linear goodness-of-fit (R^2) values (Table 2). The NSI varied between –263 and 0.43, the R^2 values ranged from 0.01 and 0.57. The best result was achieved for discharge and nutrient loads. Except for sediment, the load simulation performed better than the concentration simulation. An evaluation of the time-series of all output variables showed that, except for NH_4-N and PO_4-P concentrations, the calibration result was satisfactorily since the main features of the annual behaviour can be depicted.

Table 2. The evaluation of the calibration result at Vanhakartano, P2 – subbasin 39, for the period 1990-1994 (NSI: Nash-Sutcliffe index, R^2: linear goodness-of fit , n: number of measurement-simulation pairs).

Variable	NSI	R^2	n	Variable	NSI	R^2	n
discharge	0.43	0.57	1826	total N load	0.32	0.46	180
sediment load	-0.11	0.21	172	total N conc.	-2.2	0.01	180
sediment conc.	0.01	0.20	172	PO_4-P load	0.15	0.29	171
NH_4-N load	0.01	0.02	124	PO_4-P conc.	-9.3	0.03	171
NH_4-N conc.	-263	0.02	124	total P load	0.01	0.13	191

NO_{23}-N load	0.16	0.14	95	total P conc.	-2.0	0.07	191
NO_{23}-N conc.	-0.11	0.22	95				

When examining the singular time-series certain problems can be detected:

- Discharge: There were no systematic errors, but there was a discrepancy between the measured and simulated peak values during snow melt periods in winter and spring. Also, the low flow in summer was generally underestimated. It is possible that the use of other meteorological stations for precipitation input, even though situated outside the catchment boundaries, could improve the calibration result. The simulation of low flows was difficult due to the extremely low measured values (down to 0.03 $m^3 s^{-1}$). These values were underestimated during certain summers by a factor of five, especially towards the end of the summer. This had an enormous impact on the simulated concentrations of NH_4-N and PO_4-P which were strongly related to point sources.
- Sediment: The overall fit was rather good, the peak load events reflected simulated flow.
- NH_4-N: When SWAT was run without in-stream processes, the entire NH_4-N load could be attributed to only to point-sources. This would indicate that a stable load level can be calibrated to the measurements, but during low flow periods in summer the concentrations are over-estimated by a factor of 1000.
- NO_{23}-N: When SWAT was run without in-stream processes, the NO_2-N load was zero; the higher measured concentrations were underestimated by the simulation and this was reflected in the load simulation.
- Total N: Because total N was calculated as the sum of NH_4-N, NO_{23}-N and organic N, the effects seen in the previous variables were repeated in the totN load simulation. In the totN concentrations, the small concentrations were additionally overestimated, generally the variability in the simulation was too large when compared to the measured behaviour.
- PO_4-P: The load simulation was rather well depicted but during the low flow period the same overestimation (factor 100) observed for NH_4-N concentrations was observed.
- Total P: The simulated behaviour of totP was very close to that of totN.

The overall impression was that the constant point load that was used for scattered settlements (non-connected community waste water networks) was not working properly. It seemed to be difficult to estimate the correct unit loading. The mismatch had strong influence during low flow periods where the daily flow was usually less than 0.1 $m^3 s^{-1}$. Additionally, it was determined that individual HRUs and subbasins should be thoroughly examined for their outputs, rather than basing the calibration on a limited number of catchment or subbasin wide parameters (Table 1).

A validation of this SWAT set-up was attempted against data at the same Vanhakartano location for the period from 1995-1999. Additionally, discharge data for the period from 1985-1989 was utilised (Table 3). The validation results show that, with the exception of sediment load and concentration, the validation performance was poorer than the calibration result. The same issues as identified in the calibration period play a role here; however, in early autumn 1999 there was also a period of elevated measured nitrogen concentrations which were overestimated by the model by a factor of ten.

Table 3. The evaluation of the validation result at Vanhakartano, P2 – subbasin 39, for the period 1995-1999, additionally 1985-1989 for discharge (Q) (NSI: Nash-Sutcliffe index, R^2: linear goodness-of fit , n: number of measurement-simulation pairs).

Variable	NSI	R^2	n	Variable	NSI	R^2	n
Q (1995-1999)	0.18	0.32	1826	NO_{23}-N conc	-53	0.03	157
Q (1985-1989)	0.24	0.42	1826	totN load	-2.7	0.33	191
sediment load	-0.18	0.21	191	totN conc	-34	0.07	191
sediment conc	0.10	0.11	191	PO_4-P load	-0.39	0.10	181
NH_4-N load	0.0	0.00	155	PO_4-P conc	-17	0.01	181
NH_4-N conc	-401	0.01	155	totP load	-3.5	0.05	189
NO_{23}-N load	-8.3	0.37	157	totP conc	-21	0.00	189

A second validation was performed for the same time period as the calibration (1990-1994) but for six additional monitoring points within the catchment. Since there were no discharge measurements for these points, only concentrations were considered, including measurements for sediment and total nutrient. Three agricultural dominated sub-catchments with monitoring points at S10 (subbasin 7), S12 (subbasin 14) and S13 (subbasin 42) and three forestry dominated catchments with monitoring points at S1 (subbasin 38), S3 (subbasin 22) and S4 (subbasin 21) were chosen for the second validation (Figure 1). The percentage of agricultural land in the monitoring scheme and simulation vary between 6% and 54% and 0% and 81%, respectively (Table 4).

Table 4. Percentage of agricultural land in the subbasin contributing to the monitoring point (measurement) or the SWAT subbasin outlet (simulated).

subbasin	measured	simulated	subbasin	measured	simulated
S10 / SB7	32	37	S1 / SB38	18	15
S12 / SB14	54	81	S3 / SB22	6	0
S13 / SB42	47	50	S4 / SB21	9	13

The NSI for all subbasins indicates the inability of the model set-up to describe the measured sediment and total nutrient concentrations: -2.0 to -0.78 for sediment, -7.3 to -0.62 for total N, and -3.7 to -1.5 for total P. When the pairs of simulated and measured values were compared (n = 43-47 pairs in the three-year-period 1991-1994) the largest difference was in sediment concentration in S3/SB22 where the measured average concentration was 124 times higher and, related to this, totP was nine times higher, than the simulated average concentration (Figure 2). For all the remaining subbasins and variables the measured concentrations were 1.6-4.6 times higher than the simulated ones. For S3/SB22 the reason for the discrepancy was that erosion (and sediment bound nutrients) from forested soils was parameterised in a way that nearly no erosion was expected. Including no agricultural land in the discretisation would change the results radically, even in subbasin 22 which consists of only 6% agricultural land. The main reason for the failure in validation for all subbasins was that even if the maximum concentrations were rather well described by the simulation, there were long periods during the summer where no loading was simulated (zero concentrations). Therefore, the measured concentration levels hardly differ from the rest of the year. In the end, this issue led to the underestimation of mean annual concentrations and most likely to an underestimation of loads. This cannot, however, be proven due to the missing discharge measurement at the subbasin level.

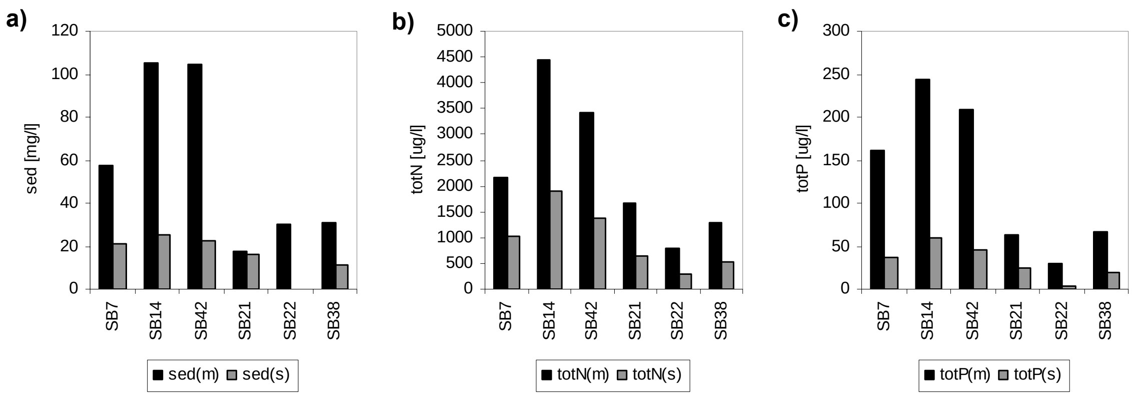

Figure 2. Average concentrations of suspended sediments (a), total N (b) and total P (c) at three agriculturally dominated and three forestry dominated subbasins in 1991-1994.

A further validation was completed for the average concentrations of total nutrients along the main stream (points P1-P4). This analysis revealed further issues in the present model set-up in describing catchment dynamics (Figure 3). The measured average concentrations for the years 1991-1994 indicated a rise from the river mouth to the agriculturally intensive upper parts of the catchment; however, the simulation results showed just the opposite. These results indicated that the main variables affecting the simulation results were the processes in the stream, not the loading from land reflecting land use. The agricultural land was discretised as spring barley with a moderate inorganic fertilisation practise. Also, the in-stream processes were missing for nutrients but seem to play an important role. The effect of this calibration can be seen as the best fit found at P2.

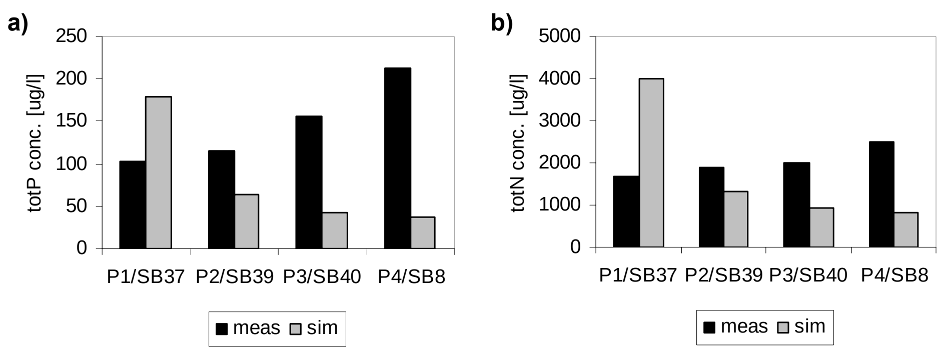

Figure 3. Average concentrations of total P (a) and total N (b) at four monitoring points along the main stream in 1991-1994.

Conclusion

The approach to assess the SWAT model performance in the Finnish Yläneenjoki Catchment revealed that the model can be calibrated to a certain extent to discharge and nutrient loads using a limited parameter set of about 30 input parameters. Validation at the same Vanhakartano point indicated that the calibration performance directly translates into validation performance. Therefore, based on these findings it was determined that the SWAT set-up would be acceptable for end-users in evaluating management practices such as implementation of buffer strips. Further validation within the catchment showed, however, that the calibration and validation at one point was not enough to provide an accurate understanding of the dynamics of such a complex model like SWAT. Three options remain: 1) improve calibration using subbasin and HRU level information more efficiently and pay attention to the in-stream processes; 2) improve the model by changing e.g. snow accumulation and melting routines and the description of forested areas on organic soils; 3) choose another model. Giving that the availability of models in Finland which fulfill the requirements of simulating both P and N on catchment scale and include agricultural management actions is limited and that the simple exercises performed thus far using the present set-up for buffer strip efficiency demonstrations is what local water managers are interested in, further consideration of the model and improvement of the calibration are recommended. The appropriate use of a model such as SWAT is time consuming and requires an experienced user. This should be considered when planning to use the model for practical water management issues.

Acknowledgment

The financial support of the 'Benchmark models for the Water Framework Directive' project through the European Commission's 5th Framework Programme (contract EVK1-CT-2001-00093) is gratefully acknowledged.

References

Arnold, J.G., Srinivasan, R., Muttiah, R.S. and Williams, J.R. 1998. Large area hydrologic modelling and Assessment part I: model development. *Journal of American Water Resources Association* 34(1): 73-89.

Bärlund, I., Kirkkala, T., Malve, O. and Kämäri, J. 2004. Assessing SWAT model performance in the evaluation of management actions for the implementation of the Water Framework Directive in a Finnish catchment. IN: Pahl-Wostl, C., Schmidt, S., Rizzoli, A.E. and Jakeman, A.J. (eds), Complexity and Integrated Resources Management, Transactions of the 2nd Biennial Meeting of the International Environmental Modelling and Software Society vol. 2: 1051-1056. [http://www.iemss.org/iemss2004/proceedings/index.html]

Dilks C.F., Dunn, S.M. and Ferrier, R.C. 2003. Benchmarking models for the Water Framework Directive: evaluation of SWAT for use in the Ythan catchment, UK. IN: Arnold, J. et al. (eds.), Condensed abstracts of the 2nd International SWAT Conference, 1.-4.7.2003, Bari, Italy, pp. 63-66.

Eckhardt K., Haverkamp, S., Fohrer, N. and Frede, H.-G. 2002. SWAT-G, a version of SWAT99.2 modified for application to low mountain range catchments. *Physics and Chemistry of the Earth* 27: 641-644.

Ekholm P., Malve, O. and Kirkkala, T. 1997. Internal and external loading as regulators of nutrient concentrations in the agriculturally loaded Lake Pyhäjärvi (southwest Finland). Hydrobiologia 345: 3-14.

Granlund, K., Rekolainen, S., Grönroos, J., Nikander, A. and Laine, Y. 2000. Estimation of the impact of fertilisation rate on nitrate leaching in Finland using a mathematical simulation model. *Agriculture, Ecosystems and Environment* 80: 1-13.

Grizzetti, B., Bouraoui, F., Granlund, K., Rekolainen, S. and Bidoglio, G. 2000. Modelling diffuse emission and retention of nutrients in the Vantaanjoki watershed (Finland) using the SWAT model. *Ecological Modelling* 169: 25-38.

Hutchins, M.G., Deflandre, A. and Boorman, D.B. submitted. Benchmarking linked diffuse pollution and in-stream water quality models. *Archiv für Hydrobiologie supplement Large Rivers*.

Hyvärinen, V., Solantie, R., Aitamurto, S. and Drebs, A. 1995. Water balance in Finnish drainage basins during 1961-1990. Publications of Water and Environment Administration – series A, 220. [in Finnish, abstract in English]

Johnsson, H., Bergström, L., Jansson, P.E. and Paustian, K. 1987. Simulated nitrogen dynamics and losses in a layered agricultural soil. *Agriculture, Ecosystems and Environment* 18: 333-356.

Knisel, W.G. 1993. GLEAMS, ground water loading effects of agricultural management systems. Version 2.1 UGA-CPES-BAED Publ. no. 5 University of Georgia, Tifton, GA.

Knisel, W.G. and Turtola, E. 2000. GLEAMS model application on a heavy clay soil in Finland. *Agricultural Water Management* 43: 285-309.

Krysanova V., Müller-Wohlfeil, D.-I. and Becker, A 1998. Development and test of a spatially distributed hydrological / water quality model for mesoscale watersheds. *Ecological Modelling* 106: 261-289.

Kämäri, J., Boorman, D., Icke, J., Perrin, C., Candela, L., Elorza, F., Ferrier, R. and Bakken, T.H. submitted. Process for benchmarking models: dialogue between water managers and modellers. *Archiv für Hydrobiologie supplement Large Rivers*.

Mattila, H., Kirkkala, T., Salomaa, E., Sarvala, J. and Haliseva-Soila, M. (eds.) 2001. Pyhäjärvi. Pyhäjärvi-instituutin julkaisuja 26. Pyhäjärven suojelurahasto. 108 p. [in Finnish]

Neitsch, S.L., Arnold, J.G., Kiniry, J.R. and Williams, J.R. 2001. Soil and Water Assessment Tool – Theoretical Documentation - Version 2000, Blackland Research Center, Agricultural Research Service, Texas, USA.

Perrin, C., Dilks, C., Bärlund, I., Payan, J.L. and Andréassian, V. submitted. Use of simple rainfall-runoff models as a baseline for the benchmarking of the hydrological component of complex catchment models. *Archiv für Hydrobiologie supplement Large Rivers*.

Puustinen, M. 1999. Effect of soil tillage on surface erosion and nutrient transport. - The Finnish Environment 285.

Pyykkönen, S., Grönroos, J., Rankinen, K., Laitinen, P., Karhu, E. and Granlund, K. 2004. Cultivation measures in 2000-2003 and their effects to the nutrient runoff to the waters in the farms committed to the Agri-Environmental Programme. The Finnish Environment 711. 119 p. [in Finnish, abstract in English]

Rankinen, K., Tattari, S. and Rekolainen, S. 2001. Modelling of vegetative filter strips in catchment scale erosion control. *Agricultural and Food Science in Finland* 10(2): 99-112.

Tattari, S., Bärlund, I., Rekolainen, S., Posch, M., Siimes, K., Tuhkanen, H.-R. and Yli-Halla, M. 2001. Modelling sediment yield and phosphorus transport in Finnish clayey soils. *Transactions of ASAE* 44(2): 297-307.

Turtola, E. and Kemppainen, E. 1998. Nitrogen and phosphorus losses in surface and drainage water after application of slurry and mineral fertilizer to perennial grass ley. *Agricultural and Food Science in Finland* 7(5-6): 569-581.

Van Griensven A., Francos, A. and Bauwens, W. 2002. Sensitivity analysis and autocalibration of an integral dynamic model for river water quality. *Water Science and Technology* 45(5): 321-328.

Application of SWAT Model to the Decision Support Framework of the Mekong River Commission

Kittipong Jirayoot[1] and Le Duc Trung[2]
[1]Technical Support Division, Mekong River Commission Secretariat, 184 Fa Ngoum Road, Vientiane 01000, Lao PDR, e-mail: kittipong@mrcmekong.org
[2]Water Utilization Programme, Mekong River Commission Secretariat, 184 Fa Ngoum Road, Vientiane 01000, Lao PDR, e-mail: trung@mrcmekong.org

Abstract

The Mekong River Commission (MRC) has been established since the Agreement on the Cooperation for the Sustainable Development of the Mekong River Basin was signed in April 1995 by The Kingdom of Cambodia, The Lao People's Democratic Republic, The Kingdom of Thailand, and The Socialist Republic of Viet Nam. According to the Agreement, the Water Utilization Programme (WUP) was established under which the Rules for Water Utilization and Inter-Basin Diversions are in the process of formulation. To help with rule formulation and implementation, the Water Utilization Programme has recently developed a computer package called the Decision Support Framework (DSF). Within the package, there are three main elements including a Knowledge Base (KB), a suite of three Simulation Models (SMs) and Impact Analysis Tools (IATs). All information can be internally transferred between each element. The SWAT (Soil and Water Assessment Tool) has been selected as the Hydrological Model for the Decision Support Framework to generate the runoff fed into the Basin Simulation Model and Hydrodynamic Model. The model was initially set-up using the dominant Hydrologic Response Unit (HRU) option based on GIS digital elevation data, a single land use map, and soil map classified according to the FAO 1988 system, which have been developed by the Mekong River Commission. SWAT has been applied to 138 subbasins in the Lower Mekong Basin (LMB) covering the areas upstream of Kratie, catchment areas around the Great Lake, and some parts of Vietnam. First, the SWAT model parameters for the headwater catchments were calibrated against naturalized flows which were calculated from gauged flows added on by estimated water usage. The calibrated parameters were transferred to the ungauged subbasins based on proximity and similarity of soil types and land uses. SWAT calibration for the subbasins of instream reaches and the mainstream was also considered. The evaluation results of the model calibration for headwater catchments show the values of Nash-Sutcliffe Coefficient for daily flows are in the range from -0.1 to 0.8 but most of the volume errors are within a ±4% range. Most of the subbasins showed the calibration results in terms of the Nash-Sutcliffe Coefficient for monthly flows lie between 0.5 to 0.9. Nevertheless, the SWAT model can be applied well inside the Decision Support Framework, especially to generate the inflows for the Basin Simulation and Hydrodynamic Models, model reset and recalibration, as well as the capabilities concerning sediment and water quality issues, which the Water Utilization Programme views as a short-term plan.

Keywords: Mekong River Commission, Water Utilization Programme, Decision Support Framework, Impact Analysis Tools, SWAT

Introduction

Mekong River Basin (MRB)

The Mekong River is the 12th longest river in the world with a length of 4,800 km and a basin area of 795,000km^2 for which it is ranked 21st. It is also ranked 8th in the world for its average annual runoff of 475,000 million m^3. The basin is composed of portions of several countries, including China 21%, Myanmar 3%, Lao PDR 25%, Thailand 23%, Cambodia 20%, and Vietnam 8%. The Lower Mekong River Basin mainly covers the areas in the four downstream riparian countries, i.e. Lao PDR, Thailand, Cambodia, and Vietnam, with a total basin area of approximately 620,000 km^2. Figure 1 shows the shape of the Mekong River Basin and the longitudinal profile of the Mekong River from the headwaters to the river mouth. The resources in the basin serve a population of over 60 million.

There are two existing hydropower dams in China, Manwan and Dachaosan, on the Mekong mainstream. The Xiaowan hydropower station is under construction, the Jinghong in Yunan will be constructed soon, and Nuozhadu is under preparation for construction. There are currently about six major tributary dams in the northeast of Thailand under operation, Ubol Ratana, Chulabhorn, Sirindhorn, Pak Mun, Lam Pao, and Nam Oun. These dams are used for hydropower production and irrigation. The part of the basin occupied by Northeast Thailand currently has significant irrigation development and potential for future development. Three major tributary dams in Lao PDR (Nam Ngum, Nam Theun Hinboun, and Huai H) are used for energy production. In addition, there are other areas with the potential for further hydropower developments. A significant part in Cambodia is made up of the Great Lake and Tonle Sap, the lake area varies from 3,000 km^2 in the dry season to 15,000 km^2 in the wet season, at which point the lake becomes the biggest source of freshwater fish in Southeast Asia. The Tonle Sap River, about 120km in length, connects the lake to the Mekong River. The reverse flow from the Mekong River to the lake causes the hydraulic and ecological processes of this area to be quite complicated. Yali Falls Dam, on the Se San River, a major tributary in the east of the basin, is one exiting Vietnam dam used for hydropower generation. However, there is high potential in the Se San area for energy production. The Mekong Delta, mostly in Vietnam, is the most important source for rice production of the country. The tide can affect areas through the delta up to Phnom Penh. An area of paddy rice, about 2.5 million hectares, has been provided with an irrigation and drainage system; however, in the dry season only a fraction of this has been fulfilled due to the limitation of freshwater and the need to control seawater intrusion.

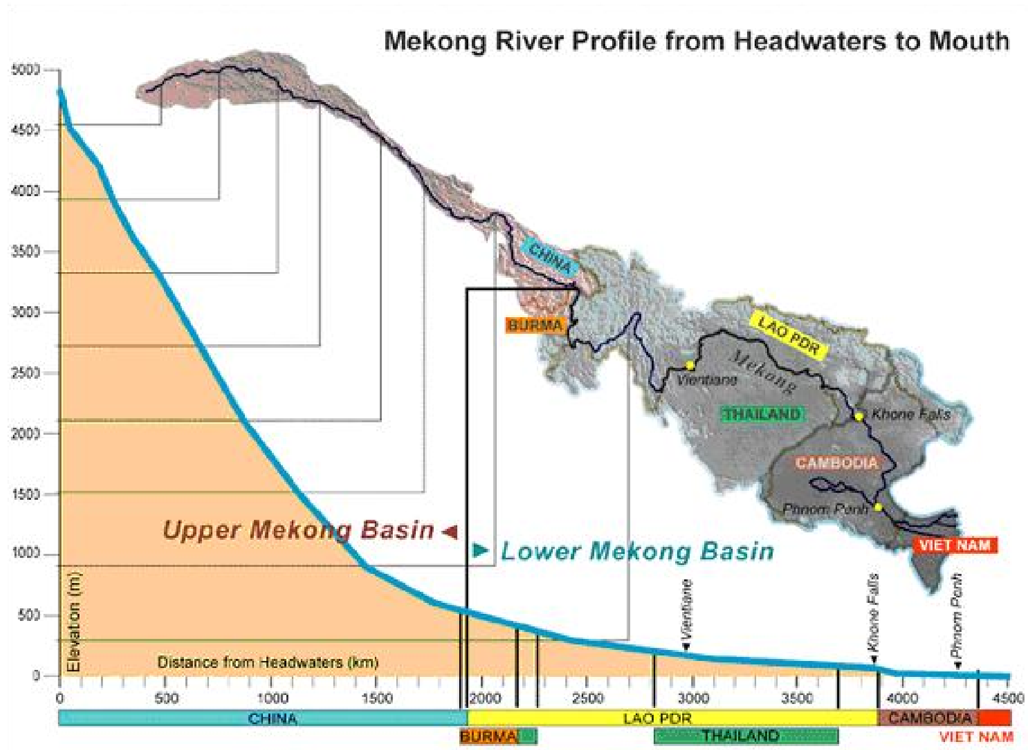

Figure 1. Mekong River Basin and longitudinal profile of the Mekong River.

Agreement on the Cooperation for the Sustainable Development of the Mekong River Basin

Four riparian countries in the Lower Mekong Basin, Cambodia, Lao PDR, Thailand, and Vietnam, signed the “Agreement on the Cooperation for the Sustainable Development of the Mekong River Basin” on April 5, 1999 in Chiang Rai, Thailand. The meaning of the agreement is “to cooperate in a constructive and mutually beneficial manner for sustainable development, utilization, conservation and management of the Mekong River Basin water and related resources”. The main content of the agreement concerning the water utilization of the Mekong River Basin includes: Article 5: Reasonable and Equitable Utilization, Article 6: Maintenance of Flows on the Mainstream, and Article 26: Rules for Water Utilization and Inter-Basin Diversions. These three main articles resulted in the establishment of the Water Utilization Programme under which a tool needs to be developed for integrated management of the resources in the basin.

Decision Support Framework (DSF)

The Decision Support Framework was developed from June 2002 to March 2004 by the Mekong River Commission under the responsibility of the Water Utilization Programme Working Group 1, and funded by the Global Environmental Facility through the World Bank. The main purpose of the Decision Support Framework is to assist planners in assessing both the magnitude of changes brought about through natural and man-made interventions in the water resource system, as well as the impacts that these will have on the natural environment and upon people's livelihoods.

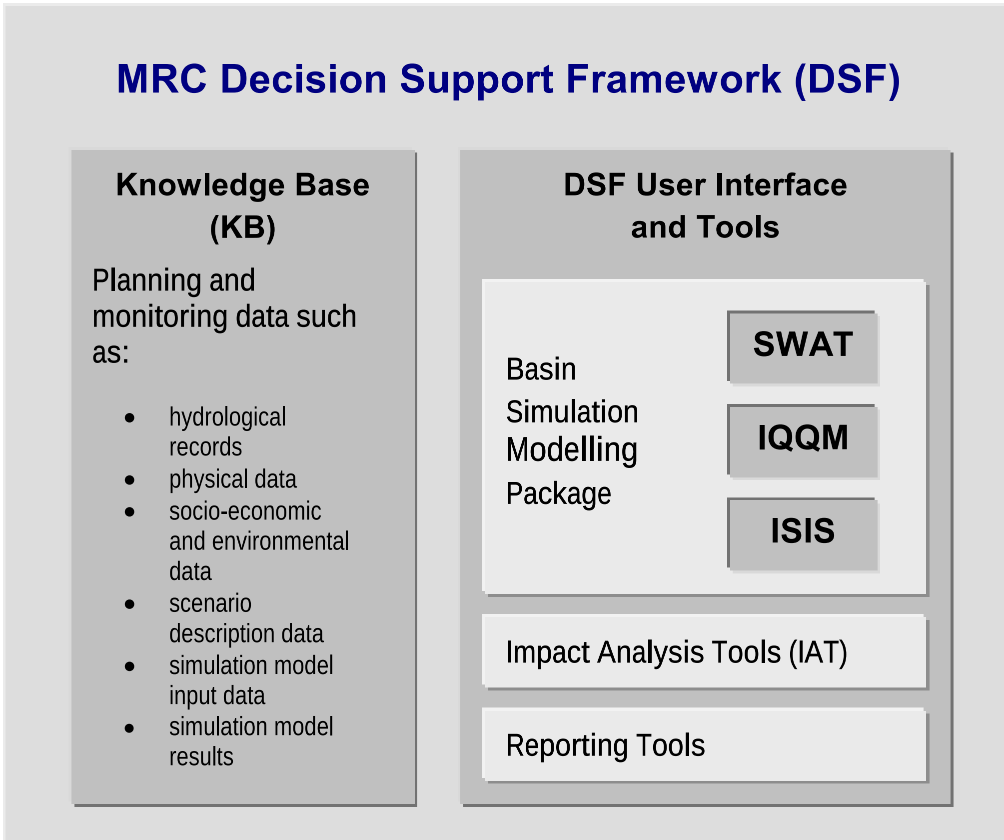

Figure 2. Structure of the decision support framework.

The structure of the Decision Support Framework, as shown in Figure 2, includes three main elements accessed through a single-user interface:

- a Knowledge Base containing information on the historical records, physical data, simulation model input data, modelling outputs, scenario description data, and when fully populated, socio-economic and environmental conditions, as well as predictions of how these may change in the future.

- a suite of Simulation Models that enable the prediction of the impacts of condition changes within the basin on the river system. The SWAT model, developed by the US Department of Agriculture, has been set up to generate subbasin runoff from rainfall and climate data. The SWAT model provides inputs to a series of basin simulation models that are based on the IQQM software originally developed for the Murray-Darling Basin in Australia. The simulation models route catchment flows through the river system, making allowances for control structures such as dams and irrigation abstractions. A hydrodynamic model, based on iSIS software developed by HR Wallingford and Halcrow, was used to simulate the downstream part of the basin, including the Great Lake and delta. The hydrodynamic model represents the complex interactions caused by tidal influences, flow reversal in the Tonle Sap River, and over-bank flow in the flood season with the varying inflows from upstream.

- a set of Impact Analysis Tools that enable the prediction of environmental and socio-economic impacts in response to condition changes of the river system. Time Series Impact Analysis Tools allow the users to carry out the impact analyses for a full range of flow regimes. In the case of the spatial analyses, the outputs produced from iSIS include flow, water level, and salinity used to derive the grid-based flood depth, flood duration, salinity concentration, and salinity duration maps produced by the mapping tools inside the Decision Support Framework. The maps can be overlain on any range of appropriately formatted spatial data using ArcView (provided with the Decision Support Framework) to make direct assessments of impacted populations, land areas or sites of specific interest.

The Decision Support Framework has being used as the planning and analytical tool for the Water Utilization Programme and Basin Development Plan (BDP) for the Mekong River Commission, especially to implement the rules for water utilization in the basin. The hydrological regimes obtained from the Decision Support Framework and the results from Impact Analysis Tools can support further analyses for various programmes, i.e Fishery, Navigation, Flood Management, Environment, Water Resources, etc. The modular architecture of the Decision Support Framework will enable the Mekong River Commission to continue to update the system as the need arises to better support specific purposes of its activities. However, in the remainder of this paper, only the SWAT model is presented for the topics of model set-up, model calibration, and discussion of the results for further improvement.

SWAT Model Set-Up

The SWAT model was set up to cover the total area (600,000 km^2) of the Lower Mekong Basin (shaded area in Figure 3). The GIS data used to set up the model included digital elevation data, a single land use map, and a soil map classified according to the FAO 1988 system, all of which were developed by the Mekong River Commission. The land use map was derived from the interpretation of hard copies of satellite images from 1993 to 1997 and was last updated in January 1999. The forest types have been mapped with a high degree of detail, however, non-forest land cover types have been mapped in lesser detail with many land cover types aggregated into one class. Therefore, before setting up the land use for SWAT, the land use/land cover map was reclassified into the appropriate equivalent classification as embedded in the SWAT database. The physical and hydraulic properties of soils were obtained from the Global Soil Database (GSB) supplemented by local soil pedon data available at the Mekong River Commission Secretariat (MRCS). Using the SWAT2000 Arcview Interface, the Lower Mekong River Basin upstream of Kratie (in Cambodia) was disaggregated into 121 subbasins. The runoff generated from these subbasins will feed into the Basin Simulation Model. Separate SWAT models were established for the 17 subbasins downstream of Kratie, 15 subbasins located around the Great Lake in Cambodia, and two subbasins in Vietnam. The runoff generated from the subbasins downstream of Kratie will directly feed into the Hydrodynamic Model. Figure 4 shows the SWAT subbasins within the Lower Mekong Basin and key monitoring stations on the Mekong mainstream.

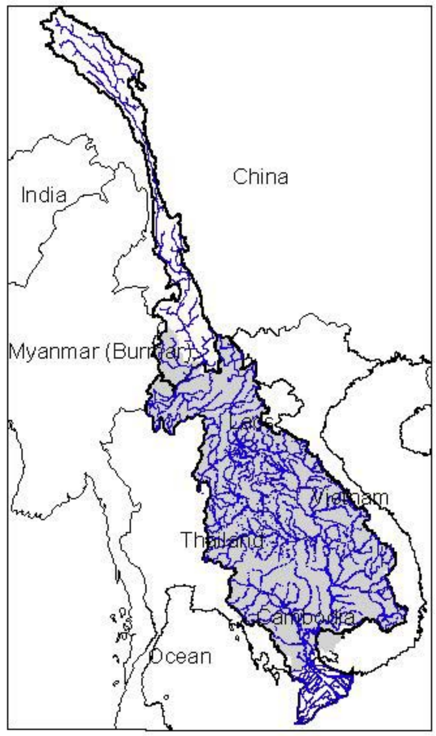

Figure 3. Part of Lower Mekong River Basin to which the SWAT has been applied (shaded area)

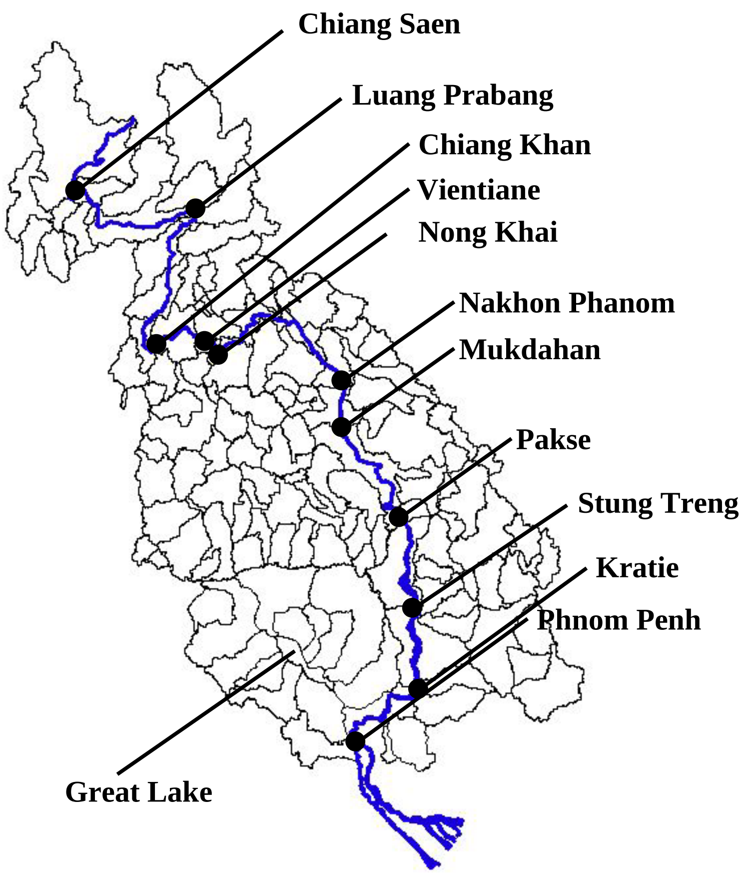

Figure 4. SWAT subbasins and key monitoring stations on Mekong mainstream.

The dominant Hydrologic Response Unit (HRU) comprising a land use/land cover type and a soil class was assigned to each subbasin to define parameters represented for the subbasin such as runoff curve number, land use/land cover properties, soil properties, etc.

The time series data of daily rainfall from 358 stations, most of them located inside the Lower Mekong Basin, was used to calculate the average subbasin rainfall for each SWAT subbasin using the MQUAD (a Multi-Quadratic Function Approach) module inside the Decision Support Framework. The MQUAD fits the observed daily rainfall with a multi-quadratic function and then integrates over each subbasin area to obtain average daily rainfall. The daily climatic parameters required by SWAT including temperature, wind speed, humidity, and radiation were obtained from only 38 stations inside the basin and the missing values were replaced by monthly values from the FAO CLIMWAT database.

SWAT Model Calibration

A total of 32 headwater subbasins with available guage data located upstream of Kratie were calibrated. The calibration was made by comparing the SWAT flow against the naturalized flow. Naturalized flow was calculated by adding on to the gauged flows with pre-estimated water usage in the basins. The water usage considered includes domestic/industrial demand and irrigation demand. The domestic/industrial demand for each subbasin was estimated using per capita water usage and the population in the subbasin. The per capita water usage was estimated from the reports available in the Mekong River Commission Secretariat, WHO, and ADB websites. The subbasin irrigation demand was estimated using the crop model in the IQQM package and based on input such as irrigation area per crop, crop pattern and calendar, crop factors, irrigation efficiency, etc.

The initial values for the SWAT model parameters were taken from the dominant land use and soil type by assuming the subbasins were homogenous. These values were refined during the model calibration to reflect non-dominant land use and soil types in the subbasins. Due to uncertainty of information, initial values of some parameters were set to zero. These parameters included GWQMN and RCHRG_DP. The values of GW_DELAY and GW_REVAP were initially set to zero and adjusted during the calibration. The initial values for REVAPMN and ALPHA_BF were derived from observed hydrographs by examining their shapes. In the absence of soil depth data, one-layer soils were assumed for all soil types. SOL_Z was assumed to be identical with SOL_ZMAX and modified during the calibration process. Similarly, the SCS curve number (CN2) was allowed to vary between expected values for the land use and dominant hydrologic soil group and the adjacent hydrologic soil group during the calibration process. Lateral flow parameters such as LAT_TTIME and SLSOIL were also modified during the calibration process.

The parameters derived for the gauged catchments were transferred to the ungauged catchments based on proximity and similarities in land uses and soil types which would give rise to similar hydrological responses. The transferred parameters of intervening subbasins were refined by secondary calibration against the residual flow. The residual flow was calculated by subtracting the downstream gauged flow with headwater gauged flows routed by IQQM. Where necessary, local knowledge was used to supplement the digital data. In particular, definitions of dominant land use in the subbasin were reviewed.

Calibration Results and Discussions

Given the insufficiency of the observed data for calibrating the subbasins downstream of Kratie, only the calibration results of the headwater subbasins upstream of Kratie are presented in this paper. The calibration results presented in Table 1 show that SWAT can predict the flow volumes within 4% accuracy for all subbasins, with the exception of 419. The calibration evaluation results in terms of the Nash-Sutcliffe Coefficient for daily flows were between -0.1 to 0.8. About one-third of the SWAT headwater subbasins have Nash-Sutcliffe Coefficient values for daily flows greater than 0.5 but for the monthly coefficient, the values range between 0.5 and 0.9. The evaluation results, especially in terms of the Nash-Sutcliffe Coefficient, were low because of poor gauging stations and unrepresentative rainfall data, particularly in mountainous areas. The errors in gauging stations varied across the flow range but were more pronounced at the extreme low and high flows. The low flow was generally affected by recording errors where the higher flows were affected by rating errors. This can be corrected by improved instrumentation and improved rating estimates. Rainfall used by the model was averaged by MQUAD using rainfall gauging network, which was sparse in some areas. Reasonable results were obtained for the areas with flat gradients of rainfall coverage. However, in mountainous regions where the gradients were steep and rainfall data were not available, there was inevitably substantial uncertainty.

Table 1. Calibration results for headwater subbasins upstream of Kratie.

SWAT sub-basin	Period	High flows				Low flows			Overall		
		Vr (%)	FDC Error at Q%			Vr (%)	FDC Error at Q%		Vr (%)	Nash-Sutcliffe (CE)	
			5	25	50		75	95		Daily	Monthly
201	1985-1999	2	0.4	2.1	0.4	3	0.6	7.1	2	0.5	0.7
206	1985-1999	-2	0.4	0.8	0.4	-3	0.1	1.6	-2	0.6	0.8
207	1985-1999	3	0.1	1.5	0.1	3	3.1	3.3	3	0.3	0.5
210	1985-1999	-4	0.2	4.2	0.2	-2	1.6	10.9	-4	0.2	0.6
211	1985-1999	0	0.7	3.4	0.7	n/a	6.7	0.0	-1	0.2	0.7
212	1985-1999	2	0.4	2.4	0.4	-6	0.5	7.2	1	0.2	0.1
304	1985-1999	2	0.2	2.2	0.2	3	0.4	1.6	2	0.6	0.8
307	1985-1999	3	0.5	2.8	0.5	n/a	2.4	0.0	2	0.2	0.6
402	1985-2000	-1	0.9	3.1	0.9	3	2.3	0.7	0	0.3	0.8
412	1985-2000	2	3.1	8.6	3.1	1	3.5	1.3	1	0.0	0.2
415	1985-1999	-5	0.4	1.0	0.4	n/a	3.1	9.1	-5	0.5	0.6
417	1985-1999	2	1.4	0.2	1.4	n/a	23.8	0.0	1	0.5	0.8
419	1985-1996	-3	0.3	1.0	0.3	-79	24.8	0.0	-11	0.3	0.8
420	1987-1999	-1	1.1	5.3	1.1	3	1.8	4.2	-1	0.4	0.9
421	1987-1999	2	0.4	0.2	0.4	0	0.2	0.4	2	0.3	0.7
422	1985-1999	0	0.6	1.2	0.6	n/a	13.7	29.6	-1	0.8	0.9
423	1986-1999	0	0.4	1.6	0.4	-4	3.1	8.3	0	0.2	0.6
424	1985-2000	1	1.0	2.6	1.0	n/a	1.4	6.2	1	0.5	0.7
427	1996-1999	0	0.3	3.5	0.3	10	1.6	5.4	0	0.6	0.9
504	1985-1997	4	0.3	1.4	0.3	n/a	0.0	0.0	4	0.1	0.5
506	1985-1999	-3	2.3	0.8	2.3	n/a	6.3	0.0	-3	0.4	0.5
509	1985-2000	0	2.2	5.1	2.2	n/a	7.3	0.0	0	0.5	0.8
510	1985-2000	2	0.6	2.7	0.6	-3	3.4	1.2	1	0.3	0.6
512	1985-1999	0	1.9	1.6	1.9	n/a	7.6	18.2	-1	0.4	0.4
514	1985-1999	-3	0.5	0.4	0.5	1	1.1	0.7	-2	0.4	0.5
515	1985-2000	1	0.3	4.6	0.3	n/a	5.6	14.4	1	0.5	0.7
608	1985-1999	0	0.4	0.4	0.4	-6	2.9	6.0	-1.0	0.3	0.5
610	1985-1999	-3	0.5	4.4	0.5	1	1.9	4.1	-2.0	0.2	0.6
614	1996-1999	-1	1.6	5.1	1.6	3	1.4	1.9	-1.0	0.4	0.6
620	1985-2000	0	1.7	3.8	1.7	-4	2.0	2.9	0.0	-0.1	0.7
700	1985-1999	0	0.8	0.4	0.8	2	0.7	1.0	1.0	0.2	0.5
800	1985-1999	1	0.7	2.8	0.7	n/a	2.3	5.9	1.0	0.2	0.6

Remarks : 1) $V_r(\%) = \frac{FlowVolume_{sim}}{FlowVolume_{obs}} 100 - 100$

2) FDC at Q% represents the % deviation of the simulated Flow Duration Curve from the observed Flow Duration Curve, at 5%, 25%, 50%, 75% and 95% probability of exceedance

Conclusions

The Decision Support Framework has been used as the planning and analytical tool for scenario impact assessment and directly supports the Water Utilization Programme and Basin Development Plan, especially in implementing rules for water utilization in the basin. The hydrological regimes obtained from the Decision Support Framework and the results from the Impact Analysis Tools can support further analyses for various programmes of the Mekong River Commission such as Fishery, Navigation, Flood Management, Environment, Water Resources, etc. The SWAT model has been embedded into the Decision Support Framework as the first official hydrological model of the Mekong River Commission and used to generate the runoff at the subbasin level. Now, SWAT has been used to generate runoff from each subbasin under historical climate conditions, climate change, and land cover change conditions. In the future, the Mekong River Commission will improve the Mekong SWAT model in various aspects, such as better calibration results and land cover change. The first priority is to redelineate existing subbasins into smaller subbasins to represent more realistic physical conditions and set-up with multiple HRUs to capture the spatial variability of land uses/land covers and soils. The SWAT2003 model was used in this redelineation and sensitivity analysis, uncertainty analysis, and auto calibration tools inside the package will be applied soon. Lastly, the SWAT capability on water quality and sedimentation will also be applied.

Acknowledgements

The Decision Support Framework was developed under the framework of Water Utilization Programme funded by the Global Environmental Facility through the World Bank. On behave of the Mekong River Commission; the authors are thankful to these two organizations for their support. Special thanks are also given to the United States Department of Agriculture for providing the free SWAT software downloaded through the internet.

References

Agreement on the Cooperation for the Sustainable Development of the Mekong River Basin, between The Kingdom of Cambodia, The Lao People's Democratic Republic, The Kingdom of Thailand and The Socialist Republic of Viet Nam, signed on 5 April 1995 at Chiang Rai, Thailand.

Mekong River Commission, Water Utilization Project Component A: Development of Basin, Modelling Package and Knowledge Base (WUP-A), Review of Available Models, Working Paper No. 4, January 2002.

Mekong River Commission, Water Utilization Project Component A: Development of Basin, Modelling Package and Knowledge Base (WUP-A), Interim Report on Development of Models, Working Paper No. 12, September 2002.

Mekong River Commission, Water Utilization Project Component A: Development of Basin, Modelling Package and Knowledge Base (WUP-A), Technical Reference Report DSF 620 – SWAT and IQQM Models, March 2004.

The European Common Agricultural Policy and Feasible Hydrological Impacts for the Dill Catchment, Germany

L. Breuer*, J.A. Huisman, and H.-G. Frede
Institute of Landscape Ecology and Resources Management, Justus-Liebig-University of Giessen, Heinrich-Buff-Ring 26, D-35392 Giessen, Germany. Email: lutz.breuer@agrar.uni-giessen.de

Introduction

Common European Agricultural Policy (CAP) for the 21st century will have a major influence on land use and management practices in many regions of Europe. In the preceding CAP, including the MacSharry reform implemented in 1992 and the Agenda 2000 reform, agricultural products such as corn, milk or sugar were subsidized per yield. This led to intensive production systems marked, for example, by high fertilization rates, unadjusted pesticide application, or exhaustive water use. With more sustainable land use and management in mind, European agricultural ministers agreed to support land use by acreage instead of produced yield in the future.

The scope of the Collaborative Research Centre 299 is to develop concepts for land use in peripheral regions. Peripheral regions in this context are regions which have economic, structural, and/or ecological drawbacks for agricultural production. The Dill Catchment, a mesoscale catchment of approximately 693 km^2 in Germany, is characterized by small acreages (due to inheriting rules over the centuries), steep slopes (unsuitable for large machinery production) and poor soils (shallow, coarse textured, stony). The 10% portion of fallow land is larger than anywhere else in Germany. It is assumed that more and more farmers will quit agricultural activity in the future. This in turn will lead to more uncultivated land, with effects on water quality, biodiversity or heritage landscapes among other landscape services. The new CAP could be a chance for farmers in such peripheral regions to continue agricultural production. But what are the consequences of changes in land use and management for economic and ecological parameters?

The hydrological model SWAT is used to investigate the effects of the CAP on water fluxes in the Dill Catchment. Land use scenarios reflecting the conditions of the Agenda 2000 as well as the new CAP are predicted by the bio-economic ProLand (Prognosis of Land use) model. These maps act as spatial differentiated model input. Hydrological objectives as calculated for the two CAP scenarios are compared to the current land use distribution.

Methods

Study Area

The Dill Catchment is a low mountainous catchment in Germany (Figure 1) with an area of 693 km^2. Digital soil data is available on the scale of a 1:50,000 for the catchment (HLUG, 1998). A multi-temporal remotely sensed land use classification from 1994/1995 was used as a baseline scenario for the present investigation (Nöhles, 2000). The catchment was characterized by a heterogeneous land use pattern with more than 50% of the area covered by forests and 20% by pasture. Details for the land use distribution of the baseline scenario are given in Table 1.

The Agro-economic Model ProLand

The land use scenarios presented were derived by the ProLand model (Kuhlmann et al., 2002). ProLand assumes that land use patterns are a function of natural, economic, and social conditions in a landscape. It postulates land rent maximizing behavior of the land user for any parcel of land. Based on the economic, social and natural, and technical boundary conditions the model calculates a set of agricultural and forestry land use systems for a parcel of land, of which the one with the highest land rent is allocated to. Land rent is defined as the sum of monetary yields including all subsidies minus input costs, depreciation, taxes, and opportunity costs for employed capital and labor. Model outputs are key indicators to describe the economic performance of the calculated set of land use systems and spatially explicit maps of land use distribution. The spatial resolution of the derived land use maps depends on the resolution of the available physical, biological and socio-economic data. In the present case, data are available on a 25 m x 25 m grid.

European Agricultural Policy-driven Land Use Scenarios

The aim of the European CAP is to provide consumers with quality food at fair prices and to provide farmers with a reasonable standard of living. The way the governments have tried to meet these aims has changed over the years. In the past, the key concept of CAP was to subsidize production of basic foodstuffs in the interests of self-sufficiency. The current CAP emphasizes direct payments to farmers as the best way of guaranteeing farmer incomes, food safety and quality, and environmentally sustainable production.

In this study, the agro-economic simulation model ProLand is used to predict land use distributions for the Dill River Catchment that are optimal from an economic point of view under past and future CAP. In the following presentation the land use distribution which should have been in existence due to ProLand theory in the past is called the Agenda 2000 land use scenario. Potential future land use distribution, as predicted by ProLand, is referred to as the CAP land use scenario. For further information on the technique of scenario development and the assets and drawbacks of the ProLand approach, refer to Kuhlmann et al. (2002) and Weinmann and Kuhlmann (2005).

Table 1. Land use distribution [%] of the Dill Catchment and three of its subcatchments.

Scenario	Baseline				Agenda 2000				CAP			
(Sub)Catchment	Dill	6	33	51	Dill	6	33	51	Dill	6	33	51
Forest [%]	53.4	64.6	45.6	38.0	74.8	77.0	81.8	55.4	59.1	65.8	48.0	38.3
Pasture [%]	20.6	18.4	21.0	47.4	6.0	9.3	5.5	12.6	30.3	30.0	48.4	58.6
Urban [%]	9.2	4.1	3.5	3.1	9.2	4.1	3.5	3.0	9.2	4.2	3.6	3.1
Fallow [%]	9.1	11.3	8.1	7.3	-	-	-	-	-	-	-	-
Cropland [%]	6.5	1.5	21.7	4.2	9.7	9.5	9.2	28.9	1.2	-	-	-
Surface waters [%]	0.3	<0.1	<0.1	<0.1	0.3	<0.1	<0.1	<0.1	0.3	<0.1	<0.1	<0.1
Area [km^2]	693	22.0	12.4	20.4								
Mean precipitation [$mm\ a^{-1}$]	952	1071	759	1231								

Hydrological Modeling

A modified version of SWAT2000 was used to assess the hydrological impacts of land use distribution changes induced by the CAP reforms. The SWAT model was adapted for the application in low mountainous catchments with its typical shallow rock aquifers and a high portion of lateral flow (Eckhardt et al., 2002). An anisotropy factor, defined as the ratio between horizontal and vertical saturated conductivity, was used to simulate this increased lateral flow. A soil horizon with a high bulk density and low available water content was added below the regular soil profile to account for the hydrogeological characteristics of the fissured rock aquifers in the Dill River Catchment. Prior to model application, SWAT was automatically calibrated by the use of the combined Scuffled Complex Evolution Metropolis algorithm (SCEM-UA) (Huisman et al., 2003). The model was run from 01.01.1980 to

31.12.2002, whereby the first three years act as a warming-up period. Results for hydrological fluxes such as discharge, groundwater recharge, and direct runoff for the two land use scenarios Agenda2000 and CAP were compared and set in relation to the baseline land use distribution.

The Dill Catchment is divided in 52 subcatchments for all scenarios. Based on the selected threshold of 3% land use and 7% soil for the definition of HRUs, the baseline scenario consisted of 765 HRUs, the Agenda 2000 of 470 and the CAP scenario of 424 HRUs. Three subcatchments were selected for further evaluation of the spatial differences of water fluxes based on the projected land use changes (Table 1). The selection of subcatchments was based on the land use distribution of the baseline scenario. Here, subcatchment six is characterized by a large share of forests (65%). One of the highest shares of cropland in the Dill Catchment was identified in subcatchment 33 (22%). Pasture was the dominating land use type in subcatchment 51 with 47%. Mean annual precipitation was substantially different for the investigated subcatchments, ranging between 759 and 1,231 mm a^{-1}, with an average of 952 mm a^{-1} for the entire Dill Catchment (Table 1).

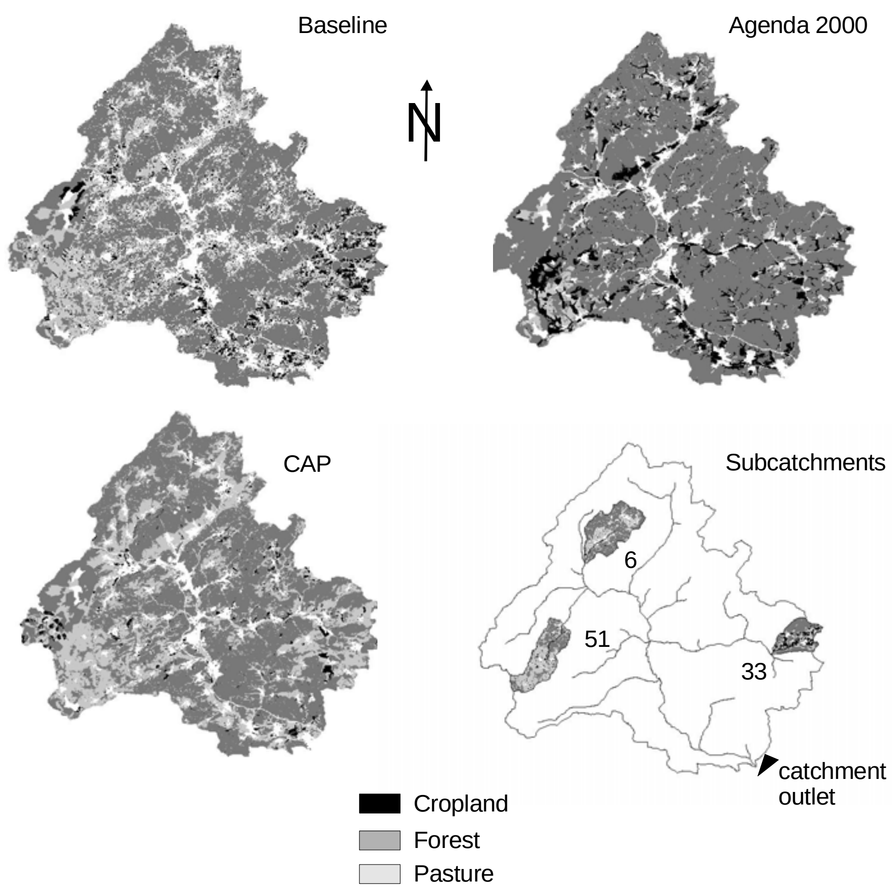

Figure 1. Land use distribution in the Dill Catchment derived from remote sensed data (Baseline, Nöhles 2000) and from ProLand simulations (Agenda 2000 and CAP). Further investigations were conducted in three selected subcatchments with the following dominant land cover types: forest [6], cropland [33] and pasture [51].

Results and Discussion

Scenario analysis with any hydrological model requires general model credibility in space and time. In the current application a split sample test was used to test for temporal model transferability (calibration period 01.11.1990 - 31.10.1993). A sufficient agreement between measured and predicted daily discharge in the Dill Catchment was achieved for the period 01.01.1983 - 31.12.2002 (Figure 2). The Nash-Sutcliffe Efficiency (NSE) of 0.737 was satisfactory, given the limitation of predicting flooding events with a daily time step model for a catchment that is characterized by an immediate response of the hydrograph to rainfalls and an average stream travel duration time of less than 24 h. A proxy-catchment test for the Dill River Catchment and the subcatchments of the Obere Dill River, the Dietzhölze River and the Aar River was performed to test for spatial model transferability. In general, NSE for all subcatchments and the Dill Catchments were within a range of 0.76 and 0.83. The results of the proxy-catchments test are described in detail by Huisman et al. (2003).

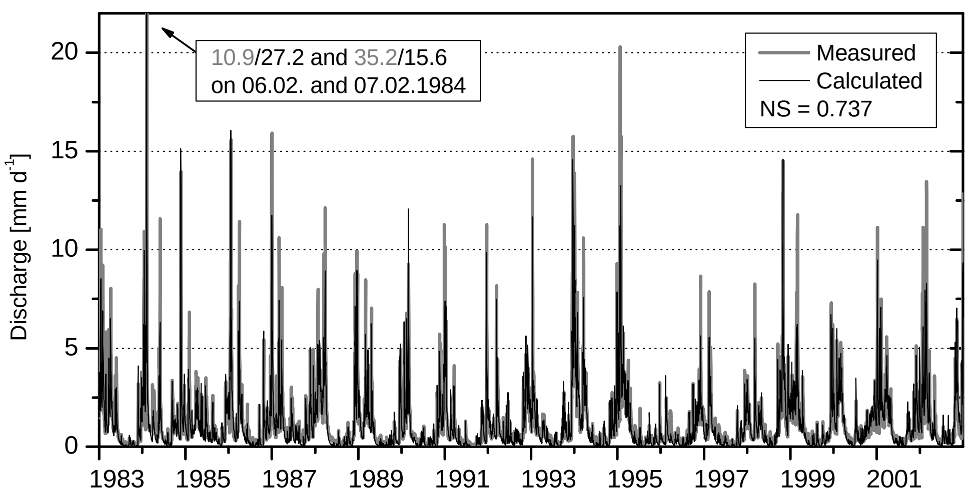

Figure 2. Measured and calculated daily discharge for the period 1983-2002. Note the flooding peaks in February, 6th and 7th 1984. NSE = Nash-Sutclife Efficiency.

A comparison of annual discharges for the Dill River in response to different land use distributions is shown in Figure 3. Calculated annual discharge matches measured discharge (NSE = 0.815), which was to be expected based on the model results for daily discharge. Despite this fact, the calculated annual mean discharge for the baseline scenario was 414 mm and underestimated by -6.4 % as compared to the measured discharge. Annual discharge based on the predicted land use distribution for the Agenda 2000 scenario was similar to the baseline scenario (-6.5 %). A slightly reduced mean annual discharge of 403 mm a^{-1} was calculated for the CAP scenario (-8.9 %).

An analysis of the hydrological flow components gives insights to the hydrological systems of the land use scenarios (Figure 4). The most obvious difference was the increased evapotranspiration and reduced surface runoff components for the CAP scenario as compared to the baseline and the Agenda 2000 scenarios. This can be explained by the fact that evapotranspiration rates are highest for pasture compared to all other land cover types simulated in this work. Pasture covers more than 30 % of the land in the CAP scenario, whereas its expansion was lower in the other two scenarios, e.g. 9 % in the Agenda 2000 scenario. Lateral flow as well as baseflow contribution to discharge was nearly the same for all scenarios, ranging between 287-293 mm a^{-1} and 47-50 mm a^{-1}, respectively. Deep aquifer recharge, a feasible indicator for maintaining a self-sufficient drinking water supply for a landscape, also remains fairly constant for all land use scenarios.

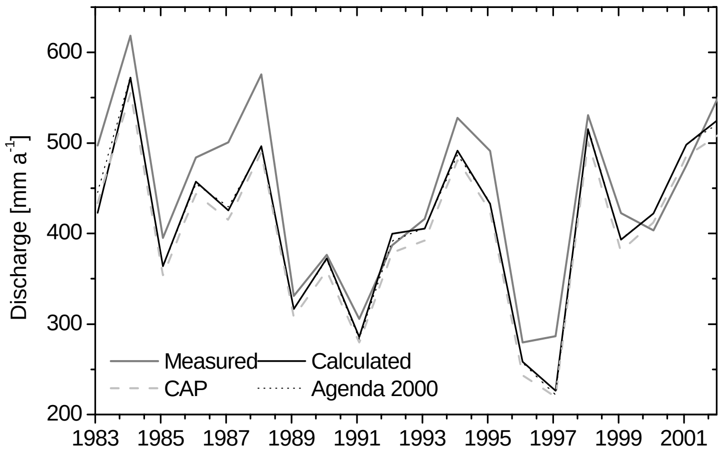

Figure 3. Comparison of measured and predicted annual discharge [mm a^{-1}] for the period 1983-2002. Predicted discharge is also shown for the Agenda 2000 and CAP scenarios.

The observed changes in discharge and other hydrological flux components were comparable to the results obtained in other studies in the area of investigation. For example, Weber et al. (2001) evaluated the effects of introducing a grassland bonus to increase livestock farming in the Aar Catchment, which is a subcatchment in the eastern part of the Dill Catchment. Even though the shares of land use types changed even more as compared to this study, reactions in the hydrological scheme were comparable. In another case study in the Aar Subcatchment, Fohrer et al. (2001) analyzed the effects of different average field sizes on land use distribution. The reactions of the hydrological components in the overall catchment were also low, with slightly increased flooding risks for larger field sizes. However, Fohrer et al. (2001) also pointed out that a spatially differentiated view of changes in hydrological patterns is necessary. For example, on small scales land use does influence flooding potential (Niehoff et al., 2002).

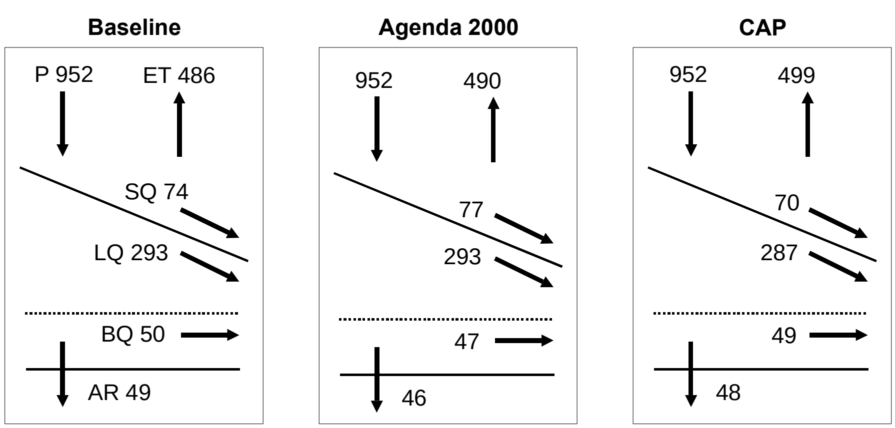

Figure 4. Calculated hydrological fluxes [mm a^{-1}] for the Dill Catchment (Baseline, left) and the two land use scenarios, Agenda 2000 (middle) and CAP (left). P = precipitation; ET = Actual evapotranspiration; SQ = Surface runoff; LQ = Lateral flow; BQ = Baseflow; AR = Aquifer recharge.

Therefore, this analysis of the Dill River Catchment was subdivided into three subcatchments. The selection of the subcatchments was based on the dominant land use types in each of the subcatchments as derived from the baseline scenario. A further distinct feature of the investigated subcatchments was the difference in mean annual precipitation (see Table 1).

Distinct differences in the water balance composition of the three subcatchments can be found for all land use scenarios. Figure 5 outlines the results for the baseline scenario. In subcatchment six evapotranspiration was approximately 47%. Discharge in this subcatchment was largely determined by lateral flow which contributes to around 80%, followed by surface runoff and baseflow with an equal share of approximately 10%. Subcatchment 33 was characterized by an even higher portion of evapotranspiration (70%). Similar to subcatchment six, discharge was mainly composed of lateral flow (74%). The pattern of the water balance in subcatchment 51 was quite different from the other two subcatchments. Here, discharge was more evenly allocated to the three different pathways, surface runoff (45%), lateral flow (27%) and baseflow (28%). The portion of discharge and evapotranspiration was 44% and 43% respectively. Groundwater recharge in subcatchments six and 33 was relatively low. This was slightly different in subcatchment 51, where groundwater accounted for 15% of the total water balance.

These results raised questions concerning the striking differences among the water balance in these subcatchments. One explanation could be in the variation of land use, as all subcatchments have very distinct patterns of land uses (Table 1). Subcatchment six, for example, was largely covered by forests (65%). Due to higher evapotranspiration rates of trees than crops, one could assume that the portion of evapotranspiration in the water balance in subcatchment six was also higher as compared to subcatchment 33. In this subcatchment, cropland accounted for 20% more area than forests. But this is not the case, as show in Figure 5. Another remarkable fact is that surface runoff was dominant in subcatchment 51, although cropland only covers 4 % of the area in the baseline scenario. Pasture and forests, both land covers protecting soil surface from runoff all year around, dominate land use distribution by more than 85% (Table 1). Among other things such as morphological or pedological subcatchment characteristics, it is most likely that differences in rainfall distribution could be responsible for the observed differences in the subcatchments. Mean annual precipitation for the selected subcatchments differs widely (Table 1). Predominant westerly weather situations and the influence of the High Westerwald Range result in mean annual sums of precipitation of 1,230 mm for subcatchment 51 as compared to 759 mm for subcatchment 33 and 1,071 mm for subcatchment six. Figure 6 shows the rainfall-runoff coefficient for the Dill Catchment. It can be seen that the eastern part, where subcatchment 51 is located, was characterized by high rainfall-runoff coefficients > 0.2. Water that cannot infiltrate into the soil generates infiltration excess overland flow. In contrast, a larger share of precipitation that falls in subcatchment 33 leaves the system by plant evapotranspiration. In addition, soils in subcatchment 33 had an elevated field capacity due to widespread loess layers. As a result larger amounts of precipitation can be stored and do not contribute directly to runoff generation in this region.

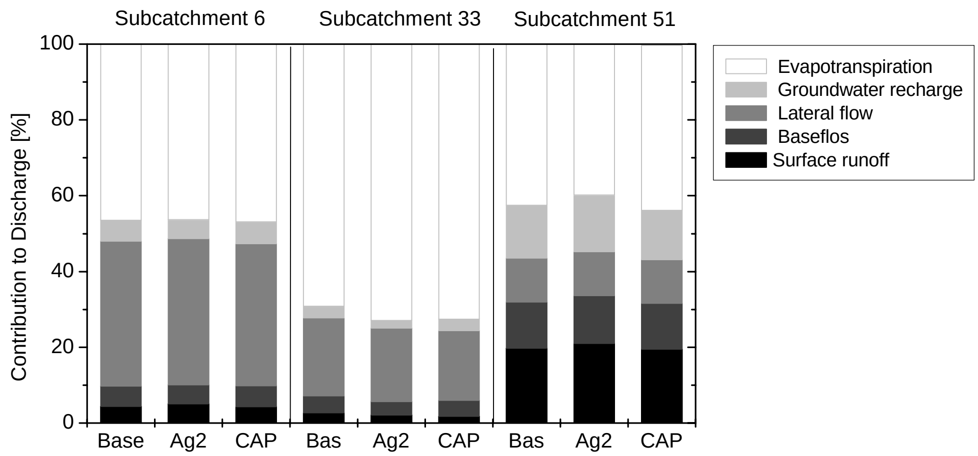

Figure 5. Relative contribution of surface runoff, baseflow, and lateral flow to discharge for three selected subcatchments of the Dill. Relative contribution is given for the current land use distribution (Baseline, Bas) as well as for the Agenda 2000 (Ag2) and the CAP land use scenarios. A detailed description of subcatchments is given in Table 1.

To come back to the problem of tracing the influence of land use on the water balance, we compared the alteration of the water balance composition within each subcatchment for all land use scenarios. As seen in Figure 5, the patterns of water balance composition remain nearly stable under different land uses for subcatchment six. For example, even though cropland area in the Agenda 2000 scenario increases to 10% and decreases to 0% in the CAP scenario (Table 1), the SWAT model calculates no change in surface runoff. It is feasible that several soil and vegetation properties in this subcatchment have an opposite influence on surface runoff generation.

Only slight increases in evapotranspiration were calculated for the Agenda 2000 and CAP scenario for both subcatchments 33 and 51. Land use changes in these two catchments were more pronounced as compared to the ones in subcatchment six (Table 1). But with respect to the amount of change, forests increased from 45% to 82% and cropland decreased from 22% to 0% in subcatchment 33, the predicted changes were rather small. Overall there were only marginal influences of predicted CAP land use scenarios on hydrological fluxes and water balance effects in the Dill River Catchment.

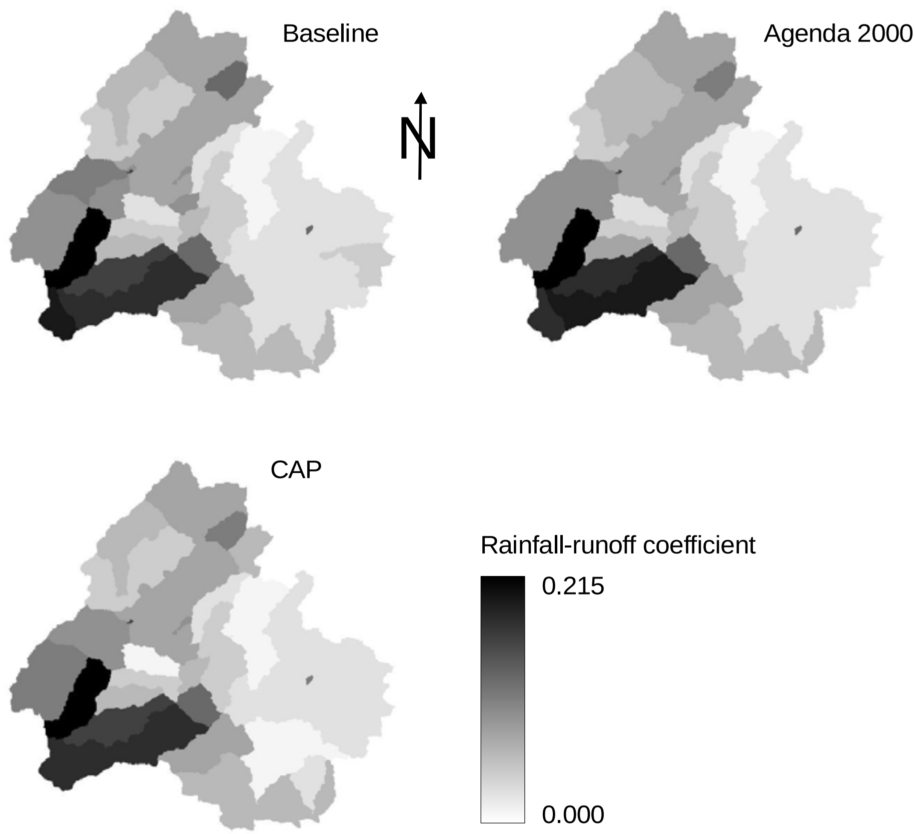

Figure 6. Rainfall-runoff coefficient for the Baseline, Agenda 2000 and CAP scenario. Rainfall-runoff coefficients were calculated for each subcatchment. Precipitation data from 12 gauging stations were allocated by nearest neighbor to the subcatchments. Runoff data were obtained from the SWAT model for each subcatchment.

Conclusions

Two different land use distribution scenarios, namely the Agenda 2000 and the new European CAP scenario, were analyzed for their potential to alter the hydrological cycle of the Dill River Catchment. A modified version of the SWAT2000 model was used to trace the effects of land use distribution on discharge components and evapotranspiration. Little difference was found for the different land use scenarios, even when subcatchments with pronounced differences in land use were investigated. But it should be noted that the observed minor differences in hydrological fluxes for several land use distributions in the Dill Catchment were not typical for all kinds of catchments in general. Generation of discharge in the Dill Catchment was first of all determined by lateral flow, a hydrological flux component that was altered little by land use change. In addition, soil and hydrogeological properties of the Dill Catchment as well as spatially heterogeneous precipitation patterns are overlying feasible hydrological changes due to differences in land use.

Acknowledgement

Land use scenarios were kindly provided by Prof. Kuhlmann and Dr. Weinmann from the Institute of Agricultural Business Administration, Justus-Liebig-University, Giessen, Germany. This study has been supported by the Deutsche Forschungsgemeinschaft within the scope of the Collaborative Research Centre (SFB) 299.

References

Eckhardt, K., Haverkamp, S., Fohrer, N., and Frede, H.-G., 2002. SWAT-G, a version of SWAT99.2 modified for application to low mountain range catchments. Physics and Chemistry of the Earth, Part B: Hydrology, Oceans and Atmosphere, 27, 641-644.

Fohrer, N., Haverkamp, S., Eckhardt, K.S., and Frede, H.-G., 2001. Hydrologic response to land use changes on the catchment scale. Physics and Chemistry of the Earth, Part B: Hydrology, Oceans and Atmosphere, 26, 577-582.

HLUG (Hessisches Landesamt für Umwelt und Geologie), 1998. Digital soil map 1:50000.

Huisman, J. A., Breuer, L., Eckhardt, K., and Frede, H.-G, 2003. Spatial consistency of automatically calibrated SWAT simulations in the Dill catchment and three of its sub-catchments. Proceedings of the second international SWAT conference, Bari, Italy, pp 168-173.

Kuhlmann, F., Möller, D., and Weinmann, B., 2002. Modellierung der Landnutzung - Regionshöfe oder Raster-Landschaft? Berichte über Landwirtschaft, 80, 351-392.

Niehoff, D., Fritsch, U., and Bronstert, A., 2002. Land-use impacts on storm-runoff generation: scenarios of land-use change and simulation of hydrological response in a meso-scale catchment in SW-Germany. Journal of Hydrology, 267, 80-93.

Nöhles, I., 2000. Landnutzungsklassifikation mit multitemporalen Landsat TM-Szenen in einer kleinstrukturierten Agrarregion. Schriftenreihe zur Bodenkunde, Landeskultur und Landschaftsökologie, Bd. 32. Justus-Liebig-Universität Gießen, 160 pp.

Weber, A., Fohrer, N., and Möller, D., 2001. Long-term land use changes in a mesoscale watershed due to socio-economic factors - effects on landscape and functions. Ecological Modelling, 140, 125-140.

Weinmann, B., Kuhlmann, F., 2005. Modelling the CAP reform at the regional level with ProLand. Modelling agricultural policies: state of the art and new challenges, 89th EAAE Seminar, Parma (Italy), 15 pp.

Session IX

35. **On the use of SWAT for the identification of the most cost-effective nitrogen abatement measures for river basins** **339**
Jan Cools and Willy Bauwens

36. **Downstream sediment response to conservation practice implementation** **349**
Michael W. Van Liew and Jeffrey G. Arnold

37. **Development of complex hydrologic response unit (HRU) schemes and management scenarios to assess environmental concentrations of agricultural pesticides using SWAT** **359**
Michael F. Winchell, Raghavan Srinivasan, Tammara L. Estes and Susan S. Alexander

On the Use of SWAT for the Identification of the Most Cost-Effective Nitrogen Abatement Measures for River Basins

Jan Cools[1,2] and Willy Bauwens[1]
[1]Department of Hydrology and Hydraulic Engineering, Faculty of Applied Sciences, Vrije Universiteit Brussel, Pleinlaan 2, B-1050 Brussels, Belgium. E-mail: wbauwens@vub.ac.be
[2]Soresma Engineering, Poortakkerstraat 41, B-9051 Ghent, Belgium

Abstract

In order to reach the water quality objectives, as set by the EU Water Framework Directive, emission loads have to be reduced and pollution abatement plans set up for river basins by 2008. Thereby, good water quality has to be reached in the most cost-effective manner. In order to define the most cost-effective set of measures that need to be implemented to meet the water quality objectives, the SWAT2005 simulator was linked to an economic optimization module. SWAT2005 simulates the in-stream load reductions of various measures. The economic module then selects that combination of measures that achieves the environmental objectives at the lowest cost. The methodology is applied for the Kleine Nete River Basin in Belgium and focuses on the abatement of nitrogen pollution.

Introduction

Given the numerous pressures on water resources, it is vital that effective legislative instruments help to secure existing resources for future generations. Since 2000, the Water Framework Directive (2000/60/EC) of the European Communities, further abbreviated as WFD, enforces the sustainable use of water throughout Europe. Its fundamental objective is to maintain a ‘high status’ of all waters, i.e. groundwater, surface water, transitional water and coastal water. Any deterioration of the existing status must be prevented, and by 2015 a ‘good status’ must be achieved for all European waters. The WFD furthermore stipulates that countries have to set up a River Basin Management Plan, including a set of abatement actions to ensure that the objectives of the WFD will be met within the given deadlines. These plans will be designed and implemented on the river basin scale – the natural geological and hydrological unit that brings together upstream and downstream interests across regional and national boundaries (European Communities, 2002).

Traditionally, pollution problems are solved on a first-come, first-serve basis. Emission permits target the worst polluters first. Yet, pollution abatement measures are often randomly applied without evidence that the environmental targets will be achieved and without considering potentially cheaper alternatives elsewhere in the basin or in other sectors. Taking into account the fact that most rivers in Belgium suffer from a high nitrate load and that older European legislation has not achieved a good water status, it is expected that traditional emission based measures will not be sufficient and that supplementary measures will be required to achieve the environmental quality objectives of the WFD. According to the WFD, a given pollution abatement measure is not considered as a goal in itself, but as a pragmatic action, established with the purpose of reaching an environmental objective.

Including economics in the development of a River Basin Management Plan is another novelty of the WFD. The cost and effectiveness of abatement plans therefore becomes important and should be optimized. Yet, the availability of useful data on costs and effects of pollution abatement measures remains a major bottleneck. Available data on costs and effects are not systematically collected and may be user- or basin-specific, only partly accessible, or fragmented. To fill this data gap, the WFD requires the development of the following documents (at the subbasin scale by 2009):

- documentation of the initial characterization of the river basin, including an economic analysis;
- supplementary information on the current status derived from chemical and biological monitoring;
- catalogues of measures at the subbasin scale, including location-specific cost information.

A practical multi-stage approach for the selection of pollution abatement measures based on a cost-effectiveness analysis was developed by Interwies et al. (2004). Similar work was done for the Rhine Basin by van der Veeren (2002) and for Belgium by Meynaerts et al. (2003).

With regard to economic optimization, cost-effectiveness analysis and cost-benefit analysis are the most common techniques used. For river basin management, a cost-effectiveness analysis is preferred to a cost-benefit analysis if the aim is to find out how the environmental standards can be achieved at the least cost (Turner, 1993, van der Veeren, 2002). This is explained by the fact that in a cost-benefit analysis, environmental standards are set by economic criteria instead of being based on eco-toxicological or environmental considerations. Cost-effectiveness is defined as the annual cost for each unit of pollution abatement (e.g. x Euro / kg N abatement). Likewise, Zanou et al. (2003) define the cost-effectiveness ratio (CE) as the ratio of cost/effectiveness. Note that the 'cost-effectiveness' of a plan can only be determined in relative terms and not in absolute terms.

The previously mentioned studies, however, focus on a methodology for economic optimization and less on the impact of the measures on the receiving waters. Little work has been done to fully integrate economic optimization and water quality modeling. Yet, with respect to in-stream water quality, where the benefit of measures is reflected to a large extent in other downstream subbasins, it is expected that the summed cost of all local combinations of measures will be higher than the total cost of the most cost-effective combination of measures at river basin level (Schleich et al., 1996). Moreover, as the size and complexity of watersheds increase, so does the exercise in finding a good implementation strategy (Srivastava et al., 2002). Within this framework, the use of modeling tools becomes imperative as a means to provide the necessary insight into the hydrologic and socio-economic heterogeneity of the river basin.

In this paper, an integrated economic-hydrologic modeling tool is presented and applied to the River Nete Basin in Belgium. To simulate the impact of pollution abatement measures on the in-stream water quality, the Soil and Water Assessment Tool – SWAT2005 (Arnold et al., 1994) - is used. For the economic optimization, cost-minimization is used as the objective function in agreement with the principle of cost-effectiveness.

Study Area: Nete River Basin (Belgium)

The 'Kleine Nete' River Basin is located in the Flemish Region of Belgium (Figure 1). It is a subbasin of the Nete Basin, which is part of the international river basin district of the River Scheldt. From the selected control section (at the city of Herentals), the Kleine Nete Basin has an area of 320 km^2. The basin is characterized by sandy soil and alluvial sediments. Having an average altitude of 20 mASL and slopes below 2%, the Nete Basin is typically a lowland area.

The Kleine Nete Basin is characterized by a high population density (200 inhabitants/km^2) and an equally high density of animals bred for dairy production (150 cows/km^2, 300 pigs/km² and 4,000 chickens/km²) (Mestbank, 2005). The food and chemical industry are the main industrial activities. The major sources of pollution are (untreated) domestic waste water and animal manure. As much as 60% of the total area is agricultural land, and high manure application rates are used. On average, 210 kgN/ha and 90 kgP_2O_5/ha are applied to the fields (Mestbank, 2005). In 2002, 65% of the population was connected to a waste water treatment plant (WWTP). At the outlet of the basin, an average concentration of 3.5 mgN/L and 0.5 mgP/L were measured for the period 2000-2002 (VMM, 2005). The mean flow during this period was 5.4 m^3/s.

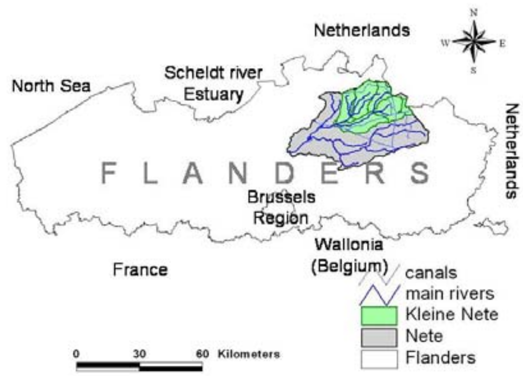

Figure 1. The Kleine Nete River Basin in Flanders (Belgium).

Methodology

The first step in the selection of potential combinations of measures is the identification stage (Figure 2). According to the WFD, the identification needs to be based on the initial characterization of the prevailing pressures and polluter categories (e.g. agriculture, households, industrial, etc.) in each surface water body (at the subbasin scale). In the next phase, measures are selected (at the subbasin scale) based on the ecological effectiveness, the likelihood of target achievement by 2015, and a prioritization on the basis of operational and economic costs. Furthermore, the efficiency of measures depends, to a large extent, on local peripheral conditions as well as technical, social, and financial conditions.

For the sake of testing the integrated economic-hydrologic tool, a 'preliminary' database of potential abatement measures was set up, consisting of information on the potential emission load reductions at the source and cost data for the different measures.

Next, for each particular pollution source and abatement measure, potential emission load reductions at the source were implemented into a calibrated SWAT model, each as a different scenario. Hence, SWAT provides the modeled in-stream load reductions at the control section(s). The modeled in-stream load reduction was consequently used to calculate the 'emission coefficient', α, which is the ratio between the load that reaches the control section and the load that was emitted at the source of the pollution. An emission coefficient can be seen as a linearized coefficient of the non-linear SWAT model.

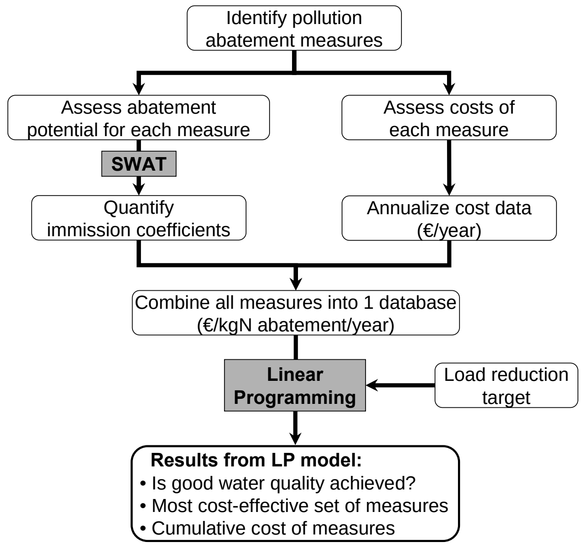

Figure 2. Methodology used in the economic module for SWAT.

In order to select the most cost-effective combination of measures to achieve the water quality objectives, an optimization algorithm was used that combines water quality and economic objective functions. Here, the SWAT simulator was linked to an economic optimization module with cost-minimization as the objective function. The optimization model was based on linear programming (LP).

Consider a set of potential measures, i, for each subbasin, sub, each having an annual cost, c_i (in Euro/year), an emission reduction potential, A_i (in kg/year), a level of implementation, x_i (measure specific units), and a maximum level of implementation (based on the current pollution load). Each subbasin was considered to be a single unit for economic optimization, having subbasin specific measures with a subbasin specific level of implementation as well as subbasin specific load reduction targets, etc. Annual costs were assumed to be homogeneous over the entire river basin.

The model optimizes the values of x_i for each measure in each subbasin. The total cost of the most cost-effective set of measures F(x) for the entire river basin is then defined as (Equation 1):

$$F(x) = \min \sum_{sub} \sum_{i} c_i * x_{i,sub} \tag{1}$$

In addition, the following constraints have to be taken into account (Equations 2-4):

$$\sum_{i} \alpha_{i,sub} A_{i,sub} x_{i,sub} \geq LR_{sub} \tag{2}$$

$$0 \leq x_{i,sub} \leq max_{i,sub} \tag{3}$$

$$\sum_{sub} LR_{sub} = LR_{tot} \tag{4}$$

The constraint in Equation 2 states that the total in-stream load reduction for the subbasin should not be less than the subbasin-specific load reduction target, LR_{sub} (in kgN/year). To ensure that the load reduction target for the entire river basin (LR_{tot}) matches the sum of subbasin-specific reduction targets, Equation 4 is set as an extra constraint. Equation 3 signifies that the level of implementation cannot exceed a given maximum level of implementation. As the interaction between measures, for now, is not considered, the combined effect of a set of measures equals the sum of the effects of the individual measures.

Linking SWAT2005 and the Economic Optimization Tool

Starting with a calibrated water quality model in SWAT2005 and the database of pollution abatement measures, the most cost-effective set of measures was obtained in a Matlab environment (Mathworks, 2002), as shown in Figure 3. By means of a newly developed pre- and postprocessor tool for SWAT2005 (see below), the load reduction targets (LR for each subbasin as well as for the entire river basin) and emission coefficients (α) were determined. Together with the database of measures, all required input data were entered into the economic optimization tool. As a result, the most cost-effective combination of measures (x_i) was returned. The combined emission reduction of the optimal selection was consequently subtracted from the respective pollution load in the initial SWAT model and entered into SWAT as a pollution abatement scenario. In this way, it was possible to assess whether the optimal selection effectively realizes a good water status. Different criteria could be used for this assessment. For the sake of testing the methodology, the assessment was based on the exceedance (EX) of the environmental standard. The latter is calculated based on of the differences between the modeled daily concentrations of total nitrogen (C_{Nt}) at the outlet of the basin and the environmental standard (C_{stand}), as shown by Equation 5. Hereby, negative exceedance values, i.e. when the pollutant loads are lower than the environmental standards, are not considered.

$$EX = \sum_t (C_{Nt} - C_{stand}) * Q_t \qquad \text{if } C_{Nt} < C_{stand} \qquad (5)$$

If the environmental standard is exceeded (EX >0) additional measures have to be applied. To force the economic optimization tool to select an alternative measure, a larger load reduction target is set most simply by increasing the load reduction targets after each optimization until EX becomes zero. As the emission coefficient is specific for a combination of measures, it is recalculated iteratively.

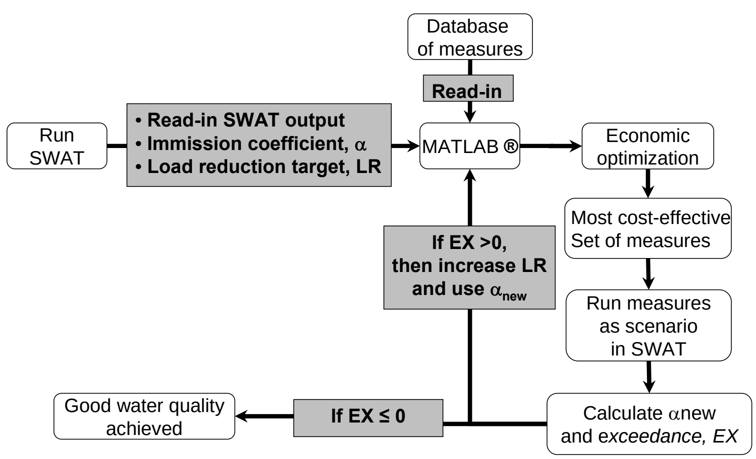

Figure 3. Methodology to link SWAT2005 to the economic optimization tool.

A Pre- and Postprocessor for SWAT2005

In order to support the above mentioned procedures, pre- and postprocessors for SWAT2005 have been developed. A version with a graphical user interface was created in Excel (Figure 4), while a second version, with more functionality and which allows for batch runs of SWAT, was developed in Matlab (Mathworks, 2002).

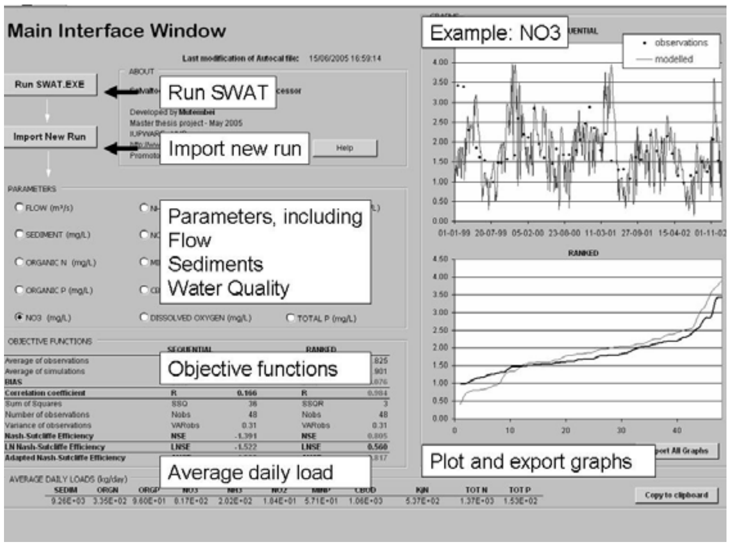

Figure 4. The pre- and postprocessor for SWAT2005, including water quality variables (Excel version).

The new tools allow users to:

- prepare input files in the specific SWAT2005 format, for the required number of HRUs. The input files for diffuse and point source pollution are included
- run SWAT automatically and iteratively from within Excel or Matlab, with no need for the existing ArcView interface. Hence, scenarios generated in the previous step can be simulated in batch mode, e.g. for calibration, sensitivity analysis or environmental impact assessment. In the Matlab version, the best run can be selected based on user-specific objective functions.
- import modeling results for flow and water quality parameters into Excel or Matlab.
- calculate objective functions and efficiency criteria (R^2, Nash-Sutcliffe, bias).
- plot time series and ranked series and export into an easily accessible format.
- link SWAT2005 to the economic optimization tool (only with the Matlab version).

Identification of Measures

For the sake of testing the economic module, only nitrogen pollution was considered in the case study. The following abatement measures were considered:
1) the connection of the remaining households to a waste water treatment plant (sewerage);
2) the subsidized reduction of the pig livestock;
3) the processing of pig manure prior to application on the field.

For each measure, load abatement characteristics and total annual costs are shown in Table 1. Cost estimates are assumed to be average, annual total costs for the entire basin. Administrative costs of designing and implementing nutrient reduction policies are not considered. It is also assumed that the measures have a constant marginal cost, which equals the average cost. Hence, the effectiveness of the measure does not depend on the initial emission load.

Information on waste water treatment and the installation of sewer systems was based on indicators made available by Aquafin, the WWTP operator for the Flemish Region. The nitrogen content of the WWTP influent was assumed to be 10 gN/IE/day and the average nitrogen removal efficiency was 56% (Aquafin, 2004). The annualized cost of sewerage was based on the construction of a semi-separated sewer system. As this is the most expensive option for sewer systems, the costs are expected to be overestimated.

Pig reduction as well as manure processing represents a farmer's management option. These measures prevent pig manure, and its nutrients, from being applied to the field. For manure processing, a small-scale unit processing 20,000 m^3 of liquid manure per year, or the manure produced by 7,000 pigs, was considered. Assuming that a unit consists of a chain of techniques (Feyaerts et al., 2002; VCM and STIM, 2004), a nitrogen removal efficiency of 100% was assumed for these units. VCM and STIM (2004) report an average cost of 25-30 €/ton dry matter. Assuming a dry matter content of 8.5%, this value corresponds to an average cost of 4 €/m³ liquid manure. Unlike other measures, the cost of removing one pig was not defined by investment and operational costs, but rather at the level of the government's compensation funds: 117.5 Euro/pig. The emission coefficient was set to a value of 11%, as suggested for diffuse sources by the Flemish EPA for the Nete Basin (VMM, 2001). Interaction between measures was not considered: the combined effect of a set of measures equals the sum of the effect of the individual measures.

Table 1. The selected pollution abatement measures.

measure	unit	abatement A (kg N/unit/yr)	emission coefficient α	total cost c (€/year/unit)
connect to WWTP	sewer units to connect 1 IE	3.65	0.56	100-200
reduce pigs	1 pig	10.8	0.11	14
manure processing	1 unit = 7,000 pigs = 20,000 m³/yr	76,000	0.11	80,000

Results

The cost/effectiveness ratio (CE) for the different abatement measures is shown in Table 2. Despite its high investment cost, manure processing proved to be the most cost-effective measure (9.6 Euro/kgN abatement). The subsidized reduction of pigs however is only slightly less cost-effective (11.8 Euro/kgN abatement). The construction of a semi-separated sewer system proved to be the most expensive in terms of N abatement (from 50-100 Euro/kgN abatement). Yet, the cost of waste water treatment itself is in the range of the other measures. The construction and operation of a new WWTP of 10.000 IE for example, has a CE ratio of about 10 Euro/kgN abatement. One should also be aware that the CE ratios are strongly affected by the emission coefficients. Obviously, the latter should thus be set carefully, e.g. as a result of SWAT modeling results.

Table 2. Cost-effectiveness ratios (CE) and ranking.

measure	CE ratio (€/kgN abatement)	rank
connect to WWTP	50-100	3
reduce pigs	11.8	2
manure processing	9.6	1

The most cost-effective set of measures as an outcome of the integrated modeling tool is given in Table 3. As confirmed by the CE ratios, manure processing was the most cost-effective measure. In total, nine units for manure processing were required to achieve the best environmental result. As with the abatement potential, costs and other optimization parameters are equally distributed over the subbasins. In the future, subbasin heterogeneity will be considered.

Table 3. Location and selection of abatement actions.

subbasin	most cost-effective measures
1	2 manure processing units
2	3 manure processing units
3	2 manure processing units
4	2 manure processing units
Total cost	**720,000 Euro/year**

As presented in Figure 3, the optimal result was achieved iteratively. Initially, the environmental standard was exceeded most of the time, as shown in Figure 5. The initial load reduction target (LR_{init}) was estimated from Equation 5 to be 63 tonN/year. If good results were not obtained, LR_{init} was increased, and a new optimization run was started. This process was repeated until the optimal result was achieved (Figure 6). In this way, the final load reduction target (LR_{final}) was increased to six times the initial value. Yet, exceedance of the peak values continues to occur. A better estimate of the load reduction target and exceedance criteria is therefore needed.

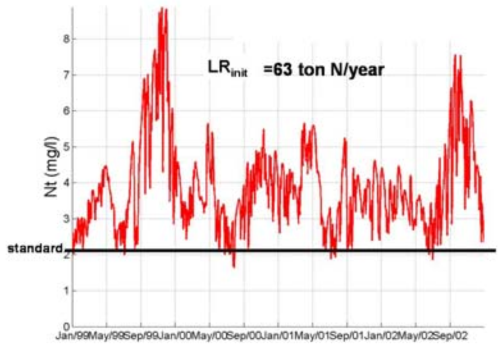

Figure 5. Time series for total nitrogen in the Kleine Nete River Basin (initial status). The environmental standard is mostly exceeded.

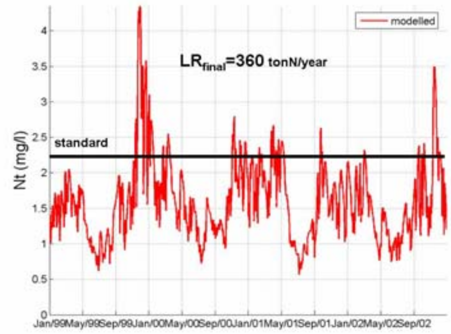

Figure 6. Time series for total nitrogen after implementation of the most cost-effective set of measures. LR_{final} is six times LR_{init}.

Discussion and Conclusions

An integrated hydrologic-economic modeling tool for the optimization of the water pollution abatement costs, in which an economic tool is linked to SWAT2005, was proposed. A linear programming (LP) framework with cost-minimization as the objective function was loosely coupled to SWAT. The most cost-effective set of measures that need to be implemented in order to meet the water quality objective, as well as the cumulative cost to achieve emission load reduction targets was calculated. SWAT was used to model the in-stream load reductions of each measure at the control section.

In order to link the economic tool to SWAT, a pre- and postprocessor for SWAT2005 was developed, using Excel and Matlab.

The economic module was applied to the Kleine Nete River Basin (Belgium), considering the following nitrogen abatement measures: 1) the connection of the remaining households to a waste water treatment plant, 2) a reduction of pigs, and 3) manure processing. Since a catalogue of pollution abatement measures with location-specific costs and pollution abatement values are currently not available, a limited set of measures having highly uncertain costs and effectiveness values was tested.

The lumped approach used in this paper, in which only the allocation to a subbasin was required, may be considered as an advantage. The Water Framework Directive does require a program of measures at the subbasin scale. The semi-lumped SWAT model can furthermore be used to assess downstream impacts. A lumped approach clearly attributes changes in emission load at the control section to abatement measures that are taken. In this way, lumped modelling results can be used to aid management decisions at the river basin scale.

The proposed method however requires the determination of emission coefficients. As these values appear to be most sensitive, SWAT will be used in a later phase to quantify these values more accurately. Likewise, alternative load reduction target functions and criteria for exceedance of the environmental standard will be integrated in the modeling tool.

Although the case study considered in this paper is a simple one, it illustrates the importance of designing policies that account for the cost implications of different strategies. When considering the fact that the number of possible implementation schemes increases as the size of the watershed and the number of variables increases, the use of an optimization algorithm for river basin management is essential.

References

Arnold JG, Williams JR, Srinivasan R & King KW (1994). SWAT: Soil and water assessment tool, USDA Agric. Res. Serv., Temple, Texas.

Aquafin (2004). Annual Report, 2004.

European Communities (2002). The Water Framework Directive. Tap into it! Office for Official Publications of the European Communities. Luxembourg. ISBN 92-894-1946-6.

Feyaerts, T, Huybrechts, D & Dijkmans, R (2002). Best Beschikbare Technieken (BBT) voor mestverwerking. VITO, 2nd Ed., 376 p.

Interwies E, Borchardt D, Kraemer A, Kranz N, Görlach B, Richter S, Willecke J & Dworak T (2003) . Basic Principles for selecting the most cost-effective combinations of measures for inclusion in the program of measures as described in Article 11 of the Water Framework Directive –Handbook. Research Report 202 21 210 (000563/engl), Federal Environment Agency (Umweltbundesamt), Berlin, Germany, 245p.

Mathworks Inc. (2002). Matlab, the language of technical computing, version 6.5.

Mestbank (2005). Based on online database at www.mestbank.be

Meynaerts E, Ochelen S & Vercaemst P (2003). Environmental Cost Model for Flanders: background document *[in Dutch: Milieukostenmodel voor Vlaanderen: achtergronddocument]*. Flemish Institute of Technological Research (Vito). Mol, Belgium.

Schleich, J, White, D & Stephenson, K (1996). Cost implications in achieving alternative water quality targets, Water Resources Research, 32(9), pp. 2879-2884.

Srivastava, P, Hamlett, JM, Robillard, PD & Day, RL (2002). Watershed optimization of best management practices using AnnAGNPS and a genetic algorithm, Water Resources Research, 38(3).

Turner, R.K. (1993). Sustainable Environmental Economics and Management: Principles and Practice. John Wiley and Sons Ltd., 390 p.

Vanderveeren, RJHM (2002). Economic analysis of nutrient abatement policies in the Rhine basin. PhD-thesis, Vrije Universiteit Amsterdam, The Netherlands, 272 p.

VCM & STIM (2004). Manure processing on-farm: opportunities and cost [*In Dutch: Mestverwerking op het landbouwbedrijf: mogelijkheden en kostprijs*], 72 p. February 2004.

VMM (2005). Based on online database at www.vmm.be

Zanou, B, Kontogianni, A & Kourtos, MA (2003). Classification approach of cost effective management measures for the improvement of watershed quality. Ocean and Coastal Management, 46, pp. 957-983.

Downstream Sediment Response to Conservation Practice Implementation

Michael W. Van Liew[1] and Jeffrey G. Arnold[2]
[1]USDA Agricultural Research Service, Grazinglands Research Laboratory, 7207 W. Cheyenne St, El Reno, OK 73036 USA. E-mail: mvanliew@grl.ars.usda.gov
[2]USDA Agricultural Research Service, Grassland Soil and Water Research Laboratory, Temple, TX USA

Abstract

In recent years watershed scale hydrologic models have been developed to assess the environmental conditions of watersheds and evaluate the impacts of Best Management Practice (BMP) implementation. In this study, the Soil and Water Assessment Tool (SWAT) is used to simulate the impact of BMP implementation on downstream sediment yields for the 136 km^2 Lake Creek Watershed in southwestern Oklahoma, USA, under dry, average, and wet climatic conditions. Changes in cultivated crops from winter wheat, sorghum-wheat, and peanut-wheat to Bermuda grass located in the uppermost portion of the watershed are implemented at BMP levels representing the most erodible 2.5%, 5.0%, and 7.5% of the total watershed area. Resultant changes in sediment yield are then simulated at three locations downstream of the proposed conversions. Of the three types of cropping system conversions simulated by the model, test results show that the largest percent reductions in sediment occur for a change from winter wheat to Bermuda, followed by changes from sorghum-wheat, and then peanut-wheat to Bermuda. Under average climatic conditions for the Lake Creek Watershed, BMP implementation on the most erodible 2.5% of land area resulted in a 15.1%, 9.2%, and 6.7% reduction in sediment yield for wheat, sorghum-wheat, and peanut-wheat, respectively. Sediment reductions were most pronounced in the upper reaches of the watershed and became increasingly less pronounced further downstream, due to the dampening effect of averaging sediment yields from larger, contributing watershed areas. At the 5.0% BMP implementation level, sediment reduction for the conversion of wheat to Bermuda under average climatic conditions was 49.3%, 36.5%, and 23.2% for contributing watershed areas of 36.5%, 62.6%, and 100%, respectively. Simulation results suggest that the impact of decadal scale variations in precipitation is minimal on percent sediment reductions for the three cropping systems. This investigation provides preliminary information that quantifies the relative changes in sediment yield that would be expected to occur downstream if conservation practices were implemented in the erodible, upper areas of the watershed.

Introduction

For many decades flooding, erosion, sedimentation, and the movement of pollutants from agricultural chemicals have contributed to environmental degradation of agricultural lands and streams throughout the United States. Pollutant loadings to streams and waters that drain agricultural lands are increasingly a cause for concern to both human and aquatic health. In response to non-point source (NPS) pollution from agricultural areas, government regulations, such as the Clean Water Act of 1972, have lead to a growing emphasis on NPS pollution control (Veith et al., 2003). Implementation of conservation practices associated with agricultural production represents one method of eliminating or sufficiently reducing NPS pollution to meet water quality criteria. Such practices that substantially reduce material losses of soil, nutrients, and pesticides from farm fields or ranches help to reduce pollutant loadings to streams and often provide enhanced wildlife and aquatic habitat.

In this study, a cursory investigation is conducted to determine the watershed scale impact of implementing a particular conservation practice on downstream sediment yields. Hypothetical changes in cultivated crops from winter wheat, sorghum-wheat, and peanut-wheat to Bermuda grass in the uppermost portions of the watershed are implemented at three Best Management Practice (BMP) levels. Resultant changes in sediment yield are simulated with the Soil and Water Assessment Tool (SWAT) at three locations downstream of the proposed changes. The setting for the study is a 136 km^2 drainage of the USDA ARS Ft. Cobb Watershed referred to as the Lake Creek subwatershed located in southwestern Oklahoma, USA. This investigation provides preliminary information that quantifies the relative changes in sediment yield that would be expected to occur downstream if conservation practices were implemented in the erodible, upper areas of the watershed.

Methodology

Test Watershed

The Lake Creek Watershed is located about 150 kilometers southwest of Oklahoma City, OK, USA, and drains an area of 136 km^2 (Figure 1). The climate in the region is sub-humid to semi-arid with an average annual precipitation of about 770 mm. Topography of the watershed is characterized by gently to moderately rolling hills, and the soil types primarily consist of silty loams, loams, fine sandy loams, and sandy loams. Land use types include rangeland/pasture (47%), winter wheat (19%), miscellaneous dry land crops (19%), irrigated crops (14%), and forest (1%). Agricultural practices in the watershed during the past few decades have contributed to excessive sediment, nitrogen, and phosphorous loadings to Lake Creek which in turn drains into Ft. Cobb Reservoir immediately to the south. Portions of the channel are 303(d) listed as impaired by the Oklahoma Dept. of Environmental Quality.

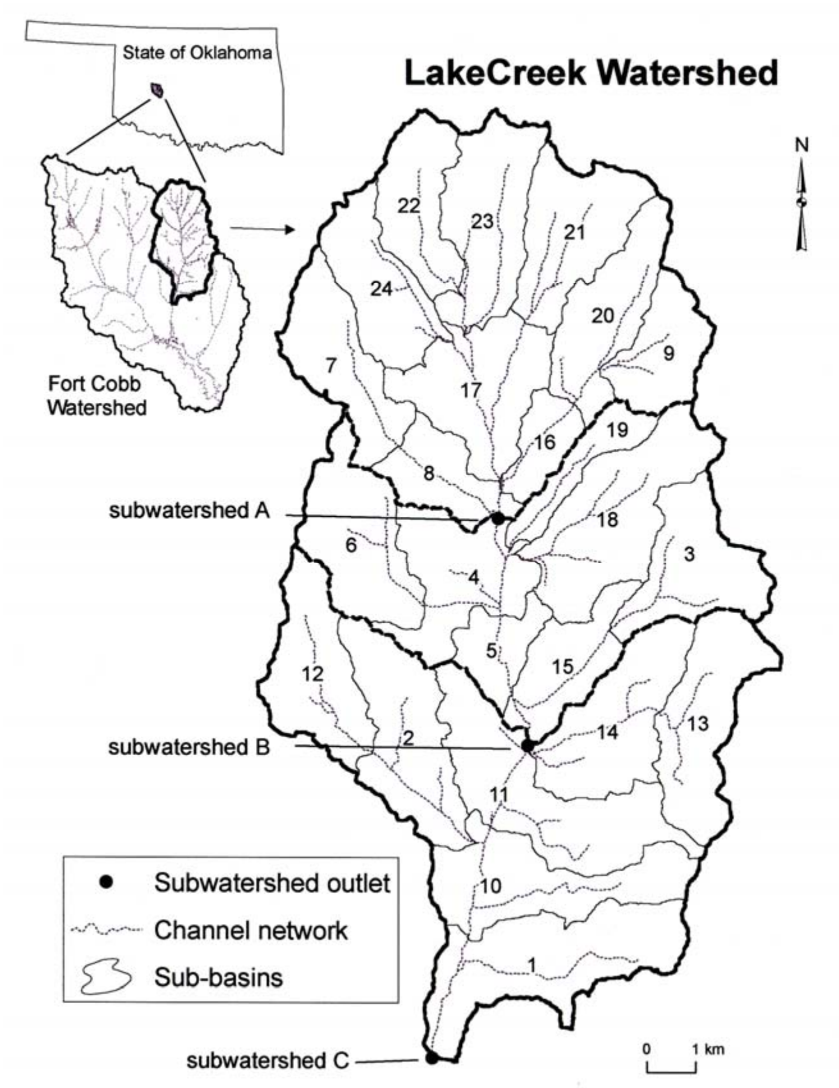

Figure 1. Location of Lake Creek Watershed and the respective subwatersheds and subbasins.

Model Description and Data Input

The Soil and Water Assessment Tool (SWAT) (Arnold et al, 1998) was used to simulate streamflow and sediment responses from the Lake Creek Watershed. For this study, the SCS runoff curve number method was used to estimate surface runoff from precipitation, with adjustments made to the curve number during simulation to reflect changes in moisture conditions on the watershed. Evapotranspiration in the model was computed using the Hargreaves (1975) method, and the variable storage method was used to route flows throughout the watershed.

The 2003 version of SWAT includes a multi-objective, automated calibration procedure that was developed by Van Griensven and Bauwens (2003). The calibration procedure is based on the shuffled complex evolution algorithm that allows for the calibration of model parameters based on a single function. For multi-objective calibrations, this function represents the global optimization criterion, which is an aggregation of several objective functions (Van Griensven and Bauwens, 2003). Eleven parameters that govern streamflow were calibrated in SWAT using the sum of squares of residuals optimization function in the autocalibration tool.

Model Calibration

The Lake Creek Watershed was subdivided into 24 subbasins and 175 hydrologic response units (HRUs) (Figure1). In addition to pasture, wooded, and miscellaneous land use types, three types of cropping systems were simulated on the watershed. These cultivated crops included winter wheat for grain, irrigated sorghum-wheat, and irrigated peanut-wheat. They are herein referred to as wheat, sorghum-wheat, and peanut-wheat. The management operations schedule and Universal Soil Loss Equation (USLE) Practice P and minimum cover-management C factors simulated by SWAT for these crops were obtained from data reported by Storm et al. (2003) for the Ft. Cobb Watershed. The management operations schedule for the three cropping systems is presented in Table 1. The USLE P factor for each cropping system was 0.8, and USLE minimum C factors were 0.07, 0.18, and 0.10 for wheat, peanuts, and sorghum, respectively (Storm et al., 2003). For pasture, Bermuda grass, forest, corn, and alfalfa, USLE P factors were set equal to 1.0, 1.0, 1.0, 0.8, and 0.8, respectively. Default values in SWAT were selected for the USLE minimum C factors for these five land cover types. USLE P and C factors were the only two parameters in SWAT that were adjusted to account for the impact of crop and management conditions on soil erosion in the model. For this preliminary investigation, the impact of channel processes on erosion was not considered.

Data from five continuous precipitation recording rain gages and a streamgage on the watershed were used to calibrate the streamflow response of the model for a four year period of record from 1974 to 1977. The autocalibration tool in SWAT was used to calibrate 11 parameters in the model that govern streamflow response. These parameters included three, six, and two parameters that primarily govern surface, subsurface, and basin response in the model, respectively. Initial lower and upper default and final calibrated values are presented in Table 2a. As noted in the table, values for the SCS runoff curve number (CN2) and available soil water capacity (SOL_AWC) are expressed as a percent change from the default values. Since SOL_AWC and CN2 were calibrated for each HRU, the calibrated data set consists of a multitude of values for these two parameters. Default and calibrated values for SOL_AWC for each soil type on the Lake Creek Watershed are listed in Table 2b. For brevity, only the default and calibrated values for CN2 for the land cover types on the Pond Creek soil are shown in the table. Results of the model simulation show that SWAT estimated annual streamflow within $\pm$ 20% for three out of the four years of record; the computed monthly coefficient of efficiency value was 0.79. Contributions of baseflow to total streamflow were 36% for both the 1974 to 1977 measured and simulated response.

BMP Implementation and Treatment Simulations

To compare the effect of BMP implementation on contributing watershed area, the Lake Creek Watershed was divided into three subwatersheds, designated as subwatershed A (49.6

km^2), subwatershed B (85.2 km^2), and subwatershed C (136 km^2) (Figure 1). An available precipitation period of record from 1963 to 1992 was used to assess the impact of BMP implementation under decadal scale variations in precipitation.

Table 1. Management operations schedule used in SWAT.

Winter Wheat for Grain		Peanut-Wheat	
Harvest Wheat	June 1	Kill Wheat	April 15
Fertilize 135 kg/ha N	Sept 20	Fertilize 30 kg/ha N	April 16
Fertilize 34 kg/ha P2O5	Sept 20	Fertilize 79 kg/ha P205	April 16
Disk	Sept 22	Disk	April 17
Springtooth harrow	Sept 24	Insecticide Aldicarb 1.1 kg/ha	April 17
Plant Wheat	Sept 25	Herbicide Alachlor 3.4 kg/ha	April 17
Grazing 0.81 au/ha for 90 days	Dec 1	Springtooth harrow	April 18
		Plant Peanuts	April 19
		Auto-irrigation	April 20
Sorghum-Wheat		Harvest Peanuts	Oct 15
		Fertilize 45 kg/ha N	Oct 17
Harvest Wheat	May 25	Fertilize 17 kg/ha P2O5	Oct 17
Fertilize 45 kg/ha N	May 27	Disk	Oct 18
Fertilize 17 kg/ha P2O5	May 27	Springtooth harrow	Oct 19
Disk	May 28	Plant Wheat	Oct 20
Insecticide Aldicarb 1.1 kg/ha	May 28	Grazing 0.81 au/ha for 130 days	Dec 1
Herbicide Alachlor 2.8 kg/ha	May 28		
Springtooth harrow	May 29		
Plant Sorghum	June 1		
Auto-irrigate	June 20		
Harvest sorghum	Oct 15		
Fertilize 92 kg/ha N	Oct 17		
Disk	Oct 18		
Springtooth harrow	Oct 19		
Plant Wheat	Oct 20		

This period of record was divided into three periods: a dryer than average period (1963 to 1972), a near average period (1973-1982), and a wetter than average period (1983 to 1992). For the Lake Creek Watershed (subwatershed C), the average annual precipitation for these three periods was 628, 771, and 896 mm, respectively (Table 3). Based on a 30-year average of precipitation equal to 770 mm, the dry, average, and wet periods specified on Lake Creek represent departures from the norm of about -16%, 0%, and +18%, respectively. Simulation results show that for existing land cover conditions, average annual runoff for subwatershed C was 27.4, 54.2, and 84.9 mm under dry, average, and wet climatic conditions, respectively (Table 3). Therefore, runoff was about two and three times greater, respectively, under average and wet climatic conditions than under dry conditions. Under dry, average, and wet climatic conditions, average annual sediment yield for subwatershed C was 1.6, 3.5 and 4.0 Tonnes/ha, respectively, where the yields under average and wet climatic conditions were about 2.2 and 2.5 times greater than those under dry conditions.

Within Lake Creek subwatershed A, the most erodible cultivated HRUs delineated by SWAT were identified and ranked. These HRUs were then summed to determine the most erodible 340, 680, and 1,020 ha within subwatershed A that represent arbitrarily chosen percentages equal to 2.5%, 5.0%, and 7.5% of the total area of the Lake Creek Watershed, respectively.

Table 2a. Parameter values calibrated in SWAT using the autocalibration tool.

Parameter	Initial Default Values Lower Bound	Initial Default Values Upper Bound	Calibrated Value	Parameter	Initial Default Values Lower Bound	Initial Default Values Upper Bound	Calibrated Value
CN2*	-10	10	+9.6%	GW_REVAP	0.02	0.2	0.072
ESCO	0	1	0.001	REVAPMN	0	500	222
SOL_AWC*	-50	50	+2.1%	GWQMN	0	5000	3561
SURLAG	0.5	10	0.642	GW_DELAY	0	500	50.4
CH_K2	0	150	51	ALPHA_BF	0	1	0.379
				RCHRG_DP	0	1	0.898

CN* and SOL_AWC* parameter values expressed as percent change from default values

Table 2b. Default and calibrated values of SOL_AWC for each soil type and CN2 for various land cover types on the Pond Creek Soil.

Soil Type	Default Value of SOL_AWC	Calibrated Value of SOL_AWC	Land Cover Type	Value for Pond Creek Soil	CN2 Value for Pond
Pond Creek	358	366	Pasture	69	75.6
Noble	237	242	Bermuda	69	75.6
Dill	118	121	Forest	60	65.8
Grant	292	298	Corn	77	84.4
St. Paul	350	357	Alfalfa	69	75.6
Knoco	154	157	Wheat	77	84.4
			Sorghum	78	85.5
			Peanut	73	80.1

Table 3. Measured average annual precipitation and simulated average annual runoff and sediment yield for existing land use conditions on Lake Creek subwatersheds A, B, and C under dry, average, and wet climatic conditions.

Subwatershed	Contributing Drainage Area (sq km)	Climatic Period	Average Annual Precipitation (mm)	Average Annual Runoff (mm)	Average Annual Sediment Yield (tonnes/ha)
		1963-1972	646	22.6	2.1
A	49.6	1973-1982	803	46.1	4.6
		1983-1992	898	75.5	5.5
		1963-1972	631	22.7	1.6
B	85.2	1973-1982	780	47.4	3.7
		1983-1992	897	77.1	4.3
		1963-1972	628	27.4	1.6
C	136	1973-1982	771	54.2	3.5
		1983-1992	896	84.9	4.0

Model simulations were performed that assigned these most erodible tracts to a given cropping system. The model was then rerun with the BMP conversions, and percent reductions in runoff and sediment yield were noted. Table 4 illustrates the percent of cover for each of the subbasins in subwatershed A under current conditions and the percent changes in winter wheat to Bermuda grass at the 2.5% BMP level.

Table 4. Percent of land cover for each subbasin in subwatershed A under current conditions and a 2.5% BMP implementation of winter wheat to Bermuda grass.

	Current Conditions					2.5% BMP Implementation on Winter Wheat					
Sub-basin	pasture range	forest	winter wheat	misc. dryland crops	irrigated peanut sorghum	pasture range	forest	winter wheat	misc. dryland crops	irrigated peanut sorghum	Bermuda grass
7	45.6	0.0	23.4	16.5	14.5	45.6	0.0	0.0	16.5	14.5	23.4
8	61.1	0.0	26.0	12.9	0.0	61.1	0.0	26.0	12.9	0.0	0.0
9	34.0	0.0	11.5	17.1	37.4	34.0	0.0	11.5	17.1	37.4	0.0
16	70.3	8.6	14.9	6.2	0.0	70.3	8.6	14.9	6.2	0.0	0.0
17	65.7	0.0	19.9	14.4	0.0	65.7	0.0	19.9	14.4	0.0	0.0
20	62.7	0.0	27.1	10.2	0.0	62.7	0.0	16.3	10.2	0.0	10.8
21	41.2	0.0	25.8	17.6	15.4	41.2	0.0	25.8	17.6	15.4	0.0
22	70.1	0.0	23.8	6.1	0.0	70.1	0.0	7.6	6.1	0.0	16.2
23	34.5	0.0	30.6	27.4	7.5	34.5	0.0	30.6	27.4	7.5	0.0
24	42.4	0.0	16.3	31.0	10.3	42.4	0.0	0.0	31.0	10.3	16.3

Results and Discussion

Percent reductions in sediment yield as a result of BMP implementation at 2.5%, 5.0%, and 7.5% levels for each of the three cropping systems are presented in Table 5. Listed in the table are changes in sediment that would be expected to occur for subwatersheds A, B, and C under dry, average, and wet climatic conditions. On a unit area basis, the greatest impact of the fraction of cultivated land that was converted to Bermuda grass was at the 2.5% BMP implementation level, with incrementally smaller impacts at the 5.0% and 7.5% levels. Of the three types of cropping system conversions simulated by the model, test results show that the largest percent reductions in sediment occur for a change in wheat to Bermuda. This larger impact on the winter wheat system is mainly attributed to the conversion of summer fallow conditions to permanent grass. Under average climatic conditions for subwatershed C, a 2.5% BMP implementation results in a 15.1%, 9.2%, and 6.7% reduction in sediment for wheat, sorghum-wheat, and peanut-wheat, respectively. Conversion of wheat to Bermuda also brought about the greatest reductions in sediment at the 5.0% and 7.5% BMP levels, when compared to the sorghum-wheat and peanut-wheat conversions (Table 5). Differences in reductions in sediment among the three cropping systems as a result of BMP implementation reflect changes in runoff amounts and USLE C factors that vary seasonally due to differences in land management practices for each system.

Test results show that the impact of decadal scale variations in precipitation was minimal on percent sediment reductions among the three cropping systems. In most cases, differences in variation in sediment reduction under dry, average, and wet climatic conditions were not appreciable at the 2.5% BMP level and only slightly more pronounced at the 7.5% level. For wheat conversion on subwatershed B, for example, reductions in sediment load at the 2.5% level were 25.0%, 23.2%, and 22.7% (range of 2.3%) under dry, average, and wet climatic conditions, respectively. For these same climatic conditions at the 7.5% BMP level, these reductions were 53.3%, 49.3%, and 47.5%, respectively, representing a range of 5.8%.

Among the three types of cultivated crops, the impact of BMP implementation was somewhat more evident under dry climatic conditions than average or wet conditions for the wheat and sorghum-wheat cropping systems. For cultivated peanut-wheat, the opposite response was observed. Although not substantiated, these differences in sediment reductions due to varying climatic conditions were mainly attributed to differences in the integrated effects of seasonal precipitation and management practices (e.g., the timing of planting, tillage and harvest) among the three cropping systems.

Table 5. Percent reductions in sediment yield on subwatersheds A, B, and C as a result of BMP implementation at 2.5%, 5.0%, and 7.5% levels for each of the three cropping systems under varying climatic conditions.

Sub-	Climatic	Wheat to Bermuda			Sorghum-Wheat to Bermuda			Peanut-Wheat to Bermuda		
watershed	Period	2.5%	5.0%	7.5%	2.5%	5.0%	7.5%	2.5%	5.0%	7.5%
A	1963-1972	-33.0	-51.7	-70.3	-27.6	-42.9	-58.2	-18.7	-28.4	-38.1
	1973-1982	-32.0	-50.5	-67.9	-24.9	-37.7	-50.6	-20.2	-31.1	-41.7
	1983-1992	-30.3	-46.8	-63.1	-23.3	-36.2	-49.0	-21.2	-32.3	-43.0
B	1963-1972	-25.0	-39.2	-53.3	-19.2	-29.7	-40.3	-11.3	-17.1	-23.0
	1973-1982	-23.2	-36.5	-49.3	-15.6	-23.7	-31.9	-12.0	-18.4	-24.7
	1983-1992	-22.7	-35.2	-47.5	-16.0	-24.9	-33.8	-14.2	-21.6	-28.7
C	1963-1972	-16.3	-25.6	-34.9	-11.4	-17.7	-24.0	-5.8	- 8.8	-12.2
	1973-1982	-15.1	-23.7	-32.0	- 9.2	-13.9	-18.6	-6.7	-10.3	-13.7
	1983-1992	-15.4	-23.8	-32.2	-10.0	-15.5	-21.0	-8.5	-13.0	-17.2

Percent reduction in sediment yield for wheat conversion to Bermuda grass under average climatic conditions was plotted against contributing watershed area, and is shown in Figure 2. The figure illustrates the impact of BMP implementation on changes in downstream sediment yield for subwatershed A and subwatersheds B and C further downstream. Not surprisingly, sediment reductions are most pronounced on subwatershed A, and became increasingly less pronounced downstream, due to the dampening effect of averaging sediment yields from larger, contributing watershed areas. At the 5.0% BMP implementation level, sediment reduction for the conversion of wheat to Bermuda under average climatic conditions is 49.3%, 36.5%, and 23.2% for contributing watershed areas of 36.5% (subwatershed A), 62.6% (subwatershed B), and 100% (subwatershed C), respectively. This same trend was also exhibited at the other BMP levels for the sorghum-wheat and peanut-wheat cropping systems under varying climatic conditions. Although BMPs could also be placed at lower portions of Lake Creek in subwatersheds B or C, preliminary testing showed that resulting sediment reductions at subwatershed C would not be appreciably different from those obtained with the BMPs located in subwatershed A. This is because topographic and soil factors that contribute to erosion on subwatersheds B and C are smaller than those existing in subwatershed A.

Model simulations performed in this study consisted of BMP conversion of a single selection of one of the three cropping systems to Bermuda grass. Under actual field conditions, BMP implementation would likely consist of various combinations of cultivated crops being converted to Bermuda grass. Based on the results of model simulations performed in this study with BMP implementation in subwatershed A under average climatic conditions, sediment yield reductions for Lake Creek (subwatershed C) at the 2.5%, 5.0%, and 7.5% level would be expected to range from about 7% to 15%, 10% to 24%, and 14% to 32%, respectively.

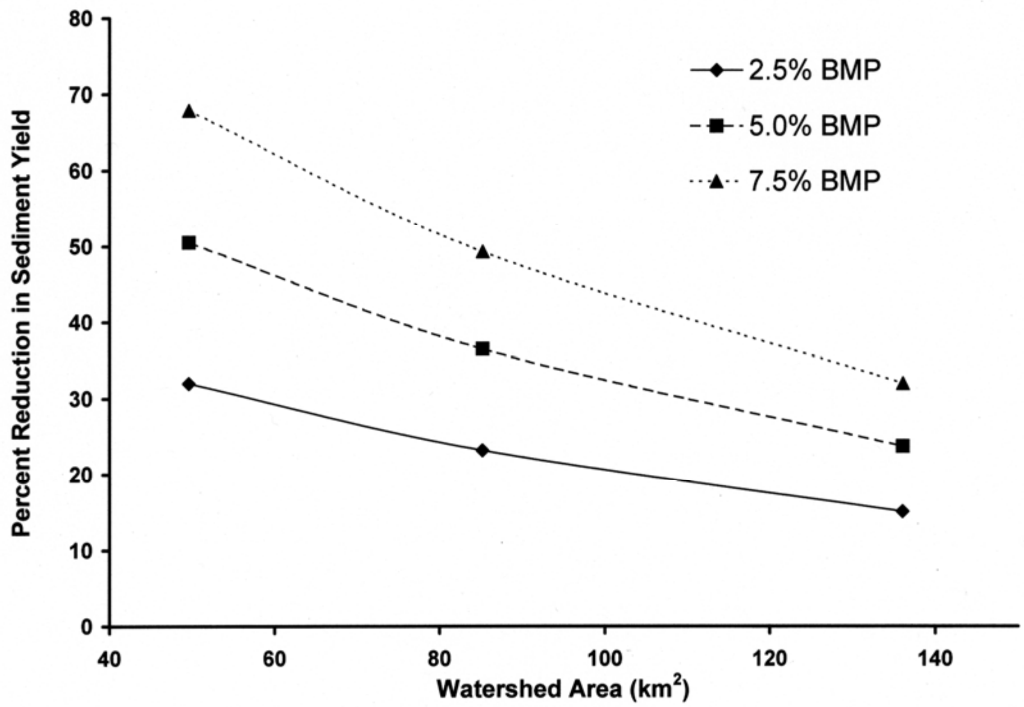

Figure 2. Impact of conversion of wheat to Bermuda grass BMP implementation on subwatersheds A, B, and C under average climatic conditions.

Summary and Conclusions

In this investigation, the Soil and Water Assessment Tool was used to simulate the impact of BMPs on downstream sediment yields for the USDA ARS Lake Creek Watershed in southwestern Oklahoma, USA. Changes in cultivated crops from winter wheat, sorghum-wheat, and peanut-wheat to Bermuda grass in the uppermost portions of the watershed were implemented at three BMP levels, and resultant changes in sediment yield were simulated at three locations downstream of the proposed changes. Of the three types of cropping system conversions simulated by the model, test results show that the largest percent reductions in sediment occurred for a change in wheat to Bermuda, followed by changes in sorghum-wheat and then peanut-wheat. Sediment reductions were strongest in the upper reaches of the watershed and became increasingly less pronounced further downstream, due to the dampening effect of averaging sediment yields from larger, contributing watershed areas. This investigation provides preliminary information that quantifies the relative changes in sediment yield that would be expected to occur downstream if conservation practices were implemented in the erodible, upper areas of the watershed. Further studies are needed to evaluate the impacts of other types of BMPs such as minimum or no till treatments, riparian buffers, and restricted grazing in riparian corridors.

References

Arnold, J.G., R. Srinivasan, R.S. Muttiah, and J.R. Williams. 1998. Large area hydrologic modeling and assessment, part I: model development. J. American Water Resources Assoc. 34(1):73-89.

Hargreaves, G.H. 1975. Moisture availability and crop production. Trans. ASAE 18:980-984.

Storm, D.E., M.J. White, and S. Stoodley. 2003. Modeling non-point source component for the Ft. Cobb TMDL. Final Report submitted to the Oklahoma Dept. of Environmental Quality. 48p.

Van Griensven, A. and W. Bauwens. 2003. Multiobjective autocalibration for semidistributed water quality models. Water Resources Research 39(12):9/1-9/9.

Veith, T.L., M.L. Wolfe, and C.D. Heatwole. 2003. Optimization procedure for cost effective BMP placement at a watershed scale. J. American Water Resources Assoc. 39(6):1331-1343.

Development of Complex Hydrologic Response Unit (HRU) Schemes and Management Scenarios to Assess Environmental Concentrations of Agricultural Pesticides Using SWAT

Michael F. Winchell[1], Raghavan Srinivasan[2], Tammara L. Estes[1], Susan S. Alexander[1]
[1]Stone Environmental, 535 Stone Cutters Way, Montpelier, VT 05602. E-mail: mwinchell@stone-env.com
[2]Texas A&M University, College Station, Texas, USA

Abstract

A large number of SWAT applications over the past decade have involved modeling of nutrients and sediment, often in support of developing best management practices to reduce the loading of these non-point source pollutants. Recently, in the United States, there has been an increased interest in applying SWAT to assess levels of exposure to agricultural pesticides. Modeling pesticide exposure presents unique challenges that are not often encountered when modeling nutrient or sediment loads. These challenges arise because evaluating pesticide exposure requires an assessment of the frequency and magnitude of short duration peak events, as opposed to the assessment of longer duration load totals that is typical for nutrients and sediment. Modeling short duration peak events requires more precise data concerning the pesticide application parameters of timing, rate, and area of application. Customized model data input procedures were created to accommodate the more rigorous input requirements of modeling pesticides to evaluate exposure and the effects of best management practices. Two different applications will be discussed, one in which spatially distributed daily pesticide application input data was available, and one in which daily pesticide application data was inferred from more general crop planting data. In both cases, capturing the temporal and spatial variability of pesticide applications required a sub-HRU approach that was flexible enough to allow subbasin-dependent HRU splitting. This presentation will consider the strategies used to develop the complex HRU and management schemes required for pesticide modeling through a review of the results from several model applications.

Introduction

Models that simulate agricultural pesticide exposure at the watershed scale must be able to adequately predict both the duration and magnitude of peak pesticide concentrations in surface waters. Both human health risks and ecological health risks are gauged at least partially on an acute exposure over durations of one day or less. In order to predict pesticide concentrations at these time scales, accurate assumptions concerning the pesticide application practices throughout the watershed must be made. The critical characteristics of pesticide applications that must be estimated for input into a watershed scale model include the application locations, application rates, and application timing. If these characteristics are poorly estimated, the calibration of the model will be extremely difficult and will suffer from bias in the inputs. As a result, the predictions will not be representative of “real world” conditions.

There are several types of challenges associated with accurately modeling pesticide application practices within SWAT. Among these are two that broadly involve the practical use of available data. The first set of challenges is associated with the raw data available to construct the SWAT management file inputs, and the second set of challenges concerns developing the SWAT model structure to handle the complex management scenarios associated with pesticide applications.

In the United States, the state of California is unique in its collection and distribution of pesticide application data. The California Department of Pesticide Regulation collects data on the date, acreage, and application rate of every pesticide application at a one square mile resolution. These one square mile areas are called sections. This high-resolution data allows very accurate, very detailed pesticide application inputs to be developed. However, for the remainder of the United States, and a large part of the remainder of the world, this level of data is unavailable. For example, in other parts of the U.S., pesticide application data can be obtained at the county level (xx square miles). The challenge then becomes estimating where, within that county area, a pesticide application occurred. This is particularly important when modeling subbasins that only partially intersect an entire county. Figure 1 shows an example of county-level pesticide data overlaid with watershed boundaries and crop locations. It is clear that the actual application location within a county will determine which subbasin receives the pesticide. The other aspect of pesticide applications that is perhaps even more difficult to estimate is application timing. Unlike California, where pesticide applications are recorded on a daily time-step, most other regions of the U.S. only report annual pesticide application acreage and pounds applied. The actual dates when those applications occurred must be inferred from characteristics of when those applications occur during the lifecycle of the crop. Figure 2 shows an example of how pesticide applications can vary within a single application season. Daily diazinon applications for two subbasins in California are plotted along with a single point for each subbasin, representing an equivalent single pesticide application in the subbasin, occurring in the middle of the application season. Daily rainfall data is also plotted in Figure 2. The timing of model application inputs relative to rainfall events will have a huge impact of the predicted concentrations and parameter calibration. The vast majority of modeling applications would not have observed daily application as depicted in Figure 2, but would need to rely on raw data similar to the single application points. The uncertainty in both the spatial and temporal patterns in pesticide applications present one of the greatest challenges in watershed scale modeling of pesticides.

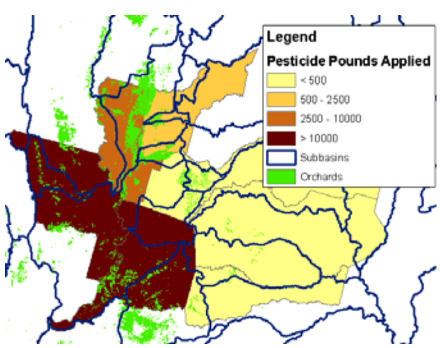

Figure 1. Pesticide application uncertainty (spatial).

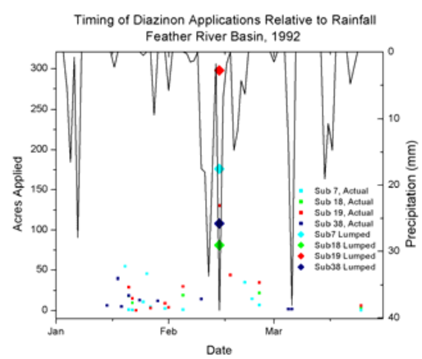

Figure 2. Pesticide application uncertainty (timing).

The second set of challenges in modeling pesticides with SWAT is developing the model structure and input files to accommodate these complex management practices. Whether using high-resolution or low-resolution datasets to develop SWAT management operations, a model structure which is more complex than a single HRU for each crop/soil combination is required. In addition, methods for efficiently constructing the SWAT management tables

(.mgt1 and .mgt2) for large numbers of subbasins and HRUs (outside of the AV-SWAT2000 interface) are necessary.

The remainder of this paper will discuss strategies for working with both high-resolution and low-resolution pesticide-use data. Two case studies will be used to illustrate techniques for working with these different types of data. The first case study will focus on a SWAT model application for diazinon in California where daily pesticide application data at a one square mile resolution was used to develop a daily time series of pesticide applications for each HRU. The second case study will discuss a SWAT model application for a pesticide in the Midwestern U.S where county-level annual pesticide-use data was used to develop application scenarios based on both crop planting date patterns and accumulated heat units. The precise study location and pesticide for the Midwestern study are confidential and will remain anonymous throughout this paper.

Methodology

The objective of any SWAT model pesticide application is to simulate the pesticide application location, area, amount, and timing as closely as possible to what can be inferred from the observed data. This observed data may be a combination of pesticide-use information and cropping practices, such as planting dates. In most cases, this will require creating sub-HRUs in SWAT. Sub-HRUs are created by splitting HRUs that have a common crop and soil type into sub-units for which different management operations can be performed. Each sub-HRU can represent a different percentage of the crop/soil area within a given subbasin. This allows a pesticide application to occur on only a fraction of a particular crop area within any given subbasin, and allows subsequent applications to occur on different dates. An example of this sub-HRU concept is shown schematically in Figure 3.

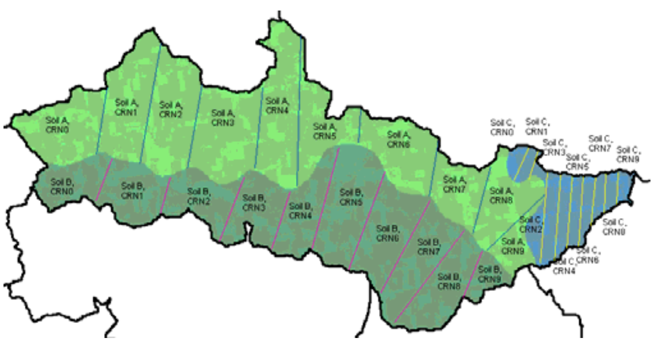

Figure 3. Creation of sub-HRUs to allow distributed pesticide applications within a subbasin.

In Figure 3, one subbasin is shown. Within that subbasin, three soils are present: Soil A, Soil B, and Soil C. Corn (shown as a shaded area within each soil) represents a significant portion of this subbasin. Instead of having only three corn HRUs within this subbasin (one for each soil), this subbasin has been split up to have 30 corn sub-HRUs (10 for each soil). Each corn sub-HRU can be equal or have varying percentages of the total corn area for a given soil. The type of scheme illustrated in Figure 3 offers great flexibility in how management operations are constructed within a subbasin. Of course, the drawback is the increase in the number of total HRUs in the model and the resulting increase in model processing time. This generic HRU framework will be adopted for both the high-resolution and low-resolution case study examples that are discussed in the following sections.

Case Study: Daily Pesticide Use Data in California

A SWAT model was developed to model diazinon concentrations in surface waters within the Feather River Watershed. The Feather River, in northern California, drains approximately 6,000 square miles and is a tributary to the Sacramento River. Much of the watershed falls in the Sierra Nevada Mountains and foothills, with only the lower portion of the watershed containing agricultural land uses. Diazinon is applied as a dormant season spray to orchard crops (almonds, walnuts, peaches, pears, prunes, and apples), typically during the months of January through March. The primary mechanism by which diazinon enters surface waters is through surface runoff. SWAT was applied only to the lower agricultural portion of the watershed. Observed inflows from streamflow gages representing the flow contributions from the headwaters were used as inputs to the model to properly simulate the flow in the downstream reaches. The objective of the modeling exercise was to simulate daily diazinon concentrations at numerous stream reaches throughout the watershed in order to estimate the exceedance frequency above target concentration levels being developed as part of a TMDL (total maximum daily load).

Daily pesticide use data at a one square mile resolution was used to construct daily time series of pesticide applications for each HRU within the SWAT model. The pesticide-use data was obtained from the California Department of Pesticide Regulation Pesticide Use Record (PUR) database for the years 1993 through 2001. The PUR database contains the acreage, pounds, crop, and location for each pesticide application. The spatial resolution of this pesticide-use data (hereafter referred to as PUR sections) relative to the size of the subbasins for a portion of the Feather River Watershed is shown in Figure 4. In general, the PUR sections are smaller than the size of a subbasin, but often are split between multiple subbasins.

The observed pesticide concentration data available for model calibration was limited to scattered storm events at eight locations throughout the watershed. The number of observations at these locations ranged from only two to as many as 100 for the period from 1993 through 2001. The number of actual diazinon detections ranged from 0 to 41. This represents a relatively small quantity of data for calibrating SWAT for daily chemical concentration predictions. Given observed data for only a limited number of storm events, misrepresentation of diazinon application practices could drastically effect the simulations and impact the ability to accurately calibrate the model. For this reason, an approach for structuring HRUs and management operations was designed to maintain as closely as possible the actual application areas, rates, and timing indicated by the PUR database.

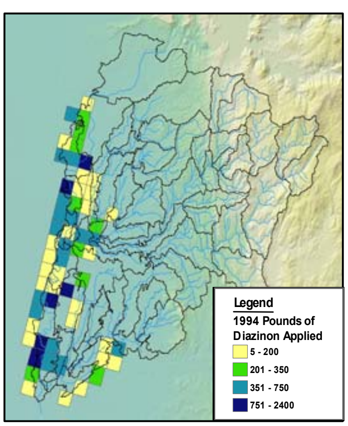

Figure 4. Diazinon use resolution and subbasins in the Feather River Watershed.

The first step in developing daily time series of pesticide applications for each HRU was to develop an HRU structure in SWAT that would accommodate a high level of detail in pesticide application inputs. A primary objective was to preserve the observed acreage and timing of pesticide applications as much as possible. To accomplish this, a sub-HRU scheme was developed that allowed any possible integer combination of orchard crop percentages within a subbasin to receive an application on any given day. This sub-HRU structure split any orchard HRU into 10 sub-HRUs representing various percentages of the total orchard HRU. These percentages are shown in Table 1.

Table 1. Orchard sub-HRU percentages of total orchard HRU area.

Sub-HRU	ORC 0	ORC 1	ORC 2	ORC 3	ORC4	ORC5	ORC6	ORC7	ORC8	ORC9
% of HRU	1%	2%	3%	4%	5%	5%	10%	20%	20%	30%

The second step was to determine the percentage of orchard crops within each subbasin receiving an application on a given day, and the application rate for that day. This is largely a GIS operation that involves spatial unioning of the boundaries of SWAT subbasins, land use, and PUR sections. This allowed calculation of the contributions of the applications from each PUR section to be allocated to the proper subbasin and land use. Combining the GIS analysis with the data in the PUR database, a table similar to Table 2 was created for each subbasin. The sub-HRUs that correspond to the observed percentage of orchards treated are also shown in this table. A script was written to automatically calculate which sub-HRUs should receive pesticide on a given day to attain the proper percentage of orchards treated in the subbasin.

Table 2. Pesticide application data table.

Subbasin	**Date**	**Orchard Acres Treated (%)**	**Application Rate (kg/ha)**	**Sub-HRUs Treated**
1	1/10/1993	1	1.5	ORC0
1	1/12/1993	5	1.74	ORC4
1	1/23/1993	10	1.85	ORC6
1	1/28/1993	23	1.45	ORC2, ORC7
1	2/10/1993	4	1.78	ORC3
1	2/26/1993	2	1.55	ORC1
1	3/5/19993	15	1.43	ORC5, ORC6

The final step was to develop a process to take the information from the pesticide application data table and to create SWAT management operations. A combination of VBA scripts and MS Access SQL operations were developed to update the SWAT mgt1.dbf and mgt2.dbf dBase tables. Once the dBase tables were updated, the ArcView Avenue scripts from the AV-SWAT interface were run to generate the SWAT .mgt text input files. This semi-automated process for populating the management input files was significantly more efficient than inputting thousands of management operations by hand through the AV-SWAT interface.

Case Study: Annual Pesticide Use Data in the Midwest U.S.

A SWAT model was developed to simulate daily pesticide concentrations in a small (< 200 mi^2) agricultural watershed in the Midwestern United States. One objective of the modeling exercise was to assess the impacts of different assumptions concerning pesticide applications on the frequency, duration, and magnitude of peak pesticide concentrations. The pesticide modeled is most commonly applied at planting.

Pesticide-use data for the study area was available at county-level spatial resolution and an annual time-step. The data included annual acres of crop treated and pounds of pesticide applied for each county in the region from 1998 through 2002. Pesticide-use data prior to 1998 were estimated based on the 1998 data. The hypothesis prior to this study was that making gross assumptions on the timing of pesticide applications would result in simulations that do not closely follow reality. The coarse resolution (both spatial and temporal) of the raw pesticide-use data required that some additional manipulation of the data be performed to construct a pesticide application scenario that results in reasonable model predictions. Two different approaches were evaluated. The first approach used state-level weekly crop planting data, and the second approach used the heat unit scheduling in SWAT to generate pesticide application timing.

In both the planting data and heat unit approaches, the first step was to calculate a subbasin-average pesticide application rate for the crop HRUs of interest. This process is primarily a GIS operation involving the union of county-level application data, subbasin boundaries, and the integration of remotely sensed land cover data to calculate the contribution of pesticide use from each county to the crop areas of each SWAT subbasin. The details of these operations are not discussed further in this paper.

The crop planting date approach used a sub-HRU strategy to split the HRUs for the crop of interest into 10 sub-HRUs each representing 10% of the total crop HRU area. The crop planting data contained the date and percent of crop planted on a weekly time-step for the entire planting season. The sub-HRU strategy allowed additional sub-HRUs to receive pesticide applications as the data indicated additional crops were being planted. Table 3 shows an example of this weekly planting data and which sub-HRUs would receive an application at certain times during the season.

Table 3. Crop plating date based pesticide applications.

Date	**% Planted**	**Sub-HRUs Treated**
4/19/1992	2	
4/26/1992	4	
5/3/1992	20	CRP0, CRP1
5/10/1992	72	CRP2 – CRP6
5/17/1992	98	CRP7, CRP8
5/24/1992	100	CRP9

The planting date data available was at the state level. The assumption was made that the state planting data statistics applied for the study watersheds. There was no variability in the planting dates across the various subbasins in the SWAT model, so pesticide application dates were uniform as well. The data presented in Table 3 was then translated to SWAT model management operations in the mgt1.dbf and mgt2.dbf.

The heat unit approach used the same sub-HRU strategy as the planting date approach (i.e., each target crop HRU was split into 10 sub-HRUs). However, instead of using the state-level crop planting dates, a distribution of fraction of potential heat unit values were used to represent when additional percentages of the crop would be planted and receive an application. Table 4 summarizes the heat unit distribution used to represent pesticide application scheduling and the corresponding sub-HRUs receiving applications. The shape of this distribution was adjusted during calibration.

Table 4. Heat unit based pesticide applications.

Fraction of Potential Heat Units	% Treated	Sub-HRUs Treated
0.05	10	CRP0
0.075	20	CRP1, CRP2
0.10	40	CRP3 – CRP6
0.125	20	CRP7, CRP8
0.15	10	CRP9

There were two reasons for investigating this approach. First, the state-level crop planting dates may not be representative of the planting dates in the region where the study watersheds are located. Second, there may be regions where local or even regional planting dates are unavailable. In these situations, the distributed heat unit scheduling approach may represent a viable option. The actual dates at which the pesticide applications occur will vary from subbasin to subbasin if the weather data and resulting growing conditions vary across subbasins. The data presented in Table 4 was translated to SWAT model management operations in the mgt1.dbf and mgt2.dbf.

Results and Discussion

The methods for developing HRU structures and pesticide application schemes for both high-resolution and low-resolution pesticide-use data were applied to the California and Midwestern U.S. study areas, respectively. The modeling results of each of these case studies will be presented and discussed in the following sections.

Case Study: Daily Pesticide-Use Data in California

SWAT was run for the Feather River Watershed using a daily diazinon application time series for each of the 177 subbasins for the period spanning 1993 through 2001. The process for the development of these time series was presented in the Methodology section of this paper. The model was calibrated first for streamflow, then for diazinon concentrations. Streamflow calibration focused on two unregulated catchments within the Feather River Watershed to obtain general parameter adjustments that were then applied to the remainder of the subbasins. Several mainstem gages were used to calibrate the routing parameters. The diazinon concentration calibration considered storm-event monitoring data at approximately eight sites. Most of the sites had data available for only one year. The results of this calibration are shown for several sites in Figure 5. The first graph on the left represents Jack Slough at Doc Adams, a small agricultural drainage. The graph on the right represents the mainstem Feather River at Yuba City.

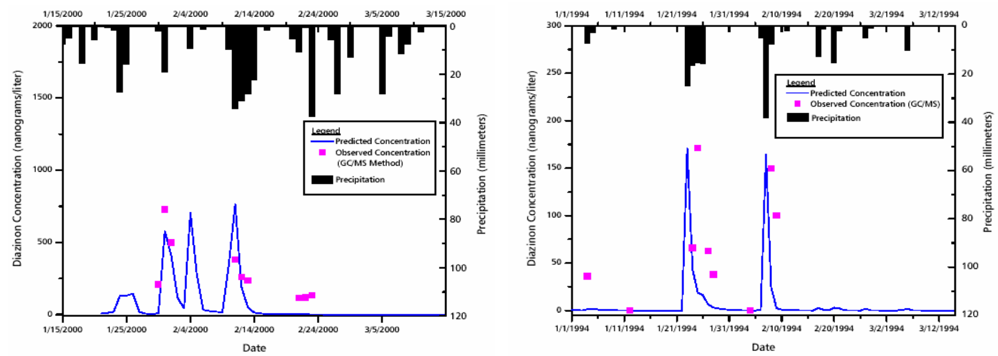

Figure 5. Observed vs. predicted diazinon concentrations, Jack Slough at Doc Adams and Feather River at Yuba City.

The results shown in Figure 5 indicate a strong match of the timing, duration, and magnitude of the peak diazinon concentrations for both Jack Slough and the mainstem Feather River. There are some small events that are not well simulated by the model, such as the February 22, 2000 event on Jack Slough and the January 5, 1994 event on the Feather River. Some of those errors are likely a result of hydrologic simulation errors. Nevertheless, it appears that the rigorous treatment of the PUR database to develop complex HRU management scenarios has resulted in a model that appropriately simulated the frequency, magnitude, and duration of diazinon peaks in this watershed.

Case Study: Annual Pesticide-Use Data in the Midwest U.S.

SWAT was run for the Midwestern watershed for a period spanning 1991 through 2002. For this application, the model was run based on the “best estimate” parameters that could be obtained from all available datasets, and was not fully calibrated. The objective was to evaluate the performance of SWAT using the various pesticide application scenarios, assuming that hydrologic and chemical parameters were estimated only based on best available data sources and not through calibration.

Figure 6 shows the results of the planting date pesticide application timing approach for two different application seasons. In addition to the weekly planting date approach (resulting in distributed applications) a simplified, single pesticide application run is presented for comparison. In general, the peak magnitudes and durations are modeled acceptably using the distributed application approach. The single application approach results in peaks that are too high and does not capture the frequency of significant peaks as well as the distributed approach.

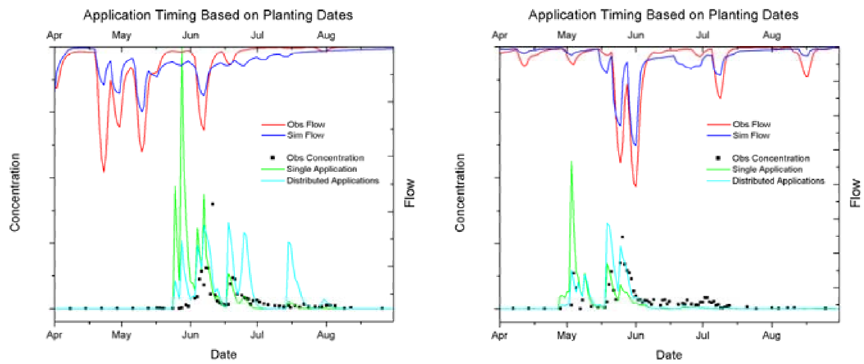

Figure 6. Observed vs. predicted concentrations; planting date scenarios.

Figure 7 shows the results of the distributed heat unit based application timing approach for the same two application seasons. Once again, a simplified, single application run (based on just a single heat unit threshold) is shown for comparison. As with the planting data approach, the distributed heat unit method results in pesticide concentrations peaks that are within a reasonable range of the observed concentrations. The advantage of distributing the pesticide applications over a range of heat units is evident based on the significant over prediction that occurs when only a single heat unit value is used to schedule applications.

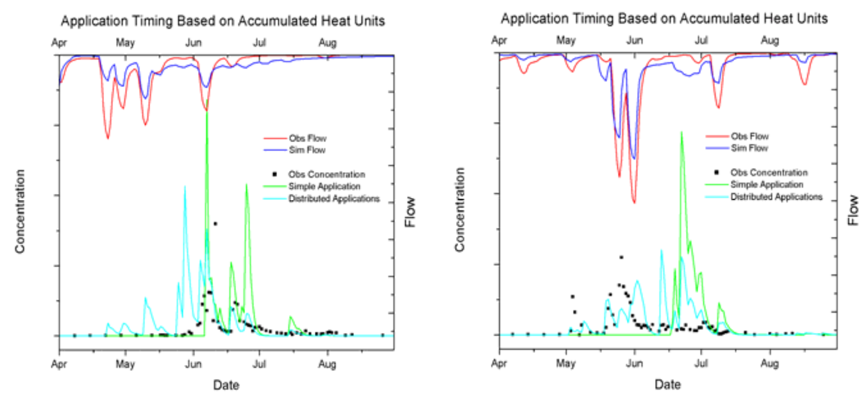

Figure 7. Observed vs. predicted concentrations; heat unit scenarios.

A final comparison was made directly between the planting date based approach and the heat unit based approach. This comparison is shown in Figure 8. In the first season, the heat unit approach appears to estimate that pesticide applications occur too early in the season, as indicated by the high early peaks. In the second season, the planting data approach may lump too many applications right before the large event that occurs in mid-June. Based upon the analysis performed in this study, it is difficult to determine which method produces the most reliable pesticide application scenarios, since in some seasons the heat unit approach performs better and in others, the planting date approach performs better. Nevertheless, if pesticide applications can be closely linked to a specific time during the crop lifecycle (e.g., planting), and observed crop planting (or other lifecycle milestone) data is available at a local level, then the recommendation would be to use this source of data for estimating pesticide applications. The heat unit approach is a viable option, but will likely require some calibration to obtain the proper distribution of heat unit thresholds for applications.

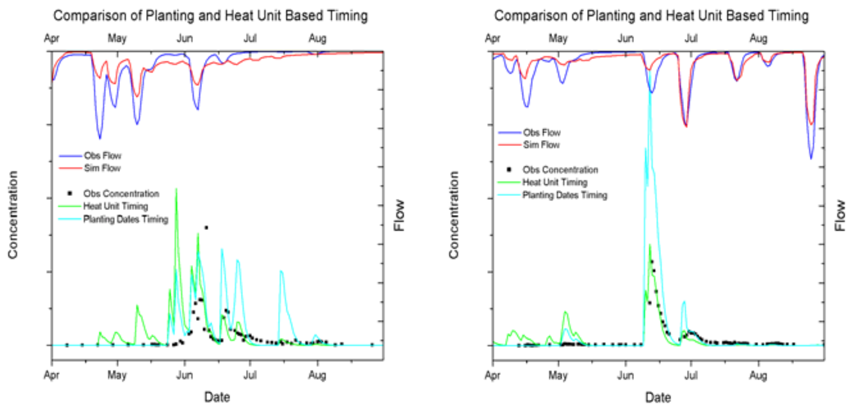

Figure 8. Observed vs. predicted concentrations; planting date and heat unit scenarios.

Conclusions

Modeling agricultural pesticides at the watershed scale can be complicated due to model input requirements and data availability for calibration. These complications are driven by the objectives of most pesticide modeling efforts, which require that the pesticide concentration peak magnitude, duration, and frequency be accurately simulated. These characteristics of concentration peaks depend significantly on the spatial and temporal variability in the pesticide applications throughout the watershed. Obtaining pesticide-use data that accurately represents the distribution of applications within a watershed is very difficult. Even for the limited areas of the world that have accurate, high-resolution pesticide-use data available, compiling those data into a format useable by watershed simulation models is not trivial. This paper focused on strategies for developing pesticide application scenarios, specifically for input to SWAT management operations, using both high-resolution and low-resolution pesticide-use data.

The most critical strategy when modeling pesticides, whether using high-resolution or low-resolution use data, was to develop a highly distributed sub-HRU scheme for the crops of interest. This type of scheme allows different proportions of a crop HRU within a subbasin to receive pesticide applications at different times during the application season, spreading applications over many different days as opposed to lumping them into a single application. This type of scheme was shown to accurately capture the frequency and magnitude of diazinon concentration peaks in the Feather River Watershed in California. In the Midwestern U.S., two different strategies for estimating pesticide application timing distribution from annual pesticide use data were explored. The first was based on weekly crop planting dates and the second was based on a distribution of accumulated potential heat units. Both methods resulted in significantly better simulations than the approaches that lumped the pesticide applications within each subbasin into a single week or single heat unit threshold.

The methods presented required significant GIS processing to estimate subbasin-level pesticide application areas and rates. Furthermore, customized scripts and SQL operations were required to translate large tables of sub-HRU pesticide application data into SWAT management operations and to make proper updates to the SWAT input files. Additional work to further develop and refine these procedures will help to make modeling realistic pesticide management scenarios more effective and efficient using SWAT.

Posters

38. **A decision support system based on the SWAT model for the Sardinian Water Authorities** 369
P. Cau and E. Lorrai

39. **Use of hydrological models at the catchment scale to predict the effect of different land management practices and point source pollution** 379
I. Contu, A. Carucci and P. Cau

40. **Scale issues, hydrological pathways, and nitrogen runoff from Agriculture-Results from the Mellupite Catchment, Latvia** 390
Johannes Deelstra, Kaspars Abramenko, Nils Vagstad and Viesturs Jansons

41. **Evaluation of SWAT for use in development of a river basin management plan for the Ythan Catchment, UK** 398
Caroline F. Dilks, Sarah M. Dunn and Robert C. Ferrier

42. **Distributed watershed modeling of a mountainous catchment-A case study in the Amameh Catchment in Iran** 408
Shaaban-Ali Gholami

43. **SWAT model development for a large agricultural watershed in Iowa** 414
C.H. Green, M. Di Luzio, J.G. Arnold and M.D. Tomer

44. **An analysis of non-point source pollution in a stock breeding area of the Heihe River Basin** 423
Fanghua Hao, Hongguang Cheng, Shengtian Yang, Ye Qi and Xiyan Ren

45. **Modeling the effects of land use and climate change on hydrology and soil erosion in a sub-humid African catchment** 434
H. Busche, Claudia Hiepe and B. Diekkrüger

46. **An assessment of alternative conservation practice and land use strategies on the hydrology and water quality of the Upper Mississippi River Basin** 444
Manoj Jha, Philip W. Gassman, Silvia Secchi, Jeff G. Arnold, Lyubov A. Kurkalova, Hong-Li Feng and Cathy L. Kling

47. **Macro-scale catchment modeling in Northwest Russia** 454
S.A. Kondratyev

48. **Sensitivity of the SWAT model to spatial variability of land use and soil data: A Lake Balaton Catchment case study** 464
Peter Laszlo, Laszlo Pasztor and Jozsef Szabo

49. **Impact of precipitation data interpolation on the quality of SWAT simulations** 472
Roberta Maletta, Johan A. Huisman, Lutz Breuer, Hans-Georg Frede and Giuseppe Mendicino

50. **SWAT modeling response of soil erosion and runoff to changes in precipitation and cover** **482**
Claire Baffaut, M.A. Nearing, V. Jetten, O. Cerdan, A. Couturier, M. Hernandez, Y. Le Bissonnais, M.H. Nichols, J.P. Nunes, C.S. Renschler, V. Souchère and K. van Oost

51. **Hydrologic modeling of a semi-arid region in Brazil** **491**
Maria Quiteria C. de Oliveira, Ramon C. de Oliveira and Yvonilde D P Medeiros

52. **Evaluation of the soil nitrogen balance model in SWAT with lysimeter data** **498**
Thorsten Pohlert, Johan A. Huisman, Lutz Breuer and Hans-Georg Frede

53. **Modeling soil carbon cycle for the assessment of carbon sequestration potentials at the river basin scale** **509**
Joachim Post, Felicitas Suckow, Valentina Krysanova and Fred F. Hattermann

54. **Evaluation of soil infiltration in furrow irrigation and determination of Kostiakov and Kostiakov-Lewis equations coefficients** **518**
A.Rahimi, H.A. Kashkuli and S. Boroomand

55. **Assessment of agricultural management practices in the Upper Maquoketa River Watershed using SWAT** **522**
Pipat Reungsang, R.S. Kanwar, M. Jha, P.W. Gassman, K. Ahmad and A. Saleh

56. **Evaluation of SWAT streamflow components for the Grote Nete River Basin (Flanders, Belgium)** **532**
Hamed Rouhani, Patrick Willems and Jan Feyen

57. **Impact of land use changes on stream flows using the SWAT model; Case study: Kasilian Catchment** **542**
Hossein Saadati, S.H. Gholami and S.A. Ayyoubzadeh

58. **Imitating model water-salt balance (IWSBM) in large watershed basins** **549**
Javad Sadatinejad and A. Ranjbarfordoi

59. **Application of SWAT and APEX models using SWAPP (SWAT/APEX program) for Upper North Bosque River Watershed in Texas** **559**
Ali Saleh

60. **A modeling approach for evaluating the water quality benefits of conservation practices at the national level** **568**
C. Santhi, N. Kannan, M. Di Luzio, S.R. Potter, J.G. Arnold, J.D. Atwood and R.L. Kellogg

61. **Transport and uptake of Cd, Cu, Pb and Zn in calcareous soil of Central Iran under wheat and safflower cultivation: A column study** **577**
Gholamabbas Sayyad, Majid Afyuni, Sayed-Farhad Mousavi, Karim C. Abbaspour Rainer Schulin

62. Prioritizing watershed development programmes in developing countries 588
Sucharita Sen and Ms. Poulomi Banerjee

63. Climate change impacts on the hydrology and water quality of the Upper Mississippi River Basin 599
Eugene S. Takle, Manoj Jha, Philip W. Gassman, Christopher J. Anderson and Silvia Secchi

64. Model for nitrogen leaching from a watershed using field scale models 609
Anatoli Vassiljev

65. A procedure to compute groundwater table depth using SWAT 616
Gabriel G. Vazquez–Amábile and Bernard A. Engel

66. Calibration and validation of the SWAT model to predict atrazine in streams in Northeast Indiana 627
Gabriel G. Vazquez–Amabile, Bernard A. Engel and Dennis C. Flanagan

67. Methods for analyzing calibration parameter uncertainty 637
T.L. Veith, L. T. Ghebremichael, M. W. Van Liew and J. G. Arnold

68. The TERRACE Project: SWAT application for diffuse chemical pollution modeling 657
S.M. White, N. Kannan, I. Beaudin, J. Hollis, A.R. Young, V. Keller and M. Whelan

69. Ensuring appropriate hydrological response for past and future nutrient load modeling in the Norfolk Broads 666
J. Whitehead, S.M. White and I. Holman

70. Groundwater resource management on the urban environment 674
Eyilachew Yitayew

A Decision Support System Based on the SWAT Model for the Sardinian Water Authorities

P. Cau*[1], E. Lorrai[1]
[1]Center for Advanced Studies, Research and Development in Sardinia (CRS4); address: Parco Scientifico e Tecnologico, POLARIS, Edificio 1, 09010 PULA (CA - Italy) email: plcau@crs4.it

Abstract

Sardinian Regional Authorities, such as the *Assessorato della Difesa dell'Ambiente*, have the demanding problem of water management and protection. Targeted to their specific needs they use alternative applications and models for their specific tasks and little communication is usually achieved. Black box models, in the past, have been the most commonly used approach to describe the hydrological cycle. Despite their wide use, these models have shown severe limitations in accounting for land use and climate changes. Physically based models can provide better predictions because different combinations of soils and land use, within the basin, have a significant effect on the hydrological cycle. The variety and complexity of alternative environmental problems found on the island, which vary from the impact of the agro-zootechnical to industrial sector, have suggested that empirical models are less suitable to predict the environmental dynamics at the catchment scale. Regional Authorities enact Regional Directives to enforce different European Directives, and no absolute limits can be drawn to separate their alternative field of application. The *Piano di Tutela delle Acque (PTA)* Regional Directives aim to enforce water policy in terms of definition on where and how water resources must be used and what water protection actions need to be enforced to improve water quality of rivers, lagoons, groundwater, lakes etc. In this context, the hydrological physically based SWAT model has been chosen and applied to estimate both the water budget of the main catchments of the island and the impact of land management practices on downstream water bodies. The performance of the model has been evaluated at several stream flow monitoring gages against observed data.

Introduction

Action plans to reduce diffuse and point water pollution is an enormous challenge to policy makers and presents an ever increasing complexity. The issue of water management, in fact, is interrelated with broader policy questions associated with social and economical development. A cross disciplinary, multisectoral approach must be adopted to collect and link together information that ranges from environmental models to imprecise background data in order to form an overview of the problem at hand. A multisectoral approach is needed to truly integrate river basin management through consideration of socio-economic and environmental aspects, through the use of modeling techniques with GIS functions, and multi-criteria decision aids (Giupponi et al., 2001).

The management of water resources is an important environmental problem in Sardinia, where water demand is steadily increasing and water resources are scarce (availability of water is a critical issue in this region, where summer water shortages are a perennial problem). Nutrients that enter the water are mostly from the zootechnical sector and agricultural land, which is, in general, the industrial sector that is still limited. Nitrate and phosphorous levels in water bodies, both ground and surface waters, are found to be increasing and local and regional authorities are now facing this awkward environmental problem. The European Directives require Member States to identify areas that are thought to be at risk of contamination and to establish Action Programmes in order to reduce and prevent further contamination. Consideration of the physical processes associated with water movement, crop growth, and nutrient cycling can be important in evaluating the gradual build up of pollutants due to different land management practices on downstream water bodies (e.g. coastal lagoons). In this framework models can give support by identifying indicators at each scale that reflect critical ecosystem processes or state variables related to the integrity and sustainability of those ecosystems.

Methodology

Description of the DSS

In 2002 a Consortium made up of CRS4, TEI srl, PROGEMISA and NAUTILUS was created for the three year project "*Piano di Tutela delle Acque*" (PTA). One of the main goals of the project was the development of a multisectoral, integrated and operational Decision Support System (DSS) for Sustainable Use of Water resources at the catchment scale.
The project had three main objectives:

1. to collect all available information (driving forces, natural and anthropogenic pressures on the water systems, historical water quality information of the main water bodies, etc.) and design a two year monitoring campaign to gather water quality indicators of the main water systems of the island;
2. to design and implement an operational decision support system for the management of water resources that is based on hydrologic modeling, multi-disciplinary indicators and a multi-criteria evaluation criteria;
3. to identify those protection actions to preserve the water quality standards of the water bodies of the island, and for those polluted, to plan actions to reduce contamination below the limits drawn by the national water directives. As a result of the project, the "*Piano di Tutela*" (PTA) regional water directives will be enacted.

A series of aspects have deviated from the original objectives to what was actually realized during the course of the project. It is, now, clearly stated that a primary goal is to build relationships between local stakeholders and end users. It was actually the collaboration with the end users that led us to an ever-increasing consideration for the relationship between water management authorities and local communities, and to structuring their contribution in the decision process.

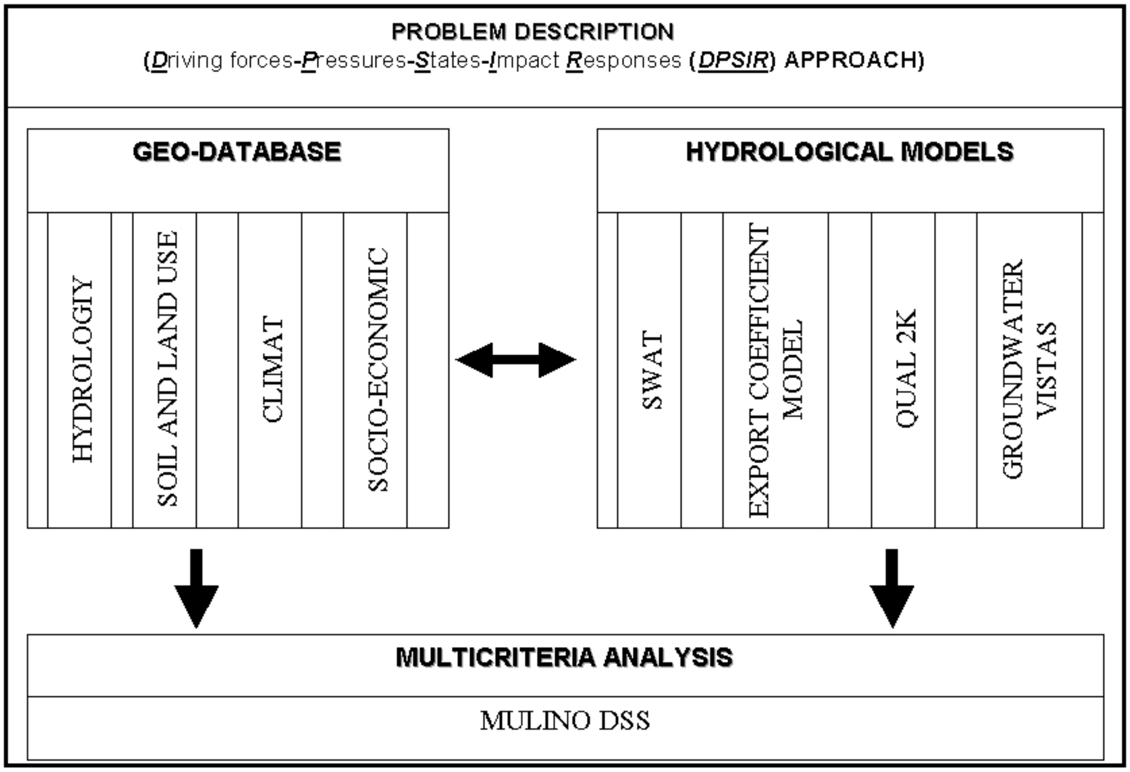

Figure 1. The DPSIR approach can be useful for organizing information that emphasizes cause-effect relationships designed for environmental problem solving. This methodological framework summarizes key information from different sectors (field data, models, and socio-economic analysis). Four alternative hydrological models and the multi-criteria decision support system (Mulino DSS) are the main modules of the system.

The specific aims of the DSS were improving the quality of decision making and achieving a truly integrated approach to river basin management. Although the integration of socio-economic and environmental modeling techniques with GIS functions and multi-criteria decision aids was a specific requirement of the DSS, the informatics architecture has been developed to be modular. The DSS has been designed with stand alone tools to solve alternative problems. With the project half complete, PTA is undergoing a transition period in which the main modules, that have been chosen, developed and/or integrated with a high level of communication, but essentially with a great degree of independence, are beginning to be used in an integrated way.

The DPSIR conceptual framework has been developed to structure decision making problems by linking Drivers – Pressures – State – Impacts – Responses, thus representing a systemic and dynamic view of the decision context. The hydrological models are used to explore interactions between pressures and states. Four alternative hydrological models have been chosen: SWAT, the Export Coefficient Model, QUAL 2K, and Groundwater Vistas. The first two models (both are catchment scale models and evaluate the impacts of diffuse and point source pollution) differ in approach, time resolution of the input-output, and space discretization criteria. QUAL2K is a comprehensive and versatile stream water quality model. Groundwater Vistas is a Windows graphical user interface for 3-D groundwater flow and transport modeling. This is a package of different groundwater models (MODFLOW,MT3DMS, etc.).

Theoretically the structuring problem requires three phases:

1. The pressures and the state of the environment are investigated and the causal links identified. In this phase models can give support to identify the cause effect relationship;
2. Alternative options for the environmental problem are defined and investigated. In this phase the decisional indicators with the use of local network analysis, model outputs, economic analysis, etc. are chosen; model results can be read directly in the multi-criteria decision support system (Mulino DSS (Giupponi et al., 2001).
3. A decisional criteria is chosen.

Description of the island

The climate of the island is Mediterranean, with long hot dry breezy summers and short mild rainy winters, except at high altitudes. Average annual temperatures range from 18 °C along the coastal belt to 14 °C inland. Precipitation is largely confined to the winter months and distribution is somewhat irregular, with as much as 1,300 mm/year in the highest areas along the east coast. The rainfall regime is typically Mediterranean, characterized by a peak rainfall in December, and a minimum in July, with an average value of about 780 mm/year. A north-westerly wind blows over the island in all seasons, particularly sweeping the west side. Lying in the Tyrrhenian Sea to the east, the Sardinian Sea to the west, and separated from Corsica to the north by the Strait of Bonifacio, Sardinia is found in the middle of the Western Mediterranean between 38°51'52" and 41°15'42" north latitude and 8°8' and 9°50' east longitude. It is one of the largest islands in the Mediterranean Sea (24,089 km^2). The morphology of the island is the result of complex tectonic processes and volcanic activity in the Cenozoic era on a mass of Paleozoic rock up thrust from the sea, later severely affected by late Paleozoic orogenesis. The Sardinian mountains are a chaotic series of deeply eroded ranges, groups, plateaus and uplands, scattered in apparent disarray. Relief alternates with deep valleys and winding riverbeds. With the notable exception of the Campidano in Sardinia there are few plains, usually of small extension. Catchments range in size, topography, climate, socio-economic and cultural context.

The water courses are characteristically fast flowing, with a relatively high water volume in winter, reduced to a trickle in summer. The principal rivers are the Flumendosa and Cedrino to the east, the Mannu-Coghinas, emptying into the Gulf of Asinara, the Tirso, which flows into the Gulf of Oristano and the Temo which flows into the sea near Bosa and is the only navigable river. Their waters have been harnessed and form artificial lakes and reservoirs (more then 50).

The most important lagoons are located in the humid areas near Cagliari (S. Gilla) and Oristano (S. Giusta, Mistras etc.), which are among the largest wetlands in Europe. The waters which flow underground and appear as karst springs both in the open and in caves are also of great interest. Equally important are the mineral springs flowing from fractures in the terrain due to ancient processes of volcanism dating back to the Tertiary and Quaternary; these waters have therapeutic properties and are marketed in the form of mineral water.

The island is sparsely populated, with a density of about of 68 people/km^2, which is slightly higher than a third of the Italian national average. The industrial sector is limited to a few areas of the Island. Agriculture is generally extensive with the cultivation of cereal, wheat, olives, etc. The zootechnical sector is predominant, with mostly cows and sheep. Rivers, lakes, and groundwater have been classified into homogeneous groups according to the concentration of contaminants of the waters with regards to the quality limits drawn by the national water directives (152/99). The export coefficient model has been applied on a regional scale to highlight the cause-effect relationship between pressures and states.

The main problems found on the island are associated with an irregular precipitation regime and water scarcity, which affects the availability of water supplies to the main users. Agriculture is competing with other sectors for the use of water, rendering the management of water quantity and the preservation of water quality very significant issues.

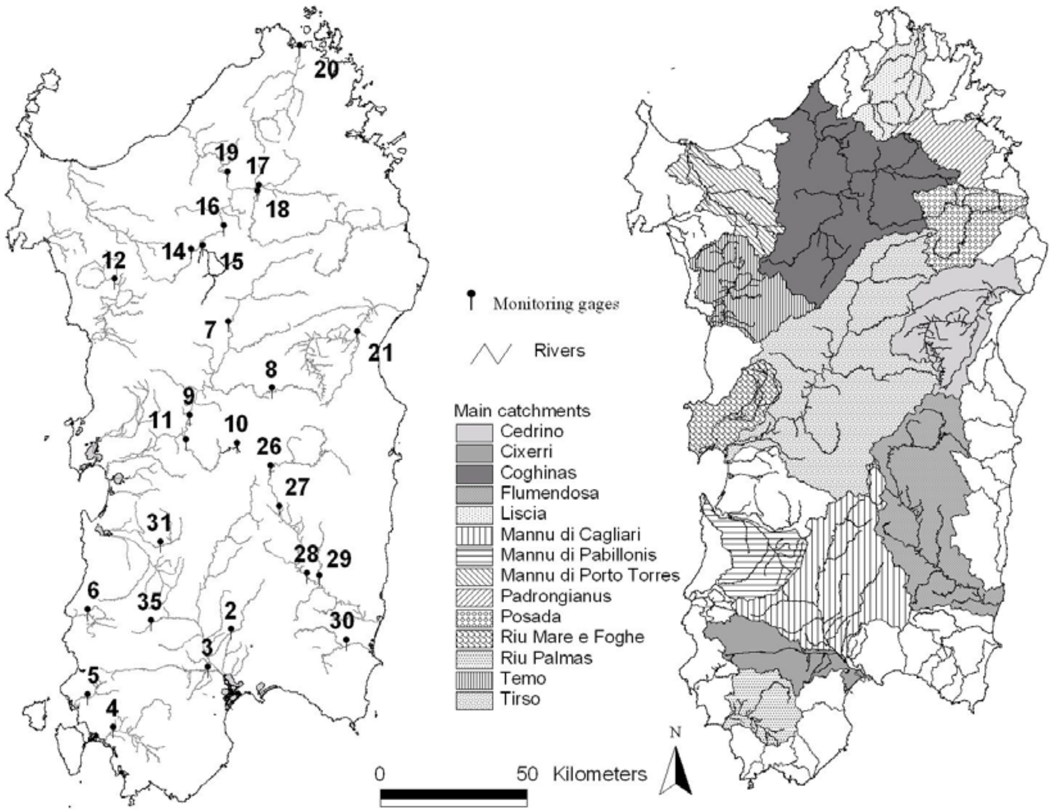

Figure 2. Main rivers, stream flow monitoring gages, and main catchments of the island.

Data Availability and Climate, Soil and Land Cover Characterization

A large effort was needed to collect the available information concerning soils, land cover, land use, and climate of the island. Rather than organizing the information necessary for SWAT on a catchment scale, a regional scale approach was followed. In this context, a geographical information system (GIS) dataset was created and formatted for SWAT. The developed system greatly reduces GIS initializations and offers the possibility to simply rely on a regional framework database without being an expert user of the SWAT model.

For the characterization of the geo-pedologic facies of the region we referred to the soil vector map of Sardinia (Aru et al.,1991) and the land classification for irrigation of Sardinia (Arangino et al., 1986). Forty representative soil profiles were described and classified according to the USDA and FAO guidelines. Classical pedotransfer functions were used to calculate dependent variables (field capacity, permanent wilting point, available water capacity, and saturated hydraulic conductivity) from the three independent variables: sand, silt and clay content (Saxton et al., 1986). Other complementary information was obtained, for the same class of soils, using the State Soil Geographic (STATSGO) Database (1994). Finally all information was placed in a soil database for the entire region formatted for the SWAT model (Cau et al, 2003; Cadeddu and Lecca, 2003).

The influence the land use on the water cycle is a function of the density of plant cover, the morphology of the plant species, etc. The CORINE Land Cover 1:100,000 vector map (www.centrointerregionale.it) was used in this analysis. The CORINE Land Cover consists of a geographical database describing vegetation and land use in 44 classes, grouped into three nomenclature levels. It covers the entire spectrum of Europe and gives information on the status and the changes of the environment. We converted the CORINE land cover classification codes to the SWAT land cover/plant codes (Cadeddu et al., 2003).

The available rainfall and climatic databases are on a monthly time resolution (Cao et al. 1998). For this reason a statistical analysis to describe the climate of the island was carried out using the available, but incomplete, daily records. For each month, average daily maximum air temperature (ºC), average daily minimum air temperature, standard deviation for daily maximum and minimum air temperature (ºC), average daily solar radiation, etc. were assessed and placed in the *userwgn* database. For the rainfall characterization a stochastic time generator was developed on the basis of the rainfall statistical characteristics of Sardinia (Cau et al., 2003). By means of the Markov chain procedure, the time distribution of wet days was determined and then a skewed distribution was used to generate the amount of precipitation occurring in each wet day. Finally, the sum of the daily precipitation of each month of each year was scaled to match the monthly registered rainfall for each station. The Sardinian rain gages were grouped in two different homogeneous classes, referred to in this study as East and West rain gages, using a cluster technique based on the spatial distribution of standard deviation and skew of daily rainfall data. This was essential to produce realistic rainfall events at rain gages which were determined to be climatically correlated. Finally all rainfall series were formatted for the SWAT model (Cau et. al., 2003).

Calibration of the Stream flow component

Thirty one monitoring gages are found scattered along the main rivers of the island. Previous studies were used to compare to the results of this study, show limitations, and plan future work. Water budget calculations were performed, using the SWAT model (Neitsch et al., 2001; Di Luzio et al., 2001), for 15 Sardinian catchments, having different climatic and hydrologic conditions. Twenty seven monitoring gages are found within the basins under investigation.

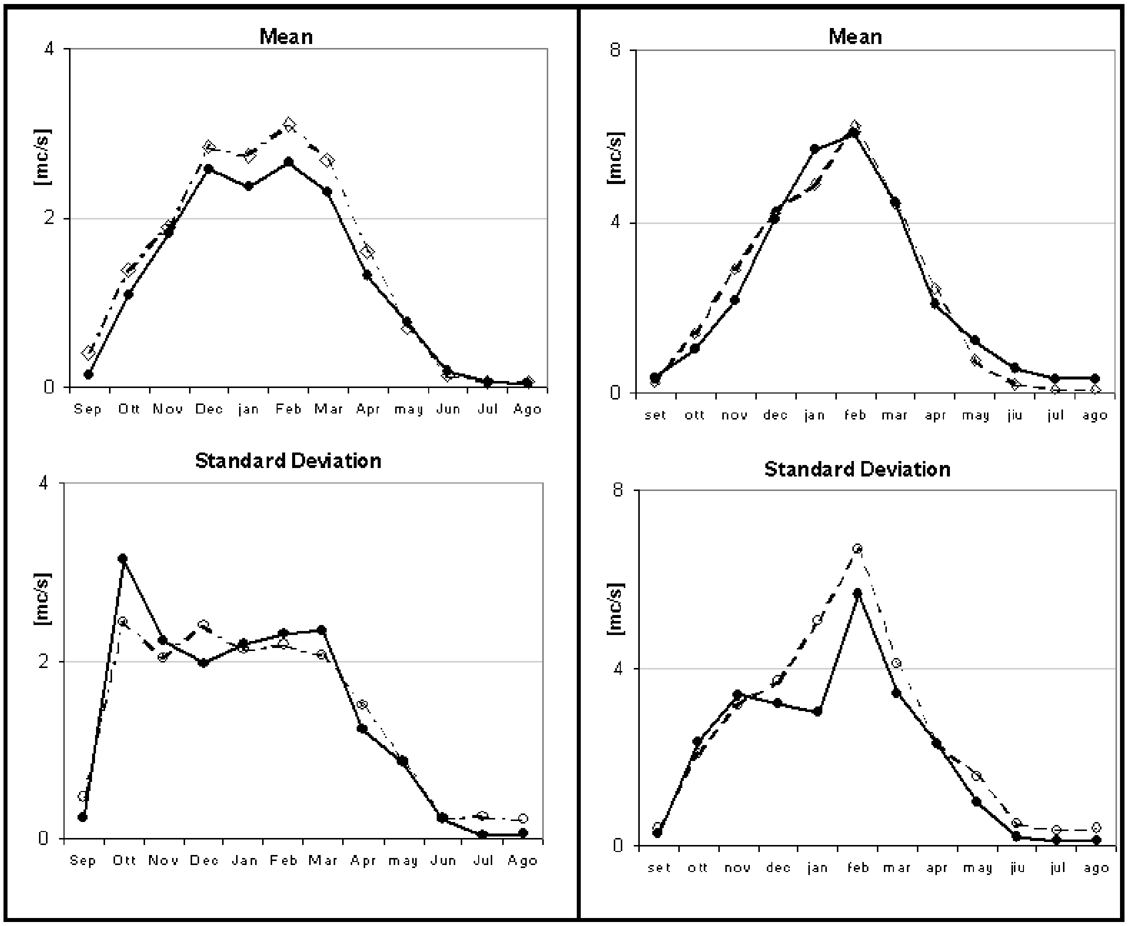

Figure 3. Gage N. 30 (left) and Gage N. 4 (right). Comparison between observed (continuous line) and simulated (dotted line) flow rates after calibration. The mean (above) and the standard deviation (below) are shown on a monthly basis.

Before calibration, it was determined that the stream flow component was always over estimated, while the evapotranspiration was highly under estimated. Calibration of the stream flow component was first completed for average annual conditions. Once the stream flow component was calibrated for these conditions, monthly records were used to fine-tune the calibration (Figure 3). When calibrating a watershed with multiple stream gages, streamflow should be tuned first for the gage furthest upstream. Once this gage is calibrated, the downstream gages can be calibrated. The parameters that were modified in the calibration procedure were ESCO, GW-QMN, GWREVAP and CN2. The case studies were used to test methodologies applied on the regional level, to improve the understanding of the recharge-discharge transformation and to estimate basin-averaged hydrologic values for a 70 year historical period (1922-1992).

Results

Calibration of the stream flow component, performed for the main catchments of the island, was the first step for investigating the effect of all complementary phenomena related to the water cycle. The quantification of performance of the model was therefore essential to evaluate the model outputs and their limits. The performance of the model was assessed through the following ensemble statistical indicators (Equations 1 and 2):

$$K_{Nash-Sutcliffe} = 1 - \left(\frac{\sum_{i=1}^{N} (Q_{1,i} - Q_{2,i})^2}{\sum_{i=1}^{N} (Q_{1,i} - \overline{Q}_1)^2} \right) \text{ (Nash-Sutcliffe index)} \quad (1)$$

$$\overline{Er} = \frac{\sum_{i=1}^{N} \left| \frac{Q_{1,i} - Q_{2,i}}{Q_{1,i}} \right|}{N} \text{ (average error)} \quad (2)$$

Where N represents the years of registered stream flow data, $Q_{1,i}$ is the registered stream flow at time i, $Q_{2,i}$ is the correspondent simulated stream flow. The Nash-Sutcliffe index ranges between $-\infty$ and 1. When $Q_{1,i} = Q_{2,i}$, $K_{Nash-Sutcliffe} = 1$. In our case, the Nash-Sutcliffe index was 0.77, while the estimated average error was 13%, showing a good match between the simulated and the observed stream flow rates.

The model reasonably simulated monthly water flow over a 70-year period and accurately captured the timing and magnitude of seasonal water yields under current land use/land cover conditions. These results were accomplished with little calibration of free parameters. Figure 4 shows the comparison between observed and simulated annual flow rate (1922-1992) based on the contribution of all basins under investigation. Due to less permeable soils, steeper slopes and a different rainfall distribution, the water yields of the east basins are higher than the west basins (Figure 5). The yearly average number of wet days for the west rain gages, in fact, was 80 (70 between September and April and 10 for the period from May-August) with a yearly precipitation value of 687 mm. The yearly average number of wet days for the east rain gages was 74 (64 between September and April and 10 for the period from May-August) with a yearly precipitation value of 828 mm.

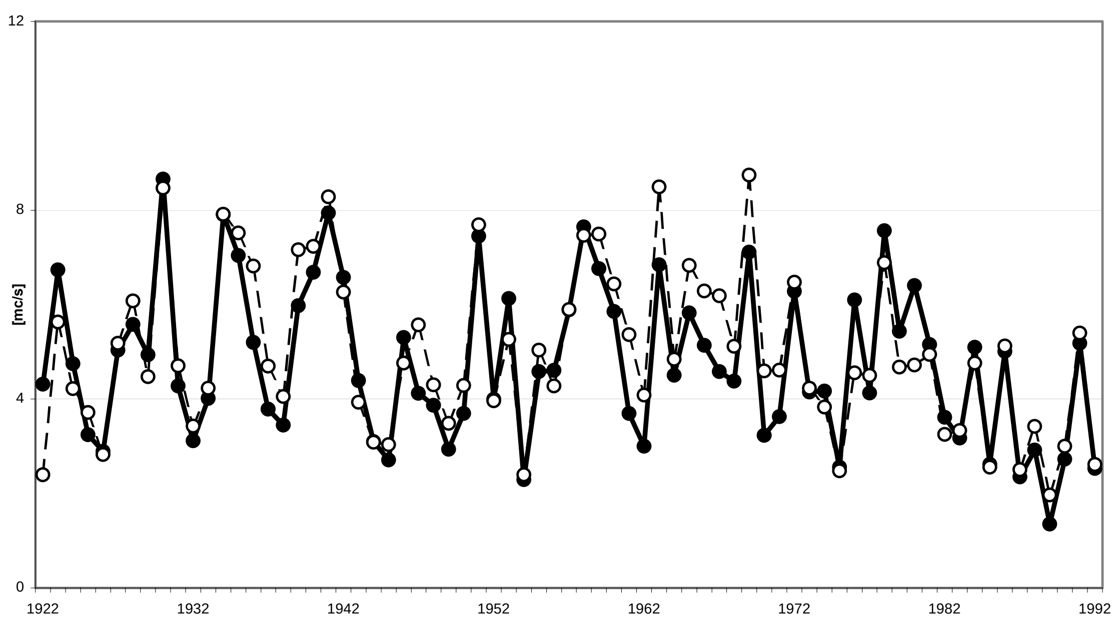

Figure 4. Comparison between observed (continuous line) and simulated (dotted line) annual flow rate (1922-1992).

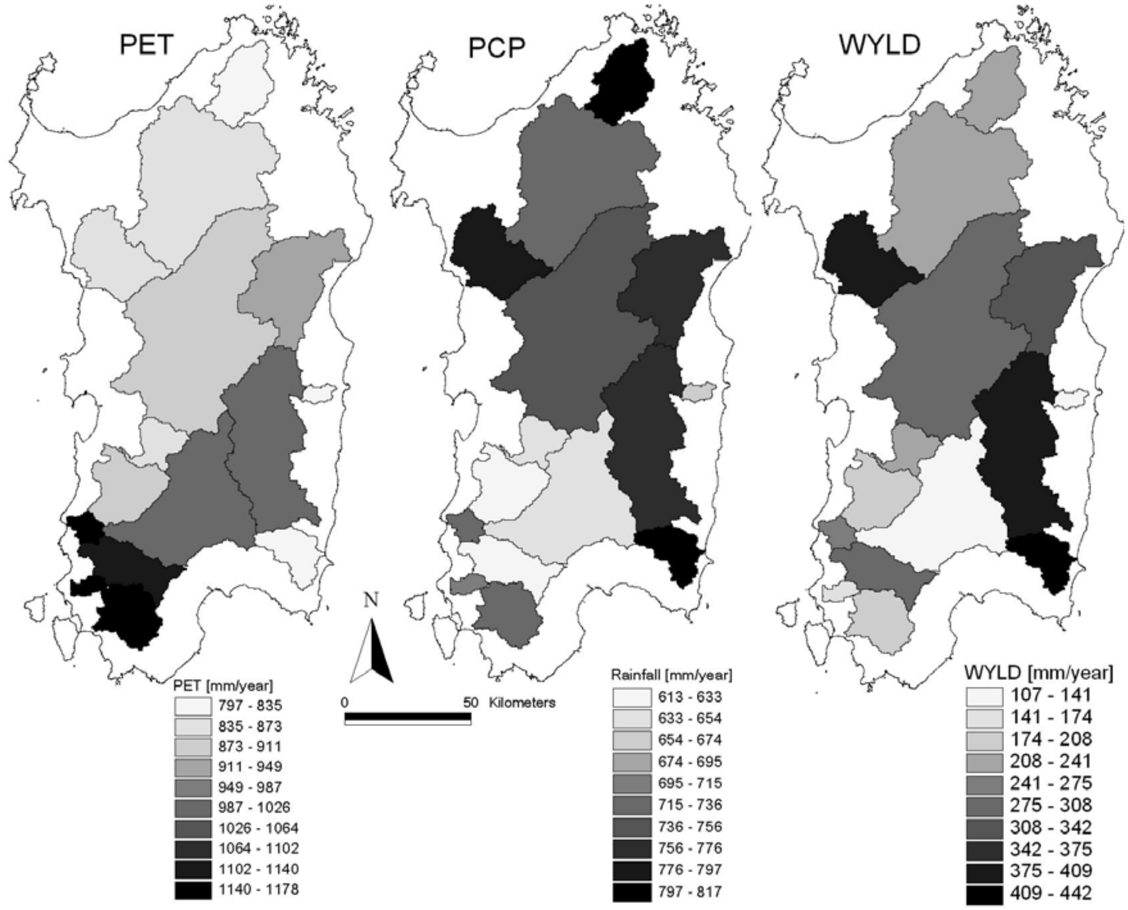

Figure 5. The Multi-catch.avx extension (for more details see "*A user firendly multi-catchments tool for the SWAT model*") has been used to map the spatial distribution of the average precipitation (1922-1992), potential evapotranspiration and water yield on a yearly basis.

Conclusion and Future Developments

Land use changes and irrigation schemes need to be managed so as to minimize the risk of water and soil contamination. Water resource management is a complex task, and the lack of data and information on the system has an important role in policy design. The complexity of the problems found on the island has shown that a multidisciplinary approach must be adopted to have an overview of the problem at hand. The use of hydrological models at a catchments scale, such as SWAT, can be important in reproducing the water cycle and evaluating the impact of land management practices on downstream water bodies. Models help to identify indicators at each scale that reflect critical ecosystem processes or state variables related to the integrity and sustainability of those ecosystems. Moreover models can provide support in identifying the cause-effect relationship, highlighting the causal links between human activities, pressures, and the state of the environment. With the project half complete, SWAT has been used to estimate the water budget for the main watersheds of the island. In this context, a regional scale approach was used to assess the geographical information. This offers the possibility to simply rely on databases concerning soils, land cover, climate and precipitation on a regional scale. Model results have shown that SWAT reasonably simulates monthly water flow and accurately captures the timing and magnitude of seasonal water yields under current land cover, soil and climate conditions. The next step is to investigate those situations where waters are highly contaminated.

Acknowledgement
The study has been partially funded by the Sardinian Regional Authorities.

References

Arangino, F., A. Aru, P. Baldaccini, & S. Vacca. *I suoli delle aree irrigabili della Sardegna* (Piano Generale delle Acque, Regione Autonoma della Sardegna), Cagliari, 1986.

Aru, A., Baldaccini, P. Vacca, A. *Nota illustrativa alla carta dei suoli della Sardegna, con carta illustrata 1:250.000*. Regione Autonoma della Sardegna, 1991.

Box, G.E.P. & G.M. Jenkins, Time series Analysis: Forecasting and Control, Holden-Day, 1976.

Cadeddu A., P. Cau, C. Gallo, G. Lecca, M. Marrocu, and M. Sulis. Implementazione di una procedura per la stima delle componenti del bilancio idrologico a scala di bacino per la Regione Sardegna. Technical Report 03/82. CRS4, Italy, Aprile 2003. Progetto MURST nr. 30 Cluster 11, workpackage 4).

Cadeddu A. & G. Lecca Sistema Informativo dei Suoli della Sardegna da interfacciare al modello idrologico SWAT. Report interno del CRS4 - Centro di Ricerca Sviluppo e Studi Superiori in Sardegna (2003)

Cau P., Cadeddu A., Gallo C., Lecca G. & M. Marrocu. Estimating available water resources of the Sardinian island using the SWAT model. Proceedings of the Second International SWAT conference, Bari, Italy, pag. 64 - 70, Luglio 2003.

Di Luzio M., M. Srinivasan & J. Arnold. *ARCVIEW interface for SWAT2000 – User's Guide*, USDA Agricultural Research Service, Temple, Texas, 2001.

Cao Pinna, C., A. Petruso, R. Silvano, A. Fadda, F. Buffa, N. Orrù (eds.), *Studio dell'Idrologia Superficiale della Sardegna (SISS)*, Ente Autonomo del Flumendosa (EAF), Cagliari, Italy, 1998.

Giupponi, C., Mysiak, J., Fassio, A., and Cogan, V., MULINO: *Multi-sectoral, Integrated and Operational Decision Support System for Sustainable Use of Water Resources at the Catchment Scale*. In F. Ghassemi et al. (Eds) (Ed). Proceedings of MODSIM 2001 - International Congress on Modelling and Simulation. MSSA-NZ, 1183-1188, 2001.

Neitsch, S. L., J. G. Arnold, J. R. Kiniry & J. R. Williams. *Soil and Water Assessment Tool (SWAT) – Theoretical Documentation* (version 2000), USDA Agricultural Research Service, Temple, Texas, 2001.

Nicks, A.D. *Stochastic generation of the occurrence, pattern and location of maximum amount of daily rainfall*. p. 154-171. In Proc. Symp. Statistical Hydrology, Tucson, AZ. Aug.-Sept. 1971. USDA Misc. Publ. 1275. U.S. Gov. Print. Office, Washington, DC, 1974.

Saxton K.E., W.J. Rawls, J.S. Romberger, and R.I. Papendick. *Estimating generalized soil-water characteristics from texture*. Soil Science Society of America Journal 50(4) , 1986, pag. 1031-1036.

USDA & NRCS Soil Survey Division. State Soil Geographic (STATSG0) Data Base - Data use information. Miscellaneous Publication Number 1492, 1994.

Use of Hydrological Models at the Catchment Scale to Predict the Effect of Different Land Management Practices and Point Source Pollution

I. Contu*[1], A. Carucci[1], and P. Cau[2]
[1]University of Cagliari, Department of Geoengineering and Enviromental Technologies; address: Digita, Piazza d'Armi - 09123 Cagliari. Email: irene@crs4.it
[2]Center for Advanced Studies, Research and Development in Sardinia (CRS4); address: Parco Scientifico e Tecnologico, Polaris, Edificio 1, 09010 PULA (CA - Italy). Email: plcau@crs4.it

Abstract

Creating action plans to reduce water pollution is a strategic task for European Countries, mostly in Mediterranean areas, where water demand is steadily increasing and water resources are limited. Contamination levels in water bodies, both ground and surface waters, are found to be increasing and local and regional authorities are now facing this awkward environmental problem. Most of the nutrients that enter the water are from the agro-zootechnical and the industrial sectors. Consideration of the physical processes associated with water movement, crop growth, and nutrient cycling can be essential to evaluate the gradual build up of pollutants due to alternative land management practices on downstream water bodies (e.g. rivers and coastal lagoons). In this framework, models can give support to identify, among alternative choices, those that will not lower the integrity and sustainability of the ecosystems.

In this study, the SWAT model was used to estimate the effects of point and diffuse source pollution on the 520 km^2 Santa Sperate Basin (southwestern part of Sardinia, Italy). High levels of P, NH_4, and COD, etc. were found at the two monitoring gages located on the Flumini Mannu of the South Sperate River (the main river of the plain) within the basin. This contamination was assumed to be due to the civil and industrial sectors, as well as to the agro-zootechnical sector in the basin. The objective of this work was to apply the physically based hydrological model, SWAT 2000, to the basin to predict the impact of alternative land management practices and point source pollution on water bodies. To this end a statistical analysis of the climatic data has been carried out and daily rainfall data was downscaled from monthly pluviometric records in order to generate daily weather inputs for the SWAT model. The resulting model input data along with the watershed and HRU (hydrologic response unit) spatial discretization criteria were carefully checked to ensure global consistency at the overall scale. The calibration and validation of the model was performed against monthly measured stream flows for the period 1922–1992.

The performance of the model was then compared with the results of the black box “export coefficient” model. This comparison was used to improve identifying methods, tools, and indicators at each scale that reflect critical ecosystem processes or state variables related to the integrity and sustainability of those ecosystems.

Introduction

The use of hydrological models can be important in supporting decision making in a complex region, threatened by point and nonpoint source pollution. Models help with investigations on the causal links between human activities, pressures, and the state of the environment, highlighting cause and effect relationships. After more than 30 years of `classical' model development, the use of a new generation of hydrological models, that make use of distributed information about a catchment's characteristics, is steadily increasing. Although the "physically based" approach might be useful in terms of process knowledge, it has limitations when applied in an operational context. One, in fact, is faced with the task of accurately representing the inherent complexity of real systems, because the predictive and descriptive potential of distributed models is limited especially to data availability and their quality. Conversely, simple catchment models that lump a catchment's heterogeneities and represent the transformation input/output, conceptually or empirically, are generally easy-to-use tools with lower data requirements. In spite of the crude approximation resulting from their lumped nature and simple structure, simple models can still be efficient. In many case studies reported in the literature, simple models are undoubtedly useful for engineers and water managers.

In this work, the impact of civil, industrial and agro-zootechnical pollution sources has been assessed with the export coefficient (simple) model and the SWAT (semi-distributed) model (Neitsch et al., 2001). The basin under investigation is the Santa Sperate Basin located in the southwest part of Sardinia.

The export coefficient model describes the environmental system using empirical connections between input and output data, with no concern for the physical processes. The SWAT model, instead, is a semi-distributed model that describes the environmental core system structure in all its parts, and permits evaluation of the water cycle, and other related phenomena, at the catchment and sub-catchment scale. This discussion underlines the limits and potentials of both models.

Methodology

Description of the Study Site

The study site is the 520 km^2 Flumini Mannu of the Santa Sperate Basin (Sardinia, Italy), which is part of the larger Flumini Mannu of the Cagliari Basin. High levels of contamination, due to the civil, industrial, and agro-zootechnical sectors were found at the two monitoring gages (PMP 20801 and PMP 20802) located on the river within the basin. The Italian water directives (Dlgs 152/99) group waters into five classes, where the first class is for uncontaminated waters and the fifth is for the highly contaminated ones. The water quality of the river assessed through a yearly monitoring campaign at the 20802 and the 20801 gages belongs to the third and fifth classes, respectively.

The Flumini Mannu of the Santa Sperate Basin is located in the south part of Sardinia and is delimited by the Sarcidano Plateau to the north, the Sarrabus relief to the east, and the last layer of Iglesiente Massif to the west. The watershed is characterized by a significant variation in terms of altitude (from 13 to 972 m a.s.l.). The main river is a tributary of the Flumini Mannu of the Cagliari River which discharges its waters into the Santa Gilla humid area near the Gulf of Cagliari (Figure 1). Santa Gilla is a very important humid area in Sardinia and is among the largest wetlands in Europe. The Santa Sperate River is characteristically fast flowing, with a relatively high water volume in winter, reduced to a trickle in summer. The monthly water volume is characterized by a peak in February (4 mc/s) and a minimum in August (0.16 mc/s) (values registered in the 02 stream flow monitoring gage).

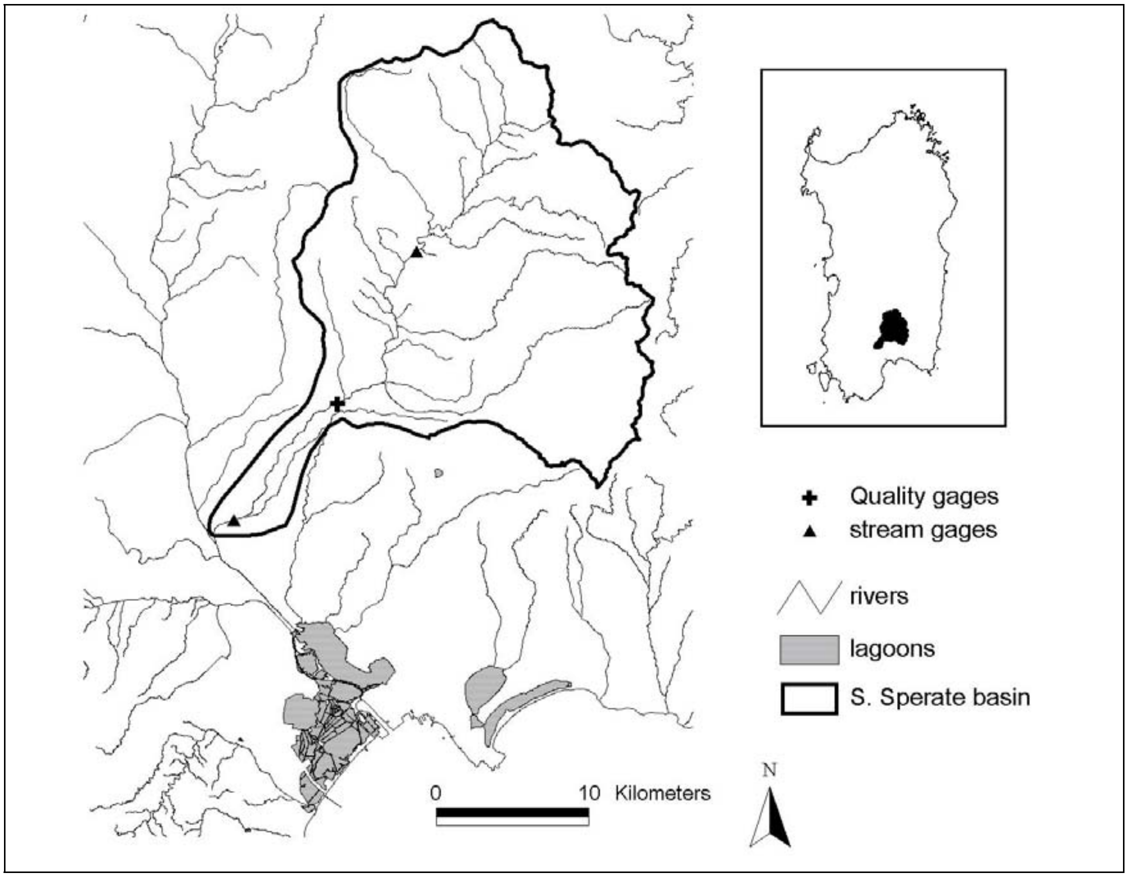

Figure 1. Location of the study site, the 20801 and 20802 water quality monitoring gages, and the 02 stream gage.

The climate of the area is Mediterranean with long hot dry breezy summers and short mild rainy winters. The temperature regime was recorded by the Donori S. Michele climatic gage, located close to the basin. Average monthly temperature ranges from 8°C (January and February) to 25°C (July and August). Precipitation is largely confined to the winter months; the rainfall regime is characterized by a peak rainfall in December (83 mm) and a minimum in July (8 mm), with an average value of 591 mm/year. Land is primarily used for agricultural purposes. Large areas are used for crop cultivation, predominantly cereal (9,091 ha). The south is mainly characterized by vineyards (1,709 ha), olive groves (2,383 ha) and orchards 1,709 ha). The eastern portions of the basin are predominantly forest and pastures, although the zootechnical sector on this part of the island is limited (about 75,000 ovine and 4,500 bovines). The S. Sperate is sparsely populated, with a density of about 68 p/km2. This is in accordance with the regional average, and slightly higher than a third of the Italian national average.

Decisional Contest

The theoretical infrastructure chosen to conceptualize the environmental problem is based on the DPSIR approach (Driving forces, Pressure, State, Impact and Responses), and consists of the identification of all possible DPS chains that describe the system. The decision problem is therefore described and the cause and effect relationship between the relevant socio-economic and environmental indicators, at each scale, accessed. This task is particularly relevant in the management of multisectoral conflicts of water resources, where the lack of multisectoral perspective can result in socio-economic damages to the different local users.

The model, in this phase, was used to evaluate human impacts to the environment and the actions needed to reduce those impacts.

Each change generates new impacts to the human health and economy, which require responses by society. A response can have an effect on the entire system, e.g. on driving forces through structural actions, pressure through technological actions, state through land reclamation works, impacts through damage economic compensation, etc..

Alternative strategies, that were evaluated, include:

I) routing waste water produced by the civil/industrial sector, currently collected at small treatment plants scattered within the basin, to a larger water treatment plant. By doing so, the dispersion of point pollution will be reduced (in general larger treatment plants work better);
II) reducing areas used in extensive and intensive agriculture;
III) planning protection zones close to the river and the main tributaries;
IV) identifying alternative land management practices that are eco-compatible with the environment.

Description of the Export Coefficient Model

The export coefficient model works in three phases:

- Phase 1. Agro-zootechnical and industrial potential loads (*PL*) are calculated from loading factors;
- Phase 2. Agro-zootechnical and industrial effective loads (*EL*) that enter the reach are calculated with the use of the export coefficients;
- Phase 3. The impact of the effective loads (*TL*) to the river is calculated from the *EL* that enters water, taking into account the reduction of the pollutants due to self-purification, algal growth (part of the nutrients are used by algae to grow), etc., through the use of reduction coefficients.

In the first phase the pollution loads (PL) impacting the land are calculated with the use of loading factors (IRSA-CNR, 1991). The loading factors allow modelers to obtain the loads with respect to all pollutants of interest. The potential load of a generic chemical impacting the land from agriculture (*CH*) is calculated with the following formula (Equation 1):

$$PL._{CH} = SAU \cdot LF_{CH} \left[{kg}/{year} \right] \qquad (1)$$

where *SAU* is the exploited land extension and *LFCH* is the loading factor for the chemical *CH*. The loading factor depends on the plant or animal species, etc., and varies for each pollutant. In this phase, the origins of pollution and the potential dangers are identified. No consideration is given to structural actions or geological, morphologic or climatic contexts that reduce the impact of the potential pollution.

The effective load (*EL*), or portion entering the stream, is then calculated from the potential load, considering all the reduction factors connected with the land phase where the pollution originates (Equation 2).

$$EL._{CH} = PL_{CH} \cdot (EC \cdot a \cdot b \cdot c)_{CH} \left[{kg}/{year} \right] \qquad (2)$$

where *EC* is the export coefficient, and *a*, *b* and *c* are reduction factors depending on soil permeability, basin topography, and rainfall regime.

The contaminant load in the river is calculated as (Equation 3):

$$TL_{CH} = EL_{CH} \cdot RC_{CH} \left[{kg}/{year} \right] \qquad (3)$$

where *TL* is the contaminant load in the river. This is calculated reducing *EL* with reduction coefficients (RC), which take into consideration all of the reduction phenomena occurring to the different pollutants in the reach (routing phase).

The export coefficient model is not a distributed model; therefore, it is not possible to locate in space and time the pollution sources. Output data are available only according to limited outlets (for the Santa Sperate Basin the PMP monitoring gages are the only possible outlets and the impacts are assessed on an annual basis). The model needs to be calibrated in order to make reliable predictions. Although the model appears to be very simple, it is important to highlight that the calibration is performed with optimization procedures which are easy to implement. The model requires geographical data at the catchment scale (e.g. total number of animals and inhabitants within the basin, the agricultural land, cultivation types, etc.). In Figure 2 the flow chart of the model is shown.

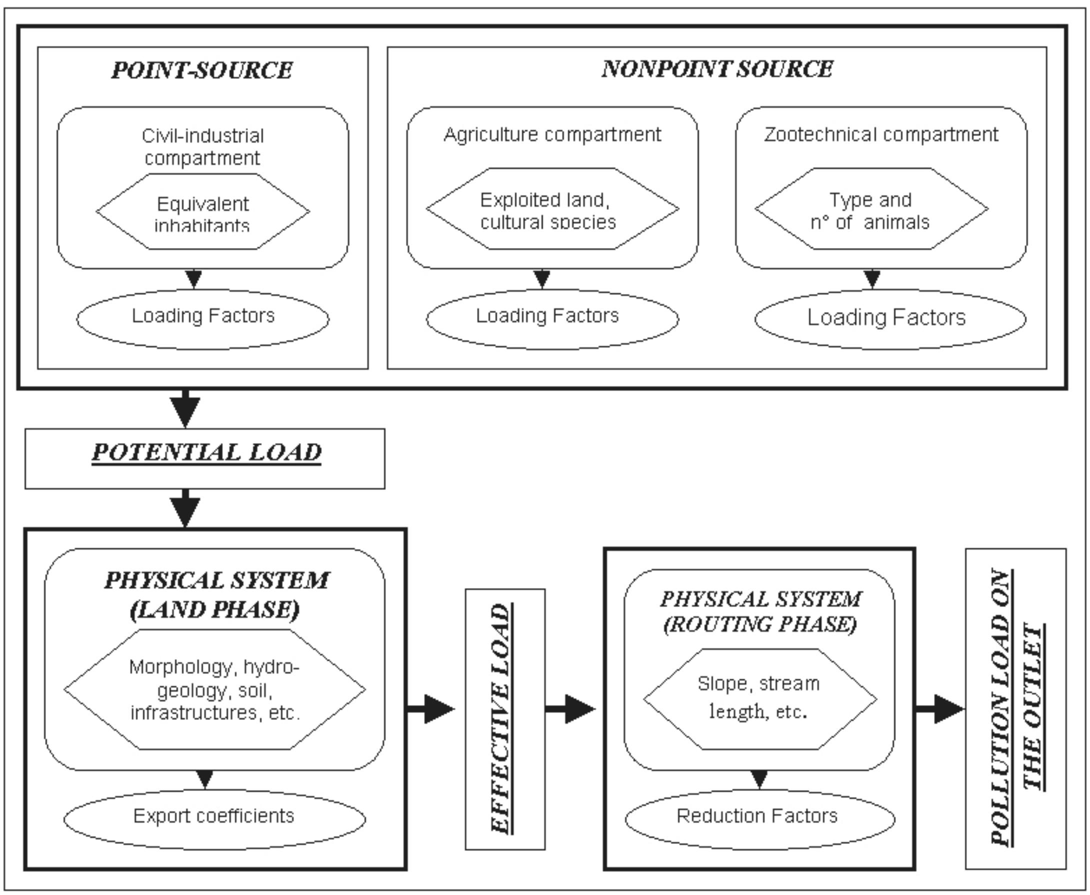

Figure 2. The export coefficient model works in three phases. Potential loads (CP) are calculated by means of loading factors. The effective loads are calculated by multiplying (CP) for the export coefficient, which represents the purification capacity of the territory (soil, infrastructures and rivers) of the pollution load.

Model Calibration

An extensive quality assessment of the available climatic, soil and land use data was carried out for the study area. For this, a geographical information system (GIS) was set up. The SWAT model requires daily precipitation records, but the available climatic data in

Sardinia are accessible on a monthly or yearly basis (Cao et al., 1998). In this study, the synthetic daily precipitation series (Cau et al., 2003) was downscaled from the monthly series using a Markov chain-skewed generator (Nicks, 1974). These series have the same monthly cumulative values as the measured ones. The export coefficient model, instead, requires average annual rainfall values.

The hydrological behavior of soil is related to a number of physical soil properties (USDA-NRCS Soil Survey Division, 1994). To obtain information about the soil properties of the S. Sperate Basin, a 1:250,000 soil vector map (Arangino et al., 1986) (Aru et al., 1991) was used, where each cartographic unit was associated with one or two delineations corresponding to subgroups of USDA soil taxonomy (Cadeddu et al., 2003). Land cover significantly affects the water cycle. In this study, the CORINE Land Cover 1:100,000 vector map (Commissione Europea, Ministero dell'Ambiente, 1996) was used. It consists of a geographical database describing vegetation and land use in 44 classes, grouped into three nomenclature levels. CORINE covers the entire spectrum of Europe and gives information on the status and the changes of the environment (Cumer, 1999).

Calibration of the export coefficient model was performed through an optimization procedure. Optimization was performed by varying the export coefficients (land phase calibration) and the reduction factors (stream calibration) in accordance with a fixed range.

The SWAT model was first roughly calibrated on a yearly basis for stream flow and then tuned on a monthly basis. Calibration was performed with a trial and error approach, taking into consideration potential/real evapotranspiration and the stream flow component (slow and fast). The no calibration simulation showed that real evapotranspiration was under-estimated with regard to literature values for the area, and the stream flow component was over-estimated.

The real evapotranspiration was controlled at the HRU scale level with the ESCO and CAN_MAX parameters. Runoff and base flow was controlled varying GW_REVAP and GW_QMIN. A correlation factor of about 0.83 was found between monthly simulated and measured stream flows, showing a good accuracy in reproducing the hydrologic regime.

Results

The nutrient cycle was assessed by taking into consideration point and nonpoint source pollution (Figure 5). In this paper only NO_3 will be shown. The model has been run with the following hypotheses:

- land use and water management are constant during the seventy year simulation
- the thermo-pluviometric regime is stationary.

With these hypotheses the impact of point and nonpoint source pollution was assessed with the thermo-pluviometric synthetic regime (Cau et al., 2003) for the time period 1922-1992, while measurements were for the time period 2002-2004.

The SWAT and export coefficient model results were compared, considering the simulated mean of NO_3 concentration for the SWAT model and the simulated mean load for the export coefficient model on a yearly basis. Results on a yearly basis are shown in Table 1 and 2. Mean NO_3 concentrations ($\overline{C_{mis}}$) were available for the 20801 and 20802 PMP monitoring gages.

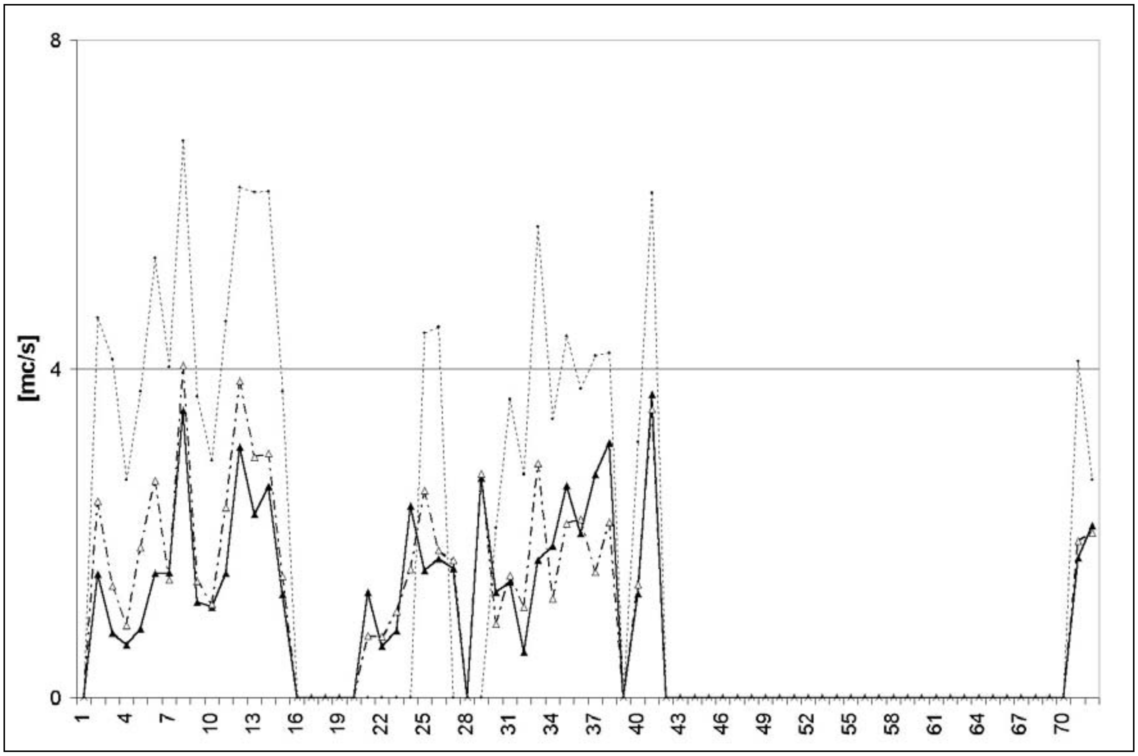

Figure 3. Non-calibrated (dotted line), calibrated (dashed line), and observed (continuous line) stream flow component on a yearly basis.

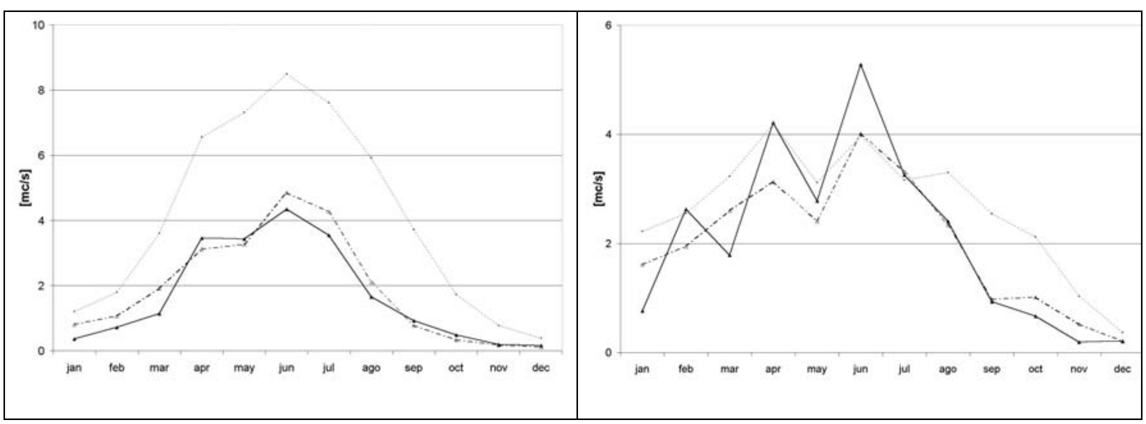

Figure 4. Comparison between average (left) and standard deviation (right) values for the measured (continuous line) and simulated stream flow before (dotted line) and after calibration (dashed line) on a monthly basis.

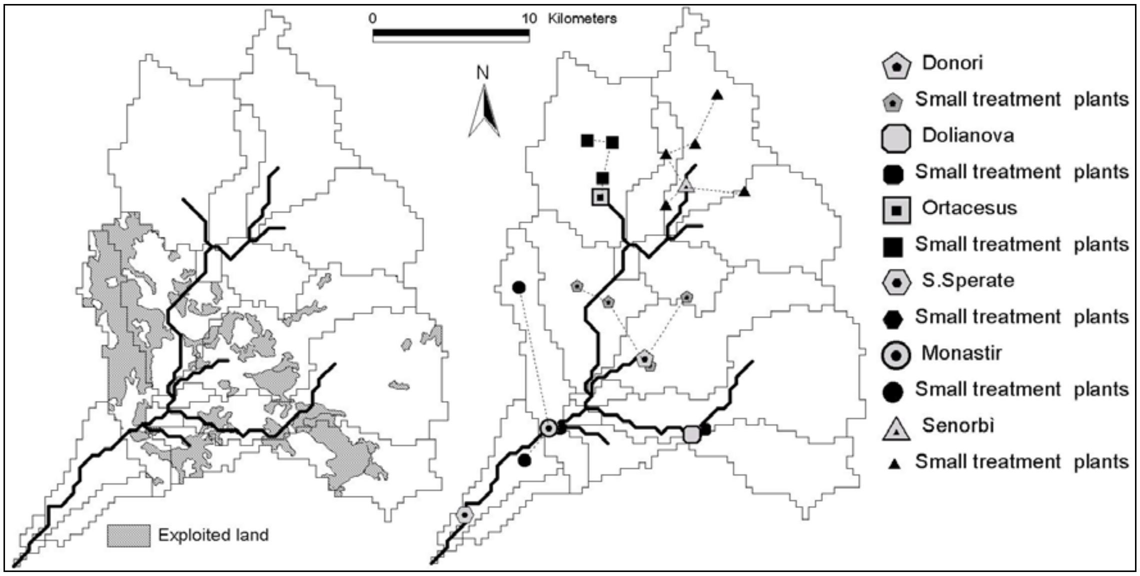

Figure 5. Nonpoint (left) and point (right) source pollution. The exploited land used for corn cultivation is about 86 km^2. In the Santa Sperate SWAT project, the major point sources (Donori, Dolianova, Ortacesus, S. Sperate, Monastir, Senorbì) were activated. Also included are the small water treatment plants (small points) within the basin.

Table 1. Export coefficient model results For measured and simulated mean NO_3 loads calculated on a yearly basis.

PMP	$Load_{sim}$ [t/year]	$\overline{C_{mis}} \cdot (\overline{Q} - STD(Q))$ [t/year]	$\overline{C_{mis}} \cdot \overline{Q}$ [t/year]	$\overline{C_{mis}} \cdot (\overline{Q} + STD(Q))$ [t/year]
20801	122.87	22.82	78.71	134.59
20802	42.65	10.44	28.51	46.58

$Load_{sim}$ is the simulated NO_3 load; $\overline{C_{mis}}$ is the measured mean concentration; $\overline{Q}$ is the mean stream flow simulated by SWAT for the 20801 and 20802 monitoring gages.

Table 2. SWAT results for measured and simulated NO_3 concentrations calculated on a yearly basis.

ID	$\overline{C_{mis}}$ [mg/l]	$\overline{C_{sim}} - STD(C_{sim})$ [mg/l]	$\overline{C_{sim}}$ [mg/l]	$\overline{C_{sim}} + STD(C_{sim})$ [mg/l]
20801	1.25	0.32	0.98	1.63
20802	0.97	0.75	1.22	1.97

$\overline{C_{mis}}$ is the measured mean concentration; $\overline{C_{sim}}$ is the simulated mean concentration; and 20801 and 20802 are the ID of the two monitoring gages in the basin.

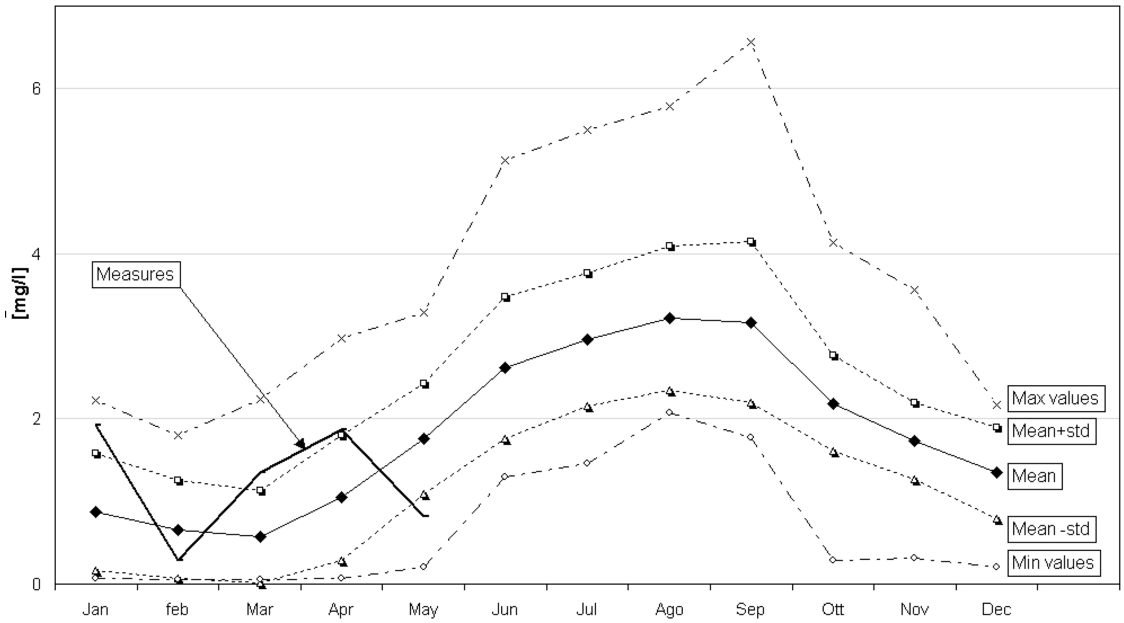

Figure 6. Comparison between the simulated and measured NO_3 concentrations for the 20801 gage.

The SWAT model allows for an analysis of results on a monthly basis (Figure 6) for all the sub-basins within the Santa Sperate Basin. This can help identify indicators at each scale (temporal and spatial) that reflect critical ecosystem processes or state variables related to the integrity and sustainability of those ecosystems.

The measured concentration is not always included between the average simulated NO_3 concentrations ($\pm STD(C_{sim})$) on a monthly basis. It does, however, fall within the monthly maximum and minimum simulated values interval (the only exception is in May for the 20802 gage, not shown). Simulations show that the most critical period for the water system is during the summer, when point source pollution is predominant.

Conclusions

Models can give support to identify the cause and effect relationships and the causal links between human activities, pressures, and the state of the environment. In this context, the export coefficient and SWAT models can be used to evaluate human impacts on the environment and actions to reduce those impacts.

Although the export coefficient model lumps a catchment's heterogeneities and represents the transformation input/output empirically, it is generally easy-to-use and has low data requirements. In spite of the crude approximation resulting from its lumped nature and simple structure, it can still be efficient and useful for engineers and water managers.

This study confirmed that the SWAT model could accurately simulate runoff and nutrient losses. The SWAT model can be efficiently employed to identify the critical sub-watersheds that are major contributors to nutrient losses and prioritize these in order to develop a multi-year management plan. This can be essential in reducing the nutrient impact from point and nonpoint source pollution to downstream water bodies. Future work will be done to plan and analyze the remediation actions to restore the integrity of the system.

Acknowledgement

The study was partially funded by the Sardinian Regional Authorities.

References

Arangino, F., A. Aru, P. Baldaccini, and S. Vacca. I suoli delle aree irrigabili della Sardegna (Piano Generale delle Acque, Regione Autonoma della Sardegna), Cagliari, 1986.

Aru, A., P. Baldaccini, A. Vacca. Nota illustrativa alla carta dei suoli della Sardegna, con carta illustrata 1:250.000. Regione Autonoma della Sardegna, 1991.

Cadeddu A., P. Cau, C. Gallo, G. Lecca, M. Marrocu, and M. Sulis. Implementazione di una procedura per la stima delle componenti del bilancio idrologico a scala di bacino per la Regione Sardegna. Technical Report 03/82. CRS4, Italy, Aprile 2003. Progetto MURST nr. 30 Cluster 11, workpackage 4).

Cadeddu, A. and G. Lecca. Sistema Informativo dei Suoli della Sardegna da interfacciare al modello idrologico SWAT. Report interno del CRS4 - Centro di Ricerca Sviluppo e Studi Superiori in Sardegna (2003)

Cao Silvano, R., A. Fadda, F. Buffa, and N. Orrù. Nuovo studio dell'idrologia superficiale della Sardegna. Regione Autonoma della Sardegna, Assessorato della Programmazione, Bilancio ed Assetto del Territorio - Centro Regionale di Programmazione - Ente Autonomo del Flumendosa (1998).

Cau P., A. Cadeddu, C. Gallo, G. Lecca, and M. Marrocu. Estimating available water resources of the Sardinian island using the SWAT model. Atti della conferenza Second International SWAT conference, Bari, Italy, pag. 64 - 70, Luglio 2003.

Commissione Europea, Ministero dell'Ambiente, Regioni coordinate dal Centro Interregionale. CORINE – Land Cover. Carta della Copertura del Suolo Scala 1:100.000. Shape file della Sardegna. Liberamente disponibile su http://www.centrointerregionale.it/download/corine/ (1996).

Cumer, A. Le evoluzioni del Land Cover CORINE in Italia. MondoGIS, numero 16, 1999.

IRSA-CNR. (1991). Valutazione dei carichi inquinanti potenziali per i principali bacini idrografici italiani: Adige, Arno, Po e Tevere. Quaderno N. 90.

Neitsch, S.L., J.G. Arnold, J.R. Kiniry, J.R. Williams. Soil and Water Assessment Tool. Theoretical documentation. Version 2000. Blackland research center - Texas agricultural experiment station. Grassland, soil and water research laboratory - USDA agricultural research service (2001).

Neitsch, S.L., J.G. Arnold, J.R. Kiniry, J.R. Williams. Soil and Water Assessment Tool. User's manual. Version 2000. Blackland research center - Texas agricultural experiment station. Grassland, soil and water research laboratory - USDA agricultural research service (2001).

Nicks, A.D. Stochastic generation of the occurrence, pattern and location of maximum amount of daily rainfall. p. 154-171. In Proc. Symp. Statistical Hydrology, Tucson, AZ. Aug.-Sept. 1971. USDA Misc. Publ. 1275. U.S. Gov. Print. Office, Washington, DC, 1974.

USDA & NRCS Soil Survey Division. State Soil Geographic (STATSG0) Data Base - Data use information. Miscellaneous Publication Number 1492, 1994.

Scale Issues, Hydrological Pathways, and Nitrogen Runoff from Agriculture – Results from the Mellupite Catchment, Latvia

Johannes Deelstra*[1], Kaspars Abramenko[2], Nils Vagstad[3], and Viesturs Jansons[2]
[1] Jordforsk, Centre for Soil and Environmental Research, 1432 Aas, Norway,
e-mail: johannes.deelstra@jordforsk.no
[2]Latvia University of Agriculture, Department of Env. Engineering
[3] NIVA, Norwegian Institute for Water Research. N-0411 Oslo, Norway,

Abstract

A comparison of measured N loads in small agricultural catchments in the Nordic and Baltic regions has revealed large differences which could not be explained only by differences in agricultural practices. This paper presents the results of measurements of nitrogen runoff in relation to the hydrological processes in a Latvian catchment. Measurements were carried out at three spatial scales: plot, drainage field, and catchment. The nitrogen concentrations and loads decreased with an increase in scale, which could be a result of hydrological pathways. Comparison of runoff showed a delayed response in runoff at increasing scale while recession curve analysis revealed an increase in residence coefficient, indicating the possible presence of different flow paths involved in nitrogen runoff generation. This paper highlights the importance of understanding the hydrological flow processes across spatial scales in catchments and the possible effects this can have on nitrogen transport and loads into surface waters. The results suggest that the hydrological processes and scale issues need to be carefully considered when *(i)* designing monitoring strategies in the implementation of the Water Framework Directive (WFD), and *(ii)* defining measures to control diffuse N losses.

Introduction

Description of the catchment

The results presented are from a small agricultural catchment in Latvia. The Mellupite catchment (Figure 1) is located in western Latvia, approximately 160 km southeast from Riga, located in the Venta river basin, part of the Latvian plateau of Permian limestone deposits, covered with a 10-20 m thick quaternary sediment layer. The soils are classified as Luvisols according to the FAO soil classification system with silt loam as the main soil type. The texture varies between the different horizons from loam to sandy/silt clay loam with higher silt contents in the upper horizons. The moraine is rich in carbonate with calcium carbonate normally present in the uppermost 1.5 m., which also has an effect on the pH (6.7-6.8 in the topsoil). The organic matter content in the topsoil ranges from 1.0-1.2%, while the C/N - ratio varies from 11-13. Discharge measurements at Mellupite were initiated during 1995-1996 and are carried out at three levels: main catchment, drainage field and small plots. At the main catchment, a Crump weir was used for discharge measurements, while a V-notch and tipping buckets were used at the drainage field and small plots, respectively. At all levels, water samples were collected on a volume proportional basis. Discharges were recorded using a data logger in combination with a pressure transducer or counter at catchment/drainage and plot scale, respectively.

The land use in the Mellupite catchment is characterised by moderately intensive farming representing the average situation in Latvia. Arable land constitutes 60-70% of the main catchment. The major part of the agricultural land in the catchment is drained with artificial drains with a spacing of L = 22–24 m and a depth of approximately 1 m below the soil surface. Some open drains are used in the upper reaches of the catchment. The Mellupite catchment area is 9.64 km^2. The total area of the tile drained field is 12 ha. The dimensions of the drainage system in the field are similar to the catchment. A total of 16 experimental plots have been established, each having an area of 0.12 ha, and are equipped with a subsurface drainage systems with drain spacing of L = 12 m and a depth of d = 1.4 m below the soil surface.

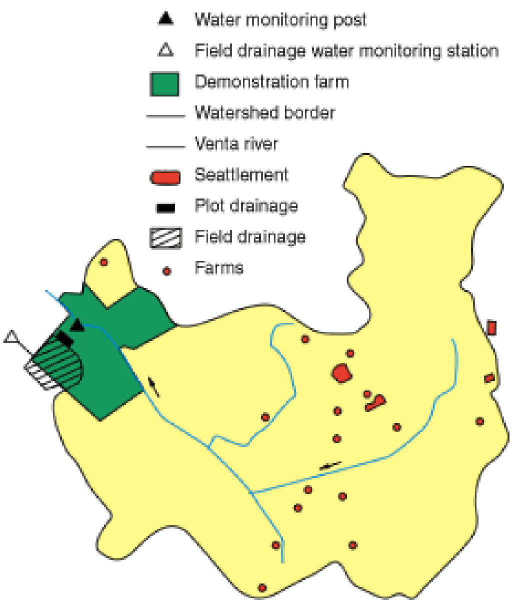

Figure 1. The Mellupite Catchment.

Cropping patterns at the catchment scale

Land use in the catchment is comprised of agricultural land (658 ha, 68%) and forests (306 ha, 32%). The total arable land shows yearly variations of 230-330 ha for grains, 80-130 ha for leys, ± 10 ha for potatoes and ± 5 ha for beets (sugar/fodder), making a total area of ± 350-460 ha (Table 1). Agricultural land includes pastures and other agricultural land as well. The most important grain crops in the catchment are winter wheat and barley.

Table 1. Land use in the Mellupite Catchment.

Crop	Area (ha)				
	1998	2000	2001	2002	2003
Winter wheat	182	138	126	167	162
Barley	86	125	81	148	138
Summer wheat	10		13	3	1
Oat	41	8	10	12	19
Sum grains	319	271	230	331	320
Potatoes	9	7	7	6	12
Fodder beets	5	5	3	3	3
Ley	132	118	120	112	83
Sum of arable land	464	401	358	452	417

The average yield for grain crops varied from 1.5-3.9 t ha^{-1} (Table 2). The variation in yield can be due to a variety of reasons but the main reason is often based on weather conditions, especially during the growing season. For example, during the growing season of 2002, the low yield for grain crops was most likely due to the low rainfall during the early stages of the growing season.

Table 2. Average yield for grain crops (t ha^{-1}).

Crop	1998	2000	2001	2002	2003
Winter wheat	3.6	3.7	2.7	3.6	3.5
Barley	3.0	2.8	2.7	2.1	3.3
Summer wheat	2.6		2.3	1.5	2
Oat	3.2	1.6	1.8	2.5	3.9

Nitrogen fertiliser application to the main grain crops varies roughly from 40-70 kg ha^{-1}, while the phosphorus application varies from 6-24 kg ha^{-1} (Table 3). In general, the fertiliser applications have shown a dramatic decrease since the beginning of the 1990s after the collapse of the Soviet Union (Vagstad et al, 2001).

Table 3. Fertiliser application to the main grain crops (kg ha^{-1}).

	1998		1999		2000		2001		2002		2003	
	N	P	N	P	N	P	N	P	N	P	N	P
Winter wheat	70	24	73	19	45	14	47	10	47	22	63	18
Barley	66	7	49	24	62	13	48	6	38	17	57	19

Cropping patterns in the drainage field

The drainage field is divided into two major farmer fields with similar land use (Table 4). The main crop type is grain. Fertiliser application is slightly higher compared to the main catchment and varies from 40-110 kg ha^{-1}, with a high of 168 kg ha^{-1}, for nitrogen and 8-30 kg ha^{-1} for phosphorus. Yields are on the same order of magnitude and vary from 1.3-4.4 t ha^{-1}.

Methodology

Small plots/demonstration field

A total of 16 demonstration trials were constructed at Mellupite, with the main objective of measuring the effect of different fertiliser application treatments on nutrient runoff and the water quality. A total of five treatments were applied (three replicates), including normal fertiliser application in addition to non-fertilised, double fertilising rate and two different forms of manure application. In this case only “normal” fertiliser application was considered to have a fertiliser application similar to that in the drainage field and main catchment. Fertiliser applications to grain crops are on the same order of magnitude as for the drainage field and catchment (Table 5).

Table 4. Land use in the drainage field.

	Crop type	Area (ha)	Yield (t ha^{-1})	Fertiliser Application (kg ha^{-1})	
				N	P
1998	Winter wheat	6.58	3.9	100	30
	Spring barley	5.39	4.4	108	12
1999	Spring barley	3.29	1.3	75	13
	Spring wheat	3.29	3.9	168	30
	Oates	5.39	1.9	108	12
2000	Spring barley	6.58	3.4	70	8
	Bare fallow	5.39	-	-	-
2001	Bare fallow	6.58	-	-	-
	Winter wheat	5.39	3.8	112	23
2002	Winter wheat	6.58	3.3	79	23
	Spring barley	5.39	1.6	38	16
2003	Peas	1.20	2.7	39	23
	Spring barley	5.38	4.4	92	23
	Bare fallow	5.39	-	-	-

Table 5. Cropping system and fertiliser application (kg ha $^{-1}$) in demonstration field.

Year	Crop	N	P
1998	Winter wheat	70	20
1999	Barley	70	20
2000	Winter rape	80	20
2001	Peas	8	17
2002	Barley	12	20
2003	Barley + clover	60	30

Results and conclusions

The average yearly runoff, measured at different scales, was quite similar (Table 6). There was great variation in annual runoff varying from a minimum of ± 130 mm to a maximum of ± 350 mm. Also the monthly runoff showed a large variation (Figure 2). The same variation was measured at the drainage field scale (not shown here).

Table 6. Yearly measured runoff (mm) at different scales.

	1998	1999	2000	2001	2002	2003	Average
catchment	328	258	153	243	288	130	233
drainage field	349	223	174	246	270	137	233

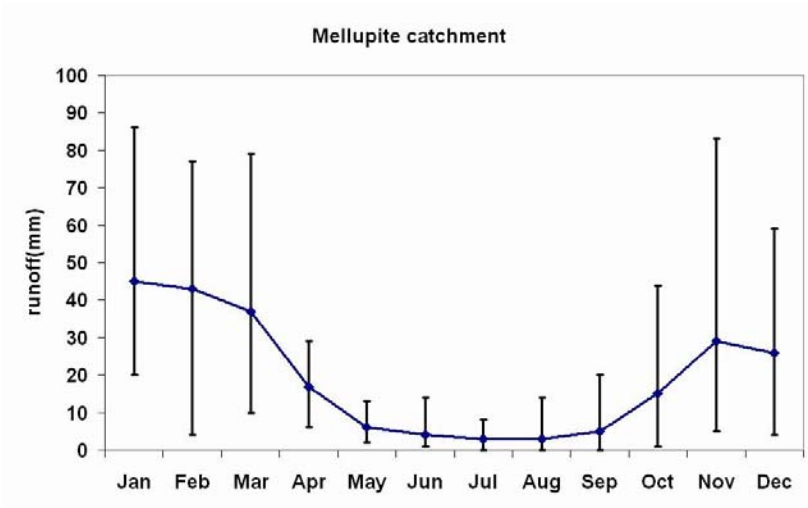

Figure 2. Average monthly, maximum and minimum runoff at the catchment scale.

Nutrient concentration and losses at different scales

Nutrient losses differ, depending on the scale of measurement. During the entire measurement period, the N-losses were highest at the drainage field scale. The average N-loss at the catchment scale was approximately 50% of the loss at the drainage field scale (Table 7).

The same applies to the P-losses, which showed reduced average annual losses with an increase in scale (Table 8). However, when considering the individual years, this difference was less significant, and the maximum annual loss also occured at the largest scale (i.e. 1999)

Table 7. Average N- losses (kg ha^{-1}) at the catchment, drainage and demonstration field scale.

	1998	1999	2000	2001	2002	2003	Average
Catchment	9.6	8.3	7.0	10.9	10.1	7.2	8.9
drainage field	20.7	14.4	17.9	22.4	16.5	12.4	17.4

Table 8. Average P losses (kg ha^{-1}) at the catchment, drainage and demonstration field scale.

	1998	1999	2000	2001	2002	2003	Average
catchment	0.238	0.270	0.089	0.125	0.155	0.162	0.173
drainage field	0.768	0.178	0.103	0.128	0.260	0.107	0.257

Nitrate concentrations were highest at the plot scale and decreased with an increase in scale (Figure 3) and a decrease in load was also observed. To be able to capture the major portion of root zone leakage at the demonstration plot, the drainage intensity was increased by a 50% reduction in the drain spacing. The decrease in N-concentration at the drainage field scale might be due to an increase in denitrification as a consequence of the increased drain spacing compared to the demonstration field scale. Larger spacing leads to longer residence times, in which case the soil is maintained at saturated or almost saturated conditions for longer time periods during periods with excess precipitation and/or snowmelt. This in turn leads to anaerobic conditions in the soils and a possible increase in denitrification rates. First, a number of runoff recession periods were analysed, measured at different scales but identical time periods. The main principle behind this analysis was that during the recession period, the discharge at time (t) and time (t +1) relate to each other as (Equation 1):

$$Q_{t+1} = Q_t \text{ x } e^{-\alpha} \text{ or } Q_{t+1} = Q_t \text{ x } A \tag{1}$$

where $e^{-\alpha}$ is a constant, based on the assumption that the system behaves as a linear reservoir. A comparison shows a decrease in the recession coefficient with an increase in scale, indicating a longer residence time or slower flow process at the drainage field and catchment scale (Table 9). Similar findings were made by Skaggs et al. (1994), showing that an increased drain spacing reduced nitrate leaching significantly, most likely due to increased denitrification losses. Reduction in nitrogen runoff was also artificially created through a system of controlled drainage, creating saturated conditions in the root zone (Breve et al., 1998; Evans et al., 1995; Wesström, 2002).

Table 9. Recession coefficients (a) measured at different scales.

	$e^{-\alpha}$	A	number of observations
catchment	0.96	0.04	12
drainage	0.94	0.06	12
demonstration field	0.86	0.15	19

Nitrate concentrations at the catchment scale were considerably lower compared to those at the drainage field and demonstration plot scales. This could be because the flow paths involved in runoff generation at the catchment scale are different than those at the drainage and demonstration field scales. which is reflected by the lowest recession coefficient (Table 9). Similar observations were also made in Estonia where N-losses from subsurface drainage systems were considerably larger when compared to measurements at a larger scale. Possible reasons for the differences were attributed to nitrogen retention processes in the unsaturated/saturated zones (Iital and Loigu, 2001). Deelstra et al. (1998) found that hydrology played an important role in explaining the N-loss differences between Norwegian and Baltic catchments and that the low N-loss in the Baltic countries was partly explained by the different flow paths due to the geo-hydrological settings. When considering the N-loss at the catchment scale, retention processes, such as in open streams and groundwater, might need to be considered.

Further analysis on recession curves was carried out to get more insight into flow processes at different scales in this catchment and will be reported at a later stage. Also other means of assessing hydrological differences with increase in scale should be assessed. Runoff and loads for the demonstration field have not been presented due to large variations in discharge. Further analysis needs to be carried out.

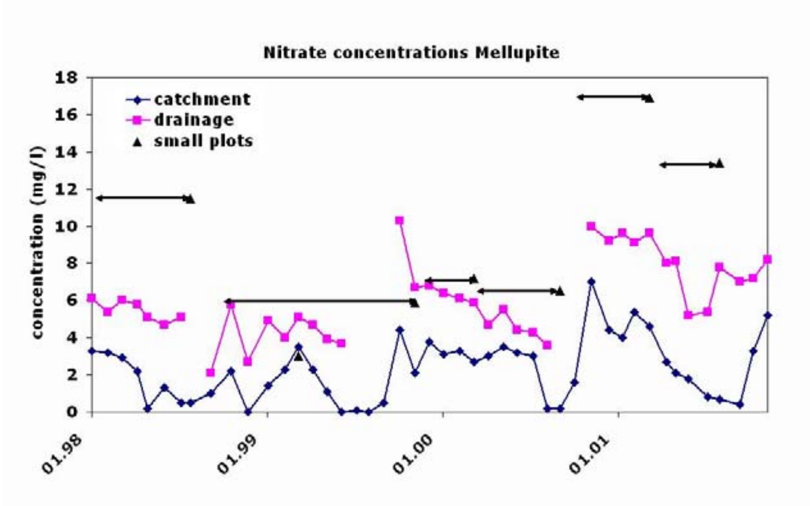

Figure 3. Nitrate concentrations at three different scales.

Another important reason for the low N-loss at the catchment scale was due to the fact that part of the catchment is predominately forest. The area grown with fertilised crops varied during the observation period from 37-48%. Pastures and other agricultural land varied during the same period from 20-31%. The rest of the area was occupied by forest. The N-losses from non-agricultural lands are unknown and therefore accurate estimates of the N-loss from agricultural land at the catchment scale are difficult to provide. If one assumes the N-loss from forest to be equal to 10% of that from the agricultural land (Vandsemb et al., 2003), the calculated N-loss from agriculture is ± 12.5 kg ha^{-1}, which is about 28% lower than the measured losses at the drainage field scale. Whether this is the true loss from agricultural land is uncertain due to lack of information on background losses and uncertainty about possible retention processes in ground and surface water, as described by Deelstra et al. (1998) and Iital and Loigu (2001).

References

Breve, M.A., Skaggs, R.W., Parsons, J.E. Gilliam, J.W., 1998. Using the Drainmod-N Model to Study Effects of Drainage System Design and Management on Crop Productivity, Profitability and NO3-N Losses in Drainage Water. *Agricultural Water Management* 35, 227 - 243.

Deelstra, J., Vagstad, N., Loigu, E., Vasiljev, A., Jansons, V. 1998. Interactions between hydrology and nutrient runoff in small agricultural catchments. A comparative study of Estonian, Latvian and Norwegian catchments. *20th Nordic Hydrological Conference. Helsinki*, *August 1998*, volume 1, 120 – 129.

Evans, R.O., Skaggs, R.W., Gilliam, J.W., 1995. Controlled versus conventional drainage effects on water-quality. *Journal of irrigation and drainage engineering-ASCE* 121, 271-276.

Iital, A. and Loigu, E. 2001. Agricultural runoff monitoring in Estonia. In: *Proceedings of the Symposium dedicated to the 40th Anniversary of the Institute of Environmental Engineering at the Tallinn Technical University.* 24-26 September, Tallinn, 67-76.

Skaggs, R.W., Breve, M.A., and J.W. Gilliam, 1994. Hydrologic and water quality impacts of agricultural drainage. Critical Reviews in Environmental Science and Technology, 24(1):1-32 (1994).

Vagstad, N., Stålnacke, P., Andersen, H-E., Deelstra, J., Gustafson, A., Ital, A., Jansons, V., Kyllmar, K., Loigu, E., Rekolainen, S., Tumas, R. and Vuorenmaa, J., 2001. Nutrient losses from agriculture in the Nordic and Baltic countries - Results of measurements in small agricultural catchments and national agro-environmental statistics. *TemaNord 2001:591. 74 p.*

Vandsemb, S.M., Bechmann, M., Eggestad, H.O., Øygarden, L., Deelstra, J. 2003. Erosion and nutrient losses from agricultural areas (In Norwegian). *Jordforsk report nr. 102/03, 47 pp.*

Wesström, I. 2002. Controlled Drainage. *Effects on subsurface runoff and nitrogen flows*. Doctoral Thesis. Swedish University of Agriculture Sciences. Uppsala.

Evaluation of SWAT for Use in Development of a River Basin Management Plan for the Ythan Catchment, UK

Caroline F. Dilks[1*], Sarah M. Dunn[1] and Robert C. Ferrier[1]
[1] Macaulay Institute, Craigiebuckler, Aberdeen AB15 8QH, U.K.
Email:c.dilks@macaulay.ac.uk

Abstract

The implementation of the EU Water Framework Directive (WFD) introduced an integrated approach to the protection and improvement of Europe's aquatic environment. The successful execution of the Directive is centred around a new river basin management planning system. Application of numerical models for predicting current and future trends in pollutants entering the aquatic environment under a variety of management regimes has been identified as key to development of successful river basin management plans (RBMP). Given the extensive range of model codes available, the EU project Benchmark Models for the Water Framework Directive (BMW) developed a model evaluation tool (MET) aimed at helping modellers and policy makers select appropriate model codes for specific model applications. The MET was used to select a model code to evaluate management practices for mitigation of in-stream NO_3 in the Ythan Catchment, UK (Dilks et al., 2003); a rural, agricultural catchment designated as a nitrate vulnerable zone in 2000. The selected model, SWAT, was calibrated and validated for discharge and in-stream NO_3 load. Model performance was satisfactory. A series of land management practices, recommended for reduction of NO_3 runoff and leaching in the Ythan Catchment have been simulated. These measures fell into three categories, fertiliser reduction, tillage practice, and cropping patterns. Reductions in inorganic fertiliser use were predicted to be the most successful option in terms of reducing annual in-stream NO_3 load and leaching, whilst planting spring instead of autumn-sown cereals, was more effective at reducing NO_3 load during the most ecologically sensitive period of the year. Limitations to the application of SWAT in the Ythan Catchment have been identified. These limitations include requirements for a comprehensive groundwater component for tracing leached nutrients through the underlying aquifer. Coupling of SWAT with a detailed groundwater model has been recognised as a potential solution to increasing groundwater representation in the region. Evaluation of model performance and simulation of various management options provided an opportunity to investigate the suitability of SWAT for development of a RBMP for the Ythan region.

Introduction

The EU Water Framework Directive (WFD) is an ambitious piece of legislation that establishes an integrated approach to the protection, improvement, and sustainable use of Europe's aquatic environment (SEPA, 2002). The principal objective of the Directive is to achieve good chemical and ecological status for receiving waters by 2015. Central to the successful implementation of the WFD is a new river basin management planning system. This planning mechanism is intended to ensure integrated management of the water environment, providing a decision-making framework for setting environmental objectives. Mathematical modelling has been recognised as an important tool in the implementation of the WFD with different stages of the legislative process requiring the application of different types of model codes (Rekolainen et al., 2004). For example, relatively simple representations will be needed during the characterisation phase of the WFD with more complex, processed-based representations required during the river basin management planning stage (Dunn and Dilks, submitted). Development of successful river basin management plans (RBMP) is dependent on detailed evaluation of pollutant fluxes under a variety of environmental conditions. Such assessments will require application of mathematical models that go beyond prediction of current conditions and are capable of forecasting both short and long-term change. In terms of diffuse agricultural pollution, models will be required to quantify the effectiveness of various land management options for addressing pollution issues (Dunn and Dilks, submitted).

Given the extensive range of model codes available, selecting an appropriate code for a given modelling objective can be a difficult task. Recognising this, the EU commissioned, under Framework V, the "*Benchmark Models for the Water Framework Directive*" (BMW) project (EK1 – CT2001-00093). The principal objective of BMW was to provide guidance for selection of model codes for use in the field of water management, specifically in the context of the WFD. This guidance has been provided through the development of a model evaluation tool (MET) to be used by modellers, water managers, and policy makers (Hutchins et al., submitted; http://www.rbm-toolbox.net). The BMW MET was used *a priori* to select a model code to evaluate land management scenarios for reducing NO_3 load in the River Ythan, UK. The Ythan Catchment was designated a nitrate vulnerable zone (NVZ) in 2000 as a result of evidence of elevated NO_3 concentrations in the surface waters and the estuary displaying characteristics typical of eutrophic waters.

This paper describes the application of the selected model, the Soil and Water Assessment Tool (SWAT) in the Ythan Catchment. The model was applied to assess the effectiveness of a variety of management practices proposed for reducing NO_3 runoff and leaching in the area (SEERAD, 2001). The suitability of SWAT for use in development of a RBMP for the Ythan has been evaluated in terms of (1) model performance and (2) the ability of the model to simulate relevant land management scenarios for the region. Assessment of uncertainty surrounding model predictions is beyond the scope of this article.

Study Area

Located in northeast Scotland, the River Ythan is situated approximately 20km north of the city of Aberdeen. The watershed extends to 680km^2, 540km^2 of which is above the tidal limit. The area, characterised by gently rolling lowland, ranges in altitude from 0 - 300m a.s.l. (Figure 1). Soils comprise of a mixture of humus-iron podzols, brown forest soils, and non-calcareous gleys. Approximately 95% of the Ythan Catchment is agricultural land (arable including grassland, improved pasture, rough grazing) (Figure 1). In total, 65% of the agricultural area is used for arable cropping; the remaining 35% is grassland used for grazing and mowing. Mean annual rainfall and water yield (at Ellon) are 815 and 450mm (mean discharge 7.8m^{3}s^{-1}), respectively. Discharge is dominated by slow subsurface response, baseflow comprising 75 to 80% of total annual discharge. The majority of the fast response is generated by flow through preferential subsurface pathways such as agricultural drains. In general, peak discharges occur in spring and autumn with extended periods of low flow typical during the summer months.

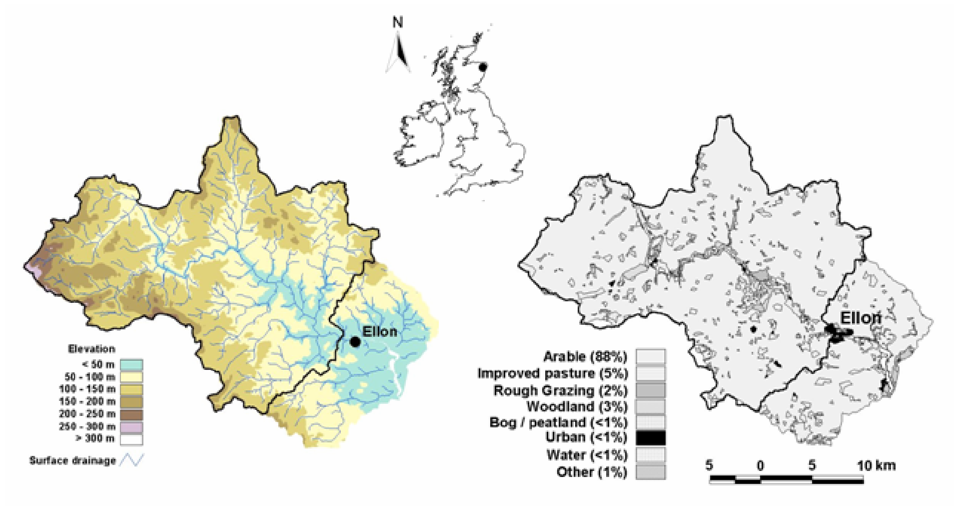

Figure 1. The Ythan catchment (location, topography, land use and modelled area).

Over the past 40 years average in-stream NO_3 concentrations in the Ythan main channel have increased three-fold (2.5 to 7.5 mgl^{-1} NO_3-N). This increase, mirrored in the estuary (Balls et al, 1995), is thought to reflect changing land use, intensification of agriculture, and an increase in the use of inorganic fertilisers (Edwards et al., 2003; Raffaelli et al., 1989). The elevated NO_3 levels have been linked to the development of extensive weed mats of macro-algae on the estuary mud flats.

Methodology

The BMW MET was employed to select a model code for use in the Ythan Catchment (Dilks et al., 2003). Following calibration and validation, SWAT, was used to evaluate a series of land management options recommended for mitigation of NO_3 runoff and leaching.

Model Description

SWAT is a physically based, spatially distributed, watershed model developed in the US to predict long-term effects of management on water, sediment, nutrient, and pesticide yields within large complex rural agricultural river basins. The main driving force behind SWAT is the hydrological component. The hydrological processes are divided into two phases, the land phase, which controls the amount of water, sediment, and nutrient loading in receiving waters, and the water routing phase which simulates movement though the channel network. SWAT considers both natural sources (e.g. mineralisation of organic matter and N-fixation) and anthropogenic contributions (fertilisers, manures and point sources) as nutrient inputs. The nutrient transformation component of SWAT is detailed by Neitsch et al. (2002).

Data

Table 1 presents the key input datasets, topographical, meteorological, soils, land use, and land management available for the Ythan Catchment.

Table 1. Input data sets available for the Ythan Catchment.

Input data	Description
Topography	50m DEM
Soil	Soil series map (1:25 000)
	Soils database for Scotland
Land use	Land cover map for Scotland (LCS88)
	Parish Census data (1989 – 1999)
Meteorological	Daily precipitation data (1980 – 1999), 8 stations
	Daily maximum and minimum air temperature (1980 – 1999), 3 stations
Management	Fertiliser use survey (DEFRA, 2001)
	Farm management handbook (Chadwick, 2000)
	Local knowledge

In addition, daily discharge and approximately monthly spot water quality samples were available (1983 – 1999) for one site (Ellon) on the Ythan. This site was used as the watershed outlet for the modelling. NO_3 constituted almost 100% of total in-stream N; therefore, for the remainder of this paper the symbol N will be taken as synonymous with in-stream NO_3. Observed water quality data were generally biased towards low flows. As such, a linear regression model (R^2 = 0.92) (Eq.1) was derived from the relationship between discharge Q (m^3s^{-1}) and in-stream N load ($Tday^{-1}$) enabling daily N loads to be estimated for the calibration and validation periods.

$$N = 0.6822Q - 0.135 \qquad \text{Eq.1}$$

The regression estimated daily dataset provided an indication of the timing of peaks and troughs in the N load time series that were not well represented in the observed data. This regression dataset therefore helped calibrate and validate SWAT for N load but was not used in the calculation of model performance indices.

Model Parameterisation

The SWAT ArcView Interface was used to subdivide the Ythan Catchment (above Ellon) into 32 subbasins using a 50m DEM. Each subbasin was parameterised using hydrological response units (HRUs), defined from soil and land use maps. Soil maps for the Ythan region are available at the soil series level, while the land cover map was produced as a combination of two datasets, LCS88 and Parish Census data. In total, the watershed was divided into 695 HRUs. Management strategies were determined for each crop type grown within the catchment. In general, crops were planted in either spring or autumn following a tillage operation and harvested in late summer. Plant residues were either removed or incorporated into the soil with an additional tillage operation following harvest. Inorganic fertiliser was applied as detailed by DEFRA (2001) and organic fertiliser (animal slurries) was spread three times per year. Sheep and cattle were assumed to graze for 365 and 180 days, respectively, while pigs and poultry were housed all year.

Default values were used for many model parameters, although calibration, based on local conditions, was necessary. To reduce the influence of initial conditions, a four-year model warm-up period was allowed prior to simulation.

Calibration and Validation

SWAT was calibrated (1984 - 1992) and validated (1992 - 1999) at Ellon using a standard split sample technique. Calibration focused on the water balance before considering N load and N concentration. Nash-Sutcliffe efficiency coefficients (E) for daily model performance are presented in Table 2.

Table 2. Nash-Sutcliffe efficiency coefficients for calibration and validation.

	Calibration	Validation
Discharge	0.80	0.73
N load	0.65	0.63
N concentration	-5.23	-3.92

During calibration, discharge parameters affecting the split between groundwater and surface water contributions (e.g. CN2) were found to exert the greatest influence on the stream hydrograph. Baseflow comprises approximately 75% of total annual discharge in the Ythan and as such dominates the flow regime. Other groundwater parameters, specifically groundwater delay (GW_DELAY) and the groundwater recession factor (ALPHA_BF) exerted a considerable influence on the daily hydrograph. Tile drains were simulated underneath all arable and improved grassland to mimic the fast hydrograph response known to occur in the catchment (Dunn et al., 1998). Surface runoff peaks were calibrated using SURLAG (surface runoff lag time). In general, SWAT predictions of low flow periods were in line with observed values; however, a number of discharge peaks were underestimated (Figure 2a). Good performances for discharge were obtained during both calibration (E = 0.80) and validation (E = 0.73).

Calibration of N load focused on three main parameters, GWNO3 (groundwater NO_3 concentration), NPERCO (N percolation coefficient), and BIOMIX (biological mixing efficiency). Groundwater NO_3 concentrations for the Ythan were estimated (on a subbasin basis) as the average concentration recorded during summer low flow months when groundwater constitutes 100% of flow. Groundwater NO_3 concentrations were significant, ranging between 5.0 and 7.5mgl^{-1}. Under low flow conditions N load exhibited a good match with observed values (Figure 2b). However, numerous peaks were underestimated in comparison to the regression estimated daily data. In general, underestimated N peaks corresponded to underestimated discharge peaks, reflecting the strong relationship between flow and N load (R^2 = 0.92 for Eq.1). Model performance for N load (determined in relation to observed data) was considered to be satisfactory for both the calibration (E = 0.65) and validation (E = 0.63) periods.

Having achieved satisfactory predictions of both flow and N load, N concentrations were calculated using the SWAT predicted flow (m^{3}s^{-1}) and N load (tday^{-1}). Examination of N concentration provided a more rigorous test of the N dynamics of the SWAT model that were, in this case, drowned out by the flow effect when load was considered. Nash-Sutcliffe efficiency coefficients for in-stream N concentration were -5.23 for the calibration and -3.92 validation periods, respectively. Substantial differences were seen between the predicted and observed time series (Figure 2c). SWAT predicted concentrations were notably lower than observed concentrations from late autumn to late spring when measured values were at their highest. Concentrations tended to be more similar during the summer months when the groundwater is the main source of in-stream N. Generally in the Ythan catchment, higher precipitation occurs in spring and autumn with lower precipitation typical of the summer period. Flow through agricultural drains, transporting NO_3 to the surface drainage network, is associated with precipitation events. Under-predication of N concentration during the autumn to spring period may result from the absence of a routine in the SWAT code for nutrient transport through agricultural drains.

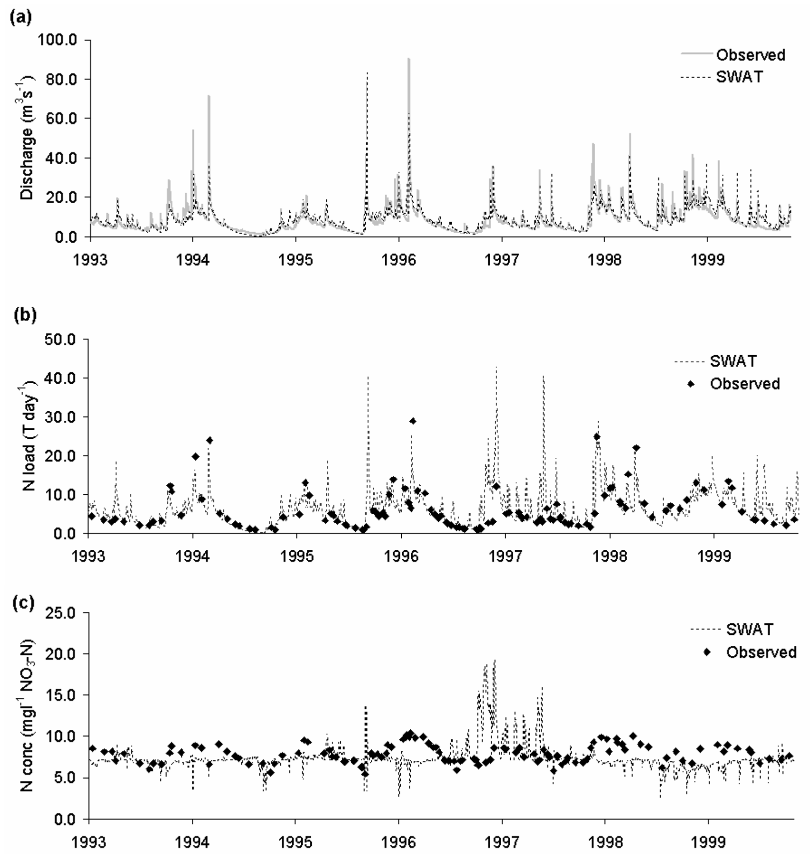

Figure 2. Simulated and observed (a) discharge, (b) N load (c) N concentration at Ellon on a daily time step (validation period).

Management Scenarios

Following designation of the Ythan Catchment as an NVZ a number of land management practices aimed at reducing NO_3 runoff and leaching were proposed (SEERAD 2001). A subset of these management practices have been simulated and average annual reductions in N load examined in relation to a no change or reference scenario (Table 3). Since N concentrations were poorly represented they have not been considered further. Simulations were conducted over a 12 year period, looking towards 2015 when objectives of the WFD are to be met.

Table 3. Land management scenarios simulated in the Ythan Catchment.

Scenario	**Description**
No change / reference	Reference scenario. Inorganic fertiliser applied according to levels detailed by the DEFRA fertiliser use survey (DEFRA, 2001). Organic fertilisers (slurries) are applied in addition to inorganic fertilisers.
Organic N accounting	Nutrient content of organic fertilisers is accounted for and inorganic fertiliser use reduced accordingly.
Fertiliser reduction	5, 10, 20 and 30% reduction in inorganic fertiliser levels below the organic N accounting level.
Direct drilling	Autumn crops sowed using direct drilling.
No tillage	No tillage operations.
No winter cereals	Winter-sown cereals are replaced by spring-sown cereals.

Results

Figure 3 presents average annual percentage changes in in-stream N load (Figure 3a), NO_3 leaching (Figure 3b), and discharge (Figure 3c) under the nine simulated management scenarios. Percentage change, a measure of effectiveness, was calculated in relation to the no change reference scenario. Changes in monthly N loads and average monthly discharge (also calculated in relation to the no change scenario) are given in Figure 4 for three of the scenarios, organic N accounting, direct drilling, and no winter cereals. For clarity, the additional fertiliser reduction scenarios (5, 10, 20, 30% reductions below the organic N accounting level) have not been presented in Figure 4. The same monthly pattern of N load reduction, although larger amounts, were predicted for the additional reduction scenarios as for organic N accounting scenario.

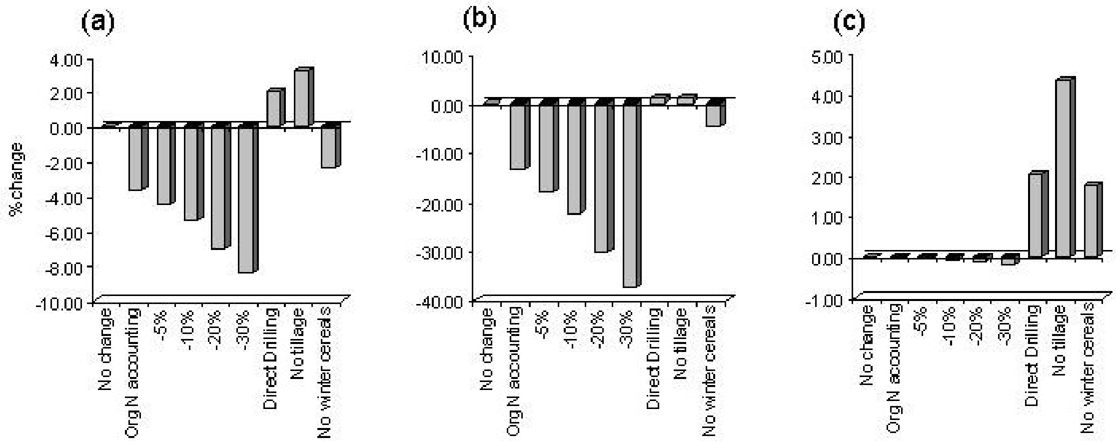

Figure 3. Predicated average annual % change in (a) N load, (b) NO_3 leaching, (c) discharge under different management scenarios.

Simulations indicate that fertiliser reduction scenarios will be the most effective in terms of reducing annual N load and NO_3 leaching (Figure 3). Reductions in average annual N load were small compared to decreases in fertiliser application. However, the reduction in NO_3 leaching was substantial, in excess of reductions in fertiliser use. Since SWAT does not trace leached nitrate through the shallow aquifer the model does not account for changes in groundwater NO_3 concentrations during a simulation. This is a significant limitation with regard to prediction of long-term changes in surface water NO_3 concentrations in the Ythan Catchment. The impact of reduced NO_3 leaching on the NO_3 concentration of groundwater entering streams will depend on the residence time of groundwater within the aquifer and subsurface storage. The largest monthly reductions were seen in September, October, November, and December indicating that less N remained in the soil at the end of the growing season (Figure 4). Little change was seen in the flow regime under the fertiliser reduction scenarios.

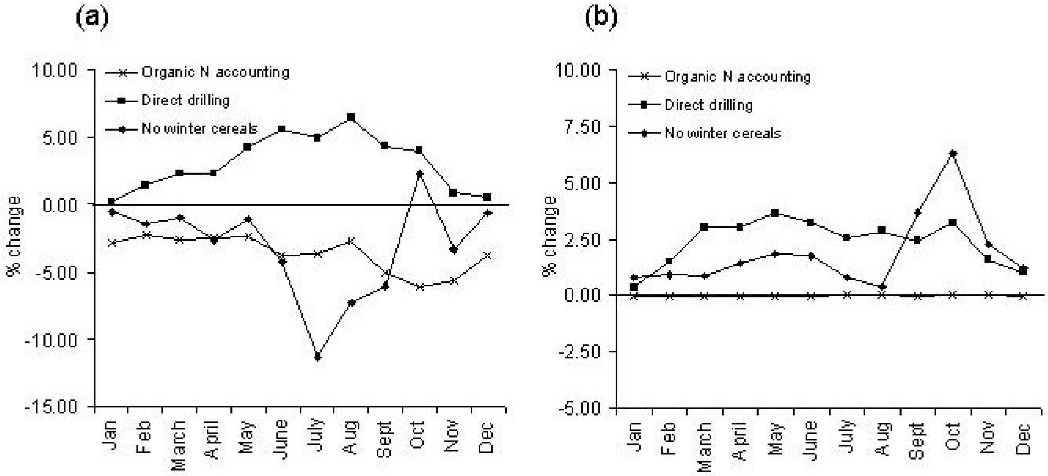

Figure 4. Predicted average monthly % change in (a) N load and (b) discharge under three of the management scenarios.

Changing cropping patterns, replacing winter-sown with spring-sown cereals, was estimated to result in an approximately 2.5 and 5% decrease in average annual N load and NO_3 leaching (Figure 3). Average annual discharge was predicted to increase in the order of 1.75% under this regime. The largest reductions in monthly N load were predicted to occur in the summer months (June to September) and November during which monthly discharge increased between 0.4% (August) and 3.7% (September) (Figure 4). Given the positive relationship between discharge and N load in the catchment, these results suggest that the predicted reduction in N load is associated with changes in management rather than changes in discharge. The monthly reductions in N load can be explained by differences in the timing of (1) fertiliser applications and (2) fertiliser uptake by winter versus spring crops.

Scenarios related to tillage practice (direct drilling and no tillage) were predicted to increase N load, NO_3 leaching and discharge (Figures 3 and 4). Increases were thought to reflect predicted decreases in crop yield and as such reduced water and nutrient uptake under these tillage regimes compared to the no change scenario.

Discussion

SWAT was successfully calibrated and validated for daily discharge and N load indicating that the model is suitable for prediction of current conditions within the Ythan catchment. In general the simulated time series were in line with observed data although some N load peaks were thought to be underestimated. A strong relationship was seen between discharge and N load, highlighting the importance of achieving a good prediction of discharge before considering water quality parameters. Predictions of N concentrations, on the other hand were poor, indicating that there were problems simulating the nitrogen dynamics in the region, particularly during the winter months. Agricultural drainage has been identified as a potentially important pathway for N transport in the Ythan Catchment. Included as a hydrological pathway only, there is currently no routine within SWAT to simulate nutrient, sediment or pesticide transport through agricultural drains.

The suitability of SWAT for use in development of a WFD RBMP for the Ythan Catchment depends on the ability to predict pollutant fluxes under a variety of environmental conditions. Prediction capability has been examined through the simulation of a number of policy-relevant land management scenarios for the reduction of NO_3 runoff and leaching. In total, nine scenarios, falling into three general categories (fertiliser reduction, cropping patterns, and tillage) were simulated. On an average annual basis fertiliser reductions were found to be most effective in terms of reducing in-stream N load and leaching. Also, switching from winter-sown to spring-sown cereals resulted in more targeted monthly reductions in N load focused around the more biologically active months of the year (July, August) when NO_3 uptake by algae is greatest. No data was available to validate these model forecasts. The uncertainty associated with these scenario predictions has yet to be quantified.

Following simulation of the management scenarios, a potential limitation of the SWAT model for use in simulating long-term scenarios was identified. SWAT does not trace nutrients through the shallow aquifer. Therefore, any nutrients leaching out of the bottom of the soil profile are lost from the simulation. In a groundwater dominated catchment with high groundwater NO_3 concentrations, like the Ythan, this can have a notable impact on in-stream N load. Simulations indicate a substantial decrease in NO_3 leaching out of the bottom of the soil profile under reduced fertiliser regimes. This reduction in leaching is, however, not reflected in groundwater NO_3 concentrations that remain static throughout the duration of the SWAT simulation. The time taken for reductions in NO_3 leaching to become evident in baseflow NO_3 concentrations will depend on the residence time of the groundwater and volume of storage in the subsurface. The groundwater model, MODFLOW has been successfully linked with SWAT (Conan et al.,2003; Sophocleous and Perkins, 2000; Sophocleous et al., 1999). Coupling SWAT with a suitable groundwater model may enable more accurate predictions of in-stream N load in the Ythan. However, as little is known about the properties of the shallow aquifer, additional experimental work will be required to enable parameterisation of a groundwater model application in the Ythan Catchment. Additionally, model predictions are likely to be improved by increased knowledge of land management practices, particularly the amount and timing of fertiliser and slurry applications, in the regions that have a significant influence on both N load and N leaching. Currently, only general management information is available for the Ythan. Detailed land management data is rarely available.

The scenarios simulated in this study were all characterised by broad catchment scale changes to land management. In reality, however, many changes to farm management practice are likely to occur at the field scale. Installation of buffer strips along the edge of watercourses, for example, has been identified as a practice capable of reducing in-stream sediment in addition to nutrient (N and P) load concentration. Small scale practices such as these can be difficult to simulate effectively within catchment scale models due to differences in the scale at which the processes occur and models operate. Given that SWAT uses HRUs that are not spatially located within subbasins; simulation of management practices associated with specific land parcels cannot be easily achieved.

Conclusions

Although successfully applied to predict current conditions within the Ythan catchment, the suitability of SWAT for long-term forecasting of N load under different land management regimes in the Ythan region has been questioned. Two limitations to the current model set-up have been identified (1) lack of a comprehensive groundwater component for tracing leached nutrients through the underlying aquifer and (2) problems associated with simulation of more localised management practices such as buffer strips. Despite these limitations the SWAT model proved a useful tool for evaluating a number of land management practices within the Ythan Catchment. Difficulties associated with prediction of small-scale management options are typical of many large-scale catchment scale models. In terms of the development of RBMPs, a nested modelling approach may be more effective. This approach would involve the use of catchment scale models to evaluate broad-scale management changes and farm or field scale models to evaluate more small-scale practices.

Acknowledgements

This research was jointly funded by the Commission of European Communities under Framework V as part of the Benchmark Models for the Water Framework Directive (BMW) project (contract no: EK1 – CT2001-00093) and the Scottish Executive Environment and Rural Affairs Department (SEERAD).

References

Balls, P.W., Macdonald, A., Pugh, K. and Edwards, A.C. 1995. Long-term nutrient enrichment of an estuarine system, Ythan Scotland 1958 – 1993. Environmental Pollution, 90: 311-321.

Chadwick, L. (Ed). 2000. The farm management handbook 1999/2000. SAC, Edinburgh, UK. I SBN: 1 85482 961 3.

Conan C, Bouraoui F, Turpin N, de Marsily G, and Bidoglio G. 2003. Modelling flow and nitrate fate at catchment scale in Brittany (France). Journal of Environmental Quality, 32(6): 2026-2032.

DEFRA. 2001. Fertiliser Practice: Fertiliser use on farm crops for crop year 2000. http://www.defra.gov.uk.

Dilks, C.F., Dunn, S.M., Ferrier, R.C. 2003. Benchmarking models for the Water Framework Directive: evaluation of SWAT for use in the Ythan catchment, UK. Proceedings of 2nd International SWAT Conference, Bari, Italy. 1 – 4 July, 2003.

Dunn, S.M., and Dilks, C.F. Submitted. Benchmark models for diffuse pollution: the challenges. Large Rivers Supplement.

Dunn, S.M., McAlister, E. and Ferrier, R.C. 1998. Development and application of a distributed catchment-scale hydrological model for the River Ythan, NE Scotland. Hydrological Processes, 12: 401-416.

Edwards, A.C., Sinclair, A.H. and Domburg, P. 2003. Identification, designation and formulation of an action plan for a nitrate vulnerable zone: a case study of the Ythan catchment, NE Scotland. European Journal of Agronomy, 20: 165-172.

Hutchins, M. , Urama, K., Penning, E., Icke, J., Dilks, C., Bakken, T., Perrin, C., Saloranta, T. and Candela, L. Submitted. The BMW model evaluation tool: a guidance document. Large Rivers Supplement.

Neitsch, S.L., Arnold, J. G., Kiniry, J.R., Williams, J.R. and King, K.W. 2002. Soil and water assessment tool theoretical documentation version 2000, Texan Water Resources Institute, Texas, US.

Raffaelli, D., Hull, S., Milne, H. 1989. Long term changes in nutrients, weed mats and shorebirds in an estuarine system. Cahiers de Biologie Marine, 30: 259-270.

Rekolainen, S., Kamari, J. and Hiltunen, M. 2004. A conceptual framework for identifying the need and role of models in the implementation of the Water Framework Directive. International Journal of River Basin Management, 4: 347-352.

SEERAD. 2001. Draft regulations establishing the action programme measures to apply in the Ythan nitrate vulnerable zone. Paper No. 1/ 2001. UK.

SEPA. 2002. *The future for Scotland's waters*. Scottish Environment Protection Agency, UK.

Sophocleous, M. and Perkins, S.P. 2000. Methodology and application of combined watershed and ground-water models in Kansas. Journal of Hydrology, 236: 185-201.

Sophocleous, M.A., Koelliker, J.K., Govindaraju, R.S., Birdie, T., Ramireddygari, S.R. and Perkins, S.P. 1999. Integrated numerical modelling for basin-wide water management: the case of the Rattlesnake Creek basin in south-central Kansas. Journal of Hydrology, 214: 179-196.

Distributed Watershed Modeling of Mountainous Catchment - A Case Study in the Amameh Catchment in Iran

Shaban Ali Gholami*[1] and A.K. Gosain[2]
[1]Assistant Professor of Soil Conservation and Watershed Management Research Center (SCWRC) Tehran, Iran. Email: ali_gholami@hotmail.com
[2]Professor of Civil Engineering, Indian Institute of Technology, Delhi 110 016, India. E-mail: gosain@civil.iitd.ernet.in, (91) (011) 2659 1186, Fax: (91) (011) 2658 1117

Abstract

Watershed management is a widely accepted approach for optimal use of soil and water resources. Therefore, watershed modeling incorporating hydrological processes plays a crucial role in proper planning and development of local resources. Invariably, one of the major difficulties encountered with the use of hydrological models is the requirement to calibrate the model in the target area. For the purpose of calibration, most of the hydrological models require a long series of observed runoff data. These series of data are usually not available for small watersheds. Therefore, it is imperative that hydrological models which can overcome this requirement be identified. One such hydrological model, SWAT (Soil and Water Assessment Tool), has been identified and implemented in Tehran-Amameh, a mountainous, snow-bound, 37.20 km^2 watershed in Iran.

This study provides insight into the working of the continuous, distributed water-balance model SWAT. The major objective of this study was to assess the applicability of the model in ungauged watersheds. These findings are important in view of the fact that it is impractical to gauge small watersheds, which are accepted as viable planning and management units throughout the world.

It has been shown that use of the model on ungauged watersheds is not optimal since it is not always possible to define model parameters. However, through the use of a small series of observed flow data (about one year), the model performance has been appreciably enhanced. The character of the watershed is reflected through the observed flow and is not attainable from any other information. The structure of the SWAT model proved to be very stable, but the snow component of the model needed improvement and was therefore modified.

During the course of simulation analysis it was observed that the selection of an appropriate interval for analysis is very important. For example, if the simulation results appear to be adequate at the monthly interval, they may not necessarily be adequate at the daily interval, and vice versa.

The capability of the model to simulate the sediment yield is shown. Interestingly, the improvement in water yield simulations corresponded to improvements in sediment yield, which shows that the model is sufficient for sediment yield simulations.

Introduction

Soil and water are among the basic natural resources necessary for human survival. Unfortunately, these resources are being depleted due to unchecked growth in population, thereby accelerating changes in land units and overall mismanagement of the watershed. The consumption of food increases as the population grows; therefore, agricultural production must increase. To produce more, farmers must make use of inconvenient lands such as those on steep slopes of hills and mountains.

During the later half of the 19th and the first half of the 20th century, many engineers' empirical methods or models were derived from empirical observations. But they could not solve the problems at a generic level because each watershed has different hydrological behavior and topographically specific characteristics. Also, only inadequate or incomplete data, and at times no data, are available for ungauged catchments. In this study an effort has been made to bridge the gap created by the unavailability of this data. A physically based model is needed, which can be used for ungauged watersheds. In this study the SWAT model is applied to the Amameh Catchment (one of biggest subcatchments of the Latian Basin) located in Tehran, Iran.

The first goal of this study was to identify a hydrological model which is capable of simulating the small watersheds and thereby is suitable to be used as a watershed management tool. Secondly, the SWAT model was evaluated in one specific watershed, the Amameh Catchment, with respect to ease of calibration.

Methodology

A topographic map, areal photo, field data, recording station and GIS tools were used in this study. The extent of the catchment data plays a major role in deciding the type of model that can be used. In the selected catchment, the extent of the data was reasonable for SWAT simulation. Data on physio-topography as well as the hydro-meteorological parameters of the catchment were collected. The physio-topography data are static, and were measured and organized in the field. This data includes parameters such as topography, physiographic data, geology, soils, erosion, and land use changes. Land use is very important in this study; therefore, measurements of this parameter were completed with great precision.

The dynamic data was organized into meteorological and hydrological data. These data were gathered from two recording stations, Baghtangeh and Kamarkhani. All of the input and output files for each subunit of the basin were organized in a file with a CIO extension. The analysis was then carried out with selected model parameters.

Results and Conclusions

In several tests within the study area it was found that, in general, eleven parameters influence the model. Some of these are shown in Figure 1. One of the major objectives of this study was to assess the applicability of SWAT in ungauged watersheds. The various steps taken to achieve this objective are as follows:

1. It was assumed that the SWAT model is fully capable of simulating the catchment through the parameter set defined with respect to the observable and derived characteristics as per the recommended procedure. This evaluation was performed on a monthly scale.

2. It is important to have some minimum observed flow data, and as little as one year of collected data has been demonstrated to be sufficient for understanding the characteristics of the catchment. An attempt was made to identify which processes of the model need improvement.
3. The important issue of interval of simulation was also addressed. The desired simulation interval might change with respect to the problem in question. In some situations, the monthly flow volume may suffice, whereas in other situations, the daily flow rates may be required. SWAT is a daily time-step model. Moreover, the real response of some of the model components can only be observed at the daily interval. It was demonstrated that at some stages the analysis of daily output can be quite useful.

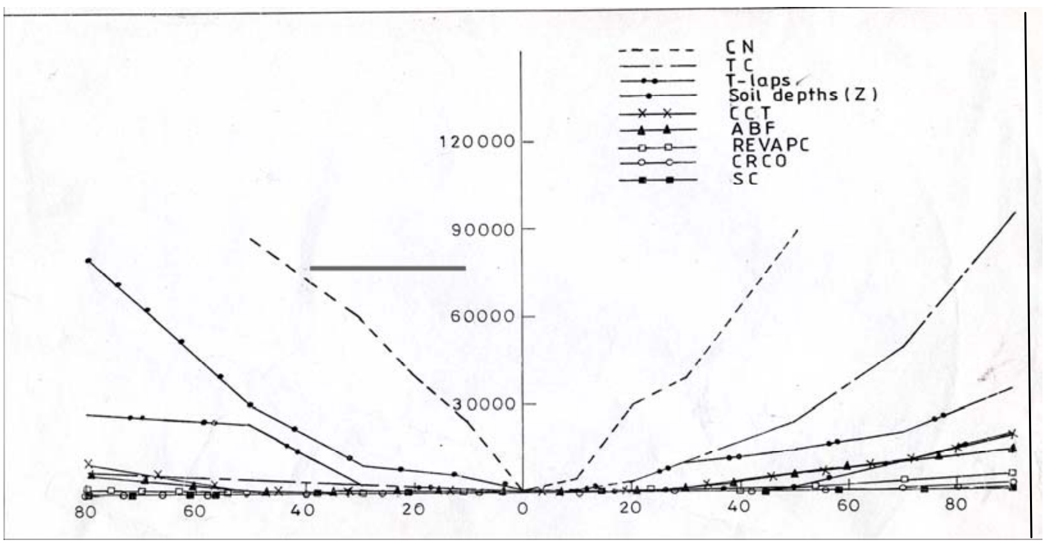

Figure 1. Sensitivity of the model to parameters using the total sum of squared residual (TSSR) statistics.

Water Yield Simulation

Emphasis was given to two aspects of yield simulation, water and sediment. The first element of yield in a watershed is the water yield. As a first step, the validity of the SWAT model, in terms of ungauged catchment simulations, was explored.

Simulation of an Ungauged Catchment

In this step, although some observed data was available for the study area, it was assumed that the study area was an ungauged watershed. Therefore, the observed flow data was not used in these simulations.

Two questions were posed for evaluating the model:

1) How much error can exist in the simulation results if there is no observed data to measure against?
2) What is the minimum duration for observed flow data required to sufficiently identify the characteristics of a watershed?

For the first question, the upper subcatchment of the Amameh Catchment was used. The Amameh Catchment is in a mountainous region and most of the land has been allocated to rangeland with a variety of range plants. Four years of observed flow data for this catchment, 1973 to 1976, was utilized for comparison with the simulated results. It appears that at least two years of data are sufficient for such a comparison. The first year of simulation was highly affected by the assumed initial conditions of the watershed, and serves as a "warm-up" period for the model. However, two additional years were also included in this analysis. Table 1 outlines the salient parameters, which were arrived at using the procedures recommended for the SWAT model.

Table 1. Summary of runs depicting improvement in model performance in the Amameh Catchment.

No	Parameters of the model		Run 1	Run 2	Run 3	Run 4	Run 5	Run 6	Run 7	Run 8	Run 9	Run 10
1	FFC		* 2	2	2	*3	3	*2	2.oo	*1.15	1.15	1.15
2	TC		*2.5	2.5	2.5	2.5	2.5	2.5	2.5	*2.00	2.00	2.00
3	CCT		X	**0.31	0.31	0.31	0.31	0.31	*0.416	0.416	0.416	0.416
4	T-Laps		X	X	**7.3	7.3	7.3	*5.65	5.65	*744	7.44	7.44
5	CN II		81	81	81	**81	*72	72	72	*60	60	60
6	ABF		0.065	0.065	0.065	*0.065	*0.0065	0.0065	**0.49	0.049	0.049	*0.037
7	Soil Depth (z)		590	590	*640	640	*683	683	683	683	*966.7	966.7
8	Revape		0.00	0.00	0.00	0.00	0.00	0.85	*0.115	0.115	0.115	0.115
9	Crack-flow		X	X	X	X	X	X	2	2	*1	1
10	Sc		* 1.65	1.64	1.64	1.64	*14.84	14.84	14.84	*6.98	6.98	6.98
11	K		0.2	*0.01	0.01	0.01	*0.15	0.15	*0.25	0.25	0.25	0.25
12	Mgt (No Crop) OBS		23-19	23-19	23-19	23-19	23-19	23-19	23-19	23-19	23-19	23-19
	1973	583	357.4	799.4	542.6	520.70	525.05	711.80	712.90	649.6	596.00	563.20
	1974	564	341.3	598.9	442.9	420.60	414.40	560.50	555.80	559.50	352.00	538.84
	1975	726	466.4	846.5	613.10	566.90	596.10	805.60	788.20	806.74	449.0	744.00
	1976	643	662.02	753.0	493.20	489.04	473.30	629.30	602.40	615.50	673.0	723.00
TSSR 1973 to 1976		Month	125361	314690	82019	53765	48057	52422	43817	43788.0	37240	13318
		Year	168.54	66464	51430	73389	71392	23137	22267	11769	11336	1793
NS 1973 to 1976		Month	0.063	-1.35	0.387	0.59	0.641	0.608	0.668	0.67	0.722	0.900
		Year	-9.54	-3.17	-2.22	-3.6	-3.47	-0.45	-0.39	0.26	0.289	0.887

* the value of a parameter was changed

** the input parameter value changed from an annual to monthly interval (Same value is given 12 times)

Improvement in Simulation

Having obtained poor results for the ungauged simulation, it was decided to add minimum flow data for the catchment. This was achieved through manual calibration where visual interpretation was made for the monthly simulation results. Although the simulation plots for four consecutive years of observed and simulated monthly flow depths were used, a shorter sequence of about two years of data would have been sufficient.

Eight parameters played a significant role in the model. These are CCT, CNII, Z (Depth of Soil), T-laps, SC, ABF, TC and REVAPC (Figure 1). The following sections demonstrate the systematic sequence in which improvements were made through the visual interpretation of the simulation results. The improvements in the model are also quite appreciable in the daily simulation. The final simulation could be considered quite good by any standard, be it the NS value of 0.90 or the flow simulation at the monthly or the daily time-step.

Simulation of the Entire Catchment

The simulation for the same years, 1973 to 1976, was also performed for the entire Amameh Catchment using the general common parameters of run 10, along with the local parameters of the Kamarkhani sub-catchment. Table 2 shows the summary results of the Baghlangeh sub-catchment and the entire Amameh Catchment, including the Kamarkhani sub-catchment.

Table 2. Summary of water yield simulations in the Amameh Catchment with 10 years of data.

Baghtangeh Sub-catchment		Entire catchment	
R2	= 0.906	R2	= 0.785
Reg. Slope	= 930	Reg. Slope	= 1.093
Test of TSSR	= 13318	Test of TSSR	= 22233
Test of NS	= 0.90	Test of NS	= 0.717
Mean Measurement	= 52.4	Mean Measurement	= 41
Mean predicted	= 51.4	Mean predicted	= 31
STD DEV Measurement	= 53	STD DEV Measurement	= 41
STD DEV Predicted	= 55	STD DEV Predicted	= 33

Simulation Performance on the Remaining Period

Because four years of data were used to improve the parameters of the model, it was useful to evaluate the performance of the model using these parameters for the remaining years. The philosophy of simulation dictates that if the representative set of model parameters has been obtained, then the same set should produce acceptable simulation results for any period in the future, provided no man-made changes occur in the study area.

The performance of the entire catchment was obtained by extending the characteristics for the upper sub-catchment to the lower sub-catchment. The results were not as good due to the fact that the lower sub-catchment may not be representative of the upper area. However, the performance was not terrible. This brings us back to the same premise that it is essential to explore the true characteristics of the basin using the observed hydrological response before any reasonable water yield simulation is attempted.

Sediment Yield Simulation

In this step, the capability of the SWAT model to simulate soil erosion rates and sediment yield (suspended sediment load) was evaluated. Land use/land cover in the Amameh Catchment includes rangeland, rock, urban, and agricultural land. Rangeland covers 72% of the catchment area, 26% is covered by rock, 1% by urban area, and the rest of the area is covered with agricultural and orchard lands. A litho formation called marl is very prevalent and creates a type of erosion called Hezar-darreh. This is the main source of fine sediment in the catchment. Because the soil parameters were so completely identified for the catchment in question, only the soil erodibility factor (K) was changed in this analysis. The results for the subcatchments Baghtangeh and Kamarkhani are shown in Table 3.

Table 3. Summary of Results of Sediment Yields for the Amaneh Catchment.

Baghtangeh Sub-catchment			**Kamar khani Sub-catchment**	
Duration	**Subject**	**Result**	**Subject**	**Result**
Monthly	**R2**	**0.761**	**R2**	**0.051**
	TSSR	**0.72**	**TSSR**	**11.5**
	NS	**0.412**	**NS**	**0.93**
Annually	**R2**	**0.631**	**R2**	**0.010**
	TSSR	**0.47**	**TSSR**	**16.2**
	NS	**10.9**	**NS**	**3.167**
	Sediment Yield T/h	**0.48**	**Sediment Yield T/h**	**0.65**

References

Arnold, J. G., B. A. Engel and R. Srinivasan, 1993. A Continuous Time, Grid Cell Watershed Model. In: Application of Advanced Information Technologton, June 17-19, 1993. ASAE, St. Joseph, Michigan.

Arnold, J.G., Williams, J.R. Sirinivasan, R.and. King, K.W 1996. SWAT-Soil and Water Assessment Tool, USDA, Ageiculture Research service.

Bathurst, J.C., 1986b. Sensitivity analysis of the Systeme Hydrologique Europeen for an upland catchment. J.Hydrol., 87 : 103-123.

Burnash, R.J.C., Ferral, RL. And. Mc Guirem, R. A, 1973, A generalized streamflow somulation system conceptual modelling for digital computers, export by the joint Federal State River Forecast centre, Sacremento, califor.,

Chiew, F.H.S. and McMahon, T.A., 1994. The optimisation of parameters of the daily rainfall- runoff model MODHYDROLOG in 28 Australian Catchments. J.Hy. Irol., 153:383-416.

Ffolliott, P.F. & Guertin P.D. 1988. Yield II : An interactive computer model to simulate water yield from southwestern ecosystem. In: Modelling Agricultural. Forest, and Rangeland Hydrology. ASAE publication 07-88: 72-78.

Ewen, J. (1990) Basis for the sub- surface contaminant migration component of the catchment water flow, contaminant transport, and contaminant migra- tion modelling system SHETRAN-UK. NIREX Research Report NSS/R229, NIREX, Harwell.

Helvey, J.D., 1971. A summary of rainfall interception by certain conifers of North America. In Biological effects of the hydrological cycle. E.J> Monke, E.J. Monke, Ed. West Lafayette : Purdue University.

Kuchmwnt. L.S., 1980. A two- dimensional rainfall-runoff model: identification of parameters and possible use for hydrological forecasts. IAHS-AISH Publ., 129: 215-219.

Massman, W.j., 1983. The derivation and validation of a new model for the interception of rainfall by forests. Agric. Meteorol., 28: 261-286.

Moore, R.J., and Clarke, R.T., 1981. A distribution function approach to rainfall- runoff modelling. Water Resour. Res. 17(5):1367-1382.

Richardson, C. W., 1981. Stochastic Simulation of Daily Precipitation, Temperature, and Solar Radiation. Water Resources Research 17(1): 182-190.

Rockwood, D.M., and Nelson, M.L. 1966, Computer application to strwamflow synthesis and reservoir regulation. IV International Conference on Irrigation and Drainage

Shanholtz, V.O. & Younos, 1994. A soil water balance model for no-tillage and conventional till systems. Agricultural Water Management, 26:155-168.

Solan, P.G., Morre, I.D., Coltharp, G.B., and. Eigel, J.D.,1983. Modeling Surface and Subsruface Stormflow on Steeply. Sloping Forested Watersheds. Water Resources Inst. Report 142, University of Kentucky, Lexington, Kentucky.

Srinivasn, R., J. Arnold, W. Rosenthal, and R. S. Muttiah, 1993. Hydrologic Modeling of Texas Gulf Basin Using GIS. In: Proceedings of Second International GIS and Environmental Modeling, Breckinridge, Colorado, pp.213-212.

Todini, E. 1996. The ARNO. Rainfall Runoff Model, Journal of Hydrology, Vol. 175:339-382.

Venetis, C. 1969. A study of the recession of unconfirmed aquifers. Bull. Intl. Assoc. Sci. Hydrol. 14(4):119-125.

Williams, J.R., Nicks A.D. and Arnold, J.G., 1985. Simulation for water resoruces in rural basins, Journal of Hydrolic Engineering, 111(6):970-986

SWAT Model Development for a Large Agricultural Watershed in Iowa

C.H. Green*[1], M. Di Luzio[2], J.G. Arnold[1], and M.D. Tomer[3]
[1]USDA-ARS/SPA. Email: chgreen@spa.ars.usda.gov Phone: (254) 770-6507
[2]Texas A & M University
[3]USDA-ARS/NSTL

Abstract

The SWAT (Soil and Water Assessment Tool) water quality model is designed to assess nonpoint and point pollution and conduct agricultural management scenario comparisons. The model's simulation accuracy was evaluated with hydrologic monitoring data collected from the South Fork watershed in Iowa. This watershed represents the most intensive region for row-crop and livestock production in the Midwest. The model, in its latest version, was applied using AVSWAT-X, the interface with ArcView 3.3 GIS software. AVSWAT-X provides an extendable environment including the optional usage of SSURGO data maps and derived soil parameters. Land use-land cover input maps and classes were primarily based on the NASS Crop Data Layer 2002 enhanced by Iowa Gap analysis data. Climate data from 1990 to 2004 were incorporated. Three years of crop rotation and conservation practice data were combined to establish Management scenarios' effects on the impairment of South Fork watershed waters. Initial results of hydrologic validation will be presented.

Introduction

The Natural Resources Conservation Service (NRCS) and Agricultural Research Service (ARS) are quantifying the benefits of the USDA conservation programs, under the Conservation Effects Assessment Program (CEAP). The impacts of conservation practices exist at the field level; however CEAP is designed to measure conservation effects for larger areas, such as watersheds, due to their inclusion of more complex interactions. The South Fork of the Iowa River is one of the ARS Benchmark Watersheds.

The SWAT model is being enhanced to optimize its ability to accurately simulate water quality processes affected by best management practices (BMPs). This version of SWAT2003 includes the tile drain component and modifications related to streamflow. The tile drainage component (Arnold et al., 2003) is important for the watershed water balance as well as its role in agricultural pollution transport (Baker et al., 1975; Logan et al., 1994). Du et al. (2003) assessed the applicability of tile flow in SWAT2003 for nine years. They found that SWAT2003 estimated monthly flow reasonably well (E value up to 0.75). The daily flow had lower accuracy with E values from 0.43 to 0.52. The objective of this study was to evaluate the model's accuracy in simulating streamflow with the tile flow component and additional parameters for the South Fork watershed (SFW) located in central Iowa. The evaluation and refinement of N and P routines in SWAT2003 are next on the agenda.

Watershed Description

The South Fork of the Iowa River covers about 78,000 ha, including tributaries of Tipton and Beaver Creeks (Figure 1). It is representative of the Des Moines Lobe, the dominant landform region of north-central Iowa. The terrain is young (about 10^4 y since the last glacial retreat), and therefore natural stream incision and development of alluvial valleys has only occurred in the lower parts of the watershed. The upper parts of the watershed are occupied by till plains and marginal moraines that have many internally drained “prairie potholes.”

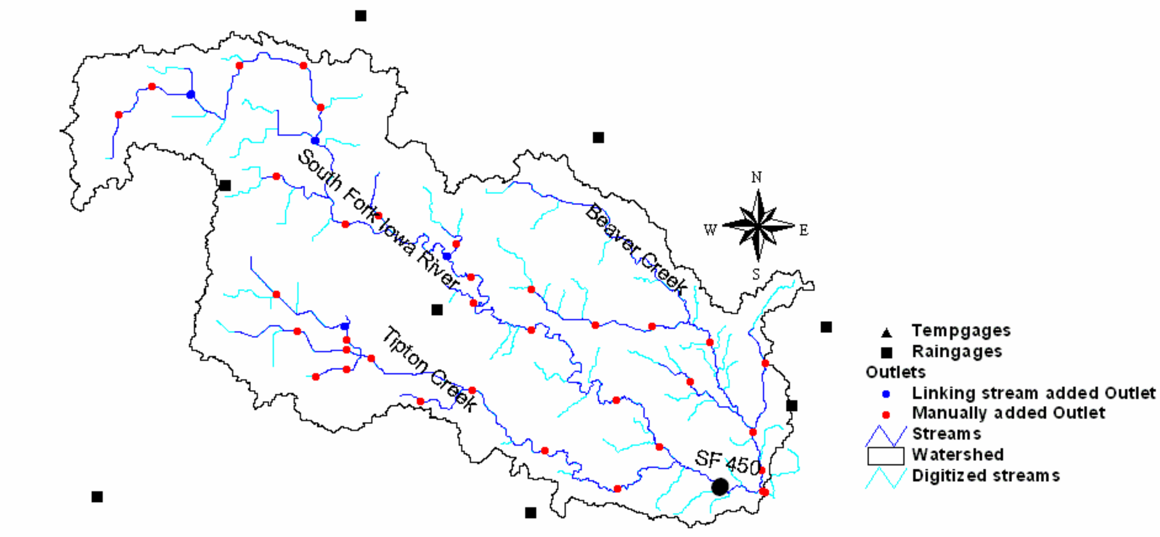

Figure 1. Distribution of temperature, raingages, and USGS gage SF450 and sampling locations in the SFW, IA used by SWAT2003.

Soil wetness is a major concern for land management and agricultural production for this region. Hydric soils occupy about 54% of the watershed. Artificial drainage was installed to allow agricultural production, beginning more than 100 years ago. Subsurface tile drainage and dug ditches have significantly decreased surface water storage and hastened the routing of water from the watershed. Today about 85% of the land area is under corn and soybean rotations. The South Fork watershed contains some of the most intensive row-crop and livestock production in the Midwest. There are nearly 100 confined animal feeding operations in the watershed, most producing swine. Two major subbasins, Tipton Creek (19,850 ha) and the upper South Fork (25,600 ha), contain most of the livestock.

The soils are highly productive, with the Clarion-Nicollet-Webster soil association being dominant, forming a sequence (respectively) of well-drained Typic Hapludolls, somewhat poorly drained Aquic Hapludolls, and poorly drained Typic Haplaquolls (National Cooperative Soil Survey, 1986; Soil Survey Staff, 2003). The potholes are occupied by very poorly drained Okoboji soils (Cumulic Haplaquolls), often with calcareous and poorly drained Harps soils (Typic Calciaquolls) on their margins.

Methodology

Input Data
Hydrologic discharge data

The USGS established a gauging station near New Providence in 1995, as part of the Eastern Iowa Basins NAWQA program (Becher et al., 2001). Hydrologic and water-quality monitoring were expanded, and by early 2001 additional gauging stations were established (Figure 1). Stream stage height was determined using bubbler-type water level recorders. Periodic measurements of cross-sectional depths and flow velocities under varying flow conditions were used to establish and maintain rating curves defining a relationship between stage height and discharge at each station. These cross-sectional measurements were made during and/or after major events, to identify changes in the rating curves that can be affected by changes in the stream bed. Hydrologic data were maintained in a WISKI hydrologic database (http://www.jbsenergy.com/Instruments/WISKI/wiski.html), which includes customized software that automatically accounts for changes in rating curves, and interpolates missing or aberrant data using methods that conform to USGS protocols for processing hydrologic data.

Precipitation and temperature data

Daily precipitation totals were obtained from the National Oceanic and Atmospheric Administration's (NOAA) National Climatic Data Center (NCDC) (http://www.ncdc.noaa.gov) for the eight raingage stations within and adjacent to the watershed (Figure 1). Daily maximum and minimum temperatures were obtained from two NCDC stations. The time period for this data ranged from 1995 to 2004. The Penman-Monteith method was selected for potential ET calculation.

Land use data

Cropping rotations were determined using annual classified satellite data made available by the National Agricultural Statistics Service (USDA-NASS) (http://www.nass.usda.gov/research/Cropland/SARS1a.htm). The classification is carried out by NASS to estimate acreages of different crops that are planted in several states each year. Two years of classified data (2002-2003) were overlaid to map the dominant crop rotations occurring on agricultural lands within the watershed. Agricultural lands were identified using digitized agricultural field boundaries within the watershed obtained from local Farm Service Agency (USDA-FSA) offices. These overlay combinations were grouped to represent cover types of crops. The crop rotations were further divided according to whether manure or commercial fertilizer applications would be expected. The land use classes plotted included: corn-soybean (CNBN (no manure)and CBMN (with manure)); soybean-corn (BNCN and BCMN); continuous corn (CCRN and CCMN) on the agricultural lands, plus pasture (PAST), wetlands (WETN), forest (FRSD) and urban (UTRN) areas on the non-agricultural land. Rotations were defined based on the sequence of crops observed in each field across the two years of record. The urban class was assigned to roadways, towns, and farmsteads.

Animal feeding operations were digitized, based on the interpretation of a rectified mosaic of infrared photographs acquired in May 2002 by Iowa's DNR (http://ortho.gis.iastate.edu/cir/cir.html). The digitized buildings allowed location and size (floor area) of the confinement buildings to be estimated. Agricultural areas surrounding the CAFOs were classified as receiving manure, based on their size, number, and distance to nearby confinement buildings. We assumed that all confinement buildings produced swine, with a deep pit, wean to finish operation. A livestock density of one animal per 0.75 m^2 was assigned (B. Kerr, USDA/ARS, personal communication, April 2004). Although we do not have information on the exact types of operations in the watershed, finishing operations are the most common type, and nearly all of the CAFOs produce swine. Most CAFOs (approximately 60 out of 110) lack external manure storage (i.e. lagoons were not present on the photos) and are presumed to be deep pits. Nutrient excretion rates per animal per day of 23 g N d^{-1} and 18 g P d^{-1}, typical of pumped deep-pit manure (Lorimer et al., 2000), were used to estimate the potential load of nutrients that could be produced by each operation assuming full livestock occupancy. This totals approximately 9.9 kg N y^{-1} and 6.6 kg P y^{-1} per square meter of building area. Assuming an N-based manure application of 200 kg N ha^{-1} for each year of corn, with about 433,500 m^2 of confined feeding operations in the watershed (based on digitized data), we estimate that 21,350 ha (27% of the watershed) has manure applied. This allows for NH_3 volatilization losses of 10%, which is a conservative value for injection, the dominant practice in the area. The application results in an estimated volumetric rate of slurry application of 41.1 m^3 ha^{-1}, which is within the range of injection application rates, reported by Lory et al. (2004), for a representative set of confined swine operations with deep-pit manure storage in this region.

The locations of manure-applied land were modeled by spreading N from each facility to increasingly sized circles (in 40 m radius increments, without overlap) (Figure 2) until the area could accept the N loading from the facility at a 200 kg N ha^{-1} rate for corn (100 kg N ha^{-1} y^{-1}). The rates were modified for the rotation by assigning the full rate to continuous corn, and half the rate to the corn-soybean and soybean-corn rotation areas. This reflects the relative (and estimated) frequency of corn and assumes manure is not applied to soybeans.

Topographic Data

The basin was divided into 45 subbasins using the automated delineation tool in AVSWAT-X (DiLuzio et al., 2004a) based on the 30 m DEM (digital elevation model).

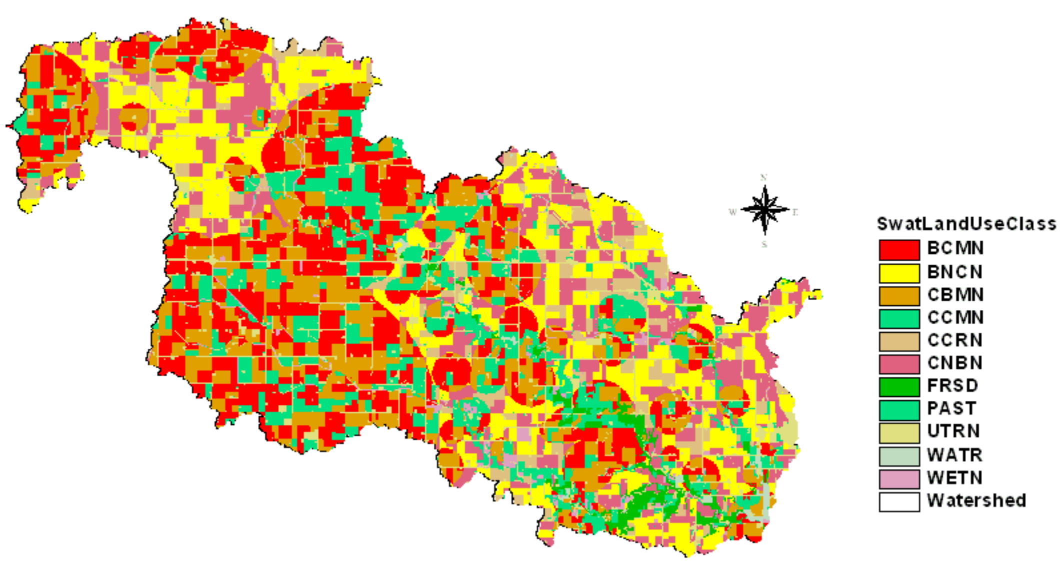

Figure 2. Land use classification and manure application areas for the SFW.

The tile mains are digitized from county records. The drainage districts tend to follow the watershed subbasins where there are intrinsically poorly drained soils. Approximately 80% of the agricultural land is tile drained. A standard tile drain depth of 2.5 m (depth to impermeable layer (depimp)) for the entire basin was used in this study to account for tile flow (Table 1). The tile drains were used to reduce the water content to field capacity with 24 hours; therefore, the time to drain (tdrain) soil to field capacity was set at 24 hours. The drain tile lag time (gdrain) and depth to drainage (ddrain) were set to 96 hours and 1 m, respectively (Table 1).

AVSWAT-X

The SWAT model was set up using AVSWAT-X, an upgrade of AVSWAT (ArcView GIS – SWAT) (Di Luzio et al., 2004a), a software system linking ArcView 3.x Geographic Information System software and the model. AVSWAT is designed to define watershed hydrologic features; store, organize, and manipulate the related spatial and tabular data; and analyze management scenarios. AVSWAT-X provides an extendable environment including optional customized capabilities, such as the SEA (SSURGO Extension for AVSWAT), automatic calibration tool, the Land Use / Land Cover class splitting tool and others in preparation.

In AVSWAT-X, the SEA extension (Di Luzio et al., 2004b) has been applied to process and manage the variously formatted SSURGO (Soil Survey Geographic) data sets and to create the needed digital soil maps, generate and store the required soil physical and hydraulic model input parameters derived from pedo-transfer functions, and seamlessly include them in the South Fork watershed modeling framework. The soil surveys data sets processed for the South Fork watershed include Hardin and Hamilton counties.

Model Evaluation and Calibration Methods

SWAT2003 was calibrated to the South Fork watershed's average annual flow. The SF450 USGS gage station discharge data from 1996-2001 were used for the calibration and validated from 2002 and 2003. The parameters adjusted for calibration are listed in Table 1. Due to tile flow, more parameters were altered for calibration than are usually required. The soil evaporation compensation coefficient (esco), CN2 (condition II runoff curve number), FFCB (initial soil water storage expressed as a fraction of field capacity water content), PHU (potential heat unit), Surlag (surface runoff lag time), and ICN (based on the SCS runoff curve number procedure and a soil moisture accounting technique) and its CNcoeff (curve number coefficient) (Williams and LaSeuer, 1976) were kept within reasonable ranges.

Table 1. SWAT2003 Input parameters for calibration and validation for South Fork Watershed site 450.

ESCO	FFCB	CN2	CNcoeff	Surlag (days)	Depimp (mm)	Ddrain (mm)	Tdrain (h)	Gdrain (h)	PHU
0.5	0.8	-12	0.5	0.35	2500	1000	24	96	1500

Results and Discussion

Water Balance

Initial calibrations of SWAT were performed based on the measured annual stream discharge data at the 450 site of SFW from 1996-1999 (Table 2). The annually averaged simulated stream discharge (251.8 mm) is 98% of the measured average value (257.2 mm). The validation period of 2000 through September, 2004 resulted in the simulated average discharge (171.6 mm) accounting for 88% of the measured average discharge (194.1 mm). The water balance breaks down accordingly: precipitation 787.4 mm; ET 557 mm; groundwater flow 10.6 mm; tile flow 102.9 mm; lateral soil flow 5.7 mm; and surface flow 109.7 mm. The baseflow ratios for the USGS filtered and SWAT2003 simulation were 65% and 53%, respectively. We assumed that baseflow from SWAT included tile flow, lateral soil flow, and groundwater flow. The lower value for the SWAT2003 simulated baseflow ratio may indicate that the tile flow component could be higher, therefore resulting in a greater baseflow value.

Table 2. Comparison of measured and simulated stream discharge for SFW.

Year	Measured (mm)	Simulated (mm)
1996	179.0	129.6
1997	295.7	257.8
1998	424.5	389.0
1999	331.7	328.0
2000	37.6	83.7
2001	274.5	322.4
2002	221.4	187.9
2003	170.0	203.3
2004	191.0	123.6
Ave.	236.2	225.0

Table 3 provides the descriptive statistics demonstrating that there is no statistically significant difference (α=0.05) between the means and variance for the measured and simulated values annually or monthly. The annual comparison included all of the values from 1996 to 2004 while the monthly included the events (22) that had measured stream discharge values greater than 30 mm. Du et al. (2003) also found a lack of statistical significance between the measured and SWAT2003 simulated annual data. They found that SWAT2003's simulated discharge values were closer to measured values than that of SWAT2000.

Table 3. Annually and monthly comparisons of the measured and simulated data for the SFW at USGS site SF450.

	Measured	Simulated	Measured	Simulated
	Annually (mm)		Monthly (mm)	
Mean	236.2	225.0	54.5	55.8
Standard deviation	111.2	105.7	1.8	4.2

The coefficient of determination, R^2, and Nash-Sutcliffe coefficient, E_{NS}, (Nash et al., 1970) are included in Table 4. With the exception of 2000 and 2004 the average relative percent difference between measured and simulated values was 14.6% ranging from 1.1% (1999) to 27.6% (1996). The yearly R^2 values are acceptable while the validation E value raises concern regarding SWAT2003's ability to accurately simulate discharge through 2003 and September, 2004. E values for the annual calibration and validation periods were 0.95 and 0.25, respectively, indicating that SWAT2003 did not satisfactorily simulate annual streamflow; however, the water balance values are within the appropriate ranges.

Table 4. E and R^2 values for monthly and annual discharge at SF450 of SFW.

	R^2	E_{NS}	R^2	E_{NS}
	Annually		Monthly	
Calibration (96-99)	0.98	0.95	0.87	0.57
Validation (00-04)	0.72	0.25	0.84	0.23

To gain insight into this annual discrepancy, we evaluated the monthly flows (Figure 3).

The largest measured and simulated monthly discharge event (June, 1998) had the values of 148.4 mm and 145.5 mm, respectively. The second largest event (May, 1999) had less than a 4% flow difference. After these two events, the disparity between the measured and simulated flows varies considerably for nine out of the next 15 events. SWAT2003 overestimated discharge by an average of 37 mm (64% of simulated data) for five out of 15 of the largest events and underestimated four of the 15 largest events by 31 mm (56% of measured data). This indicates that no clear trend existed for over- or underestimation by SWAT2003.

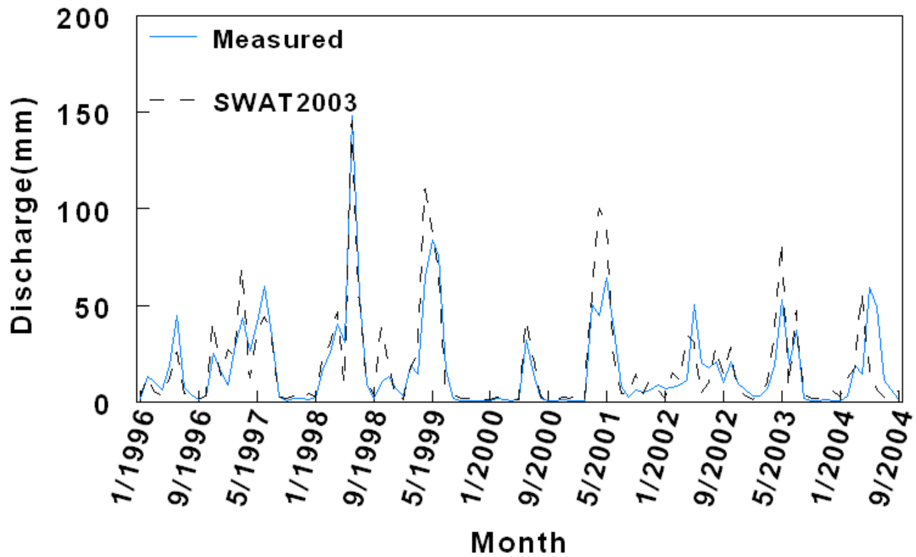

Figure 3. Monthly simulated and measured discharge at USGS site SF450 of SFW.

The calibration period contained one dry year which was balanced by the other years which included large discharge events resulting in a high E value. Because the validation period did not contain discharge events as large as the ones in 1998 and 1999, we reevaluated which years should be considered the calibration and validation periods. These periods were also assessed since an extended dry period did not exist in the calibration years. As a result, the calibration period was changed from 1996 to 1998 and the validation period from 1999-2002. With this new division, each period contained one of the two largest events and the dry years that were not present during the calibration period were removed. The annual calibration and validation R^2 values became 0.97 and 0.88 and the E values became 0.84 and 0.52, respectively. The monthly calibration and validation R^2 values changed to 0.86 and 0.81 while the E values became 0.86 and 0.62, respectively. These E value improvements reveal that the simulated yearly and monthly streamflows for the calibration and validation periods were well matched to the measured data. The alteration to the calibration and validation years indicates that in order to satisfactorily validate cyclic data, the calibration period must contain those cycles as well.

Conclusion

The SWAT2003 model with a modified tile drain component was evaluated for nine years of measured flow in SFW. A downstream USGS gaging station (SF450) was used as the outlet site of the SFW and was selected to investigate the overall performance of SWAT2003. The presence of subsurface tile drainage systems can facilitate nutrient transport thereby increasing environmental pollution concerns. For this paper, the interest in tile drainage was for its contribution to the water balance. Without its inclusion, the surface flow was overestimated resulting in a disproportioned water balance. The baseflow ratio for the SWAT2003 simulation's first pass was slightly low, indicating that additional work is needed in the tile drainage portion. While the initial calibration descriptive statistics (R^2 values, means, standard deviations, and average annual discharge) for streamflow were promising, the validation E values demonstrated that the monthly (and daily) parameters should be further evaluated. However, after reallocating the calibration and validation periods to include both wet and dry cycles, the validation E values increased significantly. Overall, the monthly results were not as good as the annual results.

References

Arnold, J.G., B. Du, A. Saleh, and D.B. Jaynes. 2003. Application of Soil and Water Assessment Tool (SWAT) to landscapes with tiles and potholes. Part I. Development of new procedures. (Submitted).

Baker, J.L., K.L. Campbell, H.P Johnson, and J.J. Hanway. 1975. Nitrate, phosphorus, and sulfate in subsurface drainage water. J. Environ. Qual. 4:406-412.

Becher, K.D., S.J. Kalkhoff, D.J. Schnoebelen, K.K. Barnes, and V.E. Miller. 2001. Water-Quality Assessment of the Eastern Iowa Basins – Nitrogen, Phosphorus, Suspended Sediment, and Organic Carbon in Surface Water, 1996-98. U.S. Geological Survey Water-Resources Investigations Report 01-4175. Iowa City, IA.

Di Luzio, M., J.G. Arnold, and R. Srinivasan 2004b. Integration of SSURGO maps and soil parameters within a geographic information system and nonpoint source pollution model system. Journal of Soil and Water Conservation, 59: 123-133.

Di Luzio, M., Srinivasan R., Arnold J.G. 2004a. A GIS-Coupled Hydrological Model System for the Watershed Assessment of Agricultural Nonpoint and Point Sources of Pollution. Transactions in GIS, 8: 113-136.

Logan, T.J., D.J. Eckert, and D.G. Beak. 1994. Tillage, crop and climatic effects on runoff and tile drainage losses of nitrate and four herbicides: Soil Tillage Res. 30:75-103.

Lorimer, J., W. Powers, and A. Sutton. 2000. Manure Characteristics. MWPS-18. Midwest Plan Service. Ames IA.

Lory, J.A., R.E. Massey, J.M. Zulovich, J.A. Hoehne, A.M. Schmidt, M.C. Carlson, and C.D. Fulhage. 2004. An assessment of nitrogen-based manure application rates on 39 US swine operations. J. Environmental Quality. 33:1106-1113.

Mausbach, M.J. and A.R. Dedrick. 2004. The length we go: Measuring environmental benefits of conservation practices. J. Soil and Water Conservation. Vol. 59, p. 96-103.

Nash, J.E. and J.E. Sutcliffe. 1970. River flow forecasting through conceptual models. Part I – A discussion of principles. J. Hydrol. (Amsterdam) 10:282-290.

National Cooperative Soil Survey. 1985. Soil Survey of Hardin County Iowa. USDA- Soil Conservation Service, and Iowa State University Cooperative Extension Service. U.S. Govt. Printing Office, Washington, D.C.

Soil Survey Staff. 2003. Keys to Soil Taxonomy, 9th Ed. [Online] Available at: Http://soils.usda.gov/technical/classification/tax_keys/keysweb.pdf . NRCS, Washington, D.C.

Williams, J.R. and W.V. LaSeuer. 1976. Water Yield Model Using SCS Curve Numbers. J. Hydraulics Division, ASCE, 102 (HY9), Proc. Paper 12377. pp. 1241-1253.

Wood, E.D., F.A.J. Armstrong, and F.A. Richards. 1967. Determination of nitrate in seawater by cadmium-copper reduction to nitrite. J. Marine Biology. 47:23-31.

An Analysis of Non-point Source Pollution in a Stock Breeding Area of the Heihe River Basin

Fanghua Hao*[1], Hongguang Cheng[1], Shengtian Yang[1], Ye Qi[1], and Xiyan Ren[1]
[1]School of Environment, State Key Laboratory of Water Environment Simulation, Beijing Normal University, Beijing, 100875, China. Email: fanghua@bnu.edu.cn

Abstract

A GIS-based distributed SWAT (Soil and Water Assessment Tool) model was used to simulate the runoff, sediment yield and non-point source pollution load in the Heihe River Basin. The Heihe River is a tributary and the main water supply source of the Yellow River. The Heihe River Basin is a typical stock breeding area, and the industry and agriculture are not developed. The main pollution source of the Heihe River is non-point source pollution from raising livestock. With GIS and RS techniques, the non-point source pollution database in the Heihe River Basin was established. Analysis of the SWAT model and typical parameters for the Heihe River Basin were examined. Pollution load and transportation rules for pollutants such as nitrogen are illustrated.

Key words: Non-point source pollution, stock breeding, SWAT, Heihe River

Introduction

Studies of non-point source pollution were extended to several aspects such as the investigation, model theory, pollution load evaluation, effective factors, best management practices for pollution control, and load cutting measurements. All of the aspects of agricultural non-point source pollution studies were sufficient; however, the study of the non-point source pollution from the stock breeding was not. Thus, it is important to study the processes in the pasture.

The Heihe River Basin is the main runoff supplier for the Yellow River and is located in the Sichuan Province, which is the main pasturing area in China. It plays a key role in water protection for the Yellow River Basin.

SWAT (Soil and Water Assessment Tool), a distributed hydrological model, was selected to simulate long-term runoff and sediment yield in the study area. The model has been used in several projects by the USEPA, NOAA, NRCS and others to estimate the off-site impacts of climate and management on water use and non-point source loads, and has been extensively validated across the United States for stream flow and sediment yields (Arnold *et al.*, 1998).

Methodology

SWAT Model Description

SWAT is a hydrological water quality model developed by the United States Department of Agriculture-Agricultural Research Service (USDA-ARS) (Santhi *et al.*, 2001). It is a continuous time model that operates on a daily time-step. A modified version of the SCS CN method was used in SWAT for predicting surface runoff yield (USDA-SCS, 1972) (Equations 1 and 2):

$$Q = \frac{(R - 0.2S)^2}{(R + 0.8S)} \qquad R > 0.2\mathrm{S} \qquad (1)$$

$$Q = 0 \qquad R \leqq 0.2\mathrm{S} \qquad (2)$$

where Q is the daily surface runoff (mm), R is the daily rainfall (mm), and S is a retention parameter. S varies among basins under various soil, land use, management, and slope conditions, and over time responding to changes in soil water content. The parameter S is related to curve number (CN) by (Equation 3):

$$S = 25.4\left(\frac{1000}{CN} - 10\right) \qquad (3)$$

Erosion and sediment yield are estimated for each subbasin with the Modified Universal Soil Loss Equation (MUSLE) (Williams, 1975) (Equation 4):

$$Y = 11.8(Vq_p)^{0.56}(K)(C)(PE)(LS) \qquad (4)$$

where Y is the sediment yield from the subbasin, V is the surface runoff column for the subbasin in m^3, q_p is the peak flow rate for the subbasin in $m^3\ s^{-1}$, K is the soil erodibility factor, C is the crop management factor, PE is the erosion control practice factor, and LS is the slope length and steepness factor.

Channel routing consists of flood and sediment routing. The flood routing model uses a variable storage coefficient method developed by Williams (Williams, 1969). Channel inputs include the reach length, channel slope, bankfull width and depth, channel side slope, flood plain slope, and Manning's *n* for channel and floodplain. Flow rate and average velocity are calculated using Manning's equation, and travel time is computed by dividing channel length by velocity. Outflow from a channel is also adjusted for transmission losses, evaporation, diversions, and return flow. The channel sediment routing equation uses a modification of Bagnold's sediment transport equation that estimates the transport concentration capacity as a function of velocity (Bagnold, 1977) (Equation 5):

$$CY_u = SPCON * V^{SPEXP} \qquad (5)$$

where CY_u is the sediment transport concentration capacity in g m^{-3}; $SPCON$ is the concentration capacity in g m^{-3} at a velocity of 1m s^{-1}; V is flow velocity in m s^{-1}; and $SPEXP$

is a constant in Bagnold's equation. The SWAT model either deposits excess sediment or reentrains sediments through channel erosion depending on the sediment load entering the channel.

Study Area Description

The Heihe River Basin (Figure 1) with an area of 7,241 km^2 is characterized by grassland and swamp landscape. The Ruoergai Grassland is located in the south part of the basin, the Maqu Grassland in the north. This area belongs to the altiplano seasonal climate zone, and the annual average precipitation is about 400–650 mm. Land uses in this basin are mostly pasture and swamp in the upper reaches while pasture and forest are widely spread in the lower reaches. The major soil types are peat bog from the low to high elevation area.

Development of the Database for Heihe River Basin

The basic database for the Heihe River Basin was established using ArcView, which mainly includes topography, soil and land use maps, as well as climate and land management data (Table 1). Initially, the basin was delineated into subbasins using the digital elevation map. The delineated subbasin map was then overlaid with land use and soil maps. The SWAT model simulates different land use classes in each subbasin.

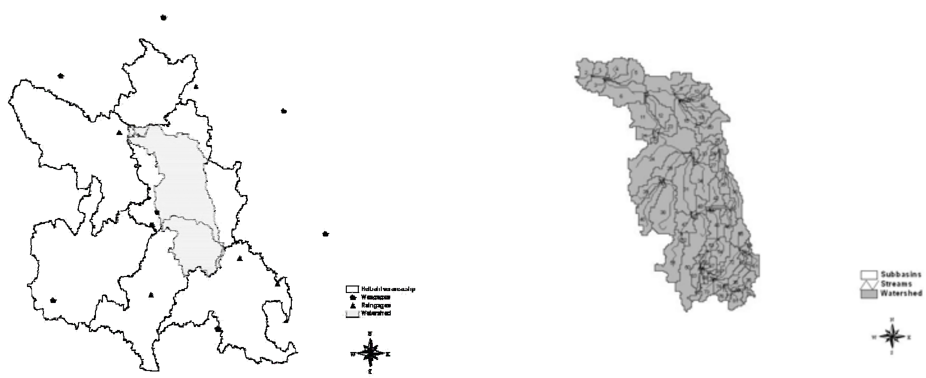

Figure 1. Map of the study area.

Evaluation of model output

Mean, Relative error (*Re*), coefficient of determination (R^2), and Nash-Sutcliffe efficiency (E_{ns}) (Nash & Sutcliffe, 1970) were used to evaluate model performance. The R^2 is an indicator of strength of relationship between the observed and simulated values. E_{ns} indicates how well the plot of the observed value versus the simulated value fits the 1:1 line. If the R^2 and E_{ns} values are less than or very close to zero, the model performance is considered "unacceptable or poor". If the values are equal to one, then the model prediction is considered to be "perfect".

Table 1. Data sources for the Heihe River Basin.

Data Type	Source	Scale	Data Description/Properties
Topography	National Geomatics Center of China	1:250,000	Elevation, overland, and channel slopes, lengths, etc.
Soil	Institute of Soil Science, Chinese Academy of Sciences (CAS)	1:4,000,000	Soil classifications and physical properties such as bulk density, texture, saturated conductivity, etc.
Land use	Institute of Geographical Sciences and Natural Resources Research, CAS	1:1,000,000	Land use classifications such as cropland, pasture, forest, etc.
Weather	Water Resources Conservancy Committee of the Yellow River Basin	–	Daily precipitation, air temperature, relative humidity, solar radiation and wind speed, etc.
Land Management	On-site surveys	–	Tillage, planting and harvesting dates for different crops.

Model Calibration

SWAT is not a "parametric model" with a formal optimization procedure (as part of the calibration process) to fit any data. Instead, a few important variables that are not well defined physically such as runoff curve number and Universal Soil Loss Equation's cover and management factor, or *C* factor, may be adjusted to provide a better fit. A two stage "Brute Force" optimization procedure is used to find the optimum parameter values (Allred & Haan, 1999). This "brute force" optimization procedure, despite its lower computational efficiency than other methods, has the advantage of being insensitive to local minimums in the objective function.

Initially, baseflow was separated from surface flow for both observed and simulated streamflow using an automated digital filter technique (Arnold & Allen, 1999). Calibration parameters for various model outputs are constrained within the ranges shown in Table 2. Model outputs are calibrated to fall within a percentage of average measured values and then regression statistics (R^2 and E_{ns}) are evaluated for monthly data. If all parameters were pushed to the limit of their ranges for a model output (i.e., flow or sediment) and the calibration criteria were still not met, then calibration would be terminated for that output.

Table 2. Inputs used in model calibration.

Variable	Processes	Description	Range	Value/Change
CN_2	Flow	Curve Number	±4	Pasture: +3 Forest: -2 Bare land: +2
REVAPC	Flow	Ground water re-vaporize coefficient	0.00 to 1.00	0.20
ESCO	Flow	Soil Evaporation compensation factor	0.00 to 1.00	0.6
EPCO	Flow	Plant uptake compensation factor	0.00 to 1.00	0.2
SMFMN	Flow	Melt factor for snow on December 21	0 to 10	6.5
C Factor	Sediment	Cover or management factor	0.003 to 0.45	Pasture: 0.01 Forest: 0.08
SPCON	Sediment	Linear factor for channel sediment routing	0.0001 to 0.01	0.0006
SPEXP	Sediment	Exponential factor for channel sediment routing	1.0 to 1.5	1.2

Flow: With the combination of the stream flow from 1993 to 1997, obtained from the Water Conservancy Committee of the Yellow River's monitoring station (Dashui hydrological station), the SWAT model was calibrated. The runoff curve number (CN_2) was adjusted using surface runoff data to allow a range of ±4 from the tabulated curve numbers to reflect the impact of conservation tillage practices and soil residue cover conditions in the basin (Table 2). For base flow, related model parameters such as the re-evaporation coefficient (*REVAPC*) for ground water that represents the water that moves from the shallow aquifer back to the soil profile/root zone and plant uptake from deep roots, soil evaporation compensation factor (*ESCO*), and plant evaporation compensation factor (*EPCO*) were adjusted from the initial estimates to match the simulated and observed baseflow (Table 2). Finally, in order to match the streamflow, minimum melt factor for snow (SMFMN) was adjusted for snow-melt periods.

Sediment: The cover, or *C* factor, of the Universal Soil Loss Equation was adjusted to match observed and simulated sediment loads. The *C* factor was adjusted to better represent the surface (Table 2). Channel sediment routing variables such as the linear factor (*SPCON*) and the exponential factor (*SPEXP*) for calculating the maximum amount of sediment reentrained during channel sediment routing are also adjusted (Table 2) in the process of sediment calibration. These two variables are adjusted to represent the cohesive nature of the channels.

Model Validation

In the validation process, the model is operated with parameters obtained in the process of calibration without any change and the results are compared with the remaining observational data (from January 1998 to December 1999) to evaluate the model performance. The same statistical measures are used to assess the model performance.

Model Calibration and Validation Results

Calibration

Flow: The measured and simulated monthly flow at the Dashui hydrological station match well (Figure 2(a)). Further agreement between observed and simulated flows are shown by the R^2 and E_{ns}, both are larger than 0.75 (Table 3). These results show that the hydrological processes in SWAT are simulated realistically in the study area.

Sediment: The temporal variations of sediment load at the Dashui station are represented in Figure 2(b). Means of observed and simulated sediment are within a difference of 15% (Table 3). The values for R^2 and E_{ns} are both larger than 0.70 (Table 3), which indicates that the simulated sediment is close to the observed sediment and this model is able to predict sediment loads well.

Validation

Flow: The observed and simulated flows at the Dashui hydrological station matched well (Figure 3(a)). *Re* is -9.2%, R^2 and E_{ns} are all greater than 0.75. The difference might result from the spatial variability of precipitation. However, the prediction statistics are acceptable (Table 4).

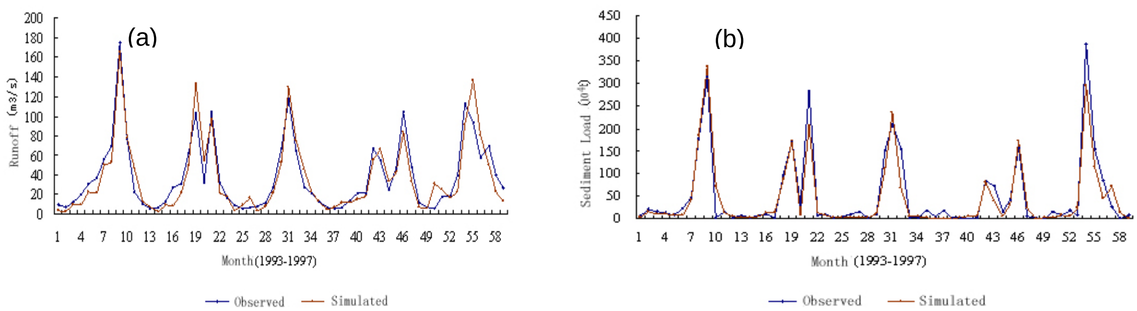

Figure. 2 Observed and simulated monthly flow and sediment loads during the calibration period.

Table 3. Calibration results at the Dashui hydrological station for the period from 1992 to 1997.

Variable (units)	Annual mean observed	Annual mean simulated	Re	R^2	E_{ns}
Flow (m^3/s)	38.46	37.01	-3.8%	0.80	0.78
Sediment (10^4 t)	10.5	8.82	11.2%	0.70	0.74

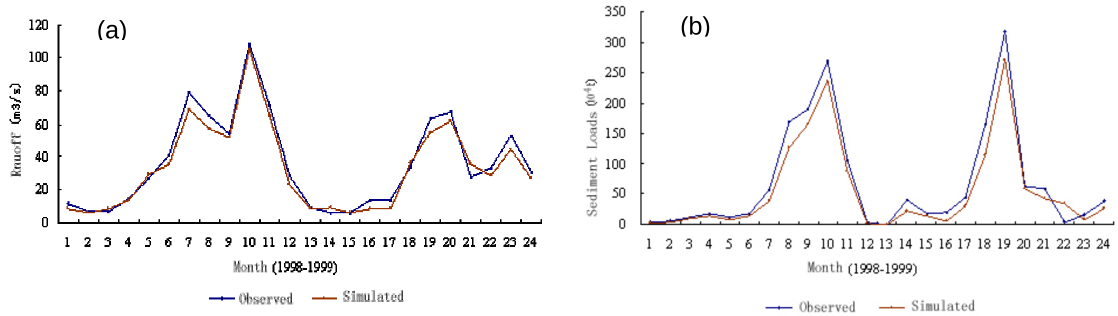

Figure 3. Observed and simulated monthly flow, and sediment loads during the validation period.

Table 4. Validation results at the Dashui hydrological station for the period from 1998 to 1999.

Variable (units)	Annual mean observed	Annual mean simulated	*Re*	R^2	E_{ns}
Flow (m^3/s)	31.01	28.18	-9.2%	0.78	0.76
Sediment (10^4 t)	13.22	11.12	–19.2%	0.78	0.76

Sediment: The observed and simulated sediment loads match well (Figure 3b). The values of R^2 and E_{ns} are both above 0.9, which indicates that the model is able to predict sediment reasonably well. The reason for high R^2 and E_{ns} values may be that the sediment yield in 1998 was much greater than the sediment yield in 1999. As the "goodness-of-fit" of observed and simulated data in 1998 is good, the results are acceptable even though the results do not match well in 1999. The results to some extent indicate that the SWAT model is more suitable for high flow years than low flow years

Calibration and Validation of NH3-N

The observed monthly NH_3-N average loading from 1998 was used for model parameter calibration (Figure 4(a)) while the data from 1999 was used for model validation (Figure 4(b)). The difference might result from the spatial variability of precipitation. However, the prediction statistics are acceptable (Table 5).

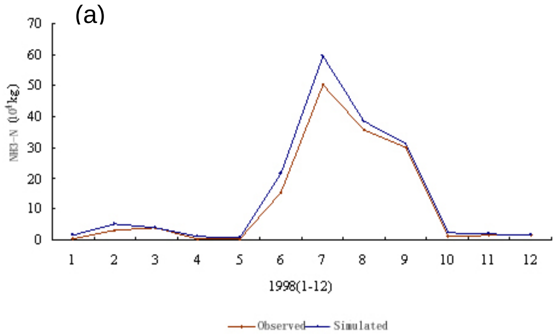

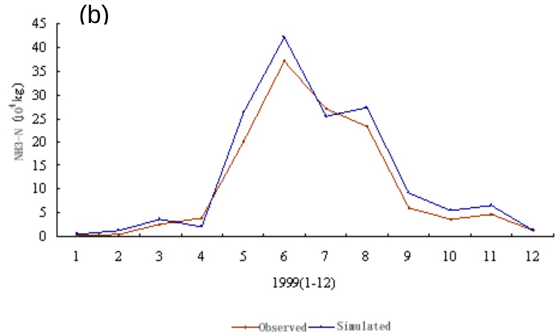

Figure 4. Observed and simulated monthly NH3-N during the calibration and validation periods.

Table 5. NH3-N results at the Dashui hydrological station for the period from 1998 to 1999 (10^4kg).

Period	Annual mean		*Re*	R^2	E_{ns}
	observed	simulated			
Calibration	2.62	1.29	-12.2%	0.75	0.76
Validation	2.52	1.06	-16.7%	0.74	0.72

Status of Stock breeding in the Heihe River Basin

According to the stock breeding status of the Heihe River Basin, including two counties, the percentage of cows was 45.6%, the percentage of horses was 12.7%, and the percentage of goats was 38.6%. The percentage of poultry was 3.1%. The actual number for stock breeding is 216.38×10^4. The coefficient of pollution is determined by the livestock breeding book (Tables 6 and 7).

Table 6. Annual soil load for livestock in the Sichuan Province (kg/livestock).

Livestock	Ordure	BOD_5	COD_{Cr}	NH_3-N
Cow	14,600	292	401.5	73
Horse	1,080	36	47.88	7.2
Goat	600	24	33	6.1
Poultry	2.75	0.2475	0.495	0.033

Table 7. Average content of nitrogen in Ordure and Stale of livestock (kg/ton).

Livestock	Cow		Horse		Goat		Poultry
Index	Ordure	Stale	Ordure	Stale	Ordure	Stale	
Total Nitrogen	4.37	8	5.88	3.3	7.5	14	9.84

The pollution capacity of the livestock is calculated by the following formula (Equation 6):

$$Q_i = q_i \times S_i \times N \qquad (6)$$

where Q_i is the pollution capacity; q_i is the average content of nitrogen in Ordure and Stale of livestock; S_i is the percentage of the livestock in the stock breeding structure; N is the number for stock breeding.

Results and Discussion

Table 8. The loads of non-point source pollution in 2000 in the Heihe River Basin (10^4kg).

Year	Adsorption Nitrogen	Solve Nitrogen	NH3-N
2000	231.8	106.0	28.4

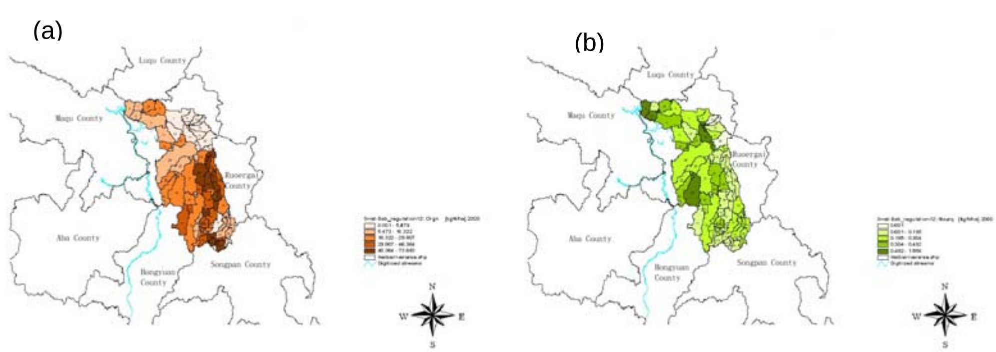

Figure 5. The distribution of Nitrogen (a) Adsorbed Nitrogen; (b) Dissolved Nitrogen.

The non-point source load and the rules for pollution load distribution in the Heihe River Basin in 2000 were analyzed. The most distributed areas were in the southeast part of the basin. This is because the pasturing areas are located in the southeast portions of Ruoergai county and in the northern portions of Hongyuan county. Furthermore, the precipitation and sediment load are also heavy in these areas.

Conclusions

The observed monthly runoff and sediment yield data from the Dashui Hydrological gauge during 1993-1997 was used for parameter calibrations; data from 1998-1999 was used for model validation. From the model results, the relative simulated error was less than 15%; both the relative coefficient and Nash-Sutcliffe coefficient were greater than 0.7, indicating that the model can simulate the runoff and sediment outputs in the study area satisfactorily.

The suitable parameters of stock breeding in Heihe River Basin were formulated and can be used for other similar basins if validated.

The spatial distribution of the non-point source pollution was different from the stock breeding distribution.

Acknowledgements

This study was supported by the Major State Basic Research Development Program, “Evolving Law and Maintaining Mechanism of Renewable Capacity of Water Resources in the Yellow River Basin” (no. G1999043601). The authors would like to thank Dr. Yiguo Han from the Stockholm Environment Institute, Sweden, for providing detailed advice that contributions to improving and refining the paper.

References

Allred, B. & Haan, C. T. (1996) Small watershed monthly hydrologic modeling system. Users Manual, Biosystems and Agricultural Engineering Department, Oklahoma State University, Stillwater, Oklahoma, USA.

Arnold, J.G. & Allen, P.M. (1999) Automated methods for estimating baseflow and groundwater recharge from stream flow records. *J. Am. Water Resour. Assoc.* 35(2), 411–424.

Arnold, J.G., Srinivasan, R., Muttiah, R.S. & Williams, J.R. (1998) Large area hydrologic modelling and assessment part i: model development. *J. Am. Water Resour. Assoc.* 34(1), 73–89.

Bagnold, R.A. (1977) Bedload transport in natural rivers. *Water Resour. Res.* 13(2), 303–312.

Chaubey, I., Haan, C.T., Grunwald, S. & Salisbury J. M. (1999) Uncertainty in the model parameters due to spatial variability of rainfall. *J. Hydrol.* 220, 48–61.

FitzHugh, T.W. & Mackayb, D.S. (2000) Impacts of input parameter spatial aggregation on an agricultural nonpoint source pollution model. *J. Hydrol.* 236, 35–53.

Guo, J.M. & Zheng J.L. (1995) *Yearbook of Yiluohe River*. China Science and Technology Press, Beijing, China.

Liu G.H, Cai Q.G, Zhu, H.Y. & Tang Z.H. (2003) Simulation of runoff and sediment flow in a catchment based on landunit flow networks. *Progr. Geogr.* 22(1), 71–78 (in Chinese).

Nash, J.E. & Sutcliffe J.V. (1970) River flow forecasting through conceptual models, Part I.

A discussion of principles. *J. Hydrol.* 10(3), 282–290.
Niu, Z.M., Xie, M.S., Sun G., McNulty, S.G. (2001) Applying ANSWERS2000 to Simulate Soil Erosion Process on Two Watersheds of Three Gorges Area. *J. Soil Water Conserv.* 15(3), 56–60 (in Chinese).
Saleh, A; Arnold, JG; Gassman, PW;hauck, LM; Rosenthal, WD; Williams, JR;mcFarland, AMS. Application of SWAT for the upper North Bosque River Watershed. Transactions of the ASAE [Trans ASAE], vol. 43, no. 5, pp. 1077-1087, Sep 2000.
Santhi, C., Arnold, J.G., Williams J.R., Dugas W.A., Srinivasan R. & Hauck L.M. (2001) Validation of the SWAT model on large river basin with point and nonpoint sources. *J. Am. Water Resour. Assoc.* 37(5), 1169–1188.
Srinivasan, Raghavan; Ramanarayanan, Tharacad; Arnold, Jeffrey; Bednarz, Steven. Simulation ofhydrology and erosion in a Texas watershed using SWAT. IAHS Publication (International Association ofhydrological Sciences) [IAHS Publ], no. 253, pp. 175-183, 1998.
USDA-SCS (1972). *National Engineering Handbook*, hydrology Section 4, chap. 4–10. US Dept. of Agriculture, Soil Conservation Service, Washington, DC, USA.
Williams, J.R. (1969) Flood routing with variable travel time or variable storage coefficients. *Trans. ASAE* 12(1), 100–103.
Williams, J.R. (1975) Sediment routing for agricultural watersheds. *Water Resour. Bull.* 11(5), 965–974.

Modelling the Effects of Land Use and Climate Change on Hydrology and Soil Erosion in a Sub-humid African Catchment

H. Busche*, C. Hiepe and B. Diekkrüger
* Department of Geography, University of Bonn, Meckenheimer Allee 166, 53115 Bonn, Germany. E-mail: hbusche@giub.uni-bonn.de

Abstract

Facing aggravating climatic and socioeconomic conditions the sustainable management of water and soil resources is becoming increasingly important for West Africa. This study analyzes hydrological and erosive processes caused by water in the Terou Catchment in the sub-humid savannah zone of Benin, West Africa, considering land use and precipitation changes for the period 2000 to 2025.

The land use scenarios describe a continuous expansion of farmland. A simple method for disaggregating the coarse data has been developed and assessed. The precipitation scenarios generally indicated a decrease in rainfall in the study area. Considering the high interannual and interdecadal variability of rainfall in the study area, a continuous simulation is desirable. Using a weather generator, precipitation series were generated, which included the changes in monthly precipitation derived from the regional climate model REMO. Due to the fact that the weather generator performed poorly in matching the extreme events, the erosion rates that were simulated on the basis of simulated rainfalls had to be regarded critically. It was found that the SWAT2003 model is appropriate to consider changes in land use and precipitation. The land use scenarios resulted in an increase in surface runoff, whereas the baseflow decreased. Additionally, increases in runoff variability led to a higher flood risk. The changes in precipitation account for changes in total runoff, especially for the years 2020 and 2025, which showed very low runoff. This can be explained by the high levels of evapotranspiration, despite decreased precipitation.

The land use scenarios showed a significant increase in erosion rates. However, erosion rates on savannah that was recently converted to farmland were lower than on farmland that was cultivated for several decades. These differences can be attributed to spatial variations in physical soil properties.

Introduction

Water and soil are basic requirements for life on earth. It is well known that, especially in the periphery of dry zones, these resources are most susceptible. West Africa suffers periodically from droughts, which cause considerable damage to the environment and economy. Less obvious, but as hazardous as drought, is the process of soil erosion, which has the capability to endanger food security irreversibly. The development of these processes is highly dependent on issues referred to as Global Change. On the one hand, altered socioeconomic conditions lead to changes in land use patterns, on the other hand, changes in climate affect the hydrological cycle. Hence, the application of a hydrological model in the sub-humid savannahs of Benin is in the interest of both integrated water resources management and Global Change research.

This study was integrated with the IMPETUS project which investigates the effects of global change on the water cycle in two catchments in West Africa: the Drâa Catchment in Morocco and the Ouémé Catchment in Benin (SPETH et al. 2002). Within the project land use and climate scenarios have been generated in high spatial and temporal resolution. These scenarios enable modelling and quantifying the effects of Global Change on hydrological and erosive processes.

Below, the study area is briefly characterized; thereafter, the processing of the scenarios is described. After the discussion of the results further research activities are pointed out.

Study Area

The Terou Catchment is a subcatchment of the Ouémé River and is located between 9°N and 10°N (Figure 1). It is characterized by one rainy season from March to October. Dominating types of precipitation are squall-lines marking the beginning and end of the rainy season and monsoonal rainfalls in the central rainy season (Weischet and Endlcher, 2000). Squall-lines leading to convective spatially limited rainfalls of high intensity account for most of the precipitation in the study area (Leroux, 2001).

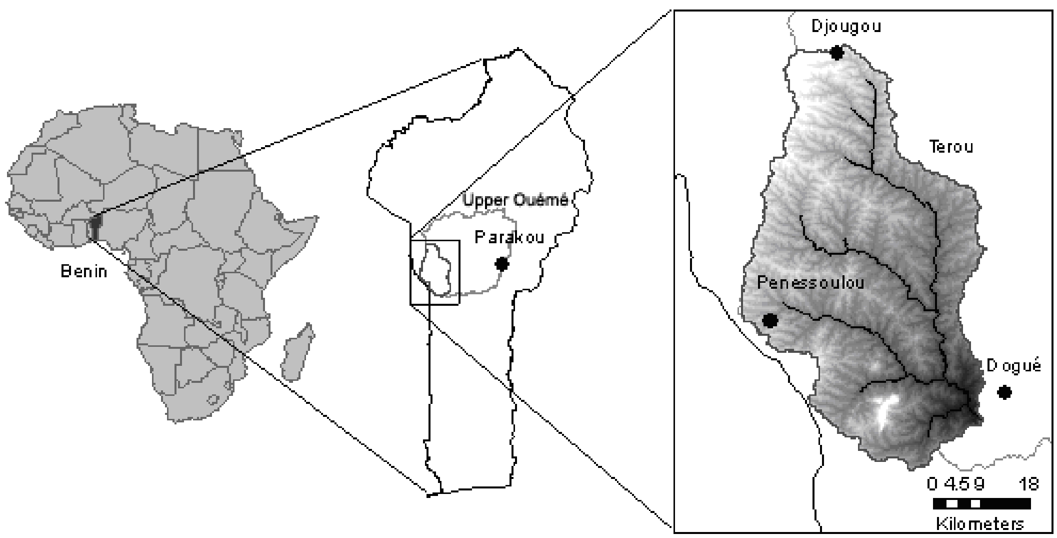

Figure 1. Terou Catchment (2,336 km², dark grey) within the Upper Ouémé Catchment (14,325 km², white).

Average annual rainfall in Parakou is about 1,100 mm, but is subject to considerable variation (1983: 642 mm, 1988: 1,614 mm) as precipitation shows high interannual and interdecadal variability in Western Africa (HULME et al. 2001). The study area is part of the Guinea-Sudan transition zone (Adjanohoun, 1989). Dense dry forests represent the climax vegetation, but have been widely replaced by different savannah types. Naturally, savannahs only appear where shallow or wet soils prevent the development of forests, but due to human activities such as burning, logging, farming, and raising cattle, savannahs represent the dominant land cover in the region (Will, 1996).

The local topography is dominated by a gently undulating pediplain with slopes less than three degrees. The landscape has been shaped by the alternation of sub-humid and sub-arid conditions which lead to polycyclic cutting of the inclined plane (Runge, 1990). Under present conditions no cutting takes place (Rohdenburg, 1969). The raw material for soil formation consists of layered fine-grained and gravely substrates over saprolite (Junge, 2004). The hill slopes are characterized by a typical catena which consists of plinthitic Acrisols on the upland, well-drained loamy and sandy Acrisols overlaying an impermeable crust on the mid-slope and predominantly sandy Gleysols in the hydromorphic zone of the valley bottom (Junge, 2004). Due to prevailing crusts, interflow constitutes a major fraction of runoff processes in the study area, whereas surface runoff only represents an important process in agricultural areas, but not in catchments with natural vegetation (Giertz, 2004).

Methodology

A comparison of different modelling approaches for the Terou Catchment with regard to modelling scenarios recommended a distributed approach for considering land use changes and a conceptual approach for simplifying upscaling (Bormann and Diekkrüger, 2003). SWAT fulfils both demands; hence, it is principally suited for this study. The model has already been successfully applied to the Terou Catchment (Sintondji, 2005). The data used are a global SRTM digital elevation model, a soil map 1:200,000 (Faurè and Volkoff, 1998), and a land use classification derived from satellite images. Soil and land use databases have been set up using field measurements or literature values. Precipitation data from five stations within the study area were used. Additional climate parameters were generated using data from Dogué and Parakou (Figure 1). The model was calibrated against discharge data at the catchment outlet for the period 1998-2001 and validated for the period 2002-2003. On a weekly time-step it performed satisfactory for the validation period (R^2=0.64, Coefficient of Model Efficiency=0.52, Index of Agreement=0.88). However, discharge was still overestimated, especially in the late rainy season, as displayed in the discharge hydrograph (Figure 2).

Additionally, the simulation was biased by a poor representation of interflow. The average fraction of simulated interflow for the period 1998-2003 was only 2.6%, which differs significantly from measured values (Giertz, 2004). It was found that the major part of the interflow was included in the simulated baseflow, whereas simulated surface runoff, crucial for determining erosion rates, was within a realistic range.

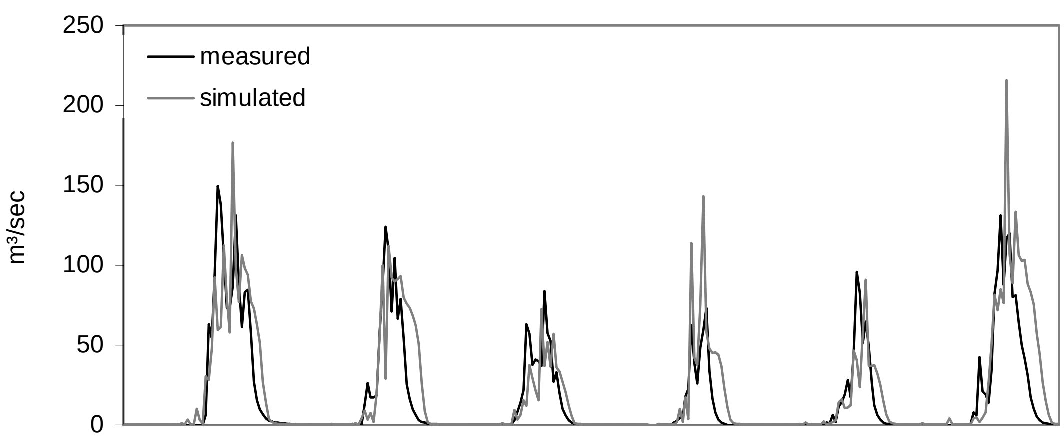

Figure 2. Weekly mean of simulated and measured discharge of the Terou Catchment (2.336 km²). Calibration period 1998-2001, validation period 2002-2003.

The precipitation scenarios have been generated with the regional climate model REMO (Paeth, 2004). They were based on assumptions similar to the IPCC Scenario B2 but have been adapted to regional conditions considering land degradation (IPCC, 2001; Paeth, 2004). REMO produced precipitation data for a 0.5° grid covering West Africa. Two of these grid cells have been selected for this work. Figure 3 displays the simulated monthly precipitation for the years 2000, 2005, 2010, 2015, 2020 and 2025.

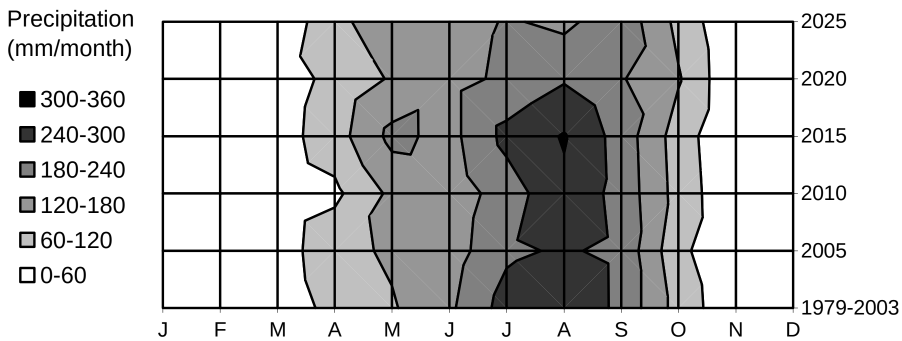

Figure 3. Simulated monthly precipitation as well as measured mean values (1979-2003) in the Terou Catchment.

Generally, the scenarios tend toward an increase in precipitation in May and October, and a decrease in August and September (Figure 3). The REMO data could not be used in SWAT directly, as they represent areal and not site-specific precipitation. This led to a considerable underestimation of rainfall intensities (Figure 4). Therefore a weather generator, set up with records from the Djougou and Penessoulou stations, was used to generate a site-specific precipitation series of 100 years, which reflects the forecasted changes in monthly precipitation. A comparison of the weather-generators WXGEN (implemented in SWAT) and LARS-WG (stand-alone) confirmed the latter to be me more exact because of the semi-empiric approach used in LARS-WG. This makes LARS-WG more flexible in simulating precipitation distributions than the Markov-chain used in WXGEN. This result is supported by findings from other climate zones (Semenov et al., 1998). Rainfall series generated with LARS-WG represent the rainfall intensities well for the observed period (Figure 4). However, extreme events of the future rainfall series may have been misjudged, as LARS-WG scales daily precipitation with a factor derived from monthly data, decreasing or increasing every event. The comparison of the generated rainfall series intensities from 2015 and 2025 illustrates this. The increase in total precipitation in 2015 leads to a curve of rainfall intensities which is shifted to the right, whereas the decreased amount of total rainfall in 2025 leads to a curve shifted to the left (Figure 4). Although average values are within the range of standard deviation for measured values, erosion rates derived from simulated rainfalls have to be interpreted carefully. But as no other information concerning the future change in frequency distribution is available this approach seems to be adequate.

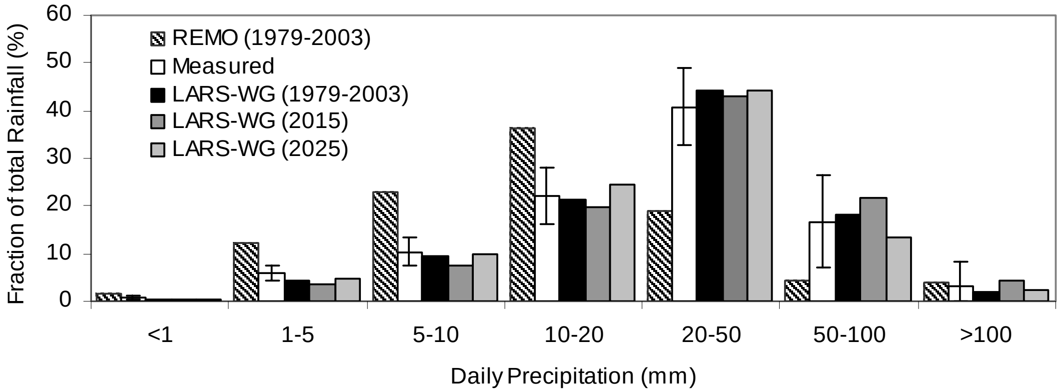

Figure 4. Simulated (REMO, mean over 25 years) and generated (LARS-WG, mean over 100 years) compared to measured (mean over 25 years including standard deviation) daily precipitation at Parakou, 100 km east of the study area.

Within the IMPETUS project, future trends in land use in the Upper Ouémé Catchment were calculated with the model CLUE-S (Verburg et al., 1999). The assumptions were also based on the IPCC scenario B2. A major driving force in the study area was a projected increase of population by 67% within the period 2000-2025. Therefore, the expansion of farmland was the most notable development. The simulation delivered land use scenarios for the same years as REMO with a 500 m spatial resolution. Figure 5 displays the land use in 2000 and 2025. The highest increase in farmland took place near the axis Djougou-Penessoulou (western study area, Figure 1) and in the central study area. The center was widely dominated by savannahs in 2000, but the ongoing development of infrastructure will facilitate the expansion of farmland through 2050. In contrast, the northeast portion of the study area will, even in 2025, be widely dominated by savannahs, due to poor infrastructure.

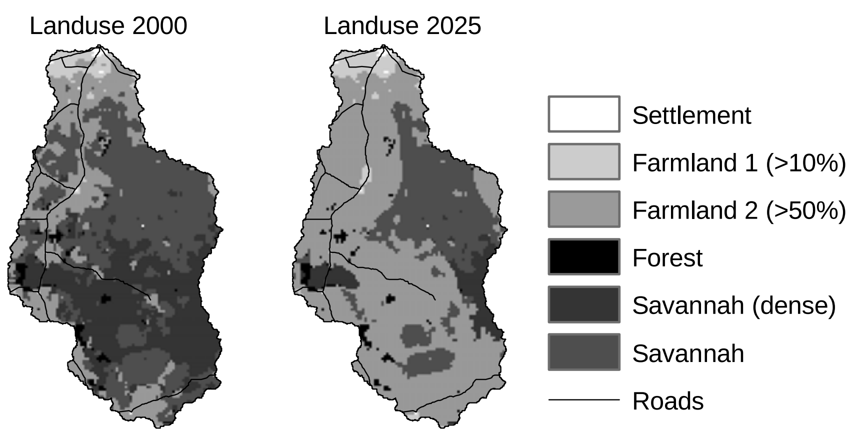

Figure 5. Land use scenarios for the years 2000 and 2025.

An exact determination of farmland was necessary for this work. Therefore, the 500 m resolution was too coarse, as it only displayed the dominat land use. For example, the class “Farmland 1” consist of only 10-50% true farmland. If SWAT had been run with this map, erosion would have been severely overestimated.

To solve this problem the simulated land use maps were disaggregated to a 50 m grid with differentiated land use classes. At first it was determined which fraction of land use types in the satellite classification were represented in the CLUE-S land use types by comparing the CLUE-S map from the year 2000 with the satellite image of the same year. Next, this distribution was transferred to each grid cell of the simulated land use maps. Figure 6 displays the scheme of disaggregation.

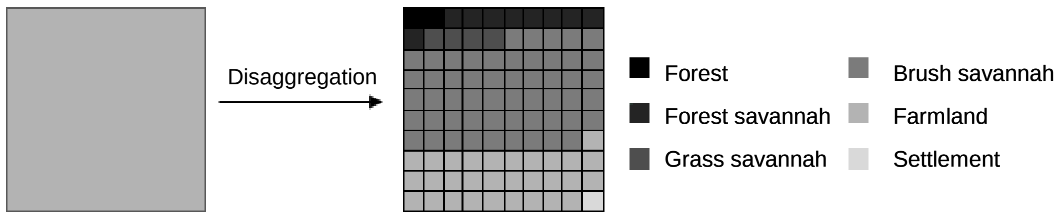

Figure 6. Land use disaggregation scheme applied to a typical cell type "Farmland 1" with 2% forest, 9% forest savannah, 4% grass savannah, 55% brush savannah, 30% farmland and 1% settlement.

Results

A comparison between the original model and a model that used a) the generated land use map of the year 2000, b) the generated precipitation series of the year 2000, and c) both generated datasets indicated a satisfactory representation of the present state. The results of the scenario runs are summarized in Table 1. The land use scenarios describe an expansion of farmland, which would lead to an increase in the mean erosion rate from 2.84 t/ha/yr in 2000 to 4.68 t/ha/yr in 2025. Figure 7 displays the erosion rates for each subbasin for the land use scenarios 2000 and 2025. It can be stated that the erosion risk increased mainly in the western and southern parts of the study area, but remained lower than in the areas in the vicinity of Djougou (northern part of the catchment). This is due to the soils under the savannah being less vulnerable to erosion than soils that have already been under cultivation for centuries. This development can be attributed to two soil properties, available water capacity and the USLE soil erodibility. The available water capacity ranges from 300 mm to 400 mm in areas that show low erosion rates and from 200 mm to 300 mm in areas that show high rates. The USLE soil erodibility factor ranges from 0.43-0.52 in the northern and 0.26- 0.46 in the southern and central study area. For that reason the average erosion rate on farmland decreased in the land use scenario from 17 to 12 t/ha/yr. The average erosion rate of 12 t/ha/yr on farmland equalled a loss of 1 mm topsoil per year (given a bulk density of 1.2 g/cm^3).

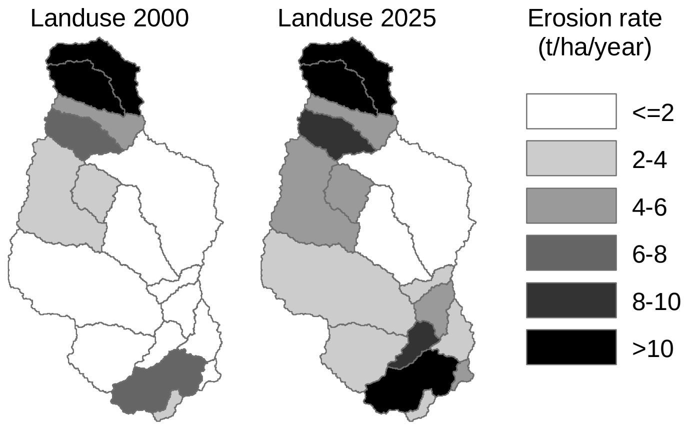

Figure 7. Erosion rates in the Terou Catchment: Land use scenarios 2000 and 2025.

Surface runoff steadily increased from 108 mm in 2000 to 134 mm in 2025, whereas baseflow decreased from 154 to 139 mm (Table 1). This includes a change in the runoff dynamic. On the one hand, the increasing surface runoff induced earlier runoff and higher runoff rates in the mid-rainy season; on the other hand, the decreasing baseflow led to an earlier end of runoff.

The precipitation scenarios described an inconsistent development: low precipitation in 2020 and 2025 is contrasted by above-average rainfall in 2015. As the evaporation remained almost constant, changes in precipitation had a strong impact on total runoff (Figure 9). Therefore the runoff coefficient fluctuated between 0.10 (2025) and 0.22 (2015), which is within the range of measured values in the region. The ratio of runoff components was not affected by changes in precipitation. Baseflow and surface runoff responded to changes in precipitation on the same magnitude. Erosion rates corresponded strongly to the total amount of precipitation, which is partly caused by the insufficient reproduction of extreme events by LARS-WG; hence, erosion rates in the precipitation scenarios are significantly lower in 2020 and 2025 and higher in 2015.

Table 1. Results of the different scenarios 2000-2025 including standard deviation for total runoff and erosion rates.

		Runoff Components (mm/yr)				
Scenario	**Year**	**Precipitation**	**Surface Runoff**	**Baseflow**	**Total Runoff**	**Erosion rate (t/ha/yr)**
Original	1998-2003	1141	114	152	271	2,75
Land use	2000	1141	108	154	267	2.85
	2005		113	149	268	3.33
	2010		117	147	270	3.66
	2015		119	147	271	4.01
	2020		128	140	274	4.41
	2025		134	139	279	4.68
Precipitation	2000	1275	121	125	251 (+/- 118)	2.92 (+/- 1.23)
	2005	1190	94	94	193 (+/- 100)	2.77 (+/- 1.29)
	2010	1160	96	95	196 (+/- 98)	2.77 (+/- 1.22)
	2015	1332	140	142	288 (+/- 112)	3.78 (+/- 1.36)
	2020	1117	67	68	140 (+/- 79)	1.99 (+/- 0.94)

	2025	1062	52	49	107 (+/- 64)	1.44 (+/- 0.74)
Land use + Precipitation	2000	1275	113	122	241 (+/- 118)	2.94 (+/-1.29)
	2005	1190	92	87	184 (+/- 99)	3.17 (+/- 1.48)
	2010	1160	97	87	189 (+/- 98)	3.50 (+/- 1.51)
	2015	1332	147	132	285 (+/- 112)	5.61 (+/- 1.97)
	2020	1117	76	59	139 (+/- 79)	3.02 (+/- 1.39)
	2025	1062	63	39	106 (+/- 64)	2.49 (+/- 1.34)

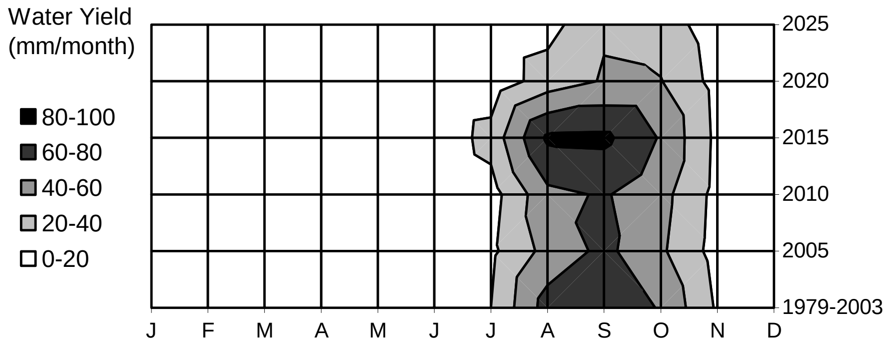

Figure 8. Simulated monthly water yield in the Terou Catchment using simulated precipitation.

The results of the combined scenarios were determined by the outlined developments: a decrease in total runoff and a relative increase in surface runoff compared to baseflow (Figure 9). The discharge hydrographs were similar to those generated by using only simulated precipitation, which can be explained by the fact that total discharge was only slightly influenced by land use changes. Since changes in land use patterns and precipitation cause contradictory effects on erosion rates, neither a clear increase due to land use changes nor a clear decrease due to precipitation changes could be observed.

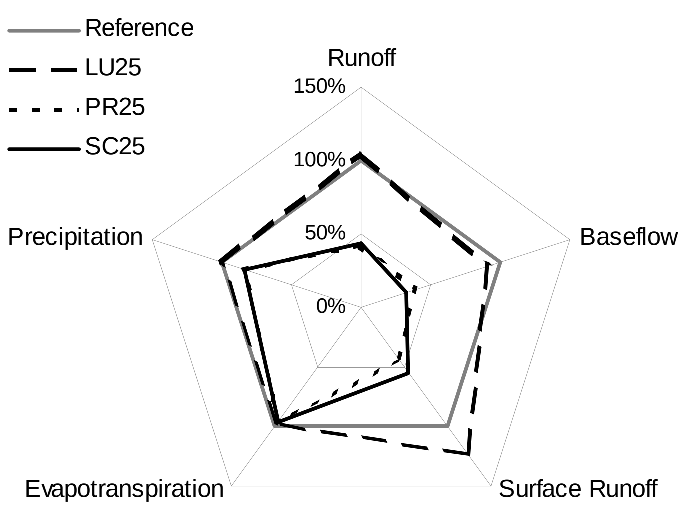

Figure 9. Comparison of the scenario results for 2025 (LU25: Land use, PR25: Precipitation, SC25: Combined, Reference: year 2000).

Conclusions

It can be stated that the SWAT2003 model is appropriate to adequately simulate changes in land use and precipitation. Reasonable values for future changes in runoff and erosion rates were obtained. The land use scenarios showed an increase of surface runoff, whereas baseflow decreased. The runoff variability and erosion rates increased significantly. The changes in precipitation led to changes in total runoff, especially for the years 2020 and 2025 which showed very low runoff compared to the year 2000. Consequently, the forecasted changes in land use and precipitation showed opposite effects on soil erosion. The effect of increased runoff due to expansion of agricultural fields was overcompensated by the decrease in total runoff due to climate change. The combined effect on soil erosion could not be quantified with a high certainty due to limitations in the weather generator and unknown development of future frequency distributions of daily rainfall. For mid- and long-term assessments of soil erosion one has to keep in mind that the loss of topsoil may result in positive feedbacks, as already shown on a coarser scale (Feddema and Freire, 2001). Assuming constant soil profiles for decades can result in an underestimation of soil erosion, based on the influence of soil water capacity.

In future work, the scenario results could be improved by using land use scenarios with a higher resolution (100 m) and continuous simulations of precipitation from REMO. The continuous climate simulation would eliminate the imponderability caused by high climate variability. Furthermore, attempts should be made to disaggregate the precipitation output from the regional climate model for direct use in SWAT. Additionally, the sediment budget for the original model will be calibrated and validated with continuous suspended sediment measurements and the scenarios will be extended to the entire upper Ouémé Catchment. All of the results from the scenario analysis will be processed for stakeholders in Benin for decision support.

Acknowledgements

The authors would like to thank the German ministry of education and research (BMBF, Grant number 07 GWK 02) as well as the MSWF Northrine-Westfalia (Grant number 514-21200200) for funding the IMPETUS project in the framework of the GLOWA program. Thanks also to H.-P. Thamm and M. Judex, University of Bonn, for providing the land use classification and scenarios of the upper Ouémé valley, H. Paeth for providing the REMO data and to L.O. Sintondji for providing a version of the SWAT model parameterized for the study area.

References

Adjanohoun, E.J. (1989): Contribution aux études ethnobotaniques et floristiques en République Populaire du Bénin. Agence de Coopération Culturelle et Technique. Paris. 895 pp.

Bormann, H. and B. Diekkrüger (2003): Possibilities and limitations of regional hydrological models applied within an environmental change study in Benin. Physics

and Chemistry of the Earth (B) 28. p. 1323-1332.
Fauré, P. and B. Volkoff (1998): Some factors affecting regional differentiation of the soils in the Republic of Benin (West Africa). Catena 32, p. 281–306.
Feddema, J. and S. Freire (2001): Soil degradation, global warming and climate impacts. Climate Research 17. p. 209–216.
Giertz, S. (2004): Analyse der hydrologischen Prozesse in den sub-humiden Tropen Westafrikas unter besonderer Berücksichtigung der Landnutzung am Beispiel des Aguima-Einzugsgebietes in Benin. Dissertation. Bonn. 249 pp. Available at http://hss.ulb.uni-bonn.de/diss_online/math_nat_fak/2004/giertz_simone/giertz.htm
Hulme, M.; R. Doherty, T. Ngara, M. New and D. Lister (2001): African Climate Change: 1900-2100. Climate Research 17. p. 145-168
IPCC (2001): Climate Change 2001: The Scientific Basis. Cambridge University Press. Cambridge. 881 pp.
Junge, B. (2004): Die Böden im oberen Ouémé-Einzugsgebiet: Pedogenese, Klassifikation, Nutzung und Degradierung. Dissertation. Bonn. 217 pp. Available at http://hss.ulb.uni-bonn.de/diss_online/landw_fak/2004/junge_birte/index.htm
Leroux, M. (2001): The meteorology and climate of tropical Africa. Springer, London. 548 pp.
Paeth, H. (2004): Key factors in African climate change evaluated by a regional climate model. Erdkunde 58. p. 290-315
Rohdenburg, H. (1969): Hangpedimentation und Klimawechsel als wichtigste Faktoren der Flächen- und Stufenbildung in den wechselfeuchten Tropen an Beispielen aus Westafrika, besonders aus dem Schichtstufenland Südost-Nigerias. Giessener Geographische Schriften 20. p. 57-152.
Runge, J. (1990): Morphogenese und Morphodynamik in Nord-Togo (9°-11°N) unter dem Einfluss spätquartären Klimawandels. Göttinger Geographische Abhandlungen 90. Goltze. Göttingen. 115 pp.
Sintondji, L. (2005): Modelling of process rainfall-runoff in the Upper Quémé catchment area (Terou) in a context of climate change: extrapolation from the local scale to a regional scale. Dissertation. Bonn.
Semenov, M.; R. Brooks, E. Barrow and C. Richardson (1998): Comparison of the WGEN and LARS-WG stochastic weather generators for diverse climates. Climate Research 10. p. 95-107.
Speth, P.; Diekkrüger, B. and M. Christoph (2002): IMPETUS West Africa – An integrated approach to the efficient management of scarce water in West Africa – Case studies for selected river catchments in different climatic zones. In: GSF – Forschungszentrum für Umwelt und Gesundheit GmbH (Hrsg.): GLOWA – German Programme on Global Change in the Hydrological Cycle. Status Report. p. 61-67.
Verburg, P.; G. De Koning, K. Kok, A. Veldekamp and J. Bouma (1999): A spatial explicit allocation procedure for modelling the pattern of land use change based upon actual land use. Ecological Modelling 116. p. 45-61
Weischet, W. and W. Endlicher (2000): Regionale Klimatologie. Bd. 2. Die Alte Welt (Europa, Afrika, Asien). Stuttgart. 625 pp.
Will, H. (1996): Fernerkundung und Weideökologie in der subhumiden Savannenzone NW-Benins. Karlsruher Schriften zur Geographie und Geoökologie 4. 118 pp.

An Asssessment of Alternative Conservation Practice and Land Use Strategies on the Hydrology and Water Quality of the Upper Mississippi River Basin

Manoj Jha[1], Philip W. Gassman*[1], Silvia Secchi[1], Jeff G. Arnold[2], Lyubov A. Kurkalova[1], Hong-Li Feng[1], and Cathy L. Kling[1]
[1]Center for Agricultural and Rural Development (CARD), Dept. of Economics, Iowa State University, Ames, Iowa 50011, U.S. Email: pwgassma@iastate.edu
[2]Grasslands Soil and Water Research Laboratory, USDA-ARS, Temple, Texas, U.S.

Abstract

The Upper Mississippi River Basin (UMRB) is dominated by agricultural land use, which is a major source of sediment and nutrient pollutant loadings to the regional stream system and ultimately to the Gulf of Mexico. An integrated modeling framework has been constructed for the UMRB that consists of the Soil and Water Assessment Tool (SWAT) model, the interactive SWAT (i_SWAT) software package, and other supporting software and databases. The simulation framework facilitates execution of alternative policy scenarios for the region by incorporating detailed crop rotations and an array of nutrient and tillage management schemes, derived from the USDA National Resources Inventory (NRI) database and other sources. Calibration and validation of SWAT for the UMRB annual streamflows for 1982-90 and 1991-97, respectively, resulted in R^2 and modeling efficiency (E) values that ranged from 0.92 to 0.96; corresponding monthly R^2 and E statistics ranged from 0.58 to 0.74. The calibrated model was then used to assess the impact of increasing the amount of land area managed with the following conservation practices: land set aside, terraces, contouring, grassed waterways, and conservation tillage. Percentage reductions of 35, 7, 43, and 13% were predicted for sediment, nitrate, organic N, and total N loads, respectively, at the UMRB outlet. The effects of reducing nitrogen fertilizer applications on corn by 10%, in tandem with the conservation practice scenario, resulted in greater predicted nitrate and total N reductions of 15 and 20%, respectively.

Introduction

The Mississippi River Watershed covers 3.2 million km^2 across parts or all of 31 states and two Canadian provinces (Figure 1). Excess nitrogen, phosphorus, and sediment loadings have resulted in water quality degradation within the Mississippi and its tributaries. The nitrate load discharged from the mouth of the Mississippi River has also been implicated as the primary cause of the Gulf of Mexico seasonal oxygen-depleted hypoxic zone, which according to Rabalais et al. (2002) covered nearly 20,000 km^2 in 1999 (Figure 1). Approximately 90% of the nitrate load to the Gulf is attributed to diffuse pollution. A significant portion of this load originates from the Upper Mississippi River Basin (UMRB), which covers only 15% of the total Mississippi drainage area (Figure 1). Goolsby et al. (1999) estimated that the UMRB was the source of nearly 39% of the Mississippi nitrate load discharged to the Gulf between 1980 and 1996; 35% of this load was attributed solely to Iowa and Illinois tributary rivers for average discharge years during the same time period (Goolsby et al., 2001).

Nutrient inputs via fertilizer and/or livestock manure on cropland and pasture areas are the primary sources of diffuse nutrient pollution in the UMRB stream system. Sediment losses to the UMRB stream system are a function of erosion from upland soils, especially from cropland areas, and stream bank erosion. These nonpoint source pollution problems persist throughout the region, despite a wide range of water quality initiatives that have been undertaken at different watershed and regional scales by federal, state and/or local agencies. This underscores the need for continued assessments of specific subwatersheds and of the entire region, to determine which management and land use strategies will be the most effective approaches for mitigating UMRB diffuse pollution problems.

A simulation study using the Soil and Water Assessment Tool (SWAT) model (Arnold et al., 1998) has been initiated to address UMRB water quality issues, by providing insights that could help mitigate nutrient and sediment losses from UMRB cropland and pastures. The objectives of this research are: (1) to calibrate and validate streamflows predicted with SWAT at the UMRB outlet at Grafton, Illinois, and (2) to estimate the impact of a suite of conservation practices and land use changes on sediment and nitrogen loadings at the UMRB outlet.

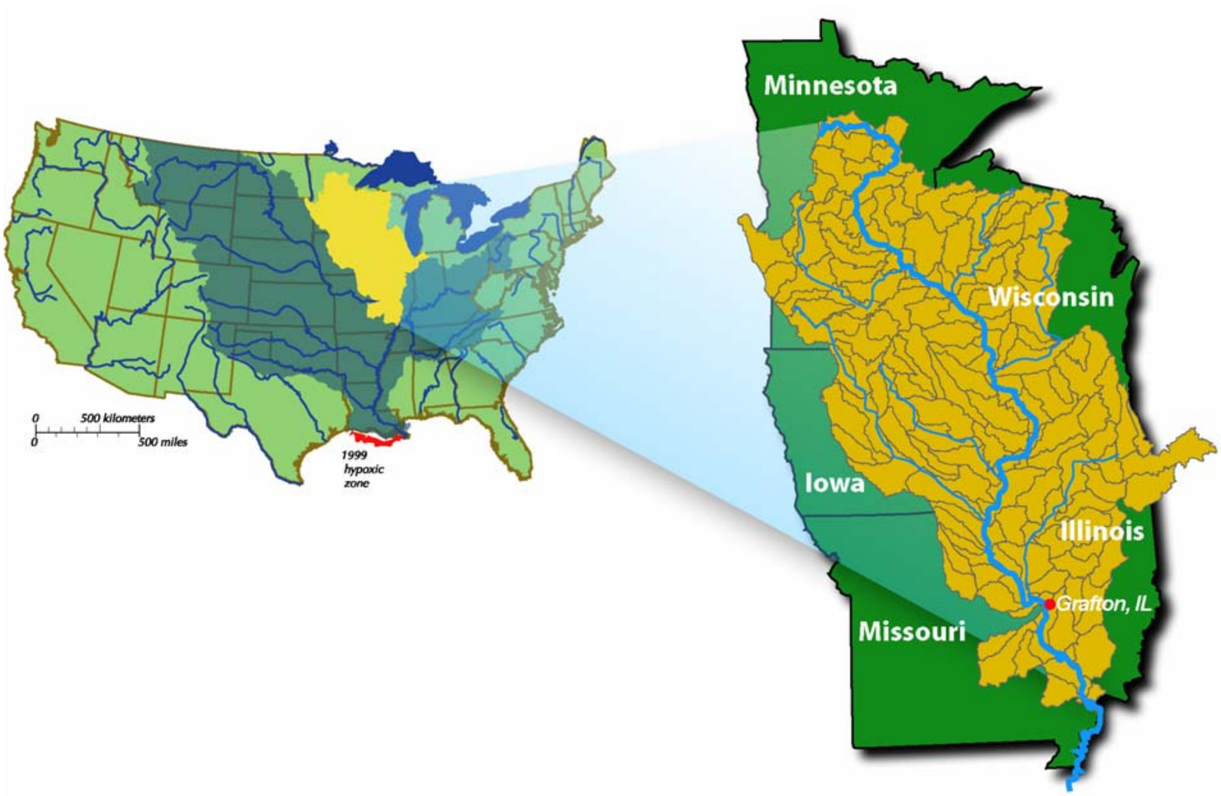

Figure 1. Location of the Upper Mississippi River Basin (UMRB) within the Mississippi River Basin, the 131 8-digit watersheds located within the UMRB, and the location of Grafton, IL.

Watershed Description

The UMRB extends from the source of the Mississippi River at Lake Itasca in Minnesota to a point just north of Cairo, Illinois. The total drainage area is nearly 492,000 km^2, which lies primarily in parts of Minnesota, Wisconsin, Iowa, Illinois, and Missouri (Figure 1). The assumed UMRB outlet for this study was Grafton, Illinois, which lies just above the confluence of the Mississippi River and Missouri River and covers an area of 431,000 km^2 that drains approximately 90% of the entire UMRB. The major UMRB land use categories shown in Table 1 are based on land use data obtained from the USDA 1997 National

Resources Inventory (NRI) database (http://www.nrcs.usda.gov/technical/NRI/; Nusser and Goebel, 1997). According to the 1997 NRI, the dominant land areas are cropland (42.7%), forest (20.2%), and pasture/hay/range (18.6%). The total NRI UMRB agricultural area (cropland, pasture/hay/range, and Conservation Reserve Program (CRP) land) is estimated to be 64.6%, which is slightly lower than the estimate of 67% provided by NAS (2000) and an estimate of 66% derived from the USGS 1992 National Land Cover Data set (Vogelmann et al., 2001) by C. Santhi (2004, Unpublished research data, Blacklands Research and Extension Center (BREC), Temple, Texas).

Table 1. 1997 NRI broad land use categories for the UMRB.

Land Use	Area (km^2)	% of Total Area	Comments
Cropland	210,049	42.7	Row crop and small grains
Pasture/hay/range	91,463	18.6	Includes alfalfa rotated with corn
CRP	16,375	3.3	Conservation Reserve Program
Forest	99,157	20.2	About 85% of forests are deciduous trees
Urban/barren	43,002	8.7	Includes farmsteads & rural roads
Water	14,678	3.0	Streams, reservoirs, etc.
Wetlands	7,647	1.6	Rural marshland and rice
Federal land	9,494	1.9	No actual land use data provided
Total	491,836	100.0	

Methodology

A simulation framework has been constructed for the UMRB using 131 subwatersheds (Figure 1) that coincide with the boundaries of the USGS 8-digit Hydrologic Cataloging Unit (HCU) watersheds (Seaber et al., 1987; http://www.nrcs.usda.gov/technical/land/meta/m3862.html) and builds on previous UMRB SWAT research reported by Arnold et al. (2000). Only 119 8-digit watersheds were simulated in this study, due to the assumption that the UMRB outlet was located at Grafton, Illinois. The primary data source for the modeling system was the 1997 NRI, which contains soil type, landscape features, cropping histories, conservation practices and other information for roughly 800,000 nonfederal land points for the entire U.S. Each point represents an area that generally ranges from a few hundred to several thousand hectares in size and which consists of homogeneous land use, soil, and other characteristics.

The simulated tillage practices were obtained from data reported in the USDA 1990-95 Cropping Practices Survey (CPS) data (http://usda.mannlib.cornell.edu/usda/ess_entry.html). The assumed fertilizer application rates used in the analysis were based on statewide average application rates obtained from 1996-98 Agricultural Resource Management Survey (ARMS) data (http://www.ers.usda.gov/data/arms/). Applications of nutrients via livestock manure were not simulated in this study. Precipitation, maximum temperature, and minimum temperature data were obtained from C. Santhi (2002. Personal communication, BREC, Temple, Texas) for a single representative climate station for each 8-digit watershed, and were used for both the SWAT baseline and scenario simulations. The climate records span from 1967-98; however, only a 17-year portion (1981-97) was used for the SWAT simulations reported here. The soil layer data required for the SWAT simulations was obtained from a soil database that contains soil properties consistent with those described by Baumer et al. (1994), that includes ID codes that allow direct linkage to NRI points.

Delineation of the UMRB into smaller spatial units required for the SWAT simulations consists of two steps: (1) subdividing the overall basin into 131 subwatersheds (Figure 1), and (2) creating smaller HRUs located within each of the 131 8-digit watersheds. The HRUs required for the SWAT UMRB baseline simulation were created by aggregating NRI points together on the basis of common soil, land use, and management characteristics. Common soil types were aggregated at the 8-digit level via a statistically-based soil clustering process that was performed for NRI-linked soils for most of the U.S. (Sanabria and Goss, 1997), and reduced the number of possible HRU combinations. For land use, all of the points within a given category such as forest, urban, pasture, and land set aside (defined as part of the Conservation Reserve Program or CRP) land were clustered together, except for the cultivated cropland. For the cultivated cropland, the NRI points were first aggregated into several crop rotation land use clusters within each 8-digit watershed, based on the NRI cropping histories. The final step of developing HRUs required aggregation across NRI points according to the management characteristics, such as tile drainage (yes or no), conservation practices (terracing, contouring, and/or strip cropping), and type of tillage (conventional, reduced, mulch, or no-till). Over 18,000 HRUs were included in the SWAT simulations performed for this study.

The conservation practice scenario was based on an algorithm developed for an assessment of conservation practices in Iowa (Gassman et al., 2005). The key steps in the algorithm were:

1) Retire all cropland within 100 ft. of a waterway.
2) Retire additional cropland until 10% is retired statewide, based on the NRI Erosion Index.
3) Terrace remaining cropland with slopes above 5%.
4) Implement contouring on all remaining cropland with slopes above 4%.
5) Install grassed waterways (GWs) on remaining cropland with 2 to 4% slopes.
6) Implement conservation tillage (20% notill and 80% mulch till) on all non-retired cropland with slopes $\geq$ 2%.

The scenario was applied to the URMB by implementing the algorithm at the USGS 4-digit HCU watershed level (Figure 2). The resulting additional new land area that was shifted into these conservation practices is listed in Table 2. The scenario was then executed a second time with an additional simplistic nutrient management (NM) scheme in which it was assumed that the nitrogen fertilizer rates were reduced on all corn acres by 10% (The total nitrogen applied to corn was by far the most significant source of nitrogen in the region).

The SWAT model was calibrated and validated using measured streamflow data collected at a USGS stream gauge located on the Mississippi River near Grafton, IL (Station # 05587450). The total simulation period (1981-1997) was divided into two time periods: nine years (1982-1990) for the calibration period (1981 was assumed to be an initialization year) and seven years for the validation period (1991-1997). The coefficient of determination (R^2) and Nash-Sutcliffe simulation efficiency (E) were used to evaluate the model predictions for both time periods. The R^2 value is an indicator of strength of relationship between the observed and simulated values. The E value indicates how well the plot of the observed versus the simulated values fits the 1:1 line. If the R^2 values are close to zero, and the E values are less than or close to zero, then the model prediction is unacceptable. If the values equal one, the model predictions are considered perfect. No attempt was made to calibrate and validate the pollutant loadings for this study. However, this step will be carried out in the next stage of UMRB SWAT simulation research with additional climate data for 1999-2004, which is the period with the most reliable measured sediment and nutrient loads.

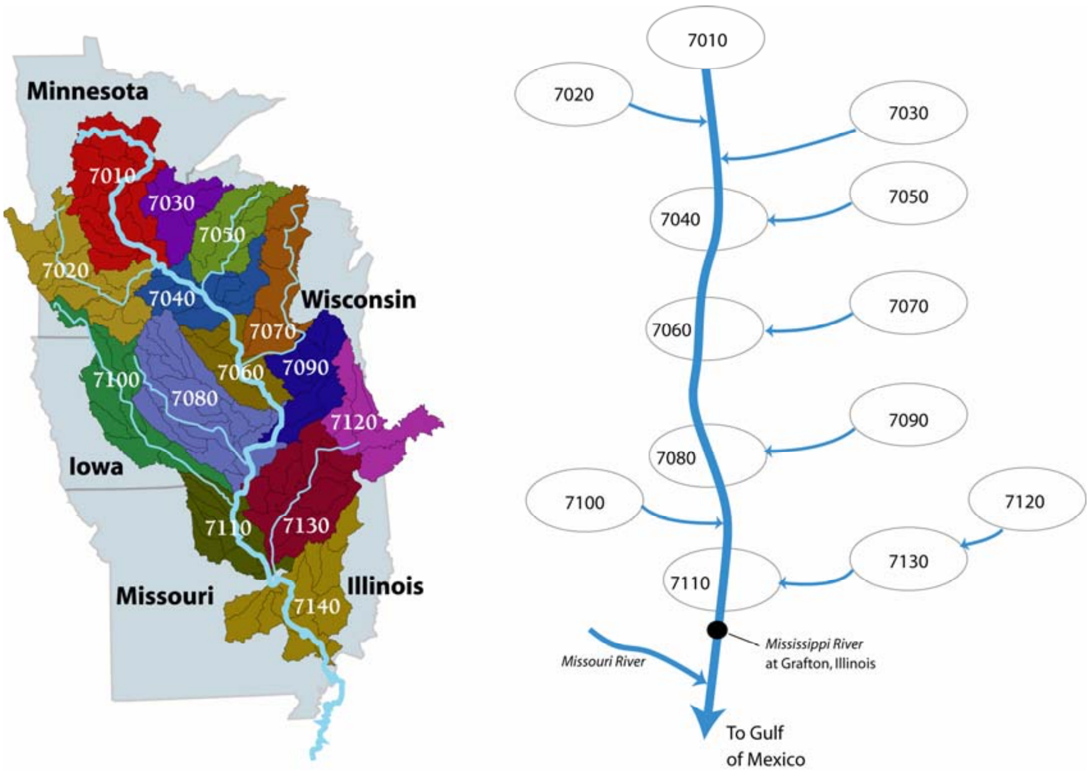

Figure 2. The 14 4-digit watersheds that are located within the UMRB and the flow chart showing the routing structure between the watersheds; wateshed 0714 lies below Grafton, Illinois (the assumed UMRB outlet) and was not included in the SWAT simulations.

Table 2. Total area of additional land selected for each conservation practice by UMRB 4-digit watershed, in response to the application of the conservation practice algorithm.

4-digit wateshed	Conservation tillage	Land set aside	Contouring	Terraces	Grassed Waterways
			1,000 ha		
7010	735	34	55	77	469
7020	1,459	154	81	116	1,016
7030	204	6	25	47	107
7040	925	12	52	303	380
7050	360	12	37	87	186
7060	1,058	6	53	420	300
7070	503	4	24	167	217
7080	3,551	173	212	512	1,431
7090	1,265	71	119	239	587
7100	1,935	92	91	192	793
7110	883	14	64	160	289
7120	1,011	141	8	1	426
7130	2,473	278	82	36	1,028
Totals	32,722	1,990	1,807	4,716	14,456

Results and Discussion

SWAT was calibrated and validated for streamflow by comparing the simulated outputs with measured data collected at Grafton, Illinois. The initial step was a baseflow-surface runoff separation analysis that was performed with an automated digital filter technique developed by Arnold and Allen (1999). This calibration phase was performed using several hydrologic parameters including the soil evaporation compensation factor, curve numbers, and soil available water capacity values, which were adjusted within acceptable ranges relative to their initial estimates to achieve the desired proportion of surface runoff to baseflow on an annual basis. Based on these procedures, baseflow was found to comprise over 70% of the total annual average streamflow. Once this ratio was determined, several other model parameters were adjusted to match the seasonal variation of the simulated flow with the measured flow on a monthly basis, including snowmelt parameters, the groundwater delay factor, and recession coefficients. The calibration (1982-1990) yielded a strong correlation in annual streamflow (Figure 3) as indicated by an R^2 of 0.93 and an E value of 0.93. The calculated statistics were of similar strength for the validation period (1991-97) of the annual flows, as evidenced by the R^2 and E values of 0.96 and 0.92. The calibration monthly time-series comparison (Figure 4) for 1982-90 also reveals a strong correspondence between the predicted and measured streamflows, with resulting R^2 and E values of 0.74 and 0.67. The performance of the model was somewhat weaker for the monthly streamflow validation period (1991-97), although the R^2 and E values of 0.66 and 0.58 show that the model generally tracked the observed streamflows accurately.

A baseline simulation was performed for the UMRB following the calibration and validation procedure. The predicted sediment and nitrogen (N) loads are listed for each four digit watershed in Table 3. The predicted baseline loadings ranged greatly between the 4-digit watersheds, reflecting differences in land use throughout the region (e.g., less cropland in the northern areas), the presence of reservoirs that trap sediment (e.g. watershed 7100), and other factors. The overall loads range from about 119 thousand tons for organic N to over 46 million tons for sediment at the UMRB outlet. The large nitrate losses relative to the organic N losses are generally consistent with measured data reported for 1997-2004 at Grafton. However, it is probable that the nitrate loads are being overpredicted at present, based on initial investigation of measured data for the period of 1997-2003.

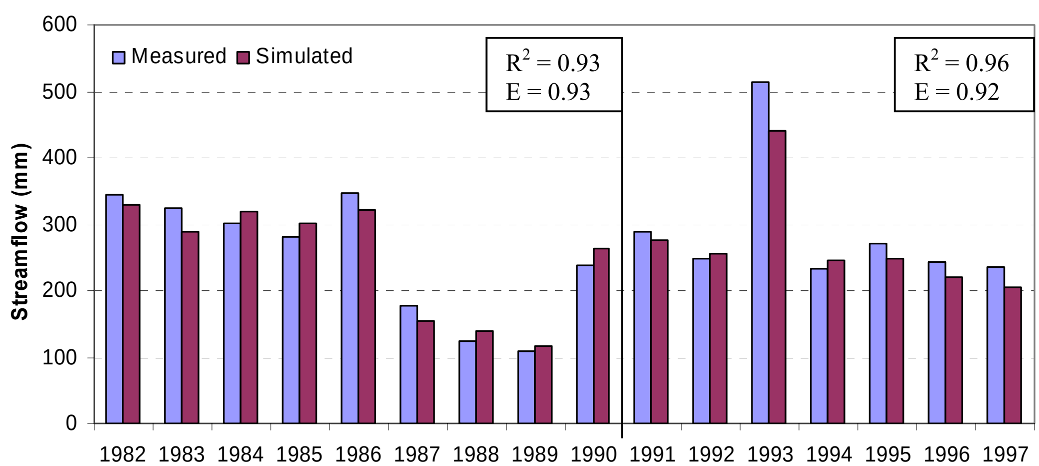

Figure 3. Comparison of simulated versus measured annual streamflows at Grafton, Illinois for the calibration period (1982-1990) and validation period (1991-1997).

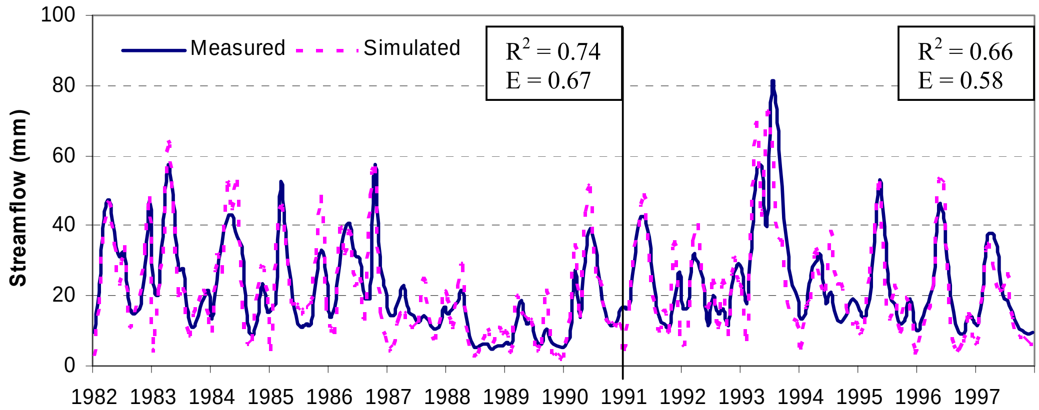

Figure 4. Comparison of simulated versus measured monthly streamflows at Grafton, Illinois for the calibration period (1982-1990) and validation period (1991-1997).

Table 3. Baseline loadings predicted at the outlets of the 4-digit watersheds.

4-digit watershed	Sediment	Nitrate	Organic N	Total Nitrogen
		Metric tons		
7010	3,443,603	49,847	21,373	71,220
7020	2,261,387	26,426	19,048	45,474
7030	336,137	4,821	1,355	6,176
7040	9,101,316	94,690	24,657	119,347
7050	760,550	9,729	2,209	11,937
7060	17,452,539	146,652	31,347	177,999
7070	1,143,156	12,713	4,874	17,587
7080	28,979,658	288,691	81,378	370,069
7090	2,707,139	32,246	22,319	54,565
7100	913,502	50,919	21,157	72,076
7110[a]	**46,034,087**	**562,684**	**118,848**	**681,531**
7120	3,227,018	59,675	24,426	84,101
7130	14,424,650	148,524	52,869	201,393

[a]The watershed 7110 outlet is the UMRB outlet at Grafton, Illinois (see Figure 2b).

The impacts of conservation practice scenarios are reported in Tables 4 and 5. Essentially no impact on streamflows was predicted in response to the scenarios. Reductions in the sediment loads were predicted to range from 4% in watershed 7100 to 54% in watershed 7030. The impact for watershed 7100 reflects the effect of two large reservoirs located on the main stem of the Des Moines River, which trap the majority of the sediment. The effects of the conservation practices on nitrate were minor in the first scenario; the nitrate reductions ranged from -3 to 7%. The negative numbers indicate that slight increases in nitrate movement to stream systems were predicted to occur in three of the 4-digit watersheds, which could occur due to greater nitrate leaching (in response to more terraces, etc.) and subsequently greater amounts of nitrate moving to the streams in subsurface flow. The predicted relative reductions on organic N losses ranged from 25 to 56% for the initial scenario; the 43% reduction predicted for watershed 7100 may be questionable due to the sediment-trapping reservoirs. The estimated reductions in total nitrogen losses were much lower (9-19%) across the 4-digit watersheds (Table 4), reflecting the fact that nitrate is the dominant component of the nitrogen losses. The overall impacts on the sediment, nitrate, organic N, and total N for the first scenario at the UMRB outlet (watershed 7110) were 35, 7, 43, and 13%, respectively. The inclusion of a 10% reduction in the corn fertilizer application rates resulted in estimated nitrate, organic N, and total N decreases of 2-15, 26-56, and 10-27% between the 13 4-digit watersheds (Table 5). Overall reductions of 15, 44, and 20% were predicted at the UMRB outlet for the second scenario.

Table 4. Relative reductions of simulated pollutants to the baseline for each 4-digit watershed in response to the conservation practice scenario.

4-digit watershed	Flow	Sediment	Nitrate	Organic N	Total Nitrogen
			%		
7010	-1	41	3	39	14
7020	-3	36	3	39	18
7030	0	54	-3	56	10
7040	-1	50	5	45	14
7050	0	53	0	48	9
7060	0	48	6	47	13
7070	0	40	-1	37	10
7080	0	42	6	49	15
7090	-1	32	-2	50	19
7100	1	4	1	43	13
7110[a]	**0**	**35**	**7**	**43**	**13**
7120	0	27	2	25	9
7130	0	39	3	39	12

[a]The 4-digit watershed 7110 outlet is the UMRB outlet at Grafton, Illinois (see Figure 2b).

Table 5. Relative reductions of simulated pollutants to the baseline for each 4-digit watershed in response to the conservation practice scenario plus the 10% nitrogen fertilizer reduction.

4-digit watershed	Flow	Sediment	Nitrate	Organic N	Total Nitrogen
			%		
7010	-1	41	8	40	17
7020	-3	36	7	39	21
7030	0	54	2	56	14
7040	-1	50	10	45	17
7050	0	53	2	48	10
7060	-1	48	12	47	18
7070	0	40	2	37	12
7080	-1	42	13	49	21
7090	-2	32	11	50	27
7100	1	4	9	43	19
7110[a]	**0**	**35**	**15**	**44**	**20**
7120	0	27	15	26	18
7130	0	39	13	40	20

[a]The 4-digit watershed 7110 outlet is the UMRB outlet at Grafton, Illinois (see Figure 2b).

Conclusions

The SWAT modeling framework constructed for the UMRB proved to be a flexible and useful tool for evaluating the impact of the two scenarios on sediment loads and nitrogen losses at the UMRB outlet and the outlet of other major upstream watersheds. The results reported here are preliminary; further calibration and validation of sediment and nutrient losses is needed to confirm the reliability of the model estimates. Additional climate data is being obtained for the period 1998-2003 to enable a complete test of the model with the observed pollutant loadings available for 1997-2003 at Grafton and elsewhere in the UMRB. It is interesting to note that the conservation practices did significantly impact the sediment losses and sediment bound nitrogen, as would be expected, and that the 10% decrease in the corn nitrogen fertilizer application rates resulted in a doubling of the predicted nitrate reductions at Grafton. This result was significantly less than estimated by McIssac et al. (2001), who state that a 12% reduction in nitrogen fertilizer over 1960-1998 for the entire Mississippi River Basin would have reduced the nitrate flux to the Gulf Mexico by 33%. Clearly, further investigation of alternative fertilizer and conservation practice effects is needed to determine the best options to reduce diffuse pollution in the UMRB and other major Mississippi River Basin subregions.

References

Arnold, J.G., and P.M. Allen. 1999. Automated methods for estimating baseflow and groundwater recharge from streamflow records. *J. of the American Water Resources Association* 35(2):411-424.

Arnold, J.G., R.S. Muttiah, R. Srinivasan, and P.M. Allen. 2000. Regional estimation of base flow and groundwater recharge in the upper Mississippi basin. *J. of Hydrology* 227(2000):21-40.

Arnold, J.G., R. Srinivasan, R.S. Muttiah and J.R. Williams. 1998. Large area hydrologic modeling and assessment part I: model development. *J. Amer. Water Resour. Assoc.* 34(1):73-89.

Baumer, O., P. Kenyon, and J. Bettis. 1994. MUUF v2.14 User's Manual. U.S. Department of Agriculture, Natural Resources Conservation Service, National Soil Survey Center, Lincoln, Nebraska.

Gassman, P.W., S. Secchi, C.L. Kling, M. Jha, L.A. Kurkalova and H.L. Feng. 2005. An Analysis of the 2004 Iowa Diffuse Pollution Needs Assessment using SWAT. Proceedings of the 3rd International SWAT Conference, Swiss Federal Institute of Environmental Science and Technology, Dubendorf, Switzerland.

Goolsby, D.A., W.A. Battaglin, B.T. Aulenbach, and R.P. Hooper. 2001. Nitrogen input to the Gulf of Mexico. *Journal of Environmental Quality* 30: 329-336.

Goolsby, D.A., W.A. Battaglin, G.B. Lawrence, R.S. Artz, B.T. Aulenbach, R.P. Hooper, D.R. Keeney and G.J. Stensland. 1999. Flux and sources of nutrients in the Mississippi-Atchafalaya River Basin: Topic 3 report for the integrated assessment on hypoxia in the Gulf of Mexico. NOAA Coastal Ocean Program Decision Analysis Series No. 17. U.S. Department of Commerce, National Oceanic and Atmospheric Administration, National Centers for Coastal Ocean Science, Silver Spring, Maryland. http://www.nos.noaa.gov/products/pubs_hypox.html.

NAS. 2000. The changing face of the UMR Basin; agriculture: Selected profiles of farming and farm practices. National Audubon Society, Upper Mississippi River Campaign, St. Paul, Minnesota. http://www.umbsn.org/news/documents/chg_face.pdf.

Nusser, S.M. and J.J. Goebel. 1997. The national resources inventory: a long-term multi-resource monitoring programme. *Environ. Ecol. Stat.* 4:181-204.

McIssac, G.F., M.B. David, G.Z. Gertner and D.A. Goolsby. 2001. Nitrate Flux in the Mississippi River. *Nature* 414(8):166-167.

Rabalais, N.N., R.E. Turner and D. Scavia. 2002. Beyond science into policy: Gulf of Mexico hypoxia and the Mississippi River. *BioScience* 52(2): 129-142.

Sanabria, J. and D.W. Goss. 1997. Construction of input for environmental simulation models using multivariate analysis. *In Proc. South Central SAS (Statistical Analysis System) Users Meeting*, 217-234. Houston, TX.

Seaber, P.R., F.P. Kapinos and G.L. Knapp. 1987. Hydrologic Units Maps. U.S. Geological Survey, Water-Supply Paper 2294.

Vogelmann, J.E., S.M. Howard, L. Yang, C.R. Larson, B.K. Wylie and N. Van Driel. 2001. Completion of the 1990s National Land Cover Data Set for the conterminous United States from Landsat Thematic Mapper Data and ancillary data sources. *Photogramm. Eng. Remote Sens.* 67(6):650-655, 657-659,661-662.

Macro-scale Catchment Modeling in Northwest Russia

S.A. Kondratyev[1]
[1]Institute of Limnology of the Russian Academy of Sciences, Sevastyanova 9, St. Petersburg, 196105 Russia. Email: kondratyev@limno.org.ru

Abstract

A model of phosphorus balance of a large aquatic system and its catchment was developed. The model was tested for the freshwater system of Lake Ladoga and Neva Bay of the Gulf of Finland with a total catchment area of about 29,500 km^2. An assessment of the influence of load from point and nonpoint sources of phosphorus in the system was conducted. It was shown that present total phosphorus concentration in Lake Ladoga is far from the corresponding critical value. Eutrophic status and phosphorus levels in the Neva Bay depend mainly on outflow from Lake Ladoga and are impacted by the waste waters of St. Petersburg.

Introduction

The aim of this study was to develop a model for the phosphorus balance of a macro-scale catchment in order to test the water systems of Lake Ladoga and the Neva Bay of the Gulf of Finland. The role of various elements of landscapes, land cover, point sources of load, changes in formation of phosphorus load and phosphorus regime of surface waters in this aquatic system were explored. The main objective in model development was to couple a phosphorus balance model with physically-based models like SWAT for assessment of distributed parameters in sub-catchments

Methodology

Catchment Modeling: General Approach

There are two ways of constructing catchment models with various levels of complexity. The first involves development of hydrodynamic, hydraulic and chemical kinetic equations, and their analytical solutions. As a rule, this approach can be used for simple basins, small temporal intervals and a large amount of initial data. The models are called physically-based or deterministic (Kuchment, 1980) models. The second approach is empirical or semi-empirical generalization of knowledge, concerning the phenomena under study at various spatial and temporal levels, in the form of simple equations. The structure of empirical models depends on the amount of initial data that are available. It is better to use the physically-based models for describing processes at the micro-scale in catchments with diurnal variability. Empirical or semi-empirical models are usually better for estimation of annual changes in large, macro-scale catchments. Different combinations of physically-based and empirical models are called conceptual models, usually these models include empirical equations based on physical concepts.

The procedure for catchment model development is shown in Figure 1. The main factors defining the structure of the model are spatial and temporal. The selection of scales depends on the requirements of the task, the initial data available, the phenomena of interest, and a particular catchment. Ideally, a scientist should have a bank of models, consisting of sub-models with various levels of complexity, which influence the model selection. The temporal scale of a model depends substantially on the range of variability of investigated processes, which is defined by scale of process variability, and the step-type behavior and scale of averaging of the initial data (Rozhkov & Trapeznikov, 1990).

There are three basic categories of spatial scales of modeling: macro, meso, and micro. Continents, states, catchments of the large rivers and reservoirs, and spatial cells of global circulation atmospheric models can be related to number of macro-scale catchments. Meso-scale objects of modeling (landscape structures, the administrative formations, river catchments) represent the most extensive category of catchment, which are considered at the decision of practical tasks. The micro-scale objects include small homogeneous catchments, research plots, and point objects. They, as a rule, are objects of special experimental research and detailed verification of models.

The choice of a schematization of the catchments surface is the important factor that determines structure of model. Such ways of a schematization of a surface, as 'the open book', 'the kinematic cascade', 'uniform grid', 'homogeneous basins + channel', etc. frequently were used on the initial stages of development of catchment modeling (Kondratyev, 1992). The schematizations of a catchments surface on the basis of a 'finite elements' method (Kuchment et al., 2000) and runoff formations complexes (Vinogradov, 1988) are widely distributed. The allocation of elementary and cascade landscapes-geochemical systems is seemed perspective also (Kosheleva, 2003). Perfection of computer facilities and wide introduction of geoinformational technologies into modeling practice have allowed to automate labor-consuming enough procedures of a spatial schematization of catchment and to unite existing databases with mathematical models.

All mentioned methods are quite suitable for micro- and meso-scale modeling. Macro-scale areas with hundreds or thousands rivers and lakes usually need special approach of model development. Volume of available initial data is of great importance for structure of this model. For macro-scale modeling it is very important to define (i) the spatial structure of the model as a set of sub-models for selected sub-catchment and water bodies, (ii) the interaction between these sub-models. Well known and verified models like SWAT, AGWA or MIKE-SHE can be used as sub-models. At present study a special attention is paid for definition of interaction between sub-models for selected sub-catchment and water bodies in the framework of macro-scale model of large "rivers-lakes" system. Future development of each sub-model by using physically-based distributed models is the next step of research.

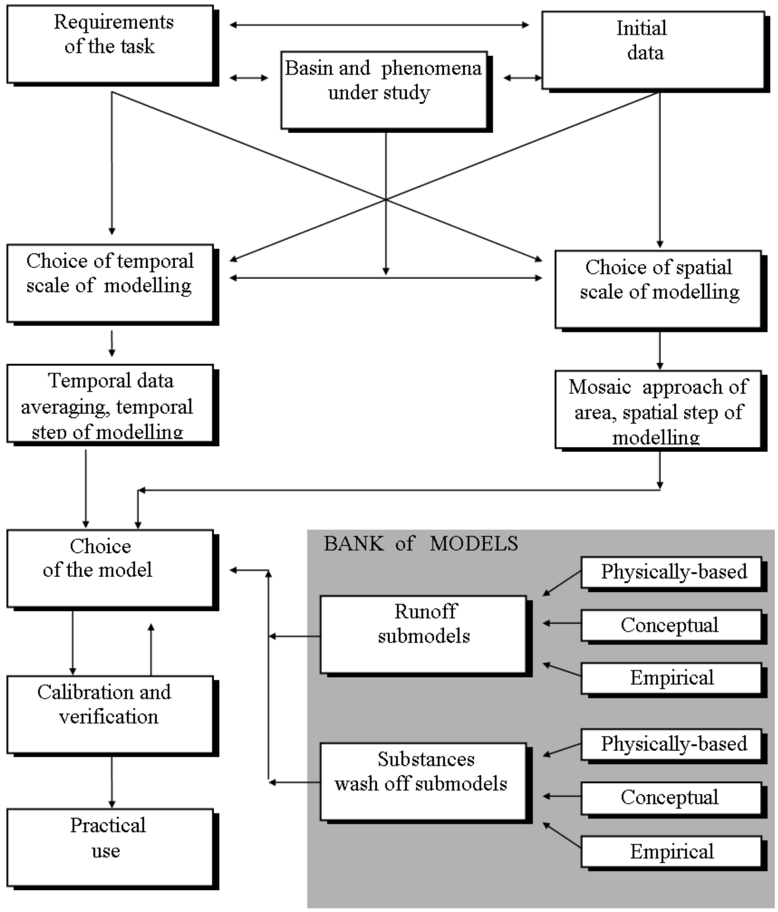

Figure 1. General structure of catchment model development (Kondratyev & Mendel, 1997).

Studied Area and Description of the Model

Lake Ladoga is the largest European lake with surface area about 18 000 km^2. The lake volume is 908 km^3, and its average and maximum depths are 51 m and 230 m, respectively. The catchment of Lake Ladoga has an area more than 280 000 km^2 and 20% of this area is located in Finland. The water system of Lake Ladoga includes the catchments of lakes Saimaa (Finland), Onega and Ilmen (North-west Russia) connected by large rivers: Vuoksa, Svir and Volkhov. The case study catchment is located on the territory of 7 administrative regions of Russia and 4 provinces of Finland. The Neva Bay (400 km^2) is a freshwater part of the Gulf of Finland of the Baltic Sea. Water quality and ecological state of the Neva Bay depend on Lake Ladoga outflow and impact of St. Petersburg. Phosphorus is an element which defines the eutrophication of studied freshwater system, that is why a special model of phosphorus balance was developed.

There are about 50 000 lakes and 60 000 rivers at studied area. Traditional scheme of catchment model as a set of slopes and river channels is not valid in this case. Five main water bodies (lakes Saimaa, Onega, Lagoga, Ilmen and Neva Bay) and five sub-catchments were selected as a main units for the modeling (Fig. 2). Areas of studied water bodies ($\boldsymbol{F_{wb}}$), their catchments ($\boldsymbol{F_c}$), and water surface in catchments ($\boldsymbol{F_{cw}}$) are presented in Table 1.

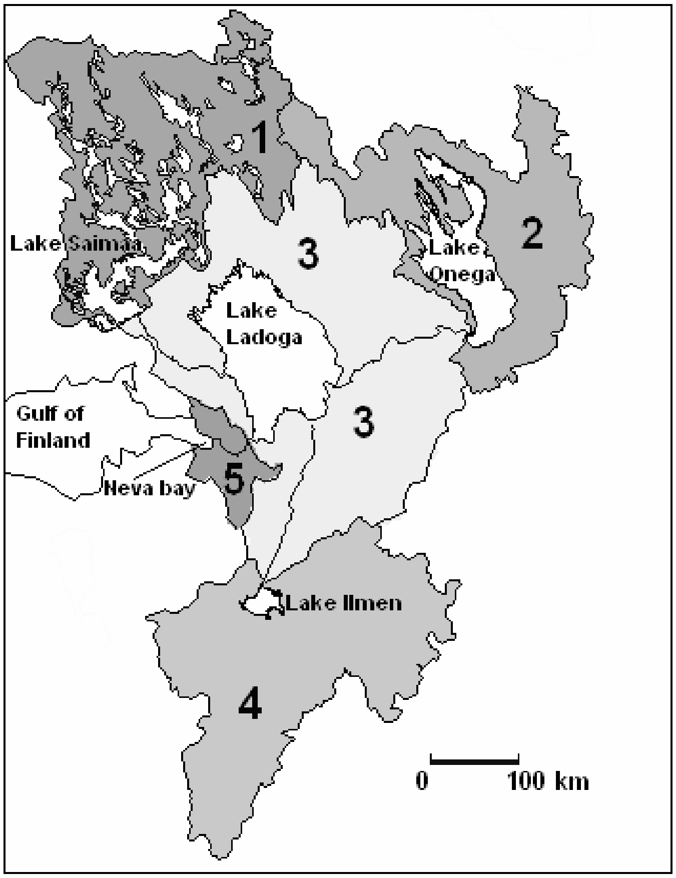

Figure 2. Water system of Lake Ladoga and Neva Bay of the Gulf of Finland (numbers of sub-catchments – according Table 1).

Table 1. Areas of studied water bodies, their catchments and water surface in catchments.

№	Name	Area (km^2)
1	Saimaa catchment / including water surface	56130 / 8419
2	Onega catchment / including water surface	41770 / 3721
3	Ladoga immediate catchment / including water surface	93058 / 2857
4	Ilmen catchment / including water surface	66190 / 1215
5	Neva river and Neva Bay catchment / including water surface	6660 / 36
6	Lake Saimaa	4460
7	Lake Onega	9720
8	Lake Ladoga	17329
9	Lake Ilmen	1200
10	Neva Bay of the Gulf of Finland	400
	Total	296917

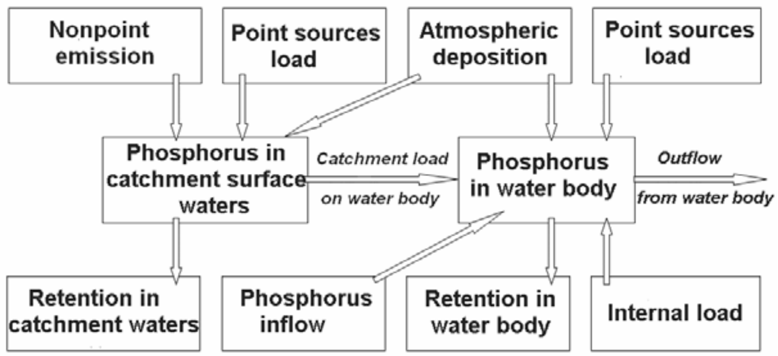

Figure 3. The scheme of phosphorus balance model for catchment – water body system.

The main components of phosphorus balance of the catchment-water body system with main interactions described by developed model are shown in Figure 3.

Annual total phosphorus (P_{tot}) load on water body from catchment area f_1 is:

$$f_1 = (\sum_{i=1}^{n} k_i F_i + L_p + l_a F_{cw})(1 - R_c)\,, \tag{1}$$

where k_i is coefficient of P_{tot} emission in water bodies for i–type of land cover, F_i - area of i-type land cover, L_p – point sources load, l_a- atmospheric specific load, F_{cw} – area of surface waters in catchment, R_c – coefficient of P_{tot} retention in catchment surface waters. The following empirical relationship was used for R_c assessment (Ostrofsky, 1978):

$$R_c = \frac{24}{(30 + \frac{wF_c}{F_{cw}})}\,, \tag{2}$$

where w is runoff depth. The equation of P_{tot} annual balance in water body is:

$$\frac{d(C_p V)}{dt} = f_1 + f_2 + f_3 + f_4 + f_5 + f_6 - f_7 - f_8\,, \tag{3}$$

where C_P is annual P_{tot} concentration in water body, V – water volume, f_2 – P_{tot} inflow from upper parts of water system (for Lake Ladoga it is a sum of inflows from lakes Saimaa, Onega and Ilmen, for the Neva Bay – inflow from Lake Ladoga), f_3 – P_{tot} inflow from lower parts of water system (it is equals 0 for all water bodies excepting the Neva Bay where inflow from the Eastern Gulf of Finland is very important as a result of reverse fluxes), f_4 - P_{tot} input from bottom sediments (internal load), f_5 – atmospheric deposition, f_6 – P_{tot} direct point sources inputs, f_7 – P_{tot} retention in water body, f_8 - P_{tot} outflow. Annual phosphorus retention in water body f_7 is:

$$f_7 = R_w \sum_{i=1}^{5} r_i\,, \tag{4}$$

where R_w is coefficient of P_{tot} retention in water body, calculated by using the equation similar like above mentioned:

$$R_w = \frac{24}{(30 + \frac{wF_c}{F_{wb}})}\,. \tag{5}$$

Changes of various land cover areas F_i were taken from State Statistical Committee (Social…, 2003). Information about land covers of the Finnish part of studied area was taken from web-site “Statistics Finland” (http://www.tilastokeskus.fi/index_en.html). Dynamic of agricultural areas in studied catchments is presented in Fig.4a. Point sources load on catchment surface waters (Fig. 4b) $\boldsymbol{L_p}$ was taken from the results of previous study (Kondratyev et al., 2002) and materials of State Statistic Committee (Social…, 2003). Values of coefficient of P_{tot} emission in water body $\boldsymbol{k_i}$ for selected types of land cover are presented in Table 2.

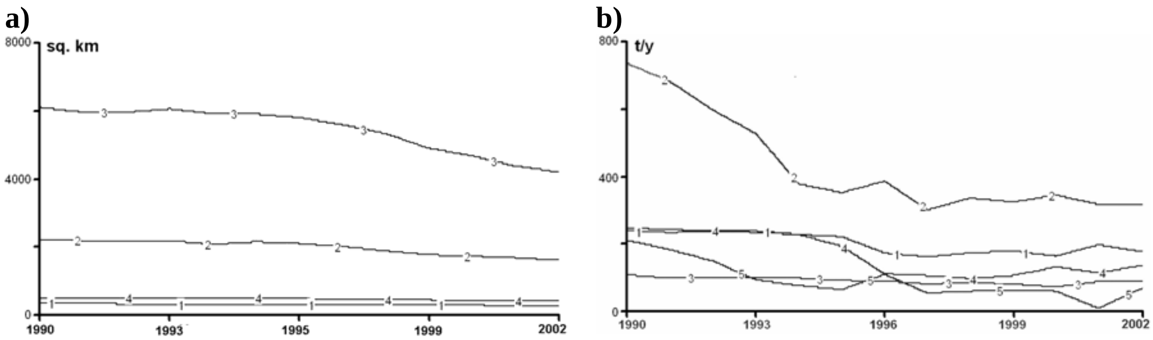

Fig.4. Dynamics of agricultural areas (a) and point sources load (b) water in Lake Onega catchment (1), Lake Ilmen catchment (2), Lake Ladoga immediate catchment (3), Neva River and Neva Bay catchment (4).

Table 2. Coefficients of nonpoint emission (k_i) of P_{tot} in surface waters for various land covers in the Gulf of Finland catchment (Kondratyev et al., 2003)

№	Land cover	k_i - kg km^{-2}year^{-1}
1	Marshes	29
2	Forest	35
3	Agriculture	110
4	Urban	90
5	Others	30

Atmospheric specific phosphorus load on catchment area $\boldsymbol{l_a}$ is equal to 1.9 kg km^{-2} y^{-1}. Annual characteristics of runoff were constant for selected catchments: $\boldsymbol{w}$ = 0.28 m y^{-1} for Lake Ilmen catchment, $\boldsymbol{w}$ = 0.30 m y^{-1} for Lake Saimaa catchment, Lake Ladoga immediate catchment and Neva Bay catchment, $\boldsymbol{w}$ = 0.32 m y^{-1} for Lake Onega catchment. Annual P_{tot} inflow from upper parts $\boldsymbol{f_2}$ is equal to 0 for Lake Saimaa, Lake Onega and Lake Ilmen. For Lake Ladoga $\boldsymbol{f_2}$ is equal to P_{tot} outflows from above mentioned lakes. For Neva Bay $\boldsymbol{f_2}$ is equal to outflow from Lake Ladoga. Annual P_{tot} inflow from lower parts $\boldsymbol{f_3}$ is calculated only for Neva Bay. About 30% of annual inflow comes in bay from eastern part of the Gulf of Finland as a result of reverse fluxes ($\boldsymbol{f_3}$=0.3 $\boldsymbol{f_2}$). Annual P_{tot} inflow from bottom sediments ($\boldsymbol{f_4}$ - internal load) was assessed by using results of previous studied (Kondratyev et al., 1997; Ignatieva, 1996; 1999): $\boldsymbol{f_4}$ = 790 t y^{-1} for Lake Ladoga and 60 t y^{-1} for Neva Bay. Dynamics of direct P_{tot} inputs $\boldsymbol{f_6}$ in Lake Ladoga and in Neva Bay from St. Petersburg according State Enterprise “Vodokanal of St. Petersburg” plan of municipal wastewaters treatment (Environmental…, 2003) are shown in Fig.5 a & b.

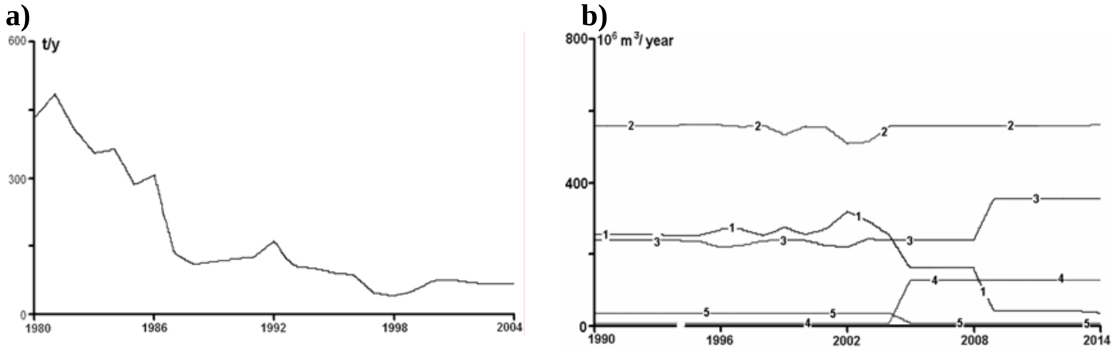

Fig. 5. Dynamics of direct P_{tot} inputs in Lake Ladoga (a) and in Neva Bay (b): untreated wastewaters (1), outputs of Central treatment plant (2), Northern treatment plant (3), South-Eastern treatment plant (4) and Krasnoselskaya treatment plant (5).

Results and Discussion

Calculation of phosphorus balance of studied water system was made for period 1980 – 2014. The comparison between calculated and measured P_{tot} concentrations in Lake Ladoga (Figure 6a) shows that the model is quite adequate. Decrease of P_{tot} concentration in Lake Ladoga can be explained by decrease of components of external load. Main reasons of this decrease were effective environmental protection measures in 80^{th} and economical crisis in 90^{th}.

Calculated dynamic of main components of P_{tot} balance in the Neva Bay is shown in Fig .6b. It is possible to note that phosphorus loads on the Neva Bay from St. Petersburg' wastewaters are 25-30% higher than load from the Neva river and Lake Ladoga. P_{tot} inflow from the Eastern Gulf of Finland as a result of reverse fluxes is also important part of phosphorus load on the Neva Bay (up to 1250 t y^{-1}). High rate of water exchange and low residence time are the reasons of low phosphorus retention in the Neva Bay calculated by using equation (5).

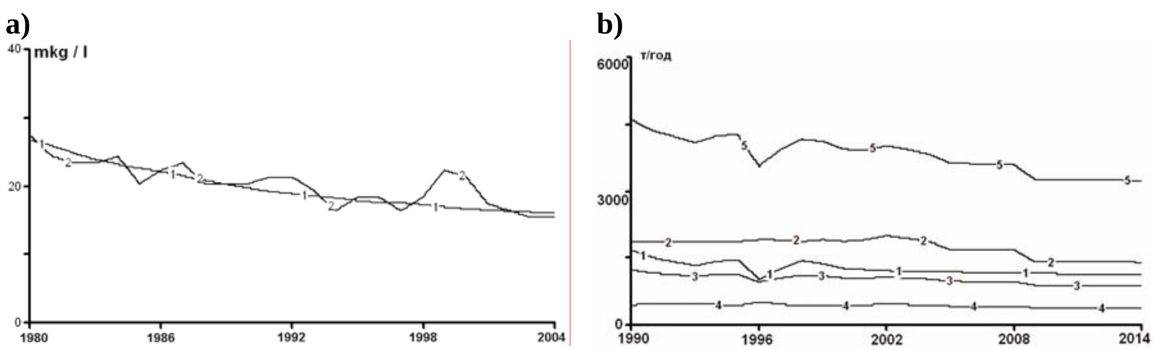

Fig.6. Calculated (1) and measured (2) P_{tot} concentration in Lake Ladoga (a); calculated components of P_{tot} balance in the Neva Bay (b): inflow with Neva runoff (1), municipal wastewaters (2), inflow from the Easter Gulf of Finland with reverse fluxes (3), retention in the Neva Bay (4), outflow to the Easter Gulf of Finland (5).

Developed model can be used for assessment of the role of different land covers and elements of landscapes in water quality formation for studied water bodies. For example, it is possible to assess P_{tot} retention in catchment surface waters and water bodies, which are the important elements of landscape. Calculated values of coefficient of P_{tot} retention for studied sub-catchments and water bodies are presented in Table 3. Lake Onega has the highest value of coefficients of P_{tot} retention, because its residence time (time of water exchange) is about eighteen years. $\boldsymbol{R_w}$ for Lake Ladoga is equals to 0.71, its retention time is about 11 years. At the same time the residence time for Neva Bay is about one week, that is why P_{tot} retention in Neva Bay is less the 10% (Fig. 6b).

Table 3. Coefficients of P_{tot} retention in water bodies (R_w) and catchment surface waters (R_c).

№	Name	Coefficients of P_{tot} retention
1	Lake Saimaa	0.71
2	Lake Saimaa catchment surface waters	0.75
3	Lake Onega	0.76
4	Lake Onega catchment surface waters	0.71
5	Lake Ladoga	0.71
6	Lake Ladoga immediate catchment surface waters	0.60
7	Lake Ilmen	0.53
8	Lake Ilmen catchment surface waters	0.53
9	Neva Bay	0.09
10	River Neva and Neva Bay catchment surface waters	0.32
	Mean	0.57

Present P_{tot} load forms the concentration in Lake Ladoga equals to 14.3 mkg l^{-1}. The load consists of natural and anthropogenic parts. If the direct point load will be excluded and if coefficients of P_{tot} emission from urban and agricultural areas will be changed on coefficients of emission from natural land cover, results of calculation will show the response of the lake on natural part of load. In this case the P_{tot} concentration in Lake Ladoga will equal to13.2 mkg l^{-1}. This value corresponds the impact of natural landscapes and land covers. Man-made part of load increase the P_{tot} concentration in Lake Ladoga only on 8%.

Assessment of expecting P_{tot} concentration in the Neva Bay depending on various scenarios of wastewaters treatment in St. Petersburg is presented in Table.4. Wastewaters treatment under HELCOM recommendations (1.5 mg P_{tot} l^{-1} for all outlets of municipal treatment plants) together with implementation of State Enterprise "Vodokanal of St. Petersburg" scenario will lead to decrease of P_{tot} content in the Neva Bay only about 5 % to 2004 level. It is worse then results of calculation with present degree of treatment. Additional treatment of wastewaters at all treatment plants according the EU recommendations (1.0 mg P_{tot} l^{-1} in treated waters) will lead to decrease of P_{tot} content in The Neva Bay about 22 %. Extra treatment up to 0.8 mg P_{tot} l^{-1} in treated waters will decrease P_{tot} content in the Neva Bay on 29 % to 2004 level. The obtained results can be use to decision makers for evaluation of perspectives of practical application of new and very expensive technologies of municipal wastewaters treatment taking into account possible response of the Neva Bay's water quality.

Table 4. Results of simulation modeling with the aim of assessment of future changes of P_{tot} concentration in Neva Bay depending on scenarios of wastewaters treatment in St. Petersburg.

Scenario	% from 2004 value (39.8 mkg l^{-1})
Without treatment	153
State Enterprise "Vodokanal of St. Petersburg" treatment plan	85
P_{tot} concentration in treated waters - 1.5 mg l^{-1} (HELCOM recommendation)	95
P_{tot} concentration in treated waters - 1.0 mg l^{-1} (EU recommendation)	78
P_{tot} concentration in treated waters - 0.8 mg l^{-1}	71

Conclusions

The model of phosphorus balance of large water system and its catchment area was developed and tested for freshwater system of Lake Ladoga and Neva Bay of the Gulf of Finland. The model was used for assessment of the role of point and nonpoint sources of phosphorus loading in water quality formation for the system. Phosphorus retention in catchment surface waters and water bodies was assessed: the water bodies with high residence time are characterized by high values of coefficients of phosphorus retention. An assessment was made of potential future phosphorus concentration in Neva Bay depending on various scenarios of wastewaters treatment in St. Petersburg.

The nearest perspectives of the model development are (i) to couple the model of phosphorus balance with physically-based models like SWAT for assessment of distributed hydrological parameters in sub-catchments, (ii) to assess the influence of hydrological changes on phosphorus fluxes and (iii) to investigate spatial distribution of nonpoint phosphorus emission from various land covers in the studied water system.

Acknowledgment

The study was carried out with partial financial support from the Russian Fund for Basic Research (project 05-05-65097-2) "Estimation and forecast of phosphorus balance of Lake Ladoga and Neva Bay water system".

References

Becker A. (1992) Criteria for a hydrologically sound structuring of large scale land surface process model. – In: Advances in theoretical hydrology (ed J.P.O'Kane), Elsevier, 98-111.

Environmental Report 1997-2001 (2002) State Enterprise "Vodokanal of St. Petersburg", 63 p.

Ignatieva N. (1996) Distribution and release of sedimentary phosphorus in Lake Ladoga. Hydrobiologia, 322:129-136.

Ignatieva N. (1999) Nutrient exchange across the sediment-water interface in the eastern Gulf of Finland. Boreal Environment research, 4: 295-305.

Kondratyev S. (1992) Mathematical modeling of runoff and pollution washout in catchments. - D.Sc. Thesis, Institute of Limnology, St. Petersburg (In Russian).
Kondratyev S., Efremova L., Raspletina G., Tchernikh O., Veselova M., Kulibaba V., Svistov P. (1997) Assessment of external load on Lake Ladoga. Ecological Chemistry, 6(2):73-84, (in Russian).
Kondratyev S., Gronskaya T., Ignatieva N., Blinova I., Telesh I., Yefremova L. (2002) Assessment of present state of water resources of Lake Ladoga and its drainage basin using Sustainable Development indicators. Ecological Indicators, 2: 79-92.
Kondratyev S., Mendel O. (1997) Modelling runoff and leaching at various temporal scales. - Proc. of Int. Symp."Freshwater Contamination", 5-th Scientific Assembly of IAHS, Rabat, Marocco, IAHS Publ. N 243, pp. 341 - 347.
Kondratyev S.A., Alyabina G.A., Sorokin I.N., Moiseenkov A.I., Izmailova A.V. (2003) Assessment of external load on aquatic systems depending on the land cover of catchments (Northwest Russia as a case study). EcoSys (Beiträge zur Őkosystemforschung), 10: 107-115.
Kosheleva N.E. (2003) Mathematical modeling of migration processes in landscape-geochemical systems. – D.Sc. Thesis, Moscow State University (in Russian).
Kuchment L.S. (1980) Models of river runoff formation. – Leningrad, Hydrometeoizdat Publ. House, 142 p. (in Russian)
Kuchment L.S., Gelfan A.N., Demidov V.N. (2000) A distributed model of runoff generation in the permafrost regions. – J.Hydrology 240, pp. 1-22.
Ostrofsky M.L. (1978) Modification of phosphorus retention models for use with lakes with low water loading. J. Fish. Res. Board Canada, 35(12):1532-1536.
Rozhkov V.F., Trapeznikov Yu.A., (1990) Probabilistic models of the ocean processes. – Leningrad, Hydrometeoizdat Publ. House, 272 p.(in Russian).
Social and economic characteristics of Northwest Russian regions in 1995-2002 (2003) - Goskomstat Proceedings, Russia, 160 p. (in Russian).
Vinogradov Y.B. (1988) Mathematical modeling of runoff formation. – Leningrad, Hydrometeoizdat Publ. House, 312 p. (in Russian).

Sensitivity of the SWAT Model to Spatial Variability of Land Use and Soil Data: A Lake Balaton Catchment Case Study

Peter Laszlo*[1], Laszlo Pasztor[1] and Jozsef Szabo[1]
[1]Research Institute for Soil Science and Agricultural Chemistry of the Hungarian Academy of Sciences, H-1022 Budapest, Herman Otto 15, Hungary. E-mail: laszlo@rissac.hu

Abstract

Soil erosion has special importance in the watershed of Lake Balaton, Hungary, since the sediment, rich in organic matter and nutrients, can accelerate eutrophication of the lake. Non-point source pollution of the lake has become recognized as an important environmental problem associated with agricultural production. The agricultural diffuse phosphorus loading of Lake Balaton must be further decreased in order to maintain good water quality. Modeling phosphorus (P) loss from agricultural watersheds is key to quantifying the long-term water quality benefits of alternative best management practices. The goal of the 3/024/2001 NKFP project was to develop policy scenarios that may result in significant reduction of P loads. Three major objectives were set up: i) the mechanism of phosphorus transport should be clarified and modeled because the mechanisms associated with this process are not sufficiently known, ii) build a coherent watershed database and publish it on the homepage of the project so that it can meet different levels of demand on information. iii) develop these new services, to work out environmentally friendly farming alternatives and test the farmers` acceptance.

The Soil and Water Assessment Tool (SWAT) was chosen to study soil erosion in a subwatershed on long-term simulations for management purposes. The model requires satisfactory spatial information on topography, hydrography, land use, soil characteristics, management, etc. Large-scale spatial information on soil properties, which significantly affects formulation of runoff and soil loss, can provide suitable information with the expected accuracy. To create DDM and for compilation of a land cover map 1:10,000 scale topographic maps were used. A 1:10,000 scale soil map and the National 1:25,000 Scale Spatial Soil Information System were used as basic information for soil characteristics with new laboratory data from the area for compilation of soilscape and generation of soil input parameters. To control the land use and soil data, a characteristic study catchment was selected. In order to model calibration, the outlet of the pilot area has been equipped with an automatic flow meter, a rainfall collector, and sediment samplers. The process of map compilation and results of soil input parameter generation achieved in a pilot area (Somogybabod) in a subwatershed (Tetves) of Lake Balaton are presented in this paper.

Introduction

Physically based, distributed hydrological models (PDHMs), whose input parameters have a physical interpretation and explicit representation of spatial variability (Abbott et al., 1986) are increasingly being used to solve complex problems in water resource applications. However, problems with PDHMs include a lack of sufficient data to fully characterize spatial variability, scale problems of field measurements and model parameter elements, and imperfect representations of real processes in models (Beven, 1989). These factors result in the requirement of model calibration and validation (Anderton et al., 2003). Unfortunately, the use of this kind of modeling requires spatially distributed databases and advanced GIS applications. There is a lack of understanding of the robustness, sensitivity and validation of these models in relation to different parameterizations. In particular, questions are raised about the appropriate resolution of the spatial soil and land use input data.

The goal of the 3/024/2001 NKFP project is to identify which alternate management practices or land use changes can potentially help mitigate diffuse phosphorous pollution of Lake Balaton, Hungary.

The Soil and Water Assessment Tool (SWAT) was chosen to study soil erosion in a subwatershed on long-term simulations for management purposes. The objective of this paper is to describe primary results of applying the SWAT model to a study catchment. The SWAT model was developed as a river basin scale model to quantify and predict the effects from different land management practices in large, complex catchments (Arnold et al., 1998). In this study we compare different approaches of watershed delineation processes. More precisely, we will analyze the sensitivity of AVSWAT to the spatial variability of soil and land use map information by comparing the pre-processed data results to a pilot area.

Methodology

Model Description

In this case study, the AVSWAT version of the SWAT2000 model was used (Di Luzio, 2002). This version is integrated with ArcView GIS and applies some of the ArcView functions.

The Study Catchment and the Pilot Area

The study catchment (Tetves) is situated in the south part of the Lake Balaton Watershed in Hungary (Figure 1). The total surface area of the study catchment is 74 km^2. The average elevation of the catchment is 206 m a.s.l. and the terrain is gently undulating. As reference for the HRU (Hydrological Response Unit) distribution and for further calibration, a pilot area (Somogybabod) in the study catchment was selected. The total area of the pilot area is 7 km^2 and the outlet was equipped with an automatic flow meter, rainfall collector and sediment samplers.

Figure 1. The study catchment and the pilot area.

General Input Data for SWAT Simulations

The digital elevation model (DEM) was used for delineation and topographic characterization of the watershed (Figure 2). The DEM of the watershed was obtained by digitizing topographic maps at a scale of 1:10,000. The maps were rasterized and georeferenced, and then elevation contour lines and spot heights were vectorized in order to obtain the geographic database for topography. The DEM was built by processing the digital topographic data through the TIN and "topogrid" procedures implemented in the ESRI ARC/INFO software.

The weather data were obtained from the Hungarian Meteorological Service. The data set includes the daily precipitation rate and the daily maximum/minimum temperature. The simulated year was a typical climate year (1992) with 635 mm precipitation.

The land use map was created using the European CORINE Land Cover 1:50,000 vector map (CLC50) dataset (Figure 3). The CLC50 consists of a geographical database describing vegetation and land use in 87 classes. The initial classification of the CLC land use was not in agreement with the model classification; therefore, a reclassification of the land use (based on its specification) was done.

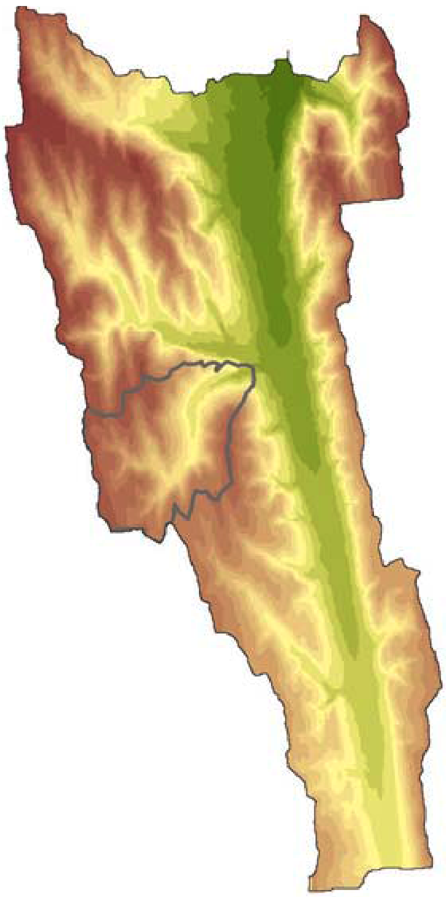

Figure 2. DEM.

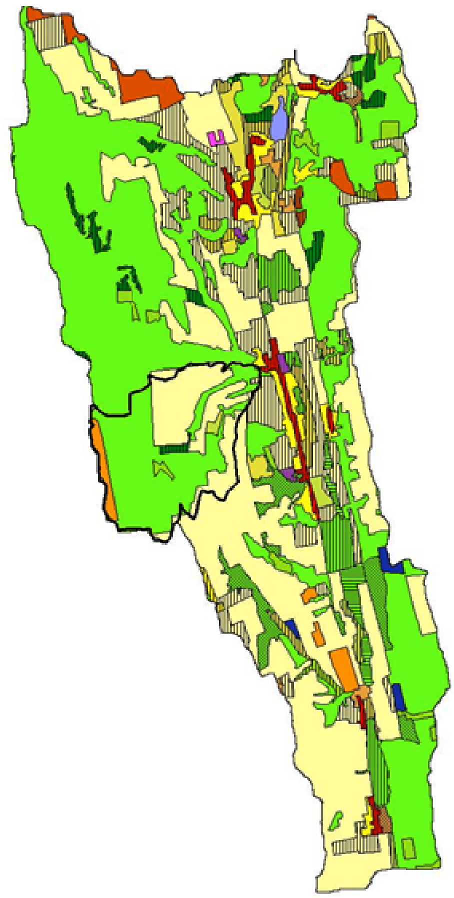

Figure 3. CORINE.

At the beginning of the study, no suitable soil map for the area was available. The only sufficiently detailed map of soils for the study area was acquired from an association map. The map, developed by Kreybig (1937) at a scale of 1:25,000, does not strictly show the individual soil types. Instead the map shows compound soil-landform units, referred to as map units, which are characterized by different and particular collections or associations of soils (Figure 4). Each soil type is characterized via the "representative profile" with layers. The underlying attributes of the map consist of field descriptions of the soil profile, physical properties such as moisture, structure, texture, extractions and measured laboratory data (organic carbon content, pH and nutrients) in each diagnostic horizon. The soil layer was obtained using the digitalized KREYBIG map at the scale of 1:25,000. Physical and hydrological properties of the soil profiles were related to the corresponding cartographic units using taxonomy categories. Soil parameterization was taken from the laboratory-measured data of the KREYBIG dataset. After extraction of the soil data, the missing soil parameters for each soil layer were estimated by using pedotransfer functions (Fodor and Rajkai, 2004). Management input data were combined from information provided by several farmers and experts. In the case of flow data, water quality data, forested area management, and some of the crop parameters, the SWAT database values were used.

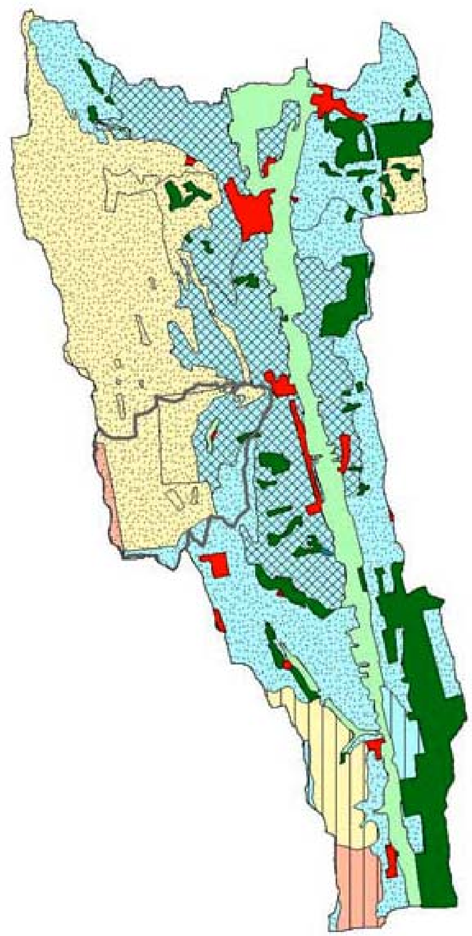

Figure 4. DKSIS.

Modeling Scenarios

The subbasin size threshold value (CSTV) plays an important role in determining the detail of the stream network and the size and number of subbasins. The interface lists a minimum, maximum, and suggested subbasin area in hectares. The number of subbasins and HRUs was determined after some investigation of the scale effect. In the first option, the study catchment was subdivided into subbasins based on a threshold area suggested by the SWAT model. The initial stream network defined by watershed delineation was refined adding outlet locations in the study catchment and the pilot area which corresponded to the stream flow gages. Several combinations of threshold values were tested for HRU delineation. The HRU distribution procedure subdivides the catchment into areas having unique land use and soil combinations, and enables the model to reflect differences in evapotranspiration and other hydrologic conditions for different land cover/crops and soils. Runoff is predicted separately for each HRU and routed to obtain the total runoff for the watershed. This increases the accuracy of load predictions and provides a much better physical description of the water balance. The user has two options in determining the HRU distribution: assign a single HRU to each subbasin or assign multiple HRUs to each subbasin. For characterizing the soil type and land use in each HRU, the dominant and multiple soil/land use distributions were considered.

Results and Discussion

In the first option, the entire Tetves Stream Catchment was subdivided into 15 subbasins based on a threshold area of 200 hectares, as suggested by the model. The total number of HRUs in the study catchment and the pilot area, according to the different HRU distributions, are shown in Table 1.

If multiple HRUs are selected, the user may specify sensitivities for the land use and soil data that will be used to determine the number and kind of HRUs in each subbasin. All of the land use and soil type classes will be considered if the user determines zero for the Land Use (%) over the subbasin area and zero for the Soil Class (%) over Land Use. If a single HRU per subbasin is selected, the dominant land use category and soil type within each subbasin determines the HRU distribution. These options produced different cover for the land uses and soil types for the study catchment area and for the pilot area, and are shown in Tables 2 and 3.

To analyze the sensitivity of the model to the spatial variability of land use and soil data, the CSTV200 and CSTV100 were compared. The suggested value (CSTV200) was not detailed enough because the results were analyzed in the pilot area. In this case, the CSTV100 was needed.

Table 1. CSTV and LandUse/Soil options.

CSTV (ha)	Study catchment (TETVES)			Pilot area (SOMOGYBABOD)		
	Number of Sub-basins	DOMINANT LandUse/Soil OPTION	MULTIPLE HRUs LandUse/Soil OPTION	Number of Sub-basins	DOMINANT LandUse/Soil OPTION	MULTIPLE HRUs LandUse/Soil OPTION
100	41	41	520	3	3	25
200 (suggested)	15	15	273	1	1	18

Table 2. Land use classes in SWAT land cover/plant codes.

Land Use	Study catchment %Wat. Area				Pilot area %Sub. Area
	CSTV 200		CSTV 100		CSTV 100
	multiple HRU’s	single HRU	multiple HRUs	single HRU	single HRU
Range-Brush (RNGB)	0.27	-	-	-	-
Agricultural Land-Generic (AGRL)	29.13	-	34.01	-	52.34
Agricultural Land-Row Crops (AGRR)	9.19	40.22	0.69	-	-
Forest-Deciduous (FRSD)	45.42	59.56	58.08	100	47.66
Forest-Evergreen (FRSE)	1.47	-	1.28	-	-
Forest-Mixed (FRST)	0.34	-	-	-	-
Orchard (ORCD)	2.54	-	4.51	-	-
Pasture (PAST)	1.30	-	-	-	-
Italian (Annual) Ryegrass (RYEG)	3.11	-	1.04	-	-
Water (WATR)	0.26	-	-	-	-
Wetlands-Forested (WETF)	3.11	-	-	-	-
Residential-Low Density (URLD)	3.57	0.22	0.39	-	-
Industrial (UIDU)	0.29	-	-	-	-

Table 3. Soil types.

Soil	study catchment %Wat. Area				pilot area %Sub. Area
	CSTV 200		CSTV 100		CSTV 100
	multiple HRUs	single HRUs	multiple HRUs	single HRUs	single HRUs
SB1	51.13	68.68	79.51	100	100
SB113	6.16	9.87	-	-	-
SB114	19.92	16.25	18.63	-	-
SB116	9.74	4.98	0.87	-	-
SB117	10.62	-	0.37	-	-
SB118	0.03	-	-	-	-
SB206	2.41	0.22	0.60	-	-

Conclusions

This study has shown that there are differences in the HRU distributions in subbasins according to the subbasin size threshold value. Due to high variability in soil types and land uses (and also some inaccuracy) a higher threshold value than what was suggested was needed for a realistic HRU distribution. It seems that the CLC50 land use and KREYBIG soil maps are sufficient for this modeling exercise because more detailed land use and soil maps would not be useful in SWAT (only the most common combinations appear in the HRUs and less common soil types disappear). Therefore, it is advised to take precautions before applying an integrated model.

Acknowledgement

The study was funded by the Hungarian Ministry of Education, contract No. 3/024/2001 NKFP project.

References

Abbott M.B., J.C. Bathurst, J.A. Cunge, P.E. O'Connel, and J. Rasmussen. 1986. An introduction to the European Hydrological System 1. History and philosophy of a physically based distributed modeling system. J. Hydrol. 87:45-59.

Anderton S., J. Latron, F. Gallart. 2002. Sensitivity analysis and multy-response, multi-criteria evaluation of a physical based distributed model. Hydrol. Process. 16:333-353.

Arnold, J.G., R. Srinivasan, R.S. Muttiah, and J.R. Williams. 1998. Large area hydrologic modeling and assessment. I. Model development. J. Am Water Resour. Assoc. 34:73-89.

Bernoux, M., D. Arrouays, C.C. Cern, and H. Bourennane, 1998. Modeling vertical distribution of carbon in oxisols of the western Brazilian Amazon (Rondonia). Soil Science 163, 941-951.

Beven K.J. 1989. Changing ideas in hydrology: the case of physically based models. J. Hydrol. 105:157-172.

Di Luzio, M., R. Srinivasan, J.G. Arnold , and S.L. Neitsch. 2002. Soil and Water Assessment Tool. ArcView GIS Interface Manual: Version 2000. GSWRL Report 02-03, BRC Report 02-07, Published by Texas Water Resources Institute TR-193, College Station, TX. 346p.

Fodor N. and K. Rajkai 2004. Talajfizikai tulajdonságok becslése és alkalmazásuk modellekben. Agrokémia és Talajtan. 53:225-448.

Grayson R.B., I.D. Moore, T.A. McMahon. 1992. Physically based hydrologic modeling I. A terrain-based model for investigative purposes. Water Resour. Res. 28:2639-2658.

Impact of Precipitation Data Interpolation on the Quality of SWAT Simulations

Roberta Maletta*[1], Johan A. Huisman[2], Lutz Breuer[2], Hans-Georg Frede[2], and Giuseppe Mendicino[1]
[1]Department of Soil Conservation,University of Calabria, Italy. Email: betta.maletta@libero.it.
[2]Institute of Landscape Ecology and Resources Management, University of Giessen, Germany.

Abstract

Precipitation is the most important driving factor for rainfall-runoff models. Typically, only point measurements made with rain gauges are available. Interpolation is required to estimate precipitation in other parts of the catchment. The current version of SWAT uses a nearest neighbour approach. However, many other interpolation methods, such as inverse distance weighting, inverse square distance weighting, kriging with a time-stable variogram, and kriging with daily variograms are available. The first objective of this work was to compare the interpolation accuracy of these five interpolation methods through cross-validation. Daily precipitation time series from a network of 18 stations in the Lahn-Dill Region (Germany) were used in this study. Cross-validation showed that all interpolation schemes had a similar accuracy, except for the nearest neighbour interpolation characterised by a lower accuracy. The second objective was to analyze the impact of different interpolation schemes on the quality of automatically calibrated SWAT simulations both with respect to different components of the water cycle and the optimised model parameters. All of the interpolation methods were used to generate precipitation input data for the Aar Catchment, a 134 km^2 catchment within the Lahn-Dill Region. The interpolation methods resulted in different water balances with the strongest relative increase in the deep aquifer recharge. Despite our expectations, the automatic calibration was only partly able to compensate for the differences in the precipitation values, which was attributed to the dominance of the lateral flow component in the Aar Catchment.

Introduction

Precipitation at daily time-step is the most important component in hydrological modelling. Although precipitation has a high degree of variability both in space and time, in most areas the density of rain gauges is low. Interpolation is required to estimate precipitation in other parts of the catchment. The current version of SWAT uses a nearest neighbour approach. However, many other interpolation methods are available in the literature.

The first objective of this work is to compare the interpolation accuracy of five interpolation methods based on daily precipitation data recorded from a network of 18 precipitation stations in the Lahn-Dill Region (Germany). The second objective is to analyze the impact of the different interpolation schemes on the quality of automatically calibrated SWAT simulations, both with respect to different components of the water cycle and the optimised model parameters. To achieve this, the interpolation methods were used to generate five different sets of precipitation input values. Then, each precipitation field was used to automatically calibrate a modified version of the SWAT2000 model (Eckhardt et al., 2002).

Methodology

Interpolation Methods

In this paper, five methods used to interpolate precipitation were compared. The first method is based on the nearest neighbour. In nearest neighbour interpolation, it is assumed that values at unsampled locations are equal to the value at the nearest sampled point. This is the interpolation method used in SWAT2000. Since this method only considers measurements at the nearest station and does not include measurements from other nearby stations, it is often considered as a crude interpolation method, showing unrealistic and discontinuous precipitation fields.

In the inverse distance and inverse square distance interpolation methods, the values at unsampled locations are achieved by weighting the measurements at each precipitation station with the inverse of the distance or the inverse of the squared distance, respectively. The inverse square distance interpolation puts more weight on nearby measurements. In their simplest form when all precipitation stations in an area are considered, these methods distort the occurrence frequency of precipitation because precipitation will be predicted at the unsampled location, once precipitation was measured at any one of the stations. To avoid this distortion, a limited number of four nearest stations were included in these interpolation methods.

The final two methods are based on ordinary kriging, where the weights for each measurement location are achieved through a function that describes the dependence of the variance on the distance between sample locations. This function is known as the variogram and it must be estimated from the precipitation data. Typically, a large number of measurements (>150) is required to accurately estimate this variogram and clearly such a large number of precipitation stations is seldom available. In this paper, two approaches to estimating the variogram were considered. In the first approach, a time-stable variogram was hypothesised. This allows the use of precipitation measurements from all dates, which strongly increases the amount of measurements to estimate the variogram. Of course, this is a rather crude assumption because it is well known that convective rainfall events are much more spatially variable than advective rainfall events. In the second approach, a variogram was estimated separately for each day. Although this approach potentially considers the spatial variability of different rainfall events, it is very inaccurate to estimate the variogram from only a small number of precipitation stations. Therefore, it is questionable whether the second approach is more accurate than the first one. Both ordinary kriging methods also suffer from the same distortion of the precipitation occurrence frequency described earlier, albeit to a lesser extent than interpolation methods based on the distance only. Therefore, the number of stations included in the interpolation has been limited to a search radius of 10 km.

Aar Catchment

The Aar Catchment is a subcatchment of the low mountainous Dill Catchment in Germany. It has an area of 131 km^2 with an elevation range from 220 to 596 m a.s.l, and an average altitude of about 349 m (Figure 1). The Aar Catchment is covered by 29% deciduous forest, 23% coniferous forest, 19% pasture, 6% cropland and 9% urban area, as determined from a composite of Landsat TM5-scenes from 1994 and 1995 (Nöhles, 2000). Soil data are available in a 1:50,000 scale soil map (HLUG, 1998). For the SWAT simulations, the Aar Catchment was divided into 10 subbasins and 151 hydrological response units.

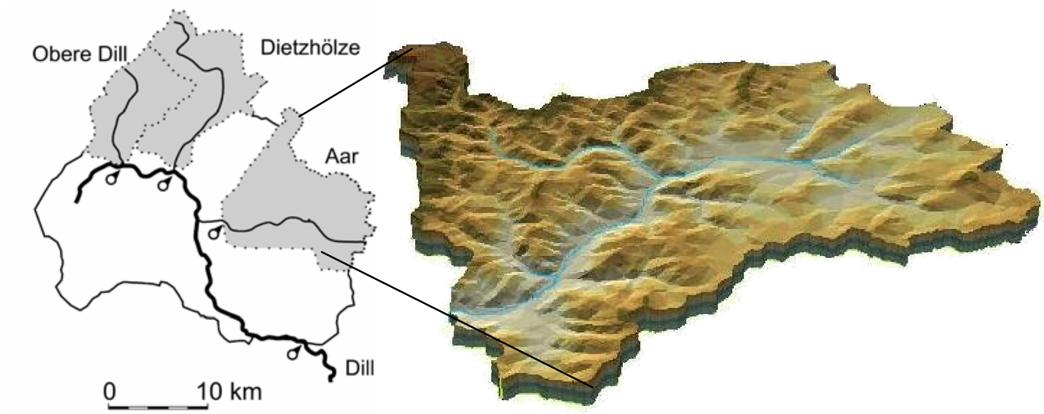

Figure 1. The Aar Catchment, Germany.

For the automated calibration of the Aar Catchment, a version of the Shuffled Complex Evolution Metropolis (SCEM) algorithm coupled with SWAT2000 in a Matlab environment was used. SCEM-UA is an effective and efficient optimisation algorithm that simultaneously finds the optimal model parameters and their uncertainty bounds within a parameter space defined by upper and lower values for each calibrated model parameter (Table 1). For more information on this optimisation algorithm, refer to Vrugt et al. (2003).

A modified version of SWAT2000, SWAT-G, adapted to low mountainous regions in Germany (Eckhardt et al., 2002) was used for these simulations. One of the main differences between SWAT-G and other versions of SWAT is that SWAT-G includes an anisotropy factor between vertical and horizontal saturated hydraulic conductivity to account for the strong tendency for lateral flow in this type of catchment. SWAT-G was calibrated to three years of daily discharge measurements (1991-1993) available at the outlet of the catchment by minimizing the sum of squared residuals (SSR) between measured and simulated discharge. Validation was performed on seven years of daily discharge measurements (1983-1989).

To assess the impact of different precipitation data interpolation methods on the quality of the SWAT simulations for the catchment, precipitation data from 17 stations located in the Lahn-Dill Region were used. Figure 2 shows the dependence of mean yearly precipitation on altitude within this area. It can be seen that mean yearly precipitation ranges from about 700 to 1300 mm and is strongly dependent on altitude. Due to the dominance of west winds and the high Westerwald area to the west of the catchment, the mean yearly precipitation is also dependent on the longitude with decreasing precipitation from west to east.

Table 1. Lower and upper bound of the user-defined parameter space and the optimised parameters for each interpolation method.

	Lower bound	Upper Bound	Nearest Neighbour	Inverse Distance	Inv. Sq. Distance	Ordinary Kriging	Ord. Krig. (daily)
Surface runoff lag time (d^{-1})	1.00	2.00	1.00	1.00	1.00	1.00	1.00
Groundwater recession coefficient (d^{-1})	0.03	0.06	0.05	0.05	0.05	0.05	0.04
Delay of groundwater recharge (d)	1.0	20.0	1.0	1.2	1.0	1.1	1.2
Deep aquifer percolation factor (-)	0.00	0.80	0.42	0.68	0.70	0.71	0.59
*Bulk density soil (g cm^{-3})	1.50	1.60	1.55	1.55	1.55	1.55	1.56
Bulk density bedrock (g cm^{-3})	2.51	2.64	2.64	2.64	2.64	2.64	2.64
*Available water content (m^3 m^{-3})	0.10	0.30	0.29	0.30	0.30	0.30	0.30
*Saturated hydraulic conductivity Soil I (mm/hr)	1.0	45.0	42.5	44.6	43.7	43.6	44.4
*Saturated hydraulic conductivity Soil II (mm/hr)	10.0	85.0	65.7	63.8	64.7	67.0	66.0
Anisotropy factor (-)	2.00	8.00	2.78	2.22	2.38	2.48	2.21
Manning N surface runoff ($m^{-1/3}$ s)	0.10	0.50	0.50	0.50	0.49	0.50	0.50

* the value of the upper soil layer of one particular soil was calibrated and the values for the other layers of the same soil and other soils were adjusted according to this change (Eckhardt and Arnold, 2001).

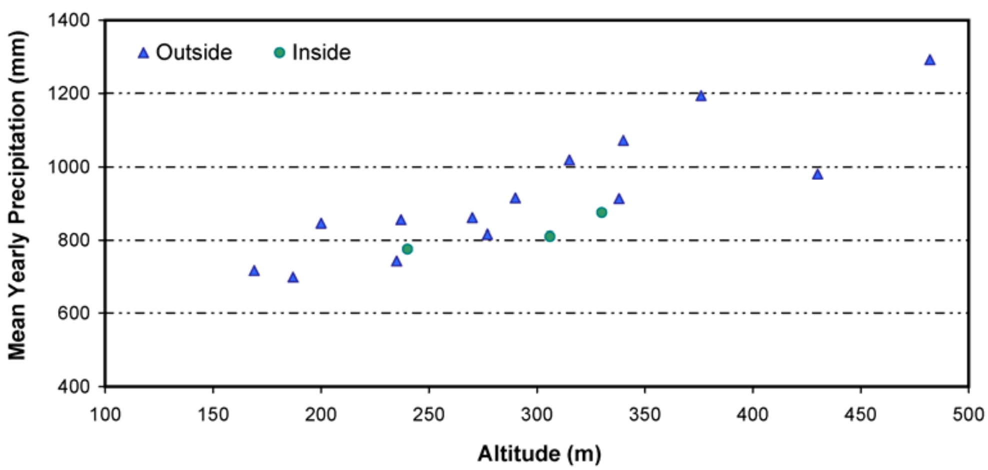

Figure 2. Dependence of mean yearly precipitation on altitude for the 17 precipitation stations in the Lahn-Dill Region for the period 1980-1994. The circles indicate stations that are located within the Aar Catchment. Triangles indicate stations in the Lahn-Dill Region but outside the Aar Catchment.

In order to compare different interpolation methods, a pseudo-precipitation station located at the centroid of each of the 10 subbasins within the catchment was created. The five interpolation methods were then used to generate precipitation data time series for each pseudo-precipitation station. This way, the nearest neighbour interpolation implemented in the SWAT2000 interface was circumvented. The nearest neighbourhood, the inverse distance and the inverse square distance interpolation methods included a precipitation correction for the altitude difference between the pseudo- and actual precipitation stations based on a linear precipitation lapse rate of 3.54 mm/day per km. This lapse rate was derived from the dependence of mean annual precipitation on altitude. The two ordinary kriging approaches cannot be combined with this altitude correction. Therefore, an altitude correction was not included in the two geostatistical interpolation methods. The small number of precipitation stations hampers the use of more advanced geostatistical methods that are able to include the precipitation trends (e.g. cokriging or universal kriging).

To quantitatively evaluate the modelling results, different statistical measures were determined. These measures were calculated on a daily basis for the calibration and validation period for each interpolation technique. The statistical measures included a linear regression equation ($Y = aX + b$) between simulated (Y) and observed discharge (X). Ideally, the coefficients a and b should be 1 and 0, respectively. The coefficient of determination, R^2, summarizes how well the regression line represents the data. Moreover, the Mean Squared Error (MSE) and the Nash and Sutcliffe (NS) coefficient were calculated from the observed daily discharge (q_o), the simulated daily discharge (q_s) and the number of observations (n) (Equations 1 and 2):

$$MSE = \frac{1}{n}\sum_{i=1}^{n}(q_o - q_s)^2 \qquad (1)$$

$$NS = 1 - \left(\frac{\sum_{i=1}^{n}(q_o - q_s)^2}{\sum_{i=1}^{n}(q_o - \overline{q}_o)^2} \right) \qquad (2)$$

To assess the accuracy of the different interpolation methods independently of the SWAT simulations, a cross-validation on the 17 rain gauge stations was also carried out. In this cross-validation, one station at a time was removed from the dataset and the remaining 17 stations were used to predict the precipitation at the location of the station that was removed. A comparison of the actual and predicted precipitation for all 17 precipitation stations provides information on interpolation quality.

Results and Discussion

Figure 3 presents the results of the cross-validation. The left panel shows the bias for each of the interpolation methods. The bias was close to zero for all methods, which suggests that all methods provide unbiased estimates. However, the standard deviation of the bias, which is indicated by the error bars in the left panel, was considerable. The standard deviation of the bias was highest for the nearest neighbour interpolation (138 mm) and lowest for the inverse distance interpolation (106 mm). The largest bias was –365 mm per year for one precipitation station interpolated with ordinary kriging using a time-stable variogram.

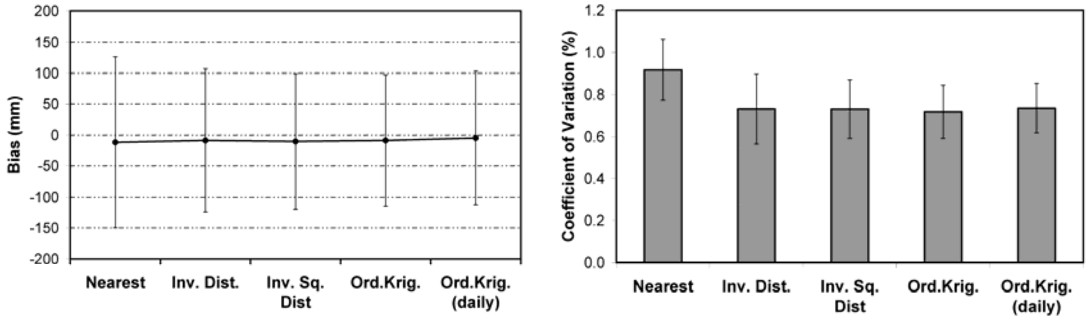

Figure 3. Bias and coefficients of variation for the cross-validation with the 17 precipitation stations within the Lahn-Dill Bergland.

The right panel of Figure 3 shows the coefficient of variation for each of the interpolation methods. The coefficient of variation (CV) is defined as the root mean squared error between measured and predicted precipitation divided by the average precipitation at that station. It can be seen that the nearest neighbour interpolation had the highest CV. This means that the interpolation quality was lower than the quality of the other interpolation methods, which all have a similar CV (0.72 - 0.74). These CV values were much higher than those reported by Dirks et al. (1998), who found CV values on the order of 0.30 - 0.40. This is due to the larger extent of this study area, approximately 1000 km^2 for the Lahn-Dill Region and 35 km^2 in the Dirks et al. (1998) study on Norfolk Island.

There is a large body of literature on the use of geostatistical interpolation methods on precipitation data (Goovaerts, 2000 and references therein). Generally, these studies have found that more advanced interpolation methods outperform simpler interpolation methods. However, the focus of these studies has mostly been on average monthly or even average yearly precipitation. Also, these studies tend to use data sets with a large number of precipitation stations and a high station density. In this study, the higher accuracy of the precipitation interpolation with more advanced interpolation methods could not be confirmed. A similar conclusion was reached by Dirks et al. (1998). In this study, and that of Dirks et al. (1998), the focus was on interpolation of daily precipitation with only a small number of stations (<18). We believe that these contrasting results are due to problems with defining appropriate variograms. First of all, this is due to the small number of precipitation stations available. However, the problem might also be inherent to daily precipitation data. It is assumed that a time-stable variogram results in a well-defined variogram, but neglects changes in spatial variability for different precipitation event types. Potentially, these changes in spatial variability for different precipitation event types can be addressed by calculating the variogram separately for each day. However, for a 15 year time period this means that more than 5,000 variograms need to be determined. This can only be achieved by an unsupervised determination, which can seriously affect the quality of the interpolations. Our results reconfirm the finding of the Dirks et al. (1998) study, that the complications with the ordinary kriging method lead to a interpolation quality that is similar to that of the simpler inverse distance interpolation. Therefore, the results of the cross-validation suggest that inverse distance interpolation is the most appropriate interpolation method in this study.

The five precipitation data sets were also used to calibrate the SWAT model. Figure 4 shows the observed and the simulated discharge obtained with the five optimised SWAT models in the calibration period. All five models show a good agreement with the measured data. It can also be seen that the difference between the five simulations is much smaller than the difference between the simulations and the measurements.

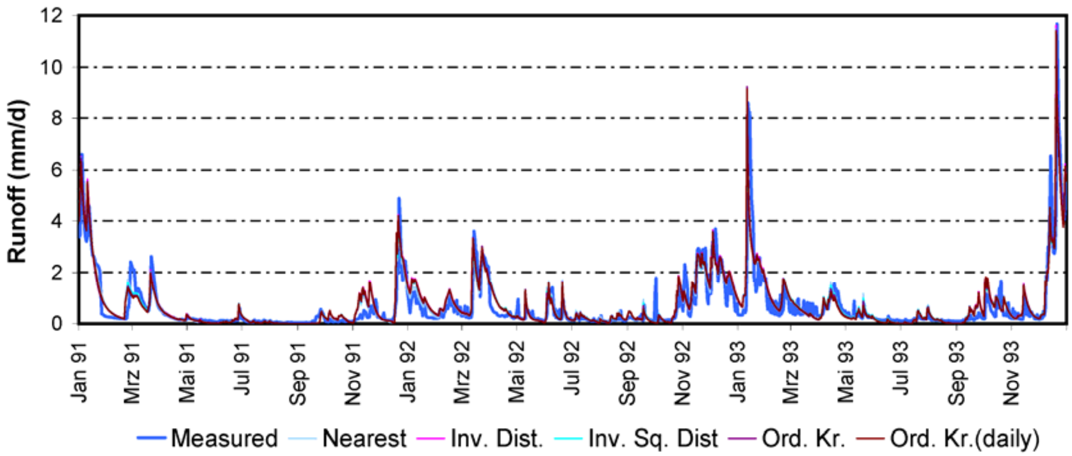

Figure 4. Runoff in the calibration period for different rainfall interpolation methods after automatic model calibration.

Table 2 presents the statistical measures for the simulated flows for all five interpolation methods for the calibration period. These measures confirm the visual impression that all five simulations have a similar quality in the calibration period. The parameters *a* and *b* of the regression equation indicate that the peak flows are underestimated by SWAT. This is typical for many hydrological models and is often attributed to timing issues when using a daily time-step, inaccuracy in precipitation measurements at high intensities, and the higher percentage of error in discharge measurements during high flows.

Table 2. Statistical measures for simulated flow for five interpolation methods for the calibration and the validation period.

	Calibration period			Validation period		
	MSE	Linear Regression	NS	MSE	Linear Regression	NS
Nearest Neighbour	0.28	$y = 0.84x + 0.16$ $R^2 = 0.80$	0.79	0.72	$y = 0.66x + 0.26$ $R^2 = 0.73$	0.72
Inverse Distance	0.30	$y = 0.86x + 0.18$ $R^2 = 0.79$	0.78	0.70	$y = 0.69x + 0.29$ $R^2 = 0.73$	0.73
Inverse Squared Distance	0.29	$y = 0.85x + 0.17$ $R^2 = 0.79$	0.78	0.70	$y = 0.68x + 0.28$ $R^2 = 0.73$	0.73
Ordinary Kriging	0.29	$y = 0.86x + 0.16$ $R^2 = 0.79$	0.78	0.69	$y = 0.69x + 0.26$ $R^2 = 0.74$	0.73
Ordinary Kriging (daily)	0.30	$y = 0.84x + 0.17$ $R^2 = 0.79$	0.78	0.71	$y = 0.67x + 0.27$ $R^2 = 0.73$	0.73

Table 2 also shows the statistical measures for the validation period. It can be seen that there is a relatively strong increase in the MSE between the calibration and the validation period, although this decrease is similar for all interpolation methods. The higher MSE values in the validation period are due to three flood events in 1984. If the simulations for these events were removed, the MSE would drop to approximately 0.38. The underestimation of the three flood peaks also has a strong impact on the slope of the regression equation, which dropped from approximately 0.85 to 0.68. The NS efficiency for the validation period was less affected by these flood events because the MSE was normalized by the variance of the measurements, which also strongly increased due to these flood events.

The results for the calibration and validation period do not indicate that there is a better interpolation method when the quality of the simulated flow is considered. The nearest neighbour interpolation, which performed worst in the cross-validation, resulted in the best flow simulations in the calibration period. However, it was slightly outperformed by the other methods in the validation period. Of course, one might wonder whether this similarity in model quality was caused by some kind of error compensation within the model calibration. The remaining part of the paper attempts to address this question.

In order to better understand the performance of the SWAT simulations based on the five interpolation methods, water balance for each method according to the long-term average annual values were calculated (Equation 3):

$$\Delta SW = P - ET - Q_{surf} - Q_{lat} - Q_{base} - GWR \qquad (3)$$

where P is precipitation, ET is actual evapotranspiration, Q_{surf} is surface runoff, Q_{lat} is lateral flow, Q_{base} is the base flow, GWR is the deep aquifer recharge, and ΔSW is the change in soil and snow water storage. These water balance components are presented in Table 3 for the validation period. It can be seen that the nearest neighbour interpolation resulted in the lowest amount of mean yearly precipitation (850.6 mm), whereas the inverse distance interpolation resulted in the highest precipitation (888.8 mm). The difference in precipitation was distributed among all water balance components, with the strongest relative increase in the deep ground water recharge. This seems to indicate that the model calibration partly compensates for the differences in precipitation input by adjusting the amount of deep aquifer recharge, which makes sense since the deep aquifer system is a disconnected sink in the SWAT model. This guess is further supported by a close inspection of the optimised model parameters provided in Table 1, which indicate that the deep aquifer percolation factor is lowest for the nearest neighbour interpolation and higher for the other interpolation methods.

To further investigate the extent to which the model calibration compensates for the differences in precipitation input, all five optimal parameter sets provided in Table 1 were applied to all precipitation fields. The NS efficiency of each model run in this cross-application is provided in Table 4. Table 4 shows that the variability of the NS efficiencies was smaller when different parameter sets were applied to a single precipitation field (columns) than when a single parameter set was applied to different precipitation fields (rows). This implies that model calibration can only compensate for the different precipitation input to a small extent. If significant compensation had occurred, the within-row and within-column variability should have been similar. This contradicts the common opinion that complex (semi-) distributed models can compensate for input errors.

Table 3. Water balance components for each interpolation technique in the validation period.

	P (mm)	ET (mm)	Q_{surf} (mm)	Q_{lat} (mm)	Q_{base} (mm)	GWR (mm)	ΔSW (mm)
Nearest Neighbour	850.6	486.0	27.7	281.8	40.8	17.7	-3.4
Inverse Distance	888.8	492.0	31.7	291.3	47.7	28.6	-2.5
Inverse Square Distance	877.5	490.5	30.5	288.1	44.4	26.8	-2.8
Ordinary Kriging	870.7	488.8	30.1	286.8	42.3	25.2	-2.5
Ordinary Kriging (daily)	874.2	488.9	30.2	284.2	43.7	29.4	-2.2

Table 4. NS efficiency for cross-application of optimised parameter sets (Table 1). Rows indicate the different optimised parameter sets. Columns indicate the different precipitation fields.

		Precipitation Fields				
		Nearest Neighbour	Inverse Distance	Inv. Sq. Distance	Ordinary Kriging	Ord. Kr. (daily)
Parameter Sets	Nearest Neighbour	0.795	0.773	0.783	0.781	0.777
	Inverse Distance	0.792	0.777	0.785	0.783	0.780
	Inverse Square Distance	0.793	0.777	0.785	0.784	0.780
	Ordinary Kriging	0.795	0.777	0.785	0.784	0.780
	Ordinary Kriging (daily)	0.791	0.777	0.784	0.783	0.779

To a certain extent, the results presented in this case study were due to the typical properties of the Aar Catchment. Although the optimised model parameters seem to indicate some error compensation through the deep aquifer recharge, this mechanism was not very strong in our study because the system is dominated by lateral flow. In a groundwater flow dominated system, the deep aquifer recharge could compensate much more for the different precipitation inputs. Therefore, it seems appropriate to disable deep aquifer recharge in future applications of SWAT, unless there is solid experimental evidence that this recharge is actually occurring.

Conclusions

Five different methods for the interpolation of precipitation were compared with respect to 1) their interpolation accuracy in a cross-validation and 2) the quality of the SWAT simulation after model calibration. The cross-validation showed that nearest neighbour interpolation had the lowest accuracy, and that the other four methods had a similar accuracy.

In this study, with daily precipitation data for 17 precipitation stations, advanced geostatistical methods did not result in more accurate interpolations than simple inverse distance interpolation. The quality of the flow simulations with SWAT after model calibration with different precipitation fields was similar, although there were differences in the water balance. A closer inspection of the calibration results indicated that model calibration only partly compensated for the different precipitation input.

Acknowledgements

This study was supported by the Deutsche Forschungsgemeinschaft within the scope of the Collaborative Research Center (SFB) 299 and the ModeCI master programme of the Università degli Studi della Calabria.

References

Dirks K.N., J.E. Hay, C.D. Stow, D. Harris. 1998. High-resolution studies of rainfall on Norfolk Island Part II: Interpolation of rainfall data. Journal of Hydrology, 208, 187-193.

Eckhardt K., J.G. Arnold. 2001. Automatic calibration of a distributed catchment model. Journal of Hydrology, 251, 103-109.

Eckhardt K., S. Haverkamp, N. Fohrer, H.-G. Frede. 2002. SWAT-G: a version of SWAT 99.2 modified for application to low mountain range catchments. Physics and Chemistry of the Earth, 27, 641-644.

Goovaerts, P. 2000. Geostatistical approaches for incorporating elevation into the spatial interpolation of rainfall. Journal of Hydrology, 228, 113-129.

HLUG (Hessisches Landesamt für Umwelt und Geologie). 2002. Digital soil map 1:50000.

Nöhles, I. 2000. Landnutzungsklassifikation mit multitemporalen Landsat TM-Szenen in einer kleinstrukturierten Agrarregion. PhD-thesis Justus-Liebig Universität Giessen, Germany (in German).

Vrugt, J.A., H.V. Gupta, W. Bouten, S. Sorooshian. 2003. A shuffled complex evolution metropolis algorithm for optimization and uncertainty assessment of hydrologic model parameters. Water Resources Research, 39, 1201.

SWAT Modeling Response of Soil Erosion and Runoff to Changes in Precipitation and Cover

C. Baffaut[1*], M.A. Nearing[2], V. Jetten[3], O. Cerdan[4], A. Couturier[4], M. Hernandez[1], Y. Le Bissonnais[5], M.H. Nichols[1], J.P. Nunes[6], C.S. Renschler[7], V. Souchère[8], K. van Oost[9]
[1] Food and Agricultural Policy Research Institute, Univ. Missouri, 101 Park DeVille Drive, Suite E, Columbia, MO 65211 USA, email: baffautc@missouri.edu.
[2] USDA-ARS Southwest Watershed Research Center,Tucson, AZ, USA.
[3] Univ. Utrecht, Fysische Geografie, The Netherlands.
[4] BRGM ARN, Orléans, France.
[5] INRA, Olivet, France.
[6] Dept. Environmental Sciences and Eng., New Univ. Lisbon, Caparica, Portugal.
[7] Dept. of Geography, University at Buffalo - The State University of New York, Buffalo, NY, USA.
[8] UMR SAD APT, Thiverval Grignon, France
[9] Laboratory for Experimental Geomorphology, Leuven, Belgium

Abstract

Global climate has changed over the past century. Precipitation amounts and intensities are increasing. In this study, we investigated the SWAT model response to a few basic precipitation and vegetation related parameters using common data from one semi-arid rangeland watershed in Arizona. We compared it to the response of six other models. The seven models: SWAT, WEPP, LISEM, MEFIDIS, RUSLE, STREAM, and KINEROS were calibrated using flow data and sediment loadings from three storms. Information on topography, soils, land use, land management, and weather was provided to the modelers but no calibration criteria and application style was specified. Perturbations were made to inputs for rainfall intensities and amounts, and to ground surface and canopy cover. The model response to an input perturbation was quantified by its sensitivity, expressed as percentage change in either runoff or sediment response relative to percentage change in input value. All models were sensitive to rainfall depth, rainfall intensity, and ground cover, but were less sensitive to canopy cover. Sensitivities were generally larger for the smaller events even though the magnitude of change was larger for the larger events. In spite of the differences between the models in terms of process descriptions, data sets to develop and validate the models, and differences in the modelers' application style and calibration criteria, the similarities in the responses of these models give credibility to the use of such models for studying climate change impacts on runoff and erosion.

Introduction

The consensus of atmospheric scientists is that the earth is warming, and as global temperatures increase the hydrologic cycle is becoming more vigorous. The IPPC reported that there has likely been an increase (probability 90 to 99%) in precipitation during the 20th century in the mid-to-high latitudes of the Northern Hemisphere. Much of the increase in precipitation that has been observed worldwide has been in the form of heavy precipitation events (IPCC Working Group I, 2001; Easterling et al., 2000a, b; Karl and Knight, 1998). Climate models are predicting a continued increase in intense precipitation events during the 21st century (IPCC Working Group II, 2001).

Soil erosion rates may change in response to changes in climate for a variety of reasons, the most direct of which is the change in the erosive power of rainfall (Williams et al., 1996; Nearing, 2001; Pruski and Nearing, 2002a). Soil erosion responds both to the total amount of rainfall and to differences in rainfall intensity; however, the dominant variable appears to be rainfall intensity rather than rainfall amount alone. A second dominant climate change influence is brought about by changes in plant biomass. The mechanisms by which climate changes affect biomass, and by which biomass changes impact runoff and erosion, are complex (Williams et al., 1996; Pruski and Nearing, 2002b). For example, anthropogenic increases in atmospheric carbon dioxide concentrations cause increases in plant production rates and changes in plant transpiration rates (Rosenzweig and Hillel, 1998), which translate to an increase in soil surface canopy cover and, more importantly, biological ground cover. The Soil and Water Conservation Society recently published a comprehensive review on the conservation implications of climate change on soil erosion and runoff from cropland (SWCS, 2003).

Every soil erosion model has limitations in terms of its representation of erosion processes (Jetten et al., 1999, 2003); thus there is always a level of uncertainty in interpreting the results of studies that look at climate change impacts on soil erosion. The objective of this analysis was to compare the response of the SWAT model and a variety of different soil erosion models to a few key variables related to climate change, i.e. to a few basic precipitation and vegetation related parameters. Seven different erosion models were calibrated by scientists familiar with those models to common data from a semi-arid watershed in the southwest United States. Perturbations were then made to rainfall intensities and amounts, and to ground surface and plant canopy covers in order to assess and compare the sensitivities of the models to runoff and erosion.

Methodology

Data were provided to modelers for the watershed, including information on topography, soils, land use, and weather for a specific time period. A cropped watershed in Ganspoel, Belgium was also selected for analysis but was not modeled with the SWAT model and is not reported here. Three storms were selected from each of the data sets for analysis in the exercise. Results for the Ganspoel watershed are presented in Nearing et al. (2004). Scenarios were designated as perturbations to the climate and land cover information for those storms as described below. The modelers then gathered at a meeting of the Soil Erosion Network in Tucson, AZ, USA on November 17-19, 2003 and presented an overview and the results of the exercise for their model.

Watershed Description

Lucky Hills watershed 103 is located within the Walnut Gulch Experimental Watershed in southeastern Arizona, U.S.A. Cattle grazing is the primary land use with mining, limited urbanization, and recreation making up the remaining uses. Mean annual temperature is 17.6 ^{o}C and mean annual precipitation is approximately 300 mm. Lucky Hills watershed 103 is approximately 3.7 ha in size. Land cover is shrub dominated, semi-arid rangeland characterized by mounds under shrub and lower inter-shrub areas. Cover during the rainy season is approximately 25% bare soil, 25% canopy, and 50% erosion pavement (rocks). The dominant soil is a McNeal Gravelly Sandy Loam, with approximately 25% rock fragments in the surface layer. Sediment from the watershed is monitored with a supercritical flume with an automatic traversing slot sampler. Precipitation is monitored in Walnut Gulch with a network of 88 weighing-type recording rain gauges, one of which was located within the

Lucky Hills area. Data on precipitation, runoff amounts, peak runoff rates, runoff duration, and sediment amounts were provided to the modelers for storms occurring from 1982 through 1992. The storms of September 1, 1984, September 10, 1982, and August 12, 1982 were selected to be used for the modeling comparison exercise. These represent large, medium, and small storms, respectively, from the record (Table 1).

Table 1. Observed runoff and sediment at Lucky Hills 103 watershed for the storms used in the model comparison.

Year	Month	Day	Rainfall Depth (mm)	Runoff Volume (mm)	Peak Runoff Rate (mm/hr)	Runoff Duration (min)	Event Sediment (kg/ha)
1984	9	1	32.8	15.0	46.0	78	3075
1982	9	10	18.8	3.3	8.7	133	721
1982	8	12	6.6	0.3	2.9	22	82

Modeling Scenarios

The intention of the modeling exercise was to perform a sensitivity analysis as the first step in looking at climate change impacts on erosion. Sensitivity of runoff amounts, peak runoff rates, gross erosion, and net sediment yield were assessed relative to changes in rainfall intensities and amounts and differences in canopy and ground cover.

Space limitations in this paper preclude detailed descriptions of the models. Models used included the Limburg Soil Erosion Model (LISEM) (De Roo et al., 1989; Jetten et al., 1998), the Physically-Based Spatially-Distributed Erosion Model (MEFIDIS) (Nunes and Seixas, 2004), the Revised Universal Soil Loss Equation (RUSLE) (Renard et al., 1997), Sealing and Transfer by Runoff and Erosion related to Agricultural Management (STREAM) (Cerdan et al., 2002; Souchère et al., 1998), Kinematic Runoff and Erosion (KINEROS) (Smith et al., 1995), the Soil and Water Assessment Tool (SWAT) (Arnold et al., 1999), and the Water Erosion Prediction Project (WEPP) (Flanagan and Nearing, 1995; Renschler, 2003). One of the models was not able to represent the watershed scale, and could only be applied at a hill slope scale. In this case calibration was not performed in the same manner as the other models, and only a sensitivity analysis was performed.

For the SWAT model, the watershed was represented as one subbasin with the McNeal soil and typical Southwest range vegetation. Soil properties, in addition to what was specified in the data supplied for the exercise, were taken from the Map Unit Use File (MUUF) database (Baumer et al., 1994). The crop properties of a generic land representation of the southwestern US (arid) rangeland found in the SWAT crop file were used. The supplied daily precipitation values at gauge stations 83 and 80 were used in the model. Daily measured temperature data was obtained from the Douglas airport weather station. Additional weather parameters were generated by the model using monthly characteristics from the Douglas airport station. The curve number method, the Hargreaves evapo-transpiration method, and a Muskingum routing method were used in this analysis. Channel degradation and deposition were active.

In order to capture the erosion occurring in the primary channel, modifications to the SWAT model were made to force the routing of the sediment yields from the subbasin through the first-order channel. The SWAT model makes the assumption that MUSLE takes this into account. Therefore, the model code was modified in order to simulate the high channel erosion and degradation that takes place in this watershed.

The basic methodology was to calibrate the model to measured data from the watershed and then superimpose change scenarios on those baseline simulations. Precipitation, flow, and sediment data was provided from July 1982 to August 1992. No event was recorded in 1986, 1990, or 1991. The monitored events all occurred between June and October of each year. We used the years 1982 through 1984 to calibrate the models (23 recorded events) and the rest to validate it (22 recorded events).

Table 2 shows the calibration and validation results along with the results specific to the events selected for the analysis. The choice of the years 1982 to 1984 for model calibration, a period characterized by several large events, made the model a much more reliable tool for simulating medium and large events. The model does not perform well for small events, as is shown by the results for the validation period and for the storm event of August 12, 1982.

Table 2. Calibration and validation results.

	Total Measured Flow (mm)	Measured Sediment (kg/ha)	Predicted Flow (mm)	Predicted Sediment (kg/ha)	% error runoff volume	% error sediment yield	Nash-Sutcliffe
82-84	44.09	5398	33.82	8884	-3%	-39%	0.77
85-92	38.33	9563	51.16	9837	33%	3%	-3.55
9/1/84	15.0	3075	13.4	3242.5	-10%	5%	
9/10/82	3.3	721	3.3	264.5	1%	-63%	
8/12/82	0.3	82	0.001	~0	-100%	-100%	

The scenarios tested are listed in Table 3. Scenario 1A was simulated by adjusting the rainfall depth in the daily precipitation file and the maximum half-hour intensities in the weather file by the required amount. Scenario 1B was simulated by only adjusting the rainfall depth in the precipitation file. A limitation of the SWAT model with the curve number method is the insensitivity of the estimated runoff volume to event intensity and duration. Maximum half-hour intensities are utilized by the model to estimate a peak runoff rate that is then used to estimate the sediment yield. We, therefore, did not expect to see any sensitivity in the runoff volume to rain intensity but did expect some sensitivity in the sediment yields. Lack of time prevented developing the model with the Green and Ampt runoff estimation method. In this exercise, the maximum half-hour intensities were increased or decreased by 10% or 20% when intensities had to be adjusted.

A further limitation of the SWAT model is the difficulty to distinguish between ground cover and canopy cover. It was not possible to investigate scenarios 3A, 3B, and 3C separately, and only a change in both the ground and canopy cover was investigated (scenario 3C). The scenario was simulated by simultaneously adjusting the curve number and the USLE_C factor.

Analyses of Data

The basic methodology used to interpret the results of the study was linear sensitivity analysis. All the results of the models were analyzed in terms of relative changes in runoff volume and erosion from the zero change, or baseline, conditions. Specifically, the ratios of changes in predicted runoff and erosion for the -20%, -10%, +10%, and +20% cases to the corresponding values for the zero change condition were calculated for each model for each storm and each change scenario. Then, linear sensitivity values were calculated using linear regression between the percent change of response variable to the percentage change of input variable for each model and each scenario.

We used the median values for sensitivities between the models as an index to represent the sample set of model responses for each storm and scenario. It was apparent that the model results followed a skewed distribution type, and attempts to use standard means testing between model results did not give sensible results.

Table 3. Definitions of rainfall and cover change scenarios tested for model sensitivity.

Scenario	Variable	Instructions for Conducting Scenarios
1A	Rainfall Amount and Intensity	Change in rainfall depth (total rainfall amount) by -20%, -10%, 0, +10%, and +20% by changing rainfall intensity by -20%, -10%, 0, +10%, and +20%, holding rainfall duration (time) constant.
1B	Rainfall Amount and Duration	Change in rainfall depth (total rainfall amount) by -20%, -10%, 0, +10%, and +20% by changing rainfall duration (time) by +20%, +10%, 0, -10%, and -20%, holding rainfall intensities constant.
2	Rainfall Intensity Alone	Hold total rainfall depth (amount) per storm constant, looking at rainfall intensity effects separate from rainfall amount effects bysimultaneously changing rainfall intensities and durations as: • -20% intensity with +25% duration (0.8*1.25=1); • -10% intensity with +11.1% duration (0.9*1.11=1.0); • 0% intensity with 0% duration; • +10% intensity with -9.1% duration (0.909*1.1=1.0); • +20% intensity with -16.7% duration changes (1.2*0.833=1.0).
3A	Ground Cover	Ground cover change by -20%, -10%, 0, +10%, and +20%, rainfall unchanged; OR Manning’s n change by -20%, -10%, 0, +10%, and +20% where ground cover information was not available or not used by a model, rainfall unchanged.
3B	Canopy Cover	Plant canopy cover change by -20%, -10%, 0, +10%, and +20%, rainfall unchanged.
3C	Ground and Canopy Cover	Both ground cover (or Manning's n) and canopy cover change by -20%, -10%, 0, +10%, and +20%, rainfall unchanged.

Results and Discussion

Table 4 shows the linear sensitivities (non-dimensional) of model sediment predictions relative to changes in inputs for the various scenarios for the Lucky Hills watershed. Because of the poor performance of the calibration for smaller events, we only present the results for the largest and medium events. These results represent the average percentage change in sediment response to each percentage change in the respective input values for each scenario (Table 3).

Precipitation and intensities: All of the models, including SWAT, responded with positive sensitivities to scenarios 1A, 1B, and 2, which means that predicted erosion increased with increases in both precipitation amount and intensity (Table 4). Sensitivities for runoff response of the models followed many of the same patterns as did sensitivities for erosion, but in nearly every case the median sensitivity values for the models were less for runoff than for erosion. This makes sense in terms of the processes. Erosion is affected by the runoff amounts as well as directly by rainfall energy and cover, thus the overall response to rainfall changes will be greater for erosion than for runoff amounts. These results are consistent with the expectation that erosion should increase as the driving force (rainfall) increases.

As expected, with the SWAT model, runoff volume was not sensitive to changes in rain intensity (scenario 2). For erosion, other models showed more sensitivity to an increase in storm rainfall amounts by way of an increase in rainfall intensity (scenario 1A) than by way of an increase in rainfall duration (scenario 1B). As expected, SWAT sensitivity values for scenarios 1A and 1B were similar for runoff. The values were similar also for erosion, which indicates that the effect of the half-hour maximum intensities is limited if at all detectable. Sediment yields should be affected since the peak runoff rates used in the MUSLE equation are affected by the half-hour maximum intensity. Indeed, scenario 2 shows that the sensitivity of SWAT to changes in maximum half-hour rainfall intensities is very low.

In general, the results indicate that rainfall increases associated with increased rainfall intensity and/or rainfall duration are quite important relative to potential changes in erosion rates. These results point out the importance of rainfall relative to climate change impacts on soil erosion, and the potential implications of historically observed increases in intense precipitation events (IPCC Working Group I, 2001; Easterling et al., 2000a, b; Karl and Knight, 1998) and predictions of a continued increase in intense precipitation during the 21st century (IPCC Working Group II, 2001).

Sensitivity values were greater for the larger storms with SWAT while, in general, they were greater for the smaller storms with the other models. Note that while the models predicted a greater relative change (i.e. sensitivity) for the smaller storm, the absolute changes in magnitude of erosion were greater for the larger storms. For example, for scenario 1A, the median of the model results would indicate a 5.8% increase in erosion for every 1% change in rainfall amount and intensity for the storm on September 10, 1982, and only a 2.3% change in erosion for the storm on September 1, 1984. However, a 5.8% change in erosion for the storm on September 10, 1982 translates to 41.9 kg ha^{-1}, while a 2.4% change in erosion for the storm on September 1, 1984 translates to 69.6 kg ha^{-1}.

Ground cover and canopy: The models were all sensitive to cover changes. All the models responded with negative sensitivities to scenario 3C, which means that predicted erosion decreased with increases in both ground cover and canopy cover.

Ground and canopy cover increase the water uptake, slow down runoff, and increase infiltration, thus decreasing the amount of runoff. Ground and canopy cover also reduce the energy of falling raindrops, which will produce a decrease in soil erosion by splash. Ground cover, though, also acts as a significant deterrent to rill erosion by both protecting the soil surface from the forces of flowing water and by dissipating energy of flow that would otherwise be available to transport sediment.

There was a great deal of coherence between the seven models in terms of their relative responses of predicted runoff and erosion as a function of the simulated changes in rainfall and cover. As mentioned above, most of the models showed the greater sensitivity to rainfall changes, particularly to changes in the combination of rainfall amount and intensity (scenario 1). All of the models showed a general tendency to have a greater relative influence, though a lesser absolute difference, on the medium storms.

Table 4. Sensitivities (non-dimensional) of model sediment and runoff predictions relative to changes in inputs for the various scenarios for the Lucky Hills watershed, expressed as percentage change in response to each percentage change in input values calculated using linear regression.

Scenario	Storm	Sediment		Runoff	
		Median of Models Sensitivities	SWAT Model Sensitivity	Median of Models Sensitivities	SWAT Model Sensitivity
1A	1-Sep-84	2.26	4.47	2.27	2.60
	10-Sep-82	5.81	7.88	4.80	5.23
1B	1-Sep-84	1.94	4.37	2.13	2.54
	10-Sep-82	2.95	7.61	2.40	5.15
2	1-Sep-84	0.80	0.12	0.57	0.07
	10-Sep-82	2.73	0.25	2.13	0.14
3C	1-Sep-84	-1.20	-3.21	-0.18	-1.83
	10-Sep-82	-1.67	-9.41	-0.39	-5.70

Conclusions and Implications

The results of this study are alarming. If the trends reported for precipitation in the United States and Europe over the last century continue, significant consequences will incur. If, as a rough estimate, we compute the average of the sensitivities for scenarios 1A and 1B for all storms, the sensitivity value would be 3.24 (324%). Even the smallest value for the two scenarios gives a sensitivity of 1.94 (194%). If rainfall amounts during the erosive times of the year were to increase roughly as they did during the last century in the United States, the increase in rainfall would be on the order of 10%, with greater than 50% of that increase due to increase in storm intensity. If these numbers are correct, and if no changes in land cover occurred, erosion could increase by something on the order of 19 to 32% over the next century. Correspondent values for runoff are 21 to 29%. Obviously these are not well defined values, nor scientifically defendable in an absolute sense, but the trends are clear. Both storm water runoff and soil erosion are likely to increase significantly under climate change unless offsetting amelioration measures are taken.

Some conclusions specific to the SWAT model include:

1. The SWAT model behaved in a coherent fashion compared to other models to estimate the effect of rainfall amounts.
2. Changes in maximum half-hour intensity had little impact on sediment yields. It is difficult to accurately estimate the effect of rainfall intensities with the SWAT model using the Curve Number method.
3. The proposed adjustment of the curve number and the USLE_C factor to reflect the changes in canopy and ground cover produced a much larger response than predicted by other models.

The basic conclusions from the overall results include:

1. Erosion is likely to be more affected by changes in rainfall and cover than in runoff, though both are likely impacted in similar ways.
2. On a purely percentage basis, erosion and runoff will change more for each percentage change in rainfall amount and intensity of a storm than to each percentage change in either canopy or ground cover.

3. Changes in rainfall amount associated with changes in storm rainfall intensity will likely have a much greater impact on runoff and erosion than changes in rainfall amount alone.
4. Changes in ground cover (cover in contact with the soil surface) have a greater impact on both runoff and erosion than changes in canopy cover alone.

References

Arnold, J.G., R. Srinivasan, R.S. Muttiah, and P.M. Allen. 1999. Continental Space Simulation of the Hydrologic Balance. *J. Am. Water Resources Assoc.* 35(5): 1037-1051.

Baumer, O., P. Kenyon, and J. Bettis. 1994. Map Unit Use File (MUUF) v2.14 User's Manual. Natural Resource Conservation Service, National Soil Survey Center, Lincoln, Nebraska.

Cerdan, O., V. Souchère, V. Lecomte, A. Couturier, and Y. Le Bissonnais. 2002. Incorporating soil surface crusting processes in an expert-based runoff model: STREAM (Sealing and Transfer by Runoff and Erosion related to Agricultural Management). *Catena*, 46: 189-205.

De Roo, A.P.J., L. Hazelhoff, and P.A. Burrough. 1989. Soil erosion modeling using ANSWERS and geographical information systems. *Earth Surface Processes and Landforms.* 14(6-7): 517-532.

Easterling, D.R., G.A. Meehl, C. Parmesan, S.A. Changnon, T.R. Karl, and L.O. Mearns. 2000a. Climate extremes: Observations, modeling, and impacts. *Science* 289(5487): 2068-2074.

Easterling, D.R., J.L. Evans, P.Ya. Groisman, T.R. Karl, K.E. Kunkel, and P. Ambenje. 2000b. Observed variability and trends in extreme climate events: A brief review. *Bulletin of the American Meteorological Society* 81(3):417-425.

Favis-Mortlock, D.T. 1998. Validation of field-scale soil erosion models using common data sets. In: *"Modelling Soil Erosion by Water"*, eds. J. Boardman and D. Favis-Mortlock, NATO ASI series I: Global Environmental Change, Vol 55:89-127.

Flanagan, D.C, and M.A. Nearing. 1995. USDA-Water Erosion Prediction project: Hill slope profile and watershed model documentation. *NSERL Report No. 10.* USDA-ARS National Soil Erosion Research Laboratory, West Lafayette, IN 47097-1196.

Intergovernmental Panel on Climate Change, Working Group I. 2001. Climate Change 2001: The Scientific Basis. Contribution of Working Group I to the Third Assessment Report of the IPPC. Cambridge University Press.

Intergovernmental Panel on Climate Change, Working Group II. 2001. Climate Change 2001: Impacts, Adaptation, and Vulnerability. Contribution of Working Group II to the Third Assessment Report of the IPPC. Cambridge University Press.

Jetten, V.G., A.P.J. De Roo, and J. Guerif. 1998. Sensitivity of the model LISEM to variables related to agriculture. In: "*Modelling Soil Erosion by Water*", eds. J. Boardman and D. Favis-Mortlock, NATO ASI series I: Global Environmental Change, Vol 55:339-350.

Jetten, V., A. De Roo and D. Favis-Mortlock. 1999. Evaluation of field-scale and catchment-scale soil erosion models. *Catena* 37: 521-541.

Jetten, V., G. Govers, and R. Hessel. 2003. Erosion models: quality of spatial predictions. *Hydrological Processes* 17:887-900.

Karl,T.R., and R.W. Knight. 1998. Secular trends of precipitation amount, frequency, and intensity in the USA. *Bulletin of the Am. Meteorological Soc.* 79:231-241.

Nearing, M.A. 2001. Potential changes in rainfall erosivity in the U.S. with climate change during the 21st century. *Journal of Soil and Water Conservation* 56(3), 229-232.

Nearing, M.A., V. Jetten, C. Baffaut, O. Cerdan, A. Couturier, M. Hernandez, Y. Le Bissonnais, M.H. Nichols, J.P. Nunes, C.S. Renschler, V. Souchère, K. van Oost. 2004. Modeling Response of Sol Erosion and Runoff to Changes in Precipitation and Cover, submitted to CATENA, 2004.

Nunes, J.P., and J. Seixas, 2004. Impacts of Extreme Rainfall Events on Hydrological Soil Erosion Patterns: Application to a Mediterranean Watershed. *World Resource Review* 15 (3): 336-351.

Pruski, F. F. and M.A. Nearing. 2002a. Climate-induced changes in erosion during the 21st century for eight U.S. locations. *Water Resources Research*. 1298.

Pruski, F. F. and M.A. Nearing. 2002b. Runoff and soil loss responses to changes in precipitation: a computer simulation study. *Journal of Soil and Water Conservation* 57(1), 7-16.

Renard, K.G., G.R. Foster, G.A. Weesies, D.K. McCool, and D.C. Yoder. 1997. *Predicting soil erosion by water – a guide to conservation planning with the revised universal soil loss equation (RUSLE)*. Agricultural Handbook No. 703, U.S. Government Printing Office, Washington, D.C.

Renschler, C.S. 2003. Designing geo-spatial interfaces to scale process models: The GeoWEPP approach. *Hydrological Processes* 17, p. 1005–1017.

Rosenzweig, C. and D. Hillel. 1998. *Climate change and the global harvest. Potential impacts of the greenhouse effect on agriculture.* Oxford University Press, Inc. New York.

Smith, R.E., D.C. Goodrich, D.A. Woolhiser, and C.L. Unkrich. 1995. KINEROS: A kinematic runoff and erosion model. Pages 697-732 in V. P. Singh, editor. *Computer Models of Watershed Hydrology.* Water Resources Publications, Highlands Ranch, Colorado.

SWCS (Soil and Water Conservation Society). 2003. *Conservation Implications of Climate Change: Soil Erosion and Runoff.* Soil and Water Conservation Society. 945 Southwest Ankeny Road, Ankeny, Iowa 50021

Souchère, V., D. King, J. Daroussin, F. Papy, and A. Capillon. 1998. Effect of tillage on runoff direction: consequences on runoff contributing area within agricultural catchments. *Journal of Hydrology*, 206: 256-267.

Williams, J.R., M. A. Nearing, A. Nicks, E. Skidmore, C. Valentine, K. King, and R. Savabi. 1996. Using soil erosion models for global change studies. *Journal of Soil and Water Conservation* 51(5):381-385.

Hydrologic Modeling of a Semi-Arid Region in Brazil

Maria Quiteria C. de Oliveira*[1], Ramon C. de Oliveira[2], and Yvonilde D P Medeiros[3]
[1]Superintendência de Recursos Hídricos, Av. ACM, 357, Itaigara, CEP: 41.825-000, Salvador, Bahia, Brazil. Email: quiteria@srh.ba.gov.br
[2]UFC Engenharia, Bahia, Brazil. Email: ramonco@ufba.br
[3]Universidade Federal da Bahia, Brazil. Email: yvonild@ufba.br

Abstract

The Salitre River Watershed is located in the semi-arid state of Bahia (Brazil) and presents problems related to the water availability because of the small amount and irregular seasonal distribution of precipitation. It is notable that in this region, data for streamflow is scarce, making it difficult to measure water availability in the basin. Studies from mathematical rain-flow models are necessary to resolve this problem. This research presents an application of the hydrologic model Soil and Water Assessment Tool (SWAT), associated with a Geographic Information System (GIS) in the Salitre River Watershed. The simulated results were compared to the observed data at select points in the basin and the results were satisfactory. The monthly time series comparison of measured and predicted streamflows at the Junco gage explains the general trend of the time series very well. The results demonstrate that this model can sufficiently represent the climatic and physical conditions of the semi-arid regions in Brazil.

Introduction

Historically, the Northeast Region of Brazil has been characterized by low water availability due to its semi-arid geographical location. This characteristic has been a restrictive element to socioeconomic development. In the search for solutions for better water conservation and management which ensure minimization of waste and thereby an improvement in the water use efficiency, it is important to know the evolution of water availability. This information is generally obtained from long-term flow gage measurements. However in some regions of Brazil the historical measurements are scarce. In this case, some mathematical models of watershed hydrology have been used to estimate long-term mean monthly flow.

The application of conceptual and distributed mathematical models, such as SWAT, has revealed a powerful tool because model parameters can be related directly to physical, geological, and biological attributes of a watershed and can theoretically be used without calibration.

Giving continuity to the research developed in the Integrated Management Plan for the Salitre River Watershed (ANA/GEF/PNUMA/OEA, 2003), the Salitre Rive Basin was chosen for this case study. It is located in the semi-arid region of Bahia (Brazil).

Salitre River Basin

The Salitre River Basin has an area of roughly 13,470 square kilometers (Figure 1). It is situated between the coordinates -9º 27' and -11º 30' latitude and -40º 22' and -41º 30' longitude. The Salitre River has little natural water availability. In this region, the lack of regular rainfall, not only throughout the year but also in multi-annual periods, further worsens the dispute over water and the regions social problems. It is located in the semi-arid areas of these regions that drought hits hardest and water means survival. The Salitre River and its tributaries have intermittent flow regimes that are fed by constant rains from February through April and become empty riverbeds during the dry season. The driest period is from August through October, thus this period does not contribute to baseflow.

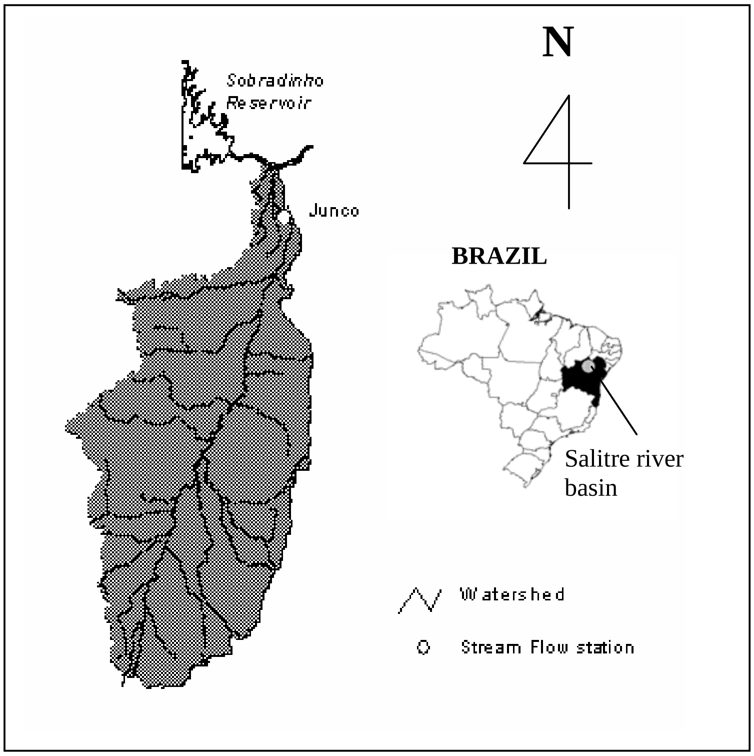

Figure 1. Location of the Salitre River Basin in Brazil.

Methodology

Description SWAT

SWAT is a mathematical model, developed in 1996 by the USDA-Agricultural Research Service (USDA-ARS) and Texas A&M University, objectifying the analysis of the impacts of alterations in land use on hydrology, sediment transport, and water quality. To satisfy these objectives the model: (i) is based on physical characteristics of the basin, (ii) uses available input data, (iii) is computationally efficient to operate on average to large basins (> 1,000 km^2), and (iv) is continuous in time, and capable of simulating long periods (> 50 years). Therefore SWAT is able to compute the effect of alterations in land use on hydrological processes. The SWAT model is distributed, and watersheds can be divided into subbasins in order to reflect varying soils, land use, and management conditions. This is possible through the subdivision of cells (each cell representing a subbasin). The physical processes directly modeled by SWAT are hydrology, weather, sedimentation, crop growth, nutrient conditions in the soil, pesticide and agricultural management, and channel/reservoir routing of flood, sediment, and nutrients. The hydrology component of SWAT uses a modification of the Soil Conservation Service (SCS) curve number method (USDA-SCS, 1972) to determine surface runoff. Sediment yield is computed for each subbasin using the Modified Universal Soil Loss Equation (MUSLE) (Williams & Berndt, 1977). A detailed description of the different components of SWAT can be found in Arnold *et al*. (1995) and Diluzio & Neitsch (1999).

The graphical interface used in this research was the SWAT ArcView Interface. This interface was used to collect, edit and store the basin information to be formatted into SWAT input and output files.

Hydrographic and Geographic Maps and Databases

The basic data required by the model are spatial and temporal data on topography, soil, land use, and weather. The elevation and the slope were obtained from GTOPO30 Global digital elevation model (DEM). The horizontal grid spacing is 30-arc seconds, about 0.00833333 degrees, resulting in a DEM with 21,600 rows and 43,200 columns. The data was processed and projected into a Geographic projection (Decimal degrees). Soils data for the Salitre River Basin were derived from the ANA/GEF/PNUMA/OEA (2003) soil map produced by the Water Resource Group/UFBa, 1:250,000 scale. It was necessary to create a soils database for model input. The soil parameters required by SWAT were obtained from MME (1981). Land use data was extracted from the ANA/GEF/PNUMA/OEA (2003) vegetation map produced by the Water Resource Group/UFBa, 1:250,000 scale. Measured daily precipitation and streamflow were obtained from the Agência Nacional de Águas (ANA), (records available on their website). A new weather generator was created and added to the database by setting parameters obtained from the Instituto Nacional de Meteorologia - INMET.

The Salitre River Basin was divided into 63 homogeneous areas according to the predominant characteristics of land use and soil type. The curve number parameter was used by the model to estimate the potential maximum retention of rainfall, which varies according to soil type, land use class, and antecedent moisture conditions. Soil type maps available in the basin did not provide enough information to classify the soils listed into SCS categories; therefore, a table was created with alternative categories for soil use based on the values presented in Tucci (1997) and Oliveira (1999). For different land uses and hydrolithical categories the CN values are presented in Table 1 (antecedent moisture condition II). These values were obtained according to the following:

I - Water: in this category the wetlands were included, with a value of 100 for the Curve Number;
II – Regular plantations: in this category cultivated areas were included;
III – Permanent Campos: in this category the Cerrado dense vegetations were considered;
IV – Forests: in this category the medium-scale vegetation was included;
V – Fallow lands: in this category the exposed soils and relief were included;
VI – Pasture: in this category scarce vegetation was considered.

Results

The model was applied to the Salitre Watershed, which has a low density of streamflow gages. Surface water flow was calibrated against the Junco gaging station where streamflow data has been collected for only a few years. Separate time periods were modeled for calibration and validation. The calibration time period ran from January 1977 to December 1979, while the validation time period ran from January 1969 to December 1973.

Table 1. Runoff curve numbers for hydrologic soil groups in the Salitre Watershed.

Land Use Description	Curve Number for Hydrologic Soil Group			
	A	B	C	D
Water/Wetlands	100	100	100	100
Cultivated areas	65	76	84	88
Cerrado dense vegetations	34	60	73	79
Medium-scale vegetation	41	64	74	80
Exposed soils	39	61	74	80
Pasture (scarce vegetation)	26	54	75	83

The hydrologic groups are classified as:
Group A: High infiltration, low runoff, for deep sand or loess.
Group B: Moderate infiltration, for moderately fine to coarse textured soils such as sandy loam.
Group C: Slow infiltration, for fine textured soils such as clay loam and shallow sandy loam.
Group D: Very slow infiltration, for clay soils.

Model Calibration

In this study, the calibration procedures formulated consisted of finding the most appropriate parameters for baseflow and the travel time for hydrologic routing model components. The accuracy of baseflow separation depends on the length of stream gage recorded data that is processed. As longer periods of data provide more reliable separation than shorter periods, average monthly values were used in this study because they provided better results than daily predictions.

The calibration process can provide important insight into both local conditions and model performance; if correction factors are large or inconsistent across several study areas, this suggests that some significant component of the hydrologic system or its controls was neglected. Figure 1 shows the location along the Salitre River Basin where SWAT predicted streamflow was compared to the Agência Nacional de Águas (ANA) measured streamflow.

To test the calibration models developed in this study, two coefficients were used: Correlation and Determination. A comparison of monthly measured and predicted streamflow statistics for the Junco Station are shown in Table 2.

Table 2. Measured and predicted yield statistics for the Junco Station, Bahia, Brazil (1977-1979).

Variable	Meas. Mean	Pred. Mean	Meas. St. Dev	Pred. St. Dev	Coef. Correlation	Coef. Determination
Water Yield (m3/s)	1.26	1.36	0.84	1.08	0.95	0.88

Figure 2 shows the monthly time series comparison of measured and predicted streamflow at the Junco gage. The SWAT model explains the general trend in the time series well, within correlation coefficient of 95% and determination coefficient of 88%.

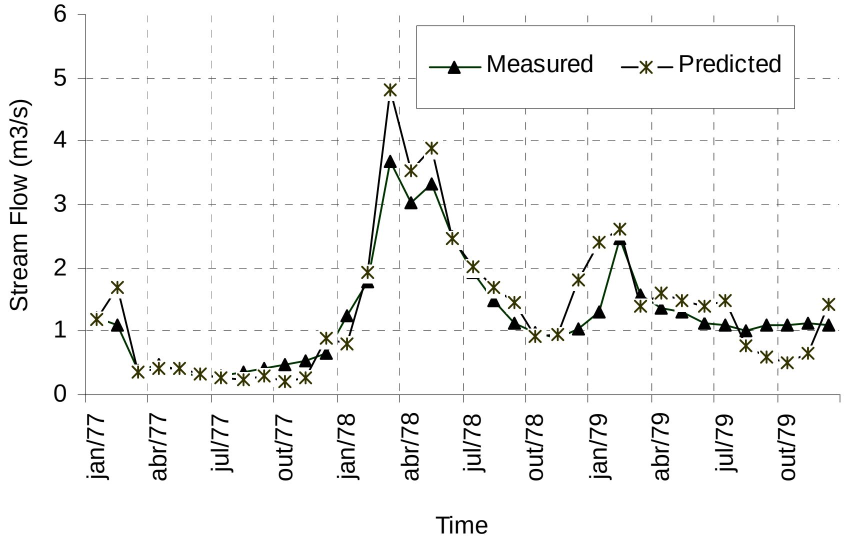

Figure 2. Monthly time series comparison for measured and predicted streamflow at the Junco gage (calibration).

Model Verification

In the verification process, the necessary parameters to characterize the system were specified and model output was compared to experimental observations. A comparison of monthly measured and predicted streamflow statistics for the Junco Station are shown in Table 3.

Table 3. Measured and predicted yield statistics for the Junco Station, Bahia, Brazil (1969-1973).

Variable	Meas. Mean	Pred. Mean	Meas. St. Dev	Pred. St. Dev	Coef. Correlation	Coef. Determination
Water Yield (m3/s)	1.23	1.75	1.17	1.55	0.78	0.70

Figure 3 shows the monthly time series comparison for measured and predicted streamflow at the Junco gage. The SWAT model explains the general trend of the time series well, within correlation coefficient of 78% and determination coefficient of 70%.

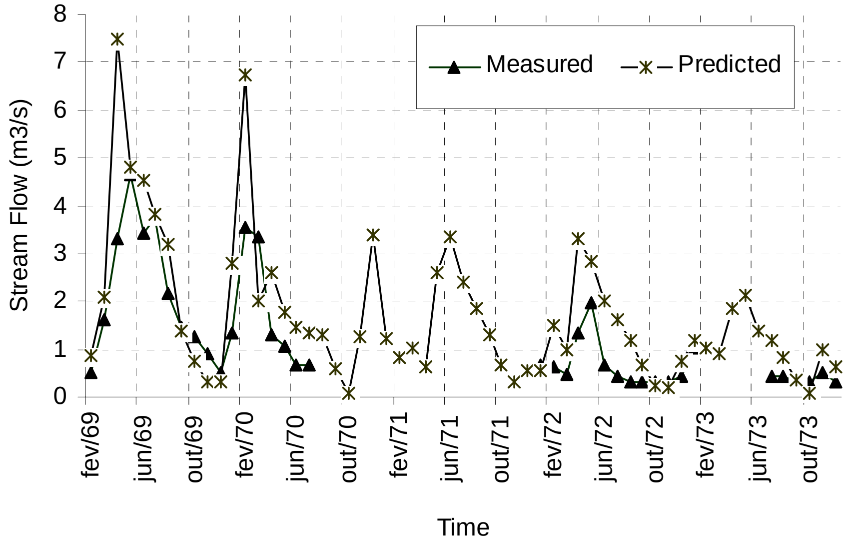

Figure 3. Monthly time series comparison of measured and predicted streamflow at the Junco gage (verification).

Conclusions

A GIS-linked SWAT model provides significant advances in the generated product quality and facilitates the storage of information as well as periodic updates. The SWAT model was applied to of the Salitre River Basin to simulate the hydrology in a semi-arid region of Brazil. The simulated results were compared to observed data at select points in the basin and the results were satisfactory with no complicated processing required in the calibration process. Nevertheless, the model tends to overestimate streamflow. This difference could be attributed to two factors: 1) the SWAT model is based on the CN method, which was initially developed for agricultural and natural watersheds in the U.S., so extending it to "extensive" world watersheds (for which the existing CNs are not representative) can cause the model to predict high runoff; 2) the quality of land use data used may be low. If the land use data used are not representative of the period's ground conditions, runoff predictions will be skewed. As annual land use data are rarely available, there is a good chance that land use change was not adequately represented by the data, and significant changes may occur more quickly than can be captured by linear interpolation.

Acknowledgements

The authors would like to acknowledge the support for this project provided by Bahia Federal University (UFBa) and the Science and Technology Council in Brazil (CNPq)

References

ANA/GEF/PNUMA/OEA. 2003. Projeto de gerenciamento integrado das atividades desenvolvidas em terra na bacia do São Francisco. 383p.

Arnold J.G., K.W. King, J.R. Williams, and R. Srinivasan. 1995. Soil and Water Assessment

Tool–SWAT. USDA, Agricultural Research Service. 450p.
Diluzio, M. and S.L. Neitsch. 1999. ArcView Interface for SWAT 99.2: User's Guide. 185p.
Ministério De Minas E Energia (MME). 1981a. Projeto RADAMBRASIL.
Oliveira, M.Q.C. 1999. Impacto de Mudanças no Uso do Solo nas Características Hidrossedimentológicas da Bacia Hidrográfica do Rio Joanes e sua Repercussão na Zona Costeira. Salvador, Dissertação de Mestrado, Universidade Federal da Bahia. 92p
Tucci, C.E.M. 1997. Escoamento Superficial. In: Tucci, C.E.M., J. Kelman. Hidrologia ciência e Aplicação. 2e. Porto Alegre: Editora da Universidade: ABRH. P.391-441.
U.S. Departament Of Agriculture, Soil Conservation Service (USDA-SCS). 1972. Engineering Handbook: Section 4, Hydrology. Washington: USDA, Supplement A. 250p.
Williams, J.R. and H.D. Berndt. 1977. Sediment Yield Prediction Based on Watershed Hydrology. American Society of Agricultural Engineers, 20(6): p.1100-1104.

Evaluation of the Soil Nitrogen Balance Model in SWAT with Lysimeter Data

Thorsten Pohlert*[1], Johan A. Huisman[1], Lutz Breuer[1] and Hans-Georg Frede[1]
[1]Institute of Landscape Ecology and Resources Management, University of Giessen, Heinrich-Buff-Ring 26, D-35392 Giessen, Germany. Email: Thorsten.Pohlert@agrar.uni-giessen

Abstract

In this study we evaluated the soil nitrogen balance algorithms incorporated in SWAT2000 on the micro scale. Therefore we applied SWAT2000 on a long term German lysimeter experiment to compare predicted with observed monthly actual evapotranspiration, percolation and nitrate leaching. The agreement between SWAT2000 simulated and observed nitrate leaching was poor. A discussion about the constraints of the existing nitrogen balance routines in SWAT2000 is given in this paper. Consequently, we replaced the existing SWAT algorithms with algorithms for both ammonification and nitrification from the DNDC (Denitrification-Decomposition) model and algorithms for denitrification from the CropSyst (Cropping Systems Simulation Model) model. The new model is referred to as SWAT-DNDC. The same dataset was reevaluated, which provided an increase in Nash-Sutcliffe-efficiency for the six year validation period from -0.218 to 0.619.

Introduction

Eco-hydrological simulation models such as SWAT2000 are essential tools for decision support in water resources planning. They can be used to simulate the effects of land use scenarios on both water and matter fluxes, provided that all relevant key processes and interactions of the soil-vegetation-water-system are considered and valid. SWAT2000 has already been applied for decision support with respect to diffusive nitrate emissions in various countries (e.g. Santhi et al., 2001; Chaplot et al., 2004; Grizzetti et al., 2003).

SWAT2000 is also employed within the collaborative research center (CRC 299) at the University of Giessen, Germany. The scope of the CRC 299 is to develop sustainable land use options for peripheral regions. The economic model ProLand (Möller and Kuhlmann, 1999) provides potential land use maps based on specific agro-economic scenarios. The potential land use maps are used as input data for SWAT2000 and various other ecological models to analyze the impact of land use on specific landscape services. For example the impact of potential land use changes on streamflow, actual evapotranspiration, surface runoff and groundwater recharge was analyzed by Weber et al.(2001) for the Aar Catchment, a subcatchment of the Dill Catchment in Mid-Germany.

Using an application of SWAT2000 for the analysis of the nitrogen cycle on the catchment scale, we provide a critical evaluation of the implemented nitrogen balance algorithms. We examined those processes which are simulated on the scale of a Hydrological Response Unit (HRU) in SWAT2000. A lysimeter dataset was obtained to test the performance of SWAT2000 on nitrate leaching, actual evapotranspiration, and percolation. We created an artificial catchment with zero slope and a single HRU. Since an HRU is a unique land use and soil type combination with a specific farm management, the simulated HRU represents the lysimeter.

Lysimeter Station Brandis

The lysimeter station Brandis is located 15 km southeast of Leipzig in Eastern Germany. From 1980 to 1992 a long term fertilizer experiment was employed on various local soil types to test both the impact of soils and water use of crops on yield and the impact of farming practices on nitrate leaching (Haferkorn, 2000). In this study we used the data for the lysimeter group 5, which consists of three undisturbed soil monoliths with an area of 1 m^2 and a depth of 3 m. The soil was classified as an eroded Cambisol (Table 1). Percolate for the three monoliths, gravimetric soil water content, and precipitation was measured on a daily basis. Mineral nitrogen in the percolate was analyzed on a monthly basis (Haferkorn, 2000). The resulting dataset consisted of averaged monthly totals of percolation, nitrate leaching and evapotranspiration calculated from three replicates for the years 1980 to 1992.
The same dataset was used earlier in a competitive workshop to evaluate various soil nitrogen models from Germany and Austria (Dreyhaupt, 2000).

Table 1. Soil physical parameters of lysimeter group 5 at Brandis (Haferkorn, 2000).

Horizon	Depth [cm]	Clay [%]	Silt [%]	Humus [%]	K_{SAT} [mm hr^{-1}]	Bulk density [g cm^{-3}]
Ap	0 – 35	8.0	30.0	2.1	635	1.49
C1	35 – 175	2.0	2.0		782.9	1.67
C2	175 - 300	4.0	2.0		391.7	1.53

Daily records for measured precipitation at a height of 1 m, humidity, wind velocity, and maximum and minimum temperature were obtained from the weather station at Leipzig. Rainfall and sunshine duration was measured directly in the field. Global radiation was calculated according to Angstrøm (1924), where global radiation is a function of extra terrestrial radiation and the proportion of hours of bright sunshine for a given location. The systematic underestimation of precipitation due to measurements with a rain gauge at a level of 1 m was corrected in accordance to Richter (1995). Information on farming management consisted of crop rotation, planting and harvesting dates, fertilizer application amounts, and timing (Table 2). Wet deposition of mineral nitrogen was recorded by analyzing mineral nitrogen in the precipitation collected from the rain gauge during the entire research period (Haferkorn, 2000).

Model Elaboration

When SWAT2000 was tested on the lysimeter data, the model was not capable of accurately simulating percolation. The soil water in the model drained quicker than in the experiment. This can be attributed to the proposed cascaded soil moisture balance model in SWAT2000, where a reduction of saturated hydraulic conductivity according to the moisture status of the individual soil layer is omitted. Consequently, a function which reduces hydraulic conductivity under non-saturated moisture conditions in SWAT2000 was implemented.

Table 2. Crop rotation, precipitation, nitrogen input and output for lysimeter group 5 (after Haferkorn, 2000 and Dreyhaupt, 2000).

Year	Crop	Precipitation [mm a^{-1}]	N-Fertilization [kg N ha^{-1} a^{-1}]	N-Deposition [kg N ha^{-1} a^{-1}]	N-Leaching [kg N ha^{-1} a^{-1}]	N-Uptake [kg N ha^{-1} a^{-1}]
1980	Maize	657	140	44	-	97
1981	Sugar beet	727	160	53	88	111
1982	Winter wheat	390	120	28	60	90
1983	Winter barley	672	120	33	47	117
1984	Grass	536	175	42	14	118
1985	Potato	477	100	69	17	73
1986	Winter wheat	581	120	35	61	94
1987	Potato	629	100	37	98	131
1988	Winter wheat	574	140	46	56	72
1989	Winter barley	546	120	46	34	124
1990	Sugar beet	579	140	44	21	155
1991	Winter wheat	417	140	37	25	101
1992	Winter barley	583	120	29	35	50

SWAT2000 simulated surprisingly high annual denitrification losses of up to 135 kg N ha^{-1} a^{-1} for the total model period. In the conceptualization of SWAT2000, denitrification occurs in a given soil layer if 95% of field capacity is exceeded (Neitsch et al., 2001). This threshold is always exceeded if water moves from upper to underlying soil layers in the cascaded soil moisture balance model. Hence, in SWAT2000 leaching and denitrification are two competing processes. The extraordinarily high denitrification rates led to a rapid and complete depletion of the nitrate pool in each layer.

A further constraint of the SWAT2000 model is that under limiting nitrogen conditions crops can accumulate their nutrient deficiency as long as this condition continues. As soon as the nitrate pool in the soil is increased by fertilization, the plant can take up an amount equal to its accumulated deficiency. This happens in the model because a sink limitation for nitrogen uptake is missing.

To overcome the aforementioned constraints, a new nitrogen balance model was implemented in SWAT2000 and is further referred to as SWAT-DNDC (Figure 1). SWAT-DNDC distinguishes between three organic litter pools with respect to their decomposability. The allocation of litter and organic fertilizer to the three litter pools depends on their C-N ratios. The ammonium and nitrate content of mineral fertilizers are added to their corresponding pools in the top soil of the model as is the case for mineral nitrogen in rainfall. In SWAT-DNDC crops take up both, nitrate and ammonium. Furthermore, a constant sink limitation with respect to maximum daily crop nitrogen uptake was implemented. Nitrogen can leave the soil-vegetation system through leaching, lateral transport, surface transport and gaseous emissions.

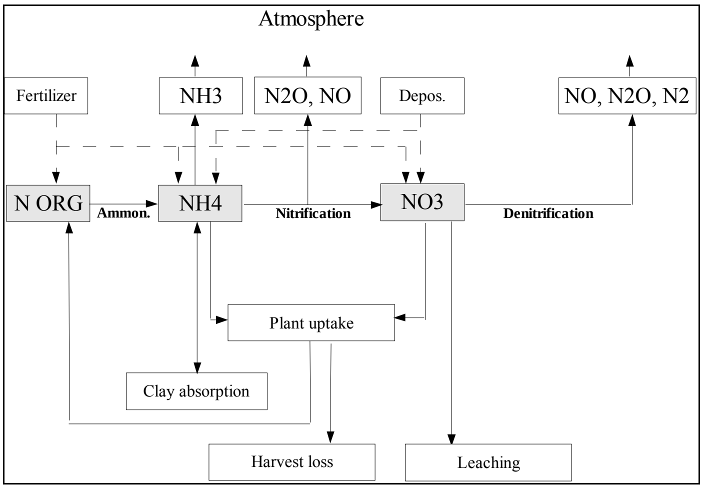

Figure 1. Conceptualization of the nitrogen turnover model implemented in SWAT-DNDC (after Zhang et al., 2002).

Decomposition

Decomposition is the production of mineral C and ammonium from soil organic matter mediated by microorganisms. The algorithms for decomposition were incorporated from Li et al. (1992) and Li et al. (2000). As mentioned before, the model distinguishes between three organic litter pools. Each litter pool is characterized by both a specific rate constant $k_{C,i}$ and a specific C-N ratio. The gross decomposed carbon for any litter pool is calculated in accordance with Equation 1:

$$F_{C,l}=k_{C,i}\ f_{(1,l\ 2,l)}\ C_i \tag{1}$$

where $F_{C,l}$ is the decomposed organic carbon available for growth of nitrifying bacteria [kg C ha^{-1}] at soil layer l, C_i is the organic carbon content of the decomposable litter pool i [kg C ha^{-1}], $f_{(1,l\ 2,l)}$ is the combined moisture and temperature factor for soil layer l, and $k_{C,i}$ is the rate constant at optimum temperature and moisture conditions for litter pool i. The combined moisture and temperature factor is calculated in accordance to Stange (2001) (Equation 2):

$$f_{(1,l\ 2,l)}=\ 2\ /\ \left(\frac{1}{f_{1,l}}+\frac{1}{f_{2,l}}\right) \tag{2}$$

where $f_{(1,l)}$ is the moisture factor and $f_{(2,l)}$ is the temperature factor of soil layer l. The moisture factor is calculated with the WEIBULL-function (Equation 3):

$$f_{1,l}=\ 1\ -\ \left(1\ +\ \exp\frac{\Theta_{ACT,l}\ -\ \Theta_{CRIT}}{\gamma}\right)^{-1} \tag{3}$$

where $\Theta_{ACT,l}$ is the actual soil moisture of soil layer l [WFPS], Θ_{CRIT} is the critical soil moisture content [WFPS], and γ is the parameter for the WEIBULL-function. The temperature reduction function is calculated with the O'NEILL-function as proposed by Stange (2001) (Equation 4).

$$f_{2,l} = \left(\frac{t_{MX} - t_{S,l}}{t_{MX} - t_{OPT}} \right)^{t_A} e^{\,t_A[(t_{S,l} - t_{OPT}) \;/\; (t_{MX} - t_{OPT})]} \tag{4}$$

where t_{MX} is the maximum temperature of the O'NEILL-function [°C], t_{OPT} optimum temperature of the O'NEILL-function [°C], t_A scale parameter and $t_{S,l}$ soil temperature of layer l [°C]. The decomposed carbon is partly used for the formation of microbial biomass. Since a C-N ratio of 8-12 exists for microbes, one can estimate the resulting nitrogen demand for microbial growth. If the released ammonium meets the demand for microbial growth, a net mineral nitrogen surplus will occur. Otherwise the microbes will reduce nitrate to meet their nitrogen demand, consequently, a net mineral nitrogen loss will occur in this case. Net ammonification is calculated as given by Equation 5:

$$F_{NH_4N,l} = \left(\frac{F_{C,l} + D_{BC,l}}{CN_{i,l}} \right) - D_{BN,l} \tag{5}$$

where F_{NH4N} is the flux of organic nitrogen into the ammonium pool in layer l [kg N ha^{-1} d^{-1}], $D_{BC,l}$ is the surplus of microbial biomass in layer l [kg C ha^{-1} d^{-1}], $CN_{i,l}$ is the C/N ratio for litter pool i in layer l, and $D_{BN,l}$ is the microbial N demand for biomass formation [kg N ha^{-1} d^{-1}].

Nitrification

Nitrification is a multi-step oxidation process mediated by several autotrophic organisms, namely *Nitrosomas* spp. and *Nitrobacter* spp. Ammonium is sequentially oxidized to nitrite and nitrate. However, in SWAT-DNDC, nitrification is modelled as a one step oxidation where nitrate is produced directly. Since SWAT-DNDC is a gross nitrogen balance model the available ammonium for nitrification needs to be estimated. A portion of the ammonified nitrogen is adsorbed to clay minerals in the model. Furthermore the dissociation of ammonium to ammonia, depending on soil pH, is calculated. A fraction of the ammonia can volatilize to the atmosphere. The remaining ammonium in a given soil layer can be nitrified. The gross nitrification is calculated in accordance with Zhang (2002). It depends on moisture, temperature and pH values for the soil (Equation 6).

$$F_{NO_3N,l} = N_{NH_4N,l} \left[1 - \exp^{(k_{35} \;\; f_{3,l})} \right] \; f_{4,l} \quad f_{5,l} \tag{6}$$

where $F_{NO3N,l}$ is the gross flux from the ammonium pool, k_{35} is the rate constant for nitrification at 35 °C, $f_{3,l}$ is the temperature factor, $f_{4,l}$ is the moisture factor, and $f_{5,l}$ is the pH factor for nitrification. The temperature factor and the moisture factor are calculated in accordance with the factors for ammonification, though the parameters for the given functions differ. The pH factor $f_{5,l}$ is calculated with a second order polynomial in accordance with Zhang (2002) (Equation 7).

$$f_{5,l} = -0.0604\, pH^2 + 0.7347\, pH - 1.2314 \tag{7}$$

During ammonification gaseous losses of N_2O and NO can occur. This is considered in the model with the following equation (Equation 8):

$$N_{ox,l} = k_{ox} \ F_{NO_3N,l} \ \Theta_{ACT,l} \ 2.72^{(34.6-9615) \ / \ (t_{s,l}+273.15)} \qquad (8)$$

where N_{ox} is N_2O or NO production, and k_{ox} is the coefficient for N_2O production (6 x 10^4) and NO production (2.5 x 10^{-3}), respectively. The remaining $F_{NO3N,l}$ is the net flux of mineral nitrogen into the nitrate pool of soil layer *i*.

Denitrification

Denitrification is the reduction of nitrate to gaseous N compounds, namely N_2O, NO and N_2. The algorithms for denitrification were taken from Stöckle and Campbell (1989); they are also incorporated in the model CropSyst (Stöckle and Nelson, 1995). Denitrification is modeled as a 1st order kinetic depending on moisture content and temperature for each soil layer. Additionally, denitrification only occurs in the model, if organic carbon is present in the soil layer. This implicitly accounts for the necessary substrate for the reduction of nitrate catalyzed by denitrifying bacteria (Equation 9):

$$DN_l = NO_3N_l[1-\exp^{(-k_{15} f_{6,l} f_{7,l})}] \qquad (9)$$

where DN_l is denitrification loss to the atmosphere of soil layer l [kg ha^{-1}], NO_3N_l is the nitrate content of soil layer l [kg ha^{-1}], k_{15} is the denitrification rate constant at 15°C, $f_{6,l}$ is moisture and $f_{7,l}$ is the temperature factor for denitrification. The moisture factor is calculated as (Equation 10):

$$f_{6,l} = \exp[0.304 + 2.94(\Theta_{SAT,l} - \Theta_{ACT,l}) - 47(\Theta_{SAT,l} - \Theta_{ACT,l})^2] \qquad (10)$$

where $\Theta_{SAT,l}$ is the volumetric soil moisture content at saturation for soil layer l [m^3 m^{-3}] and $\Theta_{ACT,l}$ is the actual volumetric soil moisture content of soil layer l [m^3 m^{-3}]. The temperature factor is calculated as given in Equation 11:

$$f_{7,l} = \begin{array}{ll} 0.67\exp[0.43(T_{S,l}-10)] & \forall \quad T_{S,l} \leq 10 \\ \exp[0.08(T_{S,l}-15)] & \forall \quad T_{S,l} > 10 \end{array} \qquad (11)$$

Experimental Design

In accordance with Dreyhaupt (2000), a split sample test was employed with a calibration period from 1980 to 1986 and a validation period from 1987 to 1992. A warm-up-period of three years was simulated prior to calibration using three copies of the climatic data for 1980. SWAT-DNDC was calibrated with a two step approach. First, a multi-objective calibration was performed considering parameters which are important in the processes of evapotranspiration and percolation. The automatic calibration procedure was similar to that proposed by Huisman et al. (2003). Second, parameters controlling nitrogen balance in SWAT-DNDC were manually calibrated (Table 3), and the resulting nitrate leaching was visually compared with plotted observed data.

Table 3. Initial and calibrated parameter values.

Parameter	Definition	Initial value	Calibrated value
BD *	Bulk density [g cm^{-3}]	1.490	1.479
AWC *	Available water capacity [m^3 m^{-3}]	0.168	0.188
A	Albedo	0.250	0.219
K_{SAT} *	Saturated hydraulic conductivity [mm hr^{-1}]	635	747
ESCO	Soil evaporation compensation factor	0.000	0.528
EPCO	Plant uptake compensation factor	0.000	0.297
krcvl +	Rate factor for decomposition of very labile litter	0.25	10^{-4}
krcl +	Rate factor for decomposition of labile litter	0.074	10^{-4}
krcr +	Rate factor for decomposition of stabile litter	0.02	5×10^{-6}
k_{35} +	Rate factor for nitrification	25	10
DNH3 +	Diffussion coefficient for ammonia	0.025	0.015
MaxNup +	Maximum daily N uptake of a crop [kg N ha^{-1} d^{-1}]	3.5	1.5
PORFRAC	Porous volume from which anions are excluded	0.5	0.9

* Parameters of the top soil layer were calibrated and the parameters of the underlying layers were adjusted according to the change ratio of the top soil layer as proposed by Eckhardt and Arnold (2001).
+ New parameters in SWAT-DNDC.

Results and Discussion

As shown in Figure 2a, the SWAT-DNDC model accurately predicted actual monthly evapotranspiration. It should also be noted that remarkable uncertainties exist in the observed data set for the extreme evapotranspiration rates. The coefficient of variance (cv) for the three replicates was up to 79% during the winter period and 20% during the summer period. The average cv was 9.25% for the entire study period. The model efficiencies from Nash and Sutcliffe (1970) were 0.746, 0.715 and 0.732 for the calibration, validation, and total period, respectively.

As mentioned in the previous section SWAT2000 was not able to predict percolation accurately through the constraints of the cascaded soil moisture balance model. After the modifications, SWAT-DNDC accurately predicted timing and amount of percolation, although predicted monthly percolation was less precise than predicted actual monthly evapotranspiration. Percolation in the lysimeter group 5 occurred almost entirely during the period from October to March during each year. The average cv for the three replicates for percolation during the total period was 27.8%. The agreement was high between predicted and observed monthly percolation in the beginning of the period when maize, sugar beet, winter wheat and winter barley grew (Figure 2b). However, when grass grew, in 1984, SWAT-DNDC poorly predicted monthly percolation, which can be attributed to uncertainties in the parameterization of the crop. The model efficiencies for the calibration, validation and total period were 0.584, 0.632, and 0.609, respectively

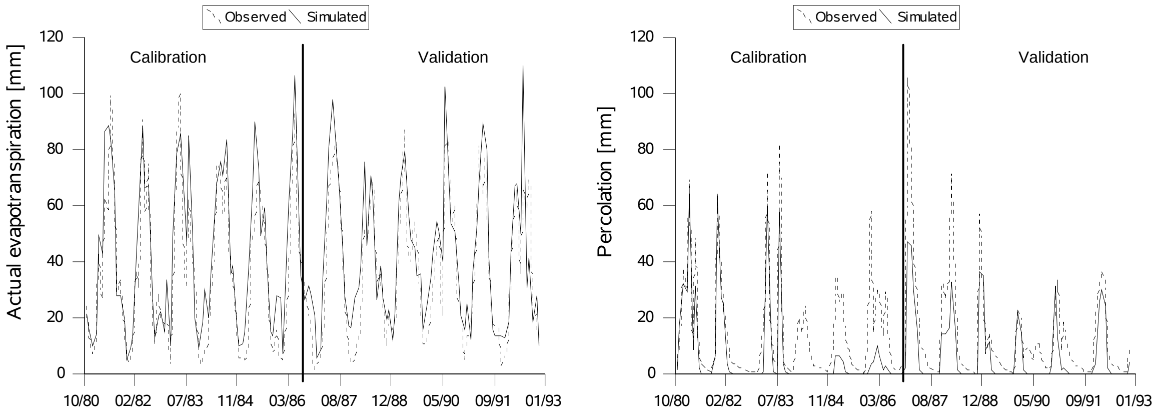

Figure 2. (a) Observed and simulated monthly actual evapotranspiration using SWAT-DNDC. (b) Observed and simulated monthly percolation using SWAT-DNDC.

The accuracy of nitrate leaching prediction strongly depends on the accuracy of predicted percolation, since nitrate leaching is the transport of nitrate in soil water solution. As shown in Figure 3a, the original SWAT2000 version was not capable of simulating the leaching of nitrate reasonably well. The efficiencies were -0.264, -0.218, and -0.234 for the calibration, validation and total period, respectively. Furthermore, average annual nitrate leaching differed strongly between observed (46.8 kg N ha^{-1} a^{-1}) and simulated data (2.4 kg N ha^{-1} a^{-1}).

To overcome these problems, the new SWAT-DNDC model was developed and tested on the Brandis lysimeter data set. The performance of the SWAT-DNDC model is provided in Figure 3b. The model efficiencies were 0.185, 0.619, and 0.443 for calibration, validation and the entire period, respectively, consequently the model efficiency was enhanced through the newly implemented algorithms. A complete depletion of mineral nitrogen in the modeled soil profile, as was the case in SWAT2000, did not occur in SWAT-DNDC. Mineral nitrogen content in the entire modelled soil profile varied between 10 kg N ha^{-1} a^{-1} and 180 kg N ha^{-1} a^{-1}.

However, the model tends to underestimate the observed peaks during the calibration period (Figure 5). On the other hand, the model overestimated nitrate leaching in the validation period. Both can be attributed to our simplified assumption that mineral nitrogen concentration in rainfall (calculated and implemented as the daily average concentration in SWAT-DNDC) remains constant over the entire simulation period. As shown in Table 2, a clear decline of wet nitrogen deposition was visible. Hence, the model underestimated incoming mineral nitrogen in the beginning and overestimated it at the end of the simulation period. A further reason for remaining imperfections in the model performance was the noteworthy uncertainty in observed nitrate leaching. The cv for the three replicates of observed nitrate leaching during the total period was 32.5%.

As shown in Figure 3, percolation was accurately predicted by SWAT-DNDC for the first two seasons, but predicted nitrogen leaching was imprecise (Figure 5). This can be attributed to an imperfect representation of the nitrate concentration in the modelled soil monolith. Predicted average annual nitrate leaching was 24 kg N ha^{-1} a^{-1}, which still represents a 50% underestimation of observed data. But one has to keep in mind that the available dataset has some limitations for model development. First of all, a comparison with daily data was not possible since the dataset consists of monthly totals only. In addition, measured data for model testing and model input data are prone to data uncertainty, an issue that has not been addressed in the present work. Nevertheless, the detailed comparison of the old SWAT2000 and the new SWAT-DNDC version clearly reveals that the internal process description is improved. The status of the soil nitrogen pools and the nitrogen fluxes are now more consistent and SWAT-DNDC is able to simulate long term series with crop rotation.

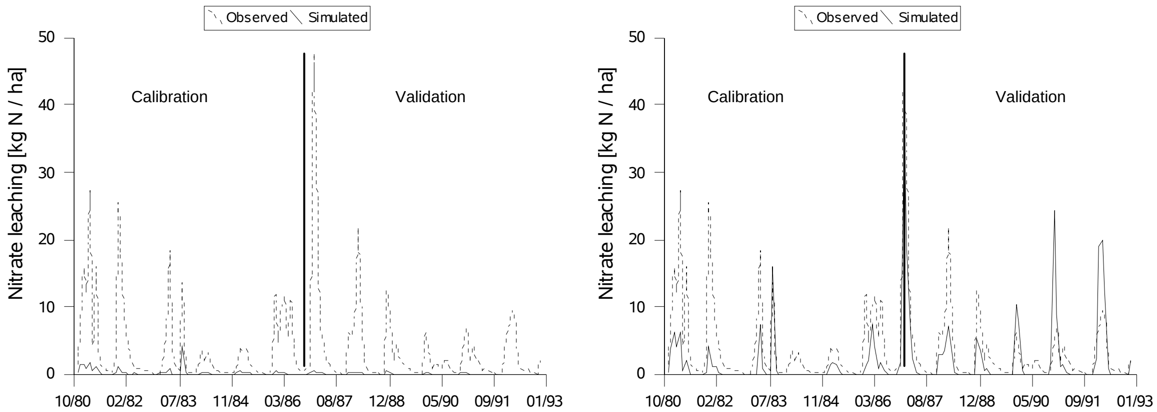

Figure 3. (a) Simulated and observed nitrate leaching using SWAT2000. (b) Simulated and observed nitrate leaching using SWAT-DNDC.

Conclusion

In this study we examined the internal fluxes and cycles of nitrogen compounds and elaborated a new, detailed model for nitrogen balance on the HRU scale. The constraints of the SWAT2000 model regarding the representation of the nitrogen cycle became apparent after detailed analysis of the nitrogen turnover processes on the microscale. This was attempted in the present work by investigating a lysimeter data set. The constraints would have likely remained unnoticed with the classical approach of comparing simulated with observed nitrate load on a river basin outlet only. Hence, scale dependent simulated processes should be evaluated with appropriate measurements on corresponding scales.

Through the implementation of algorithms for decomposition, nitrification and denitrification from both the DNDC and CropSyst model in SWAT, the model efficiency increased from -0.218 to 0.619 for nitrate leaching for the validation period. A sound sensitivity study, a further test on both the field and catchment scale, as well as the application of the coupled SWAT-DNDC model for land use scenarios will be accomplished in the near future.

Acknowledgements

This study was supported by the Deutsche Forschungsgemeinschaft within the scope of the Collaborative Research Center (SFB) 299. We thank Dr. Ulrike Haferkorn and Dr. Uwe Franko (both UFZ-Leipzig) for the provision of lysimeter data from the research station Brandis.

References

Angstrøm, A. 1924. Solar and terrestrial radiation. Q. J. R. Meteorol. Soc. 50, 121-125
Chaplot, V., A. Saleh, D. Jaynes, and J. Arnold. 2004. Predicting water, sediment and NO_3-N

loads under scenarios of land-use and management practices in a flat watershed. Water Air Soil Pollut. 154, 271-293.
Dreyhaupt, J. (ed.). 2000. Stickstoffmodellierung für Lysimeter des Parthe-Bebietes. Ergebnisse des Workshops "Stickstoffmodellierung" vom 8.6.1999 bis 10.6.1999 am UFZ Leipzig-Halle. UFZ Bericht 17/2000. Leipzig. (in German).
Eckhardt, K., and J. Arnold. 2001. Automatic calibration of a distributed catchment model. J. Hydrol. 251, 103-109.
Eckhardt, K., S. Haverkamp, N. Fohrer, and H.-G. Frede. 2002. SWAT-G, a version of SWAT 99.2 modified for application to low mountain range catchments. Phys. Chem. Earth 27, 641-644.
Grizzetti, B., F. Bouraoui, K. Granlund, S. Rekolainen, and G. Bidoglio. 2003. Modelling diffuse emissions and retention of nutrients in the Vantaanjoki watershed (Finland) using the SWAT model. Ecol. Model. 169, 25-38.
Haferkorn, U. 2000. Größen des Wasserhaushaltes verschiedener Böden unter landwirtschaftlicher
Nutzung im klimatischen Grenzraum des Mitteldeutschen Trockengebietes – Ergebnisse der Lysimeterstation Brandis. PhD-thesis University of Göttingen. (in German).
Huisman, J.A., L. Breuer, K. Eckhardt, and H.-G. Frede. 2003. Spatial consistency of automatically calibrated SWAT simulations in the Dill catchment and three of its subcatchments. Proceeding of the second international SWAT conference, Bari, Italy, 78-81.
Li, C., S. Frolking, and T.A. Frolking. 1992. A model of nitrous oxide evolution from soil driven by rainfall events: 1. model structure and sensitivity. J. Geophys. Res., 97, 9759-9776.
Li, C., J. Aber, F. Stange, K. Butterbach-Bahl and H. Papen. 2000. A process-oriented model of N_2O and NO emissions from forest soils: 1. Model development. J. Geophys. Res., 105, 4369-4384.
Möller, D., and F. Kuhlmann. 1999. ProLand: A new approach to generate and evaluate land use options. IX European congress of agricultural economists, Warsaw, Poland August 24-28, 1998.
Nash, J.E., and J.V. Sutcliffe. 1970. River flow forecasting through conceptual models. 1. A discussion of principles. J. Hydrol. 10, 282-290.
Neitsch, S., J.G. Arnold, J.R. Kiniry, and J.R. Williams. 2001. Soil and water assessment tool. Version 2000. Theoretical documentation. Temple, TX.
Richter, D. 1995. Ergebnisse methodischer Untersuchungen zur Korrektur des systematischen Meßfehlers des Hellmann-Niederschlagsmessers. Berichte DWD 194. (in German).
Santhi, C., J. Arnold, J. Williams, W. Dugas, R. Srinivasan, and L. Hauck. 2001. Validation of the SWAT model on a large river basin with point and nonpoint sources, J. Am. Water Resour. Assoc. 37, 1169-1188.
Stange, F. 2001. Entwicklung und Anwendung eines prozessorientierten Modells zu Beschreibung der N_2O und NO-Emissionen aus Böden temperater Wälder. PhD-thesis University of Freiburg. (in German).
Stöckle, C.O. and R. Nelson. 1995. CropSyst. Cropping Systems Simulation Model. User's Manual (Ver. 1.04). Washington State Univ., Biol. Syst. Eng. Dep., Pullman, WA.
Stöckle, C. and G. Campbell. 1989. Simulation of crop response to water and nitrogen: An example using spring wheat. Trans. ASAE, 32, 66-68.
Weber, A., N. Fohrer, and D. Möller. 2001. Long-term land use changes in a mesoscale watershed due to socio-economic factors - effects on landscape structures and functions. Ecol. Modell. 140, 125-140.
Zhang, Y., C. Li, X. Zhou, and B. Moore. 2002. A simulation model linking crop growth and

soil biogeochemistry for sustainable agriculture. Ecol. Model., 151, 75-108.

Modelling Soil Carbon Cycle for the Assessment of Carbon Sequestration Potentials at the River Basin Scale

Joachim Post*[1], Felicitas Suckow[2], Valentina Krysanova[2] and Fred F. Hattermann[2]
[1]Potsdam Institute for Climate Impact Research, Dep.: Global Change and Natural Systems, P.O. Box 60 12 03, 14412 Potsdam, Germany, phone: +49 (0) 331-288-2417, Fax: +49 (0) 331-288-2695, Email: joachim.post@pik-potsdam.de
[2]Potsdam Institute for Climate Impact Research, Germany

Abstract

To investigate the effects of different land use management practices and land use change on carbon fluxes in river basins, a soil organic matter model (Soil-Carbon-Nitrogen model, a submodel of the forest growth model 4C) has been integrated into the eco-hydrological river basin model SWIM (Soil and Water Integrated Model). The extended integrated model combines hydrological processes, crop and vegetation growth, carbon, nitrogen, phosphorus cycles and soil organic matter turnover. The direct connection to land use, soil and climate data provides a possibility to use the model for analyses of climate change and land use change impacts on hydrology, vegetation growth (e.g. crop yield) and soil biogeochemistry. The aim of this study was to test the model performance and its capability to simulate the magnitude and temporal behaviour of carbon pools and fluxes at the regional scale. As a first step, a sensitivity analysis has been performed and the model has been parameterised and verified for conditions in East Germany, using values known from literature and regionally available time series of carbon pools and fluxes. This provides verification of carbon pools and fluxes in the landscape and verifies the correct representation of the environmental processes therein. Additionally, uncertainty analysis on model results has been performed using a Monte Carlo type approach. This led to a quantification of uncertainty bounds attached to spatial and temporal model results.

Based on this, different land management strategies and land use change options can be simulated to assess the behaviour of water and carbon fluxes as well as carbon sequestration options within the river basin or at the landscape level. For agricultural areas, the impacts of land management changes on the carbon balance have been investigated. It has been found that different crop rotations and fertilisation practices show a considerable effect on long term soil organic carbon dynamics.

Keywords: Eco-hydrological modelling, soil carbon, soil nitrogen, soil organic matter turnover, land use change, land management, carbon sequestration

Introduction

To answer questions related to soil carbon (C) sequestration and soil quality, soil nutrient and water uptake by plants, soil nutrient loss and water quality issues, soil disturbance and land management and climatic impacts on ecosystems, the application of ecosystem models are seen as a useful tool. Referring to terrestrial carbon cycling, soils are of high importance as they are considered as potential accumulation medium for C and could help to mitigate the continuous increase of atmospheric CO_2 (Lal, 2004). Most of the C in soil organic matter (SOM) is plant-derived through root exudates and decomposition of root, shoots and litter (Johnston and Groffman, 2004). The combination of these inputs and outputs (e.g.

decomposition, mineralization, and erosion) determines the C balance in the SOM pool and the productivity below and above ground. Environmental changes may directly affect allocation of C from plant to soil and the decomposition and mineralization processes, as well as lateral and vertical translocations. To assess soil C development for a certain region it is necessary to consider relevant processes and feedbacks between them, namely plant growth and plant derived soil C returns, soil nutrient status, soil temperature, and soil water driven by land management and climate.

To investigate the effects of different land use management practices on carbon fluxes at the regional scale we developed an integrated model by coupling the eco-hydrological river basin model SWIM (Soil and Water Integrated Model; Krysanova et al., 1998) and the soil organic matter model SCN (Soil-Carbon-Nitrogen model). The latter is a sub-model of the forest growth model 4C (Lasch et al. 2002). The extended integrated model (SWIM-SCN) combines hydrological processes, crop and vegetation growth, soil erosion, soil temperature, carbon, nitrogen, phosphorus cycles, and soil organic matter turnover.

Methodology

The Eco-hydrological Model SWIM

SWIM (Krysanova et al., 1998) is a continuous-time, spatially distributed model. SWIM works on a daily time-step and integrates hydrology, vegetation, erosion, and nutrients at the river basin scale. The spatial aggregation units are subbasins, which are delineated from digital elevation data. The subbasins are further disaggregated into hydrotopes, hydrologically homogenous areas. The hydrotopes are defined by uniform combinations of subbasin, land use and soil type (Krysanova et al. 2000). The model is connected to meteorological, land use, soil and agricultural management data. For detailed process descriptions of validation studies and data requirements, refer to publications by Krysanova et al. (1998, 2000) and Hattermann (2004).

The Extended Soil Carbon and Nitrogen Module

The new carbon and nitrogen cycle module is based on the tight relationship between the soil and the vegetation. On the one hand, organic matter is added to the soil through accumulating litter, dead fine roots, and organic fertiliser. On the other hand, there is a withdrawal of water and nitrogen from the soil by the vegetation, release of CO_2 into the atmosphere, and export of inorganic nitrogen by soil water flows (e.g. percolation into the groundwater and lateral flow processes).

To describe the carbon (C) and nitrogen (N) budget, organic matter is differentiated into Active Organic Matter (AOM) as the soil organic matter pool and Primary Organic Matter (POM) as the litter pool. The latter is separated into five fractions for each vegetation and crop type (stems, twigs and branches, foliage, coarse roots and fine roots). For all pools of active and primary organic matter, the carbon and nitrogen content is considered.

The carbon and nitrogen turnover into different stages (pools) is pictured as a first order reaction (Chertov and Komarov, 1997; Franko, 1990; Parton et al., 1987). The processes are controlled by matter specific reaction coefficients. Heterotrophic (substrate induced) soil respiration is calculated through the decay of C_{POM} and C_{AOM} pools per day. The effects of soil temperature, soil water content and soil pH status on mineralisation and nitrification is considered through reduction functions (Franko, 1990).

Model Parameterisation

The model parameterisation was done to simulate soil organic matter and relevant processes for eastern German conditions. Therefore, related environmental studies in the region and literature were used for parameterisation. The reaction coefficients controlling the turnover of soil organic matter have to be determined for each plant species (forest and crop types) and organic primary matter fraction (fine roots, coarse roots, twigs and branches, foliage and stems). Determination of these coefficients is mainly done by either field experiments (litter bag experiments) or under laboratory conditions (incubation experiments). Main source for these parameters for the region under study are from agricultural plant investigations by Klimanek (1990 a,b) and Franko (1990) and from forest type information by Bergmann (1999) and Berg & Staaf (1980).

Sensitivity and Uncertainty Analysis

In order to get a better understanding of the model behaviour, the sensitivity of the main input parameters to model results have been tested, and an uncertainty analysis has been performed. The analysis is based on a Monte Carlo type global sensitivity and uncertainty analysis of model parameters using the Latin Hypercube Sampling (LHS) method (McKay et al., 1979). LHS allows interactions between different parameter combinations to be studied and can identify the contributions of parameters alone and in combination with the uncertainty of the modelled results (Saltelli, 1999). Correlations between parameters can be considered in the sensitivity and uncertainty assessment. To generate the appropriate sample sets, which are fed into the SWIM model, the software tool SimLab was applied (Saltelli, 2004). Analysis of sensitivity and uncertainty of model parameters to model results also has been performed using SimLab.

The sensitivity of model results to the parameters was estimated using the partial ranked correlation coefficient (PRCC) (Saltelli, 2004). Uncertainty was analysed using histogram plots of model results based on 500 realisations.

Results and Discussion

Sensitivity Analysis

Based on two output variables, namely total soil C storage (CTOT, Figure 1a) and soil respiration (CRESP, Figure 1b), the sensitivity of SWIM-SCN model parameters was determined. A high absolute PRCC value indicates a high sensitivity of the respective model parameter.

It turned out that the most sensitive parameters are the turnover coefficient of soil organic matter (determining the rate of mineralization (k_{aom}) and a parameter which determines the amount of organic matter transformed from dead plant material to soil organic matter (k_{syn}). The latter shows higher sensitivity for above-ground litter fractions (k_{syn} litter) than below-ground fractions (k_{syn} roots) (Figure 1a and b). Besides these two parameters, the amount of litter entering the soil as plant residuals has a high influence on the output variables in the model (Figure 1a, “fraction litter”). The parameter k_{pom} (determining the turnover coefficient of primary organic matter) shows the least sensitivity (lowest absolute PRCC values) both for above-ground (litter) and below-ground (roots) plant fractions.

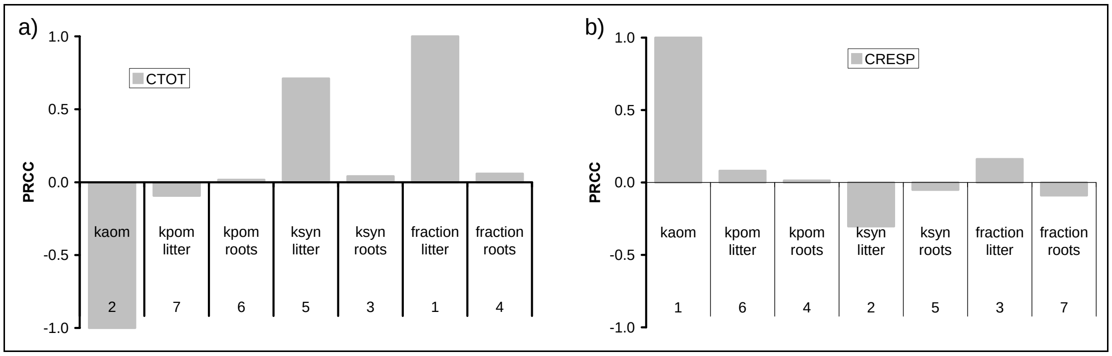

Figure 1. Sensitivity analysis of main SWIM-SCN model parameters.

This analysis gives important information on the relative importance of relevant model parameters. Therefore, the highest accuracy in model parameterisation has to be conducted for the parameters showing the highest sensitivity (Figure 1). Additionally, the most sensitive parameters are contributing the most to model uncertainty. Besides the determination of k_{aom} and k_{syn}, the calculation of crop/vegetation growth and therefore the calculation of plant material entering the soil as primary organic matter is crucial.

Verification of the Extended Model

All processes related to the turnover of soil organic matter have to be evaluated against observed data. Therefore, the extended SWIM model was evaluated against data on soil temperature, soil hydrology, crop yield, soil nitrogen and long-term soil organic matter dynamics at the plot scale. The model was run predominantly without calibration except for the use of some parameterisation data provided for the experimental field plots used (e.g. soil physical parameters).

For soil temperature, soil water dynamics, comparison of modelled and simulated crop yields, and nitrogen dynamics at the plot scale, the verification results are summarized in Post et al. (2005).

Further verification has been performed on decomposition studies of dead plant material, which showed good results for two crop types (winter wheat and summer barley) and one evergreen forest type (Scots Pine). For soil respiration simulations, the verification showed satisfactory results. On a yearly basis and for broad land use classes (cropland ecosystems, deciduous, and evergreen forests), the magnitudes of simulated values are in agreement with the measured data (Post et al. 2004). Figure 2 shows results for daily comparisons of simulated and modeled soil respiration on an agricultural field site of the Leibniz Institute for Agricultural Engineering Bornim (ATB), Germany (Hellebrand et al. 2003).

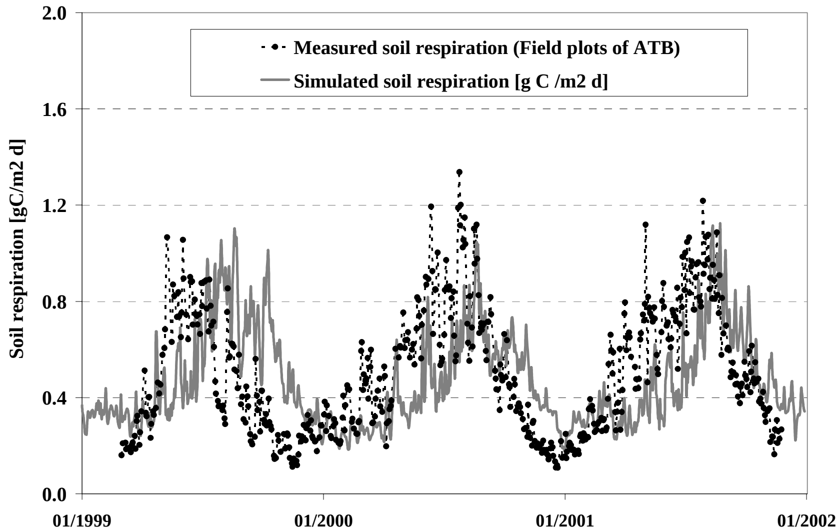

Figure 2. Comparison of simulated and measured soil respiration at an agricultural field site in Brandenburg (Germany) for the years 1999 - 2001, data provided by the Leibniz Institute for Agricultural Engineering (ATB).

It has to be mentioned that simulated soil respiration does not include root respiration. To account for root respiration, values cited in Hanson et al. (2000) were used to subtract the portion of root respiration in the measurements. This allowed for direct comparison with the simulation results. The temporal dynamics represented reasonably well based on comparisons between the measurements and simulation results (Figure 2). Although there is a shift from higher soil respiration rates in spring to a quicker decrease in soil respiration rates in autumn, the shift between simulations and measurements is most likely due to an incorrect simulation of soil warming effects in spring and cooling in autumn of this sandy soil site. Therefore, the soil temperature effects on decomposition are not satisfactory for the site conditions.

Long-term soil organic carbon dynamics have been simulated for the long-term static fertiliser experiment at Bad Lauchstädt, Germany (100 years, 51 simulations) and for the long-term experiment V140 at Müncheberg, Germany (35 years). Results of the comparison of simulated and measured data are shown in Figure 3a for a fertilised and unfertilised plot at the Müncheberg site (150 kg N ha^{-1} a^{-1} inorganic and about 25 t ha^{-1} farmyard manure every two years). The Bad Lauchstädt site, representing a fertilised plot (30 t ha^{-1} farmyard manure every two years and varying rates of inorganic fertiliser (NPK)) and an unfertilised plot, is shown in Figure 3b. The simulations adequately reproduced the impacts of organic fertilisation on soil organic carbon dynamics. The pattern of the measurements reasonably matched the simulation for both verification sites. The simulated values lie between the standard error for most of the measured data. The long-term trends in measured SOC contents are met by the simulations (Figure 3a and b).

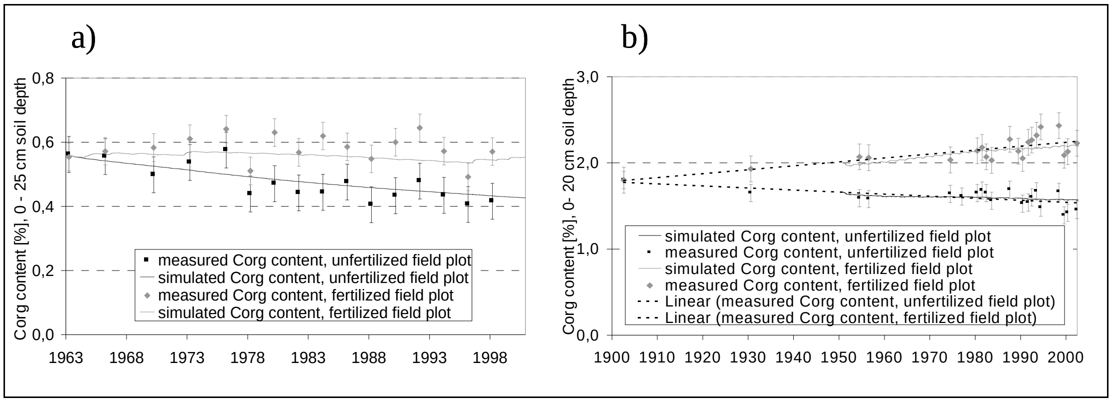

Figure 3: Comparison of measured and simulated values of total soil organic carbon [%] in the top 25 cm of soil at the Müncheberg site (a) and the in the top 20 cm of soil at the Bad Lauchstädt site (b).

Uncertainty Analysis

Following the concept described for the sensitivity assessment, one can assess the uncertainty in model results due to model parameterisation. The parameter used was the same as in the sensitivity assessment, and the same parameter value ranges were derived from literature. As an example, the histogram of model outputs (500 realisations) for simulated annual soil respiration is shown in Figure 4.

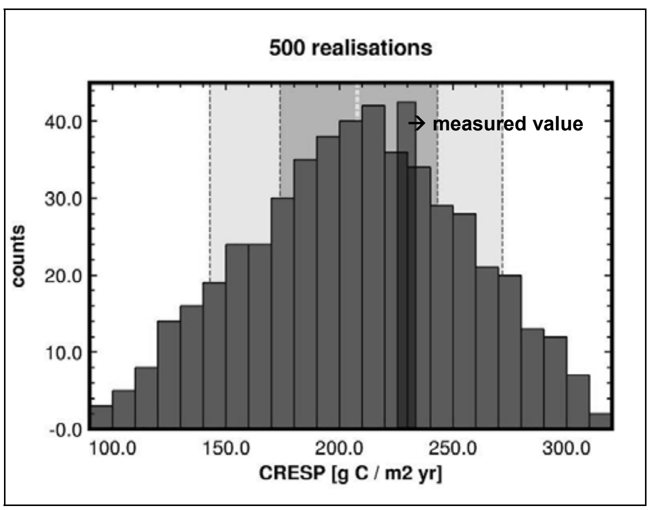

Figure 4: Histogram of modelled annual soil respiration [g C/m2/yr] based on 500 realisations.

Measured values were again derived from the agricultural field site of the Leibniz Institute for Agricultural Engineering Bornim, Germany. It can be seen that 80% of simulated values are within a range of 260-150 g C/m^2/year (light grey area in Figure 4). The measured reference value for this case is 236 g C/m^2 with a mean for the 500 realizations of 207 g C/m^2. This can be interpreted as relatively low uncertainty in model results in terms of the parameters used. For this site, simulated values show a standard variation for 500 realisations of 48 g C/m^2/year. This gives additional information on the magnitude of uncertainty (at least for this site's conditions), which should receive attention in the interpretation of model results.

Land Management

Figure 5 shows the influence of different crop rotations on soil organic carbon dynamics at the Bad Lauchstädt unfertilised experimental plot. Different crop rotations show an influence on soil C development. The black line in Figure 5 represents the original crop rotation of summer barley, potato, winter wheat, and sugar beets on an unfertilised plot. Rotations with only two crops shows a decreasing trend in soil C content (light grey line in Figure 5, rotation winter wheat to rape). This is mainly due to the fact that this rotation has a longer fallow period than a crop rotation which incorporates more crops. This rotation shows a decrease of soil C of 0.037 t C ha^{-1} yr^{-1}. A more complex rotation with reduced fallow periods may act as a C sink, with increasing soil C content (dark grey line, Figure 5). Here a rotation with summer barley, potato, winter wheat, rye, silage, and maize shows an increasing soil C content of 0.02 t C ha^{-1} yr^{-1}.

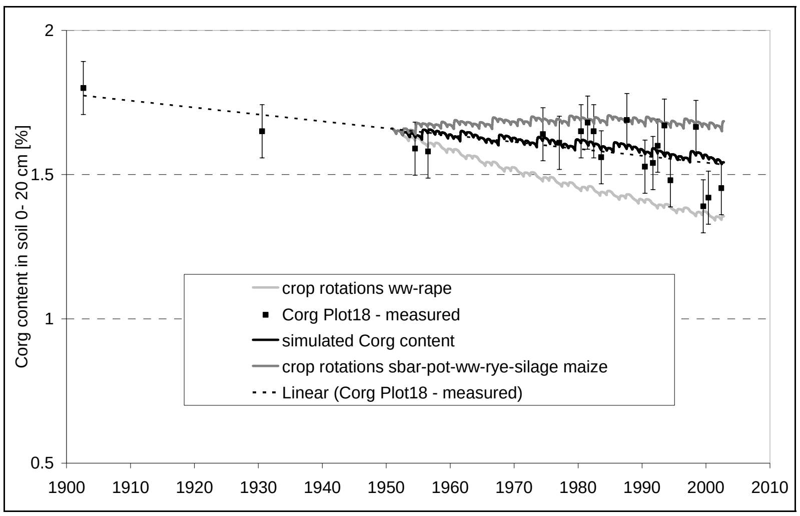

Figure 5: Impacts of different crop rotations on soil organic carbon development for the long term static fertiliser experiment, Bad Lauchstädt, Germany.

Conclusions

This paper presents a model extension for the simulation of soil organic matter dynamics at the river basin scale. Verification showed the ability of the model to correctly represent the relevant processes for soil organic matter dynamics, such as soil temperature, soil water, soil nitrogen, soil carbon dynamics, and crop yields at the plot scale using the standard model parameter values as derived from the literature. This forms the base to assess impacts of regional environmental changes on eco-hydrology and biogeochemical cycles in river basins.

Through the aid of sensitivity and uncertainty analysis of model parameters, important information is gained with respect to the relevance of model parameters, interactions between parameters, their influence on model results, and error bounds of these model results. The point scale assessment of uncertainty has to be enlarged to other environmental conditions and to a spatial assessment of uncertainty for river basins.

The extended model is able to consider cropland management practices, such as fertilisation, different crop rotations, some soil cultivation techniques, and crop residue returns. The use of different crop types and amounts of crops in rotations shows a considerable influence on the long-term soil organic carbon trend. A rotation with two crops in the demonstrated case shows a decreasing trend, whereas rotations incorporating more crops and reducing the fallow period exhibit an increasing trend in soil organic carbon. Factors such as a high rotational complexity, reduction of fallow period, and inclusion of a winter cover crop increase soil organic carbon contents as shown here. This result is in agreement with West et al. (2004).

These point scale findings now have to be translated into regional or river basin scale assessments of eco-hydrology and soil organic matter turnover. This would provide useful information on carbon sequestration potentials to mitigate climate change and to enhance soil fertility (Lal, 2004) in relation to other ecosystem services such as water quantity and quality in river basins.

Acknowledgements

The authors would like to thank the Leibniz – Institute of Agricultural Engineering Bornim (ATB), Germany, the Leibniz-Centre for Agricultural Landscape and Land Use Research (ZALF), Müncheberg, Germany, and the Centre for Environmental Research Leipzig-Halle (UFZ), Germany for the provision of data from their experimental field sites. This work was supported by the HSP fund of the federal state of Brandenburg, Germany.

References

Berg, B. and H. Staaf (1980). Decomposition rate and chemical changes of Scots pine needle litter. I. Influence of stand age. Structure and function of northern coniferous forests - An ecosystem study. T. Persson. Stockholm. 32: 363-372.

Bergmann, C., T. Fischer, et al. (1999). Decomposition of needle-, herb-, root-litter, and Of-layer-humus in three Scots pine stands. Changes of Atmospheric Chemistry and Effects on Forest Ecosystems. A Roof Experiment Without Roof. R.F. Hüttl and K. Bellmann. Dordrecht, Kluwer. 3: 151-176.

Chertov, O.G. and A.S. Komarov (1997). “SOMM: A model of soil organic matter dynamics.” Ecol. Modell. 94(2-3): 177-189.

Franko, U. (1990). C- und N-Dynamik beim Umsatz organischer Substanz im Boden. Berlin, Akademie der Landwirtschaftswissenschaften der DDR.

Hanson, P.J., N.T. Edwards, et al. (2000). "Separating root and soil microbial contributions to soil respiration: A review of methods and observations." Biogeochemistry 48: 115-146.

Hattermann, F.F., M. Wattenbach, et al. (2005). "Runoff simulations on the macroscale with the ecohydrological model SWIM in the Elbe catchment-validation and uncertainty analysis." Hydrological Processes 19: 693-714.

Hellebrand, H.J., J. Kern, et al. (2003). "Long-term studies on greenhouse gas fluxes during cultivation of energy crops on sandy soils." Atmospheric Environment 37(12): 1635-1644.

Johnston, C.A. and P. Groffman (2004). “Carbon cycling in soil.” Frontiers in Ecology and the Environment 2(10): 522 - 528.

Klimanek, E.M. (1990 a). “Umsetzungsverhalten der Wurzeln landwirtschaftlich genutzter Pflanzenarten.” Arch. Acker- Pfl. Boden 34(8): 569-577.

Klimanek, E.M. (1990 b). “Umsetzungsverhalten von Ernterückständen.” Arch. Acker- Pfl. Boden 34(8): 559-567.

Krysanova, V., D.-I. Müller-Wohlfeil, et al. (1998). “Development and test of a spatially distributed hydrological/water quality model for mesoscale watersheds.” Ecological Modelling 106: 263-289.

Krysanova, V. and A. Becker (2000). “Integrated modelling of hydrological processes and nutrient dynamics at the river basin scale.” Hydrobiologia 410: 131 - 138.

Lal, R. (2004). “Soil Carbon Sequestration Impacts on Global Climate Change and Food Security.” Science 304(5677): 1623-1627.

Lasch, P., F.-W. Badeck, et al. (2002). “Sensitivity of simulated forest growth to changes in climate and atmospheric CO2.” Forstwiss. Centralblatt 121(Supplement 1): 155-171.

McKay, M., R. Beckman, et al. (1979). “A comparison of three methods of selecting values of input variables in the analysis of output from a computer code.” Technometrics 21: 239-245.

Parton, W.J., D.S. Schimel, et al. (1987). “Analysis of factors controlling soil organic matter levels in Great Plain grasslands.” Soil Sci. Soc. Am. J. 51: 1173-1179.

Post, J., V. Krysanova & F. Suckow (2004). “Simulation of water and carbon fluxes in agro- and forest ecosystems at the regional scale”. In: C. Pahl-Wostl, S. Schmidt, A. E. Rizzoli & T. Jakeman (Eds.) Complexity and Integrated Resources Management. Transactions of the 2nd Biennial Meeting of the International Environmental Modelling and Software Society (iEMSs), Manno, Switzerland, pp. 730-736.

Post, J., A. Habeck, F.F. Hattermann, et al. (2005). “Evaluation of water and nutrient dynamics in soil-crop systems using the eco-hydrological catchment model SWIM (Soil and Water Integrated Model).” submitted to Nutrient Cycling in Agroecosystems.

Saltelli, A. (1999). "Sensitivity analysis: Could better methods be used?" Journal of Geophysical Research 104(D3): 3789 - 3793.

Saltelli, A., S. Tarantola, et al. (2004). “Sensitivity Analysis in Practice: A Guide to Assessing Scientific Models”. Hoboken, NJ, Wiley.

West, T.O., G. Marland, et al. (2004). "Carbon Management Response Curves: Estimates of Temporal Soil Carbon Dynamics." Environmental Management 33(4): 507.

Evaluation of Soil Infiltration in Furrow Irrigation and Determination of Kostiakov and Kostiakov-Lewis Equation Coefficients

Rahimi, A.*[1], Kashkuli H.A.[2], Boroomand Nasab S.[3]
[1]Dept.of Irrigation Agricultural Faculty, Islamic Azad University, Sanandaj –Iran. Email: abobakrr@hotmail.com
[2]Dept.of Irrigation, Shaheed Chamran University, Ahwaz-Iran. Email: HAKASHKULI1@yahoo.com
[3]Dept.of Irrigation, Shaheed Chamran University, Ahwaz-Iran), Email: boroomand@hotmail.com

Abstract

A major step in the design and evaluation of a furrow irrigation system is the determination of infiltration function. The purpose of this study is to compare infiltration measurement results, using double ring and inflow-outflow methods following consecutive irrigation events. Study of bulk density variation, after each irrigation, was another aim of this investigation. Experiments were conducted on a site near the agricultural facility of Shaheed Chamran University in Ahwaz. Results indicate that correlation coefficient in the first irrigation period is low in comparison with the others periods. Cumulative infiltration is reduced in the second irrigation in comparison with the first irrigation 180 minutes after irrigation started. Cumulative infiltration is also reduced in the third irrigation in comparison with the second irrigation. During the fourth irrigation, cumulative infiltration increased in comparison with the third irrigation which was due to weed growth in the furrows. Results show that calculated basic infiltration rate using inflow-outflow method is 4.4 times greater than the double ring method. Results also show that for short time periods (less than 180 minutes), Kostiakov method is in a better agreement with Kostiakov-Lewis method. Cumulative infiltration was shown to be higher using Kostiakov-Lewis method in comparison to actual measurement for long time periods (more than 180 minutes).

Key Words: Furrow irrigation, Infiltration, inflow-outflow method, double rings, Kostiakov and Kostiakov-Lewis equations

Introduction

With the application of infiltration equation modeling of surface flow and the process of surface irrigation, design and evaluation become easier tasks. In order to find the relationship between equation coefficients in different soils under different surface soil conditions, it is essential to conduct field tests. Infiltration equations under different soil conditions are classified into 3 major groups; i.e. theoretical, physical, and empirical equations. Authors such as Clemens (1983) and Walker et al. (1983) have suggested using empirical infiltration equations for design and evaluation of surface irrigation systems. In this study, the empirical models of Kostiakov and Kostiakov-Lewis have been applied to a series of inflow-outflow and double ring methods of measuring soil infiltration. Kostiakov (1939) presented the following equation for determining cumulative depth of infiltration into soils.

$$Z = KT^{n} \tag{1}$$

Where Z = cumulative infiltration depth, T = elapsed time, and K and n = empirical constants. Equation (1) is widely used due to its simplicity and ease of application. However, infiltration rate estimated with this equation at large times tends to zero which is not realistic. In order to resolve this, the following Kostiakov-Lewis equation was presented

$$Z = KT^{n} + f_0 T \tag{2}$$

Where $f_0 =$ basic infiltration rate.

Methodology

Infiltration experiments were conducted at Shaheed Chamran University research plots during fall of 1998, using the inflow-outflow and double ring methods. Relevant information about the experiments is as follows.

- soil texture for 0-25 cm layer was "clay loam "and for 25-100 cm layer was loam
- number of furrows 15
- length of furrows 80m
- width of furrows 75cm
- number of irrigation tests 4
- number of double ring tests 30

The amount of water used in each irrigation was based on readily available moisture and non-erosive inflow rate to furrows (1.1-1.5 lit/s), considering soil texture and furrow slope. Infiltration coefficients for Kostiakov and Kostiakov-Lewis equations in the double ring method were derived using the methods of Garcia and Walker. In the inflow-outflow method however, the volume balance method was used as given in Table 1. The measured and estimated values of infiltration rate and cumulative infiltration depths are given in Table 2 for comparison.

Results and Conclusions

Results indicate that the correlation coefficient in the first irrigation period is low in comparison with the other periods. Cumulative infiltration is reduced in the second irrigation in comparison with the first irrigation 180 minutes after irrigation started. Also, cumulative infiltration is reduced in the third irrigation in comparison with the second irrigation. During the fourth irrigation, cumulative infiltration increased in comparison with the third irrigation which was due to weed growth in the furrows. Results show that calculated basic infiltration rate using inflow-outflow method is 4.4 times greater than double ring method. The results also show that for short time periods (less than 180 minutes), Kostiakov method is in a better agreement with Kostiakov-Lewis method. Cumulative infiltration was shown to be higher using Kostiakov-Lewis method compared to actual measurement for long time periods (more than 180 minutes). .

Table 1. Kostiakov and Kostiakov -Lewis Coefficients for furrows inflow-outflow, and double ring methods.

Description	Number Furrow	Kostiakov		Kostiakov -Lewis		
		$k(\frac{cm}{\min^n})$	n	$k(\frac{cm}{\min^n})$	n	$f_0(\frac{cm}{\min})$
First Irrigation	F1					
	F2					
	F3	0.124	0.996	0.00373	0.747	0.1212
	F4	0.143	0.937	0.177	0.301	0.1003
	F5	0.1516	0.915	0.0826	0.61	0.09173
	Average	0.1395	0.949	0.0877	0.553	0.1044
Second Irrigation	F1	0.413	0.739	1.779	0.106	0.0964
	F2	0.603	0.714	2.397	0.138	0.1174
	F3	0.539	0.705	1.176	0.279	0. 0988
	F4	0.125	0.956	0.0542	0.559	0.0971
	F5	0.181	0.828	0.222	0.439	0.0679
	Average	0.372	0.788	1.1246	0.304	0.09572
Third Irrigation	F1	0.1425	0.82	0.178	0.488	0.0477
	F2	0.1044	0.96	0.0514	0.679	0.07438
	F3	0.215	0.849	0.466	0.247	0.0931
	F4	0.125	0.965	0.0264	0.666	0.089
	F5	0.258	0.7048	0.2603	0.52	0.0438
	Average	0.169	0.859	0.19655	0.52	0.06959
Fourth Irrigation	F1	0.1504	0.916	0.253	0.55	0.0546
	F2	0.2105	0.88	0.241	0.419	0.1071
	F3	0.3586	0.777	0.89	0.255	0.0995
	F4	0.1536	0.913	0.063	0.697	0.0923
	F5	0.2069	0.776	0.2014	0.492	0.0613
	Average	0.216	0.852	0.3297	0.482	0.0829
Double Rings	F1	0.331	0.565	0.372	0.433	0.0158
	F2	0.288	0.614	0.322	0.466	0.0195
	F3	0.377	0.542	0.429	0.41	0.0159
	F4	0.395	0.551	0.467	0.387	0.0197
	F5	0.187	0.715	0.208	0.513	0.0258
	Average	0.316	0.597	0.36	0.436	0.0193
	Irrigation Average	0.224	0.862	0.435	0.464	0.088

Table 2. The comparison of cumulative average depth of infiltration at different times (average depth of infiltration (cm) and Time (Minutes)).

Description	Cumulative average depth of infiltration at different times								
	10	30	60	90	120	150	180	240	300
First Irrigation	1.23b	3.204b	6.13ab	9.008ab	11.86ab	14.74ab	17.56ab	23.25ab	28.88ab
Second Irrigation	2.67a	5.01a	8.24a	11.34a	14.41a	17.44a	20.45a	26.33a	32.36a
Third Irrigation	1.21b	2.95a	5.38bc	7.75b	10.04b	12.34b	14.6b	19.1b	22.58b
Fourth Irrigation	1.64ab	3.79ab	6.76ab	9.6ab	12.4ab	15.25ab	17.89ab	23.29ab	28.67ab
Double Rings	1.27b	2.3b	3.43c	4.31c	5.2c	6.08c	6.78c	8.1c	9.22c

***Letters indicate significant differences at one percent level.**

References

Clemmens, A.J.1983.Infiltration equation for border irrigation. In: Advances in infiltration proceedings of the National Conference on Advances in infiltration Michigan, ASAE, pp.266-274.

Bautista, E. & W.W. Wallender.1993.Calculation of infiltration in furrow irrigation numerical simulation models. Journal of the irrigation and drainage division, ASCE, 119(2):95-266.

Bautista, E. & W.W. Wallender.1993.Optimal management strategies for cut back furrow irrigation. Journal of the irrigation and drainage division, ASCE, 119(6):1099-1114.

Childs, J.L, W.W. Wallender, & J.W. Hofmans.1993.Spatial and temporal variation of furrow infiltration. Journal of the irrigation and drainage Eng., ASAE, 119(1):74-90

Walker, W.R. & L.Willardson.1983.Iinfiltration measurements for simulation furrow irrigation .in advance in infiltration proceedings of the national conference on advances in infiltration Michigan, ASAE.PP.241-248.

Assessment of Agricultural Management Practices in the Upper Maquoketa River Watershed using SWAT

P. Reungsang[1], R.S. Kanwar[2], M. Jha[3], P.W. Gassman[3], K. Ahmad[2], and A. Saleh[4]
[1]Dept. of Agricultural and Biosystems Engineering, Iowa State University, Ames, IA, 50011, USA. Email: preungsa@iastate.edu.
[2]Dept. of Agricultural and Biosystems Engineering, Iowa State University, USA.
[3]Center of Agricultural and Rural Development, Dept. of Economics, Iowa State University, USA.
[4]Texas Institute for Applied Environmental Research, Tarleton State University, USA.

Abstract

A validation study has been performed using the Soil and Water Assessment Tool (SWAT) model with data collected for the Upper Maquoketa River Watershed (UMRW), which drains over 16,000 ha in northeast Iowa. This validation assessment builds on a previous nested modeling study for the UMRW that required both the Agricultural Policy EXtender (APEX) model and SWAT. In the nested modeling approach, edge-of-field flows and pollutant load estimates were generated for manure application fields with APEX and then subsequently routed to the watershed outlet in SWAT, along with flows and pollutant loadings estimated for the rest of the watershed to the watershed outlet. In the current study, the entire UMRW cropland area was simulated in SWAT, which required translating the APEX subareas into SWAT hydrologic response units (HRUs). Calibration and validation of the SWAT output was performed by comparing predicted flow and NO_3-N loadings with corresponding in-stream measurements at the watershed outlet during 1999-2001. Annual stream flows measured at the watershed outlet were greatly under-predicted when precipitation data collected within the watershed during 1999-2001 were used to drive SWAT. Selection of alternative climate data resulted in greatly improved average annual stream predictions, and also relatively strong r^2 values of 0.73 and 0.72 for the predicted average monthly flows and NO_3-N loads, respectively. The results of this study show that SWAT can replicate measured trends for this watershed and that climate inputs are very important for validating SWAT and other water quality models.

Introduction

Water quality modeling is emerging as a key component of Total Maximum Daily Load (TMDL) assessments and other watershed-based water quality studies. Numerous water quality models have been developed that differ greatly in terms of simulation capabilities, documentation, and technical support. One of the more widely used water quality models is the Soil and Water Assessment Tool (SWAT), which was developed to assess the water quality impacts of agriculture and other landuses for a range of watershed scales, including large river basins (Arnold et al., 1998). Detailed documentation on the model inputs is provided in Neitsch et al. (2002a); model theory documentation is presented in Neitsch et al. (2002b) and Arnold et al. (1998). Previous applications of SWAT have compared favorably with measured data for a variety of watershed scales and conditions (Arnold and Allen, 1996; Srinivasan et al.,1998;

Kirsch et al., 2002; Arnold et al., 1999; Saleh et al., 2000; Santhi et al. 2001). However, an ongoing need regarding the use of SWAT is to test it with measured data for different scales, land use, topography, climate, and soil conditions.

The objective of this study was to test SWAT by comparing predicted stream flows and nitrate (NO_3-N) levels with corresponding measured values at the outlet of the Upper Maquoketa River Watershed (UMRW), which is a row-crop dominated watershed that is typical of much of Iowa. An overview of the data inputs and modeling assumptions is provided first, including a description regarding how some of the SWAT inputs were derived from a previous UMRW modeling study that used both the Agricultural Policy EXtender (APEX) model (Williams et al., 2001) and SWAT. The calibration and validation process is then described, including the effect of selecting alternative climate data inputs to achieve a more accurate replication of measured data at the watershed outlet.

Methodology

Watershed Description

The UMRW covers an area of about 162 km^2 in portions of Buchanan, Clayton, Fayette, and Delaware counties, and lies within the upper reaches of the Maquoketa River Watershed (MRW) that drains a total of 4,867 km^2 of predominantly agricultural land (Figure 1). In 1998, the MRW was listed as a priority watershed within the Iowa Department of Natural Resources Unified Watershed Assessment with the primary concern being nutrient and sediment losses from agricultural nonpoint sources. Surface monitoring at the UMRW outlet (sampling site 4) located in Backbone State Park showed elevated NO_3-N and phosphate-phosphorus (PO_4-P), depending on the flow conditions (Baker et al., 1999). Tile drains are a key conduit of NO_3-N to the UMRW stream system.

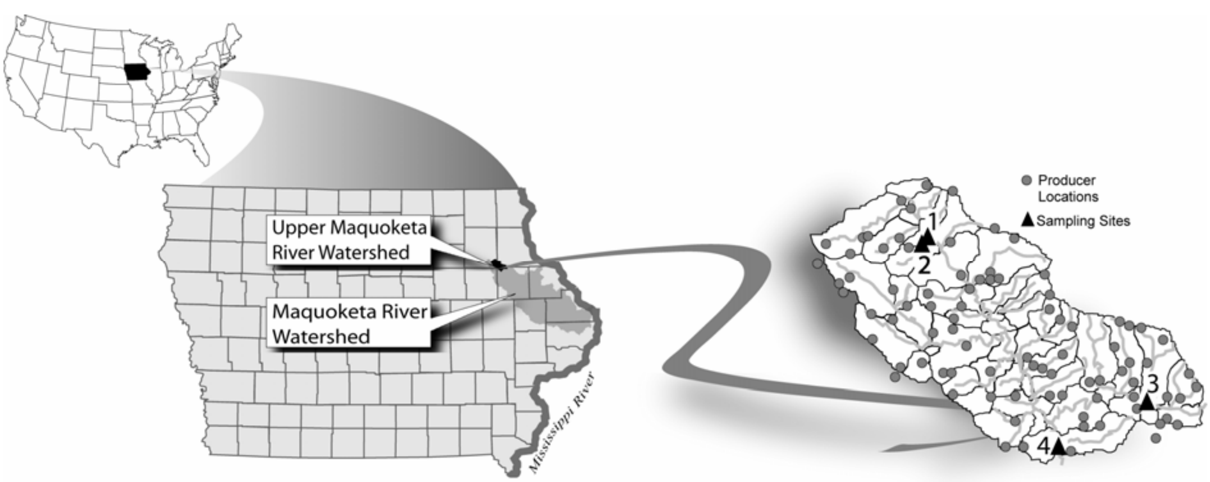

Figure 1. Location of the Upper Maquoketa River Watershed with reference to the Maquoketa River Watershed and the Mississippi River, the locations of the UMRW livestock operations and sampling sites.

Corn and soybean are the major crops in the UMRW, accounting for 66% of the total land use (Gassman et al, 2002). Other key land uses included woodland (8.9%), alfalfa (7.5%), Conservation Reserve Program (CRP) land (4.1%), and pasture (4.0%). A total of 90 operations were identified in 1999 (Osei et al, 2002a) having one or more types of livestock (Figure 1), with production focused primarily on swine, dairy cows, beef cattle, feeder cattle, and/or calves and heifers. The survey also discovered that most of the livestock producers were not taking enough credit for the nutrient content from manure when it was applied to the crop fields.

SWAT Input Data and Management Assumptions

This SWAT validation study builds on the original UMRW simulation study, in which a nested APEX-SWAT modeling approach was used (Saleh et al., 2003; Gassman et al., 2002). APEX was used to simulate the manured cropland and pasture areas due to its enhanced flexibility in simulating different manure application scenarios relative to SWAT. Edge-of-field sediment and nutrient losses simulated in APEX, coupled with losses simulated in SWAT from other land uses, were routed in SWAT through the stream system to the watershed outlet. This approach was also used in two other previous watershed studies that were conducted in Texas, as described in Gassman et al. (2002). In this study the entire watershed was simulated in SWAT for 1997-2001, which provides an initial two-year “stabilization period” and also includes the three years that the monitoring data were collected (1999-2001) which were used for calibrating and validating the model.

The land use/cover, topographic, and soil data required for the SWAT simulations were generated as part of the previous UMRW modeling study, from maps developed within the Geographical Resource Analysis Support System (GRASS) Geographic Information System (GIS) using the GRASS/SWAT Interface Program (Gassman et al., 2002). A total of 52 subwatersheds were created with the GRASS GIS for the UMRW (Figure 1), with the watershed outlet (sampling site 4) located in Backbone State Park. Each subwatershed delineated within SWAT is simulated as a homogeneous area in terms of climatic inputs. However, the subwatersheds were further subdivided into hydrologic response units (HRUs) that were assumed to consist of homogeneous land use and soils. The percent of the subwatershed that is covered by a specific HRU is input to SWAT; however, the exact spatial location is not accounted for. A land use threshold of 10% was used when the HRUs were created, which limited the land use to categories that covered at least 10% of a given subwatershed. The HRU land use categories generated in SWAT/GRASS included pasture, urban land, continuous corn, corn-soybean, and a five-year rotation of corn and alfalfa. A total of 646 HRUs were used for the UMRW.

As previously noted, the manured cropland and pasture areas were originally simulated in APEX. These APEX areas were translated into SWAT HRUs for this analysis as described in Kanwar et al. (2003). Small open lot and buffer strip areas that were simulated in APEX for swine open lot and cattle feeder operations were assumed to be non-grazed pasture areas in SWAT. The remaining pasture areas simulated within each SWAT subwatershed were split into separate dairy, calf/heifer, and beef cow pasture HRUs, to preserve differences in manure deposition rates and grazing periods that were assumed to occur between these different livestock species. The manure was assumed to be applied to cropland that was planted in corn. Manure generated by beef pasture and calf/heifer operations was relatively minor compared to the other types of operations and assumed to be deposited on pastures and/or corn fields via grazing rather than applied with a manure spreader. It was assumed that the livestock producers applied solid manure at an annual rate of 44.8 t/ha and liquid manure at a rate of 46,745 l/ha, resulting in the N and P application rates shown in Table 1.

Table 1. Manure N and P rates (kg/ha) applied to corn by farm type for the UMRW baseline simulations[a].

Nutrient	Tie stall dairies	Small swine (open lot)	Large swine (confinements)	Cattle feeder
Manure N	234	278	293	262
Manure P	49	96	101	71

[a]Baseline manure application rate = 22.4 t/ha; liquid rate of 46,745 l/ha used for swine confinements.

The main N fertilizer applications were applied at the same rate for manured fields relative to nonmanured cropland (Table 2). An N fertilizer rate of 159 kg/ha was assumed for continuous corn. Assumed fertilizer rates applied to corn following soybean and alfalfa were 128 and 100 kg/ha, respectively, reflecting some accounting of N credit from the legume crops. Additional “crop-removal” N and phosphate (P_2O_5) fertilizer were simulated for both manured and nonmanured fields following corn harvest (Table 2), for continuous corn, corn-soybean, and the second year of corn when rotated with alfalfa for the manured cropland. Smaller starter N and P fertilizer amounts of 10 and 11 kg/ha were assumed applied for corn in all rotations, regardless of manure inputs.

Additional details regarding the distribution of livestock in the watershed and the nutrient management assumptions are given in Osei et al. (2000) and Gassman et al. (2002).

Table 2. Expected yields and fertilizer rates based on UMRW survey results.

Crop	Crop sequence	Expected yield (bu/ac)	Main N fertilizer application (kg/ha)[a]	Fall crop removal fertilization applications (kg/ha)			
				Manured fields		Nonmanured fields	
				N	P_2O_5	N	P_2O_5
Corn	after corn	155	159	18	46	28	68
Corn	after soybean	160	128	10	26	28	68
Corn	after alfalfa	158	100	10	26	28	68
soybean	after corn	55	0	15	39	28	68

[a]The same rate was assumed to be applied to both manured and nonmanured fields.

Soil and Climate Inputs

The soil map and associated soil layer data used for the UMRW SWAT simulation were obtained from the Iowa Department of Natural Resources (http://www.igsb.uiowa.edu/nrgislibx/). The soil slope length and percent slopes were determined from an assessment of mean slope lengths that are given in the 1992 National Resource Inventory (NRI) database (http://www.nrcs.usda.gov/technical/NRI/; Nusser and Goebel, 1997).

Daily precipitation data were collected at sampling sites 2 and 3 (Figure 1) within the UMRW for the same three year period (1999-2001) that the in-stream monitoring data was collected. Two five-year average daily precipitation records for 1997-2001 were then constructed by collating 1997-98 precipitation data collected at Fayette and Manchester (obtained from the Iowa Environmental Mesonet at http://mesonet.agron.iastate.edu/) onto the site 2 and site 3 data, respectively. Fayette and Manchester were determined to be the two closest climate stations based on a Thiessen Polygon analysis; the locations of both stations are shown in Figure 2. Two other five-year precipitation records were also constructed using only data measured at Fayette and Manchester, to provide an alternative source of climate data inputs for the SWAT simulation. A comparison of 1999-2001 annual precipitation amounts (Table 3) shows that the precipitation levels measured at sites 2 and 3 were considerably lower than those measured at Fayette and Manchester, and precipitation amounts collected at other climate stations in the region. Thus it was of interest to assess the effects of the two different sets of precipitation data on the SWAT hydrologic estimates. The assignment of a specific precipitation record to a given subwatershed was determined on the basis of which rain gage or weather station was closest to the subwatershed.

Table 3. Total annual precipitation (mm) for 1999-2001 (and overall total) for UMRW climate sources.

Year	Rain Gauge[a] or Climate Stations[b]							
	Site 2[a]	Site 3[a]	Fayette	Manchester	Oelwein	Tripoli	Dubuque	Independence
1999	814.3	807.2	1,052.1	943.6	987.3	1054.1	910.3	1,057.1
2000	750.9	839.4	967.0	834.9	955.5	958.1	820.7	840.0
2001	794.7	795.4	1,042.7	893.1	987.8	811.3	933.7	970.8
Total	2,359.87	2,442.0	3,061.8	2,671.6	2,930.6	2,823.5	2,664.7	2,867.9

[a]Measured within the watershed at sampling sites 2 and 3 (Figure 2)
[b]Climate station data was obtained from http://mesonet.agron.iastate.edu/.

Maximum and minimum temperature data for 1997-2001 were again obtained from the Iowa Environmental Mesonet for Fayette and Manchester, and were used for all of the SWAT simulations. The daily air temperature inputs were used in the SWAT crop growth algorithms and the evapotranspiration computations. The Hargreaves Method (Neitsch et al., 2002b) was used to estimate daily evapotranspiration rates. Solar radiation, relative humidity, and wind speed were generated internally in SWAT with the built-in weather generator.

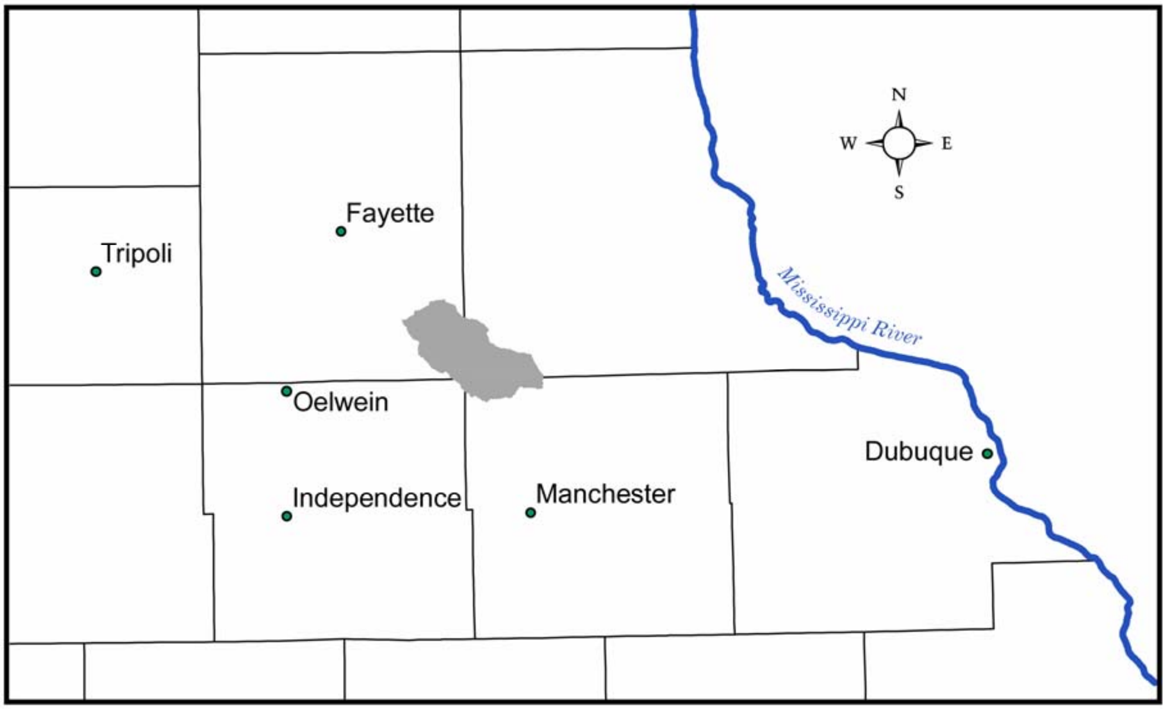

Figure 2. Climate stations located near the UMRW (including Fayette and Manchester) and county boundaries.

Results and Discussion

Each SWAT simulation was executed for 1997-2001 to encompass a complete cycle of the five-year corn and alfalfa rotations and to provide a two-year "initialization period". Calibration of SWAT was performed for 1999 while 2000 and 2001 were used as the validation years. Figure 3 shows that the annual average stream flows were greatly under-predicted using the five-year precipitation records that included the 1999-2001 site 2 and site 3 rain gage data. Additional monthly comparisons (not shown) further revealed that low flow periods were especially under-predicted using these precipitation data. The annual average stream flows were more accurately predicted when the precipitation records based solely on the Fayette and Manchester climate station measurements were used (Figure 4). A slight under-prediction of 0.74% was predicted for the three-year average (Figure 4) when using the alternative precipitation data. The annual average results shown in Figures 3 and 4 could indicate that measurement error occurred for the rain gage data collected at sites 2 and 3. Further analysis was performed only with the five-year records that consisted entirely of precipitation data collected at Fayette and Manchester.

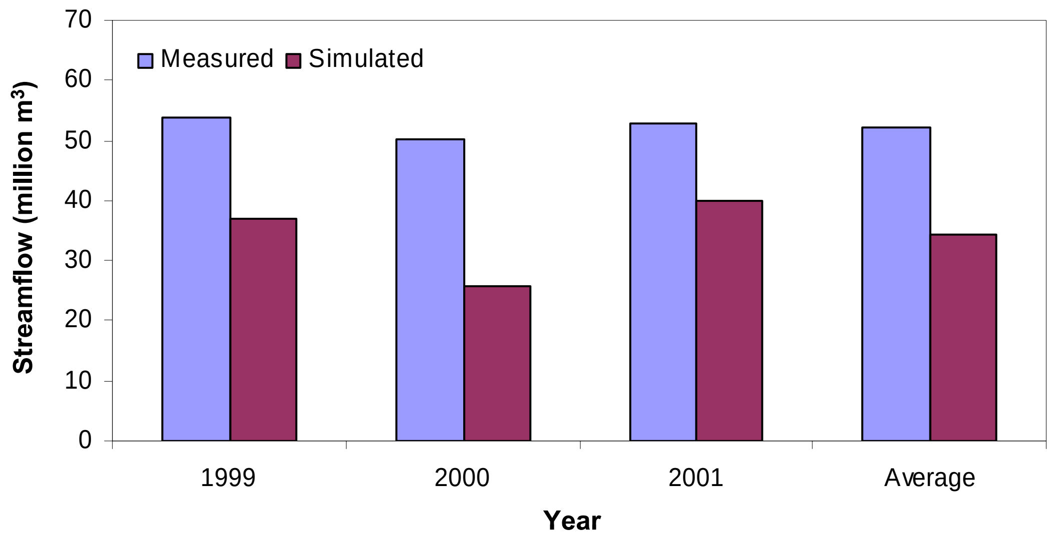

Figure 3. Simulated versus measured UMRW annual stream flows in response to the five-year precipitation records that include the site 2 and site 3 rain gage data.

Simulated daily flows are shown relative to corresponding measured flows for 1999-2001 at the UMRW outlet (Figure 5). The model accurately tracked most of the peak flow events that occurred during the year, although the peaks were usually over-predicted. In contrast, the majority of the low-flow periods were under-predicted by SWAT. Figure 6 shows the predicted and measured average monthly flows for 1999 to 2001. Some of the high flow periods were over-predicted while other high flow periods were under-predicted. The regression of the measured and simulated average monthly flow resulted in an r^2 value of 0.73, indicating that the model accurately tracked the average monthly flow trends during the simulation period.

The predicted versus measured average monthly NO_3-N levels are plotted in Figure 7. The NO_3-N trend was again accurately tracked by SWAT, as reflected in the r^2 value of 0.72. However, the majority of the months with observed high NO_3-N levels were over-predicted by the model. The cumulative three-year NO_3-N load was under-predicted by SWAT by 7.3%.

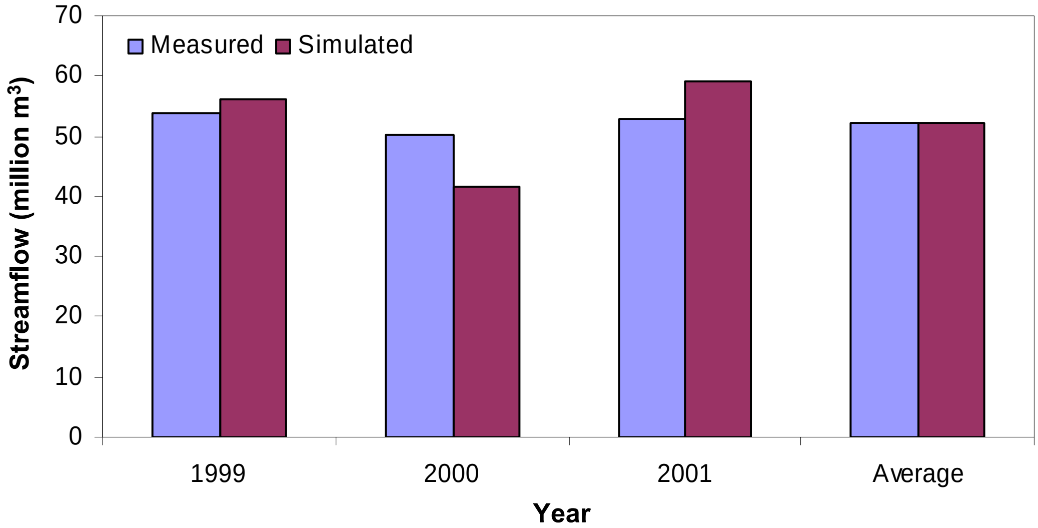

Figure 4. Simulated versus measured UMRW annual stream flows in response to the five-year precipitation records that consist only of data measured at Fayette or Manchester.

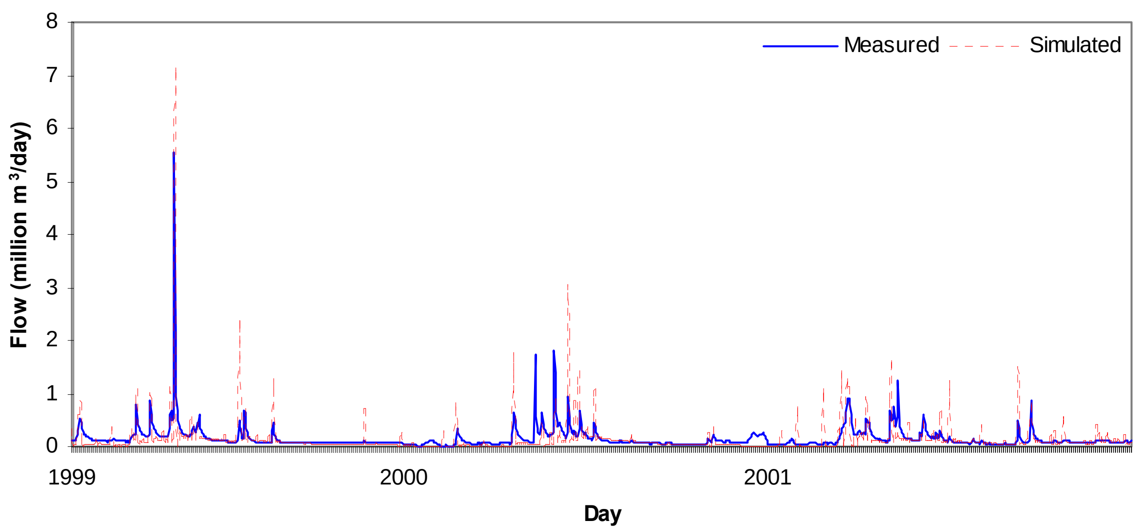

Figure 5. Simulated versus measured daily stream flows at the UMRW outlet (1999-2001).

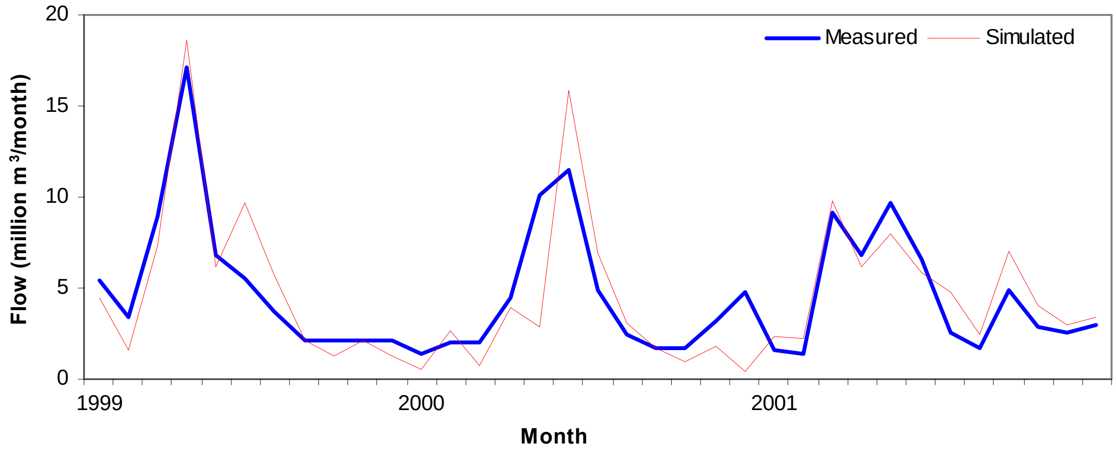

Figure 6. Simulated versus measured monthly stream flows at the UMRW outlet (1999-2001).

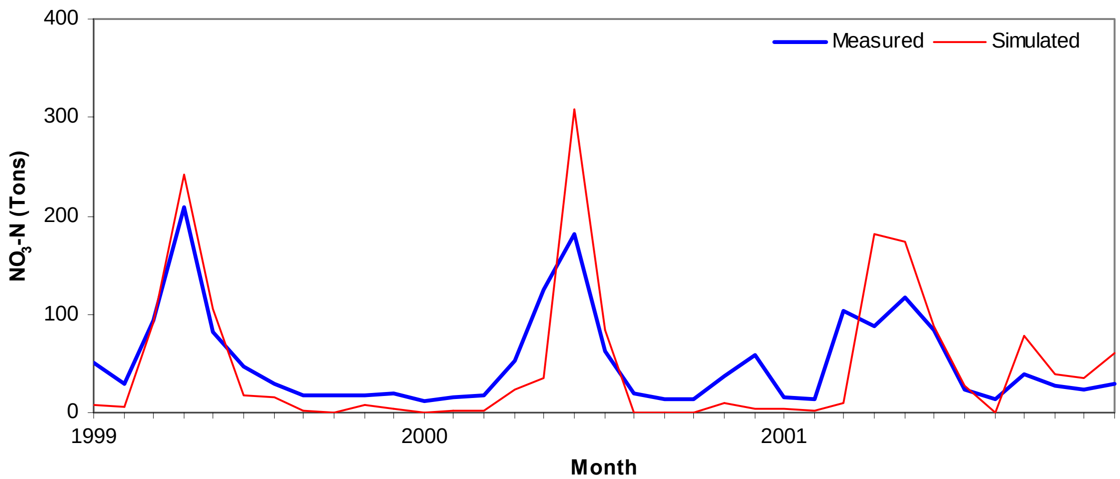

Figure 7. Observed and simulated monthly NO_3-N loads at the watershed outlet during 1999-2001.

Conclusions

Annual stream flows measured at the UMRW outlet for 1999-2001 were greatly under-predicted when precipitation data collected within the watershed during 1999-2001 were used as input to SWAT. The predicted annual stream flows improved greatly when precipitation data measured at climate stations outside the watershed were used. These results do not follow expectations and pose the question as to whether measurement error may have occurred regarding the precipitation data collected at UMRW sampling sites 2 and 3. Further investigation is needed to verify why the large discrepancies exist between the sites 2 and 3 precipitation data and the corresponding data collected at other climate stations in the region. Further simulations with SWAT using only the climate data collected at the Fayette and

Manchester climate stations showed that the model was able to accurately track monthly measured stream flows and nitrate losses at the watershed outlet. The r^2 statistics found for the stream flows and NO_3-N losses were equal to 0.73 and 0.72, respectively. These results compare favorably with previous r^2 values reported by Saleh et al. (2003) of 0.79 for stream flows and 0.74 for the NO_3-N loads, using the APEX-SWAT approach. However, the annual stream flows and three-average annual stream flow were more accurately simulated in this study. It can be concluded that both the APEX-SWAT and SWAT-only methods can be viable simulation approaches. However, the SWAT-only approach may be better suited for investigating the long-term watershed-level impacts of agricultural management practices due to less complexity in terms of managing model input and output when compared with APEX-SWAT approach.

References

Arnold, J.G., R. Srinivasan, R.S. Muttiah, and J.R. Williams. 1998. Large Area Hydrologic Modeling and Assessment. Part I. Model Development. J. Am. Water Resour. Assoc. 34: 73-89.

Arnold, J.G., R. Srinivasan, R.S. Muttiah, and P.M. Allen. 1999. Continental scale simulation of the hydrologic balance. J. Am. Water Resour. Assoc. 35(5): 1037-1051.

Arnold, J.G. and P.M. Allen. 1996. Estimating hydrologic budgets for three Illinois watersheds. J. Hydr. 176: 57-77.

Arnold, J.G., R.S. Muttiah, R. Srinivasan, and P.M. Allen. 2000. Regional Estimating of Base Flow and Groundwater Recharge in the Mississippi River Basin. J. Hydr. 227: 21-40.

Baker, J.L., S.W. Melvin, M.M. Agua, J. Rodecap, A. Saleh, and T. Jones, 1999. Collection of Water Quality Data for Modeling the Upper Maquoketa River watershed. ASAE Paper No. 99-2222, St. Joseph, Michigan.

Gassman, P.W., E. Osei, A. Saleh, and L.M. Hauck. 2002. Application of an Environmental and Economic Modeling System for Watershed Assessments. J. Am. Water Resour. Assoc. 38(2): 423-438.

Kanwar, R., P.W. Gassman, and A. Saleh. 2003. Completion Report for the Component #3 on the "Use of the SWAT Model" of the Iowa Water Quality Protection Project. Submitted to the Iowa Department of Natural Resources, Des Moines, Iowa.

Kirsch, K., A. Kirsch, and J.G. Arnold. 2002. Predicting sediment and phosphorus loads in the Rock River Basin using SWAT. Trans. ASAE 45(6): 1757-1769.

Neitsch, S.L., J.G. Arnold, J.R. Kiniry, and J.R. Williams. 2002a. Soil and Water Assessment Tool User's Manual, Version 2000. Blackland Research Center. Texas Agricultural Experiment Station, Temple, Texas. http://www.brc.tamus.edu/swat/swat2000doc.html

Neitsch, S.L., J.G. Arnold, J.R. Kiniry, J.R. Williams, and K.W. King. 2002b. Soil and Water Assessment Tool Theoretical Documentation, Version 2000. Blackland Research Center. Texas Agricultural Experiment Station, Temple, Texas. http://www.brc.tamus.edu/swat/swat2000doc.html.

Nusser, S.M., and J.J. Goebel. 1997. The national resources inventory: a long-term multi-resource monitoring programme. Environ. Ecol. Stat.. 4: 181-204.

Osei, E., P. Gassman, and A. Saleh. 2000. Livestock and the Environment: a National Pilot Project: CEEOT-LP Modeling for the Upper Maquoketa River Watershed, Iowa: Technical

Report. Report No. RR0001. Texas Institute for Applied Environmental Research, Tarleton State Univ., Stephenville, TX.

Santhi, C., J.G. Arnold, J.R. Williams, W.A. Dugas, and L. Hauck. 2001. Validation of the SWAT model on a large river basin with point and nonpoint sources J. Am. Water Resour. Assoc. 37(5): 1169-1188.

Saleh, A., J.G. Arnold, P.W. Gassman, L.M. Hauck, W.D. Rosenthal, J.R. Williams, and A.M.S. McFarland, 2000. Application of SWAT for Upper North Bosque River Watershed. Trans. ASAE 45(3): 1077-1087.

Saleh, A., P.W. Gassman, J. Abraham, and J. Rodecap, 2003. Application of SWAT and APEX model for Upper Maquoketa River Watershed. ASAE Paper No. 032063. http://asae.frymulti.com/.

Srinivasan, R.S., J.G. Arnold, and C.A. Jones. 1998. Hydrologic modeling of the United States with the soil and water assessment tool. Water Resources Development 14(3): 315-325.

Williams, J.R. 2002. The APEX manure management component. In Proceedings of the Total Maximum Daily Load (TMDL) Environmental Regulations Conf., 44-51. A. Saleh, ed. ASAE Publication No. 701P0102. St. Joseph, MI: ASAE. http://asae.frymulti.com/.

Evaluation of SWAT Stream Flow Components for the Grote Nete River Basin (Flanders, Belgium)

Hamed Rouhani*[1], Patrick Willems[2] and Jan Feyen[1]
[1]Department of Land Management, K.U. Leuven, Vital Decosterstraat 102, B-3000 Leuven, Belgium. E-mail: hamed.rouhani@student.kuleuven.be
[2]Department of Civil Engineering, K.U. Leuven, Kasteelpark Arenberg 40, B-3001 Heverlee, Belgium

Abstract

A simulation study using the Soil and Water Assessment Tool (SWAT) model was initiated to estimate daily flow components in the Grote Nete River Basin, Belgium. The parameters of hydrologic models often are not exactly known and therefore have to be determined by calibration. In this study, the procedure considers multiple calibration objectives including calibrated components for flow, such as the total flow and base flow, considering indirectly the overland flow component being the difference between total and base flow. Model calibrations were pursued on the basis of comparing the simulated output with the observed total and base flow using qualitative (graphical) assessments and quantitative (statistical) indicators.

This analysis was conducted in order to obtain some insight into the relative importance of the surface and base flow components of observed hydrographs in an effort to improve the predictive capability of the model for the study site. The study was conducted using a 10-year historical flow record (1986-1995); in which the period 1986-1989 was used for calibration and 1990-1995 for validation. The predicted daily total flow and base flow matched the observed values, with a Nash-Sutcliff coefficient of 0.62 during calibration and 0.77 during validation, and with a Nash-Sutcliff coefficient of 0.56 during calibration and 0.65 during validation, respectively. Analysis of high flows and low flows indicated that the model was unbiased.

The results indicate that the SWAT model is a suitable model for use in the Grote Nete River Basin. The calibration focuses on matching simultaneously the total and base flow and has a very good potential for being used as a tool to study stream flows in Belgium.

Introduction

SWAT is a physically-based watershed model that is integrated into the ArcView geographic information system (GIS) software as an extension. The model is capable of simulating a high level of spatial detail by allowing the division of a watershed into a large number of sub-watersheds (Gassman et al., 2003). It also provides an example for distributed models relying on a physically based description of the runoff generation and the effects of different land covers (Eckhardt et al., 2001). A comprehensive description of all of the components in SWAT can be found in the literature (Arnold et al., 1994, Arnold et al., 1998, Neitsch, 2001 and 2002). According to previous research, SWAT has good potential for being used as a tool to study stream flow in Belgium (Abu El-Nasr et al., 2004, Van Griensven, 2002).

Methodology

Description of the Study Area and Model Setup

A model for the Grote Nete River Basin in Belgium was established. This basin covers approximately 383 km², and the altitude of the catchment varies between 12 and 75 meters above sea level. While the most common slopes in the watershed are lower than 1%, slope varies between 0 and 5%. Based on a digital elevation model, the catchment was divided into 41 subbasins. The multiple HRU option was used to enable the creation of multiple HRUs for each subbasin (the default threshold values of 20% for land use and 10% for soil were applied); in total, 277 HRUs were used with varying sizes. Also six different land use categories were distinguished within the catchment. The most dominant land use is forest (37.17%). Table 1 summarizes different land uses in the basin.

Table1. Summary of land uses within the basin.

Land use	Percent of Basin
Forests	37.17
Cultivated land	20.73
Pasture	14.62
No data (military domain)	10.73
Urban area	9.74
Physical infrastructure	5.80
Wetlands and water bodies	1.20

Sandy soils (49.57%) are dominant in the Grote Nete River Basin watersheds. Sandy loam soils (23.28%) and clay soils (17.49%) occupy a smaller fraction of the basin. Loamy soils are rare, representing only 0.62% of the basin area. Sandy soils occupy the northern part of the catchment, while sandy loam soils are found in the southern part of the basin. Clay soils are mainly located as a small strip along the river branches. Artificial soils (9.04 %) are located inside the territory of the Hechtel-Eksel and Leopoldsburg communities, which are military bases.

The collected data for this study included stream-gauging records, land use information, soil data, hydrologic data, topographic information, climate records, and daily precipitation. Potential evapotranspiration was obtained from data reported by Timmerman (Timmerman et al., 2001). All data were gathered from the monitoring sites and available data bases of the Royal Meteorological Institute, AMINAL, National Geographic Institute, Flemish Land Agency. Also, the AARDEWERD database was used to derive basic soil attributes (Van Orshoven et al., 1993). Soil hydraulic parameters were calculated from these basic attributes using the pedo-transferfunctions of Vereecken et al. (1990).

Model Calibration and Validation

A calibration/validation procedure was applied to the Grote Nete River Basin using the daily average flow rates measured in the Varendonk outlet station for comparison against the simulated model output.

Traditionally, physically based distributed models are rarely calibrated and validated thoroughly because of lack of data (Feyen et al., 2000). In practice, model testing is limited to the comparison of simulated and predicted discharges in a catchment. Rarely, models are calibrated with respect to the flow components composing the total river flow as opposed to observed basin variables such as well data, the soil water content of the unsaturated zone, or any other state variable that might have been observed in space and time. Given the internal compensating effects, it is likely that with a set of parameters derived from a manual or automatic calibration, a good estimate can be obtained of the observed total discharge, but the base flow will be overestimated and the intermittent and overland flow underestimated, or vice-versa (Vázquez and Feyen, 2004).

The purpose of this study was to conduct the calibration/validation in such a way that not only a good agreement between the simulated and observed total daily discharge was obtained, but also between the components making up the total discharge. Given the characteristics of the study basin, the total flow was assumed to consist of a quick and slow flow component, whereby the slow flow component was considered as the sum of what classically is considered as intermittent and base flow. The justification for this is based on the fact that the basin is relatively flat, composed of primarily sandy soils with high hydraulic conductivity, and is intensively drained by a network of ditches and pipe drainage systems. If the land in the basin is not properly drained the water table in the winter season would rise close to the surface constraining the agricultural exploitation. Given the local conditions, it is difficult to physically discern the intermittent flow from the base flow. Therefore, both components in this study were summed and considered as the slow flow component, whereas the difference between the total flow and the slow flow component was defined as the quick flow component. The observed total daily average flow was split into observed slow and quick flow using the flow separation program of Arnold et al. (1999). The SWAT output, consisting of the three flow components among other simulated state variables, was reduced to the daily average overland flow, or quick flow component and slow flow component.

The performance assessment in this study was based on the following criteria:

- Agreement between the average observed and simulated catchment runoff volume (i.e. control of the overall water balance)
- Agreement of the overall shape of the time series of daily discharge together with the accumulated total and slow flow volumes and
- Agreement of observed and simulated extreme quick and extreme slow flows.

Time series of extreme quick and extreme slow flows was constructed using the partial duration series (PDS); i.e. the peak over (extreme quick flows) and under (extreme low flows) threshold (POT) approach. The application of the POT approach involves two main steps: selection of the threshold and estimation of the tail index. The Water Engineering Time Series Processing tool (WETSPRO) was used in this study to extract the extreme quick and slow flows (Willems, 2003). It has been observed that the estimators in extreme-value theory can be subject to serious bias. Moreover, graphical representations of extreme data often show an erratic behavior. The statistical literature advises to use a Box-Cox transformation to reduce the bias (Box and Cox, 1964) and to ensure approximate Gaussian behavior.

In addition to the visual graphical interpretation of the agreement between observed and simulated time series of daily and cumulative flows, four statistical performance indicators were used to quantify the goodness of fit. The indicators used are the modeling efficiency (EF), the goodness of fit (R^2), the overall volume error, and the root mean square error (RMSE) (Nash and Sutcliffe, 1970; Gupta et al., 1998; Madsen, 2002; Abu El-Nasr et al., 2004; Ajami et al., 2004).

When using multiple objectives, the solution to the calibration problem will not, in general, be a single unique set of parameters but will consist of the set of Pareto optimal (non-dominated) solutions. To illustrate the Pareto optimal solutions to a multi-objective calibration problem the calibration routine has been applied for optimization of two objectives, the RMSE of extreme quick flows and the RMSE of extreme low flows. Also, the different objectives were transformed into a single aggregated objective measure (Madsen, 2000) (Equation 1):

$$F_{agg}(\theta) = \left[(F_1(\theta))^2 + (F_2(\theta))^2 + ... + (F_p(\theta))^2\right]^{1/2} \tag{1}$$

The objective functions integrated in Equation 1 were optimized manually, meanwhile the result was compared with EF and R^2 to select the best simulation run.

The hydrologic components of the SWAT model were calibrated to fit the observed daily stream flow data of the Grote Nete River in Belgium, for the period 1986-1989. This period was chosen because it represents a combination of dry, average, and wet years (annual precipitation ranged from 646.5 to 988.7 mm). The model was run for a five-year period (1985-1989), of which the first year (1985) was used for the warming up-stabilization of the model runs. The values of selected model parameters were varied iteratively within a reasonable range during various calibration runs until a satisfactory agreement was obtained between the observed and simulated stream flow data. The model validation was done using the observed flow data for the years 1990-1995. Model performance was assessed with respect to the following three basin characteristics: total flow, slow flow, and extreme quick and slow flows. Calibration of each hydrologic characteristic involved methodically adjusting the input parameters and then evaluating the model performance.

Determining and considering only sensitive parameters was the first step in reducing the number of calibrated parameters and thus keeping the run time of the optimized parameter in reasonable bounds. A preliminary model run showed which parameters should be given priority in the optimization. In terms of land use and soils these are the curve number, available water capacity, Manning's coefficient for tributary channel, groundwater delay, base flow alpha factor, threshold depth of water in shallow aquifer for "return follow" and "revap" to occur, the "groundwater revap" coefficient, and deep aquifer percolation fraction. Furthermore, parameters determining the delay of the surface runoff, the ground water recharge, and the base flow recession were optimized. The sensitivity analysis was conducted to identify the most sensitive model parameters and to identify the ranking among those parameters. The sensitivity analysis was conducted in a standard manner after calibration, and while all parameters were kept constant one single parameter was altered by ± 10% and 20%. The climatic inputs to the model were constant for all iterations.

Results and Discussion

Model Calibration and Validation

Examination of the calibrated data indicated that SWAT results were less accurate, but removal of the 1989 data from the calibration data set considerably increased the coefficient of efficiency. Because of uncertainty in discharge observations for the year 1989, the value of discharge observation during 1989 was highest while precipitation was lowest. Thus, it was decided to limit the calibration period from 1986 to 1988. Also the results in the validation period showed that removal of 1991 from the analysis improved the results. Therefore, the years 1989 and 1991 were not included in the statistical analysis.

The solutions of the Pareto approach were obtained by manually calibrating the parameters of the SWAT model while optimizing simultaneously the RMSE for extreme quick and slow flows. The results of the Pareto multi-objective calibration analysis were plotted and three points were considered. The first two points corresponded to the lowest RMSE for extreme slow and quick flows, and the third intermediate point was located between the above mentioned points. According to Equation 1, the difference between the error (RMSE) for extreme quick flows, slow flows, total flow and slow flow estimates is a measure of improvement in the model performance. The parameters of the model run with the lowest extreme slow flows yielded the best performance. For each run in the Pareto front, the EF and R^2 were examined. As shown in Figures 1 and 2, the scatter plots of the extreme quick and extreme slow flows after Box-Cox transformation of the observed and simulated flows are underestimated for extreme quick flow while overestimated for extreme slow flow. The result shows that the overall performance of the model is good, but the extreme high and extreme slow flows are systematically underestimated and overestimated, respectively.

The model calibration and validation statistics for daily total and slow flows are presented in Table 2. The SWAT model simulated the mean daily total flow satisfactorily during the calibration period, with an $R^2 = 0.86$ and an $EF = 0.73$, and the mean daily slow flow with an $R^2 = 0.85$ and an $EF = 0.71$. Over the three-year simulation period (1986-1988) the model slightly overestimated the total flow by 1.03% (Table 3). Daily slow flow volumes were also simulated well, with three out of four years having a percent error of slightly over 1.02%.

Also, simulated daily flows matched well with observed flows but some difficulties were encountered in matching exactly the magnitude or timing of storm events. Difficulties in matching exactly the timing or magnitude of storm flows can largely be attributed to the spatial and temporal uncertainties in the input climatic data.
There are numerous additional uncertainties including aerial rainfall estimation errors, parameter estimation/calibration uncertainties due to overparameterization, and consequently the subjectivity of the manual calibration. Other causes of uncertainties which should be noted are evapotranspiration input estimation errors, spatial

resolution and scale of the spatially distributed parameters and input, and macroscopic and semi-distributed description of the physical processes.

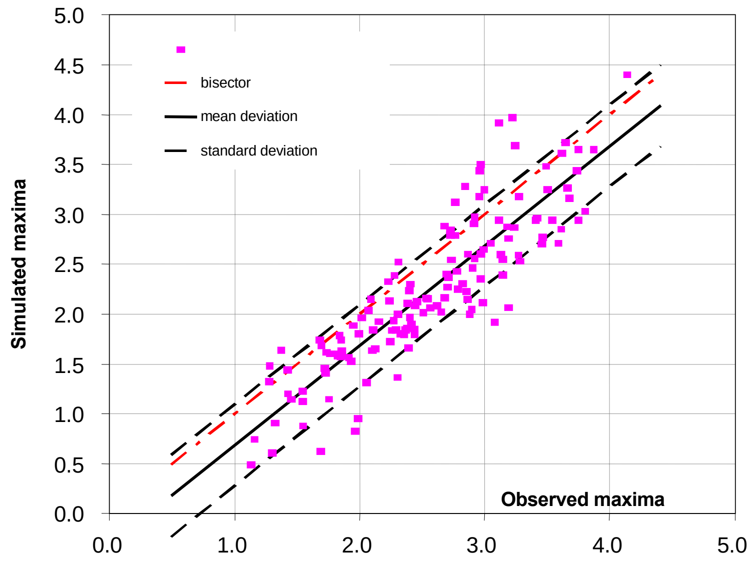

Figure 1. Scatter plots of Box-Cox transformed independent observed and simulated extreme quick flow during the calibration and validation periods.

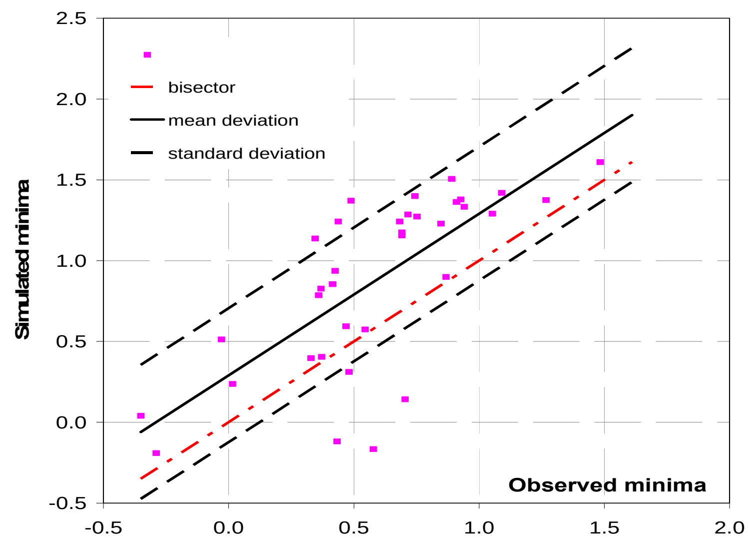

Figure 2. Scatter plots of Box-Cox transformed independent observed and simulated extreme slow flow during the calibration and validation periods.

The procedure based on the multi-objective optimization has the best overall performance but the worst performance for extreme quick and extreme slow flows.

During model validation (1990-1995) the statistical analysis revealed that the model performance was quite good, with an $R^2 = 0.82$ and an EF = 0.64 for the mean total flow (Table 2). The slow flow was reasonably well estimated over the five-year validation period, as can be concluded from the relatively high values for EF and R^2, low value for RMSE, and a -0.97% error (Tables 2 and 3). The good model performance during the validation period indicates that the SWAT model accurately replicates the daily stream flows measured at Varendonk for the 10-year simulation period.

It is obvious that the simulated daily total flow shows a good correspondence with the observed daily stream flow. In general, peak discharge was underestimated, which could be explained by the smoothing effect of the Digital Elevation Model, used for representing the basin topography. Furthermore, it was observed that there was always a small flow in the central section of the basin that does not reach the outlet due to re-infiltration in the sandy soils.

Table 2. Summary statistics from flow calibration and validation periods in the Grote Nete Catchment.

Statistical index	Total flow		Slow flow	
	Calibration	Validation	Calibration	Validation
RMSE	1.33	1.41	0.88	0.70
EF	0.73	0.64	0.71	0.66
R^2	0.86	0.82	0.85	0.82
Overall volume error	0.15	0.07	-0.008	-0.11

Table 3. Comparisons between measured and predicted daily stream flows.

Period	Total flow (m^3/s)		Slow flow (m^3/s)	
	Observed	Simulated	Observed	Simulated
Calibration	4.70	4.85	3.78	3.77
Validation	3.74	3.81	3.08	2.98

Sensitivity Analysis

The sensitivity analysis was conducted using the data from the calibration period (1986-1988). This simple test consisted of changing one parameter at a time, while keeping other parameters constant. The optimal parameter values were altered by both an increase and decrease of 10 and 20%. The levels of 10 and 20% change were chosen arbitrarily. The impact of the change in parameter value was measured by the change in EF of the model output as compared to no change in parameter values. The effects of the changes in parameter values on total and slow flows are depicted in the Tables 4 and 5.

Table 4. Most important parameters in total flow and their sensitivity ranking.

Parameter	Variation	Rank
RDHRGDP	0.298	1
REVAPMN	0.288	2
Soil _AWC	0.255	3
GW_QMN	0.237	4
CH_N1	0.237	5
GW_Delay	0.193	6
CN2	0.185	7
GW_REVAP	0.181	8
ALPHA_BF	0.177	9

Table 5. Most important parameters in slow flow and their sensitivity ranking.

Parameter	Variation	Rank
RDHRGDP	0.377	1
GW_Delay	0.357	2
REVAPMN	0.201	3
Soil _AWC	0.182	4
GW_QMN	0.143	5
CH_N1	0.127	6
CN2	0.107	7
GW_REVAP	0.060	8
ALPHA_BF	0.011	9

Conclusion

This study reveals that the semi-distributed SWAT model performed satisfactorily using the hydrological data of the Grote Nete River Basin. Its distributed nature proved to be valuable for a correct representation of the sharp and rapid increase of the stream flows observed at the Varendonk limnigraphic station. The hydrological components of the SWAT model, such as total flow and slow flow, were calibrated and validated at the catchment scale of the basin. Daily discharge records and base flow data, determined by using an automatic base flow separation algorithm (Arnold *et al.*, 1999)) for the period January 1985 - December 1995 were used for the model calibration and validation. With respect to all objective functions used in this study, the model was able to adequately simulate the total and base flows. Notwithstanding the precipitation variability, the integrated calibration and validation process indicated that the agreement between predicted and observed total stream flow and slow flow were quite good. The model efficiency reached, measured by the EF between 0.73 and 0.71 for total and base flow in the period of study, the same order of magnitude as reported for model runs in regions f the U.S., Germany and Belgium (Srinivasan et al., 1998; Van Griensven, 2002; Michel et al., 2003; Van Liew and Garbrecht, 2003; Di Luzio and Arnold, 2004). The results of the study demonstrate that the hydrodynamic component of SWAT can be applied successfully in flat and sandy soil environments on daily time scales.

This study is a first-step in the development of a calibration/validation procedure, which not only uses total discharge as a variable in the calibration of the model parameters, but also observed and simulated base flow values agree, and the extreme quick and slow flows are not over or underestimated. In the next phase of this research, the automatic calibration and validation for total and base flow will be pursued, as well as nitrogen and phosphorous variables

References

Abu El-Nasr, A., Arnold, J.G., Feyen, J., Berlamont, J., 2004. Modeling the hydrology of a catchment using a distributed and a semi-distributed model. Hydrol. Process., 18.

Ajami, N.K., Gupta, H., Wagener, T., Sorooshian, S., 2004. Calibration of a semi-distributed hydrologic model for streamflow estimation along a river system. J. of Hydrol., 298: 112-135.

Arnold, J.G., Williams, J.R., Srinisavan, R., King, K.W., 1994. SWAT: soil ad water assessment tool." U.S. Dept. of Agric., Agricultural Research Service, Temple, Texas, USA.

Arnold, J.G., Srinivasan, R., Muttiah, R.S., Williams, J.R., 1998. Large area hydrologic modelling and assessment. Part 1: Model development. J. Am. Water Resources Assoc., 34(1): 73-89.

Arnold, J.G., Allen, P.M., 1999. Automated methods for estimating base flow and ground water recharge from stream flow records. J. Am. Water Resources Assoc., 35(2): 411-424.

Di Luzio, M., Arnold, J.G., 2004. Formulation of a hybrid calibration approach for a physically based distributed model with NEXRAD data input. J. of Hydrol., 298: 136-154.

Eckhardt, K., Arnold, J.G., 2001. Automatic calibration of a distributed catchment model. J. of Hydrol., 251:103-109.

Feyen, L., Vázquez, R., Cristianes, K., Sels, O., Feyen, J., 2000. Application of a distributed physically-based hydrological model to a médium size catchment. Hydr. and Earth Syst. Sc., 4(1): 47-63.

Gassman, P.W., Jha, M., Secchi, S., Arnold, J., 2003. Initial calibration and validation of the SWAT model for the upper Mississippi river basin. 7th International Conference on Diffuse Pollution and Basin Management in Dublin, 17-22 August 2003: 10-40.

Gupta, H.V., Sorooshian, S., Yapo, P.O., 1998. Toward improved calibration of hydrologic models: multiple and non-commensurable measures of information. Water Resour. Res., 34(4): 751-763.

Madsen, H.,2000. Automatic calibration and uncertainty assessment in rainfall-runoff modeling. 2000 Joint Conference on Water Resources Planning and Management, Hyatt Regency, Minneapolis, USA, July 30-August 2: 1-10.

Madsen, H. ,2002. Automatic calibration of a conceptual rainfall-runoff model using multiple objectives. J. of Hydrol., 235: 276-88.

Madsen, H., 2003. Parameter estimation in distributed hydrological catchment modelling using automatic calibration with multiple objectives. Adv. in Water Resour., 26: 205-216.

Michel, W., Liew, V., Garbrecht J., 2003. Hydrologic simulation of the little Washita River experimental watershed using SWAT. J. Am. Water Resources Assoc., 39 (2): 413-426.
Nash, J.E., Sutcliffe, J.V., 1970. River flow forecasting through conceptual models. I. A discussion of principles. J. of Hydrol., 10: 282-290.
Neitsch, S.L., Arnold, J.G., Kiniry, J.R., Williams, J.R., 2001. Soil and Water Assessment Tool theoretical Documentation. Blackland Research Center, Texas Agricultural Experiment Station. Temple, Texas, USA: 93-115.
Neitsch, S.L., Arnold, J.G., Kiniry, J.R., Srinivasan, R., Williams, J.R., 2002. Soil and Water Assessment Tool User's Manual: Version 2000. GSWRL Report 02-02, BRC Report 02-06, Publ. Texas Water Resources Institute, TR-192, College Station, Texas, USA., 438 pp.
Timmerman, A., J. Mertens, J.G. Kroes en T. Vandenbosch, 2001. Eindrapport projectonderdeel B. Watermanagement op bedrijfsniveau : "integratie van het beregeningsadviessysteem met het peil- en nutriëntenbeheer". Interregprogramma voor het Benelux Middengebied, 113pp.
Srinivasan, R., Ramanarayanan, T.S., Arnold, J.G., Bednarz, S.T., 1998. Large area hydrological modeling and assessment. Part II: Model application. J. Am. Water Resources Assoc., 34 (1): 91-101.
Willems, P., 2003. WETSPRO: Water Engineering Time Series PROcessing tool. Methodology and User's Manual. K.U.Leuven, Hydraulics Laboratory, Leuven, Belgium.
Van Liew, M.W., Garbrecht, J., 2003. Hydrologic simulation of the Little Washita River Experimental Watershed using SWAT. J. Am. Water Resources Assoc., 39(2): 413-426.
Van Griensven, A., 2002. Developments toward integrated water quality modeling for river basins. PhD Dissertation, VUB Hydrologie Nr. 40. Vrije Universiteit Brussels, Faculty of Applied Sciences, Department of Hydrology and Hydraulic Engineering, 236pp.
Van Orshoven, J., Deckers, J.A., Vandenbroucke, D., Feyen, J., 1993. The completed database of Belgian soil profile data and its applicability in planning and management of rural land. Bulletin Recherche Agronomie Gembloux, 28(2-3): 197-222.
Vázquez, R.F., Feyen, J., 2004. Potential evapotranspiration for the distributed modelling of Belgium catchments. ASCE J. Irrig. and Drain. Engng, 130 (1): 1-8.
Vereecken, H. Feyen, J. Maes, J., 1990. Estimating the hydraulic conductivity soil water content relationship from easy to measure soil properties. Soil Sc., 149(1): 1-12.

Impact of Land Use Changes on Stream Flows using the SWAT Model; Case Study: Kasilian Catchment

Saadati H.*[1], Gholami S.H.[2], Ayyoubzadeh S.A.[3]
[1]Member of Scientific Staff of Islamic Ardebil Azad University. Email: saadati55@yahoo.com
[2]Assistant Prof. of Soil Conservation and Watershed Management Research Center,
[3]Assistant Prof. of River & Sediment Eng., Dept. of Water Structures Eng., TMU.

Abstract

Based on the availability of daily data, the physically based structure, and superior conceptual basis, the Soil and Water Assessment Tool (SWAT) hydrological model was selected to simulate the effect of land use alteration on surface runoff in the Kasilian Catchment located in northern Iran. Ten years of daily data were used in this analysis. The rainfall data were first divided into three periods, the set up, calibration (4 years), and validation (6 years) periods. In the next stage, six scenarios, including both positive and negative environmental tendencies, were studied. An optimization procedure was carried out by minimizing the sum of squared differences between the observed and calculated results.

The results showed that the model simulated the high flow runoff more satisfactorily than low flow conditions. Furthermore, the study revealed that the model, with its corresponding optimum set of parameters, was able to predict runoff values which have similar properties to the recorded runoff. The coefficient of determination between actual and simulated runoff was 0.69. In addition, further analysis showed that the ABF, CN2, and REVAPC parameters were the most sensitive. Finally, the effect of hydrological parameters on stream flow was evaluated. In general, a better simulation for mean and maximum stream flow values may be obtained in the catchment under consideration. Increasing the values of stream flow runoff (monthly and annually) under the two land use scenarios, Cases 1 and 2, in comparison with the current land use shows that the future land use conditions could have negative effects and natural resources would be damaged. On the contrary, the results of Case 4, describing conditions that occurred in the past with positive effects, show the model simulating the condition with less runoff. In spite of the fact that Case 3 indicates positive conditions and Case 6 shows negative conditions (Table 2), the model could not simulate more reasonable runoff values. The results also highlighted that the hydrological processes are simulated in agricultural areas and rangelands better than forested areas. In conclusion, the SWAT model should be regarded as a promising model to simulate the hydrological processes in other similar Iranian catchments.

Keywords*:* Hydrological parameters, Kasilian, Iran, Runoff, Simulation, SWAT model.

Introduction

In order to establish a reasonable balance in the water cycle through appropriate land use management, a powerful hydrological model in collaboration with an effective database is fundamental. The Soil and Water Assessment Tool (SWAT) is a model developed to simulate the effect of different land management scenarios on runoff, sediment yield, and pollution in large complex watersheds with various soil types, land uses, and management conditions over long periods of time. The model is a multipurpose simulation model for watershed management and is capable of simulating runoff discharge originating from any land use alteration. The model simulated yearly mean runoff over a ten year period successfully in the Mississippi watershed at Good Win Creek with a correlation coefficient of 76% (Bings et al., 1989). The same correlation coefficient was obtained in another research study using the model to simulate daily sediment runoff in the Amameh Catchment in Iran (Gholami, 2000). The SWAT model has been integrated with the ArcView Geographic Information System (GIS) software in order to facilitate development of model inputs and analysis of model output (Di Luzio and Neitsch, 1999).

This research was aimed at investigating the effects of land use alteration on various hydrological components. The study area is composed of four types of land use classes, urban, cultivated, forests, and rangeland. Runoff discharge in these areas can be different due to any alteration in land use. This difference was investigated using the SWAT model following model calibration. The study includes estimation of daily, monthly, and annual water discharge for northern watersheds in Iran, such as the Kasilian Catchment, influenced by given alteration in land uses and species types. The hydrologic components used for calibration and validation include precipitation, temperature, potential evapotranspiration (PET), total water yield, and groundwater flow.

Methodology

Physiographical data were determined from 1:50,000 scale topographic maps obtained from the country geographical organization using ILWIS and ArcView modules in a GIS environment. The data includes a soil map, geology map, vegetation map, hydrographical network map, slope of the basin, slope tendency, and erosion maps. Dynamic data, including rainfall, discharge, and sediment yield, have been obtained from hydrological recording stations in the catchment or in its bounded area. Daily and monthly data were collected from the four hydrological stations located in the catchment. A twenty year data duration period was selected to apply the model. Therefore, a decision was made to provide all data within the same 20 years, and some data was corrected or completed accordingly. As previously mentioned, the catchment under study consist of four land use areas, forest, rangeland, cultivated, and urban areas (Table 1). All required data for the model in each land use area were collected through field measurements. Once required field measurements were collected, they were linked to data obtained from the maps and other hydrological data. Calibration of the parameters, model validation, and sensitivity analyses were performed in the next steps, and the results were evaluated. It should be noted that the sensitivity analyses were conducted using well-known sensitivity models, including the NS, TASAR, TSSR, and PBIS models.

In this study, three steps were conducted including calibration, validation, and alternative studies. In alternative studies, some combinations of crop pattern management and land use were considered, and the alternatives were consequently defined. Table 2 shows alternatives considered in this research as Case 0 (the current case) to Case 6. The model was then employed to determine the hydrological processes and components and the values of stream flows were obtained and analyzed accordingly. Land use management was studied in the two general prescribed manners; one with positive and the other with negative conditions. Crop pattern management was investigated by changing the current crop, winter and summer wheat, to one of the other seven crop types, including soy beans, corn and sunflower, grain sorghum, barley oats, stripper and picker cotton, rice, potato and pea, only in the cultivated subbasins 3 and 4.

Table 1. Landuse areas in the Kasilian Catchment subbasins.

subbasin	Land use	Area(ha)	Percentage
1	Range-Rock	840	12.15
2	Forest	1742	26.5
3	Forest-Agricultural	3431	51.5
4	Agricultural	665	9.85
Total		6678	100

Table 2. Definition of alternative scenarios.

Alternative	*Case0*	*Case1*	*Case2*	*Case3*	*Case4*	*Case5*	*Case6*
Description	Current landuse	Alteration of both the forest and rangeland to cultivated land	Alteration of the rangeland only to cultivated land	Alteration of the cultivated land to forest	Alteration of the rangeland to forest	Alteration of both the cultivated land and forest to rangeland	Alteration of the forest only to rangeland

In calibration procedures for model parameters the best fitting method is used to obtain the minimum difference between the model results and the corresponding observed data. In this stage, the best fit was achieved with an R^2 = 0.69, PBIAS = 5.2, and NS = 0.72. The validation test was also performed using other datasets not used in the calibration procedure with the results of R^2 = 0.57, NS = 0.54, and PBIS = 3.4 between simulated and observed values. As can be seen in Figure 1, a good fit was obtained between observed and the calibrated model results. In the SWAT model, the results of simulated daily runoff for each subbasin as an output of the model are stored in two files with the extensions SBS and BSB. Another important output file of the model is the STD file, which includes daily, monthly, and annual runoff for all subbasins with some additional parameters such as sub-surface runoff, evapotranspiration, water, and sediment yield. The management (MGT) program for cultivated scenarios was analyzed similar to Arnold et al. (1996) using codes in the MGT principle file including IGRO, NROT, NPTOT and HUSE.

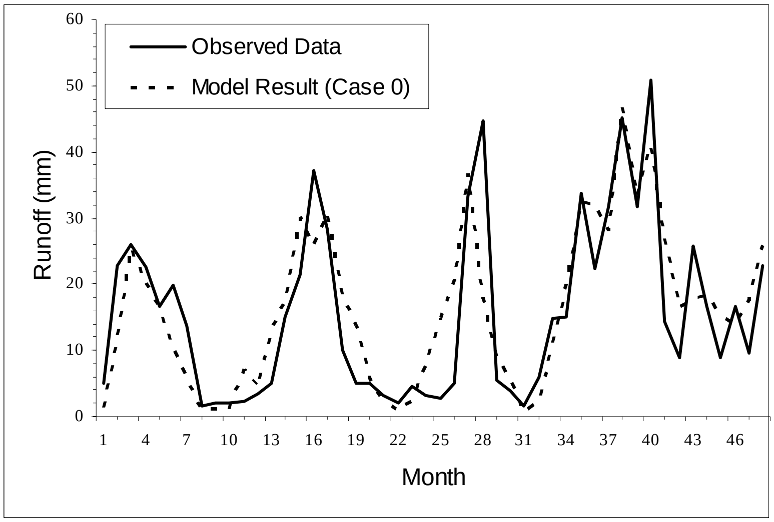

Figure 1. Model calibration: comparison between observed and corresponding simulated monthly runoff in the Kasilian Basin using the SWAT Model (Case 0).

Results

Land Use Management Studies

Once the CIO file, as a control file for SWAT, was completed, the model was run using various alterations in land use areas. In each run, some file name components of the CIO principle file were altered and the model was then executed for each subbasin considering the desired changes in land use as in Table 2. The hydrological results of the six alternatives, as previously mentioned, were then obtained. The minimum, mean, and maximum runoff results for land use alteration cases are shown in Figure 2, by which a trend can be seen when compared with the results for the current land use case, Case 0. Also, Figure 3 shows the simulated monthly runoff for the six cases under consideration in comparison with the current land use.

Crop Pattern Management Studies

As previously mentioned, various scenarios for crop management were investigated. The percent change in the hydrological and soil parameters for each crop management scenario are shown in Table 3.

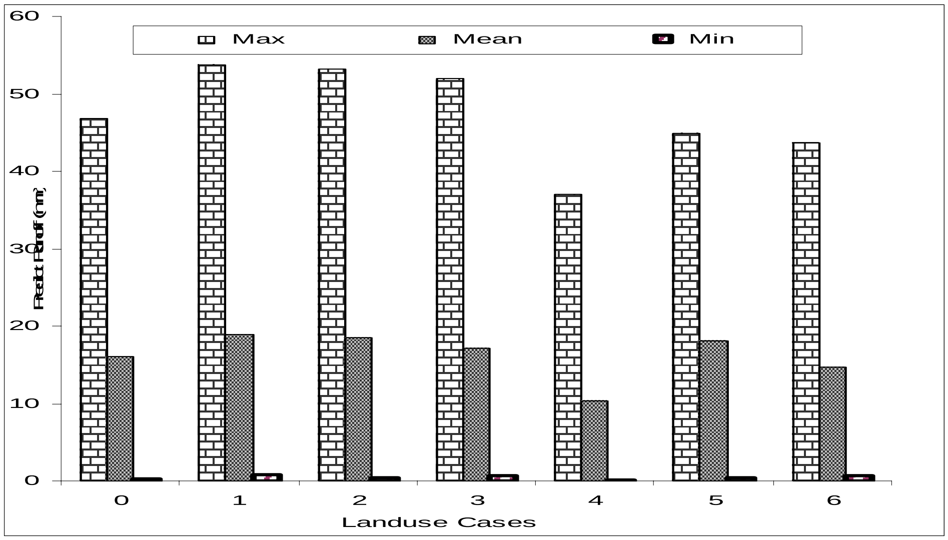

Figure 2. Minimum, mean and maximum simulated runoff for each land use alteration in comparison with the current case (Case 0).

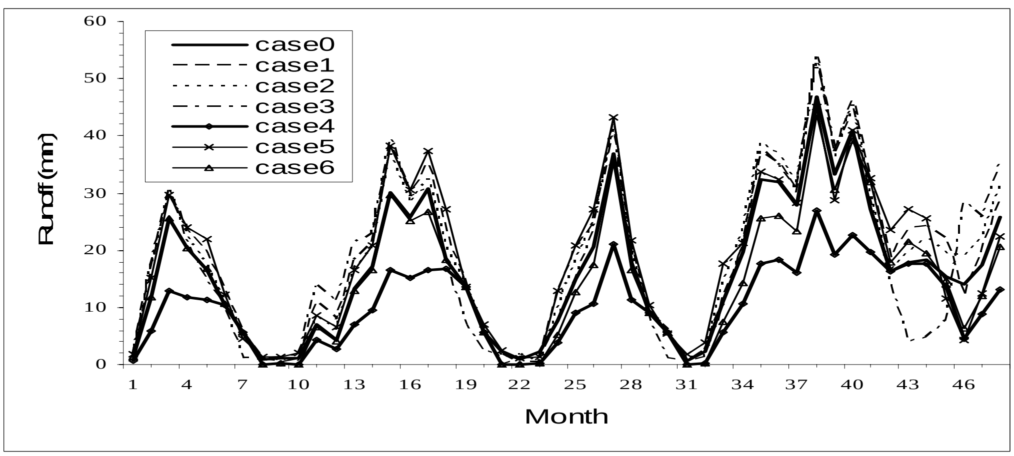

Figure 3. Comparison between simulated monthly runoff results from various landuse alterations and the current land use in the Kasilian Basin.

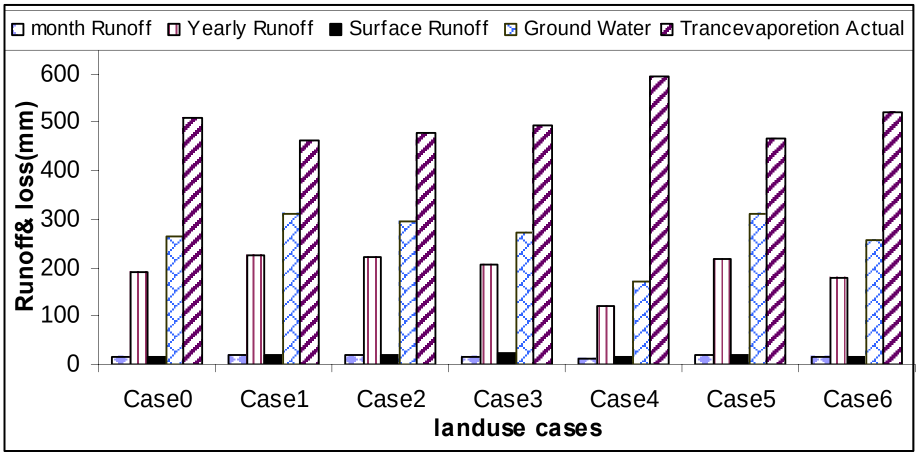

Figure 4. Output results for various hydrological parameters in the cases under consideration for land use alterations in the Kasilian Basin.

	Crop Type						
Investigated Parameter	Soya beans	Corn Sunflower	Grain Sorghum	Barley oats	Stripper Cotton Picker Cotton	Rice	Potato Pea
Crop %	-10.96	-82.27	252.97	-4.91	-50.50	-3.64	-52.74
Biomass %	2.19	51.01	63.99	0.46	-27.52	28.94	-32.01
ET %	-1.00	-5.18	-4.38	-0.20	0.40	-2.99	1.20
Q_{sur} %	2.20	10.36	13.33	1.19	0.00	9.52	-1.19
Q_{lat} %	1.24	3.05	2.86	0.00	0.00	1.90	18.57
GRW shallow %	1.09	8.18	6.72	0.55	-1.02	4.82	-1.72
Water Yield %	0.81	8.59	9.10	0.35	-2.38	5.31	-2.38
Mean Predicted Monthly%	0.91	8.42	7.94	0.00	-2.42	4.85	-2.42

Table 3. Percent changes in hydrological and soil parameters for each crop management scenario.

Discussion and Conclusions

In this study, the impact of land use and crop management were investigated using the SWAT model in the Kasillian Catchment in northern Iran. The study first included a calibration procedure using observed monthly runoff, and the model result achieved a squared correlation coefficient of 0.69 (Figure 1).

The application of the model in the first step of the study showed that the model was capable of simulating the stream flow under various positive and negative scenarios of land use as given by Figures 2-4. Figure 2 shows that, in general, better simulation for mean and maximum stream flow values may be obtained in the catchment under consideration. According to Figure 3, the values for stream flow in subbasins 1 (rangeland) and 4 (cultivated land) were better simulated than the forest subbasin.

Some detailed information on hydrological characteristics for the various cases of land use, including annual and monthly runoff, evapotranspiration, and ground water flow were obtained and are shown in Figure 4. Increasing the values of stream flow runoff (monthly and annual) under two land use scenarios, Cases 1 and 2, in comparison with the current land use showed that the future land use scenarios with negative conditions could occur and the natural resources would be damaged. However, the results of Case 4, with a positive scenario, showed that the model simulated the condition with less runoff. In spite of the fact that Case 3 indicated positive conditions and Case 6 showed negative conditions (Table 2), the model could not simulate more reasonable runoff values. The results also highlight the fact that the hydrological processes are simulated in agricultural areas and rangelands better than forested areas.

References

Arnold, J.G. 1996, Estimating Hydrologic Budgets for Three Illinois Watersheds. Journal of Hydrology, 176:57-77.

Arnold, J.G., J. Williams, R. Srinivasan, and K.W. King (1996), “SWAT Simulation Model-Soil and Water Assessment Tool”, USDA, Agriculture Research Service, p. 213.

Bathurst, J.C. 1977. Sensitivity analysis of the System Hydrologic European for an upland catchment. J. Hydrology, 87:103-123.

Bingner, R.L. 1996, “Runoff Simulation from Goodwin Creek Watershed Using SWAT, ASAE 59 1 : 85-90

Diluzio, M., Neitsch, S.L. 1999. ArcView Interface for SWAT 99.2: User’s Guide. p. 185.

Gholami, S.A. 1998, “Distributed Watershed Modelling of Mountainous Catchment.” Synopsis of ph. D Thesis. Dept of Civil Engineering, Indian Institute Technology New Delhe, p. 469.

Helvey, J.D. 1971. A summary of rainfall interception by certain conifers of North America. In Biological effects of the hydrological cycle, E.J. Monke, Ed. West Lafayette : Purdue University, p. 584.

Leonard, P.B.A. 1979 A stable and accurate convective modelling procedure based on quadratic upstream interpolation. Computer Methods in Applied Mechanics and Engineering, pp. 59-98.

Mahdavi, M. 1999. Applied hydrology, publication Tehran University, Iran.

Nash, J.E. and T.E. Sutcliff, 1970, “River Flow Forecasting Through Conceptual Model”, Part I.A Discussion of Principles. J. Hydrol. 10(3):282-290.

Royappan, M. 1984, “Survey of effect of change of land use to runoff by SWAT model in South Africa “Kentucky University, p. 482.

Shanholtz, V.O. 1994. A soil water balance model for no-tillage and conventional till systems. Agricultural Water Management, 26:155-168.

Solan, P.G. et al., 1983. Modeling Surface and Subsurface Stormflow on Steeply. Sloping Forested Watersheds. Water Resources Inst. Report 142, University of Kentucky, Lexington, Kentucky, p. 345.

Tamab, C. E. 1978-1687. Water comprehensive plan. Tehran, Iran.

Williams, J.R. 1984. Simulation for water resources in rural basins, Journal of Hydraulic Engineering, 111(6):970-986.

Imitating Model Water-salt Balance (IWSBM) in Large Watershed Basins

Sadatinejad S.J.*[1] and Ranjbarfordoi A.[1]
[1]Faculty of agriculture, Department of Natural Resources, ShahreKord university, P.O.Box: 115, ShahreKord, Iran. Email: sadatinejad@agr.sku.ac.ir

Abstract

Water-salt balance (WSB) in watershed basin is an indication of the way of human activity utilization from soil and water resources in river basin. Therefore the outcome of each type of unreasonable exploitation from natural resources in watershed basin can be investigated through water and salt regime in the main river. Due to complexity of relation among the WSB components in watershed basin, especially in large scale, in this research was tried to offer an applied and simple model for these basins. The imitating Water and salt balance offered in this research, is a combination of balance in two sections of the main river and basin lands. The connecting factor in these two sections is: intake water from the main river to lands and return water from lands to the main river (a reciprocal relationship). The land balance comprises calculations in three sections including land surface, aeration and saturation zones. A compliment of these equations under IWSBM in frame of software is prepaid in order to use. The mention package (IWSBM) was used for estimation of outflow and its salt content in Syrdarya River Basin. The achieved results show that estimating and observational outflow are closed correlated (with coefficient R=0.99), relative error was around %7.7, estimating and observational salt content having a correlation coefficient R=0.84 and relative error was %13.3, which demonstrates a high precise of the model.

Introduction

Agricultural activities affected nature of the earth and induce changing in natural parameters. The produced alterations by anthropological activities especially agricultural activities could be studied through investigation of water-salt balance. In general, in agricultural regions due to some related parameters such as land irrigation, natural land-balance is varied and has much differences with land where no any changing in its nature has. Study of water-salt balance (WSB) in detailed is so complicated. Soil and water-input varies and in view of time scale has an extended range, from seconds to years. Therefore, in some cases, for calculation of detailed balance in a region, some thirty factors should be consulted (Kharchenko, 1975)

In a large scale and extended areas, distribution of effective parameters in natural balance, in view of time and place, there are lots of problems. Due to these problems the parameters should be used in average (Sadatinejad, 2001). Therefore the first step in study of WSB in agricultural areas is: determination of the areas in where formation of balance parameters is the similar. These regions are varied in view of surface area, ranging from a small plan to a country area.

Irrigation on agricultural lands induces water infiltration to soil and causes reservation of moisture in the soil whish is evaporated through capillary tubs, consumed by plants and joint to the under ground water. On this basis the depth of soil could be divided in two zones comprising aeration and saturation zone. With respect to the subject, for calculation of WSB in agricultural areas, it should be investigated in three sections: on the soil surface, aeration and saturated zones (Budagovsky, 1994 and 1998)

Among the above-mentioned sections exchange of water is vertically carried out. In watershed basins, the isolator territories in two later zones, on the contrary of lateral territory, are not permanently definite and affects by water table. With respect to time scale, WSB has different time period such as daily, hourly, monthly, seasonal and yearly. However, the period time depends to scope of the area. For instance in large basins, time periods like month and year are used.

The equation for WSB is written as follows:

$$\frac{\partial W}{\partial T} = W_{IN} - W_{OUT} \quad (1)$$

Where W is water volume storage in given area, W_{in} is input water to the area, W_{out} is outflow water from the area.Figure1schematic presentation from watershed basin and the WSB parameters.

On basis of the figure, watershed basins are divided in two zones comprising zone of formation flow , and consumption zone include plains and agricultural areas. Therefore with respect to the figure, WSB is separated in two sections (1) WSB on lands and (2)WSB in main rivers. In this study WSB in the two sections are separately investigated and our proposal model in these sections is IWSBM. (Sadatinejad,2001)

The base for IWSBM is the protection and transportation law of water and salts. This law could be written as integral and differential equations if the parameters are used as average, the equation can be changed into a simple form. The simple form of the equation comprises the following parameters: (1) input water through precipitation and irrigating water to watershed basin surface, (2) inflow and outflow from ground water, (3) infiltration and evaporation, (4) saving of moisture into soil and ground water.

So these equations complete so precise and application of them due to averaging is easier. That is why before using these models, the watershed basin have to separate in analogous peaces. The only substantial relationship among the mentioned peaces is current of water and salt in the main river.

In this relation, in frame of an imitating model, IWSBM must be calculated in the following sections: (1) on lands(agriculture and non agriculture) and (2), the main river in watershed basin.

The relationships between these two sections are: water transported from the main river, irrigated on the agricultural land and then the current of salt and water return to the main river in different ways. Regardless the both mentioned cases, in land section, water exchange among the active water exchange zones, comprises soil surface, aeration zone, and saturated zone must be considered. In this model time period for WSB parameters is month. The general equations for water balance in land section (agricultural and non-agricultural areas) of watershed are come as: (Glubash,1989)

$$W_{i.l} + W_{l.in} + W_{iw.r} + W_p = W_{f.l} + W_{iva} + W_{out.l} \quad (2)$$

where $W_{i.l}$ = initial water storage; $W_{l.in}$ = lateral inflow; $W_{iw.r}$ = intake water from river channel; W_p = precipitation; $W_{f.l}$ = final water storage (at the end of time period); W_{iva} = evaporation; $W_{out.t}$ = territory outflow. Unit for the parameters in above equation is mm. With imposing amount of salts (C_j) to the above equation (2), equation for WSB is as follows:

$$W_{i.l}S_{i.l} + W_{l.in}S_{l.in} + W_{iw.r}S_{iw.r} + W_p s_p = W_{ef.l}S_{f.l} + W_{iva}S_{iva} + W_{out.l}S_{out.l} \quad (3)$$

Inflow and outflow of water and salt in watershed basins is horizontally down but current of evaporation from watershed surface and infiltration to aeration and saturation zones is vertically carried out. Therefore it seem instead of using general WSB equations in agricultural and non-agricultural lands , the modified equation is used for different soil layers (comprising soil surface, saturation and aeration zones). These equations are as follows:

Water balance equation of soil surface:

$$\Delta W_l = W_p + W_{wi} + W_{in.gr} + W_{l.in} - W_{iva} - W_{out.t} \quad (4)$$

Water balance equation of aeration zone:

$$\Delta W_{ae} = W_p + W_{wi} + W_{su.ae} - W_{iva} - W_{ae.su} \quad (5)$$

Water balance equation of saturation zone:

$$\Delta W_{su} = W_{in.su} + W_{l.in.res} + W_{inf\,ch} + W_{ae\,.su} - W_{su.ae} - W_{out.su} \quad (6)$$

Where W_p = precipitation; W_{wi} = water intake for irrigation; $W_{in.gr}$ = inflow from ground water; $W_{l.in.res}$ = residual of lateral inflow; W_{iva} = total evaporation; $W_{out.l}$ = outflow from agricultural and non-agri, lands to river channel; $W_{su.ae}$ = inflow from saturation to aeration zone; $W_{ae.su}$ = inflow from aeration zone to ground water (saturation zone); $W_{inf.ch}$ = infiltration from irrigating channels; ΔW_l, ΔW_{ae}, ΔW_{su} = storage volume of water on soil surface, aeration and saturation zones which is calculated from the difference between initial storage and storage at the end of time period.

All of water balance parameters are expressed in mm per month or million cubic meters per month. Salt balance is calculated as balance parameters by salt content (Cj) and is expressed as follows:

Water-salt balance equation of soil surface

$$W_pS_p + W_{wi}\,S_r + W_{in.gr}\,S_{in.gr} + W_{l.in.res}\,S_{l.in} - W_{out.s}S_{out.s} + \Delta W_sS_s = 0 \quad (7)$$

Water-salt balance equation of aeration zone

$$W_pS_p + W_{wi}S_r + W_{su.ae}\,S_{su} - W_{ae.su}S_{ae} + \Delta W_{ae}S_{ae} = 0 \quad (8)$$

Water-salt balance equation of saturation zone

$$W_{in.su}\,S_{insu} + W_{l.in.res}\,S_{l.in} + W_{inf.ch}\,S_{wi} + W_{ae.su}S_{ae} - W_{su.ae}S_{su} + \Delta W_{su}S_{su} = 0 \quad (9)$$

Where S_p = salt content in precipitation; S_{li} = salt content in lateral inflow; S_r = salt content in main river; S_{ae} = salt content in aeration zone; S_{su} = salt content in saturation zone; S_{wi} = salt content in irrigating water.

Measurement of salt unit is expressed in g/l. In order to evaluation of agricultural activity effects on water resources in watershed basin, alteration in outflow and it's salt rate in the basin must be considered. It is necessary to mention these changes rises from expansion of agricultural land in the basin and their balances are respected in the above mentioned equations. Therefore in the second section the effects of WSB are investigated. The dominant equations in the second section of WSB are expressed as:

Water balance equation of main river channel

$$W_{in.r} - W_{wi.r} + W_{out.t} + \Delta W_{r.ch} = W_{out.r} \tag{10}$$

Water-salt balance equation of main river channel

$$W_{in.r}S_{in.r} - W_{wi}S_r + W_{out.t}\,S_{out.t} + \Delta W_r S_r = W_{out.r}\,S_{out.r} \tag{11}$$

Where $W_{in.r}$ and $S_{in.r}$ = river channel inflow and it's salt content; $W_{out.r}$ and $S_{out.r}$ = river channel outflow and it's salt content; $W_{out.l}$ $S_{out.l}$ = return flow from lands to the river channel and it's salt content; $W_{wi.r}S_r$ = water intake from river channel and it's salt content; $\Delta W_{r.ch}S_r$ = water storage in river channel and it's salt content.

Among the parameters effective in WSB, both parameters, precipitation and evaporation, are more independent and variable and the other parameters are estimated with respect to these two parameters (Ismaylov,1996).

Methodology

Content of reserved moisture in aeration zone and alterations in water table are determined on inflow and outflow of moisture basis in saturation and aeration zones. If content of inflow induce to increase in soil moisture (higher than field capacity) water table increases ($-\Delta H_{wt\,(1)}$) and due to moisture exchange from saturation to aeration zones, water table gets down ($+\Delta H_{wt\,(2)}$). Some other parameters such as drainage and outflow from underground result in decrease water table ($\Delta H_{wt\,(3)}$). General changing in water table is equal to algebraic amount of $-\Delta H_{wt\,(1)}$, $+\Delta H_{wt\,(2)}$ and $+\Delta H_{wt\,(3)}$. In aeration zone, due to output and input of water, moisture store alters from minimum to maximum rate. These two rates (at least and up most moisture) are explained by field capacity (Fc) and permanent wilting point (PwP).

Difference between FC and PwP shows the water holding capacity in soil (WHC).

$$WHC = (Fc\text{-}PwP) \times D \tag{12}$$

$$WHC = (w_{ae.i} - PwP) \times D \qquad \text{if} \qquad (W_{ae.i} < FC) \tag{13}$$

Where D = soil layer depth.

In general, the amount of entering water from aeration zone to saturation zone which induces an increasing to water table is equal to:

$$h_{ae.gr} = \begin{cases} 0 & \textit{if} \quad h_{in.ae} \le h_{fc} \\ h_{ae.i} + h_p + h_{wi} - h_{fc} & \textit{if} \quad h > h_{fc} \end{cases} \tag{14}$$

Where $H_{t.i.n.ae}$ = total input water to aeration zone; h_{wi} = content of irrigating water; h_{fc} = content of water in field capacity condition; h_{pwp} = content of water in permanent wilting point condition.

In saturated zone, inflow from ground water($h_{in.gr}$) and infiltration from irrigating channels ($h_{inf.ch}$) cause increase of water table in this zone. Total input to this zone ($h_{t.in.ag}$) is:

$$h_{t.in.su} = h_{ae.su} + h_{in.su} + h_{inf.ch} \tag{15}$$

and the amount of increase in water table is:

$$\Delta h_{(1)} = (h_{ae.su} + h_{in.gr} + h_{inf.ch}) / \mu \tag{16}$$

Where μ is specific yield.

In order to determination of aeration zone enrichment through saturation zone, the Averianov empirical formula is used (Averianov, 1956).

$$h_{su.ae} = \begin{cases} h_{iva.o}\left(1 - \dfrac{H_{wt(1)}}{H_{wt.cr}}\right)^n & if \quad H_{wt(1)} \langle H_{wt.cr} \\ 0 & if \quad H_{wt(1)} \geq H_{wt.cr} \end{cases} \tag{17}$$

Where $H_{wt.cr}$ = the maximum depth in which direct evaporation from ground water is carried out; n = a coefficient dependent to type of soil which varies from 1 to 3; $h_{iva.\ 0}$ = potential evaporation.

Through input of under saturated zone to aeration zone, water table (H_{wt}) declines.

$$\Delta h_{(2)} = H_{su.ae} / \mu \tag{18}$$

$$H_{Wt\,(2)} = H_{wt\,(1)} + \Delta H_{(2)} \tag{19}$$

After the mentioned moisture exchange, amount of moisture in aeration zone alters from initial condition ($h_{ae.i}$) to final condition ($h_{ae.f}$).

$$h_{ae.f} = h_{ae.i} + h_p + h_{wi} + h_{su.ae} - h_{iva}\text{-}h_{ae.su} \tag{20}$$

Outflow of saturation zone through drainage in agricultural lands, and by pumping through wells increase water table. The following formula expresses the relation between outflow from underground water and water table.

$$H_{out.su} = f\,(H_{wt\,(2)}) \tag{21}$$

Final alteration in water table can be written as:

$$H_{wt.f} = H_{wt(2)} + (h_{out.su})/\mu \tag{22}$$

Regard salt balance, content of salts exist in saturation zone charges through aeration zone or inflow to this zone and salts in aeration zone are transferred from rainfall and irrigating water. The following mathematical relation expresses the content of input salts from aeration zone to saturated zone.

$$S_{ae.su} = \frac{S_{ae.i}h_{ae.i-1} + S_{wi}h_{wi.i} + S_{p.i}h_{p.i}}{h_{ae.i-1} + h_{wi.i} + h_{p.i}} \tag{23}$$

Where $h_{ae.i-1}$ and $S_{ae.i-1}$ are initial moisture in aeration zone and content of salts in initial condition (g/lit); $S_{p.i}$ and S_{wi} are content of salts in precipitation and salts exist in irrigating water (g/lit).

After infiltration of water to saturated zone salt content in this zone is as below:

$$S_{gr.i} = \frac{(s_{gr.i-1} \times \mu(H_{\max} - h_{wt.i-1}) + S_{ae.gr.i} h_{ae.gr.i} + S_{iw.i} h_{\inf.ch})}{\mu(H_{\max} - h_{wt.i-1}) + h_{ai.gr.i} + h_{\inf.i}} \tag{24}$$

Where H_{max} = maximum drop off in water table (in the area under study); $\mu(H_{max}-h_{wt.i-1})$ = water volume that participate in water exchange process and S_{su} = content of salt in saturation zone.

Content of salt exist in aeration zone at end of water transfer process is expressed as below:

$$S_{ae.e} = \frac{S_{ae.i} h_{ae.i} + S_{p.i} h_{p.i} + S_{wi.i} h_{wi.i} + S_{su.ae.i} h_{su.ae.i} - S_{ae.su.i} h_{ae.gr.i}}{h_{ae.f}} \tag{25}$$

Sum equations from (4) to (25) allow determining WSBM components in a watershed basin. Integration of all the above mentioned equations in a frame of calculating chart makes an algorithm by which the theoretical conditions in a watershed basin are changed to real conditions which it make the base of IWSBM. On algorithm basis WSBM, parameters WSB are calculated in lands and, main river. The inputs IWSBM model are: soil specifications in moisture exchange zone such FC, PWP and critical depth in water table, specifications of technical irrigating system such as delivery and application efficiencies (E_d,E_a), content of initial moisture in land surface, aeration zone and water table at the beginning of study (first month of first year) (Sadatinejad,2001).

The other input parameters are: precipitation ($h_{p.i}$), evaporation from land surface ($h_{iva.i}$), lateral inflow ($h_{lw.i}$)', input ground water inflow ($h_{in.gr.i}$), main river inflow ($h_{in.r}$) and water intake for irrigation ($h_{wl.ag}$). Unit for all the abovementioned parameters is mm/month.

In computing processes of IWSBM the below parameters are continuously calculated: Loss of water from irrigating channels ($h_{inf.i}$), rising water table due to water infiltration through irrigating channels ($\Delta H_{wt(1)i}$), accumulation of moisture in aeration zone due to water table rising ($h_{ae(1)i}$), input moisture through infiltration of precipitation and infiltration through irrigating channels, water table alterations (ΔH_{wt}), amount of moisture in aeration zone after evaporation from this zone($h_{gr.ai.i}$), evaporation from under ground water, outflow from ground water to main river ($h_{out.gr.i}$), water table at the end of calculation time ($h_{t.wt.f.i}$), moisture content in aeration zone at the end of calculation ($h_{ae.e.i}$), outflow from surface and under ground lands to main river ($h_{out.l.i}$) and outflow at basin outlet ($h_{out.r.}$). By this method calculation of water balance in sections of basin (lands and river) in first month and first year are calculated and it is repeated for the coming years.

For calculation of salt balance the input data are: Content of precipitation salts, content of irrigating salts, content of salts in underground flow and main river at entrance section, content of salts in aeration zone at beginning of calculations ($S_{ae.i}$) and initial salts content in saturation zone ($S_{su.i.i}$). WSBM output data are: salt content in saturation zone due to salt input from lateral tributary stream ($\Delta S_{su(1)}$), salt content in saturation zone after infiltration of water through irrigating channels and precipitation($\Delta S_{su(2)}$), content of salt in saturated zone after inflow from aeration zone($\Delta S_{su(3)}$), salt content in aeration zone after inflow from underground zone($Sai_{(1)}$)h, salt content of outflow from underground water to main river

($S_{out.gr.i}$), salt content of outflow from surface and under ground lands to main river ($S_{out.l.i}$) and salt content of outflow at basin outlet ($S_{out.r}$).Like the method mentioned for water balance, after calculations for first month, it repeated for the other months and years. Algorithm Model of Water and Salt Balance has been prepared as a package (IWSBM) to use in PC computers. Input data as a constant and balance parameters in from tables are given to the model. Out put of the models are Tables and graphs for WSB parameters.

The Model Verification

For verification in IWSBM model, Syrdarya watershed basin (in Uzbekistan) was chosen that has an area around 24150 square kilometers. Eighteen-years hydrometeorological data (1968-1986) used for verification of the model. The drainage information used in the model comprise water table at the end of each month from 1968-1981.

For calculation of WSB in the Syrdarya watershed basin, content of salt (g L^{-1} $month^{-1}$) in main river and precipitation, underground water, and Lateral tributary stream were considered and given to the model. Invariable input data used in the model (IWSBM) in Syrdarya Basin are shown in Table 1.

For verification of model, estimated data was evaluated with observational data using the below criteria:

1- Correlation coefficient (r_{mo}) between estimating and observational water-salt balance components.

2- relative error

$$\left|1-\frac{\sigma_m}{\sigma_o}\right| = 1-\sqrt{\frac{\sum\left(\chi_{im}-\overline{\chi_m}\right)^2}{\sum\left(\chi_{io}-\overline{\chi_o}\right)^{2)}}} \tag{26}$$

Where σ_m = standard deviation of estimating data; σ_o = standard deviation of observation data; X_{im} = estimating parameters in a given month; $\overline{\chi_m}$ = mean of estimating parameters; X_{i0} = observed parameter in a given month; $\overline{\chi_o}$ = mean of observed parameter in a given month.

3- Relative error in calculated parameters $$A = \frac{\chi_{im}}{\chi_{io}} \times 100 \tag{27}$$

The model can be verified and eventually used in watershed basins, if the following conditions are met in the criteria: $|r_{mo} 1 \geq 0.8|$, $|1- 1- (\sigma m / \sigma 0)| \leq 0.30$, A≤10-20% (Ismaylov,1995).

On above criteria basis observational and estimating parameters are evaluated. In this study, the outflow from Syrdarya River on Forghana Valley and its content of salts are tested by the model.

Table 2 shows predicting and observational outflow and it's salt content in Syrdarya river. With respect to the results from these results, good agreement between predicting and observational data exists (for outflow: r_{mo} = 0.99> 0.80, $\left|1-\frac{\sigma_m}{\sigma_o}\right| = 021 \langle 03$, A=7.7% and for Salt r_{mo} = 0.84>0.8, $\left|1-\frac{\sigma_m}{\sigma_o}\right| = 0.62 \rangle 0.3$, A= +13.8%).

Figure2 shows the agreement between estimated and observed outflow from Syrdarya River. It is necessary to mention in some special years amount of error reach to 20-40%. For conformity of estimated underground water data at the end of each month and it's comparison with observational data, a good relation was observed. Correlation coefficient (r_{mo}=0.929) shows a strong conformity between estimating and observational data.

Conclusions

Table 2 shows that IWSBM for estimation of the balance in watershed basin is précised. Although this model is not highly precise for estimation of salt. Nonetheless, imitating model can be used to investigate the effect of agricultural activities on content of salts in river flow. Verification results show that, in addition of convenience the use of the IWSBM, it has enough efficiency to estimate of outflow and water table. By this model and using hydrometeorological and irrigating data (are accessible in watershed basin), a suitable estimation could be available for WSB basin and this subject is important for estimation of anthropological activities in water and soil resources in watershed basin.

References

Averianov S.F., Irrigated agriculture in Europe parts of SSUR, AN SSUR publishes, 1965. p. 151.

Averianov S.F., Effects of irrigation system in ground water regime, AN SSUR publish, 1956. p. 447.

Budagovsky A.I., Golubash T.Yu. Influence of water factor on the production process of vegetable covered, Water resources, Volume 21,№ 2, 1994. pp.133-143.

Budagovsky A.I.Basis of calculation methodic of irrigation norm and regime, Water resources, № 1, 1998. p. 38-48.

Budagovsky A., Djogan L.Ja. Mean of consistent making more precise of calculation methodic of irrigation norm, Water resources, № 6, 1980. pp. 29-51.

Golubash T. Yu., Ismayilov G, Kh., Lazareva E.V. Reclamation block in the water economic model of arid zone, Water resources, № 5, 1989. pp. 144-155.

Ismaylov G. Kh., Sensova n.I. Simulation of water and salt regime formation of an area: the Aral Sea Basin case study, Water resources, vol. 23, № 5, 1996. pp. 616-627.

Ismaylov G. Kh., Sensova n.I. Anthropogenic effects on the regime and quality of natural waters in irrigated regions., Environmental and socio-economic consequences of water resources development and management: proceeding of the Moscow symposium(15-20 may 1995).-UNSCO. Paris, 1996. pp.65-68.

Kharchenko S. I. Hydrology of irrigated lands. Leningrad, hydrometeopublish, 1975. p. 342.

Sadatinejad,S.J., methodical approach for construction imitating water-salt model: proceeding of the second international Iran and Russia conference" Agriculture and Natural Resources",Moscow,2001. pp. 372-375.

Sensova N.i. A method for prospective assessment of the water-salt balance of an irrigated area, Water Resources, vol.21, № 3,1994. pp.21-270.

Yeliseeva I.I, Neverozhkina L.I.,, Statistical theory with foundations of probability theory, Unitypublish, Moscow,2001. p. 446.

Zone of Flow Formation

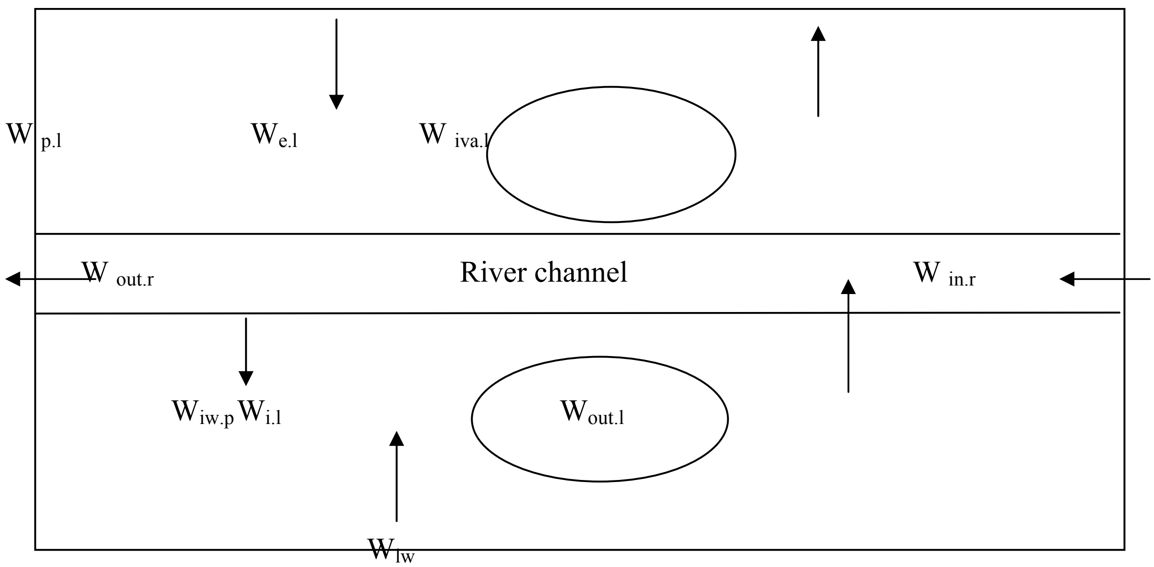

Figure 1. Schematic presentation of river basin.

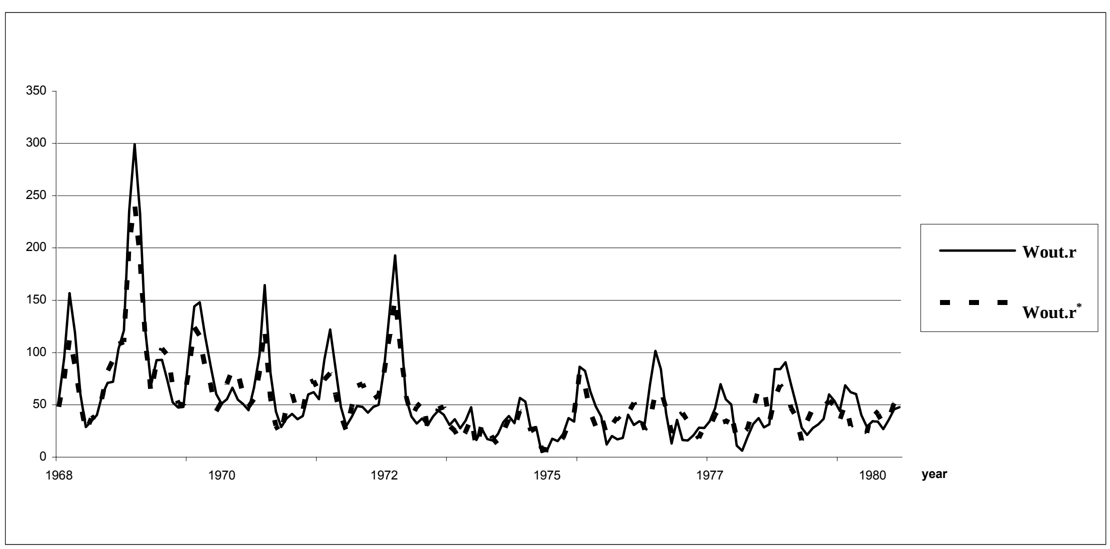

Figure 2. Conformity of outflow in Syrdarya River in both calculation and observational status Wout.r – observation data, Wout.r*- predicting data.

Table 1. Inputs data used in IWSBM model in Syrdarya basin.

h_{wt} (mm)	$H_{ae.i}$ (mm)	$S_{ae.i}$ (g /lit)	$S_{gr.i}$ (g/lit)	Fc	PWP	H_{wt}.(mm)	μ	E_d	E_{at}
109	541	1	1.25	0.69	0.34	300	0.17	0.69	0.8

Table2. Comparison between estimating data and observed data.

Year	Syrdarya River outflow			Salt content of Syrdarya River outflow			Water table in end of year		
	Observation data	Predicting data	A%	Observation data	Predicting data	A%	Observation data	Predicting data	A%
1968/69	820	896	+9,3	-	0,88		153	169	+10,4
1969/70	1383	1488	+10,8	-	0,84		164	170	+3,6
1970/71	917	975	+10,6	-	0,87		175	180	+2,8
1971/72	707	756	+6,9	1,04	1,00	-3,8	178	183	+2,8
1972/73	695	708	+1,9	1,20	1,02	-15,0	176	181	+2,8
1973/74	807	862	+6,8	1,03	0,92	-10,7	189	186	-2,6
1974/75	290	346	+19,3	1,24	1,20	-3,2	194	200	+3,1
1975/76	288	334	+16,0	1,28	1,31	+2,3	199	205	+3,0
1976/77	572	490	-4,3	1,45	1,36	-6,2	201	196	-2,5
1977/78	441	486	+10,2	1,58	1,35	-14,6	188	197	+4,8
1978/79	460	420	-8,7	1,34	1,61	+20,1	192	192	0
1979/80	570	638	+11,9	1,24	1,39	+7,8	188	188	0
1980/81	462	528	+14,3	1,73	1,70	-1,7	184	184	0
1981/82	656	689	+5,0	1,60	1,66	+3,8	-	-	-
1982/83	589	649	+10,2	1,59	1,88	+18,2	-	-	-
1983/84	440	565	+28,4	1,91	2,41	+26,2	-	-	-
1984/85	524	597	+13,9	1,87	2,67	+42,8	-	-	-
1985/86	470	561	+19,4	3,17	3,92	+23,6	-	-	-
Среднее	613	666	+8,6	1,46	1,64	+12,3	183	187	+2,2
σ	259	272		0,30	0,71		14	11	
Cv	0,42	0,41		0,21	0,44		0,08	0,06	
r_{mo}		0,990			0,906			0,926	
$\left\|1-\frac{\sigma_м}{\sigma_o}\right\|$		0,05			1,36			,22	

Application of SWAT and APEX Models Using SWAPP (SWAT/APEX Program) for the Upper North Bosque River Watershed in Texas

Ali Saleh[1]
[1]Texas Institute for Applied Environmental Research, Tarleton State University. P.O. Box T410, Stephenville, Texas, 76401. Email: saleh@tiaer.tarleton.edu.

Abstract

In response to the Clean Water Act, in the early 1970s, the Agricultural Research Service (ARS) branch of United States Department of Agriculture (USDA) initiated the development of several processed-based nonpoint source models. These models are used to assess and evaluate various BMPs (best management practices) at field (using the Agricultural Policy/Environmental eXtender, APEX) and watershed (using the Soil Water Assessment Tool, SWAT) levels. However, these models are capable of simulating a limited number of scenarios individually. For example, APEX is capable of simulating scenarios such as multi-cropping, filter strips, and farm-level animal production systems, which are difficult to simulate in SWAT. Therefore, in this study the SWAPP (SWAT/APEX Programs) program was developed to facilitate the simultaneous use of these two models. The SWAT (version 2000) and APEX (version 2110) models were applied using the SWAPP program to the upper North Bosque River (UNBR) watershed located in central Texas. Flow and loadings (sediment and nutrients) from various land uses, such as cropland and pasture, are simulated by APEX and then routed by SWAT within the SWAPP program. SWAT alone (SWAT-A) and combined SWAT and APEX models within the SWAPP program were calibrated and verified against historical monitoring data collected within UNBR watershed. The UNBR watershed was simulated from 1988 through 1999. Model output was calibrated for flow, sediment, and nutrients measured at the outlet of UNBR watershed for the period of January 1994 through June 1995 and verified for the period of July 1995 to July 1999. The results of this study show that output from SWAT-A and SWAPP are similar and close to measured values, which indicates that the simulated field conditions by APEX can be routed by SWAT at the watershed level using the SWAPP program.

Introduction

In response to the Clean Water Act, in the early 1970s, the Agricultural Research Service (ARS) branch of United States Department of Agriculture (USDA) initiated the development of several processed-based nonpoint source (NPS) models. Knisel (1980) developed the field scale CREAMS (Chemical, Runoff, and Erosion from Agricultural Management Systems) model to simulate the impact of land management on water, sediment, nutrients, and pesticides leaving the edges of fields. The EPIC (Erosion-Productivity Impact Calculator) model was initially developed (Williams, 1990) to simulate the impact of erosion on crop productivity, but has evolved into a comprehensive agricultural management, field scale, nonpoint source loading model. The APEX (Agricultural Policy/Environmental eXtender) model was developed for use in entire farm/small watershed management (Williams et al., 2000). The individual field simulation component of APEX is taken from the EPIC model. Continuous time watershed models such as SWRRB (Simulator for Water Resources for Rural Basins) (Williams, 1990 and Arnold et al., 1990) were developed to simulate NPS pollution from watersheds. However, these models lack sufficient spatial detail. Therefore, SWAT (Soil Water Assessment Tool, Arnold et al., 1998) was developed to simulate stream flow in much larger basins, allowing for the division of a basin into hundreds or thousands of grid cells or subwatersheds. This model is a continuous time model that operates on a daily time-step. The SWAT model was developed to evaluate management effects on water quality, sediment, and agricultural chemical yield in large ungauged basins. SWAT is based on a command structure for routing runoff and chemicals through a watershed. These commands allow the user to route and input measured data (e.g. weather) and point source pollution loadings. The major components of SWAT include hydrology, weather, sedimentation, soil temperature, crop growth, nutrients, pesticides, and agricultural management.

The hydrology component of SWAT includes surface runoff, percolation, lateral subsurface flow, groundwater flow, evapotranspiration, and transmission loss subroutines. The minimum weather inputs required by SWAT are maximum and minimum air temperature and precipitation. Sediment yield is estimated by the Modified Universal Soil Loss Equation, MUSLE (Williams, 1975). Daily average soil temperature is simulated using the maximum and minimum annual air temperatures, surface temperature, and damping depth. SWAT is also able to accept output data from other simulation models such as APEX.

APEX is a field-scale model designed to simulate edge-of-field nutrient concentration, runoff volume, and nutrient loadings from specific field management practices on a daily time-step for multiple fields within one simulation. APEX simulates weather, hydrology, soil temperature, erosion-sedimentation, nutrient cycling, tillage, dairy management practices, crop management and growth, pesticide and nutrient fate and transport, as well as costs and returns of the various management practices. APEX is applicable to a wide range of soils, climates, and cropping systems.

The advantages of using APEX at the field level within the SWAT program are: 1) APEX can provide predicted values at a more precise level than SWAT; 2) simultaneous double cropping simulation within SWAT is not possible at this time, while APEX is capable of this function; 3) scenarios such as “filter strips” are simulated within SWAT by adjusting the coefficients based on the literature, while within APEX filter strips are simulated based on physically-based functions; and 4) APEX is capable of simulating conditions in more detail, such as animal productions and economic impacts of BMPs (best management practices), and wind erosion, which is not possible with SWAT program. The strengths of SWAT are: 1) the capability of generating the required databases through the AVSWAT interface (Di Luzio et al., 2002); 2) the routing function, which allows the user to simulate various land uses and route outputs to the outlet of the watershed; and 3) the capability of accepting input from other models, such as APEX, and point sources, such as wastewater treatment plants.

Saleh et al. (2000), Osei et al. (2000), and Gassman et al. (2001) are among those who have taken advantage of the capabilities of the SWAT and APEX models. In these studies an environmental baseline and BMPs at the field level were simulated in APEX and the results and remaining land uses within a watershed were then routed to the SWAT model. This arrangement provided the opportunity to simulate scenarios, such as filter strips, at the field level using APEX, which is not possible in SWAT. Due to the manual transformation of files from SWAT to APEX, however, the simulation process was often tedious and subject to a number of assumptions that could have affected simulation results. Hence, there was a need to establish a direct link between SWAT and APEX where the simulation process is automated and results are less subject to errors. Recently, Williams et al. (2003) provided a program to convert SWAT files to APEX format for simulations. However, many parts of this program are still performed manually and a direct linkage of these two models is missing. Also, the program has not been verified by any measured data. Therefore, this study was conducted to: 1) develop an automated program to facilitate the simultaneous use of SWAT and APEX; and 2) test this program using the measured data from the upper North Bosque River (UNBR) watershed in central Texas.

Methodology

SWAPP Program Description

The SWAPP process starts with data files created by the AVSWAT program. The SWAPP process occurs in four major phases:

- Phase 1. By using the SWAT-APEX subprogram of SWAPP, all of the required APEX data files for selected land uses are transferred to proper (APEX) format. These files include management, soil, subfile, weather, and general databases including crop.dat, fert.dat, parm.dat, and till.dat data files. Also, the original areas simulated by SWAT are reduced to account for the land use areas simulated by APEX.
- Phase 2. During this phase the selected land uses that will be simulated by APEX and SWAT input files (.SWT) are produced.
- Phase 3. In this phase the output files (.SWT) from APEX are accumulated at the subbasin level using the APEX-SWAT subprogram of SWAPP. The results obtained from this process are input into SWAT as point sources at the subwatershed level.
- Phase 4. During the last phase, the SWAT program, which includes the output files from APEX, is operated. The results of simultaneous SWAT and APEX simulations are presented in the SWAT *.RCH file.

Watershed Description

The UNBR watershed is defined as the contributing drainage area above sampling site BO070 located on the North Bosque River at Hico, Texas. The UNBR watershed is 98% rural, with the primary land uses being rangeland (43%), forage fields (23%), and dairy waste application fields (7%) (McFarland and Hauck, 1999). Dairy production is the dominant agricultural activity; other important agricultural enterprises include range-fed cattle, pecan, peach, and forage hay production (peanut production has been phased out over the last decade). The watershed lies primarily in two major land resource areas, the West Cross Timbers and Grand Prairie. The soils in the West Cross Timbers are dominated by fine sandy loam with sandy clay subsoil, while calcareous clays and clay loam are the predominant soil types in the Grand Prairie (Ward et al., 1992). The elevation in the watershed ranges from 305 to 496 meters.

The City of Stephenville (population 16,000) and portions of the smaller cities of Dublin and Hico are located within the UNBR watershed. The Stephenville wastewater treatment plant (SWTP), with an average discharge of 6,380 m^3 per day during the simulation period, is the only point source permitted to discharge in the watershed.

The average annual precipitation in the area is approximately 750 mm and the average daily temperature ranges from 6^{o}C in winter to 28^{o}C in summer (McFarland and Hauck, 1999).

Winter and fall rainfall is induced by continental polar fronts, which produce low-intensity, long-duration storms. In the spring and summer, the majority of rainfall events are squall line thunderstorms, which produce high-intensity, short-duration storms that can result in flooding in smaller watersheds.

A consistent period of monitoring from October 1993 through December 2000 was available for the BO070 stream site for use in model calibration and verification. The BO070 sampling site was instrumented with an automated sampler to monitor storm events. Monthly and biweekly grab sampling was also conducted to represent base flow water quality characteristics. Routine chemical analyses of water samples using USEPA approved analytical methods included total suspended solids (TSS), total Kjeldahl-N (TKN), ammonia-nitrogen (NH_3- N), nitrate-nitrogen (NO_3-N) plus nitrite-nitrogen (NO_2-N), total-P, and soluble reactive phosphorous (PO_4-P) (USEPA, 1983). Particulate-P was estimated by subtraction of PO_4-P from total-P and organic-N was determined by subtraction of NH_3-N from TKN. Herein, total-N is defined as the sum of TKN, NO_3-N, NO_2-N, and NH_4-N. Water levels monitored at each stream site at five-minute intervals were combined with site-specific stage-discharge curves to develop a history of flow. Flow information and water quality data were then combined using a midpoint rectangular integration method to calculate nutrient and TSS loadings at each site. Specifics of the monitoring program and loading calculations are presented in McFarland and Hauck (1999).

SWAT and APEX Models Data Input Descriptions

Topographic, land use and cover, and soil data required by SWAT and APEX for this study were generated from GIS maps using AVSWAT. Topographic data were obtained from an existing 1:24,000 scale United States Geological Survey (USGS) DEM and digitized USGS 7-1/2 minute quadrangle maps. A subwatershed map required for SWAT and APEX was then generated from the topographic data with consideration of current locations of sampling sites. Based on this procedure, the UNBR watershed was divided into 41 subwatersheds.
The land use categories in the watershed were developed from the classifications of Landsat Thematic Mapper images created from an overflight taken on August 28, 1992. Ground truthing was performed to assist in the imagery classification and to verify the final results. The minimum mapping unit for land use characterization was about 0.1 hectare. Land use categories included in the final land use map were rangeland, forage fields (Coastal Bermuda grass and some double-cropped wheat and Sudan grass), woodland (trees and heavy brush), orchards and groves, peanuts, urban, and water. The size and location of animal waste application fields were obtained from the Texas Commission on Environmental Quality (TCEQ) dairy permits and available waste management plans.

Soils data used for this study were determined using a digital soil map of the UNBR watershed developed by the USDA-NRCS (1972). The major soil series in the watershed are the hydrologic group C Windthorst series (fine, mixed, thermic Udic Paleustalfs), the hydrologic group D Purves series (clayey, montmorillonitic, thermic Lithic Calciustolls), and the hydrologic group B Duffau series (fine-loamy, siliceous, thermic Udic Paleustalfs).

Daily rainfall data obtained from 14 gauges (including several National Weather Service and study associated sites, located throughout the watershed) were processed into the proper format for the simulation period. A similar procedure was used to convert daily temperature data available from the National Weather Service sites into the required SWAT and APEX input data files.

NO_3-N, NO_2-N, NH_4-N, NH_3-N, organic-N, particulate-P, and PO_4-P are common forms of nutrients simulated by SWAT and APEX. Based on surveys of local farmers the dairy waste application fields (WAF) were simulated in SWAT and APEX as receiving four applications of manure totaling an average annual rate of 35.8 t/ha. The nutrient content of manure included NO_3-N (0.17%), organic-N (2.18%), particulate-P (0.38%), and PO_4-P (0.66%). Other improved pasture fields, based on standard farming practice in the UNBR watershed, were assumed to receive four applications of N and P fertilizer at an annual rate of 336 and 49 kg/ha, respectively.

The measured daily loading of NO_3-N+NO_2-N, organic-N, PO_4-P, TSS, and flow from the SWTP were added as a point source to both models. The input data regarding the SWTP were determined from average daily discharge information reported by the treatment plant and biweekly and monthly water quality samples collected and analyzed by the Texas Institute for Applied Environmental Research.

The basic data files for APEX simulation, including subarea, management, weather, soil, control, and other required data were created through the SWAPP program. Manure and commercial N and P were applied in APEX at the same rate as those in SWAT to the surface and upper soil layers.

Model Simulations

The SWAT stand alone (SWAT-A) and combined SWAT and APEX within the SWAPP program were calibrated and validated using daily and monthly measured data from the UNBR watershed from January 1994 to July 1999 in two stages:

Stage 1 – SWAT-A Simulation for the UNBR Watershed

The flow, sediment and nutrient (NO_3-N, NO_2-N, organic-N, particulate-P, and PO_4-P) loading were simulated by SWAT-A for the UNBR watershed during the period of 1988 to 1999. The measured flow and loading data at the outlet of the UNBR watershed (site BO070) during January 1994 through June 1995 were used for calibration and from July 1995 through July 1999 were used for validation.

Stage 2 – SWAPP Simulation for the UNBR Watershed

The APEX and SWAT models within the SWAPP program were calibrated and validated for the same period as SWAT-A. The APEX output from simulation of selected land uses, including pasture and agricultural lands, were input as a point source into SWAT using the automated functions of the SWAPP program.

Measure of Model Performance

The predicted and measured values were compared using standard deviation and the Nash and Sutcliffe (1970) model efficiency (E). A value of E = 1.0 indicates a perfect prediction, while negative values indicate that the predictions are less reliable than if one had used the sample mean instead. In addition, the mean error (*ME*) was used. The *ME* measures bias where, the negative or positive *ME* indicate the under or over-prediction of simulated values, respectively.

Results and Discussions

Due to continuation of this research, the results presented here are limited to site BO070 (outlet of the watershed). The final report will include the results from other sites within this watershed.

Flow

The variation in average annual precipitation during the simulation period ranged from 600 mm in 1999 to 1200 mm in 1997, indicating the test of SWAT-A and SWAPP under different moisture regimes. Table 1 shows measured and simulated average, standard deviation, and *ME* of monthly daily-flow during the calibration (January 1994 through June 1995) and validation (July 1995 through July 1999) periods.

Table 1. SWAT-A and SWAPP mean, standard deviation (SD), and mean error (*ME*) of monthly daily flow, TSS, and nutrient loading at the outlet of UNBR watershed (BO070) during (a) calibration and (b) validation periods.

a)

Calibration Period	Measured		SWAT-A			SWAPP		
(01/94 - 06/95)	*Mean*	*SD*	*Mean*	*SD*	ME	*Mean*	*SD*	ME
Flow (M^3/s)	3.9	4.7	4.2	5.0	0.3	4.2	5.1	0.3
Sediment (t)	4323.4	7841.4	4324.3	5403.4	0.8	3010.6	3615.8	-1312.8
NO_3-N + NO_2-N (kg)	8162.6	8568.2	6907.6	7136.9	-1255.0	7579.3	9367.2	-583.3
PO_4-P (kg)	2048.2	3614.0	2406.2	3811.9	358.0	1950.6	3000.3	-97.6
Organic-N (kg)	17926.2	25394.0	17887.1	23838.8	-39.1	17523.0	21167.1	-403.2
Particulate-P (kg)	3543.3	4523.6	2186.4	3359.3	-1356.8	2544.3	3392.4	-999.0
Total-N (kg)	26088.8	33373.3	24794.7	30608.9	-1294.1	25102.3	30403.4	-986.5
Total-P (kg)	5591.5	7787.8	4592.7	7158.0	-998.8	4494.9	6302.4	-1096.6

b)

Validation Period	Measured		SWAT-A			SWAPP		
(07/95 - 7/99)	*Mean*	*SD*	*Mean*	*SD*	*ME*	*Mean*	*SD*	*ME*
Flow (M^3/s)	4.1	5.4	3.9	5.4	-0.2	3.9	5.5	-0.2
Sediment (t)	3735.3	9245.6	3737.3	5300.2	2.0	2730.1	3865.2	-1005.2
NO_3-N + NO_2-N (kg)	6924.7	10024.9	6535.6	9188.5	-389.0	7145.6	10472.7	220.9
PO_4-P (kg)	2631.3	3861.4	3151.3	6195.9	520.0	1936.1	3791.2	-695.2
Organic-N (kg)	17298.9	29548.9	19714.0	33818.4	2415.1	15774.7	26995.1	-1524.2
Particulate-P (kg)	3241.0	5891.6	2851.9	5764.6	-389.2	2662.1	4761.6	-578.9
Total-N (kg)	24223.6	38921.3	26249.6	42845.8	2026.0	22920.3	36628.4	-1303.2
Total-P (kg)	5872.4	9530.8	6003.2	11927.9	130.8	4598.2	8501.9	-1274.1

The average monthly daily-flow at the outlet of the UNBR watershed (BO070) simulated by SWAT-A (4.2 m^3/s, *ME* = 0.3 and 3.9 m^3/s, *ME* = -0.2 during the calibration and validation periods, respectively) and SWAPP (4.2 m^3/s, *ME* = 0.3 and 3.9 m^3/s, *ME* = -0.2 during the calibration and validation periods, respectively) are close to measured values (3.9 m^3/s and 4.1 m^3/s during the calibration and validation periods, respectively) (Table 1). Also, the trends in measured and predicted average monthly daily-flow by SWAPP at site BO070 are almost the same (E = 0.75 for SWAPP as compared to 0.72 for SWAT-A) as that of SWAT-A during the simulation period.

Predicted and measured TSS loading in the UNBR watershed indicates a significant TSS transport from the watershed (Table 1), as expected, since a major portion of the watershed is covered by erosive soils that are susceptible to significant erosion from stream banks. The average monthly TSS loading at site BO070 simulated by SWAT-A (4324.3 t, *ME* = 0.8 and 3737.3 t, *ME* = 2.0 during the calibration and validation periods, respectively) and SWAPP (3010.6 t, *ME* = -1312.8 and 2730.1 t, *ME* = -1005.2 during the calibration and validation periods, respectively) are close to measured values during the calibration and validation periods. The better prediction of SWAT-A is also reflected in higher E values obtained from SWAT-A (E = 0.64) than SWAPP (E = 0.49), indicating a better prediction of temporal variation of monthly TSS by SWAT-A during the simulation period (Figure 1). The lower model efficiencies for SWAPP are due to the under prediction of TSS during May 1994, September 1995, and March 1997. However, it is expected that the current calibration efforts will result in better TSS predictions by SWAPP.

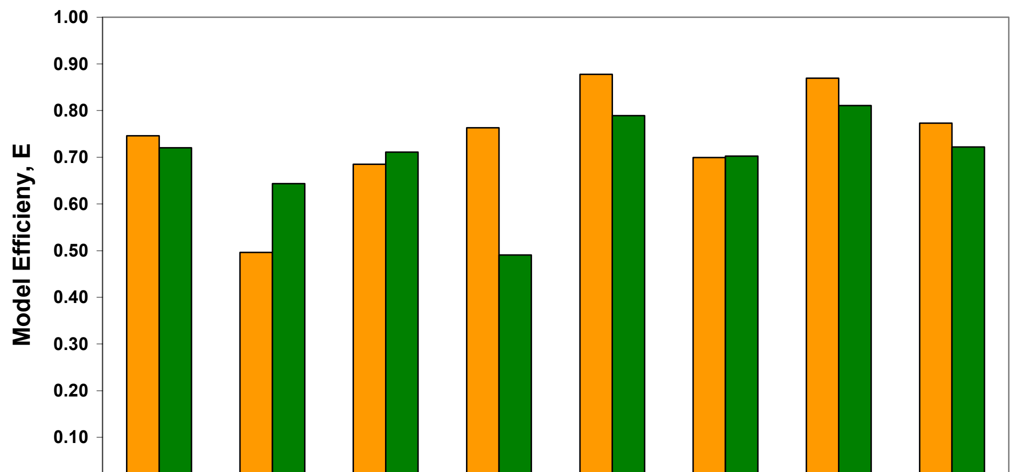

	Flow	TSS	NO_3-N + NO_2-N	PO_4	Organic-N	Particulate-P	Total-N	Total-P
SWAPP	0.75	0.50	0.69	0.76	0.88	0.70	0.87	0.77
SWAT-A	0.72	0.64	0.71	0.49	0.79	0.70	0.81	0.72

Figure 1. Model efficiency (E) of SWAT-A and SWAPP methods for monthly daily-flow, TSS, and sediment (TSS).

Nutrients

As was expected, the average monthly simulated NO_3-N+NO_2-N, organic-N, PO_4-P, and particulate P loading by SWAT-A and SWAPP at BO070 are close to measured values during both the calibration and validation periods (Table 1). However, the model efficiencies of SWAPP in predicting monthly nutrient loading are similar (NO_3-N+NO_2-N and particulate P) or higher (PO_4-P and organic-N) than those predicted by SWAT-A (Figure 1) at the outlet of the watershed.

To overcome the differences associated with different forms of N between laboratory analytical procedures and those described by equations within the models, the sum of simulated monthly NO_3-N+NO_2-N and organic-N (total-N) and PO4-P and particulate P were compared to the measured values. Table 1 shows a closer average and trend in total-N and total-P from the two models to measured values than the individual nutrient form comparisons. The efficiencies of both models also improved for total-N as compared to the individual nutrient forms. The better E values by SWAPP during the simulation period are due to the more refined calibration process at the field level by using APEX.

Summary and Conclusions

The watershed-scale SWAT stand alone (SWAT-A) and combined SWAT and field-scale APEX models within the SWAPP program were evaluated by comparing the predicted and measured flows, TSS, and nutrient loadings for the UNBR watershed; a watershed that is highly impacted by dairy operations. A GIS-based AVSWAT interface was used to generate much of the required data for both models. However, the SWAPP program was used to transfer data files of selected land uses within the watershed to and from SWAT and APEX.

SWAT-A and SWAPP provided reasonable, and relatively similar, predictions of average-monthly daily-flow during the calibration and validation periods, as indicated by the mean, standard deviations, mean error, and Nash-Sutcliffe model efficiencies for the outlet of the UNBR watershed. However, while prediction of TSS by SWAT-A was better, the trends in measured and predicted nutrient loading by SWAPP were closer to observed measurements.

The results of this study provide an opportunity to use field-scale models such as APEX to simulate the baseline and BMP scenarios (such as filter strips and multiple-cropping systems) at the field-level and use the SWAT program to route the results from APEX through a watershed stream system. The SWAPP program enables one to simulate conditions and BMP scenarios that are difficult to simulate at the field-level with SWAT at this time. The automated process of SWAPP makes it easy for users to transfer files to and from SWAT and APEX. Currently, the SWAPP program is being modified to link the latest version of SWAT (SWAT2003) and APEX (version 2110).

Acknowledgements

The author acknowledges support from the U.S. Environmental Protection Agency (USEPA) for providing funding for the project under contract No. R-82680701. The views expressed in this paper are not necessarily those of the USEPA. The author also acknowledges the valuable assistance of Mr. Oscar Gallego (Research Associate at Texas Institute for Applied Environmental Research, TIAER) on this project.

References

Arnold, J.G., R. Srinivasan, R.S. Muttiah, and J.R. Williams. 1998. Large area hydrologic modeling and assessment Part I: Model development. J. of the American Water Resource Assoc. 34(1):73-89.

Arnold, J.G., J.R. Williams, R.H. Griggs, and N.B. Sammons. 1990. SWRRB: A Basin Scale Simulation Model for Soil and Water Resources Management. Texas A&M Univ. Press, College Station, TX.

Di Luzio, M., R. Srinivasan, and J.G. Arnold. 2002. A GIS-Hydrological Model System for the Watershed Control of Agricultural Nonpoint and Point Sources for Pollution. Submitted to Transaction of ASAE

Gassman P.W., J. Abraham, A. Saleh, K. Keplinger, J.R. Williams. 2001. Simulation of nutrient losses from Chicken Litter Applications in East Central Texas with APEX. Presented at the ASAE Annual meeting. Sacremento, CA. April 30-May 2 2001

Osei, E., P. Gassman, and A. Saleh. 2000. Livestock and the Environment: A national Pilot Project: CEEOT-LP modeling for Upper Maquoketa River watershed, Iowa. Technical ReportTexas # PR0003. Stephenville, TX. Texas Institute for Applied Environmental Research Report, Tarleton State University.

Knisel, W.G. 1980. CREAMS, A field scale model for chemicals, runoff, and erosion from agricultural management systems. USDA, Conserv. Res. Rept. No. 26.

McFarland, A., and L. Hauck. 1999. Relating agricultural land uses to in-stream stormwater quality. J. Environ. Qual. 28:836-844.

Nash, J.E., and J.E. Sutcliffe. 1970. River flow forecasting through conceptual models. Part1 – A discussion of principles. J. Hydrol. 10:282-290.

Saleh A., J.G. Arnold, P. Gassman, L. Hauck, W.D. Rosenthal, J.R. Williams, and A. McFarland. 2000. Application of SWAT model for Upper North Bosque River Watershed. Transaction of the ASAE Vol. 43 (5):1077-1087.

USDA, Soil Conservation Service. 1972. National Engineering Handbook, Hydrology Section 4, Chapters 4-10.

USEPA. 1983. Method for chemical analysis of water and wastes. USEPA-600/4-79-020, Revised March 1983. Cincinnati, Ohio: USEPA, Office of Research and Development.

Ward, George, Joan D. Flowers, and Tina L. Coan. 1992. Final Report on Environmental Water Quality Monitoring Relating to Nonpoint Source Pollution in the Upper North Bosque River Watershed. Texas Institute for Applied Environmental Research, Tarleton State Univ., Stephenville, TX.

Williams, J.R. 1975. Sediment routing for agricultural watershed. Water Resource Bull. 11(5):965-974.

Williams, J.R. 1990. The erosion productivity impact calculator (EPIC) model: a case history. *Phil. Trans. R. Soc. Lond.* 329: 421-428.

Williams, J.R, J.G. Arnold, and R. Srinivasan. 2000. The APEX model. BRC Report No. 00-06. Temple, Texas: Blackland Research Center.

Williams, J.R. E. Wang., A. Meinardus, and W.L. Harman. 2003. Apex users guide (version 1310). Blackland Research Center, Temple TX.

A Modeling Approach for Evaluating the Water Quality Benefits of Conservation Practices at the National Level

C. Santhi*[1], N. Kannan[1], M. Di Luzio[1], S.R. Potter[1], J.G. Arnold[2], J.D. Atwood[3] and R.L. Kellogg[4]
[1]Blackland Research Center, 720 E. Blackland Road, Texas A&M University System, Temple, Texas, USA 76502. Email: csanthi@brc.tamus.edu
[2]United States Department of Agriculture-Agricultural Research Service, Temple, Texas, USA
[3]United States Department of Agriculture-Natural Resources Conservation Service, Temple, Texas, USA
[4]United States Department of Agriculture-Natural Resources Conservation Service, Beltsville, Maryland, USA

Abstract

The United States Department of Agriculture has initiated the Conservation Effects Assessment Project (CEAP) including a modeling effort to quantify the environmental benefits of conservation practices at the national scale in the United States. This paper focuses on the modeling approach consisting of the data sets, modeling components, and scenarios being used in the CEAP national assessment study. Data sets including weather, land use, soils, management practices, and farmer surveys were used to develop model inputs for the conterminous U.S. The modeling approach includes the farm-scale model Agricultural Policy/Environmental Extender (APEX) and the Soil and Water Assessment Tool (SWAT), along with the GIS databases. The APEX model was used to simulate conservation practices for cultivated cropland. Farmer surveys conducted on a subset of National Resource Inventory sample points provided information on current farming activities and conservation practices for APEX. Outputs from APEX will be input into the watershed scale model, SWAT in the HUMUS (Hydrologic Unit Modeling for the United States) system for routing the pollutants to the 8-digit watershed outlets. HUMUS/SWAT will be calibrated and validated using observed streamflow from the United States Geological Survey's (USGS) gauging stations and streamflow and pollutant data generated by the SPAtially Referenced Regressions on Watershed Attributes (SPARROW) model. The modeling system will be used to simulate in-stream effects for (1) a baseline scenario with conservation practices and (2) an alternative scenario without conservation practices. The off-site water quality benefits of conservation practices will be determined by comparing outputs of these scenarios for each 8-digit watershed. Benefits will be reported as reductions in in-stream concentrations and loadings of sediment, nutrients and pesticides, and reductions in the number of days that concentrations exceed human health and ecological thresholds.

Introduction

Since the 1930's, the United States Department of Agriculture (USDA) has implemented a wide range of conservation practices to assist landowners in conserving and improving soil, water, and other natural resources associated with agricultural lands. Although it is widely recognized that these conservation practices will protect the land and water resources, the environmental benefits of these practices have not been quantified at the national scale. Extensive literature and documentation exists on the effects of conservation practices at the field level. However, there is not adequate information available showing the quantitative benefits of conservation practices, especially, at the national scale. Hence, the USDA has initiated the Conservation Effects Assessment Project (CEAP) including a modeling effort to quantify the environmental benefits of conservation practices in the United States. Estimating these benefits will allow decision-makers and program managers to assess the benefits of the existing programs and to design new programs to more effectively and efficiently meet governmental goals (Mausbach and Dedrick, 2004).

Conducting field experiments or collecting long-term monitoring data to evaluate the effects of conservation practices is expensive and time consuming. It is also difficult to repeat the monitoring process without additional resources and time when corrections are warranted. In this context, a modeling approach is a potential option to assess the effects of conservation practices on water quality at different scales. Models can also be used to analyze various scenarios during the planning phase to improve the efficacy of conservation program implementation. This paper focuses on the modeling approach consisting of the modeling components, databases and scenarios being analyzed to assess the water quality effects in the CEAP national assessment study.

Methodology

HUMUS/SWAT Modeling Approach

The HUMUS (Hydrologic Unit Modeling for the United States) system is a national-scale modeling structure developed for the United States for making national and river basin scale resource assessments considering the current and future developments in soil, land and water management and issues related to point and non-point source pollution. The HUMUS system includes (a) basin-scale hydrologic model, the Soil and Water Assessment Tool (SWAT) (Arnold et al., 1998) to assess water quantity and water quality issues, and (b) databases of spatial and temporal data required for SWAT (Srinivasan et al., 1998). The HUMUS system was developed as part of the Resources Conservation Act Assessment (RCA) of 1997. The cooperators were the USDA and the Texas Agricultural Experiment Station (TAES) of the Texas A&M University System.

The HUMUS system follows the hydrologic unit accounting system of the United States. There are 18 major river basins, or 2-digit watersheds, in the conterminous U.S. (Figure 1). Each river basin is divided into several 8-digit watersheds, or Hydrologic Unit Codes (HUCs). There are 2,107 HUCs within the conterminous U.S. (Figure 2). The average area of a HUC is about 4,000 square kilometers. Approximately two-thirds of these HUCs have significant cropland acreage. Each river basin is treated as a watershed and each HUC is treated as a subbasin within the HUMUS/SWAT modeling structure. Each HUC consists of several soil-land use combinations or Hydrologic Response Units (HRUs).

For the CEAP national assessment modeling effort, revised HUMUS modeling approach is used for assessing the off-site water quality benefits of the conservation practices at the 8-digit watershed levels (Figure 3). The revised HUMUS modeling approach uses the HUMUS structure but with updated databases and a more recent version of SWAT (SWAT 2003). In addition, in the revised HUMUS modeling approach, SWAT is used to simulate the non-cultivated land and APEX (Agricultural Policy/Environmental Extender) (Williams et al., 2000) is used to simulate the conservation practices implemented on cultivated cropland.

The CEAP national assessment is primarily focused on cropland where most of the conservation practices are implemented. Hence, the CEAP approach uses the farm-scale model, APEX to simulate the various conservation practices implemented and the APEX output will be input into the watershed scale model, SWAT, to assess the off-site water quality benefits of these conservation practices. SWAT will simulate the non-cultivated land and route the pollutants from non-cultivated land and point sources along with the APEX pollutant outputs for cultivated land to the outlet of each 8-digit watershed and then to the river basin outlet (USDA-NRCS, USDA-ARS and TAES, 2004).

APEX is a physical process model and is an extension of the EPIC (Environmental Policy Impact Calculator) model (Williams et al., 1984). APEX has the capability to simulate several agricultural management and conservation practices in detail. APEX simulates agricultural management processes on multiple fields as well as the fate and transport of nitrogen, phosphorous, eroded soil and pesticides.

Databases Used

The HUMUS/SWAT system requires several databases such as land use, soils, management practices, and weather. For the CEAP effort, recently available data are processed to update the HUMUS/SWAT databases and prepare the SWAT input files for the entire country (Figure 3).

Land use: The 1992 United States Geological Survey (USGS) -National Land Cover Data Set (NLCD) is the spatial data currently available for land use at 30-m resolution for the entire country (Vogelmann et al., 2001). For the CEAP assessment, the 1992 USGS land cover data set will be used as the base, which includes agriculture, urban, pasture, range, forest, wetland, barren and water. For the calibration simulations, 1992 land use data will be used. For the CEAP baseline and alternative scenarios, 1997 land use conditions will be used. The 1992 USGS land cover data set is adjusted to represent 1997 land use conditions by using the relative changes in land use as determined by the 1992 and 1997 National Resource Inventory (NRI) data (Nusser and Goebel, 1997; USDA- Natural Resources Conservation Service (NRCS), 2000).

Soils: Each land use within an 8-digit watershed is associated with soil data. Soil data required for SWAT were processed from the State Soil Geographic (STATSGO) database (USDA-NRCS, 1992). Each STATSGO polygon contains multiple soil series and the aerial percentage of each. The soil series with the largest area was extracted and associated physical properties of the soil series were extracted for SWAT.

Topography: Topographic information on accumulated drainage area, overland field slope, overland field length, channel dimensions, channel slope, and channel length were derived from the DEM data in the previous HUMUS project (Srinivasan et al., 1998). It will be used in this modeling effort.

Management Data: Management data is important in the SWAT model. Management operations such as planting, harvesting, fertilizer application, manure and pesticides and irrigation water and tillage operations, along with timings or potential heat units are to be specified for various land uses in the management files. Management operations/inputs vary across regions. These data are being gathered for land uses such as pasture, hay and orchards that are simulated in SWAT from various sources such as the Agricultural Census Data and

USDA-National Agricultural Statistics Service's (NASS) agricultural chemical use data and Agricultural Extension Centers.

Weather: Measured daily precipitation and maximum and minimum temperature data sets from 1960 to 2001 will be used in this modeling approach. The precipitation and temperature data sets were created from a combination of point measurements of daily precipitation and temperature (maximum and minimum) (Eischeid et al., 2000) and PRISM (Parameter-elevation Regressions on Independent Slopes Model) (Daly et al., 2002). The point measurements data set is a serially complete (no missing values) data set (1895-2003) processed from the station records available from the NCDC (National Climatic Data Center). PRISM is an analytical model that uses point data and a digital elevation model (DEM) to generate gridded estimates of monthly climatic parameters. PRISM data are distributed at a resolution of approximately 4 km^2. Di Luzio (2005a) has developed a novel approach to combining the point measurements (station records) and the monthly PRSIM grids to develop the distribution of the daily records with orographic adjustments over each of the USGS 8-digit watersheds.

Other data such as solar radiation, wind speed and relative humidity will be simulated using the weather generator (Nicks, 1974; Sharpley and Williams, 1990) available within SWAT.

Point Source Data: Effluents discharged from the municipal treatment plants are major point sources of pollution. The USGS has developed a point source database for use in the 1992 SPARROW simulations and it will be used in the calibration runs. Point sources for a year near 1997 will be estimated using human population and it is assumed that these estimates are valid for 3-5 years before and after the year they were developed.

Atmospheric Nitrogen Deposition: Atmospheric deposition can be a significant component of nitrogen balance and contribution to plant growth and nitrogen runoff concentrations, especially in some of the non-agricultural land areas. Hence, estimates of nitrogen deposition (nitrate and ammonium) are to be incorporated into the SWAT and APEX models. Nitrogen deposition data set (loads and concentration) were developed from the National Atmospheric Deposition Program/National Trends Network (NADP/NTN) database (NADP/NTN, 2004), which consists of yearly deposition grids available for the entire nation. These data are processed for creating nitrogen deposition records for each of the 8-digit watersheds (Di Luzio, 2005b). Atmospheric deposition data is available from 1994 to 2001. For years prior to 1994, 1994 concentration levels will be assumed.

Model Calibration and Validation

Although SWAT inputs are physically based and can be obtained from existing landscape properties and conditions, there is still some uncertainty in the inputs that are not well defined such as curve number and the Universal Soil Loss Equation's crop cover (C) factor. Hence, there is a need to calibrate the model. Currently, there is not adequate water quality monitoring data available for model calibration at the 8-digit watershed level. The USGS has developed a regression model called SPARROW (SPAtially Referenced Regressions On Watershed attributes) to simulate flow and nutrients for the entire nation (Smith et al., 1997). SPARROW takes all of the relevant USGS stream monitoring data, watershed characteristics and various sources of nutrients, estimates of (a) runoff, sediment and nutrient loadings within each 8-digit watershed and (b) streamflow, and sediment and nutrients leaving the outlet of each 8-digit watershed into account. SPARROW estimates are based on 1992 land use. Thus, the HUMUS calibration will be performed using 1992 land use data. In addition to calibrating average annual flow and loads for each 8-digit watershed using SPARROW results, calibration of daily concentration distributions (i.e. 10, 25, 50, 85 and 90 percentiles) at a few selected gages within each of the 18 major river basins will be performed (Figure 3). This will give confidence in the model estimates on the number of days the pollutant concentrations exceed human health and ecological thresholds.

For validation, additional water quality data from a few USGS gages (not used in calibration) at major locations in the 18 river basins will be used. The models will be run without modification of input parameters. Stream gage data from years near 1992 will be selected to ensure that the 1992 land use data is representative of the measured concentration data. Model validation is critical for ensuring scientific support of the modeling approach.

For calibration and validation runs, the SWAT model will use APEX outputs for cultivated cropland obtained using the National Nutrient Loss and Soil Quality Database (NNL&SQ Database) (Potter et al., forthcoming). The 1992 land use conditions will be used for the SWAT calibration.

Scenario Analysis

The calibrated HUMUS/SWAT model will be used to develop scenarios to assess the effects of conservation practices on off-site water quality benefits (Figure 3). HUMUS/SWAT modeling inputs remain the same for all scenarios except for the variations in APEX outputs input into SWAT. SWAT will use the 1997 land use conditions for these scenarios.

Farmer surveys were conducted on a subset of National Resource Inventory sample points (30,000) to get information on current farming activities and conservation practices representing 2003-2006. Survey information will be used in APEX and the outputs will be used in Baseline and Alternative Scenario Analysis in SWAT.

CEAP Baseline Scenario: HUMUS/SWAT simulations will be made using the APEX output generated for cultivated cropland with conservation practices currently in use based on farmer surveys.

Alternative Scenario: HUMUS/SWAT simulations will be made using the APEX output generated for cultivated cropland using farmer surveys assuming no conservation practices were applied.

The off-site water quality benefits of conservation practices currently in use will be determined by comparing model outputs for the alternative scenarios to those of the CEAP Baseline for each 8-digit watershed. Benefits will be reported as (ii) reductions in in-stream concentrations and loadings of sediment, nutrients and pesticides, and (ii) reductions in the number of days that concentrations of nutrients or pesticides exceed human health and ecological thresholds.

Conclusions

Information on the quantitative benefits of conservation practices or programs on water quality is necessary for future policy planning, program development and resource allocation. Modeling is a feasible approach for assessing the effects of conservation practices on water quality benefits. This paper described the modeling approach that will be used for evaluating the water quality benefits of conservation practices at the national level in the CEAP assessment. This modeling approach is useful in addressing several “what if” situations that might be helpful for the conservation managers in planning and implementation of conservation practices.

Scenarios related to the conservation practices currently in use are discussed here. However, several other scenarios can be analyzed to support policy makers and conservation managers.

Acknowledgements

The authors acknowledge the United States Department of Agriculture for providing funding for this national scale modeling study as part of Conservation Effects Assessment Project. The authors also thank the researchers at the United States Geological Survey and other agencies for sharing the data required for this project.

References

Arnold, J.G., R. Srinivasan, R., R.S. Muttiah, J.R. Williams. 1998. Large area hydrologic modeling and assessment Part I: Model development. Journal of the American Water Resources Association 34(1), 73-89.

Daly, C., R.P. Neilson, and D.L. Phillips. 1994. A statistical-topographic model for mapping climatological precipitation over mountainous terrain. Journal of Applied Meteorology 33, 140-158.

Di Luzio, M. 2005a. Development of precipitation and temperature databases for the Conservation Effects Assessment Project: National Assessment. Blackland Research Center, Temple, TX. (Personal communication, March, 2005).

Di Luzio, M. 2005b. Development of atmospheric nitrogen deposition database for the Conservation Effects Assessment Project: National Assessment. Blackland Research Center, Temple, TX. (Personal communication, April, 2005).

Eischeid, J.K., P.A. Pasteris, H.F. Diaz, M.S. Plantico, and N.J. Lott. 2000. Creating a serially complete, national daily time series of temperature and precipitation for the Western United States. Journal of Applied Meteorology 39:1580-1591.

Mausbach, M.J., and A.R. Dedrick. 2004. The Length we go - Measuring environmental benefits of conservation practices. Journal of Soil and Water Conservation 59 (5): 96-103.

Neitsch, S.L., J.G. Arnold, J.R. Kiniry, J.R. Williams, and K.W. King. 2002. Soil and Water Assessment Tool Theoretical Documentation Version 2000. GSWRL Report 02-01, BRC Report 02-05, Published by Texas Water Resources Institute TR-191, College Station, TX. 498 pp.

National Atmospheric Deposition Program (NRSP-3)/National Trends Network. 2004. NADP Program Office, Illinois State Water Survey, 2204 Griffith Dr., Champaign, IL 61820

Nicks, A.D., 1974. Stochastic generation of the occurrence, pattern and location of maximum amount of rainfall. In Proceedings of symposium on Statistical Hydrology, Tuscon, Arizona, Aug-Sep 1971, USDA, Misc. Publ. No. 1275.

Nusser, S.M., and J.J. Goebel. 1997. The National Resources Inventory: A long-term multi-resource monitoring programme. Environmental and Ecological Statistics 4:181-204.

Potter, S., J.D. Atwood, L. Norfleet, J. Lemunyon, D. Oman, S. Andrews, R.L. Kellogg. 2005. Model simulation of soil loss, nutrient loss, and change in soil carbon associated with crop production. Texas Agricultural Experiment Station, Blackland Research and Extension Center and U.S. Dept. Agriculture-Natural Resources Conservation Service.

Sharpley, A.N., and J.R. Williams, eds. 1990. EPIC – Erosion Productivity Impact Calculator, Model Documentation, Tech. Bulletin No. 1768, USDA-ARS.

Smith, R.A., G.E. Schwarz, and R.B. Alexander, R.B. 1997. Regional Interpretation of water-quality monitoring data. Water Resources Research 33: 2781-2798.

Srinivasan, R., J.G. Arnold, and C.A. Jones. 1998. Hydrologic modeling of the United States with the Soil and Water Assessment Tool. International Journal of Water Resources Development 14(3): 315-325.

USDA-NRCS. 1992. State Soil Geographic (STATSGO) Database. United States Department of Agriculture-Natural Resources Conservation Service. (Available at http://www.ncgc.nrcs.usda.gov/products/datasets/statsgo/data/index.html)

USDA-NRCS. 2000. 1997 Natural Resources Inventory Summary Report. United States Department of Agriculture-Natural Resources Conservation Service, Washington DC. (Available at http://www.nrcs.usda.gov/technical/NRI/1997/summary_report/index.html.)

USDA-NRCS, USDA-ARS, and TAES. 2004. Review Draft of the Work Plan for the Cropland Component of the Conservation Effects Assessment Project (CEAP) National Assessment**.** United States Department of Agriculture-Natural Resources Conservation Service-Resource Inventory and Assessment Division, United States Department of Agriculture - Agricultural Research Service- Grassland, Soil & Water Research Laboratory and Texas A&M University, Texas Agricultural Experiment Station, Blackland Research and Extension Center.

Vogelmann, J.E., S.M. Howard, L. Yang, C.R. Larson, B.K. Wylie, and N. Van Driel. 2001. Completion of the 1990s National Land Cover Data Set for the Conterminous United States from Landsat Thematic Mapper Data and Ancillary Data Sources. Photogrammetric Engineering and Remote Sensing 67: 650–652.

Williams, J.R., C.A. Jones, and P.A. Dyke. 1984. A modeling approach to determine the relationship between erosion and soil productivity. Transactions of the American Society of Agricultural Engineers 27:129-144.

Williams, J.R., J.G. Arnold, and R. Srinivasan. 2000. The APEX Model. BRC Report No. 00-06, Texas Agricultural Experiment Station, Blackland Research and Extension Center, Temple, TX.

Figure 1. Major water resource regions/river basins in the Conterminous United States

Figure 2. The 8-digit watersheds (HUCs) of the Conterminous United States

INPUT DATA

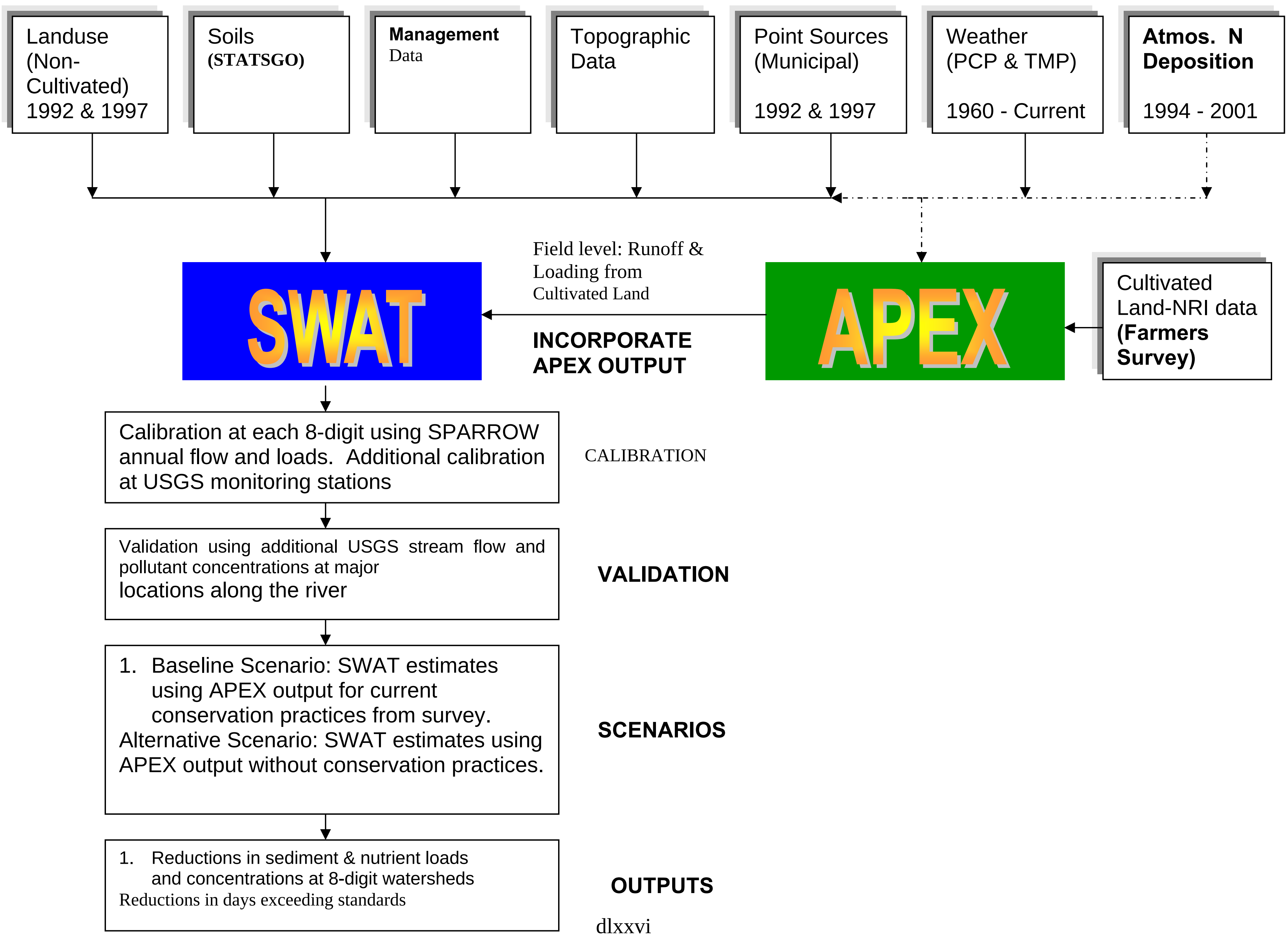

Figure 3. HUMUS/SWAT Modeling Approach for CEAP-National Assessment

Transport and Uptake of Cd, Cu, Pb and Zn in Calcareous Soil of Central Iran under Wheat and Safflower Cultivation – a Column Study

Gholamabbas Sayyad*[1], Majid Afyuni[1], Sayed-Farhad Mousavi[1], Karim C. Abbaspour[2], and Rainer Schulin[3]
[1]Isfahan University of Technology, College of Agriculture, 84156 Isfahan, Iran. Email: gsayyad@ag.iut.ac.ir
[2]Swiss Federal Institute for Environmental Science and Technology, EAWAG, Ueberlandstrasse 133 P.O. Box 611, 8600 Dübendorf, Switzerland.
[3]Institute of Terrestrial Ecology, ETHZ, Grabenstrasse 3/11a, CH-8952 Schlieren, Switzerland.

Abstract

Anthropogenic release of heavy metals (HMs) to the environment has resulted in a continuous buildup of HMs in soils. On the one hand, uptake and accumulation of HMs in plant tissue and in grains may lead to food chain transfer to humans, and on the other, transport of HMs through preferential paths to groundwater may cause groundwater contamination. The objectives of this study were to assess the mobility of Cd, Cu, Pb, and Zn under two plants with different rooting systems in the arid soils of Isfahan, Iran. The plants consisted of wheat (*Triticum aestivum*) with a fibrous rooting system and safflower (*Carthamus tinctorious*) with a taproot system. The study was conducted on undisturbed soil columns (Typic Haplocalcids). The top 10 cm of half of the columns were contaminated with Cd, Cu, Pb, and Zn at concentrations of 15, 585, 117 and 1094 mg kg^{-1}, respectively. The contaminated and uncontaminated columns were planted with wheat and safflower according to their previous cultivation history. Leachate was collected continuously and analyzed for HMs. After the crops were harvested, soil samples were collected at 10-cm intervals and analyzed for HNO3- and DTPA-extractable HM concentrations. Results showed that the presence of plants had a significant effect on HM transport. In planted columns, HM concentrations of the subsoils were greater than in fallow columns. Rooting systems also exhibited differences in HM movement, with safflower resulting in larger concentrations at deeper depths. In contaminated treatments, metal concentrations in discharge were significantly ($p<0.05$) more than controls. Metal uptake of plants in contaminated columns were also significantly ($p<0.05$) more than uncontaminated columns. The DTPA extractable levels of HMs were larger in the subsoil of contaminated soils, indicating that metals had moved from the surface layer in more soluble forms into the deeper zones in the profile. Cd was found to be the most mobile metal to plants and also in soil.

Introduction

Soil pollution by heavy metals (HMs) continues to create serious environmental risks (McBride 1998, Richards et al. 1998, Schwab et al. 2002). Industrial and agricultural activities have released large amounts of HMs into soils. The potential mobility of HMs in soils has been investigated for several decades (Emmerich et al. 1982, Richards et al. 1998). Many researchers have concluded that there is little evidence for HM leaching through the soil into the groundwater (Chang et al. 1984), but these studies have two important shortcomings. First, most of these studies were conducted in homogenized columns (Emmerich et al. 1982) not depicting real soil processes. Second, a lack of a noticeable increase in HM concentrations below the contaminated topsoil was considered as the evidence for HM immobility (Chang et al. 1984). Preferential flow has been shown to greatly increase the mobility and velocity of heavy metals and solute transport through the soil (Camobreco et al. 1996, Richards et al. 1998, Schwab et al. 2002). Another factor that could enhance metal mobility is transport of metals incorporated in soluble metal-organic complexes.

Having small permeability and large ion exchange capacity, clay and clay loams usually present a limited risk for groundwater contamination. The presence of macropores, however, can increase the hydraulic conductivity of these soils by several orders of magnitude (Topp and Davis, 1981) and may increase HM mobility through the soil by means of preferential flow.

Cropping systems can have a strong influence on the macroporosity and hydraulic properties. Plants may increase solute mobility through the soil (Caron et al., 1996), but may also retard HM leaching. From literature review it is obvious that the role of plants on metal mobility in the soil is not well understood. Also there is limited information about HM transport under plants with different rooting systems especially in calcareous soils, so there is a need for further studies. The objective of this study was to investigate the mobility of Cd, Cu, Pb and Zn under two crops with different rooting systems, wheat with a fibrous root system and safflower with a taproot system.

Methodology

The study was conducted using 24 undisturbed soil columns of 22.5 cm in diameter and 50 cm in depth in a greenhouse at Isfahan University of Technology. Soils (Fine, Mixed, Termic, Typic Haplocalcid) were sampled from two nearby farms at Kabotarabad Research Station of Isfahan Agricultural Research Center, 40 km southeast of Isfahan, central Iran, (3598500N, 572000E, UTM, Zone 39) with the elevation of 1750 meters and mean annual precipitation of 145 mm. One soil had in the previous year been cultivated with safflower and the other with wheat. Continuous macropores of 0.5-3 cm width were seen to extend from 25 cm to 60 cm depth in the field profile. The history of cultivation for the wheat farm in last four years was wheat-fallow-wheat-wheat and for the safflower farm was wheat-wheat-fallow-safflower.

In half of the columns (12), the upper 10 cm of soil was contaminated with metal solutions $CdCl_2$ (19.5 mgCd kg $^{-1}$dry soil), $CuSO_4$ (750 mgCu kg $^{-1}$ dry soil), $Pb(NO_3)_2$ (150 mgPb kg $^{-1}$ dry soil), and $ZnCl_2$ (1400 mgZn kg $^{-1}$ dry soil) by spraying and completely mixing the soil. The above values are the 50% of maximum permitted metal loading in soil established by the USEPA-503 regulations (1993). We sought to investigate metal transport and also metal uptake by plants in a large contaminated calcareous soil. After two weeks, three of the contaminated and uncontaminated wheat farm columns were sown with wheat, W+M and W, three of the contaminated and uncontaminated safflower farm columns were sown with safflower, S+M and S, and the remaining 12 were left fallow, Wf+M, Wf, Sf+M and Sf. During these weeks the columns were irrigated and the leachate was collected. The planting was done in accordance with the previous history of the cultivation in the field. Plants were seeded manually on 30 March 2003 at a density of 200 seeds per m^2 for wheat and 20 seeds per m^2 for safflower. After seeding, each column was placed on a support and equipped with a plastic funnel to collect the leachate. Water content in columns was measured using horizontal TDR probes placed at 15, 30 and 45 cm depths. Irrigation was applied using a scaled cylinder. Irrigation amount was calculated based on the 65% depletion of the available soil water capacity determined by measuring the moisture release curve at 10, 30, 50, 100, 300, 500, 1000 and 1500 kPa (Klute, 1986).

Leachate was continuously collected and analyzed for heavy metals. Water balance for the duration of the experiment was calculated using the following expression:

$$E = I - D + \Delta S \qquad (1)$$

where E is the actual evaporation for unplanted columns and actual evapotranspiration for planted columns (mm), I is irrigation (mm), D is discharge (mm), and ΔS is the change in column water storage (mm).

Soils were fertilized with the rate of 60 mg N kg^{-1} and 40 mg K kg^{-1} by addition of Urea and potassium nitrate. No P was applied, as initial soil analysis had shown that the available soil P was sufficient for plant growth. Plants were harvested after 75 days at the end of pollination period. Later harvest would have made HM mass balancing more difficult due to gradual loss of leaves. Plant samples were washed carefully with distilled water to remove dust and then oven dried at 60 °C and then ground. Sub-samples of 0.2 g were digested in 6 ml solution of 65% HNO_3, 2 ml solution of 2% H_2O_2 and 2 ml of distilled water. The solution was then filtrated using No. 42 Wattman filter paper and analyzed for metals by a graphite furnace AAS (Varian Spectra 300-400). The roots, shoots (stems plus leaves) and heads (spike in wheat and head in safflower) of plants were analyzed separately

After the plants had been harvested, soil columns were cut into 10-cm sections, air dried, crushed and sieved to <2 mm. Sub-samples were collected from each section and analyzed for HNO_3-extraction (Sposito et al., 1981) and diethylenetriaminepenta acetic acid (DTPA)-extractable metal concentrations (Soltanpour, 1991). The metal concentrations in the extracts were analyzed using atomic absorption spectrometry or inductively coupled plasma (ICP).

Mass balance for heavy metals was performed according to the following expression:

$$M_A = M_S + M_U + M_D \qquad (2)$$

where M_A is the applied metal (mg), M_S is the metal in the soil at the end of the experiment (mg), M_U is the metal taken up by plants (mg), and M_D is the metal in discharged water (mg). Statistical studies were conducted with SAS software (Version 6.12). Multiple comparisons of variables were made by using LSD's separation of means procedure. A probability level of $p<0.05$ was chosen to establish statistical significance.

Results and Discussion

The soils have large cation exchange capacity (CEC) with the average of 14 cmol kg^{-1} and pH values (the average of 7.7 in saturated paste). Organic matter content of these soils is generally less than 1%. The large $CaCO_3$ (with the average of 35%) imparts a large pH buffering capacity, which decreases the possibility of metal movement in soluble free form. The dominant anion is Cl^-, with the average of 1.5%, which can form soluble complexes with Cd and Pb (Khoshgoftar, 2004), hence increasing their mobility. HNO3-extractable Cd concentration (the average is 1.6 mg kg^{-1}) in the soil was more than threshold of 0.8 mg kg^{-1}

set by VBBo (FOEFL, 1998). Chemical and physical properties of the soils, under wheat and safflower in the field, show small differences as indicated by the values in Table 1. We intended to have similar soil profiles so as to reveal the differences in the two different rooting systems although as mentioned before, theses soil have been affected by same plants with different rooting system for years, which in this study must be reflected in their metal transport behavior. Therefore, we could say they are “wheat soil” and “safflower soil”.

During the experiment, each soil column received a total of 588.5 mm water. In fallow columns, discharges were in general larger than evaporation as shown. On the average about 35% of the applied irrigation water was collected as discharge for planted columns and 56% for the unplanted columns. In the planted columns more water was lost by evapotranspiration than by discharge. The discharge rate varied significantly between different treatments, a difference that evolved with time as the plants developed and consumed more water during the growing period. Although irrigation was increased during the growing period, columns with plants often had no leachate in contrast to unplanted columns. As we have also found in this study, wheat and safflower are reported to have similar water consumption in the literature (Doorenbos and Pruitt, 1977). However, under metal stress, there appears to be a significant difference between the uptake behavior of these crops as wheat shows a 14% decrease in water uptake while the decrease for safflower is only 6%. This indicates that safflower is more tolerant to HM stress than wheat, a reason why safflower performs better than wheat in this region, which has large HM levels (Amini et al., 2004), and its cultivation is promoted.

Metal Concentrations in Plants

Metal concentrations in different parts of the plants were different, depending on the plant and metal types. The highest metal concentrations were always measured in roots in both plants. The metals in roots increased in the order of Zn> Cu> Cd> Pb in both plants. The root metal concentrations of wheat increased significantly ($p<0.05$) in contaminated columns so that, Cd increased 12-fold, Cu 2-fold, Pb 5-fold and Zn 3-fold. The same trend was found for safflower, where Cd increased 14 times, Cu 1.5 times, Pb 1.2 times and Zn 2.3 times in contaminated columns. As the values show the wheat roots have more potential for metal uptake in contaminated situation than safflower except for cadmium. The same trend was observed for metals concentration in shoots in both plants. Cadmium, Cu, Pb, and Zn increased in wheat shoot by 17, 1.8, 2.8 and 2-fold in contaminated columns. These values for safflower were 13, 1.8, 1.3 and 1.9-fold for Cd, Cu, Pb and Zn, respectively.

The effect of artificial metal contamination on plant dry biomass was different for plants. Wheat dry biomass decreased significantly ($p<0.05$) in contaminated columns (mean 12.4 gplant column^{-1}) by 50% than uncontaminated columns (mean 27.6 g plant column^{-1}), while safflower dry biomass, with means of 29.8 and 27.4 gplant column^{-1} for uncontaminated and contaminated columns respectively, was not affected significantly ($p<0.05$).

Metal Concentrations in Soil Profiles

For evaluating the effects of active rooting systems on metal mobility, the difference between metal concentrations in soil profiles in fallow and planted columns were shown in Figure 1. Although in uncontaminated soils, wheat was more effective in increasing metal transport through the soil than safflower for all the metals, but in contaminated soil, the presence of safflower caused more metal mobility in the soil profile, especially in deeper depths, than wheat. In an uncontaminated situation, it seems that the role of metal uptaking by plants is more than the role of plants on enhancing metal mobility so that for all the metals the differences among metal concentrations were around zero. In general, metal concentrations in safflower planted columns were less than wheat. The points about metal concentrations in plant tissues also confirm the point as metal concentrations in safflower tissues were more than wheat. However, in contaminated situations, the role of safflower in metal mobility (except Pb) was more than wheat. This fact was more obvious for Cd in subsoil of safflower planted columns, with mean HNO_3- and DTPA-extractable concentrations of 0.30 and 0.1 mg kg^{-1} for Cd and 8.00 and 2.00 mg kg^{-1} for Cu.

The absolute values of metal concentrations in safflower tissues were more than wheat (except Pb), but compared with plant tissues in uncontaminated soil, the mean ratios of metal concentrations for wheat tissues were more than safflower (except Cu). The values were 14.6 for Cd, 1.64 for Cu, 2.8 for Pb and 2 for Zn while for safflower were 12.5 for Cd, 2 for Cu, 1.8 for Pb and 1.4 for Zn. This point plus the results discussed about metal stress effects on dry biomass and evapotranspiration on wheat, 50% decrease in dry biomass and 14% decrease in evapotranspiration, confirms the hypothesis that in contaminated situations, metal stress could alter plant metabolism and so decrease its chemical, physical, and biological efficiency. In our study, the results support this point about wheat with its fibrous rooting system. However, safflower with its taproot could tolerate metal stress more than wheat. This could be a good explanation for different behaviors of wheat in two different situations, uncontaminated vs. contaminated soil. Plants in undisturbed soils will try to avoid growing roots in the contaminated zones, the top layer in our case (Palazzo et al., 2003). This will obviously be easier for safflower with its tap root system, so our results are consistent with this theory. The taproot of safflower could affect metal mobility in deeper depths than wheat.

The ratio of DTPA to HNO_3-concentration showed much larger DTPA-extractable metal concentrations at the surface than at further depths. This could cause a problem of food chain poisoning. Cadmium had the largest ratio in safflower, while Pb had similar ratios in both safflower and wheat columns. It is interesting to note that, as might be expected, the DTPA-extractable metal concentrations in the contaminated columns was larger than the uncontaminated columns, which, with only the background concentration, had longer time to reach equilibrium between the solid and soluble phases of HMs (Lim et al., 2002).

Relative Metal Mobility

For comparing metal mobility, it is necessary to normalize metal concentrations in the soil profile because applied rate of metals were different and metals with larger concentrations will show larger concentrations (like Zn) in subsoil than those with lower concentrations (like Cd). To normalize the measured total HM concentrations in contaminated columns, we divided these values by their respective uncontaminated ones (background contamination) plus the applied amount of HMs. Relative mobility of the HMs showed Cd to be the most mobile followed by Pb, Cu, and Zn. For Cd the normalized ratio was at least 25 times larger than other HMs. The depth of movement of all HMs is larger in planted than fallow columns indicating root influence in HM transport, especially in view of the substantially greater percolation occurring in the fallow columns. In wheat planted columns, Cd moved to a depth of 35 cm, while in safflower planted columns, a deeper movement is evident up to 45 cm. There is no difference in the movement of Cu in planted and fallow treatments, although this difference is still larger in safflower. In the wheat column Pb had an effective movement down to a depth of 35 cm. In general, Pb showed a more significant movement in the wheat (fibrous) rooting system than in the tap rooting system. In both wheat and safflower, Zn did not show any significant movement.

Metal Concentrations in Discharge

Substantial variation between replicate columns with undisturbed subsoils can be expected due to variable macropore distributions (Akhtar et al., 2003). Metal contamination of the topsoil significantly ($p<0.05$) increased metal concentrations in the discharge for both planted and fallow treatments than their respective controls. In the contaminated wheat planted columns, W+M, as the result of contamination, Cd concentration in the leachate increased 9.1-fold, while Cu increased 1.2-fold, Pb increased 3.6-fold, and Zn 2.1-fold. These ratios for safflower were, respectively, 11.6, 1.6, 2.0, and 1.6. The relative increase in the concentration of safflower leachate can partly be explained by larger HM mobility in their columns as discussed before. Comparing discharge metal concentrations in planted and fallow treatments also confirms the metal stress effects on wheat. Although planted columns, ignoring some exceptions, in general caused more HM concentrations in discharge in both plants and for contaminated and uncontaminated treatments, however metal concentrations in contaminated planted wheat columns were less than fallow wheat columns (except Zn).

Metal Mass Balance

Metal mass balance calculated for soil-plant-discharge system is shown in Table 1. For calculating metal mass recovered, metal concentrations in each part were multiplied by the respective media mass (plant and soil), or volume (discharge) to change the concentration units into mass units. For calculating the metal fraction recovered in each part, the total metal mass recovered in each part were divided by their respective uncontaminated ones (background contamination) plus the applied amount of HMs. As it is obvious, most part of metals were left in the soil and then in the plant and discharge. The minimum recovered metal was for Zn (61%) in S treatment and the maximum for Cu (107.27%) in Wf+M treatment. For Cd the range of retaining metal in 50 cm depths soil for different treatments was 61.1% in S+M treatment to 92.7% in Sf+M. For Cu the range was 60.5-107.8% in W and Wf+M respectively, for Pb 81.0-102.0% for W and Wf+M and for Zn 59.2-91.9% for S and Wf+M treatments. In average about 25-30% of metals were lost in the mass balance calculation. The main sources of error for the loss of the missing fractions could be incomplete extraction of soil and plant samples, and sorption to columns. Comparing the recovered mass with the other studies (Chang et al. 1984, Baveye et al. 1999, Richards et al. 1998) shows that in different situations, the recovered metal mass was variable and analytical metal recovery from the soil is difficult.

Table 1 also gives the percentage of HMs taken up by the plants, i.e. the masses of HMs in the plants divided by the total applied plus background HM. Artificial contamination of topsoil significantly increased the accumulation of all four metals by both crops (Table 1). The increase in metal uptake of wheat in contaminated columns as compared with uncontaminated ones was 21-fold for Cd, 2-fold for Cu, 6-fold for Pb, and 7-fold for Zn. For safflower, the increase in plant uptake was 14-fold for Cd, 1.4-fold for Cu, 1.2-fold for Pb, and 2-fold for Zn. This smaller increase in metal uptake by safflower than control partly explains its more tolerant to metal stress and so its more efficiency in metal mobility in soil than wheat. As alluded to before, safflower is found to be the crop of choice in the region of study and its production is greatly encouraged. As the heavy metal concentration of pollutants such as Cd and Pb are large in the region of study (Amini et al., 2004), one reason for the success of safflower could be its smaller increase in uptake of HMs than control. This point is interesting because water uptake of safflower has only decreased by 6% as a result of contamination as compared to 14% by wheat. This can definitely be an advantage in areas of large heavy metal concentrations.

From Table 1, it can be concluded that with increasing metal uptake by plants, metal mass in the leachate decreased (except Cd and Pb). Safflower absorbed more metals than wheat and so less metal masses were measured in leachate. It is important to note that these values are the result of multiplication of discharge volume by metal concentration in discharge, and as mentioned before in contaminated soil, wheat caused more discharge than safflower and so metal output was more in wheat planted columns than safflower. Comparing metal masses in planted and fallow treatments shows that due to larger discharge volumes, metal transported by fallow columns were more than planted columns. This could mostly be due to the larger discharge volumes. However, this increase is not very large for Cu, and for Zn the planted column even shows a larger amount in the leachate. For safflower the difference between HMs in planted and fallow columns is even smaller. As we noted before, safflower has a greater ability to mobilize HMs than wheat.

Conclusions

This study showed that even in calcareous soils, plants could enhance HM mobility through the soil profile. Metal concentrations in discharge were higher in contaminated than uncontaminated columns. Metal movements, in general, in planted columns were greater than fallow columns showing the significant effects of active rooting systems on enhancement of metal transport through the soil. Safflower produces deeper roots than wheat and has more fine roots at the bottom of the columns, which could explain why metal displacement in safflower columns was in general more than wheat. Due to higher volume of discharge, a metal amount in fallow column leachate was greater than those from planted columns. However, due to the higher mobility of HMs in the safflower columns, the difference between planted and fallow columns was not substantial. Future work in this area should focus more on the measurement of root distribution, and the effect of root exudates on mobilizing various HMs, and in situ measurement of HMs concentration near roots. Measurement of dissolved organic carbon, biological oxygen demand (BOD) or chemical oxygen demand (COD) in the leachate could enhance interpretation of root-HM interaction.

References

Akhtar, M.S., T.S. Steenhuis, B.K. Richards, and M.B. McBride. 2003. Chloride and lithium transport in large arrays of undisturbed silt loam and sandy loam soil columns. Vadose Zone Journal 2:715-727.

Amini, M., M. Afyuni, N. Fathianpour, H. Khademi, and H. Fluhler. 2004. Continuous soil pollution using fuzzy logic and spatial interpolations. Geoderma 124:223-233.

Baveye, P., M.B. McBride, D. Bouldin, T.D. Hinesly, M.S.A. Dahdoh, M.F. Abdel-Sabour. 1999. Mass balance and distribution of sludge-born trace elements in a silt loam soil following long-term applications of sewage sludge. Sci. of Total Envrion. 227: 13-28.

Camobreco, V.J., B.K Richards., T.S. Steenhuis, J.H. Peverly, and M.B. McBride. 1996. Movement of heavy metals through undisturbed and homogenized soil columns. Soil Sci. 161:740-750.

Caron, J., O. Banton, D.A. Angers, and J.P. Villeneuve. 1996. Preferential bromide transport through a clay loam under alfalfa and corn. Geoderma 69:175-191.

Chang, A.C., J.E. Warneke, A.L. Page, and L.J. Lund. 1984. Accumulation of heavy metals in sewage sludge-treated soils. J. Environ. Qual. 13**:**87-91.
Doorenbos, J. and W.O. Pruitt. 1977. Crop Water Requirements. FAO Irrigation and Drainage Paper No. 24. United Nations Food and Agriculture Organization, Rome.
FOEFL (Swiss Federal Office of Environment, Forest and Landscape). 1998. Commentary on the Ordinance Relating to Pollutants in Soils. VBBo of July 1. Bern.
Emmerich, W.E., L.J. Lund, A.L. Page, and A.C. Chang. 1982. Movement of heavy metals in sewage sludge treated soils. J. Environ. Qual. 11:174-178.
Khoshgoftar, A.H., H. Shariatmadari, N. Karimian, M. Kalbasi, S.E.A.T.M.van der Zee, and D.R Parker. 2004. Salinity and zinc application effects on phytoavailability of cadmium and zinc. Soil Sci. Soc. Am. J. 68: 1885-1889.
Klute, A. 1986. Water retention: Laboratory methods. P. 635-662. *In* A Klute (ed.) Methods of Soil Analysis: Part 1. 2nd ed. Agron. Monogr. 9. ASA and SSSA, Madison, WI.
Lim, T.T., J.H Tay, and C.I. Teh. 2002. Contamination time effect on lead and cadmium fractionation in a tropical coastal clay. J. Environ. Qual. 31:806–812
McBride, M. 1998. Soluble trace metals in alkaline stabilized sludge products. J. Environ. Qual. 27:578-584.
Palazzo, A. J., T.J Cary., S.E. Hardy, and C.R. Lee. 2003. Root growth and metal uptake in four grasses grown on zinc-contaminated soils. J. Environ. Qual. 32:834-840.
Richards, B.K., T.S Steenhuis., J.H. Peverly, and M.B. McBride. 1998. Metal mobility at an old, heavily loaded sludge application site. Environ Pollut. 99:365-377.
Schwab, A. P., M.K. Banks, and L.E. Erickson. 2002. Fate and transport of heavy metals and radionuclides in soil: The impact of vegetation [online]. Available at http//www.engg.ksu.edu/HSRC/ fate.html.
Soltanpour, P.N. 1991. Determination of nutrient availability and element toxicity by AB-DTPA soil test and ICPS. Adv. Soil Sci. 16:165-190.
Sposito, G., L.J. Lund, and A.C. Chang. 1981. Trace metal chemistry in arid-zone field soils amended with sewage sludge: I. Fractionation of Ni, Cu, Zn, Cd and Pb in solid phases. Soil Sci. Soc. Am. J. 46: 260-264.
Topp, G.C. and Davis J.L. 1981. Detecting infiltration of water through soil cracks by time domain reflectometery. Geoderma 26: 13-23.
U.S. Environmental Protection Agency. 1993. Clean water act. Section 503. Vol. 58. No. 32. USEPA, Washington, DC.

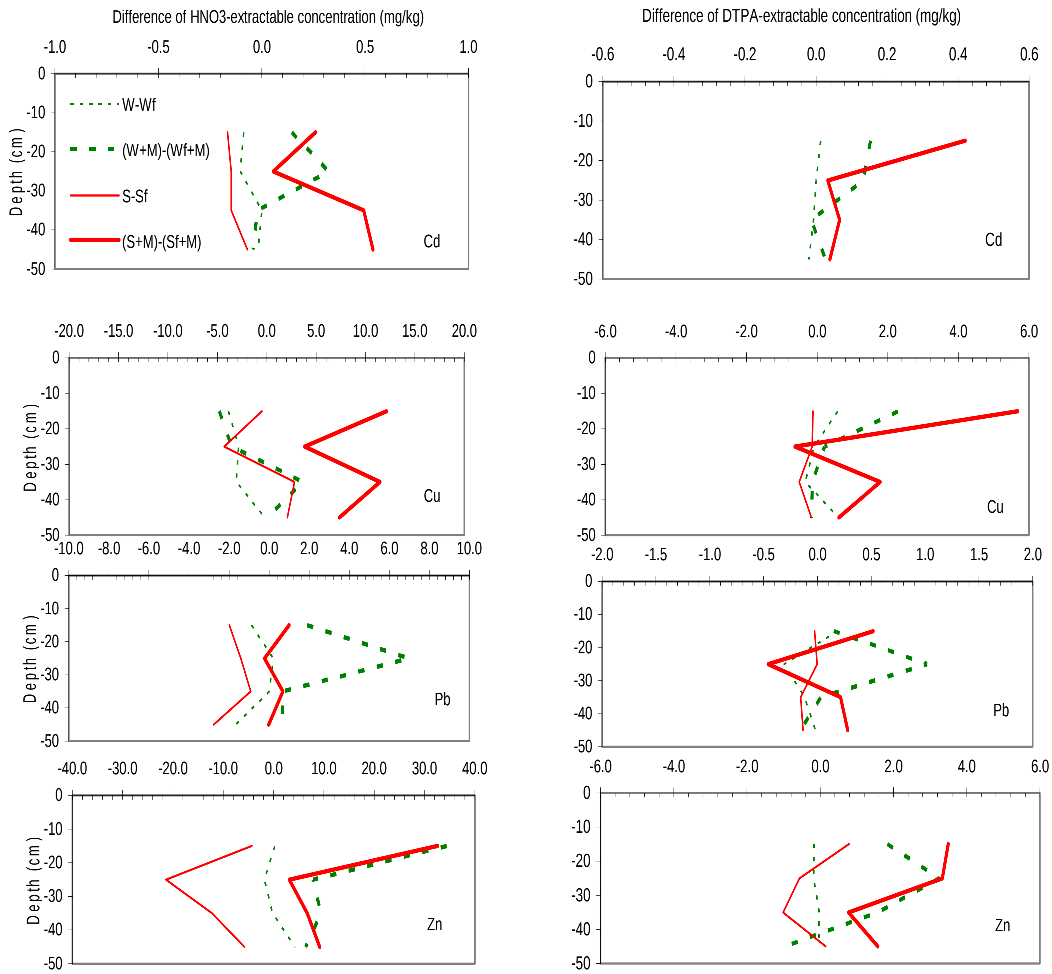

Figure 1. Differences between HNO_3-(left) and DTPA-extractable (right) metal concentrations in planted and fallow treatments. W: planted wheat columns; Wf: fallow wheat columns, S: planted safflower columns; Sf: fallow safflower columns, M: Metal contaminated.

Table 1. Metal mass balance calculated for the soil-plant-discharge system.

Treatment	system	Recovered Cd (mg)	Recovered Cu (mg)	Recovered Pb (mg)	Recovered Zn (mg)	Fraction recovered (%)			
						Cd	Cu	Pb	Zn
	Soil	35.38±1.10	529.57±48.71	407.66±1.43	1216.15±174.10	79.47	60.53	81.00	71.77
W	plant	0.04±0.08	0.85±0.39	0.06±0.03	3.42±7.79	0.08	0.10	0.01	0.20
	discharge	0.02±0.01	4.91±0.85	0.68±0.03	14.22±2.70	0.05	0.59	0.14	0.05
	Sum					79.60	61.22	81.15	72.02
	Soil	37.68±3.76	636.37±185.98	429.88±64.97	1220.97±74.29	83.84	75.94	86.37	72.04
Wf	discharge	0.03±0.00	6.98±0.58	1.26±0.11	12.70±4.22	0.07	0.83	0.25	0.79
	Sum					83.91	76.77	86.62	72.38
	Soil	108.51±32.43	3846.62±263.48	967.62±172.45	5750.72±526.06	88.62	100.74	88.46	79.23
W+M	plant	0.83±0.15	1.91±0.41	0.35±0.18	25.52±4.05	0.68	0.05	0.03	0.35
	discharge	0.18±0.04	8.06±2.85	2.53±0.45	43.67±7.53	0.15	0.21	0.23	0.60
	Sum					89.45	101.00	88.70	80.18
	Soil	111.86±26.28	4086.80±727.10	1117.66±139.18	6668.93±474.01	91.35	107.02	102.18	91.88
Wf+M	discharge	0.43±0.16	9.51±2.74	7.08±0.30	28.86±8.60	0.35	0.25	0.65	0.40
	Sum					91.70	107.27	102.73	92.28
	Soil	33.87±3.85	566.02±42.88	366.69±9.04	1008.74±70.05	75.35	67.54	73.68	59.52
S	plant	0.05±0.01	2.47±0.32	0.08±0.03	14.34±2.36	0.11	0.29	0.02	0.85
	discharge	0.01±0.53	1.70±0.33	0.29±0.05	13.33±7.80	0.02	0.20	0.06	0.79
	Sum					72.48	68.03	73.76	61.16
	Soil	37.34±3.13	576.42±32.82	430.02±53.80	1386.59±160.33	83.07	68.78	86.40	81.82
Sf	discharge	0.08±0.01	2.63±1.00	1.07±0.25	21.78±5.02	0.18	0.23	0.23	1.42
	Sum					83.25	69.01	86.63	83.24
	Soil	74.76±7.21	3146.85±191.36	985.84±719.58	5507.77±378.18	61.06	82.41	90.13	75.88
S+M	plant	0.70±0.36	3.47±0.89	0.10±0.08	31.65±9.37	0.57	0.09	0.01	0.44

	discharge	0.32±0.03	4.27±0.05	1.66±0.01	36.39±10.15	0.27	0.11	0.15	0.50
	Sum					61.90	82.61	90.29	76.93
	Soil	113.53±5.01	3729.32±152.40	1055.96±33.40	5547.21±87.34	92.72	97.66	96.54	76.43
Sf+M	discharge	0.18±0.01	5.17±0.70	1.52±0.13	41.33±10.44	0.14	0.14	0.14	0.62
	Sum					92.86	97.80	96.68	77.05

W: planted wheat columns; Wf: fallow wheat columns, S: planted safflower columns; Sf: fallow safflower columns, M: Metal contaminated.

Prioritising Watershed Development Programmes in Developing Countries

Dr. Sucharita Sen and Ms. Poulomi Banerjee
Centre for Study of Regional Development, School of Social Sciences, Jawaharlal Nehru University, New Delhi-10067, India. E-mail: ssen@mail.jnu.ac.in

Abstract

The complexities associated with implementation of watershed development programmes (WDP) in India, coupled with scarcity of financial resources make it essential to prioritise the programmes undertaken with the watershed approach. In this context, the degree of ecological and socioeconomic fragility of respective regions can be the basis for prioritizing allocation of funds. The focus of this paper is the development of a framework for prioritizing the watershed development programmes and to empirically assess whether selected watershed programmes have been prioritized as per any norm of requirement of different regions. *Need based indices* indicating natural resource base, demographic aspects, status of economic living standard, and overall index of fragility have been developed by using Principle Component Analysis. The exercise has been attempted both across agro-climatic zones/states at the macro level and across villages at the micro level. While published data sufficed for developing a need-based index at the macro level; remote sensing data, along with some secondary data was used to carry out this exercise at the micro level. Prioritisation accorded in watershed projects were evaluated by taking into consideration 1) spatial coverage and per hectare financial allocation *at the macro level* and 2) year of implementation of the project in villages within the duration of the IWDP implementation *at the micro level.* The study concludes that one of the important reasons for inconsistent impact of WDPs across regions could be rooted in ad-hoc allocation of resources for watershed management in India.

Introduction

Planning in the context of land and water resource management in India has been governed by the need for self-reliance in food production, improving resource-use efficiency, productivity, and equity. There is a growing realisation, both among policy-makers and public policy analysts, that development of rain-fed areas would be crucial, *inter-alia,* to ensure food and nutritional security of India's growing population. In India, watershed programmes were initiated primarily to resolve the increasing environmental crisis and to ensure sustainability of agricultural operations especially in the rain-fed and arid/semi-arid regions (Rajagopalan, 1991).

The integrated approach of watershed development focuses on conservation and development of three natural resources, namely land, water, and vegetation. However, these projects are also associated with a large number of complexities due to the their thrust on both environmental and livelihood sustainability, particularly after adoption of the 1994 common guidelines for watershed programmes (GOI, 2000); these complexities include emphasis on resource conservation rather than utilization, conflicting interests between private and common properties, and implied trade-offs between stakeholders from different economic and social strata. (Shah, 2000). These problems necessitate prioritization of programmes undertaken with the watershed approach, particularly in developing countries, where sufficient resources cannot be allocated to all regions. In this context, the degree of ecological and socioeconomic fragility of respective regions can be the basis for prioritizing allocation of funds. Giving priority to such fragile areas has been integral, at least implicitly, to the objectives of most of the watershed development programmes (GOI 2001a and 2001b). In India, at a macro level, prioritization should largely be the responsibility of the central government, (Ministry of Agriculture or Ministry of Rural Development, as the case may be) as the funds flow from the Centre to the states for implementation of the programmes. Within the state, the same criteria can be adopted to distribute the funds within different watersheds by the state government. At the watershed level, the project implementing agency (PIA) once again needs to classify the villages based on similar principles.

The focus of this paper is to develop a framework for prioritizing the watershed development programmes, both at the macro and the micro levels, and assess whether relative emphasis given to different regions in selected watershed programmes[i] are in conformity with their relative levels of requirements, i.e. with their ranking in terms of the need-based indices developed for this purpose.

Importance of a Need-Based Index

The degree of fragility of a region should ideally be based on the requirement of the area measured in terms of the natural resource base, demographic aspects, and the status of economic living standard. For the purpose of our analysis, *need based indices* have been developed by aggregating variables encompassing ecological fragility, demographic pressure, and economic vulnerability. The aggregation has been attempted by means of Principle Component Analysis, using the composite index associated with the first principle component. In this method, the eigen vector, which are derived from the degree of association between the variables considered, are used as the weights for these variables to achieve the aggregation. Table 1 lists the indicators used for constructing the index; while some variables has a positive relationship with the need for undertaking measures for ecological and livelihood sustainability of a respective region (i.e. percent of total wasteland, incidence of poverty, density of population etc), some other variables have a negative association with its requirement (rainfall, share of net sown area, land and labour productivity). Reciprocals of the latter set of variables have been used for deriving the composite index such that the composite index thus created is consistent in reflecting the needs of the respective regions.

Table 1. Component score coefficient matrix for the overall index.

Variables	Nature of Variable	Score Coefficient For Principal Component 1
Population Density	Demographic	.387
Labour Productivity	Standard of Living Index	.160

Land Productivity	Standard of Living Index	.422
Rural Poverty	Standard of Living Index	.201
Ground Water balance	Resource Variable	.120
Net Sown Area	Resource Variable	.188
Total Waste land	Resource Variable	.060
Rainfall	Resource Variable	.211

Both at the level of agro-climatic zones and states, four indices were worked out, the three mentioned in Table 1 and an overall composite index encompassing all the variables[ii]. The purpose for this exercise was to develop physical/natural, demographic, socio-economic as well as overall criteria for allocating resources under watershed development programmes. Table 1 also provides the weightages used to derive the overall composite index, which is the correlation coefficient between the variables and the overall index. Population density and land productivity has got the maximum weightages in deriving this index, both of which can be linked to carrying capacity sustainability concept (Bell and Moorse, 1999). The emphasis given to the different regions of the country representing diverse ecological settings and varying levels of development through the programmes undertaken with the watershed approach can conceivably encompass two aspects; firstly, the extent covered by the programme or the expansion aspect and secondly, the nature of work undertaken within the watershed, or the qualitative aspect. To encapsulate these aspects at the macro level, the data available with the Ministry of Agriculture was utilized for this paper. For spatial coverage, cumulative percentage of area covered under NWDPRA from the inception of the project[iii] until 2002 to the total geographical area across agro-climatic zones[iv] have been taken into consideration. To capture the qualitative aspect, the financial allocation per unit area has been used as a proxy variable; the higher the amount per hectare, the better would be the scope for undertaking more effective activities under the programme. The above ‘implementation indicators’ were compared with these indices at agro-climatic zone level and state level respectively[v]; the purpose was to assess whether watershed programmes (NWDPRA taken as a case) are implemented with respect to these indicators. In other words, one of the important objectives of this study was to examine whether the resources in WDPs are allocated using some norm, and if so, identify the nature of this norm.

Table 2. Correlation coefficients of efficiency indicators of watershed implementation and need-based indices of agro-climatic zones/states.

Variables	Resource base	Demographic	Standard of living	Overall index
Cumulative Spatial Spatial Coverage under NWDPRA $	-0.23*	-0.063	-0.243*	-0.283*
Expenditure Per Hectare of 8th	-0.37	0.167	-0.015	0.167

over 9th plan #					

Note: # State level; $ Agro-climatic zone level; * significant five percent level.

Table 2 attempts to capture the above-mentioned problem; coverage of area under the NWDPRA programme shows negative and significant relation with most of the need based indices while state-wise per hectare undertaken with the same programme reveal no relationship with the requirement resource-fragility, demographic, standard of living or overall requirement norms. Thus, the relative emphasis accorded in terms of spatial extent coverage under the project appear to be greater in the regions that are better off and lower in the ones that are worse off. Therefore, it may not be an over-statement to note that NWDPRA seems to have been implemented in an ad-hoc manner, without taking into consideration any norms for allocating resources across regions

The region and state-wise positions for spatial expansion and expenditure per hectare emerges more clearly from Figure 1 and Table 3 respectively. Table 4 has been derived from computing the deviation of ranks of agro-climatic zones in terms of spatial coverage and the overall need-based index.

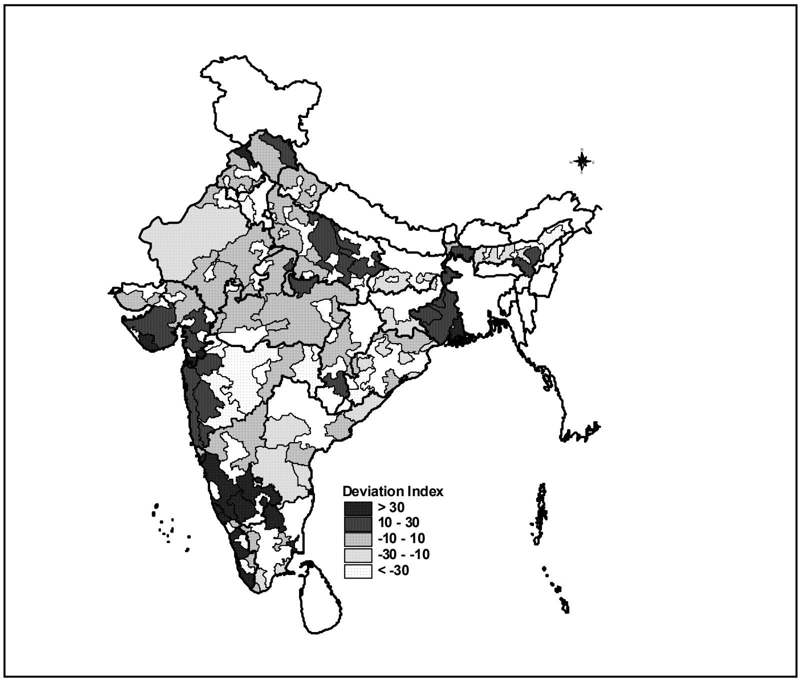

Figure 1. Deviation index for area coverage among agro-climatic zones.

A high positive deviation for any region would place it in the category of a relatively favoured region, where the WDP coverage rank is higher than that of its need-based rank. Similarly, a region with a very low negative value would indicate that it has been neglected relative to its requirement position vis-à-vis the rest of the regions. A region characterized by no deviation or a zero its relative priority in implementation as per its need-rank.

Figure 1 shows the deviation across all agro-climatic zones of India and as can be observed, the entire western coastal region, West Bengal, parts of Punjab and Uttar Pradesh, are the more favoured regions. While some states like Maharastra, Andhra Pradesh, Assam, and Uttar Pradesh show substantial disparity in the deviation across the state. States such as West Bengal, Kerala, Rajasthan, and Madhya Pradesh have performed more uniformly in terms of watershed area coverage vis-à-vis the requirement of their agro-climatic zones.

Table 3. Comparison of expenditure per hectare and need-based index among various states of India.

		High	Medium	Low
Expenditure	High	Maharastra	Orissa, Karnataka,	Kerala
	Medium	Andhra Pradesh, Himachal Pradesh	Bihar, Assam	
	Low	Madhya Pradesh	Gujarat	Goa, Harayana, Punjab, West Bengal

Table 3 portrays the situation with respect to per hectare expenditure within the watershed area, which may be treated as the proxy variable for quality of work done within the watershed area, at least in terms of policy decisions. While some of the states spend as per their relative position with respect to the need-based index, states like Kerala and Madhya Pradesh represent two extremes of note. While Kerala gets to spend much more per unit of area in relation to its position in relation to its need based position, Madhya Pradesh is the most neglected state, where the need is extremely high and the per hectare expenditure very low.

Watershed Level Prioritisation: Framework Using Remote Sensing Data

The prioritization of villages at the watershed level rests with the Project Implementing Agency (PIA), the constitution of which varies from watershed to watershed, depending of the degree of involvement of the state Governments, non-governmental organisations, international funding agencies, etc. However, at this level, at least as per the new Watershed Guidelines put in place by the Hanumantha Rao Committee in 1994, some form of participation of people living within the watershed is mandatory. Thus, prioritisation at this level is important and has direct bearing to the success of the programmes, given the limited resources. Prioritization within a watershed cannot adopt the same criteria as used for the macro-framework, as the selected villages within a watershed usually get full coverage and uniform financial allocation per unit of area. However, funding for any watershed development programme is usually available in phases. Initially, it needs to be decided whether all villages within the watershed need to be covered by the programme; in the next step, villages where the programme is to be implemented need to be grouped using some objective criteria as the programme cannot be started at all villages at the same time and has to be synchronized with the phases in which the funds are released. There would be no contention about the concept that villages having early implementation are in a distinctly advantageous position, as the activities undertaken in these villages can be monitored and corrected within the duration of the programme[vi].

For this section, we suggest a framework for categorising villages into groups, once again using a need-based approach and taking into account the several criteria that are related directly to the specific objectives of the watershed development programme. For this purpose, an empirical example of Dangri Watershed located in Panchkula District in Haryana has been used, where Integrated Watershed Development Programme funded by the World Bank and Haryana Government (70 percent and 30 percent respectively) and implemented entirely by the Department of Agriculture, Haryana was in operation between 1999 and 2004. Keeping in line with the earlier section, we also assess the efficiency of prioritization of this project with respect to the framework of efficiency developed in this study. Here the access to the database is crucial, and we have, to a large extent depended on remote sensing data to derive relevant indicators at the village-level to construct the index (Table 6).

One of the primary objectives of a watershed development programme undertaken in semi-arid tropics is to arrest the process of soil erosion, which is known to have a multiplier effect on rural natural resource management, which in turn has a direct bearing on rural livelihood status. For this reason, susceptibility to soil erosion can be used as one of the basic criterion for watershed prioritisation.

Soil erosion modeling is an important component for analyzing the efficacy of WDP. GIS has gained in importance in terms of providing a tool for soil erosion modeling which uses both processed remote sensing and ancillary data. A number of modeling approaches, both quantitative and qualitative are currently used. Morgan, Morgan and Finney (MMF) model is a process-based model which has been used for our purpose. Physical process-based models predict the spatial distribution of runoff and sediment over the land surface during individual storms in addition to the total runoff and soil loss.

The MMF model has been divided into a water phase and a sediment phase. The sediment phase computes the soil loss as a result of detachment of soil particles as a result of overland flow, while the water phase computes the rate of soil detachment due to the splash effect of erosion. The input parameters used in the MMF model are provided in Table 4. For calculating the A, E_t/E_o and C values, time weighted averages have been used for different cropping systems. Some of the important examples of the values taken are shown in Table 5.

Table 4. Parameters used in MMF model for soil erosion.

Sl. No.	*Parameters*	**Description**
1	MS	Soil moisture content at field capacity (%w/w)
2	BD	Bulk density of the top soil (Mg/m^3)
3	RD	Top soil rooting depth (m)
4	K	Soil detachability index (g/J) (weight of soil detached from the soil mass per unit of rainfall energy)

5	S	Steepness of the ground slope expressed as the slope angle (in radians)
6	R	Annual rainfall (mm)
7	R_n	Number of rainy days
8	I	Typical value for intensity of erosive rain
9	A	Percentage rainfall contributing to permanent interception and stemflow.
10	E_t/E_0	Ratio of actual to potential evapotranspiration
11	C	Crop cover management factor

Table 5. The weights and values given for selected parameters in MMF model.

Crops/land use	Time weight	A	E_t/E_o	C
Forest	12	20	1	0.001
Paddy	4	43	1.35	0.72
Wheat	5	43	0.5	0.65
Scrub	5	15	0.15	0.90
Barren	-	0	0.05	1.00
Other Crops	4	25	0.7	0.47

NB: Adopted from Morgan, Morgan, Finney, 1984[vii].

Operating functions for the Morgan, Morgan, and Finney method of prediction of soil-loss.

Water Phase:
$E = R\,(11.9+8.7\,log_{10}(J))$ and $Q = R\exp(-R_c/R_o)$
Where, $Rc = 1000\ MS.BD.RD\ (E_t/E_o)^{0.5}$ & $Ro = R/R_n$

Sediment Phase:
$F = K(Ee^{-aA})^b.10^{-3}$ & $G = C\,Q^d \sin(S).\,10^{-3}$

E= Kinetic energy of rainfall (J/m^2); Q = volume of overland flow (mm)
G = transport capacity of overland flow (kg/m^2); F = rate of soil detachment by raindrop impact (kg/m^2)

To carry out the soil erosion modeling, the basic layers that are required are soil, the satellite-derived land use map, and the digital elevation model. The flow diagram for this model has been provided in the Appendix. The soil-loss was worked out for 1998 and 2003. From the results derived from the MMF model, which provides estimates of both periods, area weighted average of soil loss was derived for each village within the watershed. These average soil losses for both periods were ranked and divided into clusters of villages, going by the number of villages selected each year in IWDP of the Dangri Watershed. The numbers of villages in different categories accordingly were 11 for highest priority, 14 for high priority, eight for moderately high priority, eight for moderate priority, and 35 for low priority. These category classes (0, 1, 2, 3, and 4) were then subtracted from the ranks of the IWDP rankings.

The second criteria that was used for prioritization was an overall need-based index adopting similar method as in the earlier section; the variables and their data source has been provided in Table 6. The first principal component explains about 40 percent of the variation in the data set.

Table 6. Variables selected for composition of overall WDP prioritization.

Sl. No.	***Variables***	***Specifications***	Data Source
1.	Soil erosion (tons/hac)	Resource variable (1997-98, derived from MMF model)	Remote sensing & GIS
2	Female literacy (%)	Indicator for social awareness	Census
3	Proportion of cultivated area to total area (%)	Resource variable	Remote sensing
4	Cultivable area per household (ha/hh)	Demographic variable	Remote sensing and Census
5	Percent of cultivable area under double crop	Economic variable	Remote sensing

The soil-erosion criterion (1997-98) shows a reasonable degree of correspondence with the watershed prioritisation (Table 7), with around 43 percent of the villages showing no deviation in the hierarchical group classification between the two sets of clusters. Around 18 percent of the villages show a deviation greater than three, out of which only around seven percent of the villages are such which have been given lower priority in relation to their position of ecological fragility measured by soil erosion criterion. The soil erosion (2001-03) based ranking show a marginally higher degree of correspondence compared with WDP ranking compared to the earlier season.

Table 7. Rank correlation between ranks of need-based index and actual prioritization.

	Soil erosion Criteria	Overall Index
Correlation Coefficient	0.40	0.58
Significance (2-tailed)	0.00	0.00
N	75	73

Rank correlation between soil erosion criteria for both years shows reasonably high correlation both of which are significant at one percent level of significance. Thus, as per the soil erosion criterion, the prioritisation of WDP villages can be said to be fairly efficient. Figure 2, however, shows that the according to the overall criteria, the hilly underdeveloped villages of Morni Block (Nagal, Morni and Balig) have been neglected, where watershed development programmes should have been undertaken on the first phase of implementation.

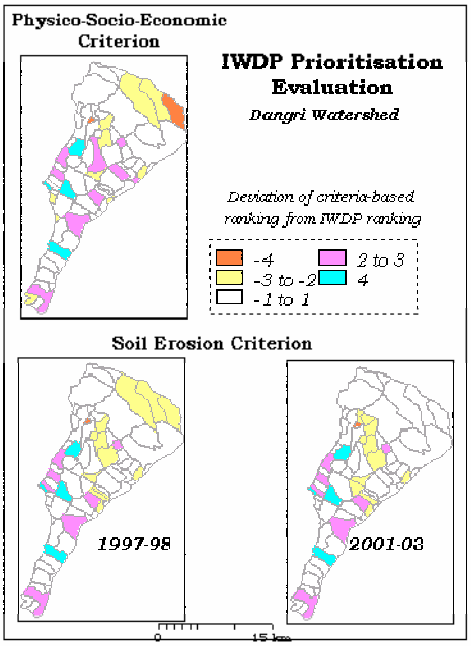

Figure 2.

The prioritisation criteria can be further improved by including infrastructure variables as percentage of irrigated area, connectivity of villages, percentage of households electrified, percentages of population served by primary health care centers, and proportion of population having middle or high school education. There are nevertheless clear indications that an overall perspective of development has been followed in the Dangri Watershed for prioritisation of villages.

Conclusions

Our analysis brings out the need to adopt a framework for ranking macro and micro regions to enhance the efficacy of watershed development programmes in India. As case studies, we have evaluated NWDPRA, one of the most important watershed development programmes in India in terms of its spatial coverage that is implemented by the Ministry of Agriculture at the macro level, and IWDP undertaken in an ecologically fragile zone of a developed state in India at the micro level. The case studies were attempted primarily to demonstrate the feasibility of evaluation of prioritisation of WDPs both at the macro and micro levels and not precisely for the purpose of assessing watershed development programmes in India. However, our findings do shed some light on the state of implementation of WDPs in India. First, it appears that the central government has had no particular norm in allocating resources for watershed programmes. Experience in terms of impact of these projects varies from region to region, and, project to project; undoubtedly, some projects have been far less effective than others (Rao, 2000; Deshpande and Reddy, 1991). One of the important reasons, other than that of varying

degrees of peoples' participation that have been explicitly brought out by recent literature (Reddy, et al, 2004; Kolavalli and Kerr, 2002; Shah, 2000), could be allocation of watershed resources in an ad-hoc manner.
While no generalization can be made from the finding of the micro level case study, its successful prioritization points toward the fact that contrary to the notion that state governments are by and large ineffective implementers of land development programmes, state machinery can be adequate and efficient provided that the monitoring system in place is rigorous.[viii]

The findings of our study point toward the need to review the current policy implementation and include relative fragility of different agro-climatic zones as a criterion for resource allocation within its policy framework. In this context, a careful evaluation of indicators reflecting vulnerability position or risk status of different regions would be necessary.

Given the objectives set out by the common guidelines set out by all watershed development programmes (GOI, 2000), which takes into account a holistic perspective of rural livelihood, it is clear that while the physical processes determining ecological fragility is extremely important, the social and economic position of the states/agro-climatic regions/villages are crucial for prioritisation. Ideally, such a holistic perspective should take into account, along with socio-economic standing of the villages, the infrastructural conditions too, such as connectivity, irrigation, and electricity facilities. Understandably, data availability at different levels would vary and there is a need to work out consistent need-based indices at different levels of prioritization as much as possible. Remote sensing data at the village-level prioritization offers interesting possibilities and has the potential to greatly contribute to more efficient policy formulation.

References

Bell, S and S. Morse. 1999. 'Sustainability Indicators: Measuring the Immeasurable', Earthscan, London.

Government of India. 1991. 'Agro-climatic Regional Planning at the State Level:Profiles, Issues, Strategies and Programmes', ARPU Working Paper no 5, Agro-climatic Regional Planning Unit, Planning Commission, Ahmedabad.

Government of India. 2000. *Common Approach for Watershed Development*. New Delhi: Ministry of Agriculture.

Government of India. 2001a. *Guidelines for Watershed Development, Revised (2001*). New Delhi: Ministry of Rural Development.

Government of India. 2001b. *Report of the Working Group on Watershed Development, Rain-fed Farming and Natural Resource Management for the Tenth Five-Year Plan*, New Delhi: Ministry of Rural Development.

Kolavalli,S.L. and J.Kerr. 2002., 'Mainstreaming Participatory Watershed Development', *Economic and Political Weekly,* 37(3): 225-42.

Morgan, R.P.C., D.D.V. Morgan and H.J. Finney (1984), "A predictive Model for the Assessment of Soil Erosion Risk" *Journal of Agricultural Engineering Research,* 30, 245-253.

Rajagopalan V.1991. 'Integrated Watershed Development in India: Some Problems and Perspectives', *Indian Journal of Agricultural Economics*, 46(3):241-50.

Rao, C.H.H. 2000., 'Watershed Development in India: Recent Experience and Emerging Issues', *Economic and Political Weekly*, 35(45): 3943-47.

Reddy, V.R., Reddy, M.G, Galab, S., Soussan, J and Springate-Baginski, O 2004. 'Participatory Watershed Development in India: Can it sustain Rural Livelihoods?' *Development and Change*, 35(2), 297-326.

Shah, A. 2000. 'Watershed Programmes: A Long Way to Go', *Economic and Political Weekly*, 35(35-36): 3155-64.

---

[i] National Watershed Development Programme for Rainfed Areas (NWDPRA) implemented by the Ministry of Agriculture at the macro-level and Integrated Watershed Development Programme implemented in Dangri Watershed in Panchkula district in Haryana at the micro-level has been selected for the purpose.

[ii] The composite index associated with the first principle component explains about 59.6 percent of the variation of the variables in case of the overall index.

[iii] NWDPRA has been functional from 1990-91. We have here derived the cumulative percentage for spatial extent by clubbing the 8[th] and the 9[th] Plan area under the project.

[iv] Data in the block level has been aggregated to the district level and further to the level of agro-climatic zones.

[v] The data for the financial allocation is not available at the level of the agro-climatic zone, as the Central Government allocates this fund to various states. The responsibility to further allocate the same within the state rests with the state Government.

[vi] Usually watershed projects have a duration of five years.

[vii] It needs to be mentioned here that it has been assumed that for the area classified as barren with or without scrub, the scrub has covered the ground for the duration of the rainy season. Thus the A,C and Et/Eo values assumed for scrub is an approximation derived crudely from the other values provided in Morgan, Morgan and Finney (1984).

[viii] In this case, the World Bank, the primary funding body for the project had put up an efficient system of monitoring the project.

Climate Change Impacts on the Hydrology and Water Quality of the Upper Mississippi River Basin

Eugene S. Takle[1,2]*, Manoj Jha[3], Philip W. Gassman[3], Christopher J. Anderson[1], and Silvia Secchi[3]
[1]Department of Agronomy, 3010 Agronomy Hall, Iowa State University, Ames, IA 50011. Email: gstakle@iastate.edu
[2]Department of Geological and Atmospheric Sciences, Iowa State University, Ames, IA 50011
[3]Center for Agricultural and Rural Development (CARD), Department of Economics, Iowa State University, Ames, IA 50011

Abstract

Output from an ensemble of seven global climate models for contemporary and future scenario climates was used to drive the Soil and Water Assessment Tool (SWAT) to examine components of the hydrologic budget for the Upper Mississippi River Basin (UMRB). Results showed only modest increases in precipitation (+6%) and streamflow (+3%) but substantial reduction in snowfall (-37%) for the UMRB for the end of the 21st century. The low-resolution of global models contributes to biases in some but not all hydrologic components, most notably evapotranspiration, potential evapotranspiration, and baseflow. Ensemble results indicate an increase in baseflow (+12%) and decrease in runoff (-20%) for the future scenario. Such changes would likely decrease sediment loading of streams, but influences on the fate of fugitive nitrates are indeterminate from this preliminary study.

Introduction

Recent observations and modeling suggests acceleration of the hydrological cycle at high latitudes in the Northern Hemisphere (Stocker and Raible, 2005; Wu et al., 2005). Detailed evaluation of the spectrum of precipitation events for the central US (Groisman, et al, 2005) reveal that the occurrence of extreme intense precipitation events has increased over the twentieth century. Most notably, however, all of this increase (20% increase, statistically significant at the 0.01 level) occurred during the last 30 years of the twentieth century. Assessments of local and regional impacts of changes in the hydrological cycle in future climates call for improved capabilities for modeling the hydrological cycle and its individual components at the subwatershed level.

Takle et al. (2005) report a preliminary study to determine the ability of global models to produce suitable inputs for the Soil and Water Assessment Tool (SWAT) watershed model (Arnold and Fohrer, 2005) to simulate components of the hydrological cycle in the Upper Mississippi River Basin (UMRB). By comparing observations of streamflow at Grafton, Illinois with simulated results, we found that no individual low-resolution global model was able to give a distribution of annual flows that was not statistically different from the mean of observed values. However, the ensemble of nine models did produce credible distribution that was statistically significant. Also, the one model for which we had both high-resolution and low-resolution versions produced annual streamflows not statistically different from observations at high resolutions even though results from its low-resolution sister model were statistically different from observations.

Streamflow models such as SWAT accept a wide range of meteorological datasets and use internal weather generators to fill in key missing values and create refined details, such as the partitioning of daily precipitation between rain and snow. Because Jha et al. (2004) showed that UMRB SWAT provided good results for annual streamflow while having larger uncertainty of monthly values, it is not clear whether either spatial or temporal refinement of global model results is warranted for simulating streamflow for this watershed. Use of data directly from global climate models is an alternative to using regional climate models or statistical models to downscale global results. Coupled atmosphere-ocean global climate models have improved physical process models and process resolution since the last assessment of the Intergovernmental Panel on Climate Change (2001). Furthermore, advances in computing capabilities now permit the use of multi-model ensembles, which we have shown (at least for one region and one period) to provide a reliable source of weather data for assessing streamflow (Takle et al., 2005).

We report herein an extension of the results reported by Takle et al. (2005) in that we examine a subset of the global ensemble used in that study to evaluate impacts of increases in atmospheric greenhouse gas concentrations on future streamflow in the UMRB. We use 21st century results of seven global climate models being made directly available for the IPCC 4th Assessment Report [PCMDI, 2005] as input to SWAT for calculating components of the hydrological cycle in the region experiencing changes in the hydrological regime over the last 30 years (Pan et al., 2004; Groisman et al., 2005).

Domain

The UMRB has a drainage area of 447,500 km^2 up to the point just before the confluence of the Missouri and Mississippi Rivers near Grafton, Illinois (Figure 1). Land cover in the basin is diverse and includes agricultural lands, forests, wetlands, lakes, prairies, and urban areas. The river system supports commercial navigation, recreation, and a wide variety of ecosystems.

For modeling with SWAT, the basin is divided into 119 subwatersheds, with each subwatershed being subdivided into hydrological response units (HRUs) such that the basin consists of 474 HRUs. One hundred eleven weather stations relatively uniformly distributed throughout the basin provide observed climate data used as input to the hydrological model for simulating baseline streamflows. Details of land use, soils, and topography data for the UMRB are provided in Jha et al. (2004). Our study domain lacks fine-scale orographic features that would surely otherwise compromise the ability of GCMs to describe the spatial distribution of hydrological processes over a region containing only a few GCM grid points.

Figure 1. The Upper Mississippi River Basin (UMRB) and delineated subwatersheds.

Models

SWAT Model

SWAT (Arnold and Fohrer, 2005) is a continuous time, long-term, watershed scale hydrology and water quality model. The model was developed to predict the impact of land management practices on water, sediment and agricultural chemical yields in large complex watersheds with varying soils, land use and management conditions over long periods of time. It is a physically-based model and uses readily available inputs. It operates on a daily time-step and is computationally efficient. The model is not designed to simulate detailed, single-event flood routing.

Subdivision of the watershed into HRUs enables SWAT to reflect differences in evapotranspiration for various crops and soils. Flow generation, sediment yield, and non-point-source loadings estimated for each HRU in a subwatershed are summed, and the resulting loads are routed through channels, ponds, and/or reservoirs to the watershed outlet. Upland components include hydrology, weather, erosion/sedimentation, soil temperature, plant growth, nutrients, pesticides, and land and water management. Stream processes considered in SWAT include channel flood routing, channel sediment routing, and nutrient and pesticide routing and transformation. The ponds and reservoirs component contains water balance, routing, sediment settling, and simplified nutrient and pesticide transformation routines.

Meteorological input to SWAT includes daily values of maximum and minimum temperature, total precipitation, mean wind speed, total solar radiation, and mean relative humidity. The hydrologic cycle, as simulated by SWAT at the HRU level, is based on the balance of precipitation, surface runoff, percolation, evapotranspiration, and soil water storage. SWAT takes total daily precipitation from models or observations and classifies it as rain or snow using the average daily temperature. The snow cover component allows non-uniform cover due to shading, drifting, topography, and land cover and is allowed to decline non-linearly based on an areal depletion curve. Snowmelt, a critical factor in partitioning between runoff and baseflow, is controlled by the air and snow pack temperature, the melting rate, and the areal coverage of snow. On days when the maximum temperature exceeds 0°C, snow melts according to a linear relationship of the difference between the average snow pack maximum temperature and the base or threshold temperature for snowmelt. The melt factor varies seasonally, and melted snow is treated the same as rainfall for estimating runoff and percolation. SWAT simulates surface runoff volumes for each HRU using a modified SCS curve number method (USDA Soil Conservation Service, 1972). Further details can also be found in the SWAT User's manual (Neitsch et al., 2002). The version of SWAT used to produce results reported herein is the same model calibrated for the UMRB baseline conditions that was reported in Jha et al. (2004).

Global Climate Models

Global model results that included daily values needed for our simulations of future scenarios were available from seven models (see Table 1) in the IPCC Data Archive (PCMDI, 2005), including two versions of models from two of the laboratories. While not spanning the full range of model variability and giving disproportionate weight to models from these two laboratories, the results do provide a useful and preliminary view of the hydrologic cycle components resulting from direct use of data generated by multiple GCMs. Takle et al. (2005) found that streamflow data resulting from the GCM ensemble consisting of models used here plus two more were serially uncorrelated at all lags and formed unimodal distributions, suggesting that the data may be modeled as independent samples from an identical normal distribution. The test of the hypothesis of zero difference between mean annual streamflow of the pooled GCM/SWAT and OBS/SWAT results gave a p-value of 0.5979. This suggests that use of GCM ensemble results may provide a valid approach for assessing annual streamflow in the UMRB. Model outputs from runs of seven of the nine models examined by Takle et al. (2005), i.e. those having output for the twenty-first century (21C) A1B emission scenario (IPCC, 2001) for the period 2082-2099, were used in this analysis.

Influence of Model Resolution

The UMRB has nominal dimensions of 7° N-S by 5° E-W. A comparison of these dimensions with the model resolutions in Table 1 shows that the number of grid points "representing" the basin for the low-resolution models ranges from about two for the NASA model to seven for the GFDL model, and that the high-resolution MIROC model has about 27. By contrast, 111 weather stations were used to represent baseline climate in the region (corresponding to a grid spacing of about 0.6^o x 0.6^o, if they were uniformly distributed).

Table 1. Global models used in the SWAT-UMRB simulations.

Institution	Model Name	Long. x Lat. Resolution	W/m2 Cl. Sens.
NOAA Geophysical Fluid Dynamics Laboratory (USA)	GFDL-CM 2.0	2.5^o x 2.0^o	2.9
Center for Climate System Research (Japan)	MIROC3.2 (medres)	2.8^o x 2.8^o	1.3
Center for Climate System Research (Japan)	MIROC3.2 (hires)	1.125^o x 1.125^o	1.4
Meteorological Research Institute (Japan)	MRI	2.8^o x 2.8^o	0.86
NASA Goddard Institute for Space Studies (USA)	GISS-AOM	4^o x 3^o	2.6
NASA Goddard Institute for Space Studies (USA)	GISS-ER	5^o x 4^o	2.7
Institut Pierre Simon Laplace (France)	IPSL-CM4.0	3.75^o x 2.5^o	1.25

Ideally, a simulation with SWAT would have at least one weather station per subbasin. While this condition is approximately met for the observing network in the UMRB, this requirement needs to be reconsidered when climate model data are used. It is instructive to consider the impact of model resolution on simulated hydrology.

Evapotranspiration (ET) and potential evapotranspiration (PET) generally will be under-predicted when low-resolution weather data are supplied to SWAT (assuming no changes due to orographic influences and the model does not have a high temperature bias). The Clausius-Clapeyron equation is an exponential function of temperature, so high temperatures proportionately lead to more evaporation/transpiration than low temperatures compared to a linear dependence. Low-resolution models do not capture temperature extremes (either high or low) as well as high-resolution models, and missing extreme high temperatures has a much larger impact than missing extreme low temperatures.

Influence of Model Biases

It is noteworthy that precipitation, snowfall, and runoff are "events" whereas snowmelt, baseflow, ET, PET, and total water yield are continuous values. Snowfall (partitioning of precipitation to snow fraction) depends on temperature on the day of snowfall. ET and PET depend on temperature every day (more so in the warm season). Other components are not directly (although they are indirectly) dependent on temperature.

A cool bias in the cold season of a GCM model will lead to excessive snowfall (assuming total precipitation is accurately simulated). A comparable warm bias would result in too little snow, of a more-or-less comparable amount. A cool bias will also lead to reduced ET and PET, particularly if the bias is in the warm season. A comparable warm bias would produce excessive ET and PET of an amount exceeding the reduced values for a cool bias, as previously discussed. Since the basin has no permanent snow, annual snowmelt tracks annual snowfall and is unaffected by temperature bias. Likewise, runoff is unaffected by temperature bias. Baseflow and total water yield are not directly affected by temperature but are affected indirectly. High bias on temperature will elevate ET and PET and consequently reduce baseflow, without impact on runoff, thereby reducing total water yield. Likewise low bias on temperature will increase water yield (other factors being equal, of course).

Climate models generally produce too many light rain events and too few intense events (Gutowski et al., 2003) even if rainfall totals are accurate. The impact of this bias, compared to the true intensity spectrum, is to reduce runoff and increase ET and/or baseflow. Low bias on rainfall likely would lead to low runoff, baseflow, ET, and hence water yield, while excess rain would have the opposite effect. Biases in wind speed, solar radiation, and humidity would likely have less prominent effects in this basin.

We sometimes casually consider observations to be unbiased, but they too may have systematic errors. Cooperative weather stations from which data are collected in the UMRB have operators that check instruments once daily, either at 7 AM (morning station) or at 5 PM (afternoon station). Morning stations tend to have a low-temperature bias and afternoon stations a high-temperature bias (Takle, 1995), which could impact SWAT through calculation of snow fraction in winter and ET and PET in the warm season. For the present study we expect observational biases to be less than model biases.

Results

Biases

Rainfall gauges from the 111 locations in the UMRB provided measurements of precipitation, and gauge data from Grafton, IL provided measurements of streamflow. However, since no other hydrologic components were measured, we estimate these with SWAT-derived hydrologic components created with weather station input (OBS/SWAT). Comparison of calculations of streamflow by SWAT using observed weather input with gauge data revealed that SWAT introduces a slight positive bias to annual streamflow but represents the interannual variability quite well (Takle et al., 2005). Biases generated by the combination of GCM and SWAT (Table 2) were calculated by comparing GCM/SWAT results with OBS/SWAT results.

The GCMs generally underestimate annual precipitation in the region on average, by a modest amount, but overestimate streamflow. Most models produce too much snow but are quite inconsistent regarding the amount of runoff produced. Baseflow is uniformly high compared to SWAT results produced by station-derived weather, but PET and ET are uniformly low. Total water yield was overestimated by all but one model.

The discussion presented in the previous section and data from Table 2 provide insight for interpreting these results. The components for which the models produce the most consistent results are ET and PET, which are quite uniformly underestimated (by 25% and 38%, respectively). Although this could signal a uniform positive temperature bias in the warm season, we suggest the more likely cause is the coarse resolution of the models (see previous section). It is noteworthy that the only high-resolution model of the ensemble (MIROC3.2-hires) has the lowest bias of all models for both ET and PET. The deficiency in ET forces a model to partition more soil water input to baseflow, which is a likely explanation for uniformly excessive baseflow across the ensemble. And because baseflow is the dominant contributor to total water yield, which also is over-predicted by all but two models, we can say with some confidence that streamflow is over-predicted in this basin by global models because of failure to resolve daily maximum temperatures in summer due to coarse resolution.

Table 2. Model biases and climate change for each hydrological cycle component.

Hydrologic Comp/Model	Bias(%)	Change (%)	Hydrologic Comp/Model	Bias(%)	Change (%)
Precipitation			Snowfall		
GFDL 2.0	22	1	GFDL 2.0	81	-32
GISS AOM	-12	17	GISS AOM	6	-22
GISS ER	-12	25	GISS ER	-19	3
IPSL	-6	0	IPSL	71	-43
MIROC-hi	-3	-4	MIROC-hi	-12	-80
MIROC-med	-13	-12	MIROC-med	-7	-65
MRI	-16	16	MRI	13	-18
Mean	-6	6	Mean	19	-37
Snowmelt			Runoff		
GFDL 2.0	83	-32	GFDL 2.0	155	-30
GISS AOM	5	-20	GISS AOM	-24	-2
GISS ER	-19	5	GISS ER	-39	32
IPSL	73	-43	IPSL	73	-31
MIROC-hi	-12	-79	MIROC-hi	-9	-38
MIROC-med	-6	-65	MIROC-med	-30	-63
MRI	13	-17	MRI	-21	-7
Mean	20	-36	Mean	15	-20
Baseflow			Potential ET		
GFDL 2.0	176	4	GFDL 2.0	-54	45
GISS AOM	50	43	GISS AOM	-42	5
GISS ER	76	45	GISS ER	-49	5
IPSL	22	-5	IPSL	-34	46
MIROC-hi	63	-12	MIROC-hi	-24	37
MIROC-med	27	-32	MIROC-med	-29	32
MRI	11	38	MRI	-34	14
Mean	61	12	Mean	-38	27
ET			Total Water		
GFDL 2.0	-37	16	GFDL 2.0	154	-8
GISS AOM	-26	7	GISS AOM	16	33

GISS ER	-30	12	GISS ER	27	43
IPSL	-25	12	IPSL	33	-17
MIROC-hi	-18	6	MIROC-hi	29	-18
MIROC-med	-20	3	MIROC-med	0	-40
MRI	-22	12	MRI	-7	25
Mean	-25	10	Mean	36	3

Climate Change

Although there is inconsistency among models, the mean precipitation created by the ensemble suggests an increase of 6% due to climate change. ET and PET calculations give positive changes for all models, with more uniformity in ET. These changes likely result from temperature increases in the warm season. Substantial decreases in snowfall suggest that warming is strong in winter as well. Runoff decreases substantially for most models, possibly due to enhanced drying of soils (due to enhance ET) between rains, which then can hold more precipitation when the next event occurs. Total water yield shows wide variance among the models, with the ensemble mean showing almost no change from the contemporary climate.

Impact on Water Quality

Although a detailed study of changes in water quality with climate change was beyond the scope of this study, we can infer some possible trends from the hydrologic components. Fugitive nitrates and sediment from the landscape are both carried by overland flow related to runoff. However, the dominant pathway for nitrate loss is through leaching to groundwater and then via baseflow or tile drains (Randall, 2001). Results show a substantial decrease in runoff in the future climate but increase in baseflow, although with less agreement among models. From this we might speculate that both sediment and nitrate loading of streams would decrease due to decreased runoff but that nitrate leaching might increase. Therefore, although water quality might improve due to reduced sediment, the loading due to nitrates is less clear but might increase.

A caveat to the previous analysis is related to the spectrum of intensity of rainfall events that is likely to occur. Recent observations (Groisman et al., 2005) and projections by regional climate models of future scenario climates (Gutowski et al., 2003) suggest an increase in extreme rainfall events, even if there is no change in total annual rainfall. In Europe, in fact, reports (Christensen and Christensen, 2003) suggest that this effect could lead to more flooding and, at the same time, more droughts due to fewer but more intense precipitation events that are more widely separated in time. If this should be the future for the UMRB as well, the reduced runoff might mask a more subtle mechanism for increasing overland loss of sediment and nitrate.

Conclusions

Output from an ensemble of seven GCMs was examined for use in driving a regional hydrological model for contemporary and future scenario climates. Ensemble mean results showed only modest changes in precipitation and streamflow for the UMRB for the end of the 21^{st} century (increases of 6% and 3%, respectively). Snowfall is substantially reduced over the basin in the future scenario climate (down 37%). Low resolution of global model results contributes to low biases in ET and PET, which, in turn, give high biases for baseflow. Despite these biases an increase in baseflow of 12% and decrease of runoff of 20% are simulated for the future scenario. These results suggest that both sediment and nitrate loading of streams would decrease due to decreased runoff, but that nitrate leaching to groundwater and eventually to streams might increase. Therefore, water quality might increase due to reduced sediment, but further studies are needed to determine whether increased nitrate leaching would be more than offset by reduced nitrate overland flow. These results do not account for possible changes in storm intensity that might increase overland flow even with no change in total precipitation.

Acknowledgement

We acknowledge the international modeling groups for providing their data for analysis, the Program for Climate Model Diagnosis and Intercomparison (PCMDI) for collecting and archiving the model data, the JSC/CLIVAR Working Group on Coupled Modelling (WGCM) and their Coupled Model Intercomparison Project (CMIP) and Climate Simulation Panel for organizing the model data analysis activity, and the IPCC WG1 TSU for technical support. The IPCC Data Archive at Lawrence Livermore National Laboratory is supported by the Office of Science, U.S. Department of Energy.

References

Arnold, J.G., and N. Fohrer. 2005. Current capabilities and research opportunities in applied watershed modeling. Hydrolog. Processes, 19, 563-572.

Christensen, J.H., and O.B. Christensen. 2003. Severe summertime flooding in Europe. *Nature*, 421, 805.

Intergovernmental Panel on Climate Change (IPCC). 2001. Climate change 2001 - The scientific basis, J.T. Houghton, T.Y. Ding, D.J. Griggs, M. Noguer, P.J. van der Linden, and D. Xiaosu (Eds.), 944pp., Cambridge Univ. Press, Cambridge.

Groisman, P.Y., R.W. Knight, D.R. Easterling, T.R. Karl, G.C. Hegerl, and V.N. Razuvaev. 2005. Trends in intense precipitation in the climate record. J. Climate, 18, 1326-1350.

Gutowski, W.J. Jr., S.G. Decker, R.A. Donavon, Z. Pan, R.W. Arritt, and E.S. Takle. 2003. Temporal-spatial scale of precipitation errors in central US climate simulation. J. Climate, 16, 3841-3847.

Global Energy and Water Cycle Experiment (GEWEX). 2005. http://www.gewex.org/gewex_overview.html.

Jha, M., Z. Pan, E.S. Takle, R. Gu. 2004. Impact of climate change on stream flow in the Upper Mississippi River Basin: A regional climate model perspective, J. Geophys. Res., *109*, D09105, doi:10.1029/2003JD003686.

Neitsch, S.L., J.G. Arnold, J.R. Kiniry, R. Srinivasan, and J.R. Williams. 2002. Soil and Water Assessment Tool: User Manual, Version 2000. Texas Water Resour. Inst. TR-192. GSWRL 02-02, BRC 02-06. 455 pages.

Pan, Z., R.W. Arritt, E.S. Takle, W.J. Gutowski, Jr., C.J. Anderson, and M. Segal. 2004. Altered hydrologic feedback in a warming climate introduces a “warming hole”. Geophys. Res. Lett.*31*, L17109, doi:10.1029/2004GL020528.

Program for Climate Model Diagnosis and Intercomparison (PCMDI). 2005. http://www-pcmdi.llnl.gov/

Randall, G.W. 2001. Factors affecting nitrate losses to subsurface tile drainage and surface waters in Minnesota. Presented at Summit for Finding Common Ground in Controlling Agricultural Nonpoint Sources of Nutrients, 7-9 October, Queenstown, Maryland.

Stocker, T.F. and C.C. Raible. 2005. Water cycle shifts gear, Nature, *434*, 830-833.

Takle, E.S. and L.O. Mearns. 1995. Midwest Temperature Means, Extremes, and Variability: Analysis of Observed Data. In G. R. Carmichael, G. E. Folk, and J. L. Schnoor, ed., Preparing for Global Change: A Midwestern Perspective. Academic Publishing bv, Amsterdam, p . 129-134.

Takle, E.S., M. Jha and C.J. Anderson. 2005. Hydrological cycle in the Upper Mississippi River Basin: 20th century simulations by multiple GCMs. Submitted to Geophysical Research Letters (May 2005).

US Department of Agriculture (USDA) Soil Conservation Service. 1972. National Engineering Handbook, Section 4 Hydrology, chapters 4-10.

Wu, P., R. Wood and P. Stott. 2005. Human influence on increasing Arctic river discharges, Geophys. Res. Lett., 32, L02703, doi:10.1029/2004GL021570.

Modelling of Nitrogen Leaching from a Watershed using Field Scale Models

Anatoli Vassiljev
Department of Mechanics, Tallinn University of Technology, Ehitajate tee 5, 19086, Tallinn, Estonia E-mail: avasil@edu.ttu.ee

Abstract

Many comprehensive models have been developed for use at the small scale (field, patch); however, there is a need for models applicable to the watershed scale. Most conceptual hydrological models cannot provide the data needed to calculate the nitrogen transformations in soils, and it is difficult to couple them with the comprehensive nitrogen-leaching models. Furthermore, some researchers show that the mobile-immobile water concept, or a division of the soil pore space into slow and fast flowing regions can improve the results of nitrogen modelling. Hydrological models developed for watersheds usually ignore the non-equilibrium water movement. MACRO model has been developed in Sweden for water and solute transport, which takes into account the non-equilibrium fluxes of water in soils with macropores. This model has been elaborated for use on the field scale and it is coupled with another well-known field scale model SOILN, which simulates nitrogen turnover and leaching. The objective of this paper was to show that field scale models may be adapted to the watershed scale. The differences between the small homogeneous fields and the heterogeneous watersheds are very significant.

1. The zone of aeration is usually thin in areas located close to permanent streams, and quite thick in areas located far from streams and especially on hills. The soil profile with a thin zone of aeration will be saturated very quickly, and will start producing the surface runoff. On the other hand, the soil profile with a thick zone of aeration needs much more water for saturation and very rarely produces surface runoff.

2. The discharge at the watershed outlet depends on the performance of its river system. The larger the watershed, the more time is needed for water to reach the outlet of watershed. This leads to differences in the time lags between water flows to the outlet of a small field and to the outlet of the whole watershed. The time lag may vary from several hours for small watersheds with areas of several square kilometers to several days for watersheds with areas of several thousands a square kilometers. Moreover, the river system usually acts as a chain of reservoirs that smooth variations in water flow and quality.

Two different field scale models were tested on the watershed scale. One of them is based on the mobile-immobile water concept and other one ignores the non-equilibrium water movement.

Introduction

Elevated nitrate concentrations in surface and ground waters continue to be a matter of concern throughout the developed world (e.g. Burt et al., 1993; Worrall &Burt., 1999). High nitrate content can degrade surface water quality by promoting eutrophication. The river water in agricultural areas often contains high nitrate amounts due to anthropogenic sources such as manure and fertilizers used on arable land. In many countries, non-point source pollution from agriculture represents the major source of nitrate pollution (Pfenning & McMahon, 1996). Therefore, there is a need to understand and predict the influence of agricultural practices on nitrogen export from catchments. Usually the modelling of nitrogen leaching includes two main tasks. The first is the modelling of water fluxes, because water is a carrier of nitrogen. The second task is the modelling of the nitrogen fate. Many comprehensive one-dimensional models have been developed for water flow and solute transport. Some of them may be found in Rood, 2004. The well-known SOILN model (Johnsson et al., 1987) describes fate of nitrogen in soil. This model works in conjunction with the SOIL model, which simulates water fluxes. Some researchers showed that division of the soil pore space into slow and fast flowing regions can improve the results of nitrogen modelling (Addiscott et al., 1992; Larsson & Jarvis, 1999). Therefore, other variants of the SOILN model has been developed, which works in conjunction with the MACRO model and takes into account the non-equilibrium fluxes of water in soils with macropores (Jarvis, 1994). Some of the one-dimensional models work on the field scale. For example, the models MACRO, SOIL simulate horizontal fluxes to field drainage system and consequently, they are rather at field scale than pure one-dimensional models. Vassiljev at al. (2004) have proposed the method to adapt a field scale model for use at the watershed scale. The method is based on the assumption that a watershed may be represented by set of typical fields. Water and solute from these fields go directly into the river system and to watershed outlet. The method has been tested for MACRO and SOILN models developed (Larsson & Jarvis, 1999) for use in the case of dual-porosity soil profile. Calculations of interchange between micro and macro pores need much computer time. The objective of this study was to test the method of adaptation of the field scale model for the watershed for another couple of models – SOIL and SOILN. The SOIL model does not simulate water exchange between macropores and micropores and therefore needs less time for calculations. Moreover, SOIL model simulates many more situations than MACRO model. Therefore, SOIL model would be preferred one in case it gives results, which do not differ much from results of the MACRO model.

Method of Calculation

The models MACRO (Jarvis, 1994), SOIL (Jansson, 1991) and SOILN (Johnsson et *al.*, 1987) are one-dimensional models developed for use at the field scale. In all of them, the soil profile is divided into homogeneous layers characterized by their physical and biological properties. The models are used in series such that the results from the hydrological model (MACRO or SOIL) are used as input data for the SOILN model. The driving input data for the hydrological model (MACRO or SOIL) include daily meteorological information: precipitation, air temperature, wind speed, vapour pressure, and solar radiation.

The soil profile in the MACRO model is divided into two separate but interacting pore regions, the macropores and micropores, each characterized by the conductivity, vertical flow rate, and degree of saturation. The SOIL model does not simulate water exchange between macropores and micropores.

To adjust the MACRO and SOILN models to the watershed scale, some procedures have been proposed in Vassiljev et al. (2004). They take into account the influence of a relief and river network. The differences between the small homogeneous fields and the heterogeneous watersheds are quite significant. Field scale models deal with one soil profile. Vassiljev et al. (2004) showed that even watersheds with one soil type and one land use type needs several soil profiles to represent different thicknesses of the zone of aeration within a watershed. The soil profile with a thin zone of aeration will be saturated very quickly and will start producing surface runoff. Conversely, the soil profile with a thick zone of aeration needs much more water for saturation and very rarely produces surface runoff.

The discharge at the watershed outlet depends also on the performance of the river system. The larger the watershed, the more time is needed for water to reach the outlet. This leads to differences in the time lags between water flows to the outlet of a small field and to the outlet of the whole watershed. The time lag may vary from several hours for small watersheds with areas of several square kilometres to several days for watersheds with areas of several thousands square kilometres. Moreover, the river system usually acts as a chain of reservoirs that smooth variations in water flow and quality.

Vassiljev et al. (2004) used set of different soil profiles to take into account various thicknesses of the zone of aeration. Fractions of the watershed represented by each profile are calculated on the base of results obtained by hydrological model for each of them and measured water flow. Response functions have been used to model processes in the river system. The aim of this study was to test this approach for coupling of the one-dimensional models (SOIL and SOILN), which are used very often to simulate nitrogen leaching. This coupling of models takes less computer time for calculations but does not simulate nitrogen exchange between micropores and macropores. Therefore, the second aim was to compare results obtained in this study with ones obtained by the model, which simulates nitrogen exchange between micropores and macropores. Calculations have been performed for the watershed of the River Odense in Denmark with a watershed area 496 km^2.

Results and Discussion

Vassiljev et al. (2004) have proposed to represent watersheds as a set of the typical, non-interacting fields with different one-dimensional profiles. Water and nitrogen flows are calculated for each typical field (represented by their own soil profile) using the field scale model. Water and nitrogen flows for the whole watershed are calculated by equations

$$Q_t = \sum_{\tau=1}^{M}\left[\sum_{i=1}^{N}\left(I_{i,t-\tau+1}k_i a\right) + P_{t-\tau+1}WAa\right]h_\tau + Q_b \tag{1}$$

$$Q_t \cdot c_t = \sum_{\tau=1}^{M}\left[\sum_{i=1}^{N}\left(I_{i,t-\tau+1}k_i a c_{i,t-\tau+1}\right) + P_{t-\tau+1}WAac_p)\right]h_\tau + Q_b c_b \tag{2}$$

where Q_t is water discharge at the watershed outlet at time t (days), $I_{i,t}$ is water flow from the area represented by the ith soil profile at time t (in mm depth per day), and k_i is the dimensionless coefficient representing areal fraction occupied by the ith soil profile (typical field), τ is the consecutive number of the ordinate of the response function (from 1 to M, and h_τ is the dimensionless ordinate of the response function, P is precipitation (mm), WA is the share of watershed area occupied with the streams (fraction of one), a is a coefficient for transformation of mm depth per day into m^3/s (= F/86400/1000, where F is watershed area in m^2 and 86400 is the number of seconds in 24 h), Q_b is base flow, c_t is concentration at the watershed outlet (g/m^3), $c_{i,t}$ is concentration at the outlet of the ith typical field, and c_b is concentration in baseflow. Response function h_τ is approximated by function with two parameters (Kalinin & Miljukov, 1957).

$$h_\tau = \frac{1}{r\Gamma(n)}\left(\frac{\tau}{r}\right)^{n-1}\exp\left(-\frac{\tau}{r}\right) \tag{3}$$

where $\Gamma(n)$ is a gamma function, and n and r are dimensionless parameters.

Coefficients k_i, representing areal fraction occupied by the I-th soil profile, are obtained from the GIS system or by means of calibration. Calibration is possible only if there are data on measured water discharges during several years. Automatic calibration (Vassiljev at al., 2004) especially needs a great deal of information on measured discharges. Besides, automatic calibration is based on comparison of the measured and simulated hydrographs and therefore coefficients, obtained by calibration, depend on the model as well (different models – different coefficients).

Five different soil profiles have been used to represent differences in relief (Table 1).

Table 1. Set of the soil profiles selected to represent the watershed.

Profile	A	B	C	D	E	F (area of the river network)
Whole depth (cm)	170	95	65	30	15	0
Depth of the drainage system (artificial or natural) (cm)	95	80	50	20	10	0

Solver procedures from Microsoft Excel were used to evaluate the parameters by minimizing the objective function, OF.

$$OF = \min \sum_{t=b}^{e} (Q_{t,\text{obs}} - Q_{t,\text{sim}})^2 \tag{4}$$

where b and e indicate the beginning and end of the time series used for optimization; and $Q_{t,\text{obs}}$, $Q_{t,\text{sim}}$ are observed and simulated water discharge at the outlet of the watershed ($m^3\ s^{-1}$).

The time series divided into two parts. The first part (1991–1993) was used to calibrate the model. The second part (1994–1996) was used for validation, i.e. the parameters obtained by calibration on the first part of series were used in the calculations for the second half of series, to verify the model performance on independent data. The efficiency of the model was evaluated according to the formula used by Loague & Green (1991):

$$EF = \left[\sum_{i=1}^{NN} (O_i - O_{av})^2 - \sum_{i=1}^{NN} (C_i - O_i)^2 \right] / \sum_{i=1}^{NN} (O_i - O_{av})^2 \tag{5}$$

where C_i are the predicted values, O_i are the observed values, NN is the number of values, and O_{av} is the mean of the observed data.

The efficiency of the model for the first half of the time series (calibration part) equals 0.90 for the watershed model based on the SOIL model and 0.92 for the one based on the MACRO model. The efficiency for the second half of the time series (validation part) equals 0.88 and 0.90 respectively. Figure 1 shows the comparison of the observed and simulated hydrographs for the period 1993–1994. One can see that the simulated discharges coincide quite well with the measured values for both models. Results obtained by MACRO and SOIL models are indistinguishable for the most part of hydrograph. High efficiency of the watershed model based on the SOIL model shows that SOIL model may be adapted for the watershed scale.

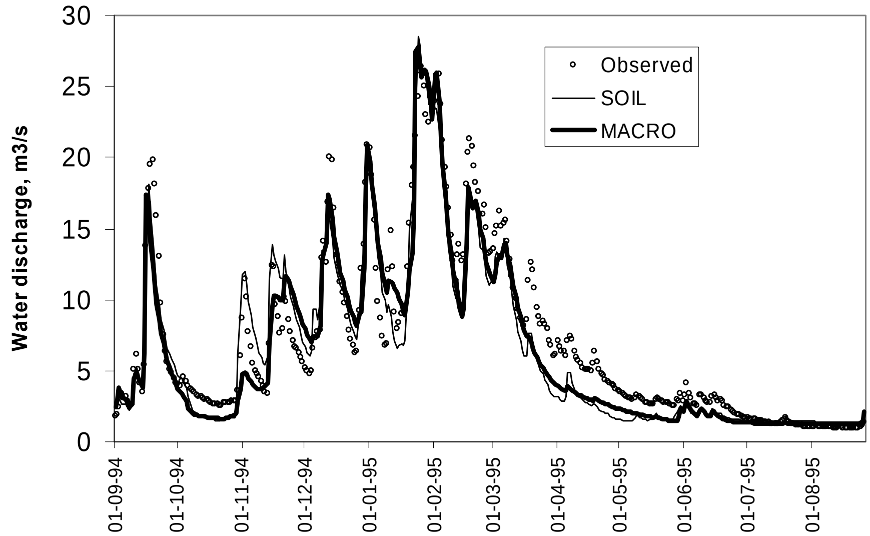

Figure 1. Discharge simulated by the SOIL and MACRO models (both adapted for modelling on the watershed scale) and observed water discharge in the River Odense (F = 496 km2).

The water flow simulated by the SOIL / MACRO model was used to calculate the concentrations of nitrogen. The modelling of nitrogen concentration was performed using the same categories of the soil profiles (Table 1) with the corresponding SOILN model (it was mentioned above that SOILN model working with MACRO model adjusted for use in the case of dual-porosity soil profile (Larsson & Jarvis, 1999)). The fertilization rate was 140 kg ha^{-1} year^{-1}. The leaching of nitrates was calculated for each typical profile. The transport (flow) of nitrates at the watershed outlet was calculated using Equation (2). The concentrations at the watershed outlet are estimated by dividing the flow of nitrates (Equation (2)) by water discharge (Equation (1)). Figure 2 shows the results for the period 1993–1994.

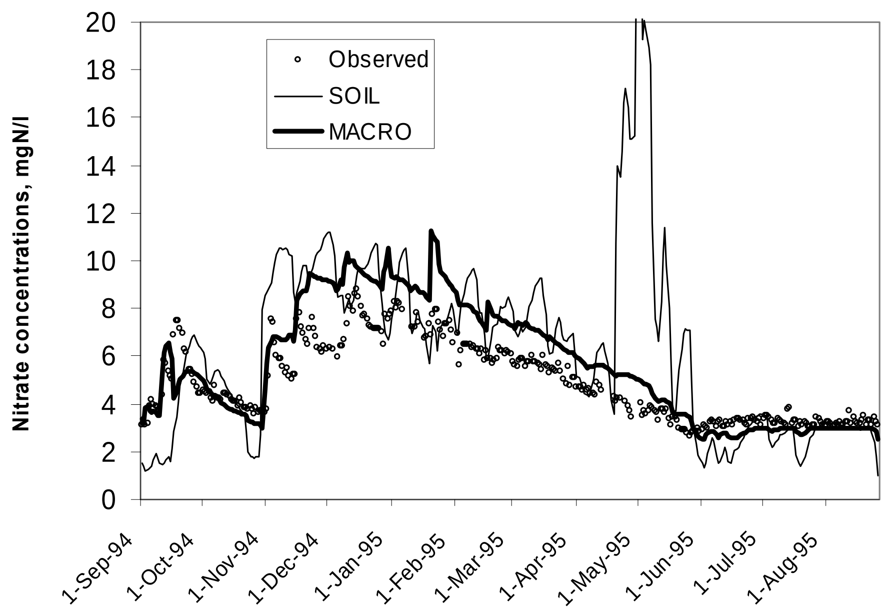

Figure 2. Simulated by SOIL + SOILN and MACRO +SOILN (all adapted for modelling on the watershed scale) and observed nitrate concentrations in the River Odense.

One can see that results, obtained by MACRO and corresponding SOILN model, are closer to observed values. Concentrations obtained by SOIL and SOILN models oscillate around concentrations obtained by MACRO and SOILN models. There are also obvious reactions on fertilization in each year (peaks of simulated concentrations with values above 20 mg/l). These oscillations show, in our opinion, that use of dual-porosity soil profile improves results. Thus, MACRO model is preferable to SOIL for simulation of the daily concentrations. Both models can be used for the simulation of the mean concentrations for the longer time (2-3 months).

Summary and Conclusions

The investigation showed that the one-dimensional models SOIL and SOILN may be used on the watershed scale after adaptation by the method proposed in Vassiljev et al., (2004). Comparison of the results with results obtained by MACRO model showed that SOIL model simulates water flow with the same precision as the MACRO model. Results also showed that use of dual-porosity soil profile in MACRO model with corresponding SOILN model improves simulation of the daily concentrations significantly. Thus, MACRO model is preferable to SOIL for simulation of the daily concentrations. Both models can be used for the simulation of the mean concentrations for the longer time (2-3 months).

Acknowledgements

This work was financially supported by the Estonian Scientific Fund (grant 6199).

References

Addiscott, T.M., Whitmore, A.P., Powlson, D.S. (1992) *Farming, Fertilizers and Nitrate Problem*. CABI Publishing, Wallingford, UK.

Burt, T.P., Heathwaite, A L. & Trudgill S.T. (eds) (1993) *Nitrate. Processes, Patterns and Management*. John Wiley & Sons Ltd, Chichester, West Sussex, UK.

Jansson, P-E. (1991) SOIL water and heat model, technical description. Internal paper from Soil Science Department, Swed. Univ. of Agricultural Sciences., 46 pp.

Jarvis, N. (1994) The MACRO model (Version 3.1). Technical description and sample simulations. Reports and Dissertations 19, Dept of Soil Sci., SLU, Uppsala, Sweden.

Johnsson, H., Bergström, L., Jansson, P.-E. & Paustian, K. (1987) Simulated nitrogen dynamics and losses in a layered agricultural soil. *Agric. Ecosyst. Environ.* 18, 333–356.

Kalinin, G.P. & Miljukov, P.I. (1957) On the computation of unsteady flow in open channels. *Met. Gidrol.* 10**,** 10–18 (in Russian).

Larsson, M.H. & Jarvis, J. (1999) A dual-porosity model to quantify macropore flow effects on nitrate leaching. *J. Environ. Qual.* 28, 1298–1307.

Loague, K. & Green, R.E. (1991) Statistical and graphical methods for evaluating solute transport models: overview and application. In: *Validation of Flow and Transport Models for Unsaturated Zone* (guest ed. by P. J. Wierenga). *J. Contam. Hydrol.* 7, 51–73.

Pfenning, K.S. & McMahon, P.B. (1996) Effect of nitrate, organic carbon, and temperature on potential denitrification rates in nitrate-rich riverbed sediments. *J. Hydrol.* 187, 283–295.

Rood, A.S. (2004) A Mixing-Cell Model for Assessment of Contaminant Transport in the Unsaturated Zone Under Steady-State and Transient Flow Conditions. *Environmental Engineering Science.* 21 (6), 661-677

Worrall, F. & Burt, T.P. (1999) The impact of land-use change on water quality at the catchment scale: the use of export coefficient and structural models. *J. Hydrol.* 221, 75–90.

Vassiljev, A., Grimvall, A. & Larson, M. (2004) A dual-porosity model for nitrogen leaching from a watershed. *Hydrological Sciences Journal* 49(2), 313-322

Calibration and Validation of the SWAT Model to Predict Atrazine Load in Streams in Northeast Indiana

Gabriel Vazquez–Amabile[1], Bernard A. Engel[1], Dennis C. Flanagan[2]

[1]Agricultural and Biological Engineering department. Purdue University, ABE Bldg. 225 University St. West Lafayette, IN 47907-2093 USA. E-mail: engelb@purdue.edu

[2]USDA, ARS, National Soil Erosion Research Laboratory, W. Lafayette, Indiana, USA

Abstract

SWAT was calibrated and validated to predict atrazine loads in streams for the period 1996-2004 at eleven sampling sites, in northeast Indiana. This study was carried out within a comprehensive water quality monitoring and BMP research and assessment project, led by the USDA-ARS National Soil Erosion Laboratory (West Lafayette, Indiana), for the Source Water Protection Initiative in the St. Joseph River Watershed (268,000 ha).

SWAT performed well in predicting the general trend of atrazine concentration in streams over time, for daily and monthly time intervals. Daily streamflow calibration and validation had to be accomplished before starting pesticide calibration. During the validation period, Nash-Sutcliffe values varied from 0.33 to 0.60 for daily streamflow and between 0.64 and 0.74 for monthly streamflow. Even though the model was not accurate for predicting atrazine levels at specific points, showing low Nash-Sutcliffe values, SWAT was consistent in presenting high coefficients of determination (R^2), despite over and under predicting values. Monthly predictions were better than daily predictions, but three month running averages were not better than monthly average concentrations.

During the calibration period, monthly atrazine concentrations were predicted with an average R^2 of 0.60 and a average Nash Sutcliffe coefficient of 0.38. In the validation period atrazine was predicted with an average R^2 of 0.49 and an average Nash-Sutcliffe value of -0.91. Large watersheds were not consistently better predicted than smaller watersheds, or vice versa. After validation, the total mass of atrazine released by the entire basin between 2000 and 2003, for the period April-September, was closely predicted by the model in two of the four years. The observed average amount of atrazine released during the four seasons was 1,002.1 kg/season, whereas SWAT predicted 950.1 kg/season.

Introduction

The general goal of this study was to analyze the capabilities and performance of the SWAT model (Soil Water Assessment Tool, Arnold et al., 1998) to predict atrazine levels in streams and carry out a nonpoint source (NPS) pollution risk analysis for this pesticide, to be used as a complement of the NAPRA-GLEAMS system (Lim et al., 2001), at the basin scale.

SWAT was calibrated and validated for the period 1996-2004 at 11 sampling sites in northeast Indiana. This study was carried out within a comprehensive water quality monitoring and BMP research and assessment project, led by the USDA-ARS National Soil Erosion Laboratory (West Lafayette, Indiana), for the Source Water Protection Initiative in the St. Joseph River Watershed. Watershed modeling is an integral component of the project, and the main purpose of this study was to evaluate the SWAT model for water quality modeling and its use in risk analysis.

The St. Joseph River watershed is located in northeast Indiana, northwest Ohio, and south central Michigan, and encompasses 2,808.5 km^2. The main stream of the watershed is the St. Joseph River, approximately 100 km long, which runs in a NE-SW direction until joining the Maumee River at Fort Wayne, IN. Since 1995, agricultural chemicals have been detected in the St. Joseph River at Fort Wayne. This river represents the source of drinking water for approximately 200,000 residents in Fort Wayne (SJRWI, 2004). Peak levels of atrazine higher than 3 ppb, (the EPA drinking water standard, EPA, 2004) have been reported at different sites in the watershed between 1995 and 1998 by a network of environmental groups (Environmental Working Group-EWG) and the St. Joseph River Watershed Initiative (SJRWI).

Water quality data recorded by SJRWI between 1996 and 2002 offer the possibility for calibration and validation of hydrologic models for the entire watershed, which may be used to simulate the impact of different management practices or any other kind of scenarios. In 2002, the USDA-Agricultural Research Service started a program to study the transport and fate of agricultural chemicals in the sources of the water supply, as well as the impact of best management practices (BMP) implementation, in the St. Joseph River Watershed (Flanagan et al., 2003).

In previous evaluations, SWAT has shown good results when predicting runoff (Saleh et al., 2000; Spruill et al., 2000) and nitrogen and phosphorus levels in streams (Saleh et al., 2000; Saleh and Du, 2002; Saleh et al., 2003). SWAT daily predictions for atrazine were evaluated in Sugar Creek, Indiana by Neitsch et al. (2002) who reported an R^2 of 0.21 and 0.41 in the calibration and validation periods, respectively.

Methodology

This project consisted of two parts. First, SWAT was calibrated and validated for streamflow at four USGS gauges. Then, the model was calibrated and validated at 10 sampling sites within the study area for atrazine level in streams. Additionally, SWAT was validated for the entire basin at the main outlet for the period 2000-2004 using a more detailed daily dataset for the St. Joseph River. This data was recorded by personnel at the Three Rivers Filtration Plant, at Fort Wayne.

The St. Joseph River watershed is largely agricultural with major crops being corn and soybeans. Land use was grouped in five major classes where agriculture and pasture represent 79.9% of the total area, forest 13.1%, wetlands 3.9%, and urban 3.1% of the total watershed area.

Soils in the watershed are generally poorly drained and the parent material is compacted glacial till. The topography of the watershed varies from rolling to nearly level plains. Erosion and over-saturation are the major soil limitations (SJRWI, 2004), and tile drainage is an important practice in some sectors of the basin. The average slope varies between 0 to 2%, and the predominant soil hydrologic groups are classes B and C on 24% and 73% of the area, respectively. The remaining 3% correspond to class A.

Input files for SWAT were organized based on GIS data supplied by the SJRWI. Weather data recorded at Butler, Garret, and Waterloo in Indiana and Montpellier in Ohio were used in this study. Daily streamflow recorded by the USGS at four of the five gages in the watershed were used to calibrate SWAT for streamflow. Those gages were located at Cedar Creek near Cedarville, Cedar Creek near Newville, the St. Joseph River near Ft. Wayne, and Fish Creek near Artic. Data from Fish Creek near Hamilton was not used in this study because of the presence of Hamilton Lake and the lack of information to calibrate the reservoir, which has an extension of 300 hectares.

As for atrazine, SJRWI has been collecting water quality data since 1996 at 40 sampling stations throughout the watershed. For this study, only 10 sampling stations were selected, which provide continuous sets of observations of atrazine for the period 1996-2002. Model calibration and validation for atrazine were conducted at these sampling sites. To obtain monthly atrazine concentrations, average weighted values were calculated from weekly streamflow observation.

Additionally, data recorded by the Three Rivers Filtration Plant at Fort Wayne were used to validate the model at the main outlet of the watershed for the period 2000-2004. This dataset was supplied by the Office of the Indiana State Chemist.

Atrazine Application Rates and Dates

Corn and soybean acreages have been assigned based on the proportion they are represented in the watershed according to the information supplied by the USDS-National Agriculture Statistics Service (NASS, 2004a). Since SWAT cannot grow two different crops in the same Hydrologic Response Unit in the same year, two rotations (Corn-Soybean and Soybean-Corn) were assigned to different HRUs. This was done in order to get an average constant area of corn and soybeans according to the actual crop distribution. This is an important step in making a more realistic simulation of pesticide (atrazine in corn) and nutrient (N and P in corn and soybean) losses, since both crops require different rates and produce different biomass. Usual tillage, planting dates, and rates of application were set according to current farmer practices and information published by USDA-NASS.

For the simulation, the corn-soybeans rotation (corn in the first year and soybeans in the second year) represented 54% of the cropping area, and the soybeans-corn rotation the represented the remaining 46%. Thus, average corn acreage was 52% for the period 1986-2004, which is slightly higher than the 48% recorded by NASS for the same period.

After establishing the corn and soybean acreage for the basin, two rotation scenarios were set to input the distribution of atrazine applications according to the planting dates of every year for the period 1996-2004, supplied by the NASS (NASS, 2004 a). The corn planted area progress, reported weekly for northeast Indiana, was used to set the application dates for atrazine for each year. Atrazine was applied three days after the reported planting date, at a rate of 1.46 kg/ha in only one application, according to the average use of that pesticide in northeast Indiana for 1996-2002 (NASS, 2004 b). In every hydrologic response unit (HRU) planted with corn, atrazine was applied weekly, proportional to the increment of the planted area. For example, an increment of 10% planted area resulted in an application of 0.146 kg/ha, which means that 1.46 kg atrazine /ha was applied randomly to 10% of the corn area. Thus, atrazine was applied from April to June according to the progress of corn planting, which had a different pattern every year due to weather (Figure 1).

This input information was extremely important in the calibration process, improving model predictions when atrazine was applied following the actual pattern of corn planting in every season, instead of using an overall average pattern of application. As can be observed in Figures 1a and b, the planting distribution was completely different from one year to another, which has an effect on the application of atrazine and its release to the stream after every storm.

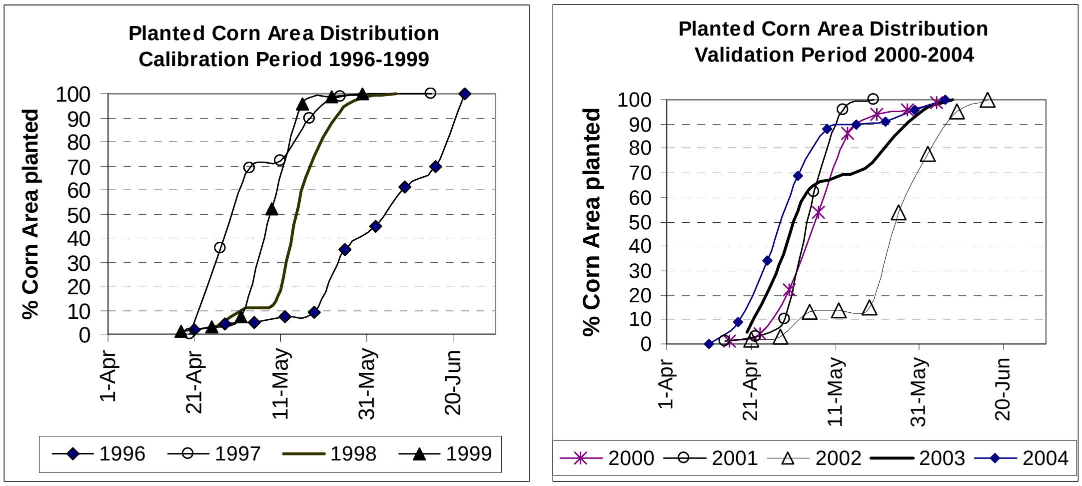

a b

Figure 1. Planting date distribution according to NASS (NASS, 2004a) for northeast Indiana between 1996 and 1999 (a) and from 2000 to 2004 (b).

Calibration and Validation

The model was first calibrated and validated for streamflow and then atrazine. For streamflow, the model was calibrated for the period 1989-1998 at three USGS gages: Cedar Creek near Cedarville, and the St. Joseph River near Ft. Wayne and near Newville. Streamflow validation was accomplished for the period 1999-2002 at those gages as well as at Fish Creek near Artic, using records from 1998-2002.

As for atrazine, data from 10 sampling sites were used for model calibration and 11 sampling sites for validation. The calibration period was 1996-1999, and the validation period was 2000-2003 for the SJRWI stations. Furthermore, the entire basin was validated at the main outlet for the period 2000-2004, using data recorded by the Three Rivers Filtration Plant at Fort Wayne. All model runs were started three years before the period of analysis to be sure the model results were stabilized at the beginning of the study period.

Streamflow calibration was accomplished by adjusting the model for all subbasins simultaneously, without changing settings for each subbasin. This strategy was adopted for two reasons. First, the watershed is fairly uniform, in terms of landscape, slope, drainage pattern, and land use. Thus, there is no reason to calibrate the model for different subbasins. Second, if SWAT is calibrated for the entire watershed regardless of the subbasin boundaries, the model results will not depend on the watershed subdivisions, and model settings will remain the same if a different criterion is adopted to define subbasins. This was important in this project because USGS gages and SJRWI sampling sites were placed at different locations. Since SWAT computes pesticide load in streams at every subbasin outlet, two different subbasin subdivisions were used for streamflow and atrazine calibration, respectively.

For streamflow calibration and validation, a SWAT project was created defining six subbasins for the five USGS gages and the main outlet of the St. Joseph River Watershed (HUA 8-digit # 04100003). After finishing streamflow calibration, a new SWAT project was built for atrazine calibration, keeping the model settings but redefining subbasin boundaries, using the 10 water quality sampling sites as subbasin outlets. Figure 2 shows the subbasin outlets for streamflow and for atrazine calibration.

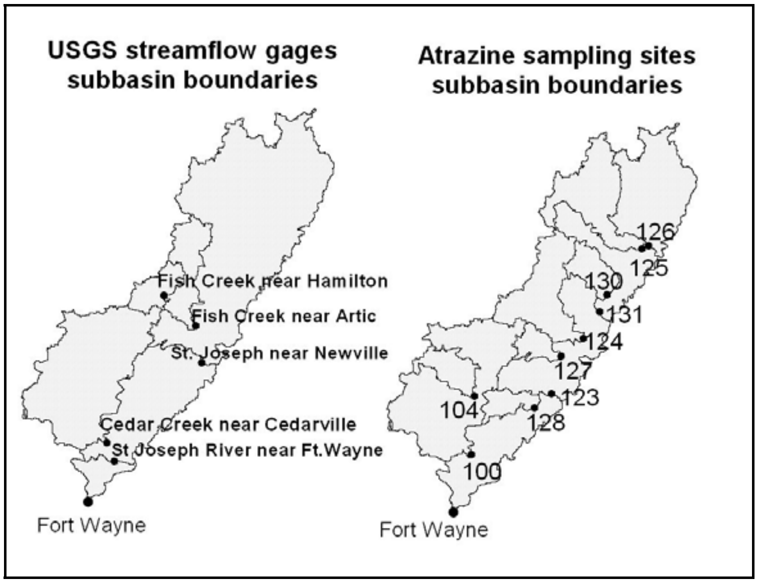

Figure 2. Subbasin boundaries for streamflow and atrazine calibration.

Daily and Monthly Streamflow: Calibration and Validation

Prior to calibrating SWAT for atrazine, streamflow was calibrated. Daily streamflow calibration is important in predicting atrazine release to the streams during and after each precipitation event. A good calibration for monthly streamflow is not useful to predict atrazine movement to the streams if the model is not reasonably well calibrated for daily streamflow.

In the calibration process for streamflow, the curve number was reduced by five for all HRUs, and the Manning's coefficients for overland flow, the main and tributary channels, and groundwater inputs were calibrated.

In Table 1, R^2 values and the Nash-Sutcliffe model efficiencies (R^2_N) (Nash and Sutcliffe, 1970) are presented for the validation periods at four of the USGS gages, for daily and monthly streamflow.

Table 1. Nash-Sutcliffe model efficiency for monthly streamflow predictions for the validation period (1999-2002).

Validation Sites (1999-2003)	Drainage Area (ha)	Daily		Monthly	
		R^2	R^2_N	R^2	R^2_N
Fish Creek near Artic	24,430	0.62	0.60	0.73	0.72
Cedar Creek near Cedarville	64,039	0.60	0.53	0.73	0.64
St. Joseph River near Newville	148,108	0.50	0.33	0.73	0.68
St. Joseph River near Ft. Wayne	255,310	0.66	0.59	0.76	0.74

Model Calibration and Validation to Predict Atrazine Concentration on Streams

As previously mentioned, a new SWAT project was built, keeping the former settings but using the water quality sampling sites to define the subbasin outlets (Figure 2).

Predicted atrazine values are given by the model in milligrams per day. Thus, atrazine concentration in ppb was computed dividing the pesticide given in milligrams by the total daily volume of water (computed from flow in m^3/sec). Daily and monthly predicted values were computed for atrazine loads at the 10 sampling sites and at the main basin outlet. During the calibration process, many adjustments were attempted, including modification of pesticide solubility (g/L), application efficiency, and delaying pesticide application for three, five, and eight days after planting. However, the only adjustments that had a major impact on the model predictions were the PERCOP (pesticide percolation coefficient) coefficient and the distribution and rate of atrazine throughout the planting season. The PERCOP coefficient was set at 0.04, and the atrazine application dates and rates were set for each year, delaying it three days after planting, according to the corn planted area progress reported by NASS for northeast Indiana (NASS, 2004a). Even though there were different applications dates, there was just one corn planting date, since SWAT does not allow more than one crop growing at the same time in the same HRU. Therefore, the last application of atrazine might be done on a crop planted earlier, and some pesticide might be intercepted by leaves. SWAT monitors the amount of pesticide intercepted by foliage and washed off during rain events according to a pesticide constant coefficient, or WOF (wash-off fraction for pesticide). To solve this problem, the WOF for atrazine was set to 1 in order to wash off all pesticide remaining on the crop leaves in the following rain event. Thus, PERCOP and WOF were the only model coefficients modified after streamflow calibration to predict atrazine concentration in streams.

R^2, Nash-Sutcliffe model efficiency (R^2_N), and root mean squared error (RMSE) for daily, monthly and three-month running average atrazine concentrations, between April and September, are presented in Table 2 for the calibration period (1996-1999) and Table 3 for the validation period. Both tables show the upstream area corresponding to each sampling station or subbasin outlet. In some cases the sampling stations were placed on the St. Joseph River (123, 131 and Ft. Wayne); in other cases samples were taken in a tributary stream before joining the St. Joseph River. For that reason, at some points, observed atrazine load comes from the pesticide released in one subbasin and, at other points, comes from the atrazine routed from more than one upstream subbasin.

Table 2. Model calibration results for atrazine concentration at streams sites for 1996-1999.

Site	Upstream Area (ha)	Daily			Monthly			Three-month running average		
		R^2	R^2_N	RMSE (ppb)	R^2	R^2_N	RMSE (ppb)	R^2	R^2_N	RMSE (ppb)
100	64,180	0.45	0.42	1.78	0.71	0.69	0.88	0.83	0.76	0.87
104	9,909	0.36	0.33	2.10	0.68	0.66	0.97	0.67	0.57	0.88
123	162,000	0.36	0.30	1.97	0.77	0.60	1.10	0.78	0.57	1.04
124	27,280	0.00	-0.46	3.41	0.12	-0.14	1.91	0.01	-0.49	1.94
125	27,880	0.15	-0.04	2.40	0.53	0.16	1.42	0.39	-0.30	1.50
126	38,660	0.15	0.08	2.77	0.50	0.37	1.42	0.25	-0.04	1.58
127	6,252	0.18	0.11	3.45	0.40	0.32	1.89	0.57	0.49	1.49
128	6,770	0.29	-0.37	3.61	0.74	0.29	1.83	0.82	0.18	1.85
130	9,348	0.54	0.49	1.79	0.85	0.76	0.88	0.78	0.63	0.84
131	96,100	0.23	-0.07	3.83	0.71	0.12	2.08	0.81	-0.09	2.04
Mean		**0.27**	**0.08**	**2.71**	**0.60**	**0.38**	**1.44**	**0.59**	**0.23**	**1.40**
Mean area weighted		**0.29**	**0.14**	**2.57**	**0.66**	**0.42**	**1.39**	**0.67**	**0.28**	**1.37**

SWAT performed better for monthly predictions than for daily predictions, and the R^2 values were also better than the Nash-Sutcliffe model efficiency, based on the disagreement with the 1:1 line between observed and predicted values.

There are many sources of uncertainty when modeling NPS pollution caused by atrazine. Some of them come from the input data and others from the model itself. It is important to provide the model with accurate atrazine rates and application dates. The quality of the recorded data, regarding the frequency of the water sampling, during and between rainfall events, is also a key issue in the calibration-validation process. Precipitation data is also of importance because of the spatial variability of this variable and the consequent variation of runoff and NPS pollution throughout the watershed.

However, SWAT estimates resembled the general pattern of daily and monthly atrazine loads in streams over time, but either under or over-predicted daily and monthly loads (Figures 3 and 4). Part of the error might be due to the prediction of streamflow, which adds to the error in the atrazine load prediction.

Table 3. Model validation results for atrazine concentration at streams sites for 1999-2003 for SJRWI sampling stations and 2000-2004 for the Fort Wayne water treatment plant.

Site	Upstream Area (ha)	Daily			Monthly			Three-month running average		
		R^2	R^2_N	RMSE (ppb)	R^2	R^2_N	RMSE (ppb)	R^2	R^2_N	RMSE (ppb)
100	64,180	0.77	-2.49	2.57	0.63	-2.01	1.99	0.45	-0.64	0.85
104	9,909	0.80	-2.37	2.95	0.20	-2.08	2.40	0.20	0.03	0.95
123	162,000	0.25	0.40	1.44	0.53	0.40	1.15	0.25	-0.01	0.63
124	27,280	0.73	-1.94	2.56	0.39	-2.11	1.88	0.54	-3.54	1.99
125	27,880	0.35	0.21	1.29	0.63	0.36	0.90	0.66	0.32	0.93
126	38,660	0.81	-0.70	1.70	0.58	-0.28	1.20	0.71	-0.50	1.21
127	6,252	0.63	-0.78	2.51	0.38	-1.25	2.14	0.17	-1.81	1.87
128	6,770	0.66	-1.02	2.70	0.61	-3.69	2.60	0.72	-4.76	1.58
130	9,348	0.30	0.09	2.15	0.33	0.17	1.32	0.66	0.10	1.21
131	96,100	0.10	0.05	2.10	0.48	0.18	1.48	0.20	-0.88	1.62
Fort Wayne (Basin outlet)	262,000	0.27	-0.31	1.06	0.59	0.28	1.34	0.58	0.24	0.91
Mean		**0.52**	**-0.80**	**2.09**	**0.49**	**-0.91**	**1.67**	**0.46**	**-1.17**	**1.28**
Mean area weighted		**0.35**	**-0.40**	**1.59**	**0.33**	**-0.22**	**0.91**	**0.23**	**-0.39**	**0.68**

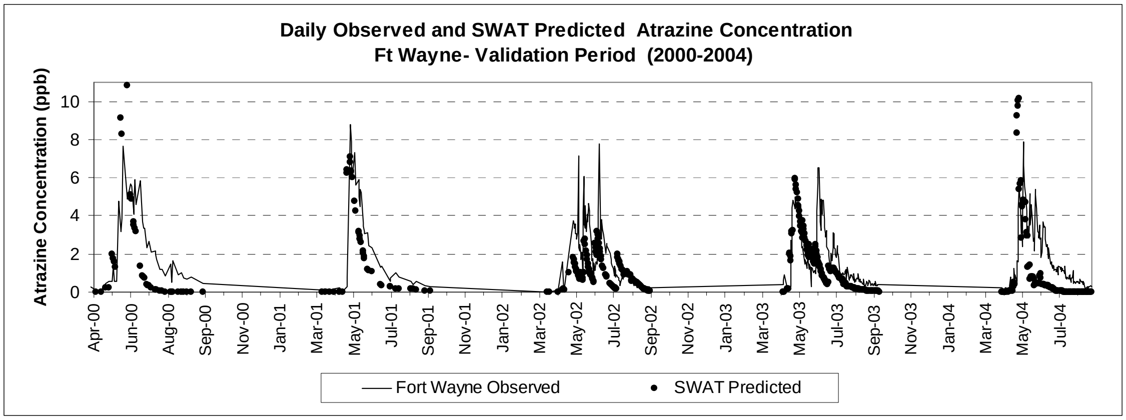

Figure 3. Observed and SWAT predicted daily atrazine concentration in the St. Joseph River at Fort Wayne, for the validation period 2000-2004.

As for the total mass of atrazine released by the entire basin to the river during the crop season (April-September) in the period 2000-2003, Table 4 shows the SWAT predicted values and the observed values at Fort Wayne. Although the atrazine concentration for the crop season 2004 is known, the total mass of atrazine was not computed, because the USGS flow data for that season were not available at the time of this report.

Assuming an average annual mass of atrazine of 120,000 kg applied to the entire basin, (a rate of 1.46 kg/ha applied to 50% of the agriculture area, or 59% of the total area), the released mass of the pesticide would represent 0.9% of the total applied (Table 4). This proportion agrees with similar values reported in other studies (Hubber, 1993; Zhang et al., 1997; Christensen and Ziegler, 1998).

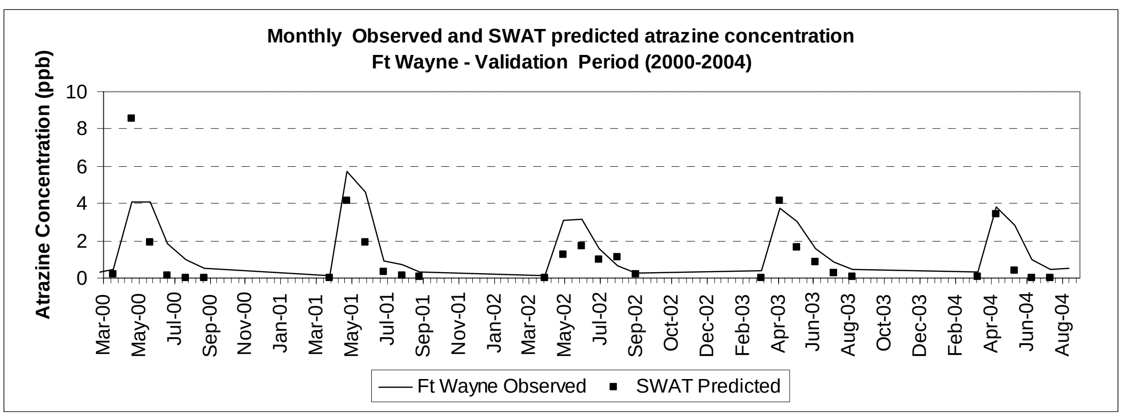

Figure 4. Observed and SWAT predicted monthly atrazine concentrations in the St. Joseph River at Fort Wayne for the validation period 2000-2004.

Table 4. Total Mass and proportion of applied atrazine released to the St. Joseph River during the crop season in the period 2000-2003.

Year	Total mass (kg) of atrazine released to streams (April-September)		Proportion (%) of the applied mass of atrazine released to streams (April-September)	
	Observed	SWAT predicted	Observed	SWAT predicted
2000	1,391.0	1,864.9	1.15%	1.55%
2001	989.9	531.4	0.82%	0.44%
2002	698.8	354.8	0.58%	0.29%
2003	928.9	1,052.8	0.77%	0.87%
Average 2000-2003	1002.1	951.0	0.83%	0.79%
Total 2000-2003	4,008.5	3,803.9		

Conclusions

SWAT performed well in predicting the general trend of atrazine concentrations in streams over time, for daily and monthly time intervals. Daily streamflow calibration and validation had to be accomplished before starting pesticide calibration. During the validation period, Nash-Sutcliffe values varied from 0.33 to 0.60 for daily streamflow and between 0.64 and 0.74 for monthly streamflow.
Even though the model was not accurate for predicting atrazine levels at specific points, showing low Nash-Sutcliffe values, SWAT was consistent in presenting high coefficients of determination (R^2), despite over and under predicting values. Monthly predictions were better than daily predictions, but three month running averages were not better than monthly average concentration predictions.

During the calibration period, monthly atrazine concentrations were predicted with an average R^2 of 0.60 and an average Nash Sutcliffe coefficient of 0.38. In the validation period, atrazine was predicted showing an average R^2 of 0.49 and an average Nash-Sutcliffe value of -0.91. These results agreed with those reported by Neitsch et al. (2002) in Sugar Creek, east-central Indiana.

Large watersheds were not consistently better predicted than smaller watersheds, or vice versa. At validation, the total mass of atrazine released by the entire basin between 2000 and 2003, for the period April-September, was closely predicted by the model in two of the four years. The observed average amount of atrazine released during the four seasons was 1,002.1 kg/season, whereas SWAT predicted 950.1 kg/season.

Likewise, the model was suitable to carry out an NPS pollution risk analysis for atrazine, to be used as a complement of the NAPRA-GLEAMS system, at a basin scale. Additional research will be necessary to evaluate the model sensitivity to predict the effects of best management practices on NPS pollution. This represents a key question for NPS pollution modeling and an essential step before using SWAT as a tool for comparing different management scenarios.

As a recommendation for future research and model improvements, it can be said that the model does not generate any output variable that describes the level of pesticides in shallow groundwater. This is very important to predict pesticide loads not only in shallow aquifers, but also in the baseflow between rainfall events, particularly in those watersheds that deliver pesticides through tile drain systems.

Finally, the amount of atrazine released to the St. Joseph River during the period 2000-2003, represented around 1% of the total applied in the entire basin. Therefore, model inputs sampling method and frequency required to predict such a proportion should be as accurate as possible so as not to introduce additional sources of uncertainty in the processes of model calibration and validation.

References

Arnold, J.G., R.Srinavasan, R.S.Muttiah, and J.R.Williams. 1998. Large Area hydrologic modeling and assessment part I: model development. J.American Water Resources Association. 34(1):73-89.

Christensen, V. G. , A. G. Ziegler Atrazine in source water intended for artificial ground-water recharge, south central Kansas. USGS fact-sheet FS-074-98.

Engel, B. A., and J. Lee. 1998 WWW-based hydrologic/water quality modeling decision supports system. In: Seventh International Conference on Computes in Agriculture. F.Zazueta and J. Xin (eds.) ASAE, St. Joseph, MI. pp:359-367.

EPA, 2004. Consumer fact-sheet on Atrazine http://www.epa.gov/safewater/contaminants/dw_contamfs/atrazine.html Accessed July 7th, 2004

Flanagan, D. C., S.J.Livingston, C.H. Huang, and E.A.Warnemuende. 2003. ASAE Paper No.03-2006 . Runoff and Pesticide Discharge from Agricultural Watersheds in NE Indiana. Las Vegas, Nevada: ASAE

Huber, W. Ecological relevance of atrazine in aquatic systems. 1993. Environ. Toxicol. Chem. 12:1865-1881.

Lim, K.J, B. Engel, and A. Hertzron. 2001. Incorporation and Evaluation of a River Quality Model to NAPRA WWW Decision Support System No 01-2127 International ASAE Annual Meeting, Sacramento, California.

NASS, 2004 a. Indiana Agricultural Statistics. Available at http://www.nass.usda.gov/in/publications.html Accesed on July 2004

NASS, 2004 b. NASS Agricultural Chemical Database. Available at http://www.pestmanagement.info/nass/app_usage.cfm. Accesed on July 2004.

Neitsch, s., J. G. Arnold and R. Srinavasan. 2002. Pesticides Fate and Transport Predicted by the Soil and Water Assessment Tool (SWAT)Atrazine, Metolachlor and Trifluralin in the Sugar Creek watershed. BRC Publication #2002-03. Office of Pesticide Programs Environmental Protection Agency. Available at http://www.brc.tamus.edu/swat/applications/SugarCreekIN.pdf

Saleh A., J. G. Arnold, P. W. Gassman, L. M. Hauck, W. D. Rosenthal, J. R. Williams and A. M. S. McFarland. 2000. Application of SWAT for the upper North Bosque River watershed. Transactions of the ASAE. 43(5): 1077-1087.

Spruill, C.A., S.R. Workman, and J. L.Taraba. 2000. Simulation of daily and monthly stream discharge from small watersheds using the SWAT model. Transactions of the ASAE 43(6): 1431-1439.

St. Joseph River Watershed Initiative. 2004. http://www.sjrwi.org/watershed.htm (Accessed 2/12/2004)

Zhang, X.C., L.D. Norton and M. Hickman. 1997. Rain pattern and soil moisture content effects on atrazine and metolachlor losses in runoff. Journal of Environmental Quality. 26:1539-1547.

A Procedure to Compute Groundwater Table Depth Using SWAT

Gabriel G. Vazquez-Amábile[1] and Bernard A. Engel[1]
[1]Agricultural and Biological Engineering Department. Purdue University, ABE Bldg. 225 University St. West Lafayette, IN 47907-2093 USA. E-mail: engelb@purdue.edu

Abstract

A procedure to compute perched groundwater table depth, using SWAT inputs and outputs, is proposed based on the theory used by DRAINMOD, in order to expand SWAT capabilities. SWAT was calibrated and validated for streamflow for three watersheds, and for groundwater table depth for three soils, at sites located within the Muscatatuck River Basin in southeast Indiana. The Nash-Sutcliffe model efficiency (R^2_N) for monthly streamflow was 0.49, 0.61 and 0.81 for the three watersheds for the validation period (1995-2002). SWAT predicted groundwater table depths provided R^2_N values of 0.61, 0.36, and 0.40 for the three soils in the calibration period (1992-1994), and 0.10, -0.51 and 0.38 for the validation period (1995-1996). Even though the model performance for predicting groundwater table depth was not as good as for streamflow, SWAT predictions resembled the seasonal variation of the groundwater table with correlation coefficients (r) of 0.68, 0.67, and 0.45 for the three wells during the validation period.

Introduction

In rural watersheds, groundwater table rises can decrease total productivity by reducing the farming area, affecting the development of crops, and delaying or stopping field-work (tillage, planting, and harvest) and can degrade the soil properties for the next crop season (Pivot et al., 2002). In the long run, groundwater table rises increase the risk of groundwater contamination by nutrients and pesticides and may also bring about soil salinization, depending on the groundwater quality.

The objective of the work presented here was to extend the SWAT model to compute groundwater table depth, which is a variable of interest when rural watersheds are analyzed at river basin scales. Thus, the main goal of this study was to incorporate some knowledge from DRAINMOD (Skaggs, 1980) into SWAT in order to expand its capabilities respecting the essence of the model. The intention of computing groundwater table depth, which is not computed by SWAT, is not to change the model soil water balance, but provides an additional variable of interest.

In this study, SWAT input and outputs were used to compute groundwater table depth for three soil series in southeast Indiana based on the theory used by DRAINMOD. AVSWAT2000 version was used for this purpose (Di Luzio et al., 2001). Primarily, SWAT was calibrated and validated for streamflow on three watersheds within the Muscatatuck River Watershed, located in southeast Indiana. Then, SWAT was tested to compute water table depth on a smaller watershed in the Muscatatuck Wildlife Refuge.

Groundwater table depth is a variable of interest for basin level studies, and SWAT might be an efficient tool to compute it, making it possible to evaluate the impact of tile drainage and other practices on this variable. The main advantage of modeling groundwater table depth with SWAT lies in the fact that SWAT does not necessarily require sub-daily precipitation data, does not require the retention curve for the soils, and can model more than one soil simultaneously in different subbasins in large watersheds, comparing scenarios and generating thematic maps.

Methodology

Study Area and Input Data

The study area was the Muscatatuck River Watershed, defined by the USGS as 8-digit HUA #05120207. It has an area of 295,221 hectares and is located in southeast Indiana (Figure 1) in Decatur, Jennings, Ripley, Jefferson, Scott, and Jackson counties. The SWAT model calibration and validation for streamflow was carried out using data recorded at the three USGS stream gages in the watershed, located at Vernon, Deputy, and Harberts Creek. Groundwater table depth calibration and validation were conducted using data from three observation wells located in the Storm Creek Lower Watershed (14 digit HUA #05120207080040) (Figure 1). Daily weather data were obtained from the records of the weather stations located at Greensburg and North Vernon as shown in Figure 1 for the period 1976-2002.

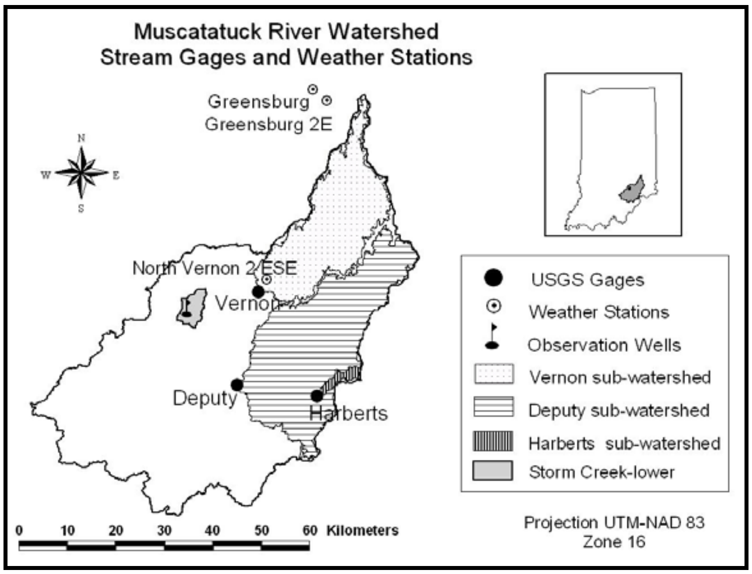

Figure 1. Weather stations and USGS gages for the Muscatatuck River Watershed.

SWAT calibration and validation were accomplished using daily streamflow data recorded by USGS for the period 1976-2002 at gages 03369500 (Vernon), 03366500 (Deputy), and 03366200 (Harberts Creek near Madison) (USGS, 2003a). Elevation data used in the project was the National Elevation Dataset (NED-NAD 83) DEM with a resolution of one arc-second (approximately 30 meters), developed by USGS.

Groundwater table data recorded by Jenkinson (1998) during the period 1992-1996 were used for groundwater table depth calibration and validation. The groundwater table was measured at three observation wells located in three soil series, Avonburg, Rossmoyne, and Cobbsfork, at the Muscatatuck Wildlife Refuge in the Storm Creek Lower Watershed (14 digit HUA 05120207080040) as depicted in Figure 1.

Two sources of soil data were used in this study. Soil data from the State Soil Geographic Database for the Conterminous United States (STATSGO), approximate scale 1:250,000, were used when the 8-digit HUA area was analyzed for streamflow calibration and validation, because more detailed information from SSURGO (Soil Survey Geographic database) was not available for the six counties included in the watershed. SSURGO data were available for Jennings and Jackson counties, and used for the groundwater table depth calibration and validation at the Muscatatuck Wildlife Refuge, located in the 14 digit-HUA watershed Storm Creek Lower.

As for groundwater inputs, "baseflow days" were computed using the RECESS model (USGS, 2003b), a program developed by Rutledge (1993) to determine the recession index and the master recession curve from daily streamflow records. The "groundwater delay" was set at zero days assuming there was not a vadose zone between the lower limit of the soil bottom layer and the shallow aquifer, which fluctuated from the surface to 2.5 m during the year. The default value for the shallow aquifer specific yield (0.003) was replaced by 0.18, corresponding to the average specific yield for silt (Johnson, 1967), according to the high proportion of that material in the subsoil. The remaining groundwater inputs were set to model default values.

Procedure to Calculate Groundwater Table Depth from Soil Moisture in SWAT

SWAT calculates the daily soil water balance. Every day the model updates the amount of water stored in every soil layer for every Hydrologic Response Unit (HRU). However, soil water content is an output variable for the soil profile as a whole, but not layer by layer. For this project, a special modification in the code was provided by the authors of SWAT in order to provide soil water content by layer of every hydrologic response unit, in an additional output file. Using this special output file, it was possible to convert soil moisture into groundwater table level following the theory used by DRAINMOD (Skaggs, 1980), using a spreadsheet without modifying the main code of the SWAT model and without additional inputs.

This procedure is based on the relationship between water table depth and drainage volume, which is the effective air volume above the water table. This relationship can be calculated for every soil from the drainage volume of every layer, building the curve that depicts that relationship. In DRAINMOD this relationship is used to determine the water table fall or rise when a given amount of water is removed or added from the soil profile. Drainage volume can be computed from the soil water characteristics for each soil horizon. However, when this information is not available, drainage volume can be calculated from the estimated drainage porosity of each soil layer (Skaggs, 1980). The later approach is useful in regional studies when detailed soil information is not available, and it was evaluated in this study because of its compatibility with the SWAT soil input data.

The drainage volume is the void space that holds water between field capacity and saturation. It can be understood as the volume of voids filled with air at field capacity. The volume of water stored in the void space always drains by gravity, and it will be termed "drainable volume". Even though both terms, drainage volume and drainable volume, are similar and therefore may be confusing, they were used here as defined for DRAINMOD in order to maintain the same terminology. Drainage volume is the volume of "air" held in macro pores, and drainable water is the volume of "water" held in macro pores.

If a completely saturated soil is left to drain under the force of gravity, the volume that drains (drainable volume) is equal to the "drainage volume". That drainage volume expressed as a fraction of the bulk volume is termed "Specific Yield" (Sy) or drainage porosity (Charbeneau, 2000). It is also important to keep in mind that soils are rarely fully saturated because of entrapped air. Thus, total saturation is usually around 90 or 95% of the soil porosity (Skaggs, 1980).

The drainage volume is related to groundwater table depth. Below the groundwater table, the drainage volume is equal to zero, because there is not air in the macro pores. Thus, if the water table is lowered by an amount of ΔH (mm), the water drained by the soil, in terms of water depth (mm), will be equal to the drainage porosity (Sy) multiplied by ΔH (Equation 1):

$$\text{Drainage volume (mm)} = Sy * \Delta H \qquad (1)$$

Below the groundwater table the soil is saturated and all the voids are filled with water. Then, the saturation upper limit was calculated as equal to the soil porosity, and soil porosity (%) was calculated as (Equation 2):

$$\text{Porosity (\%)} = 1 - (\text{Bulk density}/ 2.65) *100 \qquad (2)$$

Thus, the drainage porosity for each layer is given by the relationship (Equation 3):

$$\text{Drainage Porosity} = \text{Porosity} - \text{Field Capacity} \qquad (3)$$

Using the variables defined in SWAT, field capacity will be equal to the available water content plus the wilting point. Thus, Equation 3 can be written as (Equation 4):

$$\text{Drainage Porosity} = \text{Porosity} - \text{AWC} - \text{WP} \qquad (4)$$

where AWC is soil available water content, which is a model soil input, also termed as water retention difference (WRD) by NRCS, and equivalent to the amount of water stored between wilting point and field capacity. WP is the wilting point that is the fraction of micro pores that hold water at high pressures, which is not available to the crops. SWAT estimates WP as (Neitsch et al., 2001) (Equation 5):

$$\text{WP} = 0.4*\text{Clay (\%)} * \text{Bulk density} / 100 \qquad (5)$$

Drainage porosity was initially calculated for each layer of the three soils, and drainage volume (mm) was computed daily from the soil water stored for every layer (Equation 6a) and for the soil profile (Equation 6b).

$$\text{Layer Drainage Volume (mm)} = \text{Drainage Porosity} * \text{Layer Depth (mm)} \qquad (6a)$$

$$\text{Total Drainage Volume (mm)} = \Sigma \text{ Layer Drainage Volume} \qquad (6b)$$

Therefore, "Total Drainage Volume" is referred to as the volume of voids filled with air in the soil profile at field capacity (FC). The total drainage volume changes depending on the degree of saturation of the soil above FC. If the soil water content is at 100% of AWC, the "actual" drainage volume is equal to the soil Total Drainage Volume at FC. However, if the soil is above 100% AWC, the "actual" drainage volume will be smaller than the soil Total Drainage Volume.

The relationship "Total drainage volume – water table depth" was calculated using the layer drainage volume (mm) and the layer depth. Each layer has a special relationship which is defined by the specific yield. This relationship can be simplified as a linear function where the specific yield, or drainage porosity, is the slope (Skaggs, 1980). In Figure 2, the horizontal axis represents the water table depth, and also soil depth, and the vertical axis represents the total drainage volume. In that plot, the curve of each layer is drawn separately and the composite curve for the soil profile can be observed. If the points of cumulative drainage volume of each layer are joined, the cumulative curve for the soil profile is obtained. Thus, graphically, intercepting the curve for any drainage volume of soil profile, the groundwater table depth can be obtained. Figure 2 presents the curve for the Avonburg series and the same procedure was followed to build the curves for the other soils series, Cobbsfork and Rossmoyne. The graphical method is simple, but is cumbersome when there is a large amount of data. In this study, there were 3,650 daily data values, corresponding to the daily soil drainage volume values of a simulation of 10 years for each soil of the watershed.

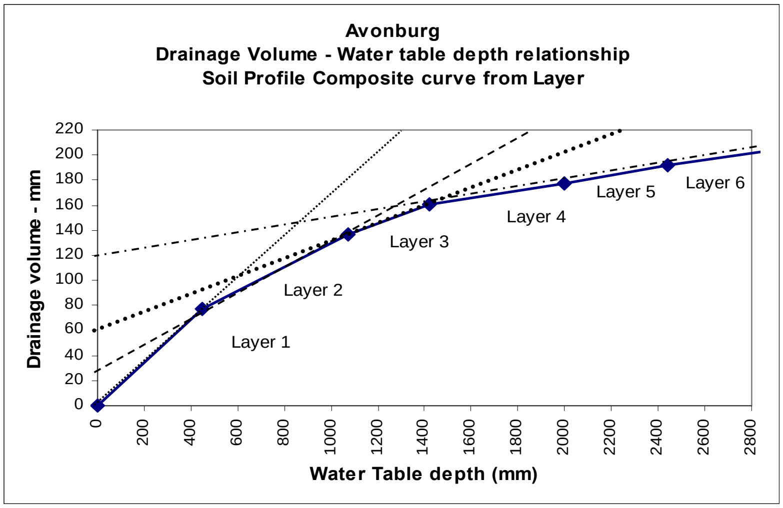

Figure 2. Soil profile water yield curve for the Avonburg series.

Thus, groundwater table depth was determined analytically using soil input data to compute the cumulative drainage volume of the soil from top to the bottom and soil output file to compute the total drainage volume. The total drainage volume was computed for the three soils for every day of the simulation based on the daily values of soil water content for each layer and the amount of water stored above field capacity at the end of the day. Groundwater table depth was computed daily for each soil according to its drainage volume.

This approach allows estimating the relationship between water table depth and drainage volume, but it is important to point out its limitations. The curves computed for the three soils depict a simplified linear relationship between soil drainage volume and water table depth. The slope of that relationship is depicted by the drainage porosity assuming that the soil is completely drained immediately above the water table. However, there is a transition zone, or capillary fringe, above the water table, which is at saturation near its base while its upper extent is near field capacity (Charbeneau, 2000). This transition zone above the water table is more important in fine soils than in coarse soils, and it is not considered in this approach.

Therefore, for a given drainage volume, the curve estimated in this way will under-predict the water table depth. This underestimation will be more important as the silt and clay content increase. Conversely, for a given water table depth the drainage volume will be overestimated. Since all three curves were built based on this assumption, and the slope of every layer were given by the drainage porosity, the shape of the curves differ from those curves computed using the soil characteristic curves. This underestimation was partially corrected in the calibration process, as discussed later.

Since this procedure is based on the relationship between water table depth and the soil drainage volume, water table depth oscillation can only be computed from the soil surface down to the lower limit of the bottom layer defined in the soil input information. When the water table is located below the lower limit, its depth cannot be computed because there is not information to compute water stored beyond the defined layers. In the case of the Avonburg soil, for example, the maximum observed depth of the shallow aquifer was 2.5 m, and therefore the lower limit of the soil profile was defined at 2.8 m.

It is important to keep this point in mind when the model is calibrated in order to provide enough soil information to compute water table oscillation. All soils of the watershed should be defined considering this point and also individually calibrated, if possible. For that reason, the definition of soil inputs and the calibration of soil and groundwater input parameters are very important steps in the process of predicting this variable using SWAT.

Results and Discussion

Streamflow Calibration and Validation

Streamflow calibration was completed using data recorded by the USGS at three watershed stream gages between 1980 and 1994. This process was conducted comparing monthly and daily observed streamflow with monthly and daily water yield predicted by SWAT. Observed and simulated results were compared by means of the correlation coefficients, the root mean square error (RMSE) and the Nash-Sutcliffe model efficiency (Nash and Sutcliffe, 1970), which estimates the agreement between the 1:1 line and the observed vs. simulated points. The correlation coefficients depicted the strength of the relationship between observed and predicted values indicating if both variables varied together or separately. Validation of SWAT predicted streamflow was carried out for the period January 1995 - September 2002. The final results for the three watersheds are presented in Tables 1 and 2 for calibration and validation periods, respectively. Model efficiency values for monthly streamflow were similar to those found by other authors (Saleh et al., 2000). Spruill et al. (2000) also found similar model efficiencies for daily streamflow between -0.14 and 0.19 and between 0.58 and 0.89 for monthly total flow.

Although streamflow calibration was not the main purpose of this study, it was carried out first to get a reasonable set of parameters to be used later in three observation wells located downstream 15 km southwest from Vernon, outside of the watersheds. Streamflow daily calibration could have been better if a different set of parameters would have been applied for each watershed. However, in that case, the problem is which setting we should have used for the observation wells.

Table 1. RMSE (mm) and Nash-Sutcliffe Model Efficiency (R^2_N) values for streamflow for the calibration period (1980-1994).

	RMSE (mm)		r		R^2_N	
Watershed	Daily	Monthly	Daily	Monthly	Daily	Monthly
Harberts	3.66	27.7	0.59	0.78	0.19	0.59
Deputy	3.53	19.8	0.47	0.85	-0.23	0.73
Vernon	2.43	15.1	0.70	0.90	0.28	0.80

Table 2. RMSE (mm), correlation coefficient (R) and Nash-Sutcliffe Model Efficiency (R^2_N) values for streamflow for the validation period (1995-2002).

	RMSE (mm)		r		R^2_N	
Watershed	Daily	Monthly	Daily	Monthly	Daily	Monthly
Harberts	5.25	38.4	0.52	0.70	0.05	0.49
Deputy	4.26	27.6	0.54	0.78	-0.35	0.61
Vernon	3.10	19.1	0.74	0.91	0.48	0.81

Groundwater Table Depth Calibration and Validation

After calibrating and validating the model for runoff for the whole watershed, daily and monthly groundwater table depth were calculated and compared with data recorded by

Jenkinson (1998) at the Muscatatuck Wildlife Refuge between January of 1992 and December of 1997, for three soil series: Avonburg, Rossmoyne, and Cobbsfork. The data recorded between 1992 and 1994 were used for the model calibration, and data for the period 1995-1997 for model validation.

Calibration was carried out varying bulk density layer by layer in a range of ± 10%. When this variation was not enough, available water content (AWC) was changed within a range of ± 10%. Bulk density variation has an effect on the soil porosity and then on the drainage porosity. Varying these soil parameters, the drainage volume-water table depth curve was modified in the three soils.

Once the soils were calibrated for the period 1992-1994, SWAT was run for the period 1995-1996 to validate the model. RMSE, correlation coefficient and R^2_N were computed comparing observed and predicted data. The data were compared using the daily measurements and by grouping the daily observations to create monthly observations. The results can be observed in Tables 3 and 4 and by looking at Figures 4, 5, and 6.

SWAT was again more efficient for monthly estimation than daily estimations. Even though SWAT presented RMSE from 42 cm to 84 cm for monthly estimations, the model was able to predict the groundwater table oscillation over time. This can be observed by looking at Figures 4, 5, and 6, and reading the correlation coefficients (r) from Tables 3 and 4. The correlation coefficients inform about the correlation between observed and SWAT predicted daily and monthly groundwater table depth throughout the calibration and validation periods. Correlation values varied from 0.46 to 0.82 for daily estimation and from 0.45 to 0.88 for monthly estimation. The magnitude of the correlation coefficient indicated the strength of the relationship between the observed and predicted data, in terms of whether they change together or separately, and Nash Sutcliffe coefficients explained how far all model predictions were from the reality.

Table 3. RMSE, model efficiency (R^2_N) and correlation coefficient (R) for groundwater table depth for calibration period (1992-1994).

	Daily			Monthly		
	RMSE (m)	R^2_N	R	RMSE (m)	R^2_N	R
Avonburg	0.51	0.28	0.82	0.42	0.61	0.88
Cobssfork	0.74	-0.12	0.60	0.59	0.36	0.71
Rossmoyne	0.69	0.15	0.46	0.65	0.40	0.64

Table 4. RMSE, model efficiency (R^2_N) and correlation coefficient (R) for groundwater table depth for validation period (1995-1996).

	Daily			Monthly		
	RMSE (m)	R^2_N	r	RMSE (m)	R^2_N	r
Avonburg	0.80	-0.05	0.71	0.79	0.10	0.68
Cobssfork	0.92	-0.74	0.41	0.84	-0.51	0.45
Rossmoyne	0.69	0.33	0.63	0.65	0.38	0.67

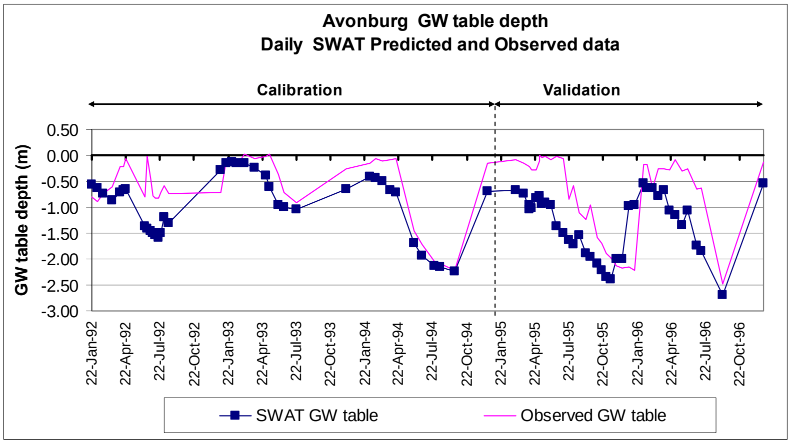

Figure 4. Observed and predicted data for the calibration and validation periods for the observation well located on the Avonburg soil.

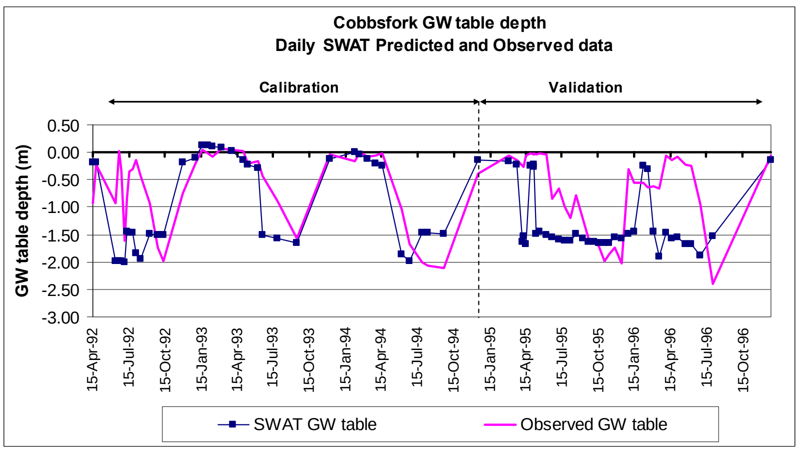

Figure 5. Observed and predicted data for the calibration and validation periods for the observation well located on the Cobbsfork soil.

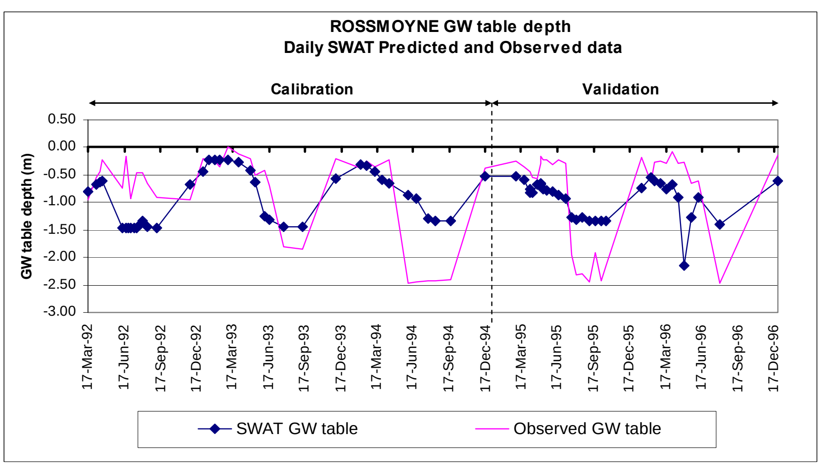

Figure 6. Observed and simulated data for the calibration and validation periods for the observation well located on the Rossmoyne soil.

The differences between observed and predicted values could be explained by the variability of soil properties, such as bulk density and available water content (AWC). The model was very sensitive to adjustments in AWC and bulk density when groundwater table depth was calibrated. The soil data were taken from NRCS reports (NRCS, 1976 and 1990), because soil measurements taken in situ were not available. Thus, even though the three soils were in situ classified as Avonburg, Rossmoyne, and Cobbsfork, NRCS soil data represent a mode profile and might not represent the properties of the series at the observation wells. This could be a source of error in the model calibration. Amatya et al. (2003) found that DRAINMOD performed poorly in predicting groundwater table depth during two years when the model was not calibrated using in situ soil measurements.

It was also difficult to estimate a unique cause for the errors, because there was not a common pattern in the error for the three soils. In Avonburg, the groundwater table was mostly underestimated, but fairly well predicted. In Cobbsfork it was under and over estimated and in Rossmoyne it was mostly overestimated. Over and underestimations of the model were not associated with any season, so that the error did not seem to be associated with a deficiency in the computation of the evapotranspiration. These differences between predicted and observed data could be due to several sources of uncertainty such as inaccurate soil data, lack of precipitation records taken in situ, and the assumptions of the estimated drainage volume-water table curve.

Conclusions and Recommendations for Future Research

The model showed a better performance in predicting monthly streamflow than daily streamflow. The better predictions were for the Vernon and Deputy Watersheds which were the largest watersheds and nearest the weather station.

A procedure to compute the water table depth of a shallow aquifer, using the soil input data and the SWAT output "daily soil water content by layer," was proposed based on the relationship drainage volume-water table depth. This procedure allowed prediction of shallow aquifer oscillations between the soil surface and the lower limit of the soil bottom layer. Thus, groundwater table depth was computed daily for each soil based on the relationship for water table depth-drainage volume. The model efficiency (R^2_N) for monthly groundwater table depth was 0.61, 0.36 and 0.40 for the three wells in the calibration period and 0.10, -0.51 and 0.38 for the validation period. The performance of the model to predict groundwater table depth was not as good as for streamflow. However, the model was able to predict the seasonal variation of groundwater table presenting correlation coefficients that varied between 0.46 and 0.88 in the calibration period and between 0.41 and 0.71 in the validation period. Inaccurate soil data, lack of precipitation records taken in situ, and the assumptions of the estimated drainage volume-water table curve were identified as the main sources of error to predict groundwater table. Another potential source of error is the contribution of the surrounding soil units to the groundwater table depth. Even though this should be included in the lateral flow from units located upstream, it still needs to be clarified.

Based to these results, the prediction of groundwater table depth based on daily soil water content might be an interesting capability for inclusion in SWAT, which would compute this variable for all soils of a watershed without using sub-daily precipitation data and soil retention curves. Furthermore, it makes it possible to analyze the impact of different scenarios, such as land use changes, weather change or management practices, on the variation of the shallow aquifer at different points of a basin. However, further studies using additional data, along with precipitation and soil measurements taken in situ are recommended to better analyze the performance of SWAT to predict this variable. A good understanding of the prediction of groundwater table depth by SWAT would be useful in the study of the performance of the model's soil water balance.

References

Amatya D.M., G. Sun, R.W. Skaggs, and C.C. Trettin. 2003. Testing of DRAINMOD for forested watersheds with non-pattern drainage. ASAE Paper No 032046, Las Vegas, Nevada: ASAE.

Charbeneau, R.J. 2000. Groundwater hydraulics and pollutant transport. Upper Saddle River, New Jersey: Prentice Hall.

Di Luzio M., R. Srinavasan, and J.G. Arnold. 2001. ArcView Interface for SWAT2000, User's Guide. Temple, Texas: Blackland Research Center-Texas Agricultural Experiment Station. http://www.brc.tamus.edu/swat/swatdoc.html.

Jenkinson, B.J. 1998. Wet soil monitoring project on two till plains in south and west central Indiana. M.S Thesis, Purdue University, West Lafayette, Indiana.

Johnson, A.I. 1967. Specific yield- compilation of specific yields for various materials. U.S. Geological Survey Water Supply. Paper 1662-D, 74 pp.

Nash, J.E. and J.E Sutcliffe. 1970. River flow forecasting through conceptual models. Part 1- A discussion of principles. Journal of Hydrology 10:282-290.

Neitsch, S.L., J.G. Arnold, J.R. Kiniry and J.R. Williams. 2001. Soil and Water Assessment Tool Theoretical Documentation version 2000. Temple, Texas: Blackland Research Center-Texas Agricultural Experiment Station. http://www.brc.tamus.edu/swat/swatdoc.html.

NRCS. 1976.Soil Survey of Jennings County, Indiana. USDA, Soil Conservation Service.

NRCS. 1990. Soil Survey of Jackson County, Indiana. USDA, Soil Conservation Service.

Pivot, J.M., E. Josien and P. Martin. 2002. Farms adaptation to changes in flood risk: a management approach. Journal of Hydrology 267 (1-2):12-25.

Rutledge, A.T. 1993. Computer programs for describing the recession of groundwater discharge and for estimating mean groundwater recharge and discharge from streamflow records: U.S. Geological Survey Water-Resources Investigations Report 93-4121.45p.

Saleh A., J.G. Arnold, P.W. Gassman, L.M. Hauck, W.D. Rosenthal, J.R. Williams and A.M. S. McFarland. 2000. Application of SWAT for the upper North Bosque River watershed. Transactions of the ASAE 43(5): 1077-1087.

Skaggs R.W. 1980. DRAINMOD reference report. USDA. Soil Conservation Service.

Spruill, C.A., S.R. Workman, and J.L.Taraba. 2000. Simulation of daily and monthly stream discharge from small watersheds using the SWAT model. Transactions of the ASAE 43(6): 1431-1439.

USGS, 2003a. NWISWeb Data for the Nation.http://waterdata.usgs.gov/nwis accessed 20 May.2003.

USGS, 2003b. Ground water information pages http://water.usgs.gov/ogw/gwsw.html. Accessed 15 Jun 2003.

Vazquez-Amábile, G. 2004. Computation of Groundwater table depth and flood risk on farm fields using SWAT. M.S Thesis, Purdue University, West Lafayette, Indiana.

Methods for Analyzing Calibration Parameter Uncertainty

T. L. Veith,[1] L. T. Ghebremichael,[2] M. W. Van Liew,[3] J. G. Arnold[4]
[1]USDA-ARS Pasture Systems and Watershed Management Research Unit, Curtin Rd.-Bldg. 3702, University Park, PA 16802, USA. E-mail: Tamie.Veith@ars.usda.gov.
[2]Pennsylvania State University, University Park, USA.
[3]USDA-ARS Grazinglands Research Laboratory, El Reno, OK, USA.
[4]USDA-ARS Grassland, Soil & Water Research Laboratory, Temple, TX, USA.

Abstract

Natural variation in any agricultural ecosystem impacts the degree to which a simulation model can accurately and precisely represent the system. However, due to time, expense, and repeatability limitations with field work, simulation modeling is often the most practical technique for predicting and comparing watershed-scale land management impacts on downstream water quantity and quality. Thus, it is important to understand, as fully as possible, the uncertainties within model input parameters and how these uncertainties affect model outputs. Of particular interest are surface and subsurface hydrologic and nonpoint source parameters to which previous studies have found a particular model is sensitive. The aim of this study is to use current and literature-based modeling efforts to begin a development of guidelines on uncertainty analysis which are understandable to a wide range of modelers.

Introduction

Watershed-level nonpoint source (NPS) simulation models are crucial in evaluating best management practice effects at the watershed scale, for which field studies become unfeasibly labor intensive. Such models also provide the ability to predict impacts of alternative management scenarios over time. However, simulation models contain multiple types of error, which can be related to three basic categories: physically-based input data, model processes, and non-physically related "calibration" parameters. Such errors can be significant in research involving natural systems, which are neither fully understood nor can be fully controlled by humankind, and thus should be considered when interpreting model results.

Input data contain errors due to collection and reporting as well as application errors of extrapolation of scale or quantification of a more general attribute. These uncertainties, as well as uncertainties in measurement and reporting methods, are transferred through to the model. Errors within the model process, assuming that all coding correctly performs the calculations intended by the model designer, likewise stem from the inability to completely know and quantify system processes and interactions accurately and precisely. The impossibility of such a task results in necessary simplifications in temporal and spatial scale and in simplifying from stochastic to discrete information. For further discussion on model error see Warwick (1991), Haan et al. (1995), Klepper (1997), and Gupta et al. (1998).

Additionally, many current NPS models require some level of calibration of a number of parameters. By uniquely combining nonlinear and evolutionary optimization techniques, Duan et al. (1993) developed the Shuffled Complex Evolution heuristic specifically to meet the needs of autocalibration of complex NPS models. Van Griensven and Meixner (2003) incorporated this heuristic into a suite of tools for performing sensitivity analysis, autocalibration, and uncertainty analysis on the Soil and Water Assessment Tool (SWAT; Arnold et al., 1998). Although autocalibration is much less labor intensive than manual calibration, both methods are still time consuming and require knowledge of processes characteristic to the watershed to create a realistic, physically-based representation. Additionally, for locations without monitored data, researchers have to rely on calibration values that have been determined for watersheds similar in physiographic region, climate, geology, and land use.

As autocalibration techniques become more widely validated in the literature, determining uncertainty ranges of calibrated parameters becomes of increasing interest. Such information is particularly valuable for modeling non-calibrated watersheds. By knowing which parameters are most uncertain, one can plan field data collection more efficiently and better assess where the modeled system will most likely vary from the natural system. Due to the absence of reported uncertainty values related to model processes and physically-based input data, calibration parameters have typically been used to account for all model error. Fortunately, research in assessing and portraying error, or uncertainty, within non-physically related input parameters (i.e., "calibration" parameters) has advanced notably in the past three decades as models have become increasingly complex and computer technology has facilitated more rapid and complex calculations. This paper will present a broad synthesis of uncertainty analysis literature for calibrating NPS models in an attempt to provide the necessary background for further discussion and development of clear uncertainty analysis guidelines.

Methods and Complexity of Calibration

Discussion of uncertainty analysis in complex models requires some prior consideration of methods of calibration employed. Manual calibration may only involve one specifically calculated measure but typically involves multiple implicit or draft calculations by the nature of human intuition and assessment. Most likely the expert is not even explicitly aware of many such measures, such as all the assessments made to determine and maintain a water balance. However autocalibration measures must be explicitly stated and those are generally reduced to one measure during the optimization process and perhaps one or two additional measures afterwards (Boyle et al., 2000). A fraction of possible calibration possibilities are shown in Figure 1. The solid bold line indicates the most simple path of calibrating for a single output (streamflow) to address a single optimization goal (minimize daily difference) by using a single objective function (sum of squares error). The resulting solution is tested by one or two statistics (Nash-Sutcliffe and the R^2 coefficient of determination). The solid thin line shows a route in which two functions are used to evaluate a single goal. The dashed line traces a more involved calibration process in which two outputs (stormflow and baseflow) are calibrated against. Stormflow is then calibrated using two optimization goals, each measured by a single function.

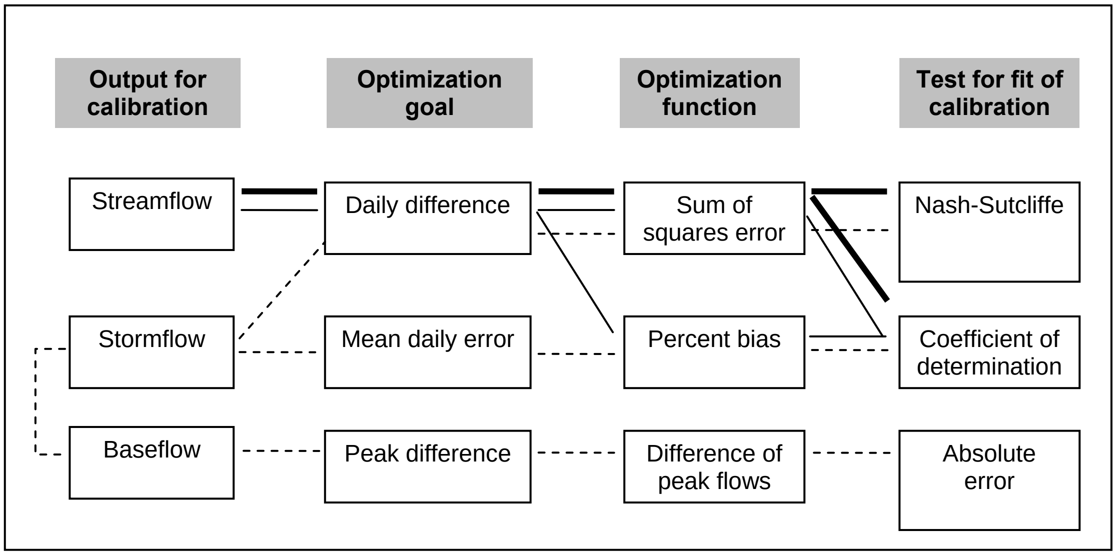

Figure 1. Three possible routes of model calibration, designated by solid bold, solid thin, and dashed lines.

While the single output/single objective/single function path is the simplest in terms of options and alternatives to evaluate, it is certainly not trivial. Substantial work has been done in developing, comparing, and fine-tuning optimization techniques to solve the calibration problem efficiently and effectively. Three basic routes have been taken: 1) methods focused largely on first-order, second-moment evaluations (Nofziger et al., 1994; Haan et al., 1995); 2) Markov chain Monte Carlo approaches such as the Metropolis algorithm (Klepper, 1997); or 3) single-objective optimization heuristics. Gupta et al. (1998) presented a concise report of progress along the first two routes for single-output calibration of hydrological models. Calibration methods involving optimization techniques such as response surface methodology, simulated annealing, genetic algorithms, and shuffled complex evolution have been demonstrated and compared (Duan et al., 1993; Ibrahim and Liong, 1992; Liong et al., 1995; Sumner et al., 1997; Mulligan and Brown, 1998; Gupta et al., 1999; Thyer et al., 1999). Most recently, researchers have worked to benefit from multiple routes by combining techniques; for example, the SCEM-UA algorithm (Vrugt et al., 2003) was created to incorporate benefits of the Metropolis algorithm into shuffled complex evolution.

Selecting the most suitable objective function ultimately depends on the question the model user is trying to answer (Klepper, 1997; Gupta et al., 1998). Willmott (1984), Martinec and Rango (1989), and ASCE (1993) provide guidance on selecting functions to evaluate hydrologic models. However, guidance related to other components of NPS models, and to which functions best address which optimization goals, remains limited. Perhaps this is why users appear to most often select those functions with which they are most familiar and/or which most frequently occur in the literature (which becomes, in itself, self-fulfilling). Thus, there appears a need for those conversant in mathematical implications of model-evaluation functions to help develop guidelines on which functions best or most completely address which goals and which test functions are most appropriate in given situations.

The next step of complexity is to evaluate a goal with multiple functions. In order to evaluate multiple goals while minimizing an increase in computational complexity, objective functions which combine the goals through some means of weighting have been developed (e.g., Van Griensven and Bauwens, 2003). In this situation a single "preferred" solution is provided at the end of the calibration run. Although techniques which maintain unique equations for the multiple criteria are typically more complex to evaluate and interpret, they are valuable in providing an ability to better fit the entire hydrograph (Klepper, 1997; Boyle et al., 2000). In particular, Liong et al. (1995) demonstrates this effect for peak flow. To address the need for multi-objective evaluation, Gupta et al. (1998) and Boyle et al. (2000) motivated the need for and demonstrated a multi-objective model, MOCOM-UA, which is presented in Yapo et al. (1998) and is an extension of SCE-UA. Cooper et al. (1997) and Abdulla et al. (1999) evaluated the abilities of multiple optimization methods to solve calibration problems with multiple objective functions.

The most complete approach to model calibration is to consider multiple goals, each evaluated with one or more objective functions. This is very much like adding another layer or dimension to the previous step. Such an evaluation, while providing a thorough evaluation of uncertainty within and among parameters and a good understanding of the model's response to the particular study, is likely to be more complex and involved than is feasible or even needed to sufficiently address ongoing research questions. Thus, as the number of outputs increases, feasibility likely will require a reduction in the numbers of objectives and functions evaluated for each output.

Uncertainty Analysis through Multiple Solutions

Solution sets from multiple output or multiple function techniques form pareto-curves of nondominated solutions. The pareto-curves show the trade-off among different optimal results with respect to the outputs or functions. In Figure 2, solution point "S1" on the curve is more optimal in minimizing Function #1 while solution point "S2" is more optimal in minimizing Function #2. Although solutions in between are less optimal within at least one of the functions as compared to points "S1" and "S2", there are no solutions that are more optimal within either function than those shown on the curve.

In some cases, different optimization runs result in equivalent or nearly equivalent objective solutions. This is particularly likely when input specifications for the optimization runs differ slightly. Such differences might include changes in the seed used to generate random numbers for the optimization algorithm, changes in optimization population sizes or mutation rates, or use of multiple objective functions to test the same objective goal. Although optimal solution values across runs may be equivalent in such cases, parameter values may vary widely. Calibrated values of eight parameters corresponding to optimal solutions of four SWAT 2003 optimization runs were plotted, each optimization run indicated by a different symbol and the letters "G", "M", "N", and "O" (Figure 3). Although calibrated values for a given parameter, such as "SMFMX," differed across runs, input specifications of these four runs differed only in the random number seed and the optimal objective function values for all runs were equivalent. Mathematically it follows that when two (or more) such parameter sets differ there is another optimal goal or function which more completely describes each parameter sets. In this case, the parameter sets will plot at the same location on the 2-dimensional pareto-curve (i.e., points "S3a" and "S3b" on the "function #1-function #2" plane shown in Figure 2). However, when additionally plotted with regard to a third, previously unconsidered objective function, such as along the "function #3" axis shown in Figure 4, points "S3a" and "S3b" plot at distinct locations.

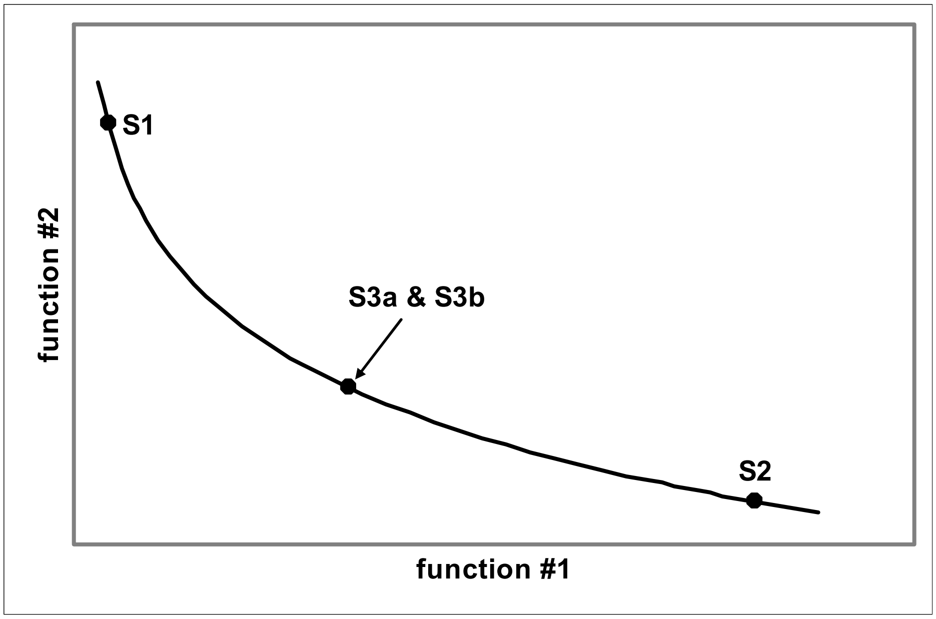

Figure 2. Pareto-curve for a two-objective or two-function minimization problem.

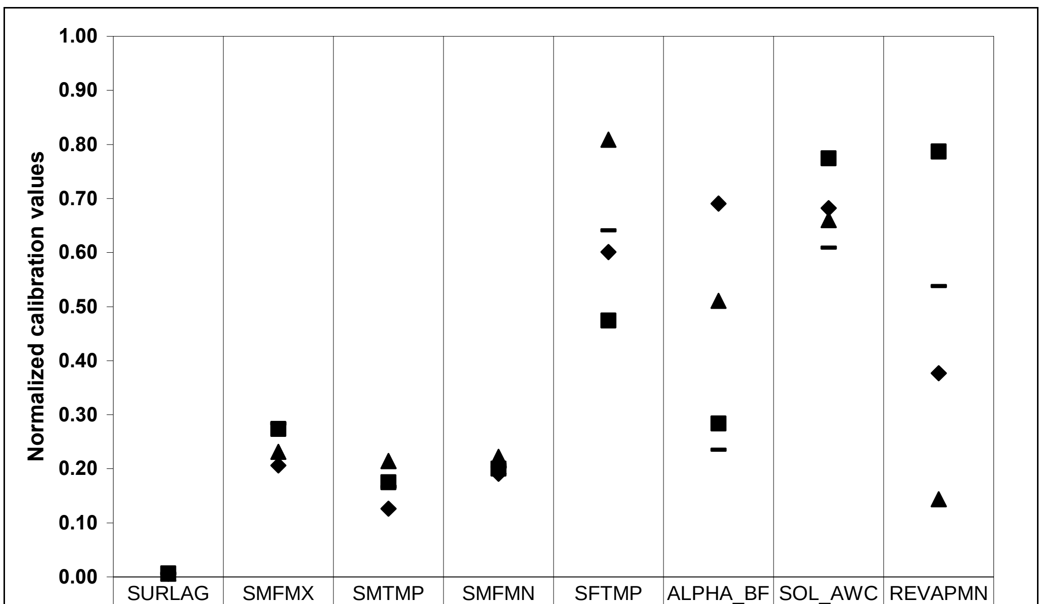

	SURLAG	SMFMX	SMTMP	SMFMN	SFTMP	ALPHA_BF	SOL_AWC	REVAPMN
━ G	0.01	0.28	0.17	0.20	0.64	0.24	0.61	0.54
◆ M	0.01	0.21	0.13	0.19	0.60	0.69	0.68	0.38
■ N	0.01	0.27	0.17	0.20	0.47	0.28	0.77	0.79
▲ O	0.01	0.23	0.21	0.22	0.81	0.51	0.66	0.14

Figure 3. Normalized calibration values for eight SWAT2003 parameters, corresponding to four optimization runs (G, M, N, O) whose input specifications differed only by random number generator seed.

In many cases, differences among parameter sets may be insignificant to warrant further exploration. Certainly, the potential objective functions that completely describe each parameter set are often infeasible to locate, particularly for the number of calibration parameters within SWAT or other models. However, differences in parameter values can provide valuable information on parameter uncertainty ranges with respect to the evaluated objective functions. For example, in Figure 3, the ALPHA_BF and REVPMN parameters have wide value ranges for the evaluated objective function and consequently are not likely to be very sensitive to that function. This can result in a high level of uncertainty as to how well the calibrated values for these parameters help fit the model to the system. In contrast, the SURLAG parameter values are equivalent at the second decimal; the uncertainty in this parameter value then is quite minimal with respect to the optimization function.

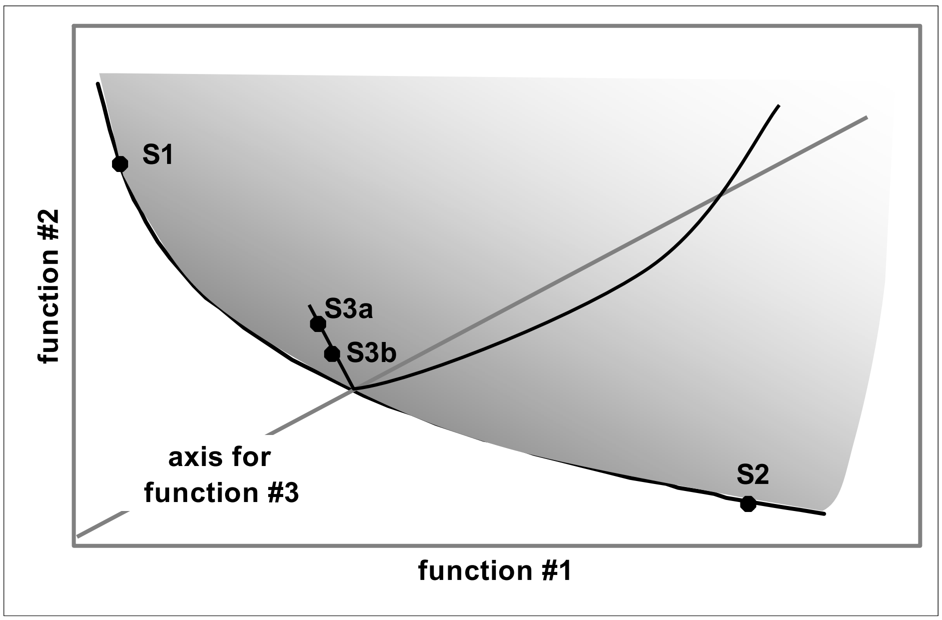

Figure 4. Three-dimensional graph depicting two solutions ("S3a" and "S3b"), which have identical objective solutions in the "function #1-function #2" plane but unique solutions with respect to function #3, indicating variation in one or more parameter values.

Uncertainty Analysis through Confidence Intervals

Another way of evaluating parameter uncertainty is to compare the variance in optimized parameter values with the range of the initial upper and lower bounds set for each parameter. Computerized optimization runs are coded to save the inputs and outputs of each NPS model evaluation throughout the optimization process. Confidence intervals around the optimal solution of a given run are determined with classical statistics, such as the chi-square statistic. This enables all NPS model evaluations for which the objective function values are within the specified confidence interval to be extracted. Each such evaluation contains an output value or data series (such as a daily time series of streamflow) and the corresponding model-determined calibration parameter set. The minimums and maximums of all output values within the confidence interval and of the corresponding calibration parameters are determined. The uncertainty range for each parameter is simply the range between its minimum and maximum value.

The output range, when plotted with the optimal solution time series can show which areas of the hydrograph (or pollutogragh) may have not been well captured by the objective goals or functions chosen. For examples see Gupta et al. (1998), Vrugt et al. (2003), and Yapo et al. (1998).

For plotting and simplified evaluation purposes, the uncertainty range for each calibration parameter is typically normalized by dividing the uncertainty range by the calibration range initially provided to the autocalibration routine by the user. A normalized uncertainty range is calculated by: (*x*-*lb*)/(*ub*-*lb*) where *x* is the value in question, *lb* and *ub* are lower and upper bounds, respectively, of the user-input parameter range. By definition then, the normalized input range for any parameter will be {0,1.0}. For example, the second parameter shown in Figure 5, "SMFMX," was given an initial (not shown) calibration range of 0 to 10 by user input. When the optimization run finished, the optimal "SMFMX" calibration value was determined to be 1.6 and 4.4 was the largest "SMFMX" calibration value of all model evaluations having an objective function value within 2.5% of the optimal solution. For "SMFMX" the normalized parameter range for the optimal solution was {(1.6-0)/(10-0), (4.4-0)/(10-0)} = {0.16, 0.44}.

Normalized uncertainty ranges for a calibration of streamflow in SWAT2003 using eight parameters are shown graphically in two formats (Figure 5). The format of Figure 5a (patterned after Gupta et al., 1998) caters to the tendency of reading left to right. Also, it enables a more vivid picture of how one parameter range varies as compared to another. It is perhaps a more accurate portrayal of the combined difference between the initial input ranges (portrayed by the total graph area) and the final uncertainty ranges (portrayed by the shaded area). In contrast, Figure 5b graphs each parameter with an individual bar on the vertical scale. This format, perhaps, lessens the tendency to assign meaning to the order in which the parameters are graphed.

Wide ranges of uncertainty indicate which calibration parameters can vary widely and still produce near-optimal results. In the case shown (Figure 5), better information could clearly be gained by reducing the input bounds since most of the uncertainty ranges reach the initial upper or lower bound. Guidelines on initial boundaries for each calibration parameter may vary by model depending on whether the scale is hydrologic response unit or some combination, such as farm, subbasin, or basin. Sensitivity analysis can help determine parameters and boundary guidelines. For example, Klepper (1997) discussed the complexity involved in satisfactory calibration and presents a theoretical method to group parameters similar in sensitivity to reduce computational complexity and gain a possible insight into model behavior. Any previous work, when available, that has determined parameters that greatly impact certain features of the model response can serve as an additional guide to parameter selection and boundary determination

Summary and Conclusions

Much work has been done on uncertainty analysis for calibration parameters of complex environmental simulation models such as SWAT. Much of this research provides detailed discussion related to a specific study area, model, or related techniques being explored. This is crucial in enabling others to understand, replicate, and further explore such methods. However, this paper attempts to meet a need indicated by SWAT users for identifying a method for uncertainty analysis that can be applied without in-depth knowledge of the techniques involved.

Two approaches for uncertainty analysis, which have been demonstrated in the literature, are presented in simple terms: evaluation of multiple optimization runs, and creation of single run uncertainty ranges. The need for clear guidance on a peer-accepted method of assessing and presenting uncertainty analysis is only partially met by this paper, as a conference paper of limited length. However, this paper will hopefully serve as a backboard for critical discussion by researchers well-versed in autocalibration and uncertainty analysis techniques at the annual SWAT conference and, as such, provide the authors with feedback needed to further develop clear guidelines for performing sufficient uncertainty analyses on SWAT modeling applications.

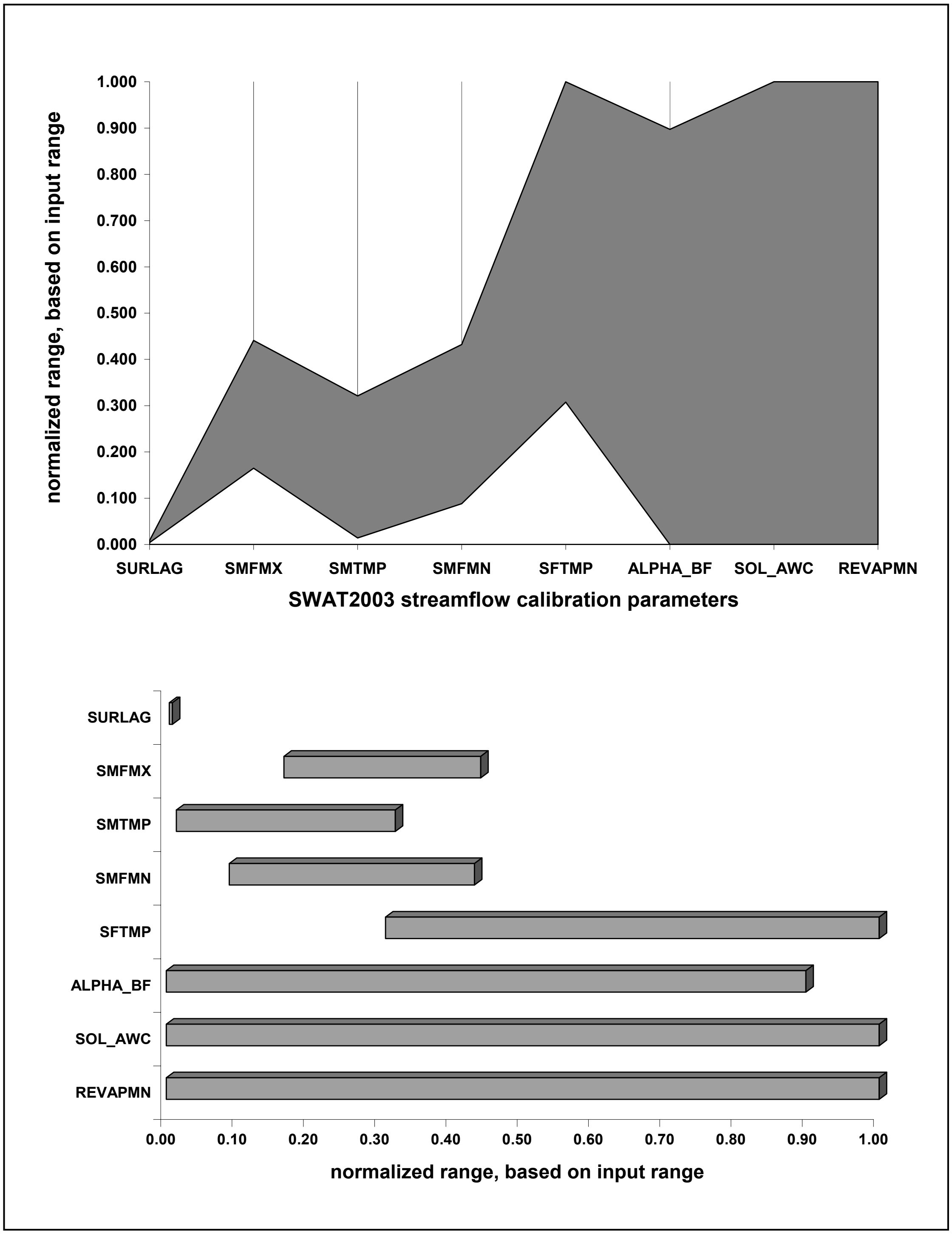

Figure 5. Two methods of displaying uncertainty ranges; 5a) top graph, 5b) bottom graph.

References

Abdulla, F.A., D.P. Lettenmaier, and X. Liang. 1999. Estimation of the ARNO model baseflow parameters using daily streamflow data. *J. Hydro.* 222(1-4): 37-54.

Arnold, J.G., R. Srinivasan, R.S. Muttiah, and J.R. Williams. 1998. Large-area hydrologic modeling and assessment: Part 1. Model development. *J. Amer. Water Resour. Assoc.* 34(1): 73-89.

ASCE Task Committee. 1993. Criteria for evaluation of watershed models. *J. Irrig. Drain. Eng.* 119(3): 429-442.

Boyle, D.P., H.V. Gupta, and 01S. Sorooshian. 2000. Toward improved calibration of hydrologic models: combining the strengths of manual and automatic methods. *Water Resour. Res.* 36(12): 3663-3674.

Cooper, V.A, V.T.V. Nguyen, and J.A. Nicell. 1997. Evaluation of global optimization methods for conceptual rainfall-runoff model calibration. *Water Sci. Tech.* 36(5): 53-60.

Duan, Q.Y., V.K. Gupta, and S. Sorooshian. 1993. Shuffled complex evolution approach for effective and efficient global minimization. *J. Opt. Theory Appl.* 76(3): 501-521.

Gupta, H.V., S. Sorooshian, and P.O. Yapo. 1998. Toward improved calibration of hydrologic models: multiple and noncommensurable measures of information. *Water Resour. Res.* 34(4): 751-763.

Gupta, H.V., S. Sorooshian, P.O. Yapo. 1999. Status of automatic calibration for hydrologic models: comparison with multilevel expert calibration. *J. Hydro. Eng.* 4(2): 135-143.

Haan, C.T., B. Allred, D.E. Storm, G.J. Sabbagh, and S. Prabhu. 1995. Statistical procedure for evaluating hydrologic/water quality models. *Trans. ASAE* 38(3): 725-733.

Ibrahim, Y. and S. Liong. 1992. Calibration strategy for urban catchment parameters. *J. Hydraulic Eng.* 118(11): 1550-1570.

Klepper, O. 1997. Multivariate aspects of model uncertainty analysis: tools for sensitivity analysis and calibration. *Ecol. Mod.* 101: 1-13.

Liong, S., W.T. Chan, and J. ShreeRam. 1995. Peak-flow forecasting with genetic algorithm and SWMM. *J. Hydraulic Eng.* 121(8): 613-617.

Martinec, J. and A. Rango. 1989. Merits of statistical criteria for the performance of hydrological models. *Water Resour. Bull.* 25(2): 421-432.

Mulligan, A.E. and L.C. Brown. 1998. Algorithms for calibrating water quality models. *J. Environ. Eng.* 124(3): 202-211.

Nofziger, D.L., J. Chen, and C.T. Haan. 1994. Evaluation of unsaturated/vadose zone models for superfund sites. U.S. Environmental Protection Agency report CR-818709, Robert S. Kerr Environmental Research Laboratory, Ada OK.

Sumner, N.R., P.M. Fleming, and B.C. Bates. 1997. Calibration of a modified SFB model for twenty-five Australian catchments using simulated annealing. *J. Hydro.* 197(1-4): 166-188.

Thyer, M., G. Kuczera, and B.C. Bates. 1999. Probabilistic optimization for conceptual rainfall-runoff models: a comparison of the shuffled complex evolution and simulated annealing algorithms. *Water Resour. Res.* 35(3): 767-773.

Van Griensven, A. and T. Meixner. 2003. Statistical methods developed for SWAT2003. White Paper. Dept. of Environmental Sciences, Univ. of CA, Riverside, CA.

Van Griensven, A. and W. Bauwens. 2003. Multiobjective autocalibration for semidistributed water quality models. *Water Resour. Res.* 39(12): 1348-1356.

Vrugt, J.A., H.V. Gupta, L.A. Bastidas, W. Bouten, and S. Sorooshian. 2003. Effective and efficient algorithm for multiobjective optimization of hydrologic models. *Water Resour. Res.* 39(8): 1214-1233.

Yapo, P.O., H.V. Gupta, S. Sorooshian. 1998. Multi-objective global optimization for hydrologic models. *J. Hydro.* 204(1-4): 83-97.

Warwick, J. J. 1991. Optimizing water quality modeling in an uncertain environment. *Water Sci. Tech.* 24(6): 41-48.

Willmott, C. J. 1984. On the evaluation of model performance in physical geography. *In:* G. L. Gaile and C. J. Willmott (eds.), Spatial Statistics and Models, pg 443-460, D. Reidel Publishing Company.

The TERRACE Project: SWAT Application for Diffuse Chemical Pollution Modelling

S.M. White[1*], N. Kannan[2], I. Beaudin[3], J. Hollis[4], A.R.Young[5], V. Keller[5] and M. Whelan[6]
[1]Institute of Water and Environment, Cranfield University, Silsoe, Bedfordshire, MK45 4DT, U.K. E-mail: Sue.White@cranfield.ac.uk
[2]Blackland Research and Extension Centre, 720, East Blackland Road, Temple, TX, 76502, U.S.A
[3]Formerly: Institute of Water and Environment, Cranfield University, Silsoe, Bedfordshire, MK45 4DT, U.K.
[4]National Soil Resources Institute, Cranfield University, Silsoe, Bedfordshire, MK45 4DT, U.K.
[5]CEH-Wallingford, Maclean Building, Crowmarsh Gifford, Wallingford, Oxfordshire, OX10 8BB, UK
[6]Unilever Safety and Environmental Assurance Centre, Colworth House, Sharnbrook, Bedfordshire, MK44 1LQ. U.K.

Abstract

SWAT has been adopted as the diffuse-source component of the European Chemicals Industries Council (CEFIC) Long-range Research Initiative (LRI) environmental modelling suite. In order to make SWAT applicable across Europe, the diffuse-source LRI project (TERRACE) has identified a number of consistent data sources at a European level which could be used to generate model parameters and driving variables. In addition, linkages have been built with other LRI model components, specifically the point-source river model, GREAT-ER, and the atmospheric model, ADEPT.

The linkage with ADEPT is fairly straightforward with contaminant inputs being applied to the land either by dry deposition or with rainfall on a temporally and spatially varying basis. Linkage with the river model is more complex because of a dichotomy in modelling approaches between SWAT (Soil and Water Assessment Tool) and GREAT-ER. GREAT-ER is a steady-state stochastic model where contaminant concentrations are modelled for different flow percentiles whereas SWAT is dynamic. The solution to interfacing these different models was to generate a series of flow and contaminant-transfer probability distributions using SWAT, to calibrate the flow frequency distributions used by GREAT-ER using the SWAT flows, and then to use the contaminant transfer distributions as inputs to GREAT-ER. The link developed between these models opens possibilities for other dynamic-stochastic model linkages, and for the way in which SWAT is calibrated and validated. The model was developed using data from the Exe Catchment in southwest England.

Introduction

The overall aim of the TERRACE (Terrestrial Runoff modelling for Risk Assessment of Chemical Exposure) project was to develop a simulation model for evaluation of diffuse-source chemical runoff at the regional scale across Europe. The TERRACE model should be capable of integration with the GREAT-ER system (Boeije et al., 1997; Boeije et al., 2000; Feijtel et al., 1997; Feijtel et al., 1998). The ultimate aim for development of GREAT-ER and its associated models (Figure 1) is to provide a comprehensive modelling tool for use in environmental risk assessment at the regional level throughout Europe. GREAT-ER and its components are spatially distributed, thereby allowing more accurate prediction of regional-scale Predicted Environmental Concentrations (PECs) than the lumped models presently used in environmental risk assessment for new compounds (Knopfler, 1994). The requirement for more accurate prediction of PECs is especially pressing given the more restrictive licensing environment which stems from the European Commission's proposed Water Framework Directive[1] and the White Paper setting out a future 'Community Policy for Chemicals'[2].

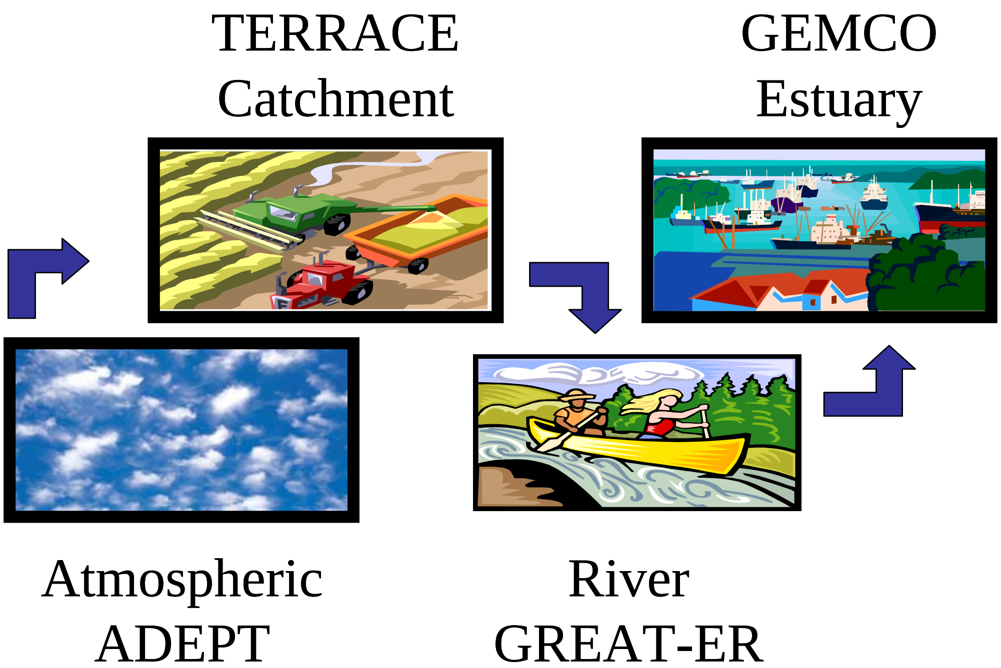

Figure 1. The CEFIC-LRI Tier II models.

Given the above rationale, the four objectives of the TERRACE project were:

1. To review the current state-of-the-art in runoff and contaminant transport modelling. This includes an assessment of the validation status of models examined, and of their compatibility with commonly used risk assessment strategies.
2. To integrate selected runoff and contaminant transport models with a geo-referenced database of model parameters within a geographical information system (GIS).
3. To carry out a preliminary application of this system to an example river basin, in order to demonstrate its utility to potential end-users.
4. To specify a plan for validation of the modelling system.

[1] http://www.wwffreshwater.org/pdf/wfd.pdf
[2] http://www.europa.eu.int/comm/environment/chemicals/index.htm

Review of the Current State-of-the-Art in Runoff and Contaminant Transport Modelling

An extensive review of the state-of-the-art in contaminant transport modelling for application at the catchment scale was carried out (White et al., 2001). The study examined the background, structure, and applicability of a wide variety of contaminant transport modelling approaches. Models were grouped into three classes, which essentially represent their three spatial scales of application: soil profile, field, and catchment. At an early stage, the first of these three scales was excluded from further consideration. Some models from the other groups were also excluded, because of their lack of recent development, their complexity or their empirical nature. This left a long list of nine models for further consideration. These were:

Field scale:	EPIC, GLEAMS, Opus, PRZM, PELMO & RZWQM
Catchment scale:	ANSWERS-2000, SWAT-2000 & SWATCATCH

These models encompassed a range of modelling strategies, from empirical to physically-based at spatial scales which are relevant to TERRACE. An assessment of the validation status of these nine models, with detailed descriptions of validation results, was then carried out, and important issues arising from this review were discussed and reported. The report then proceeded to a consideration of model data requirements and data availability within Europe and at a national level. Again issues arising from this review were highlighted.

Finally, a model shortlist for further evaluation and development in TERRACE was presented. This shortlist included three models - ANSWERS-2000, SWAT-2000, and SWATCATCH - which provide examples of three very different approaches to catchment scale modelling. Of these, SWAT-2000 was the preferred option for the TERRACE project. The other two models would enable assessment of Predicted Environmental Concentrations in very different ways. Details of the SWAT model can be found in Neitsch et al. (2001) and White et al. (2002).

With this model shortlist in mind, compatibility of the TERRACE models with GREAT-ER and options for development environments were considered. None of the evaluated models explicitly includes the capability to model organic compounds or dioxins resulting from atmospheric deposition or sewage sludge application to land. However, the basic structure of SWAT means that modification of existing model components was not an unrealistic prospect.

Integration of the Selected Model with a Geo-referenced Database of Model Parameters

Two of the reasons for selecting SWAT for the TERRACE study were the ability to run SWAT within a GIS environment and the use of databases within the model structure. This meant that databases for European conditions could be constructed to replace the default US databases.

SWAT requires a wide range of temporal and spatial data inputs, together with characteristic data for contaminants, soils, and plants. The second year report (White et al., 2002) details data requirements and identifies European and national datasets which satisfy these requirements. In many cases the data are not available directly but have to be transformed into the format required by the model. A number of model parameter estimation routines have been defined in order to estimate model parameter values from available pan-European datasets.

A Preliminary Application to an Example River Basin

SWAT was set up for the Exe Catchment in southwest England (Figure 2) with the aim of running an example application of the diffuse-source model and demonstrating how the SWAT software could be used to provide contaminant inputs to the GREAT-ER model.

In order for the TERRACE and GREAT-ER models to be compatible it was necessary to first link the flow components of the two models. TERRACE will not deliver water to the GREAT-ER model, but should be able to deliver the contaminant loads associated with each percentile flow in each reach in the GREAT-ER set-up for a catchment. It was decided early in the project that the diffuse-source contaminant-flow relationships would be better defined at the monthly, rather than the annual level. This is because similar rainfall events cause different runoff profiles carrying different levels of contaminant at different times of the year, dependent on a complex mixture of antecedent soil moisture conditions, evaporative demand, and vegetative cover. The existing GREAT-ER model at the start of this project used LowFlows to provide hydrological data for each reach. This was provided at the reach level and was on an annual basis, as annual flow duration curves. However, an upgrade of the LowFlows software, LowFlows2000, provides flow-duration curves at the monthly level and is currently being incorporated into an updated version of GREAT-ER. LowFlows2000 has been developed and tested on the Exe Catchment, making this an obvious choice for an application of TERRACE.

The modelling procedure for the Exe therefore included various principal steps:

1. Obtaining, checking, and processing all input data required by the SWAT model.
2. Setting up the model databases and spatial data inputs.
3. Calibration and validation of the model for a recent period, for which better quality validation data were available. Flow data were naturalised (i.e. adjusted for abstraction from and discharge to the river) by the UK Environment Agency. Spatially the model was discretised into 11 subbasins based on gauging station locations (Figure 2).
4. Comparison of flows and concentrations of contaminants at monitoring stations in the catchment.
5. Discretisation of the catchment by GREAT-ER reach definitions, giving 63 subbasins. This is not every river reach defined in LowFlows2000, but a subset which will be produced for future inputs to the GREAT-ERII package.
6. Setting up the model for a 30-year run for the period concurrent with Low-Flows2000.
7. Calibration/validation of the 30-year model run against flow-duration curves per reach provided by LowFlows2000.
8. Production of contaminant load duration curves linked to the flow duration curves for input to GREAT-ER.

An initial model run for the Exe was made for the period 1997-1999 because for this period better quality data are available for model set-up (land use, pesticide and nutrient usage statistics, climate inputs), calibration (flow and water quality), and validation (flow and water quality). This allows determination of parameter values for the model in order to obtain the best possible results at HRU, subcatchment, and catchment levels so that there is confidence in the way the model reproduces the important phases of the hydrological cycle which act as transport modes for various contaminants. Once set, these parameters are used for a longer model run for a period compatible with the LowFlows2000 application to the Exe Catchment (1961-1990).

The catchment was discretised for this exercise into 11 subcatchments, defined by nine principal and two intermittent flow gauging stations. The outlet of a subcatchment in SWAT is the first geographically located point at which time series and summary information can be extracted from the model. Data output is also possible for each HRU, but unless HRUs are explicitly defined as individual fields (as in the application for Colworth; Kannan et al., 2005) the HRUs are not geographically located in space and may consist of a number of non-contiguous areas with the same soil and land use combination within a subcatchment. Therefore, the number of HRUs always exceeds the number of subcatchments, and the same HRU land use-soil combination may occur within every subcatchment and will be assigned a separate HRU identifier.

Data output at the subcatchment level allows comparison of the observed and predicted time series of flow and water quality at the catchment outlet as well as allowing the expected and actual hydrological process response to be compared. Thus, a baseflow time series extracted from the observed flow series can be compared with the SWAT groundwater component of flow output from the subcatchment. Flow through drains can be compared with any information on drain flow from the catchment (e.g. at what time of year drain flow occurs or how long it persists). Surface response largely controls the rapid rises and falls in flow hydrographs and can therefore be checked against the occurrence of such peaks. Flow or contaminant outputs can also be viewed as exceedance curves (Figure 3), which is of direct use for linkage with GREAT-ER.

Figure 2. Exe Catchment location and discretisation.

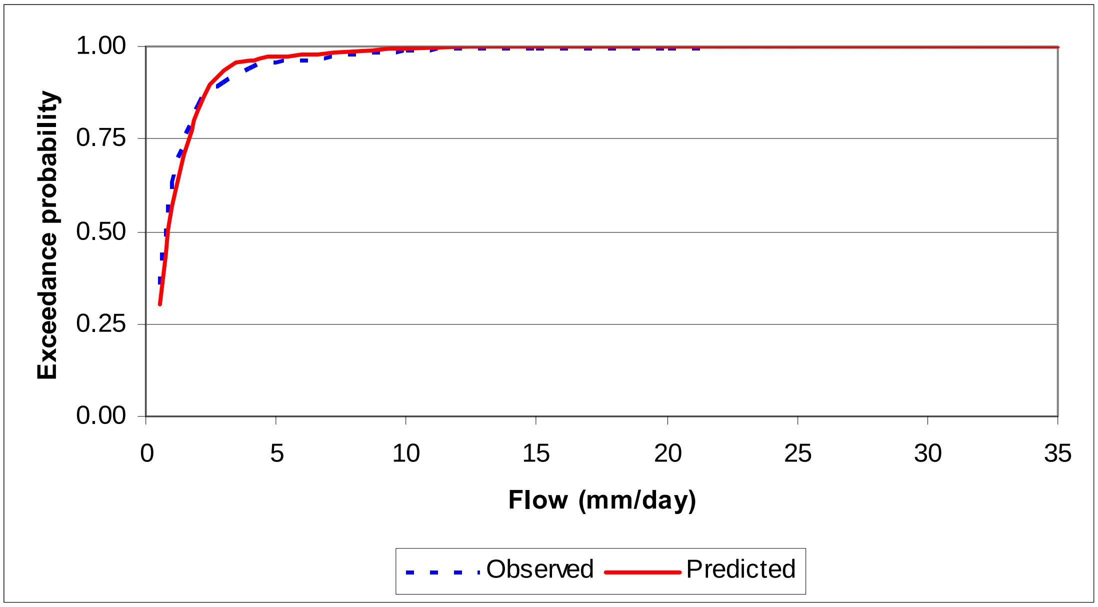

Figure 3. Flow exceedance curve for the Cowley Subcatchment.

At the HRU level a range of statistics such as crop growth, date of reaching and leaving field capacity, and maximum soil moisture deficit were used to check model performance.
By using the full range of outputs from SWAT at HRU, subcatchment and catchment levels to check against expected or observed behaviour patterns it is possible to build confidence in the way the model represents process rather than how good it is at matching final output. This is important for TERRACE and for CEFIC because a model that predicted the right outputs at a large scale, but with the wrong process mechanisms at any or all levels within the model, would risk rejection of the proposed methodology by the responsible European authorities.

SWAT has another major advantage for LRI. The model is sensitive to changes in land management practices and crop rotations. Although this demands a high level of data input and hydrological competence in setting up and running the model, it also means that more confidence can be placed in the model outputs. There will always be uncertainty in many of the data inputs. Our knowledge of the spatial variation in soils and their hydrological behaviour, for example, is incomplete. Information will never be available to define exactly what is happening (or worse what did happen) on every day of the year in every field in a large catchment. These uncertainties will remain for a long time to come. By having a model which can be shown to robustly reproduce the hydrological behaviour at HRU, subcatchment, and catchment levels the level of uncertainty in the model predictions can be restricted.

Linkage of SWAT to GREAT-ER

In order to demonstrate the methodology results from the three-year simple model set-up are given here for the Woodmill Subcatchment and the pesticide Mecoprop (see White et al., 2005a for details of pesticide modelling). The first stage is to produce flow duration curves for a site for comparison with those from LowFlows2000 (Figure 5). Only annual data are presented here as with only two years of valid run the monthly level curves are not statistically valid.

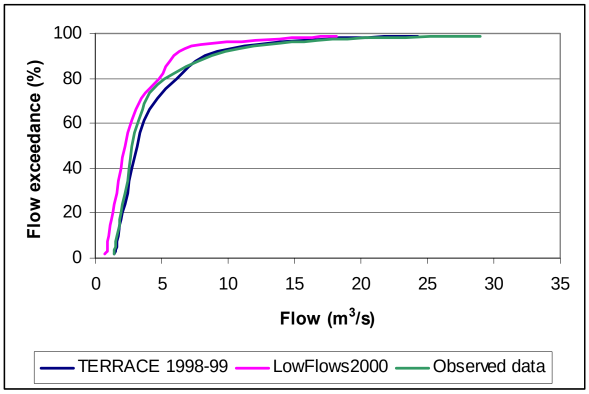

Figure 5. Flow exceedance curves for the Woodmill Subcatchment.

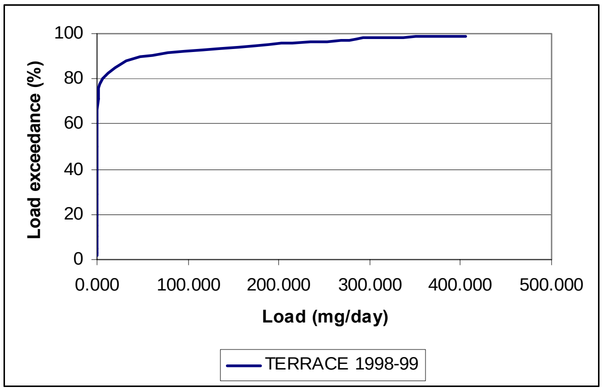

Figure 6. Mecoprop load exceedance curves for the Woodmill Subcatchment.

Mecoprop load duration curves are also prepared for the same sites (Figure 6). As may be expected there is little or no response at the low frequency end of the graph, indicating that Mecoprop is only moving in high flow events which will have a large surface flow component.

The final step in the analysis procedure is to link the flow and load duration curves for each node. Again examples are given for Woodmill. Figure 7 shows the load exceedance-flow exceedance relationship for the site. From the model results it is clear that high water flows do not always relate to high Mecoprop loads. The additional control on the relationship is Mecoprop availability. If data are studied by month of occurrence it is clear that a seasonal variation is present in the load-flow relationship requiring data to be analysed at a monthly level.

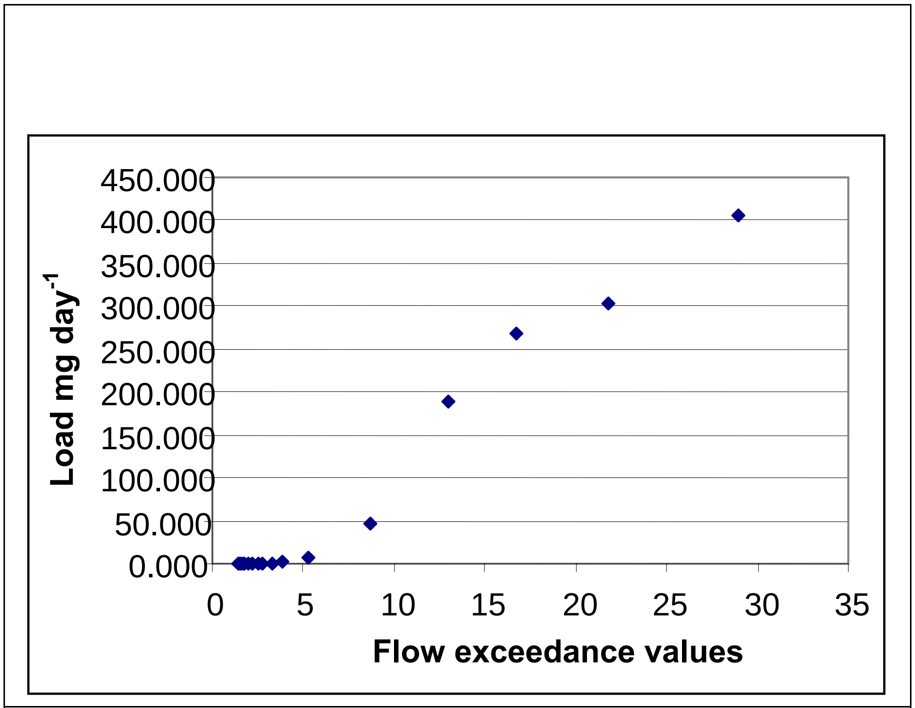

Figure 7. Linkage between flow and load exceedance for Woodmill, Cowley, and Thorverton.

A Plan for Future Use of the Modelling System

The impetus for the CEFIC-LRI programme has been the requirement by the EU for the chemicals industries to develop methodologies for demonstrating the likely impacts of chemicals in the environment via the estimation of Predicted Environmental Concentration (PEC). The EU has accepted in outline the approaches developed under LRI subject to “extensive validation”.

Implementation

Once the TERRACE approach is validated there is still the question about how it will be implemented and used within LRI and REACH (a computer-based set of data and models in support of EC Chemicals Directives objectives). SWAT-2000 is a complex model which requires a high level of hydrological expertise to set up, calibrate, and validate for hydrological performance before any contaminant movement can be modelled. It is suggested that this is best achieved through a series of focus sites across Europe. These should be selected to represent key combinations of land use, climate, soil, and land management. This approach is the same as that approved by the EU as part of their FOCUS initiative for both groundwater (vertical) and surface water (to edge-of-field) analysis of pesticide transfer. Details of the FOCUS scenario selection methodology are given Linders et al. (2003). Such an approach fits well alongside the proposed validation scheme.

Conclusions

SWAT was identified as a suitable model for Tier II diffuse pollution modelling in support of the EC Chemicals Directive. Pan-European and UK national datasets have been identified which allow SWAT to be applied in a consistent way to any river basin. Where these datasets did not contain the parameters needed for SWAT applications, pedo-transfer functions have been developed to convert available values to required parameters. A method of extensive model calibration, verification and validation has been described and implemented for a trial catchment, the Exe, in southwest England. A methodology for linking a distributed dynamic catchment model with a stochastic river water quality model has been defined and applied for the Exe. Further use of SWAT, in its TERRACE guise, within the REACH system depends on identifying focus catchments across Europe where the model can be extensively calibrated and validated. These catchments would then provide test-bed sites for testing the predicted environmental concentrations form diffuse sources of new and existing chemicals.

References

Boeije, G., Vanrolleghem, P. and Matthies, M., 1997. A geo-referenced aquatic exposure prediction methodology for ‘down-the-drain’ chemicals. *Wat. Sci. Tech.*, 36, 251-258.

Boeije, G.M., Wagner, J-O., Koormann, F., Vanrolleghem, P. A., Schowanek, D.R. and Feijtel, T.C.J., 2000. New PEC definitions for river basins applicable to GIS-based environmental exposure assessment. *Chemosphere*, 40, 255-265.

Feijtel, T., Boeije, G., Matthies, M., Young, A., Morris, G., Gandolfi, C., Hansen, B., Fox, K., Holt, M., Koch, V., Schroder, R., Cassani, G., Schowanek, D., Rosenblom, J. and

Niessen, H., 1997. Development of a geography-referenced regional exposure assessment tool for European rivers – GREAT-ER. Contribution to GREAT-ER #1. *Chemosphere*, 34, 2351-2373.

Feijtel, T., Boeije, G., Matthies, M., Young, A., Morris, G., Gandolfi, C., Hansen, B., Fox, K., Matthijs, E., Koch, V., Schroder, R., Cassani, G., Schowanek, D., Rosenblom, J. & Holt, M., 1998. Development of a geography-referenced regional exposure assessment tool for European rivers – GREAT-ER. *J. Hazardous Materials*, 61, 59-65.

Kannan, N., White, S.M & Whelan, M.J., 2005. Predicting diffuse-source transfers of sewage-sludge- associated chemicals to surface waters using SWAT. *Proceedings SWAT 2005, 3rd International Conference*, Zurich, Switzerland, July 11th – 15th 2005.

Knopfler, W., 1994, Environmental Hazard - Assessment of Chemicals and Products. *Environmental Science & Pollution Research*, 1, 47-53.

Linders, J., Adriaanse, P., Allen, R., Capri, E., Gouy, V., Hollis, J., Jarvis, N., Klein, M., Lolos, P. Maier, W.-M., Maund, S., Pais, C., Russell, M., Smeets, L., Teixera, J.-L., Vizantinopoulos, S. & Yon, D., 2003. *FOCUS Surface Water Scenarios in the EU evaluation process under 91/414/EEC*. Report prepared by the FOCUS Working Group on Surface Water Scenarios. 238 pp.

Neitsch, S.L., Arnold, J.G., Kiniry, J.R., Williams, J.R. 2001. *Soil and Water Assessment Tool - Theoretical Documentation. Version 2000*.

Smith, L.P., 1976 *The agricultural climate of England and Wales, Technical Bulletin 35*, Ministry of Agriculture, Fisheries and Food, U.K.

White, S.M., Anderton, S.P, Ishemo, C., Worrall, F., Hollis, J., Hallett, S., 2001. *TERRACE: TErrestrial Runoff modelling for Risk Assessment of Chemical Exposure. Review of State of the Art: Assessment of Modelling Software and Available Geodata*. University of Durham, Unpublished report.

White, S.M., Beaudin, I, Hollis, J., Hallett, S. & Worrall, F., 2002. TERRACE: TErrestrial *Runoff modelling for Risk Assessment of Chemical Exposure. Development of SWAT-2000 and Database development.* Cranfield University, Unpublished report.

White, S.M., Kannan, N., Grizzetti, B. & Hollis, J.M., 2005a. Catchment scale modeling of pesticide losses with imperfect data – a case study from the UK. *Proceedings SWAT 2005, 3rd International Conference*, Zurich, Switzerland, July 11th – 15th 2005.

White, S.M., Kannan, N., Holman, I., Whitehead, J., Beaudin' I., Carter, J. & Hollis, J.M., 2005b. Using SWAT in English catchments: experience and lessons. *Proceedings SWAT 2005, 3rd International Conference*, Zurich, Switzerland, July 11th – 15th 2005.

Ensuring Appropriate Hydrological Response for Past and Future Nutrient Load Modelling in the Norfolk Broads

J. Whitehead[1*], S.M.White[1] and I. Holman[1]
[1]Institute of Water and Environment, Cranfield University, Silsoe, Bedfordshire, MK45 4DT, U.K.

Abstract

SWAT is being used to model past and future land use and climate scenarios for river basins supplying water and nutrients to the ecologically important low-lying lakes of the Norfolk Broads area of eastern England. These lakes suffer from high nutrient loading, both via the groundwater and in surface response in soluble and sorbed forms. Eutrophication and sedimentation in the shallow lakes (known as broads) are of major concern.

One problem with using the nationally available crop type and soil data for England and Wales is that data are supplied in grid format with an associated dominant crop type or soil group, and a range of sub-dominant classes. In this context dominant is used in a spatial sense rather than a hydrological one, but sometimes a soil or crop which covers less of the area is more important in controlling either hydrological or erosional response, or both. As this study is focused on potential future conditions it is essential that past and current conditions are modelled as accurately as possible, and that we ensure that the responses we get at the subbasin and basin level actually reflect the processes we expect to find.

Techniques to define the controlling soil-vegetation cover from within the range of possible combinations have been developed and tested. The importance of such care in model set-up will be discussed in the context of the nutrient modelling required for these basins.

Introduction

The Norfolk Broads are a group of important low-lying lakes in eastern England (Figure 1); they form a very fragile ecosystem with two main pressures. These pressures are key to the more ecologically desirable clear water, plant dominated system that characterized the Broadlands until the 1960’s.

The structure of the river ecosystem has been destroyed in the past from boats, although boating activities are better managed now. The current water quality of the system is not compatible with diverse biological plant communities that are remembered from 50 years or more ago. There are over 200 sewage treatment works in the Norfolk Broads, many of which serve less than 1,000 people and which therefore do not fall under the Urban Waste Water Treatment legislation requiring works to undertake phosphorus stripping. Therefore, there is still a great deal of phosphorus being released into the Broadland system from sewage effluent, but legislation exists, were it to be used, to eliminate this source almost entirely.

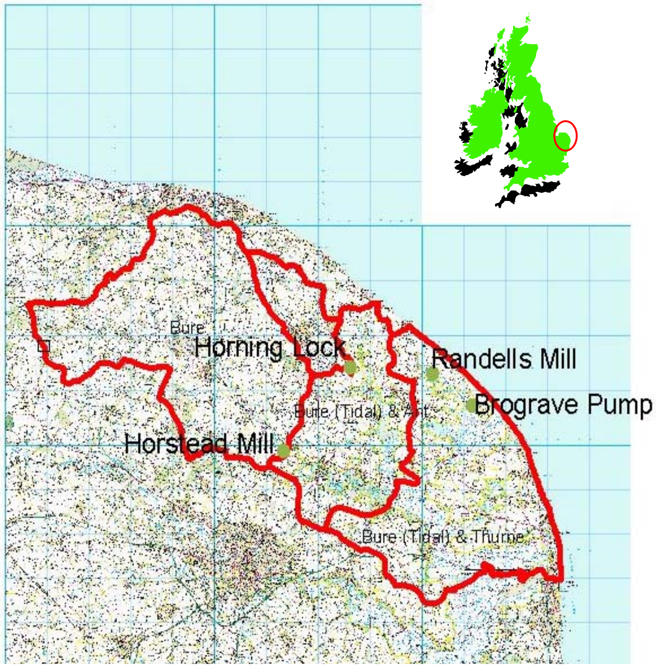

Diffuse sources of nutrients from cultivated land, stock wastes, sediments, and agricultural drainage systems are less easy to control but do however need to be addressed. Until water quality can be improved at the river basin scale it is not worth attempting restoration measures such as the use of bio-manipulation in the Broads. SWAT is therefore being used to model past and future land use and climate scenarios for river basins supplying water and nutrients to Broadlands.

Figure 1: The study area.

Methodology

Soil and crop type data are only available at a national or regional level. This data is supplied in grid format with an associated dominant crop type or soil group, and a range of sub-dominant classes. In this context dominant is used in a spatial sense rather than a hydrological one, but sometimes a soil or crop which covers less of the area is more important in controlling either hydrological or erosional response, or both. As this study is focused on potential future conditions it is essential that past and current conditions are modelled as accurately as possible, and that we ensure that the responses we get at the subbasin and basin level actually reflect the processes we expect to find. SWAT is a comprehensive model that requires a diversity of information in order to run; therefore, great care has been taken in selecting data for use in the model setup.

Soil Data

The data required by SWAT encompasses a large number of paper soil reports, maps, and digital soil information. The NSRI LandIS database incorporates all these data sources and has been utilized to gain the appropriate data for SWAT. Within LandIS, soil profile characteristics are used to define soils at four levels in a hierarchical system, general characteristics being used at the highest level to give broad separations, and more specific ones at the lower levels to give increasingly precise subdivisions. Soil associations are made up of a number of soil series but are named after the dominant soil series. For example, Wick 2 is made up of Wickmere, Sheringham and Aylsham series (see Table 1).

Table 1. Soil associations within the study area.

Soil Association	Areas In SWAT (ha)	Ancillary Subgroups	Proportions (%)	Proportions based on SWAT areas (ha)
Wallasea 1	116.06	813 Wallasea	75	87.05
		814 Newchurch	25	29.02
Newport 4	3787.68	551 Newport	76	2878.63
		631 Redlodge	24	909.04
Isleham 2	1463.04	861 Isleham	31	453.54
		1024 Adventurers	29	424.28
		552 Ollerton	20	292.61
		821 Blackwood	20	292.61
Wick 3	17645.72	541 Wick	61	10763.89
		541 Sheringham	28	4940.80
		551 Newport	11	1941.03
Wick 2	31279.82	541 Wick	38	11886.33
		572 Wickmere	36	11260.74
		541 Sheringham	16	5004.77
		543 Aylsham	10	3127.98
Hanworth	2038.96	871 Hanworth	40	815.58
		831 Sustead	30	611.69
		1024 Adventurers	30	611.69
Gresham	1547.74	711 Gresham	63	975.08
		711 Prolleymoor	21	325.03
		831 Sustead	16	247.64
Beccles 1	1039.76	711 Beccles	65	675.85
		712 Ragdale	35	363.92
Altcar 2	621.58	1022 Altcar	50	310.79
		1024 Adventurers	30	186.47
		1025 Mendham	20	124.32
Felthorpe	1674.01	643 Felthorpe	40	669.60
		642 Lakenheath	27	451.98
		821 Blackwood	33	552.42

As can be seen from Table 1, each soil series within Wick 2 contributes a percentage to the total soil association; however each series has different characteristics. At the moment the soil database in SWAT is made up of the dominant soil series for each association found in the study area, thus the database doesn’t take into consideration the characteristics of the other soil series making up the association. Soils which are highly erodible could therefore be missed from the model giving unreliable results. To assess this problem USLE calculations have been undertaken for each soil series within each subbasin within the SWAT model.

USLE calculations showed that some soil series such as Sheringham have high erodibilty factors. The Sheringham series makes up approximately 28% of the Wick 3 association and 16% of the Wick 2 association, and therefore potentially covers 9,945 ha of the SWAT river basin. By only modelling the soil association, soil series such as Sheringham are not incorporated into the model; therefore, model results could be underestimating soil erosion. The difference between the Sheringham soil series and the Wick association are nominal (see Hodge et al., 1984). The only difference being the percentage of stones in the soil, therefore the differences being shown in the USLE calculations may be artificial, although it is thought that Sheringham, with no stones within it, will be more erodible than Wick.

The modeling of the soil subgroups within SWAT does however prove problematic. The SWAT ArcView interface requires a soil map linked to the soil database, to provide spatial information on the soil distribution within the river basin. These maps need to be prepared prior to running the interface. Unfortunately, the only digital soil map available is that of the National Soil Map, which only displays soil associations. Neither is any quantitative information available on the spatial distribution of the soil subgroups within each soil association.

Management Files

Quantifying the impact of land management and land use on water supply and quality is a primary focus of environmental modelling. Crop rotation is a system of regularly changing the crops grown on a piece of land. However, there are no mandatory rotations, and no single rotation necessarily represents best practice. Individual farmers will deviate from them to allow for their own machinery/labour availability, personal preferences, prices, or because of weather and soil moisture conditions in a given year.

Originally, typical rotations for the eastern region of the UK were used to vary crops grown from year to year within the SWAT model. These were taken from ADAS standard rotation information and based on soil type (Table 2).

Table 2. ADAS standard crop rotations (Holman, 2004).

Soil	Rotation	Crops	Soil	Rotation	Crops
Sandy	Primary	pts/ww/sb/sbt/ww/wb	Deep Silty	Primary	pts/ww/p/ww/sbt/ww
	Secondary	sbt/ww/osr/wb		Secondary	ww/sb/osr
	Set-aside	sbt/ww/sa		Set-aside	p/ww/sa/ww/sbt/ww
Peaty	Primary	sbt/ww/p/ww	Clay	Primary	osr/ww/ww/wbn/ww/ww
	Secondary	wbn/ww/osr/ww		Secondary	osr/ww/ww/wbn/ww/ww
	Set-aside	pts/ww/sa/sbt/ww		Set-aside	osr/ww/ww/sa/ww/wb
Organic	Primary	sbt/ww/p/ww	Shallow	Primary	pts/ww/sb/sbt/ww/wb
	Secondary	wbn/ww/osr/ww		Secondary	sbt/ww/osr/wb
	Set-aside	pts/ww/sa/sbt/ww		Set-aside	sbt/ww/sa
Other Mineral	Primary	osr/ww/ww/wbn/ww/wb	Key: osr = oilseed rape ww = winter wheat wb = winter barley sb = spring barley p = peas sa = set aside pts = potatoes sbt = sugar beet wbn = winter field beans		
	Secondary	osr/ww/ww/sbt/ww/wb			
	Set-aside	osr/ww/ww/sa/ww/wb			

The use of these rotations in the SWAT model did not give a good representation of the crops known to have grown in the study area from EDL data. There was far too much winter wheat being represented in the model due to Wick 2 and Wick 3 soils (which cover the majority of the study area) being classified as 'other mineral' under ADAS standard rotations (Table 3).

Table 3. ADAS soil texture classes (MAFF, 2000).

Predominant Soils	ADAS Texture Class	Area (ha) in SWAT
Altcar	Peaty	621.58
Beccles	Other Mineral	1039.76
Felthrope	Organic	1674.01
Gresham	Other Mineral	1547.74
Hanworth	Organic	2038.95
Isleham	Organic	1463.04
Newport 4	Sandy	3787.67
Wallesea	Clayey	116.06
Wick 2	Other Mineral	31279.82
Wick 3	Other Mineral	17645.70

To better represent EDL data, Wick soils were reclassified as 'sandy soils' to help reduce the quantity of winter wheat being grown in the river basin and to increase the area of other crops such as potatoes, spring barley, and sugar beets. The Wick soils were chosen as they are usually sandy at depth, and therefore could easily fall into either the ‘sandy’ or ‘other mineral’ category.

Rotations were also slightly adjusted to increase or decrease the amount of certain crops within the SWAT model. Set-aside rotations were not used within the model, instead the 5,500 ha which was counted as set-aside in the 2000 EDL data was primarily allocated to the wettest soils in the river basin as permanent set-aside, based on the soil wetness class (Table 4). The system of *wetness class* grades soils from Wetness class I, well drained to Wetness class VI, almost permanently waterlogged within 40cm depth (Hodge et al., 1984).

Table 4. Soil wetness classes (Hodge et al., 1984).

Soil	Wetness Class
Beccles	III
Hanworth	III to V
Wallesea	IV

Maize was not incorporated in the ADAS rotations but is a crop known to grow in the study area, being represented by 282 ha in the EDL data. Maize is recognized as having a higher risk of soil erosion and runoff than most other crops. The late drilling of maize means that the land is not ‘covered’ with a growing crop until late into June which results in the ground being more vulnerable than winter cereal crops to an intense summer thunderstorm which can lead to flash flooding. With late harvesting it is also necessary for machinery to access the land when it is generally wet and close to field capacity, causing an increased vulnerability to compaction in the soil. Compaction in the soil reduces permeability, increasing the risk or erosion and runoff. As maize is best suited to sandy soils, it was allocated to Newport soil series within the SWAT model.

Therefore, to give a good representation of EDL data within the SWAT model (Figure 2), 13 rotations have been created based on the ADAS standard rotation information, taking into account the soil type (Table 5).

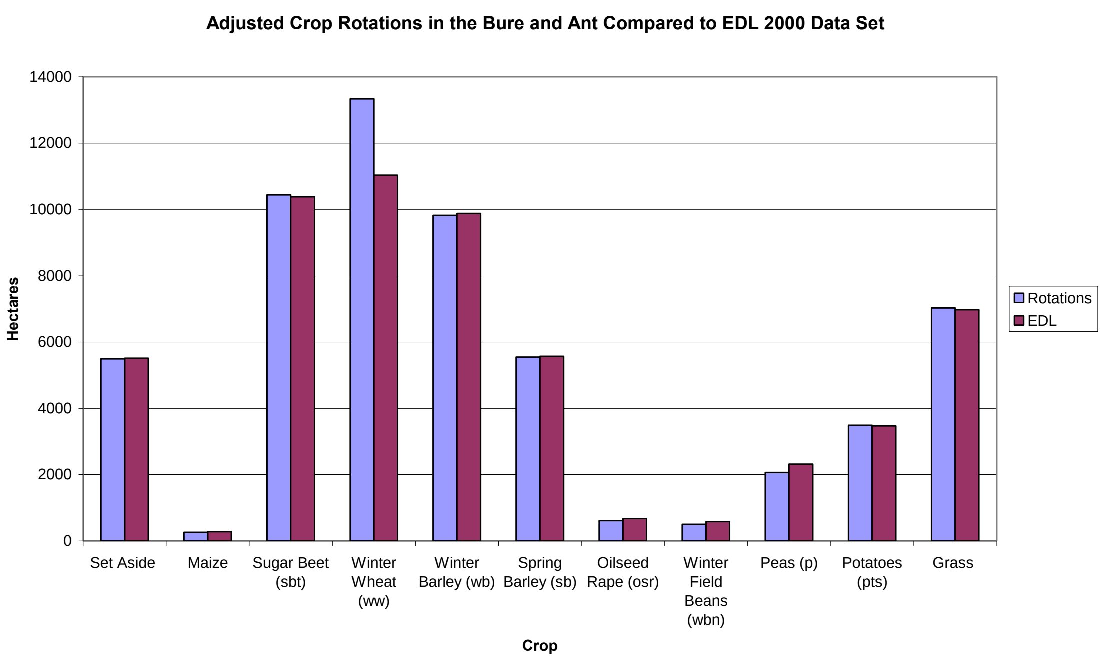

Figure 2. Comparison of modeled and actual crop areas.

Table 5. Adjusted crop rotations.

Other Mineral	Sandy	Organic	Peaty
osr/ww/wb/wbn/ww/wb	pts/ww/sb/sbt/ww/wb	sbt/ww/sb/ww	wbn/ww/p/ww
osr/ww/sbt/wbn/ww/wb	pts/ww/wb/wbn/ww/wb	sbt/ww/p/ww	
	wbn/ww/sb/sbt/ww/wb		
	sbt/ww/sbt/wb		
	sbt/ww/p/wb		
	Maize		
	sbt/ww/osr/wb		
	sbt/ww/sb/wb		

Information on dates of planting along with harvest dates was not available for the study area. Indicative crop calendar dates (Holman et al., 2004) were therefore used in creating the management files for the SWAT model. Fertiliser information has been gathered from a number of sources. Application dates have been taken from published reviews for example 'Agrometeorological Aspects of Crops in the UK and Ireland'. Fertiliser type and application rates have been taken from best practices guidelines - "Fertiliser recommendations: for agricultural and horticultural crops (RB209)" published by the Stationery Office on behalf of MAFF.

Irrigation Schedule

It was hoped that irrigation could be applied automatically by SWAT because inputting irrigation dates and amount for crops such as potatoes could be very time consuming. It was not possible to use the auto irrigation as when attempted, irrigation would only occur within the first year of the crop rotation. Therefore, irrigation had to be scheduled manually.

A program called CropWat (Smith, 1992) has been utilized to produce irrigation schedules for each crop which can be transferred to the SWAT management files. CropWat for Windows is a program that uses the FAO (1992) Penman-Monteith methods for calculating reference crop evapotranspiration. These estimates are used to develop irrigation schedules under various management conditions.

CropWat requires monthly climate data (temperatures, humidity, wind speed, and sunshine), crop files with planting dates, and monthly rainfall data. Data used for SWAT were transferred to CropWat. Climate data was taken from BADC data for Coltishall as this is the only climate gauge in the river basin. Monthly rainfall was taken from the Alysham rain gauge for 1990 as this gauge had data nearest the annual areal average, and 1990 was the closest to the annual average over a ten year period.

Default soil types were used within the model for light and medium soils. Irrigation scheduling criteria was set to irrigate when 100% of readily available soil moisture depletion occurred. Application depth was set to refill 100% of readily available soil moisture. Irrigation application date and net irrigation (mm) were used to schedule irrigation treatment within the SWAT management files for each crop within the HRU.

Results and Discussion

As no daily time series data are available at the outlet of the river basin being modeled, initial calibration has been undertaken at three gauged sites within the river basin (Ingworth, Horstead Mill, and Honing Lock). Measured streamflow for the period 1996 – 1998 was used for the calibration of SWAT. In the calibration procedure, baseflow was separated from surface flow for measured streamflows using two methods. These are Base flow Index (BFI) from the soil HOST groups (Boorman et al., 1995) and the Turning Points Method (Gustard et al., 1980). The two techniques estimated the baseflow to be approximately 83% and 84%, respectively for the study area. Model parameters were adjusted from the SWAT initial estimates within acceptable ranges to achieve the desired proportion of surface runoff to baseflow. Increasing the deep aquifer percolation fraction (RCHRG_DP) to 0.7 and the baseflow alpha factor (ALPHA_BF) to 0.3 resulted in a proportion of 81% baseflow and 19% surface runoff on an annual basis. Table 6 shows that the model is able to accurately predict the overall contributions of groundwater flow to total flow at Ingworth. A good correlation is indicated by R^2 of 0.63 and E_{NS} of 0.53. However, it should be noted that this is only at an annual level.

Table 6. Ground flow contributions to total flow.

	Groundwater Flow		**Total Stream Flow**		**% of total stream flow from groundwater**	
Year	**Separated (mm)**	**Predicted (mm)**	**Observed (mm)**	**Predicted (mm)**	**Separated**	**Predicted**
1996	40.76	43.97	46.69	54.90	87.33	80.10
1997	38.60	43.48	44.63	53.28	86.49	81.63
1998	50.04	46.02	67.05	57.22	74.64	80.44
Total	**129.4**	**133.47**	**158.35**	**165.38**	**82.82**	**80.72**
					Average Values	

Table 7 shows annual summary statistics for the calibration period, at Ingworth. Exact agreement is unlikely to be reached because of uncertainty involved in estimating which crops are grown from year to year. This will therefore affect the amount of water leaving as evapotranspiration, and thus the amount of water left to contribute to streamflow.

Table 7. Annual summary statistics.

Year	**Observed flow (mm)**	**Predicted flow (mm)**	**Pred/Obs (mm)**	**Precipitation (mm)**	**ET (mm)**	**P-ET (mm)**
1996	46.69	54.9	1.18	560.10	317.07	243.03
1997	44.63	53.28	1.19	599.30	425.88	173.42
1998	67.05	57.22	0.85	826.98	543.08	283.90

Conclusions

The SWAT model was applied to two river basins in the Norfolk Broads, which is located in the east of England. The model was built with great consideration given to the management and soil files. The model has been initially calibrated for annual base and surface flow. The model was found to predict flow well. However, further sensitivity work is to be carried out on the distribution of soil associations and their soil series within the river basin. The use of dominant soil associations has shown that the use of a soil which covers less of the area is more important in controlling either hydrological or erosional response, or both. Further successful calibration of SWAT for non-point sources in the river basin will provide further insight as to which management and/or land use strategies could potentially help mitigate eutrophication problems now and in the future within the Norfolk Broads National Park.

References

Boorman, Hollis, Lily (1995) Hydrology of Soil Types: A hydrologically based classification of the soils of the UK, Institute of Hydrology Report No. 126, Wallingford, UK

Gustard, Bullock and Dixon (1980) Low Flow Estimation in the UK, Institute of Hydrology Report 108, Wallingford, UK

Hodge, Burton, Corbett, Evans and Seal (1984) Soils and their use in Eastern England, Soil Survey of England and Wales

Holman, Quinn and Knox (2004) National Groundwater Recharge Assessment – Crop Calendar Dataset R&D Technical Report, Technical Report Task 1f: The development of the crop calendar dataset, Cranfield University, Unpublished

Hough (1990) Agrometeorological Aspects of Crops in the UK and Ireland - A review for Sugar Beet, Oilseed Rape, Peas, Wheat, Barley, Oats, Apples and Pears. Luxembourg: Commission of the European Communities.MAFF (2000) Fertiliser Recommendations for Agricultural and Horticultural Crops (RB209), The Stationary Office, London

Smith (1992) Cropwat: a computer program for irrigation planning and management, FAO irrigation and drainage paper; 46, Food and Agriculture Organization of the United Nations

Groundwater Resource Management on the Urban Environment

Mr. Eyilachew Yitayew
P.O. Box 41742, Addis Ababa, Ethiopia. E-mail: eyilachew@yahoo.com

Introduction

Water is a fundamental resource for socio-economic development and is essential for maintaining healthy environment and ecosystems. Consequently, there is a rising demand for fresh water resources as a result of increasing population and advancement of technology, and it is becoming increasingly difficult to satisfy in the current context of growing pollution worldwide. This is a matter requiring urgent attention, since water is such an important and scarce resource that it needs detailed scientific research all over the world in order to sustain and protect the water resource from pollution and for its wise utilization.

Natural fresh water is a finite resource, essential for agriculture, industry, and human/domestic existence. Without fresh water of adequate quantity and quality, sustainable development will be impossible and life is in danger. But human intervention in the natural system has a significant effect on the quality of natural water. Human activities like discharge of untreated toxic chemical and industrial waste into streams, unplanned urban development, lack of sewerage system, over pumping of aquifers, contamination of water bodies with substances that promote algal growth (possibly leading to eutrophication), and global circulation (heating) are some of the prevailing causes of water quality degradation.

Dire Dawa is the second largest urbanized centre in Ethiopia, next to Addis Ababa, along the Addis Ababa-Djibuti railway, with a population of more than 270,000. It has an enormous development potential. Industries mainly comprise food-processing plants, textile, and cement factories. The main source of water for domestic supply is groundwater (Sabiyan well-field) within the urbanized part of the town**.** In addition, there is water supply from the springs and hand-dug wells. Although easier to exploit, it has to be treated before it meets the WHO standards for domestic supply. Hence, the water supply from the Dire Dawa and its vicinity is not completely safe due to the presence of different sources of pollutants that increase the risk of chemical pollution of the water resource.

Objectives

1) Determine water quality of the aquifers and impacts of the present and future exploitation
2) To identify the different sources of pollutants affecting the quality of groundwater
3) Give recommendation on the strategy of groundwater resources development and protection

Methodology

The methods applied are:

1) Data collection and review of previous studies i.e. geological, hydrogeological, urbanization
2) Water points inventory, sampling & field measurements (location, EC, PH, EH, temperature)

3) Water quality survey, hydrochemical, isotope analysis, and pollution source identification by applying different software

Urbanization and Groundwater Pollution in Dire Dawa Town

General Situation

The geomorphologic, geologic, and hydrogeologic characteristics of the basin facilitate the effect of pollution. The town consists of mainly unconsolidated permeable alluvium deposit that can easily be penetrated by disposing wastewater. Percolation of wastewater is also facilitated by a gently dipping or almost flat nature of the topography of the town. The groundwater table is encountered at shallow depth in the northern part of the town that is as low as ten meters below ground level. Such distance is covered within a short time interval by descending pollutants.

Degradation of the town's groundwater quality may be caused by urban agriculture in the south (valley) -western and eastern sides of the basin, or by point sources such as septic tanks, pit latrines, garbage disposal sites, and cemeteries. Line sources such as poor quality water; wastewater drainages from factories and seepage from polluted streams affect the hydrogeologic system in a considerably high magnitude which tends to move laterally in the direction sources of the pollution.

The present contamination may be at its early stage because the movement of both groundwater and pollutants is so slow that it takes many years to be in contact. After the contact is made, it is difficult to clean up and rehabilitate from the aquifer since the degree of contamination will show a growing/pluming trend.

Spatial Conditions and Urbanization

Dire Dawa is the second largest and one of the fast growing towns in Ethiopia. It has recorded a dramatic growth since its foundation. The first master plan of Dire Dawa was prepared in 1967 that has now become obsolete. The land use master plan that dates back to late 1967 and 1994 (NUPI) indicates that the total planned area was 2,928 and 3,241 hectares respectively. Presently (2004), it is extended to 8,386 hectares. The existing and future land use for Dire Dawa town is shown on the land use map.

The land use of the town is dominantly mixed, especially residential areas with commercial activities. This is true, notably in the central part of the town, where almost all buildings along the streets are used for commercial activities and their backyards or internal courtyards are used for dwelling purposes. Residential areas cover around 680 ha (10.38%), squatter settlement is estimated 980 ha (12%) and all about consists of 50.14% of the total built-up area.

The sanitation situation in Ethiopia is very low; the development is limited and has not been a major concern. Most of the population in rural and urban areas do not have access to safe and reliable sanitation facilities. As a result, above 75% of the health problems in Ethiopia are due to contagious diseases attributed to unsafe and inadequate water supply, and unhygienic waste management, particularly human excreta.

In Dire Dawa town, there is no municipal sewerage system at present. The sanitary system and practice in the town is very poor; unlined, traditional pit latrines are the most common technology in use. At present the town doesn't have any system for the safe disposal of wastewater. Each household is in charge of disposing of its own waste. It is clear that the existing facilities do not cover the needs of the town in terms of sanitation.

Sanitation in Dire Dawa town at the moment is the responsibility of both the Water Supply and Sewerage and the Health Offices, even though they have insufficient means at their disposal to adequately execute their role. In the town there are three trucks and 84 transfer containers for refuse collection and two vacuum trucks for emptying the filled toilets. Sullage is domestic wastewater used for body washing, laundries, and cleaning of cooking utensils. Sullage water represents a significant proportion of water consumption in the town and the volume produced is greatly dependent on the volume of domestic water used. In Dire Dawa town, washing is mostly carried out at the entrance of households and the resulting wastewater is disposed on the ground or into drainage ditches outside the compound.

Table 3.1. Solid waste disposal situations in Dire Dawa and rural as per 1998 CSA.

Status	Vehicle container	Dug out	Thrown away	Others	Total
Rural	3.1%	1.1%	93%	2.8%	100%
Urban	46.55	11%	37.4%	5.1%	100%

Source: 1998 CSA WMS

Solid waste disposal sites are not selected according to hydrogeological priorities. The main solid waste disposal area is the sandy dry stream Channel of Dechatu River that divides the town into two almost equal parts. Solid waste stack is clearly seen in the dry river channel starting from the upper part of the town (Addis Ketema) to the lower part (Kebelle 22).

Dire Dawa textile, meat factory, and soft drinks factory discharge untreated wastewater into the drainage. All of them drain northward unprotected and open to additional surface contaminations. Due to the highly permeable nature of the geological formations, there is a sharp drop in the amount of wastewater into the system from the initial points.

It is noted that dysentery and malaria are the second and the third causes of death in the region, which are caused by ingestion of contaminated water. Even the first cause of death TB- the barometer of the living standard is highly connected with water, sanitation, and environment.

Sources of Pollution

Due to the rapid growth and urbanization in Dire Dawa, there is an increase in the size of population, number of commercial establishments, and number of industries. Consequently, the amount of waste generated has also increased since there is no good integrated waste management system (no recycling, sewage network, and landfill sites) in the town. The geology and aquifer system is easily exposed for contamination. The major pollution sources are related to anthropogenic activities that are domestic, industrial, and agricultural. On the other hand, natural hardness is a major problem of the region since it is a sedimentary terrain and the major aquifer is limestone with Ca-Mg bicarbonate of water type is dominant.

Industry is the second important economic activity in urban area. There are six major industries and more than 100 small-scale manufacturing industries in the town of Dire Dawa. These are Dire Dawa textile, Dire Dawa food complex, ELFORA meat processing, East Africa bottling (soft drink), and Dire Dawa Cement.

Major wastes and by products of the factory are carbon dioxide, carbon monoxide, dust, and sometimes sulfur dioxide. Carbon monoxide is produced when there is incomplete combustion of raw material. The main raw material is lime ($CaCO_3$). When partially combusted, the lime gives off cement, CO_2, and CO. Both CO_2 and CO liberate to the air, which ultimately contributes to the greenhouse effect in the atmosphere. Another nuisance waste product is sulfur dioxide that liberates from the furnace when there is less air or less ventilation. This gas has been causing bad smells for the nearby residents.

The Dire Dawa textile factory is the main source of contamination in the urban area. The chemicals used in this factory pollute the ground and surface water. The factory has no waste treatment plant and it directly releases all sorts of wastes into the nearby stream. Most of the time, PH of the waste is more than 12. The following table shows the type and amount of different chemicals used in the factory.

In the town, there are about 98 medium and small-scale factories. All medium and large-scale industries do not treat their effluent or liquid waste. They merely discharge into open fields, nearby the Dry River or sandy stream channel, which is a threat for the groundwater source. The cumulative and long-term effects of these pollutants in the environment, particularly in the surface and ground water resource potentials of the town would be significant.

There is no waste treatment and proper waste disposal system in Dire Dawa town. Domestic as well as industrial wastes have been discharged directly into the open ditches and sandy streams. From the nature of its topography and soil, the groundwater resource is very vulnerable to pollution. Degradation of groundwater quality is exacerbated by point-source contamination such as septic tanks, pit latrines, and industrial effluents.

Table 3.2. Urban toilet facilities of Dire Dawa by housing unit, as to 1994 census.

Towns	All Housing units	Type of toilet facilities					
		Has no Toilet	Flushed Toilet private	Flushed Toilet shared	Pit Private	Pit Shared	Not stated
Dire Dawa	34680	21.6%	4.7%	2.4%	29.7%	39.6%	1.9%
MelkaJebdu	1702	61.4%	-	0.5%	31.1%	5.4%	1.4%
DDAC	36382	8531	1662	851	10831	13811	696

According to CSA (1994), about 68% of the household in Dire Dawa use pit latrines. This situation is increasing the risk of the groundwater contamination by human wastes. These pollution problems are clearly observed from the water quality analysis in the past 30 years. Water quality tests from different sites of the town (bore holes) show that nitrate concentration of water samples from Sabiyan and inner parts of the town highly exceeds the WHO and Ethiopian Drinking Water Quality Guideline Values.

In the town and its vicinity, there are numerous urban and rural agricultural activities such as Tony farm, chat farm, Amdael diary farm, Hafecat diary, and other small-scale cattle breeding and horticulture producers in the town. Generally, the agricultural inputs and by-products constitute the greatest amount of wastes and have a chance to contact the groundwater system.

Animal wastes are classified as solid and liquid. Such animal waste may become the source of groundwater pollution. The groundwater quality is directly affected by microorganisms in organic fertilizers, particularly when raw animal feces are applied without being subjected to thermal and anaerobic stabilization prior to application (Castany, Groba, Tomija, 1986; and references therein).

In the Dire Dawa area, in addition to the above-mentioned potential sources, there are also possible pollution sources like markets, cemeteries, fuel stations, garages, etc. Urban activities produce numerous sources of contamination to the environment.

The other possible source of water pollution is cemeteries. Most of the churches in Dire Dawa have graveyards/cemeteries away from their compounds. There are two main cemeteries associated with the religious consideration such as Muslim and Christian. But both cemetery sites are in the inner part of the town and near the Dechatu River.

Sources of Groundwater Contamination

The chemical, biological, and physical properties of natural water are variable and depend on the composition of precipitation, geology, climate, biological activities, geochemical processes, the contact surface and contact time between water and rocks, and human factors. As a result of disposal of liquid, gaseous and solid wastes, chemical substances, and pathogens pollute water sources; and their potability may be impaired by troublesome odor, test, and color. Also, substances that can be used in agriculture such as fertilizers, insecticides, and herbicides may pollute water sources. Their harmful effect on water quality can be caused by inappropriate application or the chemical nature of the substance used.

Generally, domestic as well as industrial wastes affect water quality in urban centers. In Ethiopia the degree of pollution is generally not large except the surface waters of Addis Ababa and groundwater of Dire Dawa town. In general, the influence of human activity in the wastewater in the urban centers is indicated by the increase of nitrate and chloride concentration in the water bodies.

Groundwater moves slowly and responds slowly to quality changes. The movement of pollution is determined by the movement of water, and therefore depends on physical factors. Pollution tends to attenuate as it moves through soil and groundwater systems due to physical dilution and dispersion, and a combination of chemical and biological actions. Of these, precipitation-solution, ion exchange and adsorption, and biological degradation (oxidation-reduction) are most significant to groundwater quality. The importance of the various physical, chemical or biological processes depends on the type and source of pollution, the nature of the soil and/or aquifer material, the hydrology, and the well field.

The causes, types, and extent of groundwater pollution range from wide spread agricultural sources to the primary domestic pollution sources of solid and liquid waste disposal. Individual septic tanks cause local and up to regional contamination problems of nitrate buildup if their concentration is very high. The land disposal of municipal sewage is a potential nitrate source and landfills are sources of metals and a variety of organic and inorganic compounds.

Most potential groundwater contaminants are released at or slightly beneath the land surface. Here, the wastes are subjected to the processes of leaching and percolation that may lead to their introduction into the ground water system. As they move through the unsaturated zone above the groundwater table there is the tendency to attenuate; a process that sometimes eliminates potential contamination sources as serious problems, because contamination simply does not reach the groundwater in sufficient strength.

The movement of a solute through the unsaturated zone, or zone of aeration, to the water table is primarily vertically downward from the surface, and then horizontal displacement has undergone within the saturated zone. In the unsaturated zone, hydraulic and mass transport properties influence the degree of pollutant movement (FAO-Rome, 1979).

Contaminants are solutes reaching aquifer systems as a result of human activities. Pollution occurs when contaminant concentrations reach objectionable levels. Man's interference with natural flow patterns and his introduction of chemical and biological material into the ground usually results in undesirable groundwater quality changes. Contaminant sources include: municipal sewer leakage, liquid waste disposal, solid waste disposal, urban runoff, lawn fertilizer application, industrial liquid waste disposal, tank and pipeline leakage, mining activities, chemical spills, etc.

Dire Dawa has no sewer system, well-studied waste disposal sites, and no systematic disposal methods. For the past nine decades, pit latrines have remained the main human excreta disposal facilities. There are more than 15,000 pit latrines and more than 1,000 septic tanks throughout the town. In the other part of the town, where the population density is higher, the latrines are closely spaced and this poses cumulative effects on the hydrogeologic environment. With a total population of more than 270,000 and poor feeding style, the annual tonnage of human excreta dumped is considerably high. Such exponential increase will have a direct and higher effect on the hydrogeologic system since it is only in the past few decades that the town has developed and populated. The effect of population in polluting the hydrogeologic system is still in its early stages.

Human excreta contain large amount of water, 20% organic matter, 2.5% urine, nitrogen, phosphoric acid, sulfur, and other inorganic compounds (Ehlers and steer, 1976). As can be understood from this fact, nitrogen is the main component of human excreta. Of the organic matter contained in average domestic sewage, about 40% is made up of nitrogenous substances, 50% of carbohydrates and 10% of fats (Fair and Geyer, 1971). Such high influx of nitrogenous substances will result in nitrate pollution of groundwater.

Industrial and domestic wastewater drain into the sandy stream channels and percolate within few hundreds of meters distance from their source. Dire Dawa textiles factory, meat factory, and soft drinks factory discharge untreated wastewater through drainages and into the hydrogeologic environment, unprotected, and open that makes additional surface contaminations. On the other hand, they create favorable conditions for the decomposition of organic matter dumped as a solid waste in the sandy water channels.

The laboratory analyses conducted on the water samples taken from different localities at different times indicate that the level of groundwater pollution is increasing at an alarming rate. For instance, according to the hydrochemical analysis conducted by an Israeli geologist in 1959, the maximum concentration of NO_3 at the center of the town was 45mg/l. After 22 years (1982) Ketema Tadesse has reported a NO_3 concentration of 320mg/l within the town. On the other hand, while preparing this research the water sampled from Dire Dawa food complex bore hole (FBH) at August 2003 and analyzed on October 2003 by EIGS-laboratory shows the result is still high to 266mg/l (2003).

Nitrate may also play a role in the production of nitrosomines in the stomach, which are known as carcinogens. This was considered as a possible reason for a higher death rate from gastric cancer in a group of people that had high nitrate levels in their drinking water (Bower and references their in, 1978). Point contamination also has higher contribution to the higher concentration of sulfate, sodium, and chlorine in Dire Dawa groundwater (refer nitrate map).

Presently, the factors that are assumed to cause pollution (declining of the rainfall, increment of household wastes, absence of proper waste management, etc.) are being aggravated. Hence, the level of pollution is exceeding the maximum allowable limits set by World Health Organization (WHO) and the National Standard (ENWQG).

High nitrate, chloride, and sodium concentration is observed in the wells found within Dire Dawa town. The water quality of alluvial aquifers is highly contaminated by human interferences, especially the alluvial water in the Dire Dawa town and dug wells near the community. The total dissolved solids of polluted water is from 1,000 mg/l to more than 3,000 mg/l. The spatial coverage and trend of TDS, EC, hardness, major cations, and anions of the basin in general and the Dire Dawa town in particular is explained on the maps.

From the land use map of the town and in relation with the hydrochemical evolution, the concentration of EC, TDS, chloride, nitrate, and sulfate are mainly dependent on the groundwater flow direction and anthropogenic activities. For further understanding, please see the attached figures.

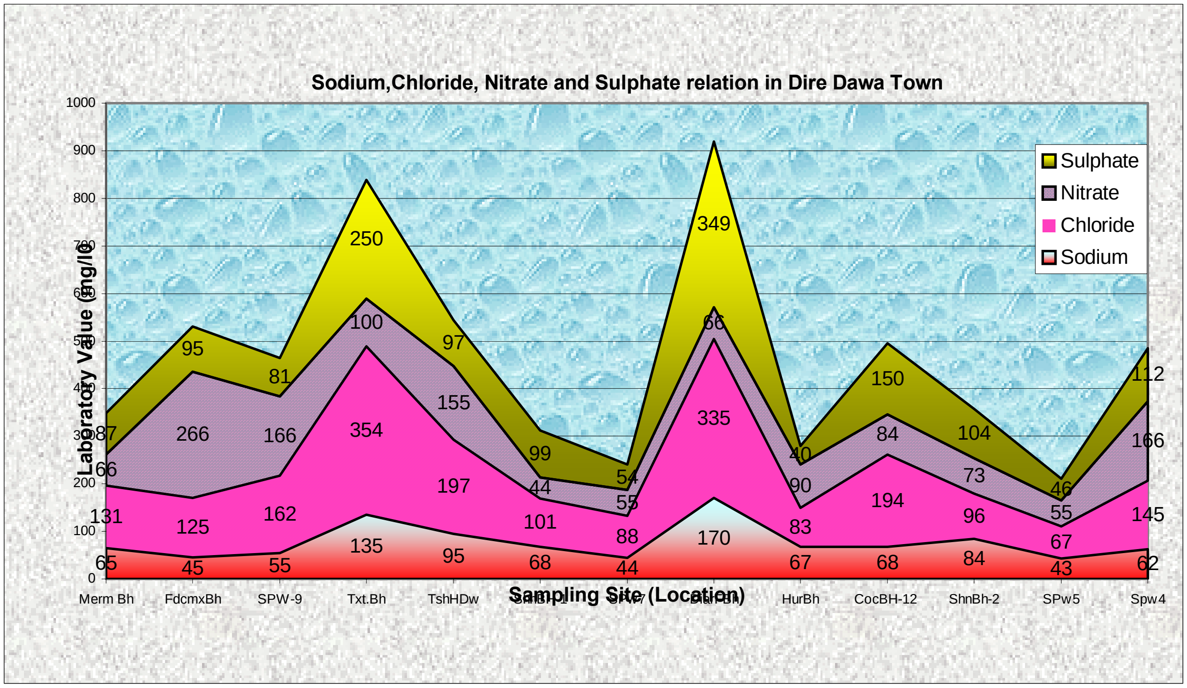

Figure 3.1. Sodium, chloride, nitrate, and sulfate relations within Dire Dawa groundwater.

Aquifers Vulnerability

There are two aquifers in Dire Dawa area that is the alluvial and the upper sandstone aquifer. The main aquifer that is exploited for the Dire Dawa town water supply is the upper sandstone. Upper sandstone is semi-confined overlaid by the alluvial aquifer. The groundwater elevation map shows that the groundwater level is deep along the Dechatu River and at the same time the overlying alluvial and the upper sandstones are highly permeable and the groundwater flow concentrates along the river. In general, the upper sandstone aquifer at Dire Dawa town is vulnerable to pollution due to the high to moderate permeability of the alluvial sediments overlying the main aquifer.

From nitrates, chlorides, and sulfate concentration distribution in the aquifer of the Dire Dawa basin, the following observations are made:

1) High concentration is directly related to high population density and industrial areas
2) The high concentration plume is flowing along the groundwater flow direction
3) At the Sabiyain well field a localized plume of nitrates, chlorides, and sulfate are flowing to the well field. At present, some of the wells in the well field are located within the zone of 50-166 mg/l of nitrates.

Impacts of Pollution on the Environment

One of the major difficulties with groundwater contamination is that it occurs underground with a complex system. The pollution sources are not easily observed nor are their effects seen until damage has occurred. The tangible effects of groundwater contamination usually come to light after the incident causing the contamination has occurred. This long lag time is a major problem.

All the scientific evidence that has been considered so far lead to the conclusion that continued disposal of wastes to the subsurface will produce progressive and largely irreversible pollution of the groundwater. Although physical, chemical, and biological processes have been identified which may attenuate pollutants, these processes have finite limits or are operative only over a limited range of physico-chemical conditions. Persistent pollutants will therefore accumulate in the groundwater until a dynamic balance is reached between the rate of input of the pollutants to the groundwater flow system and the rate of discharge of the pollutants from the system.

In order to evaluate the extent of pollution in the study area the number and distribution of possible pollutant sources, hydrogeolgical characteristics of rocks and soils, and results of water analysis have been given due emphasis. Based on these factors the study area was divided into three different areas as shown in the map (Figure 3.1). The sources of pollutants are closely associated with land use patterns and to some extent to population density in the area. Moreover, the extent of pollution also varies between the urban and suburban part of the town.

Remedial Measures and Aquifer Cleanup

The general characteristics of contaminants from common point and non-point sources are seepage pits and trenches, percolation ponds, lagoons, waste disposal facilities, streambeds, landfills, deep disposal wells, injection wells, surface spreading and irrigation areas, and farming areas.

The largest component of municipal land disposal of solid wastes is paper, but substantial food wastes, yard wastes, glass, menials, plastics, rubber, and liquid wastes are also included. Landfill leaches can contain high levels of BOD, COD, iron, manganese, chloride, nitrate, hardness, heavy metals, stable organics, and trace elements. Gases such as methane, carbon dioxide, ammonia, and hydrogen sulfide are by-products of municipal landfills. Many municipal waste disposal sites receive industrial process residuals and pollution control sludge. Radioactive, toxic, and hazardous wastes have been disposed in some municipal landfills and applied an integrated waste management system.

Municipal waste water may reach to aquifers by leakage from collecting sewers, leakage from the industries during processing, land disposal of the treatment plant effluent, disposal to surface waters which recharged aquifers, and land disposal of sludge. Sewer leakage can introduce high concentrations of BOD, COD, nitrate, organic chemicals, bacteria, and heavy metals in to groundwater. Potential contaminants form sludge includes nutrients, heavy metals, and pathogenic organisms. Potential contaminants from industrial waste disposal sites cover the full range of inorganic and organic chemicals including phenols, acids, heavy metals, and cyanide.

These remedial measures are time-consuming (months to years) and very expensive (tens of thousands to millions of dollars). It often takes longer to decontaminate an aquifer than it took to contaminate the aquifer.

Remedial measures remove or isolate point sources and/or pump and treat contaminated ground water (JRB Associates, 1982). Remedial measures include: changing the surface drainage so that runoff does not cross the source, using source subsurface drains and ditches, constructing low-permeability caps above the source, installing a low-permeability vertical barrier (slurry wall, grout curtain or sheet piling) around the source, lowering the water table where it is in contact with the source, chemical or biological in situ treatment of the source plume, modifying nearby production well discharge patterns, changing water table hydraulic gradients though the installation of injection wells, artificial recharge, and extracting contaminated ground water via production wells.

Removal of contaminated water through extraction wells with aquifer advection and dispersion mechanisms but without aquifer sorption mechanisms requires that a volume of groundwater about twice the volume of the contaminant plume be removed from the aquifer.

Biological activity is another method to identify the nitrate after investigating the issue in detail.

Conclusions and Recommendations

Chemical, physical, and biological processes in addition to the geological formation and man-made factors influence the hydrochemical variation of groundwater both spatial and temporal in water quality directly and indirectly. Due to the fact that different nuclei have seen on the hydrochemical variation maps within the basin area. Mostly, the concentration EC, TDS, and chloride are increasing along the groundwater flow direction. But total hardness and bicarbonate are directly related with the PH conditions of the groundwater and geological formation.

The poor sanitation condition together with the lack of proper waste disposal mechanisms attributed to severe effects of pollution of both surface and groundwater resources of the area. The most severe effects of pollution were observed in shallow wells, which is the reflection of all anthropogenic impact on water bodies of the area.

The existing industries should be enforced or advised to treat their wastes and good waste management systems should be established in the Dire Dawa town. When industrial establishments are considered, the budget for the treatment plant should be included (considered) in the main cost of the plant. Develop and implement effective programs of solid waste disposal and sanitation system. More solid waste containers with the required truck should be allocated as one alternative for solid waste collection and disposal. To minimize the impact on public health and environment, treat wastes down to an acceptable standard and dispose of it.

Waste generated from industries, agricultural activities, households, market centers, institutions, garages, fuel stations, and the health centers are the main sources of pollutants that may affect the quality of water in the area. In general, the causes, types and extent of waste pollution range from the wide spread agricultural use of fertilizers to a single incident of an industrial chemical spill.

Since there is a danger of potential pollutant risk of the water bodies of the area, planners and policy makers and other decision making bodies in the region should create clear environmental policies. Rules and regulation should be formulated to control utilization of groundwater, effluent standards, and properly follow the implementation of the policy; otherwise future generations will inherit these problems.

Recommendations

Based on the present investigations the following recommendations are made:

1) Artificial recharge should be done to maximize the groundwater potential and proper groundwater management should be undertaken and boreholes must be drilled outside the town to the north direction.
2) Establish environmental standards related to chemical management and develop concepts of integrated waste management strategy (source reduction, sorting, recycling, incineration, and sanitary landfill) and construct a sewerage system.
3) Remedial measures should in practices i.e. change the surface drainage so that runoff does not cross the source.
4) Aquifer cleanup/removal of contaminated water through extraction wells with aquifer advection and dispersion mechanisms, but aquifer sorption mechanisms requires that a volume of groundwater about twice the volume of the contaminant plume be removed from the aquifer. Biological activity is another method to identify the nitrate and to dismantle from the contaminated zone.

References

David K. Todd (1980) Groundwater Hydrology
Dire Dawa Feasibility study for water supply, Oct 1982 Associated Engineering services Ltd.
GIBB/Seuereca, Harar town water supply hydrogeological investigation study programme, Nov 1996
Greitzer Y, Stratigraphy, Hydrogeology and Jurrasic Ammonites of the Harar and Dire Dawa area, 1970 (Doctoral thesis)
Habteab Z. and Jiri Sima, Hydrogeology and Hydrochemistry of the Dire Dawa Area NC 37-12 Sheet, EIGS 1986
John C. Harvey (1982), The properties of Groundwater
Ketema Tadesse, 1982, Hydrogeology of the Dire Dawa Area, Unpublished Technical Report (880-551-17), EIGS
Mesfin Aytenfisu, Hydrogeology of Northeastern part of Haraghe, 1981 (Msc thesis)
MoWR, 8 towns water supply project production well drilling works, Feb 1999
Taye Alemayehu, Contamination of the Hydrogeological System in Dire Dawa, 1988
Tesfamichael Keleta, 1974, Hydrogeology of the Dire Dawa, A statement of present knowledge (880-551-07) EIGS

Non-SWAT Related Papers

71. Sugarcane crop coefficient (Ratoon) in Haft tappeh of Iran 684
Saeed Boroomand Nasab, Heidarali Kashkuli and Mohamad Reza

72. Floodwater effect on infiltration rate of a floodwater spreading system in Moosian gravelly piedmont plain in Dehloran, West Central Iran 691
Saeed Boroomand Nasab, Hossain Charkhabi and Ayoub Pirani

73. Soil physical and chemical properties as indicators of land degradation in the Kouhrang (Chelgerd) Region, Chahar-Mahal & Bakhtiary Province, Iran 697
A. Jalalian, M. Azarbin, M.K. Eghbal and S.F. Mousavi

74. Depasturation effects on soil physical and chemical properties in Isfahan and CharMahal Bakhtiari Region
Mohammad Hajabbasi

Sugarcane Crop Coefficient (Ratoon) in Haft tappeh of Iran

Saeed Boroomand Nasab*[1], Heidarali Kashkuli[1], and Mohamad Reza Khaledian[1]
[1]Associate Prof., Irrigation Department, Faculty of Water Sciences Engineering, Shahid Chamran University, Ahwaz, Iran. Email: boroomandsaeed@yahoo.com

Abstract

The sugarcane crop coefficient is necessary for estimating the water requirement in irrigation water planning and management. This study has been initiated to determine the crop coefficient (Kc) of sugarcane (Ratoon) in the Haft tappeh climate. The relationships between Kc, ETc/Ep, length growth, days after cutting (DAS) and percent days after cutting (%DAS), were also investigated.

The mid-season and late-season Kc values for sugarcane were 1.45 and 1.14, respectively. These values are somewhat higher than those values that recommended by FAO. The ratio of ETc/Ep varied between 0.64 to 1.10 from the beginning to the end of the growing season.

The maximum ratios of ETc/ET0 and ETc/Ep occurred at a length growth of 126 cm. Furthermore, second order polynomials were presented to predict the Kc values from days after cutting (DAS) and percent days after cutting (%DAS).

Keywords: Sugarcane, Haft tappeh, Crop coefficient, Irrigation and Evapotranspiration

Introduction

Sugarcane is an irrigated cash crop usually planted in Khouzestan of I.R. of Iran. Therefore, it should be included in crop pattern of irrigation projects in these regions, and its water requirement estimated for irrigation water planning and management. Crop coefficient is required for estimation of crop water requirement. As far as authors are aware, there is little data if any reported on the water requirement of sugarcane (Cp48-103) in I.R. of Iran and other parts of the world.

Crop coefficient is the ratio of actual crop evapotranspiration (ETc) to reference crop evapotranspiration (ET0). The reference crop is usually grass (Doorenbos and Pruitt, 1977). The pan evaporation method is a simple method to predict of evapotranspiration. This method has been modified by FAO (1998). Different methods estimating ET0 values have been used for the study area but a suitable method is still in doubt.

This study was initiated to measure the ETc of sugarcane using two lysimeters and to estimate the ET0 using the pan evaporation method to compute the crop coefficient of sugarcane in Haft tappeh area. The relationships between Kc and days after cutting and length growth were also investigated for sugarcane.

Methodology

Crop coefficient (Kc) can be estimated by,

$$Kc = \frac{ETc}{ET0} \qquad (1)$$

Therefore, the ETc and ET0 values were determined at the various stages of growth.

The study was conducted in Haft tappeh, I.R. of Iran. The area is a flat at 32.07(degree, N) and 48.35 (degree, E) and an altitude of 63.1 m. Climate of the study area has warm summers and most of the rain occurs in the winter months. Temperature, relative humidity, wind speed at 2 m height and sunshine duration on a daily basis were collected during the study period. A summary of the weather data is shown in Table 1.

Table 1. Summary of meteorological parameters for Haft tappeh area.

Parameters	Unit	Maximum	Minimum	Annual
Temperature	C	50	0	-
Humidity	%	99	18	56
Sunshine	hours	9.8	4.8	-
Wind speed (U2)	m/s	3.09	1.45	-
Precipitation	mm	-	-	291

ETc of sugarcane was measured by two drainable lysimeters surrounded by sugarcane plantation. The lysimeters and surrounding sugarcane plantation were located in between of a field of sugarcane during the growing season of 2000-2001(April to November). The average depth and dimension of the lysimeters were 1.9 m and 4×4.5 m^2, respectively. A Cp48-103 cultivar of sugarcane was cutted on 23 December 2000.

The weight method was used to measure the volumetric soil water contents before and after growing season. These measurements were used to determine the amount of ETc in lysimeters during the growing season. ETc was calculated by the following equation:

$$ETc=I+P-D+(M1-M2) \qquad (2)$$

where I, P and D are irrigation, precipitation and deep percolation (mm), respectively. M1 and M2 are volumetric soil water content, cm^3 / cm^{ε},at times one and two (before and after growth season). D was measured from the drain pipe, which was connected, to the lysimeters.

ET0 Calculation

ET0 for each irrigation interval was determined using the pan evaporation method modified by FAO (1998).

$$ET0=Kp \times Ep \qquad (3)$$

where ET0 is reference evapotranspiration (mm/day), Kp is the pan coefficient and Ep is pan evaporation (mm/day).

Class A pan with dry fetch applied. Kp was calculated by the following equation.

$$\begin{aligned}Kp=&0.61+0.00341(RHmean)-0.000162(U2)(RHmean)-\\&0.00000959(U2)(FET)+0.00327(U2)(LnFET)-0.00289(U2)Ln(86.4U2)-\\&0.0106Ln(86.4U2)Ln(FET)+0.00063(Ln(FET))^2 Ln(86.4U2)\end{aligned} \qquad (4)$$

where RHmean is the average daily relative humidity (%), U2 is average daily wind speed at 2 m height (m/s), and FET is the fetch or distance of green agricultural crop.

Length growth of a plant from each lysimeter was measured by a ruler at 7-days intervals throughout the growing season.

Results and Discussion

Using the monthly weather data, the amount of monthly ET0 was calculated and the amounts of monthly were determined. These results and measured values of class A pan evaporation (Ep) and lysimeter actual evapotranspiration (ETc) are shown in Fig.1. In general, the pan evaporation (Ep) was higher than the ETc and ET0.

Sugarcane Crop Coefficient

The ratio of ETc to ET0 by pan evaporation and the ratio of ETc to Ep are given in Fig.2. Furthermore, the values of Kc for all of the growing season which is not compatible with the values of Kc for sugarcane reported by FAO (1998).

The ETc and ET0 by pan evaporation and Kc values for different stages of sugarcane growth period are shown in Table 2. The values of Kc for all of the growing season are somewhat higher than that reported by FAO (1998). Therefore, these Kc values may be used for sugarcane in area of similar environmental conditions (Table 1) which occur in vast areas of I.R. of Iran and in other parts of the world.

The variation in Kc may be shown as a function of days after cutting (DAS) or Julian date (Wright,1982) and fraction of growing season (%DAS)(Elliott et al.,1988). In this study, Kc as a function of DAS and %DAS was obtained by a multiple regression procedure as follows:

$$Kc=-0.0003(\%DAS)^2+0.0451(\%DAS)-0.4189 \qquad (5)$$
$$R^2=0.9257 \qquad n=7$$

$$Kc=--3^{-5}(DAS)^2+0.0138(DAS)-0.4258 \qquad (6)$$
$$R^2=0.9317 \qquad n=7$$

Second-order polynomial equations (Eqs. (5) and (6)) were obtained with higher coefficients of determination (R^2)). The calculated values of Kc from Eqs. (5) and (6) are shown in Figs. (4) and (5) as curves which are skewed and fitted better to the data points. A third-order polynomial equation was also proposed for Spanish peanuts by Elliott et al (1988).

The monthly Kc values were calculated and the results are presented in Table 3. These values of Kc are commonly used in water requirement computation for irrigation water resource allocation projects. It also seems that there is a relationship between crop coefficient (Kc) and length growing. This relationship for sugarcane (Ratoon) was obtained as follows (Fig.3):

$$Kc=-0.8095(\text{length growth})^2+1.4053(\text{length growth})+0.7747 \qquad (7)$$
$$R^2=0.6277 \qquad n=8$$

The value of ETc/ET0=Kc is nearly equal to 1.4 at a length growth of 1 meter. In plant growth models where the evapotranspiration is estimated by length growth, Eq.(7) can be used for sugarcane.

ETc/Ep for Sugercane

The measured pan evaporation rates (Ep) during the growing season are shown in Fig.1. The values were often greater than the ETc for sugarcane. The ETc/Ep ratios for sugarcane were computed at Haft tappeh and the results are presented in Fig. 2. The minimum and maximum values of ETc/Ep ratios were 0.64 and 1.10 which occurred at the beginning and middle of the growing season, respectively.

Monthly ETc/Ep ratios were also computed. The results are given in Table 4. The minimum and maximum ratios were 0.64 and 1.10 respectively, which occurred at the beginning and middle of the growing season. The ratios of ETc/Ep at different growth stages of crops are useful as a practical tool for estimating the seasonal crop evapotranspiration where the pan evaporation data are available (Venkatachari and reddy,1978; Rao et al., 1990).

There also seems to be a relationship between ETc/Ep and length growth. This relationship for sugarcane was obtained as follows:

$$ETc/Ep=-0.5987(\text{length growth})^2+1.0975(\text{length growth})+0.5358 \quad (8)$$

$R^2=0.7932$ n=8

The value of ETc/Ep is nearly equal to 1.10 at a length growth of 1.27 m. In plant growth models, where the evapotranspiration is estimated by pan evaporation rate and length growth, Eq. (8) can be used for sugarcane (Ratoon).

Conclusions

The seasonal ETc for sugarcane (Ratoon) in the study area with an eight months growth period was 1925 mm. The pan evaporation method was preferable for estimating ET0. The mid-and late-season Kc values for sugarcane (Ratoon) were 1.45 and 1.14,respectively. These values are somewhat higher than those values that recommended by FAO. The monthly values of Kc and ETc/Ep ratios are also presented. The ratio of ETc/Ep ratios is also presented. The ratio of ETc/Ep varied between 0.64-1.10 from the beginning to the end of the growing season .

The relationship between Kc and ETc/Ep ratio and length are also shown. The maximum ratios of ETc/ET0 and ETc/Ep occurred at a length growth of 126 cm. Furthermore, second-order polynomials are presented to predict the Kc values from days after cutting (DAS) and percent days after cutting (%DAS).

Table 2. ETc, ET0 and Kc for sugarcane (Ratoon) at different stages of growing season.

Stage	Period(days)	ETc(mm)	ET0(mm)	Kc
Initial	185	996.51	932.55	1.07
Crop development	62	788.53	593.78	1.33
Mid-season	41	378.33	261.99	1.45
Late-season	45	126.16	143.38	1.14

Table 3. ETc,ETo and Kc for sugarcane (Ratoon) for different months of growing season.

Month	ETc	ET0	Kc
April	202.58	225.7	0.90
May	319.76	301.7	1.06
June	416.95	339.12	1.23
July	407.21	316	1.29
August	383.89	281.08	1.37
September	315.55	220.37	1.43
October	168.76	130.70	1.29
November	36.2	63.28	0.57

Table 4. ETc, Ep and ETc/Ep for sugarcane for different months of growing season.

Month	ETc	Ep	ETc/Ep
April	202.58	314.67	0.64
May	319.76	431	0.74
June	416.95	473.27	0.88
July	407.21	414.34	0.98
August	383.89	370.15	1.04
September	315.55	300.45	1.05
October	168.76	153.55	1.10
November	36.2	39.07	0.93

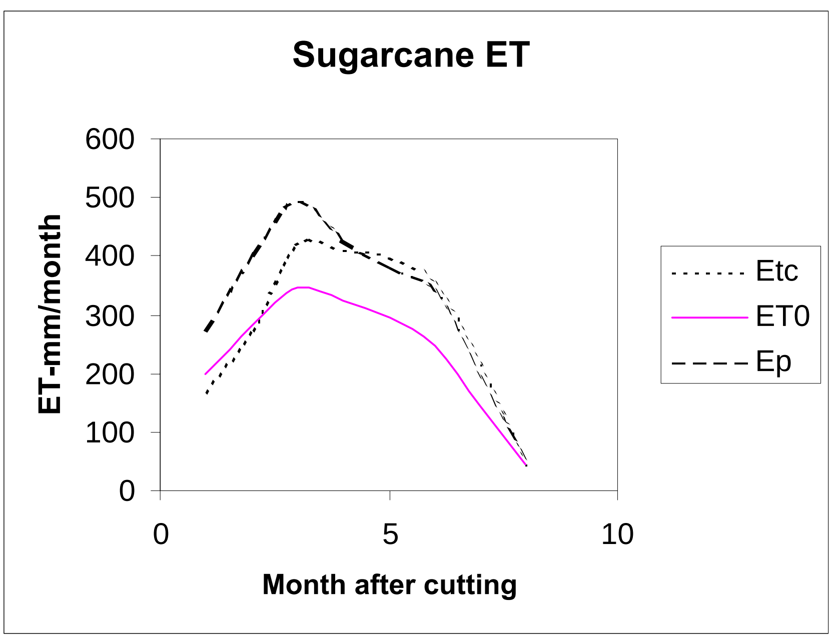

Figure 1. ETc, ET0 and Ep as a function of months after cutting.

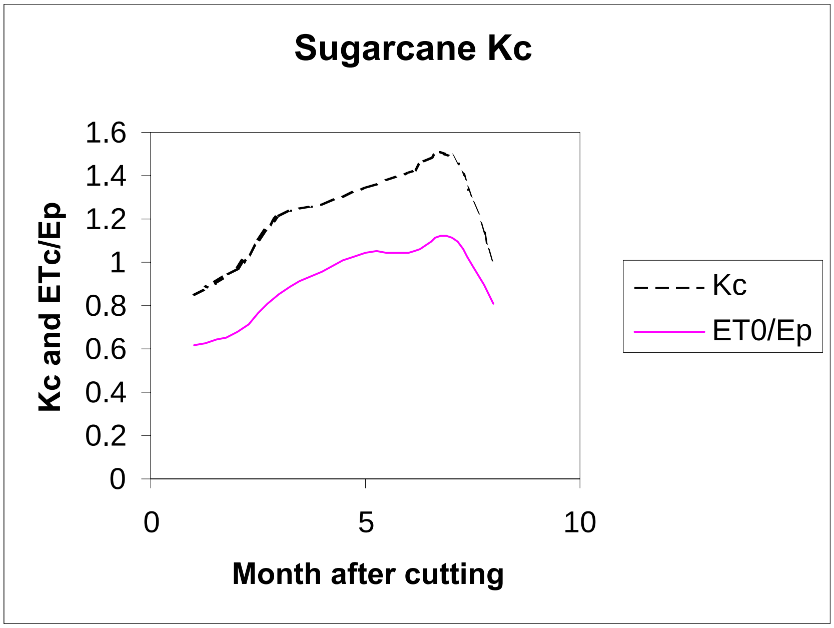

Figure 2. Kc and ETc/Ep ratio as a function of months after cutting.

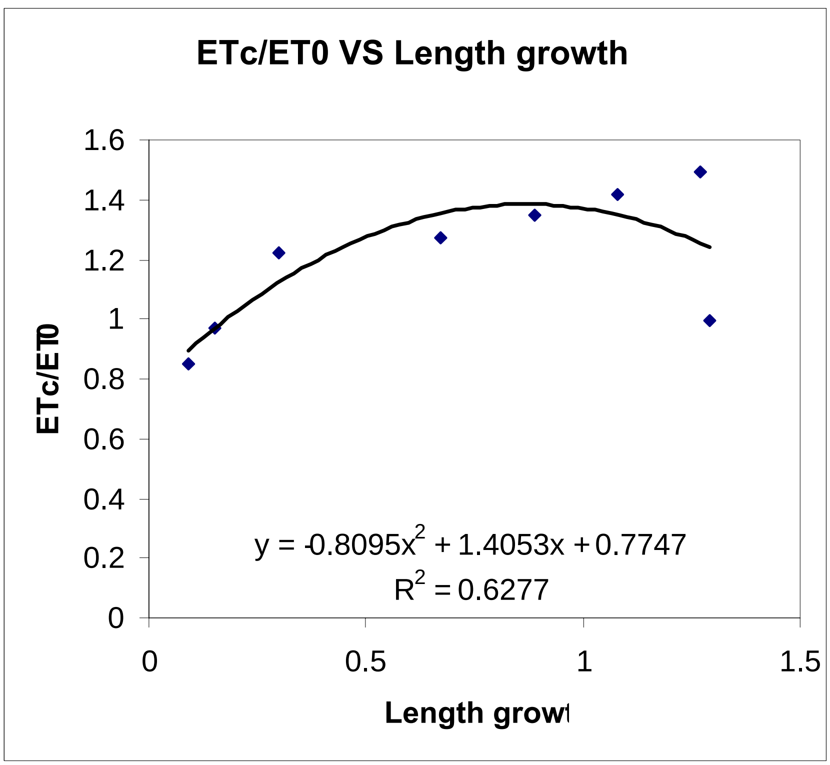

Figure 3. Measured and optimized values of Kc (ETc/ET0) as a function of length growth.

References

Aboukhaled. A., Alforo.A, Smith.M.,1982. Lysimeters:irrigation and drainage. Paper No.39, FAO, Rome, Italy.,1-20.

Allen, R.G., Pereira, L.S., Raes, D., and Smith, M.,1998. Crop evapotranspiration: irrigation and drainage. Paper No.56, FAO, Rome, Italy., 65-78.

Andam, M., 1994. Measurement of evapotranspiration, Transpiration, Crop coefficient and other parameters required in irrigation management of sesame field., Shiraz, Iran., 53-115.

Doorenbos, J., Pruitt, W.O., 1977. Crop water requirement: irrigation and drainage. Paper No.24, (Review). FAO, Rome, Italy. p. 144, 60-70.

Elliott, R.L., Harp, S.L., Grosz, G.D., Kizer, M.A., 1988. Crop coefficients for peanut evapotranspiration. Agric Water Management.15, 155-164.

Goodwin, I., 2000. Construction of an evaporation pan for irrigation scheduling. Irrigated Agriculture, Tatura.1-5.

Haft tappeh research center., 2000, Annual meteorological data.

Haft tappeh research center., 2000, Annual report.,1-40.

Kashyap, P.S.,Panda, R.K.,2001. Evaluation of evapotranspiration estimation methods and development of crop-coefficients for potato crop in a sub-humid region. Agricultural Water Management. 50 (2001), 9-25.

Rao, V.P., Raikhelkar, S.V., Sondge, V.D.,1990. Evaluation of Penman, radiation and evaporation methods for predicting sesame evapotranspiration. J. Res. APAU. 18, 131-134.

Sarami, M., 2001. Water used determination of sugarcane cultivars. Agriculture research center of Ahwaz.

Sepaskhah, A.R., and Andam, M.,2000. Crop coefficient of sesame in a semi-arid region of I.R.Iran. Agricultural Water Management. 49, (2001), 51-63.

Venkatachari, A., Reddy, K.A., 1978. Relationship of evapotranspiration with pan evaporation and evaluation of crop coefficient. Acta Agronomica Academica Scientiarum Hungaricae 27, 107-110.

Wright, J.L.,1982. New evapotranspiration crop coefficients. J. Irrig. and Drain. Div. ASCE. 108, 57-74.

Floodwater Effect on Infiltration Rate of a Floodwater Spreading System in Moosian Gravelly Piedmont Plain in Dehloran, West Central Iran

Saeed Boroomand Nasab*[1], Hossain Charkhabi[1], and Ayoub Pirani[1]
[1]Associate Prof., Irrigation Department, Faculty of Water Sciences Engineering, Shahid Chamran University, Ahwaz, Iran. Email: boroomandsaeed@yahoo.com

Abstract

In this study a floodwater-spreading system, which was constructed and started to work in 1997 on the eastern part of the Dehloran colluvial plain, was selected to measure and monitor the variation of the infiltration and clogging phenomenon. The vertical variation as well as flow direction variation of the infiltration was studied. The vertical variation of infiltration of the sediment was measured at five surfaces, (1) the surface of the whole sediment deposited since 1997 when the system started to operate, (2) the surface where the new deposited sediment is removed, (3) the surfaces when 10, (4) 20, and (5) 30 cm of the previous natural sediment were removed. To monitor infiltration in the flow direction, infiltration was measured in the desilting basin, spreading channel, spreading basin, and control points. A double ring method was used to measure infiltration at these surfaces. The statistical analyses were done using SPSS and MSTATC statistical packages. The statistical procedures used for the analyses were analysis of variance (ANOVA), Least square difference (LSD) and the Duncan method. The statistical analysis showed that the sedimentation significantly decreased the surface infiltration of the desilting basin when compared with the data obtained from the control points. The control points were selected in an intact area where the soil and geomorphic surface were similar to the selected sites. Removal of the top 10 cm of the natural surface beneath the sediment showed that the infiltration rates were significantly increased. The results found here suggests that to decrease the adverse effects of sedimentation on the infiltration rate in the desilting basin, recent sediment of the basin should be removed and the top 10cm of the natural surface should be plowed below the removed sediment. The plowing reduces the clogging phenomenon of the sediment.

Keywords: floodwater spreading, infiltration, clogging

Introduction

Uneven rainfall distribution in time and space as well as the low amount of rainfall has forced farmers to overuse ground water to maintain reliable farming practices in the southwestern plain of the Ilam province in Iran. The overuse of ground water has diminished the ground water quality in addition to lowering the ground water level in the plain. This situation has endangered the present agriculture and development, and continuing this policy has no promising future. In this scenario, ground water recharge has an important role in farming security.

One way to increase ground water quality and quantity is to use a floodwater recharging system. Floodwater spreading in an arid region with uneven distribution and lack of adequate rainfall is a possible economic solution. In Iran there is about 30 billion cubic meters of runoff flowing in the intermittent dry waterways, but it is not economically feasible to construct an expensive structure to control them. A floodwater spreading system is not expensive and takes only a few years to be constructed. However, in practice, like many other natural resource projects, this system has some real difficulties. Among the main difficulties is the clogging phenomenon, which occurs through sedimentation by fine particles over the surface of water spreading systems.

This system has the same problem of sedimentation that most of the big and mid size dams are faced with. Sedimentation not only reduces capacity of the system, it also reduces the infiltration rate of the system. The extent of this sedimentation clogging can be monitored through infiltration measurements in the system. In 1997 in the southwest part of the Dehloran plain in Ilam province, a floodwater spreading system was constructed with a total area of about 5000 hectares. Since then its operation has reduced to an area of 3000 hectares. In this part of the plain, 157 deep and semideep water wells were in use providing a total of 73.5 million cubic meters of water per year. Five years after construction of the floodwater spreading system, water table monitoring showed a balanced water table in this part of the plain.

Several studies have been done with respect to the clogging and sedimentation effects on the floodwater spreading systems in Iran in recent years. Rezai and Mossavi (1998) in Esfahan studied the effects of sediment removal from some basin surfaces of the floodwater-spreading basins. In their study, infiltration rates were measured using a double ring method. Results showed the rates were significantly different from the control basins when 15 cm of the natural underlying material was removed in addition to the removal of the recent sediment. This study showed that clogging effects reached significant depths. In general, clogging effects reduced infiltration between 10 to 40 cm depth. The degree to which the infiltration was reduced depended on the particle size distribution of the suspended materials in the floodwater, total sediment load, and the pore geometry of the underlying materials. Basirpour (1995), in the Remsheh floodwater system, measured the infiltration rate and showed that after a certain depth of sediment, increasing the depth of sediment did not have any effect on the infiltration rate of the spreading basins. He noted that the infiltration rate was reduced in the first month of the sedimentation and since then has remained relatively constant. Kamali (1998) measured the infiltration rate of several floodwater spreading systems in the Khorasan province, which was receiving sediment from different lithological materials, and found that rates were reduced by more than 2.5 times compared to the controls. Shariati (1999) measured the infiltration rates of a floodwater spreading system in the Damghan province. The mean values of the rates in three locations of the spreading channels, spreading basins, and the controls were compared. Results showed that infiltration rates were twenty times lower than the rates in the controls. Hossieni (1998) studied the effects of formation of petrogypsic and petrocalcic horizons in desert soils of Damaghan. Measuring the infiltration rates with double ring, he found that soils with these horizons had a rate four times lower than soils without these horizons. Soils with a limiting layer should be studied before any comparison of the rates. The purpose of this study was to monitor the infiltration changes in the runoff direction as well as in the soil profiles.

Characteristics of the Region

The Moosian alluvial plain is located in Dehloran County in the Ilam province which is in the midwest of Iran. It is located between 32º , 27’ and 32º , 35’ North latitude and 47º , 25’ and 47º , 42’ Eastern longitude. This plain is formed from alluvium into a syncline in a northwest to southeast direction. The elevation of the plain is about 104 m above sea level. The flood spreading system is on a piedmont plain formed from coarse gravelly materials derived from Bakhtiyari formation. Sediments in the floodwater are generally derived from the Lahbari of the Aghajari formation (Aj). This member of the Aghajari consists of light brown marls and sandstones, which could be the main reason for the light to medium texture of the sediments in the floodwater. The mean annual temperature is 31.4º C and mean annual relative humidity is 39.9%. Mean annual rainfall is 264.4 mm with a range of 422 to 174 mm. Mean annual evaporation rate is 3553 mm.

Methodology

To measure the infiltration rates, 12 points were selected (Figure 1). These points were selected as follows: 1) three control points in the area north of the system where no floodwater spreading is done, 2) three points in the sedimentation basins, 3) three points in the leveled spreading channels, and finally 4) three points in the spreading basins south of the system. These locations are shown as T0, T1, T2 and T3 in Figure 1.

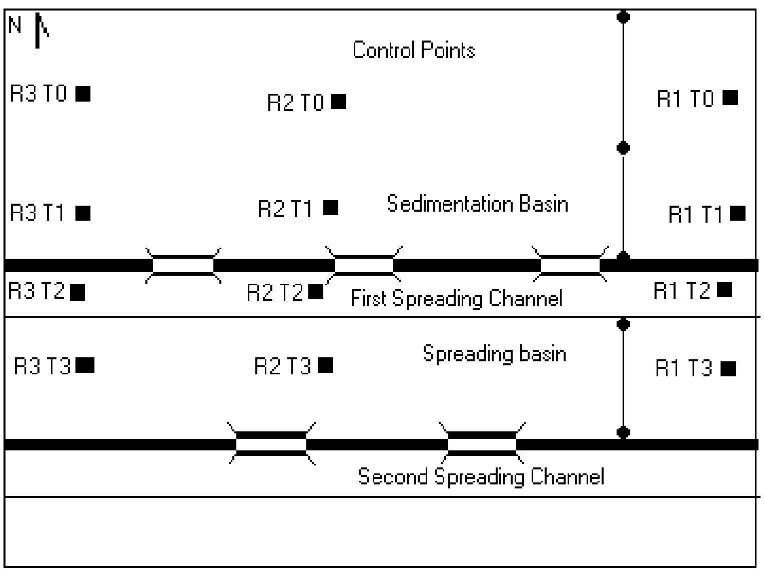

Figure 1. Layout of the test area.

Measurements of infiltration were taken on five different surfaces at each location. The surfaces were designated as Ds (recent sediment surface), D0 (natural surface), D1 (10 cm below the natural surface), D2 (20 cm below the natural surface), and finally D3 (30 cm below the natural surface). For example, T0Ds is location T0 where no flood spreading was done and the measurement was taken at the recent sediment surface. The infiltration measurements were taken in triplicates with a double ring method (Hais et al. 1956). The approximate distance between the measurement points in the east to west direction was 500m. It was difficult to push the rings into the ground surface because of the gravel texture. The bottom 10-cm of the rings were pushed into the surface and covered by fine earth to prevent leakage. Samples were taken (where measurements of infiltration were to be taken) for the top and/or subsoil for determination of particle size distribution. SPSS statistical package and Excel were used to make statistical analyses. The one-way ANOVA, multiple comparison, Duncan, and LSD tests were used for the analysis.

Results and Discussion

The results of particle size distribution analysis are shown in Table 1. Based on the AASHT system, the clay percent in the top and subsoil was less than 12 percent. The average clay percent was 5 percent. This indicates a light texture topsoil and subsoil in the selected location, which is a positive factor for a floodwater spreading system in this region. As shown in Table 1, the sediment load of floodwater does not have a high clay content. In addition, because some of the samples were taken from control points and the basin with no sediment cover, the low clay content in the samples suggests the site is a good selection for recharging the water table. Considering the characteristics of the sediment and the natural surfaces, we expect to have high infiltration rates in the spreading system, so recharging the water table should occur without difficulties. The results of 54 infiltration measurements are shown in Table 2. At each location and surface treatment, three measurements were taken and the average of each three measurements is given in Table 2. The mean infiltration rates are shown in Table 3. The vertical variation of the infiltration rates, indicates that the permeability increases with increasing depth. Means were compared using LSD and the Duncan method. The LSD test indicates that the difference between the Ds and D1, D2, and D3 was not significant. However, the difference between D0 and D1, D2, and D3 was significant at 1 percent level.

Table 1. Particle Size Distribution (AASH System).

	Depth	Clay <.002 mm	Silt .002 - .075 mm	Fine Sand 0.075- 2.000 mm	Coarse Sand 2.000 – 70.000 mm
4	0-15	12	86	2	0
5	0-20	12	86	2	0
6	0-10	12	81	4	3
10	0-15	3	57	14	26
3	0-12	6	51	27	16
2	0-20	7	46	25	22
12	0-15	4	45	16	35
1	0-10	6	44	24	26
8	0-17	10	42	30	18
9	0-10	4	25	20	51
Average		**5**	**35**	**24**	**36**
7	0-5	4	20	18	58
1	10-40	2	18	36	44
3	12-30	0	0	17	83
4	15 -100	0	0	40	60
7	5 - 100	0	0	44	56
9	10 - 100	0	0	40	60
11	15 - 100	0	0	47	53
Location No.	Cm	%			

Table 2. Infiltration rate measurements with double ring method.

	Infiltration Rates (cm/h)				
Treatments	R1	R2	R3	Average	Grand Average
T0D0	6.2	2.1	6.2	4.8	
T0D1	9.1	9.5	8.7	9.1	
T0D2	27.4	71.5	45.8	48.2	31.6
T0D3	32.1	62.1	99.3	64.5	
T1Ds	1.2	1.0	1.1	1.1	
T1D0	44.7	20.0	16.2	27.0	
T1D1	66.7	10.02	84.2	50.3	43.2
T1D2	73.5	15.2	77.1	55.3	
T0D3	178.5	24.8	44.5	82.6	
T2Ds	1.7	2.2	1.2	1.7	
T2D0	4.7	2.9	6.6	4.7	
T2D1	28.2	13.2	74.7	38.7	27.0
T2D2	25.7	11.0	86.5	41.1	
T2D3	46.8	35.5	64.5	48.9	
T3D0	10.8	3.0	6.8	6.9	
T3D1	47.1	38.4	47.0	44.2	
T3D2	48.9	40.2	60.8		
T3D3	55.9	55.2	41.8	50.9	

Table 3. Average basic infiltration rate in the selected treatments with different depths.

Treatment	Average basic Infiltration rate
D_s	1.372
D_0	10.844
D_1	36.382
D_2	48.134
D_3	61.728

Table 4. Distribution of basic infiltration rate in different places.

Treatment	Average basic Infiltration rate
T_0	4.82
T_1	1.08
T_2	1.69
T_3	6.88

The average infiltration rates of control point, T0, floodwater spreading, T1, leveled spreading channels, T2, and spreading basin, T3 are shown in Table 4. The results showed that the difference between T0 and T3 was not significant. T3 differed from T1 and T2 significantly at the 1 and 5 percent level. The results also revealed that removing the recent sediments increases the infiltration rate 2.7 times in leveled spreading channels and 4 times in the control point and spreading basin.

Conclusion

The data obtained in these experiments reveal that sedimentation had the greatest impact on the decrease of surface permeability in the basin and spreading channel in comparison to the control points and had no significant impact on spreading area. With respect to the scraping of sediments during the project five-year period, removal of more than ten centimeters can increase permeability of basins and this will lead to effective ground water recharge.

References

Basirpour, A. (1995) “Evaluation of infiltration variation affect by suspended solids in some artificial recharge basins”, MSC thesis, Agricultural college, industrial university of Isfahan, 164 P.

Haise, H.R., Donnan, J.T. Phelan, L.F. Lawhon, and D.G. Shockley (1956) “The use of cylinder Infiltrometers to Determine the Intake Characteristics of Irrigated Soils”, Publ. ARS 41-7. U.S. Department of Agriculture, Agriculture Research Service and Soil Conservation Service, Washington, D.C. 35 p.

Hossieni, E. (1998), “Study the effect of formation of petrogypsic and petro calcic horizons in desert soil of Damghan”, M.S.C thesis, Shiraz University, 148P.

Kamali, K. (1998). “Effects of receiving sediment from different lithological material on infiltration in several floodwater- spreading systems in Khorasan province”, MS.C thesis, Azad University, Tehran, 195P.

Rezai, v. and Mossavi, S.F. (1998) “ Effects of sediment removal on initial infiltration from some basin surfaces of the floodwater- spreading basins “ proceeding of ninth national conference, Irrigation and drainage committee, paper No.8, 8P.

Shariati, M.H. (1999), “Effect of flood spreading an surface infiltration in damghan province, Research project, Imam Khomenini, education center, 68P.

Soil Physical and Chemical Properties as Indicators of Land Degradation in the Kouhrang (Chelgerd) Region, Chahar-Mahal & Bakhtiary Province, Iran

A. Jalalian[1], M. Azarbin[1], M.K. Eghbal[1], and S.F. Mousavi
[1]Professor, College of Agriculture, Isfahan Univ. of Technology, Isfahan 84156, Iran.

Abstract

Water, soil, forest, and pasture are important elements of the natural ecosystem. Unfortunately, these resources are increasingly subject to degradation in most countries. The objective of this study was to investigate land degradation in the Kouhrang region located in the Zayandehroud watershed, Iran. Water erosion, especially as accelerated by other factors including overgrazing, land use change, and dry farming, is the most important agent of land degradation in the region. The factors involved were investigated on Quaternary sediments and Cretaceous limestone. Three different land uses including pasture, cultivated pasture, and degraded pasture were selected on each formation and three soil samples were taken from 0-10 and 10-20 cm depths. Soil physical properties (bulk density, infiltration rate, saturation moisture content, mean weight diameter, plasticity index, and erodibility factor) as well as chemical properties (OM, total N, and available P) were measured. The results showed a significant difference ($P<0.05$) for the bulk density and plasticity index of degraded sites. Phosphorus values did not show significant differences in the land uses of the two selected formations. The pattern of infiltration rate was similar for the formations. Infiltration in the cultivated areas was characterized by a high onset, but gradual decrease, with time. The soil erodibility factor in the degraded sites of Quaternary sediments showed a significant difference ($P<0.10$) as compared to other land uses. The highest erodibility factor was measured at degraded sites. Land use change caused soil taxonomy to change from Mollisol to Alfisol on degraded sites. On the basis of the prepared soil erosion map, 3% of the land suffered from high erosion and degradation, 40% from high erosion, 39.5% from moderate erosion, and 17.5% had only low erosion and degradation. The results indicated that this area was susceptible to erosion and land degradation and that conservation measures had to be implemented to prevent further losses.

Introduction

Population increase over the past few decades and the corresponding demand for food production have turned attention to scientific and improved management for the sustainable development of agriculture and natural resources (Hajabbasi et al., 2002). As agricultural activities have been going on throughout ages without proper knowledge of the soil environment, much disturbance has been caused in the natural environment leading to the incapacitation of soil in performing its roles. Thus, land degradation is one of the most important and most contentious issues of our modern world (Nael, 2001).

The first world map of degradation intensity called “The World Map of the Status of Human-induced Soil Degradation” was produced in 1990 by the International Soil Reference and Information Center (ISRIC) in collaboration with UNEP (Norouzi, 1999). In the evaluations on this map, five types of human interventions leading to soil degradation were identified, which include overgrazing of vegetation by livestock, improper agricultural practices, overexploitation of the natural resources, removal of vegetation cover, and industrial activities (Oldeman, 1994). Akinola (1981) carried out a study for four years in Nigeria and showed that soil degradation and tillage had reduced the organic content of soil by 19 to 33%. Change of rangeland use in most cases had led to the destruction of soil structure and reduction of the organic content, and subsequently, to reduced porosity and increased soil bulk density (Ahmadi Ilkhchi, 2001). Furthermore, the destruction of soil particles due to land use change from range to farmland further reduces the organic content and, thus, soil plastic limit retains little moisture whereas for the liquid limit it will retain a lot of moisture. Therefore, the presence of higher clay particles and lower organic content in degraded and agricultural lands entails higher values of plasticity index of the soil (Hajabbasi, 2002).

Aguilar et al. (1988) studied the effect of continuous cultivation of rangeland over a period of 44 years and found that reduced organic carbon, nitrogen, and phosphorus content in soil was due primarily to soil erosion in the cultivated sites. With land use change, soil becomes more sensitive to erosion, which is associated with a slight increase in soil sand content and a reduction in its clay content. Under scant vegetation cover, the clay part of the soil moves further down the soil profile due to selective erosion processes and causes important changes in soil texture in the long run (Loveland, 2003).

The objective of this study is to investigate the changes in soil quality parameters due to land use change and erosion, to determine the degree of soil degradation due to water erosion processes, and to develop practical solutions to reduce soil degradation in the region.

Methodology

The study area, Chelgerd, covers an area of approximately 150 km^2 between 50°-5 and 50°-15 east longitudes and 32° and 32°-30° north latitudes. It is a subbasin located in the Kouhrang region in the Chahar-Mahal and Bakhtiary Provinces. The greatest degradation observed in the region is caused by water erosion in which a multitude of factors are involved. Overgrazing by livestock and change of land use from rangeland to agricultural development and to low yield dry farms are two such factors (Management, 1986). Using the methodology recommended by the US Bureau of Land Management (BLM), an erosion map of the region was produced in order to determine the degree and intensity of land degradation. Two different formations, one sediment formation (Quaternary) taken from a site near the Gol Koushkak village, and the other of limestone material (Cretaceous) taken from a site near the Dehno village, were selected to study the impacts of land use change on degradation. On each of these formations, three different regions, each characterized by one land use, were identified: almost intact rangeland, rangeland under dry farming, and degraded rangeland. Soil samples were taken in autumn 2002 and three samples (three replications) were taken from 0-10 and 10-20 cm depths for each land use.

For soil taxonomy up to the sub-group level, profiles were dug out in the region and USDA methodology was used to classify the soils (Soil, 1999). Physical tests including bulk density, permeability (using the double-ring method), mean weight diameter, plasticity index (Casagrand method), erodability factor (Vischmeyer nomograph) as well as chemical tests including soil organic content (wet ashing method), total nitrogen (Kjeldal method), and phosphorus (Olson method) were performed on soil samples.

The analysis of the data was performed in a completly randomized design and means were compared using the LSD test with SAS software (Soil, 1999). Diagrams and graphs were prepared in EXCEL and maps were plotted using Arcview software in a GIS environment.

Results and Discussion

The map of soil degradation intensity (Figure 1) indicates that about 40% of the total area of the region suffers from high erosion, 39.5% from medium erosion, 3% from very high erosion, and 17.7% is in a low erosion state.

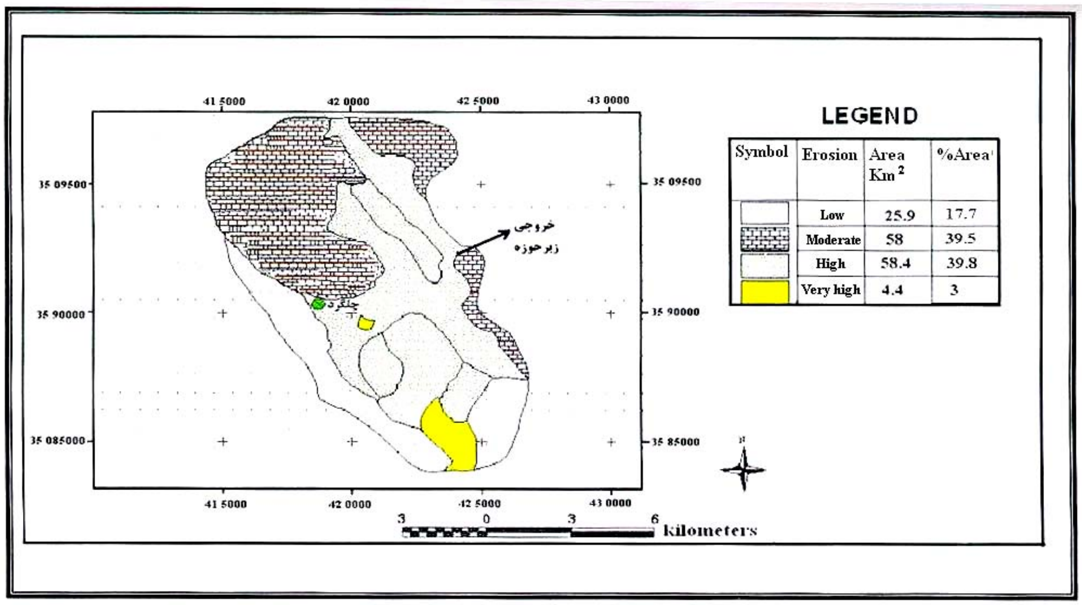

Figure 1. Map of Soil Erosion Intensity in Chelgerd Region Using BLM.

Investigations showed that most parts in the region characterized by high erosion and medium/high degradation were those in which man had serious interventions. Examples of these interventions include tillage and grooving along and parallel to steep slopes, improper dry farming practices, removal of bushes, and overgrazing by livestock. Furthermore, it was found that areas with high degradation were those where besides the impact of human interventions, low soil depth, formation materials, and the sensitivity of formations played a great role in land degradation.

Land use change from range to dry farmland has greatly influenced the sensitivity of topsoil to erosion and degradation. The change through time has caused drastic changes in topsoil properties and inflicted irreversible damages to soil quality. Tables 1 and 2 present the results from variance analysis of land degradation impacts on the measured parameters in the soils under study (0-10 cm depth) for Quaternary sediment formations and limestone Cretaceous formations, respectively. As shown in these tables, the degraded treatment shows a significant difference from the other two treatments.

Table 1. Results from analysis of variance of the effects of land degradation on measured parameters in the soils under study (0-10 cm dept) in Quaternary sediment formations.

Measured parameter	**Source Variation**	**Sum of squares**	**Degree of freedom**	**Mean squares**	**(Fischer statistic) F**
Erodibility Index	Treatment	0.03	2	0.0152	3.24
	Error	0.028	6	0.0047	
Plasticity Index	Treatment	94.719	2	47.359	8.66*
	Error	32.806	6	5.467	
Organic content	Treatment	9.146	2	4.573	10.11**
	Error	2.714	6	0.4526	
avalable phosphorus	Treatment	240.88	2	120.440	73
	Error	992	6	165.333	
Total nitrogen	Treatment	0.035	2	0.0177	4.6*
	Error	0.023	6	0.0038	
Saturation moisture percentage	Treatment	987.88	2	493.943	6.28*
	Error	479.29	6	78.715	
Mean weight Diameter of soil peds	Treatment	0.684	2	0.3422	17.36*
	Error	0.118	6	0.0197	
bulk density	Treatment	0.062	2	0.0313	8.71*
	Error	0.021	6	0.0036	

* Significant at a probability of 5%
** Significant at a probability of 1%

The results from variance analysis of the data from Quaternary sediment formations (Table 1) indicate a significant difference at a probability of 10% for the erodibility index between the degraded range and intact range at surface horizons.

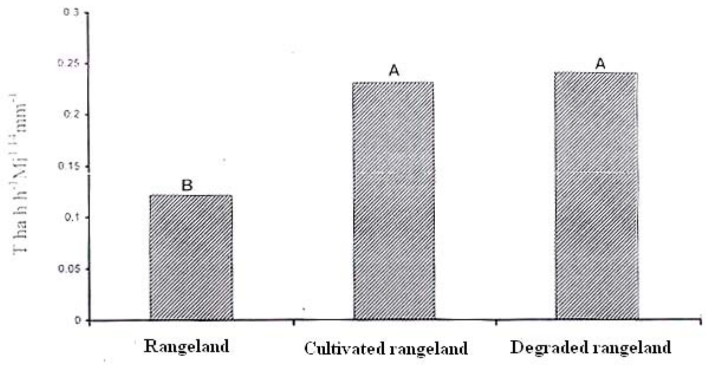

Figure 2. Fluctuations in values of soil erodibility in different landuses and on Quaternary sediment formations (0-10 cm dept).

According to Figure 2, the highest value for the erodibility index (0.24) was recorded for degraded rangeland and the lowest (0.12 t ha h h^{-1} $Mj^{1.14}$ mm^{-1}) for rangeland. No significant differences were observed at this probability level between the degraded rangeland use and the cultivated rangeland use.

No significant differences were observed, between different land uses on Cretaceous lime formations at a probability level of 10%. However, comparison of the means among different land uses indicated higher values of erodibility index for both cultivated and degraded rangelands as compared to rangeland under dry farming and almost intact rangeland (Table 2). The values for this index for degraded rangeland, rangeland under dry farming, and almost intact rangeland were 0.26, 0.22, and 0.12 t ha h h^{-1} $Mj^{1.14}$ mm^{-1} (Figure 3).

Table 2. Results from analysis of variance the effects of land degradation on measured parameters in the soils under study (0-10 cm dept) in Cretaceous lime formations.

Measured parameter	**Source Variation**	**Sum of squares**	**Degree of freedom**	**Mean squares**	**(Fischer statistic) F**
Erodibility Index	Treatment	0.03	2	0.0147	]1.47
	Error	0.06	6	0.010	
Plasticity Index	Treatment	47.75	2	23.875	5.44*
	Error	26.32	6	4.387	
Organic content	Treatment	2.08	2	1.0408	4.16*
	Error	1.5	6	0.25	
avalable phosphorus	Treatment	176.22	2	88.11	25
	Error	2086	6	347.666	
Total nitrogen	Treatment	0.022	2	0.0114	11.18*
	Error	0.006	6	0.001	

Saturation moisture percentage	Treatment	119.88	2	59.94	6.93*
	Error	51.91	6	8.65	
Mean weight Diameter of soil peds	Treatment	0.115	2	0.057	6067*
	Error	0.051	6	0.0086	
bulk density	Treatment	0.106	2	0.053	30.3*
	Error	0.01	6	0.0017	

* Significant at a probability of 5%

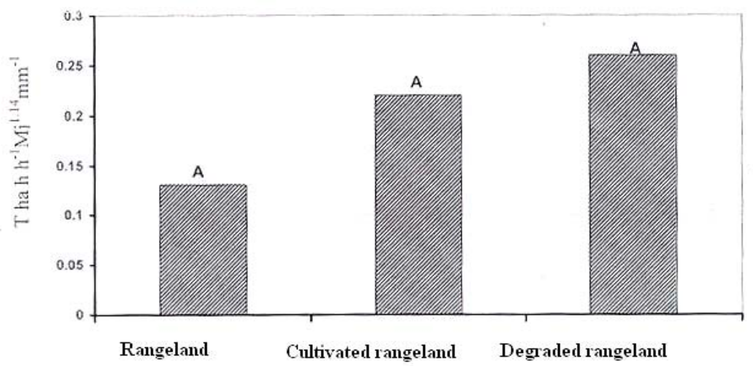

Figure 3. Fluctuations in values of soil erodibility in different landuses and on Cretaceous lime formations (0-10 cm dept).

The results from plasticity index measurements for different land uses revealed the effect of land use change and land degradation on this index. In Quaternary sediment formations, the highest value of this index was recorded for degraded rangeland and the lowest for the almost intact rangeland. The plasticity index values for degraded rangeland, rangeland under dry farming, and the almost intact rangeland were 23.6%, 18.4%, and 15.8%, respectively. The results from variance analysis of data (Table 1) show the changes in plasticity index values to be significant (Figure 4).

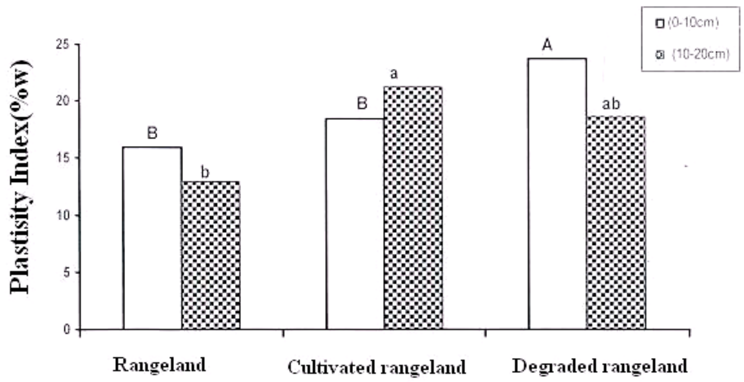

Figure 4. Fluctuations in values of soil plasticity index in different landuses and on Quaternary sediment formations.

The same situation was observed in the case of lime formations in the sense that the degraded rangeland had the highest value for plasticity index of 22.6%, rangeland under dry farming had a value of 19.1%, and degraded rangeland had a value of 17%. The results from the variance analysis of the data (Table 2) showed a significant effect on plasticity index at a depth of 0-10 cm (Figure 5). Generally speaking, the plasticity index was greater in soils with lower organic content; the clay content, of course, has a greater contribution to this situation than the organic content. The destruction of soil particles in degraded land also accounts for the high plasticity index.

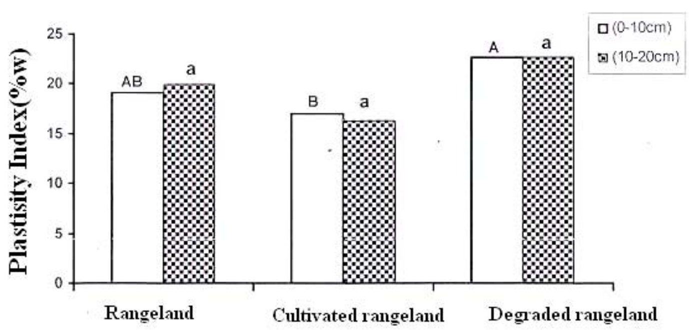

Figure 5. Fluctuations in values of soil plasticity index in different landuses and on Cretaceous lime formations.

As seen in Figures 6 and 7, permeability on both formations for the cultivated rangeland has a higher initial value than in other land uses but in the continuation of the test, the velocity reduces to a great extent to reach below the curve for the almost intact rangeland. The degraded rangeland use has the lowest permeability with a completely flat curve. The main reason for this is the unfavorable soil physical structure. The low rate of final permeability in both cultivated and degraded land causes increased runoff generation and erosion.

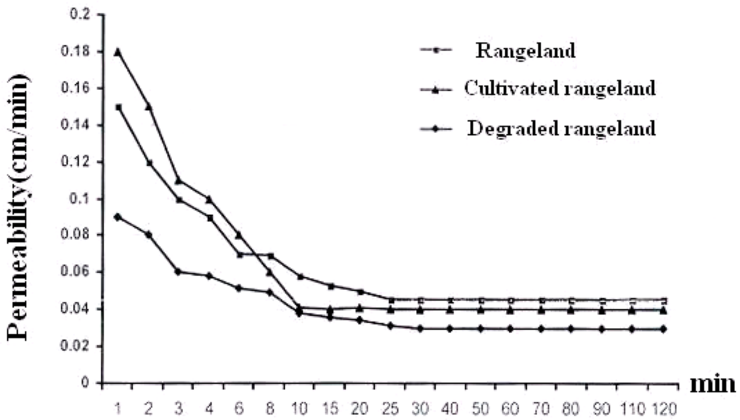

Figure 6. Fluctuations in values of soil permeability in different landuses and on Quaternary sediment formations.

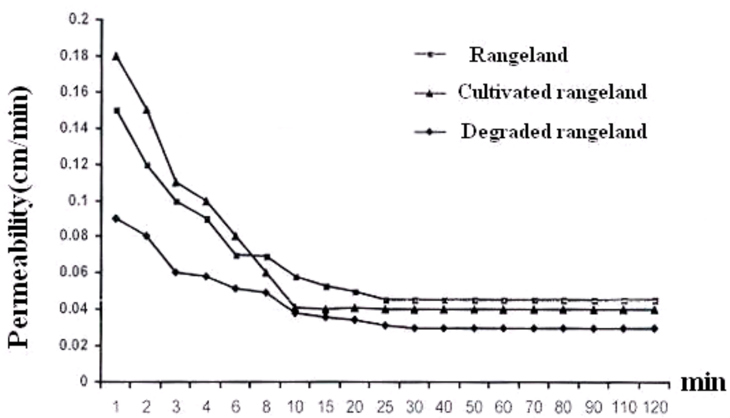

Figure 7. Fluctuations in values of soil permeability in different land uses and on Cretaceous lime formations.

The values obtained from the mean weight diameter (MWD) for different land uses in both formations at depths of 0-10 cm showed significant differences. In the Quaternary sediment formation, the maximum MWD of soil particles for the almost intact range land use was 0.92 mm and its minimum in the degraded land use was 0.24 mm. In the case of cultivated rangeland use, a value of 0.63 was obtained for this parameter. The differences among all three land uses were significant at a probability level of 5% (Figure 8).

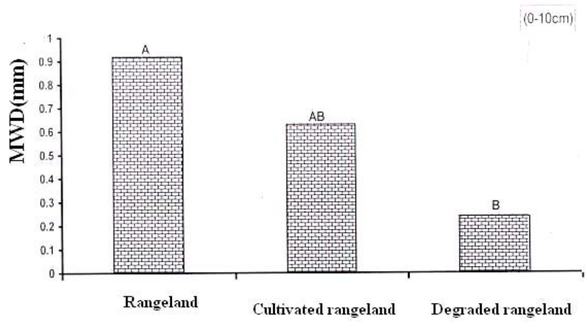

Figure 8. Fluctuations in mean weight diameter of soil particles (mm) in different land uses and on Quaternary sediment formations.

The same differences were observed in the lime formation. The maximum MWD of soil particles in the rangeland use was 0.73 mm and its minimum in the degraded land use was 0.45 mm while in cultivated rangeland use, it was 0.58 mm (Figure 9).

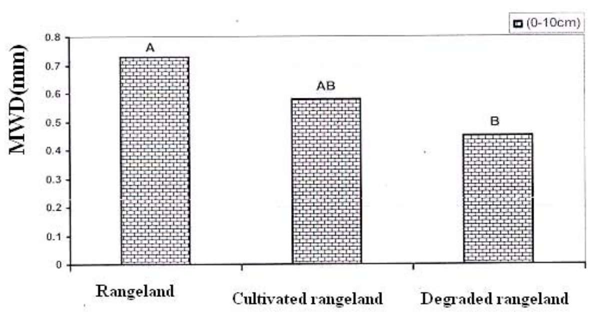

Figure 9. Fluctuations in mean weight diameter of soil particles (mm) in different land uses and on Cretaceous lime formations.

Changes in soil chemical properties, particularly in its organic content as the most important chemical property, play a great role in soil sensitivity to degradation. This is because the organic content influences most of the physio-chemical properties of soil. The values obtained for organic content measurements in different land uses showed significant differences among them. On Quaternary sediment formations, the greatest organic content was observed to be 3.8% at depths of 0-10 cm in intact rangeland, in the cultivated treatment it was 1.94%, and in degraded treatment, it was 1.5% (Figure 10).

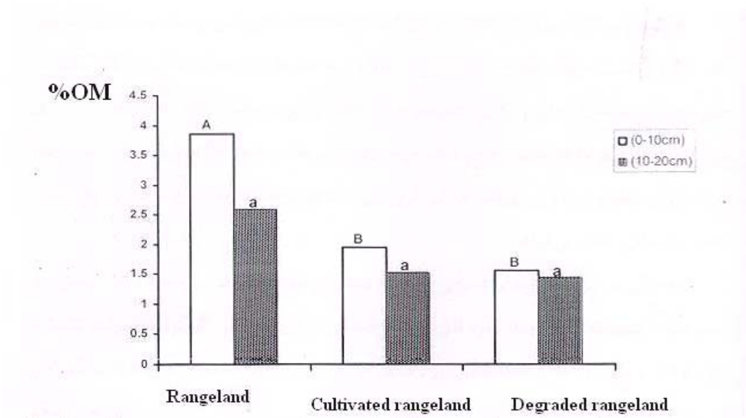

Figure 10. Fluctuations in soil organic content in different land uses and on Quaternary sediment formations.

The results from the variance analysis of the data (Table 1) showed a significant difference among different treatments at a probability level of 1%. On lime formations, the highest organic content was found to be 2.72% at depths of 0-10 cm in the rangeland use, while in the cultivated range land it was 2.13%, and in the degraded rangeland it was 1.54% (Figure 11).

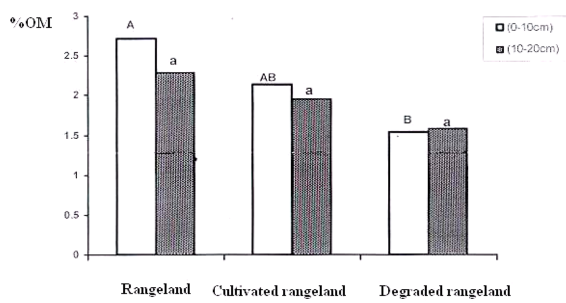

Figure 11. Fluctuations in soil organic content in different land uses and on Cretaceous lime formations.

As for other chemical properties, the land use change from range to degraded land has led to an increase of about 25% in phosphorus content and a reduction of 50 - 60% in total nitrogen in both Quaternary and Cretaceous formations.

Change of land use from range to degraded land has also had effects on soil taxonomy. As a result of this, the soil order has changed from Mollisol to Alfisol. Epipedon mollic, which is characteristic of Mollisols, deteriorates and disappears through time as a result of land use change. Mollisols are soils that receive the greatest effect on their classification due to soil erosion. The main reason for this may be the reduced organic content and a reduced mollic horizon due to erosion and degradation.

Besides land use change, overgrazing by livestock and removal of bushes have had great influences on increased land degradation. The excessive number of grazing livestock is one of these factors. From another perspective, the time the livestock step on the rangeland is also important in that the soil lacks adequate vegetation cover and has a high moisture content at that time. This state of affairs leads to compaction of the topsoil and reduction of soil permeability, which results in runoff generation and erosion.

References

Ahmadi Ilkhchi, A., 2001. (in Persian). The Effect of Range Degradation on Soil Cultivability Index and Runoff Generation in the Central Zagross Region. MSc. Thesis, College of Agriculture, Isfahan University of Technology, Iran.

Hajabbasi, M. A., Jalalian, A., Khajeddin, J. and Karimzadeh, H., 2002. (in Persian) "A Case Study of the Effect of Change of Rangeland to Farm Land on Certain Soil Physical and Productivity Properties and Cultivability Index in Boroujen, Iran". Journal of Agricultural and Natural Resources Science & Technology, Vol. VI, No.1, pp.

Management & Planning Organization, 1986 (in Persian), The Master Plan for the Development of Chahar-Mahal & Bakhtiary Province, Vols. I & II.

Nael, M., 2001. (in Persian), Investigation of Land Degradation Using Soil Quality Properties and their Spatial Changes in Range and Forest Ecosystems in Central Iran; MSc. Thesis, College of Agriculture, Isfahan University of Technology.

Norouzi, G., 1999. (in Persian), "Erosion or Regression: The Need for a New Approach". Journal of Forest and Range, No. 42, pp. 36-43.

Aguilar R., Kelly, E.F., and Heil, R.D, 1988. "Effects of Cultivation of Soils in Northern Great Plains Rangeland". Soil Sci. Soc. Am. J., Vol. 52, pp. 1081-1085.

Akinola, A., 1981. "Effects of Soil Tillage and Management Practice on the Physical and Chemical Properties of Soil and Maize Yield in a Rain Forest Zone of Western Nigeria". Agronomy J., Vol. 73, No. 2, pp. 247-251.

Loveland, P. and Webb, J., 2003 "Is There a Critical Level of Organic Matter in the Agricultural Soils of Temperate Regions: a Review". Soil & Tillage Research, Vol. 70, pp. 1-18.

Oldeman, L.R., 1994. "The Global Extent of Soil Degradation". Soil Resilience and Sustainable Landuse, CAB International, pp. 99-118.

Soil Survey Staff, 1999. "Key to Soil Taxonomy". 8th Edition, SCS, USDA, Pocahonates Press Inc, Blacksburg, Virginia, USA.

Depasturation Effects on Soil Physical and Chemical Properties in Isfahan and CharMahal Bakhtiari Region

Hajabbasi, Mohammad
Soil Science Department, Isfahan University of Technology, Isfahan 84156 Iran
E-mail: hajabbas@cc.iut.ac.ir

Abstract

Land use conversion of pasture to cropland is called depasturation. Studying soil properties during the processes of depasturation could be helpful to solve some soil and water conservation problems. A study was established in 2002 to evaluate the effects of depasturation upon soil physical and chemical properties of various regions in Isfahan and CharMahal Bakhtiari provinces. Eight regions were selected to investigate soil characteristics, including sites of virgin pasture (P); completely destroyed pasture (D); and pastures which were cultivated and cropped (C). Soil samples were taken from depths (0-10). Soil organic matter (OM), bulk density (BD), pH, EC, available cations (AC) and available anions (AA), aggregate uniformity coefficient (AUC), plasticity index (PI), and tilth index (TI) were all measured. Depasturation and tillage practices caused a 20 percent increase in bulk density of the forest soil when cultivated compared to the undisturbed pasture soil. Due to the tillage practices and exposure of pasture soil to the atmosphere a 30 percent decrease in OM, and a 10-15 percent decrease in AC and AA were observed. Total nitrogen of the pasture soil at surface (0-10 cm) was almost twice as the cultivated and cropped soil. Plasticity index of the pasture soil was 10-30 percent higher than that of the disturbed soil. The tilth index in pasture soil was 25 and 15 percent higher than depasturated and cultivated pasture respectively. Depasturation and disturbing the pasture soil caused eroding of the thin top soil, loss of productivity and thus, could perhaps leave the soil with no use for several years.

Introduction

The studying and understanding of land use systems in different regions is essential for development and implementation of appropriate crop production management, policies and procedures. In Chaharmahal-Bakhtiari region (central part of Iran), crops are mostly grown under rain-fed situations and the main limitation for crop growth is water. Of particular concern in these semi-dry areas cropping are practiced on soils with weak structural stability which minimize rainfall infiltration and thus reduces plant access to stored soil moisture. Such changes have led to examination of alternate farming practices which include lay pastures, crop rotations, and reduced tillage/controlled traffic. As soil water holding capacity and depth is generally low, when precipitation becomes scarce, available soil water diminishes rapidly and reaches a depletion level that limits and in some cases stops crop growth. Suitable soil tillage practices, therefore can affect water availability to plants, essentially via soil water capture and infiltration (Dao, 1998). Soil tillage and mulching can change the capacity of soil surface to intercept rainfall by affecting the hydraulic conductivity of the topsoil, soil roughness, and soil surface porosity. Conclusive evidence of declining soil physical, chemical, and biological fertility under conventional cropping systems is now available (Choudhary et al. 1997). Lack of sufficient information regarding the application of different tillage systems leads dominating use of conventional practice regardless of its adverse effects on soil physical, chemical, and biological properties on the marginal lands of this region. Thus, studying any alterations in the management practices which may enhance soil water and other properties, help proper decision regarding the use of different tillage practices in the region. In order to verify the effects of different methods of land use managements on soil physical properties, an experiment was established in 2002 to compare the influence of changing land use suitability (pasture and converting pasture to crop land) on some soil physical properties.

Methods and Materials

Soil samples were collected from the depths 0-15 and 15-30 cm of eight different areas with pasture in conjunction with disturbed pasture, but similar topography and parent material. Soil texture, bulk density, and organic matter were determined using the methods of hydrometer (Gee and Bauder, 1992), constant core (Blake, 1992), and digestion (Walkly and Black, 1934), respectively. Hydraulic properties like saturated hydraulic conductivity, infiltration, and moisture release curve was obtained on these soils using the methods suggested by Klute (1992). Wet sieving method of Kemper and Rosenau (1992) with a set of sieves of 2, 1, 0.5, and 0.25 mm was used to determine mean weight diameter. Mean weight diameter (MWD) was calculated by the relationship: $MWD= \sum (X_iW_i)$. Where, X (in mm) is average diameter of the pores of two consecutive sieves, and W is the weight ratio of aggregates remained on the i^{th} sieve. Analysis of variance of the results was done using the SAS (SAS, 1995) program, and the means of the results were compared using the Duncan new multiple range test.

Results and Discussion

Due to the limitations for presenting data, the results of soil texture, bulk density, mean weight diameter and soil moisture release curve will be reported. Analysis of variance (ANOVA) at 0.05 level of probability showed some significantly different effects between the land use systems. Effects of different tillage practices on soil characteristics are discussed separately in the next sections. No changes were obtained in soil texture between the disturbed and undisturbed treatments (Table 1). This might be due to the lack of suitable conditions like climate and especially the time for this component to be changed.

There were slight changes between the treatments for bulk density (Table 1). Documentation of management practices on soil bulk density is obscured by natural variations in soil type (Franzluebbers et al., 1995). Voorhees and Lindstrom (1984) hypothesized that not disturbing the soil like in the no-tillage system may result in higher bulk densities due to incomplete amelioration of compacted soil. Bauer and Black (1981) reported that cultivating could loosen the topsoil for a specific period of time, then due to heavy traffic the soil will be compacted again. According to Karlen (1990) soil compaction is considered to be the most serious problem limiting the adoption of undisturbed soils and no-till system. Hajabbasi and Hemmat (2000) concluded that although adopting the no-till system in many cases improves SOM and consequently aggregation, but due to an initially weak structure and low organic matter, a complete or at least partial amelioration of soil in winter is necessary.

A direct correlation between the stability and size of the aggregates to soil organic matter has been reported by several authors. In this study no correlation was seen between the SOM (data not shown) and MWD (Figure 1). This could be due to the initially low SOM and structurally crushed aggregates (more than 75% of aggregates were < 0.25 mm) in the region. Over all of the treatments, mean weight diameter was numerically (not significantly) higher comparing the disturbed to the undisturbed land use system. This might be because of the higher amount of residues due to cultivation, adding fertilizer, and growing crops on the land. The undisturbed pasture land in the region is usually covered by a small amount of species, less than 30%. Therefore, unlike other climatic regions, one way to increase the amount of organic matter and stabilize soil structural strength might be growing some crop, but using no or minimum tillage systems. In this way as biological activity of soil increases, at the same time soil crushing and erosion would be reduced. Soil moisture characteristic curves of the land use systems are shown in Figure 2 (the average of all eight points of study). The curve for the undisturbed treatment looks smoother compared to the disturbed land which is sharper. This indicates a better uniformity between the porous spaces of the soil for undisturbed land use treatment.

Acknowledgment

This research project has been supported by the Grant given by IUT Soil Science Center of Excellences. A special thank to the Soil Science Department of Isfahan University of Technology for the laboratory works.

References

Bauer, A., A.L. Black. 1981. Soil carbon, nitrogen, and bulk density comparison in two cropland tillage systems after 25 years in virgin grassland. *Soil Sci. Soc. Am. J.* 45: 1160-1170.

Blake, G.R. 1992. Bulk density, pp 363-375, in A. Klute, ed., *Methods of soil analysis. Part1*. American Society of Agronomy, Madison Wisconsin, USA.

Choudhary, M.A., A.R. Lal and W.A. Dick, 1997. Long-term tillage effects on runoff and erosion under simulated rainfall for a central Ohio soil. *Soil Tillage Res.* 42:175-184.

Dao, T.H. 1998. Tillage and Crop Residue Effects on Carbon Dioxide Evolution and Carbon Storage in a Paleustoll. *Soil Sci. Soc. Am. J.* 62:250–256.

Franzluebbers, A.J., F.M. Hons, and D.A. Zuberer. 1995. Tillage-induced seasonal changes on soil physical properties affecting soil CO2 evolution under intense cropping. *Soil Tillage Res.* 34:41–60.

Gee, G.W. and J.W. Bauder. 1992. Particle size analysis, pp. 383-411, in A. Klute ed., *Methods of soil analysis. Part 1*. American Society of Agronomy, Madison Wisconsin.
Hajabbasi, M.A. and A. Hemmat. 2000. Tillage impacts on aggregate stability and crop productivity in a clay-loam soil in central Iran. *Soil Till. Res*. 53(3-4): 207-214.
Karlen, D.L. 1990. Conservation tillage research needs. *J. Soil Water Conserv*. 45: 365-369.
Kemper, W.D. and R.C. Rosenau. 1992. Aggregate stability and size distribution, pp. 425-440, in A. Klute, ed., *Methods of soil analysis. Part 1*. American Society of Agronomy, Madison Wisconsin, USA.
Klute, A., 1992. *Methods of soil analysis. Part 1,* ed., Physical and Mineralogical Methods American Society of Agronomy, Madison Wisconsin.
SAS Institute. 1995. SAS/STAT guide for personal computers. Version 6. SAS Inst., Cary, NY, USA.
Voorhees, W.B., and M.J. Lindstrom. 1984. Long-term effects of tillage method on soil tilth independent of wheel traffic compaction. *Soil Sci. Soc. Am. J*. 48:152–156.
Walkly, A. and I.A. Black. 1934. An examination of digestion method for determining soil organic matter and a proposed modification of the chromic acid titration. *Soil Sci*. 37: 29-38.

Table 1. Soil texture and bulk density for the study areas as land use management differed.

Site #	Treatment	Texture	Bulk Density
1	Undisturbed	Clay	1.255
	Disturbed	Clay	1.132
2	Undisturbed	Siltyclay	1.055
	Disturbed	Siltyclay	1.212
3	Undisturbed	Clayloam	1.187
	Disturbed	Clayloam	1.192
4	Undisturbed	Clayloam	1.293
	Disturbed	Clayloam	1.254
5	Undisturbed	Clayloam	1.112
	Disturbed	Clayloam	1.085
6	Undisturbed	Clayloam	1.104
	Disturbed	Clayloam	1.204
7	Undisturbed	Clay	1.149
	Disturbed	Clay	1.063
8	Undisturbed	Clayloam	1.105
	Disturbed	Clayloam	1.184

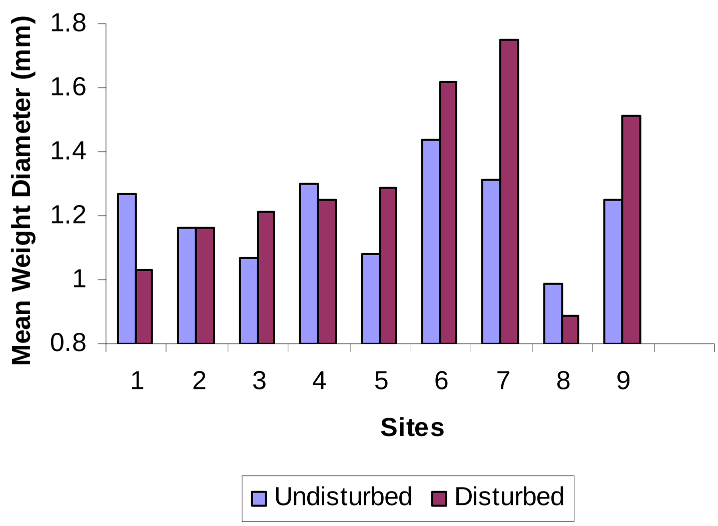

Figure 1. Mean weight diameter of soils for the study areas as a function of land use management system.

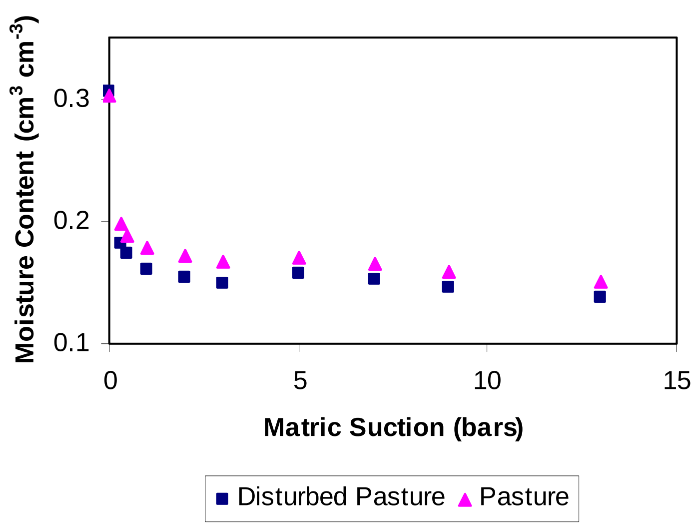

Figure 2. Moisture content vs. matric suction as a function of different land use management systems (points are average of eight sites).

APPENDIX

Author Index 708

2005 SWAT Conference Agenda 710

Conference Group Picture 717

Author Index

Abbaspour, Karim C. 40, 169, 577
Abramenko, Kaspars 390
Afyuni, Majid 577
Ahmad, K. 522
Alexander, Susan S. 359
Allen, Peter M. 107, 159
Anderson, Christopher J. 599
Arnold, Jeffrey G. 1, 107, 132, 159, 189, 349, 414, 444, 568, 637
Atwood, J.D. 568
Ayyoubzadeh, S.A. 542
Azarbin, M. 697
Baffaut, Claire 301, 482
Banerjee, Poulomi 488
Barlund, Ilona 310
Bauwens, Willy 88, 339
Beaudin, I. 657
Benson, Verel W. 301
Boroomand, Saeed 518, 684, 691
Breuer, Lutz 200, 330, 472, 498
Bruggeman, Adriana 50
Busche, H. 434
Carucci, A. 379
Cau, P. 153, 369, 379
Charkhabi, Hossain 691
Chen, Pei-Yu 159
Cheng, Hongguang 423
Chung, IL Moon 271
Cerdan, O. 482
Contu, I. 379
Cools, Jan 339
Coops, N. 142
Couturier, A. 482
De Luca, Filomena 251
de Oliveira, Maria Quiteria C. 491
de Oliveira, Ramon C. 491
Deelstra, Johannes 390
Diekkruger, B. 434
Dilks, Caroline F. 398
Di'Luzio, Mauro 189, 414, 568
Dunn, Sarah M. 398
Eghbal, M.K. 697
Engel, Bernard A. 616, 627
Estes, Tammara L. 359
Farrand, Todd D. 301
Feng, Hong-Li 291, 444
Ferrier, Robert C. 398
Feyen, Jan 221, 532
Flanagan, Dennis C. 627
Frede, Hans-Georg 200, 330, 472, 498
Gassman, Philip W. 1, 291, 444, 522, 599
Ghafouri, M. 142
Ghebremichael, L.T. 637
Gholami, Shaaban-Ali 408, 542
Girolamo, Anna Maria 251
Gosain, Ashvin K. 231, 408
Green, Colleen H. 1, 414
Grizzetti, Bruna 30
Grunwald, S. 179
Habeck, Anja 19, 114
Hao, Fanghua 423
Hatterman, Fred F. 19, 114, 509
Hernandez, M. 482
Heuvelmans, Griet 221
Hiepe, Claudia 434
Hollis, J. 30, 657
Holman, I. 666
Huisman, Johan A. 200, 330, 472, 498
Jacobs, Jennifer 98
Jalalian, A. 697
Jansons, Viesturs 390
Jetten, V. 482
Jha, Manoj 291, 444, 522, 599
Jirayoot, Kittipong 320
Kannan, N. 30, 70, 568, 657
Kanwar, R.S. 522
Kashkuli, H.A. 518, 684
Keller, V. 657
Kellogg, R.L. 568
Khaledian, Mohamad Reza 684
Killingtveit, A. 61
Kim, Nam Won 271
Kiniry, Jim 132
Kirkkala, Teija 310
Kling, Cathy L. 291, 444
Kondratyev, S. 454
Krysanova, Valentina 19, 114, 509

Kurkalova, Lyubov A. 291, 444
Laszlo, Peter 464
Le Bissonnais, Y. 482
Lee, Do Hun 271
Licciardello, Feliciana 261
Lo Porto, Antonio 251
Lorrai, E. 153, 369
Lu, Qimiao 80
MacDonald, Doug 132
Maletta, Roberta 472
McKeown, Ruth A. 132, 189
Medeiros, Yvonilde D P 491
Meixner, T. 179
Mendicino, Giuseppe 472
Mousavi, Sayed-Farhad 577, 697
Mtalo, F.W. 61
Muys, Bart 221
Ndomba, P.M. 61
Nearing, M.A. 482
Nichols, M.H. 482
Nunes, J.P. 482
Oliveira, Maria Quiteria 491
Pappagallo, Giuseppe 251
Pasztor, Laszlo 464
Pirani, Ayoub 691
Pohlert, Thorsten 200, 498
Possley, Theresa 80
Post, Joachim 19, 114, 509
Potter, S.R. 568
Prepas, Ellie 132
Putz, Gordan 132, 189
Qi, Ye 423
Rahimi, A. 518
Ranjbarfordoi, A. 549
Ray, Debajit Basu 231
Rao, Sandhya 231
Reichert, Peter 169
Ren, Xiyan 423
Renschler, C.S. 482
Reungsang, Pipat 522
Reyes, Manuel R. 1
Richardson, Clarence xiii
Rouhani, Hamed 532
Rudra, Ramesh 123
Saadati, Hossein 542
Sadatinejad, Javad 549
Saleh, Ali 522, 559
Santhi, C. 568
Sayyad, Gholamabbas 577
Schmidt, Gerd 241
Schulin, Rainer 577
Schuol, Jurgen 40
Selvalingam, S. 142
Secchi, Silvia 291, 444, 599
Sen, Sucharita 588
Shoemaker, Christine A. 210
Singh, Amanjot 123
Souchere, V. 482
Srinivasan, R. 98, 179, 261, 359
Suckow, Felicitas 509
Szabo, Jozsef 464
Takle, Gene 599
Tolson, Bryan 210
Tomer, M.D. 414
Tripathi, M.P. 279
Trung, Le Duc 320
Vagstad, Nils 390
Van Liew, Michael W. 349, 637
Vandenberghe, V. 88
van der Meijden, Geerte 50
van Griensven, Ann 88, 179
van Oost, K. 482
Vanrolleghem, Peter A. 88
Vassiljev, A. 609
Vazquez-Amabile, Gabriel G. 616, 627
Veith, T.L. 637
Volk, Martin 159, 241
Watson, Brett M. 142
Wechsung, Frank 19
Whelan, M.J. 70, 657
White, S.M. 30, 70, 657, 666
Whitehead, J. 666
Whitson, Ivan 132
Willems, Patrick 532
Winchell, Michael F. 359
Yang, Jing 169
Yang, Shengtian 423
Yang, Wanhong 123
Yitayew, Eyilachew 674
Young, A.R. 657
Zimbone, Santo Marcello 261

Agenda

3rd International SWAT Workshops & Conference
Zürich 2005

Beginners & Advanced Workshops: July 11-12

July 11

9:00	18:00	First day of the workshop at the AKADEMIE Building, EMPA-EAWAG

July 12

9:00	18:00	Second day of the workshop at the AKADEMIE building, EMPA-EAWAG
18:30	**20:00**	**REGISTRATION AND ICE BREAKING COCKTAIL PARTY AT THE AKADEMIE**

	Session Description
A	Model application
B	Directions in watershed modeling
C	SWAT development & accessories
D	Calibration, sensitivity & uncertainty
E	Comparison of SWAT & other models
F	Management scenarios & application to decision framework

First Day of Conference: July 13

8:00	**9:00**	**REGISTRATION AT THE AKADEMIE**	
9:00	9:10	Karim Abbaspour, Welcome	
9:10	9:20	Peter Reichert, Introduction to EAWAG	
9:20	9:30	Franz Stössel, DEZA	Opening remarks
9:30	9:45	Mark Weltz	Conservation effects assessment project in U.S.A
9:45	10:00	Karim Abbaspour	Application of SWAT in global freshwater availability
10:00	10:15	Faycal Bouraoui	Application of SWAT in EU 15 countries
10:15	10:30	Fanghua Hao	Application of SWAT in China
10:30	10:45	Ashvin Gosain	Application of SWAT in India
10:45	10:55	Majid Afyuni	Application of SWAT in Iran
10:55	11:10	Clarence Richardson	Modeling and monitoring watersheds in U.S.A
11:10	**11:30**	**COFFEE BREAK**	

Session I: Moderator- Jeff Arnold

B	11:30	11:50	**Philip Gassman**, Review of peer-reviewed literature on the SWAT model
B	11:50	12:10	**Valentina Krysanova**, Prerequisites for application of ecohydrological river basin models in ungaged basins and large regions
B	12:10	12:30	**S.M. White**, Using SWAT in English catchments: experience and lessons
B	12:30	12:50	**Jürgen Schuol**, Limitations, problems and solutions in the setup of a large-scale hydrological SWAT application
B	12:50	13:10	**Adriana Bruggeman**, Use of SWAT for the assessment of water productivity in Mediterranean catchments, a case study in Syria
	13:10	**14:10**	**LUNCH BREAK**
	14:10	**15:20**	**POSTER PRESENTATION**

Session II: Moderator- Nicola Fohrer

A	15:20	15:40	**P.M. Ndomba**, The suitability of SWAT model in sediment yield modeling for ungauged catchment. A case of Simiyu River subcatchment , Tanzania
A	15:40	16:00	**Katrijn Holvoet**, Dynamic modeling of pesticide fluxes to surface waters using SWAT
A	16:00	16:20	**N. Kannan**, Predicting diffuse-source transfers of surfactants to surface waters from sewage sludge using SWAT
C	16:20	16:40	**Theresa Possley**, SDA SWAT Edition: Efficient spatial data analysis & visualization for SWAT results
	16:40	**17:00**	**COFFEE BREAK**

Session III: Moderator- Valentina Krysanova

	17:00	17:20	**Jeff Arnold & Raghavan Srinivasan**, New features of SWAT 2005
A	17:20	17:40	**V. Vandenberghe**, Use of optimal experimental design for river water quality modeling to update sampling strategies in river water year by year, considering costs and practical limitations
A	17:40	18:00	**Jennifer Jacobs**, Application of SWAT in developing countries using readily available data
A	18:00	18:20	**Bruna Grizzetti,** Performance of the SWAT model in an inter-comparison of nutrient loss quantification tools throughout Europe (EUROHARP project)
C	18:20	18:40	**P.M. Allen**, SWAT-DEG and channel stability assessment

	18:40	**21:00**	**SOCIAL GATHERING AT THE AKADEMIA POSTER AREA**

Second Day of Conference: July 14

Session IV: Moderator- Lutz Breuer

C	8:30	8:50	**F.F. Hattermann**, Integrating wetlands and riparian zones in regional hydrological modeling
C	8:50	9:10	**Ramesh Rudra**, Adapting SWAT for riparian wetlands in Ontario watershed
C	9:10	9:30	**Jim Kiniry**, Developing parameters to simulate trees with SWAT
C	9:30	9:50	**Brett M.Watson**, Improved simulation of forest growth for the Soil and Water Assessment Tool (SWAT)
C	9:50	10:10	**P. Cau**, A user friendly multi-catchments tool for the SWAT model
	10:10	10:40	**COFFEE BREAK**

Session V: Moderator-Antonio Lo Porto

C	10:40	11:00	**Martin Volk,** Towards a process-oriented HRU-concept in SWAT: catchment-related control on base flow and storage of landscape units in medium to large river basins
C	11:00	11:20	**Jing Yang**, Interfacing watershed models with systems analysis tools: implementation for SWAT
C	11:20	11:40	**Ann van Griensven**, Evaluation of models using SWAT 2005
C	11:40	12:00	**Ruth. A. McKeown**, Modifications of the Soil Water and Assessment Tool (SWAT-C) for stream flow modeling in a small, forested watershed on the Canadian Boreal Plain.
D	12:00	12:20	**Francisco Olivera**, Two-step method for SWAT calibration
	12:20	**13:20**	**LUNCH BREAK**
	13:20	**14:45**	**POSTER PRESENTATION**

Session VI: Moderator- Raghavan Srinivasan

D	14:45	15:05	**Johan Huisman**, The power of multi-objective calibration: three case studies with SWAT
D	15:05	15:25	**Bryan Tolson**, Comparison of optimization algorithms for the automatic calibration of SWAT 2000
D	15:25	15:45	**Griet Heuvelmans**, A comparison of parameter regionalization strategies for the water quantity module of the SWAT with application to the Scheldt River basin

F	15:45	16:05	**A.K. Gosain**, Vulnerability assessment of climate change impact on Indian water resources using the SWAT model
	19:00	**22:00**	**SOCIAL DINNER AT UETLIBERG**

Third Day of Conference: July 15
Session VII: Moderator-Karim Abbaspour

D	8:30	8:50	**Gerd Schmidt**, Effects of the spatial resolution of input data on SWAT simulations – a case study at the Ems River Basin (Northwestern Germany)
A	8:50	9:10	**Antonio Lo Porto**, Application of water management models to Mediterranean temporary rivers
D	9:10	9:30	**Feliciana Licciardello**, Runoff-erosion modeling by SWAT of an experimental Mediterranean watershed
E	9:30	9:50	**Do Hun Lee**, Comparison of daily runoff responses between SWAT and sequentially coupled SWAT-MODFLOW model
A	9:50	10:10	**M. P. Tripathi**, Hydrological modeling for effective management of a small agricultural watershed using SWAT
	10:10	**10:30**	**COFFEE BREAK**

Session VIII: Moderator- Raghavan Srinivasan

F	10:30	10:50	**Philip Gassman**, An Analysis of the 2004 Iowa Diffuse Pollution Needs Assessment using SWAT
F	10:50	11:10	**Claire Baffaut**, Potential accuracy of water quality estimates based on non-calibrated SWAT simulations
F	11:10	11:30	**Ilona Bärlund**, Assessing SWAT model performance in the evaluation of management actions for the implementation of the Water Framework Directive in a Finnish catchment
F	11:30	11:50	**Le Duc Trung**, Application of SWAT Model to the Decision Support Framework of the Mekong River Commission
F	11:50	12:10	**Lutz Breuer**, Effects of the new European Common Agricultural Policy on water fluxes in a low mountainous catchment of Germany
	12:10	**13:10**	**LUNCH BREAK**
	13:10	**15:30**	**POSTER PRESENTATION**

Session IX: Moderator- Martin Volk

F	15:30	15:50	**Jan Cools**, On the use of SWAT for the identification of the most cost-effective pollution abatement measures for river basins
F	15:50	16:10	**Michael W. Van Liew**, A Cursory Look at Downstream Stream flow and Sediment Response to Conservation Practice Implementation
F	16:10	16:30	**Michael F Winchell**, Development of Complex Hydrologic Response Unit (HRU) Schemes and Management Scenarios to Assess Environmental Concentrations of Agricultural Pesticides Using SWAT
	16:30	17:30	**Jeff Arnold & Raghavan Srinivasan**, Future of SWAT, ArcGIS-SWAT interface

Poster Presentations

Motalib Ahsan, Global Climate Change and Future of Water Resources in Bangladesh

Majid Afyuni, Nitrate pollution of groundwater in central Iran

Manouchehr Amini, Mapping risk of cadmium and lead contamination to human healthin soils of Central Iran

Saeed Boroomand, Crop coefficients of sugarcane (Ratoon) in Haft Tappeh of Iran

Saeed Boroomand, Floodwater effect on infiltration rate of a floodwater spreading system in Moosian

P. Cau, A Decision Support System based on the SWAT model for the Sardinian Water Authorities.

Johannes Deelstra, Scale issues hydrological pathways, and nitrogen runoff from agriculture- results from the Mellupite catchment, Latvia

Thorsten Dey, Spatially differentiated calculation of the water balance in a part of the Treene watershed (Northern Germany)

Shaaban-Ali Gholami, Distributed Watershed Modeling of a mountainous catchment

C.H. Green, SWAT model development for a large agricultural watershed in Iowa

M. Hajabbasi, Depasturtation effects on soil physical and chemical properties in Isfahan and CharMahal Bakhtiari Region

Fanghua Hao, The study of the non-point source pollution in Heihe River Basin

Claudia Hiepe, Modeling soil erosion in a sub-humid tropical environment at the regional scale

Andreas L.Horn, Modeling water quality issues in the Treene catchment in northern Germany

A. Jalalian, Soil physical and chemical properties as indicators of the degree of land degradation in Kuhrang Area, Zayandehrud Watershed

Manoj Jha, An assessment of alternative conservation practice and land use strategies on the hydrology and water quality of the Upper Mississippi River Basin

S. Kondratyev, Macro-scale catchment modeling in North-West Russia

Peter Laszlo, Application of AVSWAT2000 to simulate the various management scenarios on the Lake Balaton watershed, Hungary

Roberta Maletta, Impact of precipitation data interpolation on the quality of SWAT simulations

Ivan Maximov, Modeling of hydrology and water quality in the Thur River Basin

Claire Baffaut, SWAT modeling response of soil erosion and runoff to changes in precipitation and cover

Maria Quiteria Oliveira, Hydrologic modeling semi arid region (Brazil)

Thorsten Pohlert, Evaluation of the soil nitrogen balance model in SWAT with lysimeter data

Joachim Post, Modeling soil carbon cycle for the assessment of carbon sequestration potentials at the river basin scale

A. Rahimi, Evaluation of soil infiltration in furrow irrigation and determination of Kostiakov & Kostiakov-Lewis equations coefficients

Pipat Reungsang, Assessment of agricultural management practices in the Upper Maquoketa River Watershed Northeast Iowa: using two modeling approaches

Juan G. Martínez Rodríguez, Using SWAT model to assess vegetation change effects on runoff volume in a semi arid watershed in Northern Mexico: I. model calibration and validation

Hamed Rouhani, Evaluation of SWAT stream flow components for the Grote Nete River Basin

Ramesh Rudra, Application of AVSWAT2000 to Fairchild Creek, Grand River, Ontario

H. Saadati, Investigation of the effect of land use change on simulating daily discharge flow using SWAT (case study: Kasilian catchment area)

Javad Sadatinejad, Water-salt balance in large catchments

C. Santhi, A modeling approach for evaluating the water quality benefits of conservation practices at the national level

Ivan Sarwar, Creation of monitoring system of the Dnipro River Basin to protect environment and public health

G. Sayyad, Transport and uptake of Cd, Cu, Pb and Zn in Calcareous Soil of Central Iran under wheat and safflower cultivation – a column study

Sucharita Sen, Monitoring and evaluation of integrated watershed development programs in India: a case study of Dangri Watershed, Haryana

Sucharita Sen, Prioritizing watershed development programs in developing countries

Dongil Seo, Application of Meso-Scale Land Cover Information for Nonpoint Source Pollutant Modeling of Yongdam Dam Watershed Area, Korea using AVSWAT

Gene Takle, Climate change impacts on the hydrology and water quality of the upper Mississippi River Basin

Antje Ullrich, The sensitivity of SWAT to the variation of management parameters

A. Vassiljev, Model for nitrogen leaching from a watershed using field scale models

Gabriel G. Vazquez, Use of SWAT to compute groundwater table depth and stream flow in Muscatatuck River Watershed

Gabriel G. Vazquez, Calibration and validation of the swat model to predict atrazine in streams in northeast Indiana

T. L. Veith, Method for analyzing parameter uncertainty in SWAT 2003

S.M. White, The TERRACE project: SWAT application for diffuse chemical pollution modeling

S.M. White, Catchment scale modeling of pesticide losses with imperfect data – a case study from the UK

J. Whitehead, Ensuring appropriate hydrological response for past and future nutrient load modeling in the Norfolk Broads

Eyilachew Yitayew, Groundwater resource management in the urban environment

ISBN: 1-933570-43-1